VOLUME 25 / NUMBER 16
AUGUST 23, 1987
ACC. NOS. N87-22604 TO N87-23569

STAR

AN ABSTRACT JOURNAL

Scientific and Technical Aerospace Reports

PRODUCED BY THE
SCIENTIFIC AND TECHNICAL
INFORMATION
OFFICE

NASA

NATIONAL AERONAUTICS AND SPACE ADMINISTRATION

WHAT YOU CAN DO FOR *STAR*

All users of this abstract service are urged to forward reports to be considered for announcement in *STAR*. This will aid NASA in its efforts to provide the fullest possible coverage of all scientific and technical publications that might support aeronautics and space research and development. If you have prepared relevant reports (other than those that you will transmit to NASA, DoD, or DOE through the usual contract- or grant-reporting channels), please send them for consideration to the NASA Scientific and Technical Information Facility, P.O. Box 8757, B.W.I. Airport, Maryland 21240.

Reprints of journal articles, book chapters, and conference papers are also welcome. These will be considered for announcement in *STAR's* companion journal, *International Aerospace Abstracts.*

You may specify a particular source to be included in a report announcement if you wish; otherwise the report will be placed on public sale at the National Technical Information Service. Copyrighted publications will be announced but not distributed or sold.

PURCHASE OF *STAR*

The semimonthly issues are available for sale by the Superintendent of Documents, U.S. Government Printing Office, Washington, D.C. 20402.

PUBLISHED BY:

UNITED STATES GOVERNMENT
NATIONAL AERONAUTICS AND SPACE ADMINISTRATION
SCIENTIFIC AND TECHNICAL INFORMATION OFFICE
Scientific and Technical Aerospace Reports, Volume 25, is prepared by the NASA Scientific and Technical Information Facility operated for the National Aeronautics and Space Administration by RMS Associates.

The Administrator of the National Aeronautics and Space Administration has determined that the publication of this periodical is necessary in the transaction of the public business required by law of this Agency. Use of funds for printing this periodical has been approved by the Director of the Office of Management and Budget through March 22, 1988.

US ISSN 0036-8741

INTRODUCTION

Scientific and Technical Aerospace Reports (STAR) is a major component of a comprehensive National Aeronautics and Space Administration information system covering aeronautics, space, and supporting disciplines. *STAR* is issued on the 8th and 23rd of each month and announces current publications of the following types:

- NASA, NASA contractor, and NASA grantee reports
- Reports issued by other U.S. Government Agencies, domestic and foreign institutions, universities, and private firms
- Translations in report form
- NASA-owned patents and patent applications
- Dissertations and theses

Journal, book, and conference literature, cover-to-cover journal translations, and certain foreign dissertations are announced in a companion journal, *International Aerospace Abstracts (IAA)*, available on subscription from the American Institute of Aeronautics and Astronautics, Technical Information Service, 555 West 57th Street, 12th Floor, New York, New York 10019.

SUBJECT SCOPE

Subject scope of *STAR*, and *IAA* includes all aspects of aeronautics and space research and development, supporting basic and applied research, and applications. Aerospace aspects of earth resources, energy development, conservation, oceanography, environmental protection, urban transportation, and other topics of high national priority are also covered.

OTHER NASA PUBLICATIONS

Other NASA publications and information services are described in the publication, *The NASA Scientific and Technical Information System ... and How to Use It*, available without charge from the NASA Scientific and Technical Information Facility, P.O. Box 8757, B.W.I. Airport, Maryland 21240.

HOW TO USE *STAR* SUBJECT CATEGORIES

STAR is categorized by 10 major subject divisions divided into 76 specific subject categories and one general category/division. The major subject divisions are listed in the Table of Contents, together with a note for each that defines its scope and provides any cross-references. For example:

> **AERONAUTICS**
>
> Includes aeronautics (general); aerodynamics; air transportation and safety; aircraft communications and navigation; aircraft design, testing and performance; aircraft instrumentation; aircraft propulsion and power; aircraft stability and control; and research and support facililties (air).
>
> For related information see also *Astronautics*.

Each major division is further divided into as many as nine specific categories, which are identified by category numbers.

Abstracts in *STAR* are grouped by specific category, the categories appearing in sequential order. Category breaks in the abstract section are identified by the category number and title, and a scope note. Cross-references to other categories are provided as appropriate. For example:

> **02 AERODYNAMICS**
>
> Includes aerodynamics of bodies, combinations, wings, rotors, and control surfaces; and internal flow in ducts and turbomachinery.
>
> For related information see also *34 Fluid Mechanics and Heat Transfer.*

CROSS-REFERENCES

Individual *STAR* abstracts are not ordinarily cross-referenced, except for certain conference reports or book translations that have had separate abstracts written for their component papers or chapters. Citations and abstracts of the components follow immediately after those of the parent document. When the subject content of a component differs sufficiently from the general content of the parent, a cross-reference citation also is printed at the end of the category to which it normally would have been assigned if it were independent.

DOCUMENTS ON MICROFICHE

Documents on microfiche(1) are designated by a pound sign (#) following the accession number. The pound sign is used without regard to the source or quality of the microfiche.

AVAILABILITIES

One or more sources from which a document announced in *STAR* is available to the public is given in each citation. The most commonly indicated sources and their acronyms or abbreviations are listed below. If the publication is available from a source other than those listed, the publisher and his address will be displayed on the availability line or in combination with the corporate source line.

Avail: NTIS. Sold by the National Technical Information Service. Prices for hard copy (HC) and microfiche (MF) are indicated by a price code following the letters HC or MF in the *STAR* citation. Current values for the price codes are given in the tables on page vii.

Initially distributed microfiche under the NTIS SRIM (Selected Research in Microfiche) is available at greatly reduced unit prices. For this service and for information concerning subscription to NASA printed reports, consult the NTIS Subscription Section, Springfield, Va. 22161.

NOTE ON ORDERING DOCUMENTS: When ordering NASA publications (those followed by the * symbol), use the N accession number. NASA patent applications (only the specifications are offered) should be ordered by the US-Patent-Appl-SN number. Non-NASA publications (no asterisk) should be ordered by the AD, PB, or other *report* number shown on the last line of the citation, not by the N accession number. It is also advisable to cite the title and other bibliographic identification.

Avail: SOD (or GPO). Sold by the Superintendent of Documents, U.S. Government Printing Office, in hard copy. The current price and order number are given following the availability line. (NTIS will fill microfiche requests, as indicated above, for those documents identified by a # symbol.)

---

(1) A microfiche is a transparent sheet of film, 105 by 148 mm in size, containing as many as 60 to 98 pages of information reduced to micro images (not to exceed 26:1 reduction).

Avail: BLL (formerly NLL): British Library Lending Division, Boston Spa, Wetherby, Yorkshire, England. Photocopies available from this organization at the price shown. (If none is given, inquiry should be addressed to the BLL.)

Avail: DOE Depository Libraries. Organizations in U.S. cities and abroad that maintain collections of Department of Energy reports, usually in microfiche form, are listed in *Energy Research Abstracts*. Services available from the DOE and its depositories are described in a booklet, *DOE Technical Information Center - Its Functions and Services* (TID-4660), which may be obtained without charge from the DOE Technical Information Center.

Avail: ESDU. Pricing information on specific data, computer programs, and details on ESDU topic categories can be obtained from ESDU International Ltd. Requesters in North America should use the Virginia address while all other requesters should use the London address, both of which are on page vi.

Avail: Fachinformationszentrum, Karlsruhe. Sold by the Fachinformationszentrum Energie, Physik, Mathematik GMBH, Eggenstein Leopoldshafen, Federal Republic of Germany, at the price shown in deutschmarks (DM).

Avail: HMSO. Publications of Her Majesty's Stationery Office are sold in the U.S. by Pendragon House, Inc. (PHI), Redwood City, California. The U.S. price (including a service and mailing charge) is given, or a conversion table may be obtained from PHI.

Avail: NASA Public Document Rooms. Documents so indicated may be examined at or purchased from the National Aeronautics and Space Administration, Public Documents Room (Room 126), 600 Independence Ave., S.W., Washington, D.C. 20546, or public document rooms located at each of the NASA research centers, the NASA Space Technology Laboratories, and the NASA Pasadena Office at the Jet Propulsion Laboratory.

Avail: Univ. Microfilms. Documents so indicated are dissertations selected from *Dissertation Abstracts* and are sold by University Microfilms as xerographic copy (HC) and microfilm. All requests should cite the author and the Order Number as they appear in the citation.

Avail: US Patent and Trademark Office. Sold by Commissioner of Patents and Trademarks, U.S. Patent and Trademark Office, at the standard price of $1.50 each, postage free. (See discussion of NASA patents and patent applications below.)

Avail: (US Sales Only). These foreign documents are available to users within the United States from the National Technical Information Service (NTIS). They are available to users outside the United States through the International Nuclear Information Service (INIS) representative in their country, or by applying directly to the issuing organization.

Avail: USGS. Originals of many reports from the U.S. Geological Survey, which may contain color illustrations, or otherwise may not have the quality of illustrations preserved in the microfiche or facsimile reproduction, may be examined by the public at the libraries of the USGS field offices whose addresses are listed in this Introduction. The libraries may be queried concerning the availability of specific documents and the possible utilization of local copying services, such as color reproduction.

Avail: Issuing Activity, or Corporate Author, or no indication of availability. Inquiries as to the availability of these documents should be addressed to the organization shown in the citation as the corporate author of the document.

NASA PATENTS AND PATENT APPLICATIONS

Patents and patent applications owned by NASA are announced in *STAR* under appropriate subject categories and are referenced in the *STAR* indexes. In the Report/Accession Number Index, patents are indexed by the NASA Case Number (which appears in lieu of the report number in other indexes), the U.S. Patent Number, the U.S. Patent Application Serial Number, and the U.S. Patent Class. Patent applications for which patents have not yet been issued are indexed by the NASA Case Number and the U.S. Patent Application Serial Number.

NASA *patent application specifications* are sold in paper copy by the National Technical Information Service at price code A02. Microfiche are sold at price code A01. The US-Patent-Appl-SN- number should be used in ordering either paper copy or microfiche from NTIS. Printed copies of *patents* (which are not microfiched) are available for purchase at $1.50 per copy from:

Commissioner of Patents and Trademarks
U.S. Patent and Trademark Office
Washington, D.C. 20231

When ordering patents, the U.S. Patent Number should be used, and payment must be remitted in advance, preferably by money order or check payable to the Commissioner of Patents and Trademarks. Prepaid purchase coupons for ordering are also available from the Patent and Trademark Office. The patents and patent applications announced in *STAR* are owned by NASA and are available for royalty-free licensing. Requests for licensing terms and further information should be addressed to:

Assistant General Counsel for Patent Matters/Code GP
National Aeronautics and Space Administration
Washington, D.C. 20546

ELIGIBILITY AND REGISTRATION FOR NASA INFORMATION PRODUCTS AND SERVICES

A variety of services is available to organizations of the following types that have registered with NASA to receive specific services or products:

1. NASA offices, research centers, contractors, subcontractors, grantees, and consultants;
2. Other U.S. Government agencies and their contractors;
3. Libraries in the United States that have arrangements with NASA to maintain collections of NASA documents for public reference;
4. Other organizations in the United States having a need for NASA documents in work related to aeronautics and space research;
5. Organizations abroad that have established reciprocal document exchange arrangements with NASA.

Only the central service points or central points of document acquisition and control within qualified organizations are eligible to register for NASA products and services. Domestic organizations that may be eligible to receive various classes of NASA publications and services should address their requests for registration or for further information to:

NASA Scientific and Technical Information Facility
ATTN: Registration Activity
P.O. Box 8757
B.W.I. Airport, Maryland 21240

Organizations abroad should direct requests to the same address, but to the attention of: International Exchange Program.

AVAILABILITY OF *STAR* ABSTRACTS ON MICROFICHE

Microfiche of the abstract sections of this issue and other issues of *STAR* are available on annual subscription from NTIS, Attn: Subscriptions, 5285 Port Royal Road, Springfield, Virginia 22161. Annual subscription rates are $70.00 North America; $140.00 foreign. Abstract sections for previous years retroactive to 1964 are available at the current rates. Microfiche for individual *STAR* issue abstract sections are not available.

PUBLIC COLLECTIONS OF NASA DOCUMENTS

DOMESTIC: NASA and NASA-sponsored documents and a large number of aerospace publications are available to the public for reference purposes at the library maintained by the American Institute of Aeronautics and Astronautics, Technical Information Service, 555 West 57th Street, 12th Floor, New York, New York 10019

EUROPEAN: An extensive collection of NASA and NASA-sponsored publications is maintained by the British Library Lending Division, Boston Spa, Wetherby, Yorkshire, England for public access. The British Library Lending Division also has available many of the non-NASA publications cited in *STAR*. European requesters may purchase facsimile copy or microfiche of NASA and NASA-sponsored documents, those identified by both the symbols # and * from ESA - Information Retrieval Service European Space Agency, 8-10 rue Mario-Nikis, 75738 Paris CEDEX 15, France.

FEDERAL DEPOSITORY LIBRARY PROGRAM

In order to provide the general public with greater access to U.S. Government publications, Congress established the Federal Depository Library Program under the Government Printing Office (GPO), with 50 regional depositories responsible for permanent retention of material, inter-library loan, and reference services. At least one copy of nearly every NASA and NASA-sponsored publication, either in printed or microfiche format, is received and retained by the 50 regional depositories. A list of the regional GPO libraries, arranged alphabetically by state, appears on the inside back cover. These libraries are *not* sales outlets. A local library can contact a Regional Depository to help locate specific reports, or direct contact may be made by an individual.

ADDRESSES OF ORGANIZATIONS

American Institute of Aeronautics and Astronautics
Technical Information Service
555 West 57th Street, 12th Floor
New York, New York 10019

British Library Lending Division,
Boston Spa, Wetherby, Yorkshire,
England

Commissioner of Patents and Trademarks
U.S. Patent and Trademark Office
Washington, D.C. 20231

Department of Energy
Technical Information Center
P.O. Box 62
Oak Ridge, Tennessee 37830

ESA-Information Retrieval Service
ESRIN
Via Galileo Galilei
00044 Frascati (Rome) Italy

ESDU International, Ltd.
1495 Chain Bridge Road
McLean, Virginia 22101

ESDU International, Ltd.
251-259 Regent Street
London, W1R 7AD, England

Fachinformationszentrum Energie, Physik, Mathematik GMBH
7514 Eggenstein Leopoldshafen
Federal Republic of Germany

Her Majesty's Stationery Office
P.O. Box 569, S.E. 1
London, England

NASA Scientific and Technical Information Facility
P.O. Box 8757
B.W.I. Airport, Maryland 21240

National Aeronautics and Space Administration
Scientific and Technical Information Office (NTT-1)
Washington, D.C. 20546

National Technical Information Service
5285 Port Royal Road
Springfield, Virginia 22161

Pendragon House, Inc.
899 Broadway Avenue
Redwood City, California 94063

Superintendent of Documents
U.S. Government Printing Office
Washington, D.C. 20402

University Microfilms
A Xerox Company
300 North Zeeb Road
Ann Arbor, Michigan 48106

University Microfilms, Ltd.
Tylers Green
London, England

U.S. Geological Survey Library
National Center - MS 950
12201 Sunrise Valley Drive
Reston, Virginia 22092

U.S. Geological Survey Library
2255 North Gemini Drive
Flagstaff, Arizona 86001

U.S. Geological Survey
345 Middlefield Road
Menlo Park, California 94025

U.S. Geological Survey Library
Box 25046
Denver Federal Center, MS914
Denver, Colorado 80225

NTIS PRICE SCHEDULES

(Effective January 1, 1987)

Schedule A
STANDARD PRICE DOCUMENTS AND MICROFICHE

PRICE CODE	PAGE RANGE	NORTH AMERICAN PRICE	FOREIGN PRICE
A01	Microfiche	$ 6.50	$13.00
A02	001-025	9.95	19.90
A03	026-050	11.95	23.90
A04-A05	051-100	13.95	27.90
A06-A09	101-200	18.95	37.90
A10-A13	201-300	24.95	49.90
A14-A17	301-400	30.95	61.90
A18-A21	401-500	36.95	73.90
A22-A25	501-600	42.95	85.90
A99	601-up	*	*
NO1		45.00	80.00
NO2		48.00	80.00

Schedule E
EXCEPTION PRICE DOCUMENTS AND MICROFICHE

PRICE CODE	NORTH AMERICAN PRICE	FOREIGN PRICE
E01	$ 7.50	15.00
E02	10.00	20.00
E03	11.00	22.00
E04	13.50	27.00
E05	15.50	31.00
E06	18.00	36.00
E07	20.50	41.00
E08	23.00	46.00
E09	25.50	51.00
E10	28.00	56.00
E11	30.50	61.00
E12	33.00	66.00
E13	35.50	71.00
E14	38.50	77.00
E15	42.00	84.00
E16	46.00	92.00
E17	50.00	100.00
E18	54.00	108.00
E19	60.00	120.00
E20	70.00	140.00
E99	*	*

*Contact NTIS for price quote.

IMPORTANT NOTICE

NTIS Shipping and Handling Charges

U.S., Canada, Mexico — ADD $3.00 per TOTAL ORDER

All Other Countries — ADD $4.00 per TOTAL ORDER

Exceptions — Does NOT apply to:

ORDERS REQUESTING NTIS RUSH HANDLING
ORDERS FOR SUBSCRIPTION OR STANDING ORDER PRODUCTS *ONLY*

NOTE: Each additional delivery address on an order requires a separate shipping and handling charge.

VOLUME 25 NUMBER 16 / AUGUST 23, 1987

TABLE OF CONTENTS

AERONAUTICS

Includes aeronautics (general); aerodynamics; air transportation and safety; aircraft communications and navigation; aircraft design, testing and performance; aircraft instrumentation; aircraft propulsion and power; aircraft stability and control; and research and support facilities (air).

For related information see also *Astronautics*.

01 AERONAUTICS (GENERAL) 2107

02 AERODYNAMICS 2109

Includes aerodynamics of bodies, combinations, wings, rotors, and control surfaces; and internal flow in ducts and turbomachinery.

For related information see also *34 Fluid Mechanics and Heat Transfer*

03 AIR TRANSPORTATION AND SAFETY 2111

Includes passenger and cargo air transport operations; and aircraft accidents.

For related information see also *16 Space Transportation* and *85 Urban Technology and Transportation*.

04 AIRCRAFT COMMUNICATIONS AND NAVIGATION 2116

Includes digital and voice communication with aircraft; air navigation systems (satellite and ground based); and air traffic control.

For related information see also *17 Space Communications, Spacecraft Communications, Command and Tracking* and *32 Communications and Radar.*

05 AIRCRAFT DESIGN, TESTING AND PERFORMANCE 2116

Includes aircraft simulation technology.

For related information see also *18 Spacecraft Design, Testing and Performance* and *39 Structural Mechanics*. For land transportation vehicles see *85 Urban Technology and Transportation.*

06 AIRCRAFT INSTRUMENTATION 2118

Includes cockpit and cabin display devices; and flight instruments.

For related information see also *19 Spacecraft Instrumentation* and *35 Instrumentation and Photography.*

07 AIRCRAFT PROPULSION AND POWER 2119

Includes prime propulsion systems and systems components, e.g., gas turbine engines and compressors; and onboard auxiliary power plants for aircraft.

For related information see also *20 Spacecraft Propulsion and Power, 28 Propellants and Fuels,* and *44 Energy Production and Conversion.*

08 AIRCRAFT STABILITY AND CONTROL 2120

Includes aircraft handling qualities; piloting; flight controls; and autopilots.

For related information see also *05 Aircraft Design, Testing and Performance.*

09 RESEARCH AND SUPPORT FACILITIES (AIR) 2121

Includes airports, hangars and runways; aircraft repair and overhaul facilities; wind tunnels; shock tubes; and aircraft engine test stands.

For related information see also *14 Ground Support Systems and Facilities (Space).*

ASTRONAUTICS

Includes astronautics (general); astrodynamics; ground support systems and facilities (space); launch vehicles and space vehicles; space transportation; space communications, spacecraft communications, command and tracking; spacecraft design, testing and performance; spacecraft instrumentation; and spacecraft propulsion and power.

For related information see also *Aeronautics*

12 ASTRONAUTICS (GENERAL) 2122

For extraterrestrial exploration see*lunar and planetary Exploration.*

13 ASTRODYNAMICS 2122

Includes powered and free-flight trajectories; and orbital and launching dynamics.

14 GROUND SUPPORT SYSTEMS AND FACILITIES (SPACE) 2123

Includes launch complexes, research and production facilities; ground support equipment, e.g., mobile transporters; and simulators.

For related information see also *09 Research and Support Facilities (Air).*

15 LAUNCH VEHICLES AND SPACE VEHICLES 2123

Includes boosters; operating problems of launch/space vehicle systems; and reusable vehicles.

For related information see also *20 Spacecraft Propulsion and Power.*

16 SPACE TRANSPORTATION 2131

Includes passenger and cargo space transportation, e.g., shuttle operations; and space rescue techniques.

For related information see also *03 Air Transportation and Safety* and *18 Spacecraft Design, Testing and Performance.* For space suits see *54 Man/System Technology and Life Support.*

17 SPACE COMMUNICATIONS, SPACECRAFT COMMUNICATIONS, COMMAND AND TRACKING N.A.

Includes telemetry; space communications networks; astronavigation and guidance; and radio blackout.

For related information see also *04 Aircraft Communications and Navigation* and *32 Communications and Radar.*

18 SPACECRAFT DESIGN, TESTING AND PERFORMANCE 2132

Includes satellites; space platforms; space stations; spacecraft systems and components such as thermal and environmental controls; and attitude controls.

For life support systems see *54 Man/System Technology and Life Support.* For related information see also *05 Aircraft Design, Testing and Performance, 39 Structural Mechanics,* and *16 Space Transportation.*

19 SPACECRAFT INSTRUMENTATION 2134

For related information see also *06 Aircraft Instrumentation* and *35 Instrumentation and Photography.*

20 SPACECRAFT PROPULSION AND POWER 2134

Includes main propulsion systems and components, e.g. rocket engines; and spacecraft auxiliary power sources.

For related information see also *07 Aircraft Propulsion and Power, 28 Propellants and Fuels, 44 Energy Production and Conversion,* and *15 Launch Vehicles and Space Vehicles.*

CHEMISTRY AND MATERIALS

Includes chemistry and materials (general); composite materials; inorganic and physical chemistry; metallic materials; nonmetallic materials; propellants and fuels; and materials processing.

23 CHEMISTRY AND MATERIALS (GENERAL) N.A.

24 COMPOSITE MATERIALS 2142

Includes physical, chemical, and mechanical properties of laminates and other composite materials.

For ceramic materials see *27 Nonmetallic Materials.*

25 INORGANIC AND PHYSICAL CHEMISTRY 2143

Includes chemical analysis, e.g., chromatography; combustion theory; electrochemistry; and photochemistry.

For related information see also *77 Thermodynamics and Statistical Physics.*

26 METALLIC MATERIALS 2146

Includes physical, chemical, and mechanical properties of metals, e.g., corrosion; and metallurgy.

27 NONMETALLIC MATERIALS 2149

Includes physical, chemical, and mechanical properties of plastics, elastomers, lubricants, polymers, textiles, adhesives, and ceramic materials.

For composite materials see *24 Composite Materials.*

28 PROPELLANTS AND FUELS 2152

Includes rocket propellants, igniters and oxidizers; their storage and handling procedures; and aircraft fuels.

For related information see also *07 Aircraft Propulsion and Power, 20 Spacecraft Propulsion and Power,* and *44 Energy Production and Conversion.*

29 MATERIALS PROCESSING 2152

Includes space-based development of products and processes for commercial application.

For biological materials see *55 Space Biology.*

ENGINEERING

Includes engineering (general); communications and radar; electronics and electrical engineering; fluid mechanics and heat transfer; instrumentation and photography; lasers and masers; mechanical engineering; quality assurance and reliability; and structural mechanics.

For related information see also *Physics.*

31 ENGINEERING (GENERAL) 2152

Includes vacuum technology; control engineering; display engineering; cryogenics; and fire prevention.

32 COMMUNICATIONS AND RADAR 2153

Includes radar; land and global communications; communications theory; and optical communications.

For related information see also *04 Aircraft Communications and Navigation* and *17 Space Communications, Spacecraft Communications, Command and Tracking.* For search and rescue see *03 Air Transportation and Safety,* and *16 Space Transportation.*

33 ELECTRONICS AND ELECTRICAL ENGINEERING 2157

Includes test equipment and maintainability; components, e.g., tunnel diodes and transistors; microminiaturization; and integrated circuitry.

For related information see also *60 Computer Operations and Hardware* and *76 Solid-State Physics.*

34 FLUID MECHANICS AND HEAT TRANSFER 2162

Includes boundary layers; hydrodynamics; fluidics; mass transfer and ablation cooling.

For related information see also *02 Aerodynamics* and *77 Thermodynamics and Statistical Physics.*

35 INSTRUMENTATION AND PHOTOGRAPHY 2167

Includes remote sensors; measuring instruments and gages; detectors; cameras and photographic supplies; and holography.

For aerial photography see *43 Earth Resources and Remote Sensing.* For related information see also *06 Aircraft Instrumentation* and *19 Spacecraft Instrumentation.*

36 LASERS AND MASERS 2169

Includes parametric amplifiers.

For related information see also *76 Solid-State Physics.*

37 MECHANICAL ENGINEERING 2171

Includes auxiliary systems (nonpower); machine elements and processes; and mechanical equipment.

38 QUALITY ASSURANCE AND RELIABILITY 2173

Includes product sampling procedures and techniques; and quality control.

39 STRUCTURAL MECHANICS 2173

Includes structural element design and weight analysis; fatigue; and thermal stress.

For applications see *05 Aircraft Design, Testing and Performance* and *18 Spacecraft Design, Testing and Performance.*

GEOSCIENCES

Includes geosciences (general); earth resources and remote sensing; energy production and conversion; environment pollution; geophysics; meteorology and climatology; and oceanography.

For related information see also *Space Sciences*.

42 GEOSCIENCES (GENERAL) N.A.

43 EARTH RESOURCES AND REMOTE SENSING 2179

Includes remote sensing of earth resources by aircraft and spacecraft; photogrammetry; and aerial photography.

For instrumentation see *35 Instrumentation and Photography.*

44 ENERGY PRODUCTION AND CONVERSION 2180

Includes specific energy conversion systems, e.g., fuel cells; global sources of energy; geophysical conversion; and windpower.

For related information see also *07 Aircraft Propulsion and Power, 20 Spacecraft Propulsion and Power,* and *28 Propellants and Fuels.*

45 ENVIRONMENT POLLUTION 2182

Includes atmospheric, noise, thermal, and water pollution.

46 GEOPHYSICS 2183

Includes aeronomy; upper and lower atmosphere studies; ionospheric and magnetospheric physics; and geomagnetism.

For space radiation see *93 Space Radiation.*

47 METEOROLOGY AND CLIMATOLOGY 2191

Includes weather forecasting and modification.

48 OCEANOGRAPHY 2197

Includes biological, dynamic, and physical oceanography; and marine resources.

For related information see also *43 Earth Resources and Remote Sensing.*

LIFE SCIENCES

Includes life sciences (general); aerospace medicine; behavioral sciences; man/system technology and life support; and space biology.

51 LIFE SCIENCES (GENERAL) N.A.

52 AEROSPACE MEDICINE 2198

Includes physiological factors; biological effects of radiation; and effects of weightlessness on man and animals.

53 BEHAVIORAL SCIENCES N.A.

Includes psychological factors; individual and group behavior; crew training and evaluation; and psychiatric research.

54 MAN/SYSTEM TECHNOLOGY AND LIFE SUPPORT 2204

Includes human engineering; biotechnology; and space suits and protective clothing.

For related information see also *16 Space Transportation.*

55 SPACE BIOLOGY N.A.

Includes exobiology; planetary biology; and extraterrestrial life.

MATHEMATICAL AND COMPUTER SCIENCES

Includes mathematical and computer sciences (general); computer operations and hardware; computer programming and software; computer systems; cybernetics; numerical analysis; statistics and probability; systems analysis; and theoretical mathematics.

59 MATHEMATICAL AND COMPUTER SCIENCES (GENERAL) N.A.

60 COMPUTER OPERATIONS AND HARDWARE 2206

Includes hardware for computer graphics, firmware, and data processing.

For components see *33 Electronics and Electrical Engineering.*

61 COMPUTER PROGRAMMING AND SOFTWARE 2207

Includes computer programs, routines, algorithms, and specific applications, e.g., CAD/CAM.

62 COMPUTER SYSTEMS 2213

Includes computer networks and special application computer systems.

63 CYBERNETICS 2214

Includes feedback and control theory, artificial intelligence, robotics and expert systems.

For related information see also *54 Man/System Technology and Life Support.*

64 NUMERICAL ANALYSIS 2215

Includes iteration, difference equations, and numerical approximation.

65 STATISTICS AND PROBABILITY 2218

Includes data sampling and smoothing; Monte Carlo method; and stochastic processes.

66 SYSTEMS ANALYSIS 2221

Includes mathematical modeling; network analysis; and operations research.

67 THEORETICAL MATHEMATICS N.A.

Includes topology and number theory.

PHYSICS

Includes physics (general); acoustics; atomic and molecular physics; nuclear and high-energy physics; optics; plasma physics; solid-state physics; and thermodynamics and statistical physics.

For related information see also *Engineering.*

70 PHYSICS (GENERAL) 2221

For precision time and time interval (PTTI) see *35 Instrumentation and Photography;* for geophysics, astrophysics or solar physics see *46 Geophysics, 90 Astrophysics,* or *92 Solar Physics.*

71 ACOUSTICS 2221

Includes sound generation, transmission, and attenuation.

For noise pollution see *45 Environment Pollution.*

72 ATOMIC AND MOLECULAR PHYSICS 2222

Includes atomic structure, electron properties, and molecular spectra.

73 NUCLEAR AND HIGH-ENERGY PHYSICS 2222

Includes elementary and nuclear particles; and reactor theory.

For space radiation see *93 Space Radiation.*

74 OPTICS 2223

Includes light phenomena and optical devices.

For lasers see *36 Lasers and Masers.*

75 PLASMA PHYSICS 2226

Includes magnetohydrodynamics and plasma fusion.

For ionospheric plasmas see *46 Geophysics*. For space plasmas see *90 Astrophysics.*

76 SOLID-STATE PHYSICS 2228

Includes superconductivity.

For related information see also *33 Electronics and Electrical Engineering* and *36 Lasers and Masers.*

77 THERMODYNAMICS AND STATISTICAL PHYSICS 2232

Includes quantum mechanics; theoretical physics; and Bose and Fermi statistics.

For related information see also *25 Inorganic and Physical Chemistry* and *34 Fluid Mechanics and Heat Transfer.*

SOCIAL SCIENCES

Includes social sciences (general); administration and management; documentation and information science; economics and cost analysis; law, political science, and space policy; and urban technology and transportation.

80 SOCIAL SCIENCES (GENERAL) N.A.

Includes educational matters.

81 ADMINISTRATION AND MANAGEMENT 2232

Includes management planning and research.

82 DOCUMENTATION AND INFORMATION SCIENCE 2233

Includes information management; information storage and retrieval technology; technical writing; graphic arts; and micrography.

For computer documentation see *61 Computer Programming and Software.*

83 ECONOMICS AND COST ANALYSIS N.A.

Includes cost effectiveness studies.

84 LAW, POLITICAL SCIENCE AND SPACE POLICY N.A.

Includes NASA appropriation hearings; aviation law; space law and policy; international law; international cooperation; and patent policy.

85 URBAN TECHNOLOGY AND TRANSPORTATION N.A.

Includes applications of space technology to urban problems; technology transfer; technology assessment; and surface and mass transportation.

For related information see *03 Air Transportation and Safety, 16 Space Transportation,* and *44 Energy Production and Conversion.*

SPACE SCIENCES

Includes space sciences (general); astronomy; astrophysics; lunar and planetary exploration; solar physics; and space radiation.

For related information see also *Geosciences.*

88 SPACE SCIENCES (GENERAL) 2233

89 ASTRONOMY 2237

Includes radio, gamma-ray, and infrared astronomy; and astrometry.

90 ASTROPHYSICS 2237

Includes cosmology; celestial mechanics; space plasmas; and interstellar and interplanetary gases and dust.

For related information see also *75 Plasma Physics.*

91 LUNAR AND PLANETARY EXPLORATION 2239

Includes planetology; and manned and unmanned flights.

For spacecraft design or space stations see *18 Spacecraft Design, Testing and Performance.*

92 SOLAR PHYSICS 2274

Includes solar activity, solar flares, solar radiation and sunspots.

For related information see *93 Space Radiation.*

93 SPACE RADIATION 2275

Includes cosmic radiation; and inner and outer earth's radiation belts.

For biological effects of radiation see *52 Aerospace Medicine*. For theory see *73 Nuclear and High-Energy Physics.*

GENERAL

Includes aeronautical, astronautical, and space science related histories, biographies, and pertinent reports too broad for categorization; histories or broad overviews of NASA programs.

99 GENERAL 2276

Note: N.A. means that no abstracts were assigned to this category for this issue.

SUBJECT INDEX **I-1**
PERSONAL AUTHOR INDEX **I-61**
CORPORATE SOURCE INDEX **I-69**
CONTRACT NUMBER INDEX **I-81**
REPORT/ACCESSION NUMBER INDEX **I-83**

TYPICAL CITATION AND ABSTRACT

NASA SPONSORED

ON MICROFICHE

CORPORATE SOURCE

ACCESSION NUMBER →	**N87-12542*#** Queensland Univ., St. Lucia (Australia). Dept. of Mechanical Engineering.	
TITLE →	**FURTHER SHOCK TUNNEL STUDIES OF SCRAMJET PHENOMENA**	
AUTHORS →	R. G. Morgan, A. Paull, N. A. Morris, and R. J. Stalker 12 May 1986 112 p	← **PUBLICATION DATE**
CONTRACT OR GRANT →	(Grant NAGw-674)	
REPORT NUMBER →	(NASA-CR-179937; NAS 1.26:179937; RR-10-86) Avail: NTIS	← **AVAILABILITY SOURCE**
PRICE CODE →	HC A06/MF A01 CSCL 01A	← **COSATI CODE**

Scramjet phenomena were studied using the shock tunnel T3 at the Australian National University. Simple two dimensional models were used with a combination of wall and central injectors. Silane as an additive to hydrogen fuel was studied over a range of temperatures and pressures to evaluate its effect as an ignition aid. The film cooling effect of surface injected hydrogen was measured over a wide range of equivalence. Heat transfer measurements without injection were repeated to confirm previous indications of heating rates lower than simple flat plate predictions for laminar boundary layers in equilibrium flow. The previous results were reproduced and the discrepancies are discussed in terms of the model geometry and departures of the flow from equilibrium. In the thrust producing mode, attempts were made to increase specific impulse with wall injection. Some preliminary tests were also performed on shock induced ignition, to investigate the possibility in flight of injecting fuel upstream of the combustion chamber, where it could mix but not burn. B.G.

SUBJECT INDEX

SCIENTIFIC AND TECHNICAL AEROSPACE REPORTS VOLUME 25 NUMBER 16

Typical Subject Index Listing

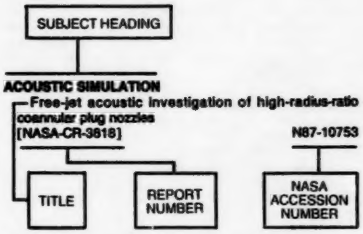

The subject heading is the key to the subject content of the document. Titles, report numbers, and accession numbers of pertinent documents are provided under each subject heading. When the title is insufficiently descriptive of the document content, a title extension has been added, separated from the title by three hyphens. The report number helps to indicate the type of document cited (e.g., NASA report, NASA translation, NASA contractor report). The NASA accession number is the number by which the document abstracts are arranged in this journal and by which the document is sold or requested. The titles, with title extensions if present, are arranged under each subject heading in ascending accession number order. The subject headings have been selected from the latest revision of the *NASA Thesaurus* (NASA SP-7053).

A

ABRASION
Aeolian abrasion on Venus: Preliminary results from the Venus simulator N87-23458
ABSORBERS (MATERIALS)
Water-absorbing capacitor system for measuring relative humidity
[NASA-CASE-NPO-16544-1-CU] N87-22953
ABSORPTION SPECTRA
New methods for obtaining scattering and absorption from tropospheric visible spectrum data
[AD-A178590] N87-23062
ABSORPTION SPECTROSCOPY
XAS (X-ray Absorption Spectroscopy) of gas phase metal-containing chemical systems
[AD-A179391] N87-22821
Plasma diagnosis by dye laser intracavity absorption
[DE87-006407] N87-23280
ABSTRACTS
A Bayesian statistics year at the Ohio State University
[AD-A178762] N87-23242
Program and abstracts of the 39th Annual Gaseous Electronics Conference
[AD-A178598] N87-23247
ABUNDANCE
SO2 on Io: A thermodynamic perspective N87-23359
Evolution of the inner asteroid belt: Paradigms and paradoxes from spectral studies N87-23372
Deconvolution of spectra for intimate mixtures N87-23428
ACCELERATION (PHYSICS)
Crew activity and motion effects on the space station N87-22744
Analytical determination of space station response to crew motion and design of suspension system for microgravity experiments N87-22752
Estimation of ICBM (intercontinental ballistic missile) performance parameters
[AD-A179204] N87-22754
Optimal shuttle altitude changes using tethers
[AD-A179205] N87-22756
Numerical modeling of on-orbit propellant motion resulting from an impulsive acceleration
[NASA-TM-89873] N87-22757
Lagrangian-like equations of hydrodynamics with mass diffusion
[DE87-007522] N87-22936
Accelerations experienced by packaged materiel during fork lift truck handling
[RDI-284/45/3] N87-22989
ACCELERATION STRESSES (PHYSIOLOGY)
Pharmacological correction of central nervous system functio during exposure to coriolis accelerations N87-23132
Reaction to vibration of rat kinesthetic analyzer neurocytes N87-23133
ACCELERATION TOLERANCE
F-16 control stick response during +G sub z-induced loss of consciousness
[AD-A178474] N87-23116
Pharmacological correction of central nervous system functio during exposure to coriolis accelerations N87-23132
ACCESS CONTROL
Throughput analysis of the IEEE 802.4 token bus standard under heavy load
[NASA-CR-180936] N87-22921
ACCRETION DISKS
Timescales for planetary accretion and the structure of the protoplanetary disk N87-23380
Generation of a dynamo magnetic field in a protoplanetary accretion disk N87-23403
ACCUMULATIONS
Analysis of the effects of impurity buildup on the performance of a reversed field pinch
[DE87-005438] N87-23277
ACOUSTIC LEVITATION
Containerless processing of glass forming melts: D-1, MEA/A-2 experiment 81F01 conducted on STS-61A flight, October 1985
[NASA-CR-179118] N87-22861
ACOUSTIC MEASUREMENT
Acoustic testing of simplified cabin box, phase 1 — helicopter cabin
[RP-698] N87-23248
ACOUSTICS
Phase space methods and path integration: A microscopic approach to direct and inverse wave propagation
[AD-A178557] N87-23249
ACOUSTO-OPTICS
The use of real-time optical processors in embedded cnmputing
[DE87-006895] N87-23153
ACTIVE CONTROL
Improved combat performance using relaxed static stability and a spin prevention system (FBW Jaguar) N87-22674
Microprocessor controlled proof-mass actuator N87-22706
Optimum mix of passive and active control of space structures N87-22714
Structural/control interaction (payload pointing and micro-g) N87-22721
Workshop on Structural Dynamics and Control Interaction of Flexible Structures N87-22728
Vibration suppression by stiffness control N87-22730
ACTUATORS
Microprocessor controlled proof-mass actuator N87-22706
On the control of structures by applied thermal gradients N87-22747
ADA (PROGRAMMING LANGUAGE)
Measuring software design
[NASA-TM-89372] N87-23189
General object-oriented software development
[NASA-TM-89375] N87-23190
Ada style guide (version 1.1)
[NASA-TM-89376] N87-23191
ADAPTATION
Convergence of relaxation algorithms by averaging
[AD-A178784] N87-23219
ADAPTIVE CONTROL
An overview of controls research on the NASA Langley Research Center grid N87-22720
Moving-bank multiple model adaptive estimation applied to flexible spacestructure control
[AD-A178870] N87-22761
Control of linear systems over commutative normed algebras with applications
[AD-A178765] N87-23205
ADAPTIVE FILTERS
A multiple model adaptive tracking algorithm for a high energy laser weapon system
[AD-A178978] N87-22974
ADDITIVES
Gas turbine combustor and engine augmentor tube sooting characteristics
[AD-A179423] N87-22679
An evaluation of metallized propellants based on vehicle performance
[NASA-TM-100104] N87-22806
ADDRESSING
A static data flow simulation study at Ames Research Center
[NASA-TM-89434] N87-23201
ADIPOSE TISSUES
Identification and validation of new anthropometric techniques for quantifying body composition
[AD-A178753] N87-23118
ADJOINTS
Generalized quantal equation of motion
[DE87-701531] N87-23307
ADRENAL GLAND
Biochemical aspects of some neurohumoral system functions during long-term antiorthostatic hypokinesia N87-23142
ADRENAL METABOLISM
Effect of short-term spaceflights on activity of renin-angiotension-aldosterone system, concentration of cyclic nucleotides and prostaglandins in blood N87-23125
ADSORPTION
The role of regolith adsorption in the transition from early to late Mars climate N87-23411
CO2: Adsorption on palagonite and the Martian regolith N87-23419
ADSORPTIVITY
Studies of the scattering/absorption of minerals N87-23423
AERIAL RECONNAISSANCE
Earth resources: A continuing bibliography with indexes (issue 53)
[NASA-SP-7041(53)] N87-23013
AERODYNAMIC CHARACTERISTICS
Analysis of structures with rotating, flexible substructures applied to rotorcraft aeroelasticity in GRASP (General Rotorcraft Aeromechanical Stability Program)
[AD-A178941] N87-22677
AERODYNAMIC COEFFICIENTS
Verification of performance results for a low-speed 15 percent elliptical circulation control airfoil
[NASA-CR-181020] N87-22633
AERODYNAMIC CONFIGURATIONS
X-29 integrating advanced technologies for tomorrow's air combat N87-22671
Improved combat performance using relaxed static stability and a spin prevention system (FBW Jaguar) N87-22674
Real-time laser holographic interferometry for aerodynamics
[NASA-TM-89462] N87-22956
AERODYNAMIC DRAG
The aerodynamic optimization of wings at subsonic speeds and the influence of wingtip design
[NASA-TM-88534] N87-22627
AERODYNAMIC HEAT TRANSFER
Numerical study of high speed viscous flows
[AD-A178639] N87-22940

AERODYNAMIC NOISE

Prediction of high-speed rotor noise with a Kirchhoff formula
[AD-A178982] N87-23250

AERODYNAMIC STALLING

Improved combat performance using relaxed static stability and a spin prevention system (FBW Jaguar)
N87-22674

Dynamic stall calculations using a Navier-Stokes solver
[AD-A178566] N87-22688

AERODYNAMICS

Improvement of Combat Performance for Existing and Future Aircraft
[AGARD-CP-409] N87-22663

Evolution of combat performance of the Hawk light combat aircraft N87-22668

Analysis of structures with rotating, flexible substructures applied to rotorcraft aeroelasticity in GRASP (General Rotorcraft Aeromechanical Stability Program)
[AD-A178941] N87-22677

The status of the vertical axis wind turbine research test bed
[DE87-005524] N87-23023

Product assurance policies and procedures for flight dynamics software development
[NASA-TM-89377] N87-23192

AEROELASTICITY

Analysis of structures with rotating, flexible substructures applied to rotorcraft aeroelasticity in GRASP (General Rotorcraft Aeromechanical Stability Program)
[AD-A178941] N87-22677

Correlation of analytical calculations from GRASP (General Rotorcraft Aeromechanical Stability Program) with torsionally-soft rotor data
[AD-A178881] N87-22689

AERONAUTICAL ENGINEERING

Description of an aeronautical geometry conversion package: Wave-drag to Langley Wireframe Geometry Standard (LaWGS) to Supersonic Implicit Marching Potential (SIMP)
[NASA-CR-178299] N87-23194

AEROSOLS

New methods for obtaining scattering and absorption from tropospheric visible spectrum data
[AD-A178590] N87-23062

Signatures from in-situ light scattering of non-homogeneous non-spherical particles
[AD-A178761] N87-23269

AEROSPACE ENVIRONMENTS

SP-100 Advanced Technology Program
[NASA-TM-89888] N87-23027

Air Force technical objectives document, fiscal year 1988
[AD-A179163] N87-23569

AEROSPACE INDUSTRY

British Aerospace: A Kingston perspective
[ETN-87-99823] N87-23308

AEROSPACE MEDICINE

Scientific goals of the German Spacelab Mission D1
[ETN-87-99669] N87-22695

Aerospace medicine and biology: A continuing bibliography with indexes (supplement 298)
[NASA-SP-7011(298)] N87-23114

F-16 control stick response during +G sub z-induced loss of consciousness
[AD-A178474] N87-23116

Air Force technical objectives document, fiscal year 1988
[AD-A179163] N87-23569

AEROSPACE TECHNOLOGY TRANSFER

Potential medical applications of TAE N87-23166

British Aerospace: A Kingston perspective
[ETN-87-99823] N87-23308

AEROTHERMODYNAMICS

Structural Integrity and Durability of Reusable Space Propulsion Systems
[NASA-CP-2471] N87-22766

Computational aerothermodynamics
[NASA-TM-89450] N87-22943

AFTERBURNING

Afterburning suppression kinetics
[AD-A178967] N87-22863

AGRICULTURE

The impact of climate change from increased atmospheric carbon dioxide on American agriculture
[DOE/NBB-0077] N87-23032

AIR DEFENSE

A partial differential equation model describing the threat to an aircraft in a one-on-Many scenario
[AD-A178641] N87-23215

AIR FILTERS

HEPA filter monitoring program
[RFP-3874] N87-22869

AIR FLOW

Diagnostic studies of meso-alpha scale flow on the Alpine northside N87-23070

On the diagnosis of a cold front observed during Alpine Experiment (ALPEX) N87-23072

Analysis of stably stratified atmospheric flow over the Dinaric Alps during the Alpine Experiment (ALPEX)
N87-23078

Dynamics and evolution of the Pyrenees lee wave event during 21-23 March 1982 N87-23079

A contribution to Bora studies using Alpine Experiment (ALPEX) aircraft data N87-23080

The Mistral-Tramuntana shear line. A satellite observation N87-23084

On the predicability of low-level flow during ALPEX — Alpine Experiment (ALPEX) N87-23088

Lagrangian turbulence measurements with constant density balloons N87-23090

Field study of the effect of orographic features on planetary boundary layer models N87-23091

The effect of the Tatra Mountains (Poland) on the atmospheric precipitation and air humidity during the northern and southern air flow N87-23094

Impact vaporization: Late time phenomena from experiments N87-23491

AIR LAND INTERACTIONS

Sensitivity of January 1983 Sea Surface Temperature (SST)-experiments to the formulation of lateral diffusion
N87-23052

Frontal interaction with orography N87-23071

Winds in the Inn Valley (Austria) N87-23074

AIR MASSES

Mesoscale analyses of temperature, pressure and wind fields over Switzerland: A case study of a Foehn
N87-23086

AIR NAVIGATION

Investigation of air transportation technology at Massachusetts Institute of Technology, 1984
N87-22605

Aircraft approach guidance using relative Loran-C navigation N87-22606

Investigation of air transportation technology at Ohio University, 1984 N87-22609

Loran-C approach considerations N87-22612

Satellite surveying for a Loran-C nonprecision approach N87-22613

AIR POLLUTION

New methods for obtaining scattering and absorption from tropospheric visible spectrum data
[AD-A178590] N87-23062

AIR QUALITY

An assessment of nitrogen oxide formation in preheated high-temperature combustion air in industrial processes
[EGG-2439] N87-23031

AIR SEA ICE INTERACTIONS

An evaluation of the polar ice prediction system
[AD-A178522] N87-23014

AIR TRAFFIC CONTROLLERS (PERSONNEL)

Investigation of hemostasis system in air traffic controllers as related to different air traffic conditions
N87-23123

AIR TRANSPORTATION

Joint University Program for Air Transportation Research, 1984
[NASA-CP-2452] N87-22604

Investigation of air transportation technology at Princeton University, 1984 N87-22619

AIR WATER INTERACTIONS

Numerical experiments on the atmospheric response to a sea surface temperature anomaly over the equatorial eastern Pacific Ocean N87-23036

Atmospheric simulations of the 1982-83 ENSO episode — El Nino Southern Oscillation (ENSO) N87-23038

Sensitivity of tropical and mid-latitude time-averaged atmospheric states to interannually varying global ocean surface temperature distribution N87-23039

Preliminary results from a Tropical Ocean Global Atmosphere (TOGA) related experiment performed at Hamburg (West Germany) with the ECWME General Circulation Model (GCM) with T21 resolution
N87-23040

Principal circulation anomalies in model atmospheres with and without interannual variations of tropical Pacific SST — sea surface temperature (SST) N87-23041

A lagged-average 60-day forecast experiment during the 1982-83 El Nino period N87-23047

Sensitivity of an Ocean General Circulation Model (OCGM) to wind forcing N87-23054

Air-sea interaction over the Mediterranean Sea during the Alpine Experiment (ALPEX) Special Observing Period N87-23073

Martian rampart craters: Morphologic clues for the physical state of the target at time of impact
N87-23507

Crater ejecta morphology and the presence of water on Mars N87-23508

AIRBORNE RADAR APPROACH

Investigation of air transportation technology at Massachusetts Institute of Technology, 1984
N87-22605

Aircraft approach guidance using relative Loran-C navigation N87-22606

Probabilistic Modeling of Loran-C for nonprecision approaches N87-22607

Investigation of air transportation technology at Ohio University, 1984 N87-22609

Loran-C approach considerations N87-22612

Satellite surveying for a Loran-C nonprecision approach N87-22613

AIRBORNE/SPACEBORNE COMPUTERS

The impact of future avionics technology on the conduct of air warfare N87-22673

The integration of spectral and spatial analysis for land use classification
[AD-A178703] N87-23015

AIRCRAFT ACCIDENTS

Integrated FAA Wind Shear Program plan
[DOT/FAA/DL-87/1] N87-23067

AIRCRAFT COMPARTMENTS

Acoustic testing of simplified cabin box, phase 1 — helicopter cabin
[RP-698] N87-23246

AIRCRAFT CONFIGURATIONS

X-29 integrating advanced technologies for tomorrow's air combat N87-22671

The assessment and evaluation of combat performance improvements N87-22675

AIRCRAFT CONSTRUCTION MATERIALS

Integrated design of structures N87-22669

AIRCRAFT CONTROL

Joint University Program for Air Transportation Research, 1984
[NASA-CP-2452] N87-22604

Investigation of air transportation technology at Princeton University, 1984 N87-22619

X-29 integrating advanced technologies for tomorrow's air combat N87-22671

Improved combat performance using relaxed static stability and a spin prevention system (FBW Jaguar)
N87-22674

Aircraft control position indicator
[NASA-CASE-LAR-12984-1] N87-22678

Evaluation of numerator lead effects on aircraft handling qualities
[AD-A179388] N87-22687

AIRCRAFT DESIGN

The aerodynamic optimization of wings at subsonic speeds and the influence of wingtip design
[NASA-TM-88534] N87-22627

Improvement of Combat Performance for Existing and Future Aircraft
[AGARD-CP-409] N87-22663

Some development trends in light ground attack aircraft N87-22666

Integrated design of structures N87-22669

Frequency-response identification of XV-15 tilt-rotor aircraft dynamics
[NASA-TM-89428] N87-22690

AIRCRAFT ENGINES

Propulsion system technologies for thrust vectoring
N87-22670

Analysis of an advanced technology subsonic turbofan incorporating revolutionary materials
[NASA-TM-89868] N87-22680

AI (Artificial Intelligence) gas turbine rotor diagnostics
[AD-A178996] N87-22683

Fiber reinforced superalloys
[NASA-TM-89865] N87-22811

AIRCRAFT FUELS

Laboratory characterization tests for antimisting fuel
[DOT/FAA/CT-86/23] N87-22684

AIRCRAFT GUIDANCE

Joint University Program for Air Transportation Research, 1984
[NASA-CP-2452] N87-22604

Investigation of air transportation technology at Massachusetts Institute of Technology, 1984
N87-22605

Aircraft approach guidance using relative Loran-C navigation N87-22606

Investigation of air transportation technology at Princeton University, 1984 N87-22619

AIRCRAFT HAZARDS

Statistics on aircraft gas turbine engine rotor failures that occurred in US commercial aviation during 1981
[DOT/FAA/CT-86/42] N87-22684

Integrated FAA Wind Shear Program plan
[DOT/FAA/DL-87/1] N87-23067

AIRCRAFT INDUSTRY

Cost analysis of aircraft projects N87-22664

AIRCRAFT LANDING
Accurate prediction of longitudinal flying qualities for landing aircraft [AD-A179069] N87-22676

AIRCRAFT LAUNCHING DEVICES
X-29 integrating advanced technologies for tomorrow's air combat N87-22671

AIRCRAFT MANEUVERS
Improved combat performance using relaxed static stability and a spin prevention system (FBW Jaguar) N87-22674
Digital control of highly augmented combat rotorcraft [NASA-TM-88346] N87-22691

AIRCRAFT NOISE
Acoustic testing of simplified cabin box, phase 1 --- helicopter cabin [RP-696] N87-23248

AIRCRAFT PERFORMANCE
A look at handling qualities of Canard configurations [NASA-TM-88354] N87-22629
Improvement of Combat Performance for Existing and Future Aircraft [AGARD-CP-409] N87-22663
Evolution of combat performance of the Hawk light combat aircraft N87-22668
Improved combat performance using relaxed static stability and a spin prevention system (FBW Jaguar) N87-22674
The assessment and evaluation of combat performance improvements N87-22675

AIRCRAFT PILOTS
Visual acuity and reaction time in navy fighter pilots [AD-A178485] N87-23117

AIRCRAFT SAFETY
Statistics on aircraft gas turbine engine rotor failures that occurred in US commercial aviation during 1981 [DOT/FAA/CT-86/42] N87-22684
Integrated FAA Wind Shear Program plan [DOT/FAA/DL-87/1] N87-23067

AIRCRAFT SPIN
Improved combat performance using relaxed static stability and a spin prevention system (FBW Jaguar) N87-22674

AIRCRAFT STABILITY
Investigation of air transportation technology at Princeton University, 1984 N87-22619
Stability boundaries for command augmentation systems N87-22622
A look at handling qualities of Canard configurations [NASA-TM-88354] N87-22629
Improved combat performance using relaxed static stability and a spin prevention system (FBW Jaguar) N87-22674
Evaluation of numerator lead effects on aircraft handling qualities [AD-A179388] N87-22687

AIRCRAFT STRUCTURES
Cost analysis of aircraft projects N87-22664
Integrated design of structures N87-22669
Prediction of service life of aircraft structural components using the half-cycle method [NASA-TM-86812] N87-23009

AIRCRAFT SURVIVABILITY
Some development trends in light ground attack aircraft N87-22666
Simulation of an integrated flight/fire control system during air-to-ground gunnery attack N87-22672

AIRFOIL PROFILES
Flutter analysis of a two-dimensional airfoil with cubic non-linear restoring force [NAE-AN-36] N87-22628

AIRFOILS
Investigation of periodic pitching through the static stall angle of attack [AD-A179512] N87-22623
Dynamic stall calculations using a Navier-Stokes solver [AD-A178566] N87-22688
Fiber reinforced superalloys [NASA-TM-89865] N87-22811
Composite velocity procedures for flows with pressure interaction [AD-A179602] N87-22929

AIRLINE OPERATIONS
Cockpit resource management training at People Express N87-22639

ALBEDO
Variations of Martian surface albedo: Evidence for yearly dust deposition and removal N87-23413
Deconvolution of spectra for intimate mixtures N87-23428
Photometric properties of lunar terrains derived from Hapke's equation N87-23432
Charged particle modification of surfaces in the outer solar system N87-23435
Sulfur-oxygen processes on Io N87-23437
Regional sources and sinks of dust on Mars: Viking observations of Cerberus, Solis Planum and Syrtis Major N87-23450
Timing of frost deposition on Martian dunes: A clue to properties of dune particles? N87-23453

ALCOHOLS
A microcrystalline growth study of solvent effects in alkoxides by dynamic laser light scattering [DE87-005710] N87-23294

ALGEBRA
Differential-algebraic equation index transformations [DE87-005543] N87-23209

ALGORITHMS
Large space structures ground experiment checkout N87-22704
Identification of large space structures: A state-of-practice report N87-22705
Flexible spacecraft simulator N87-22718
Moving-bank multiple model adaptive estimation applied to flexible spacestructure control [AD-A178670] N87-22761
Vectorizable algorithms for adaptive schemes for rapid analysis of SSME flows [NASA-CR-179082] N87-22764
Concurrent communication among multi-transceiver stations over shared media [NASA-CR-180935] N87-22890
Modeling and simulation of the WFTA (Winograd Fourier Transform Algorithm) 16 PFA (Prime Factor Algorithm) processor using the VHSIC (Very High Speed Integrated Circuit) hardware description language, volume 1 [AD-A179344] N87-22898
A multiple model adaptive tracking algorithm for a high energy laser weapon system [AD-A178978] N87-22974
Formal modeling and analysis of fault-tolerance properties for software [DE87-007006] N87-23176
An algorithm for the computation of generalized likelihood or self-critical estimators for binary data [AD-A178545] N87-23179
Design of fault tolerant prime factor algorithm array elements [AD-A178977] N87-23187
An experimental study of load balancing performance [AD-A179322] N87-23195
Parallel branch and bound on an MIMD (Multiple Instruction Stream, Multiple Data stream) system [AD-A178816] N87-23200
Control of linear systems over commutative normed algebras with applications [AD-A178765] N87-23205
A family of algorithms for the estimation of the parameters of the stable laws and the parameters of attracting stable laws [AD-A178542] N87-23214
Convergence of relaxation algorithms by averaging [AD-A178784] N87-23219
The applicability of the stable laws in collective risk theory and practice [AD-A178546] N87-23238

ALLOYS
Laser cladding of Mg and Nb alloys for improved environmental resistance [AD-A179606] N87-22833
Corrosion, wear and mechanical properties of pulse-electrodeposited alloys [AD-A178596] N87-22842
Erosion study of AM355 and Al2O3 ceramics [AD-A178882] N87-22858
Friction and wear of sintered Alpha SiC sliding against IN-718 alloy at 25 to 800 C in atmospheric air at ambient pressure [NASA-TM-87353] N87-22860
Materials Information for Science and Technology (MIST). Project overview: Phase 1 and 2 and general considerations [DE87-006799] N87-23312

ALPINE METEOROLOGY
Proceedings of the Conference on the Scientific Results of the Alpine Experiment (ALPEX), volume 2 [WMO-TD-108-VOL-2] N87-23068
Mesoscale mountain meteorology N87-23069
Diagnostic studies of meso-alpha scale flow on the Alpine northside N87-23070
On the diagnosis of a cold front observed during Alpine Experiment (ALPEX) N87-23072
Winds in the Inn Valley (Austria) N87-23074
Energy budget of an Alpine valley N87-23076
Analysis of stably stratified atmospheric flow over the Dinaric Alps during the Alpine Experiment (ALPEX) N87-23078
A contribution to Bora studies using Alpine Experiment (ALPEX) aircraft data N87-23080
Mesoscale analyses of temperature, pressure and wind fields over Switzerland: A case study of a Foehn N87-23086
Fine structure of the atmospheric boundary layer across the Alps during a high pressure period in the Alpine Experiment (ALPEX). A case study on April 22, 1982 N87-23087
On the predicability of low-level flow during ALPEX — Alpine Experiment (ALPEX) N87-23088
Synoptic-scale influence on the variability of the Alpine Experiment (ALPEX) low-level jet N87-23089

ALUMINUM
AlGaAs growth by OMCVD using an excimer laser [NASA-TM-88937] N87-23304

ALUMINUM ALLOYS
Superplasticity: A fundamental investigation on deformation mechanism and cavitation phenomena [AD-A179651] N87-22834

ALUMINUM OXIDES
Erosion study of AM355 and Al2O3 ceramics [AD-A178882] N87-22858

AMALTHEA
Cartography of irregularly shaped satellites N87-23545

AMBIENT TEMPERATURE
Friction and wear of sintered Alpha SiC sliding against IN-718 alloy at 25 to 800 C in atmospheric air at ambient pressure [NASA-TM-87353] N87-22860

AMMONIA
Low power DC arcjet operation with hydrogen/nitrogen/ammonia mixtures [NASA-TM-89676] N87-22804
High pressure cosmochemistry of major planetary interiors: Laboratory studies of the water-rich region of the system ammonia-water N87-23396
Studies of the scattering/absorption of minerals N87-23423

AMORPHOUS SILICON
Friction and wear of sintered Alpha SiC sliding against IN-718 alloy at 25 to 800 C in atmospheric air at ambient pressure [NASA-TM-87353] N87-22860

AMPLIFIERS
Programmable electronic synthesized capacitance [NASA-CASE-GSC-12961-1] N87-22895
Klystron transmitters [AD-A179068] N87-22896

ANALOG CIRCUITS
Analog fiber optic recirculating delay line [AD-A179050] N87-23272

ANALOG DATA
Measurement of the atmospheric phase coherence length, rsubo [AD-A178468] N87-23060

ANALYSIS (MATHEMATICS)
Non-linear finite element analysis program [AD-A179038] N87-23006
A method for the spatial discretization of parabolic equations in one space variable [DE87-005991] N87-23210

ANALYZERS
An implementation of a language analyzer for the very high speed integrated circuit hardware description language [AD-A178648] N87-22913

ANCHORS (FASTENERS)
Daze fasteners [NASA-CASE-LAR-13009-2] N87-22976

ANGLE OF ATTACK
Investigation of periodic pitching through the static stall angle of attack [AD-A179512] N87-22623
Hypersonic laminar boundary layer transition. Part 1: Nosetip bluntness effects on cone frustum transition. Part 2: Mach 6 experiments of transition on a cone at angle of attack [AD-A178877] N87-22625
Dynamic stall calculations using a Navier-Stokes solver [AD-A178566] N87-22688

ANGLES (GEOMETRY)
Effects of cutout orientations on natural frequencies and mode shapes of curved rectangular composite panels [AD-A178638] N87-22813
Multiple angle of incidence measurement technique for the permittivity and permeability of lossy materials at millimeter wavelengths [AD-A178851] N87-22885

ANGULAR DISTRIBUTION
Angular distribution of transition radiation in the soft X-ray spectrum [AD-A178859] N87-23255

ANGULAR MOMENTUM
Angular momentum theory applied to interactions in solids
[AD-A179366] N87-23289

ANGULAR VELOCITY
Space Station/Shuttle Orbiter dynamics during docking N87-22708

ANISOTROPY
Investigation of low-amplitude shear wave velocity in anisotropic material
[AD-A179563] N87-22994

ANNEALING
A statistical study of the combined effects of substrate temperature, bias, annealing, and a Cr3Si2 undercoating on the tribological properties of RF-sputtered MoS2 coatings
[DE87-007086] N87-23285

ANNUAL VARIATIONS
Sensitivity of tropical and mid-latitude time-averaged atmospheric states to interannually varying global ocean surface temperature distribution N87-23039
Principal circulation anomalies in model atmospheres with and without interannual variations of tropical Pacific SST — sea surface temperature (SST) N87-23041
Diagnosis of intraseasonal oscillations appearing in GCM experiments conducted at GFDL — general circulation model (GCM); Geophysical Fluid Dynamics Laboratory (GFDL) N87-23042
The 30-60 day oscillation in a perpetual January simulation with the NCAR general circulation model N87-23043
Variations of Martian surface albedo: Evidence for yearly dust deposition and removal N87-23413
Mars: Seasonally variable radar reflectivity N87-23446
Regional sources and sinks of dust on Mars: Viking observations of Cerberus, Solis Planum and Syrtis Major N87-23450
Timing of frost deposition on Martian dunes: A clue to properties of dune particles? N87-23453

ANODIC COATINGS
Corrosion, wear and mechanical properties of pulse-electrodeposited alloys
[AD-A178596] N87-22842

ANOMALIES
The delineation and interpretation of the Earth's gravity field
[NASA-CR-181015] N87-23065

ANOMALOUS TEMPERATURE ZONES
Workshop on Comparison of Simulations by Numerical Models of the Sensitivity of the Atmospheric Circulation to Sea Surface Temperature Anomalies
[WCP-121] N87-23034
Numerical experiments on the atmospheric response to a sea surface temperature anomaly over the equatorial eastern Pacific Ocean N87-23036
ENSO experiments with a two-level AGCM — El Nino Southern Oscillation (ENSO) Atmospheric General Model (AGCM) N87-23037
Atmospheric simulations of the 1982-83 ENSO episode — El Nino Southern Oscillation (ENSO) N87-23038
The impact of initial conditions and SST Anomalies on extended range predictions for the El Nino period — sea surface temperature (SST) N87-23046
The impact of SST anomalies and initial conditions on extended range predictions with an atmospheric general circulation model: A case study in early summer of 1983 N87-23051

ANTARCTIC REGIONS
Enhanced LANDSAT images of Antarctica and planetary exploration N87-23558

ANTENNA ARRAYS
Wideband parallel-plate waveguide, phased-array antenna
[AD-A179402] N87-22873
Optimization of the antenna pattern of a phased array with failed elements
[AD-A178581] N87-22878
East-west solar scans at 10-cm wavelength taken at the Algonquin Radio Observatory, Jan. 1980 to December 1985
[ARO-16] N87-23567

ANTENNA DESIGN
GPS antenna designs N87-22615

ANTENNA RADIATION PATTERNS
Detection of reflector surface error from near-field data: Effect of edge diffracted field
[NASA-TM-89920] N87-22874
Optimization of the antenna pattern of a phased array with failed elements
[AD-A178581] N87-22878

ANTENNAS
Magnitude and phase calibration of microwave sensors
[DE87-003466] N87-22955

ANTHROPOMETRY
Selection of dimensions for an anthropometric data base. Volume 2: Dimension evaluation sheets
[AD-A179472] N87-23110
Selection of dimensions for an anthropometric data base. Volume 1: Rationale, summary, and conclusions
[AD-A179566] N87-23112
Identification and validation of new anthropometric techniques for quantifying body composition
[AD-A178753] N87-23118

ANTICOAGULANTS
Investigation of hemostasis system in air traffic controllers as related to different air traffic conditions N87-23123

ANTICYCLONES
Fine structure of the atmospheric boundary layer across the Alps during a high pressure period in the Alpine Experiment (ALPEX). A case study on April 22, 1982 N87-23087

ANTIMISTING FUELS
Laboratory characterization tests for antimisting fuel
[DOT/FAA/CT-86/23] N87-22864

APERTURES
Two-point resolution criterion for multi-aperture optical systems
[AD-A178980] N87-23271

APPLICATIONS PROGRAMS (COMPUTERS)
Application of advanced computational codes in the design of an experiment for a supersonic throughflow fan rotor
[NASA-TM-88915] N87-22630
Results of the integration of a transonic full-potential analysis program with a free-wake lifting-line program for hovering rotors
[NASA-TM-89494] N87-22631
A TREETOPS simulation of the Hubble Space Telescope-High Gain Antenna interaction N87-22735
High speed simulation of flexible multibody dynamics N87-22738
Thermodynamic analysis and subscale modeling of space-based orbit transfer vehicle cryogenic propellant resupply
[NASA-TM-89921] N87-22949
An improved set of Auger data analysis programs for physical electronics Auger spectrometer systems
[DOE/TIC-4500] N87-22957
Finite element implementation of Robinson's unified viscoplastic model and its application to some uniaxial and multiaxial problems
[NASA-TM-89891] N87-23010
Sixth Annual Users' Conference --- Transportable Applications Executive (TAE)
[NASA-CP-2463] N87-23156
TAE Plus: A conceptual view of TAE in the space station era N87-23157
The evaluation end extension of TAE in the development of a user interface management system N87-23158
A design for a new catalog manager and associated file management for the Land Analysis System (LAS) N87-23159
NASA Regional Planetary Image Facility image retrieval and processing system N87-23160
SOT: A rapid prototype using TAE windows N87-23161
The 2GCHAS: A high productivity software development environment N87-23162
An overview of the catalog manager N87-23163
Display management subsystem, version 1: A user's eye view N87-23164
Rationalizing VICAR within a TAE framework: Some problems and some solutions N87-23165
Potential medical applications of TAE N87-23166
Naval applications of a TAE-derived executive N87-23167
An overview of the Land Analysis System (LAS) N87-23168
Development of Land Analysis System display modules N87-23169
Asteroid families, dynamics and astrometry N87-23370
Analysis of planetary evolution with emphasis on differentiation and dynamics N87-23382

APPROACH CONTROL
Aircraft approach guidance using relative Loran-C navigation N87-22606
Probabilistic Modeling of Loran-C for nonprecision approaches N87-22607
Advanced monitoring concepts N87-22614
Safe microburst penetration techniques: A deterministic, nonlinear, optimal control approach N87-22620
Accurate prediction of longitudinal flying qualities for landing aircraft
[AD-A179069] N87-22676

APPROXIMATION
Stationary phase approximations in Fresnel-zone magnitude-only reconstructions
[AD-A178812] N87-23270

ARC JET ENGINES
Low power DC arcjet operation with hydrogen/nitrogen/ammonia mixtures
[NASA-TM-89876] N87-22804
Langmuir probe surveys of an arcjet exhaust
[NASA-TM-89924] N87-22807

ARCHITECTURE (COMPUTERS)
The impact of future avionics technology on the conduct of air warfare N87-22673
Concurrent communication among multi-transceiver stations over shared media
[NASA-CR-180935] N87-22890
Performance comparison of four state-of-the-art computer architectures
[AD-A179071] N87-23149
The use of real-time optical processors in embedded computing
[DE87-006895] N87-23153
Optical symbolic processor for expert system execution
[AD-A179375] N87-23172
Design of fault tolerant prime factor algorithm array elements
[AD-A178977] N87-23187
Performance evaluation of parallel branch and bound search with the intel IPSC (Intel Personal SuperComputer) hypercube computer
[AD-A179384] N87-23196
An experiment in knowledge-based signal understanding using parallel architectures
[AD-A179407] N87-23197
A static data flow simulation study at Ames Research Center
[NASA-TM-89434] N87-23201

ARCTIC OCEAN
An evaluation of the polar ice prediction system
[AD-A178522] N87-23014

ARCTIC REGIONS
Atmospheric remote sensing in arctic regions
[AD-A179550] N87-23012

ARM (ANATOMY)
Workshop Symposium on Neural Models of Sensory-Motor Control
[AD-A179501] N87-23111

ARMED FORCES (UNITED STATES)
Selection of dimensions for an anthropometric data base. Volume 1: Rationale, summary, and conclusions
[AD-A179566] N87-23112
Air Force technical objectives document, fiscal year 1988
[AD-A179163] N87-23569

ARRAYS
Bipolar battery with array of sealed cells
[DE87-007194] N87-22893
Reliability of intermediate sized photovoltaic systems
[DE87-006328] N87-23024
Performance characteristics of a combination solar photovoltaic heat engine energy converter
[NASA-TM-89908] N87-23028
A static data flow simulation study at Ames Research Center
[NASA-TM-89434] N87-23201
J. VLA (Very Large Array) of a solar noise storm
[NASA-CR-180219] N87-23561
Simultaneous SMM flat crystal spectrometer and very large array observations of solar active regions
[AD-A179698] N87-23562

ARTIFICIAL INTELLIGENCE
Investigation of air transportation technology at Princeton University, 1984 N87-22619
Intelligent fault-tolerant controllers N87-22621
AI (Artificial Intelligence) gas turbine rotor diagnostics
[AD-A178996] N87-22683
Tactile feedback for teleoperator systems
[AD-A179054] N87-22983
Alternative knowledge acquisition: Developing a pulse coded neural network
[DE87-005192] N87-23145
Automatic scene analysis using hierarchical spatial frequency domain correlation with energy normalization and heuristic noise reduction
[AD-A178589] N87-23181
A prototype knowledge-based system to aid space system restoration management
[AD-A179336] N87-23203
A statistical viewpoint on the theory of evidence, revision
[AD-A178958] N87-23207
A Bayesian statistics year at the Ohio State University
[AD-A178762] N87-23242

LRS: A knowledge based approach to launch resource scheduling
[AD-A179426] N87-23310

ARTIFICIAL SATELLITES
A prototype knowledge-based system for satellite mission planning
[AD-A178873] N87-22698
A prototype expert system advisor for satellite support scheduling
[AD-A179425] N87-22760

ASPECT RATIO
Experimental evidence for non-proportional growth of large craters N87-23497

ASSOCIATIVE PROCESSING (COMPUTERS)
Optical acquisition, image and data compression
[AD-A178508] N87-23154

ASTEROID BELTS
Evolution of the inner asteroid belt: Paradigms and paradoxes from spectral studies N87-23372

ASTEROIDS
Periodic orbits about rotating asteroids in free space
[AD-A179387] N87-23338
Observations on the magnitude-frequency distribution of Earth-crossing asteroids N87-23369
Asteroid families, dynamics and astrometry N87-23370
The 1986 DA and 1986 EB: M-class asteroids in near-Earth orbits N87-23371
Meteorite spectroscopy and characterization of asteroid surface materials N87-23373
Source of the optical red-slope in iron-rich meteorites N87-23374
A search for spectral alteration effects in chondritic gas-rich breccias N87-23375
Asteroid lightcurve inversion N87-23377
Accumulation of the planets N87-23378
Solar system dynamics N87-23390
Dynamics of satellites, asteroids, and rings N87-23392
Computer simulations of 10-km-diameter asteroid impacts into oceanic and continental sites: Preliminary results on atmospheric passage, cratering and ejecta dynamics N87-23489
Impact and cratering processes on asteroids, satellites, and planets N87-23499
Crater production on Venus and Earth by asteroid and comet impact N87-23500
The surface age of Venus: Applying the terrestrial cratering rate N87-23501

ASTRO MISSIONS (STS)
Celestial target observability for astro spacelab missions
[NASA-TM-86591] N87-22696

ASTROMETRY
Asteroid families, dynamics and astrometry N87-23370

ASTRONAUTS
Developing a voice-controlled, computer-generated display to assist space station astronauts during maintenance activity
[AD-A178997] N87-22762

ASTRONOMICAL MODELS
The production of braids in Saturn's F ring N87-23363
Comet thermal modeling N87-23366
Dynamics of long period comets N87-23368
Accumulation of the planets N87-23378
Timescales for planetary accretion and the structure of the protoplanetary disk N87-23380
Formation of giant molecular clouds in global spiral structures: The role of orbital dynamics and cloud-cloud collisions N87-23381

ASTRONOMICAL PHOTOMETRY
Photometric properties of lunar terrains derived from Hapke's equation N87-23432
Io: Comparison of photometric scans produced by the Minnaert and Hapke functions N87-23436

ASTRONOMICAL SPECTROSCOPY
Compositional information for the Moon: Some characteristics of current near-IR spectra (telescopic and laboratory) N87-23429
Preliminary results of spectral reflectance studies of tycho crater N87-23430
Bidirectional reflectance spectroscopy — for Moon, asteroid, Europa, and Oberon N87-23433

ASTROPHYSICS
Timescales for planetary accretion and the structure of the protoplanetary disk N87-23380
Uranus and Neptune: Questions and possible answers N87-23386

ASYMMETRY
Waveguide junction analysis involving asymmetrical modes
[AD-A178464] N87-22909
Oklahoma downbursts and their asymmetry
[DOT/FAA/PM-87/7] N87-23095
Asymmetries in the control of saccadic eye movements to bifurcating targets
[AD-A178270] N87-23108

ASYMPTOTIC METHODS
Self-critical and robust procedures for the analysis of binary data
[AD-A178935] N87-23221

ATLANTIC OCEAN
An evaluation of the polar ice prediction system
[AD-A178522] N87-23014

ATMOSPHERIC BOUNDARY LAYER
Fine structure of the atmospheric boundary layer across the Alps during a high pressure period in the Alpine Experiment (ALPEX). A case study on April 22, 1982 N87-23087

ATMOSPHERIC CIRCULATION
Workshop on Comparison of Simulations by Numerical Models of the Sensitivity of the Atmospheric Circulation to Sea Surface Temperature Anomalies
[WCP-121] N87-23034
ENSO experiments with a two-level AGCM — El Nino Southern Oscillation (ENSO) Atmospheric General Model (AGCM) N87-23037
Preliminary results from a Tropical Ocean Global Atmosphere (TOGA) related experiment performed at Hamburg (West Germany) with the ECWME General Circulation Model (GCM) with T21 resolution N87-23040
Principal circulation anomalies in model atmospheres with and without interannual variations of tropical Pacific SST — sea surface temperature (SST) N87-23041
Diagnosis of intraseasonal oscillations appearing in GCM experiments conducted at GFDL — general circulation model (GCM); Geophysical Fluid Dynamics Laboratory (GFDL) N87-23042
The 30-60 day oscillation in a perpetual January simulation with the NCAR general circulation model N87-23043
A preliminary theory of the origin of the 40-50 day oscillation — tropical atmosphere N87-23044
Forecast and sensitivity experiments on the UK Meteorological Office GCM with El Nino SST anomalies — general circulation model (GCM) sea surface temperature (SST) N87-23045
A lagged-average 60-day forecast experiment during the 1982-83 El Nino period N87-23047
An extended forecast experiment with the CCC GCM — general climate model (GCM) N87-23050
The impact of SST anomalies and initial conditions on extended range predictions with an atmospheric general circulation model: A case study in early summer of 1983 N87-23051
Proceedings of the Conference on the Scientific Results of the Alpine Experiment (ALPEX), volume 2
[WMO-TD-108-VOL-2] N87-23068
Valley circulations as measured in the Himalaya by instrumented motor glider N87-23077
Analysis of stably stratified atmospheric flow over the Dinaric Alps during the Alpine Experiment (ALPEX) N87-23078
Field study of the effect of orographic features on planetary boundary layer models N87-23091

ATMOSPHERIC COMPOSITION
The case for a wet, warm climate on early Mars N87-23410

ATMOSPHERIC DENSITY
Wind ripples in low density atmospheres N87-23454

ATMOSPHERIC DIFFUSION
Sensitivity of January 1983 Sea Surface Temperature (SST)-experiments to the formulation of lateral diffusion N87-23052

ATMOSPHERIC HEAT BUDGET
Energy budget of an Alpine valley N87-23076

ATMOSPHERIC MODELS
Workshop on Comparison of Simulations by Numerical Models of the Sensitivity of the Atmospheric Circulation to Sea Surface Temperature Anomalies
[WCP-121] N87-23034
Simulated and observed budgets and balances during the 82/83 ENSO event — El Nino Southern Oscillation (ENSO) N87-23035
Numerical experiments on the atmospheric response to a sea surface temperature anomaly over the equatorial eastern Pacific Ocean N87-23036
ENSO experiments with a two-level AGCM — El Nino Southern Oscillation (ENSO) Atmospheric General Model (AGCM) N87-23037
Atmospheric simulations of the 1982-83 ENSO episode — El Nino Southern Oscillation (ENSO) N87-23038
Preliminary results from a Tropical Ocean Global Atmosphere (TOGA) related experiment performed at Hamburg (West Germany) with the ECWME General Circulation Model (GCM) with T21 resolution N87-23040
Principal circulation anomalies in model atmospheres with and without interannual variations of tropical Pacific SST — sea surface temperature (SST) N87-23041
Diagnosis of intraseasonal oscillations appearing in GCM experiments conducted at GFDL — general circulation model (GCM); Geophysical Fluid Dynamics Laboratory (GFDL) N87-23042
The 30-60 day oscillation in a perpetual January simulation with the NCAR general circulation model N87-23043
A preliminary theory of the origin of the 40-50 day oscillation — tropical atmosphere N87-23044
Forecast and sensitivity experiments on the UK Meteorological Office GCM with El Nino SST anomalies — general circulation model (GCM) sea surface temperature (SST) N87-23045
The impact of initial conditions and SST Anomalies on extended range predictions for the El Nino period — sea surface temperature (SST) N87-23046
A lagged-average 60-day forecast experiment during the 1982-83 El Nino period N87-23047
Sensitivity of the NMC spectral mode to the January 1983 El Nino SST — sea surface temperature N87-23048
Tropical Pacific SST experiments with the GLAS climate model — sea surface temperature (SST) N87-23049
An extended forecast experiment with the CCC GCM — general climate model (GCM) N87-23050
The impact of SST anomalies and initial conditions on extended range predictions with an atmospheric general circulation model: A case study in early summer of 1983 N87-23051
Modelling and forecasting El Nino N87-23053
The development of a coupled GCM suitable for modelling studies in TOGA — general circulation model (GCM); Tropical Ocean Global Atmosphere (TOGA) N87-23055
Numerical study of the Mistral with a mesoscale model N87-23082
Validation of a surface-layer windflow model using climatology and meteorological tower data from Vandenberg AFB, California
[AD-A178480] N87-23097

ATMOSPHERIC MOISTURE
Valley circulations as measured in the Himalaya by instrumented motor glider N87-23077

ATMOSPHERIC PHYSICS
Atmospheric remote sensing in arctic regions
[AD-A179550] N87-23012

ATMOSPHERIC PRESSURE
Friction and wear of sintered Alpha SiC sliding against IN-718 alloy at 25 to 800 C in atmospheric air at ambient pressure
[NASA-TM-87353] N87-22860
Mesoscale analyses of temperature, pressure and wind fields over Switzerland: A case study of a Foehn N87-23086

ATMOSPHERIC SOUNDING
Atmospheric remote sensing in arctic regions
[AD-A179550] N87-23012
Standard-resolution TOVS observations for the FIRE/SRB Wisconsin experiment region from October 9 through November 2, 1986
[NASA-TM-89151] N87-23101

ATMOSPHERIC TEMPERATURE
The influence of orography on the temperature and wind regime in the mountains N87-23085
Mesoscale analyses of temperature, pressure and wind fields over Switzerland: A case study of a Foehn N87-23086

ATMOSPHERIC TURBULENCE
Diagnosis of intraseasonal oscillations appearing in GCM experiments conducted at GFDL — general circulation model (GCM); Geophysical Fluid Dynamics Laboratory (GFDL) N87-23042
Air-sea interaction over the Mediterranean Sea during the Alpine Experiment (ALPEX) Special Observing Period N87-23073
Lagrangian turbulence measurements with constant density balloons N87-23090
High altitude turbulence for supersonic cruise vehicles
[NASA-TM-88285] N87-23100

ATOMIC ENERGY LEVELS
Relativistic calculations and measurements of energies, Auger rates, and lifetimes
[AD-A179137] N87-23251

ATOMIC STRUCTURE
Orbital removal method for the neutral vacancy in semiconductors
[DE87-701537] N87-23300
Submicron characterization of the atomic and electronic structure of defects in semiconductors
[AD-A178458] N87-23301

ATOMS
Non-Markovian line shapes of physisorbed atoms on a crystal
[AD-A179525] N87-23292
ATTACK AIRCRAFT
Evolution of combat performance of the Hawk light combat aircraft N87-22668
The impact of future avionics technology on the conduct of air warfare N87-22673
ATTITUDE (INCLINATION)
Accurate prediction of longitudinal flying qualities for landing aircraft
[AD-A179069] N87-22676
ATTITUDE CONTROL
Aircraft control position indicator
[NASA-CASE-LAR-12984-1] N87-22678
One Controller at a Time (1-CAT): A mimo design methodology N87-22715
Workshop on Structural Dynamics and Control Interaction of Flexible Structures N87-22728
Dual keel space station control/structures interaction study N87-22737
Space station structural dynamics/reaction control system interaction study N87-22753
AUGER SPECTROSCOPY
An improved set of Auger data analysis programs for physical electronics Auger spectrometer systems
[DOE/TIC-4500] N87-22957
AUGMENTATION
Superconducting Augmented Rail Gun (SARG)
[AD-A179269] N87-22701
AURORAL ARCS
Effect of double layers on magnetosphere-ionosphere coupling N87-23321
Anomalous transport in discrete arcs and simulation of double layers in a model auroral circuit N87-23325
Electric potential distributions at the interface between plasmasheet clouds N87-23330
AURORAS
Latitudinal motions of the aurora during substorms
[NASA-CR-180930] N87-23063
Electron acceleration in stochastic double layers
N87-23324
Weak double layers in the auroral ionosphere
N87-23326
Particle simulation of auroral double layers
N87-23327
Conditions for double layers in the Earth's magnetosphere and perhaps in other astrophysical objects N87-23328
Some aspects of double layer formation in a plasma constrained by a magnetic mirror N87-23329
Double layers above the aurora N87-23331
AUTOMATIC CONTROL
Real-time laser holographic interferometry for aerodynamics
[NASA-TM-89462] N87-22956
Automated non-destructive testing using an industrial robot
[AERE-R-12308] N87-22986
AUTOMATIC FLIGHT CONTROL
Integrated restructurable flight control system demonstration results
[NASA-CR-178305] N87-22692
AUTOMATIC FREQUENCY CONTROL
Programmable electronic synthesized capacitance
[NASA-CASE-GSC-12961-1] N87-22895
AUTOMATIC PILOTS
Effect of Gimbal friction modeling technique on control stability and performance for Centaur upper-stage
[NASA-TM-89894] N87-22755
AUTOMOBILE ENGINES
DYNA3D: A computer code for crashworthiness engineering
[DE87-003818] N87-22998
AUTOMOBILE FUELS
The autoignition of isobutane in a knocking spark ignition engine
[DE87-003241] N87-22823
AUTONOMOUS NAVIGATION
Digital Autonomous Terminal Access Communication (DATAC) system N87-22610
Star sensor fine attitude pointing model for a spinning geosynchronous satellite
[AD-A178424] N87-22763
A 3-D world modeling based on combinatorial geometry for autonomous robot navigation
[DE87-002814] N87-22980
AVIONICS
Joint University Program for Air Transportation Research, 1984
[NASA-CP-2452] N87-22604
Improvement of Combat Performance for Existing and Future Aircraft
[AGARD-CP-409] N87-22663
The impact of future avionics technology on the conduct of air warfare N87-22673
The assessment and evaluation of combat performance improvements N87-22675
Aircraft control position indicator
[NASA-CASE-LAR-12984-1] N87-22678
Electromagnetic interference (EMI) fault prevention and self recovery of digital flight control systems — helicopters
[MBB-UD-483/86] N87-22686
Digital control of highly augmented combat rotorcraft
[NASA-TM-88346] N87-22691
The integration of spectral and spatial analysis for land use classification
[AD-A178703] N87-23015
AXES OF ROTATION
Periodic orbits about rotating asteroids in free space
[AD-A179387] N87-23338
AXIAL STRESS
Investigation of low-amplitude shear wave velocity in anisotropic material
[AD-A179563] N87-22994
AXISYMMETRIC BODIES
Revised NASA axially symmetric ring model for coupled-cavity traveling-wave tubes
[NASA-TP-2675] N87-22923
AXISYMMETRIC FLOW
Axisymmetric inviscid shock tube flow simulation
[AD-A178494] N87-22937

B

BALANCING
An experimental study of load balancing performance
[AD-A179322] N87-23195
BALLISTIC TRAJECTORIES
Momentum transfer from oblique impacts N87-23493
BALLISTICS
Hybrid composite response to hydraulic ram
[AD-A178750] N87-22815
BALLOON SOUNDING
Lagrangian turbulence measurements with constant density balloons N87-23090
BANDPASS FILTERS
Envelope detection of discrete-time band-limited signals using analytic signal representations
[AD-A179307] N87-22872
BARIUM TITANATES
Reliability studies of ceramic capacitors
[AD-A179436] N87-22900
BASALT
Oxidized basalts on the surface of Venus: Compositional implications of measured spectral properties
N87-23412
Hisingerite and iddingsite on Mars: Degradation of iron-rich basalts N87-23416
Martian volcanism: Festoon-like ridges on terrestrial basalt flows and implications for Mars N87-23478
The geology of Pine and Crater Buttes: Two basaltic constructs on the far eastern Snake River Plain
N87-23487
BATCH PROCESSING
Guidelines for applying the Composite Specification Model (CSM)
[NASA-TM-89374] N87-23193
BAUXITE
Evaluation of spherical ceramic particles for solar thermal transfer media
[DE87-007432] N87-23026
BAYES THEOREM
A computer program for model verification of dynamic systems N87-22710
On Bayes selection rules for the best exponential population with type-I censored data
[AD-A178472] N87-23235
A Bayesian statistics year at the Ohio State University
[AD-A178762] N87-23242
BEAM INJECTION
A system for long pulse REB generation
[IPPJ-812] N87-23274
BEAM INTERACTIONS
Fast ion mass spectrometry and charged particle spectrography investigations of transverse ion acceleration and beam-plasma interactions
[NASA-CR-168348] N87-22817
BEAM SPLITTERS
Development of a holographic beamsplitter for use with a conventional Fresnel lens
[DE87-006770] N87-23263
BEAMS (RADIATION)
The use of the Karl sub-scale laser for Raman beam clean-up experiments
[AD-A178463] N87-22971
BEAMS (SUPPORTS)
Verification of large beam-type space structures
N87-22712
Dynamics of trusses having nonlinear joints
N87-22724
BEARING (DIRECTION)
Effects of cutout orientations on natural frequencies and mode shapes of curved rectangular composite panels
[AD-A178638] N87-22813
BEND TESTS
Influence of supporting conditions on stress intensity factors for single-edge-cracked specimens under bending
[NASA-TT-20016] N87-23008
BENDING MOMENTS
A new approach for vibration control in large space structures N87-22743
BENDING THEORY
Thermal shock resistance of mullite-based SiC-whisker composites
[AD-A179214] N87-22809
BENDING VIBRATION
Dynamic characteristics of a vibrating beam with periodic variation in bending stiffness N87-22726
BERYLLIUM ALLOYS
Characterization of rapidly solidified Al-Be-Li and Al-Be ribbons
[DE87-006613] N87-22835
BETA PARTICLES
Confinement and heating of high beta plasmas with emphasis on compact toroids. Task 2: Stellarator and heliac research
[DE87-005554] N87-23278
BIAS
A statistical study of the combined effects of substrate temperature, bias, annealing, and a Cr3Si2 undercoating on the tribological properties of RF-sputtered MoS2 coatings
[DE87-007086] N87-23285
BIBLIOGRAPHIES
Earth resources: A continuing bibliography with indexes (issue 53)
[NASA-SP-7041(53)] N87-23013
Aerospace medicine and biology: A continuing bibliography with indexes (supplement 298)
[NASA-SP-7011(298)] N87-23114
BIFURCATION (BIOLOGY)
Asymmetries in the control of saccadic eye movements to bifurcating targets
[AD-A179270] N87-23108
BINARY DATA
An algorithm for the computation of generalized likelihood or self-critical estimators for binary data
[AD-A178545] N87-23179
Self-critical and robust procedures for the analysis of binary data
[AD-A178935] N87-23221
BINARY STARS
Detection of 10^{14}-eV gamma rays from Cygnus X-3 during 1986
[DE87-006054] N87-23568
BIOCHEMISTRY
Evaluation of skeletomuscular system function in self-contained life-support system on the basis of blood biochemistry N87-23135
Some biochemical and morphological changes in rat blood with exposure to variable magnetic field at infralow frequency N87-23141
BIOELECTRICITY
Identification and validation of new anthropometric techniques for quantifying body composition
[AD-A178753] N87-23118
BIOFEEDBACK
A collection and statistical analysis of biophysical data to predict motion sickness incidence
[AD-A178874] N87-23119
BIOLOGICAL EFFECTS
Aerospace medicine and biology: A continuing bibliography with indexes (supplement 298)
[NASA-SP-7011(298)] N87-23114
USSR Report: Space Biology and Aerospace Medicine, Volume 20, No. 5, September - October 1986
[JPRS-USB-86-007] N87-23120
Reaction to vibration of rat kinesthetic analyzer neurocytes N87-23133
Hormonal and metabolic status of man in the extreme north N87-23139
Some biochemical and morphological changes in rat blood with exposure to variable magnetic field at infralow frequency N87-23141
BIOMEDICAL DATA
A collection and statistical analysis of biophysical data to predict motion sickness incidence
[AD-A178874] N87-23119

BIOPHYSICS
A collection and statistical analysis of biophysical data to predict motion sickness incidence
[AD-A178874] N87-23119

BIOTECHNOLOGY
Air Force technical objectives document, fiscal year 1988
[AD-A179163] N87-23569

BIPOLARITY
Bipolar battery with array of sealed cells
[DE87-007194] N87-22893
Development of nickel oxide/hydrogen multilayer bipolar battery for pulsed power
[AD-A178844] N87-22917
Component variations and their effects on bipolar nickel-hydrogen cell performance
[NASA-TM-89907] N87-23029

BLACKOUT (PHYSIOLOGY)
F-16 control stick response during +G sub z-induced loss of consciousness
[AD-A178474] N87-23116

BLOOD
Effect of short-term spaceflights on activity of renin-angiotensin-aldosterone system, concentration of cyclic nucleotides and prostaglandins in blood
N87-23125
Evaluation of skeletomuscular system function in self-contained life-support system on the basis of blood biochemistry N87-23135
Human blood serum proteolytic enzyme activity after stay in hypoxic environment N87-23140
Some biochemical and morphological changes in rat blood with exposure to variable magnetic field at infralow frequency N87-23141

BLOOD COAGULATION
Investigation of hemostasis system in air traffic controllers as related to different air traffic conditions
N87-23123

BLOOD FLOW
Problems and feasibility of drug correction of orthostatic tolerance in space medicine N87-23121

BLUNT BODIES
Hypersonic laminar boundary layer transition. Part 1: Nosetip bluntness effects on cone frustum transition. Part 2: Mach 6 experiments of transition on a cone at angle of attack
[AD-A178877] N87-22625
Numerical study of high speed viscous flows
[AD-A178639] N87-22940

BODY TEMPERATURE
Split circadian rhythm of simian body temperature during antiorthostatic hypokinesia N87-23128

BOMBER AIRCRAFT
Some development trends in light ground attack aircraft N87-22666
Aircrew task surveys: Selection criteria for low-cost training technology applications
[AD-A178473] N87-23146

BONDING
Microscopic study of the influence of impurities on interface bonding
[AD-A178510] N87-22841

BORON NITRIDES
Processible boron nitride preceramic polymers
[AD-A178907] N87-22859

BOUNDARY ELEMENT METHOD
Two-dimensional elastic analysis by the boundary element method
[AD-A179213] N87-22993

BOUNDARY INTEGRAL METHOD
Development of an integrated BEM (Boundary Element Mesh) for hot fluid-structure interaction N87-22799

BOUNDARY LAYER PLASMAS
Latitudinal motions of the aurora during substorms
[NASA-CR-180930] N87-23063
The generation of electrostatic noise in the plasma sheet boundary layer
[ATR-86(8433)-4] N87-23282

BOUNDARY LAYER SEPARATION
Experimental research on compressible turbulent shear layers, viscous-inviscid interactions, and flow separation
[AD-A179579] N87-22928

BOUNDARY LAYER TRANSITION
Hypersonic laminar boundary layer transition. Part 1: Nosetip bluntness effects on cone frustum transition. Part 2: Mach 6 experiments of transition on a cone at angle of attack
[AD-A178877] N87-22625
Interaction of a three-dimensional roughness element with a laminar boundary layer
[AD-A178668] N87-22941

BOUNDARY LAYERS
Millimeter wave Doppler radar observation of cloud and boundary layer structure
[AD-A178679] N87-23098

BOUNDARY VALUE PROBLEMS
A quasi-analytical method for non-iterative computation of nonlinear controls N87-22731
A new approach for vibration control in large space structures N87-22743
Vectorizable algorithms for adaptive schemes for rapid analysis of SSME flows
[NASA-CR-179082] N87-22764
Direct numerical simulations of an unpremixed turbulent jet flame
[AD-A179358] N87-22819
The impact of initial conditions and SST Anomalies on extended range predictions for the El Nino period — sea surface temperature (SST) N87-23046
The impact of SST anomalies and initial conditions on extended range predictions with an atmospheric general circulation model: A case study in early summer of 1983
N87-23051
Formation mechanisms of laboratory double layers
N87-23314
Electric fields and double layers in plasmas
N87-23323

BRAIN
Special features in regulating respiration under normal conditions and conditions of altered gas medium
[AD-A179216] N87-23106
The event related brain potential as an index of information processing and cognitive activity: A program of basic research
[AD-A179310] N87-23143

BRECCIA
A search for spectral alteration effects in chondritic gas-rich breccias N87-23375

BRIGHTNESS
The perception of brightness and colour: Neurophysiology, psychophysics and computation
[AD-A179217] N87-23107
Photometric properties of lunar terrains derived from Hapke's equation N87-23432
Bidirectional reflectance spectroscopy — for Moon, asteroid, Europa, and Oberon N87-23433

BRITTLE MATERIALS
Artificial composites for high temperature applications: A review
[DME-007] N87-22808

BRITTLENESS
Experimental and theoretical studies of the structure of grain boundaries
[DE87-007560] N87-22838

BROADBAND
Wideband parallel-plate waveguide, phased-array antenna
[AD-A179402] N87-22873

BRONZES
Circumferential hot wire TIG cladding of carbon-manganese steel with Inconel 625 and gun-metal with a tin bronze
[ARE-TM(UMD)-85574] N87-22831

BUBBLES
Thermocapillary bubble migration for large Marangoni Numbers
[NASA-CR-179628] N87-22865
Studies of vesicle distribution patterns in Hawaiian lavas N87-23484

BUCKLING
Numerical methods for imperfection sensitivity analysis of stiffened cylindrical shells. Volume 1: Development and applications
[AD-A179686] N87-22995

BULKHEADS
Tube coupling device
[NASA-CASE-MFS-25964-2] N87-22977

BUOYANCY
Flexurally-resisted uplift of the Tharsis Province, Mars
N87-23530

BURNING RATE
Afterburning suppression kinetics
[AD-A178967] N87-22863

BUTANES
The autoignition of isobutane in a knocking spark ignition engine
[DE87-003241] N87-22823

BUTT JOINTS
Residual stresses in girth butt welded pipes: Results and implications
[CUED/D-STRUCT/TR.109] N87-22992

C

CALCIUM CARBONATES
Calcium carbonate and calcium sulfate in Martian meteorite EETA79001 N87-23409

CALCULUS OF VARIATIONS
A partial differential equation model describing the threat to an aircraft in a one-on-Many scenario
[AD-A178641] N87-23215

CALIBRATING
Heat flux calibration facility capable of SSME conditions N87-22774
Numerical study of the effects of boundary conditions on the measurement and calibration of gardon type heat flux sensors N87-22775
Application of atomic fluorescence to measurement of combustion temperature in solid propellants
[AD-A179665] N87-22862
Magnitude and phase calibration of microwave sensors
[DE87-003466] N87-22955
NBS calibration services users guide, 1986-1988 edition
[NBS-SP-250] N87-22958
Calibration of the hand-held lidars used by the Naval Ocean Systems Center
[AD-A178965] N87-22973
Methodology for verification of ultrasonic inspection
[AD-A179694] N87-22988
Determination of crack initiation sites using a digital NDE workstation
[DE87-001444] N87-22997

CALLISTO
Studies of outer planet satellites, Mercury and Uranus
N87-23358
Ejecta types on Ganymede and Callisto N87-23512

CAMERAS
Design of an orbital inspection satellite
[AD-A179115] N87-22759
The Mars observer camera N87-23556

CANARD CONFIGURATIONS
A look at handling qualities of Canard configurations
[NASA-TM-88354] N87-22629
X-29 integrating advanced technologies for tomorrow's air combat N87-22671

CANTILEVER BEAMS
Experimental study of coupling between eddy curren of Tokamak limiters of tokamak limiters
[DE87-004938] N87-22999

CANYONS
Geomorphic evidence for ancient seas in west Deuteronilus Mensae, Mars-1: Regional geomorphology
N87-23471
Geomorphic evidence for ancient seas in west Deuteronilus Mensae, Mars-2: From very high resolution Viking Orbiter images N87-23472

CAPACITANCE
Programmable electronic synthesized capacitance
[NASA-CASE-GSC-12961-1] N87-22895

CAPACITORS
Reliability studies of ceramic capacitors
[AD-A179436] N87-22900
Water-absorbing capacitor system for measuring relative humidity
[NASA-CASE-NPO-16544-1-CU] N87-22953

CAPILLARY FLOW
Thermocapillary bubble migration for large Marangoni Numbers
[NASA-CR-179628] N87-22865

CARBOHYDRATE METABOLISM
Effect of hypokinesia on intensity of gluconeogenesis in cortical layer of rat kidney N87-23129

CARBON DIOXIDE
The impact of climate change from increased atmospheric carbon dioxide on American agriculture
[DOE/NBB-0077] N87-23032
The loss and depth of CO2 ice in comet nuclei
N87-23367
The case for a wet, warm climate on early Mars
N87-23410
CO2: Adsorption on palagonite and the Martian regolith N87-23419
Investigation of Martian H2O and CO2 via gamma-ray spectroscopy N87-23420

CARBON DIOXIDE LASERS
CO2 pulsed laser damage mechanism and plasma effects (focused beam)
[AD-A179201] N87-22961
Application of picosecond CO2 lasers to particle accelerators
[DE87-003711] N87-22964
A high-temperature quadrupole mass spectrometer for studying vaporization from materials heated by a CO2 laser
[LA-10744] N87-22975

CARBON FIBER REINFORCED PLASTICS
Characterization of hybridized conductive composites
[AD-A179689] N87-22810

CARBON STEELS
Circumferential hot wire TIG cladding of carbon-manganese steel with Inconel 625 and gun-metal with a tin bronze
[ARE-TM(UMD)-85574] N87-22831
CARBONACEOUS CHONDRITES
Analytical electron microscopy of fine-grained phases in primitive interplanetary dust particles and carbonaceous chondrites N87-23376
CARRIER LIFETIME
Method and apparatus for measuring minority carrier lifetime in a direct band-gap semiconductor
[NASA-CASE-NPO-16337-1-CU] N87-22894
CARTESIAN COORDINATES
The potential gradient of a plane source
[AD-A178976] N87-23223
CASCADE FLOW
Unsteady stator/rotor interaction N87-22767
A linearized Euler analysis of unsteady flows in turbomachinery
[NASA-CR-180987] N87-22948
CASTING
Mechanical properties of high gradient and hot isostatically pressed PWA 1480 N87-22781
Control systems development, research and development
[DE87-005785] N87-22868
CATALYSTS
Catalytic radiant tube. Phase 2: Proof of concept
[PB87-169835] N87-22891
CATHODES
Pulsed power for high power electron-beam pumped lasers
[DE87-004523] N87-22965
CATIONS
Novel polymeric LIT and divalent cation fast ion conducting materials
[DE87-006294] N87-23296
CAUSTICS (OPTICS)
Measurement of the J integral with caustics: An experimental and numerical investigation
[AD-A177273] N87-22990
CAVITATION FLOW
Superplasticity: A fundamental investigation on deformation mechanism and cavitation phenomena
[AD-A179651] N87-22834
CAVITIES
Experimental cavity pressure distributions at supersonic speeds
[NASA-TP-2683] N87-22626
Revised NASA axially symmetric ring model for coupled-cavity traveling-wave tubes
[NASA-TP-2675] N87-22923
CELESTIAL BODIES
Bidirectional reflectance spectroscopy — for Moon, asteroid, Europa, and Oberon N87-23433
On the sputter alteration of regoliths of outer solar system bodies N87-23434
CELESTIAL MECHANICS
Periodic orbits about rotating asteroids in free space
[AD-A179387] N87-23338
CELESTIAL NAVIGATION
Star sensor fine attitude pointing model for a spinning geosynchronous satellite
[AD-A179424] N87-22763
CELESTIAL REFERENCE SYSTEMS
Celestial target observability for astro spacelab missions
[NASA-TM-86591] N87-22696
CENSORED DATA (MATHEMATICS)
On Bayes selection rules for the best exponential population with type-I censored data
[AD-A178472] N87-23235
CENTAUR LAUNCH VEHICLE
Effect of Gimbal friction modeling technique on control stability and performance for Centaur upper-stage
[NASA-TM-89894] N87-22755
CENTRAL NERVOUS SYSTEM
Pharmacological correction of central nervous system functio during exposure to coriolis accelerations
N87-23132
Reaction to vibration of rat kinesthetic analyzer neurocytes N87-23133
CENTRIFUGES
Cross-axis synchronous flow-through coil planet centrifuge free of rotary seals: Apparatus and method for performing countercurrent chromatography
[PB87-126926] N87-22816
CENTRIFUGING
Centrifuge impact cratering experiments: Scaling laws for non-porous targets N87-23495
Centrifuge impact cratering experiments: Scaling laws for non-porous targets N87-23498
CERAMIC COATINGS
High energy high rate pulsed power processing of materials by powder consolidation and by railgun deposition
[AD-A179289] N87-22867
CERAMIC FIBERS
Processible boron nitride preceramic polymers
[AD-A178907] N87-22859
CERAMIC MATRIX COMPOSITES
Artificial composites for high temperature applications: A review
[DME-007] N87-22808
CERAMICS
Analysis of an advanced technology subsonic turbofan incorporating revolutionary materials
[NASA-TM-89868] N87-22680
Thermal shock resistance of mullite-based SiC-whisker composites
[AD-A179214] N87-22809
Experimental and theoretical studies of the structure of grain boundaries
[DE87-007560] N87-22838
The role of particle substructure in the sintering of monosized titania
[DE87-007600] N87-22839
Ceramic Technology Newsletter No. 13, October - December 1986: Ceramic technology for advanced heat engines project
[DE87-006447] N87-22852
Erosion study of AM355 and Al2O3 ceramics
[AD-A178882] N87-22858
Reliability studies of ceramic capacitors
[AD-A179436] N87-22900
Evaluation of spherical ceramic particles for solar thermal transfer media
[DE87-007432] N87-23026
CEREBELLUM
Cortical ultrastructure of rat cerebellar nodulus following flight aboard Cosmos-1514 biosatellite N87-23130
CEREBRAL CORTEX
Cortical ultrastructure of rat cerebellar nodulus following flight aboard Cosmos-1514 biosatellite N87-23130
CERENKOV COUNTERS
Cosmic ray detectors
[NASA-CR-179086] N87-22952
CERENKOV RADIATION
Cosmic ray detectors
[NASA-CR-179086] N87-22952
CERMETS
Synthesis of alumina-zirconia powders by sol-gel processing
[DE87-005721] N87-22851
CHANDRASEKHAR EQUATION
Chandrasekhar equations for infinite dimensional systems. Part 2: Unbounded input and output case
[NASA-CR-178303] N87-23208
CHANNELS (DATA TRANSMISSION)
Investigation of air transportation technology at Ohio University, 1984 N87-22609
Digital Autonomous Terminal Access Communication (DATAC) system N87-22610
Fiber optic data transmission N87-22611
A program downloader and other utility software for the DATAC bus monitor unit
[OU-TM-92] N87-22618
Concurrent communication among multi-transceiver stations over shared media
[NASA-CR-180935] N87-22890
Throughput analysis of the IEEE 802.4 token bus standard under heavy load
[NASA-CR-180936] N87-22921
Channel access schemes and fiber optic configurations for integrated-services local area networks
[NASA-CR-180934] N87-23273
CHARGED PARTICLES
Neutron scattering from charged polymer lattices
[DE87-006628] N87-22853
Charged particle modification of surfaces in the outer solar system N87-23435
CHARON
Orbital resonances, unusual configurations and exotic rotation states among planetary satellites N87-23391
CHECKOUT
Methodology for verification of ultrasonic inspection
[AD-A179694] N87-22988
CHEMICAL ANALYSIS
Calcium carbonate and calcium sulfate in Martian meteorite EETA79001 N87-23409
CHEMICAL COMPOSITION
A Simplex optimisation technique for development of rubber formulations
[ARE-TM(UMT)-86405] N87-22846
Correlations between electrical contact resistance and stages of wear in 700 Torr helium for precious metal electrical contacts
[DE87-003499] N87-22981
Experimental investigation of the process of CO2-CO-H2O-H2-N2 gas mixture breakdown in electrolysis cell with solid electrolyte N87-23137
Numerical studies of collapsing interstellar clouds
[NASA-CR-180933] N87-23340
The 1986 DA and 1986 EB: M-class asteroids in near-Earth orbits N87-23371
Evolution of the inner asteroid belt: Paradigms and paradoxes from spectral studies N87-23372
A search for spectral alteration effects in chondritic gas-rich breccias N87-23375
Analytical electron microscopy of fine-grained phases in primitive interplanetary dust particles and carbonaceous chondrites N87-23376
A chemical and petrological model of the lunar crust
N87-23408
Oxidized basalts on the surface of Venus: Compositional implications of measured spectral properties
N87-23412
Thermal-infrared spectral observations of geologic materials in emission N87-23425
Sulfur-oxygen processes on Io N87-23437
Solid sulfur in vacuum: Sublimation effects on surface microtexture, color and spectral reflectance, and applications to planetary surfaces N87-23438
Martian volcanism: Festoon-like ridges on terrestrial basalt flows and implications for Mars N87-23478
Studies of fluid instabilities in flows of lava and debris
N87-23479
The geology of Pine and Crater Buttes: Two basaltic constructs on the far eastern Snake River Plain
N87-23487
CHEMICAL DEFENSE
Air Force technical objectives document, fiscal year 1988
[AD-A179163] N87-23569
CHEMICAL ELEMENTS
Global petrologic variations of the Moon: A ternary-diagram approach N87-23407
CHEMICAL EQUILIBRIUM
Experiments pertaining to the formation and equilibration of planetary cores N87-23397
CHEMICAL EVOLUTION
Implications of convection in the Moon and the terrestrial planets N87-23406
CHEMICAL EXPLOSIONS
The effect on the strength of initiation on the corner effect — high explosives
[MBB-UA-938/86] N87-22924
CHEMICAL REACTIONS
Direct numerical simulations of an unpremixed turbulent jet flame
[AD-A179358] N87-22819
Low-pressure self-propagating high-temperature synthesis
[AD-A178593] N87-22856
CHEMOTHERAPY
Problems and feasibility of drug correction of orthostatic tolerance in space medicine N87-23121
Pharmacological correction of central nervous system functio during exposure to coriolis accelerations
N87-23132
CHIRAL DYNAMICS
The chiral symmetry aspects of supersymmetric confining gauge theories
[ETN-87-99559] N87-23305
CHONDRITES
Source of the optical red-slope in iron-rich meteorites
N87-23374
A search for spectral alteration effects in chondritic gas-rich breccias N87-23375
Magnetic flares in the protoplanetary nebula and the origin of meteorite chondrules N87-23402
CHROMATOGRAPHY
Cross-axis synchronous flow-through coil planet centrifuge free of rotary seals: Apparatus and method for performing countercurrent chromatography
[PB87-126926] N87-22816
CHROMOSPHERE
Nonlinear aspects of planar condensational instability
[AD-A178998] N87-23565
CHRONOLOGY
Timescales for planetary accretion and the structure of the protoplanetary disk N87-23380
CIRCADIAN RHYTHMS
Split circadian rhythm of simian body temperature during antiorthostatic hypokinesia N87-23128
CIRCUIT DIAGRAMS
Formal models of hardware and their applications to VLSI design automation
[AD-A178837] N87-22916
CIRCULAR CYLINDERS
Progress in the prediction of unsteady heat transfwe on turbines blades N87-22769

Computer program for electromagnetic penetration into a conducting circular cylinder through a narrow slot, TM case [AD-A178616] N87-22880

CIRCULAR ORBITS
Determining the probability of close approach between two satellites [AD-A179385] N87-22699

CIRCULATION CONTROL AIRFOILS
Verification of performance results for a low-speed 15 percent elliptical circulation control airfoil [NASA-CR-181020] N87-22633

CIVIL AVIATION
Toward the year 2000: The near future of the American civilian and military space programs [DE87-006467] N87-22697

CLADDING
Circumferential hot wire TIG cladding of carbon-manganese steel with Inconel 625 and gun-metal with a tin bronze [ARE-TM(UMD)-85574] N87-22831
Laser cladding of Mg and Nb alloys for improved environmental resistance [AD-A179606] N87-22833

CLASSIFICATIONS
Radar target classification studies [AD-A179010] N87-22889
The 1986 DA and 1986 EB: M-class asteroids in near-Earth orbits N87-23371
Natural fracture systems on planetary surfaces: Genetic classification and pattern randomness N87-23536

CLEANING
The use of the Karl sub-scale laser for Raman beam clean-up experiments [AD-A178463] N87-22971

CLIMATE
The impact of climate change from increased atmospheric carbon dioxide on American agriculture [DOE/NBB-0077] N87-23032
The case for a wet, warm climate on early Mars N87-23410
The role of regolith adsorption in the transition from early to late Mars climate N87-23411
CO2: Adsorption on palagonite and the Martian regolith N87-23419

CLIMATOLOGY
The impact of climate change from increased atmospheric carbon dioxide on American agriculture [DOE/NBB-0077] N87-23032
Validation of a surface-layer windflow model using climatology and meteorological tower data from Vandenberg AFB, California [AD-A178480] N87-23097
Standard-resolution TOVS observations for the FIRE/SRB Wisconsin experiment region from October 9 through November 2, 1986 [NASA-TM-89151] N87-23101

CLOSED ECOLOGICAL SYSTEMS
Investigation of causes of hydrogen sulfide formation in reclaimed water N87-23136

CLOSING
Gas mixtures for spark gap closing switches with emphasis on efficiency of operation [DE87-006624] N87-22906

CLOSURES
Conditional second order closure for turbulent shear flows [AD-A179661] N87-22931

CLOTHING
Selection of dimensions for an anthropometric data base. Volume 1: Rationale, summary, and conclusions [AD-A179566] N87-23112

CLOUD COVER
Millimeter wave Doppler radar observation of cloud and boundary layer structure [AD-A178679] N87-23098

CLOUD HEIGHT INDICATORS
Calibration of the hand-held lidars used by the Naval Ocean Systems Center [AD-A178965] N87-22973

CLOUD PHYSICS
Atmospheric remote sensing in arctic regions [AD-A179550] N87-23012

CLOUDS
Standard-resolution TOVS observations for the FIRE/SRB Wisconsin experiment region from October 9 through November 2, 1986 [NASA-TM-89151] N87-23101
Mass transport by Aeolian saltation on Earth, Mars and Venus: The effects of full saltation cloud development and choking N87-23456

CLUTTER
Strategies for high-resolution 3-D millimeter wave imaging [AD-A178653] N87-22882

COASTAL CURRENTS
A wind- and wave-driven nearshore current model, the one-dimensional model [AD-A178751] N87-23105

COASTS
Studies of the east Australian current off northern New South Wales [AD-A178461] N87-23103

COATINGS
Radiation damage to coatings for short wave length laser mirrors [DE87-001696] N87-22963

COBALT 60
Dose enhancement effects in the Aerospace Corporation Co-60 irradiator [AD-A178481] N87-23253

COCKPIT SIMULATORS
A feasibility study of the flexible simulation of sunlight — cockpit simulators [BR98783] N87-22693

COCKPITS
A graphics environment supporting the rapid prototyping of pictorial cockpit displays [AD-A178636] N87-23182

CODE DIVISION MULTIPLEXING
Concurrent communication among multi-transceiver stations over shared media [NASA-CR-180935] N87-22890

CODING
On 3-D inelastic analysis methods for hot section components. Volume 1: Special finite element models [NASA-CR-179494] N87-22996

COEFFICIENT OF FRICTION
Corrosion, wear and mechanical properties of pulse-electrodeposited alloys [AD-A178596] N87-22842
Friction and wear of sintered Alpha SiC sliding against IN-718 alloy at 25 to 800 C in atmospheric air at ambient pressure [NASA-TM-87353] N87-22860

COGNITION
The event related brain potential as an index of information processing and cognitive activity: A program of basic research [AD-A179310] N87-23143

COHERENT LIGHT
White-light optical information processing and holography [AD-A179489] N87-23260

COHERENT RADIATION
Why gamma rays are different: Some notes for pedestrians [DE87-004963] N87-22966

COHESION
Microscopic study of the influence of impurities on interface bonding [AD-A178510] N87-22841

COLD ACCLIMATIZATION
Hormonal and metabolic status of man in the extreme north N87-23139

COLD FRONTS
Frontal interaction with orography N87-23071
On the diagnosis of a cold front observed during Alpine Experiment (ALPEX) N87-23072

COLD PLASMAS
Pumping potential wells N87-23316
Effect of double layers on magnetosphere-ionosphere coupling N87-23321

COLLAPSE
Analysis of planetary evolution with emphasis on differentiation and dynamics N87-23382

COLLIMATORS
Measurement of the atmospheric phase coherence length, rsubo [AD-A178468] N87-23060

COLLISION RATES
Relativistic calculations and measurements of energies, Auger rates, and lifetimes [AD-A179137] N87-23251

COLLISIONAL PLASMAS
Program and abstracts of the 39th Annual Gaseous Electronics Conference [AD-A178598] N87-23247
A new hydrodynamic analysis of double layers N87-23319

COLLISIONLESS PLASMAS
Electric fields and double layers in plasmas N87-23323
Electric potential distributions at the interface between plasmasheet clouds N87-23330
Double layers and plasma-wave resistivity in extragalactic jets: Cavity formation and radio-wave emission N87-23333

COLLISIONS
Experimental studies on the impact properties of water ice N87-23364
Accumulation of the planets N87-23378
Formation of giant molecular clouds in global spiral structures: The role of orbital dynamics and cloud-cloud collisions N87-23381
Collisional and dynamical processes in moon and planet formation N87-23387
Experimental studies of collision and fragmentation phenomena N87-23494

COLOR
The perception of brightness and colour: Neurophysiology, psychophysics and computation [AD-A179217] N87-23107
Solid sulfur in vacuum: Sublimation effects on surface microtexture, color and spectral reflectance, and applications to planetary surfaces N87-23438
A preliminary analysis of the Mariner 10 color ratio map of Mercury N87-23439

COLOR PHOTOGRAPHY
White-light optical information processing and holography [AD-A179489] N87-23260

COLOR TELEVISION
Image processing for vision: An equipment requests to DOD [AD-A179261] N87-23150

COMBAT
Improvement of Combat Performance for Existing and Future Aircraft [AGARD-CP-409] N87-22663
Weapon systems polyvalence: An economic and operational challenge N87-22667

COMBINATORIAL ANALYSIS
Investigation into the use of normal and half-normal plots for interpreting results from screening experiments [AD-A179082] N87-23231

COMBUSTION
On the use of adaptive moving grid methods in combustion problems [DE87-003715] N87-22824
A high-temperature quadrupole mass spectrometer for studying vaporization from materials heated by a CO2 laser [LA-10744] N87-22975

COMBUSTION CHAMBERS
Gas turbine combustor and engine augmentor tube sooting characteristics [AD-A179423] N87-22679
Journal of Chinese Society of Astronautics (selected articles) [AD-A179690] N87-22800
Numerical simulation of the decay of swirling flow in a constant volume engine simulator [LA-10728-MS] N87-22945

COMBUSTION EFFICIENCY
Catalytic radiant tube. Phase 2: Proof of concept [PB87-169835] N87-22891
An assessment of nitrogen oxide formation in preheated high-temperature combustion air in industrial processes [EGG-2439] N87-23031

COMBUSTION PRODUCTS
An assessment of nitrogen oxide formation in preheated high-temperature combustion air in industrial processes [EGG-2439] N87-23031

COMBUSTION TEMPERATURE
Application of atomic fluorescence to measurement of combustion temperature in solid propellants [AD-A179665] N87-22862
An assessment of nitrogen oxide formation in preheated high-temperature combustion air in industrial processes [EGG-2439] N87-23031

COMET NUCLEI
Temperatures and minimum thickness of the inactive surface layer of comet Halley N87-23365
The loss and depth of CO2 ice in comet nuclei N87-23367
Dynamics of long period comets N87-23368

COMETS
Crater production on Venus and Earth by asteroid and comet impact N87-23500
The surface age of Venus: Applying the terrestrial cratering rate N87-23501

COMMUNICATION NETWORKS
The effect of multipath on digital communications systems: With application to space station [AD-A178578] N87-22876
Simulation model of a meteor burst communication system for data transmission protocol evaluation [AD-A178643] N87-22881
JANUS/Ada software implementation of a star cluster local area network of personal computers [AD-A178681] N87-23199

COMMUNICATION SATELLITES
On orbital allotments for geostationary satellites [NASA-CR-181017] N87-22700

Development of a microcomputer-based workstation for analysis of digital satellite links
[AD-A178872] N87-22888

COMPARISON

Performance comparison of four state-of-the-art computer architectures
[AD-A179071] N87-23149

Two-point resolution criterion for multi-aperture optical systems
[AD-A178980] N87-23271

COMPENSATORS

Control of linear systems over commutative normed algebras with applications
[AD-A178765] N87-23205

COMPILERS

Development of an image analysis program for the IBM PC/XT/AT
[AD-A178644] N87-23183

A development system for augmented transition network grammars and a large grammar for technical prose
[AD-A179009] N87-23188

COMPLEX COMPOUNDS

XAS (X-ray Absorption Spectroscopy) of gas phase metal-containing chemical systems
[AD-A179391] N87-22821

COMPLEX SYSTEMS

Conservative zonal schemes for patched grids in 2 and 3 dimensions
[NASA-TM-88326] N87-22932

COMPONENT RELIABILITY

Electromagnetic interference (EMI) fault prevention and self recovery of digital flight control systems — helicopters
[MBB-UD-483/86] N87-22686

Proceedings of the Instrumentation, Components, and Materials Contractors Meeting
[DE86-006596] N87-22954

Optical strain measurement system development, phase 1
[NASA-CR-179619] N87-22960

COMPOSITE MATERIALS

Thermal shock resistance of mullite-based SiC-whisker composites
[AD-A179214] N87-22809

Characterization of hybridized conductive composites
[AD-A179689] N87-22810

Electrochemical adjustment of thin film Ti-Pd resistors
[DE87-007392] N87-22837

COMPOSITE STRUCTURES

Effects of cutout orientations on natural frequencies and mode shapes of curved rectangular composite panels
[AD-A178638] N87-22813

Hybrid composite response to hydraulic ram
[AD-A178750] N87-22815

COMPRESSIBILITY

Examination of high performance polymer fibers under compressive deformation
[AD-A178640] N87-22857

COMPRESSIBLE FLOW

Flow dynamics stimulated by hairpin-like vortices in initially laminar boundary layers
[AD-A179578] N87-22927

Experimental research on compressible turbulent shear layers, viscous-inviscid interactions, and flow separation
[AD-A179579] N87-22928

A study of fluid-dynamic pressure fields on compressor reed valves
[AD-A178584] N87-22938

COMPRESSING

A fast, low resistance switch for small slapper detonators
[AD-A178562] N87-22911

COMPRESSION LOADS

Lithospheric structure on Venus from tectonic modelling of compressional features N87-23516

COMPRESSIVE STRENGTH

Examination of high performance polymer fibers under compressive deformation
[AD-A178640] N87-22857

COMPRESSOR BLADES

Preliminary investigation of the use of holographic interferometry to detect ill-fitting compressor blades
[AD-A178519] N87-22682

COMPUTATION

Dynamic stall calculations using a Navier-Stokes solver
[AD-A178566] N87-22688

Correlation of analytical calculations from GRASP (General Rotorcraft Aeromechanical Stability Program) with torsionally-soft rotor data
[AD-A178881] N87-22689

Investigate and verify the validity of mathematical formulas and procedures in relation to data obtained from theoretical investigations and experimental observations
[AD-A179564] N87-23057

Calculation of ray paths in the ionosphere using an analytic raytracing technique
[AD-A178888] N87-23064

An algorithm for the computation of generalized likelihood or self-critical estimators for binary data
[AD-A178545] N87-23179

On the least favorable configuration of a selection procedure based on ranks
[AD-A178454] N87-23234

Relativistic calculations and measurements of energies, Auger rates, and lifetimes
[AD-A179137] N87-23251

COMPUTATIONAL FLUID DYNAMICS

Application of advanced computational codes in the design of an experiment for a supersonic throughflow fan rotor
[NASA-TM-88915] N87-22630

Results of the integration of a transonic full-potential analysis program with a free-wake lifting-line program for hovering rotors
[NASA-TM-89494] N87-22631

An analysis of artificial viscosity effects on reacting flows using a spectral multi-domain technique
[NASA-CR-178308] N87-22632

Numerical modeling of on-orbit propellant motion resulting from an impulsive acceleration
[NASA-TM-89873] N87-22757

Vectorizable algorithms for adaptive schemes for rapid analysis of SSME flows
[NASA-CR-179082] N87-22764

Unsteady stator/rotor interaction N87-22767

Simulation of multistage turbine flows N87-22768

Progress in the prediction of unsteady heat transfwe on turbines blades N87-22769

Experimental and theoretical studies of time-averaged and time resolved rotor heat transfer N87-22770

Development of an integrated BEM (Boundary Element Mesh) for hot fluid-structure interaction N87-22799

Conservative zonal schemes for patched grids in 2 and 3 dimensions
[NASA-TM-88326] N87-22932

Numerical study of high speed viscous flows
[AD-A178639] N87-22940

Computational aerothermodynamics
[NASA-TM-89450] N87-22943

A three-dimensional dual potential procedure with applications to wind tunnel inlets and interacting boundary layers
[NASA-CR-180939] N87-22944

A linearized Euler analysis of unsteady flows in turbomachinery
[NASA-CR-180987] N87-22948

Protostellar disks and the primitive solar nebula
N87-23379

COMPUTATIONAL GRIDS

An overview of controls research on the NASA Langley Research Center grid N87-22720

On the use of adaptive moving grid methods in combustion problems
[DE87-003715] N87-22824

Conservative zonal schemes for patched grids in 2 and 3 dimensions
[NASA-TM-88326] N87-22932

A Godunov method for Lagrangian hydrodynamics in 1D
[DE87-005204] N87-22933

COMPUTER AIDED DESIGN

Supersonic through-flow fan design
[NASA-TM-88908] N87-22681

Probabilistic Structural Analysis Methods (PSAM) for select space propulsion system structural components
N87-22784

The NESSUS finite element code N87-22785

NESSUS/expert and NESSUS/FPI in the Probabilistic Structural Analysis Methods (PSAM) program
N87-22787

Advanced probabilistic method of development
N87-22788

Probabilistic finite elements N87-22790

Structural tailoring using the SSME/STAEBL code
N87-22795

Development of a microcomputer-based workstation for analysis of digital satellite links
[AD-A178872] N87-22888

Formal models of hardware and their applications to VLSI design automation
[AD-A178837] N87-22916

A coherent VLSI design environment
[AD-A179037] N87-22920

Research on computer aided design for maintainability
[AD-A178460] N87-23177

Multi-input/multi-output designated eigenstructure (MODES): A computer-aided control system design program
[AD-A179341] N87-23204

COMPUTER AIDED MAPPING

Computer vision research and its applications to automated cartography
[AD-A178815] N87-23017

COMPUTER GRAPHICS

Development of Land Analysis System display modules N87-23169

Parallel graph reduction on a supercomputer
[DE87-006066] N87-23173

The graphical kernel system: A standards implementation
[AD-A178583] N87-23180

A graphics environment supporting the rapid prototyping of pictorial cockpit displays
[AD-A178636] N87-23182

Development of an image analysis program for the IBM PC/XT/AT
[AD-A178644] N87-23183

Custom-made pyramids
[AD-A178955] N87-23186

COMPUTER INFORMATION SECURITY

Considerations in developing a comprehensive computer security support database system
[DE87-005527] N87-23151

Elements of a proposed security methodology for networks of computers
[DE87-006769] N87-23152

COMPUTER NETWORKS

Considerations in developing a comprehensive computer security support database system
[DE87-005527] N87-23151

Elements of a proposed security methodology for networks of computers
[DE87-006769] N87-23152

COMPUTER PROGRAM INTEGRITY

Elements of a proposed security methodology for networks of computers
[DE87-006769] N87-23152

COMPUTER PROGRAMMING

The 2GCHAS: A high productivity software development environment N87-23162

The heterogeneous machine simulator
[AD-A178771] N87-23185

Ada style guide (version 1.1)
[NASA-TM-89376] N87-23191

COMPUTER PROGRAMS

A program downloader and other utility software for the DATAC bus monitor unit
[OU-TM-92] N87-22618

Microprocessor controlled proof-mass actuator
N87-22706

Numerical modeling of on-orbit propellant motion resulting from an impulsive acceleration
[NASA-TM-89873] N87-22757

Computer program for electromagnetic penetration into a conducting circular cylinder through a narrow slot, TM case
[AD-A178616] N87-22880

On 3-D inelastic analysis methods for hot section components. Volume 1: Special finite element models
[NASA-CR-179494] N87-22996

The graphical kernel system: A standards implementation
[AD-A178583] N87-23180

General object-oriented software development
[NASA-TM-89375] N87-23190

Product assurance policies and procedures for flight dynamics software development
[NASA-TM-89377] N87-23192

Digital cartography of Mars N87-23550

COMPUTER STORAGE DEVICES

A coherent VLSI environment
[AD-A179303] N87-22897

Image processing for vision: An equipment requests to DOD
[AD-A179261] N87-23150

Convergence of relaxation algorithms by averaging
[AD-A178784] N87-23219

COMPUTER SYSTEMS DESIGN

A program downloader and other utility software for the DATAC bus monitor unit
[OU-TM-92] N87-22618

A prototype knowledge-based system for satellite mission planning
[AD-A178873] N87-22698

General object-oriented software development
[NASA-TM-89375] N87-23190

A decision support system for database management system selection
[AD-A179339] N87-23311

COMPUTER SYSTEMS PERFORMANCE

An experimental study of load balancing performance
[AD-A179322] N87-23195

COMPUTER SYSTEMS PROGRAMS
Sixth Annual Users' Conference — Transportable Applications Executive (TAE) [NASA-CP-2463] N87-23156
TAE Plus: A conceptual view of TAE in the space station era N87-23157
The evaluation and extension of TAE in the development of a user interface management system N87-23158
A design for a new catalog manager and associated file management for the Land Analysis System (LAS) N87-23159
NASA Regional Planetary Image Facility image retrieval and processing system N87-23160
SOT: A rapid prototype using TAE windows N87-23161
The 2GCHAS: A high productivity software development environment N87-23162
An overview of the catalog manager N87-23163
Display management subsystem, version 1: A user's eye view N87-23164
Rationalizing VICAR within a TAE framework: Some problems and some solutions N87-23165
Potential medical applications of TAE N87-23166
Naval applications of a TAE-derived executive N87-23167
An overview of the Land Analysis System (LAS) N87-23168
Development of Land Analysis System display modules N87-23169
Formal modeling and analysis of fault-tolerance properties for software [DE87-007006] N87-23176
JANUS/Ada software implementation of a star cluster local area network of personal computers [AD-A178681] N87-23199
COMPUTER TECHNIQUES
A program downloader and other utility software for the DATAC bus monitor unit [OU-TM-92] N87-22618
Developing a voice-controlled, computer-generated display to assist space station astronauts during maintenance activity [AD-A178997] N87-22762
Vibration analysis using shadow speckle metrology and line broadening techniques [AD-A178626] N87-23003
Research on computer aided design for maintainability [AD-A178460] N87-23177
A development system for augmented transition network grammars and a large grammar for technical prose [AD-A179009] N87-23188
Specifying functional and timing behavior for real-time applications [AD-A178769] N87-23206
COMPUTER VISION
The integration of spectral and spatial analysis for land use classification [AD-A178703] N87-23015
Computer vision research and its applications to automated cartography [AD-A178815] N87-23017
COMPUTERIZED SIMULATION
A micro-computer-based system to compute magnetic variation [OU-TM-91] N87-22617
The assessment and evaluation of combat performance improvements N87-22675
Frequency-response identification of XV-15 tilt-rotor aircraft dynamics [NASA-TM-89428] N87-22690
Transient response for interaction of two dynamic bodies N87-22709
Structural/control interaction (payload pointing and micro-g) N87-22721
Impact of space station appendage vibrations on the pointing performance of gimballed payloads N87-22733
A TREETOPS simulation of the Hubble Space Telescope-High Gain Antenna interaction N87-22735
High speed simulation of flexible multibody dynamics N87-22738
Simulation of multistage turbine flows N87-22768
Composite load spectra for select space propulsion structural components N87-22793
Direct numerical simulations of an unpremixed turbulent jet flame [AD-A179358] N87-22819
Investigation of Continuously Variable Slope Delta (CVSD) modulation for voice communications [AD-A178579] N87-22877
Simulation model of a meteor burst communication system for data transmission protocol evaluation [AD-A178643] N87-22881
Numerical simulation of the decay of swirling flow in a constant volume engine simulator [LA-10728-MS] N87-22945
DYNA3D: A computer code for crashworthiness engineering [DE87-003818] N87-22998
Atmospheric simulations of the 1982-83 ENSO episode — El Nino Southern Oscillation (ENSO) N87-23038
The 2GCHAS: A high productivity software development environment N87-23162
Patterns from models of dissipative systems [DE87-006823] N87-23175
Research on computer aided design for maintainability [AD-A178460] N87-23177
The heterogeneous machine simulator [AD-A178771] N87-23185
Automatic pattern recognition and related topics [AD-A178595] N87-23267
Development of a generalized model for a three component plasma [AD-A178979] N87-23281
Molecular-dynamics simulation of thin-film growth [DE87-006973] N87-23284
Atomistic simulation of stability properties and growth of strained layer structures [DE87-006712] N87-23297
Modeling of substrate and implantation effects on the threshold voltage of MESFET structures fabricated in semi-insulating GaAs [AD-A178550] N87-23303
Experimental observation of ion-acoustic double layers in laboratory plasma N87-23318
The cratering record at Uranus: Implications for satellite evolution and the origin of impacting objects N87-23342
Formation of giant molecular clouds in global spiral structures: The role of orbital dynamics and cloud-cloud collisions N87-23381
Eolian saltation on Mars N87-23455
Computer simulations of 10-km-diameter asteroid impacts into oceanic and continental sites: Preliminary results on atmospheric passage, cratering and ejecta dynamics N87-23489
Nonlinear aspects of planar condensational instability [AD-A178998] N87-23565
COMPUTERS
Design of fault tolerant prime factor algorithm array elements [AD-A178977] N87-23187
CONCENTRATORS
Evaluation of a heliostat tracker for linear Fresnel lens photovoltaic concentrators [DE87-006331] N87-23025
CONDUCTORS
Thermoelectric conversion with ion conductors [AD-A179353] N87-23019
CONES (VOLCANOES)
Pseudocraters as indicators of ground ice on Mars N87-23474
The geology of Pine and Crater Buttes: Two basaltic constructs on the far eastern Snake River Plain N87-23487
CONFERENCES
Improvement of Combat Performance for Existing and Future Aircraft [AGARD-CP-409] N87-22663
Structural Dynamics and Control Interaction of Flexible Structures [NASA-CP-2467-PT-2] N87-22729
Structural Integrity and Durability of Reusable Space Propulsion Systems [NASA-CP-2471] N87-22766
The Regional Electromagnetics Workshop in the USA [DE87-004709] N87-22875
Proceedings of the Instrumentation, Components, and Materials Contractors Meeting [DE86-006596] N87-22954
Workshop on Comparison of Simulations by Numerical Models of the Sensitivity of the Atmospheric Circulation to Sea Surface Temperature Anomalies [WCP-121] N87-23034
Proceedings of the Conference on the Scientific Results of the Alpine Experiment (ALPEX), volume 2 [WMO-TD-108-VOL-2] N87-23068
Workshop Symposium on Neural Models of Sensory-Motor Control [AD-A179501] N87-23111
Sixth Annual Users' Conference — Transportable Applications Executive (TAE) [NASA-CP-2463] N87-23156
A Bayesian statistics year at the Ohio State University [AD-A178762] N87-23242
Double Layers in Astrophysics [NASA-CP-2469] N87-23313
CONFIDENCE LIMITS
Development of confidence limits by pivotal functions for estimating software reliability [NASA-TP-2709] N87-23244
CONFIGURATION MANAGEMENT
Summary of the SEI (Software Engineering Institute) Workshop on Softwear Configuration Management [AD-A178770] N87-23184
The heterogeneous machine simulator [AD-A178771] N87-23185
CONSERVATION
Validation of a surface-layer windflow model using climatology and meteorological tower data from Vandenberg AFB, California [AD-A178480] N87-23097
CONSERVATION LAWS
Efficient implementation of essentially non-oscillatory shock capturing schemes [NASA-CR-178304] N87-23230
CONSTRAINTS
Physiographic constraints on the origin of lunar wrinkle ridges N87-23521
CONSTRUCTION MATERIALS
Structural panels [NASA-CASE-ARC-11429-2-CU] N87-22845
CONTACT RESISTANCE
In situ friction, wear and electrical contact resistance of precious metal alloys [DE87-001423] N87-22979
Correlations between electrical contact resistance and stages of wear in 700 Torr helium for precious metal electrical contacts [DE87-003499] N87-22981
CONTAINERLESS MELTS
Containerless processing of glass forming melts: D-1, MEA/A-2 experiment 81F01 conducted on STS-61A flight, October 1985 [NASA-CR-179118] N87-22861
CONTAMINANTS
Correlations between electrical contact resistance and stages of wear in 700 Torr helium for precious metal electrical contacts [DE87-003499] N87-22981
CONTINUOUS RADIATION
Design and operation of 140 GHz gyrotron oscillators for power levels up to 1 MW CW [DE87-006683] N87-22907
CONTINUUM MECHANICS
Equivalent beam modeling using numerical reduction techniques N87-22725
Analysis of structures with rotating, flexible substructures [AD-A178903] N87-23004
CONTOUR SENSORS
Optically Phase-Locked Electronic Speckle Pattern Interferometer (OPL-ESPI) [AD-A178652] N87-22914
CONTRACTION
Secular cooling of Earth as a source of intraplate stress N87-23519
CONTRACTORS
Proceedings of the Instrumentation, Components, and Materials Contractors Meeting [DE86-006596] N87-22954
CONTROL EQUIPMENT
Status report and preliminary results of the spacecraft control laboratory experiment N87-22717
Apparatus and method of capturing an orbiting spacecraft [NASA-CASE-MSC-20979-1] N87-22965
CONTROL SIMULATION
Flexible spacecraft simulator N87-22718
CONTROL STABILITY
Stability boundaries for command augmentation systems N87-22622
Flutter analysis of a two-dimensional airfoil with cubic non-linear restoring force [NAE-AN-36] N87-22628
Commit your works to the Lord, and your thoughts shall be established (Prov. 16:3). Inter-stable control systems N87-22716
Improving stability margins in discrete-time log controllers N87-22719
Effect of Gimbal friction modeling technique on control stability and performance for Centaur upper-stage [NASA-TM-89894] N87-22755
Control of linear systems over commutative normed algebras with applications [AD-A178765] N87-23205
CONTROL STICKS
F-16 control stick response during +G sub z-induced loss of consciousness [AD-A178474] N87-23116
CONTROL SURFACES
Integrated design of structures N87-22669
CONTROL SYSTEMS DESIGN
Digital control of highly augmented combat rotorcraft [NASA-TM-88346] N87-22691

Structural Dynamics and Control Interaction of Flexible Structures [NASA-CP-2467-PT-1] N87-22702
Status of the Mast experiment N87-22703
Large space structures ground experiment checkout N87-22704
Identification of large space structures: A state-of-practice report N87-22705
A general method for dynamic analysis of structures overview N87-22707
Space Station/Shuttle Orbiter dynamics during docking N87-22708
One Controller at a Time (1-CAT): A mimo design methodology N87-22715
Commit your works to the Lord, and your thoughts shall be established (Prov. 16:3). Inter-stable control systems N87-22716
Status report and preliminary results of the spacecraft control laboratory experiment N87-22717
An overview of controls research on the NASA Langley Research Center grid N87-22720
Solar array flight dynamic experiment N87-22722
Precision pointing and control of flexible spacecraft N87-22723
Dual keel space station control/structures interaction study N87-22737
High speed simulation of flexible multibody dynamics N87-22738
Lanczos modes for reduced-order control of flexible structures N87-22739
Slewing control experiment for a flexible panel N87-22740
Maximum Entropy/Optimal Projection (MEOP) control design synthesis: Optimal quantification of the major design tradeoffs N87-22741
Space station structures and dynamics test program N87-22751
Space station structural dynamics/reaction control system interaction study N87-22753
Control systems development, research and development [DE87-005785] N87-22868
Modeling digital control systems with MA-prefiltered measurements [NASA-TP-2732] N87-22870
Multi-input/multi-output designated eigenstructure (MODES): A computer-aided control system design program [AD-A179341] N87-23204

CONTROL THEORY
Joint University Program for Air Transportation Research, 1984 [NASA-CP-2452] N87-22604
Intelligent fault-tolerant controllers N87-22621
Flutter analysis of a two-dimensional airfoil with cubic non-linear restoring force [NAE-AN-36] N87-22628
A quasi-analytical method for non-iterative computation of nonlinear controls N87-22731
Control of flexible structures and the research community N87-22732
Maneuvering and vibration control of flexible spacecraft N87-22734
A TREETOPS simulation of the Hubble Space Telescope-High Gain Antenna interaction N87-22735
Dual keel space station control/structures interaction study N87-22737
On the control of structures by applied thermal gradients N87-22747

CONTROLLABILITY
A look at handling qualities of Canard configurations [NASA-TM-88354] N87-22629
Evaluation of numerator lead effects on aircraft handling qualities [AD-A179388] N87-22687

CONTROLLERS
Intelligent fault-tolerant controllers N87-22621
One Controller at a Time (1-CAT): A mimo design methodology N87-22715

CONVECTION
Characteristics of orographically initiated convection — Rocky Mountains N87-23092
Implications of convection in the Moon and the terrestrial planets N87-23406

CONVECTIVE HEAT TRANSFER
Numerical study of the effects of boundary conditions on the measurement and calibration of gardon type heat flux sensors N87-22775
Numerical calculation of the drag force induced by natural convection of spheres at low Grashof numbers [DE87-006791] N87-22935
Energy budget of an Alpine valley N87-23076
Venusian tectonics: Convective coupling to the lithosphere? N87-23517

CONVERGENCE
Convergence of relaxation algorithms by averaging [AD-A178784] N87-23219
Wielandt iteration as applied to the nodal expansion method [KAPL-4194] N87-23227
The exponential method [TRITA-NA-8517] N87-23228

COOLING
Numerical study of the effects of boundary conditions on the measurement and calibration of gardon type heat flux sensors N87-22775

COPOLYMERS
Physical properties and structure of ion-containing polymers [AD-A178592] N87-22855

COPPER
Investigation of the transverse-discharge copper-vapor laser [AD-A178833] N87-22972

CORIOLIS EFFECT
Pharmacological correction of central nervous system functio during exposure to coriolis accelerations N87-23132

CORONAL LOOPS
Solar active region physical parameters inferred from a thermal cyclotron line and soft X-ray spectral lines [AD-A179650] N87-23560

CORRELATION
Correlation of analytical calculations from GRASP (General Rotorcraft Aeromechanical Stability Program) with torsionally-soft rotor data [AD-A178881] N87-22689
Relationship between a two mile run and maximal oxygen uptake [AD-A179343] N87-23109
Non-Markovian line shapes of physisorbed atoms on a crystal [AD-A179525] N87-23292

CORROSION
Corrosion, wear and mechanical properties of pulse-electrodeposited alloys [AD-A178596] N87-22842

CORROSION RESISTANCE
Laser cladding of Mg and Nb alloys for improved environmental resistance [AD-A179606] N87-22833
Metalliding as an electrochemical process [AD-A178744] N87-22843

COSMIC PLASMA
The Earth's magnetosphere as a sample of the plasma universe [TRITA-EPP-86-12] N87-23337

COSMIC RAY SHOWERS
Detection of 10^{14}-eV gamma rays from Cygnus X-3 during 1986 [DE87-006054] N87-23568

COSMIC RAYS
Cosmic ray detectors [NASA-CR-179086] N87-22952

COSMOCHEMISTRY
High pressure cosmochemistry of major planetary interiors: Laboratory studies of the water-rich region of the system ammonia-water N87-23396

COSMOLOGY
Possible inflationary solution to the short distance gravity model [DE87-701559] N87-23339
Reports of Planetary Geology and Geophysics Program, 1986 [NASA-TM-89810] N87-23341
Protostellar disks and the primitive solar nebula N87-23379

COST ANALYSIS
Cost analysis of aircraft projects N87-22664

COST EFFECTIVENESS
Strategies for high-resolution 3-D millimeter wave imaging [AD-A178653] N87-22882

COST REDUCTION
Cost analysis of aircraft projects N87-22664

COUETTE FLOW
Numerical study of high speed viscous flows [AD-A178639] N87-22940

COUNTERFLOW
Cross-axis synchronous flow-through coil planet centrifuge free of rotary seals: Apparatus and method for performing countercurrent chromatography [PB87-126926] N87-22816

COUPLED MODES
Revised NASA axially symmetric ring model for coupled-cavity traveling-wave tubes [NASA-TP-2675] N87-22923

COUPLING
Full-wave analysis of isolated and coupled microwave transmission lines using the finite element method [AD-A178805] N87-22883
Waveguide junction analysis involving asymmetrical modes [AD-A178464] N87-22909
Experimental study of coupling between eddy curren of Tokamak limiters of tokamak limiters [DE87-004938] N87-22999

COUPLINGS
Tube coupling device [NASA-CASE-MFS-25964-2] N87-22977

COVARIANCE
Some robust estimates of covariance structure based on parametric density estimation [AD-A178806] N87-23220
Estimating the standard error of robust regression estimates [AD-A179099] N87-23232

CRACK INITIATION
Structural analysis demonstration of constitutive and life models N87-22780
Determination of crack initiation sites using a digital NDE workstation [DE87-001444] N87-22997
On the application of the strain energy density theory in predicting crack initiation and angle of growth [AR-004-493] N87-23011

CRACK PROPAGATION
Dynamic fracture under plane wave loading [AD-A178594] N87-23001
On the application of the strain energy density theory in predicting crack initiation and angle of growth [AR-004-493] N87-23011

CRACK TIPS
A study into the generation of temperature gradients in materials for detecting and measuring the depth of sub-surface cracks [AERE-R-12382] N87-22991
On the application of the strain energy density theory in predicting crack initiation and angle of growth [AR-004-493] N87-23011

CRACKING (FRACTURING)
Influence of supporting conditions on stress intensity factors for single-edge-cracked specimens under bending [NASA-TT-20016] N87-23008

CRACKS
Measurement of the J integral with caustics: An experimental and numerical investigation [AD-A177273] N87-22990
Two-dimensional elastic analysis by the boundary element method [AD-A179213] N87-22993

CRASHWORTHINESS
DYNA3D: A computer code for crashworthiness engineering [DE87-003818] N87-22998

CRATERING
The cratering record at Uranus: Implications for satellite evolution and the origin of impacting objects N87-23342
Cratering history of Miranda N87-23344
Geology and cratering history of Ariel N87-23348
Computer simulations of 10-km-diameter asteroid impacts into oceanic and continental sites: Preliminary results on atmospheric passage, cratering and ejecta dynamics N87-23489

CRATERS
CO2 pulsed laser damage mechanism and plasma effects (focused beam) [AD-A179201] N87-22961
The cratering record at Uranus: Implications for satellite evolution and the origin of impacting objects N87-23342
Crater morphology and morphometry on the Uranian satellites N87-23343
Orbital dynamics of the Uranian satellites based on Voyager data N87-23350
Voyager observations of 1985U1 N87-23352
Investigations of the surfaces and interiors of outer planet satellites N87-23356
Studies of outer planet satellites, Mercury and Uranus N87-23358
Lunar magnetization concentrations (MAGCONS) antipodal to young large impact basins N87-23405
Experimental evidence for non-proportional growth of large craters N87-23497
Dome craters on Ganymede N87-23510
Non-Newtonian ice rheology and the retention of craters on Ganymede N87-23511
Ejecta types on Ganymede and Callisto N87-23512
A test of the hypothesis that impact-induced fractures are preferred sites for later tectonic activity N87-23520

Characteristic structures of the highland boundary on Mars: Evidence against a single mega-impact event? N87-23523

CREEP PROPERTIES
Joint services electronics program [AD-A178599] N87-22879
Finite element implementation of Robinson's unified viscoplastic model and its application to some uniaxial and multiaxial problems [NASA-TM-89891] N87-23010
Creep of ice: Further studies N87-23540

CRITICAL VELOCITY
The formation of a double layer leading to the critical velocity phenomenon N87-23335

CROP GROWTH
The impact of climate change from increased atmospheric carbon dioxide on American agriculture [DOE/NBB-0077] N87-23032

CROSS CORRELATION
Automatic scene analysis using hierarchical spatial frequency domain correlation with energy normalization and heuristic noise reduction [AD-A178589] N87-23181
Linear time invariant system identification using a result of the Bussgang theorem [AD-A178642] N87-23216

CROSS FLOW
Analytical and experimental studies of flow-induced vibration of SSME components N87-22771

CROSSLINKING
Process for crosslinking and extending conjugated diene-containing polymers [NASA-CASE-LAR-13452-1] N87-22848

CRUSTAL FRACTURES
Quick-look guide to the crustal dynamics project's data information system [NASA-TM-87818] N87-23018
A test of the hypothesis that impact-induced fractures are preferred sites for later tectonic activity N87-23520
The Martian crustal dichotomy: Product of accretion and not a specific event? N87-23524
Implications of Viking color data for evolution of the Amenthes Region, Mars N87-23525
Thin and thick-skinned deformation in the Tharsis Region of Mars N87-23529

CRYOGENIC COOLING
Ferroelectric optically controlled millimeter-wave devices [AD-A179524] N87-22901

CRYOGENIC FLUID STORAGE
Thermodynamic analysis and subscale modeling of space-based orbit transfer vehicle cryogenic propellant resupply [NASA-TM-89921] N87-22949

CRYOGENIC ROCKET PROPELLANTS
Thermodynamic analysis and subscale modeling of space-based orbit transfer vehicle cryogenic propellant resupply [NASA-TM-89921] N87-22949

CRYSTAL DISLOCATIONS
The characterization of whiskers produced by electromigration on suspended aluminum linestripes [AD-A179383] N87-23290

CRYSTAL GROWTH
Infrared fiber optic materials [NASA-CR-180604] N87-23257
Total immersion crystal growth [NASA-CASE-NPO-15800-2] N87-23286
A microcrystalline growth study of solvent effects in alkoxides by dynamic laser light scattering [DE87-005710] N87-23294

CRYSTALLINITY
A microcrystalline growth study of solvent effects in alkoxides by dynamic laser light scattering [DE87-005710] N87-23294

CRYSTALLIZATION
The role of particle substructure in the sintering of monosized titania [DE87-007600] N87-22839
Isotactic polystyrene phase diagrams and physical gelation [DE87-002693] N87-22850
Total immersion crystal growth [NASA-CASE-NPO-15800-2] N87-23286

CRYSTALS
New laser materials [DE87-006723] N87-22970
Angular momentum theory applied to interactions in solids [AD-A179366] N87-23289
Non-Markovian line shapes of physisorbed atoms on a crystal [AD-A179525] N87-23292

CULTURE (SOCIAL SCIENCES)
Optimum culture in the cockpit N87-22643

CURRENT DENSITY
An investigation of zinc electrodes relevant to zinc-air batteries [DE87-007607] N87-22908

CURRENT DISTRIBUTION
GEMACS (general EM model for the analysis of computer systems) frequency-domain analysis to determine the lightning induced electromagnetic skin current distributions on an aircraft [AD-A178854] N87-22660

CURRENT SHEETS
Anomalous transport in discrete arcs and simulation of double layers in a model auroral circuit N87-23325

CURVATURE
Prediction of fluid flow in curved pipe using the finite element method [AD-A179538] N87-22926

CURVED PANELS
Effects of cutout orientations on natural frequencies and mode shapes of curved rectangular composite panels [AD-A178638] N87-22813

CURVES (GEOMETRY)
A theory for turbulent curved wall jets [NASA-CR-181019] N87-22951
Curvilinear ridges and related features in southwest Cydonia Mensae, Mars N87-23537

CYCLIC LOADS
Prediction of service life of aircraft structural components using the half-cycle method [NASA-TM-86812] N87-23009

CYCLOGENESIS
On the diagnosis of a cold front observed during Alpine Experiment (ALPEX) N87-23072

CYCLOTRON RADIATION
Operation of the induced resonance electron cyclotron maser at higher harmonics [AD-A179428] N87-22962

CYCLOTRON RESONANCE
Operation of the induced resonance electron cyclotron maser at higher harmonics [AD-A179428] N87-22962
Solar active region physical parameters inferred from a thermal cyclotron line and soft X-ray spectral lines [AD-A179650] N87-23560

CYCLOTRON RESONANCE DEVICES
Design and operation of 140 GHz gyrotron oscillators for power levels up to 1 MW CW [DE87-006683] N87-22907

CYCLOTRONS
Operation of the induced resonance electron cyclotron maser at higher harmonics [AD-A179428] N87-22962

CYLINDRICAL BODIES
Computer program for electromagnetic penetration into a conducting circular cylinder through a narrow slot, TM case [AD-A178616] N87-22880

CYLINDRICAL SHELLS
Numerical methods for imperfection sensitivity analysis of stiffened cylindrical shells. Volume 1: Development and applications [AD-A179686] N87-22995

CYLINDRICAL WAVES
Dual cylindrical wave laser-Doppler method for measurement of skin friction in fluid flow [AD-A178629] N87-22939

CZOCHRALSKI METHOD
Modeling of substrate and implantation effects on the threshold voltage of MESFET structures fabricated in semi-insulating GaAs [AD-A178550] N87-23303

D

DAMAGE
The use of the Karl sub-scale laser for Raman beam clean-up experiments [AD-A178463] N87-22971

DAMAGE ASSESSMENT
System identification for large space structure damage assessment N87-22750
Hybrid composite response to hydraulic ram [AD-A178750] N87-22815

DAMPING
Notes on implementation of Coulomb friction in coupled dynamical simulations N87-22746

DATA ACQUISITION
Optical acquisition, image and data compression [AD-A178508] N87-23154
Measuring software design [NASA-TM-89372] N87-23189

DATA BASE MANAGEMENT SYSTEMS
Quick-look guide to the crustal dynamics project's data information system [NASA-TM-87818] N87-23018
Considerations in developing a comprehensive computer security support database system [DE87-005527] N87-23151
A decision support system for database management system selection [AD-A179339] N87-23311
Microvax-based data management and reduction system for the regional planetary image facilities N87-23554

DATA BASES
Design of GPS (Global Positioning System) status reporting system [AD-A179334] N87-22662
Selection of dimensions for an anthropometric data base. Volume 2: Dimension evaluation sheets [AD-A179472] N87-23110
Considerations in developing a comprehensive computer security support database system [DE87-005527] N87-23151
The scale-space formulation of pyramid data structures [AD-A178960] N87-23222
Mid-infrared spectroscopic investigation N87-23424

DATA COMPRESSION
Optical acquisition, image and data compression [AD-A178508] N87-23154

DATA FLOW ANALYSIS
Guidelines for applying the Composite Specification Model (CSM) [NASA-TM-89374] N87-23193
Parallel branch and bound on an MIMD (Multiple Instruction Stream, Multiple Data stream) system [AD-A178816] N87-23200
A static data flow simulation study at Ames Research Center [NASA-TM-89434] N87-23201

DATA LINKS
Development of a microcomputer-based workstation for analysis of digital satellite links [AD-A178872] N87-22888

DATA MANAGEMENT
Human factors engineering data management handbook [AD-A179691] N87-23144
A design for a new catalog manager and associated file management for the Land Analysis System (LAS) N87-23159
An overview of the catalog manager N87-23163

DATA PROCESSING
The impact of future avionics technology on the conduct of air warfare N87-22673
Selection of dimensions for an anthropometric data base. Volume 2: Dimension evaluation sheets [AD-A179472] N87-23110
The event related brain potential as an index of information processing and cognitive activity: A program of basic research [AD-A179310] N87-23143
OMNITAB 80: An interpretive system for statistical and numerical data anlysis [PB87-172235] N87-23171
Robust data analysis based on characteristic functions [AD-A178544] N87-23178
A study of the fundamental characteristics of 2175A extinction [NASA-CR-180926] N87-23336
Lunar science from lunar laser ranging N87-23389

DATA PROCESSING TERMINALS
Digital Autonomous Terminal Access Communication (DATAC) system N87-22610

DATA REDUCTION
Robust data analysis based on characteristic functions [AD-A178544] N87-23178
Gravity data analysis N87-23400
Microvax-based data management and reduction system for the regional planetary image facilities N87-23554

DATA RETRIEVAL
NASA Regional Planetary Image Facility image retrieval and processing system N87-23160

DATA STRUCTURES
The scale-space formulation of pyramid data structures [AD-A178960] N87-23222

DATA TRANSMISSION
Fiber optic data transmission N87-22611
Simulation model of a meteor burst communication system for data transmission protocol evaluation [AD-A178643] N87-22881
Applications of fiber optics in experimental mechanics [AD-A178683] N87-23268

DEBRIS
Non-equilibrium freezing of water-ice in sandy basaltic regoliths and implications for fluidized debris flows on Mars N87-23466

DECAY RATES
Afterburning suppression kinetics
[AD-A178967] N87-22863
Relativistic calculations and measurements of energies, Auger rates, and lifetimes
[AD-A179137] N87-23251
DECISION MAKING
Design of an orbital inspection satellite
[AD-A179115] N87-22759
A prototype knowledge-based system to aid space system restoration management
[AD-A179336] N87-23203
A decision support system for database management system selection
[AD-A179339] N87-23311
DECISION THEORY
Managing uncertainty in expert systems: A probabilistic approach
[AD-A178582] N87-23246
A decision support system for database management system selection
[AD-A179339] N87-23311
DECOMPOSITION
Basic research in energetic fluorocarbons
[AD-A179676] N87-22822
Decomposition of energetic materials combustion of decoy materials
[AD-A178447] N87-22827
DECONTAMINATION
The effects of candidate chemical training agents upon service materials — chemical warfare
[MQAD-317] N87-22832
DECOYS
Decomposition of energetic materials combustion of decoy materials
[AD-A178447] N87-22827
DEFECTS
Numerical methods for imperfection sensitivity analysis of stiffened cylindrical shells. Volume 1: Development and applications
[AD-A179686] N87-22995
Radiation hardened silica-based optical fibers
[AD-A178466] N87-23266
Submicron characterization of the atomic and electronic structure of defects in semiconductors
[AD-A178458] N87-23301
DEFLECTION
Experimental study of coupling between eddy curren of Tokamak limiters of tokamak limiters
[DE87-004938] N87-22999
DEFORMATION
Analysis of structures with rotating, flexible substructures applied to rotorcraft aeroelasticity in GRASP (General Rotorcraft Aeromechanical Stability Program)
[AD-A178941] N87-22677
Deformation and fatigue behavior of SSME turbopump blade materials N87-22776
Effect of hydrogen on deformation structure and properties of CMSX-2 nickel-base single-crystal superalloy N87-22782
Development of an integrated BEM (Boundary Element Mesh) for hot fluid-structure interaction N87-22799
Examination of high performance polymer fibers under compressive deformation
[AD-A178640] N87-22857
Numerical study of high speed viscous flows
[AD-A178639] N87-22940
Thin and thick-skinned deformation in the Tharsis Region of Mars N87-23529
DEGRADATION
System identification for large space structure damage assessment N87-22750
Reliability studies of ceramic capacitors
[AD-A179436] N87-22900
Hisingerite and iddingsite on Mars: Degradation of iron-rich basalts N87-23416
Valley development on Hawaiian volcanoes
N87-23463
DEHYDRATION
Spectral effects of dehydration on phyllosilicates
N87-23422
DELAY LINES
Analog fiber optic recirculating delay line
[AD-A179050] N87-23272
DELTA MODULATION
Investigation of Continuously Variable Slope Delta (CVSD) modulation for voice communications
[AD-A178579] N87-22877
DEMAND ASSIGNMENT MULTIPLE ACCESS
Channel access schemes and fiber optic configurations for integrated-services local area networks
[NASA-CR-180934] N87-23273
DENSE PLASMAS
Opening switch research on a dense plasma focus
[AD-A179693] N87-23276
DENSITY DISTRIBUTION
Characterization of hybridized conductive composites
[AD-A179689] N87-22810
Numerical studies of collapsing interstellar clouds
[NASA-CR-180933] N87-23340
Studies of early intense cratering and possible saturation effects N87-23503
DENSITY WAVE MODEL
Hamiltonian theory of nonlinear waves in planetary rings N87-23393
DEPOSITION
Measurement of ice accretion using ultrasonic pulse echo techniques N87-22608
Plasma joining of metal matrix composites
[AD-A178731] N87-22814
Molecular reactions at the film surface in plasma polymerization
[DE87-002488] N87-22849
High energy high rate pulsed power processing of materials by powder consolidation and by railgun deposition
[AD-A179289] N87-22867
CO2 pulsed laser damage mechanism and plasma effects (focused beam)
[AD-A179201] N87-22961
A statistical study of the combined effects of substrate temperature, bias, annealing, and a Cr3Si2 undercoating on the tribological properties of RF-sputtered MoS2 coatings
[DE87-007086] N87-23285
A scaling law for accretion zone sizes N87-23385
Collisional and dynamical processes in moon and planet formation N87-23387
Variations of Martian surface albedo: Evidence for yearly dust deposition and removal N87-23413
The effect of overburden thickness on tension fracture patterns above an uplifting dome N87-23535
DEPTH
A study into the generation of temperature gradients in materials for detecting and measuring the depth of sub-surface cracks
[AERE-R-12382] N87-22991
Two and three-dimensional inversion of magnetotelluric data
[DE87-005553] N87-23058
DESIGN ANALYSIS
Application of advanced computational codes in the design of an experiment for a supersonic throughflow fan rotor
[NASA-TM-88915] N87-22630
Digital control of highly augmented combat rotorcraft
[NASA-TM-88346] N87-22691
Integrated restructurable flight control system demonstration results
[NASA-CR-178305] N87-22692
Structural Dynamics and Control Interaction of Flexible Structures
[NASA-CP-2467-PT-2] N87-22729
Design of generalised Chebyshev suspended substrate stripline filters
[AD-A178505] N87-22910
Reading patterns in online documentation: How transcript analysis reflects text design, software constraints, and user preferences
[DE87-006466] N87-23174
Fundamentals and techniques of nonimaging optics research at the University of Chicago
[DE87-006917] N87-23264
DETECTION
A study into the generation of temperature gradients in materials for detecting and measuring the depth of sub-surface cracks
[AERE-R-12382] N87-22991
Detection of 10^{14}-eV gamma rays from Cygnus X-3 during 1986
[DE87-006054] N87-23568
DETONATORS
A fast, low resistance switch for small slapper detonators
[AD-A178562] N87-22911
DEUTERIUM
Two-color, Doppler-free ionization of molecular hydrogen for isotopic analysis
[DE87-004975] N87-22825
DIAGRAMS
Global petrologic variations of the Moon: A ternary-diagram approach N87-23407
DIAMINES
Polyenamines from aromatic diacetylenic diketones and diamines
[NASA-CASE-LAR-13444-1-CU] N87-22847
DICHOTOMIES
The Martian crustal dichotomy: Product of accretion and not a specific event? N87-23524
Implications of Viking color data for evolution of the Amenthes Region, Mars N87-23525
DIELECTRIC PROPERTIES
Multiple angle of incidence measurement technique for the permittivity and permeability of lossy materials at millimeter wavelengths
[AD-A178851] N87-22885
Reliability studies of ceramic capacitors
[AD-A179436] N87-22900
DIELECTRICS
Full-wave analysis of isolated and coupled microwave transmission lines using the finite element method
[AD-A178805] N87-22883
Waveguide junction analysis involving asymmetrical modes
[AD-A178484] N87-22909
DIELS-ALDER REACTIONS
Process for crosslinking and extending conjugated diene-containing polymers
[NASA-CASE-LAR-13452-1] N87-22848
DIENES
Process for crosslinking and extending conjugated diene-containing polymers
[NASA-CASE-LAR-13452-1] N87-22848
DIFFERENCE EQUATIONS
Investigation of perturbation techniques for nonlinear difference equations and other related topics
[DE87-006663] N87-23211
DIFFERENTIAL EQUATIONS
Numerical analysis of terminal double mach reflection
[AD-A179041] N87-22942
Differential-algebraic equation index transformations
[DE87-005543] N87-23209
Oscillatory behaviour of solutions of first-order ordinary and delay differential equations
[DE87-701552] N87-23212
The exponential method
[TRITA-NA-8517] N87-23228
DIFFRACTION
Detection of reflector surface error from near-field data: Effect of edge diffracted field
[NASA-TM-89920] N87-22874
Automatic pattern recognition and related topics
[AD-A178595] N87-23267
DIFFRACTION PATTERNS
Two-point resolution criterion for multi-aperture optical systems
[AD-A178980] N87-23271
DIFFUSION ELECTRODES
Development of nickel oxide/hydrogen multilayer bipolar battery for pulsed power
[AD-A178844] N87-22917
DIGITAL DATA
Throughput analysis of the IEEE 802.4 token bus standard under heavy load
[NASA-CR-180936] N87-22921
DIGITAL FILTERS
Modeling digital control systems with MA-prefiltered measurements
[NASA-TP-2732] N87-22870
Multidimensional filtering investigations
[AD-A178745] N87-22915
DIGITAL SIMULATION
Modeling and simulation of the WFTA (Winograd Fourier Transform Algorithm) 16 PFA (Prime Factor Algorithm) processor using the VHSIC (Very High Speed Integrated Circuit) hardware description language, volume 1
[AD-A179344] N87-22898
DIGITAL SYSTEMS
Digital Autonomous Terminal Access Communication (DATAC) system N87-22610
Electromagnetic interference (EMI) fault prevention and self recovery of digital flight control systems — helicopters
[MBB-UD-483/86] N87-22686
Modeling digital control systems with MA-prefiltered measurements
[NASA-TP-2732] N87-22870
The effect of multipath on digital communications systems: With application to space station
[AD-A178578] N87-22876
Development of a microcomputer-based workstation for analysis of digital satellite links
[AD-A178872] N87-22888
Multidimensional filtering investigations
[AD-A178745] N87-22915
Mars digital terrain model N87-23549
Digital cartography of Mars N87-23550
DIGITAL TECHNIQUES
Real-time laser holographic interferometry for aerodynamics
[NASA-TM-89462] N87-22956
DILATOMETRY
Thermal expansion of epoxy-fiberglass composite specimens
[DE87-004273] N87-22812

DIMENSIONAL MEASUREMENT
Measurement of the atmospheric phase coherence length, rsubo
[AD-A178468] N87-23060

DIMENSIONS
NBS calibration services users guide, 1986-1988 edition
[NBS-SP-250] N87-22958
Two-dimensional elastic analysis by the boundary element method
[AD-A179213] N87-22993
Two and three-dimensional inversion of magnetotelluric data
[DE87-005553] N87-23058
Chandrasekhar equations for infinite dimensional systems. Part 2: Unbounded input and output case
[NASA-CR-178303] N87-23208

DIODES
The transverse dynamics of space-charge limited diodes
[AD-A179389] N87-22899
Silicon pulse sharpening diodes: Switching kilovolts in 10's of picoseconds
[DE87-005073] N87-22905

DIPLEXERS
Design of generalised Chebyshev suspended substrate stripline filters
[AD-A178505] N87-22910

DIPOLE MOMENTS
Analysis of lightning induced magnetic field penetration through protective metal screens using an equivalent magnetic dipole moment representation of an array of elliptic apertures
[AD-A178850] N87-22884

DIRECTIONAL SOLIDIFICATION (CRYSTALS)
Scientific goals of the German Spacelab Mission D1
[ETN-87-99669] N87-22695

DISCONTINUITY
Electric potential distributions at the interface between plasmasheet clouds N87-23330

DISCRETE FUNCTIONS
A separable piecewise linear upper bound for stochastic linear programs
[AD-A178694] N87-23217
A survey of mixed finite element methods
[NASA-CR-178267] N87-23229

DISCRIMINATION
On non-parametric discrimination using series expansions and projection pursuit
[AD-A178455] N87-23213

DISLOCATIONS (MATERIALS)
Submicron characterization of the atomic and electronic structure of defects in semiconductors
[AD-A178458] N87-23301

DISPLAY DEVICES
Aircraft control position indicator
[NASA-CASE-LAR-12984-1] N87-22678
Developing a voice-controlled, computer-generated display to assist space station astronauts during maintenance activity
[AD-A178997] N87-22762
Performance comparison of four state-of-the-art computer architectures
[AD-A179071] N87-23149
A graphics environment supporting the rapid prototyping of pictorial cockpit displays
[AD-A178636] N87-23182
Development of an image analysis program for the IBM PC/XT/AT
[AD-A178644] N87-23183

DISTANCE
Estimation of the parameters of mixtures via distance between densities or characteristic functions
[AD-A178623] N87-23241
Calculated viscosity-distance dependence for some actively flowing lavas N87-23482

DISTRIBUTED PROCESSING
An experimental study of load balancing performance
[AD-A179322] N87-23195

DISTRIBUTION FUNCTIONS
Robust data analysis based on characteristic functions
[AD-A178544] N87-23178
Goodness-of-fit based on integrated squared discrepancies between sample and population characteristic functions
[AD-A178763] N87-23218
Goodness of fit based on integrated squared errors in characteristic functions or densities
[AD-A179027] N87-23225
On the least favorable configuration of a selection procedure based on ranks
[AD-A178454] N87-23234
The percentiles of the stable laws
[AD-A179025] N87-23243

DISULFIDES
Lithium disulfide battery
[DE87-007183] N87-22892

DOMES (GEOLOGY)
Dome craters on Ganymede N87-23510

DOPPLER EFFECT
Considerations pertinent to the Doppler effect for space reactors
[DE87-007032] N87-23252

DOPPLER RADAR
Oklahoma downbursts and their asymmetry
[DOT/FAA/PM-87/7] N87-23095
Gravity data analysis N87-23400

DOSIMETERS
Dose enhancement effects in the Aerospace Corporation Co-60 irradiator
[AD-A178481] N87-23253

DRAG
Numerical calculation of the drag force induced by natural convection of spheres at low Grashof numbers
[DE87-006791] N87-22935

DRAG COEFFICIENTS
Numerical calculation of the drag force induced by natural convection of spheres at low Grashof numbers
[DE87-006791] N87-22935

DRAG REDUCTION
The aerodynamic optimization of wings at subsonic speeds and the influence of wingtip design
[NASA-TM-88534] N87-22627

DRAINAGE PATTERNS
Groundwater sapping channels: Summary of effects of experiments with varied stratigraphy N87-23461
Fluvial valleys on Martian volcanoes N87-23462
Valley development on Hawaiian volcanoes N87-23463

DRIVES
Direct-drive laser-fusion in the US
[DE87-005916] N87-23279

DRUGS
Problems and feasibility of drug correction of orthostatic tolerance in space medicine N87-23121

DUCTILITY
Artificial composites for high temperature applications: A review
[DME-007] N87-22808
Martensitic transformation as a deformation process
[DE87-007068] N87-22836
Experimental and theoretical studies of the structure of grain boundaries
[DE87-007560] N87-22838
Corrosion, wear and mechanical properties of pulse-electrodeposited alloys
[AD-A178596] N87-22842
Austempered ductile iron process development
[PB87-169843] N87-22866

DUCTS
Calculation of ray paths in the ionosphere using an analytic raytracing technique
[AD-A178888] N87-23064

DUNES
Mars: Morphology of Southern Hemisphere intracrater dunefields N87-23452
Timing of frost deposition on Martian dunes: A clue to properties of dune particles? N87-23453
Wind ripples in low density atmospheres N87-23454

DURABILITY
Structural Integrity and Durability of Reusable Space Propulsion Systems
[NASA-CP-2471] N87-22766

DUST
Investigations of planetary ring phenomena N87-23360
Regional sources and sinks of dust on Mars: Viking observations of Cerberus, Solis Planum and Syrtis Major N87-23450
High resolution thermal infrared mapping of Martian channels N87-23451
Mars: Morphology of Southern Hemisphere intracrater dunefields N87-23452
Timing of frost deposition on Martian dunes: A clue to properties of dune particles? N87-23453
Eolian saltation on Mars N87-23455
Mass transport by Aeolian saltation on Earth, Mars and Venus: The effects of full saltation cloud development and choking N87-23456

DUST STORMS
Variations of Martian surface albedo: Evidence for yearly dust deposition and removal N87-23413

DYE LASERS
Fundamental studies in the molecular basis of laser induced retinal damage
[AD-A178453] N87-23115
Plasma diagnosis by dye laser intracavity absorption
[DE87-006407] N87-23280

DYNAMIC CHARACTERISTICS
Investigation of periodic pitching through the static stall angle of attack
[AD-A179512] N87-22623
Frequency-response identification of XV-15 tilt-rotor aircraft dynamics
[NASA-TM-89428] N87-22690
Solar array flight dynamic experiment N87-22722
Dynamic characteristics of a vibrating beam with periodic variation in bending stiffness N87-22726
Estimation of ICBM (intercontinental ballistic missile) performance parameters
[AD-A179204] N87-22754
XAS (X-ray Absorption Spectroscopy) of gas phase metal-containing chemical systems
[AD-A179391] N87-22821
Flow dynamics stimulated by hairpin-like vortices in initially laminar boundary layers
[AD-A179578] N87-22927
Dynamic fracture under plane wave loading
[AD-A178594] N87-23001
Millimeter wave Doppler radar observation of cloud and boundary layer structure
[AD-A178679] N87-23098
Optical dynamics experiment (ODEX) data report R/V acania expedition 10 October-17 November 1982. Volume 2: Particle size distributions. Volume 6: Scalar spectral-radiometer data
[AD-A178535] N87-23104
Some dynamical properties of very strong double layers in a triple plasma device N87-23315
Dynamical constraints on the origin of the moon N87-23388

DYNAMIC CONTROL
A computer program for model verification of dynamic systems N87-22710

DYNAMIC LOADS
Analysis of structures with rotating, flexible substructures
[AD-A178903] N87-23004

DYNAMIC MODELS
Dynamic stall calculations using a Navier-Stokes solver
[AD-A178566] N87-22688
Nonlinear optical properties and subpicosecond dynamics of excitons and electron-hole plasmas in multiple quantum well structures
[AD-A179124] N87-23287

DYNAMIC PRESSURE
A study of fluid-dynamic pressure fields on compressor reed valves
[AD-A178584] N87-22938

DYNAMIC RESPONSE
A computer program for model verification of dynamic systems N87-22710
Slewing control experiment for a flexible panel N87-22740
Automated transient analysis of structural members
[AD-A179042] N87-23007

DYNAMIC STABILITY
Dynamic fracture of high strength steel
[AD-A178862] N87-22844
Periodic orbits about rotating asteroids in free space
[AD-A179387] N87-23338

DYNAMIC STRUCTURAL ANALYSIS
Flutter analysis of a two-dimensional airfoil with cubic non-linear restoring force
[NAE-AN-36] N87-22628
Flight and analytical investigations of a structural mode excitation system on the YF-12A airplane
[NASA-CR-166623] N87-22685
Structural Dynamics and Control Interaction of Flexible Structures
[NASA-CP-2467-PT-1] N87-22702
A general method for dynamic analysis of structures overview N87-22707
Considerations in the design and development of a space station scale model N87-22711
Precision pointing and control of flexible spacecraft N87-22723
Dynamics of trusses having nonlinear joints N87-22724
Dynamic characteristics of a vibrating beam with periodic variation in bending stiffness N87-22726
Structural dynamics system model reduction N87-22727
Structural Dynamics and Control Interaction of Flexible Structures
[NASA-CP-2467-PT-2] N87-22729
Vibration suppression by stiffness control N87-22730
Preliminary evaluation of a reaction control system for the space station N87-22736
High speed simulation of flexible multibody dynamics N87-22738

Maximum Entropy/Optimal Projection (MEOP) control design synthesis: Optimal quantification of the major design tradeoffs N87-22741
A new approach for vibration control in large space structures N87-22743
Modeling of controlled flexible structures with impulsive loads N87-22745
Finite element models of wire rope for vibration analysis N87-22748
Experimental characterization of deployable trusses and joints N87-22749
System identification for large space structure damage assessment N87-22750
Space station structures and dynamics test program N87-22751
Space station structural dynamics/reaction control system interaction study N87-22753
Structural Integrity and Durability of Reusable Space Propulsion Systems [NASA-CP-2471] N87-22766
Probabilistic structural analysis verification studies N87-22786
NESSUS/expert and NESSUS/FPI in the Probabilistic Structural Analysis Methods (PSAM) program N87-22787
Advanced probabilistic method of development N87-22788
Stochastic and hybrid-stress plate/shell finite elements for hot-section components N87-22789
Probabilistic finite elements N87-22790
Probabilistic SSME blades structural response under random pulse loading N87-22791
Quantifying uncertainties in the structural response of SSME blades N87-22792
Nonisothermal elasto-visco-plastic response of shell-type structures N87-22796
Dynamic characteristics of single crystal SSME blades N87-22797
The status of the vertical axis wind turbine research test bed [DE87-005524] N87-23023

DYNAMICAL SYSTEMS
A quasi-analytical method for non-iterative computation of nonlinear controls N87-22731
Notes on implementation of Coulomb friction in coupled dynamical simulations N87-22746
Quick-look guide to the crustal dynamics project's data information system [NASA-TM-87818] N87-23018
Molecular-dynamics simulation of thin-film growth [DE87-006973] N87-23284
Observational studies of Saturn's rings N87-23362

DYNAMO THEORY
The origin of polarity asymmetries in the history of the geomagnetic field N87-23401
Generation of a dynamo magnetic field in a protoplanetary accretion disk N87-23403
The steady state toroidal magnetic field at the core-mantle boundary N87-23404

E

E REGION
Calculation of ray paths in the ionosphere using an analytic raytracing technique [AD-A178888] N87-23064

EARTH (PLANET)
Observations on the magnitude-frequency distribution of Earth-crossing asteroids N87-23369

EARTH ATMOSPHERE
Measurement of the atmospheric phase coherence length, rsubo [AD-A178468] N87-23060
Millimeter wave Doppler radar observation of cloud and boundary layer structure [AD-A178679] N87-23098

EARTH CORE
Experiments pertaining to the formation and equilibration of planetary cores N87-23397
The steady state toroidal magnetic field at the core-mantle boundary N87-23404
Crustal and subcrustal nodules in ejecta from Kilbourne Hole Maar, New Mexico N87-23485

EARTH IONOSPHERE
Calculation of ray paths in the ionosphere using an analytic raytracing technique [AD-A178888] N87-23064
A preliminary study of extended magnetic field structures in the ionosphere [NASA-CR-181004] N87-23066
Effect of double layers on magnetosphere-ionosphere coupling N87-23321
Weak double layers in the auroral ionosphere N87-23326

EARTH MANTLE
Experiments pertaining to the formation and equilibration of planetary cores N87-23397
The steady state toroidal magnetic field at the core-mantle boundary N87-23404

EARTH ORBITAL ENVIRONMENTS
A preliminary study of extended magnetic field structures in the ionosphere [NASA-CR-181004] N87-23066

EARTH ORBITS
Optimal shuttle altitude changes using tethers [AD-A179205] N87-22756
Design of an orbital inspection satellite [AD-A179115] N87-22759
The 1986 DA and 1986 EB: M-class asteroids in near-Earth orbits N87-23371

EARTH PLANETARY STRUCTURE
Experiments pertaining to the formation and equilibration of planetary cores N87-23397

EARTH RESOURCES PROGRAM
Earth resources: A continuing bibliography with indexes (issue 53) [NASA-SP-7041(53)] N87-23013

EARTH ROTATION
The steady state toroidal magnetic field at the core-mantle boundary N87-23404

EARTH SURFACE
Standard-resolution TOVS observations for the FIRE/SRB Wisconsin experiment region from October 9 through November 2, 1986 [NASA-TM-89151] N87-23101
Implications of convection in the Moon and the terrestrial planets N87-23406
Bright sand/dark dust: The identification of active sand surfaces on the Earth and Mars N87-23449
Mass transport by Aeolian saltation on Earth, Mars and Venus: The effects of full saltation cloud development and choking N87-23453
Crater production on Venus and Earth by asteroid and comet impact N87-23500
Secular cooling of Earth as a source of intraplate stress N87-23519

EARTH-MOON SYSTEM
Dynamical constraints on the origin of the moon N87-23388

EARTHQUAKES
A test of the hypothesis that impact-induced fractures are preferred sites for later tectonic activity N87-23520

EASTERN HEMISPHERE
Tectonic domains in the Eastern Hemisphere of Mars N87-23531

ECONOMETRICS
A Bayesian statistics year at the Ohio State University [AD-A178762] N87-23242

ECONOMIC ANALYSIS
British Aerospace: A Kingston perspective [ETN-87-99823] N87-23308

ECONOMIC IMPACT
The impact of climate change from increased atmospheric carbon dioxide on American agriculture [DOE/NBB-0077] N87-23032

EDDY CURRENTS
The Regional Electromagnetics Workshop in the USA [DE87-004709] N87-22875
Experimental study of coupling between eddy curren of Tokamak limiters of tokamak limiters [DE87-004938] N87-22999

EDGE LOADING
Dynamic fracture under plane wave loading [AD-A178594] N87-23001

EDGES
Detection of reflector surface error from near-field data: Effect of edge diffracted field [NASA-TM-89920] N87-22674
Studies of the east Australian current off northern New South Wales [AD-A178461] N87-23103

EFFERENT NERVOUS SYSTEMS
Workshop Symposium on Neural Models of Sensory-Motor Control [AD-A179501] N87-23111

EFFICIENCY
New laser materials [DE87-006723] N87-22970

EIGENVALUES
A general method for dynamic analysis of structures overview N87-22707
Wielandt iteration as applied to the nodal expansion method [KAPL-4194] N87-23227
Estimation of the parameters of mixtures via distance between densities or characteristic functions [AD-A178623] N87-23241

EIGENVECTORS
Estimation of the parameters of mixtures via distance between densities or characteristic functions [AD-A178623] N87-23241

EJECTA
Preliminary results of spectral reflectance studies of tycho crater N87-23430
Crustal and subcrustal nodules in ejecta from Kilbourne Hole Maar, New Mexico N87-23485
Computer simulations of 10-km-diameter asteroid impacts into oceanic and continental sites: Preliminary results on atmospheric passage, cratering and ejecta dynamics N87-23489
Impacts of hemispherical granular targets: Implications for global impacts N87-23490
Impact vaporization: Late time phenomena from experiments N87-23491
Oblique impact: Projectile richochet, concomitant ejecta and momentum transfer N87-23492
Experimental studies of collision and fragmentation phenomena N87-23494
A statistical study of Mercurian crater classes applied to the emplacement of the intercrater plains N87-23502
Crater ejecta morphology and the presence of water on Mars N87-23508
Thermal inertia characteristics of the Martian crater Curie N87-23509
Ejecta types on Ganymede and Callisto N87-23512
Search for, and study of, paleozoic impact ejecta: Progress made during the past year N87-23514

EL NINO
Simulated and observed budgets and balances during the 82/83 ENSO event — El Nino Southern Oscillation (ENSO) N87-23035
ENSO experiments with a two-level AGCM — El Nino Southern Oscillation (ENSO) Atmospheric General Model (AGCM) N87-23037
Atmospheric simulations of the 1982-83 ENSO episode — El Nino Southern Oscillation (ENSO) N87-23038
Preliminary results from a Tropical Ocean Global Atmosphere (TOGA) related experiment performed at Hamburg (West Germany) with the ECWME General Circulation Model (GCM) with T21 resolution N87-23040
Forecast and sensitivity experiments on the UK Meteorological Office GCM with El Nino SST anomalies — general circulation model (GCM) sea surface temperature (SST) N87-23045
The impact of initial conditions and SST Anomalies on extended range predictions for the El Nino period — sea surface temperature (SST) N87-23046
A lagged-average 60-day forecast experiment during the 1982-83 El Nino period N87-23047
Sensitivity of the NMC spectral mode to the January 1983 El Nino SST — sea surface temperature N87-23048
An extended forecast experiment with the CCC GCM — general climate model (GCM) N87-23050
The impact of SST anomalies and initial conditions on extended range predictions with an atmospheric general circulation model: A case study in early summer of 1983 N87-23051
Modelling and forecasting El Nino N87-23053

ELASTIC BODIES
Non-linear finite element analysis program [AD-A179038] N87-23006

ELASTIC DEFORMATION
Measurement of the J integral with caustics: An experimental and numerical investigation [AD-A177273] N87-22990

ELASTIC PROPERTIES
Corrosion, wear and mechanical properties of pulse-electrodeposited alloys [AD-A178596] N87-22842
Two-dimensional elastic analysis by the boundary element method [AD-A179213] N87-22993

ELASTOPLASTICITY
Nonisothermal elasto-visco-plastic response of shell-type structures N87-22796

ELECTRIC ARCS
Coordinated research program in pulsed power physics [AD-A178625] N87-22912

ELECTRIC AUTOMOBILES
Lithium-metal sulfide battery development and submodule demonstration [DE87-004819] N87-22904
Development of advanced nickel-cadmium batteries for electric vehicle propulsion [DOE/NV/10442-1] N87-22922

ELECTRIC BATTERIES
Lithium disulfide battery [DE87-007183] N87-22892

Bipolar battery with array of sealed cells
[DE87-007194] N87-22893
Lithium-metal sulfide battery development and submodule demonstration
[DE87-004819] N87-22904
Development of nickel oxide/hydrogen multilayer bipolar battery for pulsed power
[AD-A178844] N87-22917
High temperature solid oxide regenerative fuel cell for solar photovoltaic energy storage
[NASA-TM-89872] N87-23020

ELECTRIC COILS
Superconducting Augmented Rail Gun (SARG)
[AD-A179269] N87-22701

ELECTRIC CONDUCTORS
Full-wave analysis of isolated and coupled microwave transmission lines using the finite element method
[AD-A178805] N87-22883

ELECTRIC CONTACTS
In situ friction, wear and electrical contact resistance of precious metal alloys
[DE87-001423] N87-22979
Correlations between electrical contact resistance and stages of wear in 700 Torr helium for precious metal electrical contacts
[DE87-003499] N87-22981

ELECTRIC CURRENT
GEMACS (general EM model for the analysis of computer systems) frequency-domain analysis to determine the lightning induced electromagnetic skin current distributions on an aircraft
[AD-A178854] N87-22660
SIS (Superconductor-Insulator-Superconductor) mixer research
[AD-A179604] N87-23293
Current driven weak double layers N87-23322
Electric fields and double layers in plasmas
N87-23323
Electron acceleration in stochastic double layers
N87-23324

ELECTRIC DISCHARGES
Coordinated research program in pulsed power physics
[AD-A178625] N87-22912
Transient protection of electronic circuits
[AD-A178945] N87-22919
The use of the Karl sub-scale laser for Raman beam clean-up experiments
[AD-A178463] N87-22971

ELECTRIC FIELDS
Investigation of the transverse-discharge copper-vapor laser
[AD-A178833] N87-22972
Double Layers in Astrophysics
[NASA-CP-2469] N87-23313
Formation mechanisms of laboratory double layers
N87-23314
Some dynamical properties of very strong double layers in a triple plasma device N87-23315
Pumping potential wells N87-23316
A laboratory investigation of potential double layers
N87-23317
Experimental observation of ion-acoustic double layers in laboratory plasma N87-23318
A new hydrodynamic analysis of double layers
N87-23319
Ion phase-space vortices and their relation to small amplitude double layers N87-23320
Effect of double layers on magnetosphere-ionosphere coupling N87-23321
Current driven weak double layers N87-23322
Electric fields and double layers in plasmas
N87-23323
Electron acceleration in stochastic double layers
N87-23324
Anomalous transport in discrete arcs and simulation of double layers in a model auroral circuit N87-23325
Weak double layers in the auroral ionosphere
N87-23326
Particle simulation of auroral double layers
N87-23327
Conditions for double layers in the Earth's magnetosphere and perhaps in other astrophysical objects N87-23328
Some aspects of double layer formation in a plasma constrained by a magnetic mirror N87-23329
Electric potential distributions at the interface between plasmasheet clouds N87-23330
Double layers above the aurora N87-23331
Double layers and plasma-wave resistivity in extragalactic jets: Cavity formation and radio-wave emission N87-23333
The formation of a double layer leading to the critical velocity phenomenon N87-23335

ELECTRIC GENERATORS
High energy high rate pulsed power processing of materials by powder consolidation and by railgun deposition
[AD-A179289] N87-22867

ELECTRIC POTENTIAL
SIS (Superconductor-Insulator-Superconductor) mixer research
[AD-A179604] N87-23293

ELECTRIC POWER SUPPLIES
Transient protection of electronic circuits
[AD-A178945] N87-22919

ELECTRIC PROPULSION
Low power DC arcjet operation with hydrogen/nitrogen/ammonia mixtures
[NASA-TM-89876] N87-22804
Electromagnetic emission experiences using electric propulsion systems: A survey
[NASA-TM-100120] N87-22805

ELECTRIC SWITCHES
A fast, low resistance switch for small slapper detonators
[AD-A178562] N87-22911

ELECTRICAL PROPERTIES
Characterization of hybridized conductive composites
[AD-A179689] N87-22810

ELECTRICAL RESISTANCE
Characterization of hybridized conductive composites
[AD-A179689] N87-22810
Correlations between electrical contact resistance and stages of wear in 700 Torr helium for precious metal electrical contacts
[DE87-003499] N87-22981

ELECTRICAL RESISTIVITY
Investigation of rocket powered, open cycle, magnetohydrodynamic generators for high, pulsed power needs in space
[AD-A178869] N87-22801

ELECTRO-OPTICS
Ferroelectric optically controlled millimeter-wave devices
[AD-A179524] N87-22901
Coordinated research program in pulsed power physics
[AD-A178625] N87-22912
Automatic pattern recognition and related topics
[AD-A178595] N87-23267
Analog fiber optic recirculating delay line
[AD-A179050] N87-23272

ELECTROCHEMICAL CELLS
Lithium disulfide battery
[DE87-007183] N87-22892
Component variations and their effects on bipolar nickel-hydrogen cell performance
[NASA-TM-89907] N87-23029

ELECTROCHEMICAL OXIDATION
Development of nickel oxide/hydrogen multilayer bipolar battery for pulsed power
[AD-A178844] N87-22917

ELECTROCHEMISTRY
Stochastic processes in CHEMFETs
[AD-A178841] N87-22829
Metalliding as an electrochemical process
[AD-A178744] N87-22843
Thermoelectric conversion with ion conductors
[AD-A179353] N87-23019

ELECTRODEPOSITION
Corrosion, wear and mechanical properties of pulse-electrodeposited alloys
[AD-A178596] N87-22842
Metalliding as an electrochemical process
[AD-A178744] N87-22843
An investigation of zinc electrodes relevant to zinc-air batteries
[DE87-007607] N87-22908

ELECTRODYNAMICS
Relativistic calculations and measurements of energies, Auger rates, and lifetimes
[AD-A179137] N87-23251
Collective effects in intense-field electrodynamics 1981-1986
[AD-A179490] N87-23261

ELECTROLYSIS
Metalliding as an electrochemical process
[AD-A178744] N87-22843

ELECTROLYTES
XAS (X-ray Absorption Spectroscopy) of gas phase metal-containing chemical systems
[AD-A179391] N87-22821

ELECTROLYTIC CELLS
Thermoelectric conversion with ion conductors
[AD-A179353] N87-23019
Experimental investigation of the process of CO2-CO-H2O-H2-N2 gas mixture breakdown in electrolysis cell with solid electrolyte N87-23137

ELECTROLYTIC POLARIZATION
Experimental investigation of the process of CO2-CO-H2O-H2-N2 gas mixture breakdown in electrolysis cell with solid electrolyte N87-23137

ELECTROMAGNETIC FIELDS
The Regional Electromagnetics Workshop in the USA
[DE87-004709] N87-22875

ELECTROMAGNETIC INTERACTIONS
GEMACS (general EM model for the analysis of computer systems) frequency-domain analysis to determine the lightning induced electromagnetic skin current distributions on an aircraft
[AD-A178854] N87-22660
Joint services electronics program
[AD-A178599] N87-22879

ELECTROMAGNETIC INTERFERENCE
Electromagnetic interference (EMI) fault prevention and self recovery of digital flight control systems — helicopters
[MBB-UD-483/86] N87-22686
Characterization of hybridized conductive composites
[AD-A179689] N87-22810

ELECTROMAGNETIC NOISE
The generation of electrostatic noise in the plasma sheet boundary layer
[ATR-86(8433)-4] N87-23282
SIS (Superconductor-Insulator-Superconductor) mixer research
[AD-A179604] N87-23293

ELECTROMAGNETIC PULSES
Analysis of lightning induced magnetic field penetration through protective metal screens using an equivalent magnetic dipole moment representation of an array of elliptic apertures
[AD-A178850] N87-22884
Transient protection of electronic circuits
[AD-A178945] N87-22919

ELECTROMAGNETIC RADIATION
Electromagnetic emission experiences using electric propulsion systems: A survey
[NASA-TM-100120] N87-22805
Computer program for electromagnetic penetration into a conducting circular cylinder through a narrow slot, TM case
[AD-A178616] N87-22880
Coordinated research program in pulsed power physics
[AD-A178625] N87-22912

ELECTROMAGNETIC SCATTERING
Full polarimetric non-specular scattering of flat plate structures
[AD-A178853] N87-22886

ELECTROMAGNETIC SHIELDING
Analysis of lightning induced magnetic field penetration through protective metal screens using an equivalent magnetic dipole moment representation of an array of elliptic apertures
[AD-A178850] N87-22884

ELECTROMIGRATION
The characterization of whiskers produced by electromigration on suspended aluminum linestripes
[AD-A179383] N87-23290

ELECTRON ACCELERATION
Electron acceleration in stochastic double layers
N87-23324

ELECTRON BEAMS
Coordinated research program in pulsed power physics
[AD-A178625] N87-22912
Pulsed power for high power electron-beam pumped lasers
[DE87-004523] N87-22965

ELECTRON DENSITY (CONCENTRATION)
Solar active region physical parameters inferred from a thermal cyclotron line and soft X-ray spectral lines
[AD-A179650] N87-23560

ELECTRON DISTRIBUTION
Investigations of the polar rain: Polar cap electron precipitation
[AD-A178876] N87-23099

ELECTRON ENERGY
Solar active region physical parameters inferred from a thermal cyclotron line and soft X-ray spectral lines
[AD-A179650] N87-23560

ELECTRON GUNS
The transverse dynamics of space-charge limited diodes
[AD-A179389] N87-22899

ELECTRON OSCILLATIONS
Programmable electronic synthesized capacitance
[NASA-CASE-GSC-12961-1] N87-22895

ELECTRON PLASMA
A laboratory investigation of potential double layers
N87-23317

ELECTRON SPECTROSCOPY
An improved set of Auger data analysis programs for physical electronics Auger spectrometer systems
[DOE/TIC-4500] N87-22957
On the thinning of the plasma sheet during substorms
[AD-A178484] N87-23061
ELECTRON STATES
Program and abstracts of the 39th Annual Gaseous Electronics Conference
[AD-A178598] N87-23247
Relativistic calculations and measurements of energies, Auger rates, and lifetimes
[AD-A179137] N87-23251
ELECTRON TRANSITIONS
Relativistic calculations and measurements of energies, Auger rates, and lifetimes
[AD-A179137] N87-23251
Collective effects in intense-field electrodynamics 1981-1986
[AD-A179490] N87-23261
Non-Markovian line shapes of physisorbed atoms on a crystal
[AD-A179525] N87-23292
ELECTRON TUNNELING
SIS (Superconductor-Insulator-Superconductor) mixer research
[AD-A179604] N87-23293
ELECTRONIC EQUIPMENT
Transient protection of electronic circuits
[AD-A178945] N87-22919
The use of the Kari sub-scale laser for Raman beam clean-up experiments
[AD-A178463] N87-22971
ELECTRONIC MAIL
Design of GPS (Global Positioning System) status reporting system
[AD-A179334] N87-22662
ELECTRONIC MODULES
An implementation of a language analyzer for the very high speed integrated circuit hardware description language
[AD-A178648] N87-22913
ELECTROPHYSICS
Program and abstracts of the 39th Annual Gaseous Electronics Conference
[AD-A178598] N87-23247
ELECTROSTATIC PROBES
Langmuir probe surveys of an arcjet exhaust
[NASA-TM-89924] N87-22807
ELECTROSTATIC WAVES
The generation of electrostatic noise in the plasma sheet boundary layer
[ATR-86(8433)-4] N87-23282
Double layers and plasma-wave resistivity in extragalactic jets: Cavity formation and radio-wave emission N87-23333
ELECTROSTATICS
The transverse dynamics of space-charge limited diodes
[AD-A179389] N87-22899
Experimental observation of ion-acoustic double layers in laboratory plasma N87-23318
ELEMENTARY PARTICLE INTERACTIONS
Possible inflationary solution to the short distance gravity model
[DE87-701559] N87-23339
ELLIPTICAL ORBITS
Determining the probability of close approach between two satellites
[AD-A179385] N87-22699
EMBEDDED COMPUTER SYSTEMS
The use of real-time optical processors in embedded computing
[DE87-006895] N87-23153
EMBEDDING
Heat transfer effects of longitudinal vortices embedded in a turbulent boundary layer
[DE87-006002] N87-22934
EMISSION
Submicron characterization of the atomic and electronic structure of defects in semiconductors
[AD-A178458] N87-23301
Simultaneous SMM flat crystal spectrometer and very large array observations of solar active regions
[AD-A179698] N87-23562
EMISSION SPECTRA
Laser spectroscopy of transient molecules important in explosions
[AD-A178456] N87-22828
Frequency spectrum of soft X-ray emission from transition radiation
[AD-A178858] N87-23254
Solar active region physical parameters inferred from a thermal cyclotron line and soft X-ray spectral lines
[AD-A179650] N87-23560
EMOTIONAL FACTORS
Nutritional correction of histamine and serotonin levels as related to exposure to hypokinesia and neuro-emotional stress N87-23126
ENERGETIC PARTICLES
A preliminary summary of the observations of the 16 February 1984 solar flare (STIP Interval XV, 12-21 February 1984)
[NASA-CR-180929] N87-23563
ENERGY BUDGETS
Simulated and observed budgets and balances during the 82/83 ENSO event — El Nino Southern Oscillation (ENSO) N87-23035
Standard-resolution TOVS observations for the FIRE/SRB Wisconsin experiment region from October 9 through November 2, 1986
[NASA-TM-89151] N87-23101
ENERGY CONSERVATION
Superconducting Augmented Rail Gun (SARG)
[AD-A179269] N87-22701
ENERGY CONVERSION EFFICIENCY
Superconducting Augmented Rail Gun (SARG)
[AD-A179269] N87-22701
Impact of thermal energy storage properties on solar dynamic space power conversion system mass
[NASA-TM-89909] N87-22802
An investigation of zinc electrodes relevant to zinc-air batteries
[DE87-007607] N87-22908
Reliability of intermediate sized photovoltaic systems
[DE87-006328] N87-23024
ENERGY DISSIPATION
Why gamma rays are different: Some notes for pedestrians
[DE87-004963] N87-22966
Submicron characterization of the atomic and electronic structure of defects in semiconductors
[AD-A178458] N87-23301
ENERGY DISTRIBUTION
System identification for large space structure damage assessment N87-22750
ENERGY GAPS (SOLID STATE)
Method and apparatus for measuring minority carrier lifetime in a direct band-gap semiconductor
[NASA-CASE-NPO-16337-1-CU] N87-22894
ENERGY LEVELS
Why gamma rays are different: Some notes for pedestrians
[DE87-004963] N87-22966
Program and abstracts of the 39th Annual Gaseous Electronics Conference
[AD-A178598] N87-23247
ENERGY SPECTRA
Frequency spectrum of soft X-ray emission from transition radiation
[AD-A178858] N87-23254
ENERGY TRANSFER
Magnetically insulated opening switch research
[AD-A178895] N87-22918
Program and abstracts of the 39th Annual Gaseous Electronics Conference
[AD-A178598] N87-23247
Direct-drive laser-fusion in the US
[DE87-005916] N87-23279
Double Layers in Astrophysics
[NASA-CP-2469] N87-23313
The formation of a double layer leading to the critical velocity phenomenon N87-23335
ENGINE DESIGN
Propulsion system technologies for thrust vectoring
N87-22670
NESSUS/expert and NESSUS/FPI in the Probabilistic Structural Analysis Methods (PSAM) program
N87-22787
Structural tailoring using the SSME/STAEBL code
N87-22795
High heat transfer oxidizer heat exchanger design and analysis — RL10-2B engine
[NASA-CR-179596] N87-22803
ENGINE PARTS
Analytical and experimental studies of flow-induced vibration of SSME components N87-22771
Composite load spectra for select space propulsion structural components N87-22793
High heat transfer oxidizer heat exchanger design and analysis — RL10-2B engine
[NASA-CR-179596] N87-22803
ENGINEERING MANAGEMENT
Summary of the SEI (Software Engineering Institute) Workshop on Softwear Configuration Management
[AD-A178770] N87-23184
ENGINES
Ceramic Technology Newsletter No. 13, October - December 1986: Ceramic technology for advanced heat engines project
[DE87-006447] N87-22852
Thermoelectric conversion with ion conductors
[AD-A179353] N87-23019
ENTROPY
Heat transfer in an organic heat pipe
[LA-10781-MS] N87-22946
ENVIRONMENTAL LABORATORIES
Air Force technical objectives document, fiscal year 1988
[AD-A179163] N87-23569
ENVIRONMENTAL MONITORING
HEPA filter monitoring program
[RFP-3874] N87-22869
ENVIRONMENTS
Laser cladding of Mg and Nb alloys for improved environmental resistance
[AD-A179606] N87-22833
ENZYME ACTIVITY
Evaluation of skeletomuscular system function in self-contained life-support system on the basis of blood biochemistry N87-23135
Human blood serum proteolytic enzyme activity after stay in hypoxic environment N87-23140
EPHEMERIDES
Design of GPS (Global Positioning System) status reporting system
[AD-A179334] N87-22662
EPITAXY
Superconducting thin films, composites and junctions
[AD-A179346] N87-23288
Temperature dependence of implantation damage in strained-layer superlattices
[DE87-007678] N87-23299
AlGaAs growth by OMCVD using an excimer laser
[NASA-TM-88937] N87-23304
EQUATIONS OF MOTION
Transient response for interaction of two dynamic bodies N87-22709
Structural dynamics system model reduction
N87-22727
Notes on implementation of Coulomb friction in coupled dynamical simulations N87-22746
Estimation of ICBM (intercontinental ballistic missile) performance parameters
[AD-A179204] N87-22754
Optimal shuttle altitude changes using tethers
[AD-A179205] N87-22756
Analysis of structures with rotating, flexible substructures
[AD-A178903] N87-23004
Generalized quantal equation of motion
[DE87-701531] N87-23307
Periodic orbits about rotating asteroids in free space
[AD-A179387] N87-23338
EQUATORIAL ATMOSPHERE
Numerical experiments on the atmospheric response to a sea surface temperature anomaly over the equatorial eastern Pacific Ocean N87-23036
EQUATORIAL ORBITS
Periodic orbits about rotating asteroids in free space
[AD-A179387] N87-23338
EQUIPMENT SPECIFICATIONS
Vibration isolation for line of sight performance improvement N87-22742
Optical strain measurement system development, phase 1
[NASA-CR-179619] N87-22960
A system for long pulse REB generation
[IPPJ-812] N87-23274
EROSION
Erosion study of AM355 and Al2O3 ceramics
[AD-A178882] N87-22858
Investigation of laser diagnostics of PACVD processes for depositing hard face coatings
[DE87-006292] N87-22969
Possible origin of some channels on Alba Patera, Mars N87-23465
ERROR ANALYSIS
Problems of identification
[AD-A178555] N87-23239
ERROR CORRECTING CODES
Design of fault tolerant prime factor algorithm array elements
[AD-A178977] N87-23187
ERROR DETECTION CODES
Characterization of the error performance of a QPSK (Quadrature Phase Shift Keyed) communication system in the presence of linear transmission distortion
[AD-A178855] N87-22887
ERRORS
Some integrated squared error procedures for multivariate normal data
[AD-A178985] N87-23224
Estimating the standard error of robust regression estimates
[AD-A179099] N87-23232

ESTIMATES
A family of algorithms for the estimation of the parameters of the stable laws and the parameters of attracting stable laws
[AD-A178542] N87-23214
Estimation of the parameters of a modified compound poisson distribution
[AD-A178540] N87-23236
Estimation of the parameters of mixtures via distance between densities or characteristic functions
[AD-A178623] N87-23241

ESTIMATING
An algorithm for the computation of generalized likelihood or self-critical estimators for binary data
[AD-A178545] N87-23179
Estimating the standard error of robust regression estimates
[AD-A179099] N87-23232

ETCHING
Electrochemical adjustment of thin film Ti-Pd resistors
[DE87-007392] N87-22837

EULER EQUATIONS OF MOTION
A linearized Euler analysis of unsteady flows in turbomachinery
[NASA-CR-180987] N87-22948

EULER-LAGRANGE EQUATION
Generalized quantal equation of motion
[DE87-701531] N87-23307

EVACUATING (VACUUM)
Experimental evaluation of blockage ratio and plenum evacuation system flow effects on pressure distribution for bodies of revolution in 0.1 scale model test section of NASA Lewis Research Center's proposed altitude wind tunnel
[NASA-TP-2702] N87-22694

EVALUATION
Experimental evaluation of blockage ratio and plenum evacuation system flow effects on pressure distribution for bodies of revolution in 0.1 scale model test section of NASA Lewis Research Center's proposed altitude wind tunnel
[NASA-TP-2702] N87-22694
An evaluation of the polar ice prediction system
[AD-A178522] N87-23014

EVOLUTION (DEVELOPMENT)
Investigations of the surfaces and interiors of outer planet satellites N87-23356
Meteorite spectroscopy and characterization of asteroid surface materials N87-23373
Evolution of planetesimal velocities N87-23383
Valley development on Hawaiian volcanoes N87-23463
Volatile reservoirs below the surface of the Elysium region of Mars: Geomorphic evidence N87-23467

EXCIMER LASERS
The transverse dynamics of space-charge limited diodes
[AD-A179389] N87-22899
AlGaAs growth by OMCVD using an excimer laser
[NASA-TM-88937] N87-23304

EXCITATION
Flight and analytical investigations of a structural mode excitation system on the YF-12A airplane
[NASA-CR-166623] N87-22685
Time and space resolved spectroscopy of X-ray laser experiments from 81A to 220A
[DE87-005946] N87-22968
Program and abstracts of the 39th Annual Gaseous Electronics Conference
[AD-A178598] N87-23247
Relativistic calculations and measurements of energies, Auger rates, and lifetimes
[AD-A179137] N87-23251

EXCITONS
Nonlinear optical properties and subpicosecond dynamics of excitons and electron-hole plasmas in multiple quantum well structures
[AD-A179124] N87-23287

EXHAUST EMISSION
Langmuir probe surveys of an arcjet exhaust
[NASA-TM-89924] N87-22807

EXHAUST GASES
Gas turbine combustor and engine augmentor tube sooting characteristics
[AD-A179423] N87-22679

EXOBIOLOGY
Scientific goals of the German Spacelab Mission D1
[ETN-87-99669] N87-22695
Aerospace medicine and biology: A continuing bibliography with indexes (supplement 298)
[NASA-SP-7011(298)] N87-23114

EXPANSION
On non-parametric discrimination using series expansions and projection pursuit
[AD-A178455] N87-23213

EXPERIMENT DESIGN
Infrared spectroscopy using laser and Fourier techniques of the unstable molecules SiH and NH. Determination of the molecular constants of the fundamental electronic state 3 sigma (-) of NH
[ETN-87-99552] N87-22818

EXPERT SYSTEMS
A prototype knowledge-based system for satellite mission planning
[AD-A178873] N87-22698
A prototype expert system advisor for satellite support scheduling
[AD-A179425] N87-22760
NESSUS/expert and NESSUS/FPI in the Probabilistic Structural Analysis Methods (PSAM) program N87-22787
Composite load spectra for select space propulsion structural components N87-22793
Probabilistic load model development and validation for composite load spectra for select space propulsion engines N87-22794
Programming languages for knowledge-based systems
[PB87-157228] N87-23170
Optical symbolic processor for expert system execution
[AD-A179375] N87-23172
Managing uncertainty in expert systems: A probabilistic approach
[AD-A178582] N87-23246

EXPLOSIONS
Laser spectroscopy of transient molecules important in explosions
[AD-A178456] N87-22826
A new LIHE (Light Initiated High Explosive) test capability for spherical targets
[DE87-003035] N87-23245

EXPLOSIVES
A fast, low resistance switch for small slapper detonators
[AD-A178562] N87-22911

EXPONENTIAL FUNCTIONS
The exponential method
[TRITA-NA-8517] N87-23228
On Bayes selection rules for the best exponential population with type-I censored data
[AD-A178472] N87-23235

EXTENSOMETERS
Thermal expansion of epoxy-fiberglass composite specimens
[DE87-004273] N87-22812

EXTINCTION
Bidirectional reflectance spectroscopy — for Moon, asteroid, Europa, and Oberon N87-23433

EXTINGUISHING
Collective effects in intense-field electrodynamics 1981-1986
[AD-A179490] N87-23261

EXTRAGALACTIC RADIO SOURCES
Double layers and plasma-wave resistivity in extragalactic jets: Cavity formation and radio-wave emission N87-23333

EXTREMUM VALUES
Extreme value theory for suprema of random variables with regularly varying tail probabilities
[AD-A179126] N87-23233

EYE MOVEMENTS
Workshop Symposium on Neural Models of Sensory-Motor Control
[AD-A179501] N87-23111

F

F-16 AIRCRAFT
F-16 control stick response during +G sub z-induced loss of consciousness
[AD-A178474] N87-23116

FABRICATION
Target fabrication for high density target experiments at the University of Rochester's Laboratory for Laser Energetics
[DE87-005915] N87-22967
Modeling of substrate and implantation effects on the threshold voltage of MESFET structures fabricated in semi-insulating GaAs
[AD-A178550] N87-23303

FABRY-PEROT INTERFEROMETERS
Frequency shift measurements of the Q(1) and Q(2) lines of H2 using high resolution CW Coherent Anti-Stokes Raman Spectroscopy
[AD-A179390] N87-22820

FACE (ANATOMY)
Image size and resolution in face recognition N87-23113

FAIL-SAFE SYSTEMS
Methodology for verification of ultrasonic inspection
[AD-A179694] N87-22988

FAILURE
Dynamic fracture of high strength steel
[AD-A178862] N87-22844

FAILURE ANALYSIS
Studies and analyses of the space shuttle main engine: High-pressure oxidizer turbopump failure information propagation model
[NASA-CR-179079] N87-22765
HEPA filter monitoring program
[RFP-3874] N87-22989
On the application of the strain energy density theory in predicting crack initiation and angle of growth
[AR-004-493] N87-23011
Development of confidence limits by pivotal functions for estimating software reliability
[NASA-TP-2709] N87-23244

FAILURE MODES
Statistics on aircraft gas turbine engine rotor failures that occurred in US commercial aviation during 1981
[DOT/FAA/CT-86/42] N87-22684
Studies and analyses of the space shuttle main engine: High-pressure oxidizer turbopump failure information propagation model
[NASA-CR-179079] N87-22765

FAN BLADES
Application of advanced computational codes in the design of an experiment for a supersonic throughflow fan rotor
[NASA-TM-88915] N87-22630

FAR FIELDS
Optimization of the antenna pattern of a phased array with failed elements
[AD-A178581] N87-22878

FASTENERS
Daze fasteners
[NASA-CASE-LAR-13009-2] N87-22976

FATIGUE (MATERIALS)
Structural Integrity and Durability of Reusable Space Propulsion Systems
[NASA-CP-2471] N87-22766
Dynamic characteristics of single crystal SSME blades N87-22797
Semiconductor research capabilities at the Lawrence Berkeley Laboratory
[DE87-006931] N87-23298

FATIGUE LIFE
Fatigue damage interaction behavior of PWA 1480 N87-22777
A new formulation of mean stress effects in fatigue N87-22778
Probabilistic structural analysis to evaluate the structural durability of SSME critical components N87-22783
Hydrogen and temper embrittlement interactions in fatigue of 2 1/4Cr1Mo steel
[AERE-R-12322] N87-22830
Prediction of service life of aircraft structural components using the half-cycle method
[NASA-TM-86812] N87-23009
A comparison of predicted wind turbine blade loads to test measurements
[DE87-001130] N87-23021

FATIGUE TESTS
Fatigue damage interaction behavior of PWA 1480 N87-22777

FAULT TOLERANCE
Intelligent fault-tolerant controllers N87-22621
The design of a real time operating system for a fault tolerant microcomputer
[AD-A178577] N87-23155
Formal modeling and analysis of fault-tolerance properties for software
[DE87-007006] N87-23176
Design of fault tolerant prime factor algorithm array elements
[AD-A178977] N87-23187

FEASIBILITY ANALYSIS
A prototype knowledge-based system to aid space system restoration management
[AD-A179336] N87-23203

FEEDBACK CONTROL
Safe microburst penetration techniques: A deterministic, nonlinear, optimal control approach N87-22620
Stability boundaries for command augmentation systems N87-22622
Accurate prediction of longitudinal flying qualities for landing aircraft
[AD-A179069] N87-22676
Large space structures ground experiment checkout N87-22704
One Controller at a Time (1-CAT): A mimo design methodology N87-22715
Flexible spacecraft simulator N87-22718

Improving stability margins in discrete-time log controllers N87-22719
Control of flexible structures and the research community N87-22732
Maneuvering and vibration control of flexible spacecraft N87-22734
A static data flow simulation study at Ames Research Center
[NASA-TM-89434] N87-23201
Multi-input/multi-output designated eigenstructure (MODES): A computer-aided control system design program
[AD-A179341] N87-23204
Closed loop fiber optic rotation sensor
[NASA-CASE-NPO-16558-1-CU] N87-23259

FEMALES
Identification and validation of new anthropometric techniques for quantifying body composition
[AD-A178753] N87-23118

FERMI SURFACES
Unpinning of the Fermi level on GaAs by flowing water
[AD-A178489] N87-23302

FERROELECTRICITY
Ferroelectric optically controlled millimeter-wave devices
[AD-A179524] N87-22901

FIBER OPTICS
Investigation of air transportation technology at Ohio University, 1984 N87-22609
Fiber optic data transmission N87-22611
CONMILIT (selected articles)
[AD-A179155] N87-22661
A feasibility study of the flexible simulation of sunlight — cockpit simulators
[BR98783] N87-22693
Infrared fiber optic materials
[NASA-CR-180604] N87-23257
Closed loop fiber optic rotation sensor
[NASA-CASE-NPO-16558-1-CU] N87-23259
Development of radiation hard graded index optical fibers
[AD-A178465] N87-23265
Radiation hardened silica-based optical fibers
[AD-A178466] N87-23266
Applications of fiber optics in experimental mechanics
[AD-A178683] N87-23268
Analog fiber optic recirculating delay line
[AD-A179050] N87-23272
Channel access schemes and fiber optic configurations for integrated-services local area networks
[NASA-CR-180934] N87-23273

FIBER REINFORCED COMPOSITES
Fiber reinforced superalloys
[NASA-TM-89865] N87-22811
High performance polymers: Matrix resins, high strength polyquinoxalines and conducting polyaromatics
[AD-A178457] N87-22854

FIELD EFFECT TRANSISTORS
Stochastic processes in CHEMFETs
[AD-A178841] N87-22829
Modeling of substrate and implantation effects on the threshold voltage of MESFET structures fabricated in semi-insulating GaAs
[AD-A178550] N87-23303

FIGHTER AIRCRAFT
Improvement of Combat Performance for Existing and Future Aircraft
[AGARD-CP-409] N87-22663
Performance improvement of airborne weapon systems methods, scope and limitations N87-22665
Weapon systems polyvalence: An economic and operational challenge N87-22667
The assessment and evaluation of combat performance improvements N87-22675
Visual acuity and reaction time in navy fighter pilots
[AD-A178485] N87-23117

FILE MAINTENANCE (COMPUTERS)
A design for a new catalog manager and associated file management for the Land Analysis System (LAS) N87-23159
An overview of the catalog manager N87-23163

FINE STRUCTURE
Fine structure of the atmospheric boundary layer across the Alps during a high pressure period in the Alpine Experiment (ALPEX). A case study on April 22, 1982 N87-23087

FINITE DIFFERENCE THEORY
Flutter analysis of a two-dimensional airfoil with cubic non-linear restoring force
[NAE-AN-36] N87-22628
Axisymmetric inviscid shock tube flow simulation
[AD-A178494] N87-22937
A three-dimensional dual potential procedure with applications to wind tunnel inlets and interacting boundary layers
[NASA-CR-180939] N87-22944
Bodner-Partom viscoplastic model in STEALTH finite difference code
[AD-A178994] N87-23005
Development of a generalized model for a three component plasma
[AD-A178979] N87-23281
Nonlinear aspects of planar condensational instability
[AD-A178998] N87-23565

FINITE ELEMENT METHOD
A general method for dynamic analysis of structures overview N87-22707
Equivalent beam modeling using numerical reduction techniques N87-22725
Structural dynamics system model reduction N87-22727
Dual keel space station control/structures interaction study N87-22737
Finite element models of wire rope for vibration analysis N87-22748
Nonlinear heat transfer and structural analyses of SSME turbine blades N87-22779
Structural analysis demonstration of constitutive and life models N87-22780
The NESSUS finite element code N87-22785
Probabilistic structural analysis verification studies N87-22786
Probabilistic finite elements N87-22790
Full-wave analysis of isolated and coupled microwave transmission lines using the finite element method
[AD-A178805] N87-22883
Prediction of fluid flow in curved pipe using the finite element method
[AD-A179538] N87-22926
Two-dimensional elastic analysis by the boundary element method
[AD-A179213] N87-22993
Non-linear finite element analysis program
[AD-A179038] N87-23006
Finite element implementation of Robinson's unified viscoplastic model and its application to some uniaxial and multiaxial problems
[NASA-TM-89891] N87-23010
A survey of mixed finite element methods
[NASA-CR-178267] N87-23229

FIRE CONTROL
Simulation of an integrated flight/fire control system during air-to-ground gunnery attack N87-22672

FLAME PROPAGATION
On the use of adaptive moving grid methods in combustion problems
[DE87-003715] N87-22824

FLAME RETARDANTS
Laboratory characterization tests for antimisting fuel
[DOT/FAA/CT-86/23] N87-22864

FLAMES
Direct numerical simulations of an unpremixed turbulent jet flame
[AD-A179358] N87-22819
Afterburning suppression kinetics
[AD-A178967] N87-22863

FLAT PLATES
Full polarimetric non-specular scattering of flat plate structures
[AD-A178853] N87-22886
Interaction of a three-dimensional roughness element with a laminar boundary layer
[AD-A178668] N87-22941

FLEXIBLE BODIES
Structural Dynamics and Control Interaction of Flexible Structures
[NASA-CP-2467-PT-1] N87-22702
Status of the Mast experiment N87-22703
Microprocessor controlled proof-mass actuator N87-22706
Space Station/Shuttle Orbiter dynamics during docking N87-22708
Considerations in the design and development of a space station scale model N87-22711
Verification of large beam-type space structures N87-22712
Verification of flexible structures by ground test N87-22713
Status report and preliminary results of the spacecraft control laboratory experiment N87-22717
Structural Dynamics and Control Interaction of Flexible Structures
[NASA-CP-2467-PT-2] N87-22729
Vibration suppression by stiffness control N87-22730
Control of flexible structures and the research community N87-22732
Maneuvering and vibration control of flexible spacecraft N87-22734
A TREETOPS simulation of the Hubble Space Telescope-High Gain Antenna interaction N87-22735
Lanczos modes for reduced-order control of flexible structures N87-22739
Slewing control experiment for a flexible panel N87-22740
Space station structural dynamics/reaction control system interaction study N87-22753
Analysis of structures with rotating, flexible substructures
[AD-A178903] N87-23004

FLEXIBLE SPACECRAFT
Flexible spacecraft simulator N87-22718
An overview of controls research on the NASA Langley Research Center grid N87-22720
Precision pointing and control of flexible spacecraft N87-22723

FLEXING
Flexurally-resisted uplift of the Tharsis Province, Mars N87-23530

FLIGHT CHARACTERISTICS
Accurate prediction of longitudinal flying qualities for landing aircraft
[AD-A179069] N87-22676
Evaluation of numerator lead effects on aircraft handling qualities
[AD-A179388] N87-22687
An evaluation of metallized propellants based on vehicle performance
[NASA-TM-100104] N87-22806
Product assurance policies and procedures for flight dynamics software development
[NASA-TM-89377] N87-23192

FLIGHT CONTROL
A look at handling qualities of Canard configurations
[NASA-TM-88354] N87-22629
Integrated design of structures N87-22669
X-29 integrating advanced technologies for tomorrow's air combat N87-22671
Simulation of an integrated flight/fire control system during air-to-ground gunnery attack N87-22672
Improved combat performance using relaxed static stability and a spin prevention system (FBW Jaguar) N87-22674
Accurate prediction of longitudinal flying qualities for landing aircraft
[AD-A179069] N87-22676
Aircraft control position indicator
[NASA-CASE-LAR-12984-1] N87-22678
Electromagnetic interference (EMI) fault prevention and self recovery of digital flight control systems — helicopters
[MBB-UD-483/86] N87-22686
Frequency-response identification of XV-15 tilt-rotor aircraft dynamics
[NASA-TM-89428] N87-22690
Digital control of highly augmented combat rotorcraft
[NASA-TM-88346] N87-22691
Multi-input/multi-output designated eigenstructure (MODES): A computer-aided control system design program
[AD-A179341] N87-23204

FLIGHT CREWS
Cockpit Resource Management Training
[NASA-CP-2455] N87-22634
Theory underlying CRM training: Psychological issues in flight crew performance and crew coordination N87-22635
Group-level issues in the design and training of cockpit crews N87-22636
Cockpit Resource Management (CRM): A tool for improved flight safety (United Airlines CRM training) N87-22637
The development and implementation of cockpit resource management in UAL recurrent training N87-22638
Cockpit resource management training at People Express N87-22639
Cockpit management and Specific Behavioral Objectives (SBOs) N87-22640
Pan American World Airways flight training: A new direction. Flight operations resource management N87-22641
Crew coordination concepts: Continental Airlines CRM training N87-22642
Introduction to Trans Australia Airlines CRM training N87-22644
Aircrew team management program N87-22645
Remedial training: Will CRM work for everyone N87-22646
Cockpit resource management training N87-22647
Introduction to MAC CRM training N87-22648
The application of CRM to military operations N87-22649
Cockpit Resource Management (CRM) training in the 1550th combat crew training wing N87-22650
Cockpit Resource Management (CRM) training in the 349th military airlift wing N87-22651
Cockpit Resource Management (CRM) for part 91 and 135 operations N87-22652

Cockpit Resource Management (CRM) for FAR Parts 91 and 135 operators N87-22653
The regulatory horizon N87-22654
Instructions to working groups N87-22655
Dyads and triads at 35,000 feet: Factors affecting group process and aircrew performance N87-22656
Aircrew cooperation in the Royal Air Force N87-22657
Cockpit Resource Management (CRM) and human factors training: What Air New Zealand is doing about it N87-22658
Cockpit resource management at USAir N87-22659
Aircrew task surveys: Selection criteria for low-cost training technology applications
[AD-A178473] N87-23146

FLIGHT INSTRUMENTS
Aircraft control position indicator
[NASA-CASE-LAR-12984-1] N87-22678

FLIGHT OPERATIONS
Pan American World Airways flight training: A new direction. Flight operations resource management N87-22641
Crew coordination concepts: Continental Airlines CRM training N87-22642
Optimum culture in the cockpit N87-22643

FLIGHT PATHS
Loran-C approach considerations N87-22612
Estimation of ICBM (intercontinental ballistic missile) performance parameters
[AD-A179204] N87-22754
A partial differential equation model describing the threat to an aircraft in a one-on-Many scenario
[AD-A178641] N87-23215

FLIGHT SAFETY
Cockpit Resource Management (CRM): A tool for improved flight safety (United Airlines CRM training) N87-22637
Optimum culture in the cockpit N87-22643
Introduction to Trans Australia Airlines CRM training N87-22644
Cockpit resource management training N87-22647
Cockpit Resource Management (CRM) for FAR Parts 91 and 135 operators N87-22653
Dyads and triads at 35,000 feet: Factors affecting group process and aircrew performance N87-22656
Aircrew cooperation in the Royal Air Force N87-22657
Cockpit Resource Management (CRM) and human factors training: What Air New Zealand is doing about it N87-22658
Cockpit resource management at USAir N87-22659

FLIGHT SIMULATION
Cockpit Resource Management Training
[NASA-CP-2455] N87-22634
Pan American World Airways flight training: A new direction. Flight operations resource management N87-22641
Introduction to Trans Australia Airlines CRM training N87-22644
Cockpit Resource Management (CRM) for part 91 and 135 operations N87-22652

FLIGHT SIMULATORS
Asymmetries in the control of saccadic eye movements to bifurcating targets
[AD-A178270] N87-23108

FLIGHT TESTS
Accurate prediction of longitudinal flying qualities for landing aircraft
[AD-A179069] N87-22676
Flight and analytical investigations of a structural mode excitation system on the YF-12A airplane
[NASA-CR-166623] N87-22685
Evaluation of numerator lead effects on aircraft handling qualities
[AD-A179388] N87-22687
Frequency-response identification of XV-15 tilt-rotor aircraft dynamics
[NASA-TM-89428] N87-22690
Solar array flight dynamic experiment N87-22722
High altitude turbulence for supersonic cruise vehicles
[NASA-TM-88285] N87-23100

FLIGHT TRAINING
Cockpit Resource Management Training
[NASA-CP-2455] N87-22634
Theory underlying CRM training: Psychological issues in flight crew performance and crew coordination N87-22635
Group-level issues in the design and training of cockpit crews N87-22636
Cockpit Resource Management (CRM): A tool for improved flight safety (United Airlines CRM training) N87-22637
The development and implementation of cockpit resource management in UAL recurrent training N87-22638
Cockpit resource management training at People Express N87-22639
Cockpit management and Specific Behavioral Objectives (SBOs) N87-22640
Pan American World Airways flight training: A new direction. Flight operations resource management N87-22641
Introduction to Trans Australia Airlines CRM training N87-22644
Aircrew team management program N87-22645
Remedial training: Will CRM work for everyone N87-22646
Cockpit resource management training N87-22647
Introduction to MAC CRM training N87-22648
The application of CRM to military operations N87-22649
Cockpit Resource Management (CRM) training in the 1550th combat crew training wing N87-22650
Cockpit Resource Management (CRM) training in the 349th military airlift wing N87-22651
Cockpit Resource Management (CRM) for part 91 and 135 operations N87-22652
Cockpit Resource Management (CRM) for FAR Parts 91 and 135 operators N87-22653
The regulatory horizon N87-22654
Instructions to working groups N87-22655
Aircrew cooperation in the Royal Air Force N87-22657
Cockpit Resource Management (CRM) and human factors training: What Air New Zealand is doing about it N87-22658
Cockpit resource management at USAir N87-22659
Aircrew task surveys: Selection criteria for low-cost training technology applications
[AD-A178473] N87-23146

FLOOD PLAINS
Late-stage flood lavas in the Elysium region, Mars N87-23476

FLOODS
The application of flow competence evaluations to the assessment of flood-flow velocities and stresses N87-23464

FLOW DISTRIBUTION
Numerical simulation of supersonic flow over a rotating band using flowfield blanking
[AD-A178492] N87-22624
Dynamic stall calculations using a Navier-Stokes solver
[AD-A178566] N87-22688
Unsteady stator/rotor interaction N87-22767
Simulation of multistage turbine flows N87-22768
Experimental and theoretical studies of time-averaged and time resolved rotor heat transfer N87-22770
Development of an integrated BEM (Boundary Element Mesh) for hot fluid-structure interaction N87-22799
Journal of Chinese Society of Astronautics (selected articles)
[AD-A179690] N87-22800
Conservative zonal schemes for patched grids in 2 and 3 dimensions
[NASA-TM-88326] N87-22932
On the diagnosis of a cold front observed during Alpine Experiment (ALPEX) N87-23072
Toward a model for leveed lava flows N87-23483

FLOW EQUATIONS
A study of fluid-dynamic pressure fields on compressor reed valves
[AD-A178584] N87-22938

FLOW MEASUREMENT
Toward a model for leveed lava flows N87-23483

FLOW STABILITY
An analysis of artificial viscosity effects on reacting flows using a spectral multi-domain technique
[NASA-CR-178308] N87-22632
Studies of fluid instabilities in flows of lava and debris N87-23479

FLOW THEORY
Analytical and experimental studies of flow-induced vibration of SSME components N87-22771
Long, paired A'A/Pahoehoe flows of Mauna Loa: Volcanological significance and insights they provide into volcano plumbing systems N87-23480
The 1984 Mauna Loa eruption and planetary geolgoy N87-23481

FLOW VELOCITY
Analytical and experimental studies of flow-induced vibration of SSME components N87-22771
Interaction of a three-dimensional roughness element with a laminar boundary layer
[AD-A178668] N87-22941
Numerical simulation of the decay of swirling flow in a constant volume engine simulator
[LA-10728-MS] N87-22945
Calculated viscosity-distance dependence for some actively flowing lavas N87-23482
Toward a model for leveed lava flows N87-23483

FLOWMETERS
Dual cylindrical wave laser-Doppler method for measurement of skin friction in fluid flow
[AD-A178629] N87-22939

FLUID DYNAMICS
Scientific goals of the German Spacelab Mission D1
[ETN-87-99689] N87-22695
Prediction of fluid flow in curved pipe using the finite element method
[AD-A179538] N87-22926
A study of fluid-dynamic pressure fields on compressor reed valves
[AD-A178584] N87-22938

FLUID FLOW
Experimental cavity pressure distributions at supersonic speeds
[NASA-TP-2683] N87-22626
Vectorizable algorithms for adaptive schemes for rapid analysis of SSME flows
[NASA-CR-179082] N87-22784
Prediction of fluid flow in curved pipe using the finite element method
[AD-A179538] N87-22926
Dual cylindrical wave laser-Doppler method for measurement of skin friction in fluid flow
[AD-A178629] N87-22939
Non-equilibrium freezing of water-ice in sandy basaltic regoliths and implications for fluidized debris flows on Mars N87-23466
Observations of industrial sulfur flows and implications for Io N87-23541

FLUID MANAGEMENT
Thermodynamic analysis and subscale modeling of space-based orbit transfer vehicle cryogenic propellant resupply
[NASA-TM-89921] N87-22949

FLUORESCENCE
Application of atomic fluorescence to measurement of combustion temperature in solid propellants
[AD-A179665] N87-22862

FLUOROHYDROCARBONS
Basic research in energetic fluorocarbons
[AD-A179676] N87-22822

FLUTTER ANALYSIS
Flutter analysis of a two-dimensional airfoil with cubic non-linear restoring force
[NAE-AN-36] N87-22628

FLUX (RATE)
Superconducting Augmented Rail Gun (SARG)
[AD-A179269] N87-22701
Composite velocity procedures for flows with pressure interaction
[AD-A179602] N87-22929

FLUX DENSITY
CO2 pulsed laser damage mechanism and plasma effects (focused beam)
[AD-A179201] N87-22961

FOCUSING
White-light optical information processing and holography
[AD-A179489] N87-23260

FOILS (MATERIALS)
Corrosion, wear and mechanical properties of pulse-electrodeposited alloys
[AD-A178596] N87-22842

FORCED CONVECTION
Sensitivity of tropical and mid-latitude time-averaged atmospheric states to interannually varying global ocean surface temperature distribution N87-23039
Principal circulation anomalies in model atmospheres with and without interannual variations of tropical Pacific SST — sea surface temperature (SST) N87-23041

FORCED VIBRATION
Flutter analysis of a two-dimensional airfoil with cubic non-linear restoring force
[NAE-AN-36] N87-22628

FORECASTING
An evaluation of the polar ice prediction system
[AD-A178522] N87-23014

FORMAT
Ada style guide (version 1.1)
[NASA-TM-89376] N87-23191

FORMING TECHNIQUES
High energy high rate pulsed power processing of materials by powder consolidation and by railgun deposition
[AD-A179289] N87-22867

FORMULAS (MATHEMATICS)
Investigate and verify the validity of mathematical formulas and procedures in relation to data obtained from theoretical investigations and experimental observations
[AD-A179564] N87-23057

FORTRAN
Measuring software design
[NASA-TM-89372] N87-23189

FOURIER ANALYSIS
The potential gradient of a plane source
[AD-A178976] N87-23223
FOURIER TRANSFORMATION
Laser spectroscopy of transient molecules important in explosions
[AD-A178456] N87-22828
Modeling and simulation of the WFTA (Winograd Fourier Transform Algorithm) 16 PFA (Prime Factor Algorithm) processor using the VHSIC (Very High Speed Integrated Circuit) hardware description language, volume 1
[AD-A179344] N87-22898
Design of fault tolerant prime factor algorithm array elements
[AD-A178977] N87-23187
Stationary phase approximations in Fresnel-zone magnitude-only reconstructions
[AD-A178812] N87-23270
FRACTALS
Fractal analysis of radar precipitation data over hilly terrain N87-23093
Implications of convection in the Moon and the terrestrial planets N87-23406
FRACTURE MECHANICS
Structural Integrity and Durability of Reusable Space Propulsion Systems
[NASA-CP-2471] N87-22766
Effect of hydrogen on deformation structure and properties of CMSX-2 nickel-base single-crystal superalloy N87-22782
Microscopic study of the influence of impurities on interface bonding
[AD-A178510] N87-22841
Dynamic fracture of high strength steel
[AD-A178862] N87-22844
Two-dimensional elastic analysis by the boundary element method
[AD-A179213] N87-22993
An evaluation of microgridding techniques for determining local plastic strain distributions
[AD-A178518] N87-23000
Dynamic fracture under plane wave loading
[AD-A178594] N87-23001
Failure strength of icy lithospheres N87-23357
The effect of overburden thickness on tension fracture patterns above an uplifting dome N87-23535
FRACTURE STRENGTH
Dynamic fracture of high strength steel
[AD-A178862] N87-22844
FRACTURING
Age of fracturing and mesa development in the Elysium Area, northern Martian plains N87-23532
Geometry and relative age of large patterned fractures in southern Acidalia Planitia, Mars N87-23533
Origin of fractures, Martian polygonal terrain N87-23534
Natural fracture systems on planetary surfaces: Genetic classification and pattern randomness N87-23536
FRAGMENTATION
Experimental studies of collision and fragmentation phenomena N87-23494
FREE FLOW
Investigation of periodic pitching through the static stall angle of attack
[AD-A179512] N87-22623
FREE RADICALS
Infrared spectroscopy using laser and Fourier techniques of the unstable molecules SiH and NH. Determination of the molecular constants of the fundamental electronic state 3 sigma (-) of NH
[ETN-87-99552] N87-22818
FREQUENCIES
Corrosion, wear and mechanical properties of pulse-electrodeposited alloys
[AD-A178596] N87-22842
FREQUENCY DISCRIMINATORS
Programmable electronic synthesized capacitance
[NASA-CASE-GSC-12961-1] N87-22895
FREQUENCY DISTRIBUTION
Frequency spectrum of soft X-ray emission from transition radiation
[AD-A178858] N87-23254
FREQUENCY SHIFT
Frequency shift measurements of the Q(1) and Q(2) lines of H2 using high resolution CW Coherent Anti-Stokes Raman Spectroscopy
[AD-A179390] N87-22820
FREQUENCY SHIFT KEYING
A system design requirements tool for satellite communications through nuclear-induced scintillation
[AD-A179272] N87-22871
FRESNEL LENSES
Evaluation of a heliostat tracker for linear Fresnel lens photovoltaic concentrators
[DE87-006331] N87-23025
Development of a holographic beamsplitter for use with a conventional Fresnel lens
[DE87-006770] N87-23263
FRESNEL REGION
Automatic pattern recognition and related topics
[AD-A178595] N87-23267
Stationary phase approximations in Fresnel-zone magnitude-only reconstructions
[AD-A178812] N87-23270
FRICTION
Effect of Gimbal friction modeling technique on control stability and performance for Centaur upper-stage
[NASA-TM-89894] N87-22755
SSME blade damper technology N87-22798
In situ friction, wear and electrical contact resistance of precious metal alloys
[DE87-001423] N87-22979
FRICTION MEASUREMENT
Corrosion, wear and mechanical properties of pulse-electrodeposited alloys
[AD-A178596] N87-22842
Dual cylindrical wave laser-Doppler method for measurement of skin friction in fluid flow
[AD-A178629] N87-22939
FRICTION REDUCTION
SSME blade damper technology N87-22798
FROST
Timing of frost deposition on Martian dunes: A clue to properties of dune particles? N87-23453
FRUSTRATION
Tolerance to frustration as a factor in operator performance N87-23124
FRUSTUMS
Hypersonic laminar boundary layer transition. Part 1: Nosetip bluntness effects on cone frustum transition. Part 2: Mach 6 experiments of transition on a cone at angle of attack
[AD-A178877] N87-22625
FUEL COMBUSTION
The autoignition of isobutane in a knocking spark ignition engine
[DE87-003241] N87-22823
Afterburning suppression kinetics
[AD-A178967] N87-22863
FUEL PUMPS
Gas turbine combustor and engine augmentor tube sooting characteristics
[AD-A179423] N87-22679
FUEL SYSTEMS
Simulation of multistage turbine flows N87-22768
FUEL TANKS
Hybrid composite response to hydraulic ram
[AD-A178750] N87-22815
FUNCTIONS (MATHEMATICS)
A method for the spatial discretization of parabolic equations in one space variable
[DE87-005991] N87-23210
A test of goodness of fit for multivariate normality
[AD-A178543] N87-23237
FURNACES
Low-pressure self-propagating high-temperature synthesis
[AD-A178593] N87-22856

G

GALERKIN METHOD
A method for the spatial discretization of parabolic equations in one space variable
[DE87-005991] N87-23210
GALILEAN SATELLITES
Charged particle modification of surfaces in the outer solar system N87-23435
The Galilean satellite geological mapping program, 1986 N87-23544
GALLIUM ARSENIDES
Unpinning of the Fermi level on GaAs by flowing water
[AD-A178489] N87-23302
Modeling of substrate and implantation effects on the threshold voltage of MESFET structures fabricated in semi-insulating GaAs
[AD-A178550] N87-23303
AlGaAs growth by OMCVD using an excimer laser
[NASA-TM-88937] N87-23304
GAMMA RAY ASTRONOMY
X-ray and low energy gamma-ray observations of the 16 February 1984 solar flare
[NASA-CR-180928] N87-23564
GAMMA RAY BURSTS
Beamed emission from gamma-ray burst sources N87-23332
GAMMA RAY SPECTROMETERS
Investigation of Martian H2O and CO2 via gamma-ray spectroscopy N87-23420
GAMMA RAYS
Why gamma rays are different: Some notes for pedestrians
[DE87-004963] N87-22966
Why gamma rays are different: Some notes for pedestrians
[DE87-004963] N87-22966
Detection of 10^{14}-eV gamma rays from Cygnus X-3 during 1986
[DE87-006054] N87-23568
GANYMEDE
Studies of outer planet satellites, Mercury and Uranus N87-23358
Dome craters on Ganymede N87-23510
Non-Newtonian ice rheology and the retention of craters on Ganymede N87-23511
Ejecta types on Ganymede and Callisto N87-23512
Local-scale stratigraphy of grooved terrain on Ganymede N87-23538
Stratigraphy of the south polar region of Ganymede N87-23539
GAS DISCHARGES
Program and abstracts of the 39th Annual Gaseous Electronics Conference
[AD-A178598] N87-23247
GAS DYNAMICS
Evolution of planetesimal velocities N87-23383
Accumulation of solid bodies in the solar nebula N87-23384
GAS FLOW
Journal of Chinese Society of Astronautics (selected articles)
[AD-A179690] N87-22600
The loss and depth of CO2 ice in comet nuclei N87-23367
GAS LASERS
Pulsed power for high power electron-beam pumped lasers
[DE87-004523] N87-22965
The use of the Karl sub-scale laser for Raman beam clean-up experiments
[AD-A178463] N87-22971
GAS MIXTURES
Low-pressure self-propagating high-temperature synthesis
[AD-A178593] N87-22856
Catalytic radiant tube. Phase 2: Proof of concept
[PB87-169835] N87-22891
Gas mixtures for spark gap closing switches with emphasis on efficiency of operation
[DE87-006624] N87-22906
Experimental investigation of the process of CO2-CO-H2O-H2-N2 gas mixture breakdown in electrolysis cell with solid electrolyte N87-23137
GAS POCKETS
Studies of vesicle distribution patterns in Hawaiian lavas N87-23484
GAS TUNGSTEN ARC WELDING
Circumferential hot wire TIG cladding of carbon-manganese steel with Inconel 625 and gun-metal with a tin bronze
[ARE-TM(UMD)-85574] N87-22831
GAS TURBINE ENGINES
Gas turbine combustor and engine augmentor tube sooting characteristics
[AD-A179423] N87-22679
Preliminary investigation of the use of holographic interferometry to detect ill-fitting compressor blades
[AD-A178519] N87-22682
AI (Artificial Intelligence) gas turbine rotor diagnostics
[AD-A178996] N87-22683
Statistics on aircraft gas turbine engine rotor failures that occurred in US commercial aviation during 1981
[DOT/FAA/CT-86/42] N87-22684
Experimental and theoretical studies of time-averaged and time resolved rotor heat transfer N87-22770
Nonisothermal elasto-visco-plastic response of shell-type structures N87-22796
Fiber reinforced superalloys
[NASA-TM-89865] N87-22811
GAS TURBINES
Laser anemometry techniques for turbine applications
[NASA-TM-88953] N87-22959
GAS-GAS INTERACTIONS
Program and abstracts of the 39th Annual Gaseous Electronics Conference
[AD-A178598] N87-23247
GAS-METAL INTERACTIONS
Hydrogen and temper embrittlement interactions in fatigue of 2 1/4Cr1Mo steel
[AERE-R-12322] N87-22830
GASES
Numerical analysis of terminal double mach reflection
[AD-A179041] N87-22942

Special features in regulating respiration under normal conditions and conditions of altered gas medium
[AD-A179216] N87-23106
Accumulation of the planets N87-23378

GELATION
Isotactic polystyrene phase diagrams and physical gelation
[DE87-002693] N87-22850

GELS
Isotactic polystyrene phase diagrams and physical gelation
[DE87-002693] N87-22850

GEOCHEMISTRY
Reports of Planetary Geology and Geophysics Program, 1986
[NASA-TM-89810] N87-23341
Mechanical and thermal properties of planetologically important ices N87-23346
Crustal and subcrustal nodules in ejecta from Kilbourne Hole Maar, New Mexico N87-23485
The geology of Picacho Butte, a silicic volcanic dome in northwest Arizona N87-23488

GEOCHRONOLOGY
Relative ages of lava flows at Alba Patera, Mars N87-23477
Geology of the Mohon Mountain volcanic field, Yavapai and Mohave Counties, Arizona: A preliminary report N87-23486
The geology of Picacho Butte, a silicic volcanic dome in northwest Arizona N87-23488
Impact crater scaling laws N87-23496
The surface age of Venus: Applying the terrestrial cratering rate N87-23501
Revision of the Martian relative age chronology N87-23504
Early changes in gradation styles and rates on Mars N87-23505
Cratering and obliteration history of the south polar region of Mars N87-23506
Thermal inertia characteristics of the Martian crater Curie N87-23509
Dome craters on Ganymede N87-23510
Comments on the tectonism of Venus N87-23515
Timing of ancient extensional tectonic features on Mars N87-23526
Stress history of the Tharsis Region, Mars N87-23527
History and morphology of faulting in the Noctis Labyrinthus-Claritas Fossae Region of Mars N87-23528
Age of fracturing and mesa development in the Elysium Area, northern Martian plains N87-23532
Geometry and relative age of large patterned fractures in southern Acidalia Planitia, Mars N87-23533

GEODESY
Reports of Planetary Geology and Geophysics Program, 1986
[NASA-TM-89810] N87-23341

GEODETIC SURVEYS
Altimeter measurements for the determination of the Earth's gravity field
[NASA-CR-180520] N87-23033

GEOIDS
Altimeter measurements for the determination of the Earth's gravity field
[NASA-CR-180520] N87-23033
The delineation and interpretation of the Earth's gravity field
[NASA-CR-181015] N87-23065

GEOLOGICAL FAULTS
Bilateral symmetry across Aphrodite Terra N87-23518
A test of the hypothesis that impact-induced fractures are preferred sites for later tectonic activity N87-23520
Implications of Viking color data for evolution of the Amenthes Region, Mars N87-23525
History and morphology of faulting in the Noctis Labyrinthus-Claritas Fossae Region of Mars N87-23528

GEOLOGICAL SURVEYS
Curvilinear ridges and related features in southwest Cydonia Mensae, Mars N87-23537
Geology of Io N87-23542
The Galilean satellite geological mapping program, 1986 N87-23544

GEOMAGNETISM
The origin of polarity asymmetries in the history of the geomagnetic field N87-23401
The steady state toroidal magnetic field at the core-mantle boundary N87-23404

GEOMETRICAL OPTICS
Fundamentals and techniques of nonimaging optics research at the University of Chicago
[DE87-006917] N87-23264

GEOMETRY
Conservative zonal schemes for patched grids in 2 and 3 dimensions
[NASA-TM-88326] N87-22932
Description of an aeronautical geometry conversion package: Wave-drag to Langley Wireframe Geometry Standard (LaWGS) to Supersonic Implicit Marching Potential (SIMP)
[NASA-CR-178299] N87-23194
Asteroid lightcurve inversion N87-23377
Geometry and relative age of large patterned fractures in southern Acidalia Planitia, Mars N87-23533
Cartography of irregularly shaped satellites N87-23545

GEOMORPHOLOGY
Preliminary results of geologic and remote sensing studies of Rima Mozart N87-23431
Mars: Morphology of Southern Hemisphere intracrater dunefields N87-23452
Volatile reservoirs below the surface of the Elysium region of Mars: Geomorphic evidence N87-23467
Evidence for glaciation in Elysium N87-23468
Geomorphic evidence for ancient seas in west Deuteronilus Mensae, Mars-1: Regional geomorphology N87-23471
Geomorphic evidence for ancient seas in west Deuteronilus Mensae, Mars-2: From very high resolution Viking Orbiter images N87-23472
Explosive volcanic deposits on Mars: Preliminary investigations N87-23473
Eruptive history of the Elysium Volcanic Province of Mars N87-23475
Relative ages of lava flows at Alba Patera, Mars N87-23477
Crustal and subcrustal nodules in ejecta from Kilbourne Hole Maar, New Mexico N87-23485
The geology of Pine and Crater Buttes: Two basaltic constructs on the far eastern Snake River Plain N87-23487
Cratering and obliteration history of the south polar region of Mars N87-23506
Martian rampart craters: Morphologic clues for the physical state of the target at time of impact N87-23507
Crater ejecta morphology and the presence of water on Mars N87-23508
Dome craters on Ganymede N87-23510
Ejecta types on Ganymede and Callisto N87-23512
Shatter cones in Illinois: Evidence for metoeritic impacts at Glasford and Des Plaines N87-23513
Search for, and study of, paleozoic impact ejecta: Progress made during the past year N87-23514
Physiographic constraints on the origin of lunar wrinkle ridges N87-23521

GEOPHYSICS
Reports of Planetary Geology and Geophysics Program, 1986
[NASA-TM-89810] N87-23341

GERMANIUM
Structure and properties of novel compounds of silicon germanium and tin
[AD-A179433] N87-23291

GETTERS
Extrinsic gettering for VLSI/ULSI processes
[DE87-002696] N87-22903

GIMBALS
Effect of Gimbal friction modeling technique on control stability and performance for Centaur upper-stage
[NASA-TM-89894] N87-22755

GLACIOLOGY
Evidence for glaciation in Elysium N87-23468

GLASS
Containerless processing of glass forming melts: D-1, MEA/A-2 experiment 81F01 conducted on STS-61A flight, October 1985
[NASA-CR-179118] N87-22861

GLASS FIBER REINFORCED PLASTICS
Thermal expansion of epoxy-fiberglass composite specimens
[DE87-004273] N87-22812

GLASS FIBERS
Infrared fiber optic materials
[NASA-CR-180604] N87-23257
Radiation hardened silica-based optical fibers
[AD-A178466] N87-23266

GLIDE PATHS
Advanced monitoring concepts N87-22614

GLOBAL ATMOSPHERIC RESEARCH PROGRAM
The development of a coupled GCM suitable for modelling studies in TOGA — general circulation model (GCM); Tropical Ocean Global Atmosphere (TOGA) N87-23055
Proceedings of the Conference on the Scientific Results of the Alpine Experiment (ALPEX), volume 2
[WMO-TD-108-VOL-2] N87-23068
Fine structure of the atmospheric boundary layer across the Alps during a high pressure period in the Alpine Experiment (ALPEX). A case study on April 22, 1982 N87-23087
On the predicability of low-level flow during ALPEX — Alpine Experiment (ALPEX) N87-23088

GLOBAL POSITIONING SYSTEM
Investigation of air transportation technology at Ohio University, 1984 N87-22609
GPS antenna designs N87-22615
Design of GPS (Global Positioning System) status reporting system
[AD-A179334] N87-22662

GLUCOSE
Effect of hypokinesia on intensity of gluconeogenesis in cortical layer of rat kidney N87-23129

GOLD
Electrochemical adjustment of thin film Ti-Pd resistors
[DE87-007392] N87-22837
Correlations between electrical contact resistance and stages of wear in 700 Torr helium for precious metal electrical contacts
[DE87-003499] N87-22981

GONIOMETERS
Bidirectional reflectance properties of planetary surface materials N87-23426

GOODNESS OF FIT
Goodness-of-fit based on integrated squared discrepancies between sample and population characteristic functions
[AD-A178763] N87-23218
Goodness of fit based on integrated squared errors in characteristic functions or densities
[AD-A179027] N87-23225
A modified goodness-of-fit test for the lognormal distribution with unknown scale and location parameters
[AD-A179049] N87-23226
A test of goodness of fit for multivariate normality
[AD-A178543] N87-23237

GOVERNMENT/INDUSTRY RELATIONS
Cooperative research opportunities at NBS (National Bureau of Standards)
[PB87-157236] N87-23309
The Galilean satellite geological mapping program, 1986 N87-23544

GRAIN BOUNDARIES
Experimental and theoretical studies of the structure of grain boundaries
[DE87-007560] N87-22838

GRAMMARS
A development system for augmented transition network grammars and a large grammar for technical prose
[AD-A179009] N87-23188

GRANULAR MATERIALS
Impacts of hemispherical granular targets: Implications for global impacts N87-23490

GRAPHIC ARTS
A graphics environment supporting the rapid prototyping of pictorial cockpit displays
[AD-A178636] N87-23182
A Bayesian statistics year at the Ohio State University
[AD-A178762] N87-23242

GRAPHITE
Characterization of hybridized conductive composites
[AD-A179689] N87-22810

GRASHOF NUMBER
Numerical calculation of the drag force induced by natural convection of spheres at low Grashof numbers
[DE87-006791] N87-22935

GRAVITATION
F-16 control stick response during +G sub z-induced loss of consciousness
[AD-A178474] N87-23116

GRAVITATION THEORY
Perturbative and global anomalies in supergravity theories
[DE87-701562] N87-23059

GRAVITATIONAL CONSTANT
Possible inflationary solution to the short distance gravity model
[DE87-701559] N87-23339

GRAVITATIONAL EFFECTS
Verification of large beam-type space structures N87-22712
Cortical ultrastructure of rat cerebellar nodulus following flight aboard Cosmos-1514 biosatellite N87-23130
Why no orbital resonances among the satellites of Uranus? N87-23351
Kinematics and dynamics of the Uranian rings N87-23353
Shapes of small satellites N87-23354
Protostellar disks and the primitive solar nebula N87-23379
Analysis of planetary evolution with emphasis on differentiation and dynamics N87-23382

Orbital resonances, unusual configurations and exotic rotation states among planetary satellites N87-23391
Dynamics of satellites, asteroids, and rings N87-23392
Experimental evidence for non-proportional growth of large craters N87-23497
Impact and cratering processes on asteroids, satellites, and planets N87-23499
Comments on the tectonism of Venus N87-23515

GRAVITATIONAL FIELDS
Optimal shuttle altitude changes using tethers [AD-A179205] N87-22756
Altimeter measurements for the determination of the Earth's gravity field [NASA-CR-180520] N87-23033

GRAVITATIONAL PHYSIOLOGY
Scientific goals of the German Spacelab Mission D1 [ETN-87-99669] N87-22695

GRAVITY ANOMALIES
Perturbative and global anomalies in supergravity theories [DE87-701562] N87-23059
Gravity data analysis N87-23400

GREENHOUSE EFFECT
The case for a wet, warm climate on early Mars N87-23410
The role of regolith adsorption in the transition from early to late Mars climate N87-23411
CO2: Adsorption on palagonite and the Martian regolith N87-23419

GREENLAND
An evaluation of the polar ice prediction system [AD-A178522] N87-23014

GROOVES
Local-scale stratigraphy of grooved terrain on Ganymede N87-23538

GROOVING
Stratigraphy of the south polar region of Ganymede N87-23539

GROUND HANDLING
Accelerations experienced by packaged materiel during fork lift truck handling [RDI-284/45/3] N87-22989

GROUND TESTS
Status of the Mast experiment N87-22703
Verification of flexible structures by ground test N87-22713
Applications and requirements for real-time simulators in ground-test facilities [NASA-TP-2672] N87-23202

GROUND WATER
Groundwater sapping channels: Summary of effects of experiments with varied stratigraphy N87-23461
Valley development on Hawaiian volcanoes N87-23463
Water and ice on Mars: Evidence from Valles Marineris N87-23469

GROUND WIND
Validation of a surface-layer windflow model using climatology and meteorological tower data from Vandenberg AFB, California [AD-A178480] N87-23097

GROUP DYNAMICS
Cockpit Resource Management Training [NASA-CP-2455] N87-22634
Group-level issues in the design and training of cockpit crews N87-22636
The development and implementation of cockpit resource management in UAL recurrent training N87-22638
Cockpit resource management training at People Express N87-22639
Cockpit management and Specific Behavioral Objectives (SBOs) N87-22640
Dyads and triads at 35,000 feet: Factors affecting group process and aircrew performance N87-22656
Aircrew cooperation in the Royal Air Force N87-22657
Cockpit resource management at USAir N87-22659

GROUP THEORY
Angular momentum theory applied to interactions in solids [AD-A179366] N87-23289

GROWTH
Atomistic simulation of stability properties and growth of strained layer structures [DE87-006712] N87-23297

GYROSCOPES
CONMILIT (selected articles) [AD-A179155] N87-22661

H

HALLEY'S COMET
Temperatures and minimum thickness of the inactive surface layer of comet Halley N87-23365
Comet thermal modeling N87-23366

HAMILTON-JACOBI EQUATION
Generalized quantal equation of motion [DE87-701531] N87-23307

HAMILTONIAN FUNCTIONS
Hamiltonian theory of nonlinear waves in planetary rings N87-23393

HANDBOOKS
Human factors engineering data management handbook [AD-A179691] N87-23144

HARDENING (SYSTEMS)
A new LIHE (Light Initiated High Explosive) test capability for spherical targets [DE87-003035] N87-23245

HARDNESS
Characterizing the hardness and modulus of thin films using a mechanical properties microprobe [DE87-006612] N87-22826

HARMONICS
Operation of the induced resonance electron cyclotron maser at higher harmonics [AD-A179428] N87-22962
Non-Markovian line shapes of physisorbed atoms on a crystal [AD-A179525] N87-23292
Lunar science from lunar laser ranging N87-23389

HARRIER AIRCRAFT
Propulsion system technologies for thrust vectoring N87-22670

HAWAII
Valley development on Hawaiian volcanoes N87-23463
Non-equilibrium freezing of water-ice in sandy basaltic regoliths and implications for fluidized debris flows on Mars N87-23466

HAZE
New methods for obtaining scattering and absorption from tropospheric visible spectrum data [AD-A178590] N87-23062

HEAD DOWN TILT
Some parameters of human lipid metabolism during antiorthostatic hypokinesia and their correction N87-23127
Split circadian rhythm of simian body temperature during antiorthostatic hypokinesia N87-23128
Biochemical aspects of some neurohumoral system functions during long-term antiorthostatic hypokinesia N87-23142

HEAT
Ceramic Technology Newsletter No. 13, October - December 1986: Ceramic technology for advanced heat engines project [DE87-006447] N87-22852
Thermoelectric conversion with ion conductors [AD-A179353] N87-23019

HEAT EXCHANGERS
High heat transfer oxidizer heat exchanger design and analysis — RL10-2B engine [NASA-CR-179596] N87-22803

HEAT FLUX
Heat flux calibration facility capable of SSME conditions N87-22774
Numerical study of the effects of boundary conditions on the measurement and calibration of gardon type heat flux sensors N87-22775
Air-sea interaction over the Mediterranean Sea during the Alpine Experiment (ALPEX) Special Observing Period N87-23073

HEAT OF VAPORIZATION
Pumped two-phase heat transfer loop [NASA-CASE-MSC-20841-1] N87-22950

HEAT PIPES
Heat transfer in an organic heat pipe [LA-10781-MS] N87-22946

HEAT RESISTANT ALLOYS
Progress on thin-film sensors for space propulsion technology N87-22772
Deformation and fatigue behavior of SSME turbopump blade materials N87-22776
Fatigue damage interaction behavior of PWA 1480 N87-22777
Structural analysis demonstration of constitutive and life models N87-22780
Mechanical properties of high gradient and hot isostatically pressed PWA 1480 N87-22781
Effect of hydrogen on deformation structure and properties of CMSX-2 nickel-base single-crystal superalloy N87-22782
Fiber reinforced superalloys [NASA-TM-89865] N87-22811

HEAT STORAGE
Impact of thermal energy storage properties on solar dynamic space power conversion system mass [NASA-TM-89909] N87-22802

HEAT TRANSFER
Progress in the prediction of unsteady heat transfwe on turbines blades N87-22769
Experimental and theoretical studies of time-averaged and time resolved rotor heat transfer N87-22770
Nonlinear heat transfer and structural analyses of SSME turbine blades N87-22779
Development of an integrated BEM (Boundary Element Mesh) for hot fluid-structure interaction N87-22799
High heat transfer oxidizer heat exchanger design and analysis — RL10-2B engine [NASA-CR-179596] N87-22803
Equipment for turbulent heat transfer test apparatus [AD-A179612] N87-22930
Numerical simulation of the decay of swirling flow in a constant volume engine simulator [LA-10728-MS] N87-22945
Pumped two-phase heat transfer loop [NASA-CASE-MSC-20841-1] N87-22950
Evaluation of spherical ceramic particles for solar thermal transfer media [DE87-007432] N87-23026
The delineation and interpretation of the Earth's gravity field [NASA-CR-181015] N87-23065

HEAT TRANSFER COEFFICIENTS
Heat transfer effects of longitudinal vortices embedded in a turbulent boundary layer [DE87-006002] N87-22934
Heat transfer in an organic heat pipe [LA-10781-MS] N87-22946

HEAT TRANSMISSION
Comet thermal modeling N87-23366

HEAT TREATMENT
Mechanical properties of high gradient and hot isostatically pressed PWA 1480 N87-22781

HEATING
Could Ariel have been heated by tidal friction? N87-23347
On the lack of commensurabilities in the mean motions of the satellites of Uranus and the resurfacing of Ariel N87-23349
Accretional heating of the satellites of Saturn and Uranus N87-23355
Investigations of the surfaces and interiors of outer planet satellites N87-23356

HELICAL ANTENNAS
GPS antenna designs N87-22615

HELICOPTER DESIGN
Digital control of highly augmented combat rotorcraft [NASA-TM-88346] N87-22691

HELICOPTER ENGINES
Erosion study of AM355 and Al2O3 ceramics [AD-A178882] N87-22858

HELICOPTER PERFORMANCE
The 2GCHAS: A high productivity software development environment N87-23162

HELICOPTERS
Electromagnetic interference (EMI) fault prevention and self recovery of digital flight control systems — helicopters [MBB-UD-483/86] N87-22686
Helicopter transmission testing at NASA Lewis Research Center [NASA-TM-89912] N87-22978
Acoustic testing of simplified cabin box, phase 1 — helicopter cabin [RP-698] N87-23248

HELIOSTATS
Evaluation of a heliostat tracker for linear Fresnel lens photovoltaic concentrators [DE87-006331] N87-23025

HELMETS
Effect of the neutral density helmet visor on the visual acuity of navy fighter pilots [AD-A178486] N87-23147

HEMISPHERES
Reynolds number effects on surface shear stress patterns around isolated hemispheres N87-23459

HEMOSTATICS
Investigation of hemostasis system in air traffic controllers as related to different air traffic conditions N87-23123

HETEROGENEITY
Signatures from in-situ light scattering of non-homogeneous non-spherical particles [AD-A178761] N87-23269

HEURISTIC METHODS
Automatic scene analysis using hierarchical spatial frequency domain correlation with energy normalization and heuristic noise reduction
[AD-A178589] N87-23181
HIERARCHIES
Custom-made pyramids
[AD-A178955] N87-23186
HIGH ALTITUDE
High altitude turbulence for supersonic cruise vehicles
[NASA-TM-88285] N87-23100
HIGH ENERGY ELECTRONS
Investigations of the polar rain: Polar cap electron precipitation
[AD-A178876] N87-23099
HIGH ENERGY PROPELLANTS
An evaluation of metallized propellants based on vehicle performance
[NASA-TM-100104] N87-22806
HIGH FREQUENCIES
Preliminary investigation of ionospheric modification using oblique incidence high power HF radio waves
[AD-A179174] N87-23056
SIS (Superconductor-Insulator-Superconductor) mixer research
[AD-A179604] N87-23293
HIGH GAIN
Preliminary investigation of ionospheric modification using oblique incidence high power HF radio waves
[AD-A179174] N87-23056
HIGH LEVEL LANGUAGES
An implementation of a language analyzer for the very high speed integrated circuit hardware description language
[AD-A178648] N87-22913
The design of a real time operating system for a fault tolerant microcomputer
[AD-A178577] N87-23155
Programming languages for knowledge-based systems
[PB87-157228] N87-23170
OMNITAB 80: An interpretive system for statistical and numerical data anlysis
[PB87-172235] N87-23171
Optical symbolic processor for expert system execution
[AD-A179375] N87-23172
A graphics environment supporting the rapid prototyping of pictorial cockpit displays
[AD-A178636] N87-23182
Development of an image analysis program for the IBM PC/XT/AT
[AD-A178644] N87-23183
HIGH PASS FILTERS
Design of generalised Chebyshev suspended substrate stripline filters
[AD-A178505] N87-22910
HIGH POLYMERS
High performance polymers: Matrix resins, high strength polyquinoxalines and conducting polyaromatics
[AD-A178457] N87-22854
HIGH POWER LASERS
Pulsed power for high power electron-beam pumped lasers
[DE87-004523] N87-22965
A multiple model adaptive tracking algorithm for a high energy laser weapon system
[AD-A178978] N87-22974
HIGH PRESSURE
Studies and analyses of the space shuttle main engine: High-pressure oxidizer turbopump failure information propagation model
[NASA-CR-179079] N87-22765
Investigation of the transverse-discharge copper-vapor laser
[AD-A178833] N87-22972
Fine structure of the atmospheric boundary layer across the Alps during a high pressure period in the Alpine Experiment (ALPEX). A case study on April 22, 1982
N87-23087
High pressure cosmochemistry of major planetary interiors: Laboratory studies of the water-rich region of the system ammonia-water N87-23396
Melting of troilite at high pressure in a diamond cell by laser heating N87-23398
Properties of planetary fluids at high pressure and temperature N87-23399
Creep of ice: Further studies N87-23540
HIGH RESOLUTION
Measurement of high resolution wind profiles with a minisodar
[DE87-007001] N87-23096
New very high resolution radar studies of the Moon
N87-23441
High resolution radar map of the Moon N87-23442
High resolution thermal infrared mapping of Martian channels N87-23451

Solar active region physical parameters inferred from a thermal cyclotron line and soft X-ray spectral lines
[AD-A179650] N87-23560
HIGH SPEED
An implementation of a language analyzer for the very high speed integrated circuit hardware description language
[AD-A178648] N87-22913
Prediction of high-speed rotor noise with a Kirchhoff formula
[AD-A178982] N87-23250
HIGH STRENGTH
High performance polymers: Matrix resins, high strength polyquinoxalines and conducting polyaromatics
[AD-A178457] N87-22854
HIGH STRENGTH STEELS
Dynamic fracture of high strength steel
[AD-A178862] N87-22844
HIGH TEMPERATURE
Low-pressure self-propagating high-temperature synthesis
[AD-A178593] N87-22856
A high-temperature quadrupole mass spectrometer for studying vaporization from materials heated by a CO2 laser
[LA-10744] N87-22975
On 3-D inelastic analysis methods for hot section components. Volume 1: Special finite element models
[NASA-CR-179494] N87-22996
Thermoelectric conversion with ion conductors
[AD-A179353] N87-23019
Properties of planetary fluids at high pressure and temperature N87-23399
HIGH TEMPERATURE ENVIRONMENTS
An assesement of nitrogen oxide formation in preheated high-temperature combustion air in industrial processes
[EGG-2439] N87-23031
HIGH TEMPERATURE GASES
Investigation of the transverse-discharge copper-vapor laser
[AD-A178833] N87-22972
HIGH TEMPERATURE PLASMAS
Numerical study of hybrid plume
[AD-A179561] N87-23275
Confinement and heating of high beta plasmas with emphasis on compact toroids. Task 2: Stellarator and heliac research
[DE87-005554] N87-23278
HIGHLANDS
Bilateral symmetry across Aphrodite Terra
N87-23518
Characteristic structures of the highland boundary on Mars: Evidence against a single mega-impact event?
N87-23523
HIMALAYAS
Valley circulations as measured in the Himalaya by instrumented motor glider N87-23077
HISTAMINES
Nutritional correction of histamine and serotonin levels as related to exposure to hypokinesia and neuro-emotional stress N87-23126
HISTORIES
Toward the year 2000: The near future of the American civilian and military space programs
[DE87-006467] N87-22697
HOLES (ELECTRON DEFICIENCIES)
Nonlinear optical properties and subpicosecond dynamics of excitons and electron-hole plasmas in multiple quantum well structures
[AD-A179124] N87-23287
Orbital removal method for the neutral vacancy in semiconductors
[DE87-701537] N87-23300
HOLOGRAPHIC INTERFEROMETRY
Preliminary investigation of the use of holographic interferometry to detect ill-fitting compressor blades
[AD-A178519] N87-22682
Effects of cutout orientations on natural frequencies and mode shapes of curved rectangular composite panels
[AD-A178638] N87-22813
Real-time laser holographic interferometry for aerodynamics
[NASA-TM-89462] N87-22956
HOLOGRAPHY
Development of a holographic beamsplitter for use with a conventional Fresnel lens
[DE87-006770] N87-23263
Applications of fiber optics in experimental mechanics
[AD-A178683] N87-23268
HOMEOSTASIS
Effect of hypokinesia on intensity of gluconeogenesis in cortical layer of rat kidney N87-23129
HORMONE METABOLISMS
USSR Report: Space Biology and Aerospace Medicine, Volume 20, No. 5, September - October 1986
[JPRS-USB-86-007] N87-23120

Effect of short-term spaceflights on activity of renin-angiotension-aldosterone system, concentration of cyclic nucleotides and prostaglandins in blood
N87-23125
Nutritional correction of histamine and serotonin levels as related to exposure to hypokinesia and neuro-emotional stress N87-23126
Hormonal and metabolic status of man in the extreme north N87-23139
HOT PRESSING
Mechanical properties of high gradient and hot isostatically pressed PWA 1480 N87-22781
Low-pressure self-propagating high-temperature synthesis
[AD-A178593] N87-22856
HOT SURFACES
On 3-D inelastic analysis methods for hot section components. Volume 1: Special finite element models
[NASA-CR-179494] N87-22996
HOVERING
Results of the integration of a transonic full-potential analysis program with a free-wake lifting-line program for hovering rotors
[NASA-TM-89494] N87-22631
HUBBLE SPACE TELESCOPE
Workshop on Structural Dynamics and Control Interaction of Flexible Structures N87-22728
A TREETOPS simulation of the Hubble Space Telescope-High Gain Antenna interaction N87-22735
HUMAN BEHAVIOR
Group-level issues in the design and training of cockpit crews N87-22636
Cockpit management and Specific Behavioral Objectives (SBOs) N87-22640
Optimum culture in the cockpit N87-22643
Cockpit Resource Management (CRM) and human factors training: What Air New Zealand is doing about it
N87-22658
HUMAN BEINGS
The perception of brightness and colour: Neurophysiology, psychophysics and computation
[AD-A179217] N87-23107
Selection of dimensions for an anthropometric data base. Volume 1: Rationale, summary, and conclusions
[AD-A179586] N87-23112
F-16 control stick response during +G sub z-induced loss of consciousness
[AD-A178474] N87-23116
Proceedings of the 22nd Annual Conference on Manual Control
[AD-A178627] N87-23148
HUMAN BODY
Identification and validation of new anthropometric techniques for quantifying body composition
[AD-A178753] N87-23118
HUMAN FACTORS ENGINEERING
Dyads and triads at 35,000 feet: Factors affecting group process and aircrew performance N87-22656
Cockpit Resource Management (CRM) and human factors training: What Air New Zealand is doing about it
N87-22658
Human factors engineering data management handbook
[AD-A179691] N87-23144
HUMAN FACTORS LABORATORIES
Air Force technical objectives document, fiscal year 1988
[AD-A179163] N87-23569
HUMAN PERFORMANCE
Theory underlying CRM training: Psychological issues in flight crew performance and crew coordination
N87-22635
Investigation of hemostasis system in air traffic controllers as related to different air traffic conditions
N87-23123
Aircrew task surveys: Selection criteria for low-cost training technology applications
[AD-A178473] N87-23146
Air Force technical objectives document, fiscal year 1988
[AD-A179163] N87-23569
HUMAN REACTIONS
Hormonal and metabolic status of man in the extreme north N87-23139
Human blood serum proteolytic enzyme activity after stay in hypoxic environment N87-23140
HUMAN RELATIONS
Theory underlying CRM training: Psychological issues in flight crew performance and crew coordination
N87-22635
Aircrew cooperation in the Royal Air Force
N87-22657

HUMAN RESOURCES
The event related brain potential as an index of information processing and cognitive activity: A program of basic research [AD-A179310] N87-23143
HUMAN TOLERANCES
USSR Report: Space Biology and Aerospace Medicine, Volume 20, No. 5, September - October 1986 [JPRS-USB-86-007] N87-23120
Tolerance to frustration as a factor in operator performance N87-23124
HUMIDITY
The effect of the Tatra Mountains (Poland) on the atmospheric precipitation and air humidity during the northern and southern air flow N87-23094
HUMIDITY MEASUREMENT
Water-absorbing capacitor system for measuring relative humidity [NASA-CASE-NPO-16544-1-CU] N87-22953
HYBRID PROFULSION
Numerical study of hybrid plume [AD-A179561] N87-23275
HYDRAULIC EQUIPMENT
Integrated design of structures N87-22669
Hybrid composite response to hydraulic ram [AD-A178750] N87-22815
HYDROCARBONS
Measurements of the dielectric constants for planetary volatiles N87-23447
HYDRODYNAMICS
A Godunov method for Lagrangian hydrodynamics in 1D [DE87-005204] N87-22933
Lagrangian-like equations of hydrodynamics with mass diffusion [DE87-007522] N87-22936
The potential gradient of a plane source [AD-A178976] N87-23223
Direct-drive laser-fusion in the US [DE87-005916] N87-23279
HYDROGEN
Effect of hydrogen on deformation structure and properties of CMSX-2 nickel-base single-crystal superalloy N87-22782
Low power DC arcjet operation with hydrogen/nitrogen/ammonia mixtures [NASA-TM-89876] N87-22804
Corrosion, wear and mechanical properties of pulse-electrodeposited alloys [AD-A178596] N87-22842
Development of nickel oxide/hydrogen multilayer bipolar battery for pulsed power [AD-A178844] N87-22917
Radiation hardened silica-based optical fibers [AD-A178466] N87-23266
HYDROGEN COMPOUNDS
Infrared spectroscopy using laser and Fourier techniques of the unstable molecules SiH and NH. Determination of the molecular constants of the fundamental electronic state 3 sigma (-) of NH [ETN-87-99552] N87-22818
HYDROGEN EMBRITTLEMENT
Hydrogen and temper embrittlement interactions in fatigue of 2 1/4Cr1Mo steel [AERE-R-12322] N87-22830
HYDROGEN IONS
Frequency shift measurements of the Q(1) and Q(2) lines of H2 using high resolution CW Coherent Anti-Stokes Raman Spectroscopy [AD-A179390] N87-22820
Angular momentum theory applied to interactions in solids [AD-A179366] N87-23289
HYDROGEN SULFIDE
Investigation of causes of hydrogen sulfide formation in reclaimed water N87-23136
HYDROGRAPHY
Optical dynamics experiment (ODEX) data report R/V acania expedition 10 October-17 November 1982. Volume 2: Particle size distributions. Volume 6: Scalar spectral-radiometer data [AD-A178535] N87-23104
HYDROLYSIS
A microcrystalline growth study of solvent effects in alkoxides by dynamic laser light scattering [DE87-005710] N87-23294
HYDROPONICS
Distinctions in formation of microbial complex in nutrient solutions of higher plants after use of straw mineralization products N87-23138
HYPERION
Orbital resonances, unusual configurations and exotic rotation states among planetary satellites N87-23391
HYPERSONIC FLOW
Computational aerothermodynamics [NASA-TM-89450] N87-22943
HYPERVELOCITY GUNS
Superconducting Augmented Rail Gun (SARG) [AD-A179269] N87-22701
High energy high rate pulsed power processing of materials by powder consolidation and by railgun deposition [AD-A179289] N87-22867
HYPERVELOCITY IMPACT
Experimental evidence for non-proportional growth of large craters N87-23497
HYPOKINESIA
Nutritional correction of histamine and serotonin levels as related to exposure to hypokinesia and neuro-emotional stress N87-23126
Some parameters of human lipid metabolism during antiorthostatic hypokinesia and their correction N87-23127
Split circadian rhythm of simian body temperature during antiorthostatic hypokinesia N87-23128
Effect of hypokinesia on intensity of gluconeogenesis in cortical layer of rat kidney N87-23129
Biochemical aspects of some neurohumoral system functions during long-term antiorthostatic hypokinesia N87-23142
HYPOXIA
Evaluation of effect of positive intrapulmonary pressure on respiratory function of man N87-23134
Human blood serum proteolytic enzyme activity after stay in hypoxic environment N87-23140

I

ICE
Mechanical and thermal properties of planetologically important ices N87-23346
Failure strength of icy lithospheres N87-23357
Studies of outer planet satellites, Mercury and Uranus N87-23358
Experimental studies on the impact properties of water ice N87-23364
Temperatures and minimum thickness of the inactive surface layer of comet Halley N87-23365
The loss and depth of CO2 ice in comet nuclei N87-23367
Studies of the scattering/absorption of minerals N87-23423
Non-equilibrium freezing of water-ice in sandy basaltic regoliths and implications for fluidized debris flows on Mars N87-23466
Water and ice on Mars: Evidence from Valles Marineris N87-23469
ICE ENVIRONMENTS
An evaluation of the polar ice prediction system [AD-A178522] N87-23014
Creep of ice: Further studies N87-23540
ICE FORMATION
Investigation of air transportation technology at Massachusetts Institute of Technology, 1984 N87-22605
Measurement of ice accretion using ultrasonic pulse echo techniques N87-22608
An evaluaiion of the polar ice prediction system [AD-A178522] N87-23014
ICE REPORTING
An evaluation of the polar ice prediction system [AD-A178522] N87-23014
ICY SATELLITES
Charged particle modification of surfaces in the outer solar system N87-23435
Creep of ice: Further studies N87-23540
IDENTIFYING
Investigate and verify the validity of mathematical formulas and procedures in relation to data obtained from theoretical investigations and experimental observations [AD-A179564] N87-23057
IGNEOUS ROCKS
Gossans on Mars: Spectral features attributed to jarosite N87-23417
IMAGE ANALYSIS
A design for a new catalog manager and associated file management for the Land Analysis System (LAS) N87-23159
SOT: A rapid prototype using TAE windows N87-23161
Potential medical applications of TAE N87-23166
Development of Land Analysis System display modules N87-23169
Development of an image analysis program for the IBM PC/XT/AT [AD-A178644] N87-23183
IMAGE ENHANCEMENT
Image size and resolution in face recognition N87-23113
IMAGE FILTERS
Multidimensional filtering investigations [AD-A178745] N87-22915
White-light optical information processing and holography [AD-A179489] N87-23260
IMAGE PROCESSING
Advanced monitoring concepts N87-22614
Vibration analysis using shadow speckle metrology and line broadening techniques [AD-A178626] N87-23003
The integration of spectral and spatial analysis for land use classification [AD-A178703] N87-23015
Computer vision research and its applications to automated cartography [AD-A178815] N87-23017
The perception of brightness and colour: Neurophysiology, psychophysics and computation [AD-A179217] N87-23107
Image size and resolution in face recognition N87-23113
Image processing for vision: An equipment requests to DOD [AD-A179261] N87-23150
The use of real-time optical processors in embedded computing [DE87-006895] N87-23153
Optical acquisition, image and data compression [AD-A178506] N87-23154
Sixth Annual Users' Conference — Transportable Applications Executive (TAE) [NASA-CP-2463] N87-23156
A design for a new catalog manager and associated file management for the Land Analysis System (LAS) N87-23159
NASA Regional Planetary Image Facility image retrieval and processing system N87-23160
Display management subsystem, version 1: A user's eye view N87-23164
Rationalizing VICAR within a TAE framework: Some problems and some solutions N87-23165
Potential medical applications of TAE N87-23166
Naval applications of a TAE-derived executive N87-23167
An overview of the Land Analysis System (LAS) N87-23168
Development of an image analysis program for the IBM PC/XT/AT [AD-A178644] N87-23183
Custom-made pyramids [AD-A178955] N87-23186
The scale-space formulation of pyramid data structures [AD-A178960] N87-23222
Planetary ring dynamics and morphology N87-23394
Spectral mixture modeling: Further analysis of rock and soil types at the Viking Lander sites N87-23415
A compilation system for Venus radar mission (Magellan) N87-23440
IMAGE RECONSTRUCTION
Stationary phase approximations in Fresnel-zone magnitude-only reconstructions [AD-A178812] N87-23270
IMAGE RESOLUTION
Image size and resolution in face recognition N87-23113
Custom-made pyramids [AD-A178955] N87-23186
New very high resolution radar studies of the Moon N87-23441
High resolution radar map of the Moon N87-23442
Landform identification: Lunar radar images N87-23443
IMAGERY
Real-time laser holographic interferometry for aerodynamics [NASA-TM-89462] N87-22958
IMAGES
Automatic pattern recognition and related topics [AD-A178595] N87-23267
Simultaneous SMM flat crystal spectrometer and very large array observations of solar active regions [AD-A179698] N87-23562
IMAGING TECHNIQUES
Strategies for high-resolution 3-D millimeter wave imaging [AD-A178653] N87-22882
Aspects of Voyager photogrammetry N87-23547
IMINES
Structure and properties of novel compounds of silicon germanium and tin [AD-A179433] N87-23291

IMPACT
The cratering record at Uranus: Implications for satellite evolution and the origin of impacting objects N87-23342
Experimental studies on the impact properties of water ice N87-23364
Impacts of hemispherical granular targets: Implications for global impacts N87-23490
Impact vaporization: Late time phenomena from experiments N87-23491
Oblique impact: Projectile richochet, concomitant ejecta and momentum transfer N87-23492
Centrifuge impact cratering experiments: Scaling laws for non-porous targets N87-23495
Impact crater scaling laws N87-23496
Centrifuge impact cratering experiments: Scaling laws for non-porous targets N87-23498
Crater production on Venus and Earth by asteroid and comet impact N87-23500
Martian rampart craters: Morphologic clues for the physical state of the target at time of impact N87-23507
Shatter cones in Illinois: Evidence for meteoritic impacts at Glasford and Des Plaines N87-23513
Search for, and study of, paleozoic impact ejecta: Progress made during the past year N87-23514

IMPACT DAMAGE
Computer simulations of 10-km-diameter asteroid impacts into oceanic and continental sites: Preliminary results on atmospheric passage, cratering and ejecta dynamics N87-23489
A test of the hypothesis that impact-induced fractures are preferred sites for later tectonic activity N87-23520
Characteristic structures of the highland boundary on Mars: Evidence against a single mega-impact event? N87-23523

IMPACT LOADS
Hybrid composite response to hydraulic ram [AD-A178750] N87-22815
A fast, low resistance switch for small slapper detonators [AD-A178562] N87-22911
Accelerations experienced by packaged materiel during fork lift truck handling [RDI-284/45/3] N87-22989
Experimental studies of collision and fragmentation phenomena N87-23494

IMPACT STRENGTH
Momentum transfer from oblique impacts N87-23493
Impact and cratering processes on asteroids, satellites, and planets N87-23499

IMPACT TESTS
DYNA3D: A computer code for crashworthiness engineering [DE87-003818] N87-22998
Dynamic fracture under plane wave loading [AD-A178594] N87-23001
Aeolian abrasion on Venus: Preliminary results from the Venus simulator N87-23458

IMPACTORS
Experimental evidence for non-proportional growth of large craters N87-23497

IMPEDANCE
Joint services electronics program [AD-A178599] N87-22879
Magnetically insulated opening switch research [AD-A178895] N87-22918

IMPLANTATION
Modeling of substrate and implantation effects on the threshold voltage of MESFET structures fabricated in semi-insulating GaAs [AD-A178550] N87-23303

IMPROVEMENT
The assessment and evaluation of combat performance improvements N87-22675

IMPURITIES
Thermal shock resistance of mullite-based SiC-whisker composites [AD-A179214] N87-22809
Microscopic study of the influence of impurities on interface bonding [AD-A178510] N87-22841
Analysis of the effects of impurity buildup on the performance of a reversed field pinch [DE87-005438] N87-23277
Angular momentum theory applied to interactions in solids [AD-A179366] N87-23289

INCIDENCE
Multiple angle of incidence measurement technique for the permittivity and permeability of lossy materials at millimeter wavelengths [AD-A178851] N87-22885

INCOHERENT SCATTERING
Automatic pattern recognition and related topics [AD-A178595] N87-23267

INCONEL (TRADEMARK)
Circumferential hot wire TIG cladding of carbon-manganese steel with inconel 625 and gun-metal with a tin bronze [ARE-TM(UMD)-85574] N87-22831

INDEXES (DOCUMENTATION)
Reading patterns in online documentation: How transcript analysis reflects text design, software constraints, and user preferences [DE87-006466] N87-23174

INDUCTION HEATING
Low-pressure self-propagating high-temperature synthesis [AD-A178593] N87-22856

INDUSTRIES
Automated non-destructive testing using an industrial robot [AERE-R-12308] N87-22986

INELASTIC STRESS
On 3-D inelastic analysis methods for hot section components. Volume 1: Special finite element models [NASA-CR-179494] N87-22996

INERTIA
Dynamic fracture of high strength steel [AD-A178862] N87-22844

INERTIAL NAVIGATION
CONMILIT (selected articles) [AD-A179155] N87-22661

INFINITY
Chandrasekhar equations for infinite dimensional systems. Part 2: Unbounded input and output case [NASA-CR-178303] N87-23208

INFORMATION
Alternative knowledge acquisition: Developing a pulse coded neural network [DE87-005192] N87-23145

INFORMATION FLOW
Alternative knowledge acquisition: Developing a pulse coded neural network [DE87-005192] N87-23145

INFORMATION SYSTEMS
Quick-look guide to the crustal dynamics project's data information system [NASA-TM-87818] N87-23018
Sixth Annual Users' Conference — Transportable Applications Executive (TAE) [NASA-CP-2463] N87-23156
The evaluation and extension of TAE in the development of a user interface management system N87-23158
Materials Information for Science and Technology (MIST). Project overview: Phase 1 and 2 and general considerations [DE87-006799] N87-23312

INFORMATION THEORY
A statistical viewpoint on the theory of evidence, revision [AD-A178958] N87-23207
The scale-space formulation of pyramid data structures [AD-A178960] N87-23222

INFORMATION TRANSFER
Design of GPS (Global Positioning System) status reporting system [AD-A179334] N87-22662

INFRARED ABSORPTION
Infrared fiber optic materials [NASA-CR-180604] N87-23257
Thermal-infrared spectral observations of geologic materials in emission N87-23425

INFRARED DETECTORS
A multiple model adaptive tracking algorithm for a high energy laser weapon system [AD-A178978] N87-22974
Atmospheric remote sensing in arctic regions [AD-A179550] N87-23012

INFRARED IMAGERY
Regional sources and sinks of dust on Mars: Viking observations of Cerberus, Solis Planum and Syrtis Major N87-23450
High resolution thermal infrared mapping of Martian channels N87-23451

INFRARED INSTRUMENTS
Mid-infrared spectroscopic investigation N87-23424

INFRARED RADIATION
Submicron characterization of the atomic and electronic structure of defects in semiconductors [AD-A178458] N87-23301
Mid-infrared spectroscopic investigation N87-23424

INFRARED REFLECTION
Atlas of reflectance spectra of terrestrial, lunar and meteoritic powders and frosts from 92 to 1800 •lc2)nm N87-23427
Preliminary results of spectral reflectance studies of tycho crater N87-23430
Bright sand/dark dust: The identification of active sand surfaces on the Earth and Mars N87-23449

INFRARED SIGNATURES
Mid-infrared spectroscopic investigation N87-23424

INFRARED SPECTRA
On the spectral reflectance properties of materials exposed at the Viking landing sites N87-23414
Atlas of reflectance spectra of terrestrial, lunar and meteoritic powders and frosts from 92 to 1800 •lc2)nm N87-23427
Compositional information for the Moon: Some characteristics of current near-IR spectra (telescopic and laboratory) N87-23429
Preliminary results of spectral reflectance studies of tycho crater N87-23430
Compositional stratigraphy of crustal material from near-infrared spectra N87-23559

INFRARED SPECTROSCOPY
Mid-infrared spectroscopic investigation N87-23424
Thermal-infrared spectral observations of geologic materials in emission N87-23425

INITIATION
The effect on the strength of initiation on the corner effect — high explosives [MBB-UA-938/86] N87-22924

INJECTION LASERS
The use of the Karl sub-scale laser for Raman beam clean-up experiments [AD-A178463] N87-22971

INJECTION MOLDING
Effects of machine variables on the quality of injection mouldings. An interlaboratory trial, 2: High density polyethylene [MQAD-328] N87-22987

INLET NOZZLES
Propulsion system technologies for thrust vectoring N87-22670

INLET PRESSURE
A study of fluid-dynamic pressure fields on compressor reed valves [AD-A178584] N87-22938

INPUT
Chandrasekhar equations for infinite dimensional systems. Part 2: Unbounded input and output case [NASA-CR-178303] N87-23208

INPUT/OUTPUT ROUTINES
Ada style guide (version 1.1) [NASA-TM-89376] N87-23191

INSPECTION
Design of an orbital inspection satellite [AD-A179115] N87-22759
Methodology for verification of ultrasonic inspection [AD-A179694] N87-22968

INSULATION
Magnetically insulated opening switch research [AD-A178895] N87-22918
Modeling of substrate and implantation effects on the threshold voltage of MESFET structures fabricated in semi-insulating GaAs [AD-A178550] N87-23303

INTAKE SYSTEMS
Gas turbine combustor and engine augmentor tube sooting characteristics [AD-A179423] N87-22679

INTEGRALS
A separable piecewise linear upper bound for stochastic linear programs [AD-A178694] N87-23217

INTEGRATED CIRCUITS
Extrinsic gettering for VLSI/ULSI processes [DE87-002698] N87-22903
An implementation of a language analyzer for the very high speed integrated circuit hardware description language [AD-A178648] N87-22913
Formal models of hardware and their applications to VLSI design automation [AD-A178837] N87-22916
A coherent VLSI design environment [AD-A179037] N87-22920

INTERACTIVE CONTROL
Commit your works to the Lord, and your thoughts shall be established (Prov. 16:3). Inter-stable control systems N87-22716
Flexible spacecraft simulator N87-22718
Structural/control interaction (payload pointing and micro-g) N87-22721
Structural dynamics system model reduction N87-22727

INTERCONTINENTAL BALLISTIC MISSILES
Estimation of ICBM (intercontinental ballistic missile) performance parameters [AD-A179204] N87-22754

INTERFACES
Microscopic study of the influence of impurities on interface bonding [AD-A178510] N87-22841

Proceedings of the 22nd Annual Conference on Manual Control
[AD-A178627] N87-23148
Research on computer aided design for maintainability
[AD-A178460] N87-23177
INTERFEROMETERS
Applications of fiber optics in experimental mechanics
[AD-A178683] N87-23268
Thermal-infrared spectral observations of geologic materials in emission N87-23425
INTERNAL COMBUSTION ENGINES
The autoignition of isobutane in a knocking spark ignition engine
[DE87-003241] N87-22823
Numerical simulation of the decay of swirling flow in a constant volume engine simulator
[LA-10728-MS] N87-22945
INTERNAL WAVES
The SIR-B mission: Towards an understanding of internal waves in the ocean
[ARE-TR-86122] N87-23102
INTERPLANETARY DUST
Analytical electron microscopy of fine-grained phases in primitive interplanetary dust particles and carbonaceous chondrites N87-23376
INTERPLANETARY MAGNETIC FIELDS
Latitudinal motions of the aurora during substorms
[NASA-CR-180930] N87-23063
Investigations of the polar rain: Polar cap electron precipitation
[AD-A178876] N87-23099
INTERPOLATION
The potential gradient of a plane source
[AD-A178976] N87-23223
INTERPROCESSOR COMMUNICATION
JANUS/Ada software implementation of a star cluster local area network of personal computers
[AD-A178681] N87-23199
INTERSTELLAR EXTINCTION
A study of the fundamental characteristics of 2175A extinction
[NASA-CR-180926] N87-23336
INTERSTELLAR MATTER
Formation of giant molecular clouds in global spiral structures: The role of orbital dynamics and cloud-cloud collisions N87-23381
INTERVALS
Estimation of the parameters of mixtures via distance between densities or characteristic functions
[AD-A178623] N87-23241
INVARIANCE
Linear time invariant system identification using a result of the Bussgang theorem
[AD-A178642] N87-23216
INVERSIONS
Phase space methods and path integration: A microscopic approach to direct and inverse wave propagation
[AD-A178557] N87-23249
Asteroid lightcurve inversion N87-23377
INVISCID FLOW
Experimental research on compressible turbulent shear layers, viscous-inviscid interactions, and flow separation
[AD-A179579] N87-22928
Axisymmetric inviscid shock tube flow simulation
[AD-A178494] N87-22937
Numerical analysis of terminal double mach reflection
[AD-A179041] N87-22942
IO
SO2 on Io: A thermodynamic perspective N87-23359
Orbital resonances, unusual configurations and exotic rotation states among planetary satellites N87-23391
Io: Comparison of photometric scans produced by the Minnaert and Hapke functions N87-23436
Sulfur-oxygen processes on Io N87-23437
Solid sulfur in vacuum: Sublimation effects on surface microtexture, color and spectral reflectance, and applications to planetary surfaces N87-23438
Observations of industrial sulfur flows and implications for Io N87-23541
Geology of Io N87-23542
Large scale topography of Io N87-23543
ION ACOUSTIC WAVES
Formation mechanisms of laboratory double layers
N87-23314
Experimental observation of ion-acoustic double layers in laboratory plasma N87-23318
Current driven weak double layers N87-23322
Weak double layers in the auroral ionosphere
N87-23326
Particle simulation of auroral double layers
N87-23327
ION BEAMS
The generation of electrostatic noise in the plasma sheet boundary layer
[ATR-86(8433)-4] N87-23282
ION CHARGE
Novel polymeric LIT and divalent cation fast ion conducting materials
[DE87-006294] N87-23296
ION CURRENTS
Thermoelectric conversion with ion conductors
[AD-A179353] N87-23019
ION DENSITY (CONCENTRATION)
Development of a generalized model for a three component plasma
[AD-A178979] N87-23281
ION DISTRIBUTION
Fast ion mass spectrometry and charged particle spectrography investigations of transverse ion acceleration and beam-plasma interactions
[NASA-CR-168348] N87-22817
ION ENGINES
Numerical study of hybrid plume
[AD-A179561] N87-23275
ION IMPLANTATION
Temperature dependence of implantation damage in strained-layer superlattices
[DE87-007678] N87-23299
ION IRRADIATION
On the sputter alteration of regoliths of outer solar system bodies N87-23434
ION PROPULSION
Numerical study of hybrid plume
[AD-A179561] N87-23275
IONIZATION
Two-color, Doppler-free ionization of molecular hydrogen for isotopic analysis
[DE87-004975] N87-22825
Why gamma rays are different: Some notes for pedestrians
[DE87-004963] N87-22966
Collective effects in intense-field electrodynamics 1981-1986
[AD-A179490] N87-23261
IONIZATION CROSS SECTIONS
Relativistic calculations and measurements of energies, Auger rates, and lifetimes
[AD-A179137] N87-23251
IONOSPHERIC COMPOSITION
Fast ion mass spectrometry and charged particle spectrography investigations of transverse ion acceleration and beam-plasma interactions
[NASA-CR-168348] N87-22817
IONOSPHERIC DISTURBANCES
Preliminary investigation of ionospheric modification using oblique incidence high power HF radio waves
[AD-A179174] N87-23056
On the thinning of the plasma sheet during substorms
[AD-A178484] N87-23061
J. VLA (Very Large Array) of a solar noise storm
[NASA-CR-180219] N87-23561
IONOSPHERIC PROPAGATION
Preliminary investigation of ionospheric modification using oblique incidence high power HF radio waves
[AD-A179174] N87-23056
IONS
Physical properties and structure of ion-containing polymers
[AD-A178592] N87-22855
Angular momentum theory applied to interactions in solids
[AD-A179366] N87-23289
Ion phase-space vortices and their relation to small amplitude double layers N87-23320
IRON
Austempered ductile iron process development
[PB87-169843] N87-22866
Lithium-metal sulfide battery development and submodule demonstration
[DE87-004819] N87-22904
Oxidized basalts on the surface of Venus: Compositional implications of measured spectral properties
N87-23412
Hisingerite and iddingsite on Mars: Degradation of iron-rich basalts N87-23416
IRRADIATION
Radiation damage to coatings for short wave length laser mirrors
[DE87-001696] N87-22963
Dose enhancement effects in the Aerospace Corporation Co-60 irradiator
[AD-A178481] N87-23253
Radiation hardened silica-based optical fibers
[AD-A178466] N87-23266
Two-point resolution criterion for multi-aperture optical systems
[AD-A178980] N87-23271
Charged particle modification of surfaces in the outer solar system N87-23435
Sulfur-oxygen processes on Io N87-23437
IRREGULARITIES
Cartography of irregularly shaped satellites
N87-23545
IRRIGATION
Distinctions in formation of microbial complex in nutrient solutions of higher plants after use of straw mineralization products N87-23138
ISOSTATIC PRESSURE
Low-pressure self-propagating high-temperature synthesis
[AD-A178593] N87-22856
ISOTOPES
Two-color, Doppler-free ionization of molecular hydrogen for isotopic analysis
[DE87-004975] N87-22825
ITERATION
Bodner-Partom viscoplastic model in STEALTH finite difference code
[AD-A178994] N87-23005
Stationary phase approximations in Fresnel-zone magnitude-only reconstructions
[AD-A178812] N87-23270
ITERATIVE SOLUTION
Wielandt iteration as applied to the nodal expansion method
[KAPL-4194] N87-23227

J

J INTEGRAL
Measurement of the J integral with caustics: An experimental and numerical investigation
[AD-A177273] N87-22990
JAGUAR AIRCRAFT
Improved combat performance using relaxed static stability and a spin prevention system (FBW Jaguar)
N87-22674
JAMMING
Convergence of relaxation algorithms by averaging
[AD-A178784] N87-23219
JET ENGINE FUELS
Gas turbine combustor and engine augmentor tube sooting characteristics
[AD-A179423] N87-22679
JET ENGINES
Performance improvement of airborne weapon systems methods, scope and limitations N87-22665
JET FLOW
Direct numerical simulations of an unpremixed turbulent jet flame
[AD-A179358] N87-22819
A theory for turbulent curved wall jets
[NASA-CR-181019] N87-22951
JET PROPULSION
Propulsion system technologies for thrust vectoring
N87-22670
JET STREAMS (METEOROLOGY)
Synoptic-scale influence on the variability of the Alpine Experiment (ALPEX) low-level jet N87-23089
JOINTS (JUNCTIONS)
Dynamics of trusses having nonlinear joints
N87-22724
Structural Dynamics and Control Interaction of Flexible Structures
[NASA-CP-2467-PT-2] N87-22729
Experimental characterization of deployable trusses and joints N87-22749
Analysis of structures with rotating, flexible substructures
[AD-A178903] N87-23004
JUPITER (PLANET)
Investigations of planetary ring phenomena
N87-23360
Properties of planetary fluids at high pressure and temperature N87-23399
JUPITER SATELLITES
Local-scale stratigraphy of grooved terrain on Ganymede N87-23538
Stratigraphy of the south polar region of Ganymede
N87-23539
Observations of industrial sulfur flows and implications for Io N87-23541
Geology of Io N87-23542
Large scale topography of Io N87-23543
The Galilean satellite geological mapping program, 1986 N87-23544
Cartography of irregularly shaped satellites
N87-23545
Voyager cartography N87-23546
The control networks of the satellites of Jupiter
N87-23553

K

KALMAN FILTERS
A multiple model adaptive tracking algorithm for a high energy laser weapon system [AD-A178978] N87-22974
KERNEL FUNCTIONS
The graphical kernel system: A standards implementation [AD-A178583] N87-23180
Goodness of fit based on integrated squared errors in characteristic functions or densities [AD-A179027] N87-23225
KETONES
Polyenamines from aromatic diacetylenic diketones and diamines [NASA-CASE-LAR-13444-1-CU] N87-22847
KIDNEYS
Effect of hypokinesia on intensity of gluconeogenesis in cortical layer of rat kidney N87-23129
KINEMATICS
Notes on implementation of Coulomb friction in coupled dynamical simulations N87-22746
Star sensor fine attitude pointing model for a spinning geosynchronous satellite [AD-A179424] N87-22763
Nonisothermal elasto-visco-plastic response of shell-type structures N87-22796
Millimeter wave Doppler radar observation of cloud and boundary layer structure [AD-A178679] N87-23098
Determining the kinematic parameters of a moving imaging sensor by processing spatial and temporal intensity changes [MBB-UA-914/85] N87-23256
Kinematics and dynamics of the Uranian rings N87-23353
Observational studies of Saturn's rings N87-23382
KINETIC ENERGY
System identification for large space structure damage assessment N87-22750
Lagrangian-like equations of hydrodynamics with mass diffusion [DE87-007522] N87-22936
The formation of a double layer leading to the critical velocity phenomenon N87-23335
KINETIC THEORY
Accumulation of the planets N87-23378
KINETICS
Nonisothermal elasto-visco-plastic response of shell-type structures N87-22796
KLYSTRONS
Klystron transmitters [AD-A179068] N87-22896
KNOWLEDGE
Alternative knowledge acquisition: Developing a pulse coded neural network [DE87-005192] N87-23145

L

LAGRANGE COORDINATES
Lagrangian turbulence measurements with constant density balloons N87-23090
LAMINAR BOUNDARY LAYER
Boundary layer disturbances caused by periodic heating of a thin ribbon [AD-A179342] N87-22925
Flow dynamics stimulated by hairpin-like vortices in initially laminar boundary layers [AD-A179578] N87-22927
Interaction of a three-dimensional roughness element with a laminar boundary layer [AD-A178668] N87-22941
LAMINAR FLOW
Progress in the prediction of unsteady heat transfwe on turbines blades N87-22769
Prediction of fluid flow in curved pipe using the finite element method [AD-A179538] N87-22926
Analysis of stably stratified atmospheric flow over the Dinaric Alps during the Alpine Experiment (ALPEX) N87-23078
LAND ICE
Pseudocraters as indicators of ground ice on Mars N87-23474
Crater ejecta morphology and the presence of water on Mars N87-23508
Non-Newtonian ice rheology and the retention of craters on Ganymede N87-23511
LANDFORMS
Landform identification: Lunar radar images N87-23443
Physiographic constraints on the origin of lunar wrinkle ridges N87-23521
LANDSAT SATELLITES
Enhanced LANDSAT images of Antarctica and planetary exploration N87-23558
LANDSLIDES
Water and ice on Mars: Evidence from Valles Marineris N87-23469
LARGE SPACE STRUCTURES
Structural Dynamics and Control Interaction of Flexible Structures [NASA-CP-2467-PT-1] N87-22702
Status of the Mast experiment N87-22703
Large space structures ground experiment checkout N87-22704
Identification of large space structures: A state-of-practice report N87-22705
Considerations in the design and development of a space station scale model N87-22711
Verification of large beam-type space structures N87-22712
Verification of flexible structures by ground test N87-22713
Optimum mix of passive and active control of space structures N87-22714
One Controller at a Time (1-CAT): A mimo design methodology N87-22715
Commit your works to the Lord, and your thoughts shall be established (Prov. 16:3). Inter-stable control systems N87-22716
Status report and preliminary results of the spacecraft control laboratory experiment N87-22717
An overview of controls research on the NASA Langley Research Center grid N87-22720
Precision pointing and control of flexible spacecraft N87-22723
Structural Dynamics and Control Interaction of Flexible Structures [NASA-CP-2467-PT-2] N87-22729
Vibration suppression by stiffness control N87-22730
Control of flexible structures and the research community N87-22732
A TREETOPS simulation of the Hubble Space Telescope-High Gain Antenna interaction N87-22735
High speed simulation of flexible multibody dynamics N87-22738
Maximum Entropy/Optimal Projection (MEOP) control design synthesis: Optimal quantification of the major design tradeoffs N87-22741
A new approach for vibration control in large space structures N87-22743
Modeling of controlled flexible structures with impulsive loads N87-22745
On the control of structures by applied thermal gradients N87-22747
System identification for large space structure damage assessment N87-22750
Adaptive momentum management for large space structures [NASA-CR-179085] N87-22758
LASER ALTIMETERS
Laser reflectance as a function of rough water glitter profile [AD-A178774] N87-23016
LASER ANEMOMETERS
Dual cylindrical wave laser-Doppler method for measurement of skin friction in fluid flow [AD-A178629] N87-22939
Laser anemometry techniques for turbine applications [NASA-TM-88953] N87-22959
LASER APPLICATIONS
Decomposition of energetic materials combustion of decoy materials [AD-A178447] N87-22827
HEPA filter monitoring program [RFP-3874] N87-22869
Optical strain measurement system development, phase 1 [NASA-CR-179619] N87-22960
Application of picosecond CO2 lasers to particle accelerators [DE87-003711] N87-22964
Target fabrication for high density target experiments at the University of Rochester's Laboratory for Laser Energetics [DE87-005915] N87-22967
Investigation of laser diagnostics of PACVD processes for depositing hard face coatings [DE87-006292] N87-22969
Program and abstracts of the 39th Annual Gaseous Electronics Conference [AD-A178598] N87-23247
Signatures from in-situ light scattering of non-homogeneous non-spherical particles [AD-A178761] N87-23269
LASER DAMAGE
CO2 pulsed laser damage mechanism and plasma effects (focused beam) [AD-A179201] N87-22961
Fundamental studies in the molecular basis of laser induced retinal damage [AD-A178453] N87-23115
LASER DOPPLER VELOCIMETERS
Dual cylindrical wave laser-Doppler method for measurement of skin friction in fluid flow [AD-A178629] N87-22939
Applications of fiber optics in experimental mechanics [AD-A178683] N87-23268
LASER FUSION
Direct-drive laser-fusion in the US [DE87-005916] N87-23279
LASER HEATING
Melting of troilite at high pressure in a diamond cell by laser heating N87-23398
LASER MATERIALS
New laser materials [DE87-006723] N87-22970
LASER OUTPUTS
Progress in optical strain measurement system development N87-22773
Laser cladding of Mg and Nb alloys for improved environmental resistance [AD-A179606] N87-22833
The use of the Karl sub-scale laser for Raman beam clean-up experiments [AD-A178463] N87-22971
Calibration of the hand-held lidars used by the Naval Ocean Systems Center [AD-A178965] N87-22973
Laser reflectance as a function of rough water glitter profile [AD-A178774] N87-23016
LASER PLASMA INTERACTIONS
Program and abstracts of the 39th Annual Gaseous Electronics Conference [AD-A178598] N87-23247
LASER PLASMAS
Program and abstracts of the 39th Annual Gaseous Electronics Conference [AD-A178598] N87-23247
Direct-drive laser-fusion in the US [DE87-005916] N87-23279
A new hydrodynamic analysis of double layers N87-23319
LASER PUMPING
The use of the Karl sub-scale laser for Raman beam clean-up experiments [AD-A178463] N87-22971
LASER RANGE FINDERS
A multiple model adaptive tracking algorithm for a high energy laser weapon system [AD-A178978] N87-22974
Lunar science from lunar laser ranging N87-23389
LASER SPECTROSCOPY
Laser spectroscopy of transient molecules important in explosions [AD-A178456] N87-22826
Plasma diagnosis by dye laser intracavity absorption [DE87-006407] N87-23280
LASER WEAPONS
A multiple model adaptive tracking algorithm for a high energy laser weapon system [AD-A178978] N87-22974
A new LIHE (Light Initiated High Explosive) test capability for spherical targets [DE87-003035] N87-23245
LASERS
Why gamma rays are different: Some notes for pedestrians [DE87-004963] N87-22966
LAUNCH VEHICLES
Estimation of ICBM (intercontinental ballistic missile) performance parameters [AD-A179204] N87-22754
LRS: A knowledge based approach to launch resource scheduling [AD-A179426] N87-23310
LAUNCHING
Superconducting Augmented Rail Gun (SARG) [AD-A179269] N87-22701
LAVA
Possible origin of some channels on Alba Patera, Mars N87-23465
Late-stage flood lavas in the Elysium region, Mars N87-23476
Relative ages of lava flows at Alba Patera, Mars N87-23477
Martian volcanism: Festoon-like ridges on terrestrial basalt flows and implications for Mars N87-23478
Studies of fluid instabilities in flows of lava and debris N87-23479

Long, paired A'A/Pahoehoe flows of Mauna Loa: Volcanological significance and insights they provide into volcano plumbing systems N87-23480
The 1984 Mauna Loa eruption and planetary geolgoy N87-23481
Calculated viscosity-distance dependence for some actively flowing lavas N87-23482
Toward a model for leveed lava flows N87-23483
Studies of vesicle distribution patterns in Hawaiian lavas N87-23484
The geology of Pine and Crater Buttes: Two basaltic constructs on the far eastern Snake River Plain N87-23487

LAWS
A family of algorithms for the estimation of the parameters of the stable laws and the parameters of attracting stable laws
[AD-A178542] N87-23214
The applicability of the stable laws in collective risk theory and practice
[AD-A178546] N87-23238
The percentiles of the stable laws
[AD-A179025] N87-23243

LEARNING
Summary of the SEI (Software Engineering Institute) Workshop on Softwear Configuration Management
[AD-A178770] N87-23184

LEAST SQUARES METHOD
A micro-computer-based system to compute magnetic variation
[OU-TM-91] N87-22617
A computer program for model verification of dynamic systems N87-22710
Body wave magnitudes and locations of French underground explosions at the Mururoa test site
[BR-97934] N87-22947
Deconvolution of spectra for intimate mixtures N87-23428

LEE WAVES
Dynamics and evolution of the Pyrenees lee wave event during 21-23 March 1982 N87-23079
An analysis of downslope winds in the lee of the Pyrenees on 23 March 1982 N87-23081
Cierzo: Northwesterly wind along the Ebro Valley (Spain) as a mesoscale effect induced on the lee of the Pyrenees mountain range; a case study during the Alpine Experiment (ALPEX) Special Observing Period N87-23083

LENGTH
Optimal shuttle altitude changes using tethers
[AD-A179205] N87-22756

LIE GROUPS
Optical acquisition, image and data compression
[AD-A178508] N87-23154

LIFE (DURABILITY)
Structural analysis demonstration of constitutive and life models N87-22780
Method and apparatus for measuring minority carrier lifetime in a direct band-gap semiconductor
[NASA-CASE-NPO-16337-1-CU] N87-22894

LIFT
Investigation of periodic pitching through the static stall angle of attack
[AD-A179512] N87-22623
Verification of performance results for a low-speed 15 percent elliptical circulation control airfoil
[NASA-CR-181020] N87-22633

LIFT AUGMENTATION
Verification of performance results for a low-speed 15 percent elliptical circulation control airfoil
[NASA-CR-181020] N87-22633

LIGHT AMPLIFIERS
The use of the Karl sub-scale laser for Raman beam clean-up experiments
[AD-A178463] N87-22971

LIGHT BEAMS
A microcrystalline growth study of solvent effects in alkoxides by dynamic laser light scattering
[DE87-005710] N87-23294

LIGHT CURVE
Asteroid lightcurve inversion N87-23377

LIGHT EMISSION
Nonlinear optical properties and subpicosecond dynamics of excitons and electron-hole plasmas in multiple quantum well structures
[AD-A179124] N87-23287

LIGHT SCATTERING
New methods for obtaining scattering and absorption from tropospheric visible spectrum data
[AD-A178590] N87-23062
Collective effects in intense-field electrodynamics 1981-1986
[AD-A179490] N87-23261
Workshop report on New Directions in X-ray Scattering
[DE87-006305] N87-23262
Signatures from in-situ light scattering of non-homogeneous non-spherical particles
[AD-A178761] N87-23269
A microcrystalline growth study of solvent effects in alkoxides by dynamic laser light scattering
[DE87-005710] N87-23294
Bidirectional reflectance spectroscopy — for Moon, asteroid, Europa, and Oberon N87-23433

LIGHT SOURCES
Semiconductor research capabilities at the Lawrence Berkeley Laboratory
[DE87-006931] N87-23298

LIGHTING EQUIPMENT
Design, development and deployment of public service photovoltaic power/load systems for the Gabonese Republic
[NASA-CR-179603] N87-23030

LIGHTNING
GEMACS (general EM model for the analysis of computer systems) frequency-domain analysis to determine the lightning induced electromagnetic skin current distributions on an aircraft
[AD-A178854] N87-22660
Analysis of lightning induced magnetic field penetration through protective metal screens using an equivalent magnetic dipole moment representation of an array of elliptic apertures
[AD-A178850] N87-22884
Transient protection of electronic circuits
[AD-A178945] N87-22919

LIMB DARKENING
Io: Comparison of photometric scans produced by the Minnaert and Hapke functions N87-23436

LINE OF SIGHT
Asymmetries in the control of saccadic eye movements to bifurcating targets
[AD-A179270] N87-23108

LINEAR CIRCUITS
Programmable electronic synthesized capacitance
[NASA-CASE-GSC-12961-1] N87-22895

LINEAR PROGRAMMING
On orbital allotments for geostationary satellites
[NASA-CR-181017] N87-22700
Programmable electronic synthesized capacitance
[NASA-CASE-GSC-12961-1] N87-22895
A separable piecewise linear upper bound for stochastic linear programs
[AD-A178694] N87-23217

LINEAR QUADRATIC GAUSSIAN CONTROL
Improving stability margins in discrete-time log controllers N87-22719

LINEAR QUADRATIC REGULATOR
Improving stability margins in discrete-time log controllers N87-22719

LINEAR SYSTEMS
Evaluation of a heliostat tracker for linear Fresnel lens photovoltaic concentrators
[DE87-006331] N87-23025
Control of linear systems over commutative normed algebras with applications
[AD-A178765] N87-23205
Linear time invariant system identification using a result of the Bussgang theorem
[AD-A178642] N87-23216

LINEARIZATION
A linearized Euler analysis of unsteady flows in turbomachinery
[NASA-CR-180987] N87-22948

LIPID METABOLISM
Some parameters of human lipid metabolism during antiorthostatic hypokinesia and their correction N87-23127
Some biochemical and morphological changes in rat blood with exposure to variable magnetic field at infralow frequency N87-23141

LIQUID CRYSTALS
Developing a voice-controlled, computer-generated display to assist space station astronauts during maintenance activity
[AD-A178997] N87-22762

LIQUID FLOW
Numerical modeling of on-orbit propellant motion resulting from an impulsive acceleration
[NASA-TM-89873] N87-22757

LIQUID PHASES
Pumped two-phase heat transfer loop
[NASA-CASE-MSC-20841-1] N87-22950

LIQUID PROPELLANT ROCKET ENGINES
Development of an integrated BEM (Boundary Element Mesh) for hot fluid-structure interaction N87-22799

LIQUID ROCKET PROPELLANTS
An evaluation of metallized propellants based on vehicle performance
[NASA-TM-100104] N87-22806

LIQUIDS
Properties of planetary fluids at high pressure and temperature N87-23399

LITHIUM
Lithium-metal sulfide battery development and submodule demonstration
[DE87-004819] N87-22904

LITHIUM ALLOYS
Superplasticity: A fundamental investigation on deformation mechanism and cavitation phenomena
[AD-A179651] N87-22834
Characterization of rapidly solidified Al-Be-Li and Al-Be ribbons
[DE87-006613] N87-22835

LITHIUM SULFUR BATTERIES
Lithium disulfide battery
[DE87-007183] N87-22892
Bipolar battery with array of sealed cells
[DE87-007194] N87-22893

LITHOSPHERE
The delineation and interpretation of the Earth's gravity field
[NASA-CR-181015] N87-23065
Failure strength of icy lithospheres N87-23357
Studies of outer planet satellites, Mercury and Uranus N87-23358
Lithospheric structure on Venus from tectonic modelling of compressional features N87-23516
Venusian tectonics: Convective coupling to the lithosphere? N87-23517
Lithospheric loading and tectonics of the lunar irregular maria N87-23522

LOAD DISTRIBUTION (FORCES)
Modeling of controlled flexible structures with impulsive loads N87-22745
An evaluation of microgridding techniques for determining local plastic strain distributions
[AD-A178518] N87-23000

LOADING MOMENTS
Structural dynamics system model reduction N87-22727

LOADS (FORCES)
Transient response for interaction of two dynamic bodies N87-22709
Notes on implementation of Coulomb friction in coupled dynamical simulations N87-22746
Fatigue damage interaction behavior of PWA 1480 N87-22777
Probabilistic structural analysis verification studies N87-22786
Composite load spectra for select space propulsion structural components N87-22793
Probabilistic load model development and validation for composite load spectra for select space propulsion engines N87-22794
A comparison of predicted wind turbine blade loads to test measurements
[DE87-001130] N87-23021
Lithospheric loading and tectonics of the lunar irregular maria N87-23522

LOCAL AREA NETWORKS
Digital Autonomous Terminal Access Communication (DATAC) system N87-22610
Concurrent communication among multi-transceiver stations over shared media
[NASA-CR-180935] N87-22890
Throughput analysis of the IEEE 802.4 token bus standard under heavy load
[NASA-CR-180936] N87-22921
JANUS/Ada software implementation of a star cluster local area network of personal computers
[AD-A178681] N87-23199
Channel access schemes and fiber optic configurations for integrated-services local area networks
[NASA-CR-180934] N87-23273

LOCKING
The use of the Karl sub-scale laser for Raman beam clean-up experiments
[AD-A178463] N87-22971

LOGARITHMS
A method for the spatial discretization of parabolic equations in one space variable
[DE87-005991] N87-23210

LOGIC PROGRAMMING
Experiments with OR-parallel logic programs
[DE87-006882] N87-23198

LOGISTICS
A prototype expert system advisor for satellite support scheduling
[AD-A179425] N87-22760

LONG TERM EFFECTS
Determining the probability of close approach between two satellites
[AD-A179385] N87-22699

LOOPS
Processor-controlled timing module for Loran-C receiver
[OU-TM-90] N87-22616
Pumped two-phase heat transfer loop
[NASA-CASE-MSC-20841-1] N87-22950

LORAN C
Investigation of air transportation technology at Massachusetts Institute of Technology, 1984
N87-22605
Aircraft approach guidance using relative Loran-C navigation N87-22606
Probabilistic Modeling of Loran-C for nonprecision approaches N87-22607
Investigation of air transportation technology at Ohio University, 1984 N87-22609
Loran-C approach considerations N87-22612
Satellite surveying for a Loran-C nonprecision approach N87-22613
Processor-controlled timing module for Loran-C receiver
[OU-TM-90] N87-22616
A micro-computer-based system to compute magnetic variation
[OU-TM-91] N87-22617

LOSSES
Multidimensional filtering investigations
[AD-A178745] N87-22915
Submicron characterization of the atomic and electronic structure of defects in semiconductors
[AD-A178458] N87-23301

LOSSY MEDIA
Multiple angle of incidence measurement technique for the permittivity and permeability of lossy materials at millimeter wavelengths
[AD-A178851] N87-22885

LOW FREQUENCIES
SIS (Superconductor-Insulator-Superconductor) mixer research
[AD-A179604] N87-23293

LOW GRAVITY MANUFACTURING
Analytical determination of space station response to crew motion and design of suspension system for microgravity experiments N87-22752

LOW PASS FILTERS
Design of generalised Chebyshev suspended substrate stripline filters
[AD-A178505] N87-22910

LOW TEMPERATURE ENVIRONMENTS
Hormonal and metabolic status of man in the extreme north N87-23139

LOW THRUST
High heat transfer oxidizer heat exchanger design and analysis — RL10-2B engine
[NASA-CR-179596] N87-22803

LOW VOLTAGE
Reliability studies of ceramic capacitors
[AD-A179436] N87-22900

LUMINESCENCE
Submicron characterization of the atomic and electronic structure of defects in semiconductors
[AD-A178458] N87-23301

LUMINOUS INTENSITY
Determining the kinematic parameters of a moving imaging sensor by processing spatial and temporal intensity changes
[MBB-UA-914/85] N87-23256

LUNAR COMPOSITION
A chemical and petrological model of the lunar crust
N87-23408
Atlas of reflectance spectra of terrestrial, lunar and meteoritic powders and frosts from 92 to 1800 •lc2)nm
N87-23427
Compositional information for the Moon: Some characteristics of current near-IR spectra (telescopic and laboratory) N87-23429
Preliminary results of spectral reflectance studies of tycho crater N87-23430
Compositional stratigraphy of crustal material from near-infrared spectra N87-23559

LUNAR CRATERS
Compositional stratigraphy of crustal material from near-infrared spectra N87-23559

LUNAR CRUST
Global petrologic variations of the Moon: A ternary-diagram approach N87-23407
A chemical and petrological model of the lunar crust
N87-23408
Compositional stratigraphy of crustal material from near-infrared spectra N87-23559

LUNAR DUST
Atlas of reflectance spectra of terrestrial, lunar and meteoritic powders and frosts from 92 to 1800 •lc2)nm
N87-23427

LUNAR EVOLUTION
Collisional and dynamical processes in moon and planet formation N87-23387
Dynamical constraints on the origin of the moon
N87-23388
Implications of convection in the Moon and the terrestrial planets N87-23406
A chemical and petrological model of the lunar crust
N87-23408

LUNAR GEOLOGY
Global petrologic variations of the Moon: A ternary-diagram approach N87-23407
Preliminary results of geologic and remote sensing studies of Rima Mozart N87-23431

LUNAR GRAVITATION
Lunar science from lunar laser ranging N87-23389

LUNAR LANDING SITES
New very high resolution radar studies of the Moon
N87-23441

LUNAR MAGNETIC FIELDS
Lunar magnetization concentrations (MAGCONS) antipodal to young large impact basins N87-23405

LUNAR MANTLE
Implications of convection in the Moon and the terrestrial planets N87-23406

LUNAR MAPS
Global petrologic variations of the Moon: A ternary-diagram approach N87-23407
High resolution radar map of the Moon N87-23442

LUNAR MARIA
Lithospheric loading and tectonics of the lunar irregular maria N87-23522

LUNAR RANGEFINDING
Lunar science from lunar laser ranging N87-23389

LUNAR RETROREFLECTORS
Lunar science from lunar laser ranging N87-23389

LUNAR ROCKS
Global petrologic variations of the Moon: A ternary-diagram approach N87-23407
Compositional stratigraphy of crustal material from near-infrared spectra N87-23559

LUNAR ROTATION
Lunar science from lunar laser ranging N87-23389

LUNAR SOIL
Global petrologic variations of the Moon: A ternary-diagram approach N87-23407
Compositional information for the Moon: Some characteristics of current near-IR spectra (telescopic and laboratory) N87-23429

LUNAR SURFACE
Lunar magnetization concentrations (MAGCONS) antipodal to young large impact basins N87-23405
Global petrologic variations of the Moon: A ternary-diagram approach N87-23407
Preliminary results of spectral reflectance studies of tycho crater N87-23430
Preliminary results of geologic and remote sensing studies of Rima Mozart N87-23431
Photometric properties of lunar terrains derived from Hapke's equation N87-23432
New very high resolution radar studies of the Moon
N87-23441
High resolution radar map of the Moon N87-23442
Landform identification: Lunar radar images
N87-23443
Physiographic constraints on the origin of lunar wrinkle ridges N87-23521
Lithospheric loading and tectonics of the lunar irregular maria N87-23522
A unified lunar control network N87-23552

LUNGS
Evaluation of effect of positive intrapulmonary pressure on respiratory function of man N87-23134

M

MACH REFLECTION
Numerical analysis of terminal double mach reflection
[AD-A179041] N87-22942

MACHINING
Austempered ductile iron process development
[PB87-169843] N87-22866

MAGELLAN SPACECRAFT (NASA)
A compilation system for Venus radar mission (Magellan) N87-23440

MAGMA
Studies of fluid instabilities in flows of lava and debris
N87-23479
Geology of the Mohon Mountain volcanic field, Yavapai and Mohave Counties, Arizona: A preliminary report
N87-23486

MAGNESIUM
Laser cladding of Mg and Nb alloys for improved environmental resistance
[AD-A179606] N87-22833

MAGNESIUM ALLOYS
The effects of candidate chemical training agents upon service materials — chemical warfare
[MQAD-317] N87-22832

MAGNETIC DIPOLES
Analysis of lightning induced magnetic field penetration through protective metal screens using an equivalent magnetic dipole moment representation of an array of elliptic apertures
[AD-A178850] N87-22884

MAGNETIC DISKS
Image processing for vision: An equipment requests to DOD
[AD-A179261] N87-23150

MAGNETIC FIELD CONFIGURATIONS
A preliminary study of extended magnetic field structures in the ionosphere
[NASA-CR-181004] N87-23066

MAGNETIC FIELD INVERSIONS
Two and three-dimensional inversion of magnetotelluric data
[DE87-005553] N87-23058

MAGNETIC FIELDS
A micro-computer-based system to compute magnetic variation
[OU-TM-91] N87-22617
Analysis of lightning induced magnetic field penetration through protective metal screens using an equivalent magnetic dipole moment representation of an array of elliptic apertures
[AD-A178850] N87-22884
Magnetically insulated opening switch research
[AD-A178895] N87-22918
Experimental study of coupling between eddy curren of Tokamak limiters of tokamak limiters
[DE87-004938] N87-22999
Some biochemical and morphological changes in rat blood with exposure to variable magnetic field at infralow frequency N87-23141

MAGNETIC FLUX
Analysis of lightning induced magnetic field penetration through protective metal screens using an equivalent magnetic dipole moment representation of an array of elliptic apertures
[AD-A178850] N87-22884

MAGNETIC INDUCTION
A system design requirements tool for satellite communications through nuclear-induced scintillation
[AD-A179272] N87-22871

MAGNETIC MIRRORS
Some aspects of double layer formation in a plasma constrained by a magnetic mirror N87-23329

MAGNETIC POLES
Solar active region physical parameters inferred from a thermal cyclotron line and soft X-ray spectral lines
[AD-A179650] N87-23560

MAGNETIC STORMS
On the thinning of the plasma sheet during substorms
[AD-A178484] N87-23061
Latitudinal motions of the aurora during substorms
[NASA-CR-180930] N87-23063
J. VLA (Very Large Array) of a solar noise storm
[NASA-CR-180219] N87-23561

MAGNETIC SURVEYS
Lunar magnetization concentrations (MAGCONS) antipodal to young large impact basins N87-23405

MAGNETIC TAPES
Image processing for vision: An equipment requests to DOD
[AD-A179261] N87-23150

MAGNETOHYDRODYNAMIC GENERATORS
Investigation of rocket powered, open cycle, magnetohydrodynamic generators for high, pulsed power needs in space
[AD-A178869] N87-22801

MAGNETOHYDRODYNAMIC STABILITY
Confinement and heating of high beta plasmas with emphasis on compact toroids. Task 2: Stellarator and heliac research
[DE87-005554] N87-23278
Development of a generalized model for a three component plasma
[AD-A178979] N87-23281
The generation of electrostatic noise in the plasma sheet boundary layer
[ATR-86(8433)-4] N87-23282
A laboratory investigation of potential double layers
N87-23317
Anomalous transport in discrete arcs and simulation of double layers in a model auroral circuit N87-23325
Weak double layers in the auroral ionosphere
N87-23326
Particle simulation of auroral double layers
N87-23327
Double layers above the aurora N87-23331

Double layers and plasma-wave resistivity in extragalactic jets: Cavity formation and radio-wave emission N87-23333

MAGNETOHYDRODYNAMIC WAVES
Double layers above the aurora N87-23331

MAGNETOHYDRODYNAMICS
The origin of polarity asymmetries in the history of the geomagnetic field N87-23401
Magnetic flares in the protoplanetary nebula and the origin of meteorite chondrules N87-23402

MAGNETORESISTIVITY
Two and three-dimensional inversion of magnetotelluric data [DE87-005553] N87-23058

MAGNETOSPHERE
On the thinning of the plasma sheet during substorms [AD-A178484] N87-23061
Effect of double layers on magnetosphere-ionosphere coupling N87-23321
Conditions for double layers in the Earth's magnetosphere and perhaps in other astrophysical objects N87-23328
Beamed emission from gamma-ray burst sources N87-23332
The Earth's magnetosphere as a sample of the plasma universe [TRITA-EPP-86-12] N87-23337

MAGNITUDE
Magnitude and phase calibration of microwave sensors [DE87-003466] N87-22955

MAINTAINABILITY
Research on computer aided design for maintainability [AD-A178460] N87-23177

MAINTENANCE
AI (Artificial Intelligence) gas turbine rotor diagnostics [AD-A178996] N87-22683

MAN MACHINE SYSTEMS
The event related brain potential as an index of information processing and cognitive activity: A program of basic research [AD-A179310] N87-23143
Proceedings of the 22nd Annual Conference on Manual Control [AD-A178627] N87-23148
Research on computer aided design for maintainability [AD-A178460] N87-23177
Air Force technical objectives document, fiscal year 1988 [AD-A179163] N87-23569

MAN-COMPUTER INTERFACE
Digital Autonomous Terminal Access Communication (DATAC) system N87-22610
Sixth Annual Users' Conference — Transportable Applications Executive (TAE) [NASA-CP-2463] N87-23156
TAE Plus: A conceptual view of TAE in the space station era N87-23157
The evaluation and extension of TAE in the development of a user interface management system N87-23158
NASA Regional Planetary Image Facility image retrieval and processing system N87-23160
SOT: A rapid prototype using TAE windows N87-23161
Display management subsystem, version 1: A user's eye view N87-23164
An overview of the Land Analysis System (LAS) N87-23168
Development of Land Analysis System display modules N87-23169

MANAGEMENT
Adaptive momentum management for large space structures [NASA-CR-179085] N87-22758

MANAGEMENT METHODS
Crew coordination concepts: Continental Airlines CRM training N87-22642

MANEUVERS
Lanczos modes for reduced-order control of flexible structures N87-22739

MANIPULATORS
Developing a voice-controlled, computer-generated display to assist space station astronauts during maintenance activity [AD-A178997] N87-22762

MANPOWER
Human factors engineering data management handbook [AD-A179691] N87-23144

MANUAL CONTROL
Proceedings of the 22nd Annual Conference on Manual Control [AD-A178627] N87-23148

MANY BODY PROBLEM
High speed simulation of flexible multibody dynamics N87-22738

MAPPING
A 3-D world modeling based on combinatorial geometry for autonomous robot navigation [DE87-002814] N87-22980
Altimeter measurements for the determination of the Earth's gravity field [NASA-CR-180520] N87-23033
Fluvial valleys on Martian volcanoes N87-23462
Geology of Io N87-23542
The Galilean satellite geological mapping program, 1986 N87-23544
Cartography of irregularly shaped satellites N87-23545
Voyager cartography N87-23546
Progress in compilation of the 1:2,000,000-scale topographic map N87-23548
Mars digital terrain model N87-23549
Digital cartography of Mars N87-23550
The control network of Mars: October 1986 N87-23551
A unified lunar control network N87-23552
The control networks of the satellites of Jupiter N87-23553
Microvax-based data management and reduction system for the regional planetary image facilities N87-23554
Martian terrains N87-23555

MAPS
A preliminary analysis of the Mariner 10 color ratio map of Mercury N87-23439

MARINE TECHNOLOGY
Optical dynamics experiment (ODEX) data report R/V acania expedition 10 October-17 November 1982. Volume 2: Particle size distributions. Volume 6: Scalar spectral-radiometer data [AD-A178535] N87-23104

MARKOV CHAINS
Sensitivity analysis for stationary probabilities of a Markov chain [AD-A178556] N87-23240

MARKOV PROCESSES
Non-Markovian line shapes of physisorbed atoms on a crystal [AD-A179525] N87-23292

MARS (PLANET)
Asteroid families, dynamics and astrometry N87-23370
Calcium carbonate and calcium sulfate in Martian meteorite EETA79001 N87-23409
The case for a wet, warm climate on early Mars N87-23410
The role of regolith adsorption in the transition from early to late Mars climate N87-23411
Revision of the Martian relative age chronology N87-23504

MARS ATMOSPHERE
The case for a wet, warm climate on early Mars N87-23410
The role of regolith adsorption in the transition from early to late Mars climate N87-23411
CO2: Adsorption on palagonite and the Martian regolith N87-23419
Investigation of Martian H2O and CO2 via gamma-ray spectroscopy N87-23420
The Mars observer camera N87-23556

MARS CRATERS
Mars: Morphology of Southern Hemisphere intracrater dunefields N87-23452
Pseudocraters as indicators of ground ice on Mars N87-23474
Eruptive history of the Elysium Volcanic Province of Mars N87-23475
Late-stage flood lavas in the Elysium region, Mars N87-23476
Relative ages of lava flows at Alba Patera, Mars N87-23477
Revision of the Martian relative age chronology N87-23504
Early changes in gradation styles and rates on Mars N87-23505
Cratering and obliteration history of the south polar region of Mars N87-23506
Martian rampart craters: Morphologic clues for the physical state of the target at time of impact N87-23507
Crater ejecta morphology and the presence of water on Mars N87-23508
Thermal inertia characteristics of the Martian crater Curie N87-23509

MARS GEOSCIENCE CLIMATOLOGY ORBITER
The Mars observer camera N87-23556

MARS LANDING
Martian terrains N87-23555

MARS PROBES
Investigation of Martian H2O and CO2 via gamma-ray spectroscopy N87-23420

MARS SURFACE
Calcium carbonate and calcium sulfate in Martian meteorite EETA79001 N87-23409
Variations of Martian surface albedo: Evidence for yearly dust deposition and removal N87-23413
On the spectral reflectance properties of materials exposed at the Viking landing sites N87-23414
Spectral mixture modeling: Further analysis of rock and soil types at the Viking Lander sites N87-23415
Hisingerite and iddingsite on Mars: Degradation of iron-rich basalts N87-23416
Gossans on Mars: Spectral features attributed to jarosite N87-23417
Characterization of surficial units on Mars using Viking orbiter multispectral image and thermal data N87-23418
CO2: Adsorption on palagonite and the Martian regolith N87-23419
Investigation of Martian H2O and CO2 via gamma-ray spectroscopy N87-23420
Reflectance spectra of mafic silicates and phyllosilicates from .6 to 4.6 microns N87-23421
Goldstone radar observations of Mars: The 1986 opposition N87-23444
A diffuse radar scattering model from Martian surface rocks N87-23445
Mars: Seasonally variable radar reflectivity N87-23446
Bright sand/dark dust: The identification of active sand surfaces on the Earth and Mars N87-23449
Regional sources and sinks of dust on Mars: Viking observations of Cerberus, Solis Planum and Syrtis Major N87-23450
High resolution thermal infrared mapping of Martian channels N87-23451
Mars: Morphology of Southern Hemisphere intracrater dunefields N87-23452
Timing of frost deposition on Martian dunes: A clue to properties of dune particles? N87-23453
Wind ripples in low density atmospheres N87-23454
Eolian saltation on Mars N87-23455
Mass transport by Aeolian saltation on Earth, Mars and Venus: The effects of full saltation cloud development and choking N87-23456
Fluvial valleys on Martian volcanoes N87-23462
Possible origin of some channels on Alba Patera, Mars N87-23465
Volatile reservoirs below the surface of the Elysium region of Mars: Geomorphic evidence N87-23467
Evidence for glaciation in Elysium N87-23468
Water and ice on Mars: Evidence from Valles Marineris N87-23469
Formation of the layered deposits in the Valles Marineris, Mars N87-23470
Geomorphic evidence for ancient seas in west Deuteronilus Mensae, Mars-1: Regional geomorphology N87-23471
Geomorphic evidence for ancient seas in west Deuteronilus Mensae, Mars-2: From very high resolution Viking Orbiter images N87-23472
Explosive volcanic deposits on Mars: Preliminary investigations N87-23473
Pseudocraters as indicators of ground ice on Mars N87-23474
Eruptive history of the Elysium Volcanic Province of Mars N87-23475
Late-stage flood lavas in the Elysium region, Mars N87-23476
Relative ages of lava flows at Alba Patera, Mars N87-23477
Studies of fluid instabilities in flows of lava and debris N87-23479
Revision of the Martian relative age chronology N87-23504
Early changes in gradation styles and rates on Mars N87-23505
Crater ejecta morphology and the presence of water on Mars N87-23508
Thermal inertia characteristics of the Martian crater Curie N87-23509
Characteristic structures of the highland boundary on Mars: Evidence against a single mega-impact event? N87-23523
The Martian crustal dichotomy: Product of accretion and not a specific event? N87-23524
Implications of Viking color data for evolution of the Amenthes Region, Mars N87-23525
Timing of ancient extensional tectonic features on Mars N87-23526
Stress history of the Tharsis Region, Mars N87-23527
History and morphology of faulting in the Noctis Labyrinthus-Claritas Fossae Region of Mars N87-23528
Thin and thick-skinned deformation in the Tharsis Region of Mars N87-23529

Flexurally-resisted uplift of the Tharsis Province, Mars N87-23530

Tectonic domains in the Eastern Hemisphere of Mars N87-23531

Age of fracturing and mesa development in the Elysium Area, northern Martian plains N87-23532

Geometry and relative age of large patterned fractures in southern Acidalia Planitia, Mars N87-23533

Origin of fractures, Martian polygonal terrain N87-23534

The effect of overburden thickness on tension fracture patterns above an uplifting dome N87-23535

Natural fracture systems on planetary surfaces: Genetic classification and pattern randomness N87-23536

Curvilinear ridges and related features in southwest Cydonia Mensae, Mars N87-23537

Progress in compilation of the 1:2,000,000-scale topographic map N87-23548

Mars digital terrain model N87-23549

Digital cartography of Mars N87-23550

The control network of Mars: October 1986 N87-23551

Martian terrains N87-23555

The Mars observer camera N87-23556

Enhanced LANDSAT images of Antarctica and planetary exploration N87-23558

MARS SURFACE SAMPLES

Martian terrains N87-23555

MARS VOLCANOES

The case for a wet, warm climate on early Mars N87-23410

Explosive volcanic deposits on Mars: Preliminary investigations N87-23473

Eruptive history of the Elysium Volcanic Province of Mars N87-23475

Relative ages of lava flows at Alba Patera, Mars N87-23477

Martian volcanism: Festoon-like ridges on terrestrial basalt flows and implications for Mars N87-23478

Studies of fluid instabilities in flows of lava and debris N87-23479

Long, paired A'A/Pahoehoe flows of Mauna Loa: Volcanological significance and insights they provide into volcano plumbing systems N87-23480

MARTENSITIC TRANSFORMATION

Martensitic transformation as a deformation process [DE87-007068] N87-22836

MASERS

Operation of the induced resonance electron cyclotron maser at higher harmonics [AD-A179428] N87-22962

MASS

Impact of thermal energy storage properties on solar dynamic space power conversion system mass [NASA-TM-89909] N87-22802

MASS DISTRIBUTION

Experimental evidence for non-proportional growth of large craters N87-23497

MASS FLOW

The 1984 Mauna Loa eruption and planetary geolgoy N87-23481

MASS SPECTROSCOPY

Fast ion mass spectrometry and charged particle spectrography investigations of transverse ion acceleration and beam-plasma interactions [NASA-CR-168348] N87-22817

A high-temperature quadrupole mass spectrometer for studying vaporization from materials heated by a CO2 laser [LA-10744] N87-22975

MATERIALS HANDLING

Proceedings of the Instrumentation, Components, and Materials Contractors Meeting [DE86-006596] N87-22954

A study into the generation of temperature gradients in materials for detecting and measuring the depth of sub-surface cracks [AERE-R-12382] N87-22991

Materials Information for Science and Technology (MIST). Project overview: Phase 1 and 2 and general considerations [DE87-006799] N87-23312

MATHEMATICAL LOGIC

Experiments with OR-parallel logic programs [DE87-006882] N87-23198

MATHEMATICAL MODELS

Investigation of air transportation technology at Massachusetts Institute of Technology, 1984 N87-22605

Probabilistic Modeling of Loran-C for nonprecision approaches N87-22607

A micro-computer-based system to compute magnetic variation [OU-TM-91] N87-22617

Numerical simulation of supersonic flow over a rotating band using flowfield blanking [AD-A178492] N87-22624

An analysis of artificial viscosity effects on reacting flows using a spectral multi-domain technique [NASA-CR-178308] N87-22632

Frequency-response identification of XV-15 tilt-rotor aircraft dynamics [NASA-TM-89428] N87-22690

Identification of large space structures: A state-of-practice report N87-22705

A general method for dynamic analysis of structures overview N87-22707

Verification of flexible structures by ground test N87-22713

A quasi-analytical method for non-iterative computation of nonlinear controls N87-22731

Control of flexible structures and the research community N87-22732

Lanczos modes for reduced-order control of flexible structures N87-22739

Maximum Entropy/Optimal Projection (MEOP) control design synthesis: Optimal quantification of the major design tradeoffs N87-22741

Modeling of controlled flexible structures with impulsive loads N87-22745

On the control of structures by applied thermal gradients N87-22747

Finite element models of wire rope for vibration analysis N87-22748

Experimental characterization of deployable trusses and joints N87-22749

System identification for large space structure damage assessment N87-22750

Space station structures and dynamics test program N87-22751

Space station structural dynamics/reaction control system interaction study N87-22753

Numerical modeling of on-orbit propellant motion resulting from an impulsive acceleration [NASA-TM-89873] N87-22757

Moving-bank multiple model adaptive estimation applied to flexible spacestructure control [AD-A178870] N87-22761

Simulation of multistage turbine flows N87-22768

Analytical and experimental studies of flow-induced vibration of SSME components N87-22771

Probabilistic structural analysis verification studies N87-22786

On the use of adaptive moving grid methods in combustion problems [DE87-003715] N87-22824

Axisymmetric inviscid shock tube flow simulation [AD-A178494] N87-22937

Automated transient analysis of structural members [AD-A179042] N87-23007

An elementary valley wind model N87-23075

Alternative knowledge acquisition: Developing a pulse coded neural network [DE87-005192] N87-23145

An algorithm for the computation of generalized likelihood or self-critical estimators for binary data [AD-A178545] N87-23179

A partial differential equation model describing the threat to an aircraft in a one-on-Many scenario [AD-A178641] N87-23215

A Bayesian statistics year at the Ohio State University [AD-A178762] N87-23242

Workshop report on New Directions in X-ray Scattering [DE87-006305] N87-23262

Thermodynamic properties of molten salt solutions [DE87-004948] N87-23306

Double Layers in Astrophysics [NASA-CP-2469] N87-23313

A new hydrodynamic analysis of double layers N87-23319

Effect of double layers on magnetosphere-ionosphere coupling N87-23321

Current driven weak double layers N87-23322

Electron acceleration in stochastic double layers N87-23324

Anomalous transport in discrete arcs and simulation of double layers in a model auroral circuit N87-23325

Electric potential distributions at the interface between plasmasheet clouds N87-23330

Double layers and plasma-wave resistivity in extragalactic jets: Cavity formation and radio-wave emission N87-23333

Numerical studies of collapsing interstellar clouds [NASA-CR-180933] N87-23340

Could Ariel have been heated by tidal friction? N87-23347

Investigations of the surfaces and interiors of outer planet satellites N87-23356

The loss and depth of CO2 ice in comet nuclei N87-23367

Dynamics of long period comets N87-23368

Analysis of planetary evolution with emphasis on differentiation and dynamics N87-23382

CO2: Adsorption on palagonite and the Martian regolith N87-23419

A diffuse radar scattering model from Martian surface rocks N87-23445

Application of numerical methods to planetary radiowave scattering N87-23448

Origin of fractures, Martian polygonal terrain N87-23534

MATHEMATICAL PROGRAMMING

On orbital allotments for geostationary satellites [NASA-CR-181017] N87-22700

MATRICES (MATHEMATICS)

Some robust estimates of covariance structure based on parametric density estimation [AD-A178806] N87-23220

MATRIX MATERIALS

High performance polymers: Matrix resins, high strength polyquinoxalines and conducting polyaromatics [AD-A178457] N87-22854

MAXIMUM ENTROPY METHOD

Maximum Entropy/Optimal Projection (MEOP) control design synthesis: Optimal quantification of the major design tradeoffs N87-22741

MAXIMUM LIKELIHOOD ESTIMATES

Some robust estimates of covariance structure based on parametric density estimation [AD-A178806] N87-23220

Self-critical and robust procedures for the analysis of binary data [AD-A178935] N87-23221

A modified goodness-of-fit test for the lognormal distribution with unknown scale and location parameters [AD-A179049] N87-23226

Problems of identification [AD-A178555] N87-23239

MEASURING INSTRUMENTS

Proceedings of the Instrumentation, Components, and Materials Contractors Meeting [DE86-006596] N87-22954

Dose enhancement effects in the Aerospace Corporation Co-60 irradiator [AD-A178481] N87-23253

MECHANICAL MEASUREMENT

NBS calibration services users guide, 1986-1988 edition [NBS-SP-250] N87-22958

MECHANICAL PROPERTIES

Characterizing the hardness and modulus of thin films using a mechanical properties microprobe [DE87-006612] N87-22826

Superplasticity: A fundamental investigation on deformation mechanism and cavitation phenomena [AD-A179651] N87-22834

Corrosion, wear and mechanical properties of pulse-electrodeposited alloys [AD-A178596] N87-22842

Physical properties and structure of ion-containing polymers [AD-A178592] N87-22855

Fundamental studies of the mechanical behavior of microelectronic thin film materials [AD-A179699] N87-22902

Mechanical and thermal properties of planetologically important ices N87-23346

MEDITERRANEAN SEA

Air-sea interaction over the Mediterranean Sea during the Alpine Experiment (ALPEX) Special Observing Period N87-23073

MELTING

Plasma joining of metal matrix composites [AD-A178731] N87-22814

Melting of troilite at high pressure in a diamond cell by laser heating N87-23398

MELTS (CRYSTAL GROWTH)

Total immersion crystal growth [NASA-CASE-NPO-15800-2] N87-23288

MENTAL PERFORMANCE

The event related brain potential as an index of information processing and cognitive activity: A program of basic research [AD-A179310] N87-23143

A prototype knowledge-based system to aid space system restoration management [AD-A179336] N87-23203

MERCURY SURFACE

A preliminary analysis of the Mariner 10 color ratio map of Mercury N87-23439

A statistical study of Mercurian crater classes applied to the emplacement of the intercrater plains N87-23502

MESAS
Age of fracturing and mesa development in the Elysium Area, northern Martian plains N87-23532
MESOSCALE PHENOMENA
Mesoscale mountain meteorology N87-23069
Diagnostic studies of meso-alpha scale flow on the Alpine northside N87-23070
Numerical study of the Mistral with a mesoscale model N87-23082
Cierzo: Northwesterly wind along the Ebro Valley (Spain) as a mesoscale effect induced on the lee of the Pyrenees mountain range; a case study during the Alpine Experiment (ALPEX) Special Observing Period N87-23083
The Mistral-Tramuntana shear line. A satellite observation N87-23084
Mesoscale analyses of temperature, pressure and wind fields over Switzerland: A case study of a Foehn
N87-23086
METABOLISM
Biochemical aspects of some neurohumoral system functions during long-term antiorthostatic hypokinesia
N87-23142
METAL AIR BATTERIES
An investigation of zinc electrodes relevant to zinc-air batteries
[DE87-007607] N87-22908
METAL FATIGUE
Deformation and fatigue behavior of SSME turbopump blade materials N87-22776
Fatigue damage interaction behavior of PWA 1480
N87-22777
A new formulation of mean stress effects in fatigue
N87-22778
Probabilistic structural analysis to evaluate the structural durability of SSME critical components N87-22783
An evaluation of microgridding techniques for determining local plastic strain distributions
[AD-A178518] N87-23000
METAL HYDRIDES
Development of nickel oxide/hydrogen multilayer bipolar battery for pulsed power
[AD-A178844] N87-22917
METAL MATRIX COMPOSITES
Analysis of an advanced technology subsonic turbofan incorporating revolutionary materials
[NASA-TM-89868] N87-22680
Probabilistic structural analysis to evaluate the structural durability of SSME critical components N87-22783
Artificial composites for high temperature applications: A review
[DME-007] N87-22808
Plasma joining of metal matrix composites
[AD-A178731] N87-22814
METAL OXIDE SEMICONDUCTORS
A coherent VLSI design environment
[AD-A179037] N87-22920
METAL PLATES
Stochastic and hybrid-stress plate/shell finite elements for hot-section components N87-22789
Correlations between electrical contact resistance and stages of wear in 700 Torr helium for precious metal electrical contacts
[DE87-003499] N87-22981
METAL PROPELLANTS
An evaluation of metallized propellants based on vehicle performance
[NASA-TM-100104] N87-22806
METAL SHEETS
A novel rollability test
[RFP-3901] N87-22984
METAL SHELLS
Stochastic and hybrid-stress plate/shell finite elements for hot-section components N87-22789
Nonisothermal elasto-visco-plastic response of shell-type structures N87-22796
METAL VAPOR LASERS
Investigation of the transverse-discharge copper-vapor laser
[AD-A178833] N87-22972
METAL WORKING
Austempered ductile iron process development
[PB87-169843] N87-22866
High energy high rate pulsed power processing of materials by powder consolidation and by railgun deposition
[AD-A179289] N87-22867
A novel rollability test
[RFP-3901] N87-22984
METALS
An evaluation of metallized propellants based on vehicle performance
[NASA-TM-100104] N87-22806
XAS (X-ray Absorption Spectroscopy) of gas phase metal-containing chemical systems
[AD-A179391] N87-22821
METEORITE CRATERS
Computer simulations of 10-km-diameter asteroid impacts into oceanic and continental sites: Preliminary results on atmospheric passage, cratering and ejecta dynamics N87-23489
Shatter cones in Illinois: Evidence for metoeritic impacts at Glasford and Des Plaines N87-23513
METEORITES
Meteorite spectroscopy and characterization of asteroid surface materials N87-23373
Implications of convection in the Moon and the terrestrial planets N87-23406
Calcium carbonate and calcium sulfate in Martian meteorite EETA79001 N87-23409
Search for, and study of, paleozoic impact ejecta: Progress made during the past year N87-23514
METEORITIC COMPOSITION
Atlas of reflectance spectra of terrestrial, lunar and meteoritic powders and frosts from 92 to 1800 •lc2)nm
N87-23427
METEOROLOGICAL BALLOONS
Lagrangian turbulence measurements with constant density balloons N87-23090
METEOROLOGICAL FLIGHT
A contribution to Bora studies using Alpine Experiment (ALPEX) aircraft data N87-23080
Field study of the effect of orographic features on planetary boundary layer models N87-23091
METEOROLOGICAL INSTRUMENTS
Validation of a surface-layer windflow model using climatology and meteorological tower data from Vandenberg AFB, California
[AD-A178480] N87-23097
METEOROLOGICAL RADAR
Fractal analysis of radar precipitation data over hilly terrain N87-23093
METEOROLOGICAL SATELLITES
Atmospheric remote sensing in arctic regions
[AD-A179550] N87-23012
METHOD OF MOMENTS
Joint services electronics program
[AD-A178599] N87-22879
Full polarimetric non-specular scattering of flat plate structures
[AD-A178853] N87-22886
METHYL COMPOUNDS
Decomposition of energetic materials combustion of decoy materials
[AD-A178447] N87-22827
METROLOGY
Vibration analysis using shadow speckle metrology and line broadening techniques
[AD-A178626] N87-23003
MICROANALYSIS
Characterizing the hardness and modulus of thin films using a mechanical properties microprobe
[DE87-006612] N87-22826
MICROBURSTS
Safe microburst penetration techniques: A deterministic, nonlinear, optimal control approach N87-22620
Oklahoma downbursts and their asymmetry
[DOT/FAA/PM-87/7] N87-23095
MICROCLIMATOLOGY
Validation of a surface-layer windflow model using climatology and meteorological tower data from Vandenberg AFB, California
[AD-A178480] N87-23097
MICROCOMPUTERS
Tactile feedback for teleoperator systems
[AD-A179054] N87-22983
The design of a real time operating system for a fault tolerant microcomputer
[AD-A178577] N87-23155
The graphical kernel system: A standards implementation
[AD-A178583] N87-23180
Development of an image analysis program for the IBM PC/XT/AT
[AD-A178644] N87-23183
JANUS/Ada software implementation of a star cluster local area network of personal computers
[AD-A178681] N87-23199
MICROCRYSTALS
A microcrystalline growth study of solvent effects in alkoxides by dynamic laser light scattering
[DE87-005710] N87-23294
MICRODENSITOMETERS
Potential medical applications of TAE N87-23166
MICROELECTRONICS
Electrochemical adjustment of thin film Ti-Pd resistors
[DE87-007392] N87-22837
Fundamental studies of the mechanical behavior of microelectronic thin film materials
[AD-A179699] N87-22902
MICROORGANISMS
Distinctions in formation of microbial complex in nutrient solutions of higher plants after use of straw mineralization products N87-23138
MICROPROCESSORS
Microprocessor controlled proof-mass actuator
N87-22706
MICROSCOPY
Potential medical applications of TAE N87-23166
MICROSTRUCTURE
Thermal shock resistance of mullite-based SiC-whisker composites
[AD-A179214] N87-22809
The role of particle substructure in the sintering of monosized titania
[DE87-007600] N87-22839
Investigation of the icosahedral Z-phase in aluminium transition metal alloys and rapidly solidified Al-alloys
[AD-A178451] N87-22840
Synthesis of alumina-zirconia powders by sol-gel processing
[DE87-005721] N87-22851
CO2 pulsed laser damage mechanism and plasma effects (focused beam)
[AD-A179201] N87-22961
MICROWAVE ANTENNAS
GPS antenna designs N87-22615
MICROWAVE EMISSION
A preliminary summary of the observations of the 16 February 1984 solar flare (STIP Interval XV, 12-21 February 1984)
[NASA-CR-180929] N87-23563
MICROWAVE EQUIPMENT
Atmospheric remote sensing in arctic regions
[AD-A179550] N87-23012
MICROWAVE FILTERS
Design of generalised Chebyshev suspended substrate stripline filters
[AD-A178505] N87-22910
MICROWAVE FREQUENCIES
Measurements of the dielectric constants for planetary volatiles N87-23447
MICROWAVE IMAGERY
Strategies for high-resolution 3-D millimeter wave imaging
[AD-A178653] N87-22882
MICROWAVE OSCILLATORS
Design and operation of 140 GHz gyrotron oscillators for power levels up to 1 MW CW
[DE87-006683] N87-22907
MICROWAVE SCATTERING
Application of numerical methods to planetary radiowave scattering N87-23448
MICROWAVE SENSORS
Magnitude and phase calibration of microwave sensors
[DE87-003466] N87-22955
MICROWAVE TRANSMISSION
Full-wave analysis of isolated and coupled microwave transmission lines using the finite element method
[AD-A178805] N87-22883
MIE SCATTERING
Subcentimeter-size particle distribution functions in planetary rings from Voyager radio and photopolarimeter occultation data N87-23361
MILITARY AIR FACILITIES
Air Force technical objectives document, fiscal year 1988
[AD-A179163] N87-23569
MILITARY OPERATIONS
Introduction to MAC CRM training N87-22648
The application of CRM to military operations
N87-22649
Cockpit Resource Management (CRM) training in the 1550th combat crew training wing N87-22650
Cockpit Resource Management (CRM) training in the 349th military airlift wing N87-22651
MILITARY SPACECRAFT
Toward the year 2000: The near future of the American civilian and military space programs
[DE87-006467] N87-22697
Design of an orbital inspection satellite
[AD-A179115] N87-22759
MILLIMETER WAVES
Strategies for high-resolution 3-D millimeter wave imaging
[AD-A178653] N87-22882
Multiple angle of incidence measurement technique for the permittivity and permeability of lossy materials at millimeter wavelengths
[AD-A178851] N87-22885
Ferroelectric optically controlled millimeter-wave devices
[AD-A179524] N87-22901

MIMAS
Dynamics of satellites, asteroids, and rings
N87-23392
MIMD (COMPUTERS)
Parallel branch and bound on an MIMD (Multiple Instruction Stream, Multiple Data stream) system
[AD-A178816] N87-23200
MINERALOGY
Crustal and subcrustal nodules in ejecta from Kilbourne Hole Maar, New Mexico N87-23485
Geology of the Mohon Mountain volcanic field, Yavapai and Mohave Counties, Arizona: A preliminary report
N87-23486
MINERALS
Gossans on Mars: Spectral features attributed to jarosite N87-23417
Studies of the scattering/absorption of minerals
N87-23423
Mid-infrared spectroscopic investigation N87-23424
Thermal-infrared spectral observations of geologic materials in emission N87-23425
Atlas of reflectance spectra of terrestrial, lunar and meteoritic powders and frosts from 92 to 1800 •lc2)nm
N87-23427
Deconvolution of spectra for intimate mixtures
N87-23428
Compositional information for the Moon: Some characteristics of current near-IR spectra (telescopic and laboratory) N87-23429
Preliminary results of spectral reflectance studies of tycho crater N87-23430
MIRANDA
On the lack of commensurabilities in the mean motions of the satellites of Uranus and the resurfacing of Ariel
N87-23349
Dynamics of satellites, asteroids, and rings
N87-23392
MIRRORS
Radiation damage to coatings for short wave length laser mirrors
[DE87-001696] N87-22963
MISSILE DEFENSE
A new LIHE (Light Initiated High Explosive) test capability for spherical targets
[DE87-003035] N87-23245
MISSILE TRAJECTORIES
Estimation of ICBM (intercontinental ballistic missile) performance parameters
[AD-A179204] N87-22754
MISSION PLANNING
A prototype knowledge-based system for satellite mission planning
[AD-A178873] N87-22698
MIXERS
SIS (Superconductor-Insulator-Superconductor) mixer research
[AD-A179604] N87-23293
MIXING
Studies of the east Australian current off northern New South Wales
[AD-A178461] N87-23103
MIXTURES
Estimation of the parameters of mixtures via distance between densities or characteristic functions
[AD-A178623] N87-23241
Deconvolution of spectra for intimate mixtures
N87-23428
MODAL RESPONSE
Flight and analytical investigations of a structural mode excitation system on the YF-12A airplane
[NASA-CR-166623] N87-22685
Structural dynamics system model reduction
N87-22727
MODELS
Evaluation of numerator lead effects on aircraft handling qualities
[AD-A179388] N87-22687
Studies and analyses of the space shuttle main engine: High-pressure oxidizer turbopump failure information propagation model
[NASA-CR-179079] N87-22765
Revised NASA axially symmetric ring model for coupled-cavity traveling-wave tubes
[NASA-TP-2675] N87-22923
Prediction of fluid flow in curved pipe using the finite element method
[AD-A179538] N87-22926
Modeling of substrate and implantation effects on the threshold voltage of MESFET structures fabricated in semi-insulating GaAs
[AD-A178550] N87-23303
MODES
Waveguide junction analysis involving asymmetrical modes
[AD-A178464] N87-22909
MODULES
Non-linear finite element analysis program
[AD-A179038] N87-23006
MODULUS OF ELASTICITY
Thermal shock resistance of mullite-based SiC-whisker composites
[AD-A179214] N87-22809
MOLECULAR CLOUDS
Numerical studies of collapsing interstellar clouds
[NASA-CR-180933] N87-23340
Comet thermal modeling N87-23366
Dynamics of long period comets N87-23368
Formation of giant molecular clouds in global spiral structures: The role of orbital dynamics and cloud-cloud collisions N87-23381
MOLECULAR COLLISIONS
Molecular reactions at the film surface in plasma polymerization
[DE87-002488] N87-22849
MOLECULAR INTERACTIONS
Molecular-dynamics simulation of thin-film growth
[DE87-006973] N87-23284
MOLECULAR SPECTRA
Infrared spectroscopy using laser and Fourier techniques of the unstable molecules SiH and NH. Determination of the molecular constants of the fundamental electronic state 3 sigma (-) of NH
[ETN-87-99552] N87-22818
MOLECULAR STRUCTURE
XAS (X-ray Absorption Spectroscopy) of gas phase metal-containing chemical systems
[AD-A179391] N87-22821
MOLECULAR WEIGHT
Process for crosslinking and extending conjugated diene-containing polymers
[NASA-CASE-LAR-13452-1] N87-22848
MOLECULES
Laser spectroscopy of transient molecules important in explosions
[AD-A178456] N87-22828
MOLTEN SALTS
Thermodynamic properties of molten salt solutions
[DE87-004948] N87-23306
MOMENTS
Correlation of analytical calculations from GRASP (General Rotorcraft Aeromechanical Stability Program) with torsionally-soft rotor data
[AD-A178881] N87-22689
MOMENTS OF INERTIA
Adaptive momentum management for large space structures
[NASA-CR-179085] N87-22758
MOMENTUM
Adaptive momentum management for large space structures
[NASA-CR-179085] N87-22758
MOMENTUM THEORY
Angular momentum theory applied to interactions in solids
[AD-A179366] N87-23289
MOMENTUM TRANSFER
Optimal shuttle altitude changes using tethers
[AD-A179205] N87-22756
Angular momentum theory applied to interactions in solids
[AD-A179366] N87-23289
Oblique impact: Projectile richochet, concomitant ejecta and momentum transfer N87-23492
Momentum transfer from oblique impacts N87-23493
Impact crater scaling laws N87-23496
MONITORS
Image processing for vision: An equipment requests to DOD
[AD-A179261] N87-23150
MONTE CARLO METHOD
Probabilistic SSME blades structural response under random pulse loading N87-22791
A modified goodness-of-fit test for the lognormal distribution with unknown scale and location parameters
[AD-A179049] N87-23226
Sensitivity analysis for stationary probabilities of a Markov chain
[AD-A178556] N87-23240
MOON
Collisional and dynamical processes in moon and planet formation N87-23387
Dynamical constraints on the origin of the moon
N87-23388
Lunar science from lunar laser ranging N87-23389
Lunar magnetization concentrations (MAGCONS) antipodal to young large impact basins N87-23405
Implications of convection in the Moon and the terrestrial planets N87-23406
Global petrologic variations of the Moon: A ternary-diagram approach N87-23407
MORPHINE
Chemical sensitivity of medial vestibular nuclear neurons to enkephalins, acetylcholine, GABA and L-glutamate
N87-23131
MORPHOLOGY
Some biochemical and morphological changes in rat blood with exposure to variable magnetic field at infralow frequency N87-23141
Crater morphology and morphometry on the Uranian satellites N87-23343
Cratering history of Miranda N87-23344
Geology and cratering history of Ariel N87-23348
Voyager observations of 1985U1 N87-23352
Planetary ring dynamics and morphology N87-23394
Groundwater sapping channels: Summary of effects of experiments with varied stratigraphy N87-23461
Possible origin of some channels on Alba Patera, Mars N87-23465
Non-equilibrium freezing of water-ice in sandy basaltic regoliths and implications for fluidized debris flows on Mars N87-23466
Formation of the layered deposits in the Valles Marineris, Mars N87-23470
History and morphology of faulting in the Noctis Labyrinthus-Claritas Fossae Region of Mars
N87-23528
MOTION SICKNESS
A collection and statistical analysis of biophysical data to predict motion sickness incidence
[AD-A178874] N87-23119
USSR Report: Space Biology and Aerospace Medicine, Volume 20, No. 5, September - October 1986
[JPRS-USB-86-007] N87-23120
Structure and function of otoliths N87-23122
Chemical sensitivity of medial vestibular nuclear neurons to enkephalins, acetylcholine, GABA and L-glutamate
N87-23131
MOTION STABILITY
Some dynamical properties of very strong double layers in a triple plasma device N87-23315
MOTOR VEHICLES
Advanced technology mobile robotics vehicle fleet
[DE87-007526] N87-22982
MOUNTAINS
Mesoscale mountain meteorology N87-23069
MOVING TARGET INDICATORS
On non-parametric discrimination using series expansions and projection pursuit
[AD-A178455] N87-23213
MULTILAYER INSULATION
Stochastic processes in CHEMFETs
[AD-A178841] N87-22829
MULTIPATH TRANSMISSION
The effect of multipath on digital communications systems: With application to space station
[AD-A178578] N87-22876
MULTIPROCESSING (COMPUTERS)
Performance comparison of four state-of-the-art computer architectures
[AD-A179071] N87-23149
Performance evaluation of parallel branch and bound search with the intel IPSC (Intel Personal SuperComputer) hypercube computer
[AD-A179384] N87-23196
An experiment in knowledge-based signal understanding using parallel architectures
[AD-A179407] N87-23197
MULTISPECTRAL BAND SCANNERS
Spectral mixture modeling: Further analysis of rock and soil types at the Viking Lander sites N87-23415
Characterization of surficial units on Mars using Viking orbiter multispectral image and thermal data
N87-23418
MULTISPECTRAL PHOTOGRAPHY
Enhanced LANDSAT images of Antarctica and planetary exploration N87-23558
MULTIVARIATE STATISTICAL ANALYSIS
Multidimensional filtering investigations
[AD-A178745] N87-22915
Some robust estimates of covariance structure based on parametric density estimation
[AD-A178806] N87-23220
Some integrated squared error procedures for multivariate normal data
[AD-A178985] N87-23224
Goodness of fit based on integrated squared errors in characteristic functions or densities
[AD-A179027] N87-23225
Extreme value theory for suprema of random variables with regularly varying tail probabilities
[AD-A179126] N87-23233
A test of goodness of fit for multivariate normality
[AD-A178543] N87-23237
A statistical study of Mercurian crater classes applied to the emplacement of the intercrater plains
N87-23502

MUONS
Detection of 10^{14}-eV gamma rays from Cygnus X-3 during 1986
[DE87-006054] N87-23568
MUSCULAR FUNCTION
Evaluation of effect of positive intrapulmonary pressure on respiratory function of man N87-23134
Evaluation of skeletomuscular system function in self-contained life-support system on the basis of blood biochemistry N87-23135
MUSCULOSKELETAL SYSTEM
Evaluation of skeletomuscular system function in self-contained life-support system on the basis of blood biochemistry N87-23135

N

NAPHTHALENE
Determination of surface shear stress with the naphthalene sublimation technique N87-23460
NASA SPACE PROGRAMS
Toward the year 2000: The near future of the American civilian and military space programs
[DE87-006467] N87-22697
NASTRAN
Equivalent beam modeling using numerical reduction techniques N87-22725
Dynamic characteristics of single crystal SSME blades N87-22797
NATIONAL SEVERE STORMS PROJECT
Oklahoma downbursts and their asymmetry
[DOT/FAA/PM-87/7] N87-23095
NATURAL SATELLITES
Shapes of small satellites N87-23354
Impact and cratering processes on asteroids, satellites, and planets N87-23499
NAVIER-STOKES EQUATION
Numerical simulation of supersonic flow over a rotating band using flowfield blanking
[AD-A178492] N87-22624
Application of advanced computational codes in the design of an experiment for a supersonic throughflow fan rotor
[NASA-TM-88915] N87-22630
Dynamic stall calculations using a Navier-Stokes solver
[AD-A178566] N87-22688
Composite velocity procedures for flows with pressure interaction
[AD-A179602] N87-22929
Axisymmetric inviscid shock tube flow simulation
[AD-A178494] N87-22937
NAVIGATION SATELLITES
Design of GPS (Global Positioning System) status reporting system
[AD-A179334] N87-22662
NAVY
Naval applications of a TAE-derived executive N87-23167
NEAR FIELDS
Detection of reflector surface error from near-field data: Effect of edge diffracted field
[NASA-TM-89920] N87-22874
NEAR INFRARED RADIATION
Compositional information for the Moon: Some characteristics of current near-IR spectra (telescopic and laboratory) N87-23429
Compositional stratigraphy of crustal material from near-infrared spectra N87-23559
NEBULAE
Protostellar disks and the primitive solar nebula N87-23379
NEPTUNE (PLANET)
Investigations of planetary ring phenomena N87-23360
Uranus and Neptune: Questions and possible answers N87-23386
Properties of planetary fluids at high pressure and temperature N87-23399
NERVES
Reaction to vibration of rat kinesthetic analyzer neurocytes N87-23133
NETWORK ANALYSIS
A coherent VLSI design environment
[AD-A179037] N87-22920
NETWORK CONTROL
A unified lunar control network N87-23552
The control networks of the satellites of Jupiter N87-23553
NEURONS
Workshop Symposium on Neural Models of Sensory-Motor Control
[AD-A179501] N87-23111
Chemical sensitivity of medial vestibular nuclear neurons to enkephalins, acetylcholine, GABA and L-glutamate N87-23131
Alternative knowledge acquisition: Developing a pulse coded neural network
[DE87-005192] N87-23145
NEUROPHYSIOLOGY
The perception of brightness and colour: Neurophysiology, psychophysics and computation
[AD-A179217] N87-23107
NEUROTRANSMITTERS
Chemical sensitivity of medial vestibular nuclear neurons to enkephalins, acetylcholine, GABA and L-glutamate N87-23131
Biochemical aspects of some neurohumoral system functions during long-term antiorthostatic hypokinesia N87-23142
NEUTRAL SHEETS
On the thinning of the plasma sheet during substorms
[AD-A178484] N87-23061
NEUTRON DIFFRACTION
Neutron scattering from charged polymer lattices
[DE87-006628] N87-22853
NEUTRON SCATTERING
Neutron scattering from charged polymer lattices
[DE87-006628] N87-22853
NEUTRON STARS
Beamed emission from gamma-ray burst sources N87-23332
Accretion onto neutron stars with the presence of a double layer N87-23334
NICKEL ALLOYS
Progress on thin-film sensors for space propulsion technology N87-22772
Fatigue damage interaction behavior of PWA 1480 N87-22777
Structural analysis demonstration of constitutive and life models N87-22780
Effect of hydrogen on deformation structure and properties of CMSX-2 nickel-base single-crystal superalloy N87-22782
NICKEL CADMIUM BATTERIES
Development of advanced nickel-cadmium batteries for electric vehicle propulsion
[DOE/NV/10442-1] N87-22922
NICKEL HYDROGEN BATTERIES
Component variations and their effects on bipolar nickel-hydrogen cell performance
[NASA-TM-89907] N87-23029
NICKEL OXIDES
Development of nickel oxide/hydrogen multilayer bipolar battery for pulsed power
[AD-A178844] N87-22917
NIOBIUM
Laser cladding of Mg and Nb alloys for improved environmental resistance
[AD-A179606] N87-22833
Superconducting thin films, composites and junctions
[AD-A179346] N87-23288
NITRILES
Structure and properties of novel compounds of silicon germanium and tin
[AD-A179433] N87-23291
NITROGEN
Low power DC arcjet operation with hydrogen/nitrogen/ammonia mixtures
[NASA-TM-89876] N87-22804
NITROGEN OXIDES
An assessment of nitrogen oxide formation in preheated high-temperature combustion air in industrial processes
[EGG-2439] N87-23031
NOAA SATELLITES
Standard-resolution TOVS observations for the FIRE/SRB Wisconsin experiment region from October 9 through November 2, 1986
[NASA-TM-89151] N87-23101
NOBLE METALS
In situ friction, wear and electrical contact resistance of precious metal alloys
[DE87-001423] N87-22979
NOISE GENERATORS
The generation of electrostatic noise in the plasma sheet boundary layer
[ATR-86(8433)-4] N87-23282
NOISE PREDICTION (AIRCRAFT)
Prediction of high-speed rotor noise with a Kirchhoff formula
[AD-A178962] N87-23250
NOISE REDUCTION
Automatic scene analysis using hierarchical spatial frequency domain correlation with energy normalization and heuristic noise reduction
[AD-A178589] N87-23181
Acoustic testing of simplified cabin box, phase 1 — helicopter cabin
[RP-698] N87-23248
NOMENCLATURES
Planetary nomenclature N87-23557
NONDESTRUCTIVE TESTS
Preliminary investigation of the use of holographic interferometry to detect ill-fitting compressor blades
[AD-A178519] N87-22682
Method and apparatus for measuring minority carrier lifetime in a direct band-gap semiconductor
[NASA-CASE-NPO-16337-1-CU] N87-22894
Laser anemometry techniques for turbine applications
[NASA-TM-88953] N87-22959
Automated non-destructive testing using an industrial robot
[AERE-R-12308] N87-22986
Determination of crack initiation sites using a digital NDE workstation
[DE87-001444] N87-22997
NONLINEAR EQUATIONS
Investigation of perturbation techniques for nonlinear difference equations and other related topics
[DE87-006663] N87-23211
Oscillatory behaviour of solutions of first-order ordinary and delay differential equations
[DE87-701552] N87-23212
NONLINEAR OPTICS
Nonlinear optical properties and subpicosecond dynamics of excitons and electron-hole plasmas in multiple quantum well structures
[AD-A179124] N87-23287
NONLINEAR SYSTEMS
Dynamics of trusses having nonlinear joints N87-22724
Analysis of structures with rotating, flexible substructures
[AD-A178903] N87-23004
Non-linear finite element analysis program
[AD-A179036] N87-23006
Linear time invariant system identification using a result of the Bussgang theorem
[AD-A178642] N87-23216
NONLINEARITY
Hamiltonian theory of nonlinear waves in planetary rings N87-23393
NONNEWTONIAN FLUIDS
Non-Newtonian ice rheology and the retention of craters on Ganymede N87-23511
NONOSCILLATORY ACTION
Efficient implementation of essentially non-oscillatory shock capturing schemes
[NASA-CR-178304] N87-23230
NONPARAMETRIC STATISTICS
On non-parametric discrimination using series expansions and projection pursuit
[AD-A178455] N87-23213
NORMAL DENSITY FUNCTIONS
Some robust estimates of covariance structure based on parametric density estimation
[AD-A178806] N87-23220
Some integrated squared error procedures for multivariate normal data
[AD-A178985] N87-23224
A modified goodness-of-fit test for the lognormal distribution with unknown scale and location parameters
[AD-A179049] N87-23226
NORMALIZING (STATISTICS)
Automatic scene analysis using hierarchical spatial frequency domain correlation with energy normalization and heuristic noise reduction
[AD-A178589] N87-23181
A statistical viewpoint on the theory of evidence, revision
[AD-A178958] N87-23207
NORWAY
An evaluation of the polar ice prediction system
[AD-A178522] N87-23014
NOSE TIPS
Hypersonic laminar boundary layer transition. Part 1: Nosetip bluntness effects on cone frustum transition. Part 2: Mach 6 experiments of transition on a cone at angle of attack
[AD-A178877] N87-22625
NOTCH TESTS
Influence of supporting conditions on stress intensity factors for single-edge-cracked specimens under bending
[NASA-TT-20016] N87-23008
NOZZLE DESIGN
Propulsion system technologies for thrust vectoring N87-22670
Journal of Chinese Society of Astronautics (selected articles)
[AD-A179690] N87-22800
NOZZLE FLOW
Journal of Chinese Society of Astronautics (selected articles)
[AD-A179690] N87-22800

NOZZLE GEOMETRY
Axisymmetric inviscid shock tube flow simulation [AD-A178494] N87-22937

NUCLEAR EXPLOSION EFFECT
A system design requirements tool for satellite communications through nuclear-induced scintillation [AD-A179272] N87-22871

NUCLEAR EXPLOSIONS
Body wave magnitudes and locations of French underground explosions at the Mururoa test site [BR-97934] N87-22947

NUCLEAR FUELS
Direct-drive laser-fusion in the US [DE87-005916] N87-23279

NUCLEAR POWER PLANTS
Investigation of rocket powered, open cycle, magnetohydrodynamic generators for high, pulsed power needs in space [AD-A178869] N87-22801
A 3-D world modeling based on combinatorial geometry for autonomous robot navigation [DE87-002814] N87-22980

NUCLEAR WEAPONS
Transient protection of electronic circuits [AD-A178945] N87-22919

NUCLEATION
The characterization of whiskers produced by electromigration on suspended aluminum linestripes [AD-A179383] N87-23290

NUMERICAL ANALYSIS
Numerical simulation of supersonic flow over a rotating band using flowfield blanking [AD-A178492] N87-22824
Journal of Chinese Society of Astronautics (selected articles) [AD-A179690] N87-22800
Direct numerical simulations of an unpremixed turbulent jet flame [AD-A179358] N87-22819
A Godunov method for Lagrangian hydrodynamics in 1D [DE87-005204] N87-22933
Axisymmetric inviscid shock tube flow simulation [AD-A178494] N87-22937
A three-dimensional dual potential procedure with applications to wind tunnel inlets and interacting boundary layers [NASA-CR-180939] N87-22944
Measurement of the J integral with caustics: An experimental and numerical investigation [AD-A177273] N87-22990
OMNITAB 80: An interpretive system for statistical and numerical data anlysis [PB87-172235] N87-23171
Patterns from models of dissipative systems [DE87-006823] N87-23175
Sensitivity analysis for stationary probabilities of a Markov chain [AD-A178556] N87-23240
Current driven weak double layers N87-23322
Numerical studies of collapsing interstellar clouds [NASA-CR-180933] N87-23340

NUMERICAL INTEGRATION
Some integrated squared error procedures for multivariate normal data [AD-A178965] N87-23224

NUMERICAL STABILITY
Lanczos modes for reduced-order control of flexible structures N87-22739

NUMERICAL WEATHER FORECASTING
Forecast and sensitivity experiments on the UK Meteorological Office GCM with El Nino SST anomalies — general circulation model (GCM) sea surface temperature (SST) N87-23045
The impact of initial conditions and SST Anomalies on extended range predictions for the El Nino period — sea surface temperature (SST) N87-23046
An extended forecast experiment with the CCC GCM — general climate model (GCM) N87-23050

NUTRITION
Nutritional correction of histamine and serotonin levels as related to exposure to hypokinesia and neuro-emotional stress N87-23126
Distinctions in formation of microbial complex in nutrient solutions of higher plants after use of straw mineralization products N87-23138

NUTS (FASTENERS)
Daze fasteners [NASA-CASE-LAR-13009-2] N87-22976
Tube coupling device [NASA-CASE-MFS-25964-2] N87-22977

O

OBLIQUENESS
Oblique impact: Projectile richochet, concomitant ejecta and momentum transfer N87-23492
Momentum transfer from oblique impacts N87-23493

OBSERVATION
Investigate and verify the validity of mathematical formules and procedures in relation to data obtained from theoretical investigations and experimental observations [AD-A179564] N87-23057
Problems of identification [AD-A178555] N87-23239
Simultaneous SMM flat crystal spectrometer and very large array observations of solar active regions [AD-A179698] N87-23562

OCEAN CURRENTS
Sensitivity of an Ocean General Circulation Model (OCGM) to wind forcing N87-23054
Studies of the east Australian current off northern New South Wales [AD-A178461] N87-23103

OCEAN MODELS
Modelling and forecasting El Nino N87-23053
Sensitivity of an Ocean General Circulation Model (OCGM) to wind forcing N87-23054
The development of a coupled GCM suitable for modelling studies in TOGA — general circulation model (GCM); Tropical Ocean Global Atmosphere (TOGA) N87-23055
A wind- and wave-driven nearshore current model, the one-dimensional model [AD-A178751] N87-23105

OCEAN SURFACE
Laser reflectance as a function of rough water glitter profile [AD-A178774] N87-23016
Altimeter measurements for the determination of the Earth's gravity field [NASA-CR-180520] N87-23033
The SIR-B mission: Towards an understanding of internal waves in the ocean [ARE-TR-86122] N87-23102

OCEANOGRAPHIC PARAMETERS
Simulated and observed budgets and balances during the 82/83 ENSO event — El Nino Southern Oscillation (ENSO) N87-23035
Optical dynamics experiment (ODEX) data report R/V acania expedition 10 October-17 November 1982. Volume 2: Particle size distributions. Volume 6: Scalar spectral-radiometer data [AD-A178535] N87-23104

OCEANOGRAPHY
An evaluation of the polar ice prediction system [AD-A178522] N87-23014
The SIR-B mission: Towards an understanding of internal waves in the ocean [ARE-TR-86122] N87-23102

OCULOMOTOR NERVES
Workshop Symposium on Neural Models of Sensory-Motor Control [AD-A179501] N87-23111

OKLAHOMA
Oklahoma downbursts and their asymmetry [DOT/FAA/PM-87/7] N87-23095

ON-LINE SYSTEMS
JANUS/Ada software implementation of a star cluster local area network of personal computers [AD-A178681] N87-23199

OPENINGS
Magnetically insulated opening switch research [AD-A178895] N87-22918

OPERATING SYSTEMS (COMPUTERS)
Sixth Annual Users' Conference --- Transportable Applications Executive (TAE) [NASA-CP-2463] N87-23156
TAE Plus: A conceptual view of TAE in the space station era N87-23157
The evaluation and extension of TAE in the development of a user interface management system N87-23158
A design for a new catalog manager and associated file management for the Land Analysis System (LAS) N87-23159
NASA Regional Planetary Image Facility image retrieval and processing system N87-23160
SOT: A rapid prototype using TAE windows N87-23161
The 2GCHAS: A high productivity software development environment N87-23162
An overview of the catalog manager N87-23163
Display management subsystem, version 1: A user's eye view N87-23164
Rationalizing VICAR within a TAE framework: Some problems and some solutions N87-23165
Potential medical applications of TAE N87-23166
Naval applications of a TAE-derived executive N87-23167
An overview of the Land Analysis System (LAS) N87-23168
Development of Land Analysis System display modules N87-23169

OPERATIONS RESEARCH
Cost analysis of aircraft projects N87-22664
A prototype knowledge-based system to aid space system restoration management [AD-A179336] N87-23203

OPERATOR PERFORMANCE
Crew coordination concepts: Continental Airlines CRM training N87-22642
Tolerance to frustration as a factor in operator performance N87-23124

OPTICAL COMPUTERS
The use of real-time optical processors in embedded computing [DE87-006895] N87-23153
Optical symbolic processor for expert system execution [AD-A179375] N87-23172

OPTICAL DATA PROCESSING
White-light optical information processing and holography [AD-A179489] N87-23260

OPTICAL DENSITY
Effect of the neutral density helmet visor on the visual acuity of navy fighter pilots [AD-A178486] N87-23147

OPTICAL EQUIPMENT
Progress in optical strain measurement system development N87-22773
Optically Phase-Locked Electronic Speckle Pattern Interferometer (OPL-ESPI) [AD-A178652] N87-22914
Measurement of the atmospheric phase coherence length, rsubo [AD-A178468] N87-23060
Optical symbolic processor for expert system execution [AD-A179375] N87-23172
Automatic pattern recognition and related topics [AD-A178595] N87-23267

OPTICAL GYROSCOPES
Closed loop fiber optic rotation sensor [NASA-CASE-NPO-16558-1-CU] N87-23259

OPTICAL POLARIZATION
Strategies for high-resolution 3-D millimeter wave imaging [AD-A178653] N87-22882

OPTICAL PROPERTIES
Optically Phase-Locked Electronic Speckle Pattern Interferometer (OPL-ESPI) [AD-A178652] N87-22914
Vibration analysis using shadow speckle metrology and line broadening techniques [AD-A178626] N87-23003
Optical dynamics experiment (ODEX) data report R/V acania expedition 10 October-17 November 1982. Volume 2: Particle size distributions. Volume 6: Scalar spectral-radiometer data [AD-A178535] N87-23104
Fundamentals and techniques of nonimaging optics research at the University of Chicago [DE87-006917] N87-23264
Development of radiation hard graded index optical fibers [AD-A178465] N87-23265
Nonlinear optical properties and subpicosecond dynamics of excitons and electron-hole plasmas in multiple quantum well structures [AD-A179124] N87-23287

OPTICAL PUMPING
Time and space resolved spectroscopy of X-ray laser experiments from 81A to 220A [DE87-005946] N87-22968

OPTICAL RADAR
Calibration of the hand-held lidars used by the Naval Ocean Systems Center [AD-A178965] N87-22973
Laser reflectance as a function of rough water glitter profile [AD-A178774] N87-23016

OPTICAL THICKNESS
New methods for obtaining scattering and absorption from tropospheric visible spectrum data [AD-A178590] N87-23062

OPTICAL TRACKING
Determining the kinematic parameters of a moving imaging sensor by processing spatial and temporal intensity changes [MBB-UA-914/85] N87-23256

OPTICAL WAVEGUIDES

Development of radiation hard graded index optical fibers [AD-A178465] N87-23265

OPTIMAL CONTROL

Safe microburst penetration techniques: A deterministic, nonlinear, optimal control approach N87-22620

A quasi-analytical method for non-iterative computation of nonlinear controls N87-22731

OPTIMIZATION

The aerodynamic optimization of wings at subsonic speeds and the influence of wingtip design [NASA-TM-88534] N87-22627

Equivalent beam modeling using numerical reduction techniques N87-22725

A Simplex optimisation technique for development of rubber formulations [ARE-TM(UMT)-86405] N87-22846

Optimization of the antenna pattern of a phased array with failed elements [AD-A178581] N87-22878

Automated transient analysis of structural members [AD-A179042] N87-23007

Parallel graph reduction on a supercomputer [DE87-006066] N87-23173

ORBIT PERTURBATION

Determining the probability of close approach between two satellites [AD-A179385] N87-22699

Dynamics of long period comets N87-23368

ORBIT SPECTRUM UTILIZATION

On orbital allotments for geostationary satellites [NASA-CR-181017] N87-22700

ORBIT TRANSFER VEHICLES

Thermodynamic analysis and subscale modeling of space-based orbit transfer vehicle cryogenic propellant resupply [NASA-TM-89921] N87-22949

ORBITAL MANEUVERS

Maneuvering and vibration control of flexible spacecraft N87-22734

ORBITAL MECHANICS

Solar array flight dynamic experiment N87-22722

Adaptive momentum management for large space structures [NASA-CR-179085] N87-22758

Orbital dynamics of the Uranian satellites based on Voyager data N87-23350

Formation of giant molecular clouds in global spiral structures: The role of orbital dynamics and cloud-cloud collisions N87-23381

Solar system dynamics N87-23390

Orbital resonances, unusual configurations and exotic rotation states among planetary satellites N87-23391

Dynamics of satellites, asteroids, and rings N87-23392

ORBITAL SPACE STATIONS

Structural Dynamics and Control Interaction of Flexible Structures [NASA-CP-2467-PT-2] N87-22729

Impact of space station appendage vibrations on the pointing performance of gimballed payloads N87-22733

Preliminary evaluation of a reaction control system for the space station N87-22736

Dual keel space station control/structures interaction study N87-22737

Slewing control experiment for a flexible panel N87-22740

Crew activity and motion effects on the space station N87-22744

Space station structures and dynamics test program N87-22751

Analytical determination of space station response to crew motion and design of suspension system for microgravity experiments N87-22752

Space station structural dynamics/reaction control system interaction study N87-22753

Developing a voice-controlled, computer-generated display to assist space station astronauts during maintenance activity [AD-A178997] N87-22762

ORDER-DISORDER TRANSFORMATIONS

Corrosion, wear and mechanical properties of pulse-electrodeposited alloys [AD-A178596] N87-22842

OROGRAPHY

Sensitivity of January 1983 Sea Surface Temperature (SST)-experiments to the formulation of lateral diffusion N87-23052

Frontal interaction with orography N87-23071

An analysis of downslope winds in the lee of the Pyrenees on 23 March 1982 N87-23081

The Mistral-Tramuntana shear line. A satellite observation N87-23084

The influence of orography on the temperature and wind regime in the mountains N87-23085

On the predicability of low-level flow during ALPEX — Alpine Experiment (ALPEX) N87-23088

Field study of the effect of orographic features on planetary boundary layer models N87-23091

Characteristics of orographically initiated convection — Rocky Mountains N87-23092

Fractal analysis of radar precipitation data over hilly terrain N87-23093

The effect of the Tatra Mountains (Poland) on the atmospheric precipitation and air humidity during the northern and southern air flow N87-23094

ORTHOSTATIC TOLERANCE

Problems and feasibility of drug correction of orthostatic tolerance in space medicine N87-23121

Some parameters of human lipid metabolism during antiorthostatic hypokinesia and their correction N87-23127

Split circadian rhythm of simian body temperature during antiorthostatic hypokinesia N87-23128

Biochemical aspects of some neurohumoral system functions during long-term antiorthostatic hypokinesia N87-23142

OSCILLATIONS

A coherent VLSI environment [AD-A179303] N87-22897

OSCILLATORS

Programmable electronic synthesized capacitance [NASA-CASE-GSC-12961-1] N87-22895

Water-absorbing capacitor system for measuring relative humidity [NASA-CASE-NPO-16544-1-CU] N87-22953

OTOLITH ORGANS

Structure and function of otoliths N87-23122

Cortical ultrastructure of rat cerebellar nodulus following flight aboard Cosmos-1514 biosatellite N87-23130

OUTLIERS (LANDFORMS)

Curvilinear ridges and related features in southwest Cydonia Mensae, Mars N87-23537

OUTPUT

Programmable electronic synthesized capacitance [NASA-CASE-GSC-12961-1] N87-22895

Chandrasekhar equations for infinite dimensional systems. Part 2: Unbounded input and output case [NASA-CR-178303] N87-23208

OXIDATION

Special features in regulating respiration under normal conditions and conditions of altered gas medium [AD-A179216] N87-23106

Oxidized basalts on the surface of Venus: Compositional implications of measured spectral properties N87-23412

OXIDATION-REDUCTION REACTIONS

Development of radiation hard graded index optical fibers [AD-A178465] N87-23265

OXIDES

High temperature solid oxide regenerative fuel cell for solar photovoltaic energy storage [NASA-TM-89872] N87-23020

OXYGEN CONSUMPTION

Relationship between a two mile run and maximal oxygen uptake [AD-A179343] N87-23109

OXYGEN PRODUCTION

Experimental investigation of the process of CO2-CO-H2O-H2-N2 gas mixture breakdown in electrolysis cell with solid electrolyte N87-23137

OXYGEN SUPPLY EQUIPMENT

Special features in regulating respiration under normal conditions and conditions of altered gas medium [AD-A179216] N87-23106

P

P WAVES

Body wave magnitudes and locations of French underground explosions at the Mururoa test site [BR-97934] N87-22947

PACIFIC OCEAN

Numerical experiments on the atmospheric response to a sea surface temperature anomaly over the equatorial eastern Pacific Ocean N87-23036

Principal circulation anomalies in model atmospheres with and without interannual variations of tropical Pacific SST — sea surface temperature (SST) N87-23041

Tropical Pacific SST experiments with the GLAS climate model — sea surface temperature (SST) N87-23049

The delineation and interpretation of the Earth's gravity field [NASA-CR-181015] N87-23065

PACKAGING

Semiconductor research capabilities at the Lawrence Berkeley Laboratory [DE87-006931] N87-23298

PACKET SWITCHING

Channel access schemes and fiber optic configurations for integrated-services local area networks [NASA-CR-180934] N87-23273

PACKETS (COMMUNICATION)

Throughput analysis of the IEEE 802.4 token bus standard under heavy load [NASA-CR-180936] N87-22921

PAINTS

The effects of candidate chemical training agents upon service materials — chemical warfare [MQAD-317] N87-22832

PALEOMAGNETISM

Lunar magnetization concentrations (MAGCONS) antipodal to young large impact basins N87-23405

PALEONTOLOGY

Shatter cones in Illinois: Evidence for metoeritic impacts at Glasford and Des Plaines N87-23513

Search for, and study of, paleozoic impact ejecta: Progress made during the past year N87-23514

PALLADIUM

Electrochemical adjustment of thin film Ti-Pd resistors [DE87-007392] N87-22837

PANELS

Slewing control experiment for a flexible panel N87-22740

A new approach for vibration control in large space structures N87-22743

Hybrid composite response to hydraulic ram [AD-A178750] N87-22815

Structural panels [NASA-CASE-ARC-11429-2-CU] N87-22845

PARABOLIC DIFFERENTIAL EQUATIONS

A method for the spatial discretization of parabolic equations in one space variable [DE87-005991] N87-23210

PARALLEL PLATES

Wideband parallel-plate waveguide, phased-array antenna [AD-A179402] N87-22873

PARALLEL PROCESSING (COMPUTERS)

A coherent VLSI environment [AD-A179303] N87-22897

Performance comparison of four state-of-the-art computer architectures [AD-A179071] N87-23149

Parallel graph reduction on a supercomputer [DE87-006066] N87-23173

Performance evaluation of parallel branch and bound search with the intel IPSC (Intel Personal SuperComputer) hypercube computer [AD-A179384] N87-23196

Experiments with OR-parallel logic programs [DE87-006882] N87-23198

Parallel branch and bound on an MIMD (Multiple Instruction Stream, Multiple Data stream) system [AD-A178816] N87-23200

PARALLEL PROGRAMMING

An experiment in knowledge-based signal understanding using parallel architectures [AD-A179407] N87-23197

PARAMETER IDENTIFICATION

Frequency-response identification of XV-15 tilt-rotor aircraft dynamics [NASA-TM-89428] N87-22690

A computer program for model verification of dynamic systems N87-22710

An overview of controls research on the NASA Langley Research Center grid N87-22720

Moving-bank multiple model adaptive estimation applied to flexible spacestructure control [AD-A178870] N87-22761

Problems of identification [AD-A178555] N87-23239

Determining the kinematic parameters of a moving imaging sensor by processing spatial and temporal intensity changes [MBB-UA-914/85] N87-23256

PARAMETERIZATION

The 30-60 day oscillation in a perpetual January simulation with the NCAR general circulation model N87-23043

On the predicability of low-level flow during ALPEX — Alpine Experiment (ALPEX) N87-23088

Some robust estimates of covariance structure based on parametric density estimation [AD-A178806] N87-23220

Estimation of the parameters of a modified compound poisson distribution [AD-A178540] N87-23236

Estimation of the parameters of mixtures via distance between densities or characteristic functions [AD-A178623] N87-23241

PARSING ALGORITHMS
A development system for augmented transition network grammars and a large grammar for technical prose
[AD-A179009] N87-23188
PARTIAL DIFFERENTIAL EQUATIONS
On the use of adaptive moving grid methods in combustion problems
[DE87-003715] N87-22824
A partial differential equation model describing the threat to an aircraft in a one-on-Many scenario
[AD-A178641] N87-23215
PARTICLE ACCELERATION
Beamed emission from gamma-ray burst sources
N87-23332
PARTICLE ACCELERATORS
Application of picosecond CO2 lasers to particle accelerators
[DE87-003711] N87-22964
PARTICLE IN CELL TECHNIQUE
Particle simulation of auroral double layers
N87-23327
PARTICLE PRECIPITATION
Millimeter wave Doppler radar observation of cloud and boundary layer structure
[AD-A178679] N87-23098
PARTICLE SIZE DISTRIBUTION
The role of particle substructure in the sintering of monosized titania
[DE87-007600] N87-22839
Neutron scattering from charged polymer lattices
[DE87-006628] N87-22853
Optical dynamics experiment (ODEX) data report R/V acania expedition 10 October-17 November 1982. Volume 2: Particle size distributions. Volume 6: Scalar spectral-radiometer data
[AD-A178535] N87-23104
A microcrystalline growth study of solvent effects in alkoxides by dynamic laser light scattering
[DE87-005710] N87-23294
Subcentimeter-size particle distribution functions in planetary rings from Voyager radio and photopolarimeter occultation data N87-23361
Experimental studies on the impact properties of water ice N87-23364
Dynamical studies of Saturn's rings N87-23395
Bright sand/dark dust: The identification of active sand surfaces on the Earth and Mars N87-23449
The application of flow competence evaluations to the assessment of flood-flow velocities and stresses
N87-23464
PARTICLE THEORY
Signatures from in-situ light scattering of non-homogeneous non-spherical particles
[AD-A178761] N87-23269
PARTICLE TRAJECTORIES
Impacts of hemispherical granular targets: Implications for global impacts N87-23490
PARTICLES
HEPA filter monitoring program
[RFP-3874] N87-22869
Evaluation of spherical ceramic particles for solar thermal transfer media
[DE87-007432] N87-23026
PASSIVITY
Radiation hardened silica-based optical fibers
[AD-A178466] N87-23266
PATTERN RECOGNITION
Image size and resolution in face recognition
N87-23113
Patterns from models of dissipative systems
[DE87-006823] N87-23175
Automatic scene analysis using hierarchical spatial frequency domain correlation with energy normalization and heuristic noise reduction
[AD-A178589] N87-23181
Development of an image analysis program for the IBM PC/XT/AT
[AD-A178644] N87-23183
Automatic pattern recognition and related topics
[AD-A178595] N87-23267
PECLET NUMBER
Thermocapillary bubble migration for large Marangoni Numbers
[NASA-CR-179628] N87-22865
PELLETS
Direct-drive laser-fusion in the US
[DE87-005916] N87-23279
PENETRATION
Computer program for electromagnetic penetration into a conducting circular cylinder through a narrow slot, TM case
[AD-A178616] N87-22880
PERCEPTION
The perception of brightness and colour: Neurophysiology, psychophysics and computation
[AD-A179217] N87-23107
PERFORMANCE PREDICTION
Results of the integration of a transonic full-potential analysis program with a free-wake lifting-line program for hovering rotors
[NASA-TM-89494] N87-22631
Performance improvement of airborne weapon systems methods, scope and limitations N87-22665
PERFORMANCE TESTS
Experimental characterization of deployable trusses and joints N87-22749
Helicopter transmission testing at NASA Lewis Research Center
[NASA-TM-89912] N87-22978
Component variations and their effects on bipolar nickel-hydrogen cell performance
[NASA-TM-89907] N87-23029
Analysis of the effects of impurity buildup on the performance of a reversed field pinch
[DE87-005438] N87-23277
PERIODIC VARIATIONS
Investigation of periodic pitching through the static stall angle of attack
[AD-A179512] N87-22623
PERMAFROST
Gossans on Mars: Spectral features attributed to jarosite N87-23417
Investigation of Martian H2O and CO2 via gamma-ray spectroscopy N87-23420
Evidence for glaciation in Elysium N87-23468
PERMEABILITY
Multiple angle of incidence measurement technique for the permittivity and permeability of lossy materials at millimeter wavelengths
[AD-A178851] N87-22885
PERMITTIVITY
Multiple angle of incidence measurement technique for the permittivity and permeability of lossy materials at millimeter wavelengths
[AD-A178851] N87-22885
Measurements of the dielectric constants for planetary volatiles N87-23447
PERSONAL COMPUTERS
Performance evaluation of parallel branch and bound search with the intel IPSC (Intel Personal SuperComputer) hypercube computer
[AD-A179384] N87-23196
JANUS/Ada software implementation of a star cluster local area network of personal computers
[AD-A178681] N87-23199
PERSONNEL
Selection of dimensions for an anthropometric data base. Volume 2: Dimension evaluation sheets
[AD-A179472] N87-23110
Selection of dimensions for an anthropometric data base. Volume 1: Rationale, summary, and conclusions
[AD-A179566] N87-23112
Human factors engineering data management handbook
[AD-A179691] N87-23144
Aircrew task surveys: Selection criteria for low-cost training technology applications
[AD-A178473] N87-23146
Summary of the SEI (Software Engineering Institute) Workshop on Softwear Configuration Management
[AD-A178770] N87-23184
PERSONNEL DEVELOPMENT
Aircrew task surveys: Selection criteria for low-cost training technology applications
[AD-A178473] N87-23146
PERSONNEL MANAGEMENT
Cockpit Resource Management Training
[NASA-CP-2455] N87-22634
Theory underlying CRM training: Psychological issues in flight crew performance and crew coordination
N87-22635
Group-level issues in the design and training of cockpit crews N87-22636
Cockpit Resource Management (CRM): A tool for improved flight safety (United Airlines CRM training)
N87-22637
The development and implementation of cockpit resource management in UAL recurrent training
N87-22638
Cockpit resource management training at People Express N87-22639
Cockpit management and Specific Behavioral Objectives (SBOs) N87-22640
Pan American World Airways flight training: A new direction. Flight operations resource management
N87-22641
Crew coordination concepts: Continental Airlines CRM training N87-22642
Optimum culture in the cockpit N87-22643
Introduction to Trans Australia Airlines CRM training
N87-22644
Aircrew team management program N87-22645
Remedial training: Will CRM work for everyone
N87-22646
Cockpit resource management training N87-22647
Introduction to MAC CRM training N87-22648
The application of CRM to military operations
N87-22649
Cockpit Resource Management (CRM) training in the 1550th combat crew training wing N87-22650
Cockpit Resource Management (CRM) training in the 349th military airlift wing N87-22651
Cockpit Resource Management (CRM) for part 91 and 135 operations N87-22652
Cockpit Resource Management (CRM) for FAR Parts 91 and 135 operators N87-22653
The regulatory horizon N87-22654
Instructions to working groups N87-22655
Cockpit Resource Management (CRM) and human factors training: What Air New Zealand is doing about it
N87-22658
Cockpit resource management at USAir N87-22659
PERTURBATION THEORY
Dynamic characteristics of a vibrating beam with periodic variation in bending stiffness N87-22726
Probabilistic finite elements N87-22790
Perturbative and global anomalies in supergravity theories
[DE87-701562] N87-23059
Investigation of perturbation techniques for nonlinear difference equations and other related topics
[DE87-006863] N87-23211
PETROLOGY
Reports of Planetary Geology and Geophysics Program, 1986
[NASA-TM-89810] N87-23341
Global petrologic variations of the Moon: A ternary-diagram approach N87-23407
A chemical and petrological model of the lunar crust
N87-23408
The geology of Picacho Butte, a silicic volcanic dome in northwest Arizona N87-23488
PHARMACOLOGY
Pharmacological correction of central nervous system functio during exposure to coriolis accelerations
N87-23132
PHASE COHERENCE
Measurement of the atmospheric phase coherence length, rsubo
[AD-A178468] N87-23060
PHASE DIAGRAMS
Isotactic polystyrene phase diagrams and physical gelation
[DE87-002893] N87-22850
PHASE LOCKED SYSTEMS
Optically Phase-Locked Electronic Speckle Pattern Interferometer (OPL-ESPI)
[AD-A178652] N87-22914
PHASE SHIFT
Method and apparatus for measuring minority carrier lifetime in a direct band-gap semiconductor
[NASA-CASE-NPO-16337-1-CU] N87-22894
PHASE SHIFT CIRCUITS
Ferroelectric optically controlled millimeter-wave devices
[AD-A179524] N87-22901
PHASE SHIFT KEYING
A system design requirements tool for satellite communications through nuclear-induced scintillation
[AD-A179272] N87-22871
Characterization of the error performance of a QPSK (Quadrature Phase Shift Keyed) communication system in the presence of linear transmission distortion
[AD-A178855] N87-22887
PHASE TRANSFORMATIONS
Austempered ductile iron process development
[PB87-169843] N87-22886
Non-equilibrium freezing of water-ice in sandy basaltic regoliths and implications for fluidized debris flows on Mars N87-23466
PHASE-SPACE INTEGRAL
Ion phase-space vortices and their relation to small amplitude double layers N87-23320
PHASED ARRAYS
Wideband parallel-plate waveguide, phased-array antenna
[AD-A179402] N87-22873
Optimization of the antenna pattern of a phased array with failed elements
[AD-A178581] N87-22878
PHOBOS
Cartography of irregularly shaped satellites
N87-23545
PHOTOCHEMICAL REACTIONS
The study of photochemistry at semiconductor surfaces using total internal reflection techniques
[DE87-006259] N87-23295

Unpinning of the Fermi level on GaAs by flowing water
[AD-A178489] N87-23302
PHOTOELASTICITY
Applications of fiber optics in experimental mechanics
[AD-A178683] N87-23268
PHOTOGEOLOGY
A preliminary analysis of the Mariner 10 color ratio map of Mercury N87-23439
The geology of Picacho Butte, a silicic volcanic dome in northwest Arizona N87-23488
PHOTOGRAMMETRY
Earth resources: A continuing bibliography with indexes (issue 53)
[NASA-SP-7041(53)] N87-23013
Aspects of Voyager photogrammetry N87-23547
Progress in compilation of the 1:2,000,000-scale topographic map N87-23548
PHOTOGRAPHIC FILM
White-light optical information processing and holography
[AD-A179489] N87-23260
PHOTOGRAPHY
Applications of fiber optics in experimental mechanics
[AD-A178683] N87-23268
PHOTOINTERPRETATION
Cratering and obliteration history of the south polar region of Mars N87-23506
PHOTOLUMINESCENCE
Nonlinear optical properties and subpicosecond dynamics of excitons and electron-hole plasmas in multiple quantum well structures
[AD-A179124] N87-23287
PHOTOLYSIS
Structure and properties of novel compounds of silicon germanium and tin
[AD-A179433] N87-23291
AlGaAs growth by OMCVD using an excimer laser
[NASA-TM-88937] N87-23304
PHOTOMAPPING
Tectonic domains in the Eastern Hemisphere of Mars
N87-23531
PHOTOMETERS
Optico-mechanical scanning radiometer
[DE87-007075] N87-23258
PHOTOMETRY
Dynamical studies of Saturn's rings N87-23395
PHOTOMULTIPLIER TUBES
Measurement of the atmospheric phase coherence length, rsubo
[AD-A178468] N87-23060
PHOTONS
Beamed emission from gamma-ray burst sources
N87-23332
PHOTORECEPTORS
Fundamental studies in the molecular basis of laser induced retinal damage
[AD-A178453] N87-23115
PHOTOSPHERE
East-west solar scans at 10-cm wavelength taken at the Algonquin Radio Observatory, Jan. 1980 to December 1985
[ARO-16] N87-23567
PHOTOVOLTAIC CELLS
Reliability of intermediate sized photovoltaic systems
[DE87-006328] N87-23024
Evaluation of a heliostat tracker for linear Fresnel lens photovoltaic concentrators
[DE87-006331] N87-23025
Performance characteristics of a combination solar photovoltaic heat engine energy converter
[NASA-TM-89908] N87-23028
PHOTOVOLTAIC EFFECT
Design, development and deployment of public service photovoltaic power/load systems for the Gabonese Republic
[NASA-CR-179603] N87-23030
PHYSICAL FITNESS
Relationship between a two mile run and maximal oxygen uptake
[AD-A179343] N87-23109
PHYSIOLOGICAL EFFECTS
Special features in regulating respiration under normal conditions and conditions of altered gas medium
[AD-A179216] N87-23106
PHYSIOLOGICAL FACTORS
Problems and feasibility of drug correction of orthostatic tolerance in space medicine N87-23121
PHYSIOLOGICAL RESPONSES
Workshop Symposium on Neural Models of Sensory-Motor Control
[AD-A179501] N87-23111
PHYSIOLOGY
Identification and validation of new anthropometric techniques for quantifying body composition
[AD-A178753] N87-23118
PICOSECOND PULSES
Application of picosecond CO2 lasers to particle accelerators
[DE87-003711] N87-22964
PIGMENTS
Fundamental studies in the molecular basis of laser induced retinal damage
[AD-A178453] N87-23115
PILOT PERFORMANCE
Dyads and triads at 35,000 feet: Factors affecting group process and aircrew performance N87-22656
Cockpit resource management at USAir N87-22659
Evaluation of numerator lead effects on aircraft handling qualities
[AD-A179388] N87-22687
Effect of the neutral density helmet visor on the visual acuity of navy fighter pilots
[AD-A178486] N87-23147
PILOT TRAINING
Introduction to MAC CRM training N87-22648
PINNING
Unpinning of the Fermi level on GaAs by flowing water
[AD-A178489] N87-23302
PINS
Correlations between electrical contact resistance and stages of wear in 700 Torr helium for precious metal electrical contacts
[DE87-003499] N87-22981
PIPES (TUBES)
Catalytic radiant tube. Phase 2: Proof of concept
[PB87-169835] N87-22891
Prediction of fluid flow in curved pipe using the finite element method
[AD-A179538] N87-22926
Tube coupling device
[NASA-CASE-MFS-25964-2] N87-22977
Residual stresses in girth butt welded pipes: Results and implications
[CUED/D-STRUCT/TR.109] N87-22992
PITCH (INCLINATION)
Accurate prediction of longitudinal flying qualities for landing aircraft
[AD-A179069] N87-22676
Evaluation of numerator lead effects on aircraft handling qualities
[AD-A179388] N87-22687
PITCHING MOMENTS
Investigation of periodic pitching through the static stall angle of attack
[AD-A179512] N87-22623
Verification of performance results for a low-speed 15 percent elliptical circulation control airfoil
[NASA-CR-181020] N87-22633
PLANAR STRUCTURES
Uranus and Neptune: Questions and possible answers
N87-23386
PLANE WAVES
Dynamic fracture under plane wave loading
[AD-A178594] N87-23001
PLANET EPHEMERIDES
Planetary nomenclature N87-23557
PLANETARY BOUNDARY LAYER
Field study of the effect of orographic features on planetary boundary layer models N87-23091
PLANETARY COMPOSITION
Properties of planetary fluids at high pressure and temperature N87-23399
Calcium carbonate and calcium sulfate in Martian meteorite EETA79001 N87-23409
Oxidized basalts on the surface of Venus: Compositional implications of measured spectral properties
N87-23412
On the spectral reflectance properties of materials exposed at the Viking landing sites N87-23414
Hisingerite and iddingsite on Mars: Degradation of iron-rich basalts N87-23416
Characterization of surficial units on Mars using Viking orbiter multispectral image and thermal data
N87-23418
Investigation of Martian H2O and CO2 via gamma-ray spectroscopy N87-23420
Thermal-infrared spectral observations of geologic materials in emission N87-23425
A preliminary analysis of the Mariner 10 color ratio map of Mercury N87-23439
Measurements of the dielectric constants for planetary volatiles N87-23447
PLANETARY CORES
High pressure cosmochemistry of major planetary interiors: Laboratory studies of the water-rich region of the system ammonia-water N87-23396
Lithospheric structure on Venus from tectonic modelling of compressional features N87-23516
PLANETARY CRATERS
Observations on the magnitude-frequency distribution of Earth-crossing asteroids N87-23369
PLANETARY EVOLUTION
Reports of Planetary Geology and Geophysics Program, 1986
[NASA-TM-89810] N87-23341
Analysis of planetary evolution with emphasis on differentiation and dynamics N87-23382
Accumulation of solid bodies in the solar nebula
N87-23384
Uranus and Neptune: Questions and possible answers
N87-23386
Collisional and dynamical processes in moon and planet formation N87-23387
Experiments pertaining to the formation and equilibration of planetary cores N87-23397
The origin of polarity asymmetries in the history of the geomagnetic field N87-23401
Generation of a dynamo magnetic field in a protoplanetary accretion disk N87-23403
Explosive volcanic deposits on Mars: Preliminary investigations N87-23473
Implications of Viking color data for evolution of the Amenthes Region, Mars N87-23525
PLANETARY GEOLOGY
Reports of Planetary Geology and Geophysics Program, 1986
[NASA-TM-89810] N87-23341
A preliminary analysis of the Mariner 10 color ratio map of Mercury N87-23439
High resolution thermal infrared mapping of Martian channels N87-23451
Mars: Morphology of Southern Hemisphere intracrater dunefields N87-23452
PLANETARY GRAVITATION
Dynamics of satellites, asteroids, and rings
N87-23392
Gravity data analysis N87-23400
PLANETARY MAGNETIC FIELDS
Generation of a dynamo magnetic field in a protoplanetary accretion disk N87-23403
PLANETARY MANTLES
Lithospheric structure on Venus from tectonic modelling of compressional features N87-23516
The Martian crustal dichotomy: Product of accretion and not a specific event? N87-23524
Age of fracturing and mesa development in the Elysium Area, northern Martian plains N87-23532
PLANETARY MAPPING
A compilation system for Venus radar mission (Magellan) N87-23440
Eruptive history of the Elysium Volcanic Province of Mars N87-23475
PLANETARY MASS
Accumulation of solid bodies in the solar nebula
N87-23384
A scaling law for accretion zone sizes N87-23385
PLANETARY ORBITS
Accumulation of solid bodies in the solar nebula
N87-23384
PLANETARY RINGS
Kinematics and dynamics of the Uranian rings
N87-23353
Investigations of planetary ring phenomena
N87-23360
Subcentimeter-size particle distribution functions in planetary rings from Voyager radio and photopolarimeter occultation data N87-23361
Collisional and dynamical processes in moon and planet formation N87-23387
Dynamics of satellites, asteroids, and rings
N87-23392
Hamiltonian theory of nonlinear waves in planetary rings N87-23393
Planetary ring dynamics and morphology N87-23394
Dynamical studies of Saturn's rings N87-23395
PLANETARY STRUCTURE
The production of braids in Saturn's F ring
N87-23363
High pressure cosmochemistry of major planetary interiors: Laboratory studies of the water-rich region of the system ammonia-water N87-23396
PLANETARY SURFACES
Bidirectional reflectance properties of planetary surface materials N87-23426
On the sputter alteration of regoliths of outer solar system bodies N87-23434
Solid sulfur in vacuum: Sublimation effects on surface microtexture, color and spectral reflectance, and applications to planetary surfaces N87-23438
Measurements of the dielectric constants for planetary volatiles N87-23447
Application of numerical methods to planetary radiowave scattering N87-23448
Development of wind tunnel techniques for the solution of problems in planetary Aeolian processes N87-23457
Impact and cratering processes on asteroids, satellites, and planets N87-23499

Natural fracture systems on planetary surfaces: Genetic classification and pattern randomness N87-23536
Local-scale stratigraphy of grooved terrain on Ganymede N87-23538
Stratigraphy of the south polar region of Ganymede N87-23539
Creep of ice: Further studies N87-23540
Geology of Io N87-23542
Microvax-based data management and reduction system for the regional planetary image facilities N87-23554

PLANETARY WAVES
A preliminary theory of the origin of the 40-50 day oscillation — tropical atmosphere N87-23044

PLANETOLOGY
NASA Regional Planetary Image Facility image retrieval and processing system N87-23160
Mechanical and thermal properties of planetologically important ices N87-23346

PLANETS
Collisional and dynamical processes in moon and planet formation N87-23387
High pressure cosmochemistry of major planetary interiors: Laboratory studies of the water-rich region of the system ammonia-water N87-23396

PLANNING
Elements of a proposed security methodology for networks of computers [DE87-006769] N87-23152

PLASMA CHEMISTRY
Program and abstracts of the 39th Annual Gaseous Electronics Conference [AD-A178598] N87-23247

PLASMA COMPOSITION
Nonlinear optical properties and subpicosecond dynamics of excitons and electron-hole plasmas in multiple quantum well structures [AD-A179124] N87-23287

PLASMA CONTROL
Confinement and heating of high beta plasmas with emphasis on compact toroids. Task 2: Stellarator and heliac research [DE87-005554] N87-23278
Some aspects of double layer formation in a plasma constrained by a magnetic mirror N87-23329

PLASMA CURRENTS
Some dynamical properties of very strong double layers in a triple plasma device N87-23315

PLASMA DIAGNOSTICS
Investigation of laser diagnostics of PACVD processes for depositing hard face coatings [DE87-006292] N87-22969
Confinement and heating of high beta plasmas with emphasis on compact toroids. Task 2: Stellarator and heliac research [DE87-005554] N87-23278
Plasma diagnosis by dye laser intracavity absorption [DE87-006407] N87-23280

PLASMA DIFFUSION
Development of a generalized model for a three component plasma [AD-A178979] N87-23281

PLASMA DYNAMICS
Latitudinal motions of the aurora during substorms [NASA-CR-180930] N87-23063
A preliminary study of extended magnetic field structures in the ionosphere [NASA-CR-181004] N87-23066

PLASMA ELECTRODES
Opening switch research on a dense plasma focus [AD-A179693] N87-23276

PLASMA FOCUS
Opening switch research on a dense plasma focus [AD-A179693] N87-23276

PLASMA FREQUENCIES
Numerical study of hybrid plume [AD-A179561] N87-23275
Solar active region physical parameters inferred from a thermal cyclotron line and soft X-ray spectral lines [AD-A179650] N87-23560

PLASMA GUNS
Opening switch research on a dense plasma focus [AD-A179693] N87-23276

PLASMA HEATING
Numerical study of hybrid plume [AD-A179561] N87-23275
Confinement and heating of high beta plasmas with emphasis on compact toroids. Task 2: Stellarator and heliac research [DE87-005554] N87-23278

PLASMA INTERACTIONS
Fast ion mass spectrometry and charged particle spectrography investigations of transverse ion acceleration and beam-plasma interactions [NASA-CR-168348] N87-22817
A preliminary study of extended magnetic field structures in the ionosphere [NASA-CR-181004] N87-23066
Charged particle modification of surfaces in the outer solar system N87-23435

PLASMA JETS
Double layers and plasma-wave resistivity in extragalactic jets: Cavity formation and radio-wave emission N87-23333

PLASMA LAYERS
On the thinning of the plasma sheet during substorms [AD-A178484] N87-23061
Double Layers in Astrophysics [NASA-CP-2469] N87-23313
Formation mechanisms of laboratory double layers N87-23314
Some dynamical properties of very strong double layers in a triple plasma device N87-23315
Pumping potential wells N87-23316
A laboratory investigation of potential double layers N87-23317
Experimental observation of ion-acoustic double layers in laboratory plasma N87-23318
A new hydrodynamic analysis of double layers N87-23319
Ion phase-space vortices and their relation to small amplitude double layers N87-23320
Effect of double layers on magnetosphere-ionosphere coupling N87-23321
Current driven weak double layers N87-23322
Electric fields and double layers in plasmas N87-23323
Electron acceleration in stochastic double layers N87-23324
Anomalous transport in discrete arcs and simulation of double layers in a model auroral circuit N87-23325
Weak double layers in the auroral ionosphere N87-23326
Particle simulation of auroral double layers N87-23327
Conditions for double layers in the Earth's magnetosphere and perhaps in other astrophysical objects N87-23328
Some aspects of double layer formation in a plasma constrained by a magnetic mirror N87-23329
Electric potential distributions at the interface between plasmasheet clouds N87-23330
Double layers above the aurora N87-23331
Double layers and plasma-wave resistivity in extragalactic jets: Cavity formation and radio-wave emission N87-23333
Accretion onto neutron stars with the presence of a double layer N87-23334
The formation of a double layer leading to the critical velocity phenomenon N87-23335

PLASMA OSCILLATIONS
A new hydrodynamic analysis of double layers N87-23319
Electric fields and double layers in plasmas N87-23323

PLASMA PHYSICS
Time and space resolved spectroscopy of X-ray laser experiments from 81A to 220A [DE87-005946] N87-22968
Nonlinear optical properties and subpicosecond dynamics of excitons and electron-hole plasmas in multiple quantum well structures [AD-A179124] N87-23287
Double Layers in Astrophysics [NASA-CP-2469] N87-23313

PLASMA PINCH
Opening switch research on a dense plasma focus [AD-A179693] N87-23276

PLASMA POTENTIALS
Some dynamical properties of very strong double layers in a triple plasma device N87-23315
Pumping potential wells N87-23316
A laboratory investigation of potential double layers N87-23317
Current driven weak double layers N87-23322

PLASMA PUMPING
Pumping potential wells N87-23316

PLASMA SHEATHS
Development of a generalized model for a three component plasma [AD-A178979] N87-23281

PLASMA TURBULENCE
Effect of double layers on magnetosphere-ionosphere coupling N87-23321
Some aspects of double layer formation in a plasma constrained by a magnetic mirror N87-23329

PLASMA WAVES
Magnetically insulated opening switch research [AD-A178895] N87-22918

PLASMAS (PHYSICS)
Plasma joining of metal matrix composites [AD-A178731] N87-22814
Molecular reactions at the film surface in plasma polymerization [DE87-002488] N87-22849
Some dynamical properties of very strong double layers in a triple plasma device N87-23315
Current driven weak double layers N87-23322
Electron acceleration in stochastic double layers N87-23324
Anomalous transport in discrete arcs and simulation of double layers in a model auroral circuit N87-23325
Weak double layers in the auroral ionosphere N87-23326
Particle simulation of auroral double layers N87-23327
Some aspects of double layer formation in a plasma constrained by a magnetic mirror N87-23329
The formation of a double layer leading to the critical velocity phenomenon N87-23335

PLASMASPHERE
On the thinning of the plasma sheet during substorms [AD-A178484] N87-23061

PLASTIC DEFORMATION
Superplasticity: A fundamental investigation on deformation mechanism and cavitation phenomena [AD-A179651] N87-22834
Optical strain measurement system development, phase 1 [NASA-CR-179619] N87-22960
An evaluation of microgridding techniques for determining local plastic strain distributions [AD-A178518] N87-23000

PLASTIC FLOW
Bodner-Partom viscoplastic model in STEALTH finite difference code [AD-A178994] N87-23005
Creep of ice: Further studies N87-23540

PLASTIC PROPERTIES
Superplasticity: A fundamental investigation on deformation mechanism and cavitation phenomena [AD-A179651] N87-22834
Non-linear finite element analysis program [AD-A179038] N87-23006

PLATES (TECTONICS)
Secular cooling of Earth as a source of intraplate stress N87-23519

PLENUM CHAMBERS
Experimental evaluation of blockage ratio and plenum evacuation system flow effects on pressure distribution for bodies of revolution in 0.1 scale model test section of NASA Lewis Research Center's proposed altitude wind tunnel [NASA-TP-2702] N87-22694

PLOTTING
Investigate and verify the validity of mathematical formulas and procedures in relation to data obtained from theoretical investigations and experimental observations [AD-A179564] N87-23057
Investigation into the use of normal and half-normal plots for interpreting results from screening experiments [AD-A179082] N87-23231

PLUMES
Langmuir probe surveys of an arcjet exhaust [NASA-TM-89924] N87-22807
Afterburning suppression kinetics [AD-A178967] N87-22863

POINT DEFECTS
Temperature dependence of implantation damage in strained-layer superlattices [DE87-007678] N87-23299

POINTING CONTROL SYSTEMS
Large space structures ground experiment checkout N87-22704
Structural/control interaction (payload pointing and micro-g) N87-22721
Precision pointing and control of flexible spacecraft N87-22723
Workshop on Structural Dynamics and Control Interaction of Flexible Structures N87-22728
Impact of space station appendage vibrations on the pointing performance of gimballed payloads N87-22733
Vibration isolation for line of sight performance improvement N87-22742

POISSON DENSITY FUNCTIONS
Estimation of the parameters of a modified compound poisson distribution [AD-A178540] N87-23236
Estimation of the parameters of mixtures via distance between densities or characteristic functions [AD-A178623] N87-23241

POLAND
The effect of the Tatra Mountains (Poland) on the atmospheric precipitation and air humidity during the northern and southern air flow N87-23094

POLAR CAP ABSORPTION
Investigations of the polar rain: Polar cap electron precipitation
[AD-A178876] N87-23099
POLAR CAPS
Investigations of the polar rain: Polar cap electron precipitation
[AD-A178876] N87-23099
POLAR REGIONS
Simulation model of a meteor burst communication system for data transmission protocol evaluation
[AD-A178643] N87-22881
An evaluation of the polar ice prediction system
[AD-A178522] N87-23014
Investigations of the polar rain: Polar cap electron precipitation
[AD-A178876] N87-23099
Stratigraphy of the south polar region of Ganymede
N87-23539
POLARIMETRY
Full polarimetric non-specular scattering of flat plate structures
[AD-A178853] N87-22886
POLARITY
The origin of polarity asymmetries in the history of the geomagnetic field N87-23401
POLARIZATION (WAVES)
New very high resolution radar studies of the Moon
N87-23441
POLLUTION TRANSPORT
An assessment of nitrogen oxide formation in preheated high-temperature combustion air in industrial processes
[EGG-2439] N87-23031
POLYAMIDE RESINS
Examination of high performance polymer fibers under compressive deformation
[AD-A178840] N87-22857
POLYCRYSTALS
Powder. Complex of programs for structural analysis of polycrystals
[DE87-701211] N87-23283
POLYETHYLENES
Effects of machine variables on the quality of injection mouldings. An interlaboratory trial, 2: High density polyethylene
[MOAD-328] N87-22987
POLYGONS
Origin of fractures, Martian polygonal terrain
N87-23534
POLYIMIDE RESINS
High performance polymers: Matrix resins, high strength polyquinoxalines and conducting polyaromatics
[AD-A178457] N87-22854
POLYMER CHEMISTRY
Novel polymeric LIT and divalent cation fast ion conducting materials
[DE87-006294] N87-23296
POLYMERIC FILMS
Polyenamines from aromatic diacetylenic diketones and diamines
[NASA-CASE-LAR-13444-1-CU] N87-22847
Water-absorbing capacitor system for measuring relative humidity
[NASA-CASE-NPO-16544-1-CU] N87-22953
POLYMERIZATION
Polyenamines from aromatic diacetylenic diketones and diamines
[NASA-CASE-LAR-13444-1-CU] N87-22847
Process for crosslinking and extending conjugated diene-containing polymers
[NASA-CASE-LAR-13452-1] N87-22848
Molecular reactions at the film surface in plasma polymerization
[DE87-002488] N87-22849
POLYMETHYL METHACRYLATE
The effects of candidate chemical training agents upon service materials — chemical warfare
[MOAD-317] N87-22832
POLYNOMIALS
Numerical calculation of the drag force induced by natural convection of spheres at low Grashof numbers
[DE87-006791] N87-22935
POLYPEPTIDES
Chemical sensitivity of medial vestibular nuclear neurons to enkephalins, acetylcholine, GABA and L-glutamate
N87-23131
POLYSTYRENE
Isotactic polystyrene phase diagrams and physical gelation
[DE87-002693] N87-22850
POPULATION THEORY
Robust data analysis based on characteristic functions
[AD-A178544] N87-23178
On the least favorable configuration of a selection procedure based on ranks
[AD-A178454] N87-23234
POPULATIONS
Goodness-of-fit based on integrated squared discrepancies between sample and population characteristic functions
[AD-A178763] N87-23218
On Bayes selection rules for the best exponential population with type-I censored data
[AD-A178472] N87-23235
POROSITY
Fatigue damage interaction behavior of PWA 1480
N87-22777
POROUS MATERIALS
Water-absorbing capacitor system for measuring relative humidity
[NASA-CASE-NPO-16544-1-CU] N87-22953
Centrifuge impact cratering experiments: Scaling laws for non-porous targets N87-23495
PORTABLE LIFE SUPPORT SYSTEMS
Evaluation of skeletomuscular system function in self-contained life-support system on the basis of blood biochemistry N87-23135
POSITION (LOCATION)
Estimation of ICBM (intercontinental ballistic missile) performance parameters
[AD-A179204] N87-22754
POSITION ERRORS
Probabilistic Modeling of Loran-C for nonprecision approaches N87-22607
POSITION INDICATORS
Aircraft control position indicator
[NASA-CASE-LAR-12984-1] N87-22678
POTABLE WATER
Investigation of causes of hydrogen sulfide formation in reclaimed water N87-23136
POTENTIAL GRADIENTS
The potential gradient of a plane source
[AD-A178976] N87-23223
POWDER (PARTICLES)
The role of particle substructure in the sintering of monosized titania
[DE87-007600] N87-22839
Synthesis of alumina-zirconia powders by sol-gel processing
[DE87-005721] N87-22851
Powder. Complex of programs for structural analysis of polycrystals
[DE87-701211] N87-23283
Atlas of reflectance spectra of terrestrial, lunar and meteoritic powders and frosts from 92 to 1800 •lc2)nm
N87-23427
POWDER METALLURGY
High energy high rate pulsed power processing of materials by powder consolidation and by railgun deposition
[AD-A179289] N87-22867
POWDERED ALUMINUM
Plasma joining of metal matrix composites
[AD-A178731] N87-22814
POWER CONDITIONING
SP-100 Advanced Technology Program
[NASA-TM-89888] N87-23027
POWER EFFICIENCY
Klystron transmitters
[AD-A179068] N87-22896
POWER SERIES
The exponential method
[TRITA-NA-8517] N87-23228
POWER SPECTRA
The exponential method
[TRITA-NA-8517] N87-23228
POWER SUPPLY CIRCUITS
Transient protection of electronic circuits
[AD-A178945] N87-22919
PRECIPITATION (METEOROLOGY)
Fractal analysis of radar precipitation data over hilly terrain N87-23093
The effect of the Tatra Mountains (Poland) on the atmospheric precipitation and air humidity during the northern and southern air flow N87-23094
PREDICTION ANALYSIS TECHNIQUES
Experimental characterization of deployable trusses and joints N87-22749
A three-dimensional dual potential procedure with applications to wind tunnel inlets and interacting boundary layers
[NASA-CR-180939] N87-22944
Residual stresses in girth butt welded pipes: Results and implications
[CUED/D-STRUCT/TR.109] N87-22992
On the application of the strain energy density theory in predicting crack initiation and angle of growth
[AR-004-493] N87-23011
A lagged-average 60-day forecast experiment during the 1982-83 El Nino period N87-23047
On the predicability of low-level flow during ALPEX — Alpine Experiment (ALPEX) N87-23088
PREDICTIONS
Toward the year 2000: The near future of the American civilian and military space programs
[DE87-006467] N87-22697
Progress in the prediction of unsteady heat transfwe on turbines blades N87-22769
Prediction of service life of aircraft structural components using the half-cycle method
[NASA-TM-86812] N87-23009
Development of confidence limits by pivotal functions for estimating software reliability
[NASA-TP-2709] N87-23244
PREPOLYMERS
Processible boron nitride preceramic polymers
[AD-A178907] N87-22859
PRESSURE
Composite velocity procedures for flows with pressure interaction
[AD-A179602] N87-22929
Prediction of high-speed rotor noise with a Kirchhoff formula
[AD-A178962] N87-23250
PRESSURE DISTRIBUTION
Experimental cavity pressure distributions at supersonic speeds
[NASA-TP-2683] N87-22628
Dynamic stall calculations using a Navier-Stokes solver
[AD-A178566] N87-22688
A study of fluid-dynamic pressure fields on compressor reed valves
[AD-A178584] N87-22938
PRESSURE DRAG
Investigation of periodic pitching through the static stall angle of attack
[AD-A179512] N87-22623
PRESSURE GAGES
Control systems development, research and development
[DE87-005785] N87-22868
PRESSURE OSCILLATIONS
Dynamic stall calculations using a Navier-Stokes solver
[AD-A178566] N87-22688
PROBABILITY DENSITY FUNCTIONS
Probabilistic structural analysis verification studies
N87-22786
Probabilistic load model development and validation for composite load spectra for select space propulsion engines N87-22794
PROBABILITY DISTRIBUTION FUNCTIONS
Probabilistic SSME blades structural response under random pulse loading N87-22791
Quantifying uncertainties in the structural response of SSME blades N87-22792
A modified goodness-of-fit test for the lognormal distribution with unknown scale and location parameters
[AD-A179049] N87-23226
The percentiles of the stable laws
[AD-A179025] N87-23243
PROBABILITY THEORY
Probabilistic Modeling of Loran-C for nonprecision approaches N87-22607
Determining the probability of close approach between two satellites
[AD-A179385] N87-22699
Probabilistic structural analysis to evaluate the structural durability of SSME critical components N87-22783
Probabilistic Structural Analysis Methods (PSAM) for select space propulsion system structural components
N87-22784
The NESSUS finite element code N87-22785
Advanced probabilistic method of development
N87-22788
Stochastic and hybrid-stress plate/shell finite elements for hot-section components N87-22789
Probabilistic finite elements N87-22790
Composite load spectra for select space propulsion structural components N87-22793
Probabilistic load model development and validation for composite load spectra for select space propulsion engines N87-22794
A statistical viewpoint on the theory of evidence, revision
[AD-A178958] N87-23207
Investigation into the use of normal and half-normal plots for interpreting results from screening experiments
[AD-A179082] N87-23231
Extreme value theory for suprema of random variables with regularly varying tail probabilities
[AD-A179126] N87-23233
Sensitivity analysis for stationary probabilities of a Markov chain
[AD-A178556] N87-23240

Managing uncertainty in expert systems: A probabilistic approach
[AD-A178582] N87-23246
PROBLEM SOLVING
Non-linear finite element analysis program
[AD-A179038] N87-23006
PROCESS CONTROL (INDUSTRY)
Effects of machine variables on the quality of injection mouldings. An interlaboratory trial, 2: High density polyethylene
[MQAD-328] N87-22987
PROGRAM VERIFICATION (COMPUTERS)
A program downloader and other utility software for the DATAC bus monitor unit
[OU-TM-92] N87-22618
PROGRAMMING LANGUAGES
Modeling and simulation of the WFTA (Winograd Fourier Transform Algorithm) 16 PFA (Prime Factor Algorithm) processor using the VHSIC (Very High Speed Integrated Circuit) hardware description language, volume 1
[AD-A179344] N87-22898
Programming languages for knowledge-based systems
[PB87-157228] N87-23170
OMNITAB 80: An interpretive system for statistical and numerical data anlysis
[PB87-172235] N87-23171
A graphics environment supporting the rapid prototyping of pictorial cockpit displays
[AD-A178636] N87-23182
PROJECT PLANNING
Integrated FAA Wind Shear Program plan
[DOT/FAA/DL-87/1] N87-23067
PROJECTILE CRATERING
Impacts of hemispherical granular targets: Implications for global impacts N87-23490
Impact vaporization: Late time phenomena from experiments N87-23491
Oblique impact: Projectile richochet, concomitant ejecta and momentum transfer N87-23492
Momentum transfer from oblique impacts N87-23493
Experimental studies of collision and fragmentation phenomena N87-23494
Centrifuge impact cratering experiments: Scaling laws for non-porous targets N87-23495
Impact crater scaling laws N87-23496
Centrifuge impact cratering experiments: Scaling laws for non-porous targets N87-23498
Impact and cratering processes on asteroids, satellites, and planets N87-23499
Crater production on Venus and Earth by asteroid and comet impact N87-23500
The surface age of Venus: Applying the terrestrial cratering rate N87-23501
A statistical study of Mercurian crater classes applied to the emplacement of the intercrater plains N87-23502
Studies of early intense cratering and possible saturation effects N87-23503
Early changes in gradation styles and rates on Mars N87-23505
Cratering and obliteration history of the south polar region of Mars N87-23506
Martian rampart craters: Morphologic clues for the physical state of the target at time of impact N87-23507
PROJECTILES
Numerical simulation of supersonic flow over a rotating band using flowfield blanking
[AD-A178492] N87-22624
Superconducting Augmented Rail Gun (SARG)
[AD-A179269] N87-22701
Methodology for verification of ultrasonic inspection
[AD-A179694] N87-22988
PROPELLANT TRANSFER
Thermodynamic analysis and subscale modeling of space-based orbit transfer vehicle cryogenic propellant resupply
[NASA-TM-89921] N87-22949
PROPORTIONAL COUNTERS
Cosmic ray detectors
[NASA-CR-179086] N87-22952
PROPULSION SYSTEM CONFIGURATIONS
Propulsion system technologies for thrust vectoring N87-22670
PROTECTION
Transient protection of electronic circuits
[AD-A178945] N87-22919
PROTECTIVE COATINGS
Development of advanced nickel-cadmium batteries for electric vehicle propulsion
[DOE/NV/10442-1] N87-22922
Target fabrication for high density target experiments at the University of Rochester's Laboratory for Laser Energetics
[DE87-005915] N87-22967
Investigation of laser diagnostics of PACVD processes for depositing hard face coatings
[DE87-006292] N87-22969
A statistical study of the combined effects of substrate temperature, bias, annealing, and a Cr3Si2 undercoating on the tribological properties of RF-sputtered MoS2 coatings
[DE87-007086] N87-23285
PROTEIN METABOLISM
Human blood serum proteolytic enzyme activity after stay in hypoxic environment N87-23140
PROTOCOL (COMPUTERS)
Simulation model of a meteor burst communication system for data transmission protocol evaluation
[AD-A178643] N87-22881
Throughput analysis of the IEEE 802.4 token bus standard under heavy load
[NASA-CR-180936] N87-22921
PROTOPLANETS
Accumulation of the planets N87-23378
Timescales for planetary accretion and the structure of the protoplanetary disk N87-23380
Analysis of planetary evolution with emphasis on differentiation and dynamics N87-23382
Evolution of planetesimal velocities N87-23383
Accumulation of solid bodies in the solar nebula N87-23384
A scaling law for accretion zone sizes N87-23385
Uranus and Neptune: Questions and possible answers N87-23386
Collisional and dynamical processes in moon and planet formation N87-23387
Generation of a dynamo magnetic field in a protoplanetary accretion disk N87-23403
PROTOSTARS
Protostellar disks and the primitive solar nebula N87-23379
PROTOTYPES
Microvax-based data management and reduction system for the regional planetary image facilities N87-23554
PROVING
Methodology for verification of ultrasonic inspection
[AD-A179694] N87-22988
Investigate and verify the validity of mathematical formulas and procedures in relation to data obtained from theoretical investigations and experimental observations
[AD-A179564] N87-23057
Validation of a surface-layer windflow model using climatology and meteorological tower data from Vandenberg AFB, California
[AD-A178480] N87-23097
A test of goodness of fit for multivariate normality
[AD-A178543] N87-23237
PSYCHOLOGICAL FACTORS
Theory underlying CRM training: Psychological issues in flight crew performance and crew coordination N87-22635
PSYCHOLOGICAL TESTS
Tolerance to frustration as a factor in operator performance N87-23124
PSYCHOMOTOR PERFORMANCE
Cockpit Resource Management (CRM): A tool for improved flight safety (United Airlines CRM training) N87-22637
PSYCHOPHYSICS
The perception of brightness and colour: Neurophysiology, psychophysics and computation
[AD-A179217] N87-23107
PSYCHOPHYSIOLOGY
The event related brain potential as an index of information processing and cognitive activity: A program of basic research
[AD-A179310] N87-23143
PULMONARY CIRCULATION
Evaluation of effect of positive intrapulmonary pressure on respiratory function of man N87-23134
PULSARS
Accretion onto neutron stars with the presence of a double layer N87-23334
PULSE COMMUNICATION
The effect of multipath on digital communications systems: With application to space station
[AD-A178578] N87-22876
PULSE GENERATORS
Coordinated research program in pulsed power physics
[AD-A178625] N87-22912
A system for long pulse REB generation
[IPPJ-812] N87-23274
PULSE HEATING
High energy high rate pulsed power processing of materials by powder consolidation and by railgun deposition
[AD-A179289] N87-22867
Boundary layer disturbances caused by periodic heating of a thin ribbon
[AD-A179342] N87-22925
PULSED LASERS
CO2 pulsed laser damage mechanism and plasma effects (focused beam)
[AD-A179201] N87-22961
Pulsed power for high power electron-beam pumped lasers
[DE87-004523] N87-22965
PULSES
Investigation of rocket powered, open cycle, magnetohydrodynamic generators for high, pulsed power needs in space
[AD-A178869] N87-22601
Corrosion, wear and mechanical properties of pulse-electrodeposited alloys
[AD-A178596] N87-22842
Klystron transmitters
[AD-A179068] N87-22896
Silicon pulse sharpening diodes: Switching kilovolts in 10's of picoseconds
[DE87-005073] N87-22905
PUMPS
Pumped two-phase heat transfer loop
[NASA-CASE-MSC-20841-1] N87-22950
Design, development and deployment of public service photovoltaic power/load systems for the Gabonese Republic
[NASA-CR-179603] N87-23030
PURSUIT TRACKING
On non-parametric discrimination using series expansions and projection pursuit
[AD-A178455] N87-23213
PYRAMIDS
Custom-made pyramids
[AD-A178955] N87-23186
The scale-space formulation of pyramid data structures
[AD-A178960] N87-23222
PYRENEES MOUNTAINS (EUROPE)
Dynamics and evolution of the Pyrenees lee wave event during 21-23 March 1982 N87-23079
An analysis of downslope winds in the lee of the Pyrenees on 23 March 1982 N87-23081
Cierzo: Northwesterly wind along the Ebro Valley (Spain) as a mesoscale effect induced on the lee of the Pyrenees mountain range; a case study during the Alpine Experiment (ALPEX) Special Observing Period N87-23083
PYRIDINES
Structural panels
[NASA-CASE-ARC-11429-2-CU] N87-22845
PYROLYSIS
Structure and properties of novel compounds of silicon germanium and tin
[AD-A179433] N87-23291
PYROPHORIC MATERIALS
Decomposition of energetic materials combustion of decoy materials
[AD-A178447] N87-22827

Q

QUADRATIC EQUATIONS
Characterization of the error performance of a QPSK (Quadrature Phase Shift Keyed) communication system in the presence of linear transmission distortion
[AD-A178855] N87-22887
QUALITATIVE ANALYSIS
Integrated restructurable flight control system demonstration results
[NASA-CR-178305] N87-22692
QUALITY CONTROL
Effects of machine variables on the quality of injection mouldings. An interlaboratory trial, 2: High density polyethylene
[MQAD-328] N87-22987
Methodology for verification of ultrasonic inspection
[AD-A179694] N87-22988
QUANTUM CHROMODYNAMICS
The chiral symmetry aspects of supersymmetric confining gauge theories
[ETN-87-99553] N87-23305
QUANTUM ELECTRONICS
Nonlinear optical properties and subpicosecond dynamics of excitons and electron-hole plasmas in multiple quantum well structures
[AD-A179124] N87-23287
SIS (Superconductor-Insulator-Superconductor) mixer research
[AD-A179604] N87-23293
QUANTUM THEORY
Relativistic calculations and measurements of energies, Auger rates, and lifetimes
[AD-A179137] N87-23251

QUARKS
The chiral symmetry aspects of supersymmetric confining gauge theories
[ETN-87-99553] N87-23305
QUEUEING THEORY
Specifying functional and timing behavior for real-time applications
[AD-A178769] N87-23206

R

RADAR ASTRONOMY
High resolution radar map of the Moon N87-23442
Landform identification: Lunar radar images N87-23443
Goldstone radar observations of Mars: The 1986 opposition N87-23444
Mars: Seasonally variable radar reflectivity N87-23446
RADAR CORNER REFLECTORS
Full polarimetric non-specular scattering of flat plate structures
[AD-A178853] N87-22886
RADAR ECHOES
Goldstone radar observations of Mars: The 1986 opposition N87-23444
Mars: Seasonally variable radar reflectivity N87-23446
RADAR IMAGERY
A compilation system for Venus radar mission (Magellan) N87-23440
New very high resolution radar studies of the Moon N87-23441
High resolution radar map of the Moon N87-23442
Landform identification: Lunar radar images N87-23443
RADAR MAPS
A compilation system for Venus radar mission (Magellan) N87-23440
High resolution radar map of the Moon N87-23442
RADAR MEASUREMENT
Wideband parallel-plate waveguide, phased-array antenna
[AD-A179402] N87-22873
RADAR RANGE
Wideband parallel-plate waveguide, phased-array antenna
[AD-A179402] N87-22873
RADAR RESOLUTION
New very high resolution radar studies of the Moon N87-23441
High resolution radar map of the Moon N87-23442
Landform identification: Lunar radar images N87-23443
RADAR SCATTERING
New very high resolution radar studies of the Moon N87-23441
A diffuse radar scattering model from Martian surface rocks N87-23445
Mars: Seasonally variable radar reflectivity N87-23446
RADAR TARGETS
Radar target classification studies
[AD-A179010] N87-22889
RADAR TRACKING
Millimeter wave Doppler radar observation of cloud and boundary layer structure
[AD-A178679] N87-23098
RADAR TRANSMITTERS
Klystron transmitters
[AD-A179068] N87-22896
RADIANT FLUX DENSITY
Frequency spectrum of soft X-ray emission from transition radiation
[AD-A178858] N87-23254
RADIANT HEATING
Catalytic radiant tube. Phase 2: Proof of concept
[PB87-168835] N87-22891
RADIATION ABSORPTION
New methods for obtaining scattering and absorption from tropospheric visible spectrum data
[AD-A178590] N87-23062
Frequency spectrum of soft X-ray emission from transition radiation
[AD-A178858] N87-23254
Non-Markovian line shapes of physisorbed atoms on a crystal
[AD-A179525] N87-23292
RADIATION DAMAGE
Radiation damage to coatings for short wave length laser mirrors
[DE87-001696] N87-22963
RADIATION DETECTORS
Dose enhancement effects in the Aerospace Corporation Co-60 irradiator
[AD-A178481] N87-23253
RADIATION DISTRIBUTION
Angular distribution of transition radiation in the soft X-ray spectrum
[AD-A178859] N87-23255
RADIATION DOSAGE
Dose enhancement effects in the Aerospace Corporation Co-60 irradiator
[AD-A178481] N87-23253
RADIATION EFFECTS
Development of radiation hard graded index optical fibers
[AD-A178465] N87-23265
Radiation hardened silica-based optical fibers
[AD-A178466] N87-23266
Temperature dependence of implantation damage in strained-layer superlattices
[DE87-007678] N87-23299
RADIATION HARDENING
Development of radiation hard graded index optical fibers
[AD-A178465] N87-23265
RADIATION MEASURING INSTRUMENTS
Dose enhancement effects in the Aerospace Corporation Co-60 irradiator
[AD-A178481] N87-23253
RADIATION SHIELDING
Dose enhancement effects in the Aerospace Corporation Co-60 irradiator
[AD-A178481] N87-23253
RADIATION SOURCES
Dose enhancement effects in the Aerospace Corporation Co-60 irradiator
[AD-A178481] N87-23253
RADIATION SPECTRA
Frequency spectrum of soft X-ray emission from transition radiation
[AD-A178858] N87-23254
RADIATIVE HEAT TRANSFER
Heat transfer in an organic heat pipe
[LA-10781-MS] N87-22946
RADIATIVE TRANSFER
Numerical studies of collapsing interstellar clouds
[NASA-CR-180933] N87-23340
Nonlinear aspects of planar condensational instability
[AD-A178998] N87-23565
RADIO COMMUNICATION
A system design requirements tool for satellite communications through nuclear-induced scintillation
[AD-A179272] N87-22871
RADIO FREQUENCIES
A system design requirements tool for satellite communications through nuclear-induced scintillation
[AD-A179272] N87-22871
Klystron transmitters
[AD-A179068] N87-22896
Development of nickel oxide/hydrogen multilayer bipolar battery for pulsed power
[AD-A178844] N87-22917
RADIO FREQUENCY INTERFERENCE
Electromagnetic emission experiences using electric propulsion systems: A survey
[NASA-TM-100120] N87-22805
RADIO OCCULTATION
Subcentimeter-size particle distribution functions in planetary rings from Voyager radio and photopolarimeter occultation data N87-23361
RADIO SOURCES (ASTRONOMY)
J. VLA (Very Large Array) of a solar noise storm
[NASA-CR-180219] N87-23561
RADIO TELESCOPES
J. VLA (Very Large Array) of a solar noise storm
[NASA-CR-180219] N87-23561
RADIO TRANSMITTERS
Preliminary investigation of ionospheric modification using oblique incidence high power HF radio waves
[AD-A179174] N87-23056
RADIO WAVES
A preliminary summary of the observations of the 16 February 1984 solar flare (STIP Interval XV, 12-21 February 1984)
[NASA-CR-180929] N87-23563
RADIOACTIVE ISOTOPES
Dose enhancement effects in the Aerospace Corporation Co-60 irradiator
[AD-A178481] N87-23253
RADIOMETERS
Optico-mechanical scanning radiometer
[DE87-007075] N87-23258
Fundamentals and techniques of nonimaging optics research at the University of Chicago
[DE87-006917] N87-23264
RAILGUN ACCELERATORS
Superconducting Augmented Rail Gun (SARG)
[AD-A179269] N87-22701
RAIN
Investigations of the polar rain: Polar cap electron precipitation
[AD-A178876] N87-23099
RAMAN LASERS
The use of the Karl sub-scale laser for Raman beam clean-up experiments
[AD-A178483] N87-22971
RAMAN SPECTROSCOPY
Frequency shift measurements of the Q(1) and Q(2) lines of H2 using high resolution CW Coherent Anti-Stokes Raman Spectroscopy
[AD-A179390] N87-22820
RANDOM LOADS
Probabilistic SSME blades structural response under random pulse loading N87-22791
RANDOM NOISE
Linear time invariant system identification using a result of the Bussgang theorem
[AD-A178642] N87-23216
Estimation of the parameters of a modified compound poisson distribution
[AD-A178540] N87-23236
RANDOM VARIABLES
Extreme value theory for suprema of random variables with regularly varying tail probabilities
[AD-A179126] N87-23233
Estimation of the parameters of a modified compound poisson distribution
[AD-A178540] N87-23236
RANKING
On the least favorable configuration of a selection procedure based on ranks
[AD-A178454] N87-23234
RATIOS
Magnetically insulated opening switch research
[AD-A178895] N87-22918
RAY TRACING
Calculation of ray paths in the ionosphere using an analytic raytracing technique
[AD-A178888] N87-23064
REACTION KINETICS
An analysis of artificial viscosity effects on reacting flows using a spectral multi-domain technique
[NASA-CR-178308] N87-22632
Molecular reactions at the film surface in plasma polymerization
[DE87-002488] N87-22849
Afterburning suppression kinetics
[AD-A178967] N87-22863
Development of nickel oxide/hydrogen multilayer bipolar battery for pulsed power
[AD-A178844] N87-22917
Thermodynamic properties of molten salt solutions
[DE87-004948] N87-23306
REACTION PRODUCTS
Process for crosslinking and extending conjugated diene-containing polymers
[NASA-CASE-LAR-13452-1] N87-22848
REACTION TIME
Visual acuity and reaction time in navy fighter pilots
[AD-A178485] N87-23117
REACTION WHEELS
Vibration isolation for line of sight performance improvement N87-22742
REACTOR CORES
Considerations pertinent to the Doppler effect for space reactors
[DE87-007032] N87-23252
READING
Reading patterns in online documentation: How transcript analysis reflects text design, software constraints, and user preferences
[DE87-006466] N87-23174
REAL TIME OPERATION
HEPA filter monitoring program
[RFP-3874] N87-22869
Real-time laser holographic interferometry for aerodynamics
[NASA-TM-89462] N87-22956
The use of real-time optical processors in embedded computing
[DE87-006895] N87-23153
The design of a real time operating system for a fault tolerant microcomputer
[AD-A178577] N87-23155
Applications and requirements for real-time simulators in ground-test facilities
[NASA-TP-2672] N87-23202
Specifying functional and timing behavior for real-time applications
[AD-A178769] N87-23206

RECTANGULAR PANELS
Effects of cutout orientations on natural frequencies and mode shapes of curved rectangular composite panels [AD-A178638] N87-22813

RECTIFIERS
Full-wave analysis of isolated and coupled microwave transmission lines using the finite element method [AD-A178605] N87-22883

REDUCED GRAVITY
Structural/control interaction (payload pointing and micro-g) N87-22721
Containerless processing of glass forming melts: D-1, MEA/A-2 experiment 81F01 conducted on STS-61A flight, October 1985 [NASA-CR-179118] N87-22861
Structure and function of otoliths N87-23122

REDUNDANT COMPONENTS
Analysis of structures with rotating, flexible substructures [AD-A178903] N87-23004

REENTRY VEHICLES
Computational aerothermodynamics [NASA-TM-89450] N87-22943

REFLECTANCE
Deconvolution of spectra for intimate mixtures N87-23428
Photometric properties of lunar terrains derived from Hapke's equation N87-23432
Bidirectional reflectance spectroscopy — for Moon, asteroid, Europa, and Oberon N87-23433
Charged particle modification of surfaces in the outer solar system N87-23435
Io: Comparison of photometric scans produced by the Minnaert and Hapke functions N87-23436
Mars: Seasonally variable radar reflectivity N87-23446
Bright sand/dark dust: The identification of active sand surfaces on the Earth and Mars N87-23449
Timing of frost deposition on Martian dunes: A clue to properties of dune particles? N87-23453

REFLECTION
The study of photochemistry at semiconductor surfaces using total internal reflection techniques [DE87-006259] N87-23295

REFLECTOR ANTENNAS
Detection of reflector surface error from near-field data: Effect of edge diffracted field [NASA-TM-89920] N87-22874

REFRACTORY MATERIALS
Artificial composites for high temperature applications: A review [DME-007] N87-22808
Low-pressure self-propagating high-temperature synthesis [AD-A178593] N87-22856

REFRIGERATING MACHINERY
A study of fluid-dynamic pressure fields on compressor reed valves [AD-A178584] N87-22938

REGENERATIVE FUEL CELLS
High temperature solid oxide regenerative fuel cell for solar photovoltaic energy storage [NASA-TM-89672] N87-23020

REGOLITH
A search for spectral alteration effects in chondritic gas-rich breccias N87-23375
The role of regolith adsorption in the transition from early to late Mars climate N87-23411
CO2: Adsorption on palagonite and the Martian regolith N87-23419
Photometric properties of lunar terrains derived from Hapke's equation N87-23432
On the sputter alteration of regoliths of outer solar system bodies N87-23434
Non-equilibrium freezing of water-ice in sandy basaltic regoliths and implications for fluidized debris flows on Mars N87-23466

REGRESSION ANALYSIS
A collection and statistical analysis of biophysical data to predict motion sickness incidence [AD-A178874] N87-23119
On non-parametric discrimination using series expansions and projection pursuit [AD-A178455] N87-23213
Self-critical and robust procedures for the analysis of binary data [AD-A178935] N87-23221
Estimating the standard error of robust regression estimates [AD-A179099] N87-23232
A Bayesian statistics year at the Ohio State University [AD-A178762] N87-23242

REGRESSION COEFFICIENTS
Estimating the standard error of robust regression estimates [AD-A179099] N87-23232

REGULATIONS
The regulatory horizon N87-22654

REINFORCEMENT RINGS
Tube coupling device [NASA-CASE-MFS-25964-2] N87-22977

REINFORCING FIBERS
Characterization of hybridized conductive composites [AD-A179669] N87-22810

RELATIVISTIC ELECTRON BEAMS
A system for long pulse REB generation [IPPJ-812] N87-23274

RELAXATION (MECHANICS)
Non-Newtonian ice rheology and the retention of craters on Ganymede N87-23511

RELIABILITY
Reliability studies of ceramic capacitors [AD-A179436] N87-22900
Reliability of intermediate sized photovoltaic systems [DE87-006328] N87-23024

RELIABILITY ANALYSIS
NESSUS/expert and NESSUS/FPI in the Probabilistic Structural Analysis Methods (PSAM) program N87-22787
Advanced probabilistic method of development N87-22788
Development of confidence limits by pivotal functions for estimating software reliability [NASA-TP-2709] N87-23244

RELIEF MAPS
A compilation system for Venus radar mission (Magellan) N87-23440

REMOTE CONTROL
Advanced technology mobile robotics vehicle fleet [DE87-007526] N87-22982
Apparatus and method of capturing an orbiting spacecraft [NASA-CASE-MSC-20979-1] N87-22985

REMOTE MANIPULATOR SYSTEM
Apparatus and method of capturing an orbiting spacecraft [NASA-CASE-MSC-20979-1] N87-22985

REMOTE SENSING
Investigation of air transportation technology at Ohio University, 1984 N87-22609
Earth resources: A continuing bibliography with indexes (issue 53) [NASA-SP-7041(53)] N87-23013
Development of Land Analysis System display modules N87-23169
Mid-infrared spectroscopic investigation N87-23424
Bidirectional reflectance properties of planetary surface materials N87-23426
Deconvolution of spectra for intimate mixtures N87-23428
A diffuse radar scattering model from Martian surface rocks N87-23445
Bright sand/dark dust: The identification of active sand surfaces on the Earth and Mars N87-23449
Bilateral symmetry across Aphrodite Terra N87-23518

REMOTE SENSORS
Laser reflectance as a function of rough water glitter profile [AD-A178774] N87-23016
Automatic pattern recognition and related topics [AD-A178595] N87-23267

RENAL FUNCTION
Effect of short-term spaceflights on activity of renin-angiotension-aldosterone system, concentration of cyclic nucleotides and prostaglandins in blood N87-23125

REQUIREMENTS
Guidelines for applying the Composite Specification Model (CSM) [NASA-TM-89374] N87-23193

RESCUE OPERATIONS
Apparatus and method of capturing an orbiting spacecraft [NASA-CASE-MSC-20979-1] N87-22985

RESEARCH AND DEVELOPMENT
Materials Information for Science and Technology (MIST). Project overview: Phase 1 and 2 and general considerations [DE87-006799] N87-23312

RESEARCH FACILITIES
Heat flux calibration facility capable of SSME conditions N87-22774
Helicopter transmission testing at NASA Lewis Research Center [NASA-TM-89912] N87-22978
Cooperative research opportunities at NBS (National Bureau of Standards) [PB87-157236] N87-23309
The Galilean satellite geological mapping program, 1986 N87-23544

RESEARCH MANAGEMENT
Cooperative research opportunities at NBS (National Bureau of Standards) [PB87-157236] N87-23309

RESIDUAL STRESS
Residual stresses in girth butt welded pipes: Results and implications [CUED/D-STRUCT/TR.109] N87-22992

RESISTORS
Electrochemical adjustment of thin film Ti-Pd resistors [DE87-007392] N87-22837

RESOLUTION
Two-point resolution criterion for multi-aperture optical systems [AD-A178960] N87-23271

RESONANCE
On the lack of commensurabilities in the mean motions of the satellites of Uranus and the resurfacing of Ariel N87-23349
Why no orbital resonances among the satellites of Uranus? N87-23351
Observational studies of Saturn's rings N87-23362

RESONANT FREQUENCIES
Commit your works to the Lord, and your thoughts shall be established (Prov. 16:3). Inter-stable control systems N87-22716
Effects of cutout orientations on natural frequencies and mode shapes of curved rectangular composite panels [AD-A178638] N87-22813
A coherent VLSI environment [AD-A179303] N87-22897

RESOURCE ALLOCATION
LRS: A knowledge based approach to launch resource scheduling [AD-A179426] N87-23310

RESPIRATION
Special features in regulating respiration under normal conditions and conditions of altered gas medium [AD-A179216] N87-23106

RESPIRATORY REFLEXES
Special features in regulating respiration under normal conditions and conditions of altered gas medium [AD-A179216] N87-23106
Evaluation of effect of positive intrapulmonary pressure on respiratory function of man N87-23134

RESPONSE TIME (COMPUTERS)
An experimental study of load balancing performance [AD-A179322] N87-23195

RESPONSES
Asymmetries in the control of saccadic eye movements to bifurcating targets [AD-A179270] N87-23108

RETINA
Fundamental studies in the molecular basis of laser induced retinal damage [AD-A178453] N87-23115

RETRAINING
Remedial training: Will CRM work for everyone N87-22646

REVERSE FIELD PINCH
Analysis of the effects of impurity buildup on the performance of a reversed field pinch [DE87-005436] N87-23277

REYNOLDS NUMBER
Reynolds number effects on surface shear stress patterns around isolated hemispheres N87-23459

RHEA (ASTRONOMY)
Studies of early intense cratering and possible saturation effects N87-23503

RHEOLOGY
Physical properties and structure of ion-containing polymers [AD-A178592] N87-22855
Laboratory characterization tests for antimisting fuel [DOT/FAA/CT-86/23] N87-22884
Martian volcanism: Festoon-like ridges on terrestrial basalt flows and implications for Mars N87-23478
Studies of fluid instabilities in flows of lava and debris N87-23479
Non-Newtonian ice rheology and the retention of craters on Ganymede N87-23511

RHONE DELTA (FRANCE)
Numerical study of the Mistral with a mesoscale model N87-23082

RIBBONS
Characterization of rapidly solidified Al-Be-Li and Al-Be ribbons [DE87-006613] N87-22835

RIGID STRUCTURES
Numerical methods for imperfection sensitivity analysis of stiffened cylindrical shells. Volume 1: Development and applications [AD-A179686] N87-22995

RINGS
Revised NASA axially symmetric ring model for coupled-cavity traveling-wave tubes
[NASA-TP-2675] N87-22923
RIPPLES
Wind ripples in low density atmospheres N87-23454
RISK
The applicability of the stable laws in collective risk theory and practice
[AD-A178546] N87-23238
RIVERS
The application of flow competence evaluations to the assessment of flood-flow velocities and stresses
N87-23464
RL-10 ENGINES
High heat transfer oxidizer heat exchanger design and analysis --- RL10-2B engine
[NASA-CR-179596] N87-22803
ROBOTICS
Advanced technology mobile robotics vehicle fleet
[DE87-007526] N87-22982
ROBOTS
A 3-D world modeling based on combinatorial geometry for autonomous robot navigation
[DE87-002814] N87-22980
Advanced technology mobile robotics vehicle fleet
[DE87-007526] N87-22982
Tactile feedback for teleoperator systems
[AD-A179054] N87-22983
Automated non-destructive testing using an industrial robot
[AERE-R-12308] N87-22986
ROCKET ENGINES
Optimal shuttle altitude changes using tethers
[AD-A179205] N87-22756
ROCKET EXHAUST
Afterburning suppression kinetics
[AD-A178967] N87-22863
Numerical study of hybrid plume
[AD-A179561] N87-23275
ROCKS
On the spectral reflectance properties of materials exposed at the Viking landing sites N87-23414
Spectral mixture modeling: Further analysis of rock and soil types at the Viking Lander sites N87-23415
Thermal-infrared spectral observations of geologic materials in emission N87-23425
A diffuse radar scattering model from Martian surface rocks N87-23445
ROCKY MOUNTAINS (NORTH AMERICA)
Characteristics of orographically initiated convection --- Rocky Mountains N87-23092
ROLL FORMING
A novel rollability test
[RFP-3901] N87-22984
ROTARY GYROSCOPES
Closed loop fiber optic rotation sensor
[NASA-CASE-NPO-16558-1-CU] N87-23259
ROTARY WING AIRCRAFT
Analysis of structures with rotating, flexible substructures applied to rotorcraft aeroelasticity in GRASP (General Rotorcraft Aeromechanical Stability Program)
[AD-A178941] N87-22677
Correlation of analytical calculations from GRASP (General Rotorcraft Aeromechanical Stability Program) with torsionally-soft rotor data
[AD-A178881] N87-22689
ROTARY WINGS
Prediction of high-speed rotor noise with a Kirchhoff formula
[AD-A178982] N87-23250
ROTATING BODIES
Numerical simulation of supersonic flow over a rotating band using flowfield blanking
[AD-A178492] N87-22624
ROTATION
Analysis of structures with rotating, flexible substructures
[AD-A178903] N87-23004
ROTOR AERODYNAMICS
AI (Artificial Intelligence) gas turbine rotor diagnostics
[AD-A178996] N87-22683
Unsteady stator/rotor interaction N87-22767
Prediction of high-speed rotor noise with a Kirchhoff formula
[AD-A178982] N87-23250
ROTOR BLADES
Experimental and theoretical studies of time-averaged and time resolved rotor heat transfer N87-22770
ROTOR BLADES (TURBOMACHINERY)
Application of advanced computational codes in the design of an experiment for a supersonic throughflow fan rotor
[NASA-TM-88915] N87-22630
Results of the integration of a transonic full-potential analysis program with a free-wake lifting-line program for hovering rotors
[NASA-TM-89494] N87-22631
Unsteady stator/rotor interaction N87-22767
ROTORS
Statistics on aircraft gas turbine engine rotor failures that occurred in US commercial aviation during 1981
[DOT/FAA/CT-86/42] N87-22684
A comparison of predicted wind turbine blade loads to test measurements
[DE87-001130] N87-23021
ROVING VEHICLES
Martian terrains N87-23555
RUBBER
A Simplex optimisation technique for development of rubber formulations
[ARE-TM(UMT)-86405] N87-22846
RUNNING
Relationship between a two mile run and maximal oxygen uptake
[AD-A179343] N87-23109
RUNWAY ALIGNMENT
Loran-C approach considerations N87-22612

S

S WAVES
Investigation of low-amplitude shear wave velocity in anisotropic material
[AD-A179563] N87-22994
S-N DIAGRAMS
A new formulation of mean stress effects in fatigue
N87-22778
SACCADIC EYE MOVEMENTS
Asymmetries in the control of saccadic eye movements to bifurcating targets
[AD-A179270] N87-23108
SAMPLES
Goodness-of-fit based on integrated squared discrepancies between sample and population characteristic functions
[AD-A178763] N87-23218
SAMPLING
Optical dynamics experiment (ODEX) data report R/V acania expedition 10 October-17 November 1982. Volume 2: Particle size distributions. Volume 6: Scalar spectral-radiometer data
[AD-A178535] N87-23104
A modified goodness-of-fit test for the lognormal distribution with unknown scale and location parameters
[AD-A179049] N87-23226
SANDS
Investigation of low-amplitude shear wave velocity in anisotropic material
[AD-A179563] N87-22994
Bright sand/dark dust: The identification of active sand surfaces on the Earth and Mars N87-23449
Mars: Morphology of Southern Hemisphere intracrater dunefields N87-23452
Timing of frost deposition on Martian dunes: A clue to properties of dune particles? N87-23453
Wind ripples in low density atmospheres N87-23454
Eolian saltation on Mars N87-23455
Mass transport by Aeolian saltation on Earth, Mars and Venus: The effects of full saltation cloud development and choking N87-23456
Aeolian abrasion on Venus: Preliminary results from the Venus simulator N87-23458
SATELLITE ALTIMETRY
Altimeter measurements for the determination of the Earth's gravity field
[NASA-CR-180520] N87-23033
SATELLITE ATTITUDE CONTROL
Star sensor fine attitude pointing model for a spinning geosynchronous satellite
[AD-A179424] N87-22763
SATELLITE COMMUNICATION
A system design requirements tool for satellite communications through nuclear-induced scintillation
[AD-A179272] N87-22871
SATELLITE IMAGERY
The Mistral-Tramuntana shear line. A satellite observation N87-23084
Characteristics of orographically initiated convection --- Rocky Mountains N87-23092
Naval applications of a TAE-derived executive
N87-23167
Bright sand/dark dust: The identification of active sand surfaces on the Earth and Mars N87-23449
Voyager cartography N87-23546
Aspects of Voyager photogrammetry N87-23547
The control network of Mars: October 1986
N87-23551
Microvax-based data management and reduction system for the regional planetary image facilities
N87-23554
Enhanced LANDSAT images of Antarctica and planetary exploration N87-23558
SATELLITE NETWORKS
Design of GPS (Global Positioning System) status reporting system
[AD-A179334] N87-22662
SATELLITE OBSERVATION
Satellite surveying for a Loran-C nonprecision approach N87-22613
Earth resources: A continuing bibliography with indexes (issue 53)
[NASA-SP-7041(53)] N87-23013
The Mistral-Tramuntana shear line. A satellite observation N87-23084
SATELLITE ORBITS
Determining the probability of close approach between two satellites
[AD-A179385] N87-22699
Optimal shuttle altitude changes using tethers
[AD-A179205] N87-22756
Solar system dynamics N87-23390
Dynamics of satellites, asteroids, and rings
N87-23392
SATELLITE ROTATION
Solar system dynamics N87-23390
Orbital resonances, unusual configurations and exotic rotation states among planetary satellites N87-23391
SATELLITE SOUNDING
Standard-resolution TOVS observations for the FIRE/SRB Wisconsin experiment region from October 9 through November 2, 1986
[NASA-TM-89151] N87-23101
SATELLITE SURFACES
The cratering record at Uranus: Implications for satellite evolution and the origin of impacting objects
N87-23342
Cratering history of Miranda N87-23344
On the lack of commensurabilities in the mean motions of the satellites of Uranus and the resurfacing of Ariel
N87-23349
Orbital dynamics of the Uranian satellites based on Voyager data N87-23350
Voyager observations of 1985U1 N87-23352
Accretional heating of the satellites of Saturn and Uranus N87-23355
Investigations of the surfaces and interiors of outer planet satellites N87-23356
On the sputter alteration of regoliths of outer solar system bodies N87-23434
Charged particle modification of surfaces in the outer solar system N87-23435
Io: Comparison of photometric scans produced by the Minnaert and Hapke functions N87-23436
Sulfur-oxygen processes on Io N87-23437
Solid sulfur in vacuum: Sublimation effects on surface microtexture, color and spectral reflectance, and applications to planetary surfaces N87-23438
Measurements of the dielectric constants for planetary volatiles N87-23447
Application of numerical methods to planetary radiowave scattering N87-23448
SATELLITE TRANSMISSION
A system design requirements tool for satellite communications through nuclear-induced scintillation
[AD-A179272] N87-22871
SATELLITE-BORNE PHOTOGRAPHY
The control network of Mars: October 1986
N87-23551
The Mars observer camera N87-23556
SATURN (PLANET)
Investigations of planetary ring phenomena
N87-23360
Subcentimeter-size particle distribution functions in planetary rings from Voyager radio and photopolarimeter occultation data N87-23361
Hamiltonian theory of nonlinear waves in planetary rings N87-23393
Planetary ring dynamics and morphology N87-23394
Dynamical studies of Saturn's rings N87-23395
Properties of planetary fluids at high pressure and temperature N87-23399
SATURN RINGS
Observational studies of Saturn's rings N87-23362
The production of braids in Saturn's F ring
N87-23363
SATURN SATELLITES
Accretional heating of the satellites of Saturn and Uranus N87-23355
Charged particle modification of surfaces in the outer solar system N87-23435
Voyager cartography N87-23546

SCALARS
Conditional second order closure for turbulent shear flows [AD-A179661] N87-22931
SCALE EFFECT
Development of wind tunnel techniques for the solution of problems in planetary Aeolian processes N87-23457
SCALE MODELS
Considerations in the design and development of a space station scale model N87-22711
Development of wind tunnel techniques for the solution of problems in planetary Aeolian processes N87-23457
SCALING LAWS
Verification of large beam-type space structures N87-22712
A scaling law for accretion zone sizes N87-23385
Centrifuge impact cratering experiments: Scaling laws for non-porous targets N87-23495
Impact crater scaling laws N87-23496
Centrifuge impact cratering experiments: Scaling laws for non-porous targets N87-23498
SCANNING
Wideband parallel-plate waveguide, phased-array antenna [AD-A179402] N87-22873
Optico-mechanical scanning radiometer [DE87-007075] N87-23258
Io: Comparison of photometric scans produced by the Minnaert and Hapke functions N87-23436
SCATTERING
Studies of the scattering/absorption of minerals N87-23423
SCENE ANALYSIS
Automatic scene analysis using hierarchical spatial frequency domain correlation with energy normalization and heuristic noise reduction [AD-A178589] N87-23181
SCHEDULING
A prototype expert system advisor for satellite support scheduling [AD-A179425] N87-22760
SCHROEDINGER EQUATION
Generalized quantal equation of motion [DE87-701531] N87-23307
SCIENTISTS
The Galilean satellite geological mapping program, 1986 N87-23544
SCINTILLATION
A system design requirements tool for satellite communications through nuclear-induced scintillation [AD-A179272] N87-22871
SCINTILLATION COUNTERS
Cosmic ray detectors [NASA-CR-179086] N87-22952
SEA STATES
Laser reflectance as a function of rough water glitter profile [AD-A178774] N87-23016
SEA SURFACE TEMPERATURE
Workshop on Comparison of Simulations by Numerical Models of the Sensitivity of the Atmospheric Circulation to Sea Surface Temperature Anomalies [WCP-121] N87-23034
Numerical experiments on the atmospheric response to a sea surface temperature anomaly over the equatorial eastern Pacific Ocean N87-23036
Sensitivity of tropical and mid-latitude time-averaged atmospheric states to interannually varying global ocean surface temperature distribution N87-23039
Preliminary results from a Tropical Ocean Global Atmosphere (TOGA) related experiment performed at Hamburg (West Germany) with the ECWME General Circulation Model (GCM) with T21 resolution N87-23040
Principal circulation anomalies in model atmospheres with and without interannual variations of tropical Pacific SST — sea surface temperature (SST) N87-23041
Forecast and sensitivity experiments on the UK Meteorological Office GCM with El Nino SST anomalies — general circulation model (GCM) sea surface temperature (SST) N87-23045
The impact of initial conditions and SST Anomalies on extended range predictions for the El Nino period — sea surface temperature (SST) N87-23046
A lagged-average 60-day forecast experiment during the 1982-83 El Nino period N87-23047
Sensitivity of the NMC spectral mode to the January 1983 El Nino SST — sea surface temperature N87-23048
Tropical Pacific SST experiments with the GLAS climate model — sea surface temperature (SST) N87-23049
The impact of SST anomalies and initial conditions on extended range predictions with an atmospheric general circulation model: A case study in early summer of 1983 N87-23051
Sensitivity of January 1983 Sea Surface Temperature (SST)-experiments to the formulation of lateral diffusion N87-23052
SEA TRUTH
The SIR-B mission: Towards an understanding of internal waves in the ocean [ARE-TR-86122] N87-23102
SEA WATER
Optical dynamics experiment (ODEX) data report R/V acania expedition 10 October-17 November 1982. Volume 2: Particle size distributions. Volume 6: Scalar spectral-radiometer data [AD-A178535] N87-23104
SEALS (STOPPERS)
SSME blade damper technology N87-22798
SEARCHING
Performance evaluation of parallel branch and bound search with the intel IPSC (Intel Personal SuperComputer) hypercube computer [AD-A179384] N87-23196
SEAS
Geomorphic evidence for ancient seas in west Deuteronilus Mensae, Mars-1: Regional geomorphology N87-23471
Geomorphic evidence for ancient seas in west Deuteronilus Mensae, Mars-2: From very high resolution Viking Orbiter images N87-23472
SEASONS
Mars: Seasonally variable radar reflectivity N87-23446
Regional sources and sinks of dust on Mars: Viking observations of Cerberus, Solis Planum and Syrtis Major N87-23450
Timing of frost deposition on Martian dunes: A clue to properties of dune particles? N87-23453
SEDIMENT TRANSPORT
Regional sources and sinks of dust on Mars: Viking observations of Cerberus, Solis Planum and Syrtis Major N87-23450
Wind ripples in low density atmospheres N87-23454
Eolian saltation on Mars N87-23455
Mass transport by Aeolian saltation on Earth, Mars and Venus: The effects of full saltation cloud development and choking N87-23456
Development of wind tunnel techniques for the solution of problems in planetary Aeolian processes N87-23457
Determination of surface shear stress with the naphthalene sublimation technique N87-23460
SEDIMENTARY ROCKS
Search for, and study of, paleozoic impact ejecta: Progress made during the past year N87-23514
SEDIMENTS
High resolution thermal infrared mapping of Martian channels N87-23451
The application of flow competence evaluations to the assessment of flood-flow velocities and stresses N87-23464
SEISMIC WAVES
Body wave magnitudes and locations of French underground explosions at the Mururoa test site [BR-97934] N87-22947
Investigation of low-amplitude shear wave velocity in anisotropic material [AD-A179563] N87-22994
SELECTION
On the least favorable configuration of a selection procedure based on ranks [AD-A178454] N87-23234
SEMICONDUCTOR DEVICES
On the control of structures by applied thermal gradients N87-22747
Method and apparatus for measuring minority carrier lifetime in a direct band-gap semiconductor [NASA-CASE-NPO-16337-1-CU] N87-22894
Extrinsic gettering for VLSI/ULSI processes [DE87-002696] N87-22903
SEMICONDUCTORS (MATERIALS)
Total immersion crystal growth [NASA-CASE-NPO-15800-2] N87-23286
The study of photochemistry at semiconductor surfaces using total internal reflection techniques [DE87-006259] N87-23295
Semiconductor research capabilities at the Lawrence Berkeley Laboratory [DE87-006931] N87-23298
Orbital removal method for the neutral vacancy in semiconductors [DE87-701537] N87-23300
Submicron characterization of the atomic and electronic structure of defects in semiconductors [AD-A178458] N87-23301
SENSITIVITY
Workshop on Comparison of Simulations by Numerical Models of the Sensitivity of the Atmospheric Circulation to Sea Surface Temperature Anomalies [WCP-121] N87-23034
Forecast and sensitivity experiments on the UK Meteorological Office GCM with El Nino SST anomalies — general circulation model (GCM) sea surface temperature (SST) N87-23045
Sensitivity of the NMC spectral mode to the January 1983 El Nino SST — sea surface temperature N87-23048
Sensitivity of an Ocean General Circulation Model (OCGM) to wind forcing N87-23054
A family of algorithms for the estimation of the parameters of the stable laws and the parameters of attracting stable laws [AD-A178542] N87-23214
Sensitivity analysis for stationary probabilities of a Markov chain [AD-A178556] N87-23240
SENSORIMOTOR PERFORMANCE
Workshop Symposium on Neural Models of Sensory-Motor Control [AD-A179501] N87-23111
SENSORY FEEDBACK
Tactile feedback for teleoperator systems [AD-A179054] N87-22983
SEPARATED FLOW
Experimental research on compressible turbulent shear layers, viscous-inviscid interactions, and flow separation [AD-A179579] N87-22928
SEPARATORS
Development of advanced nickel-cadmium batteries for electric vehicle propulsion [DOE/NV/10442-1] N87-22922
SEQUENCING
Performance comparison of four state-of-the-art computer architectures [AD-A179071] N87-23149
SEQUENTIAL ANALYSIS
Performance comparison of four state-of-the-art computer architectures [AD-A179071] N87-23149
SERIES (MATHEMATICS)
On non-parametric discrimination using series expansions and projection pursuit [AD-A178455] N87-23213
SEROTONIN
Nutritional correction of histamine and serotonin levels as related to exposure to hypokinesia and neuro-emotional stress N87-23126
SERUMS
Human blood serum proteolytic enzyme activity after stay in hypoxic environment N87-23140
SERVICE LIFE
Prediction of service life of aircraft structural components using the half-cycle method [NASA-TM-88812] N87-23009
SHADOWS
Vibration analysis using shadow speckle metrology and line broadening techniques [AD-A178626] N87-23003
SHAPES
Effects of cutout orientations on natural frequencies and mode shapes of curved rectangular composite panels [AD-A178638] N87-22813
Vibration analysis using shadow speckle metrology and line broadening techniques [AD-A178626] N87-23003
Non-Markovian line shapes of physisorbed atoms on a crystal [AD-A179525] N87-23292
Shapes of small satellites N87-23354
Asteroid lightcurve inversion N87-23377
Cartography of irregularly shaped satellites N87-23545
SHATTER CONES
Shatter cones in Illinois: Evidence for meteoritic impacts at Glasford and Des Plaines N87-23513
SHEAR FLOW
Experimental research on compressible turbulent shear layers, viscous-inviscid interactions, and flow separation [AD-A179579] N87-22928
Conditional second order closure for turbulent shear flows [AD-A179661] N87-22931
The Mistral-Tramuntana shear line. A satellite observation N87-23084
SHEAR LAYERS
Experimental research on compressible turbulent shear layers, viscous-inviscid interactions, and flow separation [AD-A179579] N87-22928
SHEAR PROPERTIES
Conditional second order closure for turbulent shear flows [AD-A179661] N87-22931
Analytical characterization of shear localization in thermoviscoplastic materials [AD-A178597] N87-23002

SHEAR STRESS

Reynolds number effects on surface shear stress patterns around isolated hemispheres N87-23459

Determination of surface shear stress with the naphthalene sublimation technique N87-23460

SHOCK ABSORBERS

Analytical determination of space station response to crew motion and design of suspension system for microgravity experiments N87-22752

SHOCK FRONTS

Efficient implementation of essentially non-oscillatory shock capturing schemes
[NASA-CR-178304] N87-23230

SHOCK LAYERS

A preliminary study of extended magnetic field structures in the ionosphere
[NASA-CR-181004] N87-23066

SHOCK RESISTANCE

Thermal shock resistance of mullite-based SiC-whisker composites
[AD-A179214] N87-22809

Accelerations experienced by packaged materiel during fork lift truck handling
[RDI-284/45/3] N87-22989

SHOCK TUBES

Axisymmetric inviscid shock tube flow simulation
[AD-A178494] N87-22927

SHOCK WAVE INTERACTION

The effect on the strength of initiation on the corner effect — high explosives
[MBB-UA-938/86] N87-22924

Composite velocity procedures for flows with pressure interaction
[AD-A179602] N87-22929

SHOCK WAVES

An analysis of artificial viscosity effects on reacting flows using a spectral multi-domain technique
[NASA-CR-178308] N87-22632

A fast, low resistance switch for small slapper detonators
[AD-A178562] N87-22911

A Godunov method for Lagrangian hydrodynamics in 1D
[DE87-005204] N87-22933

Numerical analysis of terminal double mach reflection
[AD-A179041] N87-22942

A linearized Euler analysis of unsteady flows in turbomachinery
[NASA-CR-180987] N87-22948

SHORELINES

A wind- and wave-driven nearshore current model, the one-dimensional model
[AD-A178751] N87-23105

SHUTTLE ENGINEERING SIMULATOR

Flexible spacecraft simulator N87-22718

SHUTTLE IMAGING RADAR

The SIR-B mission: Towards an understanding of internal waves in the ocean
[ARE-TR-86122] N87-23102

SIGNAL DETECTION

Envelope detection of discrete-time band-limited signals using analytic signal representations
[AD-A179307] N87-22872

SIGNAL DISTORTION

Characterization of the error performance of a QPSK (Quadrature Phase Shift Keyed) communication system in the presence of linear transmission distortion
[AD-A178855] N87-22887

SIGNAL GENERATORS

Envelope detection of discrete-time band-limited signals using analytic signal representations
[AD-A179307] N87-22872

SIGNAL PROCESSING

Envelope detection of discrete-time band-limited signals using analytic signal representations
[AD-A179307] N87-22872

Modeling and simulation of the WFTA (Winograd Fourier Transform Algorithm) 16 PFA (Prime Factor Algorithm) processor using the VHSIC (Very High Speed Integrated Circuit) hardware description language, volume 1
[AD-A179344] N87-22898

Optically Phase-Locked Electronic Speckle Pattern Interferometer (OPL-ESPI)
[AD-A178652] N87-22914

Multidimensional filtering investigations
[AD-A178745] N87-22915

An improved set of Auger data analysis programs for physical electronics Auger spectrometer systems
[DOE/TIC-4500] N87-22957

Calibration of the hand-held lidars used by the Naval Ocean Systems Center
[AD-A178965] N87-22973

Design of fault tolerant prime factor algorithm array elements
[AD-A178977] N87-23187

Linear time invariant system identification using a result of the Bussgang theorem
[AD-A178642] N87-23216

SIGNAL RECEPTION

GPS antenna designs N87-22615

SIGNAL REFLECTION

Measurement of ice accretion using ultrasonic pulse echo techniques N87-22608

SIGNAL TO NOISE RATIOS

Investigation of Continuously Variable Slope Delta (CVSD) modulation for voice communications
[AD-A178579] N87-22877

Characterization of the error performance of a QPSK (Quadrature Phase Shift Keyed) communication system in the presence of linear transmission distortion
[AD-A178855] N87-22887

SIGNATURE ANALYSIS

Mid-infrared spectroscopic investigation N87-23424

SILANES

Structure and properties of novel compounds of silicon germanium and tin
[AD-A179433] N87-23291

SILICA GLASS

Containerless processing of glass forming melts: D-1, MEA/A-2 experiment 81F01 conducted on STS-61A flight, October 1985
[NASA-CR-179118] N87-22861

SILICATES

Reflectance spectra of mafic silicates and phyllosilicates from .6 to 4.6 microns N87-23421

Spectral effects of dehydration on phyllosilicates
N87-23422

SILICON

Silicon pulse sharpening diodes: Switching kilovolts in 10's of picoseconds
[DE87-005073] N87-22905

Structure and properties of novel compounds of silicon germanium and tin
[AD-A179433] N87-23291

Submicron characterization of the atomic and electronic structure of defects in semiconductors
[AD-A178458] N87-23301

SILICON CARBIDES

Friction and wear of sintered Alpha SiC sliding against IN-718 alloy at 25 to 800 C in atmospheric air at ambient pressure
[NASA-TM-87353] N87-22860

SILICON COMPOUNDS

Infrared spectroscopy using laser and Fourier techniques of the unstable molecules SiH and NH. Determination of the molecular constants of the fundamental electronic state 3 sigma (-) of NH
[ETN-87-99552] N87-22818

SILICON DIOXIDE

Thermal shock resistance of mullite-based SiC-whisker composites
[AD-A179214] N87-22809

SILICON FILMS

Atomistic simulation of stability properties and growth of strained layer structures
[DE87-006712] N87-23297

SIMPLEX METHOD

A Simplex optimisation technique for development of rubber formulations
[ARE-TM(UMT)-86405] N87-22846

SIMULATION

Simulation of an integrated flight/fire control system during air-to-ground gunnery attack N87-22672

Control of flexible structures and the research community N87-22732

Flow dynamics stimulated by hairpin-like vortices in initially laminar boundary layers
[AD-A179578] N87-22927

A static data flow simulation study at Ames Research Center
[NASA-TM-89434] N87-23201

A new LIHE (Light Initiated High Explosive) test capability for spherical targets
[DE87-003035] N87-23245

Electric fields and double layers in plasmas
N87-23323

Anomalous transport in discrete arcs and simulation of double layers in a model auroral circuit N87-23325

Particle simulation of auroral double layers
N87-23327

SIMULATORS

The heterogeneous machine simulator
[AD-A178771] N87-23185

Applications and requirements for real-time simulators in ground-test facilities
[NASA-TP-2672] N87-23202

SINGLE CRYSTALS

Deformation and fatigue behavior of SSME turbopump blade materials N87-22776

Dynamic characteristics of single crystal SSME blades
N87-22797

Infrared fiber optic materials
[NASA-CR-180604] N87-23257

Total immersion crystal growth
[NASA-CASE-NPO-15800-2] N87-23286

SINGULARITY (MATHEMATICS)

On the application of the strain energy density theory in predicting crack initiation and angle of growth
[AR-004-493] N87-23011

SINTERING

Synthesis of alumina-zirconia powders by sol-gel processing
[DE87-005721] N87-22851

Friction and wear of sintered Alpha SiC sliding against IN-718 alloy at 25 to 800 C in atmospheric air at ambient pressure
[NASA-TM-87353] N87-22860

Evaluation of spherical ceramic particles for solar thermal transfer media
[DE87-007432] N87-23026

SITES

Determination of crack initiation sites using a digital NDE workstation
[DE87-001444] N87-22997

SIZE (DIMENSIONS)

Selection of dimensions for an anthropometric data base. Volume 2: Dimension evaluation sheets
[AD-A179472] N87-23110

Selection of dimensions for an anthropometric data base. Volume 1: Rationale, summary, and conclusions
[AD-A179566] N87-23112

Image size and resolution in face recognition
N87-23113

SIZE DISTRIBUTION

Studies of vesicle distribution patterns in Hawaiian lavas N87-23484

SKIN FRICTION

Dual cylindrical wave laser-Doppler method for measurement of skin friction in fluid flow
[AD-A178629] N87-22939

SLEWING

Slewing control experiment for a flexible panel
N87-22740

SLOPES

Investigation of Continuously Variable Slope Delta (CVSD) modulation for voice communications
[AD-A178579] N87-22877

SLOTS

Computer program for electromagnetic penetration into a conducting circular cylinder through a narrow slot, TM case
[AD-A178616] N87-22880

SOCIAL FACTORS

Optimum culture in the cockpit N87-22643

SODAR

Measurement of high resolution wind profiles with a minisodar
[DE87-007001] N87-23096

SOFTWARE ENGINEERING

The 2GCHAS: A high productivity software development environment N87-23162

Formal modeling and analysis of fault-tolerance properties for software
[DE87-007006] N87-23176

Summary of the SEI (Software Engineering Institute) Workshop on Softwear Configuration Management
[AD-A178770] N87-23184

Measuring software design
[NASA-TM-89372] N87-23189

General object-oriented software development
[NASA-TM-89375] N87-23190

Product assurance policies and procedures for flight dynamics software development
[NASA-TM-89377] N87-23192

Guidelines for applying the Composite Specification Model (CSM)
[NASA-TM-89374] N87-23193

Development of confidence limits by pivotal functions for estimating software reliability
[NASA-TP-2709] N87-23244

Asteroid families, dynamics and astrometry
N87-23370

SOFTWARE TOOLS

Development of a microcomputer-based workstation for analysis of digital satellite links
[AD-A178872] N87-22888

TAE Plus: A conceptual view of TAE in the space station era N87-23157

The 2GCHAS: A high productivity software development environment N87-23162

Programming languages for knowledge-based systems
[PB87-157228] N87-23170

OMNITAB 80: An interpretive system for statistical and numerical data anlysis
[PB87-172235] N87-23171

Measuring software design
[NASA-TM-89372] N87-23189

Product assurance policies and procedures for flight dynamics software development
[NASA-TM-89377] N87-23192
Guidelines for applying the Composite Specification Model (CSM)
[NASA-TM-89374] N87-23193
SOIL MECHANICS
Investigation of low-amplitude shear wave velocity in anisotropic material
[AD-A179563] N87-22994
SOILS
On the spectral reflectance properties of materials exposed at the Viking landing sites N87-23414
Spectral mixture modeling: Further analysis of rock and soil types at the Viking Lander sites N87-23415
Characterization of surficial units on Mars using Viking orbiter multispectral image and thermal data
N87-23418
CO2: Adsorption on palagonite and the Martian regolith N87-23419
Spectral effects of dehydration on phyllosilicates
N87-23422
Thermal-infrared spectral observations of geologic materials in emission N87-23425
SOL-GEL PROCESSES
Synthesis of alumina-zirconia powders by sol-gel processing
[DE87-005721] N87-22851
SOLAR ACTIVITY
Solar active region physical parameters inferred from a thermal cyclotron line and soft X-ray spectral lines
[AD-A179650] N87-23560
J. VLA (Very Large Array) of a solar noise storm
[NASA-CR-180219] N87-23561
Simultaneous SMM flat crystal spectrometer and very large array observations of solar active regions
[AD-A179698] N87-23562
A preliminary summary of the observations of the 16 February 1984 solar flare (STIP Interval XV, 12-21 February 1984)
[NASA-CR-180929] N87-23563
SOLAR ARRAYS
Solar array flight dynamic experiment N87-22722
Evaluation of a heliostat tracker for linear Fresnel lens photovoltaic concentrators
[DE87-006331] N87-23025
SOLAR ATMOSPHERE
East-west solar scans at 10-cm wavelength taken at the Algonquin Radio Observatory, Jan. 1980 to December 1985
[ARO-16] N87-23567
SOLAR CELLS
High temperature solid oxide regenerative fuel cell for solar photovoltaic energy storage
[NASA-TM-89872] N87-23020
SOLAR COLLECTORS
Evaluation of spherical ceramic particles for solar thermal transfer media
[DE87-007432] N87-23026
SOLAR CORONA
Accumulation of solid bodies in the solar nebula
N87-23384
Magnetic flares in the protoplanetary nebula and the origin of meteorite chondrules N87-23402
Nonlinear aspects of planar condensational instability
[AD-A178998] N87-23565
SOLAR DYNAMIC POWER SYSTEMS
Impact of thermal energy storage properties on solar dynamic space power conversion system mass
[NASA-TM-89909] N87-22802
SOLAR ENERGY
Impact of thermal energy storage properties on solar dynamic space power conversion system mass
[NASA-TM-89909] N87-22802
SOLAR FLARES
Magnetic flares in the protoplanetary nebula and the origin of meteorite chondrules N87-23402
A preliminary summary of the observations of the 16 February 1984 solar flare (STIP Interval XV, 12-21 February 1984)
[NASA-CR-180929] N87-23563
X-ray and low energy gamma-ray observations of the 16 February 1984 solar flare
[NASA-CR-180928] N87-23564
SOLAR FLUX
Observations of solar flux at the Algonquin Radio Observatory on 2800 MHz and the Dominion Radio Astrophysical Observatory on 2700 MHz
[ARO-15] N87-23566
East-west solar scans at 10-cm wavelength taken at the Algonquin Radio Observatory, Jan. 1980 to December 1985
[ARO-16] N87-23567
SOLAR GENERATORS
Performance characteristics of a combination solar photovoltaic heat engine energy converter
[NASA-TM-89908] N87-23028
Design, development and deployment of public service photovoltaic power/load systems for the Gabonese Republic
[NASA-CR-179603] N87-23030
Development of a holographic beamsplitter for use with a conventional Fresnel lens
[DE87-006770] N87-23263
SOLAR LIMB
X-ray and low energy gamma-ray observations of the 16 February 1984 solar flare
[NASA-CR-180928] N87-23564
East-west solar scans at 10-cm wavelength taken at the Algonquin Radio Observatory, Jan. 1980 to December 1985
[ARO-16] N87-23567
SOLAR MAGNETIC FIELD
Magnetic flares in the protoplanetary nebula and the origin of meteorite chondrules N87-23402
SOLAR OPTICAL TELESCOPE
SOT: A rapid prototype using TAE windows
N87-23161
SOLAR RADIO BURSTS
Observations of solar flux at the Algonquin Radio Observatory on 2800 MHz and the Dominion Radio Astrophysical Observatory on 2700 MHz
[ARO-15] N87-23566
SOLAR SIMULATION
A feasibility study of the flexible simulation of sunlight — cockpit simulators
[BR98783] N87-22693
SOLAR SYSTEM
Reports of Planetary Geology and Geophysics Program, 1986
[NASA-TM-89810] N87-23341
Timescales for planetary accretion and the structure of the protoplanetary disk N87-23380
Solar system dynamics N87-23390
SOLAR WIND
Investigations of the polar rain: Polar cap electron precipitation
[AD-A178876] N87-23099
SOLID ELECTROLYTES
Experimental investigation of the process of CO2-CO-H2O-H2-N2 gas mixture breakdown in electrolysis cell with solid electrolyte N87-23137
Novel polymeric LIT and divalent cation fast ion conducting materials
[DE87-006294] N87-23296
SOLID PROPELLANT COMBUSTION
Application of atomic fluorescence to measurement of combustion temperature in solid propellants
[AD-A179665] N87-22862
SOLID PROPELLANT ROCKET ENGINES
Journal of Chinese Society of Astronautics (selected articles)
[AD-A179690] N87-22800
SOLID ROCKET PROPELLANTS
Application of atomic fluorescence to measurement of combustion temperature in solid propellants
[AD-A179665] N87-22862
SOLID STATE DEVICES
Novel polymeric LIT and divalent cation fast ion conducting materials
[DE87-006294] N87-23296
SOLID STATE LASERS
New laser materials
[DE87-006723] N87-22970
SOLIDIFICATION
Characterization of rapidly solidified Al-Be-Li and Al-Be ribbons
[DE87-006613] N87-22835
Investigation of the icosahedral Z-phase in aluminium transition metal alloys and rapidly solidified Al-alloys
[AD-A178451] N87-22840
SOLIDS
Collective effects in intense-field electrodynamics 1981-1986
[AD-A179490] N87-23261
Angular momentum theory applied to interactions in solids
[AD-A179366] N87-23289
SOLUTIONS
Thermodynamic properties of molten salt solutions
[DE87-004948] N87-23306
SOLVENTS
Basic research in energetic fluorocarbons
[AD-A179676] N87-22822
A microcrystalline growth study of solvent effects in alkoxides by dynamic laser light scattering
[DE87-005710] N87-23294
SOOT
Gas turbine combustor and engine augmentor tube sooting characteristics
[AD-A179423] N87-22679
SOUND PRESSURE
Prediction of high-speed rotor noise with a Kirchhoff formula
[AD-A178982] N87-23250
SOUND TRANSMISSION
Phase space methods and path integration: A microscopic approach to direct and inverse wave propagation
[AD-A178557] N87-23249
SPACE CHARGE
The transverse dynamics of space-charge limited diodes
[AD-A179389] N87-22899
A laboratory investigation of potential double layers
N87-23317
SPACE ENVIRONMENT SIMULATION
The Earth's magnetosphere as a sample of the plasma universe
[TRITA-EPP-86-12] N87-23337
SPACE ERECTABLE STRUCTURES
Status of the Mast experiment N87-22703
SPACE EXPLORATION
Reports of Planetary Geology and Geophysics Program, 1986
[NASA-TM-89810] N87-23341
Enhanced LANDSAT images of Antarctica and planetary exploration N87-23558
SPACE FLIGHT
Toward the year 2000: The near future of the American civilian and military space programs
[DE87-006467] N87-22697
SPACE FLIGHT STRESS
USSR Report: Space Biology and Aerospace Medicine, Volume 20, No. 5, September - October 1986
[JPRS-USB-86-007] N87-23120
Problems and feasibility of drug correction of orthostatic tolerance in space medicine N87-23121
Effect of short-term spaceflights on activity of renin-angiotension-aldosterone system, concentration of cyclic nucleotides and prostaglandins in blood
N87-23125
Cortical ultrastructure of rat cerebellar nodulus following flight aboard Cosmos-1514 biosatellite N87-23130
SPACE MAINTENANCE
Developing a voice-controlled, computer-generated display to assist space station astronauts during maintenance activity
[AD-A178997] N87-22762
SPACE MISSIONS
Design of an orbital inspection satellite
[AD-A179115] N87-22759
SPACE OBSERVATIONS (FROM EARTH)
Observations of solar flux at the Algonquin Radio Observatory on 2800 MHz and the Dominion Radio Astrophysical Observatory on 2700 MHz
[ARO-15] N87-23566
East-west solar scans at 10-cm wavelength taken at the Algonquin Radio Observatory, Jan. 1980 to December 1985
[ARO-16] N87-23567
SPACE PLASMAS
A preliminary study of extended magnetic field structures in the ionosphere
[NASA-CR-181004] N87-23066
Double Layers in Astrophysics
[NASA-CP-2469] N87-23313
Formation mechanisms of laboratory double layers
N87-23314
Experimental observation of ion-acoustic double layers in laboratory plasma N87-23318
Ion phase-space vortices and their relation to small amplitude double layers N87-23320
Conditions for double layers in the Earth's magnetosphere and perhaps in other astrophysical objects N87-23328
SPACE POWER REACTORS
SP-100 Advanced Technology Program
[NASA-TM-89888] N87-23027
Considerations pertinent to the Doppler effect for space reactors
[DE87-007032] N87-23252
SPACE PROCESSING
Containerless processing of glass forming melts: D-1, MEA/A-2 experiment 81F01 conducted on STS-61A flight, October 1985
[NASA-CR-179118] N87-22861
SPACE SHUTTLE MAIN ENGINE
Vectorizable algorithms for adaptive schemes for rapid analysis of SSME flows
[NASA-CR-179082] N87-22764

Studies and analyses of the space shuttle main engine: High-pressure oxidizer turbopump failure information propagation model [NASA-CR-179079] N87-22765
Structural Integrity and Durability of Reusable Space Propulsion Systems [NASA-CP-2471] N87-22766
Unsteady stator/rotor interaction N87-22767
Simulation of multistage turbine flows N87-22768
Analytical and experimental studies of flow-induced vibration of SSME components N87-22771
Progress on thin-film sensors for space propulsion technology N87-22772
Heat flux calibration facility capable of SSME conditions N87-22774
Numerical study of the effects of boundary conditions on the measurement and calibration of gardon type heat flux sensors N87-22775
Deformation and fatigue behavior of SSME turbopump blade materials N87-22776
Nonlinear heat transfer and structural analyses of SSME turbine blades N87-22779
Structural analysis demonstration of constitutive and life models N87-22780
Mechanical properties of high gradient and hot isostatically pressed PWA 1480 N87-22781
Probabilistic structural analysis to evaluate the structural durability of SSME critical components N87-22783
Probabilistic Structural Analysis Methods (PSAM) for select space propulsion system structural components N87-22784
NESSUS/expert and NESSUS/FPI in the Probabilistic Structural Analysis Methods (PSAM) program N87-22787
Probabilistic SSME blades structural response under random pulse loading N87-22791
Quantifying uncertainties in the structural response of SSME blades N87-22792
Composite load spectra for select space propulsion structural components N87-22793
Structural tailoring using the SSME/STAEBL code N87-22795
Dynamic characteristics of single crystal SSME blades N87-22797
SSME blade damper technology N87-22798

SPACE SHUTTLE ORBITERS
Space Station/Shuttle Orbiter dynamics during docking N87-22708

SPACE SHUTTLE PAYLOADS
Structural/control interaction (payload pointing and micro-g) N87-22721

SPACE SHUTTLES
Optimal shuttle altitude changes using tethers [AD-A179205] N87-22756

SPACE STATIONS
Space Station/Shuttle Orbiter dynamics during docking N87-22708
Considerations in the design and development of a space station scale model N87-22711
Adaptive momentum management for large space structures [NASA-CR-179085] N87-22758
The effect of multipath on digital communications systems: With application to space station [AD-A178578] N87-22876
Performance characteristics of a combination solar photovoltaic heat engine energy converter [NASA-TM-89908] N87-23028

SPACEBORNE EXPERIMENTS
Analytical determination of space station response to crew motion and design of suspension system for microgravity experiments N87-22752
Containerless processing of glass forming melts: D-1, MEA/A-2 experiment 81F01 conducted on STS-61A flight, October 1985 [NASA-CR-179118] N87-22861

SPACEBORNE LASERS
Time and space resolved spectroscopy of X-ray laser experiments from 81A to 220A [DE87-005946] N87-22968

SPACEBORNE PHOTOGRAPHY
Design of an orbital inspection satellite [AD-A179115] N87-22759

SPACECRAFT
Computational aerothermodynamics [NASA-TM-89450] N87-22943

SPACECRAFT CONFIGURATIONS
Impact of space station appendage vibrations on the pointing performance of gimballed payloads N87-22733
Preliminary evaluation of a reaction control system for the space station N87-22736

SPACECRAFT CONTROL
Structural Dynamics and Control Interaction of Flexible Structures [NASA-CP-2467-PT-1] N87-22702
Status of the Mast experiment N87-22703
Microprocessor controlled proof-mass actuator N87-22706
Considerations in the design and development of a space station scale model N87-22711
Optimum mix of passive and active control of space structures N87-22714
Status report and preliminary results of the spacecraft control laboratory experiment N87-22717
Precision pointing and control of flexible spacecraft N87-22723
Control of flexible structures and the research community N87-22732
Moving-bank multiple model adaptive estimation applied to flexible spacestructure control [AD-A178870] N87-22761

SPACECRAFT DESIGN
A quasi-analytical method for non-iterative computation of nonlinear controls N87-22731

SPACECRAFT DOCKING
Space Station/Shuttle Orbiter dynamics during docking N87-22708

SPACECRAFT LAUNCHING
Transient response for interaction of two dynamic bodies N87-22709
LRS: A knowledge based approach to launch resource scheduling [AD-A179426] N87-23310

SPACECRAFT MODELS
Considerations in the design and development of a space station scale model N87-22711

SPACECRAFT MOTION
Crew activity and motion effects on the space station N87-22744
Analytical determination of space station response to crew motion and design of suspension system for microgravity experiments N87-22752
Numerical modeling of on-orbit propellant motion resulting from an impulsive acceleration [NASA-TM-89873] N87-22757

SPACECRAFT POWER SUPPLIES
Investigation of rocket powered, open cycle, magnetohydrodynamic generators for high, pulsed power needs in space [AD-A178869] N87-22801
High temperature solid oxide regenerative fuel cell for solar photovoltaic energy storage [NASA-TM-89872] N87-23020

SPACECRAFT PROPULSION
Structural Integrity and Durability of Reusable Space Propulsion Systems [NASA-CP-2471] N87-22766
Progress on thin-film sensors for space propulsion technology N87-22772
Structural analysis demonstration of constitutive and life models N87-22780
Probabilistic Structural Analysis Methods (PSAM) for select space propulsion system structural components N87-22784
Probabilistic structural analysis verification studies N87-22786
Advanced probabilistic method of development N87-22788
Composite load spectra for select space propulsion structural components N87-22793
Probabilistic load model development and validation for composite load spectra for select space propulsion engines N87-22794

SPACECRAFT RECOVERY
Apparatus and method of capturing an orbiting spacecraft [NASA-CASE-MSC-20979-1] N87-22985

SPACECREWS
Crew activity and motion effects on the space station N87-22744
Analytical determination of space station response to crew motion and design of suspension system for microgravity experiments N87-22752

SPACELAB
Celestial target observability for astro spacelab missions [NASA-TM-86591] N87-22696

SPACELAB PAYLOADS
Scientific goals of the German Spacelab Mission D1 [ETN-87-99669] N87-22695

SPANWISE BLOWING
Verification of performance results for a low-speed 15 percent elliptical circulation control airfoil [NASA-CR-181020] N87-22633

SPARK GAPS
Gas mixtures for spark gap closing switches with emphasis on efficiency of operation [DE87-006624] N87-22906

SPARK IGNITION
The autoignition of isobutane in a knocking spark ignition engine [DE87-003241] N87-22823

SPATIAL DISTRIBUTION
Dual cylindrical wave laser-Doppler method for measurement of skin friction in fluid flow [AD-A178629] N87-22939
Solar system dynamics N87-23390

SPECKLE PATTERNS
Progress in optical strain measurement system development N87-22773
Optically Phase-Locked Electronic Speckle Pattern Interferometer (OPL-ESPI) [AD-A178652] N87-22914
Optical strain measurement system development, phase 1 [NASA-CR-179619] N87-22960

SPECTRA
Reliability studies of ceramic capacitors [AD-A179436] N87-22900
Spectral effects of dehydration on phyllosilicates N87-23422

SPECTRAL ENERGY DISTRIBUTION
White-light optical information processing and holography [AD-A179489] N87-23260

SPECTRAL METHODS
Sensitivity of the NMC spectral mode to the January 1983 El Nino SST — sea surface temperature N87-23048

SPECTRAL RECONNAISSANCE
Earth resources: A continuing bibliography with indexes (issue 53) [NASA-SP-7041(53)] N87-23013

SPECTRAL REFLECTANCE
Oxidized basalts on the surface of Venus: Compositional implications of measured spectral properties N87-23412
On the spectral reflectance properties of materials exposed at the Viking landing sites N87-23414
Spectral mixture modeling: Further analysis of rock and soil types at the Viking Lander sites N87-23415
Gossans on Mars: Spectral features attributed to jarosite N87-23417
Reflectance spectra of mafic silicates and phyllosilicates from .6 to 4.6 microns N87-23421
Studies of the scattering/absorption of minerals N87-23423
Bidirectional reflectance properties of planetary surface materials N87-23426
Atlas of reflectance spectra of terrestrial, lunar and meteoritic powders and frosts from 92 to 1800 •lc2)nm N87-23427
Deconvolution of spectra for intimate mixtures N87-23428
Compositional information for the Moon: Some characteristics of current near-IR spectra (telescopic and laboratory) N87-23429
Preliminary results of spectral reflectance studies of tycho crater N87-23430
Sulfur-oxygen processes on Io N87-23437
Solid sulfur in vacuum: Sublimation effects on surface microtexture, color and spectral reflectance, and applications to planetary surfaces N87-23438
A preliminary analysis of the Mariner 10 color ratio map of Mercury N87-23439
Bright sand/dark dust: The identification of active sand surfaces on the Earth and Mars N87-23449
Regional sources and sinks of dust on Mars: Viking observations of Cerberus, Solis Planum and Syrtis Major N87-23450

SPECTRAL SIGNATURES
Signatures from in-situ light scattering of non-homogeneous non-spherical particles [AD-A178761] N87-23269

SPECTROGRAPHS
Fast ion mass spectrometry and charged particle spectrography investigations of transverse ion acceleration and beam-plasma interactions [NASA-CR-168348] N87-22817

SPECTROMETERS
Reflectance spectra of mafic silicates and phyllosilicates from .6 to 4.6 microns N87-23421
Bidirectional reflectance properties of planetary surface materials N87-23426
Simultaneous SMM flat crystal spectrometer and very large array observations of solar active regions [AD-A179698] N87-23562

SPECTROSCOPY
Time and space resolved spectroscopy of X-ray laser experiments from 81A to 220A [DE87-005946] N87-22968
Spectral effects of dehydration on phyllosilicates N87-23422
Studies of the scattering/absorption of minerals N87-23423

SPECTRUM ANALYSIS
A collection and statistical analysis of biophysical data to predict motion sickness incidence [AD-A178874] N87-23119
Applications of fiber optics in experimental mechanics [AD-A178683] N87-23268
Evolution of the inner asteroid belt: Paradigms and paradoxes from spectral studies N87-23372
Source of the optical red-slope in iron-rich meteorites N87-23374
Oxidized basalts on the surface of Venus: Compositional implications of measured spectral properties N87-23412
On the spectral reflectance properties of materials exposed at the Viking landing sites N87-23414
Hisingerite and iddingsite on Mars: Degradation of iron-rich basalts N87-23416
Gossans on Mars: Spectral features attributed to jarosite N87-23417
Characterization of surficial units on Mars using Viking orbiter multispectral image and thermal data N87-23418
Reflectance spectra of mafic silicates and phyllosilicates from .6 to 4.6 microns N87-23421

SPECULAR REFLECTION
Vibration analysis using shadow speckle metrology and line broadening techniques [AD-A178626] N87-23003
Laser reflectance as a function of rough water glitter profile [AD-A178774] N87-23016

SPEECH
Investigation of Continuously Variable Slope Delta (CVSD) modulation for voice communications [AD-A178579] N87-22877

SPEECH RECOGNITION
Developing a voice-controlled, computer-generated display to assist space station astronauts during maintenance activity [AD-A178997] N87-22762

SPHERES
Numerical calculation of the drag force induced by natural convection of spheres at low Grashof numbers [DE87-006791] N87-22935
A new LIHE (Light Initiated High Explosive) test capability for spherical targets [DE87-003035] N87-23245

SPIN DYNAMICS
Star sensor fine attitude pointing model for a spinning geosynchronous satellite [AD-A179424] N87-22763
Angular momentum theory applied to interactions in solids [AD-A179366] N87-23289

SPIN REDUCTION
Improved combat performance using relaxed static stability and a spin prevention system (FBW Jaguar) N87-22674

SPREAD SPECTRUM TRANSMISSION
GPS antenna designs N87-22615
Concurrent communication among multi-transceiver stations over shared media [NASA-CR-180935] N87-22890

SPUTTERING
A statistical study of the combined effects of substrate temperature, bias, annealing, and a Cr3Si2 undercoating on the tribological properties of RF-sputtered MoS2 coatings [DE87-007086] N87-23285
On the sputter alteration of regoliths of outer solar system bodies N87-23434

STABILITY
A family of algorithms for the estimation of the parameters of the stable laws and the parameters of attracting stable laws [AD-A178542] N87-23214
The applicability of the stable laws in collective risk theory and practice [AD-A178546] N87-23238
The percentiles of the stable laws [AD-A179025] N87-23243
Atomistic simulation of stability properties and growth of strained layer structures [DE87-006712] N87-23297

STABILITY AUGMENTATION
Stability boundaries for command augmentation systems N87-22622

STACKS
Component variations and their effects on bipolar nickel-hydrogen cell performance [NASA-TM-89907] N87-23029

STAGNATION POINT
Progress in the prediction of unsteady heat transfwe on turbines blades N87-22769

STANDARDS
Laboratory characterization tests for antimisting fuel [DOT/FAA/CT-86/23] N87-22864
NBS calibration services users guide, 1986-1988 edition [NBS-SP-250] N87-22958
The graphical kernel system: A standards implementation [AD-A178583] N87-23180
Cooperative research opportunities at NBS (National Bureau of Standards) [PB87-157236] N87-23309

STAR TRACKERS
Star sensor fine attitude pointing model for a spinning geosynchronous satellite [AD-A179424] N87-22763

STARK EFFECT
Plasma diagnosis by dye laser intracavity absorption [DE87-006407] N87-23280

STARS
Celestial target observability for astro spacelab missions [NASA-TM-86591] N87-22696

STATE VECTORS
Modeling digital control systems with MA-prefiltered measurements [NASA-TP-2732] N87-22870

STATIC CHARACTERISTICS
A static data flow simulation study at Ames Research Center [NASA-TM-89434] N87-23201

STATIC ELECTRICITY
Metalliding as an electrochemical process [AD-A178744] N87-22843

STATIC STABILITY
Improved combat performance using relaxed static stability and a spin prevention system (FBW Jaguar) N87-22674

STATISTICAL ANALYSIS
Advanced probabilistic method of development N87-22788
Radar target classification studies [AD-A179010] N87-22889
OMNITAB 80: An interpretive system for statistical and numerical data anlysis [PB87-172235] N87-23171
On Bayes selection rules for the best exponential population with type-I censored data [AD-A178472] N87-23235
A Bayesian statistics year at the Ohio State University [AD-A178762] N87-23242

STATISTICAL DISTRIBUTIONS
Self-critical and robust procedures for the analysis of binary data [AD-A178835] N87-23221
Observations on the magnitude-frequency distribution of Earth-crossing asteroids N87-23369

STATISTICAL TESTS
Quantifying uncertainties in the structural response of SSME blades N87-22792
Goodness-of-fit based on integrated squared discrepancies between sample and population characteristic functions [AD-A178763] N87-23218
Goodness of fit based on integrated squared errors in characteristic functions or densities [AD-A179027] N87-23225
A modified goodness-of-fit test for the lognormal distribution with unknown scale and location parameters [AD-A179049] N87-23226

STATOR BLADES
Unsteady stator/rotor interaction N87-22767

STEADY FLOW
Composite velocity procedures for flows with pressure interaction [AD-A179602] N87-22929

STEELS
The effects of candidate chemical training agents upon service materials — chemical warfare [MQAD-317] N87-22832
Erosion study of AM355 and Al2O3 ceramics [AD-A178882] N87-22858

STELLAR COLOR
A study of the fundamental characteristics of 2175A extinction [NASA-CR-180926] N87-23336

STELLAR EVOLUTION
Magnetic flares in the protoplanetary nebula and the origin of meteorite chondrules N87-23402

STELLAR LUMINOSITY
A study of the fundamental characteristics of 2175A extinction [NASA-CR-180926] N87-23336

STELLAR MAGNETIC FIELDS
Generation of a dynamo magnetic field in a protoplanetary accretion disk N87-23403

STELLAR MASS ACCRETION
Accretion onto neutron stars with the presence of a double layer N87-23334
Protostellar disks and the primitive solar nebula N87-23379

STELLAR OCCULTATION
Dynamical studies of Saturn's rings N87-23395

STELLARATORS
Confinement and heating of high beta plasmas with emphasis on compact toroids. Task 2: Stellarator and heliac research [DE87-005554] N87-23278

STEREOSCOPY
A compilation system for Venus radar mission (Magellan) N87-23440

STIFFNESS
Dynamic characteristics of a vibrating beam with periodic variation in bending stiffness N87-22726

STIFFNESS MATRIX
A general method for dynamic analysis of structures overview N87-22707
Transient response for interaction of two dynamic bodies N87-22709

STOCHASTIC PROCESSES
Improving stability margins in discrete-time log controllers N87-22719
Stochastic and hybrid-stress plate/shell finite elements for hot-section components N87-22789
Probabilistic load model development and validation for composite load spectra for select space propulsion engines N87-22794
Stochastic processes in CHEMFETs [AD-A178841] N87-22829
A separable piecewise linear upper bound for stochastic linear programs [AD-A178694] N87-23217
Electron acceleration in stochastic double layers N87-23324

STOKES LAW (FLUID MECHANICS)
A survey of mixed finite element methods [NASA-CR-178267] N87-23229

STORAGE BATTERIES
Development of nickel oxide/hydrogen multilayer bipolar battery for pulsed power [AD-A178844] N87-22917

STORMS (METEOROLOGY)
Air-sea interaction over the Mediterranean Sea during the Alpine Experiment (ALPEX) Special Observing Period N87-23073

STRAIN ENERGY METHODS
On the application of the strain energy density theory in predicting crack initiation and angle of growth [AR-004-493] N87-23011

STRAIN GAGES
Progress in optical strain measurement system development N87-22773
Optical strain measurement system development, phase 1 [NASA-CR-179619] N87-22960

STRAIN HARDENING
Martensitic transformation as a deformation process [DE87-007068] N87-22836
Analytical characterization of shear localization in thermoviscoplastic materials [AD-A178597] N87-23002

STRAIN MEASUREMENT
Progress in optical strain measurement system development N87-22773

STRAIN RATE
Bodner-Partom viscoplastic model in STEALTH finite difference code [AD-A178994] N87-23005

STRATEGY
A prototype knowledge-based system to aid space system restoration management [AD-A179336] N87-23203

STRATIFICATION
Formation of the layered deposits in the Valles Marineris, Mars N87-23470

STRATIGRAPHY
Groundwater sapping channels: Summary of effects of experiments with varied stratigraphy N87-23461
Formation of the layered deposits in the Valles Marineris, Mars N87-23470
Geomorphic evidence for ancient seas in west Deuteronilus Mensae, Mars-1: Regional geomorphology N87-23471
Local-scale stratigraphy of grooved terrain on Ganymede N87-23538
Stratigraphy of the south polar region of Ganymede N87-23539
Compositional stratigraphy of crustal material from near-infrared spectra N87-23559

STRATOSPHERE
High altitude turbulence for supersonic cruise vehicles [NASA-TM-88285] N87-23100

STRESS (BIOLOGY)
Some parameters of human lipid metabolism during antiorthostatic hypokinesia and their correction N87-23127
Hormonal and metabolic status of man in the extreme north N87-23139
STRESS (PSYCHOLOGY)
Nutritional correction of histamine and serotonin levels as related to exposure to hypokinesia and neuro-emotional stress N87-23126
STRESS ANALYSIS
Stochastic and hybrid-stress plate/shell finite elements for hot-section components N87-22789
Measurement of the J integral with caustics: An experimental and numerical investigation [AD-A177273] N87-22990
Residual stresses in girth butt welded pipes: Results and implications [CUED/D-STRUCT/TR.109] N87-22992
Two-dimensional elastic analysis by the boundary element method [AD-A179213] N87-22993
Investigation of low-amplitude shear wave velocity in anisotropic material [AD-A179563] N87-22994
On 3-D inelastic analysis methods for hot section components. Volume 1: Special finite element models [NASA-CR-179494] N87-22996
Secular cooling of Earth as a source of intraplate stress N87-23519
Lithospheric loading and tectonics of the lunar irregular maria N87-23522
Stress history of the Tharsis Region, Mars N87-23527
STRESS CONCENTRATION
An evaluation of microgridding techniques for determining local plastic strain distributions [AD-A178518] N87-23000
STRESS INTENSITY FACTORS
Influence of supporting conditions on stress intensity factors for single-edge-cracked specimens under bending [NASA-TT-20016] N87-23008
STRESS-STRAIN RELATIONSHIPS
Nonlinear heat transfer and structural analyses of SSME turbine blades N87-22779
Investigation of low-amplitude shear wave velocity in anisotropic material [AD-A179563] N87-22994
STRESSES
A new formulation of mean stress effects in fatigue N87-22778
Non-linear finite element analysis program [AD-A179038] N87-23006
STRIP TRANSMISSION LINES
Design of generalised Chebyshev suspended substrate stripline filters [AD-A178505] N87-22910
STRONGLY COUPLED PLASMAS
Opening switch research on a dense plasma focus [AD-A179693] N87-23276
STRUCTURAL ANALYSIS
Analysis of structures with rotating, flexible substructures applied to rotorcraft aeroelasticity in GRASP (General Rotorcraft Aeromechanical Stability Program) [AD-A178941] N87-22677
Status of the Mast experiment N87-22703
Identification of large space structures: A state-of-practice report N87-22705
Impact of space station appendage vibrations on the pointing performance of gimballed payloads N87-22733
A TREETOPS simulation of the Hubble Space Telescope-High Gain Antenna interaction N87-22735
Nonlinear heat transfer and structural analyses of SSME turbine blades N87-22779
Structural analysis demonstration of constitutive and life models N87-22780
Probabilistic structural analysis to evaluate the structural durability of SSME critical components N87-22783
Probabilistic Structural Analysis Methods (PSAM) for select space propulsion system structural components N87-22784
The NESSUS finite element code N87-22785
Experimental and theoretical studies of the structure of grain boundaries [DE87-007560] N87-22836
Non-linear finite element analysis program [AD-A179038] N87-23006
Automated transient analysis of structural members [AD-A179042] N87-23007
Finite element implementation of Robinson's unified viscoplastic model and its application to some uniaxial and multiaxial problems [NASA-TM-89891] N87-23010
Fractal analysis of radar precipitation data over hilly terrain N87-23093
Powder. Complex of programs for structural analysis of polycrystals [DE87-701211] N87-23283
Observational studies of Saturn's rings N87-23362
STRUCTURAL BASINS
Lunar magnetization concentrations (MAGCONS) antipodal to young large impact basins N87-23405
STRUCTURAL DESIGN
Probabilistic Structural Analysis Methods (PSAM) for select space propulsion system structural components N87-22784
Structural design and fabrication of the Sandia 34-meter Vertical Axis Wind Turbine [DE87-003503] N87-23022
A system for long pulse REB generation [IPPJ-812] N87-23274
STRUCTURAL DESIGN CRITERIA
Space station structures and dynamics test program N87-22751
STRUCTURAL MEMBERS
Daze fasteners [NASA-CASE-LAR-13009-2] N87-22976
Automated transient analysis of structural members [AD-A179042] N87-23007
Prediction of service life of aircraft structural components using the half-cycle method [NASA-TM-86812] N87-23009
STRUCTURAL PROPERTIES (GEOLOGY)
Crater morphology and morphometry on the Uranian satellites N87-23343
Cratering history of Miranda N87-23344
The viscosity of Miranda N87-23345
Geology and cratering history of Ariel N87-23348
Accretional heating of the satellites of Saturn and Uranus N87-23355
Studies of outer planet satellites, Mercury and Uranus N87-23358
Preliminary results of geologic and remote sensing studies of Rima Mozart N87-23431
Groundwater sapping channels: Summary of effects of experiments with varied stratigraphy N87-23461
Fluvial valleys on Martian volcanoes N87-23462
Possible origin of some channels on Alba Patera, Mars N87-23465
Evidence for glaciation in Elysium N87-23468
Water and ice on Mars: Evidence from Valles Marineris N87-23469
Geomorphic evidence for ancient seas in west Deuteronilus Mensae, Mars-1: Regional geomorphology N87-23471
Geomorphic evidence for ancient seas in west Deuteronilus Mensae, Mars-2: From very high resolution Viking Orbiter images N87-23472
STRUCTURAL RELIABILITY
Structural Integrity and Durability of Reusable Space Propulsion Systems [NASA-CP-2471] N87-22766
Probabilistic Structural Analysis Methods (PSAM) for select space propulsion system structural components N87-22784
The NESSUS finite element code N87-22785
STRUCTURAL VIBRATION
Analytical and experimental studies of flow-induced vibration of SSME components N87-22771
SUBLIMATION
Solid sulfur in vacuum: Sublimation effects on surface microtexture, color and spectral reflectance, and applications to planetary surfaces N87-23438
Determination of surface shear stress with the naphthalene sublimation technique N87-23460
SUBROUTINES
An algorithm for the computation of generalized likelihood or self-critical estimators for binary data [AD-A178545] N87-23179
SUBSONIC SPEED
The aerodynamic optimization of wings at subsonic speeds and the influence of wingtip design [NASA-TM-88534] N87-22627
SUBSTRATES
Laser cladding of Mg and Nb alloys for improved environmental resistance [AD-A179606] N87-22833
A statistical study of the combined effects of substrate temperature, bias, annealing, and a Cr3Si2 undercoating on the tribological properties of RF-sputtered MoS2 coatings [DE87-007086] N87-23285
Atomistic simulation of stability properties and growth of strained layer structures [DE87-006712] N87-23297
Modeling of substrate and implantation effects on the threshold voltage of MESFET structures fabricated in semi-insulating GaAs [AD-A178550] N87-23303
SUBSTRUCTURES
Analysis of structures with rotating, flexible substructures applied to rotorcraft aeroelasticity in GRASP (General Rotorcraft Aeromechanical Stability Program) [AD-A178941] N87-22677
Analysis of structures with rotating, flexible substructures [AD-A178903] N87-23004
SULFATES
Calcium carbonate and calcium sulfate in Martian meteorite EETA79001 N87-23409
SULFIDES
Lithium-metal sulfide battery development and submodule demonstration [DE87-004819] N87-22904
Gossans on Mars: Spectral features attributed to jarosite N87-23417
SULFUR
Sulfur-oxygen processes on Io N87-23437
Solid sulfur in vacuum: Sublimation effects on surface microtexture, color and spectral reflectance, and applications to planetary surfaces N87-23438
Observations of industrial sulfur flows and implications for Io N87-23541
SULFUR OXIDES
Sulfur-oxygen processes on Io N87-23437
SUNLIGHT
A feasibility study of the flexible simulation of sunlight — cockpit simulators [BR96783] N87-22693
SUNSPOT CYCLE
Observations of solar flux at the Algonquin Radio Observatory on 2800 MHz and the Dominion Radio Astrophysical Observatory on 2700 MHz [ARO-15] N87-23566
SUNSPOTS
Simultaneous SMM flat crystal spectrometer and very large array observations of solar active regions [AD-A179698] N87-23562
SUPERCOMPUTERS
Parallel graph reduction on a supercomputer [DE87-006066] N87-23173
Reading patterns in online documentation: How transcript analysis reflects text design, software constraints, and user preferences [DE87-006466] N87-23174
SUPERCONDUCTIVITY
Superconducting Augmented Rail Gun (SARG) [AD-A179269] N87-22701
SUPERCONDUCTORS
Superconducting thin films, composites and junctions [AD-A179346] N87-23288
SIS (Superconductor-Insulator-Superconductor) mixer research [AD-A179604] N87-23293
SUPERHIGH FREQUENCIES
Wideband parallel-plate waveguide, phased-array antenna [AD-A179402] N87-22873
Goldstone radar observations of Mars: The 1986 opposition N87-23444
SUPERLATTICES
Temperature dependence of implantation damage in strained-layer superlattices [DE87-007676] N87-23299
SUPERPLASTICITY
Superplasticity: A fundamental investigation on deformation mechanism and cavitation phenomena [AD-A179651] N87-22834
SUPERSONIC AIRCRAFT
Description of an aeronautical geometry conversion package: Wave-drag to Langley Wireframe Geometry Standard (LaWGS) to Supersonic Implicit Marching Potential (SIMP) [NASA-CR-178299] N87-23194
SUPERSONIC COMPRESSORS
A study of fluid-dynamic pressure fields on compressor reed valves [AD-A178584] N87-22938
SUPERSONIC CRUISE AIRCRAFT RESEARCH
High altitude turbulence for supersonic cruise vehicles [NASA-TM-88285] N87-23100
SUPERSONIC DRAG
Description of an aeronautical geometry conversion package: Wave-drag to Langley Wireframe Geometry Standard (LaWGS) to Supersonic Implicit Marching Potential (SIMP) [NASA-CR-178299] N87-23194
SUPERSONIC FLOW
Numerical simulation of supersonic flow over a rotating band using flowfield blanking [AD-A178492] N87-22624
Application of advanced computational codes in the design of an experiment for a supersonic throughflow fan rotor [NASA-TM-88915] N87-22630

Supersonic through-flow fan design
[NASA-TM-88908] N87-22681
Numerical study of high speed viscous flows
[AD-A178639] N87-22940
SUPERSONIC NOZZLES
Supersonic through-flow fan design
[NASA-TM-88908] N87-22681
SUPERSONIC SPEED
Experimental cavity pressure distributions at supersonic speeds
[NASA-TP-2683] N87-22626
SUPPORTS
Influence of supporting conditions on stress intensity factors for single-edge-cracked specimens under bending
[NASA-TT-20016] N87-23008
SUPPRESSORS
Afterburning suppression kinetics
[AD-A178967] N87-22863
SURFACE CRACKS
Dynamic fracture under plane wave loading
[AD-A178594] N87-23001
SURFACE LAYERS
Corrosion, wear and mechanical properties of pulse-electrodeposited alloys
[AD-A178596] N87-22842
Studies of the east Australian current off northern New South Wales
[AD-A178461] N87-23103
The characterization of whiskers produced by electromigration on suspended aluminum linestripes
[AD-A179383] N87-23290
SURFACE NAVIGATION
Joint University Program for Air Transportation Research, 1984
[NASA-CP-2452] N87-22604
SURFACE PROPERTIES
Metalliding as an electrochemical process
[AD-A178744] N87-22843
Detection of reflector surface error from near-field data: Effect of edge diffracted field
[NASA-TM-89920] N87-22874
Experimental studies on the impact properties of water ice N87-23364
Temperatures and minimum thickness of the inactive surface layer of comet Halley N87-23365
Comet thermal modeling N87-23368
Meteorite spectroscopy and characterization of asteroid surface materials N87-23373
Source of the optical red-slope in iron-rich meteorites N87-23374
SURFACE REACTIONS
Semiconductor research capabilities at the Lawrence Berkeley Laboratory
[DE87-006931] N87-23298
Unpinning of the Fermi level on GaAs by flowing water
[AD-A178489] N87-23302
On the sputter alteration of regoliths of outer solar system bodies N87-23434
SURFACE ROUGHNESS
Equipment for turbulent heat transfer test apparatus
[AD-A179612] N87-22930
Interaction of a three-dimensional roughness element with a laminar boundary layer
[AD-A178668] N87-22941
Laser reflectance as a function of rough water glitter profile
[AD-A178774] N87-23016
SURFACE TEMPERATURE
Application of atomic fluorescence to measurement of combustion temperature in solid propellants
[AD-A179665] N87-22862
Temperatures and minimum thickness of the inactive surface layer of comet Halley N87-23365
SURFACE WAVES
Joint services electronics program
[AD-A178599] N87-22879
SURGES
Laser spectroscopy of transient molecules important in explosions
[AD-A178456] N87-22828
Transient protection of electronic circuits
[AD-A178945] N87-22919
Composite velocity procedures for flows with pressure interaction
[AD-A179602] N87-22929
SURVEILLANCE
A 3-D world modeling based on combinatorial geometry for autonomous robot navigation
[DE87-002814] N87-22980
SURVEYS
Selection of dimensions for an anthropometric data base. Volume 1: Rationale, summary, and conclusions
[AD-A179566] N87-23112
Aircrew task surveys: Selection criteria for low-cost training technology applications
[AD-A178473] N87-23146
Sensitivity analysis for stationary probabilities of a Markov chain
[AD-A178556] N87-23240
SWEPT FORWARD WINGS
X-29 integrating advanced technologies for tomorrow's air combat N87-22671
SWIRLING
Numerical simulation of the decay of swirling flow in a constant volume engine simulator
[LA-10728-MS] N87-22945
SWITCHES
Gas mixtures for spark gap closing switches with emphasis on efficiency of operation
[DE87-006624] N87-22906
Magnetically insulated opening switch research
[AD-A178895] N87-22918
SWITCHING CIRCUITS
Silicon pulse sharpening diodes: Switching kilovolts in 10's of picoseconds
[DE87-005073] N87-22905
Coordinated research program in pulsed power physics
[AD-A178625] N87-22912
Opening switch research on a dense plasma focus
[AD-A179693] N87-23276
SYMBOLS
Optical symbolic processor for expert system execution
[AD-A179375] N87-23172
SYMMETRY
The chiral symmetry aspects of supersymmetric confining gauge theories
[ETN-87-99553] N87-23305
SYMPATHETIC NERVOUS SYSTEM
Biochemical aspects of some neurohumoral system functions during long-term antiorthostatic hypokinesia N87-23142
SYNCHRONISM
Cross-axis synchronous flow-through coil planet centrifuge free of rotary seals: Apparatus and method for performing countercurrent chromatography
[PB87-126926] N87-22816
SYNCHRONOUS SATELLITES
On orbital allotments for geostationary satellites
[NASA-CR-181017] N87-22700
Star sensor fine attitude pointing model for a spinning geosynchronous satellite
[AD-A179424] N87-22763
SYNOPTIC METEOROLOGY
Synoptic-scale influence on the variability of the Alpine Experiment (ALPEX) low-level jet N87-23089
SYNTAX
Specifying functional and timing behavior for real-time applications
[AD-A178769] N87-23206
SYNTHESIS (CHEMISTRY)
Basic research in energetic fluorocarbons
[AD-A179676] N87-22822
Polyenamines from aromatic diacetylenic diketones and diamines
[NASA-CASE-LAR-13444-1-CU] N87-22847
Physical properties and structure of ion-containing polymers
[AD-A178592] N87-22855
Low-pressure self-propagating high-temperature synthesis
[AD-A178593] N87-22856
Processible boron nitride preceramic polymers
[AD-A178907] N87-22859
SYNTHETIC APERTURE RADAR
A compilation system for Venus radar mission (Magellan) N87-23440
SYNTHETIC FIBERS
Examination of high performance polymer fibers under compressive deformation
[AD-A178640] N87-22857
SYSTEM FAILURES
Intelligent fault-tolerant controllers N87-22621
SYSTEM IDENTIFICATION
Identification of large space structures: A state-of-practice report N87-22705
Linear time invariant system identification using a result of the Bussgang theorem
[AD-A178642] N87-23216
SYSTEMS ANALYSIS
GEMACS (general EM model for the analysis of computer systems) frequency-domain analysis to determine the lightning induced electromagnetic skin current distributions on an aircraft
[AD-A178854] N87-22660
Performance improvement of airborne weapon systems methods, scope and limitations N87-22665
Weapon systems polyvalence: An economic and operational challenge N87-22667
Flight and analytical investigations of a structural mode excitation system on the YF-12A airplane
[NASA-CR-166623] N87-22685
Integrated restructurable flight control system demonstration results
[NASA-CR-178305] N87-22692
A quasi-analytical method for non-iterative computation of nonlinear controls N87-22731
Simulation model of a meteor burst communication system for data transmission protocol evaluation
[AD-A178643] N87-22881
Development of a microcomputer-based workstation for analysis of digital satellite links
[AD-A178872] N87-22888
SYSTEMS COMPATIBILITY
The impact of future avionics technology on the conduct of air warfare N87-22673
SYSTEMS ENGINEERING
Design of GPS (Global Positioning System) status reporting system
[AD-A179334] N87-22662
Performance improvement of airborne weapon systems methods, scope and limitations N87-22665
Weapon systems polyvalence: An economic and operational challenge N87-22667
Evolution of combat performance of the Hawk light combat aircraft N87-22668
Integrated design of structures N87-22669
Propulsion system technologies for thrust vectoring N87-22670
Probabilistic Structural Analysis Methods (PSAM) for select space propulsion system structural components N87-22784
Modeling digital control systems with MA-prefiltered measurements
[NASA-TP-2732] N87-22870
Design, development and deployment of public service photovoltaic power/load systems for the Gabonese Republic
[NASA-CR-179603] N87-23030
Proceedings of the 22nd Annual Conference on Manual Control
[AD-A178627] N87-23148
The design of a real time operating system for a fault tolerant microcomputer
[AD-A178577] N87-23155
Summary of the SEI (Software Engineering Institute) Workshop on Softwear Configuration Management
[AD-A178770] N87-23184
The heterogeneous machine simulator
[AD-A178771] N87-23185
Measuring software design
[NASA-TM-88372] N87-23189
Specifying functional and timing behavior for real-time applications
[AD-A178769] N87-23206
Linear time invariant system identification using a result of the Bussgang theorem
[AD-A178642] N87-23216
SYSTEMS INTEGRATION
Propulsion system technologies for thrust vectoring N87-22670
X-29 integrating advanced technologies for tomorrow's air combat N87-22671
Simulation of an integrated flight/fire control system during air-to-ground gunnery attack N87-22672
The impact of future avionics technology on the conduct of air warfare N87-22673
Commit your works to the Lord, and your thoughts shall be established (Prov. 16:3). Inter-stable control systems N87-22716
Rationalizing VICAR within a TAE framework: Some problems and some solutions N87-23165
SYSTEMS MANAGEMENT
Managing uncertainty in expert systems: A probabilistic approach
[AD-A178582] N87-23246

T

TANTALUM NITRIDES
Electrochemical adjustment of thin film Ti-Pd resistors
[DE87-007382] N87-22837
TARGET ACQUISITION
Celestial target observability for astro spacelab missions
[NASA-TM-86591] N87-22696
A multiple model adaptive tracking algorithm for a high energy laser weapon system
[AD-A178978] N87-22974
TARGET RECOGNITION
Radar target classification studies
[AD-A179010] N87-22889

The integration of spectral and spatial analysis for land use classification
[AD-A178703] N87-23015
Asymmetries in the control of saccadic eye movements to bifurcating targets
[AD-A179270] N87-23108
Automatic scene analysis using hierarchical spatial frequency domain correlation with energy normalization and heuristic noise reduction
[AD-A178589] N87-23181

TARGETS
CO2 pulsed laser damage mechanism and plasma effects (focused beam)
[AD-A179201] N87-22961
Target fabrication for high density target experiments at the University of Rochester's Laboratory for Laser Energetics
[DE87-005915] N87-22967
A new LIHE (Light Initiated High Explosive) test capability for spherical targets
[DE87-003035] N87-23245
Centrifuge impact cratering experiments: Scaling laws for non-porous targets N87-23495
Centrifuge impact cratering experiments: Scaling laws for non-porous targets N87-23496

TASKS
Performance evaluation of parallel branch and bound search with the intel IPSC (Intel Personal SuperComputer) hypercube computer
[AD-A179384] N87-23196

TEA LASERS
CO2 pulsed laser damage mechanism and plasma effects (focused beam)
[AD-A179201] N87-22961

TECHNICAL WRITING
A development system for augmented transition network grammars and a large grammar for technical prose
[AD-A179009] N87-23188

TECHNOLOGICAL FORECASTING
Cost analysis of aircraft projects N87-22664
Air Force technical objectives document, fiscal year 1988
[AD-A179163] N87-23569

TECHNOLOGY ASSESSMENT
The assessment and evaluation of combat performance improvements N87-22675
Performance comparison of four state-of-the-art computer architectures
[AD-A179071] N87-23149

TECHNOLOGY UTILIZATION
Potential medical applications of TAE N87-23166
Naval applications of a TAE-derived executive N87-23167

TECTONICS
Comments on the tectonism of Venus N87-23515
Lithospheric structure on Venus from tectonic modelling of compressional features N87-23516
Venusian tectonics: Convective coupling to the lithosphere? N87-23517
Lithospheric loading and tectonics of the lunar irregular maria N87-23522
Timing of ancient extensional tectonic features on Mars N87-23526
Stress history of the Tharsis Region, Mars N87-23527
History and morphology of faulting in the Noctis Labyrinthus-Claritas Fossae Region of Mars N87-23528
Thin and thick-skinned deformation in the Tharsis Region of Mars N87-23529
Flexurally-resisted uplift of the Tharsis Province, Mars N87-23530
Tectonic domains in the Eastern Hemisphere of Mars N87-23531

TELECOMMUNICATION
A system design requirements tool for satellite communications through nuclear-induced scintillation
[AD-A179272] N87-22871
The effect of multipath on digital communications systems: With application to space station
[AD-A178578] N87-22876
Simulation model of a meteor burst communication system for data transmission protocol evaluation
[AD-A178643] N87-22881

TELEOPERATORS
Advanced technology mobile robotics vehicle fleet
[DE87-007526] N87-22982
Tactile feedback for teleoperator systems
[AD-A179054] N87-22983

TELESCOPES
Two-point resolution criterion for multi-aperture optical systems
[AD-A178980] N87-23271

TELEVISION CAMERAS
Image processing for vision: An equipment requests to DOD
[AD-A179261] N87-23150

TEMPER (METALLURGY)
Hydrogen and temper embrittlement interactions in fatigue of 2 1/4Cr1Mo steel
[AERE-R-12322] N87-22830

TEMPERATE REGIONS
Sensitivity of tropical and mid-latitude time-averaged atmospheric states to interannually varying global ocean surface temperature distribution N87-23039
Preliminary results from a Tropical Ocean Global Atmosphere (TOGA) related experiment performed at Hamburg (West Germany) with the ECWME General Circulation Model (GCM) with T21 resolution N87-23040

TEMPERATURE DEPENDENCE
Temperature dependence of implantation damage in strained-layer superlattices
[DE87-007678] N87-23299

TEMPERATURE DISTRIBUTION
Thermocapillary bubble migration for large Marangoni Numbers
[NASA-CR-179628] N87-22865
Sensitivity of tropical and mid-latitude time-averaged atmospheric states to interannually varying global ocean surface temperature distribution N87-23039
Energy budget of an Alpine valley N87-23076
Valley circulations as measured in the Himalaya by instrumented motor glider N87-23077
Cierzo: Northwesterly wind along the Ebro Valley (Spain) as a mesoscale effect induced on the lee of the Pyrenees mountain range; a case study during the Alpine Experiment (ALPEX) Special Observing Period N87-23083
Numerical studies of collapsing interstellar clouds
[NASA-CR-180933] N87-23340

TEMPERATURE EFFECTS
Deformation and fatigue behavior of SSME turbopump blade materials N87-22776
Structural analysis demonstration of constitutive and life models N87-22780
Temperatures and minimum thickness of the inactive surface layer of comet Halley N87-23365

TEMPERATURE GRADIENTS
Experimental and theoretical studies of time-averaged and time resolved rotor heat transfer N87-22770
Mechanical properties of high gradient and hot isostatically pressed PWA 1480 N87-22781
Thermocapillary bubble migration for large Marangoni Numbers
[NASA-CR-179628] N87-22865
A study into the generation of temperature gradients in materials for detecting and measuring the depth of sub-surface cracks
[AERE-R-12382] N87-22991
Air-sea interaction over the Mediterranean Sea during the Alpine Experiment (ALPEX) Special Observing Period N87-23073

TEMPERATURE MEASUREMENT
Experimental and theoretical studies of time-averaged and time resolved rotor heat transfer N87-22770
Progress on thin-film sensors for space propulsion technology N87-22772
Heat flux calibration facility capable of SSME conditions N87-22774
Numerical study of the effects of boundary conditions on the measurement and calibration of gardon type heat flux sensors N87-22775

TEMPERATURE MEASURING INSTRUMENTS
Numerical study of the effects of boundary conditions on the measurement and calibration of gardon type heat flux sensors N87-22775

TEMPERING
Austempered ductile iron process development
[PB87-169843] N87-22868

TENSILE DEFORMATION
Martensitic transformation as a deformation process
[DE87-007068] N87-22836

TENSILE PROPERTIES
Dynamic fracture under plane wave loading
[AD-A178594] N87-23001

TENSILE STRENGTH
Examination of high performance polymer fibers under compressive deformation
[AD-A178640] N87-22857
Failure strength of icy lithospheres N87-23357

TENSILE STRESS
The effect of overburden thickness on tension fracture patterns above an uplifting dome N87-23535

TERRAIN
The viscosity of Miranda N87-23345
Photometric properties of lunar terrains derived from Hapke's equation N87-23432
A preliminary analysis of the Mariner 10 color ratio map of Mercury N87-23439

TERRAIN ANALYSIS
Pseudocraters as indicators of ground ice on Mars N87-23474
Late-stage flood lavas in the Elysium region, Mars N87-23476
Martian volcanism: Festoon-like ridges on terrestrial basalt flows and implications for Mars N87-23478
Revision of the Martian relative age chronology N87-23504
Early changes in gradation styles and rates on Mars N87-23505
Ejecta types on Ganymede and Callisto N87-23512
Local-scale stratigraphy of grooved terrain on Ganymede N87-23538
Mars digital terrain model N87-23549
Martian terrains N87-23555

TERRESTRIAL PLANETS
The Martian crustal dichotomy: Product of accretion and not a specific event? N87-23524

TEST FACILITIES
Target fabrication for high density target experiments at the University of Rochester's Laboratory for Laser Energetics
[DE87-005915] N87-22967
Structural design and fabrication of the Sandia 34-meter Vertical Axis Wind Turbine
[DE87-003503] N87-23022
The status of the vertical axis wind turbine research test bed
[DE87-005524] N87-23023
Applications and requirements for real-time simulators in ground-test facilities
[NASA-TP-2672] N87-23202

TEST FIRING
A fast, low resistance switch for small slapper detonators
[AD-A178562] N87-22911

TETHERING
Optimal shuttle altitude changes using tethers
[AD-A179205] N87-22756

TETHERLINES
Optimal shuttle altitude changes using tethers
[AD-A179205] N87-22756

TEXTS
Reading patterns in online documentation: How transcript analysis reflects text design, software constraints, and user preferences
[DE87-006466] N87-23174

TEXTURES
The integration of spectral and spatial analysis for land use classification
[AD-A178703] N87-23015
Solid sulfur in vacuum: Sublimation effects on surface microtexture, color and spectral reflectance, and applications to planetary surfaces N87-23438

THEMATIC MAPPING
Comments on the tectonism of Venus N87-23515

THEOREMS
The applicability of the stable laws in collective risk theory and practice
[AD-A178546] N87-23238

THERMAL BOUNDARY LAYER
Thermocapillary bubble migration for large Marangoni Numbers
[NASA-CR-179628] N87-22865

THERMAL CONDUCTIVITY
Thermal expansion of epoxy-fiberglass composite specimens
[DE87-004273] N87-22812
Analytical characterization of shear localization in thermoviscoplastic materials
[AD-A178597] N87-23002
A new hydrodynamic analysis of double layers N87-23319

THERMAL EMISSION
Thermal-infrared spectral observations of geologic materials in emission N87-23425

THERMAL EXPANSION
Thermal shock resistance of mullite-based SiC-whisker composites
[AD-A179214] N87-22809
Thermal expansion of epoxy-fiberglass composite specimens
[DE87-004273] N87-22812
Boundary layer disturbances caused by periodic heating of a thin ribbon
[AD-A179342] N87-22925

THERMAL FATIGUE
Deformation and fatigue behavior of SSME turbopump blade materials N87-22776

THERMAL MAPPING
Progress in optical strain measurement system development N87-22773
Characterization of surficial units on Mars using Viking orbiter multispectral image and thermal data N87-23418

Regional sources and sinks of dust on Mars: Viking observations of Cerberus, Solis Planum and Syrtis Major N87-23450
High resolution thermal infrared mapping of Martian channels N87-23451
Explosive volcanic deposits on Mars: Preliminary investigations N87-23473
Martian volcanism: Festoon-like ridges on terrestrial basalt flows and implications for Mars N87-23478
Thermal inertia characteristics of the Martian crater Curie N87-23509
Dome craters on Ganymede N87-23510

THERMAL PLASMAS
CO2 pulsed laser damage mechanism and plasma effects (focused beam)
[AD-A179201] N87-22961

THERMAL RESISTANCE
Thermal shock resistance of mullite-based SiC-whisker composites
[AD-A179214] N87-22809

THERMAL STRESSES
Probabilistic structural analysis verification studies N87-22786

THERMIONIC DIODES
Magnetically insulated opening switch research
[AD-A178895] N87-22918

THERMOCOUPLES
Progress on thin-film sensors for space propulsion technology N87-22772
Control systems development, research and development
[DE87-005785] N87-22868

THERMODYNAMIC PROPERTIES
Numerical study of high speed viscous flows
[AD-A178639] N87-22940
Analytical characterization of shear localization in thermoviscoplastic materials
[AD-A178597] N87-23002
The delineation and interpretation of the Earth's gravity field
[NASA-CR-181015] N87-23065
Thermodynamic properties of molten salt solutions
[DE87-004948] N87-23306
Mechanical and thermal properties of planetologically important ices N87-23346

THERMODYNAMICS
Experimental and theoretical studies of time-averaged and time resolved rotor heat transfer N87-22770
Thermocapillary bubble migration for large Marangoni Numbers
[NASA-CR-179628] N87-22865
NBS calibration services users guide, 1986-1988 edition
[NBS-SP-250] N87-22958
Thermodynamic properties of molten salt solutions
[DE87-004948] N87-23306
SO2 on Io: A thermodynamic perspective N87-23359

THERMOELECTRIC POWER GENERATION
Thermoelectric conversion with ion conductors
[AD-A179353] N87-23019

THERMOELECTRICITY
On the control of structures by applied thermal gradients N87-22747
Thermoelectric conversion with ion conductors
[AD-A179353] N87-23019

THERMOGRAPHY
Application of atomic fluorescence to measurement of combustion temperature in solid propellants
[AD-A179665] N87-22862

THERMOPLASTIC RESINS
Process for crosslinking and extending conjugated diene-containing polymers
[NASA-CASE-LAR-13452-1] N87-22848

THICKNESS
Thin and thick-skinned deformation in the Tharsis Region of Mars N87-23529
The effect of overburden thickness on tension fracture patterns above an uplifting dome N87-23535

THIN FILMS
Progress on thin-film sensors for space propulsion technology N87-22772
Characterizing the hardness and modulus of thin films using a mechanical properties microprobe
[DE87-006612] N87-22826
Electrochemical adjustment of thin film Ti-Pd resistors
[DE87-007392] N87-22837
Molecular reactions at the film surface in plasma polymerization
[DE87-002488] N87-22849
Fundamental studies of the mechanical behavior of microelectronic thin film materials
[AD-A179699] N87-22902
Molecular-dynamics simulation of thin-film growth
[DE87-006973] N87-23284
Superconducting thin films, composites and junctions
[AD-A179346] N87-23288
AlGaAs growth by OMCVD using an excimer laser
[NASA-TM-88937] N87-23304

THIN WALLED SHELLS
Nonisothermal elasto-visco-plastic response of shell-type structures N87-22796

THREE BODY PROBLEM
Solar system dynamics N87-23390
Orbital resonances, unusual configurations and exotic rotation states among planetary satellites N87-23391

THREE DIMENSIONAL BOUNDARY LAYER
Interaction of a three-dimensional roughness element with a laminar boundary layer
[AD-A178868] N87-22941

THREE DIMENSIONAL FLOW
Application of advanced computational codes in the design of an experiment for a supersonic throughflow fan rotor
[NASA-TM-88915] N87-22630
Direct numerical simulations of an unpremixed turbulent jet flame
[AD-A179358] N87-22819
A three-dimensional dual potential procedure with applications to wind tunnel inlets and interacting boundary layers
[NASA-CR-180939] N87-22944

THRESHOLD VOLTAGE
Modeling of substrate and implantation effects on the threshold voltage of MESFET structures fabricated in semi-insulating GaAs
[AD-A178550] N87-23303

THRUST
Estimation of ICBM (intercontinental ballistic missile) performance parameters
[AD-A179204] N87-22754
Investigation of rocket powered, open cycle, magnetohydrodynamic generators for high, pulsed power needs in space
[AD-A178869] N87-22801

THRUST CONTROL
Preliminary evaluation of a reaction control system for the space station N87-22736
Space station structural dynamics/reaction control system interaction study N87-22753

THRUST VECTOR CONTROL
Propulsion system technologies for thrust vectoring N87-22670

THUNDERSTORMS
Characteristics of orographically initiated convection — Rocky Mountains N87-23092

TIDES
Could Ariel have been heated by tidal friction? N87-23347
On the lack of commensurabilities in the mean motions of the satellites of Uranus and the resurfacing of Ariel N87-23349
Why no orbital resonances among the satellites of Uranus? N87-23351
Shapes of small satellites N87-23354
Investigations of the surfaces and interiors of outer planet satellites N87-23356

TIME DEPENDENCE
Possible inflationary solution to the short distance gravity model
[DE87-701559] N87-23339

TIME LAG
Control of linear systems over commutative normed algebras with applications
[AD-A178765] N87-23205

TIME MARCHING
Flow dynamics stimulated by hairpin-like vortices in initially laminar boundary layers
[AD-A179578] N87-22927

TIMING DEVICES
Processor-controlled timing module for Loran-C receiver
[OU-TM-90] N87-22616

TIN
Structure and properties of novel compounds of silicon germanium and tin
[AD-A179433] N87-23291

TITANIA
The role of particle substructure in the sintering of monosized titania
[DE87-007600] N87-22839

TITANIUM
Electrochemical adjustment of thin film Ti-Pd resistors
[DE87-007392] N87-22837

TOKAMAK DEVICES
Experimental study of coupling between eddy curren of Tokamak limiters of tokamak limiters
[DE87-004938] N87-22999

TOMOGRAPHY
Strategies for high-resolution 3-D millimeter wave imaging
[AD-A178653] N87-22882
Phase space methods and path integration: A microscopic approach to direct and inverse wave propagation
[AD-A178557] N87-23249
White-light optical information processing and holography
[AD-A179489] N87-23260

TOPOGRAPHY
The delineation and interpretation of the Earth's gravity field
[NASA-CR-181015] N87-23065
Validation of a surface-layer windflow model using climatology and meteorological tower data from Vandenberg AFB, California
[AD-A178480] N87-23097
Implications of convection in the Moon and the terrestrial planets N87-23406
Characterization of surficial units on Mars using Viking orbiter multispectral image and thermal data N87-23418
Physiographic constraints on the origin of lunar wrinkle ridges N87-23521
Curvilinear ridges and related features in southwest Cydonia Mensae, Mars N87-23537
Large scale topography of Io N87-23543
Progress in compilation of the 1:2,000,000-scale topographic map N87-23548
Mars digital terrain model N87-23549

TOROIDS
Confinement and heating of high beta plasmas with emphasis on compact toroids. Task 2: Stellarator and heliac research
[DE87-005554] N87-23278

TORSION
Correlation of analytical calculations from GRASP (General Rotorcraft Aeromechanical Stability Program) with torsionally-soft rotor data
[AD-A178881] N87-22689

TOUCH
Tactile feedback for teleoperator systems
[AD-A179054] N87-22983

TOWED BODIES
Optimal shuttle altitude changes using tethers
[AD-A179205] N87-22756

TOWERS
Validation of a surface-layer windflow model using climatology and meteorological tower data from Vandenberg AFB, California
[AD-A178480] N87-23097

TRACKING (POSITION)
Evaluation of numerator lead effects on aircraft handling qualities
[AD-A179388] N87-22687
Evaluation of a heliostat tracker for linear Fresnel lens photovoltaic concentrators
[DE87-008331] N87-23025

TRAILING EDGES
Verification of performance results for a low-speed 15 percent elliptical circulation control airfoil
[NASA-CR-181020] N87-22633

TRAINING AIRCRAFT
Evolution of combat performance of the Hawk light combat aircraft N87-22668
Evaluation of numerator lead effects on aircraft handling qualities
[AD-A179388] N87-22687

TRAINING ANALYSIS
Instructions to working groups N87-22655

TRAINING EVALUATION
Group-level issues in the design and training of cockpit crews N87-22636
Introduction to Trans Australia Airlines CRM training N87-22644
Aircrew team management program N87-22645
Cockpit Resource Management (CRM) training in the 1550th combat crew training wing N87-22650
Instructions to working groups N87-22655

TRAINING SIMULATORS
The development and implementation of cockpit resource management in UAL recurrent training N87-22638

TRAJECTORIES
Determining the probability of close approach between two satellites
[AD-A179385] N87-22699

TRAJECTORY ANALYSIS
Impacts of hemispherical granular targets: Implications for global impacts N87-23490

TRAJECTORY CONTROL
Safe microburst penetration techniques: A deterministic, nonlinear, optimal control approach N87-22620

TRAJECTORY MEASUREMENT
Investigation of air transportation technology at Massachusetts Institute of Technology, 1984 N87-22605

TRANSFER FUNCTIONS
Lanczos modes for reduced-order control of flexible structures N87-22739
TRANSFER OF TRAINING
Cockpit Resource Management (CRM): A tool for improved flight safety (United Airlines CRM training) N87-22637
Cockpit management and Specific Behavioral Objectives (SBOs) N87-22640
Pan American World Airways flight training: A new direction. Flight operations resource management N87-22641
Crew coordination concepts: Continental Airlines CRM training N87-22642
Remedial training: Will CRM work for everyone N87-22646
Cockpit Resource Management (CRM) for part 91 and 135 operations N87-22652
Cockpit Resource Management (CRM) for FAR Parts 91 and 135 operators N87-22653
TRANSFORMATIONS (MATHEMATICS)
Optical acquisition, image and data compression [AD-A178506] N87-23154
Differential-algebraic equation index transformations [DE87-005543] N87-23209
TRANSFORMERS
A coherent VLSI environment [AD-A179303] N87-22897
TRANSIENT RESPONSE
Transient response for interaction of two dynamic bodies N87-22709
TRANSITION METALS
Investigation of the icosahedral Z-phase in aluminium transition metal alloys and rapidly solidified Al-alloys [AD-A178451] N87-22840
TRANSMISSION LINES
Full-wave analysis of isolated and coupled microwave transmission lines using the finite element method [AD-A178805] N87-22883
TRANSMISSION LOSS
Characterization of the error performance of a QPSK (Quadrature Phase Shift Keyed) communication system in the presence of linear transmission distortion [AD-A178855] N87-22887
TRANSMISSIONS (MACHINE ELEMENTS)
Helicopter transmission testing at NASA Lewis Research Center [NASA-TM-89912] N87-22978
TRANSMITTER RECEIVERS
The effect of multipath on digital communications systems: With application to space station [AD-A178578] N87-22876
TRANSMITTERS
Klystron transmitters [AD-A179068] N87-22896
Preliminary investigation of ionospheric modification using oblique incidence high power HF radio waves [AD-A179174] N87-23056
TRANSONIC FLOW
Results of the integration of a transonic full-potential analysis program with a free-wake lifting-line program for hovering rotors [NASA-TM-89494] N87-22631
Composite velocity procedures for flows with pressure interaction [AD-A179602] N87-22929
Prediction of high-speed rotor noise with a Kirchhoff formula [AD-A178982] N87-23250
TRANSPORT PROPERTIES
The application of flow competence evaluations to the assessment of flood-flow velocities and stresses N87-23464
TRANSVERSE ACCELERATION
Fast ion mass spectrometry and charged particle spectrography investigations of transverse ion acceleration and beam-plasma interactions [NASA-CR-168348] N87-22817
TRAPPED PARTICLES
Formation mechanisms of laboratory double layers N87-23314
TRAVELING WAVE TUBES
Revised NASA axially symmetric ring model for coupled-cavity traveling-wave tubes [NASA-TP-2675] N87-22923
TREADMILLS
Relationship between a two mile run and maximal oxygen uptake [AD-A179343] N87-23109
TRIBOLOGY
A statistical study of the combined effects of substrate temperature, bias, annealing, and a Cr3Si2 undercoating on the tribological properties of RF-sputtered MoS2 coatings [DE87-007066] N87-23285
TRIGGER CIRCUITS
Coordinated research program in pulsed power physics [AD-A178625] N87-22912
TRITIUM
Two-color, Doppler-free ionization of molecular hydrogen for isotopic analysis [DE87-004975] N87-22825
TROILITE
Melting of troilite at high pressure in a diamond cell by laser heating N87-23398
TROPICAL METEOROLOGY
Sensitivity of tropical and mid-latitude time-averaged atmospheric states to interannually varying global ocean surface temperature distribution N87-23039
Preliminary results from a Tropical Ocean Global Atmosphere (TOGA) related experiment performed at Hamburg (West Germany) with the ECWME General Circulation Model (GCM) with T21 resolution N87-23040
Tropical Pacific SST experiments with the GLAS climate model — sea surface temperature (SST) N87-23049
The development of a coupled GCM suitable for modelling studies in TOGA — general circulation model (GCM); Tropical Ocean Global Atmosphere (TOGA) N87-23055
TROPICAL REGIONS
A preliminary theory of the origin of the 40-50 day oscillation — tropical atmosphere N87-23044
TROPOSPHERE
New methods for obtaining scattering and absorption from tropospheric visible spectrum data [AD-A178590] N87-23062
TRUCKS
Accelerations experienced by packaged materiel during fork lift truck handling [RDI-284/45/3] N87-22989
TRUSSES
Dynamics of trusses having nonlinear joints N87-22724
Equivalent beam modeling using numerical reduction techniques N87-22725
Dual keel space station control/structures interaction study N87-22737
Experimental characterization of deployable trusses and joints N87-22749
TUNGSTEN
Fiber reinforced superalloys [NASA-TM-89865] N87-22811
TUNING
Programmable electronic synthesized capacitance [NASA-CASE-GSC-12961-1] N87-22895
TURBINE BLADES
Supersonic through-flow fan design [NASA-TM-88908] N87-22681
Progress in the prediction of unsteady heat transfwe on turbines blades N87-22769
Progress on thin-film sensors for space propulsion technology N87-22772
Deformation and fatigue behavior of SSME turbopump blade materials N87-22776
Nonlinear heat transfer and structural analyses of SSME turbine blades N87-22779
Mechanical properties of high gradient and hot isostatically pressed PWA 1480 N87-22781
Probabilistic structural analysis to evaluate the structural durability of SSME critical components N87-22783
Probabilistic Structural Analysis Methods (PSAM) for select space propulsion system structural components N87-22784
Probabilistic SSME blades structural response under random pulse loading N87-22791
Quantifying uncertainties in the structural response of SSME blades N87-22792
Structural tailoring using the SSME/STAEBL code N87-22795
Dynamic characteristics of single crystal SSME blades N87-22797
SSME blade damper technology N87-22798
A linearized Euler analysis of unsteady flows in turbomachinery [NASA-CR-180987] N87-22948
A comparison of predicted wind turbine blade loads to test measurements [DE87-001130] N87-23021
Structural design and fabrication of the Sandia 34-meter Vertical Axis Wind Turbine [DE87-003503] N87-23022
The status of the vertical axis wind turbine research test bed [DE87-005524] N87-23023
TURBINE PUMPS
Studies and analyses of the space shuttle main engine: High-pressure oxidizer turbopump failure information propagation model [NASA-CR-179079] N87-22765
Heat flux calibration facility capable of SSME conditions N87-22774
Deformation and fatigue behavior of SSME turbopump blade materials N87-22776
Nonlinear heat transfer and structural analyses of SSME turbine blades N87-22779
Mechanical properties of high gradient and hot isostatically pressed PWA 1480 N87-22781
Probabilistic structural analysis to evaluate the structural durability of SSME critical components N87-22783
Probabilistic SSME blades structural response under random pulse loading N87-22791
Quantifying uncertainties in the structural response of SSME blades N87-22792
Dynamic characteristics of single crystal SSME blades N87-22797
SSME blade damper technology N87-22798
TURBINES
Simulation of multistage turbine flows N87-22768
TURBOCOMPRESSORS
Supersonic through-flow fan design [NASA-TM-88908] N87-22681
TURBOFAN ENGINES
Analysis of an advanced technology subsonic turbofan incorporating revolutionary materials [NASA-TM-89868] N87-22680
Supersonic through-flow fan design [NASA-TM-88908] N87-22681
TURBOFANS
Supersonic through-flow fan design [NASA-TM-88908] N87-22681
TURBOMACHINERY
Unsteady stator/rotor interaction N87-22767
A linearized Euler analysis of unsteady flows in turbomachinery [NASA-CR-180987] N87-22948
TURBULENCE
Dynamic stall calculations using a Navier-Stokes solver [AD-A178566] N87-22688
Prediction of fluid flow in curved pipe using the finite element method [AD-A179538] N87-22926
Conditional second order closure for turbulent shear flows [AD-A179661] N87-22931
TURBULENT BOUNDARY LAYER
Boundary layer disturbances caused by periodic heating of a thin ribbon [AD-A179342] N87-22925
Heat transfer effects of longitudinal vortices embedded in a turbulent boundary layer [DE87-006002] N87-22934
TURBULENT FLOW
Progress in the prediction of unsteady heat transfwo on turbines blades N87-22769
Analytical and experimental studies of flow-induced vibration of SSME components N87-22771
Direct numerical simulations of an unpremixed turbulent jet flame [AD-A179358] N87-22819
Prediction of fluid flow in curved pipe using the finite element method [AD-A179538] N87-22926
Experimental research on compressible turbulent shear layers, viscous-inviscid interactions, and flow separation [AD-A179579] N87-22928
Equipment for turbulent heat transfer test apparatus [AD-A179612] N87-22930
Conditional second order closure for turbulent shear flows [AD-A179661] N87-22931
Numerical simulation of the decay of swirling flow in a constant volume engine simulator [LA-10728-MS] N87-22945
TURBULENT HEAT TRANSFER
Equipment for turbulent heat transfer test apparatus [AD-A179612] N87-22930
TURBULENT JETS
A theory for turbulent curved wall jets [NASA-CR-181019] N87-22951
TWO DIMENSIONAL FLOW
Composite velocity procedures for flows with pressure interaction [AD-A179602] N87-22929
TWO PHASE FLOW
Pumped two-phase heat transfer loop [NASA-CASE-MSC-20841-1] N87-22950
TYCHO CRATER
Preliminary results of spectral reflectance studies of tycho crater N87-23430

U

ULTRAHIGH FREQUENCIES
Wideband parallel-plate waveguide, phased-array antenna [AD-A179402] N87-22873
ULTRASONIC FLAW DETECTION
Methodology for verification of ultrasonic inspection [AD-A179694] N87-22988
ULTRASONIC TESTS
Methodology for verification of ultrasonic inspection [AD-A179694] N87-22988
ULTRASONIC WAVE TRANSDUCERS
Measurement of ice accretion using ultrasonic pulse echo techniques N87-22608
ULTRASONIC WELDING
Control systems development, research and development [DE87-005785] N87-22868
ULTRASONICS
Measurement of ice accretion using ultrasonic pulse echo techniques N87-22608
Identification and validation of new anthropometric techniques for quantifying body composition [AD-A178753] N87-23118
ULTRAVIOLET ASTRONOMY
A study of the fundamental characteristics of 2175A extinction [NASA-CR-180926] N87-23336
ULTRAVIOLET REFLECTION
Atlas of reflectance spectra of terrestrial, lunar and meteoritic powders and frosts from 92 to 1800 •lc2)nm N87-23427
ULTRAVIOLET SPECTRA
Atlas of reflectance spectra of terrestrial, lunar and meteoritic powders and frosts from 92 to 1800 •lc2)nm N87-23427
UMBRIEL
Could Ariel have been heated by tidal friction? N87-23347
Geology and cratering history of Ariel N87-23348
On the lack of commensurabilities in the mean motions of the satellites of Uranus and the resurfacing of Ariel N87-23349
UNDERGROUND EXPLOSIONS
Body wave magnitudes and locations of French underground explosions at the Mururoa test site [BR-97934] N87-22947
UNITED KINGDOM
British Aerospace: A Kingston perspective [ETN-87-99823] N87-23308
UNIVERSITIES
The Galilean satellite geological mapping program, 1986 N87-23544
UNSTEADY FLOW
Unsteady stator/rotor interaction N87-22767
Experimental and theoretical studies of time-averaged and time resolved rotor heat transfer N87-22770
Analytical and experimental studies of flow-induced vibration of SSME components N87-22771
A linearized Euler analysis of unsteady flows in turbomachinery [NASA-CR-180987] N87-22948
URANIUM
A novel rollability test [RFP-3901] N87-22984
URANUS (PLANET)
Why no orbital resonances among the satellites of Uranus? N87-23351
Kinematics and dynamics of the Uranian rings N87-23353
Investigations of planetary ring phenomena N87-23360
Subcentimeter-size particle distribution functions in planetary rings from Voyager radio and photopolarimeter occultation data N87-23361
Uranus and Neptune: Questions and possible answers N87-23386
Properties of planetary fluids at high pressure and temperature N87-23399
Planetary nomenclature N87-23557
URANUS SATELLITES
The cratering record at Uranus: Implications for satellite evolution and the origin of impacting objects N87-23342
Crater morphology and morphometry on the Uranian satellites N87-23343
Cratering history of Miranda N87-23344
The viscosity of Miranda N87-23345
Orbital dynamics of the Uranian satellites based on Voyager data N87-23350
Why no orbital resonances among the satellites of Uranus? N87-23351
Voyager observations of 1985U1 N87-23352
Accretional heating of the satellites of Saturn and Uranus N87-23355
Aspects of Voyager photogrammetry N87-23547
Planetary nomenclature N87-23557
USER MANUALS (COMPUTER PROGRAMS)
Quick-look guide to the crustal dynamics project's data information system [NASA-TM-87818] N87-23018
USER REQUIREMENTS
Display management subsystem, version 1: A user's eye view N87-23164
Reading patterns in online documentation: How transcript analysis reflects text design, software constraints, and user preferences [DE87-006466] N87-23174

V

V/STOL AIRCRAFT
Propulsion system technologies for thrust vectoring N87-22670
VACANCIES (CRYSTAL DEFECTS)
Orbital removal method for the neutral vacancy in semiconductors [DE87-701537] N87-23300
VACUUM FURNACES
Control systems development, research and development [DE87-005785] N87-22868
VALLEYS
Winds in the Inn Valley (Austria) N87-23074
An elementary valley wind model N87-23075
Energy budget of an Alpine valley N87-23076
Valley circulations as measured in the Himalaya by instrumented motor glider N87-23077
Numerical study of the Mistral with a mesoscale model N87-23082
Cierzo: Northwesterly wind along the Ebro Valley (Spain) as a mesoscale effect induced on the lee of the Pyrenees mountain range; a case study during the Alpine Experiment (ALPEX) Special Observing Period N87-23083
Preliminary results of geologic and remote sensing studies of Rima Mozart N87-23431
High resolution thermal infrared mapping of Martian channels N87-23451
Fluvial valleys on Martian volcanoes N87-23462
Valley development on Hawaiian volcanoes N87-23463
Possible origin of some channels on Alba Patera, Mars N87-23465
Volatile reservoirs below the surface of the Elysium region of Mars: Geomorphic evidence N87-23467
Water and ice on Mars: Evidence from Valles Marineris N87-23469
Formation of the layered deposits in the Valles Marineris, Mars N87-23470
VALVES
A study of fluid-dynamic pressure fields on compressor reed valves [AD-A178584] N87-22938
VANADIUM
Superconducting thin films, composites and junctions [AD-A179346] N87-23288
VAPOR DEPOSITION
Investigation of laser diagnostics of PACVD processes for depositing hard face coatings [DE87-006292] N87-22969
AlGaAs growth by OMCVD using an excimer laser [NASA-TM-88937] N87-23304
VAPOR PHASES
XAS (X-ray Absorption Spectroscopy) of gas phase metal-containing chemical systems [AD-A179391] N87-22821
Pumped two-phase heat transfer loop [NASA-CASE-MSC-20841-1] N87-22950
VAPORIZING
A high-temperature quadrupole mass spectrometer for studying vaporization from materials heated by a CO2 laser [LA-10744] N87-22975
Impact vaporization: Late time phenomena from experiments N87-23491
VAPORS
SO2 on Io: A thermodynamic perspective N87-23359
VARIABILITY
Component variations and their effects on bipolar nickel-hydrogen cell performance [NASA-TM-89907] N87-23029
Synoptic-scale influence on the variability of the Alpine Experiment (ALPEX) low-level jet N87-23089
VARIABLE PITCH PROPELLERS
Evaluation of numerator lead effects on aircraft handling qualities [AD-A179388] N87-22687
VARIABLE THRUST
High heat transfer oxidizer heat exchanger design and analysis — RL10-2B engine [NASA-CR-179596] N87-22803
VARIATIONS
Lunar magnetization concentrations (MAGCONS) antipodal to young large impact basins N87-23405
Global petrologic variations of the Moon: A ternary-diagram approach N87-23407
VECTOR ANALYSIS
Estimation of ICBM (intercontinental ballistic missile) performance parameters [AD-A179204] N87-22754
VEGETATION GROWTH
Distinctions in formation of microbial complex in nutrient solutions of higher plants after use of straw mineralization products N87-23138
VELOCITY
Composite velocity procedures for flows with pressure interaction [AD-A179602] N87-22929
Evolution of planetesimal velocities N87-23383
VELOCITY DISTRIBUTION
Estimation of ICBM (intercontinental ballistic missile) performance parameters [AD-A179204] N87-22754
VELOCITY MEASUREMENT
Thermocapillary bubble migration for large Marangoni Numbers [NASA-CR-179628] N87-22865
VENUS (PLANET)
Gravity data analysis N87-23400
Lithospheric structure on Venus from tectonic modelling of compressional features N87-23516
Venusian tectonics: Convective coupling to the lithosphere? N87-23517
Bilateral symmetry across Aphrodite Terra N87-23518
VENUS SURFACE
Oxidized basalts on the surface of Venus: Compositional implications of measured spectral properties N87-23412
Mass transport by Aeolian saltation on Earth, Mars and Venus: The effects of full saltation cloud development and choking N87-23456
Aeolian abrasion on Venus: Preliminary results from the Venus simulator N87-23458
Crater production on Venus and Earth by asteroid and comet impact N87-23500
The surface age of Venus: Applying the terrestrial cratering rate N87-23501
Comments on the tectonism of Venus N87-23515
Venusian tectonics: Convective coupling to the lithosphere? N87-23517
Bilateral symmetry across Aphrodite Terra N87-23518
VERTICAL PERCEPTION
Structure and function of otoliths N87-23122
VERY LARGE SCALE INTEGRATION
A coherent VLSI environment [AD-A179303] N87-22897
Extrinsic gettering for VLSI/ULSI processes [DE87-002696] N87-22903
Formal models of hardware and their applications to VLSI design automation [AD-A178837] N87-22916
A coherent VLSI design environment [AD-A179037] N87-22920
VHSIC (CIRCUITS)
Modeling and simulation of the WFTA (Winograd Fourier Transform Algorithm) 16 PFA (Prime Factor Algorithm) processor using the VHSIC (Very High Speed Integrated Circuit) hardware description language, volume 1 [AD-A179344] N87-22898
VIBRATION
Vibration analysis using shadow speckle metrology and line broadening techniques [AD-A178626] N87-23003
VIBRATION DAMPING
Optimum mix of passive and active control of space structures N87-22714
Status report and preliminary results of the spacecraft control laboratory experiment N87-22717
Dynamics of trusses having nonlinear joints N87-22724
Workshop on Structural Dynamics and Control Interaction of Flexible Structures N87-22728
Vibration suppression by stiffness control N87-22730
Impact of space station appendage vibrations on the pointing performance of gimballed payloads N87-22733
Maneuvering and vibration control of flexible spacecraft N87-22734
Slewing control experiment for a flexible panel N87-22740
A new approach for vibration control in large space structures N87-22743

Crew activity and motion effects on the space station N87-22744
On the control of structures by applied thermal gradients N87-22747
Finite element models of wire rope for vibration analysis N87-22748
Analytical determination of space station response to crew motion and design of suspension system for microgravity experiments N87-22752

VIBRATION EFFECTS
Reaction to vibration of rat kinesthetic analyzer neurocytes N87-23133

VIBRATION ISOLATORS
Workshop on Structural Dynamics and Control Interaction of Flexible Structures N87-22728
Vibration isolation for line of sight performance improvement N87-22742
Crew activity and motion effects on the space station N87-22744
Finite element models of wire rope for vibration analysis N87-22748
Analytical determination of space station response to crew motion and design of suspension system for microgravity experiments N87-22752
SSME blade damper technology N87-22798

VIBRATION MODE
Flight and analytical investigations of a structural mode excitation system on the YF-12A airplane
[NASA-CR-166623] N87-22685
Space Station/Shuttle Orbiter dynamics during docking N87-22708
Dynamic characteristics of a vibrating beam with periodic variation in bending stiffness N87-22726
Experimental study of coupling between eddy curren of Tokamak limiters of tokamak limiters
[DE87-004936] N87-22999

VIBRATIONAL SPECTRA
Infrared spectroscopy using laser and Fourier techniques of the unstable molecules SiH and NH. Determination of the molecular constants of the fundamental electronic state 3 sigma (-) of NH
[ETN-87-99552] N87-22818

VIBRATIONAL STRESS
Accelerations experienced by packaged materiel during fork lift truck handling
[RDI-284/45/3] N87-22989

VIBRATORY LOADS
Accelerations experienced by packaged materiel during fork lift truck handling
[RDI-284/45/3] N87-22989

VIDEO DATA
Advanced monitoring concepts N87-22614

VIDEO SIGNALS
Optically Phase-Locked Electronic Speckle Pattern Interferometer (OPL-ESPI)
[AD-A178852] N87-22914
Laser reflectance as a function of rough water glitter profile
[AD-A178774] N87-23016

VIKING LANDER 1
Spectral mixture modeling: Further analysis of rock and soil types at the Viking Lander sites N87-23415

VIKING LANDER 2
Spectral mixture modeling: Further analysis of rock and soil types at the Viking Lander sites N87-23415

VINYL COPOLYMERS
Structural panels
[NASA-CASE-ARC-11429-2-CU] N87-22845

VISCOPLASTICITY
Nonisothermal elasto-visco-plastic response of shell-type structures N87-22796
Analytical characterization of shear localization in thermoviscoplastic materials
[AD-A178597] N87-23002
Bodner-Partom viscoplastic model in STEALTH finite difference code
[AD-A178994] N87-23005
Finite element implementation of Robinson's unified viscoplastic model and its application to some uniaxial and multiaxial problems
[NASA-TM-89891] N87-23010

VISCOSITY
An analysis of artificial viscosity effects on reacting flows using a spectral multi-domain technique
[NASA-CR-178308] N87-22632
The viscosity of Miranda N87-23345
Calculated viscosity-distance dependence for some actively flowing lavas N87-23482

VISCOUS FLOW
Development of an integrated BEM (Boundary Element Mesh) for hot fluid-structure interaction N87-22799
Experimental research on compressible turbulent shear layers, viscous-inviscid interactions, and flow separation
[AD-A179579] N87-22928
Numerical study of high speed viscous flows
[AD-A178639] N87-22940
Long, paired A'A/Pahoehoe flows of Mauna Loa: Volcanological significance and insights they provide into volcano plumbing systems N87-23480
The 1984 Mauna Loa eruption and planetary geolgoy N87-23481
Calculated viscosity-distance dependence for some actively flowing lavas N87-23482
Toward a model for leveed lava flows N87-23483
Studies of vesicle distribution patterns in Hawaiian lavas N87-23484

VISIBLE SPECTRUM
Optical dynamics experiment (ODEX) data report R/V acania expedition 10 October-17 November 1982. Volume 2: Particle size distributions. Volume 6: Scalar spectral-radiometer data
[AD-A178535] N87-23104

VISION
Development of an image analysis program for the IBM PC/XT/AT
[AD-A178644] N87-23163

VISORS
Effect of the neutral density helmet visor on the visual acuity of navy fighter pilots
[AD-A178486] N87-23147

VISUAL ACUITY
Visual acuity and reaction time in navy fighter pilots
[AD-A178485] N87-23117
Effect of the neutral density helmet visor on the visual acuity of navy fighter pilots
[AD-A178486] N87-23147

VISUAL PERCEPTION
Aircraft control position indicator
[NASA-CASE-LAR-12984-1] N87-22678
The integration of spectral and spatial analysis for land use classification
[AD-A178703] N87-23015
The perception of brightness and colour: Neurophysiology, psychophysics and computation
[AD-A179217] N87-23107

VOICE COMMUNICATION
Investigation of Continuously Variable Slope Delta (CVSD) modulation for voice communications
[AD-A178579] N87-22877

VOLATILITY
Volatile reservoirs below the surface of the Elysium region of Mars: Geomorphic evidence N87-23467

VOLCANOES
Fluvial valleys on Martian volcanoes N87-23462
Valley development on Hawaiian volcanoes N87-23463
Possible origin of some channels on Alba Patera, Mars N87-23465
Volatile reservoirs below the surface of the Elysium region of Mars: Geomorphic evidence N87-23467
The 1984 Mauna Loa eruption and planetary geolgoy N87-23481
Crustal and subcrustal nodules in ejecta from Kilbourne Hole Maar, New Mexico N87-23485
Geology of the Mohon Mountain volcanic field, Yavapai and Mohave Counties, Arizona: A preliminary report N87-23486
The geology of Pine and Crater Buttes: Two basaltic constructs on the far eastern Snake River Plain N87-23487
The geology of Picacho Butte, a silicic volcanic dome in northwest Arizona N87-23488
A statistical study of Mercurian crater classes applied to the emplacement of the intercrater plains N87-23502

VOLCANOLOGY
Preliminary results of geologic and remote sensing studies of Rima Mozart N87-23431

VOLT-AMPERE CHARACTERISTICS
Low power DC arcjet operation with hydrogen/nitrogen/ammonia mixtures
[NASA-TM-89876] N87-22804

VORTICES
Results of the integration of a transonic full-potential analysis program with a free-wake lifting-line program for hovering rotors
[NASA-TM-89494] N87-22631
Flow dynamics stimulated by hairpin-like vortices in initially laminar boundary layers
[AD-A179578] N87-22927
Heat transfer effects of longitudinal vortices embedded in a turbulent boundary layer
[DE87-006002] N87-22934
A three-dimensional dual potential procedure with applications to wind tunnel inlets and interacting boundary layers
[NASA-CR-180939] N87-22944
Ion phase-space vortices and their relation to small amplitude double layers N87-23320

VOYAGER PROJECT
Voyager cartography N87-23546

VOYAGER 2 SPACECRAFT
Aspects of Voyager photogrammetry N87-23547

VULNERABILITY
Hybrid composite response to hydraulic ram
[AD-A178750] N87-22815

W

WAFERS
The characterization of whiskers produced by electromigration on suspended aluminum linestripes
[AD-A179383] N87-23290

WALL JETS
A theory for turbulent curved wall jets
[NASA-CR-181019] N87-22951

WARFARE
The impact of future avionics technology on the conduct of air warfare N87-22673

WATER
Laser reflectance as a function of rough water glitter profile
[AD-A178774] N87-23016
High pressure cosmochemistry of major planetary interiors: Laboratory studies of the water-rich region of the system ammonia-water N87-23396
The role of regolith adsorption in the transition from early to late Mars climate N87-23411
Investigation of Martian H2O and CO2 via gamma-ray spectroscopy N87-23420
Studies of the scattering/absorption of minerals N87-23423

WATER EROSION
Groundwater sapping channels: Summary of effects of experiments with varied stratigraphy N87-23461
Non-equilibrium freezing of water-ice in sandy basaltic regoliths and implications for fluidized debris flows on Mars N87-23466

WATER FLOW
Unpinning of the Fermi level on GaAs by flowing water
[AD-A178489] N87-23302
The application of flow competence evaluations to the assessment of flood-flow velocities and stresses N87-23464
Possible origin of some channels on Alba Patera, Mars N87-23465

WATER QUALITY
Investigation of causes of hydrogen sulfide formation in reclaimed water N87-23136

WATER RECLAMATION
Investigation of causes of hydrogen sulfide formation in reclaimed water N87-23136

WATER RESOURCES
Design, development and deployment of public service photovoltaic power/load systems for the Gabonese Republic
[NASA-CR-179603] N87-23030

WATER WAVES
The SIR-B mission: Towards an understanding of internal waves in the ocean
[ARE-TR-86122] N87-23102

WAVE DRAG
Description of an aeronautical geometry conversion package: Wave-drag to Langley Wireframe Geometry Standard (LaWGS) to Supersonic Implicit Marching Potential (SIMP)
[NASA-CR-178299] N87-23194

WAVE EQUATIONS
Calculation of ray paths in the ionosphere using an analytic raytracing technique
[AD-A178888] N87-23064

WAVE PROPAGATION
Modeling of controlled flexible structures with impulsive loads N87-22745
A preliminary theory of the origin of the 40-50 day oscillation — tropical atmosphere N87-23044
Phase space methods and path integration: A microscopic approach to direct and inverse wave propagation
[AD-A178557] N87-23249
Double layers above the aurora N87-23331

WAVEGUIDE ANTENNAS
Wideband parallel-plate waveguide, phased-array antenna
[AD-A179402] N87-22873

WAVEGUIDES
Waveguide junction analysis involving asymmetrical modes
[AD-A178464] N87-22909

WEAPON SYSTEMS
Improvement of Combat Performance for Existing and Future Aircraft
[AGARD-CP-409] N87-22663
Performance improvement of airborne weapon systems methods, scope and limitations N87-22665

Some development trends in light ground attack aircraft N87-22666
Weapon systems polyvalence: An economic and operational challenge N87-22667
Evolution of combat performance of the Hawk light combat aircraft N87-22668
The impact of future avionics technology on the conduct of air warfare N87-22673

WEAR
Friction and wear of sintered Alpha SiC sliding against IN-718 alloy at 25 to 800 C in atmospheric air at ambient pressure
[NASA-TM-87353] N87-22860
In situ friction, wear and electrical contact resistance of precious metal alloys
[DE87-001423] N87-22979
Correlations between electrical contact resistance and stages of wear in 700 Torr helium for precious metal electrical contacts
[DE87-003499] N87-22981

WEAR RESISTANCE
In situ friction, wear and electrical contact resistance of precious metal alloys
[DE87-001423] N87-22979

WEATHER
The impact of climate change from increased atmospheric carbon dioxide on American agriculture
[DOE/NBB-0077] N87-23032

WEATHER FORECASTING
Modelling and forecasting El Nino N87-23053

WEDGE FLOW
Numerical study of high speed viscous flows
[AD-A178639] N87-22940

WEIBULL DENSITY FUNCTIONS
Self-critical and robust procedures for the analysis of binary data
[AD-A178935] N87-23221

WEIGHT REDUCTION
Fiber optic data transmission N87-22611

WEIGHTING FUNCTIONS
Robust data analysis based on characteristic functions
[AD-A178544] N87-23178
Estimation cf the parameters of mixtures via distance between densities or characteristic functions
[AD-A178623] N87-23241

WEIGHTLESSNESS
Structure and function of otoliths N87-23122
Split circadian rhythm of simian bodv temperature during antiorthostatic hypokinesia N87-23128

WELD TESTS
Circumferential hot wire TIG cladding of carbon-manganese steel with Inconel 625 and gun-metal with a tin bronze
[ARE-TM(UMD)-85574] N87-22831
Residual stresses in girth butt welded pipes: Results and implications
[CUED/D-STRUCT/TR.109] N87-22992

WELDED JOINTS
Residual stresses in girth butt welded pipes: Results and implications
[CUED/D-STRUCT/TR.109] N87-22992

WELDED STRUCTURES
Residual stresses in girth butt welded pipes: Results and implications
[CUED/D-STRUCT/TR.109] N87-22992

WHISKER COMPOSITES
Thermal shock resistance of mullite-based SiC-whisker composites
[AD-A179214] N87-22809

WHISKERS (CRYSTALS)
The characterization of whiskers produced by electromigration on suspended aluminum linestripes
[AD-A179383] N87-23290

WHITE LIGHT HOLOGRAPHY
White-light optical information processing and holography
[AD-A179489] N87-23260
Automatic pattern recognition and related topics
[AD-A178595] N87-23267

WIND (METEOROLOGY)
Winds in the Inn Valley (Austria) N87-23074
Numerical study of the Mistral with a mesoscale model N87-23082
Measurement of high resolution wind profiles with a minisoder
[DE87-007001] N87-23096
A wind- and wave-driven nearshore current model, the one-dimensional model
[AD-A178751] N87-23105

WIND DIRECTION
The effect of the Tatra Mountains (Poland) on the atmospheric precipitation and air humidity during the northern and southern air flow N87-23094

WIND EFFECTS
Sensitivity of an Ocean General Circulation Model (OCGM) to wind forcing N87-23054
Mesoscale mountain meteorology N87-23069
Bright sand/dark dust: The identification of active sand surfaces on the Earth and Mars N87-23449
Regional sources and sinks of dust on Mars: Viking observations of Cerberus, Solis Planum and Syrtis Major N87-23450
High resolution thermal infrared mapping of Martian channels N87-23451
Mars: Morphology of Southern Hemisphere intracrater dunefields N87-23452
Wind ripples in low density atmospheres N87-23454
Eolian saltation on Mars N87-23455
Mass transport by Aeolian saltation on Earth, Mars and Venus: The effects of full saltation cloud development and choking N87-23456
Development of wind tunnel techniques for the solution of problems in planetary Aeolian processes N87-23457
Aeolian abrasion on Venus: Preliminary results from the Venus simulator N87-23458
Reynolds number effects on surface shear stress patterns around isolated hemispheres N87-23459
Determination of surface shear stress with the naphthalene sublimation technique N87-23460

WIND EROSION
Aeolian abrasion on Venus: Preliminary results from the Venus simulator N87-23458

WIND MEASUREMENT
Measurement of high resolution wind profiles with a minisodar
[DE87-007001] N87-23096

WIND PROFILES
An elementary valley wind model N87-23075
Energy budget of an Alpine valley N87-23076
Valley circulations as measured in the Himalaya by instrumented motor glider N87-23077
Dynamics and evolution of the Pyrenees lee wave event during 21-23 March 1982 N87-23079
A contribution to Bora studies using Alpine Experiment (ALPEX) aircraft data N87-23080
An analysis of downslope winds in the lee of the Pyrenees on 23 March 1982 N87-23081
Cierzo: Northwesterly wind along the Ebro Valley (Spain) as a mesoscale effect induced on the lee of the Pyrenees mountain range; a case study during the Alpine Experiment (ALPEX) Special Observing Period N87-23083
The Mistral-Tramuntana shear line. A satellite observation N87-23084
The influence of orography on the temperature and wind regime in the mountains N87-23085
Mesoscale analyses of temperature, pressure and wind fields over Switzerland: A case study of a Foehn N87-23086
Measurement of high resolution wind profiles with a minisodar
[DE87-007001] N87-23096
Development of wind tunnel techniques for the solution of problems in planetary Aeolian processes N87-23457

WIND SHEAR
Safe microburst penetration techniques: A deterministic, nonlinear, optimal control approach N87-22620
Integrated FAA Wind Shear Program plan
[DOT/FAA/DL-87/1] N87-23067
Reynolds number effects on surface shear stress patterns around isolated hemispheres N87-23459
Determination of surface shear stress with the naphthalene sublimation technique N87-23460

WIND TUNNEL MODELS
Experimental evaluation of blockage ratio and plenum evacuation system flow effects on pressure distribution for bodies of revolution in 0.1 scale model test section of NASA Lewis Research Center's proposed altitude wind tunnel
[NASA-TP-2702] N87-22694

WIND TUNNEL TESTS
Hypersonic laminar boundary layer transition. Part 1: Nosetip bluntness effects on cone frustum transition. Part 2: Mach 6 experiments of transition on a cone at angle of attack
[AD-A178877] N87-22625
Verification of performance results for a low-speed 15 percent elliptical circulation control airfoil
[NASA-CR-181020] N87-22633
Experimental evaluation of blockage ratio and plenum evacuation system flow effects on pressure distribution for bodies of revolution in 0.1 scale model test section of NASA Lewis Research Center's proposed altitude wind tunnel
[NASA-TP-2702] N87-22694
Boundary layer disturbances caused by periodic heating of a thin ribbon
[AD-A179342] N87-22925
Equipment for turbulent heat transfer test apparatus
[AD-A179612] N87-22930
Interaction of a three-dimensional roughness element with a laminar boundary layer
[AD-A178668] N87-22941
Wind ripples in low density atmospheres N87-23454
Mass transport by Aeolian saltation on Earth, Mars and Venus: The effects of full saltation cloud development and choking N87-23456
Development of wind tunnel techniques for the solution of problems in planetary Aeolian processes N87-23457
Determination of surface shear stress with the naphthalene sublimation technique N87-23460

WIND TURBINES
A comparison of predicted wind turbine blade loads to test measurements
[DE87-001130] N87-23021
Structural design and fabrication of the Sandia 34-meter Vertical Axis Wind Turbine
[DE87-003503] N87-23022
The status of the vertical axis wind turbine research test bed
[DE87-005524] N87-23023

WIND VELOCITY
Development of wind tunnel techniques for the solution of problems in planetary Aeolian processes N87-23457

WING TIPS
The aerodynamic optimization of wings at subsonic speeds and the influence of wingtip design
[NASA-TM-88534] N87-22627

WINTER
Principal circulation anomalies in model atmospheres with and without interannual variations of tropical Pacific SST — sea surface temperature (SST) N87-23041
The 30-60 day oscillation in a perpetual January simulation with the NCAR general circulation model N87-23043

WIRE
Finite element models of wire rope for vibration analysis N87-22748

WIRE CLOTH
Analysis of lightning induced magnetic field penetration through protective metal screens using an equivalent magnetic dipole moment representation of an array of elliptic apertures
[AD-A178850] N87-22884

WORK CAPACITY
Tolerance to frustration as a factor in operator performance N87-23124

WORKING FLUIDS
Heat transfer in an organic heat pipe
[LA-10781-MS] N87-22946

WORKLOADS (PSYCHOPHYSIOLOGY)
Investigation of hemcstasis system in air traffic controllers as related to different air traffic conditions N87-23123

WORKSTATIONS
Determination of crack initiation sites using a digital NDE workstation
[DE87-001444] N87-22997
The evaluation and extension of TAE in the development of a user interface management system N87-23158
NASA Regional Planetary Image Facility image retrieval and processing system N87-23160
SOT: A rapid prototype using TAE windows N87-23161

WRINKLING
Physiographic constraints on the origin of lunar wrinkle ridges N87-23521

X

X RAY ABSORPTION
XAS (X-ray Absorption Spectroscopy) of gas phase metal-containing chemical systems
[AD-A179391] N87-22821

X RAY ASTRONOMY
X-ray and low energy gamma-ray observations of the 16 February 1984 solar flare
[NASA-CR-180928] N87-23564

X RAY BINARIES
Accretion onto neutron stars with the presence of a double layer N87-23334

X RAY DIFFRACTION
Examination of high performance polymer fibers under compressive deformation
[AD-A178640] N87-22857

X RAY LASERS
Time and space resolved spectroscopy of X-ray laser experiments from 81A to 220A
[DE87-005946] N87-22968
A new LIHE (Light Initiated High Explosive) test capability for spherical targets
[DE87-003035] N87-23245

X RAY SCATTERING
Workshop report on New Directions in X-ray Scattering
[DE87-006305] N87-23262

X RAY SPECTRA
Angular distribution of transition radiation in the soft X-ray spectrum
[AD-A178859] N87-23255
X RAY SPECTROSCOPY
XAS (X-ray Absorption Spectroscopy) of gas phase metal-containing chemical systems
[AD-A179391] N87-22821
X RAYS
Angular distribution of transition radiation in the soft X-ray spectrum
[AD-A178859] N87-23255
Solar active region physical parameters inferred from a thermal cyclotron line and soft X-ray spectral lines
[AD-A179650] N87-23560
Simultaneous SMM flat crystal spectrometer and very large array observations of solar active regions
[AD-A179698] N87-23562
X-29 AIRCRAFT
X-29 integrating advanced technologies for tomorrow's air combat N87-22671

Y

YF-12 AIRCRAFT
Flight and analytical investigations of a structural mode excitation system on the YF-12A airplane
[NASA-CR-166623] N87-22685
YIELD STRENGTH
Failure strength of icy lithospheres N87-23357
YTTRIUM OXIDES
Synthesis of alumina-zirconia powders by sol-gel processing
[DE87-005721] N87-22851

Z

ZEEMAN EFFECT
Plasma diagnosis by dye laser intracavity absorption
[DE87-006407] N87-23280
ZIRCONIUM
Evaluation of spherical ceramic particles for solar thermal transfer media
[DE87-007432] N87-23026
ZIRCONIUM OXIDES
Synthesis of alumina-zirconia powders by sol-gel processing
[DE87-005721] N87-22851
ZODIACAL DUST
Dynamics of satellites, asteroids, and rings
N87-23392

PERSONAL AUTHOR INDEX

Typical Personal Author Index Listing

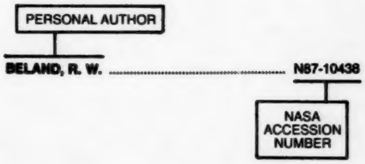

Listings in this index are arranged alphabetically by personal author. The NASA accession number denotes the number by which the citation is identified.

A

ABDUL-AZIZ, A. N87-22779
ACHUTUNI, RAO N87-23032
ACOSTA, ROBERTO J. N87-22874
ADAMCZYK, JOHN J. N87-22768
ADAMS, JOHN B. N87-23415
ADCOCK, C. B. N87-22657
AFONIN, B. V. N87-23125
AGGARWAL, B. N87-22683
AGRESTI, WILLIAM N87-23191
N87-23193
AIKEN, W. F. N87-22869
AKDENIZ, K. G. N87-23339
ALLEMEIER, R. T. N87-22997
ALLEN, JOHN L. N87-22703
ALPATOV, A. M. N87-23128
ANDERSON, DUWAYNE M. N87-23468
ANDERSON, H. U. N87-22900
ANDERSON, K. A. N87-23405
ANDERSON, L. W. N87-23247
ANDERSON, SETH B. N87-22629
ANDERSON, TODD N87-22815
ANGELL, C. A. N87-23296
ANICICH, VINCENT G. N87-23447
ANTIPOV, V. V. N87-23133
ANTOLOVICH, STEPHEN D. N87-22776
ARAKAWA, AKIO N87-23036
ARAKI, S. N87-23402
ARNOLD, G. W. N87-23298
ARNOLDUS, HENK F. N87-23292
ARON, PAUL R. N87-23304
ARPASI, DALE J. N87-23202
ARVIDSON, R. N87-23414
N87-23449
N87-23554
ARVIDSON, R. E. N87-23418
N87-23506
ARYA, V. K. N87-23010
ASHCROFT, N. W. N87-22838
ASHWILL, T. D. N87-23022
ATLURI, S. N. N87-22789
AUBERT, J. H. N87-22850
AUDEBERT, P. N87-23279
AUSTIN, F. S. N87-22957
AVAGNINA, G. M. N87-22666
AYDELOTT, JOHN C. N87-22757
N87-22949

B

BABB, LARRY N87-23162
BAGG, M. T. N87-23102
BAILEY, L. R. N87-22868
BAKER, VICTOR R. N87-23462
N87-23463
BALASUBRAMANIAM, R. N87-22865
BALOGA, STEPHEN N87-23483
BAME, S. J. N87-23061
BANERDT, W. B. N87-23357
N87-23516
BANERJEE, P. K. N87-22799
BANTA, ROBERT M. N87-23092
BANTELL, M. H., JR. N87-22723
BARBACCI, MARIO R. N87-23206
BARLOW, NADINE G. N87-23504
BARNA, B. A. N87-22997
BARNES, A. G. N87-22675
BARNES, C. N87-23326
BARNETT, R. L. N87-22869
BARNOUIN, O. N87-23279
BARRY, J. D. N87-22832
BARSZCZ, ERIC N87-23201
BARTMAN, RANDALL K. N87-23259
BASHENOV, V. K. N87-23300
BASS, ROBERT G. N87-22847
BASSETT, WILLIAM A. N87-23398
BASU, SANKAR N87-22915
BATSON, R. M. N87-23545
N87-23546
N87-23550
BATTLES, F. N87-23057
BEAVER, P. W. N87-23000
BECHER, P. F. N87-22851
BECHTEL, G. N87-22780
BEHNKE, JEANNE M. N87-23018
BEHRENS, ROBERT G. N87-22975
BELL, J. F. N87-23375
N87-23430
BELL, M. B. N87-23566
N87-23567
BELL, VERNON L. N87-22848
BELYTSCHKO, TED N87-22790
BENDERSKY, LEO N87-22840
BENHAM, R. A. N87-23245
BENNETT, J. S. N87-22679
BENSON, D. J. N87-22998
BENTS, DAVID J. N87-23020
BERANEK, J. A. N87-22685
BERLINER, MARK N87-23242
BERNATH, PETER F. N87-22628
BERNSTEIN, D. S. N87-22741
BERNSTEIN, I. M. N87-22782
BERZINS, M. N87-23210
BIEFELD, R. M. N87-23299
BIEGALSKI, CONRAD S. N87-22651
BIELER, T. N87-22834
BIER, R. N87-22907
BIGIO, I. J. N87-22964
BILSON, AMY JO N87-23113
BIRGE, JOHN R. N87-23217
BIRK, YITZHAK N87-22890
BIRKDALE, HENRY G. N87-23215
BIWER, R. L. N87-22904
BLACK, DAVID C. N87-23340
BLACKMON, MAURICE L. N87-23038
BLAKEMORE, C. B. N87-23107
BLANDER, M. N87-23306
BLECH, RICHARD A. N87-23202
BLONDIN, CHRISTIAN N87-23082
BLOUNT, H. G., II N87-23449
BLUMEN, W. N87-23079
BLUMEN, WILLIAM N87-23071
N87-23081
BODENHEIMER, PETER N87-23340
BOER, G. J. N87-23035
N87-23050
BOLTON, R. D. N87-23568
BOND, W. D. N87-22851
BOOKER, J. R. N87-23058
BOONE, STEVEN N87-23396
BORDERS, STEPHEN N87-23167
BOROVSKY, JOSEPH E. N87-23333
BORRELLO, MURRAY C. N87-23533
BOSS, A. P. N87-23388
BOUDJAADAR, DJAMEL N87-22818
BOURNE, CARLTON M. N87-23016
BOWELL, J. A. N87-23558
BOYCE, J. M. N87-23344
N87-23348
BRAATEN, ALAN J. N87-23182
BRAGAGNOLO, N. N87-22666
BREMER, S. G. N87-23171
BRESLAV, I. S. N87-23134
BRET, BERNARD N87-23082
BREZZI, F. N87-23229
BRIDGES, F. G. N87-23364
BRIDGMAN, C. N87-22812
BRINK, G. O. N87-23280
BRITT, D. N87-23505
BRITT, DANIEL T. N87-23374
BROPHY, JAMES J. N87-22829
BROTHERS, K. M. N87-23243
BROWN, DONALD D. N87-22648
BROWN, GEORGE N87-23262
BROWN, HAROLD D. N87-23197
BRUCE, KEITH D. N87-22639
BRUCKENTHAL, E. N87-23414
BRUCKENTHAL, E. A. N87-23422
BRUNNER, R. N87-22683
BRYANT, J. L. N87-23218
N87-23225
N87-23236
N87-23241
BUGG, FRANK M. N87-22751
BULLOCK, DANIEL N87-23111
BUNCH, T. N87-23379
BUNTING, JAMES T. N87-23012
BURATTI, B. N87-23426
BURKHARDT, P. N87-23057
BURKHART, BRENDA N87-23158
BURLEY, RICHARD R. N87-22694
BURMAN, R. L. N87-23568
BURNS, JOSEPH A. N87-23360
BURNS, ROGER G. N87-23416
N87-23417
BURNSIDE, O. H. N87-22787
BURRIS, HARRIS R. N87-22971
BUSS, R. J. N87-22849
BUTLER, ROY N87-22641
BUTTERFIELD, K. B. N87-23568
BUTTRAM, M. T. N87-22965
BYCHKOV, V. P. N87-23126
N87-23127
BYERS, C. H. N87-23294

C

CADY, R. N87-23568
CALVIN, W. M. N87-23445
CAMPBELL, BRUCE N87-23441
CAMPBELL, D. B. N87-23518
CANE, M. A. N87-23053
CARDELLI, JASON A. N87-23336
CARLINI, R. D. N87-23568
CARLSON, R. L. N87-22796
CARPENTER, T. N87-23315
CARROLL, J. E. N87-22637
CARTER, P. N87-22991
CASSEN, P. M. N87-23345
N87-23379
CATALDO, ROBERT L. N87-23029
CAUGHEY, THOMAS N87-22730
CAULFIELD, THOMAS N87-22811
CAVANAGH, DALE E. N87-22649
CEBECI, T. N87-22769
CEGLIO, N. M. N87-22968
CHAMBERLAIN, N. N87-22889
CHAMIS, CHRISTOS C. N87-22783
CHAN, CHUNG N87-23314
CHANG, C. Y. N87-23568
CHANG, F. R. N87-23275
CHANG, XIANQI N87-22800
CHANTEUR, GERARD N87-23322
CHAPMAN, C. R. N87-23387
CHAPMAN, CLARK R. N87-23499
CHAPMAN, J. M. N87-22724
N87-22725
CHAPMAN, M. G. N87-23555
CHATTERJEE, K. N87-23057
CHEN, J. C. N87-22727
N87-22750
CHEN, JAY N87-22730
CHEN, JAY C. N87-22712
CHEN, JAY-C. N87-22747
CHEN, S. S. N87-22771

CHEN, TIMOTHY S. N87-22845
CHERRETTE, ALAN R. N87-22874
CHERVIN, ROBERT M. N87-23039
CHILDRESS, JAMIE N87-22815
CHILENSKAS, A. A. N87-22904
CHIMA, RODRICK V. N87-22630
N87-22767
CHIPPERFIELD, K. M. N87-22831
CHISHOLM, G. H. N87-23176
CHIZHOV, S. V. N87-23136
CHOI, H. S. N87-22908
CHOKSHI, A. N87-22834
CHRISTE, K. O. N87-22822
CHRISTENSEN, P. R. N87-23418
N87-23445
N87-23449
N87-23451
CHRISTENSEN, PHILIP R. N87-23413
N87-23425
CHRISTIAN, DARRYL N87-22642
CHRISTIANSEN, ERIC H. N87-23467
CHRISTOPHOROU, L. G. N87-22906
CHROSTOWSKI, J. D. N87-22710
CHUBB, DONALD L. N87-23028
CHUMLEA, WILLIAM C. N87-23118
CHUNG, SONG-YOUNG N87-22631
CHURCH, S. M. N87-22749
CITERLEY, RICHARD L. N87-22995
CLARK, ROGER N. N87-23423
CLAUSER, CHARLES E. N87-23110
N87-23112
CLAYTON, G. R. N87-22832
CLEVELAND, W. G., JR. N87-22941
CLEVER, J. J. N87-23151
CLIFTON, R. J. N87-23001
N87-23002
CLOUTMAN, LAWRENCE D. N87-22945
COCHRAN, J. E., JR. N87-22708
N87-22743
N87-22748
COHEN, M. N87-22836
COLEMAN, CLARENCE J., JR. N87-22938
COLEMAN, HUGH W. N87-22930
COLES-HAMILTON, CAROLYN E. N87-22802
COLES, MICHAEL N87-23143
COLETTI, ALESSANDRO N87-23269
COLLINS, BERNARD F., II N87-22878
COLVIN, TIM R. N87-23552
CONKLIN, DONALD D. N87-22681
CONNELL, JOHN W. N87-22847
CONNELLY, ROBERT N87-23377
CONTRERAS, M. M. N87-22905
COOK, ED N87-22654
COOK, T. S. N87-22780
COOMBS, C. R. N87-23430
N87-23431
COOPER, CHARLES H. N87-22898
COOPER, PAUL A. N87-22737
COULTER, R. L. N87-23096
COX, K. W. N87-23079
COY, JOHN J. N87-22978
CRADDOCK, R. A. N87-23451
N87-23542
CRAIG, L. J. N87-22907
CRAIG, PETER N. N87-22914
CRAIG, ROY R., JR. N87-22739
CRASEMANN, B. N87-23251
CRAVEN, J. D. N87-23063
CRAWFORD, D. N87-23490
CRAWLEY, EDWARD F. N87-22948
CRAXTON, R. S. N87-23279
CROFT, STEVEN K. N87-23343
N87-23346
CROLEY, D. R., JR. N87-23061
CROWLEY, W. P. N87-22933
N87-22936
CROWN, D. A. N87-23473
N87-23541
N87-23542
CRUMPLER, L. S. N87-23518
CRUMPTON, KENNETH S. N87-22754
CRUSE, T. A. N87-22784
CRYSTAL, T. L. N87-23326
CUBASCH, ULRICH N87-23046
CUGINI, J. V. N87-23170
CURRAN, FRANCIS M. N87-22804
CUTCHINS, M. A. N87-22748
CUZZI, JEFFREY N. N87-23394
CYNN, HYUNCHEE N87-23396
CYR, GARRY J. N87-22813

D

DABBS, R. S. N87-22688
DAHLBURG, R. B. N87-23565
DALE-BANNISTER, M. N87-23414
DALLY, WILLIAM J. N87-22897
N87-22920
DANIELSON, G. E. N87-23556
DARBRO, W. N87-23334
DARGUSH, G. F. N87-22799
DARNELL, WAYNE L. N87-23101
DASARO, JOSEPH A. N87-22673
DAVIDSON, DENNIS R. N87-23311
DAVIDSON, JIM N87-22644
DAVIES, H. C. N87-23070
DAVIES, MERTON E. N87-23551
N87-23552
N87-23553
DAVIES, ROD N87-22645
DAVIS, D. R. N87-23384
N87-23387
N87-23494
DAVIS, DONALD R. N87-23499
DAVIS, L. P. N87-22728
DAVIS, P. A. N87-23555
DAVIS, PHILIP A. N87-23407
N87-23408
N87-23528
DAVIS, R. A. N87-22685
DAVIS, RANDALL C. N87-22976
DAVYDOVA, N. A. N87-23142
DAWSON, L. R. N87-23299
DAY, D. E. N87-22861
DEADMORE, DANIEL L. N87-22860
DEASE, C. G. N87-22905
DECKER, WAYNE L. N87-23032
DECKER, WILLIAM N87-23192
DEEKSHIT, R. V. N87-23238
DEFELICE, DAVID M. N87-22949
DEHON, R. A. N87-23539
DEIWERT, GEORGE S. N87-22943
DELAGI, BRUCE A. N87-23197
DELAHANTY, T. A. N87-23179
DELANEY, N. J. N87-23220
N87-23224
DELEHANTY, T. A. N87-23214
N87-23220
N87-23243
DELETTREZ, J. N87-23279
DELGRANDE, NANCY KERR N87-23262
DELUCA, W. H. N87-22904
DELUCIA, R. A. N87-22684
DENNIS, DALE V. N87-22678
DENNY, MICHAEL W. N87-23180
DERMOTT, STANLEY F. N87-23392
DERRIG, R. A. N87-23238
DERSTINE, MATTHEW N87-23172
DESAUSSURE, G. N87-22980
DEVORE, C. R. N87-23565
DIAL, A. L., JR. N87-23555
DIAS, J. B. N87-22785
DICKEY, J. O. N87-23389
DIMITRIADI, N. A. N87-23132
DISZ, T. N87-23198
DLUSSKAYA, I. G. N87-23140
DODD, H. M., JR. N87-23023
DODSON, B. W. N87-23297
DOLLAR, M. N87-22782
DOMNANOVICH, A. N87-22782
DOMNIKOVA, A. A. N87-23140
DONCHIN, EMANUEL N87-23143
DOTSON, KELLY J. N87-23244
DOUGHERTY, H. J. N87-22742
DOUGLAS, D. A. N87-22852
DOUGLASS, CHARLES, JR. N87-22827
DOVIAK, RICHARD J. N87-23095
DOYLE, B. L. N87-23299
DOZOIS, CLAUDE G. N87-23056
DRESS, W. B. N87-23145
DROBYSHEV, V. I. N87-23133
DRUGOVA, N. A. N87-23138
DUDAS, ALAN J. N87-22971
DUDDERAR, T. D. N87-23003
N87-23268
DUDEK, D. N87-22935
DUNN, M. G. N87-22770
DUONG-VAN, M. N87-23175
DURHAM, W. B. N87-23540
DURISEN, RICHARD H. N87-23394
DUSENBERRY, P. B. N87-23282
DUXBURY, ELIZABETH D. N87-23520
DYACHKOVA, L. N. N87-23130
DYBBS, A. N87-22775

E

EATON, J. K. N87-22934
EATOUGH, M. O. N87-23026
EBELING, P. N87-22665
EBERLY, J. H. N87-23261
EDBERG, DON N87-22747
EDELSON, L. H. N87-22839
EDELSTEIN, FRED N87-22950
EDWARDS, A. C. N87-23102
EDWARDS, BERNELL J. N87-23146
EDWARDS, K. N87-23558
EDWARDS, KATHLEEN N87-23545
EDWARDS, MARK S. N87-22877
EGGER, JOSEF N87-23074
EHERNBERGER, L. J. N87-23100
EICHMANN, GEORGE N87-23154
EIDSAUNE, DAVID W. N87-22687
EIKE, DAVID N87-23161
EILTS, MICHAEL D. N87-23095
EINHORN, JOHN K. N87-22607
EISENBERG, A. N87-22855
ELIAS, ANTONIO L. N87-22606
ELIASON, E. M. N87-23558
ELSNER, R. F. N87-23334
EMBABY, M. N87-23307
ENGEL, J. N87-23086
ENGELS, REMI C. N87-22707
EPSTEIN, R. N87-23279
N87-23332
ESBENSEN, STEVEN K. N87-23037
EVANS, D. S. N87-23330
EVANS, LARRY G. N87-23420
EVERSOLE, J. D. N87-22863

F

FADDY, D. N87-22664
FAELTHAMMAR, CARL-GUNNE N87-23337
FAHY, J. BEN N87-23166
FANALE, F. P. N87-23365
N87-23367
N87-23411
FANALE, FRASER P. N87-23359
N87-23419
FANSON, JAMES N87-22730
FARHAT, NABIL H. N87-22882
FATH, JEFFREY L. N87-22886
FEDERBUSCH, ORNA N87-23186
FEIGELSON, ROBERT S. N87-23257
FELCH, K. N87-22907
FELDE, GERALD W. N87-23012
FELDMAN, M. J. N87-23293
FENIMORE, E. E. N87-23564
FENNELL, J. F. N87-23061
FENNESSY, M. N87-23049
FERGUSON, H. M. N87-23558
FERGUSON, J. A. N87-22973
FERRARI, DOMENICO N87-23195
FERRY, DANIEL N87-23191
FETTERMAN, H. R. N87-22901
FIEDLER, MICHAEL T. N87-22650
FIMPEL, H. P. N87-23087
FINK, JONATHAN H. N87-23479
FINLEY, J. A. N87-22736
FISCHLER, MARTIN A. N87-23017
FISHER, ROBERT R. N87-22756
FISHMAN, LOUIS N87-23249
FITZ-COY, N. G. N87-22708
N87-22748
FLETCHER, T. H. N87-22935
FLOCH, JEAN-JACQUES N87-22667
FONTANA, ANTHONY N87-22703
FOREST, C. N87-23316
FORSLEY, L. N87-23279
FOUSHEE, H. CLAYTON N87-22634
N87-22655
N87-22656
FOWLER, B. L. N87-22749
FRANCIS, ROBERT A. N87-23527
FRANK, L. A. N87-23063
FRANKLIN, B. J. N87-23521
FRAUENFELDER, DEBORAH J. N87-22913
FREDIN, LEIF N87-22975
FREER, HARRISON C. N87-22662
FRENCH, RICHARD G. N87-23353
FRENKEL, I. D. N87-23126
FREY, HERBERT N87-23474
N87-23523
N87-23524
FRITZEMEIER, L. G. N87-22781
FROST, WALTER N87-23091
FUELLHAS, K. N87-22669
FULLER, M. N87-23237
FUOSS, PAUL N87-23262
FURGER, M. N87-23086
FYFE, IAN M. N87-22844

G

GAFFEY, MICHAEL J. N87-23372
N87-23373
GAGNON, H. P. N87-23566
N87-23567
GAHN, RANDALL F. N87-23029
GALPERN, A. D. N87-23258
GARBA, J. A. N87-22750
GARBA, JOHN A. N87-22712
GARBER, F. D. N87-22889
GARDNER, DALE A. N87-22965
GARNER, ERNEST L. N87-22958
GARVIN, J. N87-23412
GASKELL, R. W. N87-23543
GAULT, D. E. N87-23490
N87-23491
GAULT, DONALD E. N87-23492
N87-23493
N87-23497
GAVER, DONALD P. N87-23239
GEAR, C. W. N87-23209
GEBALLE, T. H. N87-23288
GEISLER, J. E. N87-23043
GEMEINER, RUSSEL P. N87-23029
GEORGE, FRANK L. N87-23148
GEORGE, NICHOLAS N87-23267
N87-23270
GEORGE, THOMAS F. N87-23292
GERBER, R. A. N87-22965
GERDIN, G. N87-23276
GERI, GEORGE A. N87-23106
GETZELMAN, HAROLD D. N87-22759
GHARAKHANI, V. N87-23426
GIBSON, J. N87-23370
GIBSON, W. C. N87-22817
GILBERT, J. A. N87-23268
GILBERT, JOHN A. N87-23003
GIORDANO, J. N87-22683
GIRILL, T. R. N87-23174
GIVI, P. N87-22819
GLAB, W. L. N87-22825
GLASSER, LANCE A. N87-22897
N87-22920
GLAZ, HARLAND M. N87-22942
GLOVER, R. C. N87-22765
GLYNN, PETER W. N87-23240
GOEL, PREM K. N87-23242
GOFORTH, E. A. N87-22685
GOLDBERG, WARREN M. N87-22914
GOLDSTEIN, M. N87-22980
GOLOMBEK, M. P. N87-23357
N87-23516
N87-23521
GONSALVEZ, DAVID J. A. N87-22700
GONZALEZ-SANABRIA, OLGA D. N87-23029
GOODING, J. L. N87-23409
N87-23466
GORDO, A. N87-23083
GORDON, C. N87-23055
GORDON, CLAIRE C. N87-23110
N87-23112
GORDON, DOUGLAS N87-23169
GORDON, JACQUELINE I. N87-23062
GOSS, L. P. N87-22862
GOSS, WILLIS C. N87-23259
GRADIE, JONATHAN N87-23371
GRAHAM, RONALD E. N87-22755
GRANT, L. B. N87-23489
GRATTIDGE, W. N87-23312
GREEGOR, ROBERT B. N87-22821
GREELEY, R. N87-23449
N87-23451
N87-23452
N87-23454
N87-23456
N87-23541
N87-23542
GREELEY, RONALD N87-23457
N87-23458
N87-23459
N87-23460
N87-23473
N87-23478
N87-23512
GREEN, JAMES M. N87-22806
GREEN, MICHAEL J. N87-22943
GREEN, R. M. N87-22823
GREENHAGEN, CHERYL N87-23159
GREENZWEIG, YUVAL N87-23385
GREGORY, JOHN C. N87-22852
GRIFFIN, JERRY H. N87-22798
GRIGORYEV, A. I. N87-23125
GRISHAYENKOV, B. G. N87-23137
GROSS, BRIAN N87-23071
GROSSBERG, STEPHEN N87-23111
GROVE, D. J. N87-23005
GUBEREK, MICHAEL N87-23167
GUDZ, P. N87-23073
GUINNESS, E. N87-23414
N87-23554
GUINNESS, E. A. N87-23506
GULICK, VIRGINIA C. N87-23462
N87-23463
GULLIVER, J. N87-22986
GUO, SHUMEI N87-23118
GUPTA, C. D. N87-22866
GUPTA, SHANTI S. N87-23234
N87-23235

H

HACINLIYAN, A. N87-23339
HACKMAN, J. RICHARD N87-22636
HAFNER, T. A. N87-23087
HAHN, E. N87-22758
HAILE, W. B. N87-22742
HALL, J. LYNN N87-23522
HALL, KENNETH C. N87-22948
HALLIDAY, JOHN T. N87-22651
HALLQUIST, J. O. N87-22998
HAMED, A. N87-22858
HAMILTON, D. C. N87-23399
HAMILTON, P. V. N87-23117
N87-23147
HANKS, BRANTLEY R. N87-22703
HANSEN, GEORGE P. N87-22975
HANSMAN, R. JOHN, JR. N87-22608
HAPKE, B. N87-23426
HAPKE, BRUCE N87-23427
N87-23433
N87-23434
N87-23439
HARBOR, BERNARD N87-23308
HARDT, A. P. N87-22856
HARDY, KENNETH R. N87-23012
HARDY, TERRY L. N87-22804
HARLOW, CHARLES A. N87-23015
HARRINGTON, DOUGLAS E. N87-22694
HARRINGTON, ROGER F. N87-22880
HARRIS, COLIN P. N87-23165
HARRIS, D. H. N87-22859
HARRIS, ELFRIEDA N87-23156
N87-23161
HARRIS, FOSTER R. N87-22993
HARRIS, M. T. N87-23294
HARRISON, R. F. N87-22964
HARTMANN, W. K. N87-23387
HARTMANN, WILLIAM K. N87-23494
N87-23503
HARTSOUGH, CRAIG N87-23071
HARTSOUGH, CRAIG S. N87-23081
HARVEY, KATHERINE E. N87-23184
HARWELL, WILLIAM D. N87-22985
HASEGAWA, MITSURU N87-23274
HASSELMAN, T. K. N87-22710
HASSIG, P. J. N87-23489
HATZES, A. P. N87-23364
HAUG, F. N87-22946
HAVENS, STEPHEN J. N87-22848
HAWKE, B. R. N87-23430
N87-23431
HAWKEN, M. J. N87-23107
HAYTER, J. B. N87-22853
HAYWOOD, B. C. N87-22986
HEAD, J. W. N87-23412
N87-23518
HEAD, JAMES W. N87-23538
HEARD, H. C. N87-23540
HEDDLE, D. W. N87-23247
HEDRICK, GARY D. N87-23187
HEIDMANN, K. R. N87-22778
HEIMBUCH, ALVIN H. N87-22845
HEIN, LEOPOLD A. N87-22977
HELD, MANFRED N87-22924
HELFENSTEIN, PAUL N87-23432
N87-23538
HELLMANN, J. R. N87-23026
HELMREICH, ROBERT L. N87-22635
HENNEMUTH, BARBARA N87-23076
HERGENROTHER, PAUL M. N87-22847
HERSHEY, A. V. N87-23223
HERSHKOWITZ, N. N87-23316
HESSENIUS, KRISTIN A. N87-22932
HESSLER, J. P. N87-22825
HETTMANSPERGER, THOMAS P. N87-23232
HIBLER, W. D., III N87-23014
HICKS, KERRY D. N87-23338
HILLS, C. R. N87-23285
N87-23299
HILLS, L. SCOTT N87-23534
HIPPSLEY, C. A. N87-22830
HLAVA, P. F. N87-23026
HOBDAY, J. M. N87-22954
HOCHSTEIN, JOHN I. N87-22757
HODGES, DEWEY H. N87-22677
N87-22689
HOGBEN, D. N87-23171
HOINKA, K. P. N87-23072
HOLLAREN, DOUGLAS N87-23169
HOLMES, N. C. N87-23399
HOLSAPPLE, K. A. N87-23496
HOMAN, CLARKE G. N87-22701
HONES, E. W., JR. N87-23061
HOOD, L. L. N87-23405
HOPKINS, A. S. N87-23004
HOPKINS, A. STEWART N87-22677
HOPLER, JENNIFER A. N87-23467
HOPPER, MICHAEL E. N87-23204
HORA, HEINRICH N87-23319
HORNER, GARNETT C. N87-22706
HORNER, V. M. N87-23509
N87-23512
HOROWITZ, E. N87-22840
HORTON, ROBERT S. N87-22867
HOWARD, LAURI S. N87-23201
HOWINGTON, ANNIE-ELPIS N87-23440
N87-23547
N87-23549
HSING, TAILEN N87-23233
HSU, JOHN Y. N87-22692
HSU, MING-TA S. N87-22845
HUA, T. Q. N87-22999
HUANG, CHIEN Y. N87-22621
HUANG, KAO-HUAH N87-23091
HUANG, SHANHU N87-22661
HUBER, R. N87-22665
HUBERTZ, JON M. N87-23105
HUBICKYJ, O. N87-23379
HUDSON, H. G. N87-22955
HUDSON, M. K. N87-23326
HUDSON, MARY K. N87-23321
HUEWE, LAURIE N87-23169
HUGHES, ROBERT O. N87-22733
HUMMEL, ROBERT A. N87-23186
N87-23207
N87-23222
HUMPHREYS, S. L. N87-23153
HUNTER, S. R. N87-22906
HUNTRESS, WESLEY T., JR. N87-23447
HUSSAINI, M. Y. N87-22632
HUTCHISON, R. J. N87-23279
HWANG, H. L. N87-23224
N87-23237
HWANG, HO-LING N87-23225
HWANG, R. N. N87-23252
HYLAND, D. C. N87-22741
HYMAN, J. M. N87-22824

I

IKEGAMI, R. N87-22749
INGERSOLL, A. P. N87-23556
INTRATOR, T. N87-23316
INZANA, ANTHONY N87-22651
IRANI, FREDERICK M. N87-23163
ISAYEV, G. G. N87-23134
ISHIKAWA, M. Y. N87-22697
ISLAM, M. U. N87-22806
ITO, KAZUFUMI N87-23208
ITO, Y. N87-22816
IVES, L. N87-22907
IVES, NEIL A. N87-23302
IVEY, E. W. N87-22751

J

JACKSON, ALAN N87-23272
JACKSON, L. ROBERT N87-22976
JACKSON, ROSS J. N87-22984
JACKSON, WILLIAM C. N87-22888
JACOBS, PATRICIA A. N87-23239
JACOBS, S. N87-23279
JACOT, A. D. N87-22738
JAKOSKY, B. M. N87-23445
JANATA, JIRI N87-22829
JANSA, A. N87-23083
JANSA, AGUSTIN N87-23084
JANSEN, RAINER N87-22695
JAUMANN, R. N87-23430
JEANLOZ, RAYMOND N87-23397
JELONEK, MARK P. N87-22820
JENDRZEJCZYK, J. A. N87-22771
JENSEN, DOUG N87-22639

JENSEN, R. T. N87-22869
JEWELL, R. E. N87-22728
JOCHUM, KEITH B. N87-22940
JOHNSON, C. M. N87-22869
JOHNSON, J. A. N87-22997
JOHNSON, MARK C. N87-23177
JOHNSON, MARY N87-23396
JOHNSON, R. E. N87-23435
JOHNSTON, A. N. N87-22646
JONES, D. A. N87-22911
JONES, LEE K. N87-23213
JONES, R. E. N87-22738
JONES, VERNON K. N87-23032
JORDAN, LEON N87-23192
JORDAN, RAYMOND N87-23547
N87-23548
JORGENSON, PHILIP C. E. N87-22767
JORY, H. N87-22907
JOSEPH, JOHN C. N87-22885
JOSEPH, THOMAS R. N87-23272
JOU, W.-H. N87-22619
JUANG, JER-NAN N87-22740
JUENGST, C. D. N87-22738
JUHASZ, ALBERT J. N87-22802
JUNKINS, J. L. N87-22731
JWAY, C. H. N87-22679

K

KAHN, R. N87-23506
KALANDAROV, S. N87-23126
KALAYCI, J. N87-23339
KAMEN, EDWARD W. N87-23205
KAMIS, A. J. N87-22889
KANDEIL, A. Y. N87-22808
KANE, S. R. N87-23563
N87-23564
KANG, IN-SIK N87-23041
KANG, S. Y. N87-22858
KANIC, PAUL G. N87-22803
KARDASHEV, D. L. N87-23300
KARKISHCHENKO, N. N. N87-23132
KARNICK, DREW A. N87-22761
KARPEN, J. T. N87-23565
KASTING, J. F. N87-23410
KASZETA, WILLIAM J. N87-23030
KAUCIC, ROBERT N87-23166
KAUFMAN, A. N87-22779
N87-23010
KAUL, RAJAN N87-22617
KAULA, WILLIAM M. N87-23382
KAUN, T. D. N87-22892
N87-22893
KECKLER, CLAUDE R. N87-22732
KEIL, KLAUS N87-23375
KEINHOLZ, D. A. N87-22749
KELLER, P. N87-23175
KELLER, RUSSELL L. N87-22857
KELLEY, WILLIAM H., II N87-22809
KELLY, EUGENE F. N87-23181
KENDIG, M. W. N87-22843
KENNEDY, DALE J. N87-22760
KEOUGH, J. R. N87-22866
KERTESZ, M. P. N87-22852
KHALANGOT, A. F. N87-23135
KHAYKOV, A. Z. N87-22896
KHER, SHIRISH N. N87-23006
KHOKHLOVA, O. S. N87-23127
KHOSLA, PREM K. N87-22929
KHOT, NARENDRA S. N87-22995
KIEFFER, HUGH H. N87-23366
KIELB, ROBERT E. N87-22798
KIERAS, DAVID E. N87-23188
KIM, H. N87-22967
KIM, JIN J. N87-22972
KIM, WALTER S. N87-22772
KIM, WONBECK N87-22842
KIM, YONGMIN N87-23166
KING, JOHN S. N87-23486
N87-23487
N87-23488
KING, R. J. N87-22955
KIRBY, MARK S. N87-22608
KIRBY, R. KEITH N87-22958
KIRBY, S. H. N87-23540
KIRCHNER, K. N. N87-22869
KIRK, EDILBERT N87-23040
KISIEL, ANDREW P. N87-23488
KISTLER, ROBERT E. N87-23048
KITCHEN, JAMES C. N87-23104
KITOH, AKIO N87-23036
KLAPOWA, MARIA N87-23085
KLEBANOFF, P. S. N87-22941
KLEBESADEL, R. W. N87-23564
KLEINBERG, LEONARD L. N87-22895
KLEVANS, E. H. N87-23277
KLIMOVITSKIY, V. YA. N87-23128
KLJAICH, J. N87-23176
KMIEC, THOMAS D. N87-22803
KNECHT, MARC N87-23305
KNIGHT, THOMAS F., JR. N87-22897
N87-22920
KNIP, GERALD, JR. N87-22680
KNITTLE, ELISE N87-23397
KNOWLES, STEVEN C. N87-22805
KNUE, DAVID C. N87-23246
KO, WILLIAM L. N87-23009
KOBATA, TADASUKE N87-23274
KOCH, FRED H. N87-23310
KOCHEL, R. CRAIG N87-23461
KOCHUBEYEV, A. V. N87-23134
KOLESINA, N. B. N87-23136
KOLLMANN, WOLFGANG N87-22931
KOMAR, PAUL D. N87-23464
KONDRACHUK, A. V. N87-23122
KORNEYEVA, N. V. N87-23142
KOROLEVA, A. V. N87-23258
KOZAK, R. C. N87-23515
KOZAK, RICHARD C. N87-23501
KRAFT, R. N87-22918
KRAINER, A. N87-22769
KRAMER, ARTHUR N87-23143
KRANE, M. N87-22775
KRASHUTSKIY, V. V. N87-23140
KRASNOV, I. B. N87-23130
KRATZER, R. H. N87-22859
KREY, NEIL C. N87-22652
KREYENHAGEN, K. N. N87-23489
KROLL, RICHARD W. N87-23183
KRONE-SCHMIDT, W. N87-22859
KRYLOV, YU. F. N87-23139
KRYZHANOVSKAYA, G. F. N87-23135
KUBO, SHIN N87-23274
KUDELKA, LAWRENCE N87-22925
KUETTNER, J. N87-23077
KULCINSKI, G. L. N87-22963
KUMAR, K. N87-22743
KUNIK, WILLIAM G. N87-22630
KUNZ, DONALD L. N87-22677
N87-22689
KUO, C. P. N87-22713
KUPRIIANOV, I. K. N87-23258
KURNIT, N. A. N87-22964
KURTH, R. N87-22794
KUZNETSOVA, I. V. N87-23123

L

LABURTHE, C. N87-22672
LACY, DOVIE E. N87-22802
LALLMAN, FREDERICK J. N87-22737
LAM, J. F. N87-23287
LANCASTER, N. N87-23452
N87-23541
LANDY, MICHAEL S. N87-23207
LANE, BARTON G. N87-23066
LANE, R. N87-22846
LANG, KENNETH R. N87-23560
N87-23561
N87-23562
LANG, SCOTT N87-22815
LANICCI, JOHN M. N87-23097
LANNUTTI, J. N87-22891
LANT, CHRISTIAN T. N87-22773
N87-22960
LAPUSHKIN, N. S. N87-23258
LAROS, J. G. N87-23564
LARROUTUROU, B. N87-22824
LARSON, C. R. N87-22721
LATIF, M. N87-23054
LAU, K. M. N87-23044
LAU, NGAR-CHEUNG N87-23041
N87-23042
LAUBE, SAMUEL J. P. N87-22615
LAUE, ERIC G. N87-22953
LAVALLEE, DAVID N87-23191
LAW, ROBERT L. N87-22914
LAWRENCE, C. E. N87-23221
N87-23224
LAWRIE, B. N87-22682
LAXPATI, S. R. N87-22873
LEBLANC, P. N87-22628
LECROY, STUART R. N87-23101
LEE, B. H. K. N87-22628
LEE, E. M. N87-23546
LEE, GEORGE N87-22956
LEE, J. A. N87-23459
N87-23460
LEE, JEFFREY N87-23457
LEE, RONALD W. N87-23149
LEE, S. W. N87-23541
LEE, SHANNON H. N87-22994
LEE, SHONG W. N87-22874
LEE, STEVEN W. N87-23450
LEFF, C. E. N87-23531
LEHNER, DAVID L. N87-23003
LEIGHTON, F. T. N87-22897
LEISERSON, CHARLES E. N87-22920
LEMAIRE, J. N87-23330
LENNARTSSON, W. N87-23329
LESHIN, L. A. N87-23473
N87-23542
LEUNG, MARTIN S. N87-23302
LEUNG, PHILIP N87-23317
LEVUSH, B. N87-22962
LEVY, E. H. N87-23401
N87-23402
N87-23403
N87-23404
LEWICKI, DAVID G. N87-22978
LEWIS, AARON N87-23115
LEWIS, TIMOTHY H. N87-23216
LHERMITTE, ROGER M. N87-23098
LIANG, TACHEN N87-23235
LIEBERT, CURT H. N87-22774
LIJEWSKI, MICHAEL J. N87-22942
LIKINS, PETER N87-23004
LILLEY, ROBERT W. N87-22612
N87-22614
N87-22616
LILWALL, R. C. N87-22947
LIMANOWKA, D. N87-23094
LIN, C. C. N87-23247
LIN, D. N. C. N87-23364
LIN, R. P. N87-23405
LIN, W. W. N87-22810
LINDER, HENRY G. N87-23018
LINDER, SCOTT L. N87-23290
LIOUTAS, NICK N87-22910
LIPKIN, H. J. N87-22966
LISSAUER, JACK J. N87-23363
N87-23380
N87-23385
LIU, FRANK C. N87-22752
LIU, N. S. N87-22927
LOJACONO, E. N87-22666
LOPEZ, N. N87-22907
LOTKO, W. N87-23326
LOTKO, WILLIAM N87-23324
LOVE, KAREN N87-23502
LU, YUN-CHI N87-23168
LUCAS, J. C. N87-22715
LUCAS, JOHN C. N87-23281
LUCCHITTA, B. K. N87-23469
N87-23544
N87-23558
LUCERNA, J. J. N87-22869
LUCEY, P. G. N87-23430
LUK, C. H. N87-23174
LUSK, E. N87-23198
LUSTBERG, E. A. N87-23258
LUTH, SHARON J. N87-23425
LYONS, J. E. N87-23285
LYONS, L. R. N87-23282
N87-23328
LYSAK, ROBERT L. N87-23321
LYTLE, FARREL W. N87-22821

M

MACARAEG, M. G. N87-22632
MACKINNON, D. J. N87-23455
MACKINNON, IAN D. R. N87-23376
MAHONEY, A. R. N87-23026
MAITIN, CHRISTOPHER B. N87-22926
MAKAREVICH, O. F. N87-23124
MAKAROVSKIY, V. V. N87-23135
MAKLAD, MOKHTAR S. N87-23265
MALIN, M. C. N87-23510
N87-23556
MALLETT, JOHN H. N87-23262
MANN, MARY J. N87-22975
MANSON, S. S. N87-22778
MANZO, MICHELLE A. N87-23029
MARCUS, H. L. N87-22867
MARCUS, HARRIS L. N87-22841
MARESCA, PAUL N87-23191
MARGERISON, CHARLES N87-22645
MARGRAVE, JOHN L. N87-22975
MARISKA, J. T. N87-23565
MAROUF, ESSAM A. N87-23361
MARQUES, EDWARD C. N87-22821
MARSH, BRUCE D. N87-23065
MARSHALL, J. A. N87-22817
MARSHALL, J. R. N87-23454
N87-23458

MARSHALL, M. N87-22832
MARSHALL, P. D. N87-22947
MARTIN, T. J. N87-23096
MARTZ, JAMES J. N87-22676
MARVAKOV, D. I. N87-23300
MASSE, SERGE N87-23167
MASURSKY, H. N87-23556
MASURSKY, HAROLD N87-23555
N87-23557
MATSUI, TAKASHI N87-23234
MATTHYS, DONALD R. N87-23003
MAUTZ, JOSEPH R. N87-22880
MAXWELL, T. A. N87-23524
MAXWELL, TED A. N87-23525
N87-23531
MAYER, JOHN N87-23188
MAZIERSKI, PAUL F. N87-23487
MAZUMDER, J. N87-22833
MCAVOY, H. N87-23057
MCCALL, DARYL L. N87-22613
MCCANN, DICK N87-22645
MCCARTHY, J. N87-23312
MCCOMMONS, R. B. N87-23144
MCCONVILLE, JOHN T. N87-23110
N87-23112
MCCORD, THOMAS B. N87-23421
MCCORKLE, D. L. N87-22906
MCCRORY, R. L. N87-23279
MCDONALD, H. N87-22927
MCELROY, D. L. N87-22812
MCFARLAND, RICHARD H. N87-22609
MCFARLANE, R. A. N87-23287
MCGARRY, FRANK E. N87-23192
MCGAW, MICHAEL A. N87-22777
MCGEOCH, M. W. N87-22918
MCGILL, GEORGE E. N87-23532
MCGOVERN, D. E. N87-22982
MCGOWAN, PAUL E. N87-22711
MCHARGUE, C. J. N87-22826
MCHONE, JOHN F. N87-23513
MCKAY, DAVID S. N87-23376
MCKINNON, WILLIAM B. N87-23358
MCKNIGHT, R. L. N87-22780
MCLEOD, R. R. N87-22955
MCPHERSON, MICHAEL R. N87-23119
MECHOSO, CARLOS R. N87-23036
MEDECKI, H. N87-22968
MEDERNACH, J. W. N87-22903
MEDKOVA, I. L. N87-23127
MEIROVITCH, L. N87-22734
MELDRUM, A. N87-23239
MELLO, ROBERT P. N87-23109
MENZIES, DAVID W. N87-23104
MERCHANT, R. W. N87-22957
METCALFE, R. W. N87-22819
MEYER, DONALD L. N87-23552
MEYER, GERARD G. N87-23219
MICHAUD, R. N87-23052
MICHELSEN, R. N87-23173
MICHL, JOSEF N87-23291
MICKENS, R. E. N87-23211
MIHOK, EDWARD J. N87-22988
MIKHAIL, AMEER G. N87-22937
MILLER, DANA N87-23161
MILLER, J. S. N87-23454
MILLIGAN, WALTER W. N87-22776
MILNE, J. M. N87-22991
MINISCALCO, W. J. N87-23266
MITCHELL, J. R. N87-22715
MITTRA, RAJ N87-22883
MJOLSNESS, RAYMOND C. N87-22757
MODIN, A. YU. N87-23121
MOFFATT, D. L. N87-22889
MOHRI, AKIHIRO N87-23274
MOINS, P. N87-23379
MOLCHANOVSKIY, V. V. N87-23132
MOLINARI, A. N87-23002
MOLLEY, P. A. N87-23153
MOLTENI, F. N87-23047
MONTGOMERY, RAYMOND C. N87-22720
MOORE, C. J. N87-22751
MOORE, HENRY J. N87-23443
N87-23481
MOORE, J. D. N87-23566
N87-23567
MOORE, J. M. N87-23510
MOORE, ROYCE D. N87-22681
MOOREHEAD, TAUNA W. N87-23313
MOORTHI, SHRINIVAS N87-23036
MORAN, STEVEN E. N87-22914
MORGAN, ALICE N87-22642
MORI, KAZUYA N87-23008
MORRELL, FREDERICK R. N87-22604
MORRIS, A. N87-23117
N87-23147
MORRISON, ANDREW D. N87-23286
MORRISON, CLYDE A. N87-23289
MORSY, M. W. N87-23307
MOSES, M. N87-23057
MOSS, L. A. N87-22797
MOSYAKINA, L. I. N87-23127
MOUGINIS-MARK, P. N87-23465
MOUGINIS-MARK, PETER J. N87-23441
N87-23507
MOUNT-CAMPBELL, CLARK A. N87-22700
MOZER, F. S. N87-23331
MRAZ, RICHARD T. N87-23196
MUDGE, R. W. N87-22640
MUKHERJEE, A. K. N87-22834
MULAC, RICHARD A. N87-22768
MULFORD, R. A. N87-22957
MULHERAN, P. J. N87-23103
MULLINS, K. F. N87-23546
MULLINS, LARRY D. N87-22696
MURCHIE, SCOTT L. N87-23538
MURPHY, MICHELLE M. N87-23109
MURPHY, R. C. N87-22685
MURRAY, J. N87-22753
MUSTARD, JOHN F. N87-23428
MYERS, D. R. N87-23299
MYERS, WILLIAM N. N87-22977

N

NAGIEGAAL, J. C. N87-22785
NAGLE, D. E. N87-23568
NAGPAL, VINOD K. N87-22791
N87-22792
NAKAZAWA, S. N87-22785
N87-22996
NAQWI, AMIR A. N87-22939
NARASIMHAN, R. N87-22990
NARIHARA, KAZUMICHI N87-23274
NASH, D. B. N87-23438
NASSEHI, M. MEHDI N87-23273
NEDELL, SUSAN S. N87-23470
NEININGER, B. N87-23077
NEININGER, BRUNO N87-23090
NELLIS, W. J. N87-23399
NELSON, J. R. N87-22674
NELSON, R. N87-23426
NELSON, ROBERT N87-23191
NELSON, ROBERT M. N87-23437
NELSON, W. JOHN N87-23513
NERHEIM, NOBLE M. N87-23259
NETZER, D. W. N87-22679
NEUKUM, G. N87-23430
NEWELL, J. F. N87-22793
N87-22794
NEWHALL, X. X. N87-23389
NEWMAN, WILLIAM I. N87-23382
NICHOLSON, PHILIP D. N87-23395
NICOL, M. N87-23399
NICOL, MALCOLM N87-23396
NIEH, T. G. N87-22835
NIETUBICZ, CHARLES J. N87-22937
NISITANI, HIROMOBU N87-23008
NIX, WILLIAM D. N87-22902
NOLL, CAREY E. N87-23018
NORTHRUP, C., JR. N87-23312
NORTON, S. N87-23174
NORWOOD, D. P. N87-22837
NOVACKI, STANLEY M., III N87-22610
N87-22618

O

OBERLE, LAWRENCE G. N87-22959
OCHILTREE, B. C. N87-22846
ODEN, J. TINSLEY N87-22764
OGALLAGHER, J. N87-23264
OKUDA, HIDEO N87-23327
OLIVER, W. C. N87-22826
N87-22835
OLSON, G. B. N87-22836
OMUIRCHEARTAIGH, I. N87-23239
ONEAL, JAMES L. N87-22884
ONORATO, P. I. N87-23266
ORANC, B. TARIK N87-22719
ORLADY, HARRY W. N87-22634
ORR, RICHARD S. N87-22871
OSHER, STANLEY N87-23230
OSTRO, STEVEN J. N87-23377
OVERBEEK, R. N87-23198
OWEN, J. A. N87-23045

P

PABICH, PAUL J. N87-22762
PACIOREK, K. J. N87-22859
PAEGLE, JAN N87-23088
PAGE, GERALD N87-23192
PAK, HASONG N87-23104
PALERMO, L. G. N87-22709
PALMER, T. N. N87-23045
PANG, JOSEPH N87-22921
PANITZ, J. K. G. N87-23285
PANTIC, ZORICA N87-22883
PARHI, N. N87-23212
PARKER, A. J. N87-23107
PARKER, ALICE C. N87-22916
PARKER, C. D. N87-22823
PARKER, DOLORES N87-23164
PARKER, JOHN A. N87-22845
PARKER, TIMOTHY J. N87-23471
N87-23472
N87-23537
PATTERSON, W. N87-23412
PAULSON, A. S. N87-23178
N87-23179
N87-23214
N87-23218
N87-23220
N87-23221
N87-23224
N87-23225
N87-23236
N87-23237
N87-23238
N87-23241
N87-23243
PAULSON, M. R. N87-22973
PAVLOVA, E. A. N87-23125
PEALE, S. J. N87-23347
N87-23349
N87-23351
N87-23388
N87-23391
PEALE, STANTON J. N87-23363
PEARCE, R. J. N87-22989
PEARCE, S. J. N87-23404
PEAVY, S. T. N87-23171
PECKHAM, RICHARD J. N87-22803
PECSELI, HANS L. N87-23320
PEEBLES, D. E. N87-22979
N87-22981
PELEG, SHMUEL N87-23186
PELTON, A. R. N87-22835
PENFIELD, PAUL, JR. N87-22897
N87-22920
PENG, L. N87-23044
PERALES, DAVID E. N87-22698
PERRY, J. R. N87-23102
PERRY, SANDRA N87-23192
PERSAD, C. N87-22867
PERTZBORN, D. N87-22963
PETRASEK, DONALD W. N87-22811
PETTRE, PAUL N87-23060
PHILLIPS, BARBARA A. N87-23203
PHILLIPS, CHARLES L. N87-22719
PHILLIPS, R. J. N87-23517
N87-23530
PICONE, J. M. N87-23565
PIERI, DAVID N87-23482
PIERI, DAVID C. N87-23471
N87-23472
N87-23477
N87-23537
PIERSON, L. G. N87-23152
PIETERS, C. M. N87-23412
PIETERS, CARLE M. N87-23374
N87-23428
N87-23429
N87-23430
N87-23559
PILKEY, WALTER D. N87-23007
PIN, F. G. N87-22980
PINNAMANENI, M. N87-22753
PITCHER, E. J. N87-23043
PITCHER, ERIC J. N87-23038
PITZ, W. J. N87-22823
PLATZER, M. F. N87-22769
PLAUT, J. J. N87-23506
PLESCIA, J. B. N87-23344
N87-23348
N87-23350
N87-23476
PLESCIA, JEFFREY B. N87-23538
PLETCHER, R. H. N87-22944
PLUMB, F. J. N87-22831
POCHA, M. D. N87-22905
PODOLAK, M. N87-23386
POLIAKOFF, K. N87-23410
POLITES, MICHAEL E. N87-22870
POLLACK, J. B. N87-23379
N87-23410
N87-23458

POPE, L. E. N87-22979
N87-22981
N87-23265
POPOV, I. G. N87-23136
POPOV, YU. N87-23073
PORCO, CAROLYN C. N87-23362
N87-23395
POST, RICHARD S. N87-23066
POSTAWKO, S. E. N87-23411
N87-23465
POSTAWKO, SUSAN E. N87-23419
POUCH, JOHN J. N87-23304
POWER, JOHN W. N87-22801
POWERS, ROBERT K. N87-23206
PRABHAKAR, A. N87-22709
PRAMSTALLER, D. M. N87-22866
PRANGER, H., II N87-23535
PRATT, RICHARD N87-23262
PRATT, S. N87-23412
PRATT, STEPHEN F. N87-23428
PRAVDIVTSEV, V. A. N87-23131
PRESLEY, M. A. N87-23418
PRESSER, M. A. N87-23221
PRIEBE, STEPHEN J. N87-23031
PRINZ, F. N87-22782
PRUNER, JAMES R. N87-22671
PRYBYLOWSKI, SALLI L. N87-22964
PSIAKI, MARK L. N87-22620
PURCELL, TIMOTHY W. N87-23250
PYLE, JON S. N87-22732

Q

QAQISH, WALID N87-22773
N87-22960
QUIMBY, KELVIN N87-23191
QUINN, R. D. N87-22734

R

RADOUSKY, H. B. N87-23399
RAE, W. J. N87-22770
RAHMAN, A. N87-23284
RAJA, S. N87-22833
RAJAGOPAL, K. R. N87-22766
RAJENDRAN, A. M. N87-23005
RALEIGH, D. O. N87-22843
RAO, J. B. N87-22873
RAO, K. V. N87-22944
RAVA, BARRY N87-23439
RAVICHANDRAN, G. N87-23001
RAVINE, M. N87-23556
RAY, C. S. N87-22861
READ, WILLIAM F. N87-23514
REE, F. H. N87-23399
REED, WILLIAM P. N87-22958
REILLY, CHARLES H. N87-22700
REILLY, J. J. N87-22810
REINHARDT, M. N87-23077
REINHARDT, M. E. N87-23087
REINISCH, BODO W. N87-23056
REYNOLDS, G. H. N87-22814
REYNOLDS, R. T. N87-23345
N87-23386
REYNOLDS, RAY T. N87-23355
REYNOLDS, WILLIAM C. N87-22939
RIBE, F. L. N87-23278
RICHARDS, KEN N87-22714
RICHARDS, WHITMAN N87-23150
RICHARDSON, D. D N87-22911
RICHARDSON, S. M. N87-23410
RICHEY, RANDAL L. N87-22699
RICHLEN, SCOTT L. N87-23031
RICHNER, HANS N87-23090
RIEHL, KEVIN B. N87-23099
RIETMEIJER, FRANS J. M. N87-23376
RIFF, R. N87-22796
RIGBY, D. L. N87-22770
RIOSALIDO, R. N87-23083
RITTER, PAUL D. N87-23031
RIYOPOULOS, S. N87-22962
ROBERTS, LEONARD N87-22951
ROBERTS, W. W., JR. N87-23381
ROCHE, ALEXANDER F. N87-23118
ROCHON, BRIAN V. N87-22744
RODDEN, J. J. N87-22742
RODDY, D. J. N87-23489
RODGERS, DON N87-22652
RODMAN, L. C. N87-22633
ROGERS, LYNN N87-22714
ROLLESTON, ROBERT N87-23270
ROMAN, W. C. N87-22969
ROOHAN, P. J. N87-23237
ROSAKIS, ARES J. N87-22990
ROSE, T. L. N87-22727
ROSENBERG, JACOB N87-23191
ROSENBLATT, MARTIN N87-23489
ROSS, M. N87-23399
ROSSALL, A. W. N87-23248
ROSSBACHER, LISA A. N87-23536
ROTH, L. E. N87-23446
ROTH, M. N87-23330
ROUND, P. N87-22670
ROUSH, TED L. N87-23421
ROWLAND, SCOTT K. N87-23480
ROY, DANIEL N87-23191
RUBIN, STANLEY G. N87-22929
RUBINSTEIN, ROBERT N87-22791
N87-22795
RUDY, S. W. N87-22765
RUMBLE, J., JR. N87-23312
RUMBLE, S. J. N87-22682
RUSSELL, W. C. N87-22724
RUSSO, T. N87-22684
RYAN, ROBERT S. N87-22702
N87-22729

S

SADOURNY, R. N87-23052
SAHM, PETER R. N87-22695
SAHU, JUBARAJ N87-22624
SALES, GARY S. N87-23056
SALISBURY, JOHN W. N87-23424
SALVAIL, J. R. N87-23365
N87-23367
N87-23411
SALVINA, J. T. N87-22684
SAMPSON, MADELINE P. N87-22975
SANDBERG, V. D. N87-23568
SANDSTROM, DONALD R. N87-22821
SARGENT, MICHAEL L. N87-23513
SASS, S. L. N87-22838
SAUNDERS, R. S. N87-23446
SAUNDERS, R. STEPHEN N87-23471
N87-23472
N87-23537
SAVAGE, BLAIR D. N87-23336
SAXENA, Y. C. N87-23318
SCHAAF, CRYSTAL BARKER N87-23092
SCHABER, G. G. N87-23515
N87-23542
SCHABER, GERALD G. N87-23501
SCHACK, C. J. N87-22822
SCHAEFER, THOMAS M. N87-22899
SCHAFER, FRANCIS J. N87-23440
N87-23547
N87-23548
SCHEER, STEVEN A. N87-22744
SCHENK, PAUL M. N87-23358
SCHLESE, ULRICH N87-23040
SCHMIDINGER, G. N87-22669
SCHMIDT, JAMES F. N87-22630
N87-22681
SCHMIDT, ROBERT M. N87-23495
N87-23498
SCHNEEBERGER, DALE M. N87-23471
N87-23472
N87-23477
N87-23537
SCHNEIDER, M. N87-23284
SCHNITTGRUND, G. D. N87-22781
SCHOCK, RICHARD W. N87-22722
SCHOEN, ERIC N87-23197
SCHOLZ, WILFRED N87-22701
SCHREIBER, R. N87-22891
SCHUBERT, GERALD N87-23356
N87-23511
SCHULLER, I. K. N87-23284
SCHULMAN, M. B. N87-23247
SCHULTZ, P. H. N87-23490
N87-23491
SCHULTZ, PETER H. N87-23374
N87-23492
N87-23493
N87-23497
N87-23505
N87-23508
N87-23526
SCHULTZ, R. A. N87-23524
SCHUNK, R. W. N87-23323
SCHUSTER, S. H. N87-23489
SCHUTZ, B. E. N87-23033
SCHWARTZ, DOUGLAS N87-22653
SCOFIELD, HAROLD N. N87-22702
N87-22729
SCOTT-MILLIGAN, FIONNA N87-22658
SCOTT, DAVID H. N87-23475
SCOTT, J. C. N87-23102
SCRAMANGAS, A. N87-22992
SEIDEWITZ, EDWIN V. N87-23190
N87-23191
SELLARDS, ROBERT N87-22659
SEMENIUK, ANN MARIE N87-23523
SENSBURG, O. N87-22669
SERGIYEVSKIY, M. V. N87-23106
SERYKH, V. P. N87-23283
SETTLES, GARY S. N87-22928
SEZGIN, E. N87-23059
SHAFRANSKIY, YU. A. N87-23135
SHAMROTH, S. J. N87-22927
SHARKEY, JOHN P. N87-22735
SHARP, D. J. N87-22837
SHARPTON, FRANCIS A. N87-23247
SHASHKOV, V. S. N87-23121
SHAW, F. H. N87-22724
N87-22725
SHAYDOROV, YU. I. N87-23138
SHEATHER, SIMON J. N87-23232
SHECHTMAN, DAN N87-22840
SHELL, ALLYN N87-23191
SHIAO, MICHAEL N87-22791
SHIH, CHOON-FOO N87-22712
SHIKINA, M. I. N87-23136
SHIMADA, T. N87-22964
SHIPOV, A. A. N87-23122
SHISHKINA, S. K. N87-23142
SHOEMAKER, CAROLYN S. N87-23369
SHOEMAKER, EUGENE M. N87-23369
N87-23500
N87-23501
SHREVE, STEVEN T. N87-22611
SHRIVASTAVA, P. C. N87-22622
SHROYER, DAVID H. N87-22638
SHU, CHI-WANG N87-23230
SHU, FRANK H. N87-23394
SHUKLA, J. N87-23048
SHUM, C. K. N87-23033
SHUNG, FELIX N87-23355
SIDYAKIN, V. G. N87-23141
SIGMON, THOMAS W. N87-23303
SIGNORELLI, ROBERT A. N87-22811
SIMITSES, G. J. N87-22796
SIMMONS, ARDYTH M. N87-23486
SIMMONS, DAVID W. N87-23461
SIMON, CHARLES W. N87-23231
SIMONEAU, R. J. N87-22769
SIMONELLI, DAMON P. N87-23436
SIMPSON, RICHARD A. N87-23448
SIMPSON, ROBERT W. N87-22605
SINGER, R. N87-23414
SINGER, R. B. N87-23422
SINGER, ROBERT B. N87-23421
SINGH, J. N87-22833
SINGH, NAGENDRA N87-23323
SINGH, R. P. N87-22746
SINGH, T. S. N87-22663
SINSKY, MARK S. N87-22647
SINYAK, YU. YE. N87-23136
SJOGREN, WILLIAM L. N87-23400
SKEEL, R. D. N87-23210
SKODA, GEORG N87-23093
SLAVNEY, S. N87-23554
SLAVNEY, SUSAN N87-23160
SLEEP, N. H. N87-23530
SLINEY, HAROLD E. N87-22860
SMAGA, J. A. N87-22893
SMIRL, A. L. N87-23267
SMIRNOV, K. V. N87-23127
SMITH, A. A. N87-22862
SMITH, B. T. N87-23176
SMITH, BRUCE L. N87-23327
SMITH, KERMIT L. N87-23560
N87-23562
SMITH, L. N87-23173
SMITH, MILTON O. N87-23415
SMITH, ROBERT A. N87-23325
SMITH, RONALD B. N87-23069
SMITH, T. D. N87-22674
SMITH, T. E. N87-22797
SMYTHE, W. N87-23426
SMYTHE, WILLIAM D. N87-23437
SOEDERLIND, GUSTAF N87-23228
SOKOL, YE. A. N87-23134
SOLOMON, SEAN C. N87-23519
N87-23520
N87-23522
SOULANILLE, T. N87-23556
SOURES, J. M. N87-22967
N87-23279
SOVEY, JAMES S. N87-22805
SOVIE, RONALD J. N87-23027
SPANG, S. N87-22907
SPAUTE, D. N87-23387
SPENCE, J. C. N87-23301

SPITLER, M. T. N87-23295
SPRANGLE, P. N87-22962
SPUDIS, PAUL D. N87-23407
N87-23408
SQUYRES, S. W. N87-23345
SQUYRES, STEVEN W. N87-23355
N87-23420
N87-23470
STACEY, J. A. N87-23102
STALEY, D. J. N87-23285
STALKER, K. T. N87-23153
STALLINGS, ROBERT L., JR. N87-22626
STANDLER, R. B. N87-22919
STAPLETON, S. F. N87-22868
STARK, MIKE N87-23190
STEGER, J. L. N87-22944
STEINKE, RONALD J. N87-22630
N87-22681
STENGEL, ROBERT F. N87-22619
STEPANOVA, T. P. N87-23133
STEPHEN, ERIC C. N87-22623
STEPHENS, MARK N87-23161
STEPINSKI, T. N87-23403
STETSON, KENNETH F. N87-22625
STEWART, G. R. N87-23381
N87-23393
STEWART, GLEN R. N87-23383
STICHMAN, J. H. N87-23153
STILLE, J. K. N87-22854
STOCK, MICHAEL N87-22686
STOCKTON, ROBERT G. N87-23185
STOKOE, KENNETH H., II N87-22994
STRAWN, ROGER C. N87-23250
STREETT, C. L. N87-22632
STROBELL, M. E. N87-23555
N87-23557
STROM, ROBERT G. N87-23342
STRONG, KEITH T. N87-23560
N87-23562
STUPIAN, GARY W. N87-23302
SUCIU, DAN F. N87-23031
SUGAR, ROSS N87-23158
SULLIVAN, JAMES D. N87-23066
SULLIVAN, ROBERT N87-23457
SUMMERS, AUDREY L. N87-23355
SUPRUNOVA, YE. V. N87-23142
SUTHERLAND, P. G. N87-23334
SUTTON, T. M. N87-23227
SYNNOTT, S. P. N87-23543
SZCZUR, MARTHA N87-23156
N87-23157

T

TABAKOFF, W. N87-22858
TAGGART, WILLIAM R. N87-22637
TAMPIERI, F. N87-23078
TANAKA, KENNETH L. N87-23475
N87-23528
TANG, C. M. N87-22962
TAPE, R. F. N87-22670
TAPLEY, B. D. N87-23033
TARRANT, A. N87-22693
TATTERSALL, J. M. N87-22872
TAU, CYRUS N. N87-22909
TAYLOR, ALLAN H. N87-22976
TAYLOR, JOHN V., IV N87-22763
TAYLOR, P. A. N87-23297
TEBBETTS, ILSE O. N87-23110
N87-23112
TECZA, J. N87-22683
TEDESCO, EDWARD N87-23371
TEMERIN, M. N87-23331
TEMPLETON, DAVID N87-23262
TEMURYANTS, N. A. N87-23141
THEILIG, E. N87-23478
THEON, JOHN S. N87-23091
THIEMANN, H. N87-23323
THOMAN, S. J. N87-22810
THOMAS, J. O. N87-23102
THOMAS, P. N87-23352
N87-23354
N87-23453
THOMAS, P. J. N87-23345
THOMAS, PAUL J. N87-23511
THOMPSON, R. C. N87-22731
THOMPSON, T. W. N87-23442
N87-23443
N87-23444
N87-23446
THRESHER, R. W. N87-23021
TIBALDI, S. N87-23047
TICKNER, R. L. N87-22987
TIDBALL, R. N87-22891
TIDSTRON, K. D. N87-22941
TIEN, JOHN K. N87-22811
TIGRANYAN, R. A. N87-23139
TIPTON, M. T. N87-22780
TISCHER, A. E. N87-22765
TISCHLER, MARK B. N87-22690
N87-22691
TOBAGI, FOUAD N87-22921
TOBIAS, R. W. N87-22987
TOBIN, DAVID M. N87-22974
TOKIOKA, T. N87-23051
TOMITA, YUKIHIRO N87-23274
TOMKO, FRANK G. N87-22660
TOMLINSON, W. M. N87-22817
TONINI, R. N87-22666
TORREY, MARTIN D. N87-22757
TORVEN, S. N87-23315
TOTI, WILLIAM J. N87-22876
TOWNE, DOUGLAS M. N87-23177
TOWNSEND, JOHN S. N87-22726
N87-22751
TRIENEKENS, HARRY W. N87-23200
TROMBETTI, F. N87-23078
TSUZUKI, TETSUYA N87-23274
TUCKER, D. W. N87-23458
TUCKER, W. B., III N87-23014
TURCOTTE, DONALD L. N87-23406
TURNER, J. D. N87-22731
TURNER, L. R. N87-22875
N87-22999
TURNER, ROBERT E. N87-23091
TURNER, RUSSELL M. N87-22739
TYLER, G. LEONARD N87-23448
TYLER, LEONARD G. N87-23361

U

ULSETH, G. W. N87-23238
URBARZ, H. W. N87-23563
URIANO, GEORGE A. N87-22958
URICH, D. J. N87-22679
USHAKOV, A. S. N87-23142
USHAKOV, I. B. N87-23133

V

VAKALYUK, YU. N87-23073
VALDES, JAMES E. N87-22688
VALETT, JON N87-23192
VANDALSEM, W. R. N87-22944
VANDERVOORT, R. J. N87-22746
VARNER, R. N. N87-23171
VAZQUEZ, L. N87-23083
VERCRUYSSEN, M. N87-22983
VERGEINER, I. N87-23075
VERGO, NORMA N87-23424
VEVERKA, J. N87-23352
N87-23556
VEVERKA, JOSEPH N87-23432
N87-23436
VIGIL, DEBBIE N87-22975
VILLERE, KAREN R. N87-23340
VINOGRADOVA, L. A. N87-23136
VLASOV, V. D. N87-23140
VLODAVETS, V. V. N87-23136
VOGEL, JAMES A. N87-23109
VOIGT, ROBERT J. N87-23155
VONPRAGENAU, GEORGE L. N87-22716
VONROOS, OLDWIG N87-22894
VONSTORCH, HANS N87-23040
VU, B. DANG N87-22672
VUKICEVIC, TOMISLAVA N87-23088

W

WADA, B. K. N87-22727
WADA, BEN K. N87-22713
WADSWORTH, J. N87-22835
WAGNER, JEFFREY N87-23427
WAITES, HENRY B. N87-22704
WALKER, GEORGE P. L. N87-23480
N87-23484
WALLACE, STEIN W. N87-23217
WALLACE, W. N87-22808
WALSTON, S. N87-22782
WALTER, LOUIS N87-23424
WALTON, E. K. N87-22889
WAMBSGANSS, M. W. N87-22771
WANG, E. Y. N87-23316
WANNER, H. N87-23086
WARBURTON, PENELOPE J. N87-22947
WARNER, JOSEPH D. N87-23304
WATSON, STEVEN M. N87-23271
WATTERS, THOMAS R. N87-23529
WEATHERS, MAURA S. N87-23398
WEAVER, D. P. N87-22863
WEAVER, F. J. N87-22812
WEBER, HARALD N87-23097
WEEKS, THOMAS M. N87-22671
WEI, T. N87-23266
WEIDENSCHILLING, S. J. N87-23384
N87-23387
N87-23494
WEIDENSCHILLING, STUART J. N87-23499
WEIL, ROLF N87-22842
WEISBIN, C. R. N87-22960
WEISEL, E. L. N87-23087
N87-23089
WEISS, B. N87-23554
WEISS, JEROLD L. N87-22692
WEISSKOPF, M. C. N87-23334
WEISSMAN, PAUL R. N87-23366
N87-23368
WELDON, W. F. N87-22867
WELLS, EDDIE N87-23427
WENTWORTH, S. J. N87-23409
WERNET, MARK P. N87-22959
WESTBROOK, C. K. N87-22823
WESTBROOK, J. N87-23312
WESTON, RICHARD L. N87-22961
WETHERILL, G. W. N87-23378
WETHERILL, GEORGE W. N87-23383
WETZEL, PAUL A. N87-23108
WHINNERY, JAMES E. N87-23116
WHITE, LAWSON C. N87-22647
WHITFORD-STARK, J. L. N87-23485
WHITLOCK, CHARLES H. N87-23101
WHITSEL, LYNNETTE T. N87-23226
WICHMAN, R. N87-23526
WIEDWALD, J. D. N87-22905
WIESE, MICHAEL R. N87-23194
WILCOX, FLOYD J., JR. N87-22626
WILKINS, GARY D. N87-23060
WILKINSON, C. N87-23568
WILLIAMS, A. C. N87-23334
N87-23335
WILLIAMS, ALTON C. N87-23313
WILLIAMS, E. N87-23173
WILLIAMS, J. G. N87-23370
N87-23389
WILLIAMS, JEFFREY P. N87-22717
WILLIAMS, KENNETH R. N87-22649
WILLIAMS, QUENTIN N87-23397
WILLIAMS, R. A. N87-23568
WILLIAMS, S. H. N87-23456
WILLSON, ROBERT F. N87-23560
N87-23561
N87-23562
WILSON, J. F. N87-22728
WILSON, JEFFREY D. N87-22923
WILSON, JOSEPH N87-22664
WILT, DAVID M. N87-23304
WING, JEANNETTE M. N87-23206
WING, KAM LIU N87-22790
WINSTON, R. N87-23264
WIRSCHING, P. H. N87-22788
WISDOM, JACK N87-23390
WITHERSPOON, L. L. N87-22903
WITZKE, E. L. N87-23152
WOJCIK, A. S. N87-23176
WOLFE, RUTH F. N87-23500
WONG, A. K. N87-23011
WOO, H. H. N87-22736
WOOD, JERRY R. N87-22630
N87-22681
WOOD, L. L. N87-22697
WOOD, N. J. N87-22633
WORKS, THOMAS V. N87-23199
WORONOW, ALEX N87-23502
WRIGHT, A. D. N87-23021
WRIGHT, B. D. N87-22873
WRIGHT, D. G. M. N87-22987
WU, SHERMAN S. C. N87-23440
N87-23547
N87-23548
N87-23549
WYATT, JOHN L., JR. N87-22920
WYNESS, BRYAN N87-22658

X

XU, GUOZHEN N87-22661
XU, WENG-AN N87-22800

Y

YAMAMORI, HISAAKI N87-22643
YANG, L. N87-22814
YANG, SHI-XUE N87-22800

YANG, T. F. N87-23275
YANTIS, B. N87-23173
YASNETSOV, V. V. N87-23131
YERSHIKOV, S. M. N87-23129
YEVSTAFYEVA, YE. V. N87-23141
YIM, CHANG H. N87-23255
YOON, SEOG K. N87-23254
YOUMANS, BRUCE R. N87-23259
YOUNG, D. A. N87-23399
YOUNG, JOHN W. N87-22737
YU, FRANCIS T. N87-23260
YU, YUNG H. N87-23250
YUAN, C. N87-23379
YUKON, STANFORD P. N87-23064
YUNUSOVA, L. S. N87-23138

Z

ZAK, M. N87-22745
ZANA, LYNNETTE M. N87-22805
N87-22807

ZEBIAK, S. E. N87-23053
ZEBKER, HOWARD A. N87-23361
ZEEVI, YEHOSHUA Y. N87-23108
ZEHNDER, ALAN T. N87-22990
ZENT, A. P. N87-23411
ZENT, AARON P. N87-23359
N87-23419

ZHIZNEVSKAYA, O. V. N87-23127
ZHOU, SONGNIAN N87-23195
ZIETLOW, THOMAS C. N87-23253
ZIMBELMAN, J. R. N87-23509
ZIMMER, H. N87-22627
ZINNER, HELMUT N87-23256
ZIPPEL, RICHARD E. N87-22920
ZORINA, N. G. N87-23137
ZURAWSKI, ROBERT L. N87-22806

CORPORATE SOURCE INDEX

SCIENTIFIC AND TECHNICAL AEROSPACE REPORTS VOLUME 25 NUMBER 16

Typical Corporate Source Index Listing

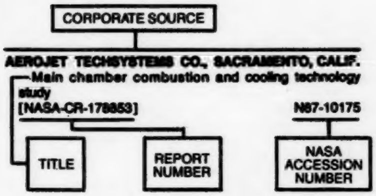
CORPORATE SOURCE
AEROJET TECHSYSTEMS CO., SACRAMENTO, CALIF.
Main chamber combustion and cooling technology study
[NASA-CR-178853]
N87-10175
TITLE
REPORT NUMBER
NASA ACCESSION NUMBER

Listings in this index are arranged alphabetically by corporate source. The title of the document provides the user with a brief description of the subject matter. The report number helps to indicate the type of document cited (e.g., NASA report, translation, NASA contractor report). The NASA accession number denotes the number by which the citation is identified. The titles are arranged under each corporate source in ascending accession number order.

A

ADMIRALTY RESEARCH ESTABLISHMENT, PORTLAND (ENGLAND).

A Simplex optimisation technique for development of rubber formulations
[ARE-TM(UMT)-86405] N87-22846

The SIR-B mission: Towards an understanding of internal waves in the ocean
[ARE-TR-86122] N87-23102

ADMIRALTY RESEARCH ESTABLISHMENT, PORTSMOUTH (ENGLAND).

Circumferential hot wire TIG cladding of carbon-manganese steel with Inconel 625 and gun-metal with a tin bronze
[ARE-TM(UMD)-85574] N87-22831

ADVISORY GROUP FOR AEROSPACE RESEARCH AND DEVELOPMENT, NEUILLY-SUR-SEINE (FRANCE).

Improvement of Combat Performance for Existing and Future Aircraft
[AGARD-CP-409] N87-22663

AERONAUTICAL RESEARCH LABS., MELBOURNE (AUSTRALIA).

Preliminary investigation of the use of holographic interferometry to detect ill-fitting compressor blades
[AD-A178519] N87-22682

An evaluation of microgridding techniques for determining local plastic strain distributions
[AD-A178518] N87-23000

On the application of the strain energy density theory in predicting crack initiation and angle of growth
[AR-004-493] N87-23011

AEROSPACE CORP., EL SEGUNDO, CALIF.

On the thinning of the plasma sheet during substorms
[AD-A178484] N87-23061

Dose enhancement effects in the Aerospace Corporation Co-60 irradiator
[AD-A178481] N87-23253

The generation of electrostatic noise in the plasma sheet boundary layer
[ATR-86(8433)-4] N87-23262

Unpinning of the Fermi level on GaAs by flowing water
[AD-A178489] N87-23302

AEROSPACE CORP., LOS ANGELES, CALIF.

Conditions for double layers in the Earth's magnetosphere and perhaps in other astrophysical objects N87-23328

AIR FORCE GEOPHYSICS LAB., HANSCOM AFB, MASS.

Atmospheric remote sensing in arctic regions
[AD-A179550] N87-23012

Characteristics of orographically initiated convection
N87-23092

Validation of a surface-layer windflow model using climatology and meteorological tower data from Vandenberg AFB, California
[AD-A178480] N87-23097

AIR FORCE HUMAN RESOURCES LAB., BROOKS AFB, TEX.

Aircrew task surveys: Selection criteria for low-cost training technology applications
[AD-A178473] N87-23146

AIR FORCE INST. OF TECH., WRIGHT-PATTERSON AFB, OHIO.

Investigation of periodic pitching through the static stall angle of attack
[AD-A179512] N87-22623

GEMACS (general EM model for the analysis of computer systems) frequency-domain analysis to determine the lightning induced electromagnetic skin current distributions on an aircraft
[AD-A178854] N87-22660

Design of GPS (Global Positioning System) status reporting system
[AD-A179334] N87-22662

Accurate prediction of longitudinal flying qualities for landing aircraft
[AD-A179069] N87-22676

Evaluation of numerator lead effects on aircraft handling qualities
[AD-A179368] N87-22687

A prototype knowledge-based system for satellite mission planning
[AD-A178873] N87-22698

Determining the probability of close approach between two satellites
[AD-A179385] N87-22699

Estimation of ICBM (intercontinental ballistic missile) performance parameters
[AD-A179204] N87-22754

Optimal shuttle altitude changes using tethers
[AD-A179205] N87-22756

Design of an orbital inspection satellite
[AD-A179115] N87-22759

A prototype expert system advisor for satellite support scheduling
[AD-A179425] N87-22760

Moving-bank multiple model adaptive estimation applied to flexible spacestructure control
[AD-A178870] N87-22761

Developing a voice-controlled, computer-generated display to assist space station astronauts during maintenance activity
[AD-A178997] N87-22762

Star sensor fine attitude pointing model for a spinning geosynchronous satellite
[AD-A179424] N87-22763

Investigation of rocket powered, open cycle, magnetohydrodynamic generators for high, pulsed power needs in space
[AD-A178869] N87-22801

Thermal shock resistance of mullite-based SiC-whisker composites
[AD-A179214] N87-22809

Effects of cutout orientations on natural frequencies and mode shapes of curved rectangular composite panels
[AD-A178838] N87-22813

Frequency shift measurements of the Q(1) and Q(2) lines of H2 using high resolution CW Coherent Anti-Stokes Raman Spectroscopy
[AD-A179390] N87-22820

Examination of high performance polymer fibers under compressive deformation
[AD-A178640] N87-22857

Investigation of Continuously Variable Slope Delta (CVSD) modulation for voice communications
[AD-A178579] N87-22877

Optimization of the antenna pattern of a phased array with failed elements
[AD-A178581] N87-22878

Simulation model of a meteor burst communication system for data transmission protocol evaluation
[AD-A178843] N87-22881

Analysis of lightning induced magnetic field penetration through protective metal screens using an equivalent magnetic dipole moment representation of an array of elliptic apertures
[AD-A178850] N87-22884

Multiple angle of incidence measurement technique for the permittivity and permeability of lossy materials at millimeter wavelengths
[AD-A178851] N87-22885

Full polarimetric non-specular scattering of flat plate structures
[AD-A178853] N87-22886

Characterization of the error performance of a QPSK (Quadrature Phase Shift Keyed) communication system in the presence of linear transmission distortion
[AD-A178855] N87-22887

Development of a microcomputer-based workstation for analysis of digital satellite links
[AD-A178872] N87-22888

Modeling and simulation of the WFTA (Winograd Fourier Transform Algorithm) 16 PFA (Prime Factor Algorithm) processor using the VHSIC (Very High Speed Integrated Circuit) hardware description language, volume 1
[AD-A179344] N87-22896

The transverse dynamics of space-charge limited diodes
[AD-A179389] N87-22899

An implementation of a language analyzer for the very high speed integrated circuit hardware description language
[AD-A178648] N87-22913

Boundary layer disturbances caused by periodic heating of a thin ribbon
[AD-A179342] N87-22925

A study of fluid-dynamic pressure fields on compressor reed valves
[AD-A178584] N87-22938

Numerical study of high speed viscous flows
[AD-A178639] N87-22940

A multiple model adaptive tracking algorithm for a high energy laser weapon system
[AD-A178978] N87-22974

Two-dimensional elastic analysis by the boundary element method
[AD-A179213] N87-22993

Investigations of the polar rain: Polar cap electron precipitation
[AD-A178876] N87-23099

A collection and statistical analysis of biophysical data to predict motion sickness incidence
[AD-A178874] N87-23119

Performance comparison of four state-of-the-art computer architectures
[AD-A179071] N87-23149

The graphical kernel system: A standards implementation
[AD-A178583] N87-23180

Automatic scene analysis using hierarchical spatial frequency domain correlation with energy normalization and heuristic noise reduction
[AD-A178589] N87-23181

A graphics environment supporting the rapid prototyping of pictorial cockpit displays
[AD-A178636] N87-23182

Development of an image analysis program for the IBM PC/XT/AT
[AD-A178844] N87-23183

Design of fault tolerant prime factor algorithm array elements
[AD-A178977] N87-23187

Performance evaluation of parallel branch and bound search with the intel IPSC (Intel Personal SuperComputer) hypercube computer
[AD-A179384] N87-23196

A prototype knowledge-based system to aid space system restoration management
[AD-A179336] N87-23203

Multi-input/multi-output designated eigenstructure (MODES): A computer-aided control system design program
[AD-A179341] N87-23204

A partial differential equation model describing the threat to an aircraft in a one-on-Many scenario
[AD-A178641] N87-23215
Linear time invariant system identification using a result of the Bussgang theorem
[AD-A178642] N87-23216
A modified goodness-of-fit test for the lognormal distribution with unknown scale and location parameters
[AD-A179049] N87-23226
Managing uncertainty in expert systems: A probabilistic approach
[AD-A178582] N87-23246
Two-point resolution criterion for multi-aperture optical systems
[AD-A178960] N87-23271
Development of a generalized model for a three component plasma
[AD-A178979] N87-23281
The characterization of whiskers produced by electromigration on suspended aluminum linestripes
[AD-A179383] N87-23290
LRS: A knowledge based approach to launch resource scheduling
[AD-A179426] N87-23310
A decision support system for database management system selection
[AD-A179339] N87-23311
Periodic orbits about rotating asteroids in free space
[AD-A179387] N87-23338

AIR FORCE ROCKET PROPULSION LAB., EDWARDS AFB, CALIF.
Identification of large space structures: A state-of-practice report N87-22705
Afterburning suppression kinetics
[AD-A178967] N87-22863

AIR FORCE SYSTEMS COMMAND, BROOKS AFB, TEX.
Air Force technical objectives document, fiscal year 1988
[AD-A179163] N87-23569

AIR FORCE SYSTEMS COMMAND, WRIGHT-PATTERSON AFB, OHIO.
CONMILIT (selected articles)
[AD-A179155] N87-22661
Journal of Chinese Society of Astronautics (selected articles)
[AD-A179690] N87-22800
Klystron transmitters
[AD-A179068] N87-22836
Special features in regulating respiration under normal conditions and conditions of altered gas medium
[AD-A179216] N87-23106

AIR FORCE WEAPONS LAB., KIRTLAND AFB, N. MEX.
Transient protection of electronic circuits
[AD-A178945] N87-22919

AIR FORCE WRIGHT AERONAUTICAL LABS., WRIGHT-PATTERSON AFB, OHIO.
Hypersonic laminar boundary layer transition. Part 1: Nosetip bluntness effects on cone frustum transition. Part 2: Mach 6 experiments of transition on a cone at angle of attack
[AD-A178877] N87-22625
X-29 integrating advanced technologies for tomorrow's air combat N87-22671
Optimum mix of passive and active control of space structures N87-22714
Proceedings of the 22nd Annual Conference on Manual Control
[AD-A178627] N87-23148

AIR NEW ZEALAND, AUCKLAND.
Cockpit Resource Management (CRM) and human factors training: What Air New Zealand is doing about it N87-22658

ALABAMA UNIV., HUNTSVILLE.
Analytical determination of space station response to crew motion and design of suspension system for microgravity experiments N87-22752
Cosmic ray detectors
[NASA-CR-179086] N87-22952
Vibration analysis using shadow speckle metrology and line broadening techniques
[AD-A178626] N87-23003
Applications of fiber optics in experimental mechanics
[AD-A178683] N87-23268

ALLIED BENDIX AEROSPACE, TETERBORO, N.J.
Adaptive momentum management for large space structures
[NASA-CR-179085] N87-22758

ALLIED CORP., MORRISTOWN, N.J.
New laser materials
[DE87-006723] N87-22970

ALPHATECH, INC., BURLINGTON, MASS.
Integrated restructurable flight control system demonstration results
[NASA-CR-178305] N87-22692

ALZETA CORP., SANTA CLARA, CALIF.
Catalytic radiant tube. Phase 2: Proof of concept
[PB87-169835] N87-22891

ANAMET LABS., INC., SAN CARLOS, CALIF.
Numerical methods for imperfection sensitivity analysis of stiffened cylindrical shells. Volume 1: Development and applications
[AD-A179686] N87-22995

ANTHROPOLOGY RESEARCH PROJECT, YELLOW SPRINGS, OHIO.
Selection of dimensions for an anthropometric data base. Volume 2: Dimension evaluation sheets
[AD-A179472] N87-23110
Selection of dimensions for an anthropometric data base. Volume 1: Rationale, summary, and conclusions
[AD-A179566] N87-23112

APPLIED RESEARCH CORP., LANDOVER, MD.
Decomposition of energetic materials combustion of decoy materials
[AD-A178447] N87-22827

ARGONNE NATIONAL LAB., ILL.
Analytical and experimental studies of flow-induced vibration of SSME components N87-22771
Two-color, Doppler-free ionization of molecular hydrogen for isotopic analysis
[DE87-004975] N87-22825
The Regional Electromagnetics Workshop in the USA
[DE87-004709] N87-22875
Lithium-metal sulfide battery development and submodule demonstration
[DE87-004819] N87-22904
Why gamma rays are different: Some notes for pedestrians
[DE87-004963] N87-22966
Experimental study of coupling between eddy curren of Tokamak limiters of tokamak limiters
[DE87-004938] N87-22999
Measurement of high resolution wind profiles with a minisodar
[DE87-007001] N87-23096
Formal modeling and analysis of fault-tolerance properties for software
[DE87-007006] N87-23176
Experiments with OR-parallel logic programs
[DE87-006882] N87-23198
Considerations pertinent to the Doppler effect for space reactors
[DE87-007032] N87-23252
Molecular-dynamics simulation of thin-film growth
[DE87-006973] N87-23284
Thermodynamic properties of molten salt solutions
[DE87-004948] N87-23306

ARIZONA STATE UNIV., TEMPE.
Submicron characterization of the atomic and electronic structure of defects in semiconductors
[AD-A178458] N87-23301
Variations of Martian surface albedo: Evidence for yearly dust deposition and removal N87-23413
Thermal-infrared spectral observations of geologic materials in emission N87-23425
Bright sand/dark dust: The identification of active sand surfaces on the Earth and Mars N87-23449
Regional sources and sinks of dust on Mars: Viking observations of Cerberus, Solis Planum and Syrtis Major N87-23450
High resolution thermal infrared mapping of Martian channels N87-23451
Mars: Morphology of Southern Hemisphere intracrater dunefields N87-23452
Mass transport by Aeolian saltation on Earth, Mars and Venus: The effects of full saltation cloud development and choking N87-23456
Development of wind tunnel techniques for the solution of problems in planetary Aeolian processes N87-23457
Aeolian abrasion on Venus: Preliminary results from the Venus simulator N87-23458
Reynolds number effects on surface shear stress patterns around isolated hemispheres N87-23459
Determination of surface shear stress with the naphthalene sublimation technique N87-23460
Explosive volcanic deposits on Mars: Preliminary investigations N87-23473
Martian volcanism: Festoon-like ridges on terrestrial basalt flows and implications for Mars N87-23478
Studies of fluid instabilities in flows of lava and debris N87-23479
Thermal inertia characteristics of the Martian crater Curie N87-23509
Dome craters on Ganymede N87-23510
Ejecta types on Ganymede and Callisto N87-23512
Shatter cones in Illinois: Evidence for metoeritic impacts at Glasford and Des Plaines N87-23513
Observations of industrial sulfur flows and implications for Io N87-23541
Geology of Io N87-23542
The Mars observer camera N87-23556

ARIZONA UNIV., TUCSON.
Advanced probabilistic method of development N87-22788
Laser spectroscopy of transient molecules important in explosions
[AD-A178456] N87-22828
The cratering record at Uranus: Implications for satellite evolution and the origin of impacting objects N87-23342
Crater morphology and morphometry on the Uranian satellites N87-23343
Mechanical and thermal properties of planetologically important ices N87-23346
Observational studies of Saturn's rings N87-23362
The origin of polarity asymmetries in the history of the geomagnetic field N87-23401
Magnetic flares in the protoplanetary nebula and the origin of meteorite chondrules N87-23402
Generation of a dynamo magnetic field in a protoplanetary accretion disk N87-23403
The steady state toroidal magnetic field at the core-mantle boundary N87-23404
Fluvial valleys on Martian volcanoes N87-23462
Valley development on Hawaiian volcanoes N87-23463
Revision of the Martian relative age chronology N87-23504

ARMY ARMAMENT RESEARCH AND DEVELOPMENT COMMAND, DOVER, N. J.
Methodology for verification of ultrasonic inspection
[AD-A179694] N87-22988

ARMY ARMAMENT RESEARCH AND DEVELOPMENT COMMAND, WATERVLIET, N. Y.
Superconducting Augmented Rail Gun (SARG)
[AD-A179269] N87-22701

ARMY AVIATION RESEARCH AND DEVELOPMENT COMMAND, MOFFETT FIELD, CALIF.
Correlation of analytical calculations from GRASP (General Rotorcraft Aeromechanical Stability Program) with torsionally-soft rotor data
[AD-A178881] N87-22689
Prediction of high-speed rotor noise with a Kirchhoff formula
[AD-A178982] N87-23250

ARMY AVIATION SYSTEMS COMMAND, MOFFETT FIELD, CALIF.
Frequency-response identification of XV-15 tilt-rotor aircraft dynamics
[NASA-TM-89428] N87-22690
Digital control of highly augmented combat rotorcraft
[NASA-TM-88346] N87-22691

ARMY AVIATION SYSTEMS COMMAND, ST. LOUIS, MO.
Analysis of structures with rotating, flexible substructures
[AD-A178903] N87-23004

ARMY AVIONICS RESEARCH AND DEVELOPMENT ACTIVITY, FORT MONMOUTH, N. J.
The impact of future avionics technology on the conduct of air warfare N87-22673

ARMY COLD REGIONS RESEARCH AND ENGINEERING LAB., HANOVER, N. H.
An evaluation of the polar ice prediction system
[AD-A178522] N87-23014

ARMY MILITARY PERSONNEL CENTER, ALEXANDRIA, VA.
Prediction of fluid flow in curved pipe using the finite element method
[AD-A179538] N87-22926

ARMY RESEARCH INST. OF ENVIRONMENTAL MEDICINE, NATICK, MASS.
Relationship between a two mile run and maximal oxygen uptake
[AD-A179343] N87-23109

ARNOLD ENGINEERING DEVELOPMENT CENTER, ARNOLD AIR FORCE STATION, TENN.
Interaction of a three-dimensional roughness element with a laminar boundary layer
[AD-A178668] N87-22941

ATLANTA UNIV., GA.
Investigation of perturbation techniques for nonlinear difference equations and other related topics
[DE87-006663] N87-23211

ATMOSPHERE FURNACE CO., WIXOM, PA.
Austempered ductile iron process development
[PB87-169843] N87-22866

ATOMIC WEAPONS RESEARCH ESTABLISHMENT, ALDERMASTON (ENGLAND).
Body wave magnitudes and locations of French underground explosions at the Mururoa test site
[BR-97934] N87-22947

AUBURN UNIV., ALA.
Space Station/Shuttle Orbiter dynamics during docking N87-22708
Improving stability margins in discrete-time log controllers N87-22719

A new approach for vibration control in large space structures N87-22743

AVCO-EVERETT RESEARCH LAB., MASS.
Magnetically insulated opening switch research
[AD-A178695] N87-22918

B

BALLISTIC RESEARCH LABS., ABERDEEN PROVING GROUND, MD.
Numerical simulation of supersonic flow over a rotating band using flowfield blanking
[AD-A178492] N87-22624
Axisymmetric inviscid shock tube flow simulation
[AD-A178494] N87-22937

BATTELLE COLUMBUS LABS., OHIO.
Studies and analyses of the space shuttle main engine: High-pressure oxidizer turbopump failure information propagation model
[NASA-CR-179079] N87-22765
Probabilistic load model development and validation for composite load spectra for select space propulsion engines N87-22794

BEDFORD RESEARCH ASSOCIATES, MASS.
Investigate and verify the validity of mathematical formulas and procedures in relation to data obtained from theoretical investigations and experimental observations
[AD-A179564] N87-23057

BELL TELEPHONE LABS., INC., HOLMDEL, N. J.
Workshop report on New Directions in X-ray Scattering
[DE87-006305] N87-23262

BERN UNIV. (SWITZERLAND).
Mesoscale analyses of temperature, pressure and wind fields over Switzerland: A case study of a Foehn N87-23086

BOEING AEROSPACE CO., SEATTLE, WASH.
Flexible spacecraft simulator N87-22718
Precision pointing and control of flexible spacecraft N87-22723
Dynamics of trusses having nonlinear joints N87-22724
Equivalent beam modeling using numerical reduction techniques N87-22725
High speed simulation of flexible multibody dynamics N87-22738
Experimental characterization of deployable trusses and joints N87-22749
XAS (X-ray Absorption Spectroscopy) of gas phase metal-containing chemical systems
[AD-A179391] N87-22821
Centrifuge impact cratering experiments: Scaling laws for non-porous targets N87-23495
Centrifuge impact cratering experiments: Scaling laws for non-porous targets N87-23498

BOSTON UNIV., MASS.
Workshop Symposium on Neural Models of Sensory-Motor Control
[AD-A179501] N87-23111

BRIGHAM YOUNG UNIV., PROVO, UTAH.
Volatile reservoirs below the surface of the Elysium region of Mars: Geomorphic evidence N87-23467

BRITISH AEROSPACE PUBLIC LTD. CO., KINGSTON-UPON-THAMES (ENGLAND).
Evolution of combat performance of the Hawk light combat aircraft N87-22668
British Aerospace: A Kingston perspective
[ETN-87-99823] N87-23308

BRITISH AEROSPACE PUBLIC LTD. CO., LANCASHIRE (ENGLAND).
The assessment and evaluation of combat performance improvements N87-22675

BRITISH AEROSPACE PUBLIC LTD. CO., PRESTON (ENGLAND).
Improved combat performance using relaxed static stability and a spin prevention system (FBW Jaguar) N87-22674

BROWN UNIV., PROVIDENCE, R. I.
Dynamic fracture under plane wave loading
[AD-A178594] N87-23001
Analytical characterization of shear localization in thermoviscoplastic materials
[AD-A178597] N87-23002
Source of the optical red-slope in iron-rich meteorites N87-23374
Deconvolution of spectra for intimate mixtures N87-23428
Impacts of hemispherical granular targets: Implications for global impacts N87-23490
Impact vaporization: Late time phenomena from experiments N87-23491
Momentum transfer from oblique impacts N87-23493
Experimental evidence for non-proportional growth of large craters N87-23497
Early changes in gradation styles and rates on Mars N87-23505
Crater ejecta morphology and the presence of water on Mars N87-23508
Bilateral symmetry across Aphrodite Terra N87-23518
Local-scale stratigraphy of grooved terrain on Ganymede N87-23538

C

CALIFORNIA INST. OF TECH., PASADENA.
Vibration suppression by stiffness control N87-22730
Measurement of the J integral with caustics: An experimental and numerical investigation
[AD-A177273] N87-22990

CALIFORNIA STATE POLYTECHNIC UNIV., POMONA.
Natural fracture systems on planetary surfaces: Genetic classification and pattern randomness N87-23536

CALIFORNIA UNIV., BERKELEY.
The role of particle substructure in the sintering of monosized titania
[DE87-007600] N87-22839
An investigation of zinc electrodes relevant to zinc-air batteries
[DE87-007607] N87-22908
An experimental study of load balancing performance
[AD-A179322] N87-23195
Double layers above the aurora N87-23331
Experiments pertaining to the formation and equilibration of planetary cores N87-23397
Lunar magnetization concentrations (MAGCONS) antipodal to young large impact basins N87-23405
A preliminary summary of the observations of the 16 February 1984 solar flare (STIP Interval XV, 12-21 February 1984)
[NASA-CR-180929] N87-23563
X-ray and low energy gamma-ray observations of the 16 February 1984 solar flare
[NASA-CR-180928] N87-23564

CALIFORNIA UNIV., BERKELEY. LAWRENCE BERKELEY LAB.
Workshop report on New Directions in X-ray Scattering
[DE87-006305] N87-23262
Materials Information for Science and Technology (MIST). Project overview: Phase 1 and 2 and general considerations
[DE87-006799] N87-23312

CALIFORNIA UNIV., DAVIS.
Superplasticity: A fundamental investigation on deformation mechanism and cavitation phenomena
[AD-A179651] N87-22834
Conditional second order closure for turbulent shear flows
[AD-A179661] N87-22931

CALIFORNIA UNIV., IRVINE.
Detection of 10^{14}-eV gamma rays from Cygnus X-3 during 1986
[DE87-006054] N87-23568

CALIFORNIA UNIV., LOS ANGELES.
Ferroelectric optically controlled millimeter-wave devices
[AD-A179524] N87-22901
Numerical experiments on the atmospheric response to a sea surface temperature anomaly over the equatorial eastern Pacific Ocean N87-23036
Investigations of the surfaces and interiors of outer planet satellites N87-23356
Analysis of planetary evolution with emphasis on differentiation and dynamics N87-23382
High pressure cosmochemistry of major planetary interiors: Laboratory studies of the water-rich region of the system ammonia-water N87-23396

CALIFORNIA UNIV., SANTA BARBARA.
Could Ariel have been heated by tidal friction? N87-23347
On the lack of commensurabilities in the mean motions of the satellites of Uranus and the resurfacing of Ariel N87-23349
Why no orbital resonances among the satellites of Uranus? N87-23351
The production of braids in Saturn's F ring N87-23363
Timescales for planetary accretion and the structure of the protoplanetary disk N87-23380
Orbital resonances, unusual configurations and exotic rotation states among planetary satellites N87-23391

CALIFORNIA UNIV., SANTA CRUZ.
Numerical studies of collapsing interstellar clouds
[NASA-CR-180933] N87-23340
Experimental studies on the impact properties of water ice N87-23364

CALSPAN-BUFFALO UNIV. RESEARCH CENTER, N.Y.
Experimental and theoretical studies of time-averaged and time resolved rotor heat transfer N87-22770

CAMBRIDGE UNIV. (ENGLAND).
Residual stresses in girth butt welded pipes: Results and implications
[CUED/D-STRUCT/TR.109] N87-22992

CANADIAN CLIMATE CENTRE, DOWNSVIEW (ONTARIO).
Simulated and observed budgets and balances during the 82/83 ENSO event N87-23035
An extended forecast experiment with the CCC GCM N87-23050

CARNEGIE INSTITUTION OF WASHINGTON, D. C.
Accumulation of the planets N87-23378

CARNEGIE-MELLON UNIV., PITTSBURGH, PA.
Effect of hydrogen on deformation structure and properties of CMSX-2 nickel-base single-crystal superalloy N87-22782
Summary of the SEI (Software Engineering Institute) Workshop on Softwear Configuration Management
[AD-A178770] N87-23184
The heterogeneous machine simulator
[AD-A178771] N87-23185
Specifying functional and timing behavior for real-time applications
[AD-A178769] N87-23206

CASE WESTERN RESERVE UNIV., CLEVELAND, OHIO.
Numerical study of the effects of boundary conditions on the measurement and calibration of gardon type heat flux sensors N87-22775
A new formulation of mean stress effects in fatigue N87-22778
Thermocapillary bubble migration for large Marangoni Numbers
[NASA-CR-179628] N87-22865

CATHOLIC UNIV. OF AMERICA, WASHINGTON, D.C.
On non-parametric discrimination using series expansions and projection pursuit
[AD-A178455] N87-23213
Phase space methods and path integration: A microscopic approach to direct and inverse wave propagation
[AD-A178557] N87-23249

CENTRE NATIONAL D'ETUDES DES TELECOMMUNICATIONS, ISSY-LES-MOULINEAUX (FRANCE).
Current driven weak double layers N87-23322

CENTRE NATIONAL DE RECHERCHES METEOROLOGIQUES, TOULOUSE (FRANCE).
A contribution to Bora studies using Alpine Experiment (ALPEX) aircraft data N87-23080
Numerical study of the Mistral with a mesoscale model N87-23082

CERAMATEC, INC., SALT LAKE CITY, UTAH.
Thermoelectric conversion with ion conductors
[AD-A179353] N87-23019

CHICAGO UNIV., ILL.
Fundamentals and techniques of nonimaging optics research at the University of Chicago
[DE87-006917] N87-23264

CINCINNATI UNIV., OHIO.
Erosion study of AM355 and Al2O3 ceramics
[AD-A178882] N87-22858
Composite velocity procedures for flows with pressure interaction
[AD-A179602] N87-22929

CITY COLL. OF THE CITY UNIV. OF NEW YORK.
Optical acquisition, image and data compression
[AD-A178508] N87-23154

COASTAL ENGINEERING RESEARCH CENTER, VICKSBURG, MISS.
A wind- and wave-driven nearshore current model, the one-dimensional model
[AD-A178751] N87-23105

COCKPIT MANAGEMENT RESOURCES, INC.
Cockpit management and Specific Behavioral Objectives (SBOs) N87-22640

COLORADO STATE UNIV., FORT COLLINS.
The effect of overburden thickness on tension fracture patterns above an uplifting dome N87-23535

COLORADO UNIV., BOULDER.
High performance polymers: Matrix resins, high strength polyquinoxalines and conducting polyaromatics
[AD-A178457] N87-22854
Frontal interaction with orography N87-23071
Dynamics and evolution of the Pyrenees lee wave event during 21-23 March 1982 N87-23079
An analysis of downslope winds in the lee of the Pyrenees on 23 March 1982 N87-23081
Parallel branch and bound on an MIMD (Multiple Instruction Stream, Multiple Data stream) system
[AD-A178816] N87-23200
The generation of electrostatic noise in the plasma sheet boundary layer
[ATR-86(8433)-4] N87-23282

A diffuse radar scattering model from Martian surface rocks N87-23445

COMBAT CREW TRAINING WING (1550TH), KIRTLAND AFB, N. MEX.

Cockpit Resource Management (CRM) training in the 1550th combat crew training wing N87-22650

COMPUTATIONAL MECHANICS CONSULTANTS, AUSTIN, TEX.

Vectorizable algorithms for adaptive schemes for rapid analysis of SSME flows
[NASA-CR-179082] N87-22764

COMPUTER SCIENCES CORP., HAMPTON, VA.

Description of an aeronautical geometry conversion package: Wave-drag to Langley Wireframe Geometry Standard (LaWGS) to Supersonic Implicit Marching Potential (SIMP)
[NASA-CR-178299] N87-23194

COMPUTER SCIENCES CORP., MOUNTAIN VIEW, CALIF.

The 2GCHAS: A high productivity software development environment N87-23162

CONSIGLIO NAZIONALE DELLE RICERCHE, BOLOGNA (ITALY).

Analysis of stably stratified atmospheric flow over the Dinaric Alps during the Alpine Experiment (ALPEX) N87-23078

CONTINENTAL AIRLINES, INC., LOS ANGELES, CALIF.

Crew coordination concepts: Continental Airlines CRM training N87-22642

CONTROL DYNAMICS CO., HUNTSVILLE, ALA.

One Controller at a Time (1-CAT): A mimo design methodology N87-22715

CORNELL UNIV., ITHACA, N.Y.

Experimental and theoretical studies of the structure of grain boundaries
[DE87-007560] N87-22838

Voyager observations of 1985U1 N87-23352

Shapes of small satellites N87-23354

Investigations of planetary ring phenomena N87-23360

Dynamics of satellites, asteroids, and rings N87-23392

Dynamical studies of Saturn's rings N87-23395

Melting of troilite at high pressure in a diamond cell by laser heating N87-23398

Implications of convection in the Moon and the terrestrial planets N87-23406

Investigation of Martian H2O and CO2 via gamma-ray spectroscopy N87-23420

Photometric properties of lunar terrains derived from Hapke's equation N87-23432

Io: Comparison of photometric scans produced by the Minnaert and Hapke functions N87-23436

Timing of frost deposition on Martian dunes: A clue to properties of dune particles? N87-23453

CORNELL UNIV., NEW YORK, N.Y.

Fundamental studies in the molecular basis of laser induced retinal damage
[AD-A178453] N87-23115

CRM CO.

Cockpit Resource Management (CRM): A tool for improved flight safety (United Airlines CRM training) N87-22637

D

DARTMOUTH COLL., HANOVER, N.H.

Electron acceleration in stochastic double layers N87-23324

Weak double layers in the auroral ionosphere N87-23326

DAYTON UNIV., OHIO.

Bodner-Partom viscoplastic model in STEALTH finite difference code
[AD-A178994] N87-23005

Asymmetries in the control of saccadic eye movements to bifurcating targets
[AD-A179270] N87-23108

DEPARTMENT OF DEFENSE, FORT MEADE, MD.

Parallel graph reduction on a supercomputer
[DE87-006066] N87-23173

DEPARTMENT OF ENERGY, MORGANTOWN, W. VA.

Proceedings of the Instrumentation, Components, and Materials Contractors Meeting
[DE86-006596] N87-22954

DEPARTMENT OF ENERGY, WASHINGTON, D. C.

Lithium disulfide battery
[DE87-007183] N87-22892

Bipolar battery with array of sealed cells
[DE87-007194] N87-22893

DEPARTMENT OF HEALTH, EDUCATION, AND WELFARE, WASHINGTON, D.C.

Cross-axis synchronous flow-through coil planet centrifuge free of rotary seals: Apparatus and method for performing countercurrent chromatography
[PB87-126926] N87-22816

DEUTSCHE FORSCHUNGS- UND VERSUCHSANSTALT FUER LUFT- UND RAUMFAHRT, OBERPFAFFENHOFEN (WEST GERMANY).

On the diagnosis of a cold front observed during Alpine Experiment (ALPEX) N87-23072

DEUTSCHE FORSCHUNGS- UND VERSUCHSANSTALT FUER LUFT- UND RAUMFAHRT, WESSELING (WEST GERMANY).

Fine structure of the atmospheric boundary layer across the Alps during a high pressure period in the Alpine Experiment (ALPEX). A case study on April 22, 1982 N87-23087

DOKKYO UNIV., SAITAMA (JAPAN).

On the least favorable configuration of a selection procedure based on ranks
[AD-A178454] N87-23234

DYNACS ENGINEERING CO., INC., CLEARWATER, FLA.

Notes on implementation of Coulomb friction in coupled dynamical simulations N87-22746

E

EDGERTON, GERMESHAUSEN AND GRIER, INC., IDAHO FALLS, IDAHO.

Determination of crack initiation sites using a digital NDE workstation
[DE87-001444] N87-22997

An assessment of nitrogen oxide formation in preheated high-temperature combustion air in industrial processes
[EGG-2439] N87-23031

EIC, INC., NORWOOD, MASS.

Development of nickel oxide/hydrogen multilayer bipolar battery for pulsed power
[AD-A178844] N87-22917

EIDGENOESSISCHE TECHNISCHE HOCHSCHULE, ZURICH (SWITZERLAND).

Diagnostic studies of meso-alpha scale flow on the Alpine northside N87-23070

Valley circulations as measured in the Himalaya by instrumented motor glider N87-23077

Lagrangian turbulence measurements with constant density balloons N87-23090

ELECTRONICS RESEARCH LAB., ADELAIDE (AUSTRALIA).

Design of generalised Chebyshev suspended substrate stripline filters
[AD-A178505] N87-22910

ENERGY RESEARCH CORP., DANBURY, CONN.

Development of advanced nickel-cadmium batteries for electric vehicle propulsion
[DOE/NV/10442-1] N87-22922

ENGINEERING MECHANICS ASSOCIATION, INC., TORRANCE, CALIF.

A computer program for model verification of dynamic systems N87-22710

ENTECH CORP., DALLAS-FORT WORTH AIRPORT, TEX.

Evaluation of a heliostat tracker for linear Fresnel lens photovoltaic concentrators
[DE87-006331] N87-23025

EOTEC CORP., WEST HAVEN, CONN.

Development of radiation hard graded index optical fibers
[AD-A178465] N87-23265

EROS DATA CENTER, SIOUX FALLS, S. DAK.

A design for a new catalog manager and associated file management for the Land Analysis System (LAS) N87-23159

Development of Land Analysis System display modules N87-23169

ESSEX CORP., ORLANDO, FLA.

Investigation into the use of normal and half-normal plots for interpreting results from screening experiments
[AD-A179082] N87-23231

EUROPEAN CENTRE FOR MEDIUM-RANGE WEATHER FORECASTS, READING (ENGLAND).

The impact of initial conditions and SST Anomalies on extended range predictions for the El Nino period N87-23046

A lagged-average 60-day forecast experiment during the 1982-83 El Nino period N87-23047

F

FEDERAL AVIATION ADMINISTRATION, WASHINGTON, D.C.

The regulatory horizon N87-22654

Integrated FAA Wind Shear Program plan
[DOT/FAA/DL-87/1] N87-23067

FEDERAL AVIATION AGENCY, ATLANTIC CITY, N.J.

Statistics on aircraft gas turbine engine rotor failures that occurred in US commercial aviation during 1981
[DOT/FAA/CT-86/42] N87-22684

Laboratory characterization tests for antimisting fuel
[DOT/FAA/CT-86/23] N87-22864

FLIGHT SAFETY INTERNATIONAL, INC., LAGUARDIA AIRPORT, N.Y.

Cockpit Resource Management (CRM) for FAR Parts 91 and 135 operators N87-22653

FLORIDA UNIV., GAINESVILLE.

Control of linear systems over commutative normed algebras with applications
[AD-A178765] N87-23205

FLOW RESEARCH, INC., KENT, WASH.

Direct numerical simulations of an unpremixed turbulent jet flame
[AD-A179358] N87-22819

FRENCH AIR FORCE, PARIS.

Weapon systems polyvalence: An economic and operational challenge N87-22667

G

GENERAL ELECTRIC CO., CINCINNATI, OHIO.

Structural analysis demonstration of constitutive and life models N87-22780

GENERAL ELECTRIC CO., PHILADELPHIA, PA.

Impact of space station appendage vibrations on the pointing performance of gimballed payloads N87-22733

GENERAL ELECTRIC CO., SCHENECTADY, N.Y.

An improved set of Auger data analysis programs for physical electronics Auger spectrometer systems
[DOE/TIC-4500] N87-22957

Wielandt iteration as applied to the nodal expansion method
[KAPL-4194] N87-23227

GEOLOGICAL SURVEY, DENVER, COLO.

Studies of the scattering/absorption of minerals N87-23423

GEOLOGICAL SURVEY, FLAGSTAFF, ARIZ.

Orbital dynamics of the Uranian satellites based on Voyager data N87-23350

Observations on the magnitude-frequency distribution of Earth-crossing asteroids N87-23369

Global petrologic variations of the Moon: A ternary-diagram approach N87-23407

A compilation system for Venus radar mission (Magellan) N87-23440

Eolian saltation on Mars N87-23455

Water and ice on Mars: Evidence from Valles Marineris N87-23469

Eruptive history of the Elysium Volcanic Province of Mars N87-23475

Late-stage flood lavas in the Elysium region, Mars N87-23476

Computer simulations of 10-km-diameter asteroid impacts into oceanic and continental sites: Preliminary results on atmospheric passage, cratering and ejecta dynamics N87-23489

Crater production on Venus and Earth by asteroid and comet impact N87-23500

The surface age of Venus: Applying the terrestrial cratering rate N87-23501

Comments on the tectonism of Venus N87-23515

History and morphology of faulting in the Noctis Labyrinthus-Claritas Fossae Region of Mars N87-23528

The Galilean satellite geological mapping program, 1986 N87-23544

Cartography of irregularly shaped satellites N87-23545

Voyager cartography N87-23546

Aspects of Voyager photogrammetry N87-23547

Progress in compilation of the 1:2,000,000-scale topographic map N87-23548

Mars digital terrain model N87-23549

Digital cartography of Mars N87-23550

Martian terrains N87-23555

Planetary nomenclature N87-23557

Enhanced LANDSAT images of Antarctica and planetary exploration N87-23558

GEOLOGICAL SURVEY, MENLO PARK, CALIF.

Landform identification: Lunar radar images N87-23443

The 1984 Mauna Loa eruption and planetary geolgoy N87-23481

GEORGE MASON UNIV., FAIRFAX, VA.

Detection of 10^{14}-eV gamma rays from Cygnus X-3 during 1986
[DE87-006054] N87-23568

GEORGIA INST. OF TECH., ATLANTA.
Analysis of structures with rotating, flexible substructures applied to rotorcraft aeroelasticity in GRASP (General Rotorcraft Aeromechanical Stability Program)
[AD-A178941] N87-22677
Deformation and fatigue behavior of SSME turbopump blade materials N87-22776
Stochastic and hybrid-stress plate/shell finite elements for hot-section components N87-22789
Nonisothermal elasto-visco-plastic response of shell-type structures N87-22796
Signatures from in-situ light scattering of non-homogeneous non-spherical particles
[AD-A178761] N87-23269

GILTSPUR PACKAGING LTD., TOTTON (ENGLAND).
Accelerations experienced by packaged material during fork lift truck handling
[RDI-284/45/3] N87-22969

GLOBAL IMAGING, INC., SOLANA BEACH, CALIF.
Naval applications of a TAE-derived executive N87-23167

GRUMMAN AEROSPACE CORP., BETHPAGE, N.Y.
Thermal expansion of epoxy-fiberglass composite specimens
[DE87-004273] N87-22812

GTE LABS., INC., WALTHAM, MASS.
Radiation hardened silica-based optical fibers
[AD-A178466] N87-23266

H

HAMBURG UNIV. (WEST GERMANY).
Preliminary results from a Tropical Ocean Global Atmosphere (TOGA) related experiment performed at Hamburg (West Germany) with the ECWME General Circulation Model (GCM) with T21 resolution N87-23040

HARRIS CORP., MELBOURNE, FLA.
Maximum Entropy/Optimal Projection (MEOP) control design synthesis: Optimal quantification of the major design tradeoffs N87-22741

HARRY DIAMOND LABS., ADELPHI, MD.
Angular momentum theory applied to interactions in solids
[AD-A179366] N87-23289

HARVARD UNIV., CAMBRIDGE, MASS.
Group-level issues in the design and training of cockpit crews N87-22636

HAWAII INST. OF GEOPHYSICS, HONOLULU.
SO2 on Io: A thermodynamic perspective N87-23359
Temperatures and minimum thickness of the inactive surface layer of comet Halley N87-23365
The loss and depth of CO2 ice in comet nuclei N87-23367
The 1986 DA and 1986 EB: M-class asteroids in near-Earth orbits N87-23371
The role of regolith adsorption in the transition from early to late Mars climate N87-23411
CO2: Adsorption on palagonite and the Martian regolith N87-23419
Reflectance spectra of mafic silicates and phyllosilicates from .6 to 4.6 microns N87-23421
Spectral effects of dehydration on phyllosilicates N87-23422
Preliminary results of spectral reflectance studies of tycho crater N87-23430
Preliminary results of geologic and remote sensing studies of Rima Mozart N87-23431
New very high resolution radar studies of the Moon N87-23441
Possible origin of some channels on Alba Patera, Mars N87-23465
Long, paired A'A/Pahoehoe flows of Mauna Loa: Volcanological significance and insights they provide into volcano plumbing systems N87-23480
Studies of vesicle distribution patterns in Hawaiian lavas N87-23484
Martian rampart craters: Morphologic clues for the physical state of the target at time of impact N87-23507

HERZBERG INST. OF ASTROPHYSICS, OTTAWA (ONTARIO).
Observations of solar flux at the Algonquin Radio Observatory on 2800 MHz and the Dominion Radio Astrophysical Observatory on 2700 MHz
[ARO-15] N87-23566
East-west solar scans at 10-cm wavelength taken at the Algonquin Radio Observatory, Jan. 1980 to December 1985
[ARO-16] N87-23567

HONEYWELL, INC., BLOOMINGTON, MINN.
Optical symbolic processor for expert system execution
[AD-A179375] N87-23172

HOUSTON UNIV., TEX.
A statistical study of Mercurian crater classes applied to the emplacement of the intercrater plains N87-23502

HUGHES AIRCRAFT CO., EL SEGUNDO, CALIF.
Development of a holographic beamsplitter for use with a conventional Fresnel lens
[DE87-006770] N87-23263

HUGHES RESEARCH LABS., MALIBU, CALIF.
Nonlinear optical properties and subpicosecond dynamics of excitons and electron-hole plasmas in multiple quantum well structures
[AD-A179124] N87-23287

HUMAN ENGINEERING LABS., ABERDEEN PROVING GROUND, MD.
Human factors engineering data management handbook
[AD-A179691] N87-23144

I

ILLINOIS UNIV., CHAMPAIGN.
The event related brain potential as an index of information processing and cognitive activity: A program of basic research
[AD-A179310] N87-23143

ILLINOIS UNIV., URBANA.
Laser cladding of Mg and Nb alloys for improved environmental resistance
[AD-A179606] N87-22833
Full-wave analysis of isolated and coupled microwave transmission lines using the finite element method
[AD-A178605] N87-22883
Differential-algebraic equation index transformations
[DE87-005543] N87-23209
A method for the spatial discretization of parabolic equations in one space variable
[DE87-005991] N87-23210
Opening switch research on a dense plasma focus
[AD-A179693] N87-23276

IMPERIAL COLL. OF SCIENCE AND TECHNOLOGY, LONDON (ENGLAND).
Rationalizing VICAR within a TAE framework: Some problems and some solutions N87-23165

INDUSTRIEANLAGEN-BETRIEBSGESELLSCHAFT M.B.H., OTTOBRUNN (WEST GERMANY).
Performance improvement of airborne weapon systems methods, scope and limitations N87-22665

INNSBRUCK UNIV. (AUSTRIA).
An elementary valley wind model N87-23075

INSTITUT NATIONAL DE RECHERCHE D'INFORMATIQUE ET D'AUTOMATIQUE, VALBONNE (FRANCE).
On the use of adaptive moving grid methods in combustion problems
[DE87-003715] N87-22824

INSTITUTE OF METEOROLOGY AND WATER MANAGEMENT, KRAKOW (POLAND).
The effect of the Tatra Mountains (Poland) on the atmospheric precipitation and air humidity during the northern and southern air flow N87-23094

INSTITUTE OF METEOROLOGY AND WATER MANAGEMENT, ZAKOPANE (POLAND).
The influence of orography on the temperature and wind regime in the mountains N87-23085

INTERNATIONAL AIR TRANSPORT ASSOCIATION, MONTREAL (QUEBEC).
Cockpit resource management training N87-22647

INTERNATIONAL ATOMIC ENERGY AGENCY, VIENNA (AUSTRIA).
Direct-drive laser-fusion in the US
[DE87-005916] N87-23279

INTERNATIONAL CENTRE FOR THEORETICAL PHYSICS, TRIESTE (ITALY).
Perturbative and global anomalies in supergravity theories
[DE87-701562] N87-23059
Oscillatory behaviour of solutions of first-order ordinary and delay differential equations
[DE87-701552] N87-23212
Orbital removal method for the neutral vacancy in semiconductors
[DE87-701537] N87-23300
Generalized quantal equation of motion
[DE87-701531] N87-23307
Possible inflationary solution to the short distance gravity model
[DE87-701559] N87-23339

INTERNATIONAL COUNCIL OF SCIENTIFIC UNIONS, ROME (ITALY).
Workshop on Comparison of Simulations by Numerical Models of the Sensitivity of the Atmospheric Circulation to Sea Surface Temperature Anomalies
[WCP-121] N87-23034
Proceedings of the Conference on the Scientific Results of the Alpine Experiment (ALPEX), volume 2
[WMO-TD-108-VOL-2] N87-23068

INTERNATIONAL FEDERATION OF AIR LINE PILOT ASSOCIATIONS, EGHAM (ENGLAND).
Remedial training: Will CRM work for everyone N87-22646

IOWA STATE UNIV. OF SCIENCE AND TECHNOLOGY, AMES.
A three-dimensional dual potential procedure with applications to wind tunnel inlets and interacting boundary layers
[NASA-CR-180939] N87-22944

IOWA UNIV., IOWA CITY.
Latitudinal motions of the aurora during substorms
[NASA-CR-180930] N87-23063
Some dynamical properties of very strong double layers in a triple plasma device N87-23315
A new hydrodynamic analysis of double layers N87-23319

ITALIAN AIR STAFF, ROME.
Some development trends in light ground attack aircraft N87-22668

J

JACKSON STATE UNIV., MISS.
The autoignition of isobutane in a knocking spark ignition engine
[DE87-003241] N87-22823

JAPAN AIR LINES CO. LTD., TOKYO.
Optimum culture in the cockpit N87-22643

JAYCOR, VIENNA, VA.
The use of the Karl sub-scale laser for Raman beam clean-up experiments
[AD-A178463] N87-22971

JET PROPULSION LAB., CALIFORNIA INST. OF TECH., PASADENA.
Verification of large beam-type space structures N87-22712
Verification of flexible structures by ground test N87-22713
Structural dynamics system model reduction N87-22727
Modeling of controlled flexible structures with impulsive loads N87-22745
On the control of structures by applied thermal gradients N87-22747
The evaluation and extension of TAE in the development of a user interface management system N87-23158
A laboratory investigation of potential double layers N87-23317
Failure strength of icy lithospheres N87-23357
Comet thermal modeling N87-23366
Dynamics of long period comets N87-23368
Asteroid families, dynamics and astrometry N87-23370
Asteroid lightcurve inversion N87-23377
Lunar science from lunar laser ranging N87-23389
Gravity data analysis N87-23400
Bidirectional reflectance properties of planetary surface materials N87-23426
Sulfur-oxygen processes on Io N87-23437
Solid sulfur in vacuum: Sublimation effects on surface microtexture, color and spectral reflectance, and applications to planetary surfaces N87-23438
High resolution radar map of the Moon N87-23442
Goldstone radar observations of Mars: The 1986 opposition N87-23444
Mars: Seasonally variable radar reflectivity N87-23446
Measurements of the dielectric constants for planetary volatiles N87-23447
Geomorphic evidence for ancient seas in west Deuteronilus Mensae, Mars-1: Regional geomorphology N87-23471
Geomorphic evidence for ancient seas in west Deuteronilus Mensae, Mars-2: From very high resolution Viking Orbiter images N87-23472
Relative ages of lava flows at Alba Patera, Mars N87-23477
Calculated viscosity-distance dependence for some actively flowing lavas N87-23482
Toward a model for leveed lava flows N87-23483
Lithospheric structure on Venus from tectonic modelling of compressional features N87-23516
Physiographic constraints on the origin of lunar wrinkle ridges N87-23521
Curvilinear ridges and related features in southwest Cydonia Mensae, Mars N87-23537
Large scale topography of Io N87-23543

JOHNS HOPKINS UNIV., BALTIMORE, MD.
Investigation of the icosahedral Z-phase in aluminium transition metal alloys and rapidly solidified Al-alloys
[AD-A178451] N87-22840

The delineation and interpretation of the Earth's gravity field
[NASA-CR-181015] N87-23065

Convergence of relaxation algorithms by averaging
[AD-A178784] N87-23219

JOINT PUBLICATIONS RESEARCH SERVICE, ARLINGTON, VA.

USSR Report: Space Biology and Aerospace Medicine, Volume 20, No. 5, September - October 1986
[JPRS-USB-86-007] N87-23120

Problems and feasibility of drug correction of orthostatic tolerance in space medicine N87-23121

Structure and function of otoliths N87-23122

Investigation of hemostasis system in air traffic controllers as related to different air traffic conditions
N87-23123

Tolerance to frustration as a factor in operator performance N87-23124

Effect of short-term spaceflights on activity of renin-angiotension-aldosterone system, concentration of cyclic nucleotides and prostaglandins in blood
N87-23125

Nutritional correction of histamine and serotonin levels as related to exposure to hypokinesia and neuro-emotional stress N87-23126

Some parameters of human lipid metabolism during antiorthostatic hypokinesia and their correction
N87-23127

Split circadian rhythm of simian body temperature during antiorthostatic hypokinesia N87-23128

Effect of hypokinesia on intensity of gluconeogenesis in cortical layer of rat kidney N87-23129

Cortical ultrastructure of rat cerebellar nodulus following flight aboard Cosmos-1514 biosatellite N87-23130

Chemical sensitivity of medial vestibular nuclear neurons to enkephalins, acetylcholine, GABA and L-glutamate
N87-23131

Pharmacological correction of central nervous system functio during exposure to coriolis accelerations
N87-23132

Reaction to vibration of rat kinesthetic analyzer neurocytes N87-23133

Evaluation of effect of positive intrapulmonary pressure on respiratory function of man N87-23134

Evaluation of skeletomuscular system function in self-contained life-support system on the basis of blood biochemistry N87-23135

Investigation of causes of hydrogen sulfide formation in reclaimed water N87-23136

Experimental investigation of the process of CO2-CO-H2O-H2-N2 gas mixture breakdown in electrolysis cell with solid electrolyte N87-23137

Distinctions in formation of microbial complex in nutrient solutions of higher plants after use of straw mineralization products N87-23138

Hormonal and metabolic status of man in the extreme north N87-23139

Human blood serum proteolytic enzyme activity after stay in hypoxic environment N87-23140

Some biochemical and morphological changes in rat blood with exposure to variable magnetic field at infralow frequency N87-23141

Biochemical aspects of some neurohumoral system functions during long-term antiorthostatic hypokinesia
N87-23142

JOINT TECHNICAL COORDINATING GROUP FOR AIRCRAFT SURVIVABILITY, WASHINGTON, D.C.

Hybrid composite response to hydraulic ram
[AD-A178750] N87-22815

K

KARLSRUHE UNIV. (WEST GERMANY).

Synoptic-scale influence on the variability of the Alpine Experiment (ALPEX) low-level jet N87-23089

KMI, INC., ALBUQUERQUE, N. MEX.

Extrinsic gettering for VLSI/ULSI processes
[DE87-002696] N87-22903

L

LABORATOIRE DE METEOROLOGIE DYNAMIQUE, PARIS (FRANCE).

Sensitivity of January 1983 Sea Surface Temperature (SST)-experiments to the formulation of lateral diffusion
N87-23052

LAMONT-DOHERTY GEOLOGICAL OBSERVATORY, PALISADES, N.Y.

Modelling and forecasting El Nino N87-23053

LAWRENCE LIVERMORE NATIONAL LAB., CALIF.

Toward the year 2000: The near future of the American civilian and military space programs
[DE87-006467] N87-22697

The autoignition of isobutane in a knocking spark ignition engine
[DE87-003241] N87-22823

Silicon pulse sharpening diodes: Switching kilovolts in 10's of picoseconds
[DE87-005073] N87-22905

Design and operation of 140 GHz gyrotron oscillators for power levels up to 1 MW CW
[DE87-006683] N87-22907

A Godunov method for Lagrangian hydrodynamics in 1D
[DE87-005204] N87-22933

Lagrangian-like equations of hydrodynamics with mass diffusion
[DE87-007522] N87-22936

Magnitude and phase calibration of microwave sensors
[DE87-003466] N87-22955

Time and space resolved spectroscopy of X-ray laser experiments from 81A to 220A
[DE87-005946] N87-22968

New laser materials
[DE87-006723] N87-22970

DYNA3D: A computer code for crashworthiness engineering
[DE87-003818] N87-22998

Reading patterns in online documentation: How transcript analysis reflects text design, software constraints, and user preferences
[DE87-006466] N87-23174

Patterns from models of dissipative systems
[DE87-006823] N87-23175

Workshop report on New Directions in X-ray Scattering
[DE87-006305] N87-23262

Semiconductor research capabilities at the Lawrence Berkeley Laboratory
[DE87-006931] N87-23298

Properties of planetary fluids at high pressure and temperature N87-23399

Creep of ice: Further studies N87-23540

LAWRENCE UNIV., APPLETON, WIS.

Search for, and study of, paleozoic impact ejecta: Progress made during the past year N87-23514

LOCKHEED-CALIFORNIA CO., BURBANK.

Flight and analytical investigations of a structural mode excitation system on the YF-12A airplane
[NASA-CR-166623] N87-22685

LOCKHEED ENGINEERING AND MANAGEMENT SERVICES CO., INC., HOUSTON, TEX.

Crew activity and motion effects on the space station
N87-22744

LOCKHEED MISSILES AND SPACE CO., PALO ALTO, CALIF.

Characterization of rapidly solidified Al-Be-Li and Al-Be ribbons
[DE87-006613] N87-22835

Low-pressure self-propagating high-temperature synthesis
[AD-A178593] N87-22856

Some aspects of double layer formation in a plasma constrained by a magnetic mirror N87-23329

Solar active region physical parameters inferred from a thermal cyclotron line and soft X-ray spectral lines
[AD-A179650] N87-23560

Simultaneous SMM flat crystal spectrometer and very large array observations of solar active regions
[AD-A179698] N87-23562

LOCKHEED MISSILES AND SPACE CO., SUNNYVALE, CALIF.

Vibration isolation for line of sight performance improvement N87-22742

LOS ALAMOS NATIONAL LAB., N. MEX.

On the use of adaptive moving grid methods in combustion problems
[DE87-003715] N87-22824

Numerical simulation of the decay of swirling flow in a constant volume engine simulator
[LA-10728-MS] N87-22945

Heat transfer in an organic heat pipe
[LA-10781-MS] N87-22946

Application of picosecond CO2 lasers to particle accelerators
[DE87-003711] N87-22964

A high-temperature quadrupole mass spectrometer for studying vaporization from materials heated by a CO2 laser
[LA-10744] N87-22975

Parallel graph reduction on a supercomputer
[DE87-006066] N87-23173

Optico-mechanical scanning radiometer
[DE87-007075] N87-23258

Beamed emission from gamma-ray burst sources
N87-23332

Double layers and plasma-wave resistivity in extragalactic jets: Cavity formation and radio-wave emission N87-23333

Detection of 10^{14}-eV gamma rays from Cygnus X-3 during 1986
[DE87-006054] N87-23568

LOUISIANA STATE UNIV., BATON ROUGE.

The integration of spectral and spatial analysis for land use classification
[AD-A178703] N87-23015

LOWELL UNIV., MASS.

Preliminary investigation of ionospheric modification using oblique incidence high power HF radio waves
[AD-A179174] N87-23056

M

MARC ANALYSIS RESEARCH CORP., PALO ALTO, CALIF.

The NESSUS finite element code N87-22785

MARTIN MARIETTA AEROSPACE, DENVER, COLO.

Space station structural dynamics/reaction control system interaction study N87-22753

MARTIN MARIETTA AEROSPACE, NEW ORLEANS, LA.

Transient response for interaction of two dynamic bodies N87-22709

MARYLAND UNIV., COLLEGE PARK.

Operation of the induced resonance electron cyclotron maser at higher harmonics
[AD-A179428] N87-22962

Tropical Pacific SST experiments with the GLAS climate model N87-23049

Detection of 10^{14}-eV gamma rays from Cygnus X-3 during 1986
[DE87-006054] N87-23568

MASSACHUSETTS INST. OF TECH., CAMBRIDGE.

Investigation of air transportation technology at Massachusetts Institute of Technology, 1984
N87-22605

Aircraft approach guidance using relative Loran-C navigation N87-22606

Probabilistic Modeling of Loran-C for nonprecision approaches N87-22607

Measurement of ice accretion using ultrasonic pulse echo techniques N87-22608

Martensitic transformation as a deformation process
[DE87-007068] N87-22836

A coherent VLSI environment
[AD-A179303] N87-22897

A coherent VLSI design environment
[AD-A179037] N87-22920

Numerical calculation of the drag force induced by natural convection of spheres at low Grashof numbers
[DE87-006791] N87-22935

A linearized Euler analysis of unsteady flows in turbomachinery
[NASA-CR-180987] N87-22948

A preliminary study of extended magnetic field structures in the ionosphere
[NASA-CR-181004] N87-23066

Image processing for vision: An equipment requests to DOD
[AD-A179261] N87-23150

Numerical study of hybrid plume
[AD-A179561] N87-23275

Kinematics and dynamics of the Uranian rings
N87-23353

Solar system dynamics N87-23390

Hisingerite and iddingsite on Mars: Degradation of iron-rich basalts N87-23416

Gossans on Mars: Spectral features attributed to jarosite N87-23417

Secular cooling of Earth as a source of intraplate stress N87-23519

A test of the hypothesis that impact-induced fractures are preferred sites for later tectonic activity N87-23520

Lithospheric loading and tectonics of the lunar irregular maria N87-23522

MASSACHUSETTS UNIV., AMHERST.

Stress history of the Tharsis Region, Mars
N87-23527

Geometry and relative age of large patterned fractures in southern Acidalia Planitia, Mars N87-23533

Origin of fractures, Martian polygonal terrain
N87-23534

MATERIALS QUALITY ASSURANCE DIRECTORATE, LONDON (ENGLAND).

The effects of candidate chemical training agents upon service materials
[MQAD-317] N87-22832

Effects of machine variables on the quality of injection mouldings. An interlaboratory trial, 2: High density polyethylene
[MQAD-328] N87-22987

MATERIALS RESEARCH LABS., ASCOT VALE (AUSTRALIA).
A fast, low resistance switch for small slapper detonators
[AD-A178562] N87-22911

MAX-PLANCK-INST. FUER METEOROLOGIE, HAMBURG (WEST GERMANY).
Sensitivity of an Ocean General Circulation Model (OCGM) to wind forcing N87-23054

MCGILL UNIV., MONTREAL (QUEBEC).
Physical properties and structure of ion-containing polymers
[AD-A178592] N87-22855

MECHANICAL TECHNOLOGY, INC., LATHAM, N. Y.
AI (Artificial Intelligence) gas turbine rotor diagnostics
[AD-A178996] N87-22683

MELBOURNE UNIV., PARKVILLE (AUSTRALIA).
Estimating the standard error of robust regression estimates
[AD-A179099] N87-23232

MESSERSCHMITT-BOELKOW-BLOHM G.M.B.H., MUNICH (WEST GERMANY).
Integrated design of structures N87-22669

MESSERSCHMITT-BOELKOW-BLOHM G.M.B.H., OTTOBRUNN (WEST GERMANY).
Electromagnetic interference (EMI) fault prevention and self recovery of digital flight control systems
[MBB-UD-483/86] N87-22686
The effect on the strength of initiation on the corner effect
[MBB-UA-938/86] N87-22924
Determining the kinematic parameters of a moving imaging sensor by processing spatial and temporal intensity changes
[MBB-UA-914/85] N87-23256

METEOROLOGICAL OFFICE, BRACKNELL (ENGLAND).
Forecast and sensitivity experiments on the UK Meteorological Office GCM with El Nino SST anomalies
N87-23045

METEOROLOGICAL RESEARCH INST., TSUKUBA (JAPAN).
The impact of SST anomalies and initial conditions on extended range predictions with an atmospheric general circulation model: A case study in early summer of 1983
N87-23051

MIAMI UNIV., FLA.
Atmospheric simulations of the 1982-83 ENSO episode N87-23038
Millimeter wave Doppler radar observation of cloud and boundary layer structure
[AD-A178679] N87-23098

MICHIGAN STATE UNIV., EAST LANSING.
Formal modeling and analysis of fault-tolerance properties for software
[DE87-007006] N87-23176

MICHIGAN UNIV., ANN ARBOR.
A development system for augmented transition network grammars and a large grammar for technical prose
[AD-A179009] N87-23188

MIDWEST RESEARCH INST., GOLDEN, COLO.
A comparison of predicted wind turbine blade loads to test measurements
[DE87-001130] N87-23021

MILITARY AIRLIFT COMMAND, SCOTT AFB, ILL.
Introduction to MAC CRM training N87-22648

MILITARY AIRLIFT WING (349TH), TRAVIS AFB, CALIF.
Cockpit Resource Management (CRM) training in the 349th military airlift wing N87-22651

MINISTRY OF DEFENCE, LONDON (ENGLAND).
Cost analysis of aircraft projects N87-22664

MINNESOTA UNIV., MINNEAPOLIS.
Effect of double layers on magnetosphere-ionosphere coupling N87-23321

MISSISSIPPI STATE UNIV., MISSISSIPPI STATE.
Equipment for turbulent heat transfer test apparatus
[AD-A179612] N87-22930

MISSOURI UNIV., COLUMBIA.
The impact of climate change from increased atmospheric carbon dioxide on American agriculture
[DOE/NBB-0077] N87-23032

MISSOURI UNIV., ROLLA.
Containerless processing of glass forming melts: D-1, MEA/A-2 experiment 81F01 conducted on STS-61A flight, October 1985
[NASA-CR-179118] N87-22861
Reliability studies of ceramic capacitors
[AD-A179436] N87-22900

MOUNT HOLYOKE COLL., SOUTH HADLEY, MASS.
The study of photochemistry at semiconductor surfaces using total internal reflection techniques
[DE87-006259] N87-23295

MSNW, INC., SAN MARCOS, CALIF.
Plasma joining of metal matrix composites
[AD-A178731] N87-22814

MURPHYS CENTER OF PLANETOLOGY, CALIF.
Oblique impact: Projectile richochet, concomitant ejecta and momentum transfer N87-23492

N

NAGOYA UNIV. (JAPAN).
A system for long pulse REB generation
[IPPJ-812] N87-23274

NATIONAL AERONAUTICAL ESTABLISHMENT, OTTAWA (ONTARIO).
Flutter analysis of a two-dimensional airfoil with cubic non-linear restoring force
[NAE-AN-36] N87-22628

NATIONAL AERONAUTICS AND SPACE ADMINISTRATION, WASHINGTON, D.C.
The aerodynamic optimization of wings at subsonic speeds and the influence of wingtip design
[NASA-TM-88534] N87-22627
Influence of supporting conditions on stress intensity factors for single-edge-cracked specimens under bending
[NASA-TT-20016] N87-23008
Earth resources: A continuing bibliography with indexes (issue 53)
[NASA-SP-7041(53)] N87-23013
Field study of the effect of orographic features on planetary boundary layer models N87-23091
Aerospace medicine and biology: A continuing bibliography with indexes (supplement 298)
[NASA-SP-7011(298)] N87-23114
Reports of Planetary Geology and Geophysics Program, 1986
[NASA-TM-89810] N87-23341
Cratering history of Miranda N87-23344
Geology and cratering history of Ariel N87-23348
Subcentimeter-size particle distribution functions in planetary rings from Voyager radio and photopolarimeter occultation data N87-23361
A search for spectral alteration effects in chondritic gas-rich breccias N87-23375
A scaling law for accretion zone sizes N87-23385
Dynamical constraints on the origin of the moon
N87-23388
A chemical and petrological model of the lunar crust
N87-23408
Compositional information for the Moon: Some characteristics of current near-IR spectra (telescopic and laboratory) N87-23429
Timing of ancient extensional tectonic features on Mars N87-23526
Compositional stratigraphy of crustal material from near-infrared spectra N87-23559

NATIONAL AERONAUTICS AND SPACE ADMINISTRATION. AMES RESEARCH CENTER, MOFFETT FIELD, CALIF.
A look at handling qualities of Canard configurations
[NASA-TM-88354] N87-22629
Results of the integration of a transonic full-potential analysis program with a free-wake lifting-line program for hovering rotors
[NASA-TM-89494] N87-22631
Cockpit Resource Management Training
[NASA-CP-2455] N87-22634
Instructions to working groups N87-22655
Dyads and triads at 35,000 feet: Factors affecting group process and aircrew performance N87-22656
Frequency-response identification of XV-15 tilt-rotor aircraft dynamics
[NASA-TM-89428] N87-22690
Digital control of highly augmented combat rotorcraft
[NASA-TM-88346] N87-22691
Structural panels
[NASA-CASE-ARC-11429-2-CU] N87-22845
Conservative zonal schemes for patched grids in 2 and 3 dimensions
[NASA-TM-88326] N87-22932
Computational aerothermodynamics
[NASA-TM-89450] N87-22943
Real-time laser holographic Interferometry for aerodynamics
[NASA-TM-89462] N87-22956
Prediction of service life of aircraft structural components using the half-cycle method
[NASA-TM-86812] N87-23009
High altitude turbulence for supersonic cruise vehicles
[NASA-TM-88285] N87-23100
A static data flow simulation study at Ames Research Center
[NASA-TM-89434] N87-23201
The viscosity of Miranda N87-23345
Accretional heating of the satellites of Saturn and Uranus N87-23355
Protostellar disks and the primitive solar nebula
N87-23379
Uranus and Neptune: Questions and possible answers
N87-23386
Planetary ring dynamics and morphology N87-23394
The case for a wet, warm climate on early Mars
N87-23410
Formation of the layered deposits in the Valles Marineris, Mars N87-23470
Non-Newtonian ice rheology and the retention of craters on Ganymede N87-23511

NATIONAL AERONAUTICS AND SPACE ADMINISTRATION. GODDARD SPACE FLIGHT CENTER, GREENBELT, MD.
Programmable electronic synthesized capacitance
[NASA-CASE-GSC-12961-1] N87-22895
Quick-look guide to the crustal dynamics project's data information system
[NASA-TM-87818] N87-23018
A preliminary theory of the origin of the 40-50 day oscillation N87-23044
Sixth Annual Users' Conference
[NASA-CP-2463] N87-23156
TAE Plus: A conceptual view of TAE in the space station era N87-23157
SOT: A rapid prototype using TAE windows
N87-23161
Display management subsystem, version 1: A user's eye view N87-23164
An overview of the Land Analysis System (LAS)
N87-23168
Measuring software design
[NASA-TM-89372] N87-23189
General object-oriented software development
[NASA-TM-89375] N87-23190
Ada style guide (version 1.1)
[NASA-TM-89376] N87-23191
Product assurance policies and procedures for flight dynamics software development
[NASA-TM-89377] N87-23192
Guidelines for applying the Composite Specification Model (CSM)
[NASA-TM-89374] N87-23193
Oxidized basalts on the surface of Venus: Compositional implications of measured spectral properties
N87-23412
Mid-infrared spectroscopic investigation N87-23424
Pseudocraters as indicators of ground ice on Mars
N87-23474
Characteristic structures of the highland boundary on Mars: Evidence against a single mega-impact event?
N87-23523
The Martian crustal dichotomy: Product of accretion and not a specific event? N87-23524

NATIONAL AERONAUTICS AND SPACE ADMINISTRATION. LYNDON B. JOHNSON SPACE CENTER, HOUSTON, TEX.
Pumped two-phase heat transfer loop
[NASA-CASE-MSC-20841-1] N87-22950
Apparatus and method of capturing an orbiting spacecraft
[NASA-CASE-MSC-20979-1] N87-22985
Analytical electron microscopy of fine-grained phases in primitive interplanetary dust particles and carbonaceous chondrites N87-23376
Calcium carbonate and calcium sulfate in Martian meteorite EETA79001 N87-23409
Non-equilibrium freezing of water-ice in sandy basaltic regoliths and implications for fluidized debris flows on Mars N87-23466

NATIONAL AERONAUTICS AND SPACE ADMINISTRATION. LANGLEY RESEARCH CENTER, HAMPTON, VA.
Joint University Program for Air Transportation Research, 1984
[NASA-CP-2452] N87-22604
Experimental cavity pressure distributions at supersonic speeds
[NASA-TP-2683] N87-22626
An analysis of artificial viscosity effects on reacting flows using a spectral multi-domain technique
[NASA-CR-178308] N87-22632
Aircraft control position indicator
[NASA-CASE-LAR-12984-1] N87-22678
Status of the Mast experiment N87-22703
Microprocessor controlled proof-mass actuator
N87-22706
Considerations in the design and development of a space station scale model N87-22711
Status report and preliminary results of the spacecraft control laboratory experiment N87-22717
An overview of controls research on the NASA Langley Research Center grid N87-22720
Control of flexible structures and the research community N87-22732
Dual keel space station control/structures interaction study N87-22737

Slewing control experiment for a flexible panel
N87-22740

Polyenamines from aromatic diacetylenic diketones and diamines
[NASA-CASE-LAR-13444-1-CU] N87-22847

Process for crosslinking and extending conjugated diene-containing polymers
[NASA-CASE-LAR-13452-1] N87-22848

Daze fasteners
[NASA-CASE-LAR-13009-2] N87-22976

Standard-resolution TOVS observations for the FIRE/SRB Wisconsin experiment region from October 9 through November 2, 1986
[NASA-TM-89151] N87-23101

Chandrasekhar equations for infinite dimensional systems. Part 2: Unbounded input and output case
[NASA-CR-178303] N87-23208

A survey of mixed finite element methods
[NASA-CR-178267] N87-23229

Efficient implementation of essentially non-oscillatory shock capturing schemes
[NASA-CR-178304] N87-23230

Development of confidence limits by pivotal functions for estimating software reliability
[NASA-TP-2709] N87-23244

NATIONAL AERONAUTICS AND SPACE ADMINISTRATION. LEWIS RESEARCH CENTER, CLEVELAND, OHIO.

Application of advanced computational codes in the design of an experiment for a supersonic throughflow fan rotor
[NASA-TM-88915] N87-22630

Analysis of an advanced technology subsonic turbofan incorporating revolutionary materials
[NASA-TM-89868] N87-22680

Supersonic through-flow fan design
[NASA-TM-88908] N87-22681

Experimental evaluation of blockage ratio and plenum evacuation system flow effects on pressure distribution for bodies of revolution in 0.1 scale model test section of NASA Lewis Research Center's proposed altitude wind tunnel
[NASA-TP-2702] N87-22694

Effect of Gimbal friction modeling technique on control stability and performance for Centaur upper-stage
[NASA-TM-89894] N87-22755

Numerical modeling of on-orbit propellant motion resulting from an impulsive acceleration
[NASA-TM-89873] N87-22757

Structural Integrity and Durability of Reusable Space Propulsion Systems
[NASA-CP-2471] N87-22766

Unsteady stator/rotor interaction N87-22767

Simulation of multistage turbine flows N87-22768

Progress in the prediction of unsteady heat transfwe on turbines blades N87-22769

Progress on thin-film sensors for space propulsion technology N87-22772

Heat flux calibration facility capable of SSME conditions N87-22774

Fatigue damage interaction behavior of PWA 1480
N87-22777

Nonlinear heat transfer and structural analyses of SSME turbine blades N87-22779

Probabilistic structural analysis to evaluate the structural durability of SSME critical components N87-22783

Structural tailoring using the SSME/STAEBL code
N87-22795

SSME blade damper technology N87-22798

Impact of thermal energy storage properties on solar dynamic space power conversion system mass
[NASA-TM-89909] N87-22802

Low power DC arcjet operation with hydrogen/nitrogen/ammonia mixtures
[NASA-TM-89876] N87-22804

Electromagnetic emission experiences using electric propulsion systems: A survey
[NASA-TM-100120] N87-22805

An evaluation of metallized propellants based on vehicle performance
[NASA-TM-100104] N87-22806

Langmuir probe surveys of an arcjet exhaust
[NASA-TM-89924] N87-22807

Fiber reinforced superalloys
[NASA-TM-89865] N87-22811

Friction and wear of sintered Alpha SiC sliding against IN-718 alloy at 25 to 800 C in atmospheric air at ambient pressure
[NASA-TM-87353] N87-22860

Detection of reflector surface error from near-field data: Effect of edge diffracted field
[NASA-TM-89920] N87-22874

Revised NASA axially symmetric ring model for coupled-cavity traveling-wave tubes
[NASA-TP-2675] N87-22923

Thermodynamic analysis and subscale modeling of space-based orbit transfer vehicle cryogenic propellant resupply
[NASA-TM-89921] N87-22949

Laser anemometry techniques for turbine applications
[NASA-TM-88953] N87-22959

Helicopter transmission testing at NASA Lewis Research Center
[NASA-TM-89912] N87-22978

Finite element implementation of Robinson's unified viscoplastic model and its application to some uniaxial and multiaxial problems
[NASA-TM-89891] N87-23010

High temperature solid oxide regenerative fuel cell for solar photovoltaic energy storage
[NASA-TM-89872] N87-23020

SP-100 Advanced Technology Program
[NASA-TM-89888] N87-23027

Performance characteristics of a combination solar photovoltaic heat engine energy converter
[NASA-TM-89908] N87-23028

Component variations and their effects on bipolar nickel-hydrogen cell performance
[NASA-TM-89907] N87-23029

Applications and requirements for real-time simulators in ground-test facilities
[NASA-TP-2672] N87-23202

AlGaAs growth by OMCVD using an excimer laser
[NASA-TM-88937] N87-23304

NATIONAL AERONAUTICS AND SPACE ADMINISTRATION. MARSHALL SPACE FLIGHT CENTER, HUNTSVILLE, ALA.

Celestial target observability for astro spacelab missions
[NASA-TM-86591] N87-22696

Structural Dynamics and Control Interaction of Flexible Structures
[NASA-CP-2467-PT-1] N87-22702

Large space structures ground experiment checkout
N87-22704

Commit your works to the Lord, and your thoughts shall be established (Prov. 16:3). Inter-stable control systems
N87-22716

Solar array flight dynamic experiment N87-22722

Dynamic characteristics of a vibrating beam with periodic variation in bending stiffness N87-22726

Workshop on Structural Dynamics and Control Interaction of Flexible Structures N87-22728

Structural Dynamics and Control Interaction of Flexible Structures
[NASA-CP-2467-PT-2] N87-22729

A TREETOPS simulation of the Hubble Space Telescope-High Gain Antenna interaction N87-22735

Finite element models of wire rope for vibration analysis N87-22748

System identification for large space structure damage assessment N87-22750

Space station structures and dynamics test program
N87-22751

Modeling digital control systems with MA-prefiltered measurements
[NASA-TP-2732] N87-22870

Tube coupling device
[NASA-CASE-MFS-25964-2] N87-22977

Double Layers in Astrophysics
[NASA-CP-2469] N87-23313

Accretion onto neutron stars with the presence of a double layer N87-23334

The formation of a double layer leading to the critical velocity phenomenon N87-23335

NATIONAL AERONAUTICS AND SPACE ADMINISTRATION. PASADENA OFFICE, CALIF.

Method and apparatus for measuring minority carrier lifetime in a direct band-gap semiconductor
[NASA-CASE-NPO-16337-1-CU] N87-22894

Water-absorbing capacitor system for measuring relative humidity
[NASA-CASE-NPO-16544-1-CU] N87-22953

Closed loop fiber optic rotation sensor
[NASA-CASE-NPO-16558-1-CU] N87-23259

Total immersion crystal growth
[NASA-CASE-NPO-15800-2] N87-23286

NATIONAL AIR AND SPACE MUSEUM, WASHINGTON, D.C.

Implications of Viking color data for evolution of the Amenthes Region, Mars N87-23525

Thin and thick-skinned deformation in the Tharsis Region of Mars N87-23529

Tectonic domains in the Eastern Hemisphere of Mars
N87-23531

Age of fracturing and mesa development in the Elysium Area, northern Martian plains N87-23532

NATIONAL BUREAU OF STANDARDS, GAITHERSBURG, MD.

Interaction of a three-dimensional roughness element with a laminar boundary layer
[AD-A178668] N87-22941

NBS calibration services users guide, 1986-1988 edition
[NBS-SP-250] N87-22958

Programming languages for knowledge-based systems
[PB87-157228] N87-23170

OMNITAB 80: An interpretive system for statistical and numerical data anlysis
[PB87-172235] N87-23171

Cooperative research opportunities at NBS (National Bureau of Standards)
[PB87-157236] N87-23309

NATIONAL BUREAU OF STANDARDS, WASHINGTON, D.C.

Materials Information for Science and Technology (MIST). Project overview: Phase 1 and 2 and general considerations
[DE87-006799] N87-23312

NATIONAL CENTER FOR ATMOSPHERIC RESEARCH, BOULDER, COLO.

Sensitivity of tropical and mid-latitude time-averaged atmospheric states to interannually varying global ocean surface temperature distribution N87-23039

NATIONAL METEOROLOGICAL CENTER, WASHINGTON, D.C.

Sensitivity of the NMC spectral mode to the January 1983 El Nino SST N87-23048

NATIONAL METEOROLOGICAL INST., MADRID (SPAIN).

Cierzo: Northwesterly wind along the Ebro Valley (Spain) as a mesoscale effect induced on the lee of the Pyrenees mountain range; a case study during the Alpine Experiment (ALPEX) Special Observing Period N87-23083

The Mistral-Tramuntana shear line. A satellite observation N87-23084

NATIONAL OCEANIC AND ATMOSPHERIC ADMINISTRATION, BOULDER, COLO.

Electric potential distributions at the interface between plasmasheet clouds N87-23330

NATIONAL RESEARCH COUNCIL OF CANADA, OTTAWA (ONTARIO).

Artificial composites for high temperature applications: A review
[DME-007] N87-22808

NATIONAL SEVERE STORMS LAB., NORMAN, OKLA.

Oklahoma downbursts and their asymmetry
[DOT/FAA/PM-87/7] N87-23095

NAVAL AEROSPACE MEDICAL RESEARCH LAB., PENSACOLA, FLA.

Visual acuity and reaction time in navy fighter pilots
[AD-A178485] N87-23117

Effect of the neutral density helmet visor on the visual acuity of navy fighter pilots
[AD-A178486] N87-23147

NAVAL AIR DEVELOPMENT CENTER, WARMINSTER, PA.

Characterization of hybridized conductive composites
[AD-A179689] N87-22810

NAVAL AIR PROPULSION TEST CENTER, TRENTON, N.J.

Statistics on aircraft gas turbine engine rotor failures that occurred in US commercial aviation during 1981
[DOT/FAA/CT-86/42] N87-22684

NAVAL OCEAN SYSTEMS CENTER, SAN DIEGO, CALIF.

Optically Phase-Locked Electronic Speckle Pattern Interferometer (OPL-ESPI)
[AD-A178652] N87-22914

Calibration of the hand-held lidars used by the Naval Ocean Systems Center
[AD-A178965] N87-22973

NAVAL POSTGRADUATE SCHOOL, MONTEREY, CALIF.

Gas turbine combustor and engine augmentor tube sooting characteristics
[AD-A179423] N87-22679

Dynamic stall calculations using a Navier-Stokes solver
[AD-A178566] N87-22688

The effect of multipath on digital communications systems: With application to space station
[AD-A178578] N87-22876

CO2 pulsed laser damage mechanism and plasma effects (focused beam)
[AD-A179201] N87-22961

Laser reflectance as a function of rough water glitter profile
[AD-A178774] N87-23016

The design of a real time operating system for a fault tolerant microcomputer
[AD-A178577] N87-23155

JANUS/Ada software implementation of a star cluster local area network of personal computers
[AD-A178681] N87-23199
A separable piecewise linear upper bound for stochastic linear programs
[AD-A178694] N87-23217
The potential gradient of a plane source
[AD-A178976] N87-23223
Problems of identification
[AD-A178555] N87-23239
Frequency spectrum of soft X-ray emission from transition radiation
[AD-A178858] N87-23254
Angular distribution of transition radiation in the soft X-ray spectrum
[AD-A178859] N87-23255

NAVAL RESEARCH LAB., WASHINGTON, D. C.
Wideband parallel-plate waveguide, phased-array antenna
[AD-A179402] N87-22873
Direct-drive laser-fusion in the US
[DE87-005916] N87-23279
Nonlinear aspects of planar condensational instability
[AD-A178998] N87-23565

NAVAL SURFACE WEAPONS CENTER, SILVER SPRING, MD.
Numerical analysis of terminal double mach reflection
[AD-A179041] N87-22942

NAVAL UNDERWATER SYSTEMS CENTER, NEW LONDON, CONN.
Envelope detection of discrete-time band-limited signals using analytic signal representations
[AD-A179307] N87-22872

NAVAL WEAPONS CENTER, CHINA LAKE, CALIF.
Hybrid composite response to hydraulic ram
[AD-A178750] N87-22815

NEW MEXICO SOLAR ENERGY INST., LAS CRUCES.
Reliability of intermediate sized photovoltaic systems
[DE87-006328] N87-23024

NEW MEXICO UNIV., ALBUQUERQUE.
Silicon pulse sharpening diodes: Switching kilovolts in 10's of picoseconds
[DE87-005073] N87-22905
Investigation of the transverse-discharge copper-vapor laser
[AD-A178833] N87-22972
Detection of 10^{14}-eV gamma rays from Cygnus X-3 during 1986
[DE87-006054] N87-23568

NEW YORK UNIV., NEW YORK.
Custom-made pyramids
[AD-A178955] N87-23186
A statistical viewpoint on the theory of evidence, revision
[AD-A178958] N87-23207
The scale-space formulation of pyramid data structures
[AD-A178960] N87-23222

NORTH CAROLINA UNIV., CHAPEL HILL.
Extreme value theory for suprema of random variables with regularly varying tail probabilities
[AD-A179126] N87-23233

NORTHEAST LOUISIANA STATE COLL., MONROE.
Stratigraphy of the south polar region of Ganymede
N87-23539

NORTHEASTERN UNIV., BOSTON, MASS.
Formation mechanisms of laboratory double layers
N87-23314

NORTHWESTERN UNIV., EVANSTON, ILL.
Probabilistic finite elements N87-22790

NOTRE DAME UNIV., IND.
Characterization of rapidly solidified Al-Be-Li and Al-Be ribbons
[DE87-006613] N87-22835

O

OAK RIDGE NATIONAL LAB., TENN.
Thermal expansion of epoxy-fiberglass composite specimens
[DE87-004273] N87-22812
Characterizing the hardness and modulus of thin films using a mechanical properties microprobe
[DE87-006612] N87-22826
Characterization of rapidly solidified Al-Be-Li and Al-Be ribbons
[DE87-006613] N87-22835
Synthesis of alumina-zirconia powders by sol-gel processing
[DE87-005721] N87-22851
Ceramic Technology Newsletter No. 13, October - December 1986: Ceramic technology for advanced heat engines project
[DE87-006447] N87-22852
Neutron scattering from charged polymer lattices
[DE87-006628] N87-22853
Gas mixtures for spark gap closing switches with emphasis on efficiency of operation
[DE87-006624] N87-22906
A 3-D world modeling based on combinatorial geometry for autonomous robot navigation
[DE87-002814] N87-22980
Alternative knowledge acquisition: Developing a pulse coded neural network
[DE87-005192] N87-23145
A microcrystalline growth study of solvent effects in alkoxides by dynamic laser light scattering
[DE87-005710] N87-23294

OFFICE NATIONAL D'ETUDES ET DE RECHERCHES AEROSPATIALES, PARIS (FRANCE).
Simulation of an integrated flight/fire control system during air-to-ground gunnery attack N87-22672

OHIO STATE UNIV., COLUMBUS.
On orbital allotments for geostationary satellites
[NASA-CR-181017] N87-22700
Joint services electronics program
[AD-A178599] N87-22879
Radar target classification studies
[AD-A179010] N87-22889
A Bayesian statistics year at the Ohio State University
[AD-A178762] N87-23242

OHIO UNIV., ATHENS.
Investigation of air transportation technology at Ohio University, 1984 N87-22609
Digital Autonomous Terminal Access Communication (DATAC) system N87-22610
Fiber optic data transmission N87-22611
Loran-C approach considerations N87-22612
Satellite surveying for a Loran-C nonprecision approach N87-22613
Advanced monitoring concepts N87-22614
GPS antenna designs N87-22615
Processor-controlled timing module for Loran-C receiver
[OU-TM-90] N87-22616
A micro-computer-based system to compute magnetic variation
[OU-TM-91] N87-22617
A program downloader and other utility software for the DATAC bus monitor unit
[OU-TM-92] N87-22618

OREGON STATE UNIV., CORVALLIS.
ENSO experiments with a two-level AGCM
N87-23037
Optical dynamics experiment (ODEX) data report R/V acania expedition 10 October-17 November 1982. Volume 2: Particle size distributions. Volume 6: Scalar spectral-radiometer data
[AD-A178535] N87-23104
The application of flow competence evaluations to the assessment of flood-flow velocities and stresses
N87-23464

OREGON UNIV., EUGENE.
Relativistic calculations and measurements of energies, Auger rates, and lifetimes
[AD-A179137] N87-23251

OXFORD UNIV. (ENGLAND).
The development of a coupled GCM suitable for modelling studies in TOGA N87-23055
The perception of brightness and colour: Neurophysiology, psychophysics and computation
[AD-A179217] N87-23107

P

PAN AMERICAN WORLD AIRWAYS, INC., SAN FRANCISCO, CALIF.
Pan American World Airways flight training: A new direction. Flight operations resource management
N87-22641

PARIS-SUD UNIV., ORSAY (FRANCE).
Infrared spectroscopy using laser and Fourier techniques of the unstable molecules SiH and NH. Determination of the molecular constants of the fundamental electronic state 3 sigma (-) of NH
[ETN-87-99552] N87-22818
The chiral symmetry aspects of supersymmetric confining gauge theories
[ETN-87-99553] N87-23305

PENNSYLVANIA STATE UNIV., STATE COLLEGE.
Non-linear finite element analysis program
[AD-A179038] N87-23006

PENNSYLVANIA STATE UNIV., UNIVERSITY PARK.
Experimental research on compressible turbulent shear layers, viscous-inviscid interactions, and flow separation
[AD-A179579] N87-22928
Estimating the standard error of robust regression estimates
[AD-A179099] N87-23232
White-light optical information processing and holography
[AD-A179489] N87-23260
Analysis of the effects of impurity buildup on the performance of a reversed field pinch
[DE87-005438] N87-23277

PENNSYLVANIA UNIV., PHILADELPHIA.
Strategies for high-resolution 3-D millimeter wave imaging
[AD-A178653] N87-22882

PEOPLE EXPRESS AIRLINES, INC., NEWARK, N.J.
Cockpit resource management training at People Express N87-22639

PHYSICAL RESEARCH LAB., AHMEDABAD (INDIA).
Experimental observation of ion-acoustic double layers in laboratory plasma N87-23318

PITTSBURGH UNIV., PA.
Workshop report on New Directions in X-ray Scattering
[DE87-006305] N87-23262
Atlas of reflectance spectra of terrestrial, lunar and meteoritic powders and frosts from 92 to 1800 •lc2)nm
N87-23427
Bidirectional reflectance spectroscopy N87-23433
On the sputter alteration of regoliths of outer solar system bodies N87-23434
A preliminary analysis of the Mariner 10 color ratio map of Mercury N87-23439

PLANETARY SCIENCE INST., TUCSON, ARIZ.
Accumulation of solid bodies in the solar nebula
N87-23384
Collisional and dynamical processes in moon and planet formation N87-23387
Experimental studies of collision and fragmentation phenomena N87-23494
Impact and cratering processes on asteroids, satellites, and planets N87-23499
Studies of early intense cratering and possible saturation effects N87-23503

PRATT AND WHITNEY AIRCRAFT, EAST HARTFORD, CONN.
On 3-D inelastic analysis methods for hot section components. Volume 1: Special finite element models
[NASA-CR-179494] N87-22996

PRATT AND WHITNEY AIRCRAFT, WEST PALM BEACH, FLA.
High heat transfer oxidizer heat exchanger design and analysis
[NASA-CR-179596] N87-22803

PRINCETON UNIV., N. J.
Investigation of air transportation technology at Princeton University, 1984 N87-22619
Safe microburst penetration techniques: A deterministic, nonlinear, optimal control approach N87-22620
Intelligent fault-tolerant controllers N87-22621
Stability boundaries for command augmentation systems N87-22622
Principal circulation anomalies in model atmospheres with and without interannual variations of tropical Pacific SST N87-23041
Diagnosis of intraseasonal oscillations appearing in GCM experiments conducted at GFDL N87-23042
Particle simulation of auroral double layers
N87-23327

PURDUE UNIV., WEST LAFAYETTE, IND.
On the least favorable configuration of a selection procedure based on ranks
[AD-A178454] N87-23234
On Bayes selection rules for the best exponential population with type-I censored data
[AD-A178472] N87-23235
Novel polymeric LIT and divalent cation fast ion conducting materials
[DE87-006294] N87-23296

R

RAND CORP., SANTA MONICA, CALIF.
The control network of Mars: October 1986
N87-23551
A unified lunar control network N87-23552
The control networks of the satellites of Jupiter
N87-23553

RENSSELAER POLYTECHNIC INST., TROY, N.Y.
Robust data analysis based on characteristic functions
[AD-A178544] N87-23178
An algorithm for the computation of generalized likelihood or self-critical estimators for binary data
[AD-A178545] N87-23179
A family of algorithms for the estimation of the parameters of the stable laws and the parameters of attracting stable laws
[AD-A178542] N87-23214

Goodness-of-fit based on integrated squared discrepancies between sample and population characteristic functions
[AD-A178763] N87-23218

Some robust estimates of covariance structure based on parametric density estimation
[AD-A178806] N87-23220

Self-critical and robust procedures for the analysis of binary data
[AD-A178935] N87-23221

Some integrated squared error procedures for multivariate normal data
[AD-A178985] N87-23224

Goodness of fit based on integrated squared errors in characteristic functions or densities
[AD-A179027] N87-23225

Estimation of the parameters of a modified compound poisson distribution
[AD-A178540] N87-23236

A test of goodness of fit for multivariate normality
[AD-A178543] N87-23237

The applicability of the stable laws in collective risk theory and practice
[AD-A178546] N87-23238

Estimation of the parameters of mixtures via distance between densities or characteristic functions
[AD-A178623] N87-23241

The percentiles of the stable laws
[AD-A179025] N87-23243

Evolution of the inner asteroid belt: Paradigms and paradoxes from spectral studies N87-23372

Meteorite spectroscopy and characterization of asteroid surface materials N87-23373

RICE UNIV., HOUSTON, TEX.

A high-temperature quadrupole mass spectrometer for studying vaporization from materials heated by a CO2 laser
[LA-10744] N87-22975

RISO NATIONAL LAB., ROSKILDE (DENMARK).

Ion phase-space vortices and their relation to small amplitude double layers N87-23320

ROCHESTER UNIV., N. Y.

Target fabrication for high density target experiments at the University of Rochester's Laboratory for Laser Energetics
[DE87-005915] N87-22967

Collective effects in intense-field electrodynamics 1981-1986
[AD-A179490] N87-23261

Automatic pattern recognition and related topics
[AD-A178595] N87-23267

Stationary phase approximations in Fresnel-zone magnitude-only reconstructions
[AD-A178812] N87-23270

Direct-drive laser-fusion in the US
[DE87-005916] N87-23279

ROCKWELL INTERNATIONAL CORP., CANOGA PARK, CALIF.

Mechanical properties of high gradient and hot isostatically pressed PWA 1480 N87-22781

Probabilistic structural analysis verification studies
N87-22786

Composite load spectra for select space propulsion structural components N87-22793

Basic research in energetic fluorocarbons
[AD-A179676] N87-22822

ROCKWELL INTERNATIONAL CORP., DOWNEY, CALIF.

Structural/control interaction (payload pointing and micro-g) N87-22721

Preliminary evaluation of a reaction control system for the space station N87-22736

ROCKWELL INTERNATIONAL CORP., GOLDEN, COLO.

Control systems development, research and development
[DE87-005785] N87-22868

HEPA filter monitoring program
[RFP-3874] N87-22869

A novel rollability test
[RFP-3901] N87-22984

ROCKWELL INTERNATIONAL SCIENCE CENTER, THOUSAND OAKS, CALIF.

Metalliding as an electrochemical process
[AD-A178744] N87-22843

ROLLS-ROYCE LTD., BRISTOL (ENGLAND).

Propulsion system technologies for thrust vectoring
N87-22670

ROME AIR DEVELOPMENT CENTER, GRIFFISS AFB, N.Y.

Measurement of the atmospheric phase coherence length, rsubo
[AD-A178468] N87-23060

Calculation of ray paths in the ionosphere using an analytic raytracing technique
[AD-A178888] N87-23064

ROYAL AIR FORCE, FARNBOROUGH (ENGLAND).

Aircrew cooperation in the Royal Air Force
N87-22657

ROYAL AUSTRALIAN NAVY RESEARCH LAB., EDGECLIFF.

Studies of the east Australian current off northern New South Wales
[AD-A178461] N87-23103

ROYAL INST. OF TECH., STOCKHOLM (SWEDEN).

The exponential method
[TRITA-NA-8517] N87-23228

The Earth's magnetosphere as a sample of the plasma universe
[TRITA-EPP-86-12] N87-23337

S

SANDIA NATIONAL LABS., ALBUQUERQUE, N. MEX.

The autoignition of isobutane in a knocking spark ignition engine
[DE87-003241] N87-22823

Electrochemical adjustment of thin film Ti-Pd resistors
[DE87-007392] N87-22837

Molecular reactions at the film surface in plasma polymerization
[DE87-002488] N87-22849

Isotactic polystyrene phase diagrams and physical gelation
[DE87-002693] N87-22850

Extrinsic gettering for VLSI/ULSI processes
[DE87-002696] N87-22903

Numerical calculation of the drag force induced by natural convection of spheres at low Grashof numbers
[DE87-006791] N87-22935

Pulsed power for high power electron-beam pumped lasers
[DE87-004523] N87-22965

In situ friction, wear and electrical contact resistance of precious metal alloys
[DE87-001423] N87-22979

Correlations between electrical contact resistance and stages of wear in 700 Torr helium for precious metal electrical contacts
[DE87-003499] N87-22981

Advanced technology mobile robotics vehicle fleet
[DE87-007526] N87-22982

Structural design and fabrication of the Sandia 34-meter Vertical Axis Wind Turbine
[DE87-003503] N87-23022

The status of the vertical axis wind turbine research test bed
[DE87-005524] N87-23023

Reliability of intermediate sized photovoltaic systems
[DE87-006328] N87-23024

Evaluation of a heliostat tracker for linear Fresnel lens photovoltaic concentrators
[DE87-006331] N87-23025

Evaluation of spherical ceramic particles for solar thermal transfer media
[DE87-007432] N87-23026

Considerations in developing a comprehensive computer security support database system
[DE87-005527] N87-23151

Elements of a proposed security methodology for networks of computers
[DE87-006769] N87-23152

The use of real-time optical processors in embedded computing
[DE87-006895] N87-23153

A new LIHE (Light Initiated High Explosive) test capability for spherical targets
[DE87-003035] N87-23245

Development of a holographic beamsplitter for use with a conventional Fresnel lens
[DE87-006770] N87-23263

A statistical study of the combined effects of substrate temperature, bias, annealing, and a Cr3Si2 undercoating on the tribological properties of RF-sputtered MoS2 coatings
[DE87-007086] N87-23285

Atomistic simulation of stability properties and growth of strained layer structures
[DE87-006712] N87-23297

Temperature dependence of implantation damage in strained-layer superlattices
[DE87-007678] N87-23299

SCHOOL OF AEROSPACE MEDICINE, BROOKS AFB, TEX.

F-16 control stick response during +G sub z-induced loss of consciousness
[AD-A178474] N87-23116

SCI-TECH KNOWLEDGE SYSTEMS, SCOTIA, N.Y.

Materials Information for Science and Technology (MIST). Project overview: Phase 1 and 2 and general considerations
[DE87-006799] N87-23312

SCIENCE APPLICATIONS INTERNATIONAL CORP., MCLEAN, VA.

Operation of the induced resonance electron cyclotron maser at higher harmonics
[AD-A179428] N87-22962

Anomalous transport in discrete arcs and simulation of double layers in a model auroral circuit N87-23325

SCIENCE APPLICATIONS RESEARCH, LANHAM, MD.

An overview of the catalog manager N87-23163

SCIENTIFIC RESEARCH ASSOCIATES, INC., GLASTONBURY, CONN.

Flow dynamics stimulated by hairpin-like vortices in initially laminar boundary layers
[AD-A179578] N87-22927

SEACO, INC., KAILUA, HAWAII.

Tactile feedback for teleoperator systems
[AD-A179054] N87-22983

SIMUFLITE, INC., DALLAS/FORT WORTH AIRPORT, TEX.

Cockpit Resource Management (CRM) for part 91 and 135 operations N87-22652

SOLAVOLT INTERNATIONAL, PHOENIX, ARIZ.

Design, development and deployment of public service photovoltaic power/load systems for the Gabonese Republic
[NASA-CR-179603] N87-23030

SOUTHERN METHODIST UNIV., DALLAS, TEX.

Venusian tectonics: Convective coupling to the lithosphere? N87-23517

Flexurally-resisted uplift of the Tharsis Province, Mars
N87-23530

SOUTHWEST RESEARCH INST., SAN ANTONIO, TEX.

Probabilistic Structural Analysis Methods (PSAM) for select space propulsion system structural components
N87-22784

NESSUS/expert and NESSUS/FPI in the Probabilistic Structural Analysis Methods (PSAM) program
N87-22787

Fast ion mass spectrometry and charged particle spectrography investigations of transverse ion acceleration and beam-plasma interactions
[NASA-CR-168348] N87-22817

SRI INTERNATIONAL CORP., MENLO PARK, CALIF.

Computer vision research and its applications to automated cartography
[AD-A178815] N87-23017

STANFORD TELECOMMUNICATIONS, INC., RESTON, VA.

A system design requirements tool for satellite communications through nuclear-induced scintillation
[AD-A179272] N87-22871

STANFORD UNIV., CALIF.

Verification of performance results for a low-speed 15 percent elliptical circulation control airfoil
[NASA-CR-181020] N87-22633

Concurrent communication among multi-transceiver stations over shared media
[NASA-CR-180935] N87-22890

Fundamental studies of the mechanical behavior of microelectronic thin film materials
[AD-A179699] N87-22902

Throughput analysis of the IEEE 802.4 token bus standard under heavy load
[NASA-CR-180936] N87-22921

Heat transfer effects of longitudinal vortices embedded in a turbulent boundary layer
[DE87-006002] N87-22934

Dual cylindrical wave laser-Doppler method for measurement of skin friction in fluid flow
[AD-A178629] N87-22939

A theory for turbulent curved wall jets
[NASA-CR-181019] N87-22951

An experiment in knowledge-based signal understanding using parallel architectures
[AD-A179407] N87-23197

Sensitivity analysis for stationary probabilities of a Markov chain
[AD-A178556] N87-23240

Infrared fiber optic materials
[NASA-CR-180604] N87-23257

Workshop report on New Directions in X-ray Scattering
[DE87-006305] N87-23262

Channel access schemes and fiber optic configurations for integrated-services local area networks
[NASA-CR-180934] N87-23273

Superconducting thin films, composites and junctions
[AD-A179346] N87-23288

Modeling of substrate and implantation effects on the threshold voltage of MESFET structures fabricated in semi-insulating GaAs [AD-A178550] N87-23303

Application of numerical methods to planetary radiowave scattering N87-23448

STATE COMMITTEE ON HYDROMETEOROLOGY AND CONTROL OF THE NATURAL ENVIRONMENT, MOSCOW (USSR).

Air-sea interaction over the Mediterranean Sea during the Alpine Experiment (ALPEX) Special Observing Period N87-23073

STATE UNIV. OF NEW YORK, BUFFALO.

Development of an integrated BEM (Boundary Element Mesh) for hot fluid-structure interaction N87-22799

Plasma diagnosis by dye laser intracavity absorption [DE87-006407] N87-23280

Non-Markovian line shapes of physisorbed atoms on a crystal [AD-A179525] N87-23292

Geology of the Mohon Mountain volcanic field, Yavapai and Mohave Counties, Arizona: A preliminary report N87-23486

The geology of Pine and Crater Buttes: Two basaltic constructs on the far eastern Snake River Plain N87-23487

The geology of Picacho Butte, a silicic volcanic dome in northwest Arizona N87-23488

STEVENS INST. OF TECH., HOBOKEN, N. J.

Corrosion, wear and mechanical properties of pulse-electrodeposited alloys [AD-A178596] N87-22842

Multidimensional filtering investigations [AD-A178745] N87-22915

SUL ROSS STATE UNIV., ALPINE, TEX.

Crustal and subcrustal nodules in ejecta from Kilbourne Hole Maar, New Mexico N87-23485

SURREY UNIV., GUILDFORD (ENGLAND).

A feasibility study of the flexible simulation of sunlight [BR98783] N87-22693

SVERDRUP TECHNOLOGY, INC., MIDDLEBURG HEIGHTS, OHIO.

Progress in optical strain measurement system development N87-22773

Dynamic characteristics of single crystal SSME blades N87-22797

SVERDRUP TECHNOLOGY, INC., CLEVELAND, OHIO.

Probabilistic SSME blades structural response under random pulse loading N87-22791

Quantifying uncertainties in the structural response of SSME blades N87-22792

Optical strain measurement system development, phase 1 [NASA-CR-179619] N87-22960

SYRACUSE UNIV., N. Y.

Computer program for electromagnetic penetration into a conducting circular cylinder through a narrow slot, TM case [AD-A178616] N87-22880

SYSTEMS RESEARCH LABS., INC., DAYTON, OHIO.

Application of atomic fluorescence to measurement of combustion temperature in solid propellants [AD-A179665] N87-22862

T

TATA INST. OF FUNDAMENTAL RESEARCH, BOMBAY (INDIA).

Detection of 10^{14}-eV gamma rays from Cygnus X-3 during 1986 [DE87-006054] N87-23568

TECHNISCHE HOCHSCHULE, AACHEN (WEST GERMANY).

Scientific goals of the German Spacelab Mission D1 [ETN-87-99669] N87-22695

TECHNISCHE UNIV., MUNICH (WEST GERMANY).

Winds in the Inn Valley (Austria) N87-23074

Energy budget of an Alpine valley N87-23076

TECHNISCHE UNIV., VIENNA (AUSTRIA).

Fractal analysis of radar precipitation data over hilly terrain N87-23093

TENNESSEE UNIV., KNOXVILLE.

Gas mixtures for spark gap closing switches with emphasis on efficiency of operation [DE87-006624] N87-22906

TENNESSEE UNIV. SPACE INST., TULLAHOMA.

A general method for dynamic analysis of structures overview N87-22707

TEXAS A&M UNIV., COLLEGE STATION.

A quasi-analytical method for non-iterative computation of nonlinear controls N87-22731

Evidence for glaciation in Elysium N87-23468

TEXAS TECHNOLOGICAL UNIV., LUBBOCK.

Coordinated research program in pulsed power physics [AD-A178625] N87-22912

TEXAS UNIV., AUSTIN.

Theory underlying CRM training: Psychological issues in flight crew performance and crew coordination N87-22635

Lanczos modes for reduced-order control of flexible structures N87-22739

Microscopic study of the influence of impurities on interface bonding [AD-A178510] N87-22841

High energy high rate pulsed power processing of materials by powder consolidation and by railgun deposition [AD-A179289] N87-22867

Investigation of low-amplitude shear wave velocity in anisotropic material [AD-A179563] N87-22994

Altimeter measurements for the determination of the Earth's gravity field [NASA-CR-180520] N87-23033

TRANS-AUSTRALIA AIRLINES, MELBOURNE.

Introduction to Trans Australia Airlines CRM training N87-22644

Aircrew team management program N87-22645

TRW, INC., REDONDO BEACH, CALIF.

Analog fiber optic recirculating delay line [AD-A179050] N87-23272

TSENTRALNYJ NAUCHNO-ISSLEDOVATELSKIJ INST. INFORMATSII I TEKHNIKO-EHKONOMICHESKIKH ISSLEDOVANIJ PO ATOMNOJ NAUKE I TEKHNIKE, MOSCOW (USSR).

Powder. Complex of programs for structural analysis of polycrystals [DE87-701211] N87-23283

TUFTS UNIV., MEDFORD, MASS.

Solar active region physical parameters inferred from a thermal cyclotron line and soft X-ray spectral lines [AD-A179650] N87-23560

J. VLA (Very Large Array) of a solar noise storm [NASA-CR-180219] N87-23561

Simultaneous SMM flat crystal spectrometer and very large array observations of solar active regions [AD-A179698] N87-23562

U

ULTRASYSTEMS, INC., IRVINE, CALIF.

Processible boron nitride preceramic polymers [AD-A178907] N87-22859

UNITED AIR LINES, INC., SAN FRANCISCO, CALIF.

The development and implementation of cockpit resource management in UAL recurrent training N87-22638

The application of CRM to military operations N87-22649

UNITED KINGDOM ATOMIC ENERGY AUTHORITY, HARWELL (ENGLAND).

Hydrogen and temper embrittlement interactions in fatigue of 2 1/4Cr1Mo steel [AERE-R-12322] N87-22830

Automated non-destructive testing using an industrial robot [AERE-R-12308] N87-22986

A study into the generation of temperature gradients in materials for detecting and measuring the depth of sub-surface cracks [AERE-R-12382] N87-22991

UNITED TECHNOLOGIES RESEARCH CENTER, EAST HARTFORD, CONN.

Investigation of laser diagnostics of PACVD processes for depositing hard face coatings [DE87-006292] N87-22969

UNIVERSITY OF SOUTHERN CALIFORNIA, LOS ANGELES.

Formal models of hardware and their applications to VLSI design automation [AD-A178837] N87-22916

UNIVERSITY OF SOUTHERN CALIFORNIA, REDONDO BEACH.

Research on computer aided design for maintainability [AD-A178460] N87-23177

UNIVERSITY OF SOUTHERN ILLINOIS, CARBONDALE.

Groundwater sapping channels: Summary of effects of experiments with varied stratigraphy N87-23461

USAIR, PITTSBURGH, PA.

Cockpit resource management at USAir N87-22659

UTAH STATE UNIV., LOGAN.

Electric fields and double layers in plasmas N87-23323

UTAH UNIV., SALT LAKE CITY.

Stochastic processes in CHEMFETs [AD-A178841] N87-22829

Waveguide junction analysis involving asymmetrical modes [AD-A178464] N87-22909

The 30-60 day oscillation in a perpetual January simulation with the NCAR general circulation model N87-23043

On the predicability of low-level flow during ALPEX N87-23088

Structure and properties of novel compounds of silicon germanium and tin [AD-A179433] N87-23291

V

VARIAN ASSOCIATES, PALO ALTO, CALIF.

Design and operation of 140 GHz gyrotron oscillators for power levels up to 1 MW CW [DE87-006683] N87-22907

VIRGINIA POLYTECHNIC INST. AND STATE UNIV., BLACKSBURG.

Maneuvering and vibration control of flexible spacecraft N87-22734

VIRGINIA UNIV., CHARLOTTESVILLE.

Automated transient analysis of structural members [AD-A179042] N87-23007

SIS (Superconductor-Insulator-Superconductor) mixer research [AD-A179604] N87-23293

Formation of giant molecular clouds in global spiral structures: The role of orbital dynamics and cloud-cloud collisions N87-23381

Evolution of planetesimal velocities N87-23383

Hamiltonian theory of nonlinear waves in planetary rings N87-23393

Charged particle modification of surfaces in the outer solar system N87-23435

VIZ ABILITY, CORVALLIS, OREG.

New methods for obtaining scattering and absorption from tropospheric visible spectrum data [AD-A178590] N87-23062

W

WASHINGTON UNIV., SEATTLE.

Dynamic fracture of high strength steel [AD-A178862] N87-22844

Two and three-dimensional inversion of magnetotelluric data [DE87-005553] N87-23058

Image size and resolution in face recognition N87-23113

Potential medical applications of TAE N87-23166

Confinement and heating of high beta plasmas with emphasis on compact toroids. Task 2: Stellarator and heliac research [DE87-005554] N87-23278

Spectral mixture modeling: Further analysis of rock and soil types at the Viking Lander sites N87-23415

Characterization of surficial units on Mars using Viking orbiter multispectral image and thermal data N87-23418

Wind ripples in low density atmospheres N87-23454

Impact crater scaling laws N87-23496

WASHINGTON UNIV., ST. LOUIS, MO.

NASA Regional Planetary Image Facility image retrieval and processing system N87-23160

Studies of outer planet satellites, Mercury and Uranus N87-23358

On the spectral reflectance properties of materials exposed at the Viking landing sites N87-23414

Cratering and obliteration history of the south polar region of Mars N87-23506

Microvax-based data management and reduction system for the regional planetary image facilities N87-23554

WESTLAND HELICOPTERS LTD., YEOVIL (ENGLAND).

Acoustic testing of simplified cabin box, phase 1 [RP-698] N87-23248

WISCONSIN UNIV., MADISON.

Radiation damage to coatings for short wave length laser mirrors [DE87-001696] N87-22983

Program and abstracts of the 39th Annual Gaseous Electronics Conference [AD-A178598] N87-23247

Pumping potential wells N87-23316

A study of the fundamental characteristics of 2175A extinction [NASA-CR-180926] N87-23336

WORLD CLIMATE PROGRAMME, GENEVA (SWITZERLAND).
Workshop on Comparison of Simulations by Numerical Models of the Sensitivity of the Atmospheric Circulation to Sea Surface Temperature Anomalies
[WCP-121] N87-23034
WORLD METEOROLOGICAL ORGANIZATION, GENEVA (SWITZERLAND).
Proceedings of the Conference on the Scientific Results of the Alpine Experiment (ALPEX), volume 2
[WMO-TD-108-VOL-2] N87-23068
WRIGHT STATE UNIV., DAYTON, OHIO.
Identification and validation of new anthropometric techniques for quantifying body composition
[AD-A178753] N87-23118

Y

YALE UNIV., NEW HAVEN, CONN.
Mesoscale mountain meteorology N87-23069

CONTRACT NUMBER INDEX

SCIENTIFIC AND TECHNICAL AEROSPACE REPORTS VOLUME 25 NUMBER 16

Typical Contract Number Index Listing

N00014-81-C-0006
N87-10545
CONTRACT NUMBER
NASA ACCESSION NUMBER

Listings in this index are arranged alphanumerically by contract number. Under each contract number the NASA accession numbers denoting documents that have been produced as a result of research done under that contract are arranged in ascending order. The NASA accession number denotes the number by which the citation is identified.

AF-AFOSR-0019-83 .... N87-23560
N87-23562

AF-AFOSR-0032-84 .... N87-22912
AF-AFOSR-0034-86 .... N87-22833
AF-AFOSR-0039-84 .... N87-23208
AF-AFOSR-0051-86 .... N87-22902
AF-AFOSR-0056-86 .... N87-23293
AF-AFOSR-0062-83 .... N87-22994
AF-AFOSR-0065-84 .... N87-23291
AF-AFOSR-0075-85 .... N87-22930
AF-AFOSR-0091-86 .... N87-22834
AF-AFOSR-0097-85 .... N87-23219
AF-AFOSR-0119-84 .... N87-22901
AF-AFOSR-0140-83 .... N87-23260
AF-AFOSR-0148-81 .... N87-23260
AF-AFOSR-0184-84 .... N87-22928
AF-AFOSR-0190-84 .... N87-23275
AF-AFOSR-0204-81 .... N87-23261
AF-AFOSR-0212-85 .... N87-23154
AF-AFOSR-0219-84 .... N87-22931
AF-AFOSR-0228-86 .... N87-23111
AF-AFOSR-0266-83 .... N87-23150
AF-AFOSR-0296-85 .... N87-23107
AF-AFOSR-0303-85 .... N87-23208
AF-AFOSR-0391-84 .... N87-23276
ARPA ORDER 3672 .... N87-22897
ARPA ORDER 4871 .... N87-23195
ARPA ORDER 4976 .... N87-23185
N87-23206

ARPA ORDER 5355 .... N87-23017
ARPA ORDER 5794 .... N87-23172
DA PROJ. 1L1-61102-AH-44 .... N87-23289
DA PROJ. 3E1-62772-A-878 .... N87-23115
DA PROJ. 230-5 .... N87-23172
DAAC29-84-C-0007 .... N87-22918
DAAG29-81-K-0110 .... N87-23178
N87-23179
N87-23214
N87-23218
N87-23220
N87-23221
N87-23224
N87-23225
N87-23236
N87-23237
N87-23238
N87-23241
N87-23243
DAAG29-82-K-0029 .... N87-22858
DAAG29-82-K-0169 .... N87-23015
DAAG29-83-K-0056 .... N87-22939
DAAG29-83-K-0065 .... N87-22844
DAAG29-83-K-0067 .... N87-23301
DAAG29-83-K-0120 .... N87-22862
DAAG29-83-K-0121 .... N87-22842
DAAG29-83-K-0140 .... N87-22855
DAAG29-83-K-0147 .... N87-22916
DAAG29-83-K-0166 .... N87-23267
N87-23270

DAAG29-84-C-0006 .... N87-22843
DAAG29-84-C-0014 .... N87-23062
DAAG29-84-C-0015 .... N87-22856
DAAG29-84-K-0028 .... N87-22854
DAAG29-84-K-0030 .... N87-23240
DAAG29-84-K-0045 .... N87-23268
DAAG29-84-K-0078 .... N87-22860
DAAG29-84-K-0081 .... N87-23205
DAAG29-84-K-0115 .... N87-23269
DAAG29-84-K-0140 .... N87-23200
DAAG29-84-K-0183 .... N87-23268
DAAG29-85-C-0027 .... N87-22814
DAAG29-85-K-0002 .... N87-23249
DAAG29-85-K-0003 .... N87-23001
N87-23002

DAAG29-85-K-0145 .... N87-23098
DAAG29-85-K-0183 .... N87-22863
DAAG29-85-K-0190 .... N87-23230
DAAK60-84-C-0054 .... N87-23118
DAAK60-84-C-0086 .... N87-23110
N87-23112

DAAL03-86-G-0074 .... N87-23242
DAAL03-86-K-0014 .... N87-23003
N87-23266

DAMD17-85-C-5136 .... N87-23115
DARPA ORDER 5527 .... N87-22840
DE-AC-76-SN-00052 .... N87-22957
N87-23227

DE-AC02-76ER-02383 .... N87-23210
DE-AC02-81ER-53122 .... N87-23280
DE-AC02-83CH-10093 .... N87-23021
DE-AC03-76SF-00098 .... N87-22839
N87-22908
N87-23298

DE-AC04-76DP-00789 .... N87-22837
N87-22849
N87-22850
N87-22903
N87-22965
N87-22979
N87-22981
N87-22982
N87-23022
N87-23023
N87-23024
N87-23025
N87-23026
N87-23151
N87-23152
N87-23153
N87-23245
N87-23263
N87-23285
N87-23297
N87-23299
DE-AC04-76DP-03533 .... N87-22868
N87-22869
N87-22984
DE-AC04-76DR-00789 .... N87-22935
DE-AC05-84OR-21400 .... N87-22812
N87-22826
N87-22835
N87-22851
N87-22852
N87-22853
N87-22906
N87-22960
N87-23145
N87-23294
DE-AC07-76ID-01570 .... N87-22997
N87-23031
DE-AC08-84NV-10442 .... N87-22922
DE-AS03-83ER-13061 .... N87-22934
DE-AS05-83ER-13123 .... N87-23211
DE-AS08-85NV-10511 .... N87-22963
DE-AT06-72ET-53047 .... N87-23278
DE-FC08-85DP-40200 .... N87-22967
N87-23279
DE-FG02-84ER-13178 .... N87-23264
DE-FG02-84ER-13209 .... N87-23295
DE-FG02-84ER-45102 .... N87-23296
DE-FG02-84ER-45154 .... N87-22836
DE-FG02-85ER-45211 .... N87-22838
DE-FG02-86ER-13560 .... N87-22969
DE-FG02-86ER-53219 .... N87-23277
DE-FG02-87ER-25026 .... N87-23209
DE-FG02-87ER25026 .... N87-23210
DE-FG06-86ER-13472 .... N87-23058
DEN3-347 .... N87-23030
DFG-FI-165/21-3 .... N87-23089
DOT/FA71NA-AP98 .... N87-22884
DTFA01-80-Y-10524 .... N87-23095
F04701-85-C-0086 .... N87-23081
N87-23253
N87-23302

F04704-85-C-0147 .... N87-22871
F12878-85-C-00014 .... N87-23107
F19628-83-C-0090 .... N87-23057
F19628-83-C-0092 .... N87-23056
F19628-85-C-0050 .... N87-23268
F19628-85-C-0143 .... N87-23265
F29601-85-K-0054 .... N87-22707
F30602-81-C-0185 .... N87-22915
F30602-82-C-0161 .... N87-22909
F30602-85-C-0012 .... N87-23197
F33615-84-C-0066 .... N87-23106
F33615-84-C-3216 .... N87-22995
F33615-84-C-5045 .... N87-23005
F33615-84-C-5072 .... N87-23303
F33615-84-K-1520 .... N87-23185
F33615-84K-1520 .... N87-23206
F33615-85-C-2513 .... N87-22683
F49620-82-C-0009 .... N87-23233
F49620-82-C-0014 .... N87-23288
F49620-83-C-0138 .... N87-22862
F49620-84-C-0083 .... N87-23267
F49620-85-C-0027 .... N87-22929
F49620-85-C-0037 .... N87-22822
F49620-85-C-0040 .... N87-23251
F49620-85-C-0041 .... N87-23143
F49620-85-C-0067 .... N87-22819
F49620-86-C-0028 .... N87-22927
F49620-86-C-0082 .... N87-23172
GRI-5085-235-1183 .... N87-22866
GRI-5086-234-1257 .... N87-22891
INAG-APT-RA-82.4822 .... N87-23082
MDA903-83-C-0027 .... N87-23017
MIPR/ARO-100-86 .... N87-22912
MOD(PE)-A94C/2196 .... N87-22989
MOD(PE)-NUW-72A/1287 .... N87-23102
MOD-K/A12/1668 .... N87-23248
MOD-2064/064-XR/FS N87-22893
NAGW-77 .... N87-23323
NAGW-111 .... N87-23352
N87-23354
N87-23453

NAGW-132 .... N87-23541
NAGW-186 .... N87-23435
NAGW-275 .... N87-23316
NAGW-398 .... N87-23383
NAGW-419 .... N87-22890
N87-22921
N87-23273

NAGW-432 .... N87-23358
NAGW-658 .... N87-23514
NAGW-853 .... N87-23326
NAGW-929 .... N87-23381
N87-23383
N87-23393

NAG1-225 .... N87-22734
NAG1-270 .... N87-23230
NAG1-517 .... N87-23208
NAG2-173 .... N87-22633
NAG2-292 .... N87-22890
N87-22921
N87-23273

NAG2-368 .... N87-23340
NAG2-393 .... N87-23563
N87-23564

NAG3-159 .... N87-22700
NAG3-534 .... N87-22796
NAG3-535 .... N87-22790
NAG3-567 .... N87-22865
NAG5-32 .... N87-23065
NAG5-376 .... N87-23563
N87-23564

NAG5-483 .... N87-23063
NAG5-501 .... N87-23561

NAG5-746 .... N87-23033
NAG5-832 .... N87-23336
NAG5-874 .... N87-23066
NASA ORDER E-69204 .... N87-22685
NASA ORDER H-85080B N87-22764
NASW-861 .... N87-23328
NASW-3214 .... N87-23384
NASW-3737 .... N87-22765
NASW-3947 .... N87-23325
NASW-4004 .... N87-23008
NASW-4006 .... N87-22627
NAS1-17070 .... N87-23208
NAS1-17411 .... N87-22692
NAS1-17999 .... N87-23194
NAS1-18107 .... N87-22632
N87-23208
N87-23229
N87-23230
NAS3-23697 .... N87-22996
NAS3-24105 .... N87-22960
NAS3-24362 .... N87-22793
NAS3-24389 .... N87-22784
N87-22785
NAS3-24738 .... N87-22803
NAS5-27430 .... N87-22817
NAS5-28558 .... N87-23091
NAS7-918 .... N87-23426
NAS8-34758 .... N87-22861
NAS8-36191 .... N87-22952
NAS8-36488 .... N87-22758
NAS9-15800 .... N87-22744
NCA2-17 .... N87-22944
NCC-2-22 .... N87-23257
NCC2-55 .... N87-22951
NCC2-173 .... N87-22951
NCC2-324 .... N87-22636
NGL-05-003-017 .... N87-23563
NGL-16-001-002 .... N87-23063
NGT-01-008-021 .... N87-22752
NSF AST-82-04256 .... N87-23381
N87-23383
NSF AST-82-004256 .... N87-23393
NSF ATM-82-17797 .... N87-23081
NSF ATM-82-18215 .... N87-23036
NSF ATM-83-17710 .... N87-23329
NSF ATM-84-17880 .... N87-23323
NSF ATM-84-18625 .... N87-23071
N87-23081
NSF ATM-84-45010 .... N87-23326
NSF ATM-86-17797 .... N87-23079
NSF DCK-85-09668 .... N87-23240
NSF DCR-84-03300 .... N87-23207
N87-23222
NSF DMS-85-03294 .... N87-23230
NSF DMS-86-06964 .... N87-23235
NSF ECS-84-04809 .... N87-23240
NSF MCS-83-04459 .... N87-23383
NSF MEA-83-07785 .... N87-22990
NSG-3079 .... N87-22948
NSG-7156 .... N87-23352
N87-23436
NSG-7312 .... N87-23421
NSG-7437 .... N87-23383
NSG-7590 .... N87-23421
N87-23422
NSG-7606 .... N87-23432
N00014-75-C-0374 .... N87-23007
N00014-78-C-0049 .... N87-22879
N00014-80-C-0483 .... N87-23177
N00014-80-C-0622 .... N87-22897
N87-22920
N00014-80-C-0741 .... N87-23232
N00014-81-C-0006 .... N87-23331
N00014-81-K-0664 .... N87-22829
N00014-82-C-0402 .... N87-22859
N00014-82-K-0294 .... N87-22900
N00014-83-C-2322 .... N87-23272
N00014-83-K-0143 .... N87-22841
N00014-83-K-0180 .... N87-22972
N00014-84-C-0167 .... N87-23234
N87-23235
N00014-84-C-0218 .... N87-23104
N00014-84-C-2245 .... N87-23213
N00014-84-K-0012 .... N87-22828
N00014-85-C-0207 .... N87-22821
N00014-85-C-0659 .... N87-22859
N00014-85-C-2147 .... N87-22827
N00014-85-C-2376 .... N87-22971
N00014-85-K-0077 .... N87-23186
N87-23207
N87-23222
N00014-85-K-0321 .... N87-22889
N00014-85-K-0385 .... N87-23188
N00014-85-K-0404 .... N87-23063
N00014-85-K-0596 .... N87-22990
N00014-85-K-0779 .... N87-22840
N00014-86-C-0803 .... N87-22917
N00014-86-C-0827 .... N87-23019
N00014-86-G-0083 .... N87-23247
N00014-86-K-0043 .... N87-23292
N00014-86-K-0068 .... N87-23560
N87-23562
N00014-86-K-0691 .... N87-23230
N00024-85-C-6041 .... N87-23006
N00039-84-C-0089 .... N87-23195
N61339-85-D-0026 .... N87-23231
N62269-85-C-0222 .... N87-22867
N66001-85-D-0023 .... N87-22983
RF5-7525 .... N87-23177
RR0-1103 .... N87-22828
RR0-4206 .... N87-23188
SWRI PROJ. 15-7435 .... N87-22817
W-31-109-ENG-38 .... N87-23176
W-7405-ENG-36 .... N87-22824
N87-22945
N87-22946
N87-22964
N87-22975
N87-23173
N87-23258
N87-23568
W-7405-ENG-48 .... N87-22697
N87-22823
N87-22905
N87-22907
N87-22933
N87-22936
N87-22955
N87-22968
N87-22970
N87-22996
N87-23032
N87-23174
N87-23175
N87-23262
N87-23399
W-31109-ENG-38 .... N87-22825
N87-22875
N87-22892
N87-22893
N87-22904
N87-22966
N87-22999
N87-23096
N87-23198
N87-23252
N87-23284
N87-23306
307-07-01 .... N87-23304
505-01-00 .... N87-23201
505-40-74 .... N87-23202
505-43-01 .... N87-22629
505-43-31 .... N87-23009
505-43-81 .... N87-22685
505-60-01 .... N87-22932
505-60-01-01 .... N87-23194
505-61-01 .... N87-22956
505-61-51 .... N87-22631
N87-22690
505-62-3A N87-22694
505-62-21 .... N87-22630
505-62-61 .... N87-22681
505-63-01 .... N87-22860
505-63-51 .... N87-22978
505-63-81 .... N87-22811
505-66-01-07 .... N87-22604
505-66-21-01 .... N87-23244
505-66-41 .... N87-23100
505-67-41 .... N87-22634
505-68-91-01 .... N87-22626
505-69-41 .... N87-22680
505-90-21-01 .... N87-22632
N87-23208
N87-23229
N87-23230
506-40-11 .... N87-22943
506-41-11 .... N87-23028
506-41-21 .... N87-23029
506-41-31 .... N87-22802
N87-23020
N87-23027
506-42-11 .... N87-22806
N87-22960
506-42-21 .... N87-22757
506-42-31 .... N87-22804
N87-22805
N87-22807
506-43-11 .... N87-22943
506-44-21 .... N87-22923
506-48-21 .... N87-22949
506-58-22 .... N87-22874
533-04-11 .... N87-22959
N87-22996
553-13-00 .... N87-22766
N87-23010
656-44-10 .... N87-23156
672-22-20-70 .... N87-23101
674-24-05 .... N87-22865
992-21-01 .... N87-22691

REPORT/ACCESSION NUMBER INDEX

Typical Report Number Index Listing

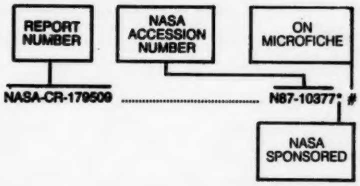

Listings in this index are arranged alphanumerically by report number. The NASA accession number denotes the number by which the citation is identified. An asterisk (*) indicates that the item is a NASA report. A pound sign (#) indicates that the item is available on microfiche.

A-86317 .... N87-22932* #
A-86332 .... N87-22629* #
A-86369 .... N87-22691* #
A-87038 .... N87-22634* #
A-87103 .... N87-22690* #
A-87129 .... N87-23201* #
A-87181 .... N87-22943* #
A-87193 .... N87-22631* #
A-87205 .... N87-22956* #

AAS-86-418 .... N87-23100* #

ACCN-74513 .... N87-23102 #

AD-A177273 .... N87-22990 #
AD-A178447 .... N87-22827 #
AD-A178451 .... N87-22840 #
AD-A178453 .... N87-23115 #
AD-A178454 .... N87-23234 #
AD-A178455 .... N87-23213 #
AD-A178456 .... N87-22828 #
AD-A178457 .... N87-22854 #
AD-A178458 .... N87-23301 #
AD-A178460 .... N87-23177 #
AD-A178461 .... N87-23103 #
AD-A178463 .... N87-22971 #
AD-A178464 .... N87-22909 #
AD-A178465 .... N87-23265 #
AD-A178466 .... N87-23266 #
AD-A178468 .... N87-23060 #
AD-A178472 .... N87-23235 #
AD-A178473 .... N87-23146 #
AD-A178474 .... N87-23116 #
AD-A178480 .... N87-23097 #
AD-A178481 .... N87-23253 #
AD-A178484 .... N87-23061 #
AD-A178485 .... N87-23117 #
AD-A178486 .... N87-23147 #
AD-A178489 .... N87-23302 #
AD-A178492 .... N87-22624 #
AD-A178494 .... N87-22937 #
AD-A178505 .... N87-22910 #
AD-A178508 .... N87-23154 #
AD-A178510 .... N87-22841 #
AD-A178518 .... N87-23000 #
AD-A178519 .... N87-22682 #
AD-A178522 .... N87-23014 #
AD-A178535 .... N87-23104 #
AD-A178540 .... N87-23236 #
AD-A178542 .... N87-23214 #
AD-A178543 .... N87-23237 #
AD-A178544 .... N87-23178 #
AD-A178545 .... N87-23179 #
AD-A178546 .... N87-23238 #
AD-A178550 .... N87-23303 #
AD-A178555 .... N87-23239 #
AD-A178556 .... N87-23240 #
AD-A178557 .... N87-23249 #
AD-A178562 .... N87-22911 #
AD-A178566 .... N87-22688 #
AD-A178577 .... N87-23155 #
AD-A178578 .... N87-22876 #
AD-A178579 .... N87-22877 #
AD-A178581 .... N87-22878 #
AD-A178582 .... N87-23246 #
AD-A178583 .... N87-23180 #
AD-A178584 .... N87-22938 #
AD-A178589 .... N87-23181 #
AD-A178590 .... N87-23062 #
AD-A178592 .... N87-22855 #
AD-A178593 .... N87-22856 #
AD-A178594 .... N87-23001 #
AD-A178595 .... N87-23267 #
AD-A178596 .... N87-22842 #
AD-A178597 .... N87-23002 #
AD-A178598 .... N87-23247 #
AD-A178599 .... N87-22879 #
AD-A178616 .... N87-22880 #
AD-A178623 .... N87-23241 #
AD-A178625 .... N87-22912 #
AD-A178626 .... N87-23003 #
AD-A178627 .... N87-23148 #
AD-A178629 .... N87-22939 #
AD-A178636 .... N87-23182 #
AD-A178638 .... N87-22813 #
AD-A178639 .... N87-22940 #
AD-A178640 .... N87-22857 #
AD-A178641 .... N87-23215 #
AD-A178642 .... N87-23216 #
AD-A178643 .... N87-22881 #
AD-A178644 .... N87-23183 #
AD-A178648 .... N87-22913 #
AD-A178651 .... N87-23063* #
AD-A178652 .... N87-22914 #
AD-A178653 .... N87-22882 #
AD-A178668 .... N87-22941 #
AD-A178679 .... N87-23098 #
AD-A178681 .... N87-23199 #
AD-A178683 .... N87-23268 #
AD-A178694 .... N87-23217 #
AD-A178703 .... N87-23015 #
AD-A178731 .... N87-22814 #
AD-A178744 .... N87-22843 #
AD-A178745 .... N87-22915 #
AD-A178750 .... N87-22815 #
AD-A178751 .... N87-23105 #
AD-A178753 .... N87-23118 #
AD-A178761 .... N87-23269 #
AD-A178762 .... N87-23242 #
AD-A178763 .... N87-23218 #
AD-A178765 .... N87-23205 #
AD-A178769 .... N87-23206 #
AD-A178770 .... N87-23184 #
AD-A178771 .... N87-23185 #
AD-A178774 .... N87-23016 #
AD-A178784 .... N87-23219 #
AD-A178805 .... N87-22883 #
AD-A178806 .... N87-23220 #
AD-A178812 .... N87-23270 #
AD-A178815 .... N87-23017 #
AD-A178816 .... N87-23200 #
AD-A178833 .... N87-22972 #
AD-A178837 .... N87-22916 #
AD-A178841 .... N87-22829 #
AD-A178844 .... N87-22917 #
AD-A178850 .... N87-22884 #
AD-A178851 .... N87-22885 #
AD-A178853 .... N87-22886 #
AD-A178854 .... N87-22660 #
AD-A178855 .... N87-22887 #
AD-A178858 .... N87-23254 #
AD-A178859 .... N87-23255 #
AD-A178862 .... N87-22844 #
AD-A178869 .... N87-22801 #
AD-A178870 .... N87-22761 #
AD-A178872 .... N87-22888 #
AD-A178873 .... N87-22698 #
AD-A178874 .... N87-23119 #
AD-A178876 .... N87-23099 #
AD-A178877 .... N87-22625 #
AD-A178881 .... N87-22689 #
AD-A178882 .... N87-22858 #
AD-A178888 .... N87-23064 #
AD-A178895 .... N87-22918 #
AD-A178903 .... N87-23004 #
AD-A178907 .... N87-22859 #
AD-A178935 .... N87-23221 #
AD-A178941 .... N87-22677 #
AD-A178945 .... N87-22919 #
AD-A178955 .... N87-23186 #
AD-A178958 .... N87-23207 #
AD-A178960 .... N87-23222 #
AD-A178965 .... N87-22973 #
AD-A178967 .... N87-22863 #
AD-A178976 .... N87-23223 #
AD-A178977 .... N87-23187 #
AD-A178978 .... N87-22974 #
AD-A178979 .... N87-23281 #
AD-A178980 .... N87-23271 #
AD-A178982 .... N87-23250 #
AD-A178985 .... N87-23224 #
AD-A178994 .... N87-23005 #
AD-A178996 .... N87-22683 #
AD-A178997 .... N87-22762 #
AD-A178998 .... N87-23565 #
AD-A179009 .... N87-23188 #
AD-A179010 .... N87-22889 #
AD-A179025 .... N87-23243 #
AD-A179027 .... N87-23225 #
AD-A179037 .... N87-22920 #
AD-A179038 .... N87-23006 #
AD-A179041 .... N87-22942 #
AD-A179042 .... N87-23007 #
AD-A179049 .... N87-23226 #
AD-A179050 .... N87-23272 #
AD-A179054 .... N87-22963 #
AD-A179068 .... N87-22696 #
AD-A179069 .... N87-22676 #
AD-A179071 .... N87-23149 #
AD-A179082 .... N87-23231 #
AD-A179099 .... N87-23232 #
AD-A179115 .... N87-22759 #
AD-A179124 .... N87-23287 #
AD-A179126 .... N87-23233 #
AD-A179137 .... N87-23251 #
AD-A179155 .... N87-22661 #
AD-A179163 .... N87-23569 #
AD-A179174 .... N87-23056 #
AD-A179201 .... N87-22961 #
AD-A179204 .... N87-22754 #
AD-A179205 .... N87-22756 #
AD-A179213 .... N87-22993 #
AD-A179214 .... N87-22809 #
AD-A179216 .... N87-23106 #
AD-A179217 .... N87-23107 #
AD-A179261 .... N87-23150 #
AD-A179269 .... N87-22701 #
AD-A179270 .... N87-23108 #
AD-A179272 .... N87-22871 #
AD-A179289 .... N87-22867 #
AD-A179303 .... N87-22897 #
AD-A179307 .... N87-22872 #
AD-A179310 .... N87-23143 #
AD-A179322 .... N87-23195 #
AD-A179334 .... N87-22662 #
AD-A179336 .... N87-23203 #
AD-A179339 .... N87-23311 #
AD-A179341 .... N87-23204 #
AD-A179342 .... N87-22925 #
AD-A179343 .... N87-23109 #
AD-A179344 .... N87-22898 #
AD-A179346 .... N87-23288 #
AD-A179353 .... N87-23019 #
AD-A179358 .... N87-22819 #
AD-A179366 .... N87-23289 #
AD-A179375 .... N87-23172 #
AD-A179383 .... N87-23290 #
AD-A179384 .... N87-23196 #
AD-A179385 .... N87-22699 #
AD-A179387 .... N87-23338 #
AD-A179388 .... N87-22687 #
AD-A179389 .... N87-22899 #
AD-A179390 .... N87-22820 #
AD-A179391 .... N87-22821 #
AD-A179402 .... N87-22873 #
AD-A179407 .... N87-23197 #
AD-A179423 .... N87-22679 #

AD-A179424 .... N87-22763 #
AD-A179425 .... N87-22760 #
AD-A179426 .... N87-23310 #
AD-A179428 .... N87-22962 #
AD-A179433 .... N87-23291 #
AD-A179436 .... N87-22900 #
AD-A179472 .... N87-23110 #
AD-A179489 .... N87-23260 #
AD-A179490 .... N87-23261 #
AD-A179501 .... N87-23111 #
AD-A179512 .... N87-22623 #
AD-A179524 .... N87-22901 #
AD-A179525 .... N87-23292 #
AD-A179536 .... N87-22926 #
AD-A179550 .... N87-23012 #
AD-A179561 .... N87-23275 #
AD-A179563 .... N87-22994 #
AD-A179564 .... N87-23057 #
AD-A179566 .... N87-23112 #
AD-A179578 .... N87-22927 #
AD-A179579 .... N87-22928 #
AD-A179602 .... N87-22929 #
AD-A179604 .... N87-23293 #
AD-A179606 .... N87-22833 #
AD-A179612 .... N87-22930 #
AD-A179650 .... N87-23560 #
AD-A179651 .... N87-22834 #
AD-A179661 .... N87-22931 #
AD-A179664 .... N87-23561* #
AD-A179665 .... N87-22862 #
AD-A179676 .... N87-22822 #
AD-A179686 .... N87-22995 #
AD-A179689 .... N87-22810 #
AD-A179690 .... N87-22800 #
AD-A179691 .... N87-23144 #
AD-A179693 .... N87-23276 #
AD-A179694 .... N87-22988 #
AD-A179698 .... N87-23562 #
AD-A179699 .... N87-22902 #

AEDC-TR-87-7 .... N87-22941 #

AERE-R-12308 .... N87-22986 #
AERE-R-12322 .... N87-22830 #
AERE-R-12382 .... N87-22991 #

AFC-30001-ANNUAL .... N87-22866 #

AFGL-ERP-963 .... N87-23097 #

AFGL-TR-86-0203 .... N87-23056 #
AFGL-TR-86-0210 .... N87-23097 #
AFGL-TR-86-0213 .... N87-23057 #
AFGL-TR-87-0128 .... N87-23012 #

AFHRL-TR-86-52 .... N87-23146 #
AFHRL-TR-86-54 .... N87-23108 #

AFIT/CS/ENG/86D-12 .... N87-23311 #

AFIT/GA/AA/85D-8 .... N87-22899 #
AFIT/GA/AA/86D-3 .... N87-22754 #
AFIT/GA/AA/86D-5 .... N87-22756 #
AFIT/GA/AA/86D-6 .... N87-22993 #
AFIT/GA/AA/86D-7 .... N87-23338 #
AFIT/GA/AA/86D-14 .... N87-22763 #

AFIT/GAE/AA/86-02 .... N87-22938 #
AFIT/GAE/AA/86D-3 .... N87-22813 #
AFIT/GAE/AA/86D-4 .... N87-22940 #
AFIT/GAE/AA/86D-5 .... N87-22857 #
AFIT/GAE/AA/86D-6 .... N87-22809 #
AFIT/GAE/AA/86D-7 .... N87-22925 #
AFIT/GAE/AA/86J-2 .... N87-22687 #
AFIT/GAE/AA/87M-2 .... N87-23204 #
AFIT/GAE/AA/87M-4 .... N87-22623 #

AFIT/GAE/ENG/87M-1 .... N87-22676 #

AFIT/GCE/ENG/86D-2 .... N87-23196 #

AFIT/GCE/MA/86D-1 .... N87-22913 #

AFIT/GCS/ENG/86D-8 .... N87-23181 #
AFIT/GCS/ENG/86D-17 .... N87-23149 #
AFIT/GCS/ENG/86D-19 .... N87-23180 #
AFIT/GCS/ENG/86D-21 .... N87-23119 #

AFIT/GCS/MA/86D-1 .... N87-23182 #

AFIT/GE/EE/86D-31 .... N87-22887 #

AFIT/GE/ENG/86D-10 .... N87-22660 #
AFIT/GE/ENG/86D-17 .... N87-22698 #
AFIT/GE/ENG/86D-25 .... N87-23183 #
AFIT/GE/ENG/86D-26 .... N87-22886 #
AFIT/GE/ENG/86D-29 .... N87-22881 #
AFIT/GE/ENG/86D-30 .... N87-22884 #
AFIT/GE/ENG/86D-34 .... N87-22878 #
AFIT/GE/ENG/86D-35 .... N87-23290 #
AFIT/GE/ENG/86D-37 .... N87-22974 #
AFIT/GE/ENG/86D-38 .... N87-22888 #
AFIT/GE/ENG/86D-41 .... N87-22761 #
AFIT/GE/ENG/86D-44-VOL-1 .... N87-22898 #
AFIT/GE/ENG/86D-45 .... N87-23187 #
AFIT/GE/ENG/86D-49 .... N87-23216 #
AFIT/GE/ENG/86D-52 .... N87-22877 #
AFIT/GE/ENG/86D-58 .... N87-22885 #

AFIT/GEP/ENP/86D-5 .... N87-22820 #
AFIT/GEP/ENP/86D-8 .... N87-23099 #
AFIT/GEP/ENP/86D-10 .... N87-22899 #
AFIT/GEP/ENP/87M-1 .... N87-23271 #

AFIT/GNE/EN/87M-4 .... N87-23281 #

AFIT/GOR/MA/86D-2 .... N87-23215 #
AFIT/GOR/MA/86D-5 .... N87-23246 #
AFIT/GOR/MA/86D-6 .... N87-23226 #

AFIT/GOR/OS/86-12 .... N87-23203 #
AFIT/GOR/OS/86D-5 .... N87-22760 #

AFIT/GSO/AA/86D-4 .... N87-22759 #

AFIT/GSO/ENG/86D-1 .... N87-22762 #

AFIT/GSO/ENP/86D-1 .... N87-22801 #

AFIT/GSO/ENS-ENG/86D-1 .... N87-22662 #

AFIT/GSO/ENS/86D-4 .... N87-23310 #

AFOSR-86-1041TR .... N87-23154 #
AFOSR-87-0319TR .... N87-23233 #
AFOSR-87-0322TR .... N87-23143 #
AFOSR-87-0329TR .... N87-23251 #
AFOSR-87-0332TR .... N87-23287 #
AFOSR-87-0341TR .... N87-23288 #
AFOSR-87-0357TR .... N87-22929 #
AFOSR-87-0368TR .... N87-22822 #
AFOSR-87-0411TR .... N87-22902 #
AFOSR-87-0414TR .... N87-23276 #
AFOSR-87-0428TR .... N87-22931 #
AFOSR-87-0436TR .... N87-22834 #
AFOSR-87-0441TR .... N87-22833 #
AFOSR-87-0447TR .... N87-23293 #
AFOSR-87-0452TR .... N87-22928 #
AFOSR-87-0455TR .... N87-22901 #
AFOSR-87-0456TR .... N87-23260 #
AFOSR-87-0457TR .... N87-23111 #
AFOSR-87-0460TR .... N87-22819 #
AFOSR-87-0461TR .... N87-23172 #
AFOSR-87-0463TR .... N87-23150 #
AFOSR-87-0483TR .... N87-22994 #
AFOSR-87-0494TR .... N87-23261 #
AFOSR-87-0521TR .... N87-23291 #
AFOSR-87-0524TR .... N87-23275 #
AFOSR-87-0555TR .... N87-22930 #
AFOSR-87-0563TR .... N87-22927 #
AFOSR-87-0565TR .... N87-22862 #

AFRPL-TR-87-001 .... N87-22863 #

AFWAL-TR-86-2072 .... N87-22683 #
AFWAL-TR-86-3032-VOL-1 .... N87-22995 #
AFWAL-TR-86-3089-PT-1-PT-2 .... N87-22625 #
AFWAL-TR-86-3093 .... N87-23148 #
AFWAL-TR-86-4098 .... N87-23005 #
AFWAL-TR-86-4103 .... N87-23303 #

AFWL-TR-85-34 .... N87-22919 #

AGARD-CP-409 .... N87-22663 #

AIAA-87-1746 .... N87-22681* #
AIAA-87-1764 .... N87-22949* #
AIAA-87-1766 .... N87-22757* #
AIAA-87-1773 .... N87-22806* #
AIAA-87-1948 .... N87-22804* #
AIAA-87-1950 .... N87-22807* #
AIAA-87-2028 .... N87-22805* #
AIAA-87-9035 .... N87-23028* #
AIAA-87-9203 .... N87-23020* #
AIAA-87-9232 .... N87-23027* #
AIAA-87-9260 .... N87-23029* #
AIAA-87-9442 .... N87-22802* #

ALZETA-86-722-129 .... N87-22891 #

ANAMET-ASIAC-585.1A-VOL-1 .... N87-22995 #

ANL-HEP-CP-86-132 .... N87-22966 #

ANL/MCS-TM-87 .... N87-23196 #

AR-9 .... N87-22879 #
AR-004-493 .... N87-23011 #

ARC-87-154 .... N87-22827 #

ARCCB-TR-87003 .... N87-22701 #

ARE-TM(UMD)-85574 .... N87-22831 #

ARE-TM(JMT)-86405 .... N87-22846 #

ARE-TR-86122 .... N87-23102 #

ARL-STRUC-R-421 .... N87-23011 #

ARL/PSU-TM-86-215 .... N87-23006 #

ARL/STRUC-TM-451 .... N87-22682 #
ARL/STRUC-TM-454 .... N87-23000 #

ARO-15 .... N87-23566 #
ARO-16 .... N87-23567 #
ARO-18072.14-MA .... N87-23237 #
ARO-18072.15-MA .... N87-23241 #
ARO-18072.17-MA .... N87-23236 #
ARO-18072.18-MA .... N87-23178 #
ARO-18072.19-MA .... N87-23218 #
ARO-18072.20-MA .... N87-23179 #
ARO-18072.21-MA .... N87-23220 #
ARO-18072.22-MA .... N87-23238 #
ARO-18072.23-MA .... N87-23224 #
ARO-18072.24-MA .... N87-23225 #
ARO-18072.25-MA .... N87-23214 #
ARO-18072.26-MA .... N87-23221 #
ARO-18072.27-MA .... N87-23243 #
ARO-18560.30-EG .... N87-22858 #
ARO-19327.9-GS .... N87-23015 #
ARO-19785.3-MS .... N87-22844 #
ARO-19976.3-EG .... N87-22939 #
ARO-20068.14-MS .... N87-23301 #
ARO-20583.13-EL .... N87-22882 #
ARO-20637.17-EL .... N87-22916 #
ARO-20642.5-MS .... N87-22842 #
ARO-20674.27-CH .... N87-22855 #
ARO-20803.7-MA .... N87-23205 #
ARO-20842.11-CH .... N87-22854 #
ARO-20910.6-MA .... N87-23249 #
ARO-20927.17-MA .... N87-23240 #
ARO-21016.1-GS .... N87-23269 #
ARO-21019.3-PH .... N87-22918 #
ARO-21051.10-PH .... N87-23270 #
ARO-21051.13-PH .... N87-23267 #
ARO-21056.34-PH .... N87-22912 #
ARO-21181.2-MS .... N87-22856 #
ARO-21289.3-MS .... N87-22843 #
ARO-21378.9-EL .... N87-22880 #
ARO-21453.8-MA .... N87-23200 #
ARO-21655.8-GS-S .... N87-23062 #
ARO-21671.6-EG .... N87-23268 #
ARO-21830.9-GS .... N87-23098 #
ARO-22148.3-EG .... N87-23268 #
ARO-22306.7-EG .... N87-23001 #
ARO-22306.8-EG .... N87-23002 #
ARO-22634.5-EL .... N87-22883 #
ARO-22817.4-MS-S .... N87-22814 #
ARO-23568.1-MA-CF .... N87-23242 #
ARO-23573.13-EG .... N87-23268 #
ARO-23573.15-EG .... N87-23003 #

ARPAD-TR-87001 .... N87-22988 #

ASR-3 .... N87-22996* #

ATR-86(8433)-4 .... N87-23282 #

AVSCOM-TR-87-C-10 .... N87-22978* #

AWRE-0-12/85 .... N87-22947 #

BCD-SSME-TR-87-1 .... N87-22765* #

BMO-TR-87-19 .... N87-22871 #

BR-97934 .... N87-22947 #

BRL-MR-3559 .... N87-22937 #
BRL-MR-3561 .... N87-22624 #

BR79765 .... N87-22832 #
BR97667 .... N87-22992 #
BR98642 .... N87-22989 #
BR98783 .... N87-22693 #

BR99605 N87-22987 #
BR100264 N87-23248 #
BR100407 N87-22846 #
BR100464 N87-22831 #
BR101469 N87-23102 #

CCEE-447222-1 N87-23154 #

CERC-87-4 N87-23105 #

CFD-18 N87-22944* #

CMU/SEI-86-TR-4 N87-23206 #
CMU/SEI-86-TR-5 N87-23184 #
CMU/SEI-86-TR-6 N87-23185 #

CONF-860198-1 N87-22955 #
CONF-860330-3 N87-22967 #
CONF-860340-16 N87-22836 #
CONF-860880-46 N87-22968 #
CONF-860961 N87-22954 #
CONF-861038-9 N87-22966 #
CONF-861106-21 N87-23279 #
CONF-861207-78 N87-22826 #
CONF-861207-79 N87-22853 #
CONF-861207-80 N87-22835 #
CONF-861207-88 N87-23284 #
CONF-861254-1 N87-22875 #
CONF-861258-1 N87-22812 #
CONF-870102-13 N87-23252 #
CONF-870114-3 N87-22905 #
CONF-870128-2 N87-23096 #
CONF-870132-3 N87-22965 #
CONF-870150-1 N87-23145 #
CONF-870157-1 N87-23568 #
CONF-870159-1 N87-23175 #
CONF-870162-1 N87-22697 #
CONF-870204-2 N87-22823 #
CONF-870254-1 N87-23294 #
CONF-870254-2 N87-22851 #
CONF-870307-7 N87-23022 #
CONF-870307-9 N87-23021 #
CONF-870354-1 N87-22980 #
CONF-870365-1 N87-23297 #
CONF-870388-2 N87-23285 #
CONF-870388-3 N87-22837 #
CONF-870398-1-SUMM N87-23245 #
CONF-870399-1 N87-23176 #
CONF-870401-2 N87-22964 #
CONF-870410-4 N87-22849 #
CONF-870410-5 N87-22850 #
CONF-870438-1 N87-23299 #
CONF-870459 N87-23262 #
CONF-870477-1 N87-23023 #
CONF-870510-1 N87-22979 #
CONF-870513-1 N87-22903 #
CONF-870513-2 N87-22981 #
CONF-870516-2 N87-22906 #
CONF-870538-4 N87-23174 #
CONF-870565-1 N87-23151 #
CONF-870574-2 N87-23153 #
CONF-870726-1 N87-23209 #
CONF-8608157-2 N87-23306 #
CONF-8609132-13 N87-22825 #
CONF-8610122-9 N87-22904 #
CONF-8610217-1 N87-22824 #
CONF-8610240-1 N87-22999 #
CONF-8610257-1 N87-23173 #
CONF-8611110-2 N87-22997 #
CONF-8611126-1 N87-22998 #

CP/8/34-507 N87-22989 #

CPL-87-1 N87-23143 #

CSL-TR-87-321 N87-22890* #
CSL-TR-87-322 N87-23273* #
CSL-TR-87-331 N87-22921* #

CU-CS-360-87 N87-23200 #

CUED/D-STRUCT/TR.109 N87-22992 #

DATA-124-VOL-2/6 N87-23104 #

DE86-006596 N87-22954 #
DE87-001130 N87-23021 #
DE87-001423 N87-22979 #
DE87-001444 N87-22997 #
DE87-001696 N87-22963 #
DE87-002488 N87-22849 #
DE87-002693 N87-22850 #
DE87-002696 N87-22903 #
DE87-002814 N87-22980 #
DE87-003035 N87-23245 #
DE87-003241 N87-22823 #
DE87-003466 N87-22955 #
DE87-003499 N87-22981 #
DE87-003503 N87-23022 #
DE87-003711 N87-22964 #
DE87-003715 N87-22824 #
DE87-003818 N87-22998 #
DE87-004273 N87-22812 #
DE87-004523 N87-22965 #
DE87-004709 N87-22875 #
DE87-004819 N87-22904 #
DE87-004938 N87-22999 #
DE87-004948 N87-23306 #
DE87-004963 N87-22966 #
DE87-004975 N87-22825 #
DE87-005073 N87-22905 #
DE87-005192 N87-23145 #
DE87-005204 N87-22933 #
DE87-005438 N87-23277 #
DE87-005524 N87-23023 #
DE87-005527 N87-23151 #
DE87-005543 N87-23209 #
DE87-005553 N87-23058 #
DE87-005554 N87-23278 #
DE87-005710 N87-23294 #
DE87-005721 N87-22851 #
DE87-005785 N87-22888 #
DE87-005915 N87-22967 #
DE87-005916 N87-23279 #
DE87-005946 N87-22968 #
DE87-005991 N87-23210 #
DE87-006002 N87-22934 #
DE87-006054 N87-23568 #
DE87-006066 N87-23173 #
DE87-006259 N87-23295 #
DE87-006292 N87-22969 #
DE87-006294 N87-23296 #
DE87-006305 N87-23262 #
DE87-006328 N87-23024 #
DE87-006331 N87-23025 #
DE87-006407 N87-23280 #
DE87-006447 N87-22852 #
DE87-006466 N87-23174 #
DE87-006467 N87-22697 #
DE87-006612 N87-22826 #
DE87-006613 N87-22835 #
DE87-006624 N87-22906 #
DE87-006628 N87-22853 #
DE87-006663 N87-23211 #
DE87-006683 N87-22907 #
DE87-006712 N87-23297 #
DE87-006723 N87-22970 #
DE87-006769 N87-23152 #
DE87-006770 N87-23263 #
DE87-006791 N87-22935 #
DE87-006799 N87-23312 #
DE87-006823 N87-23175 #
DE87-006882 N87-23198 #
DE87-006895 N87-23153 #
DE87-006917 N87-23264 #
DE87-006931 N87-23296 #
DE87-006973 N87-23284 #
DE87-007001 N87-23096 #
DE87-007006 N87-23176 #
DE87-007032 N87-23252 #
DE87-007068 N87-22836 #
DE87-007075 N87-23258 #
DE87-007086 N87-23285 #
DE87-007183 N87-22892 #
DE87-007194 N87-22893 #
DE87-007392 N87-22837 #
DE87-007432 N87-23026 #
DE87-007522 N87-22936 #
DE87-007526 N87-22982 #
DE87-007560 N87-22838 #
DE87-007600 N87-22839 #
DE87-007607 N87-22908 #
DE87-007678 N87-23299 #
DE87-701211 N87-23283 #
DE87-701531 N87-23307 #
DE87-701537 N87-23300 #
DE87-701552 N87-23212 #
DE87-701559 N87-23339 #
DE87-701562 N87-23059 #

DME-007 N87-22808 #

DOE/DP-40200/30 N87-22967 #
DOE/DP-40200/31 N87-23279 #

DOE/ER-13081/T2 N87-22934 #
DOE/ER-13123/3 N87-23211 #
DOE/ER-13178/3 N87-23264 #
DOE/ER-13209/1 N87-23295 #
DOE/ER-13472/1 N87-23058 #
DOE/ER-13560/1 N87-22969 #
DOE/ER-25026/1 N87-23209 #
DOE/ER-25026/2 N87-23210 #
DOE/ER-45102/T1 N87-23296 #
DOE/ER-45211/1 N87-22838 #
DOE/ER-53122/3 N87-23280 #
DOE/ER-53219/1 N87-23277 #

DOE/ET-53047/25 N87-23278 #

DOE/METC-86-6069 N87-22954 #

DOE/NBB-0077 N87-23032 #

DOE/NV-10511/1 N87-22963 #

DOE/NV/10442-1 N87-22922 #

DOE/TIC-4500 N87-22957 #

DOT/FAA/AT-87/1 N87-23067 #

DOT/FAA/CT-86/23 N87-22864 #
DOT/FAA/CT-86/42 N87-22684 #

DOT/FAA/DL-87/1 N87-23067 #

DOT/FAA/PM-87/7 N87-23095 #

DOT/FAA/VS-87/1 N87-23067 #

E-3107 N87-22860* #
E-3189 N87-23202* #
E-3220 N87-22923* #
E-3267 N87-22694* #
E-3339 N87-22630* #
E-3369 N87-22959* #
E-3379 N87-23304* #
E-3492 N87-22681* #
E-3512 N87-22766* #
E-3515 N87-22865* #
E-3533 N87-22811* #
E-3542 N87-22680* #
E-3547 N87-22757* #
E-3549 N87-23020* #
E-3550 N87-22960* #
E-3553 N87-22804* #
E-3576 N87-23027* #
E-3582 N87-22755* #
E-3583 N87-23010* #
E-3591 N87-23028* #
E-3600 N87-23029* #
E-3601 N87-22802* #
E-3603 N87-22978* #
E-3616 N87-22874* #
E-3617 N87-22949* #
E-3618 N87-22805* #
E-3623 N87-22807* #
E-3639 N87-22806* #

EGG-M-32586 N87-22997 #

EGG-2439 N87-23031 #

EMC-87-1 N87-22883 #

EO/MO-9 N87-22882 #

EOARD-85-0056 N87-23107 #

EOTR-87-2 N87-23231 #

ERL-0363-TM N87-22910 #

ESD-TR-86-208 N87-23206 #
ESD-TR-86-209 N87-23184 #
ESD-TR-86-212 N87-23185 #

ESL-717220-1 N87-22889 #
ESL-718109-1 N87-22879 #

ETN-87-99180 N87-23068 #
ETN-87-99182 N87-23034 #
ETN-87-99456 N87-22989 #
ETN-87-99552 N87-22818
ETN-87-99553 N87-23305
ETN-87-99669 N87-22695
ETN-87-99786 N87-23337 #
ETN-87-99809 N87-23102 #
ETN-87-99810 N87-22831 #
ETN-87-99811 N87-22846 #
ETN-87-99818 N87-22987 #
ETN-87-99819 N87-22832 #
ETN-87-99820 N87-23248 #
ETN-87-99821 N87-22992 #
ETN-87-99822 N87-22693 #
ETN-87-99823 N87-23308 #
ETN-87-99923 N87-22924 #

ETN-87-99924 N87-23256 #
ETN-87-99928 N87-22686 #

FLOW-TR-401 N87-22819 #

FR-4 N87-22828 #
FR-19289-2 N87-22803* #

FTD-ID(RS)T-0189-87 N87-23106 #
FTD-ID(RS)T-0432-86 N87-22800 #
FTD-ID(RS)T-1168-86 N87-22661 #
FTD-ID(RS)T-1312-86 N87-22896 #

GARP-PUBL-SER-27-VOL-2 N87-23068 #

GL-4157 N87-23288 #

GRI-86/0267 N87-22891 #
GRI-86/0277 N87-22886 #

H-1352 N87-23009* #
H-1361 N87-22685* #
H-1399 N87-23100* #

HAC-REF-F4767 N87-23287 #

HDL-SR-87-1 N87-23289 #

HEL-TM-6-87 N87-23144 #

HSD-TR-87-005 N87-23569 #

HTL-47 N87-22944* #

IAEA-CN-47/B-I-5 N87-23279 #

IC-86/182 N87-23307 #
IC-86/197 N87-23300 #
IC-86/238 N87-23212 #
IC-86/291 N87-23339 #
IC-86/329 N87-23059 #

ICASE-87-15 N87-23229* #
ICASE-87-32 N87-23208* #
ICASE-87-33 N87-23230* #
ICASE-87-35 N87-22632* #

IPPJ-812 N87-23274 #

ISBN-0-85518166-4 N87-22947 #
ISBN-92-835-0408-9 N87-22663 #

ISSN-0023-2718 N87-23008* #
ISSN-0348-7539 N87-23337 #
ISSN-0469-4732 N87-23274 #

ISU-ERI-AMES-87296 N87-22944* #

JAYCOR-J206-87-001/6252 N87-22971 #

JHU/ECE-87/04 N87-23219 #

JIAA-TR-56 N87-22633* #
JIAA-TR-70 N87-22951* #

JPRS-USB-86-007 N87-23120 #

JTCG/AS-86-T-001 N87-22815 #

KAPL-4193 N87-22957 #
KAPL-4194 N87-23227 #

KFTI-85-5 N87-23283 #

KK-8F-161 N87-23107 #

L-16215 N87-22626* #
L-16255 N87-22604* #
L-16264 N87-23244* #

LA-TR-87-9 N87-23258 #

LA-UR-86-3916 N87-22964 #
LA-UR-86-4043 N87-22824 #
LA-UR-87-409 N87-23568 #
LA-UR-87-673 N87-23173 #

LA-10728-MS N87-22945 #
LA-10744 N87-22975 #
LA-10781-MS N87-22946 #

LBL-PUB-606 N87-23298 #

LBL-22705 N87-22908 #
LBL-22753 N87-22839 #

LC-86-600570 N87-23309 #
LC-86-600589 N87-23171 #
LC-86-600602 N87-23170 #

LMSC-F145665 N87-22856 #

M-554-PT-1 N87-22702* #
M-554-PT-2 N87-22729* #
M-560 N87-23313* #

MBB-UA-914/85 N87-23256 #
MBB-UA-938/86 N87-22924 #

MBB-UD-483/86 N87-22686 #

MQAD-317 N87-22832 #
MQAD-328 N87-22987 #

MRL-R-1030 N87-22911 #

MTI-86-TR-36 N87-22683 #

NADC-86047-60 N87-22810 #

NAE-AN-36 N87-22628 #

NAMRL-1324 N87-23117 #
NAMRL-1325 N87-23147 #

NAPC-PE-154C N87-22684 #

NAS 1.15:86812 N87-23009* #
NAS 1.15:87353 N87-22860* #
NAS 1.15:87818 N87-23018* #
NAS 1.15:88285 N87-23100* #
NAS 1.15:88326 N87-22932* #
NAS 1.15:88346 N87-22691* #
NAS 1.15:88354 N87-22629* #
NAS 1.15:88534 N87-22627* #
NAS 1.15:88908 N87-22681* #
NAS 1.15:88915 N87-22630* #
NAS 1.15:88937 N87-23304* #
NAS 1.15:88953 N87-22959* #
NAS 1.15:89151 N87-23101* #
NAS 1.15:89372 N87-23189* #
NAS 1.15:89374 N87-23193* #
NAS 1.15:89375 N87-23190* #
NAS 1.15:89376 N87-23191* #
NAS 1.15:89377 N87-23192* #
NAS 1.15:89428 N87-22690* #
NAS 1.15:89434 N87-23201* #
NAS 1.15:89450 N87-22943* #
NAS 1.15:89462 N87-22956* #
NAS 1.15:89494 N87-22631* #
NAS 1.15:89810 N87-23341* #
NAS 1.15:89865 N87-22811* #
NAS 1.15:89868 N87-22680* #
NAS 1.15:89872 N87-23020* #
NAS 1.15:89873 N87-22757* #
NAS 1.15:89876 N87-22804* #
NAS 1.15:89888 N87-23027* #
NAS 1.15:89891 N87-23010* #
NAS 1.15:89894 N87-22755* #
NAS 1.15:89907 N87-23029* #
NAS 1.15:89908 N87-23028* #
NAS 1.15:89909 N87-22802* #
NAS 1.15:89912 N87-22978* #
NAS 1.15:89920 N87-22874* #
NAS 1.15:89921 N87-22949* #
NAS 1.15:89924 N87-22807* #
NAS 1.15:100104 N87-22806* #
NAS 1.15:100120 N87-22805* #
NAS 1.21:7011(298) N87-23114*
NAS 1.21:7041(53) N87-23013*
NAS 1.26:86591 N87-22696* #
NAS 1.26:166623 N87-22685* #
NAS 1.26:168348 N87-22817* #
NAS 1.26:178267 N87-23229* #
NAS 1.26:178299 N87-23194* #
NAS 1.26:178303 N87-23208* #
NAS 1.26:178304 N87-23230* #
NAS 1.26:178305 N87-22692* #
NAS 1.26:178308 N87-22632* #
NAS 1.26:179079 N87-22765* #
NAS 1.26:179082 N87-22764* #
NAS 1.26:179085 N87-22758* #
NAS 1.26:179086 N87-22952* #
NAS 1.26:179118 N87-22861* #
NAS 1.26:179494 N87-22996* #
NAS 1.26:179596 N87-22803* #
NAS 1.26:179603 N87-23030* #
NAS 1.26:179619 N87-22960* #
NAS 1.26:179628 N87-22865* #
NAS 1.26:180219 N87-23561* #
NAS 1.26:180520 N87-23033* #
NAS 1.26:180604 N87-23257* #

NAS 1.26:180926 N87-23336* #
NAS 1.26:180928 N87-23564* #
NAS 1.26:180929 N87-23563* #
NAS 1.26:180930 N87-23063* #
NAS 1.26:180933 N87-23340* #
NAS 1.26:180934 N87-23273* #
NAS 1.26:180935 N87-22890* #
NAS 1.26:180936 N87-22921* #
NAS 1.26:180939 N87-22944* #
NAS 1.26:180987 N87-22948* #
NAS 1.26:181004 N87-23066* #
NAS 1.26:181015 N87-23065* #
NAS 1.26:181019 N87-22951* #
NAS 1.26:181020 N87-22633* #
NAS 1.55:2452 N87-22604* #
NAS 1.55:2455 N87-22634* #
NAS 1.55:2463 N87-23156* #
NAS 1.55:2467-PT-1 N87-22702* #
NAS 1.55:2467-PT-2 N87-22729* #
NAS 1.55:2469 N87-23313* #
NAS 1.55:2471 N87-22766* #
NAS 1.60:2672 N87-23202* #
NAS 1.60:2675 N87-22923* #
NAS 1.60:2683 N87-22626* #
NAS 1.60:2702 N87-22694* #
NAS 1.60:2709 N87-23244* #
NAS 1.60:2732 N87-22870* #
NAS 1.77:20016 N87-23008* #
NAS 1.181017 N87-22700* #

NASA-CASE-ARC-11429-2-CU N87-22845*

NASA-CASE-GSC-12961-1 N87-22895*

NASA-CASE-LAR-12984-1 N87-22678*
NASA-CASE-LAR-13009-2 N87-22976*
NASA-CASE-LAR-13444-1-CU N87-22847*
NASA-CASE-LAR-13452-1 N87-22848*

NASA-CASE-MFS-25964-2 N87-22977*

NASA-CASE-MSC-20841-1 N87-22950*
NASA-CASE-MSC-20979-1 N87-22985*

NASA-CASE-NPO-15800-2 N87-23286*
NASA-CASE-NPO-16337-1-CU N87-22894*
NASA-CASE-NPO-16544-1-CU N87-22953*
NASA-CASE-NPO-16558-1-CU N87-23259* #

NASA-CP-2452 N87-22604* #
NASA-CP-2455 N87-22634* #
NASA-CP-2463 N87-23156* #
NASA-CP-2467-PT-1 N87-22702* #
NASA-CP-2467-PT-2 N87-22729* #
NASA-CP-2469 N87-23313* #
NASA-CP-2471 N87-22766* #

NASA-CR-166623 N87-22685* #
NASA-CR-168348 N87-22817* #
NASA-CR-178267 N87-23229* #
NASA-CR-178299 N87-23194* #
NASA-CR-178303 N87-23208* #
NASA-CR-178304 N87-23230* #
NASA-CR-178305 N87-22692* #
NASA-CR-178308 N87-22632* #
NASA-CR-179079 N87-22765* #
NASA-CR-179082 N87-22764* #
NASA-CR-179085 N87-22758* #
NASA-CR-179086 N87-22952* #
NASA-CR-179118 N87-22861* #
NASA-CR-179494 N87-22996* #
NASA-CR-179596 N87-22803* #
NASA-CR-179603 N87-23030* #
NASA-CR-179619 N87-22960* #
NASA-CR-179628 N87-22865* #
NASA-CR-180219 N87-23561* #
NASA-CR-180520 N87-23033* #
NASA-CR-180604 N87-23257* #
NASA-CR-180926 N87-23336* #
NASA-CR-180928 N87-23564* #
NASA-CR-180929 N87-23563* #
NASA-CR-180930 N87-23063* #
NASA-CR-180933 N87-23340* #
NASA-CR-180934 N87-23273* #
NASA-CR-180935 N87-22890* #
NASA-CR-180936 N87-22921* #
NASA-CR-180939 N87-22944* #
NASA-CR-180987 N87-22948* #
NASA-CR-181004 N87-23066* #
NASA-CR-181015 N87-23065* #
NASA-CR-181017 N87-22700* #
NASA-CR-181019 N87-22951* #
NASA-CR-181020 N87-22633* #

NASA-SP-7011(298) N87-23114*
NASA-SP-7041(53) N87-23013*

NASA-TM-86591 .... N87-22696* #
NASA-TM-86812 .... N87-23009* #
NASA-TM-87353 .... N87-22860* #
NASA-TM-87818 .... N87-23018* #
NASA-TM-88285 .... N87-23100* #
NASA-TM-88326 .... N87-22932* #
NASA-TM-88346 .... N87-22691* #
NASA-TM-88354 .... N87-22629* #
NASA-TM-88534 .... N87-22627* #
NASA-TM-88908 .... N87-22681* #
NASA-TM-88915 .... N87-22630* #
NASA-TM-88937 .... N87-23304* #
NASA-TM-88953 .... N87-22959* #
NASA-TM-89151 .... N87-23101* #
NASA-TM-89372 .... N87-23189* #
NASA-TM-89374 .... N87-23193* #
NASA-TM-89375 .... N87-23190* #
NASA-TM-89376 .... N87-23191* #
NASA-TM-89377 .... N87-23192* #
NASA-TM-89428 .... N87-22690* #
NASA-TM-89434 .... N87-23201* #
NASA-TM-89450 .... N87-22943* #
NASA-TM-89462 .... N87-22956* #
NASA-TM-89494 .... N87-22631* #
NASA-TM-89810 .... N87-23341* #
NASA-TM-89865 .... N87-22811* #
NASA-TM-89868 .... N87-22680* #
NASA-TM-89872 .... N87-23020* #
NASA-TM-89873 .... N87-22757* #
NASA-TM-89876 .... N87-22804* #
NASA-TM-89888 .... N87-23027* #
NASA-TM-89891 .... N87-23010* #
NASA-TM-89894 .... N87-22755* #
NASA-TM-89907 .... N87-23029* #
NASA-TM-89908 .... N87-23028* #
NASA-TM-89909 .... N87-22802* #
NASA-TM-89912 .... N87-22978* #
NASA-TM-89920 .... N87-22874* #
NASA-TM-89921 .... N87-22949* #
NASA-TM-89924 .... N87-22807* #
NASA-TM-100104 .... N87-22806* #
NASA-TM-100120 .... N87-22805* #

NASA-TP-2672 .... N87-23202* #
NASA-TP-2675 .... N87-22923* #
NASA-TP-2683 .... N87-22626* #
NASA-TP-2702 .... N87-22694* #
NASA-TP-2709 .... N87-23244* #
NASA-TP-2732 .... N87-22870* #

NASA-TT-20016 .... N87-23008* #

NATICK-TR-86/053-VOL-1 .... N87-23112 #
NATICK-TR-86/054 .... N87-23110 #

NBS-SP-250 .... N87-22958 #
NBS-SP-726 .... N87-23312 #

NBS/SP-500/145 .... N87-23170 #
NBS/SP-701 .... N87-23171 #
NBS/SP-723 .... N87-23309 #

NOSC-TD-1018 .... N87-22983 #

NOSC/TD-996 .... N87-22973 #

NOSC/TR-1119 .... N87-22914 #

NPS55-87-001 .... N87-23217 #
NPS55-86-021 .... N87-23239 #
NPS67-86-004 .... N87-22679 #
NPS012-86-011 .... N87-23223 #

NRC-25438 .... N87-22628 #
NRC-27323 .... N87-22808 #

NRCC-25417 .... N87-23566 #
NRCC-25466 .... N87-23567 #

NRL-MR-5922 .... N87-23565 #
NRL-MR-5947 .... N87-22962 #

NRL-9030 .... N87-22873 #

NSWC-TR-86-286 .... N87-22942 #

NUSC-TM-861161 .... N87-22872 #

ORNL/M-301 .... N87-22852 #

OS-TR-718688-2 .... N87-22700* #

OU-TM-90 .... N87-22616* #
OU-TM-91 .... N87-22617* #
OU-TM-92 .... N87-22618* #

PAT-APPL-6-915797 .... N87-22816 #

PB87-126926 .... N87-22816 #
PB87-157228 .... N87-23170 #
PB87-157236 .... N87-23309 #
PB87-169835 .... N87-22891 #
PB87-169843 .... N87-22866 #
PB87-172235 .... N87-23171 #

PERME-278 .... N87-22987 #

PSU-ME-86-R-0113 .... N87-22928 #

PWA-5940-46-VOL-1 .... N87-22996* #

QSR-3 .... N87-23172 #

QTPR-2 .... N87-23019 #

RADC-TR-86-125 .... N87-23064 #
RADC-TR-86-129 .... N87-22909 #
RADC-TR-86-181 .... N87-23266 #
RADC-TR-86-182 .... N87-23265 #
RADC-TR-86-192 .... N87-23060 #
RADC-TR-86-231 .... N87-22915 #

RANRL-TN-6/86 .... N87-23103 #

RDI-284/45/3 .... N87-22989 #

REF-86-10-VOL-2/6 .... N87-23104 #

REPT-85-08-01 .... N87-22983 #
REPT-87-58 .... N87-22858 #
REPT-87B0176 .... N87-23156* #

RFP-3814 .... N87-22868 #
RFP-3874 .... N87-22869 #
RFP-3901 .... N87-22984 #

RI/RD87-139 .... N87-22822 #

ROBOTICS-57-REV .... N87-23207 #
ROBOTICS-77 .... N87-23222 #
ROBOTICS-85 .... N87-23186 #

RP-698 .... N87-23248 #

SAND-86-0981 .... N87-23026 #
SAND-86-1322C .... N87-23022 #
SAND-86-1849C .... N87-22979 #
SAND-86-1945C .... N87-22903 #
SAND-86-2213C .... N87-23297 #
SAND-86-2366C .... N87-23245 #
SAND-86-2453 .... N87-23152 #
SAND-86-2471C .... N87-22849 #
SAND-86-2543C .... N87-23151 #
SAND-86-2555C .... N87-23285 #
SAND-86-2581C .... N87-23299 #
SAND-86-2591C .... N87-22850 #
SAND-86-2797C .... N87-22981 #
SAND-86-2926C .... N87-22965 #
SAND-86-7038 .... N87-23025 #
SAND-86-7039 .... N87-23024 #
SAND-86-7049 .... N87-23263 #
SAND-87-0033 .... N87-22982 #
SAND-87-0214C .... N87-23023 #
SAND-87-0587C .... N87-23153 #
SAND-87-0625C .... N87-22837 #
SAND-87-8201 .... N87-22935 #

SC5398.4FR .... N87-22843 #

SD-TR-87-08 .... N87-23302 #
SD-TR-87-11 .... N87-23253 #
SD-TR-87-13 .... N87-23061 #

SEL-86-002 .... N87-23190* #
SEL-86-005 .... N87-23189* #
SEL-87-001 .... N87-23192* #
SEL-87-002 .... N87-23191* #
SEL-87-003 .... N87-23193* #

SERI/TP-217-3070 .... N87-23021 #

SM-86-8 .... N87-22990 #

SR-6 .... N87-23056 #

SRL-6809 .... N87-22862 #

STAN-CS-86-1136 .... N87-23197 #

STI/E-TR-860135 .... N87-22871 #

SU-CMR-87-3 .... N87-23257* #

SYRU/DECE/TR-87/1 .... N87-22880 #

TAO-50015 .... N87-23194* #

TR-TF-28 .... N87-22939 #

TR-4 .... N87-22821 #
TR-4 .... N87-22859 #
TR-7 .... N87-22880 #
TR-14 .... N87-23240 #
TR-70 .... N87-23232 #
TR-87-2 .... N87-23234 #
TR-87-4 .... N87-23235 #
TR-87-03 .... N87-22764* #
TR-87/ONR-25 .... N87-23188 #
TR-109-ONR .... N87-23177 #
TR-140 .... N87-23233 #
TR-194-REV .... N87-23207 #
TR-239 .... N87-23222 #
TR-255 .... N87-23186 #
TR-335 .... N87-22692* #
TR-0086(6925-07)-6 .... N87-23253 #
TR-0086(6940-05)-17 .... N87-23061 #
TR-0086(6945-09)-3 .... N87-23302 #

TRITA-EPP-86-12 .... N87-23337 #

TRITA-NA-8517 .... N87-23228 #

U-OF-IOWA-86-04 .... N87-23063* #

UBUFFALO/DC/87/TR-35 .... N87-23292 #

UCID-20966 .... N87-22933 #
UCID-21006 .... N87-22936 #

UCRL-15867-VOL-2 .... N87-22970 #
UCRL-15871 .... N87-22907 #
UCRL-95152 .... N87-22998 #
UCRL-95276 .... N87-22905 #
UCRL-95475 .... N87-22955 #
UCRL-95644 .... N87-22823 #
UCRL-95706 .... N87-22968 #
UCRL-96070 .... N87-23175 #
UCRL-96188 .... N87-23174 #
UCRL-96258 .... N87-22697 #

UDR-TR-86-22 .... N87-23005 #

UILU-ENG-86-1780 .... N87-23209 #
UILU-ENG-87-1705 .... N87-23210 #
UILU-ENG-87-2542 .... N87-22883 #

UIUCDCS-R-86-1314 .... N87-23209 #
UIUCDCS-R-87-1319 .... N87-23210 #

ULRF-435/CAR .... N87-23056 #

US-PATENT-APPL-SN-442815 .... N87-23286*
US-PATENT-APPL-SN-495380 .... N87-22976*
US-PATENT-APPL-SN-553339 .... N87-22845*
US-PATENT-APPL-SN-578387 .... N87-22678*
US-PATENT-APPL-SN-674395 .... N87-23286*
US-PATENT-APPL-SN-683111 .... N87-22894*
US-PATENT-APPL-SN-692801 .... N87-22977*
US-PATENT-APPL-SN-698279 .... N87-22976*
US-PATENT-APPL-SN-725727 .... N87-22845*
US-PATENT-APPL-SN-734366 .... N87-22847*
US-PATENT-APPL-SN-746809 .... N87-22953*
US-PATENT-APPL-SN-754707 .... N87-22895*
US-PATENT-APPL-SN-755288 .... N87-22950*
US-PATENT-APPL-SN-779744 .... N87-23259* #
US-PATENT-APPL-SN-796053 .... N87-22985*
US-PATENT-APPL-SN-838655 .... N87-22848*
US-PATENT-APPL-SN-853361 .... N87-22977*
US-PATENT-APPL-SN-868388 .... N87-22892 #
US-PATENT-APPL-SN-883216 .... N87-22893 #

US-PATENT-CLASS-73-178-R N87-22678*
US-PATENT-CLASS-73-336.5 .... N87-22953*
US-PATENT-CLASS-156-607 .... N87-23286*
US-PATENT-CLASS-156-617-H N87-23286*
US-PATENT-CLASS-156-617-SP N87-23286*
US-PATENT-CLASS-165-1 .... N87-22950*
US-PATENT-CLASS-165-34 .... N87-22950*
US-PATENT-CLASS-165-104.14 .... N87-22950*
US-PATENT-CLASS-165-104.25 .... N87-22950*
US-PATENT-CLASS-165-104.26 .... N87-22950*
US-PATENT-CLASS-244-1-R N87-22678*
US-PATENT-CLASS-244/161 .... N87-22985*
US-PATENT-CLASS-250-231-GY .... N87-23259* #
US-PATENT-CLASS-285-81 .... N87-22977*
US-PATENT-CLASS-285-85 .... N87-22977*
US-PATENT-CLASS-285-91 .... N87-22977*
US-PATENT-CLASS-285-305 .... N87-22977*
US-PATENT-CLASS-307-490 .... N87-22895*

US-PATENT-CLASS-324-61-R N87-22953*
US-PATENT-CLASS-324-158-D N87-22894*
US-PATENT-CLASS-324-158-R N87-22894*
US-PATENT-CLASS-330-107 .... N87-22895*
US-PATENT-CLASS-330-294 .... N87-22895*
US-PATENT-CLASS-331-177-R N87-22895*
US-PATENT-CLASS-333-214 .... N87-22895*
US-PATENT-CLASS-333-217 .... N87-22895*
US-PATENT-CLASS-340-945 .... N87-22678*
US-PATENT-CLASS-340-971 .... N87-22678*
US-PATENT-CLASS-340-975 .... N87-22678*
US-PATENT-CLASS-356-350 .... N87-23259* #
US-PATENT-CLASS-411-166 .... N87-22976*
US-PATENT-CLASS-411-368 .... N87-22976*
US-PATENT-CLASS-411-424 .... N87-22976*
US-PATENT-CLASS-411-427 .... N87-22976*
US-PATENT-CLASS-411-531 .... N87-22976*
US-PATENT-CLASS-524-404 .... N87-22845*
US-PATENT-CLASS-524-548 .... N87-22845*
US-PATENT-CLASS-525-36 .... N87-22848*
US-PATENT-CLASS-525-182 .... N87-22845*
US-PATENT-CLASS-526-262 .... N87-22845*
US-PATENT-CLASS-528-176 .... N87-22848*
US-PATENT-CLASS-528-184 .... N87-22848*
US-PATENT-CLASS-528-192 .... N87-22848*
US-PATENT-CLASS-528-193 .... N87-22848*
US-PATENT-CLASS-528-229 .... N87-22847*
US-PATENT-CLASS-546-262 .... N87-22847*
US-PATENT-CLASS-546-264 .... N87-22847*
US-PATENT-CLASS-564-330 .... N87-22847*
US-PATENT-CLASS-564-306 .... N87-22847*
US-PATENT-CLASS-564-430 .... N87-22847*

US-PATENT-4,526,925 .... N87-22845*
US-PATENT-4,572,699 .... N87-22976*
US-PATENT-4,644,306 .... N87-22895*
US-PATENT-4,647,615 .... N87-22845*
US-PATENT-4,650,365 .... N87-22976*
US-PATENT-4,654,110 .... N87-23286*
US-PATENT-4,655,482 .... N87-22977*
US-PATENT-4,661,558 .... N87-22848*
US-PATENT-4,661,770 .... N87-22894*
US-PATENT-4,662,220 .... N87-22953*
US-PATENT-4,662,751 .... N87-23259* #
US-PATENT-4,663-627 .... N87-22678*
US-PATENT-4,663,483 .... N87-22847*
US-PATENT-4,664,177 .... N87-22950*
US-PATENT-4,664,344 .... N87-22965*

USAAVSCOM-TR-87-A-5 .... N87-22691* #

USAFSAM-TR-86-26 .... N87-23116 #

UT-CMSE-87-02 .... N87-22867 #

UTCMSE-87-1 .... N87-22841 #

UTEC-MD-86-054 .... N87-22909 #

UVA/525303/MAE86/101 .... N87-23007 #
UVA/525657/EE87/101 .... N87-23283 #

VA187-1 .... N87-23062 #

WCP-121 .... N87-23034 #

WMO-TD-108-VOL-2 .... N87-23068 #
WMO-TD-138 .... N87-23034 #

WP-37-85-P31 .... N87-23237 #
WP-37-86-P19 .... N87-23241 #
WP-37-86-P21 .... N87-23236 #
WP-37-86-P22 .... N87-23178 #
WP-37-86-P23 .... N87-23221 #
WP-37-86-P26 .... N87-23179 #
WP-37-86-P27 .... N87-23220 #
WP-37-86-P28 .... N87-23238 #
WP-37-86-P32 .... N87-23225 #
WP-37-86-P34 .... N87-23214 #

VOLUME 25 NUMBER 16 / AUGUST 23, 1987

Scientific and Technical Aerospace Reports

A Semimonthly Publication of the National Aeronautics and Space Administration

01 AERONAUTICS (GENERAL)

N87-22604*# National Aeronautics and Space Administration. Langley Research Center, Hampton, Va.
JOINT UNIVERSITY PROGRAM FOR AIR TRANSPORTATION RESEARCH, 1984
Frederick R. Morrell, comp. May 1987 165 p Meeting held in Hampton, Va., 18 Jan. 1985
(NASA-CP-2452; L-16255; NAS 1.55:2452) Avail: NTIS HC A08/MF A01 CSCL 01B

The research conducted during 1984 under the NASA/FAA sponsored Joint University Program for Air Transportation Research is summarized. The Joint University Program is a coordinated set of three grants sponsored by NASA Langley Research Center and the Federal Aviation Administration, one each with the Massachusetts Institute of Technology, Ohio University, and Princeton University. Completed works, status reports, and bibliographies are presented for research topics, which include navigation, guidance, control and display concepts. An overview of the year's activities for each of the schools is also presented. For individual titles, see N87-22605 through N87-22622.

N87-22605*# Massachusetts Inst. of Tech., Cambridge. Flight Transportation Lab.
INVESTIGATION OF AIR TRANSPORTATION TECHNOLOGY AT MASSACHUSETTS INSTITUTE OF TECHNOLOGY, 1984 c03
Robert W. Simpson *In* NASA. Langley Research Center Joint University Program for Air Transportation Research, 1984 May 1987 p 3-7 (For primary document see N87-22604 16-01)
Avail: NTIS HC A08/MF A01 CSCL 01C

Three projects sponsored by the Joint University Program at MIT are summarized. Two projects were focussed on the potential application of Loran-C in flying nonprecision approaches to general aviation runways, and the third project involved research on aircraft icing. In one Loran-C project, Aircraft Approach Guidance Using Relative Loran-C Navigation, the concept was flight tested. It used the difference in TD's from those of the touchdown point to simplify and speed navigation computer processing and took advantage of the short term accuracy of less than 100 feet for Loran-C. The goal of the project, Probabilistic Modelling of Loran-C Error for Nonprecision Approaches, was to develop a mathematical model which would predict the probability that an approach flown to a runway with a particular Loran-C receiver would fall within a given standard. The Aircraft Icing project focussed on measurement of droplet trajectories and droplet impingement/runback characteristics and measurement of real time ice accretion using ultrasonic pulse echo techniques. E.R.

N87-22606*# Massachusetts Inst. of Tech., Cambridge. Flight Transportation Lab.
AIRCRAFT APPROACH GUIDANCE USING RELATIVE LORAN-C NAVIGATION c04
Antonio L. Elias *In* NASA. Langley Research Center Joint University Program for Air Transportation Research, 1984 May 1987 p 9-16 (For primary document see N87-22604 16-01)
Avail: NTIS HC A08/MF A01 CSCL 17G

The experiments carried out at MIT during 1984 focussed on two aspects of Loran-C relative navigation that would impact system performance at the sub-microsecond level of accuracy: tracking loop bandwidth and localized field deformation. Figures are given to illustrate the results from both effects. E.R.

N87-22607*# Massachusetts Inst. of Tech., Cambridge.
PROBABILISTIC MODELING OF LORAN-C FOR NONPRECISION APPROACHES c04
John K. Einhorn *In* NASA. Langley Research Center Joint University Program for Air Transportation Research, 1984 May 1987 p 17-24 (For primary document see N87-22604 16-01)
Avail: NTIS HC A08/MF A01 CSCL 17G

The overall idea of the research was to predict the errors to be encountered during an approach using available data from the U.S. Coast Guard and standard normal distribution probability analysis for a number of airports in the North East CONUS. The research consists of two parts: an analytical model that predicts the probability of an approach falling within a given standard, and a series of flight tests designed to test the validity of the model. Author

N87-22608*# Massachusetts Inst. of Tech., Cambridge. Dept. of Aeronautics and Astronautics.
MEASUREMENT OF ICE ACCRETION USING ULTRASONIC PULSE ECHO TECHNIQUES c03
R. John Hansman, Jr. and Mark S. Kirby *In* NASA. Langley Research Center Joint University Program for Air Transportation Research, 1984 May 1987 p 25-41 (For primary document see N87-22604 16-01)
Avail: NTIS HC A08/MF A01 CSCL 01C

Many figures are given to illustrate the measurement of ice deposition using ultrasonic pulse echo techniques. The basic concept is to measure the thickness of the ice by relating the pulse echo time to the speed of sound. The measurements are made in an icing research tunnel (IRT), where echo patterns are videotaped during icing exposures under a variety of conditions. Typical echo patterns for different types of ice are illustrated. A table summarizing the icing rates measured in the IRT, along with the presence or absence of surface water is also given. E.R.

N87-22609*# Ohio Univ., Athens.
INVESTIGATION OF AIR TRANSPORTATION TECHNOLOGY AT OHIO UNIVERSITY, 1984 c03
Richard H. McFarland *In* NASA. Langley Research Center Joint University Program for Air Transportation Research, 1984 May 1987 p 45-48 (For primary document see N87-22604 16-01)
Avail: NTIS HC A08/MF A01 CSCL 01C

The operational development of Loran-C for enroute navigation and nonprecision approaches was studied, and is only one of the many projects funded by the Joint University Program for Air Transportation at Ohio University. Other projects included work on the DATAC data bus monitor, global positioning system test bed receiver development, fiber optic data bus application in general aviation aircraft, and advanced remote monitoring techniques. E.R.

N87-22610*# Ohio Univ., Athens.
DIGITAL AUTONOMOUS TERMINAL ACCESS COMMUNICATION (DATAC) SYSTEM c32
Stanley M. Novacki, III *In* NASA. Langley Research Center Joint University Program for Air Transportation Research, 1984

May 1987 p 49-56 (For primary document see N87-22604 16-01)
Avail: NTIS HC A08/MF A01 CSCL 17B

In order to accommodate the increasing number of computerized subsystems aboard today's more fuel efficient aircraft, the Boeing Co. has developed the DATAC (Digital Autonomous Terminal Access Control) bus to minimize the need for point-to-point wiring to interconnect these various systems, thereby reducing total aircraft weight and maintaining an economical flight configuration. The DATAC bus is essentially a local area network providing interconnections for any of the flight management and control systems aboard the aircraft. The task of developing a Bus Monitor Unit was broken down into four subtasks: (1) providing a hardware interface between the DATAC bus and the Z8000-based microcomputer system to be used as the bus monitor; (2) establishing a communication link between the Z8000 system and a CP/M-based computer system; (3) generation of data reduction and display software to output data to the console device; and (4) development of a DATAC Terminal Simulator to facilitate testing of the hardware and software which transfer data between the DATAC's bus and the operator's console in a near real time environment. These tasks are briefly discussed. E.R.

N87-22611*# Ohio Univ., Athens.
FIBER OPTIC DATA TRANSMISSION c32
Steven T. Shreve *In* NASA. Langley Research Center Joint University Program for Air Transportation Research, 1984 May 1987 p 57-59 (For primary document see N87-22604 16-01)
Avail: NTIS HC A08/MF A01 CSCL 17B

The Ohio University Avionics Engineering Center is currently developing a fiber optic data bus transmission and reception system that could eventually replace copper cable connections in airplanes. The original form of the system will transmit information from an encoder to a transponder via a fiber optic cable. An altimeter and an altitude display are connected to a fiber optic transmitter by copper cable. The transmitter converts the altimetry data from nine bit parallel to serial form and send these data through a fiber optic cable to a receiver. The receiver converts the data using a cable similar to that used between the altimeter and display. The transmitting and receiving ends also include a display readout. After completion and ground testing of the data bus, the system will be tested in an airborne environment. Author

N87-22612*# Ohio Univ., Athens.
LORAN-C APPROACH CONSIDERATIONS c04
Robert W. Lilley *In* NASA. Langley Research Center Joint University Program for Air Transportation Research, 1984 May 1987 p 61-63 (For primary document see N87-22604 16-01)
Avail: NTIS HC A08/MF A01 CSCL 17G

The use of Loran-C during approaches to landing is investigated. The Avionics Engineering Center has evaluated such approach applications at Galion, Ohio Municipal Airport and at Mansfield, Ohio Lahm airport. Loran-C data were referenced to ground tracker data to determine that the Loran-C approach path was straight, flyable, and parallel to the runway centerline. The Loran-C operational issues that were investigated are listed. Author

N87-22613*# Ohio Univ., Athens.
SATELLITE SURVEYING FOR A LORAN-C NONPRECISION APPROACH c04
Daryl L. McCall *In* NASA. Langley Research Center Joint University Program for Air Transportation Research, 1984 May 1987 p 65-67 (For primary document see N87-22604 16-01)
Avail: NTIS HC A08/MF A01 CSCL 17G

Work has continued to site-in a Loran-C nonprecision approach at the Ohio University Gordon K. Bush Airport located in Albany, Ohio. A survey was performed using the Motorola Mini-Ranger Satellite Surveying System, which uses the Navy's TRANSIT satellites. This position was obtained using the point-position method only, that is the position was calculated from sequential Doppler measurements as the TRANSIT satellite's passed within view of the receiver's antenna. Another method, called translocation, can use differential techniques which provide better results. The accuracies obtained, however, are sufficient to site-in a Loran-C nonprecision approach. Author

N87-22614*# Ohio Univ., Athens.
ADVANCED MONITORING CONCEPTS c04
Robert W. Lilley *In* NASA. Langley Research Center Joint University Program for Air Transportation Research, 1984 May 1987 p 69-71 (For primary document see N87-22604 16-01)
Avail: NTIS HC A08/MF A01 CSCL 17G

The emphasis in initial work will be on application of image processing techniques in the site monitoring of an ILS glide slope transmitting array. The glide slope requires a clear area in front of the antennas for use as a reflecting zone. Reflecting or scattering obstacles in this area can cause incorrect path formation and system outages. Direct video monitoring is impractical due to the narrow band nature of communication links from the ILS site to the regional maintenance location. Slow scan video is possible, but even this technique may require transmission of large amounts of data, tying up remote monitoring lines. The steps used to minimize data transmission are listed. Author

N87-22615*# Ohio Univ., Athens.
GPS ANTENNA DESIGNS c32
Samuel J. P. Laube *In* NASA. Langley Research Center Joint University Program for Air Transportation Research, 1984 May 1987 p 73-76 (For primary document see N87-22604 16-01)
Avail: NTIS HC A08/MF A01 CSCL 17B

Application of the current GPS NAVSTAR system to civilian service requires that a right hand, circularly polarized, -160 dBW spread spectrum signal be received from an orbiting satellite, where the antenna environment is also moving. This presents a design challenge when inexpensive antennas are desired. The intent of this survey is to provide information on the antennas mentioned and to construct and test prototypes to determine whether the choice made by the industry, the quadrifilar helix, is the best. The helix antenna is currently the low cost standard for GPS. Prototype versions were constructed using 12 gauge wire and subminiature coaxial hardline. The constructed antennas were tested using a signal generator and a reference turnstile. A spectrum analyzer was used to measure the level of the received signal. Author

N87-22616*# Ohio Univ., Athens. Dept. of Electrical and Computer Engineering.
PROCESSOR-CONTROLLED TIMING MODULE FOR LORAN-C RECEIVER c06
Robert W. Lilley *In* NASA. Langley Research Center Joint University Program for Air Transportation Research, 1984 May 1987 p 77-85 Previously announced as N84-20504 (For primary document see N87-22604 16-01)
(OU-TM-90) Avail: NTIS HC A08/MF A01 CSCL 01D

Hardware documentation is provided for the modified Loran-C timing module, which uses direct software control in determining loop sample times. Computer loading is reduced by eliminating polled operation of the timing loop. Author

N87-22617*# Ohio Univ., Athens. Dept. of Electrical and Computer Engineering.
A MICRO-COMPUTER-BASED SYSTEM TO COMPUTE MAGNETIC VARIATION c60
Rajan Kaul *In* NASA. Langley Research Center Joint University Program for Air Transportation Research, 1984 May 1987 p 87-112 Previously anounced as N84-20506 (For primary document see N87-22604 16-01)
(OU-TM-91) Avail: NTIS HC A08/MF A01 CSCL 09B

A mathematical model of magnetic variation in the continental United States was implemented in the Ohio University Loran-C receiver. The model is based on a least squares fit of a polynomial function. The implementation on the microprocessor based Loran-C receiver is possible with the help of a math chip which performs 32 bit floating point mathematical operations. A Peripheral Interface Adapter is used to communicate between the 6502 based microcomputer and the 9511 math chip. The implementation provides magnetic variation data to the pilot as a function of latitude and longitude. The model and the real time implementation in the receiver are described. Author

N87-22618*# Ohio Univ., Athens. Dept. of Electrical and Computer Engineering.
A PROGRAM DOWNLOADER AND OTHER UTILITY SOFTWARE FOR THE DATAC BUS MONITOR UNIT **c61**
Stanley M. Novacki, III *In* NASA. Langley Research Center Joint University Program for Air Transportation Research, 1984 May 1987 p 113-129 (For primary document see N87-22604 16-01)
(OU-TM-92) Avail: NTIS HC A08/MF A01 CSCL 09B

A set or programs designed to facilitate software testing on the DATAC Bus Monitor is described. By providing a means to simplify program loading, firmware generation, and subsequent testing of programs, the overhead involved in software evaluation is reduced and that time is used more productively in performance, analysis and improvement of current software. Author

N87-22619*# Princeton Univ., N. J. Dept. of Mechanical and Aerospace Engineering.
INVESTIGATION OF AIR TRANSPORTATION TECHNOLOGY AT PRINCETON UNIVERSITY, 1984 **c03**
Robert F. Stengel *In* NASA. Langley Research Center Joint University Program for Air Transportation Research, 1984 May 1987 p 133-137 (For primary document see N87-22604 16-01)
Avail: NTIS HC A08/MF A01 CSCL 01C

The Air Transportation Technology Program at Princeton University, a program emphasizing graduate and undergraduate student research, proceeded along four avenues during 1984: (1) guidance and control strategies for penetration of microbursts and wind shear; (2) application of artificial intelligence in flight control systems; (3) effects of control saturation on closed loop stability; and (4) response of open loop unstable aircraft. Areas of investigation relate to guidance and control of commercial transports as well as to general aviation aircraft. Interaction between the flight crew and automatic systems is a subject of principle concern. These areas of investigation are briefly discussed. Author

N87-22620*# Princeton Univ., N. J. Dept. of Mechanical and Aerospace Engineering.
SAFE MICROBURST PENETRATION TECHNIQUES: A DETERMINISTIC, NONLINEAR, OPTIMAL CONTROL APPROACH **c04**
Mark L. Psiaki *In* NASA. Langley Research Center Joint University Program for Air Transportation Research, 1984 May 1987 p 139-148 (For primary document see N87-22604 16-01)
Avail: NTIS HC A08/MF A01 CSCL 17G

A relatively large amount of computer time was used for the calculation of a optimal trajectory, but it is subject to reduction with moderate effort. The Deterministic, Nonlinear, Optimal Control algorithm yielded excellent aircraft performance in trajectory tracking for the given microburst. It did so by varying the angle of attack to counteract the lift effects of microburst induced airspeed variations. Throttle saturation and aerodynamic stall limits were not a problem for the case considered, proving that the aircraft's performance capabilities were not violated by the given wind field. All closed loop control laws previously considered performed very poorly in comparison, and therefore do not come near to taking full advantage of aircraft performance. Author

N87-22621*# Princeton Univ., N. J.
INTELLIGENT FAULT-TOLERANT CONTROLLERS **c63**
Chien Y. Huang *In* NASA. Langley Research Center Joint University Program for Air Transportation Research, 1984 May 1987 p 149-160 (For primary document see N87-22604 16-01)
Avail: NTIS HC A08/MF A01 CSCL 09B

A system with fault tolerant controls is one that can detect, isolate, and estimate failures and perform necessary control reconfiguration based on this new information. Artificial intelligence (AI) is concerned with semantic processing, and it has evolved to include the topics of expert systems and machine learning. This research represents an attempt to apply AI to fault tolerant controls, hence, the name intelligent fault tolerant control (IFTC). A generic solution to the problem is sought, providing a system based on logic in addition to analytical tools, and offering machine learning capabilities. The advantages are that redundant system specific algorithms are no longer needed, that reasonableness is used to quickly choose the correct control strategy, and that the system can adapt to new situations by learning about its effects on system dynamics. Author

N87-22622*# Princeton Univ., N. J. Dept. of Mechanical and Aerospace Engineering.
STABILITY BOUNDARIES FOR COMMAND AUGMENTATION SYSTEMS **c08**
P. C. Shrivastava *In* NASA. Langley Research Center Joint University Program for Air Transportation Research, 1984 May 1987 p 161-176 (For primary document see N87-22604 16-01)
Avail: NTIS HC A08/MF A01 CSCL 01C

The Stability Augmentation System (SAS) is a special case of the Command Augmentation System (CAS). Control saturation imposes bounds on achievable commands. The state equilibrium depends only on the open loop dynamics and control deflection. The control magnitude to achieve a desired command equilibrium is independent of the feedback gain. A feedback controller provides the desired response, maintains the system equilibrium under disturbances, but it does not affect the equilibrium values of states and control. The saturation boundaries change with commands, but the location of the equilibrium points in the saturated region remains unchanged. Nonzero command vectors yield saturation boundaries that are asymmetric with respect to the state equilibrium. Except for the saddle point case with MCE control law, the stability boundaries change with commands. For the cases of saddle point and unstable nodes, the region of stability decreases with increasing command magnitudes. Author

N87-22664# Ministry of Defence, London (England).
COST ANALYSIS OF AIRCRAFT PROJECTS
D. Faddy *In* AGARD Improvement of Combat Performance for Existing and Future Aircraft Dec. 1986 10 p (For primary document see N87-22663 16-05)
Copyright Avail: NTIS HC A07/MF A01

02 AERODYNAMICS

Includes aerodynamics of bodies, combinations, wings, rotors, and control surfaces; and internal flow in ducts and turbomachinery.

For related information see also *34 Fluid Mechanics and Heat Transfer.*

N87-22623# Air Force Inst. of Tech., Wright-Patterson AFB, Ohio. School of Engineering.
INVESTIGATION OF PERIODIC PITCHING THROUGH THE STATIC STALL ANGLE OF ATTACK M.S. Thesis
Eric C. Stephen Mar. 1987 150 p
(AD-A179512; AFIT/GAE/AA/87M-4) Avail: NTIS HC A07/MF A01 CSCL 20D

The flow over an NACA 0015 airfoil undergoing periodic pitching motions using constant pitch rate ramps was experimentally studied over a range of pitch rates and angles of attack. Surface pressure transducers coupled with a microcomputer-based data acquisition system were used to collect surface pressure data at a rate of 4000 samples per second. The data was reduced through numerical integration of the pressure data to provide graphs of the coefficients of lift, pressure drag and pitching moment versus time. Each point on the graphs represents an average of five runs. The results were compared according to their nondimensional pitch rates (defined as the product of one-half the chord length and the pitch rate divided by the freestream velocity). Data was collected in the range of nondimensional pitch up rates between 0.104 and 0.384 and the range of angles of attack between 0 and 30 degrees. GRA

N87-22624# Ballistic Research Labs., Aberdeen Proving Ground, Md.

NUMERICAL SIMULATION OF SUPERSONIC FLOW OVER A ROTATING BAND USING FLOWFIELD BLANKING

Jubaraj Sahu Dec. 1986 34 p
(AD-A178492; BRL-MR-3561) Avail: NTIS HC A03/MF A01 CSCL 20D

Implicit, approximately factored, finite difference codes have been developed for solving the Navier-Stokes equations in general body-fitted coordinates. For a protuberance such as the rotating band on artillery shell, sharp geometric variations exist which make it extremely difficult to generate body conforming grids while preserving the sharp corners. Using wrap around grids for such cases introduces geometric errors and may lead to degradation of computational efficiency and accuracy. This report describes the development and application of a computational procedure using flowfield blanking to compute the flow over a rotating band at supersonic speed with no geometric error. GRA

N87-22625# Air Force Wright Aeronautical Labs., Wright-Patterson AFB, Ohio.

HYPERSONIC LAMINAR BOUNDARY LAYER TRANSITION. PART 1: NOSETIP BLUNTNESS EFFECTS ON CONE FRUSTUM TRANSITION. PART 2: MACH 6 EXPERIMENTS OF TRANSITION ON A CONE AT ANGLE OF ATTACK Final Report, 27 Jul. 1981 - 30 Sep. 1984

Kenneth F. Stetson Dec. 1986 109 p
(AD-A178877; AFWAL-TR-86-3089-Pt-1-Pt-2) Avail: NTIS HC A06/MF A01 CSCL 20D

The effects of nosetip bluntness on cone frustrum boundary layer transition were investigated by conducting hypersonic wind tunnel experiments. Frustum transition Reynolds numbers were found to have large variations within the entropy layer swallowing region. Investigation results indicated that several nosetip blunting effects were competing for the dominant role in the frustum transition process and it was speculated that the large variations in transition Reynolds number were associated with the shifting of dominant roles. Based upon these studies, dominant nosetip bluntness effects are tentatively identified with three regions of the entropy layer. Transition movement and patterns on the frustum of a cone at small angles of attack were investigated at a Mach number of 5.9, using an 8-deg half angle cone with both sharp and blunt nosetips. Small angles of attack produced large asymmetries in the frustum transition pattern for both sharp and blunt tipped configurations. For the configurations with nosetip bluntness most of the frustum transition asymmetry occurred between meridian angles of 60 and 120 deg. Data obtained with simulated laminar ablated nosetips were generally representative of what would be expected with a larger spherically blunt nosetip. GRA

N87-22626*# National Aeronautics and Space Administration. Langley Research Center, Hampton, Va.

EXPERIMENTAL CAVITY PRESSURE DISTRIBUTIONS AT SUPERSONIC SPEEDS

Robert L. Stallings, Jr. and Floyd J. Wilcox, Jr. Jun. 1987 79 p
(NASA-TP-2683; L-16215; NAS 1.60:2683) Avail: NTIS HC A05/MF A01 CSCL 01A

An investigation was conducted to define pressure distributions for rectangular cavities over a range of free-stream Mach numbers and cavity dimensions. These pressure distributions together with schlieren photographs are used to define the critical values of cavity length-to-depth ratio that separate open type cavity flows from closed type cavity flows. For closed type cavity flow, the shear layer expands over the cavity leading edge and impinges on the cavity floor, whereas for open type cavity flow, the shear layer bridges the cavity. The tests were conducted by using a flat-plate model permitting the cavity length to be remotely varied from 0.5 to 12 in. Cavity depths and widths were varied from 0.5 to 2.5 in. The flat-plate boundary layer approaching the cavity was turbulent and had a thickness of approximately 0.2 in. at the cavity front face for the range of test Mach numbers from 1.5 to 2.86. Presented are a discussion of the results and a complete tabulation of the experimental data. Author

N87-22627*# National Aeronautics and Space Administration, Washington, D.C.

THE AERODYNAMIC OPTIMIZATION OF WINGS AT SUBSONIC SPEEDS AND THE INFLUENCE OF WINGTIP DESIGN Thesis

H. Zimmer May 1987 105 p Transl. into ENGLISH of "Die Aerodynamische Optimisrung von Tragfluegein im Unterschallgeschwindigkeitsbereich und der Einfluss der Gestaltung der Fluegelenden" Stuttgart (West Germany), 1983 122 p Original language document was announced in IAA as A84-36992 Transl. by The Corporate Word, Inc., Pittsburgh, Pa.
(Contract NASw-4006)
(NASA-TM-88534; NAS 1.15:88534) Avail: NTIS HC A06/MF A01 CSCL 01A

Some of the objectives of modern aircraft development are related to the achievement of reduced fuel consumption and aircraft noise. This investigation is mainly concerned with the aerodynamic aspects of aircraft development, i.e., reduction of induced drag. New studies of wing design, and in particular wing tips, are considered. Induced drag is important since, in cruising flight, it accounts for approximately one-third of the entire drag for the aircraft, and one-half while climbing. A survey is presented for the wing geometries and wing tip designs studied, and theoretical investigations of different planar wings with systematically varied wing tip forms are conducted. Attention is also paid to a theoretical study of some planar and nonplanar wings and their comparison with experimental data. Author

N87-22628# National Aeronautical Establishment, Ottawa (Ontario).

FLUTTER ANALYSIS OF A TWO-DIMENSIONAL AIRFOIL WITH CUBIC NON-LINEAR RESTORING FORCE

B. H. K. Lee and P. LeBlanc Feb. 1986 49 p
(NAE-AN-36; NRC-25438) Avail: NTIS HC A03/MF A01

Flutter analysis of a two dimensional airfoil with a cubic nonlinear restoring force in the pitch degree of freedom is investigated. The structural dynamic equations of motion are integrated by a time marching finite difference scheme. Flutter is determined from conditions which give rise to either a divergent or limit-amplitude solution. Case studies using various airfoil parameters and coefficients of the nonlinear term in the restoring force are carried out. The effect of initial conditions is studied by varying the displacement from equilibrium of the pitch angle at the start of the airfoil motion. For a soft spring, an increase in the initial angular displacement can induce flutter to occur below the linear flutter speed. Factors that have stabilizing and destabilizing effects are investigated. For a hard spring, divergent flutter is not encountered. Instead, the oscillations maintain a self-limited amplitude which is independent of initial angular displacement. The effects of airfoil parameters on the amplitudes of heave and pitch motions are studied. Author

N87-22629*# National Aeronautics and Space Administration. Ames Research Center, Moffett Field, Calif.

A LOOK AT HANDLING QUALITIES OF CANARD CONFIGURATIONS

Seth B. Anderson Sep. 1986 49 p Previously announced in IAA as A87-32226
(NASA-TM-88354; A-86332; NAS 1.15:88354) Avail: NTIS HC A03/MF A01 CSCL 01A

The first human-powered flight was achieved by a canard-configured aircraft (Wright Brothers). Although other canard concepts were flown with varying degrees of success over the years, the tail-aft configuration has dominated the aircraft market for both military and civil use. Reviewed are the development of several canard aircraft with emphasis on stability and control, handling qualities, and operating problems. The results show that early canard concepts suffered adversely in flight behavior because of a lack of understanding of the sensitivities of these concepts to basic stability and control principles. Modern canard designs have been made competitive with tail-aft configurations by using appropriate handling qualities design criteria. Author

N87-22630*# National Aeronautics and Space Administration. Lewis Research Center, Cleveland, Ohio.
APPLICATION OF ADVANCED COMPUTATIONAL CODES IN THE DESIGN OF AN EXPERIMENT FOR A SUPERSONIC THROUGHFLOW FAN ROTOR
Jerry R. Wood, James F. Schmidt, Ronald J. Steinke, Rodrick V. Chima, and William G. Kunik Jun. 1987 30 p Presented at the 32nd International Gas Turbine Conference and Exhibit, Anaheim, Calif., 31 May - 4 Jun. 1987; sponsored by the ASME
(NASA-TM-88915; E-3339; NAS 1.15:88915) Avail: NTIS HC A03/MF A01 CSCL 01A

Increased emphasis on sustained supersonic or hypersonic cruise has revived interest in the supersonic throughflow fan as a possible component in advanced propulsion systems. Use of a fan that can operate with a supersonic inlet axial Mach number is attractive from the standpoint of reducing the inlet losses incurred in diffusing the flow from a supersonic flight Mach number to a subsonic one at the fan face. The design of the experiment using advanced computational codes to calculate the components required is described. The rotor was designed using existing turbomachinery design and analysis codes modified to handle fully supersonic axial flow through the rotor. A two-dimensional axisymmetric throughflow design code plus a blade element code were used to generate fan rotor velocity diagrams and blade shapes. A quasi-three-dimensional, thin shear layer Navier-Stokes code was used to assess the performance of the fan rotor blade shapes. The final design was stacked and checked for three-dimensional effects using a three-dimensional Euler code interactively coupled with a two-dimensional boundary layer code. The nozzle design in the expansion region was analyzed with a three-dimensional parabolized viscous code which corroborated the results from the Euler code. A translating supersonic diffuser was designed using these same codes. Author

N87-22631*# National Aeronautics and Space Administration. Ames Research Center, Moffett Field, Calif.
RESULTS OF THE INTEGRATION OF A TRANSONIC FULL-POTENTIAL ANALYSIS PROGRAM WITH A FREE-WAKE LIFTING-LINE PROGRAM FOR HOVERING ROTORS
Song-Young Chung May 1987 22 p
(NASA-TM-89494; A-87193; NAS 1.15:89494) Avail: NTIS HC A02/MF A01 CSCL 01A

The hovering performance predictions of the TFAR1 and OPLIN codes and the experimental data are discussed. The TFAR1 program solves the full-potential equation in a rotor-fixed coordinate system by use of the line relaxation method. The OPLIN program calculates the positions of wake vortices and rotor performance using the influence-coefficient-and-lifing-line method. The two programs are combined by adding the induced velocities from the OPLIN code to the near flow-field of the rotor from the TFAR1 code. Results show that the TFAR1 program converges better with the downwash-coupling method than the twist correction method to include the wake downwash. Author

N87-22632*# National Aeronautics and Space Administration. Langley Research Center, Hampton, Va.
AN ANALYSIS OF ARTIFICIAL VISCOSITY EFFECTS ON REACTING FLOWS USING A SPECTRAL MULTI-DOMAIN TECHNIQUE
M. G. Macaraeg, C. L. Streett, and M. Y. Hussaini May 1987 17 p Submitted for publication
(Contract NAS1-18107)
(NASA-CR-178308; ICASE-87-35; NAS 1.26:178308) Avail: NTIS HC A02/MF A01 CSCL 01A

Standard techniques used to model chemically-reacting flows require an artificial viscosity for stability in the presence of strong shocks. The resulting shock is smeared over at least three computational cells, so that the thickness of the shock is dictated by the structure of the overall mesh and not the shock physics. A gas passing through a strong shock is thrown into a nonequilibrium state and subsequently relaxes down over some finite distance to an equilibrium end state. The artificial smearing of the shock envelops this relaxation zone which causes the chemical kinetics of the flow to be altered. A method is presented which can investigate these issues by following the chemical kinetics and flow kinetics of a gas passing through a fully resolved shock wave at hypersonic Mach numbers. A nonequilibrium chemistry model for air is incorporated into a spectral multidomain Navier-Stokes solution method. Since no artificial viscosity is needed for stability of the multidomain technique, the precise effect of this artifice on the chemical kinetics and relevant flow features can be determined. Author

N87-22633*# Stanford Univ., Calif. Dept. of Aeronautics and Astronautics.
VERIFICATION OF PERFORMANCE RESULTS FOR A LOW-SPEED 15 PERCENT ELLIPTICAL CIRCULATION CONTROL AIRFOIL
L. C. Rodman and N. J. Wood Feb. 1986 65 p
(Grant NAG2-173)
(NASA-CR-181020; NAS 1.26:181020; JIAA-TR-56) Avail: NTIS HC A04/MF A01 CSCL 01A

Low-speed wind tunnel tests performed by the Naval Ship Research and Development Center (NSRDC) on a circulation control airfoil model was repeated by the Joint Institute for Aerodynamics and Acoustics in an attempt to reproduce the performance results. The model used was a 15% ellipse with interchangeable trailing edges. Surface pressure measurements were taken to obtain lift and pitching moment coefficients as functions of jet blowing momentum, and the momentum deficit in the wake was measured and used to calculate the drag coefficient. The effects of spanwise slot height variation and of leading edge blowing on performance were also investigated. The performance results showed that of the three slot heights tested, a slot height/chord ratio of 0.0022 produced the most lift coefficient for a given blowing rate. Lift obtained in the current test ranged from 2 to 35% lower than the NSRDC test. However, the two data sets compared reasonably well considering wind tunnel and wall blowing scheme differences. The spanwise lift distribution showed less change in lift due to a variation in slot height than expected. The leading edge blowing results demonstrated that although lift initially decreased, a positive lift increment was possible at higher leading edge blowing rates. M.G.

03 AIR TRANSPORTATION AND SAFETY

Includes passenger and cargo air transport operations; and aircraft accidents.

For related information see also *16 Space Transportation* and *85 Urban Technology and Transportation.*

N87-22634*# National Aeronautics and Space Administration. Ames Research Center, Moffett Field, Calif.
COCKPIT RESOURCE MANAGEMENT TRAINING
Harry W. Orlady, ed. (Orlady Associates, Inc., Los Gatos, Calif.) and H. Clayton Foushee, ed. May 1987 308 p Workshop held in San Francisco, Calif., 6-8 May 1986; sponsored by NASA. Ames Research Center and Air Force Military Airlift
(NASA-CP-2455; A-87038; NAS 1.55:2455) Avail: NTIS HC A14/MF A01 CSCL 01C

Cockpit Resource Management Training is a relatively new concept in the aviation industry. Although it is still in the process of maturing, it has received widespread acceptance in all facets of the community, worldwide. Much has happened in the area since the first workshop in 1979, and NASA-Ames Aerospace Human Factors Research Division has received many requests over the years to sponsor a new workshop to review the progress. The U.S. Air Force Military Airlift Command, having undertaken resource management training on a large scale, also urged a comprehensive review and agreed to co-sponsor this workshop. This volume is an up-to-date reference for use by those interested in the subject of Cockpit Resource Management (CRM) Training. For individual titles, see N87-22635 through N87-22659.

N87-22635*# Texas Univ., Austin.

THEORY UNDERLYING CRM TRAINING: PSYCHOLOGICAL ISSUES IN FLIGHT CREW PERFORMANCE AND CREW COORDINATION

Robert L. Helmreich *In* NASA. Ames Research Center Cockpit Resource Management Training May 1987 p 15-22 (For primary document see N87-22634 16-03)
Avail: NTIS HC A14/MF A01 CSCL 01C

What psychological theory and research can reveal about training in Cockpit Resource Management (CRM) is summarized. A framework is provided for the critical analysis of current approaches to CRM training. Background factors and definitions critical to evaluating CRM are reviewed, followed by a discussion of issues directly related to CRM training effectiveness. Some of the things not known about the optimization of crew performance and the research needed to make these efforts as effective as possible are described. E.R.

N87-22636*# Harvard Univ., Cambridge, Mass.

GROUP-LEVEL ISSUES IN THE DESIGN AND TRAINING OF COCKPIT CREWS c54

J. Richard Hackman *In* NASA. Ames Research Center Cockpit Resource Management Training May 1987 p 23-39 (For primary document see N87-22634 16-03)
(Contract NCC2-324)
Avail: NTIS HC A14/MF A01 CSCL 05H

Cockpit crews always operate in an organizational context, and the transactions between the crew and representatives of that context (e.g., organizational managers, air traffic controllers) are consequential for any crew's performance. For a complete understanding of crew performance a look beyond the traditional focus on individual pilots is provided to see how team- and organization-level factors can enhance (or impede) the ability of even well-trained individuals to work together effectively. This way of thinking about cockpit crews (that is, viewing them as teams that operate in organizations) offers some potentially useful avenues for thinking about next steps in the development of CRM training programs. Those possibilities are explored, emphasizing how they can enrich (not replace) individually-focussed CRM training. Author

N87-22637*# CRM Co.

COCKPIT RESOURCE MANAGEMENT (CRM): A TOOL FOR IMPROVED FLIGHT SAFETY (UNITED AIRLINES CRM TRAINING)

J. E. Carroll and William R. Taggart *In* NASA. Ames Research Center Cockpit Reource Management Training May 1987 p 40-46 (For primary document see N87-22634 16-03)
Avail: NTIS HC A14/MF A01 CSCL 01C

The approach and methodology used in developing cockpit management skills is effective because of the following features: (1) A comparative method of learning is used enabling crewmembers to study different forms of teamwork. (2) The learning comes about as a result of crewmembers learning from one another instead of from an expert instructor. (3) Key elements of cockpit teamwork and effective management are studied so that crewmembers can determine how these elements can improve safety and problem solving. (4) Critique among the crewmembers themselves rather than from outsiders is used as a common focusing point for crews to provide feedback to one another on how each can be a more effective crewmember. (5) The training is continuous in the sense that it becomes part of recurrent, upgrade, and other forms of crewmember training and development. And (6) the training results in sound and genuine insights that come about through solid education as opposed to tutoring, coaching, or telling crewmembers how to behave more effectively. Author

N87-22638*# United Air Lines, Inc., San Francisco, Calif.

THE DEVELOPMENT AND IMPLEMENTATION OF COCKPIT RESOURCE MANAGEMENT IN UAL RECURRENT TRAINING

David H. Shroyer *In* NASA. Ames Research Center Cockpit Resource Management Training May 1987 p 47-49 (For primary document see N87-22634 16-03)
Avail: NTIS HC A14/MF A01 CSCL 01C

Line Oriented Flight Training (LOFT) for United Airlines started in 1976. At that time it was basically no more than a line-simulated training function conducted in a full-mission simulator with no attention or stress on its human factor content. Very soon after the implementation of the LOFT program concerns were voiced about certain crew behavioral situations they were observing in the flight crew's execution of cockpit duties. These duties involved emergency procedures as well as irregular and normal procedures and situations. It was evident that new information was surfacing concerning crew interaction, or its lack thereof, in the cockpit and its effect on satisfactory performance. These observations naturally raised the question of how this information translated into the safety of aircraft operations. A training system had to be repetitive, the crew interactive, and the training had to be conducted under the crew concept. The foundation had to have two other factors: (1) it was necessary to have adequate human factor content, and (2) an advanced state-of-the-art simulator and appropriate electronic devices were required. These concepts are further discussed. E.R.

N87-22639*# People Express Airlines, Inc., Newark, N.J.

COCKPIT RESOURCE MANAGEMENT TRAINING AT PEOPLE EXPRESS

Keith D. Bruce and Doug Jensen *In* NASA. Ames Research Center Cockpit Resource Management Training May 1987 p 50-55 (For primary document see N87-22634 16-03)
Avail: NTIS HC A14/MF A01 CSCL 01C

In January 1986 in a continuing effort to maintain and improve flight safety and solve some Cockpit Resource Management (CRM) problems, People Express implemented a new CRM training program. It is a continuously running program, scheduled over the next three years and includes state-of-the-art full-mission simulation (LOFT), semi-annual seminar workshops and a comprehensive academic program authored by Robert W. Mudge of Cockpit Management Resources Inc. That program is outlined and to maximize its contribution to the workshop's goals, is organized into four topic areas: (1) Program content: the essential elements of resource management training; (2) Training methods: the strengths and weaknesses of current approaches; (3) Implementation: the implementation of CRM training; and (4) Effectiveness: the effectiveness of training. It is confined as much as possible to concise descriptions of the program's basic components. Brief discussions of rationale are included, however no attempt is made to discuss or review popular CRM tenets or the supporting research. Author

N87-22640*# Cockpit Management Resources, Inc.

COCKPIT MANAGEMENT AND SPECIFIC BEHAVIORAL OBJECTIVES (SBOs)

R. W. Mudge *In* NASA. Ames Research Center Cockpit Resource Management Training May 1987 p 56-60 (For primary document see N87-22634 16-03)
Avail: NTIS HC A14/MF A01 CSCL 01C

One of the primary tools used to accomplish the task of effective training is the specific behavioral objective (SBO). An SBO is simply a statement which specifically identifies a small segment of the final behavior sought, and a little more. The key word is specific. The company pinpoints exactly what it is it wants the pilot to do after completing training, and what it should evaluate from the point of view of both the program and the pilot. It tells the junior crewmember exactly, specifically, what he should monitor and support insofar as the management function is concerned. It gives greater meaning to the term second in command. And finally, it tells the supervisory pilot exactly what he should observe, evaluate, and instruct, insofar as the management function is concerned. E.R.

N87-22641*# Pan American World Airways, Inc., San Francisco, Calif.
PAN AMERICAN WORLD AIRWAYS FLIGHT TRAINING: A NEW DIRECTION. FLIGHT OPERATIONS RESOURCE MANAGEMENT **c81**
Roy Butler *In* NASA. Ames Research Center Cockpit Resource Management Training May 1987 p 61-67 (For primary document see N87-22634 16-03)
Avail: NTIS HC A14/MF A01 CSCL 05A

The Pan Am Flight Training Department shares the experiences it is having in its attempt to integrate cockpit resource management philosophies into its training programs. A slide-tape presentation on Pan Am's new direction in flight training is presented and briefly discussed. Author

N87-22642*# Continental Airlines, Inc., Los Angeles, Calif.
CREW COORDINATION CONCEPTS: CONTINENTAL AIRLINES CRM TRAINING
Darryl Christian and Alice Morgan *In* NASA. Ames Research Center Cockpit Resource Management Training May 1987 p 68-74 (For primary document see N87-22634 16-03)
Avail: NTIS HC A14/MF A01 CSCL 01C

The outline of the crew coordination concepts at Continental airlines is: (1) Present relevant theory: Contained in a pre-work package and in lecture/discussion form during the work course, (2) Discuss case examples: Contained in the pre-work for study and use during the course; and (3) Simulate practice problems: Introduced during the course as the beginning of an ongoing process. These concepts which are designed to address the problem pilots have in understanding the interaction between situations and their own theories of practice are briefly discussed. E.R.

N87-22643*# Japan Air Lines Co. Ltd., Tokyo.
OPTIMUM CULTURE IN THE COCKPIT
Hisaaki Yamamori *In* NASA. Ames Research Center Cockpit Resource Management Training May 1987 p 75-87 (For primary document see N87-22634 16-03)
Avail: NTIS HC A14/MF A01 CSCL 01C

Even with the same program and objectives, if the culture is different, there will be different approaches to the goal of flight safety. However, the cockpit environment is culture-free so it is not as important to think of a person's cultural background as it is to think of the approach to the goal of ultimate safety. Crew members can look at their individual safety goals and compare them to their own performance to see if their behavior matches their own safety goals. The cockpit environment must be culture-free in order to obtain the ultimate safety goal. One must first realize how their culture affects their behavior before they can begin to change their attitude and actions in the cockpit. E.R.

N87-22644*# Trans-Australia Airlines, Melbourne.
INTRODUCTION TO TRANS AUSTRALIA AIRLINES CRM TRAINING
Jim Davidson *In* NASA. Ames Research Center Cockpit Resource Management Training May 1987 p 88-90 (For primary document see N87-22634 16-03)
Avail: NTIS HC A14/MF A01 CSCL 01C

Trans Australia believes that its excellent accident rate record is due to a number of factors. It has a good group of standard operating procedures, and its crews are pretty well self-disciplined and adhere to those procedures. But the other thing that it believes is a factor in its safety record is that perhaps it is also due to its preparedness to be innovative, to keep up with what is going on in the rest of the world and, if it looks to have value, then to be amongst the first to try it out. Trans Australia commenced a program similar to Line Oriented Flight Training (LOFT) fairly early in 1979--that being its first windshear program-- which leads to why they are doing a course of resource management training, which we have chosen to call Aircrew Team Management (ATM). This course is detailed in another presentation. E.R.

N87-22645*# Trans-Australia Airlines, Melbourne. Flight Standards Div.
AIRCREW TEAM MANAGEMENT PROGRAM **c81**
Charles Margerison, Dick McCann, and Rod Davies (Queensland Univ., Brisbane, Australia) *In* NASA. Ames Research Center Cockpit Resource Management Training May 1987 p 90-107 (For primary document see N87-22634 16-03)
Avail: NTIS HC A14/MF A01 CSCL 05A

The key features of the Aircrew Team Management Workshop which was designed for and in consultation with Trans Australia Airlines are outlined. Five major sections are presented dealing with: (1) A profile of the airline and the designers; (2) Aircrew consultation and involvement; (3) Educational design and development; (4) Implementation and instruction; and (5) Evaluation and assessment. These areas are detailed. E.R.

N87-22646*# International Federation of Air Line Pilot Associations, Egham (England). Human Performance Committee.
REMEDIAL TRAINING: WILL CRM WORK FOR EVERYONE
A. N. Johnston *In* NASA. Ames Research Center Cockpit Resource Management Training May 1987 p 108-122 (For primary document see N87-22634 16-03)
Avail: NTIS HC A14/MF A01 CSCL 01C

The subject of those pilots who seem unresponsive to Cockpit Resource Management (CRM) training is addressed. Attention is directed to the need and opportunity for remedial action. Emphasis is given to the requirement for new perspectives and additional training resources. It is also argued that, contrary to conventional training wisdom, such individuals do not represent a hard core which is beyond assistance. Some evidence is offered that such a new perspective will lend itself to a wider appreciation of certain specific training needs. The role of appropriately trained specialists is briefly outlined, and a selected bibliography is attached. The combined experiences of several Pilot Advisory Groups (PAG's) within IFALPA member association form the basis for this discussion. It does not purport to desribe the activities of any one PAG. While much of the activities of PAG's have no relevance to CRM, there are clearly some very important points of intersection. The relevance of these points to diagnostic skills, and remedial training in the general domain of CRM is made obvious. Author

N87-22647*# International Air Transport Association, Montreal (Quebec). Flight Operations Services.
COCKPIT RESOURCE MANAGEMENT TRAINING
Lawson C. White *In* NASA. Ames Research Center Cockpit Resources Management Training May 1987 p 123-125 (For primary document see N87-22634 16-03)
Avail: NTIS HC A14/MF A01 CSCL 01C

The 6th General Flight Crew Training Meeting held in Montreal in May, 1984 was for most IATA member airlines the first time they had been exposed to what was then a relatively new aspect of flight crew training-resource management training. In reviewing the results of this meeting the IATA Flight Crew Training SubCommittee (FCTSC), which had been responsible for the agenda and the meeting itself, concluded that because very few airlines had implemented a program or even appeared to understand the term resource management, a member airline survey should be conducted and the results analyzed. This presentation shows the results of that survey in a form which can be related to the topics of the workshop. Author

N87-22648*# Military Airlift Command, Scott AFB, Ill.
INTRODUCTION TO MAC CRM TRAINING
Donald D. Brown *In* NASA. Ames Research Center Cockpit Resource Management Training May 1987 p 132-134 (For primary document see N87-22634 16-03)
Avail: NTIS HC A14/MF A01 CSCL 01C

The author introduces the Military Airlift Command (MAC) and its mission. A brief history of Cockpit Resource Management (CRM) as it relates to MAC is given. He also states why MAC is currently interested in CRM. E.R.

N87-22649*# United Air Lines, Inc., San Francisco, Calif. Seville Training Systems Div.

THE APPLICATION OF CRM TO MILITARY OPERATIONS

Dale E. Cavanagh and Kenneth R. Williams *In* NASA. Ames Research Center Cockpit Resource Management Training May 1987 p 135-144 (For primary document see N87-22634 16-03)
Avail: NTIS HC A14/MF A01 CSCL 01C

The detailed content of the CRM training component of the C-5 Aircrew Training System (ATS) was left to the discretion of the contractor. As a part of determining what the content should be, United Airlines Services Corporation has made an effort to understand how the needs of MAC crews compare with those of civilian airline crews. There are distinct similarities between the crew roles in the cockpits of civilian airliners and military air transports. Many of the attitudes and behaviors exhibited by civil and military crew members are comparable, hence much of the training in the field referred to as Cockpit Resource Management (CRM) is equally appropriate to civil or military aircrews. At the same time, there are significant differences which require assessment to determine if modifications to what might be termed generic CRM are necessary. The investigation enabled the definition and specification of CRM training which is believed to address the needs of the C-5 operational community. The study has concentrated largely on military airlift, but the training objectives and course content of the CRM training are readily adaptable to a wider range of military cockpits than are found in strategic airlift. For instance, CRM training focusing on communication, leadership, situational awareness, and crew coordination is just as appropriate, with some modification, to the pilots manning a flight to Tactical Airlift Command A-7's as it is to the pilots, flight engineers, and loadmasters crewing a C-5. Author

N87-22650*# Combat Crew Training Wing (1550th), Kirtland AFB, N. Mex.

COCKPIT RESOURCE MANAGEMENT (CRM) TRAINING IN THE 1550TH COMBAT CREW TRAINING WING

Michael T. Fiedler *In* NASA. Ames Research Center Cockpit Resource Management Training May 1987 p 145-147 (For primary document see N87-22634 16-03)
Avail: NTIS HC A14/MF A01 CSCL 01C

The training program the 1550th Combat Crew Training Wing at Kirtland Air Force Base, New Mexico, implemented in September 1985 is discussed. The program is called Aircrew Coordination Training (ACT), and it is designed specifically to help aircrew members work more effectively as a team in their respective aircraft and hopefully to reduce human factors-related accidents. The scope of the 1550th CCTW's training responsibilities is described, the structure of the program, along with a brief look at the content of the academic part of the course. Then the Mission-Oriented Simulator Training (MOST) program is discussed; a program similar to the Line Oriented Flight Training (LOFT) programs. Finally, the future plans for the Aircrew Coordination Training Program at the 1550th is discussed. Author

N87-22651*# Military Airlift Wing (349th), Travis AFB, Calif.

COCKPIT RESOURCE MANAGEMENT (CRM) TRAINING IN THE 349TH MILITARY AIRLIFT WING

John T. Halliday, Conrad S. Biegalski, and Anthony Inzana *In* NASA. Ames Research Center Cockpit Resource Management Training May 1987 p 148-157 (For primary document see N87-22634 16-03)
Avail: NTIS HC A14/MF A01 CSCL 01C

CRM training can be done on a limited budget. It seems that everyone has a special name for their CRM program. A new program was created and entitled, Aircrew Resource Management (ARM) to emphasize the use of the full resources on our aircraft. That is meant to specifically include the loadmasters. The name also emphasizes the concept that all crewmembers are responsible for safe completion of the trip. The loadmasters have been the brightest students to date. They are a classic under-utilized resource. Together, their crew position has been credited with more ARM saves than the engineers and pilots. The seminar-based program is run by two seminar facilitators that is reinforced by Line Oriented Flight Training sessions run by the active-duty counterparts. Author

N87-22652*# SimuFlite, Inc., Dallas/Fort Worth Airport, Tex.

COCKPIT RESOURCE MANAGEMENT (CRM) FOR PART 91 AND 135 OPERATIONS

Neil C. Krey and Don Rodgers *In* NASA. Ames Research Center Cockpit Resource Management Training May 1987 p 158-169 (For primary document see N87-22634 16-03)
Avail: NTIS HC A14/MF A01 CSCL 01C

Every flight is characterized by constant change. It is the way each individual crew responds to that change that determines how effectively they will be able to manage their flight deck. The concepts of Flight Deck Management (FDM) is presented. The principles dealt with are applicable to every flight, and the occurrence of change in the conduct of every flight is given. Nothing remains as it is initially perceived. It is then shown how SimuFlite accomplishes training in these concepts. Finally the challenges which are faced as an industry to make FDM more effective are discussed. Author

N87-22653*# Flight Safety International, Inc., LaGuardia Airport, N.Y.

COCKPIT RESOURCE MANAGEMENT (CRM) FOR FAR PARTS 91 AND 135 OPERATORS

Douglas Schwartz *In* NASA. Ames Research Center Cockpit Resource Management Training May 1987 p 170-177 (For primary document see N87-22634 16-03)
Avail: NTIS HC A14/MF A01 CSCL 01C

The why, what, and how of CRM at Flight Safety International (FSI)--that is, the philosophy behind the program, the content of the program, and some insight regarding how it delivers that to the pilot is presented. A few of the concepts that are part of the program are discussed. This includes a view of statistics called the Safety Window, the concept of situational awareness, and an approach to training that we called the Cockpit Management Concept (CMC). Author

N87-22654*# Federal Aviation Administration, Washington, D.C. Training and Technical Standards Div.

THE REGULATORY HORIZON

Ed Cook *In* NASA. Ames Research Center Cockpit Resource Management Training May 1987 p 178-187 (For primary document see N87-22634 16-03)
Avail: NTIS HC A14/MF A01 CSCL 01C

The author briefly discusses the FAA's position as it relates to cockpit resource management. For example, if Cockpit Resource Management (CRM) is a positive concept, why isn't everyone required to implement it? The regulatory practice of the FAA is discussed and questions and answers are presented. E.R.

N87-22655*# National Aeronautics and Space Administration. Ames Research Center, Moffett Field, Calif.

INSTRUCTIONS TO WORKING GROUPS

H. Clayton Foushee *In its* Cockpit Resource Management Training May 1987 p 188-192 (For primary document see N87-22634 16-03)
Avail: NTIS HC A14/MF A01 CSCL 01C

The key to the success of this workshop is your active participation in the working group process. The goals of this workshop are to address four major questions regarding Cockpit Resource Management (CRM) Training. To some extent the working group topic areas parallel these issues, but in some cases they do not. However, it is important for all of the working groups to keep these general questions in mind during their deliberations: (1) What are the essential elements of an optimal CRM Training program; (2) What are the strengths and weaknesses of current approaches to CRM Training; (3) How can CRM Training best be implemented, and what barriers exist; and (4) Is CRM Training effective, do we know, and if not, how can we find out. Author

N87-22656*# National Aeronautics and Space Administration. Ames Research Center, Moffett Field, Calif.

DYADS AND TRIADS AT 35,000 FEET: FACTORS AFFECTING GROUP PROCESS AND AIRCREW PERFORMANCE

H. Clayton Foushee *In its* Cockpit Resource Management Training May 1987 p 265-279 Repr. from American Psychologist, v. 39, Aug. 1984 Previously announced in IAA as A85-21850 (For primary document see N87-22634 16-03)
Avail: NTIS HC A14/MF A01 CSCL 01C

The task of flying a multipilot transport aircraft is a classic small-group performance situation where a number of social, organizational, and personality factors are relevant to important outcome variables such as safety. The aviation community is becoming increasingly aware of the importance of these factors but is hampered in its efforts to improve the system because of research psychology's problems in defining the nature of the group process. This article identifies some of the problem areas as well as methods used to address these issues. It is argued that high fidelity flight simulators provide an environment that offers unique opportunities for work meeting both basic and applied research criteria. Author

N87-22657*# Royal Air Force, Farnborough (England).

AIRCREW COOPERATION IN THE ROYAL AIR FORCE

C. B. Adcock *In* NASA. Ames Research Center Cockpit Resource Management Training May 1987 p 280-287 (For primary document see N87-22634 16-03)
Avail: NTIS HC A14/MF A01 CSCL 01C

The progressive introduction of modern, high performance aircraft, coupled with a significant increase in the complexity of the operational environment, has highlighted crew co-operation as a critical factor in aircraft safety. Investigation into recent MAC aircraft accidents supports the conclusion reached by NASA and other U.S. research institutions that a positive training program is required to improve resource management in the cockpit and prevent a breakdown under stress of the crew process. Past training and regulation has concentrated on the attainment of individual flying skills, but group skills have been neglected through lack of knowledge and understanding of the group process. This long-standing deficiency is now being addressed in the U.S. by the progressive and widespread introduction of theoretical and practical training programs to improve crew co-operation. The RAF should provide similar training for its aircrews through the adaptation and development of existing training resources. Better crew co-operation would not only reduce the number of RAF aircraft accidents but also improve the morale of the Service. Author

N87-22658*# Air New Zealand, Auckland.

COCKPIT RESOURCE MANAGEMENT (CRM) AND HUMAN FACTORS TRAINING: WHAT AIR NEW ZEALAND IS DOING ABOUT IT

Fionna Scott-Milligan and Bryan Wyness *In* NASA. Ames Research Center Cockpit Resource Management Training May 1987 p 288-290 (For primary document see N87-22634 16-03)
Avail: NTIS HC A14/MF A01 CSCL 01C

The authors have played an integral role in Air New Zealand's evaluation of CRM and Human Factors training options available to date. As the final decision as to which course is best suited to Air New Zealand's needs has yet to be made, briefly outlined are: (1) why this form of training was considered necessary; (2) the approach taken to evaluating the options available; (3) some of the problems encountered on the way; and (4) some plans for the future. Author

N87-22659*# USAir, Pittsburgh, Pa.

COCKPIT RESOURCE MANAGEMENT AT USAIR

Robert Sellards *In* NASA. Ames Research Center Cockpit Resource Management Training May 1987 p 291-297 (For primary document see N87-22634 16-03)
Avail: NTIS HC A14/MF A01 CSCL 01C

The current USAir CRM program is presented. The lessons learned and the program issues are combined. The training material was developed after an extensive literature search and pilot interview survey to determine the problem. The investigation led to the design, implementation, and evaluation of a behavioral science awareness training program. The need was found, and the target population was identified as the pilot group. E.R.

N87-22660# Air Force Inst. of Tech., Wright-Patterson AFB, Ohio. School of Engineering.

GEMACS (GENERAL EM MODEL FOR THE ANALYSIS OF COMPUTER SYSTEMS) FREQUENCY-DOMAIN ANALYSIS TO DETERMINE THE LIGHTNING INDUCED ELECTROMAGNETIC SKIN CURRENT DISTRIBUTIONS ON AN AIRCRAFT M.S. Thesis

Frank G. Tomko Dec. 1986 132 p
(AD-A178854; AFIT/GE/ENG/86D-10) Avail: NTIS HC A07/MF A01 CSCL 01C

A frequency-domain electromagnetic (EM) analysis of an aircraft's EM interaction with lightning is performed by using the General EM Model for the Analysis of Complex Systems (GEMACS) to determine the EM skin current distributions on the surface of a FAA CV-580 aircraft. The Method of Moments (MOM) is incorporated in GEMACS to provide an approximate solution to Maxwell's integral equations and to determine the aircraft surface currents. A 384 segment wire grid model of the CV-580 and lightning channels is constructed for the analysis; two variations of modelling the channels is constructed for the analysis; two variations of modelling the channels are implemented. The GEMACS analysis is performed for frequencies of 0.5 MHz to 5.0 MHz, in 0.5 MHz increments. The GEMACS' predicted segment currents are used to derive wire grid frequency-domain transfer functions which are compared to: (1) actual aircraft transfer functions obtained from in-flight lightning measurements, and (2) transfer functions generated from a previously performed time-domain three-dimensional finite difference (T3DFD) EM program analysis. Results show that GEMACS can be implemented to adequately predict lightning induced aircraft skin current distributions and associated aircraft resonant frequencies. Also, GEMACS provides more EM interaction information than T3DFD and, based on CPU run times, predicts this information much more efficiently. GRA

N87-22605*# Massachusetts Inst. of Tech., Cambridge. Flight Transportation Lab.

INVESTIGATION OF AIR TRANSPORTATION TECHNOLOGY AT MASSACHUSETTS INSTITUTE OF TECHNOLOGY, 1984

Robert W. Simpson *In* NASA. Langley Research Center Joint University Program for Air Transportation Research, 1984 May 1987 p 3-7 (For primary document see N87-22604 16-01)
Avail: NTIS HC A08/MF A01 CSCL 01C

N87-22608*# Massachusetts Inst. of Tech., Cambridge. Dept. of Aeronautics and Astronautics.

MEASUREMENT OF ICE ACCRETION USING ULTRASONIC PULSE ECHO TECHNIQUES

R. John Hansman, Jr. and Mark S. Kirby *In* NASA. Langley Research Center Joint University Program for Air Transportation Research, 1984 May 1987 p 25-41 (For primary document see N87-22604 16-01)
Avail: NTIS HC A08/MF A01 CSCL 01C

N87-22609*# Ohio Univ., Athens.

INVESTIGATION OF AIR TRANSPORTATION TECHNOLOGY AT OHIO UNIVERSITY, 1984

Richard H. McFarland *In* NASA. Langley Research Center Joint University Program for Air Transportation Research, 1984 May 1987 p 45-48 (For primary document see N87-22604 16-01)
Avail: NTIS HC A08/MF A01 CSCL 01C

N87-22619*# Princeton Univ., N. J. Dept. of Mechanical and Aerospace Engineering.

INVESTIGATION OF AIR TRANSPORTATION TECHNOLOGY AT PRINCETON UNIVERSITY, 1984

Robert F. Stengel *In* NASA. Langley Research Center Joint University Program for Air Transportation Research, 1984 May 1987 p 133-137 (For primary document see N87-22604 16-01)
Avail: NTIS HC A08/MF A01 CSCL 01C

1987 p 133-137 (For primary document see N87-22604 16-01)
Avail: NTIS HC A08/MF A01 CSCL 01C

04 AIRCRAFT COMMUNICATIONS AND NAVIGATION

Includes digital and voice communication with aircraft; air navigation systems (satellite and ground based); and air traffic control.

For related information see also *17 Space Communications, Spacecraft Communications, Command and Tracking* and *Communications and Radar.*

N87-22661# Air Force Systems Command, Wright-Patterson AFB, Ohio. Foreign Technology Div.
CONMILIT (SELECTED ARTICLES)
Guozhen Xu and Shanhu Huang 17 Mar. 1987 38 p Transl. into ENGLISH from Conmilit (China), v. 10, no. 2, issue 13, 1 Apr. 1986 p 65-75
(AD-A179155; FTD-ID(RS)T-1168-86) Avail: NTIS HC A03/MF A01 CSCL 17G

CONMILIT (China), v. 10, no. 2, 1 Apr 1986, contains the following: Inertial navigation systems of military aircraft and their Combat Applications---Proving accurate navigational and attack parameters, and Fiberoptical gyro---The navigational instrument of the future. GRA

N87-22662# Air Force Inst. of Tech., Wright-Patterson AFB, Ohio. School of Engineering.
DESIGN OF GPS (GLOBAL POSITIONING SYSTEM) STATUS REPORTING SYSTEM M.S. Thesis
Harrison C. Freer Dec. 1986 121 p
(AD-A179334; AFIT/GSO/ENS-ENG/86D-1) Avail: NTIS HC A06/MF A01 CSCL 17G

This study sought to design a status reporting system for the NAVSTAR Global Positioning System. A systems engineering approach was used for the full satellite constellation with fully functioning user equipment. The recommended system consists of three main elements: a database, a status transmission mechanism, and microcomputer software. The database proposed has two tiers and is maintained in real time as the operational constellation changes. The first tier contains the orbital ephemeris of the active constellation; the second consists of areas and associated times of degraded coverage. Two methods of initial transmission of the status information are identified. The existing Notices to Airmen (NOTAM) system is one primary transmission system; the other recommended initial link is electronic mail. Further dissemination by appropriate agencies, using a variety of transmission methods, is also outlined. The final element of the system is software that can run on microcomputers. GRA

N87-22606*# Massachusetts Inst. of Tech., Cambridge. Flight Transportation Lab.
AIRCRAFT APPROACH GUIDANCE USING RELATIVE LORAN-C NAVIGATION
Antonio L. Elias *In* NASA. Langley Research Center Joint University Program for Air Transportation Research, 1984 May 1987 p 9-16 (For primary document see N87-22604 16-01)
Avail: NTIS HC A08/MF A01 CSCL 17G

N87-22607*# Massachusetts Inst. of Tech., Cambridge.
PROBABILISTIC MODELING OF LORAN-C FOR NONPRECISION APPROACHES
John K. Einhorn *In* NASA. Langley Research Center Joint University Program for Air Transportation Research, 1984 May 1987 p 17-24 (For primary document see N87-22604 16-01)
Avail: NTIS HC A08/MF A01 CSCL 17G

N87-22612*# Ohio Univ., Athens.
LORAN-C APPROACH CONSIDERATIONS
Robert W. Lilley *In* NASA. Langley Research Center Joint University Program for Air Transportation Research, 1984 May 1987 p 61-63 (For primary document see N87-22604 16-01)
Avail: NTIS HC A08/MF A01 CSCL 17G

N87-22613*# Ohio Univ., Athens.
SATELLITE SURVEYING FOR A LORAN-C NONPRECISION APPROACH
Daryl L. McCall *In* NASA. Langley Research Center Joint University Program for Air Transportation Research, 1984 May 1987 p 65-67 (For primary document see N87-22604 16-01)
Avail: NTIS HC A08/MF A01 CSCL 17G

N87-22614*# Ohio Univ., Athens.
ADVANCED MONITORING CONCEPTS
Robert W. Lilley *In* NASA. Langley Research Center Joint University Program for Air Transportation Research, 1984 May 1987 p 69-71 (For primary document see N87-22604 16-01)
Avail: NTIS HC A08/MF A01 CSCL 17G

N87-22620*# Princeton Univ., N. J. Dept. of Mechanical and Aerospace Engineering.
SAFE MICROBURST PENETRATION TECHNIQUES: A DETERMINISTIC, NONLINEAR, OPTIMAL CONTROL APPROACH
Mark L. Psiaki *In* NASA. Langley Research Center Joint University Program for Air Transportation Research, 1984 May 1987 p 139-148 (For primary document see N87-22604 16-01)
Avail: NTIS HC A08/MF A01 CSCL 17G

05 AIRCRAFT DESIGN, TESTING AND PERFORMANCE

Includes aircraft simulation technology.

For related information see also *18 Spacecraft Design, Testing and Performance* and *39 Structural Mechanics.*For land transportation vehicles see *85 Urban Technology and Transportation.*

N87-22663# Advisory Group for Aerospace Research and Development, Neuilly-Sur-Seine (France). Flight Mechanics Panel.
IMPROVEMENT OF COMBAT PERFORMANCE FOR EXISTING AND FUTURE AIRCRAFT
Loughton, England Dec. 1986 143 p In ENGLISH and FRENCH Symposium held in Trevisco, Italy, 14-17 Apr. 1986
(AGARD-CP-409; ISBN-92-835-0408-9) Copyright Avail: NTIS HC A07/MF A01

These proceedings contain the unclassified papers presented at the AGARD Flight Mechanics Panel Symposium on The Improvement of Combat Performance for Existing and Future Aircraft, held in Trevisco, Italy from 14 to 18 April 1986. In planning the enhancement of a defence capability to meet a growing threat within increasing financial constraints, it is invariably necessary, and is current practice in all NATO countries, to consider varying options for improvement of existing weapon systems as an alternative to embarking on totally new systems concepts. A wide range of technical options are now available to improve the overall performance of a weapon system. Many of these features are equally applicable for embodiment in new designs or in existing combat aircraft. In considering these varied options, cost and effectiveness remain the common constraints. For individual titles, see N87-22664 through N87-22675.

N87-22664# Ministry of Defence, London (England).
COST ANALYSIS OF AIRCRAFT PROJECTS c01
D. Faddy *In* AGARD Improvement of Combat Performance for Existing and Future Aircraft Dec. 1986 10 p (For primary document see N87-22663 16-05)
Copyright Avail: NTIS HC A07/MF A01

The effect of advancing technology on the cost of past aircraft and the implications for the future is reviewed. The validity of historical records for forecasting a future dominated by technological change and the consequences of continued escalation are discussed. It is argued that more priority needs to be given to the reduction of support cost and a way of looking at this as a direct contribution to military capability is suggested. The role of operations research is briefly emphasized and a more deliberately evolutionary approach to the production of aircraft is advocated. Author

N87-22665# Industrieanlagen-Betriebsgesellschaft m.b.H., Ottobrunn (West Germany).
PERFORMANCE IMPROVEMENT OF AIRBORNE WEAPON SYSTEMS METHODS, SCOPE AND LIMITATIONS
P. Ebeling and R. Huber *In* AGARD Improvement of Combat Performance for Existing and Future Aircraft Dec. 1986 11 p (For primary document see N87-22663 16-05)
Copyright Avail: NTIS HC A07/MF A01

The performance improvement and the necessity to evaluate the overall and operational system performance improvement by use of systems assessment methods are discussed. These methods are briefly discussed using simple examples of former evaluations. Author

N87-22666# Italian Air Staff, Rome.
SOME DEVELOPMENT TRENDS IN LIGHT GROUND ATTACK AIRCRAFT
R. Tonini, G. M. Avagnina, E. Lojacono, and N. Bragagnolo (Aeritalia S.p.A., Caselle Torinese, Italy) *In* AGARD Improvement of Combat Performance for Existing and Future Aircraft Dec. 1986 16 p (For primary document see N87-22663 16-05)
Copyright Avail: NTIS HC A07/MF A01

The development of a light bomber attack aircraft, AM-X, is discussed. Specific design requirements and cost effectiveness, a mission effectiveness model, effectiveness tradeoffs, weapon systems and avionics are among the topics surveyed. R.J.F.

N87-22667# French Air Force, Paris. Nouveaux Avions de Combat Div.
WEAPON SYSTEMS POLYVALENCE: AN ECONOMIC AND OPERATIONAL CHALLENGE [POLYVALENCE DES SYSTEMES D'ARMES: UN DEFI ECONOMIQUE ET OPERATIONNEL]
Jean-Jacques Floch *In* AGARD Improvement of Combat Performance for Existing and Future Aircraft Dec. 1986 5 p In FRENCH (For primary document see N87-22663 16-05)
Copyright Avail: NTIS HC A07/MF A01

With the broadening of the concept of the weapons system, air combat missions of the 1990's will include, in the course of a single mission, phases of flight during which air-to-air and air-to-ground capabilities will be alternately or even simultaneously put to the test. The notion of polyvalence is introduced and the importance of the concept to aircraft design and particularly aircraft weapon systems definition is discussed. The primary benefit of polyvalence is that it greatly extends the ability of combat aircraft to adapt to an evolving operational environment. Author

N87-22668# British Aerospace Public Ltd. Co., Kingston-upon-Thames (England). Aerodynamics Dept.
EVOLUTION OF COMBAT PERFORMANCE OF THE HAWK LIGHT COMBAT AIRCRAFT
S. F. Stapleton and R. S. Dabbs *In* AGARD Improvement of Combat Performance for Existing and Future Aircraft Dec. 1986 11 p (For primary document see N87-22663 16-05)
Copyright Avail: NTIS HC A07/MF A01

The progressive evolution of the BAe Hawk from its original concept as the advanced flying trainer aircraft for the RAF to the currently planned developments as a light attack aircraft is reviewed. The developments are described in aerodynamics propulsion and systems to give improvement in performance and weapon delivery capability appropriate to effective light attack operational roles. Author

N87-22669# Messerschmitt-Boelkow-Blohm G.m.b.H., Munich (West Germany). Helicopter and Airplane Div.
INTEGRATED DESIGN OF STRUCTURES
O. Sensburg, G. Schmidinger, and K. Fuellhas *In* AGARD Improvement of Combat Performance for Existing and Future Aircraft Dec. 1986 20 p (For primary document see N87-22663 16-05)
Copyright Avail: NTIS HC A07/MF A01

It is shown that for highly sophisticated, naturally unstable airplanes flying supersonically a joint strategy to lay out the flight control system while minimizing design loads must be adopted. The selection of control surface geometry must be performed utilizing all possibilities from overall structural optimization including aeroelastic tailoring for primary carbon fiber structures. In the proposed design philosophy the behavior of the elastic airplane structure must be introduced and optimized in the very early design stage. It is shown that the required control surface hinge moments can be reduced by optimizing mass penalties and efficiencies. Minimizing installed hydraulic power supply has also a beneficial effect on engine performance at low speed, high altitudes. Author

N87-22670# Rolls-Royce Ltd., Bristol (England).
PROPULSION SYSTEM TECHNOLOGIES FOR THRUST VECTORING c07
P. Round and R. F. Tape (Rolls-Royce, Inc., Atlanta, Ga.) *In* AGARD Improvement of Combat Performance for Existing and Future Aircraft Dec. 1986 12 p (For primary document see N87-22663 16-05)
Copyright Avail: NTIS HC A07/MF A01

The Harrier/AV-8 aircraft, with its Rolls-Royce Pegasus engine, was developed primarily for vertical or short takeoff and landing operations. To achieve this it employs nozzles capable of vectoring through more than 90 deg to provide lift and a reaction control system to provide aircraft control in low or zero forward speed operation. These features of the aircraft have also been employed to advantage during combat by vectoring in forward flight (VIFFING). Operational analysis studies have identified the potential combat advantage of post-stall maneuvering (PMS) to improve rate of turn and vehicle/weapon pointing. To achieve any or all of these capabilities will require some degree of propulsion system thrust vectoring. Some particular requirements that the need for thrust vectoring place on the engine design and the technologies involved are addressed. Author

N87-22671# Air Force Wright Aeronautical Labs., Wright-Patterson AFB, Ohio. X-29 Advanced Development Program Office.
X-29 INTEGRATING ADVANCED TECHNOLOGIES FOR TOMORROW'S AIR COMBAT
Thomas M. Weeks and James R. Pruner *In* AGARD Improvement of Combat Performance for Existing and Future Aircraft Dec. 1986 13 p (For primary document see N87-22663 16-05)
Copyright Avail: NTIS HC A07/MF A01

The X-29 Advanced Tecnnology Demonstrator Program is underway and in flight status at NASA Dryden Flight Research Facility. The joint US Air Force, NASA DARPA, Grumman Aerospace Corporation program is demonstrating a set of advanced airframe technologies for consideration by designers of tomorrow's combat aircraft. These technologies are described and preliminary quantitative results are discussed. These technologies are integrated within the X-29 airframe. Tomorrow's combat aircraft will require new, integrated technologies and will benefit from the X-29 integration experience base. The X-29 aircraft is being considered for several potential test bed demonstrations of new equipment and airframe concepts and will serve well in this role to satisfy near term requirements. Author

N87-22672# Office National d'Etudes et de Recherches Aerospatiales, Paris (France).
SIMULATION OF AN INTEGRATED FLIGHT/FIRE CONTROL SYSTEM DURING AIR-TO-GROUND GUNNERY ATTACK [SIMULATION D'UNE SYSTEME INTEGRE DE COMMANDES DE VOL ET DE CONDUITE DE TIR CANON AIR-SOL]
B. Dang Vu and C. LaBurthe *In* AGARD Improvement of Combat Performance for Existing and Future Aircraft Dec. 1986 5 p

In FRENCH (For primary document see N87-22663 16-05)
Copyright Avail: NTIS HC A07/MF A01
Copyright Avail: NTIS HC A07/MF A01

A fixed base simulation study demonstrated that an integrated flight/fire control (IFFC) system decreased pilot workload during an air-to-ground gunnery attack and improved airplane flying qualities in comparison with those of a conventional aircraft. The IFFC system was designed to use only standard on-board instrumentation, excluding sophisticated sensors (e.g., electro-optical). A preliminary investigation of direct side force showed that it does not provide significant improvements in aiming effectiveness. Author

N87-22673# Army Avionics Research and Development Activity, Fort Monmouth, N. J.
THE IMPACT OF FUTURE AVIONICS TECHNOLOGY ON THE CONDUCT OF AIR WARFARE **c06**
Joseph A. Dasaro *In* AGARD Improvement of Combat Performance for Existing and Future Aircraft Dec. 1986 9 p (For primary document see N87-22663 16-05)
Copyright Avail: NTIS HC A07/MF A01

A synopsis is given of the conclusions reached by the Systems Subpanel of the NATO AGARD workshop on the potential impact of development in electronic technology on the future conduct of air warfare. Avionic system integration technology, system architecture, data processing, data communication paths, computer programs, fault detection and isolation, and system design methodology are among the topics discussed. Author

N87-22674# British Aerospace Public Ltd. Co., Preston (England).
IMPROVED COMBAT PERFORMANCE USING RELAXED STATIC STABILITY AND A SPIN PREVENTION SYSTEM (FBW JAGUAR) **c08**
J. R. Nelson and T. D. Smith *In* AGARD Improvement of Combat Performance for Existing and Future Aircraft Dec. 1986 8 p (For primary document see N87-22663 16-05)
Copyright Avail: NTIS HC A07/MF A01

The theoretical performance benefits that can be obtained by designing an aircraft that is naturally unstable in pitch and artificially stabilized by use of active control technology including an integral stall departure and spin prevention/g limiting function are described. How many of these benefits have been successfully demonstrated during flight trials on the FBW Jaguar demonstrator aircraft is discussed. The flight trials are briefly discussed including the results of the stall departure and spin prevention system assessment with examples of severe dynamic combat maneuvers made possible by such a system. The combination of leading edge wing strakes and longitudinal instability gave improvements in aircraft turn rate, acceleration, and field performance, thus providing a practical demonstration of many of the theoretical benefits described earlier. The FBW Jaguar flight control system was designed from the outset as a production system with the aim of identifying production clearance procedures so this experience leads straight into new combat aircraft such as the EFA. Author

N87-22675# British Aerospace Public Ltd. Co., Lancashire (England). Military Aircraft Div.
THE ASSESSMENT AND EVALUATION OF COMBAT PERFORMANCE IMPROVEMENTS
A. G. Barnes *In* AGARD Improvement of Combat Performance for Existing and Future Aircraft Dec. 1986 8 p (For primary document see N87-22663 16-05)
Copyright Avail: NTIS HC A07/MF A01

Aircraft performance improvements, for combat or any other operational role, are becoming increasingly difficult to achieve. The dramatic year-by-year advances of the forties and fifties are long gone. Aerodynamicists have a much better understanding of the physical properties of the atmosphere and the shapes which can best be propelled through it. The relationships between the energy in fuel, and the conversion process into thrust are well developed. Structural engineers understand the mechanical properties of materials needed to build engines and airframes. All these factors have been exploited, and further improvements do not come cheaply. Only in the area of avionics can it be said that large benefits in the weight/cost/performance trade-off can be expected. The use of mathematical models, current simulation capabilities, tradeoff studies, and operational tactics are discussed. Author

N87-22676# Air Force Inst. of Tech., Wright-Patterson AFB, Ohio. School of Engineering.
ACCURATE PREDICTION OF LONGITUDINAL FLYING QUALITIES FOR LANDING AIRCRAFT M.S. Thesis
James J. Martz Dec. 1986 143 p
(AD-A179069; AFIT/GAE/ENG/87M-1) Avail: NTIS HC A07/MF A01 CSCL 01B

A new longitudinal flying qualities metric, called Loop Separation Parameter (LSP), is intended to correlate with pilot opinion ratings for the landing task. This parameter is based on the observed shift of pilot control emphasis from pitch attitude control during power approach to flight path control during flare to touchdown. The calculation of LSP combines simple, intuitive pilot models with classical root locus and frequency response techniques. In this research, a new criterion based on LSP to predict expected pilot ratings is presented. Although developed from data for fighter-type aircraft, the LSP criterion successfully predicts pilot ratings for large transport and space shuttle configurations as well. This criterion is developed only for aircraft using front-side of the power curve landing techniques. The prediction success of this criterion compares well with the success of MIL-F-8785C Flying Qualities criteria. Recommendations include the consideration of LSP for the Flying Qualities Handbook. GRA

N87-22677# Georgia Inst. of Tech., Atlanta.
ANALYSIS OF STRUCTURES WITH ROTATING, FLEXIBLE SUBSTRUCTURES APPLIED TO ROTORCRAFT AEROELASTICITY IN GRASP (GENERAL ROTORCRAFT AEROMECHANICAL STABILITY PROGRAM)
Dewey H. Hodges, A. Stewart Hopkins, and Donald L. Kunz (Army Aviation Research and Development Command, Moffett Field, Calif.) 1987 11 p
(AD-A178941) Avail: NTIS HC A02/MF A01 CSCL 20K

The initial version of the General Rotorcraft Aeromechanical Stability Program (GRASP) was developed for analysis of rotorcraft in steady, axial flight and ground contact conditions. In these flight regimes, the material continua of the rotorcraft may experience deformations which are independent of time. GRASP can obtain this steady-state solution and can solve the eigenproblem associated with perturbations about such a steady-state solution. GRASP is the first program implementing a new method for dynamic analysis of structures, parts of which may be experiencing discrete motion relative to other parts. Application of this new method to GRASP, including substructuring, frames of reference, nodes, finite elements and constraints, is described in the paper. The library of finite elements includes a powerful nonlinear beam element that incorporates aeroelastic effects based on a simple nonlinear, aerodynamic theory with unsteady induced inflow. GRA

06 AIRCRAFT INSTRUMENTATION

Includes cockpit and cabin display devices; and flight instruments.

For related information see also *19 Spacecraft Instrumentation* and *35 Instrumentation and Photography.*

N87-22678* National Aeronautics and Space Administration. Langley Research Center, Hampton, Va.
AIRCRAFT CONTROL POSITION INDICATOR Patent
Dale V. Dennis, inventor (to NASA) (Kentron International, Inc., Hampton, Va.) 5 May 1987 9 p Filed 8 Feb. 1984 Supersedes N84-20522 (22 - 11, p 1607)
(NASA-Case-LAR-12984-1; US-Patent-4,663-627; US-Patent-Appl-SN-578387; US-Patent-Class-340-975; US-Patent-Class-73-178-R;

US-Patent-Class-244-1-R; US-Patent-Class-340-945; US-Patent-Class-340-971) Avail: US Patent and Trademark Office CSCL 01D

An aircraft control position indicator was provided that displayed the degree of deflection of the primary flight control surfaces and the manner in which the aircraft responded. The display included a vertical elevator dot/bar graph meter display for indication whether the aircraft will pitch up or down, a horizontal aileron dot/bar graph meter display for indicating whether the aircraft will roll to the left or to the right, and a horizontal dot/bar graph meter display for indicating whether the aircraft will turn left or right. The vertical and horizontal display or displays intersect to form an up/down, left/right type display. Internal electronic display driver means received signals from transducers measuring the control surface deflections and determined the position of the meter indicators on each dot/bar graph meter display. The device allows readability at a glance, easy visual perception in sunlight or shade, near-zero lag in displaying flight control position, and is not affected by gravitational or centrifugal forces.

Official Gazette of the U.S. Patent and Trademark Office

N87-22616*# Ohio Univ., Athens. Dept. of Electrical and Computer Engineering.

PROCESSOR-CONTROLLED TIMING MODULE FOR LORAN-C RECEIVER

Robert W. Lilley *In* NASA. Langley Research Center Joint University Program for Air Transportation Research, 1984 May 1987 p 77-85 Previously announced as N84-20504 (For primary document see N87-22604 16-01)
(OU-TM-90) Avail: NTIS HC A08/MF A01 CSCL 01D

N87-22673# Army Avionics Research and Development Activity, Fort Monmouth, N. J.

THE IMPACT OF FUTURE AVIONICS TECHNOLOGY ON THE CONDUCT OF AIR WARFARE

Joseph A. Dasaro *In* AGARD Improvement of Combat Performance for Existing and Future Aircraft Dec. 1986 9 p
(For primary document see N87-22663 16-05)
Copyright Avail: NTIS HC A07/MF A01

07 AIRCRAFT PROPULSION AND POWER

Includes prime propulsion systems and systems components, e.g., gas turbine engines and compressors; and onboard auxilliary power plants for aircraft.

For related information see also *20 Spacecraft Propulsion and Power, 28 Propellants and Fuels,* and *44 Energy Production and Conversion.*

N87-22679# Naval Postgraduate School, Monterey, Calif.

GAS TURBINE COMBUSTOR AND ENGINE AUGMENTOR TUBE SOOTING CHARACTERISTICS Final Report, Oct. 1985 - Sep. 1986

J. S. Bennett, C. H. Jway, D. J. Urich, and D. W. Netzer Dec. 1986 85 p
(AD-A179423; NPS67-86-004) Avail: NTIS HC A05/MF A01 CSCL 21B

An experimental investigation was conducted to investigate the effects of smoke-suppressant fuel additives, fuel composition and combustor operating environment on the soot characteristics within the combustor and across an engine exhaust augmentor tube. A T63 combustor was used with fuel additive pumps and an exhaust augmentor tube. Soot mean diameters and concentrations were measured at two locations within the combustor and at the exhaust of the augmentor tube using three-wavelength light transmission and multiple-angle forward scattering measurements and collection probes. Fuel and air flow rates were varied and combustor inlet air temperature was varied using a hydrogen-fueled vitiated air heater. Combustor flow conditions were found to significantly change soot characteristics as well as the effects of smoke-suppressant fuel additives. D32(volume-to-surface mean diameter) varied between 0.10 and 0.30 microns within the combustor. D32 increased significantly across the engine augmentor tube, to sizes as large as 0.43 microns. GRA

N87-22680*# National Aeronautics and Space Administration. Lewis Research Center, Cleveland, Ohio.

ANALYSIS OF AN ADVANCED TECHNOLOGY SUBSONIC TURBOFAN INCORPORATING REVOLUTIONARY MATERIALS

Gerald Knip, Jr. May 1987 25 p
(NASA-TM-89868; E-3542; NAS 1.15:89868) Avail: NTIS HC A02/MF A01 CSCL 21E

Successful implementation of revolutionary composite materials in an advanced turbofan offers the possibility of further improvements in engine performance and thrust-to-weight ratio relative to current metallic materials. The present analysis determines the approximate engine cycle and configuration for an early 21st century subsonic turbofan incorporating all composite materials. The advanced engine is evaluated relative to a current technology baseline engine in terms of its potential fuel savings for an intercontinental quadjet having a design range of 5500 nmi and a payload of 500 passengers. The resultant near optimum, uncooled, two-spool, advanced engine has an overall pressure ratio of 87, a bypass ratio of 18, a geared fan, and a turbine rotor inlet temperature of 3085 R. Improvements result in a 33-percent fuel saving for the specified misssion. Various advanced composite materials are used throughout the engine. For example, advanced polymer composite materials are used for the fan and the low pressure compressor (LPC). Author

N87-22681*# National Aeronautics and Space Administration. Lewis Research Center, Cleveland, Ohio.

SUPERSONIC THROUGH-FLOW FAN DESIGN

James F. Schmidt, Royce D. Moore, Jerry R. Wood, and Ronald J. Steinke 1987 21 p Prepared for presentation at the 23rd Joint Propulsion Conference, San Diego, Calif., 29 Jun. - 2 Jul. 1987; sponsored in part by AIAA, SAE, ASME and ASEE
(NASA-TM-88908; E-3492; NAS 1.15:88908; AIAA-87-1746) Avail: NTIS HC A02/MF A01 CSCL 21E

The NASA Lewis Research Center has embarked on a program to experimentally prove the concept of a supersonic through-flow fan which is to maintain supersonic velocities throughout the compression system with only weak shock-wave flow losses. The detailed design of a supersonic through-flow fan and estimated off-design performance with the use of advanced computational codes are described. A multistage compressor facility is being modified for the newly designed supersonic through-flow fan and the major aspects of this modification are briefly described. Author

N87-22682# Aeronautical Research Labs., Melbourne (Australia).

PRELIMINARY INVESTIGATION OF THE USE OF HOLOGRAPHIC INTERFEROMETRY TO DETECT ILL-FITTING COMPRESSOR BLADES

S. J. Rumble and B. Lawrie Nov. 1986 23 p
(AD-A178519; ARL/STRUC-TM-451) Avail: NTIS HC A02/MF A01 CSCL 14B

The technique of double exposure holographic interferometry has been used to detect and investigate ill-fitting compressor blades. A brief introduction to holographic interferometry is given. Holographic interferometry has enabled the observation of the displacements of blades when the blades are subjected to a small force. The potential of a pulsed laser holographic system to be used for in-situ investigations is discussed. GRA

N87-22683# Mechanical Technology, Inc., Latham, N. Y.

AI (ARTIFICIAL INTELLIGENCE) GAS TURBINE ROTOR DIAGNOSTICS Final Report, Apr. 1985 - Jul. 1986

B. Aggarwal, J. Tecza, J. Giordano, and R. Brunner Nov. 1986 160 p
(Contract F33615-85-C-2513)
(AD-A178996; MTI-86-TR-36; AFWAL-TR-86-2072) Avail: NTIS HC A08/MF A01 CSCL 21E

With increased emphasis on improving the reliability and maintainability of gas turbine engines in the U.S. Air Force inventory and the need to operate aircraft from austere forward bases, new diagnostic tools are required. Such tools must provide reliable, consistent diagnoses and minimize training requirements for maintenance personnel. Knowledge-based diagnostic systems have the potential to meet these needs by improving the productivity of USAF maintenance personnel, affecting a standardized diagnostic approach at all maintenance facilities, and providing a wider dissemination of the benefits of accumulated USAF experience in gas turbine vibration diagnostics. Typical rotordynamic faults observed in gas turbine engines were surveyed to assess the extent of knowledge to diagnose rotordynamic faults. A set of generic rotordynamic faults was selected and a diagnostic strategy was developed for those faults. System configuration for a typical knowledge-based rotordynamic diagnostic system was defined based on the requirements identified during the survey. The diagnostic concepts developed were demonstrated using a laboratory test rig capable of having faults implanted in it. GRA

N87-22684# Naval Air Propulsion Test Center, Trenton, N.J.
STATISTICS ON AIRCRAFT GAS TURBINE ENGINE ROTOR FAILURES THAT OCCURRED IN US COMMERCIAL AVIATION DURING 1981 Final Report
R. A. DeLucia, J. T. Salvina, and T. Russo Mar. 1987 27 p
Prepared in cooperation with Federal Aviation Agency, Atlantic City, N.J.
(DOT/FA71NA-AP98)
(DOT/FAA/CT-86/42; NAPC-PE-154C) Avail: NTIS HC A03/MF A01

Statistical data relating to gas turbine engine rotor failures which occurred during 1981 in commercial aviation service use are presented. The predominant failure involved blade fragments, 83 percent of which were contained. Three disk failures occurred and all were contained. Fifty-seven percent of the 136 failures occurred during the takeoff and climb stages of flight. Author

N87-22685*# Lockheed-California Co., Burbank.
FLIGHT AND ANALYTICAL INVESTIGATIONS OF A STRUCTURAL MODE EXCITATION SYSTEM ON THE YF-12A AIRPLANE Final Report
E. A. Goforth, R. C. Murphy, J. A. Beranek, and R. A. Davis Apr. 1987 295 p
(NASA Order E-69204)
(NASA-CR-166623; H-1361; NAS 1.26:166623) Avail: NTIS HC A13/MF A01 CSCL 21E

A structural excitation system, using an oscillating canard vane to generate force, was mounted on the forebody of the YF-12A airplane. The canard vane was used to excite the airframe structural modes during flight in the subsonic, transonic, and supersonic regimes. Structural modal responses generated by the canard vane forces were measured at the flight test conditions by airframe-mounted accelerometers. Correlations of analytical and experimental aeroelastic results were made. Doublet lattice, steady state double lattice with uniform lag, Mach box, and piston theory all produced acceptable analytical aerodynamic results within the restrictions that apply to each. In general, the aerodynamic theory methods, carefully applied, were found to predict the dynamic behavior of the YF-12A aircraft adequately. Author

N87-22670# Rolls-Royce Ltd., Bristol (England).
PROPULSION SYSTEM TECHNOLOGIES FOR THRUST VECTORING
P. Round and R. F. Tape (Rolls-Royce, Inc., Atlanta, Ga.) *In* AGARD Improvement of Combat Performance for Existing and Future Aircraft Dec. 1986 12 p (For primary document see N87-22663 16-05)
Copyright Avail: NTIS HC A07/MF A01

08 AIRCRAFT STABILITY AND CONTROL

Includes aircraft handling qualities; piloting; flight controls; and autopilots.

For related information see also *05 Aircraft Design, Testing and Performance.*

N87-22686# Messerschmitt-Boelkow-Blohm G.m.b.H., Ottobrunn (West Germany). Unternehmensbereich Apparate.
ELECTROMAGNETIC INTERFERENCE (EMI) FAULT PREVENTION AND SELF RECOVERY OF DIGITAL FLIGHT CONTROL SYSTEMS
Michael Stock 1986 20 p Presented at the 12th European Rotorcraft Forum, Garmisch-Partenkirchen, West Germany, 22-25 Sep. 1986 Sponsored by DGLR
(MBB-UD-483/86; ETN-87-99928) Avail: NTIS HC A02/MF A01

Ways to achieve helicopter digital flight control system reliability and survivability are shown. Microcomputer system failures caused by electromagnetic interference (EMI) and their impact on flight control are considered. Ways to ensure self recovery after EMI induced faults are outlined. A digital flight control system designed with respect to EMI problems and flight tested on a BK-117 is presented. ESA

N87-22687# Air Force Inst. of Tech., Wright-Patterson AFB, Ohio. School of Engineering.
EVALUATION OF NUMERATOR LEAD EFFECTS ON AIRCRAFT HANDLING QUALITIES M.S. Thesis
David W. Eidsaune Nov. 1986 137 p
(AD-A179388; AFIT/GAE/AA/86J-2) Avail: NTIS HC A07/MF A01 CSCL 01A

Results of a combined analytical/flight test evaluation to investigate the effects of short period zero (T theta 2) on aircraft handling qualities are presented. Two optimal pilot models were used for the analytical portion. 1/T theta 2 was varied from 0.1 to 10 for each 4 different short period configurations. Flight testing was accomplished in the variable stability NT-33A aircraft, over a range of 1/T theta 2 values at one short period configuration. A pitch tracking task was used to generate RMS pitch errors for both the analytical and flight test phase. Cooper-Harper ratings were also collected during the flight test. Analytical results showed similar trends for all short period configurations, with pilot tracking task performance degrading at low 1/T theta 2 values. The bandwidth criterion was of limited use in predicting handling qualities levels based on T theta 2 variations alone. The dc gain variations produced minimal differences in pilot performance. Overall evaluation results indicate that T theta 2 placement is an important factor in short period handling qualities and should be included in future revisions to MIL-F-87 85C. GRA

N87-22688# Naval Postgraduate School, Monterey, Calif.
DYNAMIC STALL CALCULATIONS USING A NAVIER-STOKES SOLVER M.S. Thesis
James E. Valdes Dec. 1986 120 p
(AD-A178566) Avail: NTIS HC A06/MF A01 CSCL 20D

A Navier Stokes problem solver is installed and verified on the Cray X/MP-48 computer and is used to calculate the flow field about a NACA 0012 airfoil oscillating in pitch. Surface pressure distributions and integrated lift, pitching moment, and drag coefficients versus angle of attack are compared to existing experimental data for two cases, involving deep dynamic stall and fully attached flow at and below a freestream Mach number of .3. The flow field about the oscillating airfoil is investigated through the study of contour plots of pressure, density, Mach number, and stream function. The effect of turbulence modeling is explored through use of the Baldwin Lomax model and a modification designed to prevent underprediction by repeating the deep stall simulation at one-tenth the experimental Reynolds number and Mach numbers of .3 and 5. The latter conditions are intended for comparison with the results of wind tunnel experiments. GRA

N87-22689# Army Aviation Research and Development Command, Moffett Field, Calif. Aeroflightdynamics Directorate.
CORRELATION OF ANALYTICAL CALCULATIONS FROM GRASP (GENERAL ROTORCRAFT AEROMECHANICAL STABILITY PROGRAM) WITH TORSIONALLY-SOFT ROTOR DATA
Donald L. Kunz and Dewey H. Hodges 1987 18 p
(AD-A178881) Avail: NTIS HC A02/MF A01 CSCL 20D

As a part of the continuing effort to develop and validate the General Rotorcraft Aeromechanical Stability Program (GRASP), a correlation study is presented to compare the frequency, moment, and stability data for a model-scale, torsionally-soft, helicoptor rotor with GRASP numerical calculations. The hierarchical representation of the model rotor is discussed along with the calculations of the vacuum frequencies, the steady-state blade moments in air, and the aeroelastic stability. Correlation is generally quite good. The GRASP predictions of the first vacuum flap frequencies are outstanding and the first vacuum lag and torsion frequencies correlate reasonably well with the experimental data. Consistently outstanding results are obtained for all of the steady blade moments. The calculations of stability data are in general as good as those made by other programs, but are not quite as good as anticipated. GRA

N87-22690*# National Aeronautics and Space Administration. Ames Research Center, Moffett Field, Calif.
FREQUENCY-RESPONSE IDENTIFICATION OF XV-15 TILT-ROTOR AIRCRAFT DYNAMICS
Mark B. Tischler May 1987 191 p Prepared in cooperation with Army Aviation Systems Command, Moffett Field, Calif.
(NASA-TM-89428; A-87103; NAS 1.15:89428) Avail: NTIS HC A09/MF A01 CSCL 01C

The timely design and development of the next generation of tilt-rotor aircraft (JVX) depend heavily on the in-depth understanding of existing XV-15 dynamics and the availability of fully validated simulation models. Previous studies have considered aircraft and simulation trim characteristics, but analyses of basic flight vehicle dynamics were limited to qualitative pilot evaluation. The present study has the following objectives: documentation and evaluation of XV-15 bare-airframe dynamics; comparison of aircraft and simulation responses; and development of a validated transfer-function description of the XV-15 needed for future studies. A nonparametric frequency-response approach is used which does not depend on assumed model order or structure. Transfer-function representations are subsequently derived which fit the frequency responses in the bandwidth of greatest concern for piloted handling-qualities and control-system applications. Author

N87-22691*# National Aeronautics and Space Administration. Ames Research Center, Moffett Field, Calif.
DIGITAL CONTROL OF HIGHLY AUGMENTED COMBAT ROTORCRAFT
Mark B. Tischler May 1987 165 p
(NASA-TM-88346; A-86369; NAS 1.15:88346; USAAVSCOM-TR-87-A-5) Avail: NTIS HC A08/MF A01 CSCL 01C

Proposed concepts for the next generation of combat helicopters are to be embodied in a complex, highly maneuverable, multiroled vehicle with avionics systems. Single pilot and nap-of-the-Earth operations require handling qualities which minimize the involvement of the pilot in basic stabilization tasks. To meet these requirements will demand a full authority, high-gain, multimode, multiply-redundant, digital flight-control system. The gap between these requirements and current low-authority, low-bandwidth operational rotorcraft flight-control technology is considerable. This research aims at smoothing the transition between current technology and advanced concept requirements. The state of the art of high-bandwidth digital flight-control systems are reviewed; areas of specific concern for flight-control systems of modern combat are exposed; and the important concepts are illustrated in design and analysis of high-gain, digital systems with a detailed case study involving a current rotorcraft system. Approximate and exact methods are explained and illustrated for treating the important concerns which are unique to digital systems. Author

N87-22692*# Alphatech, Inc., Burlington, Mass.
INTEGRATED RESTRUCTURABLE FLIGHT CONTROL SYSTEM DEMONSTRATION RESULTS
Jerold L. Weiss and John Y. Hsu May 1987 134 p
(Contract NAS1-17411)
(NASA-CR-178305; NAS 1.26:178305; TR-335) Avail: NTIS HC A07/MF A01 CSCL 01C

The purpose of this study was to examine the complementary capabilities of several restructurable flight control system (RFCS) concepts through the integration of these technologies into a complete system. Performance issues were addressed through a re-examination of RFCS functional requirements, and through a qualitative analysis of the design issues that, if properly addressed during integration, will lead to the highest possible degree of fault-tolerant performance. Software developed under previous phases of this contract and under NAS1-18004 was modified and integrated into a complete RFCS subroutine for NASA's B-737 simulation. The integration of these modules involved the development of methods for dealing with the mismatch between the outputs of the failure detection module and the input requirements of the automatic control system redesign module. The performance of this demonstration system was examined through extensive simulation trials. Author

N87-22622*# Princeton Univ., N. J. Dept. of Mechanical and Aerospace Engineering.
STABILITY BOUNDARIES FOR COMMAND AUGMENTATION SYSTEMS
P. C. Shrivastava *In* NASA. Langley Research Center Joint University Program for Air Transportation Research, 1984 May 1987 p 161-176 (For primary document see N87-22604 16-01)
Avail: NTIS HC A08/MF A01 CSCL 01C

N87-22674# British Aerospace Public Ltd. Co., Preston (England).
IMPROVED COMBAT PERFORMANCE USING RELAXED STATIC STABILITY AND A SPIN PREVENTION SYSTEM (FBW JAGUAR)
J. R. Nelson and T. D. Smith *In* AGARD Improvement of Combat Performance for Existing and Future Aircraft Dec. 1986 8 p (For primary document see N87-22663 16-05)
Copyright Avail: NTIS HC A07/MF A01

09 RESEARCH AND SUPPORT FACILITIES (AIR)

Includes airports, hangars and runways; aircraft repair and overhaul facilities; wind tunnels; shock tubes; and aircraft engine test stands.

For related information see also *14 Ground Support Systems and Facilities (Space).*

N87-22693# Surrey Univ., Guildford (England). Engineering Optics Research Group.
A FEASIBILITY STUDY OF THE FLEXIBLE SIMULATION OF SUNLIGHT Final Report
A. Tarrant 1986 63 p
(Contract MOD-2064/064-XR/FS)
(BR98783; ETN-87-99822) Avail: NTIS HC A04/MF A01

A mobile sunlight simulator based on optical fibers to simulate sunlight on a fixed cockpit flight simulator was developed. For large area sunlight simulation, the system is not feasible. It needs a wide and flexible low-attenuation fiber. For small area sunlight simulation, the system should work. The test rig produces a powerful flexible light source entirely devoid of heat and free from the safety problems of trailing electric cables. ESA

N87-22694*# National Aeronautics and Space Administration. Lewis Research Center, Cleveland, Ohio.
EXPERIMENTAL EVALUATION OF BLOCKAGE RATIO AND PLENUM EVACUATION SYSTEM FLOW EFFECTS ON PRESSURE DISTRIBUTION FOR BODIES OF REVOLUTION IN 0.1 SCALE MODEL TEST SECTION OF NASA LEWIS RESEARCH CENTER'S PROPOSED ALTITUDE WIND TUNNEL
Richard R. Burley and Douglas E. Harrington Apr. 1987 26 p
(NASA-TP-2702; E-3267; NAS 1.60:2702) Avail: NTIS HC A03/MF A01 CSCL 14B

An experimental investigation was conducted in the slotted test section of the 0.1-scale model of the proposed Altitude Wind Tunnel to evaluate wall interference effects at tunnel Mach numbers from 0.70 to 0.95 on bodies of revolution with blockage rates of 0.43, 3, 6, and 12 percent. The amount of flow that had to be removed from the plenum chamber (which surrounded the slotted test section) by the plenum evacuation system (PES) to eliminate wall interference effects was determined. The effectiveness of tunnel reentry flaps in removing flow from the plenum chamber was examined. The 0.43-percent blockage model was the only one free of wall interference effects with no PES flow. Surface pressures on the forward part of the other models were greater than interference-free results and were not influenced by PES flow. Interference-free results were achieved on the aft part of the 3- and 6-percent blockage models with the proper amount of PES flow. The required PES flow was substantially reduced by opening the reentry flaps. Author

N87-22774*# National Aeronautics and Space Administration. Lewis Research Center, Cleveland, Ohio.
HEAT FLUX CALIBRATION FACILITY CAPABLE OF SSME CONDITIONS
Curt H. Liebert *In its* Structural Integrity and Durability of Reusable Space Propulsion Systems 1987 p 47-49 (For primary document see N87-22766 16-20)
Avail: NTIS HC A10/MF A01 CSCL 14B

12 ASTRONAUTICS (GENERAL)

For extraterrestrial exploration see *91 Lunar and Planetary Exploration.*

N87-22695 Technische Hochschule, Aachen (West Germany). Giesserei Inst.
SCIENTIFIC GOALS OF THE GERMAN SPACELAB MISSION D1
Peter R. Sahm, ed. and Rainer Jansen, ed. Mar. 1985 243 p
Partly in ENGLISH and GERMAN Sponsored by the BMFT
(ETN-87-99669) Copyright Avail: Issuing Activity

The Fluid physics (interface phenomena/capillarity, diffusion, critical point phenomena); solidification (solidification front dynamics, crystal growth, composites); biology (cell functions, developmental processes, graviperception (plants)); and medicine/physiology (graviperception (humans) adaption phenomena (humans)) experiments of the Spacelab D1 mission are summarized. Communications and navigation are described. ESA

N87-22696*# National Aeronautics and Space Administration. Marshall Space Flight Center, Huntsville, Ala.
CELESTIAL TARGET OBSERVABILITY FOR ASTRO SPACELAB MISSIONS
Larry D. Mullins Mar. 1987 58 p
(NASA-TM-86591; NAS 1.26:86591) Avail: NTIS HC A04/MF A01 CSCL 22A

This report presents the mathematical technique for calculating the amount of time that an astronomical object, e.g., a star, can be observed from a satellite in near Earth orbit. This includes the places and times in the orbit where the object is acquired and where it is lost. Constraints placed on the observation of the object, such as the line-of-sight from observer to the target must not come within less than some specified angle to the limb of the Earth, are included in the calculations. The equations developed within the report are then used for a detailed analysis of the observation possibilities for objects at any place on the celestial sphere for a typical Spacelab ASTRO mission. The results, presented in graphic form, are suitable for use in pre-mission planning and also for use in real-time replanning. Author

N87-22697# Lawrence Livermore National Lab., Calif.
TOWARD THE YEAR 2000: THE NEAR FUTURE OF THE AMERICAN CIVILIAN AND MILITARY SPACE PROGRAMS
L. L. Wood and M. Y. Ishikawa Jan. 1987 10 p Presented at the 3rd National Space Symposium of the US Space Foundation, Colorado Springs, Colo., 20 Jan. 1987
(Contract W-7405-eng-48)
(DE87-006467; UCRL-96258; CONF-870162-1) Avail: NTIS HC A02/MF A01

The basic features of the American civilian and military space programs at the end of this century are identified and their histories traced back to the present time, for the surprise-free scenario. Several of the more likely surprises are noted, and their probable impacts sketched. DOE

N87-22698# Air Force Inst. of Tech., Wright-Patterson AFB, Ohio. School of Engineering.
A PROTOTYPE KNOWLEDGE-BASED SYSTEM FOR SATELLITE MISSION PLANNING M.S. Thesis
David E. Perales Dec. 1986 87 p
(AD-A178873; AFIT/GE/ENG/86D-17) Avail: NTIS HC A05/MF A01 CSCL 22A

The growing complexity of modern artificial satellites and limited resources available for satellite operations has caused satellite mission planning to become a data intensive job which overwhelms mission planners. The purpose of this thesis was to determine feasibility of using Artificial Intelligence techniques, specifically knowledge-based systems, in satellite mission planning. Research was conducted to determine the type of knowledge representation that best accommodates data intensive problem domains. Using this basis, a prototype knowledge-based system for use on a microcomputer was designed, constructed, and evaluated. The satellite schedule was generated based on prioritized user requirements, the requirements' acquisitions, and available resources. Explanations were provided to enable the mission planner to understand how the schedule was generated and allow him to make changes as user requirements change. The prototype systems showed that a knowledge-based system can assist the mission planner in scheduling satellite operations. This establishes a base from which more research can be done to help determine the optimal environment required to support an operational mission planning knowledge-based system. GRA

13 ASTRODYNAMICS

Includes powered and free-flight trajectories; and orbital and launching dynamics.

N87-22699# Air Force Inst. of Tech., Wright-Patterson AFB, Ohio. School of Engineering.
DETERMINING THE PROBABILITY OF CLOSE APPROACH BETWEEN TWO SATELLITES M.S. Thesis
Randal L. Richey Dec. 1986 135 p
(AD-A179385; AFIT/GA/AA/85D-8) Avail: NTIS HC A07/MF A01 CSCL 03C

Methods to calculate probability of close approach between two satellites are developed. The investigation was restricted to satellite orbits and time intervals where the mean anomaly of both satellites can be treated as independent, uniformly distributed random variables. All orbital parameters, except for mean anomaly, were assumed to be constant over time which means that all the methods developed to calculate the probability of close approach will only be valid over very long time intervals where the ratio of the orbital periods of the two satellites can be approximated as an irrational number. Likewise, there can be no perturbations in the orbital parameters of both satellites. A general method was developed for calculating the probability of close approach between two satellites in elliptical orbits. Another method was developed for calculating the probability of close approach between two satellites in circular orbits. Both the elliptical orbit and the circular orbit methods of computing probability of close approach yielded results that compare favorably with estimates of probability of close approach derived from statistical simulations. GRA

N87-22700*# Ohio State Univ., Columbus. ElectroScience Lab.
ON ORBITAL ALLOTMENTS FOR GEOSTATIONARY SATELLITES
David J. A. Gonsalvez, Charles H. Reilly, and Clark A. Mount-Campbell Nov. 1986 151 p
(Grant NAG3-159)
(NASA-CR-181017; NAS 1.181017; OS-TR-718688-2) Avail: NTIS HC A08/MF A01 CSCL 03C

The following satellite synthesis problem is addressed: communication satellites are to be allotted positions on the geostationary arc so that interference does not exceed a given acceptable level by enforcing conservative pairwise satellite separation. A desired location is specified for each satellite, and the objective is to minimize the sum of the deviations between the satellites' prescribed and desired locations. Two mixed integer programming models for the satellite synthesis problem are presented. Four solution strategies, branch-and-bound, Benders' decomposition, linear programming with restricted basis entry, and a switching heuristic, are used to find solutions to example synthesis problems. Computational results indicate the switching algorithm yields solutions of good quality in reasonable execution times when compared to the other solution methods. It is demonstrated that the switching algorithm can be applied to synthesis problems with the objective of minimizing the largest deviation between a prescribed location and the corresponding desired location. Furthermore, it is shown that the switching heuristic can use no conservative, location-dependent satellite separations in order to satisfy interference criteria. Author

14 GROUND SUPPORT SYSTEMS AND FACILITIES (SPACE)

Includes launch complexes, research and production facilities; ground support equipment, e.g., mobile transporters; and simulators.

For related information see also *09 Research and Support Facilities (Air).*

N87-22701# Army Armament Research and Development Command, Watervliet, N. Y. Benet Weapons Lab.
SUPERCONDUCTING AUGMENTED RAIL GUN (SARG) Final Technical Report
Clarke G. Homan and Wilfred Scholz Feb. 1987 21 p Presented at the US Army Science Conference, West Point, N.Y., 17-20 Jun. 1986
(AD-A179269; ARCCB-TR-87003) Avail: NTIS HC A02/MF A01 CSCL 20C

Both the energy efficiency and projectile velocity of a rail gun system can be substantially increased by the addition of an adjunct superconducting augmentation coil system. The energy efficiency results from the superconducting coil's ability to recover the rail magnetic field energy normally dissipated at the end of launch in rail guns, by means of a unique application of the flux conservation property of superconducting coils. The increased velocity results from the augmented Lorentz force due to the augmentation coil magnetic field. In an idealized system, both the energy efficiency and projectile velocities can be increased by more than 80 percent, dependent on the magnetic coupling between the rail and augmentation coils. The theoretical evaluation has been extended to include dissipative effects which reveal that actual launch efficiencies are increased from 25 percent (rail gun) to over 50 percent (SARG). A theoretical analysis of SARG is presented here together with the progress of an experimental demonstrator developer at Benet Weapons Lab. GRA

N87-22718*# Boeing Aerospace Co., Seattle, Wash.
FLEXIBLE SPACECRAFT SIMULATOR
In NASA. Marshall Space Flight Center Structural Dynamics and Control Interaction of Flexible Structures Apr. 1987 p 399-416
(For primary document see N87-22702 16-15)
Avail: NTIS HC A99/MF E03 CSCL 14B

15 LAUNCH VEHICLES AND SPACE VEHICLES

Includes boosters; operating problems of launch/space vehicle systems; and reusable vehicles.

For related information see also *20 Spacecraft Propulsion and Power.*

N87-22702*# National Aeronautics and Space Administration. Marshall Space Flight Center, Huntsville, Ala.
STRUCTURAL DYNAMICS AND CONTROL INTERACTION OF FLEXIBLE STRUCTURES
Robert S. Ryan, ed. and Harold N. Scofield, ed. Apr. 1987 680 p Workshop held in Huntsville, ALa., 22-24 Apr. 1986
(NASA-CP-2467-Pt-1; M-554-Pt-1; NAS 1.55:2467-Pt-1) Avail: NTIS HC A99/MF E03 CSCL 22B

A workshop on structural dynamics and control interaction of flexible structures was held to promote technical exchange between the structural dynamics and control disciplines, foster joint technology, and provide a forum for discussing and focusing critical issues in the separate and combined areas. Issues and areas of emphasis were identified in structure-control interaction for the next generation of flexible systems. For individual titles, see N87-22703 through N87-22728.

N87-22703*# National Aeronautics and Space Administration. Langley Research Center, Hampton, Va.
STATUS OF THE MAST EXPERIMENT
Brantley R. Hanks, Anthony Fontana, and John L. Allen *In* NASA. Marshall Space Flight Center Structural Dynamics and Control Interaction of Flexible Structures Apr. 1987 p 29-56 (For primary document see N87-22702 16-15)
Avail: NTIS HC A99/MF E03 CSCL 22B

Many sophisticated mathematical control techniques for flexible structures have been devised. The basic problem is that most of them require a relatively accurate mathematical model of the system under control including the dynamics of both the structure and the control system components. Obtaining such a model for either subsystem traditionally has required great effort including a significant validation step based on test data. Because of the quantum increase in complexity over proven methods, promising techniques for the control of flexible structures must be validated in actual hardware experiments before committing to their use in actual spacecraft missions. The Mast experiment system serves as a focus for such validation. It is the first in a series of experiments under the Control of Flexible Structures (COFS) Program at the NASA Langley Research Center. The Mast experiment is a combination of ground tests, orbital flight test, and analysis of a deployable beam under the COFS program. It provides a vehicle for research in structures, structural dynamics, and control issues. Author

N87-22704*# National Aeronautics and Space Administration. Marshall Space Flight Center, Huntsville, Ala.
LARGE SPACE STRUCTURES GROUND EXPERIMENT CHECKOUT
Henry B. Waites *In its* Structural Dynamics and Control Interaction of Flexible Structures Apr. 1987 p 57-84 (For primary document see N87-22702 16-15)
Avail: NTIS HC A99/MF E03 CSCL 22B

NASA Marshall Space Flight Center has developed a facility in which closed loop control of Large Space Structures (LSS) can be demonstrated and verified. The main objective of the facility is to verify LSS control system techniques so that on-orbit performance can be ensured. The facility consists of an LSS test article or payload which is connected to a 3-axis angular pointing mount assembly that provides control torque commands. The angular pointing mount assembly is attached to a base excitation system which will simulate disturbances most likely to occur for Orbiter and DOD payloads. The control computer contains the calibration software, the reference systems, the alignment procedures, the telemetry software, and the control algorithms. The total system is suspended in such a fashion that the LSS test article has the characteristics common to all LSS. Author

N87-22705*# Air Force Rocket Propulsion Lab., Edwards AFB, Calif.

IDENTIFICATION OF LARGE SPACE STRUCTURES: A STATE-OF-PRACTICE REPORT

In NASA. Marshall Space Flight Center Structural Dynamics and Control Interaction of Flexible Structures Apr. 1987 p 85-98 (For primary document see N87-22702 16-15)
Avail: NTIS HC A99/MF E03 CSCL 22B

An outline of this work is presented. It begins with a schematic flow diagram and a logical flow diagram of the identification process for large space structures (LSS). Next, the task is defined by a structure model definition. A matrix polynomial formulation with a node displacement equation and a state variable formulation with node displacement and velocities are outlined. Further outlined is the identification of LSS on orbit; modeling errors and uncertainties; verification and validation of model; and noise, computations, and data collection. E.R.

N87-22706*# National Aeronautics and Space Administration. Langley Research Center, Hampton, Va.

MICROPROCESSOR CONTROLLED PROOF-MASS ACTUATOR **c35**

Garnett C. Horner *In* NASA. Marshall Space Flight Center Structural Dynamics and Control Interaction of Flexible Structures Apr. 1987 p 101-118 (For primary document see N87-22702 16-15)
Avail: NTIS HC A99/MF E03 CSCL 14B

The objective of the microprocessor controlled proof-mass actuator is to develop the capability to mount a small programmable device on laboratory models. This capability will allow research in the active control of flexible structures. The approach in developing the actuator will be to mount all components as a single unit. All sensors, electronic and control devices will be mounted with the actuator. The goal for the force output capability of the actuator will be one pound force. The programmable force actuator developed has approximately a one pound force capability over the usable frequency range, which is above 2 Hz. Author

N87-22707*# Tennessee Univ. Space Inst., Tullahoma.

A GENERAL METHOD FOR DYNAMIC ANALYSIS OF STRUCTURES OVERVIEW **c39**

Remi C. Engels *In* NASA. Marshall Space Flight Center Structural Dynamics and Control Interaction of Flexible Structures Apr. 1987 p 119-132 (For primary document see N87-22702 16-15) (Contract F29601-85-K-0054)
Avail: NTIS HC A99/MF E03 CSCL 20K

The presented research deals with the development of a dynamic analysis method for structural systems. The modeling approach is essentially a finite element method in the sense that the structure is divided into n elements. An element is defined as any structural unit whose degree of freedom (dofs) can be categorized as either interface or non-interface dofs. An element could be a fundamental unit such as a rod, a beam, a plate etc., or it could be an entire structural component. Furthermore, the parameters for the element could be distributed or lumped. The choice of elements is totally arbitrary and is a matter of user convenience. In particular, issues of accuracy and convergence do not enter on the level of example that bookkeeping is reduced to a minimum. Each element is modeled using a set of interface constraint modes (ICM) combined with a set of interface restrained normal models (IRNM). The next step is the solution of the system eigenvalue problem. The procedure calls for the sequential solution of a number of small eigenvalue problems based on a truncation principle for IRNM. In addition, the form of these eigenvalue problems is very simple such that an escalator type of eigenvalue problem solver can be used which is extremely cost-effective and fast. Author

N87-22708*# Auburn Univ., Ala.

SPACE STATION/SHUTTLE ORBITER DYNAMICS DURING DOCKING **c18**

N. G. Fitz-Coy and J. E. Cochran, Jr. *In* NASA. Marshall Space Flight Center Structural Dynamics and Control Interaction of Flexible Structures Apr. 1987 p 133-174 (For primary document see N87-22702 16-15)
Avail: NTIS HC A99/MF E03 CSCL 22B

Mathematical models of a reference space station configuration (Power Tower) and a Space Shuttle Orbiter are developed and used to study the dynamic behavior of the Space Station/Orbiter system just prior to and subsequent to an impulsive docking of the two spacecraft. The physical model of the space station is a collection of rigid and flexible bodies. The orbiter is modeled as a rigid body. An algorithm developed for use in digitally simulating the dynamics of the system is described and results of its application are presented. Author

N87-22709*# Martin Marietta Aerospace, New Orleans, La.

TRANSIENT RESPONSE FOR INTERACTION OF TWO DYNAMIC BODIES

A. Prabhakar and L. G. Palermo *In* NASA. Marshall Space Flight Center Structural Dynamics and Control Interaction of Flexible Structures Apr. 1987 p 175-198 (For primary document see N87-22702 16-15)
Avail: NTIS HC A99/MF E03 CSCL 22B

During the launch sequence of any space vehicle complicated boundary interactions occur between the vehicle and the launch stand. At the start of the sequence large forces exist between the two; contact is then broken in a short but finite time which depends on the release mechanism. The resulting vehicle response produces loads which are very high and often form the design case. It is known that the treatment of the launch pad as a second dynamic body is significant for an accurate prediction of launch response. A technique was developed for obtaining loads generated by the launch transient with the effect of pad dynamics included. The method solves uncoupled vehicle and pad equations of motion. The use of uncoupled models allows the simulation of vehicle launch in a single computer run. Modal formulation allows a closed-form solution to be written, eliminating any need for a numerical integration algorithm. When the vehicle is on the pad the uncoupled pad and vehicle equations have to be modified to account for the constraints they impose on each other. This necessitates the use of an iterative procedure to converge to a solution, using Lagrange multipliers to apply the required constraints. As the vehicle lifts off the pad the coupling between the vehicle and the pad is eliminated point by point until the vehicle flies free. Results obtained by this method were shown to be in good agreement with observed loads and other analysis methods. The resulting computer program is general, and was used without modification to solve a variety of contact problems. Author

N87-22710*# Engineering Mechanics Association, Inc., Torrance, Calif.

A COMPUTER PROGRAM FOR MODEL VERIFICATION OF DYNAMIC SYSTEMS **c61**

J. D. Chrostowski and T. K. Hasselman *In* NASA. Marshall Space Flight Center Structural Dynamics and Control Interaction of Flexible Structures Apr. 1987 p 199-214 (For primary document see N87-22702 16-15)
Avail: NTIS HC A99/MF E03 CSCL 09B

Dynamic model verification is the process whereby an analytical model of a dynamic system is compared with experimental data, and then qualified for future use in predicting system response in a different dynamic environment. There are various ways to conduct model verification. The approach adopted in MOVER II employs Bayesian statistical parameter estimation. Unlike curve fitting whose objective is to minimize the difference between some analytical function and a given quantity of test data (or curve), Bayesian estimation attempts also to minimize the difference between the parameter values of that function (the model) and their initial estimates, in a least squares sense. The objectives of dynamic model verification, therefore, are to produce a model which: (1) is in agreement with test data, (2) will assist in the interpretation of test data, (3) can be used to help verify a design, (4) will reliably predict performance, and (5) in the case of space structures, facilitate dynamic control. Author

N87-22711*# National Aeronautics and Space Administration. Langley Research Center, Hampton, Va.
CONSIDERATIONS IN THE DESIGN AND DEVELOPMENT OF A SPACE STATION SCALE MODEL **c18**
Paul E. McGowan *In* NASA. Marshall Space Flight Center Structural Dynamics and Control Interaction of Flexible Structures Apr. 1987 p 215-246 (For primary document see N87-22702 16-15)
Avail: NTIS HC A99/MF E03 CSCL 22B

Preliminary work at Langley Research Center (LaRC) related to the design, analysis and testing of a space station scale model is reviewed. Included are some rationale for focusing the scale model program on space station and the utilization of the model to achieve the program objectives. In addition, some considerations involved in designing a dynamics scale model, such as ground test facilities, sub-scale component fabrication and model replication vs. simulation are presented. Finally, some related research areas currently ongoing at LaRC in support of scale model development are discussed. Author

N87-22712*# Jet Propulsion Lab., California Inst. of Tech., Pasadena.
VERIFICATION OF LARGE BEAM-TYPE SPACE STRUCTURES **c39**
Choon-Foo Shih, Jay C. Chen, and John A. Garba *In* NASA. Marshall Space Flight Center Structural Dynamics and Control Interaction of Flexible Structures Apr. 1987 p 247-254 (For primary document see N87-22702 16-15)
Avail: NTIS HC A99/MF E03 CSCL 20K

The verification approach of large beam type space structures is verified. The proposed verification approach consists of two parts. The first part is to remove the gravity effect on the tested substructure and to identify the on-orbit dynamic characteristics of the substructure by using the measurements of the ground test. A scaling law is also established to define the critical length of the structure which can be tested in 1-g field without incurring a buckling problem. The second part is to develop an adequate scaling law to extrapolate the dynamic characteristics of the prototype structure by using results from the substructure. The verification approaches are demonstrated on two typical structural configurations, the feed support structure of a wrap-rip antenna and a candidate shuttle flight experiment. The results indicate that it is practical to verify the on-orbit dynamic characteristics of these structures by using the proposed approach. Author

N87-22713*# Jet Propulsion Lab., California Inst. of Tech., Pasadena.
VERIFICATION OF FLEXIBLE STRUCTURES BY GROUND TEST **c39**
Ben K. Wada and C. P. Kuo *In* NASA. Marshall Space Flight Center Structural Dynamics and Control Interaction of Flexible Structures Apr. 1987 p 255-274 (For primary document see N87-22702 16-15)
Avail: NTIS HC A99/MF E03 CSCL 20K

The validation of math models of large space structures (LSS) by ground tests is attempted. Concepts for two types of LSS are presented: continuous type and linked subsystems. It was concluded that ground test which simulate space conditions are not entirely reliable, that there should be an integration of testing and analyses, which then should be validated with laboratory and flight experiments. E.R.

N87-22714*# Air Force Wright Aeronautical Labs., Wright-Patterson AFB, Ohio.
OPTIMUM MIX OF PASSIVE AND ACTIVE CONTROL OF SPACE STRUCTURES **c18**
Lynn Rogers and Ken Richards (Martin Marietta Aerospace, Denver, Colo.) *In* NASA. Marshall Space Flight Center Structural Dynamics and Control Interaction of Flexible Structures Apr. 1987 p 275-292 (For primary document see N87-22702 16-15)
Avail: NTIS HC A99/MF E03 CSCL 22B

The objective of this research was to test vibration suppression (settling time and jitter) of a large space structure (LSS) characterized by low frequency high global vibration modes. Five percent passive damping in a large truss was analyzed, tested and correlated. A representative system article re-target analysis shows that modest levels of passive damping dramatically reduce the control energy required. LSS must incorporate passive damping from the outset. The LSS system performance will not be met by either active or passive damping alone. E.R.

N87-22715*# Control Dynamics Co., Huntsville, Ala.
ONE CONTROLLER AT A TIME (1-CAT): A MIMO DESIGN METHODOLOGY **c18**
J. R. Mitchell and J. C. Lucas *In* NASA. Marshall Space Flight Center Structural Dynamics and Control Interaction of Flexible Structures Apr. 1987 p 293-334 (For primary document see N87-22702 16-15)
Avail: NTIS HC A99/MF E03 CSCL 22B

The One Controller at a Time (1-CAT) methodology for designing digital controllers for Large Space Structures (LSS's) is introduced and illustrated. The flexible mode problem is first discussed. Next, desirable features of a LSS control system design methodology are delineated. The 1-CAT approach is presented, along with an analytical technique for carrying out the 1-CAT process. Next, 1-CAT is used to design digital controllers for the proposed Space Based Laser (SBL). Finally, the SBL design is evaluated for dynamical performance, noise rejection, and robustness. Author

N87-22716*# National Aeronautics and Space Administration. Marshall Space Flight Center, Huntsville, Ala.
COMMIT YOUR WORKS TO THE LORD, AND YOUR THOUGHTS SHALL BE ESTABLISHED (PROV. 16:3). INTER-STABLE CONTROL SYSTEMS
George L. vonPragenau *In its* Structural Dynamics and Control Interaction of Flexible Structures Apr. 1987 p 335-358 (For primary document see N87-22702 16-15)
Avail: NTIS HC A99/MF E03 CSCL 22B

Algebraic structures are discussed for control systems that maintain stability in the presence of resonance uncertainties. Dual algebraic operations serve as elementary connections that propagate the stability of inter-stable subsystems. Frequency responses within complex half-planes define different types of inter-stability. Dominance between incompatible types is discussed. Inter-stability produces sufficient but unnecessary stability conditions, except for conservative systems where the conditions become also necessary. Multivariable systems, colocation of actuator and sensor, and virtual colocation are treated. Instead of passivity, inter-stability relates stability to the mapping of poles and zeros by transfer functions and transfer matrices. Inter-stability determines stability on the subsystem level, is less complex even for multivariable systems, adds design flexibility, and relaxes the dynamic data problem of large systems such as space stations. Author

N87-22717*# National Aeronautics and Space Administration. Langley Research Center, Hampton, Va.
STATUS REPORT AND PRELIMINARY RESULTS OF THE SPACECRAFT CONTROL LABORATORY EXPERIMENT **c18**
Jeffrey P. Williams *In* NASA. Marshall Space Flight Center Structural Dynamics and Control Interaction of Flexible Structures Apr. 1987 p 359-398 (For primary document see N87-22702

16-15)
Avail: NTIS HC A99/MF E03 CSCL 22B

The Spacecraft Control Laboratory Experiment (SCOLE) was conceived to provide a physical test bed for investigation of control techniques for large flexible spacecraft. The SCOLE problem is defined as two design challenges. The first challenge is to design control laws for a mathematical model of a large antenna attached to the space shuttle by a long flexible mast. The second challenge is to design and implement a control scheme on a laboratory representation of the structure modelled in the first part. Control sensors and actuators are typical of those which the control designer would have to deal with on an actual spacecraft. The primary control processing computer is representative of the capacity and speed which may be expected in actual flight computers. A brief description is given of the laboratory apparatus along with some preliminary results of structural dynamics tests and actuator effectiveness tests. Author

N87-22718*# Boeing Aerospace Co., Seattle, Wash.
FLEXIBLE SPACECRAFT SIMULATOR **c14**
In NASA. Marshall Space Flight Center Structural Dynamics and Control Interaction of Flexible Structures Apr. 1987 p 399-416 (For primary document see N87-22702 16-15)
Avail: NTIS HC A99/MF E03 CSCL 14B

Verification of control algorithms for flexible spacecraft can be done only through simulation and test; these are necessary to understand control/structure interaction (C/SI) sufficiently to design robust controllers for future spacecraft. The objective persued is to develop a low-cost facility which simulates the fundamental problem of C/SI; and to provide accessibility for designs so that experience can be gained in applying various multivariable control design methods to an actual structure. A test facility is being constructed with test elements that provide 3 rigid body and 6 flexible modes, all in the horizontal plane, with frequencies below 2.5 Hz. The control force actuator are on/off air jets with sensing by optical displacement sensors. Loop closure is provided by a digital computer with control algorithms designed using the IAC and MATRIX-X. E.R.

N87-22719*# Auburn Univ., Ala. Dept. of Electrical Engineering.
IMPROVING STABILITY MARGINS IN DISCRETE-TIME LOG CONTROLLERS **c64**
B. Tarik Oranc and Charles L. Phillips *In* NASA. Marshall Space Flight Center Structural Dynamics and Control Interaction of Flexible Structures Apr. 1987 p 417-434 (For primary document see N87-22702 16-15)
Avail: NTIS HC A99/MF E03 CSCL 12A

Some of the problems are discussed which are encountered in the design of discrete-time stochastic controllers for problems that may adequately be described by the Linear Quadratic Gaussian (LQG) assumptions; namely, the problems of obtaining acceptable relative stability, robustness, and disturbance rejection properties. A dynamic compensator is proposed to replace the optimal full state feedback regulator gains at steady state, provided that all states are measurable. The compensator increases the stability margins at the plant input, which may possibly be inadequate in practical applications. Though the optimal regulator has desirable properties the observer based controller as implemented with a Kalman filter, in a noisy environment, has inadequate stability margins. The proposed compensator is designed to match the return difference matrix at the plant input to that of the optimal regulator while maintaining the optimality of the state estimates as directed by the measurement noise characteristics. Author

N87-22720*# National Aeronautics and Space Administration. Langley Research Center, Hampton, Va.
AN OVERVIEW OF CONTROLS RESEARCH ON THE NASA LANGLEY RESEARCH CENTER GRID **c39**
Raymond C. Montgomery *In* NASA. Marshall Space Flight Center Structural Dynamics and Control Interaction of Flexible Structures Apr. 1987 p 435-456 (For primary document see N87-22702 16-15)
Avail: NTIS HC A99/MF E03 CSCL 20K

The NASA Langley Research Center has assembled a flexible grid on which control systems research can be accomplished on a two-dimensional structure that has many physically distributed sensors and actuators. The grid is a rectangular planar structure that is suspended by two cables attached to one edge so that out of plane vibrations are normal to gravity. There are six torque wheel actuators mounted to it so that torque is produced in the grid plane. Also, there are six rate gyros mounted to sense angular motion in the grid plane and eight accelerometers that measure linear acceleration normal to the grid plane. All components can be relocated to meet specific control system test requirements. Digital, analog, and hybrid control systems capability is provided in the apparatus. To date, research on this grid has been conducted in the areas of system and parameter identification, model estimation, distributed modal control, hierarchical adaptive control, and advanced redundancy management algorithms. The presentation overviews each technique and presents the most significant results generated for each area. Author

N87-22721*# Rockwell International Corp., Downey, Calif. Space Station Systems Div.
STRUCTURAL/CONTROL INTERACTION (PAYLOAD POINTING AND MICRO-g) **c18**
C. R. Larson *In* NASA. Marshall Space Flight Center Structural Dynamics and Control Interaction of Flexible Structures Apr. 1987 p 457-484 (For primary document see N87-22702 16-15)
Avail: NTIS HC A99/MF E03 CSCL 22B

A 203rd order simulation model was developed to evaluate the space station customer accommodation payload pointing and micro-g requirements. The simulation shows the pointing errors on the telescope are significantly smaller than at the base of the telescope. The pointing results could change when the parametric studies are performed. The results show the micro-g requirement is met with an active isolation system. Author

N87-22722*# National Aeronautics and Space Administration. Marshall Space Flight Center, Huntsville, Ala.
SOLAR ARRAY FLIGHT DYNAMIC EXPERIMENT **c44**
Richard W. Schock *In its* Structural Dynamics and Control Interaction of Flexible Structures Apr. 1987 p 487-504 (For primary document see N87-22702 16-15)
Avail: NTIS HC A99/MF E03 CSCL 10A

The purpose of the Solar Array Flight Dynamic Experiment (SAFDE) is to demonstrate the feasibility of on-orbit measurement and ground processing of large space structures' dynamic characteristics. Test definition or verification provides the dynamic characteristic accuracy required for control systems use. An illumination/measurement system was developed to fly on space shuttle flight STS-41D. The system was designed to dynamically evaluate a large solar array called the Solar Array Flight Experiment (SAFE) that had been scheduled for this flight. The SAFDE system consisted of a set of laser diode illuminators, retroreflective targets, an intelligent star tracker receiver and the associated equipment to power, condition, and record the results. In six tests on STS-41D, data was successfully acquired from 18 retroreflector targets and ground processed, post flight, to define the solar array's dynamic characteristic. The flight experiment proved the viability of on-orbit test definition of large space structures dynamic characteristics. Future large space structures controllability should be greatly enhanced by this capability. Author

N87-22723*# Boeing Aerospace Co., Seattle, Wash.
PRECISION POINTING AND CONTROL OF FLEXIBLE SPACECRAFT **c18**
M. H. Bantell, Jr. *In* NASA. Marshall Space Flight Center Structural Dynamics and Control Interaction of Flexible Structures Apr. 1987 p 505-538 (For primary document see N87-22702 16-15)
Avail: NTIS HC A99/MF E03 CSCL 22B

The problem and long term objectives for the precision pointing and control of flexible spacecraft are given. The four basic objectives are stated in terms of two principle tasks. Under Task

1, robust low order controllers, improved structural modeling methods for control applications and identification methods for structural dynamics are being developed. Under Task 2, a lab test experiment for verification of control laws and system identification algorithms is being developed. For Task 1, work has focused on robust low order controller design and some initial considerations for structural modeling in control applications. For Task 2, work has focused on experiment design and fabrication, along with sensor selection and initial digital controller implementation. Conclusions are given. Author

N87-22724*# Boeing Aerospace Co., Seattle, Wash.
DYNAMICS OF TRUSSES HAVING NONLINEAR JOINTS c39
J. M. Chapman, F. H. Shaw, and W. C. Russell *In* NASA. Marshall Space Flight Center Structural Dynamics and Control Interaction of Flexible Structures Apr. 1987 p 539-566 (For primary document see N87-22702 16-15)
Avail: NTIS HC A99/MF E03 CSCL 20K

The transient analysis of trusses having nonlinear joints can be accomplished using the residual force technique. The technique was applied a two degree of freedom spring mass system, a four bay planar truss, and an actual ten bay deployable truss. Joints chosen for analysis were the nonlinear gap joints and the linear Voigt joints. Results from the nonlinear gap analyses generally indicate that coupling between the modes can display some interesting effects during free vibration. One particularly interesting effect was that the damping of the structure appeared to be higher than could be accounted for from modal damping alone. Energy transferral from the lower to the higher modes was found to exist as a result of the modal coupling. The apparently increased damping was due to the fact that the energy transferred to the higher modes is inherently dissipated more quickly. Another interesting phenomenon was that the lower modes could drive the higher modes even during free vibration and that these modes could display a rather large quasi-steady state behavior even when modal damping was present. Gaps were also found to increase the amplitude and period of the free vibration response as expected. Author

N87-22725*# Boeing Aerospace Co., Seattle, Wash.
EQUIVALENT BEAM MODELING USING NUMERICAL REDUCTION TECHNIQUES c39
J. M. Chapman and F. H. Shaw *In* NASA. Marshall Space Flight Center Structural Dynamics and Control Interaction of Flexible Structures Apr. 1987 p 567-594 (For primary document see N87-22702 16-15)
Avail: NTIS HC A99/MF E03 CSCL 20K

Numerical procedures that can accomplish model reductions for space trusses were developed. Three techniques are presented that can be implemented using current capabilities within NASTRAN. The proposed techniques accomplish their model reductions numerically through use of NASTRAN structural analyses and as such are termed numerical in contrast to the previously developed analytical techniques. Numerical procedures are developed that permit reductions of large truss models containing full modeling detail of the truss and its joints. Three techniques are presented that accomplish these model reductions with various levels of structural accuracy. These numerical techniques are designated as equivalent beam, truss element reduction, and post-assembly reduction methods. These techniques are discussed in detail. E.R.

N87-22726*# National Aeronautics and Space Administration. Marshall Space Flight Center, Huntsville, Ala.
DYNAMIC CHARACTERISTICS OF A VIBRATING BEAM WITH PERIODIC VARIATION IN BENDING STIFFNESS c39
John S. Townsend *In its* Structural Dynamics and Control Interaction of Flexible Structures Apr. 1987 p 595-624 (For primary document see N87-22702 16-15)
Avail: NTIS HC A99/MF E03 CSCL 20K

A detailed dynamic analysis is performed of a vibrating beam with bending stiffness periodic in the spatial coordinate. Using a perturbation expansion technique the free vibration solution is obtained in a closed-form, and the effects of system parameters on beam response are explored. It is found that periodic stiffness acts to modulate the modal displacements from the characteristic shape of a simple sine wave. The results are verified by a finite element solution and through experimental testing. Author

N87-22727*# Jet Propulsion Lab., California Inst. of Tech., Pasadena.
STRUCTURAL DYNAMICS SYSTEM MODEL REDUCTION c39
J. C. Chen, T. L. Rose, and B. K. Wada *In* NASA. Marshall Space Flight Center Structural Dynamics and Control Interaction of Flexible Structures Apr. 1987 p 625-668 (For primary document see N87-22702 16-15)
Avail: NTIS HC A99/MF E03 CSCL 20K

Loads analysis for structural dynamic systems is usually performed by finite element models. Because of the complexity of the structural system, the model contains large number of degree-of-freedom. The large model is necessary since details of the stress, loads and responses due to mission environments are computed. However, a simplified model is needed for other tasks such as pre-test analysis for modal testing, and control-structural interaction studies. A systematic method of model reduction for modal test analysis is presented. Perhaps it will be of some help in developing a simplified model for the control studies. Author

N87-22728*# National Aeronautics and Space Administration. Marshall Space Flight Center, Huntsville, Ala.
WORKSHOP ON STRUCTURAL DYNAMICS AND CONTROL INTERACTION OF FLEXIBLE STRUCTURES c39
L. P. Davis, J. F. Wilson (Sperry Corp., Phoenix, Ariz.), and R. E. Jewell *In its* Structural Dynamics and Control Interaction of Flexible Structures Apr. 1987 p 669-690 Reprinted from Vibration Damping Workshop, 6 Mar. 1986 (For primary document see N87-22702 16-15)
Avail: NTIS HC A99/MF E03 CSCL 20K

The Hubble Space Telescope features the most exacting line of sight jitter requirement thus far imposed on a spacecraft pointing system. Consideration of the fine pointing requirements prompted an attempt to isolate the telescope from the low level vibration disturbances generated by the attitude control system reaction wheels. The primary goal was to provide isolation from axial component of wheel disturbance without compromising the control system bandwidth. A passive isolation system employing metal springs in parallel with viscous fluid dampers was designed, fabricated, and space qualified. Stiffness and damping characteristics are deterministic, controlled independently, and were demonstrated to remain constant over at least five orders of input disturbance magnitude. The damping remained purely viscous even at the data collection threshold of .16 x .000001 in input displacement, a level much lower than the anticipated Hubble Space Telescope disturbance amplitude. Vibration attenuation goals were obtained and ground test of the vehicle has demonstrated the isolators are transparent to the attitude control system. Author

N87-22729*# National Aeronautics and Space Administration. Marshall Space Flight Center, Huntsville, Ala.
STRUCTURAL DYNAMICS AND CONTROL INTERACTION OF FLEXIBLE STRUCTURES
Robert S. Ryan, ed. and Harold N. Scofield, ed. Apr. 1987 729 p Workshop held in Huntsville, Ala., 22-24 Apr. 1986 (NASA-CP-2467-Pt-2; M-554-Pt-2; NAS 1.55:2467-Pt-2) Avail: NTIS HC A99/MF E03 CSCL 22B

A Workshop was held to promote technical exchange between the structural dynamic and control disciplines, foster joint technology, and provide a forum for discussing and focusing critical issues in the separate and combined areas. The workshop was closed by a panel meeting. Panel members' viewpoints and their responses to questions are included. For individual titles, see N87-22730 through N87-22753.

N87-22730*# California Inst. of Tech., Pasadena.
VIBRATION SUPPRESSION BY STIFFNESS CONTROL c39

James Fanson, Thomas Caughey, and Jay Chen *In* NASA. Marshall Space Flight Center Structural Dynamics and Control Interaction of Flexible Structures Apr. 1987 p 693-758 (For primary document see N87-22729 16-15)
Avail: NTIS HC A99/MF E03 CSCL 20K

The feasibility of using piezoelectric ceramics as both sensors and actuators for vibration suppression in a lightweight, flimsy structure was demonstrated. Multimode control was achieved using one sensor and actuator pair. The Positive Position Feedback control strategy requires only knowledge of the natural frequencies of the structure. Implementation of the Positive Position Feedback used only strain measurements to achieve damping, no velocities, or acceleration are needed. All spillover is stabilizing for sufficient small gains. B.G.

N87-22731*# Texas A&M Univ., College Station.
A QUASI-ANALYTICAL METHOD FOR NON-ITERATIVE COMPUTATION OF NONLINEAR CONTROLS **c18**
J. L. Junkins, R. C. Thompson, and J. D. Turner (Cambridge Research Associates, Mass.) *In* NASA. Marshall Space Flight Center Structural Dynamics and Control Interaction of Flexible Structures Apr. 1987 p 759-774 (For primary document see N87-22729 16-15)
Avail: NTIS HC A99/MF E03 CSCL 22B

An optimal control solution process was developed for a general class of nonlinear dynamical systems. The method combines control theory, perturbation methods, and Van Loan's recent matrix exponential results. A variety of applications support the practical utility of this method. Nonlinear rigid body optimal maneuvers are routinely solved. Flexible body dynamical systems of an order greater than 40 were solved. The method fails occasionally due to poor convergence of the perturbation expansion or numerical difficulties associated with computing the matrix exponential. The method is attractive because it appears to be a good candidate for semi-automation; no initial guess is required, and it usually converges at 2nd or 3rd order in minutes of machine time. B.G.

N87-22732*# National Aeronautics and Space Administration. Langley Research Center, Hampton, Va.
CONTROL OF FLEXIBLE STRUCTURES AND THE RESEARCH COMMUNITY **c18**
Claude R. Keckler and Jon S. Pyle *In* NASA. Marshall Space Flight Center Structural Dynamics and Control Interaction of Flexible Structures Apr. 1987 p 789-840 (For primary document see N87-22729 16-15)
Avail: NTIS HC A99/MF E03 CSCL 22B

The Control of Flexible Structures II (CPFS) program is a complex and ambitious undertaking which addresses several critical technology areas. Among them are modeling, structural dynamics, control, and ground testing issues, which are also applicable to other large space structure programs being contemplated. This effort requires early integration of controls and structural dynamic considerations. Several technological advances must be achieved in the areas of system modeling, control synthesis and methodology, sensor/actuator development, and ground testing techniques for system evaluation and on-orbit performance prediction and verification. This program offers an opportunity for the integration of several disciplines to produce technology advances which will benefit many future programs. B.G.

N87-22733*# General Electric Co., Philadelphia, Pa. Space Div.
IMPACT OF SPACE STATION APPENDAGE VIBRATIONS ON THE POINTING PERFORMANCE OF GIMBALLED PAYLOADS **c18**
Robert O. Hughes *In* NASA. Marshall Space Flight Center Structural Dynamics and Control Interaction of Flexible Structures (date) 841-866 (SEE N87-22729 16-15) Apr. 1987 (For primary document see N87-22729 16-15)
Avail: NTIS HC A99/MF E03 CSCL 22B

A study of the interface problems between the Space Station Structure (vibrations) and the Payload Pointing Control System was undertaken. A major goal of the study was to identify any bounding factors that might limit the achievement of required pointing accuracies. A major result is that the space station will have a disturbance-rich environment and the background levels will be large enough to impact the pointing of some of the payloads. The need for an interface vibration specification between the structure and the payloads was identified. Author

N87-22734*# Virginia Polytechnic Inst. and State Univ., Blacksburg. Dept. of Engineering Science and Mechanics.
MANEUVERING AND VIBRATION CONTROL OF FLEXIBLE SPACECRAFT **c18**
L. Meirovitch and R. D. Quinn *In* NASA. Marshall Space Flight Center Structural Dynamics and Control Interaction of Flexible Structures Apr. 1987 p 867-880 (For primary document see N87-22729 16-15)
(Grant NAG1-225)
Avail: NTIS HC A99/MF E03 CSCL 22B

Equations of motion, control strategy, perturbation, rigid-body maneuvers, quasi-modal equations, and vibration control are discussed for flexible spacecraft. B.G.

N87-22735*# National Aeronautics and Space Administration. Marshall Space Flight Center, Huntsville, Ala.
A TREETOPS SIMULATION OF THE HUBBLE SPACE TELESCOPE-HIGH GAIN ANTENNA INTERACTION **c39**
John P. Sharkey *In its* Structural Dynamics and Control Interaction of Flexible Structures Apr. 1987 p 881-902 (For primary document see N87-22729 16-15)
Avail: NTIS HC A99/MF E03 CSCL 20K

Virtually any project dealing with the control of a Large Space Structure (LSS) will involve some level of verification by digital computer simulation. While the Hubble Space Telescope might not normally be included in a discussion of LSS, it is presented to highlight a recently developed simulation and analysis program named TREETOPS. TREETOPS provides digital simulation, linearization, and control system interaction of flexible, multibody spacecraft which admit to a point-connected tree topology. The HST application of TREETOPS is intended to familiarize the LSS community with TREETOPS by presenting a user perspective of its key features. B.G.

N87-22736*# Rockwell International Corp., Downey, Calif. Space Station Systems Div.
PRELIMINARY EVALUATION OF A REACTION CONTROL SYSTEM FOR THE SPACE STATION **c18**
H. H. Woo and J. A. Finley *In* NASA. Marshall Space Flight Center Structural Dynamics and Control Interaction of Flexible Structures Apr. 1987 p 930-942 (For primary document see N87-22729 16-15)
Avail: NTIS HC A99/MF E03 CSCL 22B

The challenge, ground rules and criteria, some of the Reaction Control System (RCS) concepts, classical and modern design analysis, and simulation results which are applicable to the space station are presented. B.G.

N87-22737*# National Aeronautics and Space Administration. Langley Research Center, Hampton, Va.
DUAL KEEL SPACE STATION CONTROL/STRUCTURES INTERACTION STUDY **c18**
John W. Young, Frederick J. Lallman, and Paul A. Cooper *In* NASA. Marshall Space Flight Center Structural Dynamics and Control Interaction of Flexible Structures Apr. 1987 p 945-978 (For primary document see N87-22729 16-15)
Avail: NTIS HC A99/MF E03 CSCL 22B

A study was made to determine the influence of truss bay size on the performance of the space station control system. The objective was to determine if any control problems existed during reboost and to assess the level of potential control/structures interaction during operation of the control moment gyros used for vertical stabilization. The models analyzed were detailed finite-element representations of the 5 meter and 9 foot growth versions of the 300 kW dual keel station. Results are presented comparing the performance of the reboost control system for both versions of the space station. Standards for comparison include flexible effects at the attitude control sensor locations and flexible contributions to pointing error at the solar collectors. Bode analysis results are presented for the attitude control system and control, structural, and damping sensitivities are examined. Author

N87-22738*# Boeing Aerospace Co., Seattle, Wash.
HIGH SPEED SIMULATION OF FLEXIBLE MULTIBODY DYNAMICS c61
A. D. Jacot, R. E. Jones, and C. D. Juengst *In* NASA. Marshall Space Flight Center Structural Dynamics and Control Interaction of Flexible Structures Apr. 1987 p 979-998 (For primary document see N87-22729 16-15)
Avail: NTIS HC A99/MF E03 CSCL 09B

A multiflexible body dynamics code intended for fast turnaround control design trades is described. Nonlinear rigid body dynamics and linearized flexible dynamics combine to provide efficient solution of the equations of motion. Comparison with results from the DISCOS code provide verification of accuracy. Author

N87-22739*# Texas Univ., Austin. Dept. of ASE-EM.
LANCZOS MODES FOR REDUCED-ORDER CONTROL OF FLEXIBLE STRUCTURES
Roy R. Craig, Jr. and Russell M. Turner *In* NASA. Marshall Space Flight Center Structural Dynamics and Control Interaction of Flexible Structures Apr. 1987 p 999-1012 (For primary document see N87-22729 16-15)
Avail: NTIS HC A99/MF E03 CSCL 22B

Lanczos mode models represent low-frequency forced response better than do normal mode models and can be developed for both continuous and finite element structural representations. It was recommended that Lanczos mode models for systems with multiple input and/or rigid body modes should be developed; numerical stability of the Lanczos algorithm should be assessed; and control system designs employing the Lanczos mode models should be attempted. B.G.

N87-22740*# National Aeronautics and Space Administration. Langley Research Center, Hampton, Va.
SLEWING CONTROL EXPERIMENT FOR A FLEXIBLE PANEL
Jer-Nan Juang *In* NASA. Marshall Space Flight Center Structural Dynamics and Control Interaction of Flexible Structures Apr. 1987 p 1013-1032 (For primary document see N87-22729 16-15)
Avail: NTIS HC A99/MF E03 CSCL 22B

Technology areas are identified in which better analytical and/or experimental methods are needed to adequately and accurately control the dynamic responses of multibody space platforms such as the space station. A generic space station solar panel is used to experimentally evaluate current control technologies. Active suppression of solar panel vibrations induced by large angle maneuvers is studied with a torque actuator at the root of the solar panel. These active suppression tests will identify the hardware requirements and adequacy of various controller designs. Author

N87-22741*# Harris Corp., Melbourne, Fla. Government Aerospace Systems Div.
MAXIMUM ENTROPY/OPTIMAL PROJECTION (MEOP) CONTROL DESIGN SYNTHESIS: OPTIMAL QUANTIFICATION OF THE MAJOR DESIGN TRADEOFFS c18
D. C. Hyland and D. S. Bernstein *In* NASA. Marshall Space Flight Center Structural Dynamics and Control Interaction of Flexible Structures Apr. 1987 p 1033-1070 (For primary document see N87-22729 16-15)
Avail: NTIS HC A99/MF E03 CSCL 22B

The underlying philosophy and motivation of the optimal projection/maximum entropy (OP/ME) stochastic modeling and reduced control design methodology for high order systems with parameter uncertainties are discussed. The OP/ME design equations for reduced-order dynamic compensation including the effect of parameter uncertainties are reviewed. The application of the methodology to several Large Space Structures (LSS) problems of representative complexity is illustrated. B.G.

N87-22742*# Lockheed Missiles and Space Co., Sunnyvale, Calif. Space Systems Div.
VIBRATION ISOLATION FOR LINE OF SIGHT PERFORMANCE IMPROVEMENT c39
J. J. Rodden, H. J. Dougherty, and W. B. Haile *In* NASA. Marshall Space Flight Center Structural Dynamics and Control Interaction of Flexible Structures Apr. 1987 p 1071-1078 (For primary document see N87-22729 16-15)
Avail: NTIS HC A99/MF E03 CSCL 20K

Diagrams of the Reaction Wheel Assembly (RWA) are presented along with charts and graphs illustrating jitter error model, induced vibration tests, radial displacement transfer function, and axial displacement power spectra density. The RWA isolator specification requirements are listed. B.G.

N87-22743*# Auburn Univ., Ala. Dept. of Aerospace Engineering.
A NEW APPROACH FOR VIBRATION CONTROL IN LARGE SPACE STRUCTURES c39
K. Kumar and J. E. Cochran, Jr. *In* NASA. Marshall Space Flight Center Structural Dynamics and Control Interaction of Flexible Structures Apr. 1987 p 1079-1094 (For primary document see N87-22729 16-15)
Avail: NTIS HC A99/MF E03 CSCL 20K

An approach for augmenting vibration damping characteristics in space structures with large panels is presented. It is based on generation of bending moments rather than forces. The moments are generated using bimetallic strips, suitably mounted at selected stations on both sides of the large panels, under the influence of differential solar heating, giving rise to thermal gradients and stresses. The collocated angular velocity sensors are utilized in conjunction with mini-servos to regulate the control moments by flipping the bimetallic strips. A simple computation of the rate of dissipation of vibrational energy is undertaken to assess the effectiveness of the proposed approach. Author

N87-22744*# Lockheed Engineering and Management Services Co., Inc., Houston, Tex.
CREW ACTIVITY AND MOTION EFFECTS ON THE SPACE STATION c18
Brian V. Rochon and Steven A. Scheer *In* NASA. Marshall Space Flight Center Structural Dynamics and Control Interaction of Flexible Structures Apr. 1987 p 1095-1160 (For primary document see N87-22729 16-15)
(Contract NAS9-15800)
Avail: NTIS HC A99/MF E03 CSCL 22B

Among the significant sources of internal disturbances that must be considered in the design of space station vibration control systems are the loads induced on the structure from various crew activities. Flight experiment T013, flown on the second manned mission of Skylab, measured force and moment time histories for a range of preplanned crew motions and activities. This experiment has proved itself invaluable as a source of on-orbit crew induced loads that has allowed a space station forcing function data base to be built. This will enable forced response such as acceleration and deflections, attributable to crew activity, to be calculated. The flight experiment, resultant database and structural model pre-processor, analysis examples and areas of combined research shall be described. Author

N87-22745*# Jet Propulsion Lab., California Inst. of Tech., Pasadena.
MODELING OF CONTROLLED FLEXIBLE STRUCTURES WITH IMPULSIVE LOADS c18
M. Zak *In* NASA. Marshall Space Flight Center Structural Dynamics and Control Interaction of Flexible Structures Apr. 1987 p 1161-1178 (For primary document see N87-22729 16-15)
Avail: NTIS HC A99/MF E03 CSCL 22B

The characteristic wave approach is developed as an alternative to modal methods which may lead to significant errors in the presence of impulsive or concentrated loads. The method is applied to periodic structures. Some special phenomena like cumulation effects and transitions to ergodicity are analyzed. Author

N87-22746*# DYNACS Engineering Co., Inc., Clearwater, Fla.
NOTES ON IMPLEMENTATION OF COULOMB FRICTION IN COUPLED DYNAMICAL SIMULATIONS **c39**
R. J. VanderVoort and R. P. Singh *In* NASA. Marshall Space Flight Center Structural Dynamics and Control Interaction of Flexible Structures Apr. 1987 p 1197-1213 (For primary document see N87-22729 16-15)
Avail: NTIS HC A99/MF E03 CSCL 20K

A coupled dynamical system is defined as an assembly of rigid/flexible bodies that may be coupled by kinematic connections. The interfaces between bodies are modeled using hinges having 0 to 6 degrees of freedom. The equations of motion are presented for a mechanical system of n flexible bodies in a topological tree configuration. The Lagrange form of the D'Alembert principle was employed to derive the equations. The equations of motion are augmented by the kinematic constraint equations. This augmentation is accomplished via the method of singular value decomposition. B.G.

N87-22747*# Jet Propulsion Lab., California Inst. of Tech., Pasadena.
ON THE CONTROL OF STRUCTURES BY APPLIED THERMAL GRADIENTS **c39**
Don Edberg and Jay-C. Chen *In* NASA. Marshall Space Flight Center Structural Dynamics and Control Interaction of Flexible Structures Apr. 1987 p 1214-1250 (For primary document see N87-22729 16-15)
Avail: NTIS HC A99/MF E03 CSCL 20K

Some preliminary results of research on control of flexible structures performed at the Jet Propulsion Laboratory are presented. It was shown that the thermoelectric device is a feasible actuator and may effectively be used to control structures, provided the structure has a relatively low thermal inertia. The control law only depends on the open-loop system natural frequency. B.G.

N87-22748*# National Aeronautics and Space Administration. Marshall Space Flight Center, Huntsville, Ala.
FINITE ELEMENT MODELS OF WIRE ROPE FOR VIBRATION ANALYSIS **c39**
J. E. Cochran, Jr., N. G. Fitz-Coy, and M. A. Cutchins *In* NASA. Marshall Space Flight Center Structural Dynamics and Control Interaction of Flexible Structures Apr. 1987 p 1251-1270 (For primary document see N87-22729 16-15)
Avail: NTIS HC A99/MF E03 CSCL 20K

The usefulness of wire rope in shock and vibration isolation is briefly reviewed and its modeling for the purpose of vibration analysis is addressed. A model of a nominally straight segment of wire rope is described in which the rope structure is represented by a maiden, or central, strand of wire with one (or more) strand(s) wrapped around it in a helix (helices). The individual strands are modeled using finite elements and MSC NASTRAN. Small linear segments of each wire are modeled mathematically by dividing them lengthwise into triangular prisms representing each prism by a solid NASTRAN element. To model pretensioning and allow for extraction of internal force information from the NASTRAN model, the wound strands are connected to the maiden strand and each other using spring (scalar elastic) elements. Mode shapes for a length of wire rope with one and fixed to a moving base and the other attached to a point mass, are presented. The use of the NASTRAN derived mode shapes to approximate internal normal forces in equations of motion for vibration analyses is considered. Author

N87-22749*# Boeing Aerospace Co., Seattle, Wash.
EXPERIMENTAL CHARACTERIZATION OF DEPLOYABLE TRUSSES AND JOINTS **c39**
R. Ikegami, S. M. Church, D. A. Keinholz, and B. L. Fowler (CSA Engineering, Inc., Palo Alto, Calif.) *In* NASA. Marshall Space Flight Center Structural Dynamics and Control Interaction of Flexible Structures Apr. 1987 p 1271-1288 (For primary document see N87-22729 16-15)
Avail: NTIS HC A99/MF E03 CSCL 20K

The structural dynamic properties of trusses are strongly affected by the characteristics of joints connecting the individual beam elements. Joints are particularly significant in that they are often the source of nonlinearities and energy dissipation. While the joints themselves may be physically simple, direct measurement is often necessary to obtain a mathematical description suitable for inclusion in a system model. Force state mapping is a flexible, practical test method for obtaining such a description, particularly when significant nonlinear effects are present. It involves measurement of the relationship, nonlinear or linear, between force transmitted through a joint and the relative displacement and velocity across it. An apparatus and procedure for force state mapping are described. Results are presented from tests of joints used in a lightweight, composite, deployable truss built by the Boeing Aerospace Company. The results from the joint tests are used to develop a model of a full 4-bay truss segment. The truss segment was statically and dynamically tested. The results of the truss tests are presented and compared with the analytical predictions from the model. Author

N87-22750*# National Aeronautics and Space Administration. Marshall Space Flight Center, Huntsville, Ala.
SYSTEM IDENTIFICATION FOR LARGE SPACE STRUCTURE DAMAGE ASSESSMENT **c18**
J. C. Chen and J. A. Garba *In* NASA. Marshall Space Flight Center Structural Dynamics and Control Interaction of Flexible Structures Apr. 1987 p 1289-1318 (For primary document see N87-22729 16-15)
Avail: NTIS HC A99/MF E03 CSCL 22B

The need for monitoring the dynamic characteristics of large structural systems for purposes of assessing the potential degradation of structural properties was established. A theory for assessing the occurrence, location, and extent of potential damage was developed utilizing on-orbit response measurements. Feasibility of the method is demonstrated using a simple structural system as an example. Author

N87-22751*# National Aeronautics and Space Administration. Marshall Space Flight Center, Huntsville, Ala.
SPACE STATION STRUCTURES AND DYNAMICS TEST PROGRAM **c18**
Frank M. Bugg, E. W. Ivey, C. J. Moore, and John S. Townsend *In its* Structural Dynamics and Control Interaction of Flexible Structures Apr. 1987 p 1319-1332 (For primary document see N87-22729 16-15)
Avail: NTIS HC A99/MF E03 CSCL 22B

The design, construction, and operation of a low-Earth orbit space station poses challenges for development and implementation of technology. One specific challenge is the development of a dynamics test program for defining the space station design requirements, and identifying and characterizing phenomena affecting the space station's design and development. The test proposal, as outlined, is a comprehensive structural dynamics program to be launched in support of the space station (SS). Development of a parametric data base and verification of the mathematical models and analytical analysis tools necessary for engineering support of the station's design, construction, and operation provide the impetus for the dynamics test program. The four test phases planned are discussed: testing of SS applicable structural concepts; testing of SS prototypes; testing of actual SS structural hardware; and on-orbit testing of SS construction. B.G.

N87-22752*# Alabama Univ., Huntsville. Dept. of Mechanical Engineering.
ANALYTICAL DETERMINATION OF SPACE STATION RESPONSE TO CREW MOTION AND DESIGN OF SUSPENSION SYSTEM FOR MICROGRAVITY EXPERIMENTS **c18**
Frank C. Liu *In* NASA. Marshall Space Flight Center Structural

Dynamics and Control Interaction of Flexible Structures Apr. 1987 p 1333-1366 Previously announced as N86-24535 (For primary document see N87-22729 16-15)
(Grant NGT-01-008-021)
Avail: NTIS HC A99/MF E03 CSCL 22B

The objective of this investigation is to make analytical determination of the acceleration produced by crew motion in an orbiting space station and define design parameters for the suspension system of microgravity experiments. A simple structural model for simulation of the IOC space station is proposed. Mathematical formulation of this model provides the engineers a simple and direct tool for designing an effective suspension system. Author

N87-22753*# Martin Marietta Aerospace, Denver, Colo. Analytical Mechanics.
SPACE STATION STRUCTURAL DYNAMICS/REACTION CONTROL SYSTEM INTERACTION STUDY **c18**
M. Pinnamaneni and J. Murray *In* NASA. Marshall Space Flight Center Structural Dynamics and Control Interaction of Flexible Structures Apr. 1987 p 1367-1394 (For primary document see N87-22729 16-15)
Avail: NTIS HC A99/MF E03 CSCL 22B

The performance of the Reaction Control System is impacted by the extreme flexibility of the space station structure. The method used to analyze the periodic thrust profile of a simple form of phase plane logic is presented. The results illustrate the effect on flexible body response of the type of phase plane logic utilized and the choice of control parameters: cycle period and attitude deadband. Author

N87-22754# Air Force Inst. of Tech., Wright-Patterson AFB, Ohio. School of Engineering.
ESTIMATION OF ICBM (INTERCONTINENTAL BALLISTIC MISSILE) PERFORMANCE PARAMETERS M.S. Thesis
Kenneth S. Crumpton Dec. 1986 45 p
(AD-A179204; AFIT/GA/AA/86D-3) Avail: NTIS HC A03/MF A01 CSCL 16B

The estimation of launch vehicle performance parameters was explored through the use of a Bayes Filter. The missile dynamics were modeled using a seven state system consisting of the vehicle position and velocity vectors, and the acceleration due to thrust. An assumed solution was used in the model obviating the need for a numerical integration subroutine. The filter was run with two different missile flight profiles. The program produced good approximations of the missile thrust acceleration even through staging events. The results of the Bayes filter were improved with the use of fading memory. The fading memory values were adjusted until the filter closely approximated the missile acceleration values. The filter was able to handle the second missile flight profile without any adjustment in the fading memory and with no degradation of results. GRA

N87-22755*# National Aeronautics and Space Administration. Lewis Research Center, Cleveland, Ohio.
EFFECT OF GIMBAL FRICTION MODELING TECHNIQUE ON CONTROL STABILITY AND PERFORMANCE FOR CENTAUR UPPER-STAGE
Ronald E. Graham 1987 10 p Prepared for presentation at the Guidance, Navigation and Control Conference, Monterey, Calif., 17-19 Aug. 1987; sponsored by AIAA
(NASA-TM-89894; E-3582; NAS 1.15:89894) Avail: NTIS HC A02/MF A01 CSCL 22B

The powered-phase autopilot for the Centaur upper stage rocket uses an autopilot forward loop gain scheduler that decreases the proportional gain as propellant mass is depleted. Nonlinear time response simulation studies revealed that Centaur vehicles with low-gain autopilots would have large attitude error limit cycles. These limit cycles were due to the assumed presence of Coulomb friction in the engine gimbals. This situation could be corrected through the use of an harmonic dither, programmed into the on-board digital computer and added to the engine command signal. This would introduce impending motion to the engines, allowing control of the engines even under small commands. Control authority was found to be restored when dither was used. A concern arose that the Centaur could be unacceptably excited at resonances near the dither frequency, if the dither amplitude was to be chosen on the basis of friction level present, a test was conducted to measure this level. Dither characteristics were to be based on the test results. The test results showed that the gimbal friction characteristic was actually hysteretic rather than the assumed Coulomb friction. The simulation results showed that, using this new model of gimbal friction, dither would no longer be necessary. Author

16 SPACE TRANSPORTATION

Includes passenger and cargo space transportation, e.g., shuttle operations; and space rescue techniques.

For related information see also *03 Air Transportation and Safety* and *18 Spacecraft Design, Testing and Performance.* For space suits see *54 Man/System Technology and Life Support.*

N87-22756# Air Force Inst. of Tech., Wright-Patterson AFB, Ohio. School of Engineering.
OPTIMAL SHUTTLE ALTITUDE CHANGES USING TETHERS M.S. Thesis
Robert R. Fisher Dec. 1986 64 p
(AD-A179205; AFIT/GA/AA/86D-5) Avail: NTIS HC A04/MF A01 CSCL 22A

The use of tethers in space has been proposed for many years. While much work has been done recently on the use of tethers for towed satellites from the Space Shuttle, little has been done to determine the possible benefits of using tethers as propulsive devices to supplement or replace rocket engines for boost from Low Earth Orbit. Orbit insertion parameters such as velocity and final altitude for the space shuttle are limited by operational constraints on the possible delta V that can be supplied from the engines. The possibility of increasing the performance of the shuttle exists in using an inter-connecting tether to serve as a momentum transfer device between the External Tank and the Shuttle. This added momentum would widen the possible orbit options presently available by boosting the shuttle to a higher orbit. This project derives the equations of motion for a three-body connected dynamical system to include the Shuttle, the external tank, and the cable in orbit around a spherical Earth. Due to current material limitations the tether length will be limited to 100 kilometers. The possible envelope of orbital changes is investigated. GRA

N87-22757*# National Aeronautics and Space Administration. Lewis Research Center, Cleveland, Ohio.
NUMERICAL MODELING OF ON-ORBIT PROPELLANT MOTION RESULTING FROM AN IMPULSIVE ACCELERATION
John C. Aydelott, Raymond C. Mjolsness, Martin D. Torrey, and John I. Hochstein (Washington Univ., St. Louis, Mo.) 1987 24 p Prepared for the 23rd Joint Propulsion Conference, San Diego, Calif., 29 Jun. - 2 Jul. 1987; cosponsored by AIAA, SAE, ASME, and ASEE
(NASA-TM-89873; E-3547; NAS 1.15:89873; AIAA-87-1766) Avail: NTIS HC A02/MF A01 CSCL 22A

In-space docking and separation maneuvers of spacecraft that have large fluid mass fractions may cause undesirable spacecraft motion in response to the impulsive-acceleration-induced fluid motion. An example of this potential low gravity fluid management problem arose during the development of the shuttle/Centaur vehicle. Experimentally verified numerical modeling techniques were developed to establish the propellant dynamics, and subsequent vehicle motion, associated with the separation of the Centaur vehicle from the shuttle orbiter cargo bay. Although the shuttle/Centaur development activity was suspended, the numerical modeling techniques are available to predict on-orbit liquid motion resulting from impulsive accelerations for other missions and spacecraft. Author

17 SPACE COMM., SPACECRAFT COMM., COMMAND & TRACKING

Includes telemetry; space communications networks; astronavigation and guidance; and radio blackout.

For related information see also *04 Aircraft Communications and Navigation* and *32 Communications and Radar.*

No abstracts in this category.

18 SPACECRAFT DESIGN, TESTING AND PERFORMANCE

Includes satellites; space platforms; space stations; spacecraft systems and components such as thermal and environmental controls; and attitude controls.

For life support systems see *54 Man/System Technology and Life Support.* For related information see also *05 Aircraft Design, Testing and Performance, 39 Structural Mechanics,* and *16 Space Transportation.*

N87-22758*# Allied Bendix Aerospace, Teterboro, N.J. Guidance Systems Div.
ADAPTIVE MOMENTUM MANAGEMENT FOR LARGE SPACE STRUCTURES Final Report, 1 May 1986 - 31 Jan. 1987
E. Hahn 10 Feb. 1987 43 p
(Contract NAS8-36488)
(NASA-CR-179085; NAS 1.26:179085) Avail: NTIS HC A03/MF A01 CSCL 22B

Momentum management is discussed for a Large Space Structure (LSS) with the structure selected configuration being the Initial Orbital Configuration (IOC) of the dual keel space station. The external forces considered were gravity gradient and aerodynamic torques. The goal of the momentum management scheme developed is to remove the bias components of the external torques and center the cyclic components of the stored angular momentum. The scheme investigated is adaptive to uncertainties of the inertia tensor and requires only approximate knowledge of principle moments of inertia. Computational requirements are minimal and should present no implementation problem in a flight type computer and the method proposed is shown to be effective in the presence of attitude control bandwidths as low as .01 radian/sec. Author

N87-22759# Air Force Inst. of Tech., Wright-Patterson AFB, Ohio. School of Engineering.
DESIGN OF AN ORBITAL INSPECTION SATELLITE M.S. Thesis
Harold D. Getzelman Dec. 1986 125 p
(AD-A179115; AFIT/GSO/AA/86D-4) Avail: NTIS HC A06/MF A01 CSCL 22B

The need for the inspection of space objects by satellite is identified. The historical and legal context of the inspection satellite is discussed and its implications on the design of the satellite are understood. Systems engineering tools are used to identify the basic design of an orbital inspection satellite. The satellite is partitioned into six major subsystems for analysis. The interactions between subsystems is investigated. An orbital inspection satellite composed of the best systems and supporting subsystems is described. Finally, recommendations for further study and the impact of key decisions are described. Author (GRA)

N87-22760# Air Force Inst. of Tech., Wright-Patterson AFB, Ohio. School of Engineering.
A PROTOTYPE EXPERT SYSTEM ADVISOR FOR SATELLITE SUPPORT SCHEDULING M.S. Thesis
Dale J. Kennedy Dec. 1986 227 p
(AD-A179425; AFIT/GOR/OS/86D-5) Avail: NTIS HC A11/MF A01 CSCL 05H

This report documents the research conducted to develop a prototype expert system advisor for scheduling satellite supports. The purpose of this research is to demonstrate the feasibility of applying expert system technology to scheduling satellite supports. The Global Positioning System satellite program is used as the model program for the research. The development process included three main phases. First, knowledge engineering was conducted to acquire the facts, rules and heuristics the expert uses to schedule the supports. Second, an expert system development tool is selected and a system design established. Third, the expert system is built using the selected tool and tested using cases of schedules prepared by the expert. Finally, the results of the research are presented with recommendations for future work. Author (GRA)

N87-22761# Air Force Inst. of Tech., Wright-Patterson AFB, Ohio. School of Engineering.
MOVING-BANK MULTIPLE MODEL ADAPTIVE ESTIMATION APPLIED TO FLEXIBLE SPACESTRUCTURE CONTROL M.S. Thesis
Drew A. Karnick Dec. 1986 213 p
(AD-A178870; AFIT/GE/ENG/86D-41) Avail: NTIS HC A10/MF A01 CSCL 22B

A significant problem in estimation and control is the uncertainty of parameters in the mathematical model used in the design of controllers and/or estimators. These parameters may be unknown, varying slowly, or changing abruptly due to a failure in the physical system. These changes in parameters often necessitate the identification of parameters within the mathematical model and changing the mathematical model during a real-time control problem. This is often referred to as adaptive control and/or estimation. This thesis investigates methods of adaptive control implementing a moving-bank multiple model adaptive estimator. GRA

N87-22762# Air Force Inst. of Tech., Wright-Patterson AFB, Ohio. School of Engineering.
DEVELOPING A VOICE-CONTROLLED COMPUTER-GENERATED DISPLAY TO ASSIST SPACE STATION ASTRONAUTS DURING MAINTENANCE ACTIVITY M.S. Thesis
Paul J. Pabich Dec. 1986 240 p
(AD-A178997; AFIT/GSO/ENG/86D-1) Avail: NTIS HC A11/MF A01 CSCL 22B

This thesis illustrated a planning strategy for a voice-controlled, computer-generated maintenance display which would be used by astronauts when completing maintenance activity outside the proposed U.S. space station. After justifying the usefulness of a proposed systems engineering approach, five main objectives were provided: (1) the vertical stanchion of the Manipulator Foot Restraint would provide an adequate base for the display so it could be moved to and from the worksite; (2) liquid crystal display technology should be used; (3) for voice-controlled operations, the best type of recognition unit to use would be one where the unit understands only one speaker at a time and only one word at a time; (4) experimental data suggest that a hierarchical scheme should be used for the menu format; (5) use of text, audio, graphics, and color for the proposed display. Only text and graphics were recommended for use. A proposed display format was presented showing the placement of the menu, text and graphics using some known data about how the human brain processes information. GRA

N87-22708*# Auburn Univ., Ala.
SPACE STATION/SHUTTLE ORBITER DYNAMICS DURING DOCKING
N. G. Fitz-Coy and J. E. Cochran, Jr. *In* NASA. Marshall Space Flight Center Structural Dynamics and Control Interaction of Flexible Structures Apr. 1987 p 133-174 (For primary document see N87-22702 16-15)
Avail: NTIS HC A99/MF E03 CSCL 22B

N87-22711*# National Aeronautics and Space Administration. Langley Research Center, Hampton, Va.
CONSIDERATIONS IN THE DESIGN AND DEVELOPMENT OF A SPACE STATION SCALE MODEL
Paul E. McGowan *In* NASA. Marshall Space Flight Center Structural Dynamics and Control Interaction of Flexible Structures Apr. 1987 p 215-246 (For primary document see N87-22702 16-15)
Avail: NTIS HC A99/MF E03 CSCL 22B

N87-22714*# Air Force Wright Aeronautical Labs., Wright-Patterson AFB, Ohio.
OPTIMUM MIX OF PASSIVE AND ACTIVE CONTROL OF SPACE STRUCTURES
Lynn Rogers and Ken Richards (Martin Marietta Aerospace, Denver, Colo.) *In* NASA. Marshall Space Flight Center Structural Dynamics and Control Interaction of Flexible Structures Apr. 1987 p 275-292 (For primary document see N87-22702 16-15)
Avail: NTIS HC A99/MF E03 CSCL 22B

N87-22715*# Control Dynamics Co., Huntsville, Ala.
ONE CONTROLLER AT A TIME (1-CAT): A MIMO DESIGN METHODOLOGY
J. R. Mitchell and J. C. Lucas *In* NASA. Marshall Space Flight Center Structural Dynamics and Control Interaction of Flexible Structures Apr. 1987 p 293-334 (For primary document see N87-22702 16-15)
Avail: NTIS HC A99/MF E03 CSCL 22B

N87-22717*# National Aeronautics and Space Administration. Langley Research Center, Hampton, Va.
STATUS REPORT AND PRELIMINARY RESULTS OF THE SPACECRAFT CONTROL LABORATORY EXPERIMENT
Jeffrey P. Williams *In* NASA. Marshall Space Flight Center Structural Dynamics and Control Interaction of Flexible Structures Apr. 1987 p 359-398 (For primary document see N87-22702 16-15)
Avail: NTIS HC A99/MF E03 CSCL 22B

N87-22721*# Rockwell International Corp., Downey, Calif. Space Station Systems Div.
STRUCTURAL/CONTROL INTERACTION (PAYLOAD POINTING AND MICRO-g)
C. R. Larson *In* NASA. Marshall Space Flight Center Structural Dynamics and Control Interaction of Flexible Structures Apr. 1987 p 457-484 (For primary document see N87-22702 16-15)
Avail: NTIS HC A99/MF E03 CSCL 22B

N87-22723*# Boeing Aerospace Co., Seattle, Wash.
PRECISION POINTING AND CONTROL OF FLEXIBLE SPACECRAFT
M. H. Bantell, Jr. *In* NASA. Marshall Space Flight Center Structural Dynamics and Control Interaction of Flexible Structures Apr. 1987 p 505-538 (For primary document see N87-22702 16-15)
Avail: NTIS HC A99/MF E03 CSCL 22B

N87-22731*# Texas A&M Univ., College Station.
A QUASI-ANALYTICAL METHOD FOR NON-ITERATIVE COMPUTATION OF NONLINEAR CONTROLS
J. L. Junkins, R. C. Thompson, and J. D. Turner (Cambridge Research Associates, Mass.) *In* NASA. Marshall Space Flight Center Structural Dynamics and Control Interaction of Flexible Structures Apr. 1987 p 759-774 (For primary document see N87-22729 16-15)
Avail: NTIS HC A99/MF E03 CSCL 22B

N87-22732*# National Aeronautics and Space Administration. Langley Research Center, Hampton, Va.
CONTROL OF FLEXIBLE STRUCTURES AND THE RESEARCH COMMUNITY
Claude R. Keckler and Jon S. Pyle *In* NASA. Marshall Space Flight Center Structural Dynamics and Control Interaction of Flexible Structures Apr. 1987 p 789-840 (For primary document see N87-22729 16-15)
Avail: NTIS HC A99/MF E03 CSCL 22B

N87-22729 16-15)
Avail: NTIS HC A99/MF E03 CSCL 22B

N87-22733*# General Electric Co., Philadelphia, Pa. Space Div.
IMPACT OF SPACE STATION APPENDAGE VIBRATIONS ON THE POINTING PERFORMANCE OF GIMBALLED PAYLOADS
Robert O. Hughes *In* NASA. Marshall Space Flight Center Structural Dynamics and Control Interaction of Flexible Structures (date) 841-866 (SEE N87-22729 16-15) Apr. 1987 (For primary document see N87-22729 16-15)
Avail: NTIS HC A99/MF E03 CSCL 22B

N87-22734*# Virginia Polytechnic Inst. and State Univ., Blacksburg. Dept. of Engineering Science and Mechanics.
MANEUVERING AND VIBRATION CONTROL OF FLEXIBLE SPACECRAFT
L. Meirovitch and R. D. Quinn *In* NASA. Marshall Space Flight Center Structural Dynamics and Control Interaction of Flexible Structures Apr. 1987 p 867-880 (For primary document see N87-22729 16-15)
(Grant NAG1-225)
Avail: NTIS HC A99/MF E03 CSCL 22B

N87-22736*# Rockwell International Corp., Downey, Calif. Space Station Systems Div.
PRELIMINARY EVALUATION OF A REACTION CONTROL SYSTEM FOR THE SPACE STATION
H. H. Woo and J. A. Finley *In* NASA. Marshall Space Flight Center Structural Dynamics and Control Interaction of Flexible Structures Apr. 1987 p 930-942 (For primary document see N87-22729 16-15)
Avail: NTIS HC A99/MF E03 CSCL 22B

N87-22737*# National Aeronautics and Space Administration. Langley Research Center, Hampton, Va.
DUAL KEEL SPACE STATION CONTROL/STRUCTURES INTERACTION STUDY
John W. Young, Frederick J. Lallman, and Paul A. Cooper *In* NASA. Marshall Space Flight Center Structural Dynamics and Control Interaction of Flexible Structures Apr. 1987 p 945-978 (For primary document see N87-22729 16-15)
Avail: NTIS HC A99/MF E03 CSCL 22B

N87-22741*# Harris Corp., Melbourne, Fla. Government Aerospace Systems Div.
MAXIMUM ENTROPY/OPTIMAL PROJECTION (MEOP) CONTROL DESIGN SYNTHESIS: OPTIMAL QUANTIFICATION OF THE MAJOR DESIGN TRADEOFFS
D. C. Hyland and D. S. Bernstein *In* NASA. Marshall Space Flight Center Structural Dynamics and Control Interaction of Flexible Structures Apr. 1987 p 1033-1070 (For primary document see N87-22729 16-15)
Avail: NTIS HC A99/MF E03 CSCL 22B

N87-22744*# Lockheed Engineering and Management Services Co., Inc., Houston, Tex.
CREW ACTIVITY AND MOTION EFFECTS ON THE SPACE STATION
Brian V. Rochon and Steven A. Scheer *In* NASA. Marshall Space Flight Center Structural Dynamics and Control Interaction of Flexible Structures Apr. 1987 p 1095-1160 (For primary document see N87-22729 16-15)
(Contract NAS9-15800)
Avail: NTIS HC A99/MF E03 CSCL 22B

N87-22745*# Jet Propulsion Lab., California Inst. of Tech., Pasadena.
MODELING OF CONTROLLED FLEXIBLE STRUCTURES WITH IMPULSIVE LOADS
M. Zak *In* NASA. Marshall Space Flight Center Structural Dynamics and Control Interaction of Flexible Structures Apr. 1987 p 1161-1178 (For primary document see N87-22729 16-15)
Avail: NTIS HC A99/MF E03 CSCL 22B

16-15)
Avail: NTIS HC A99/MF E03 CSCL 22B

N87-22750*# National Aeronautics and Space Administration. Marshall Space Flight Center, Huntsville, Ala.
SYSTEM IDENTIFICATION FOR LARGE SPACE STRUCTURE DAMAGE ASSESSMENT
J. C. Chen and J. A. Garba *In* NASA. Marshall Space Flight Center Structural Dynamics and Control Interaction of Flexible Structures Apr. 1987 p 1289-1318 (For primary document see N87-22729 16-15)
Avail: NTIS HC A99/MF E03 CSCL 22B

N87-22751*# National Aeronautics and Space Administration. Marshall Space Flight Center, Huntsville, Ala.
SPACE STATION STRUCTURES AND DYNAMICS TEST PROGRAM
Frank M. Bugg, E. W. Ivey, C. J. Moore, and John S. Townsend *In its* Structural Dynamics and Control Interaction of Flexible Structures Apr. 1987 p 1319-1332 (For primary document see N87-22729 16-15)
Avail: NTIS HC A99/MF E03 CSCL 22B

N87-22752*# Alabama Univ., Huntsville. Dept. of Mechanical Engineering.
ANALYTICAL DETERMINATION OF SPACE STATION RESPONSE TO CREW MOTION AND DESIGN OF SUSPENSION SYSTEM FOR MICROGRAVITY EXPERIMENTS
Frank C. Liu *In* NASA. Marshall Space Flight Center Structural Dynamics and Control Interaction of Flexible Structures Apr. 1987 p 1333-1366 Previously announced as N86-24535 (For primary document see N87-22729 16-15)
(Grant NGT-01-008-021)
Avail: NTIS HC A99/MF E03 CSCL 22B

N87-22753*# Martin Marietta Aerospace, Denver, Colo. Analytical Mechanics.
SPACE STATION STRUCTURAL DYNAMICS/REACTION CONTROL SYSTEM INTERACTION STUDY
M. Pinnamaneni and J. Murray *In* NASA. Marshall Space Flight Center Structural Dynamics and Control Interaction of Flexible Structures Apr. 1987 p 1367-1394 (For primary document see N87-22729 16-15)
Avail: NTIS HC A99/MF E03 CSCL 22B

19 SPACECRAFT INSTRUMENTATION

For related information see also *06 Aircraft Instrumentation* and *35 Instrumentation and Photography.*

N87-22763# Air Force Inst. of Tech., Wright-Patterson AFB, Ohio. School of Engineering.
STAR SENSOR FINE ATTITUDE POINTING MODEL FOR A SPINNING GEOSYNCHRONOUS SATELLITE M.S. Thesis
John V. Taylor, IV Dec. 1986 152 p
(AD-A179424; AFIT/GA/AA/86D-14) Avail: NTIS HC A08/MF A01 CSCL 22A

A fine attitude determination model is developed for a spinning geosynchronous satellite, based upon stellar observations from a V-slit star scanner and ground supplied satellite ephemerides. A true attitude model is determined through numerical integration of Euler's moment equations for a torque-free, rigid, axisymmetric body, and kinematic relations which consist of pitch, roll, yaw, orientation angles. Next, the closed form solutions to the Euler equations are coupled with first-order approximate solutions of the kinematic relations to develop a second order kinematics model. Observation relations, relating stellar slit-plane crossing times, (a priori star identification assumed), to attitude states, are then developed. Finally, a nonlinear least-squares estimation algorithm is used to identify the full satellite attitude state. Simulation is tested for single scan and multiple-scan capability using exact and noise ridden data. GRA

20 SPACECRAFT PROPULSION AND POWER

Includes main propulsion systems and components, e.g., rocket engines; and spacecraft auxilliary power sources.

For related information see also *07 Aircraft Propulsion and Power, 28 Propellants and Fuels, 44 Energy Production and Conversion,* and *15 Launch Vehicles and Space Vehicles.*

N87-22764*# Computational Mechanics Consultants, Austin, Tex.
VECTORIZABLE ALGORITHMS FOR ADAPTIVE SCHEMES FOR RAPID ANALYSIS OF SSME FLOWS Final Report
J. Tinsley Oden Apr. 1987 30 p
(NASA Order H-85080B)
(NASA-CR-179082; NAS 1.26:179082; TR-87-03) Avail: NTIS HC A03/MF A01 CSCL 21H

An initial study into vectorizable algorithms for use in adaptive schemes for various types of boundary value problems is described. The focus is on two key aspects of adaptive computational methods which are crucial in the use of such methods (for complex flow simulations such as those in the Space Shuttle Main Engine): the adaptive scheme itself and the applicability of element-by-element matrix computations in a vectorizable format for rapid calculations in adaptive mesh procedures. B.G.

N87-22765*# Battelle Columbus Labs., Ohio.
STUDIES AND ANALYSES OF THE SPACE SHUTTLE MAIN ENGINE: HIGH-PRESSURE OXIDIZER TURBOPUMP FAILURE INFORMATION PROPAGATION MODEL
R. C. Glover, S. W. Rudy, and A. E. Tischer 20 Apr. 1987 511 p
(Contract NASw-3737)
(NASA-CR-179079; NAS 1.26:179079; BCD-SSME-TR-87-1) Avail: NTIS HC A22/MF A01 CSCL 21H

The high-pressure oxidizer turbopump (HPOTP) failure information propagation model (FIPM) is presented. The text includes a brief discussion of the FIPM methodology and the various elements which comprise a model. Specific details of the HPOTP FIPM are described. Listings of all the HPOTP data records are included as appendices. Author

N87-22766*# National Aeronautics and Space Administration. Lewis Research Center, Cleveland, Ohio.
STRUCTURAL INTEGRITY AND DURABILITY OF REUSABLE SPACE PROPULSION SYSTEMS
1987 205 p Conference held in Cleveland, Ohio, 12-13 May 1987
(NASA-CP-2471; E-3512; NAS 1.55:2471) Avail: NTIS HC A10/MF A01 CSCL 21H

A two-day conference on the structural integrity and durability of reusable space propulsion systems was held on May 12 and 13, 1987, at the NASA Lewis research Center. Aerothermodynamic loads; instrumentation; fatigue, fracture, and constitutive modeling; and structural dynamics were discussed. For individual titles, see N87-22767 through N87-22799.

N87-22767*# National Aeronautics and Space Administration. Lewis Research Center, Cleveland, Ohio.
UNSTEADY STATOR/ROTOR INTERACTION **c34**
Philip C. E. Jorgenson and Rodrick V. Chima *In its* Structural Integrity and Durability of Reusable Space Propulsion Systems 1987 p 5-11 (For primary document see N87-22766 16-20)
Avail: NTIS HC A10/MF A01 CSCL 20D

The major thrust of the computational analysis of turbomachinery to date has been the steady-state solution of isolated blades using mass-averaged inlet and exit conditions. Unsteady flows differ from the steady solution due to interaction of pressure waves and wakes between blade rows. To predict the actual complex flow conditions one must look at the time accurate solution of the entire turbomachine. Three quasi-three-dimensional Euler and thin layer Navier-Stokes equations are solved for unsteady turbomachinery flows. Author

N87-22768*# National Aeronautics and Space Administration. Lewis Research Center, Cleveland, Ohio.
SIMULATION OF MULTISTAGE TURBINE FLOWS c34
John J. Adamczyk and Richard A. Mulac (Sverdrup Technology, Inc., Middleburg Heights, Ohio.) *In its* Structural Integrity and Durability of Reusable Space Propulsion Systems 1987 p 13-20 (For primary document see N87-22766 16-20)
Avail: NTIS HC A10/MF A01 CSCL 20D

A flow model has been developed for analyzing multistage turbomachinery flows. This model, referred to as the average passage flow model, describes the time-averaged flow field with a typical passage of a blade row embedded within a multistage configuration. Computer resource requirements, supporting empirical modeling, formulation code development, and multitasking and storage are discussed. Illustrations from simulations of the space shuttle main engine (SSME) fuel turbine performed to date are given. Author

N87-22769*# National Aeronautics and Space Administration. Lewis Research Center, Cleveland, Ohio.
PROGRESS IN THE PREDICTION OF UNSTEADY HEAT TRANSFWE ON TURBINES BLADES c34
T. Cebeci, R. J. Simoneau, A. Krainer, and M. F. Platzer (Naval Postgraduate School, Monterey, Calif.) *In its* Structural Integrity and Durability of Reusable Space Propulsion Systems 1987 p 21-27 (For primary document see N87-22766 16-20)
Avail: NTIS HC A10/MF A01 CSCL 20D

Progress toward developing a general method for predicting unsteady heat transfer on turbine blades subject to blade-passing frequencies and Reynolds numbers relevant to the Space Shuttle Main Engine (SSME) is discussed. The method employs an invisid/viscous interactive procedure which has been tested extensively for steady subsonic and transonic external airfoil problems. One such example is shown. The agreement with experimental data and with Navier-Stokes calculations yields confidence in the method. The technique is extended to account for wake generated unsteadiness. The flow reversals around the stagnation point caused by the nonuniform onset velocity are accounted for by using the Characteristic Box scheme developed by Cebeci and Stewartson. The coupling between the inviscid and viscous methods is achieved by using a special procedure, which, with a novel inverse finite-difference boundary-layer method, allows the calculations to be performed for a wide range of flow conditions, including separation. Preliminary results are presented for the stagnation region of turbine blades for both laminar and turbulent flows. A laminar model problem corresponding to a flow on a circular cylinder which experiences the periodic passing of wakes from turbine blades is presented to demonstrate the ability of the method to calculate flow reversals around the stagnation region. Author

N87-22770*# Calspan-Buffalo Univ. Research Center, N.Y.
EXPERIMENTAL AND THEORETICAL STUDIES OF TIME-AVERAGED AND TIME RESOLVED ROTOR HEAT TRANSFER c34
M. G. Dunn, W. J. Rae, and D. L. Rigby *In* NASA. Lewis Research Center Structural Integrity and Durability of Reusable Space Propulsion Systems 1987 p 29-32 (For primary document see N87-22766 16-20)
Avail: NTIS HC A10/MF A01 CSCL 20D

Efforts in support of the Space Shuttle Main Engine (SSME) structural durability program have concentrated on obtaining detailed time-averaged and time-resolved (or phase-locked) measurements on a full-scale rotating turbine both with and without cold gas injection and on theoretical studies designed to improve the prediction capability for these turbine flows. The experimental efforts have concentrated on use of the Garrett TFE 731-2 hp turbine. However, it has been possible to apply the theoretical efforts to predicting heat-flux distributions obtained for two additional turbines - i.e., (1) the Garrett low aspect ratio turbine (LART) and (2) the Teledyne 702 turbine. The experimental technique is the short duration, shock-tunnel approach, in which fast-response, thin-film resistance thermometers are used to measure surface temperature histories at prescribed locations on the turbine component parts. Heat-flux values are then inferred from the temperature histories by using standard data reduction procedures. The turbine being used is the Garrett TFE 731-2 hp stage, and both the nozzle guide vanes and the rotor blades are heavily instrumented with thin-film heat-flux gauges. Depending on how the data from a particular heat-flux gauge are recorded, one can get either time-resolved (or phase-locked) or time-averaged results. Both types of data are illustrated. Author

N87-22771*# Argonne National Lab., Ill.
ANALYTICAL AND EXPERIMENTAL STUDIES OF FLOW-INDUCED VIBRATION OF SSME COMPONENTS c39
S. S. Chen, J. A. Jendrzejczyk, and M. W. Wambsganss *In* NASA. Lewis Research Center Structural Integrity and Durability of Reusable Space Propulsion Systems 1987 p 33-36 Sponsored in part by DOE (For primary document see N87-22766 16-20)
Avail: NTIS HC A10/MF A01 CSCL 20K

Components of the Space Shuttle Main Engines (SSMEs) are subjected to a severe environment that includes high-temperature, high-velocity flows. Such flows represent a source of energy that can induce and sustain large-amplitude vibratory stresses and/or result in fluidelastic instabilities. Three components are already known to have experienced failures in evaluation tests as a result of flow-induced structural motion. These components include the liquid-oxygen (LOX) posts, the fuel turbine bellows shield, and the internal inlet tee splitter vane. Researchers considered the dynamic behavior of each of these components with varying degrees of effort: (1) a theoretical and experimental study of LOX post vibration excited by a fluid flow; (2) an assessment of the internal inlet tee splitter vane vibration (referred to as the 4000-Hz vibration problem); and (3) a preliminary consideration of the bellows shield problem. Efforts to resolve flow-induced vibration problems associated with the SSMEs are summarized. Author

N87-22772*# National Aeronautics and Space Administration. Lewis Research Center, Cleveland, Ohio.
PROGRESS ON THIN-FILM SENSORS FOR SPACE PROPULSION TECHNOLOGY c35
Walter S. Kim *In its* Structural Integrity and Durability of Reusable Space Propulsion Systems 1987 p 39-42 (For primary document see N87-22766 16-20)
Avail: NTIS HC A10/MF A01 CSCL 14B

The objective is to develop thin-film thermocouples for Space Shuttle Main Engine (SSME) components. Thin-film thermocouples have been developed for aircraft gas turbine engines and are in use for temperature measurement on turbine blades to 1800 F. The technology established for aircraft gas turbine engines will be adapted to the materials and environment encountered in the SSME. Specific goals are to expand the existing in-house thin-film sensor technology and to test the survivability and durability of thin-film sensors in the SSME environment. Author

N87-22773*# Sverdrup Technology, Inc., Middleburg Heights, Ohio.
PROGRESS IN OPTICAL STRAIN MEASUREMENT SYSTEM DEVELOPMENT c35
Christian T. Lant and Walid Qaqish *In* NASA. Lewis Research Center Structural Integrity and Durability of Reusable Space Propulsion Systems 1987 p 45-46 (For primary document see N87-22766 16-20)
Avail: NTIS HC A10/MF A01 CSCL 14B

A laser speckle strain measurement system has been built and tested for the NASA Lewis Research Center. The system is based on a speckle shift technique, which automatically corrects for error due to rigid body motion, and provides a near real time measure of strain. The first stage of a multiphase effort to develop an optical strain gauge capable of mapping in two dimensions the strain on the surface of a hot specimen is discussed. The objectives of this first phase have been to provide a noncontact, one-dimensional, differential strain gauge for experimental purposes, and to determine the maximum open air temperature limit of the system. Author

N87-22774*# National Aeronautics and Space Administration. Lewis Research Center, Cleveland, Ohio.
HEAT FLUX CALIBRATION FACILITY CAPABLE OF SSME CONDITIONS c09
Curt H. Liebert *In its* Structural Integrity and Durability of Reusable Space Propulsion Systems 1987 p 47-49 (For primary document see N87-22766 16-20)
Avail: NTIS HC A10/MF A01 CSCL 14B

There is a need to more thoroughly characterize the hostile space shuttle main engine (SSME) turbopump environment. It has been estimated that component surface heat flux in the hot-gas environment is about 10 MW/square meter, and this is about 50 times that encountered in aircraft engines. Also, material temperature transients can be as high as 1000 K in about 1 second. These transients can cause durability problems such as material cracking. Heat flux sensors placed in the turbopump components can partially characterize this environment by measuring surface heat flux. These heat flux data can be used to verify analytical-stress, boundary-layer, and heat-transfer design models. Preliminary plans were discussed at the first SSME durablity conference for designing and fabricating a new facility for the calibration and durability testing of prototype heat flux sensors for the SSME. This facility, which is necessary for assessment of new heat flux gauge concepts needed in the hostile SSME turbopump environment, is described. Author

N87-22775*# Case Western Reserve Univ., Cleveland, Ohio.
NUMERICAL STUDY OF THE EFFECTS OF BOUNDARY CONDITIONS ON THE MEASUREMENT AND CALIBRATION OF GARDON TYPE HEAT FLUX SENSORS c35
M. Krane and A. Dybbs *In* NASA. Lewis Research Center Structural Integrity and Durability of Reusable Space Propulsion Systems 1987 p 51-57 (For primary document see N87-22766 16-20)
Avail: NTIS HC A10/MF A01 CSCL 14B

To monitor the high-intensity heat flux conditions that occur in the space shuttle main engine (SSME), it is necessary to use specifically designed heat flux sensors. These sensors, which are of the Gardon-type, are exposed on the measuring face to high-intensity radiative and convective heat fluxes and on the other face to convective cooling. To improve the calibration and measurement accuracy of these gauges, researchers are studing the effect that the thermal boundary conditions have on gauge performance. In particular, they are studying how convective cooling effects the field inside the sensor and the measured heat flux. The first phase of this study involves a numerical study of these effects. Subsequent phases will involve experimental verification. A computer model of the heat transfer around a Garden-type heat flux sensor was developed. Two specific geometries are being considered are: (1) heat flux sensor mounted on a flat-plate; and (2) heat flux sensor mounted at the stagnation point of a circular cylinder. Both of these configurations are representative of the use of heat flux sensors in the components of the SSME. The purpose of the analysis is to obtain a temperature distribution as a function of the boundary conditions. Author

N87-22776*# Georgia Inst. of Tech., Atlanta.
DEFORMATION AND FATIGUE BEHAVIOR OF SSME TURBOPUMP BLADE MATERIALS c26
Walter W. Milligan and Stephen D. Antolovich *In* NASA. Lewis Research Center Structural Integrity and Durability of Reusable Space Propulsion Systems 1987 p 65-81 (For primary document see N87-22766 16-20)
Avail: NTIS HC A10/MF A01 CSCL 11F

Directionally solidified and single crystal superalloys which are intended for use as turbopump blade materials are anisotropic both elastically and plastically. Therefore, isotropic constitutive models must be modified. Several models which are now being developed are based on metallurgical theories of deformation in these types of alloys. However, these theories have not been fully justified, and the temperature and strain regimes over which they may be valid are poorly defined. The objective of this work is to study the deformation behavior of the alloys, in order to determine the validity of these models and to thereby support the ongoing research efforts in solid mechanics. Author

N87-22777*# National Aeronautics and Space Administration. Lewis Research Center, Cleveland, Ohio.
FATIGUE DAMAGE INTERACTION BEHAVIOR OF PWA 1480 c26
Michael A. McGaw *In its* Structural Integrity and Durability of Reusable Space Propulsion Systems 1987 p 83-87 (For primary document see N87-22766 16-20)
Avail: NTIS HC A10/MF A01 CSCL 11F

The fatigue damage interaction behavior of PWA 1480 single crystal alloy has been experimentally established for the two-level loading case in which a block of low-cycle fatigue loading is followed by high-cycle fatigue loading to failure. A relative life ratio N1/N2 (where N1 and N2 are the low- and high-cycle fatigue baseline lives, respectively) of approximately 0.002 was explored to assess the interaction behavior. The experimental results thus far show evidence of a loading order interaction effect to a similar degree of detriment as has been observed in polycrystalline materials. Current generation single crystal alloys in general, and PWA 1480 in particular, contain pores; indeed, it was observed in all cases that specimen failure initiated from pores connected with or immediately below the surface. Detailed fractographic and metallographic studies are currently being made to assess the nature of the porosity in terms of its effect on fatigue life. Author

N87-22778*# Case Western Reserve Univ., Cleveland, Ohio.
A NEW FORMULATION OF MEAN STRESS EFFECTS IN FATIGUE c39
S. S. Manson and K. R. Heidmann (Steelcase Corp., Grand Rapids, Mich.) *In* NASA. Lewis Research Center Structural Integrity and Durability of Reusable Space Propulsion Systems 1987 p 89-93 (For primary document see N87-22766 16-20)
Avail: NTIS HC A10/MF A01 CSCL 20K

A common method of treating the mean stress effect on fatigue life is to displace the elastic line on a Manson-Coffin-Basquin diagram while retaining the position of the plastic line. Manson and Halford pointed out that this procedure implies that mean stress significantly affects the cyclic stress-strain curve. Actually, however, they showed experimentally and by more general reasoning, that mean stress has little, if any, effect on the cyclic stress-strain curve. Thus, they concluded that it is necessary to displace the plastic line as well as the elastic line in order to keep the cyclic stress-strain curve unaltered. Another way to express the common displacement of the two lines is to keep the lines in place and change the horizontal coordinate to include a term relating to the displacement. Thus, instead of life, 2N sub f, as the horizontal coordinate, a new coordinate can become 2N sub f (1-sigma sub m/sigma sub f) superscript 1/b, thereby displacing both the elastic and plastic lines by an amount (1-sigma sub m/sigma sub f) superscript 1/b where sigma sub m is the mean stress and sigma sub f is the intercept of the elastic line at N sub f = 1/2 cycles and b is the slope of the elastic line.

N87-22779*# National Aeronautics and Space Administration. Lewis Research Center, Cleveland, Ohio.
NONLINEAR HEAT TRANSFER AND STRUCTURAL ANALYSES OF SSME TURBINE BLADES c39
A. Abdul-Aziz (Sverdrup Technology, Inc., Middleburg Heights, Ohio.) and A. Kaufman *In its* Structural Integrity and Durability of Reusable Space Propulsion Systems 1987 p 95-104 (For primary document see N87-22766 16-20)
Avail: NTIS HC A10/MF A01 CSCL 20K

Three-dimensional nonlinear finite-element heat transfer and structural analyses were performed for the first stage high-pressure fuel turbopump blade of the space shuttle main engine (SSME).

Directionally solidified (DS) MAR-M 246 material properties were considered for the analyses. Analytical conditions were based on a typical test stand engine cycle. Blade temperature and stress-strain histories were calculated using MARC finite-element computer code. The study was undertaken to assess the structural response of an SSME turbine blade and to gain greater understanding of blade damage mechanisms, convective cooling effects, and the thermal-mechanical effects. Author

N87-22780*# General Electric Co., Cincinnati, Ohio.

STRUCTURAL ANALYSIS DEMONSTRATION OF CONSTITUTIVE AND LIFE MODELS c39

G. Bechtel, T. S. Cook, M. T. Tipton, and R. L. McKnight *In* NASA. Lewis Research Center Structural Integrity and Durability of Reusable Space Propulsion Systems 1987 p 105-106 (For primary document see N87-22766 16-20)

Avail: NTIS HC A10/MF A01 CSCL 20K

The overall objective of this program is to demonstrate the applicability of NASA-developed advanced constitutive and life damage models for calculating cyclic structural response and crack initiation in selected components of reusable space propulsion systems. The computer model resulting from this program will enable the user to produce an accurate life prediction of hot gas path, life limiting components of propulsion systems such as the space shuttle main engine (SSME). Previously developed computer models addressing constitutive modeling and life damage will be combined in an advanced finite element analysis to generate a sophisticated baseline life prediction program. A material data base will be established for the constitutive and life models parametrically involving temperature, strain range, strain rate, mean strain/stress, and dwell time. The verified computer program will be used to accomplish the life predictions of three SSME critical components as evidence of the model functionality. Author

N87-22781*# Rockwell International Corp., Canoga Park, Calif.

MECHANICAL PROPERTIES OF HIGH GRADIENT AND HOT ISOSTATICALLY PRESSED PWA 1480 c26

L. G. Fritzemeier and G. D. Schnittgrund *In* NASA. Lewis Research Center Structural Integrity and Durability of Reusable Space Propulsion Systems 1987 p 107-108 (For primary document see N87-22766 16-20)

Avail: NTIS HC A10/MF A01 CSCL 11F

This program has been designed to evaluate the potential benefits to alloy 1480 material properties due to high thermal gradient casting, hot isostatic pressing, and alternative heat treatment. Alloy 1480 castings have been obtained from vendors representing the extremes of commercial casting thermal gradients. Quantitative characterization of the dendrite arm spacing (DAS) and pore distributions has been conducted. A hot isostatic pressing (HIP) schedule, which avoids the many pitfalls of single crystal HIP has been devised for alloy 1480. In addition, an alternate heat treatment for alloy 1480 has been devised which provides benefits in mechanical properties. The standard gradient cast test material is being evaluated in the standard heat treat condition as a baseline and in the HIP plus alternate heat treated condition. The fhigh gradient cast material is being evaluated in alternate heat treat and HIP plus alternate heat treated conditions. Evaluations focus on demonstration of the benefits due to the applied processes, especially in the area of cyclic life. Author

N87-22782*# Carnegie-Mellon Univ., Pittsburgh, Pa.

EFFECT OF HYDROGEN ON DEFORMATION STRUCTURE AND PROPERTIES OF CMSX-2 NICKEL-BASE SINGLE-CRYSTAL SUPERALLOY c26

M. Dollar, I. M. Bernstein, S. Walston, F. Prinz, and A. Domnanovich *In* NASA. Lewis Research Center Structural Integrity and Durability of Reusable Space Propulsion Systems 1987 p 109-115 (For primary document see N87-22766 16-20)

Avail: NTIS HC A10/MF A01 CSCL 11F

Material used in this study was a heat of the alloy CMSX-2. This nickel-based superalloy was provided in the form of oriented single crystals, solutionized for 3 hrs at 1315 C. It was then usually heat treated as follows: 1050 C/16h/air cool + 850 C/48h/air cool. The resulting microstructure is dominated by cuboidal, ordered gamma precipitates with a volume fraction of about 75% and an average size of 0.5 microns. In brief, the most compelling hydrogen induced-changes in deformation structure are: (1) enhanced dislocation accumulation in the gamma matrix; and (2) more extensive cross-slip of superdislocations in the gamma precipitates. The enhanced dislocation density in gamma acts to decrease the mean free path of a superdislocation, while easier cross slip hinders superdislocation movement by providing pinning points in the form of sessile jobs. Both processes contribute to the increase of flow stress and the notable work hardening that occurs prior to fracture. Author

N87-22783*# National Aeronautics and Space Administration. Lewis Research Center, Cleveland, Ohio.

PROBABILISTIC STRUCTURAL ANALYSIS TO EVALUATE THE STRUCTURAL DURABILITY OF SSME CRITICAL COMPONENTS

Christos C. Chamis *In its* Structural Integrity and Durability of Reusable Space Propulsion Systems 1987 p 117-119 (For primary document see N87-22766 16-20)

Avail: NTIS HC A10/MF A01 CSCL 21H

NASA Lewis Research Center is currently developing probabilistic structural analysis methods for select Space Shuttle Main Engine (SSME) structural components. Briefly, the deterministic, three-dimensional, inelastic analysis methodology developed under the Hot Section Technology (HOST) and R and T Base Programs is being augmented to accommodate the complex probabilistic loading spectra, the thermoviscoplastic material behavior, and the material degradation associated with the environment of space propulsion system structural components representative of the SSME such as turbine blades, transfer ducts, and liquid-oxygen posts. The development of probabilistic structural analysis methodology consists of the following program elements: (1) composite load spectra; (2) probabilistic structural analysis methods; (3) probabilistic finite element theory - new variational principles; and (4) probabilistic structural analysis application. In addition, the program includes deterministic analysis elements: (1) development of structural tailoring computer codes (SSME/STAEBL); (2) development of dynamic creep buckling/ratcheting theory; (3) evaluation of the dynamic characteristics of single-crystal SSME blades; (4) development of SSME blade damper technology; and (5) development of integrated boundary elements for hotfluid structure interaction. Author

N87-22784*# Southwest Research Inst., San Antonio, Tex.

PROBABILISTIC STRUCTURAL ANALYSIS METHODS (PSAM) FOR SELECT SPACE PROPULSION SYSTEM STRUCTURAL COMPONENTS

T. A. Cruse *In* NASA. Lewis Research Center Structural Integrity and Durability of Reusable Space Propulsion Systems 1987 p 121-125 (For primary document see N87-22766 16-20)

(Contract NAS3-24389)

Avail: NTIS HC A10/MF A01 CSCL 21H

The objective is the development of several modular structural analysis packages capable of predicting the probabilistic response distribution for key structural variables such as maximum stress, natural frequencies, transient response, etc. The structural analysis packages are to include stochastic modeling of loads, material properties, geometry (tolerances), and boundary conditions. The solution is to be in terms of the cumulative probability of exceedance distribution (CDF) and confidence bounds. Two methods of probability modeling are to be included as well as three types of structural models - probabilistic finite-element method (PFEM); probabilistic approximate analysis methods (PAAM); and probabilistic boundary element methods (PBEM). The purpose in doing probabilistic structural analysis is to provide the designer with a more realistic ability to assess the importance of uncertainty in the response of a high performance structure. Probabilistic Structural Analysis Method (PSAM) tools will estimate structural safety and reliability, while providing the engineer with information on the confidence that should be given to the predicted behavior. Perhaps most critically, the PSAM results will directly provide information on the sensitivity of the design response to those variables which are seen to be uncertain. Author

N87-22785*# MARC Analysis Research Corp., Palo Alto, Calif.
THE NESSUS FINITE ELEMENT CODE c39
J. B. Dias, J. C. Nagiegaal, and S. Nakazawa *In* NASA. Lewis Research Center Structural Integrity and Durability of Reusable Space Propulsion Systems 1987 p 127-131 (For primary document see N87-22766 16-20)
(Contract NAS3-24389)
Avail: NTIS HC A10/MF A01 CSCL 20K

The objective of this development is to provide a new analysis tool which integrates the structural modeling versatility of a modern finite element code with the latest advances in the area of probabilistic modeling and structural reliability. Version 2.0 of the NESSUS finite element code was released last February, and is currently being exercised on a set of problems which are representative of typical Space Shuttle Main Engine (SSME) applications. NESSUS 2.0 allows linear elastostatic and eigenvalue analysis of structures with uncertain geometry, material properties and boundary conditions, which are subjected to a random mechanical and thermal loading environment. The NESSUS finite element code is a key component in a broader software system consisting of five major modules. NESSUS/EXPERT is an expert system under development at Southwest Research Institute, with the objective of centralizing all component-specific knowledge useful for conducting probabilistic analysis of typical Space Shuttle Main Engine (SSME) components. NESSUS/FEM contains the finite element code used for the structural analysis and parameter sensitivity evaluation of these components. The task of parametrizing a finite element mesh in terms of the random variables present is facilitated with the use of the probabilistic data preprocessor in NESSUS/PRE. An external database file is used for managing the bulk of the data generated by NESSUS/FEM. Author

N87-22786*# Rockwell International Corp., Canoga Park, Calif. Rocketdyne Div.
PROBABILISTIC STRUCTURAL ANALYSIS VERIFICATION STUDIES c39
K. R. Rajagopal *In* NASA. Lewis Research Center Structural Integrity and Durability of Reusable Space Propulsion Systems 1987 p 133-137 (For primary document see N87-22766 16-20)
Avail: NTIS HC A10/MF A01 CSCL 20K

The basic objective of this verification effort is to apply probabilistic structural analysis methods developed and implemented in the Numerical Evaluation of Stochastic Structures Under Stress (NESSUS) code to typical space propulsion components. The chosen typical components are turbine blade, high pressure duct, Lox post, and transfer tube liners. Since analysis options of increasing levels of sophistication are implemented in NESSUS incrementally, the verification efforts are also tailored to have increasing levels of sophistication during the progression of the contract. The current released version of the code is limited to linear structural analysis. Author

N87-22787*# Southwest Research Inst., San Antonio, Tex.
NESSUS/EXPERT AND NESSUS/FPI IN THE PROBABILISTIC STRUCTURAL ANALYSIS METHODS (PSAM) PROGRAM c39
O. H. Burnside *In* NASA. Lewis Research Center Structural Integrity and Durability of Reusable Space Propulsion Systems 1987 p 139-143 (For primary document see N87-22766 16-20)
Avail: NTIS HC A10/MF A01 CSCL 20K

The Numerical Evaluation of Stochastic Structures under Stress (NESSUS) is the primary computer code being developed in the NASA Probabilistic Structural Analysis Methods (PSAM) project. It consists of four modules NESSUS/EXPERT, NESSUS/FPI, NESSUS/PRE and NESSUS/FEM. This presentation concentrates on EXPERT and FPI. To provide an effective interface between NESSUS and the user, an expert system module called NESSUS/EXPERT is being developed. That system uses the CLIPS artificial intelligence code developed to NASA-JSC. The code is compatible with FORTRAN, the standard language for codes in PSAM. The user interacts with the CLIPS inference engine, which is linked to the knowledge database. The perturbation database generated by NESSUS/FEM and managed in EXPERT is used to develop the so-called response or performance model in the random variables. Two independent probabilistic methods are available in PSAM for the computation of the probabilistic structural response. These are the Fast Probability Integration (FPI) method and Monte Carlo simulation. FPI is classified as an advanced reliability method and has been developed over the past ten years by researchers addressing the reliability of civil engineering structures. Monte Carlo is a well-established technique for computing probabilities by conducting a number of deterministic analyses with specified input distributional information. Author

N87-22788*# Arizona Univ., Tucson.
ADVANCED PROBABILISTIC METHOD OF DEVELOPMENT
P. H. Wirsching *In* NASA. Lewis Research Center Structural Integrity and Durability of Reusable Space Propulsion Systems 1987 p 145-149 (For primary document see N87-22766 16-20)
Avail: NTIS HC A10/MF A01 CSCL 21H

Advanced structural reliability methods are utilized on the Probabilistic Structural Analysis Methods (PSAM) project to provide a tool for analysis and design of space propulsion system hardware. The role of the effort at the University of Arizona is to provide reliability technology support to this project. PSAM computer programs will provide a design tool for analyzing uncertainty associated with thermal and mechanical loading, material behavior, geometry, and the analysis methods used. Specifically, reliability methods are employed to perform sensitivity analyses, to establish the distribution of a critical response variable (e.g., stress, deflection), to perform reliability assessment, and ultimately to produce a design which will minimize cost and/or weight. Uncertainties in the design factors of space propulsion hardware are described by probability models constructed using statistical analysis of data. Statistical methods are employed to produce a probability model, i.e., a statistical synthesis or summary of each design variable in a format suitable for reliability analysis and ultimately, design decisions. Author

N87-22789*# Georgia Inst. of Tech., Atlanta.
STOCHASTIC AND HYBRID-STRESS PLATE/SHELL FINITE ELEMENTS FOR HOT-SECTION COMPONENTS c39
S. N. Atluri *In* NASA. Lewis Research Center Structural Integrity and Durability of Reusable Space Propulsion Systems 1987 p 151-152 (For primary document see N87-22766 16-20)
Avail: NTIS HC A10/MF A01 CSCL 20K

The research effort in the Center for the Advancement of Computational Mechanics at Georgia Tech has two main thrusts. The first of these is the development of special approaches for the numerical stress analysis of solids and structures whose material and geometric properties are uncertain. The second seeks to develop and implement high-efficiency plate and shell elements. The stochastic element method, currently being implemented, will be able to more accurately portray the probabilistic nature of stress, strain, and displacement in actual structures. Current research has provided a hybrid-stress shell element whose behavior is acceptable for aspect ratios as high as 30 to 1. Thus, substantially more complex analyses will be practicable as soon as this element is fully implemented. An additional advantage of the hybrid approach is that it permits more accurate stress-recovery at the upper and lower surfaces of the shell, an important consideration in high thickness-gradient applications. The software associated with the above research is being implemented in the form of extensions to the Nessus code. The hybrid shell element has been successfully tested in several small-deformation elastic analyses. The theoretical formulation of the stochastic elements is essentially complete; its implementation is just beginning. Author

N87-22790*# Northwestern Univ., Evanston, Ill.
PROBABILISTIC FINITE ELEMENTS c39
Ted Belytschko and Kam Liu Wing *In* NASA. Lewis Research Center Structural Integrity and Durability of Reusable Space

Propulsion Systems 1987 p 153-159 (For primary document see N87-22766 16-20)
(Grant NAG3-535)
Avail: NTIS HC A10/MF A01 CSCL 20K

In the Probabilistic Finite Element Method (PFEM), finite element methods have been efficiently combined with second-order perturbation techniques to provide an effective method for informing the designer of the range of response which is likely in a given problem. The designer must provide as input the statistical character of the input variables, such as yield strength, load magnitude, and Young's modulus, by specifying their mean values and their variances. The output then consists of the mean response and the variance in the response. Thus the designer is given a much broader picture of the predicted performance than with simply a single response curve. These methods are applicable to a wide class of problems, provided that the scale of randomness is not too large and the probabilistic density functions possess decaying tails. By incorporating the computational techniques we have developed in the past 3 years for efficiency, the probabilistic finite element methods are capable of handling large systems with many sources of uncertainties. Sample results for an elastic-plastic ten-bar structure and an elastic-plastic plane continuum with a circular hole subject to cyclic loadings with the yield stress on the random field are given. Author

N87-22791*# Sverdrup Technology, Inc., Cleveland, Ohio.
PROBABILISTIC SSME BLADES STRUCTURAL RESPONSE UNDER RANDOM PULSE LOADING
Michael Shiao, Robert Rubinstein, and Vinod K. Nagpal *In* NASA. Lewis Research Center Structural Integrity and Durability of Reusable Space Propulsion Systems 1987 p 161-166 (For primary document see N87-22766 16-20)
Avail: NTIS HC A10/MF A01 CSCL 21H

The purpose is to develop models of random impacts on a Space Shuttle Main Engine (SSME) turbopump blade and to predict the probabilistic structural response of the blade to these impacts. The random loading is caused by the impact of debris. The probabilistic structural response is characterized by distribution functions for stress and displacements as functions of the loading parameters which determine the random pulse model. These parameters include pulse arrival, amplitude, and location. The analysis can be extended to predict level crossing rates. This requires knowledge of the joint distribution of the response and its derivative. The model of random impacts chosen allows the pulse arrivals, pulse amplitudes, and pulse locations to be random. Specifically, the pulse arrivals are assumed to be governed by a Poisson process, which is characterized by a mean arrival rate. The pulse intensity is modelled as a normally distributed random variable with a zero mean chosen independently at each arrival. The standard deviation of the distribution is a measure of pulse intensity. Several different models were used for the pulse locations. For example, three points near the blade tip were chosen at which pulses were allowed to arrive with equal probability. Again, the locations were chosen independently at each arrival. The structural response was analyzed both by direct Monte Carlo simulation and by a semi-analytical method. Author

N87-22792*# Sverdrup Technology, Inc., Cleveland, Ohio.
QUANTIFYING UNCERTAINTIES IN THE STRUCTURAL RESPONSE OF SSME BLADES
Vinod K. Nagpal *In* NASA. Lewis Research Center Structural Integrity and Durability of Reusable Space Propulsion Systems 1987 p 167-173 (For primary document see N87-22766 16-20)
Avail: NTIS HC A10/MF A01 CSCL 21H

To quantify the uncertainties associated with the geometry and material properties of a Space Shuttle Main Engine (SSME) turbopump blade, a computer code known as STAEBL was used. A finite element model of the blade used 80 triangular shell elements with 55 nodes and five degrees of freedom per node. The whole study was simulated on the computer and no real experiments were conducted. The structural response has been evaluated in terms of three variables which are natural frequencies, root (maximum) stress, and blade tip displacements. The results of the study indicate that only the geometric uncertainties have significant effects on the response. Uncertainties in material properties have insignificant effects. Author

N87-22793*# Rockwell International Corp., Canoga Park, Calif. Rocketdyne Div.
COMPOSITE LOAD SPECTRA FOR SELECT SPACE PROPULSION STRUCTURAL COMPONENTS
J. F. Newell *In* NASA. Lewis Research Center Structural Integrity and Durability of Reusable Space Propulsion Systems 1987 p 175-187 (For primary document see N87-22766 16-20)
(Contract NAS3-24382)
Avail: NTIS HC A10/MF A01 CSCL 21H

The objective of this program is to develop generic load models to simulate the composite load spectra (CLS) that are induced in space propulsion system components representative of the space shuttle main engines (SSME). These models are being developed through describing individual component loads with an appropriate mix of deterministic and state-of-the-art probabilistic models that are related to key generic variables. Combinations of the individual loads are used to synthesize the composite loads spectra. A second approach for developing the composite loads spectra load model simulation, the option portion of the contract will develop coupled models which combine the individual load models. Statistically varying coefficients of the physical models will be used to obtain the composite load spectra. Author

N87-22794*# Battelle Columbus Labs., Ohio.
PROBABILISTIC LOAD MODEL DEVELOPMENT AND VALIDATION FOR COMPOSITE LOAD SPECTRA FOR SELECT SPACE PROPULSION ENGINES
R. Kurth and J. F. Newell (Rockwell International Corp., Canoga Park, Calif.) *In* NASA. Lewis Research Center Structural Integrity and Durability of Reusable Space Propulsion Systems 1987 p 189-199 (For primary document see N87-22766 16-20)
Avail: NTIS HC A10/MF A01 CSCL 21H

A major task of the program to develop an expert system to predict the loads on selected components of a generic space propulsion engine is the design development and application of a probabililic loads model. This model is being developed in order to account for the random nature of the loads and assess the variable load ranges' effect on the engine performance. A probabilistic model has been developed. The model is based primarily on simulation methods, but also has a Gaussian algebra method (if all variables are near normal), a fast probability integrator routine (for the calculation of low probability events), and a separate, stand alone program for performing barrier crossing calculations. Each of these probabilistic methods has been verified with theoretical calculations using assumed distributional forms. Author

N87-22795*# National Aeronautics and Space Administration. Lewis Research Center, Cleveland, Ohio.
STRUCTURAL TAILORING USING THE SSME/STAEBL CODE
Robert Rubinstein *In its* Structural Integrity and Durability of Reusable Space Propulsion Systems 1987 p 201-205 (For primary document see N87-22766 16-20)
Avail: NTIS HC A10/MF A01 CSCL 21H

Space Shuttle Main Engine/Structural Tailoring of Engine Blades (SSME/STAEBL) was developed by systematically modifying and enhancing the STAEBL code developed by Pratt and Whitney under contract to NASA Lewis Research Center. STAEBL was designed for application to gas turbine blade design. Typical design variables include blade thickness distribution and root chord. Typical constraints include resonance margins, root stress, and root to chord ratios. In this program, the blade is loaded by centrifugal forces only. Additions and modifications of STAEBL included in SSME/STAEBL include (1) thermal stress analysis; (2) gas dynamic (pressure) loads; (3) temperature dependent material and thermal properties; (4) forced vibrations; (5) tip displacement constraints; (6) single crystal material analysis; (7) blade cross section stacking offsets; and (8) direct time integration algorithm for transient dynamic response. Capabilities are also included which permit data transfer from finite element models and stand-alone analysis.

N87-22796*# Georgia Inst. of Tech., Atlanta.
NONISOTHERMAL ELASTO-VISCO-PLASTIC RESPONSE OF SHELL-TYPE STRUCTURES c39
G. J. Simitses, R. L. Carlson, and R. Riff *In* NASA. Lewis Research Center Structural Integrity and Durability of Reusable Space Propulsion Systems 1987 p 207-214 (For primary document see N87-22766 16-20)
(Grant NAG3-534)
Avail: NTIS HC A10/MF A01 CSCL 20K

A mathematical model and solution methodologies for analyzing structural response of thin, metallic shell-type structures under large transient, cyclic or static thermomechanical loads is disussed. Among the system responses, which are associated with these load conditions, are thermal buckling and creep buckling. Thus, geometric as well as material-type nonlinearities (of high order) can be anticipated and have been considered in the development of the mathematical model. Furthermore, this was accommodated in the solution procedures. A complete true ab-inito rate theory of kinematics and kinetics for continuum and curved thin structures, without any restriction on the magnitude of the strains or the deformation, was formulated. The time dependence and large strain behavior are incorporated through the introduction of the time rates of the metric and curvature in two coordinate systems, a fixed (spatial) one and a convected (material) coordinate system. The relations between the time derivative and the covariant derivatives (gradients) have been developed for curved space and motion, so that the velocity components supply the connection between the equations of motion and the time rate of change of the metric and curvature tensors. Author

N87-22797*# Sverdrup Technology, Inc., Middleburg Heights, Ohio.
DYNAMIC CHARACTERISTICS OF SINGLE CRYSTAL SSME BLADES c39
L. A. Moss and T. E. Smith *In* NASA. Lewis Research Center Structural Integrity and Durability of Reusable Space Propulsion Systems 1987 p 211-214 (For primary document see N87-22766 16-20)
Avail: NTIS HC A10/MF A01 CSCL 20K

The Space Shuttle Main Engine (SSME) High Pressure Fuel Turbopump (HPFTP) blades are currently manufactured using a directionally solidified (DS) material, MAR-M-246+Hf. However, a necessity to reduce the occurrence of fatigue cracking within the DS blades has lead to an interest in the use of a single crystal (SC) material, PWA-1480. A study was initiated to determine the dynamic characteristics of the HPFTP blades made of SC material and find possible critical engine order excitations. This study examined both the first and second stage drive turbine blades of the HPFTP. The dynamic characterization was done analytically as well as experimentally. The analytical study examined the SC first stage HPFTP blade dynamic characteristics under typical operating conditions. The blades were analyzed using MSC/NASTRAN and a finite element model. Two operating conditions, 27500 RPM and 35000 RPM, were investigated. Author

N87-22798*# National Aeronautics and Space Administration. Lewis Research Center, Cleveland, Ohio.
SSME BLADE DAMPER TECHNOLOGY
Robert E. Kielb and Jerry H. Griffin (Carnegie-Mellon Univ., Pittsburgh, Pa.) *In its* Structural Integrity and Durability of Reusable Space Propulsion Systems 1987 p 215-217 (For primary document see N87-22766 16-20)
Avail: NTIS HC A10/MF A01 CSCL 21H

Before 1975 turbine blade damper designs were based on experience and very simple mathematical models. Failure of the dampers to perform as expected showed the need to gain a better understanding of the physical mechanism of friction dampers. Over the last 10 years research on friction dampers for aeronautical propulsion systems has resulted in methods to optimize damper designs. The first-stage turbine blades on the Space Shuttle Main Engine (SSME) high-pressure oxygen pump have experienced cracking problems due to excessive vibration. A solution is to incorporate a well-designed friction dampers to attenuate blade vibration. The subject study, a cooperative effort between NASA Lewis and Carnegie-Mellon University, represents an application of recently developed friction damper technology to the SSME high-pressure oxygen turbopump. The major emphasis was the contractor's design known as the two-piece damper. Damping occurs at the frictional interface between the top half of the damper and the underside of the platforms of the adjacent blades. The lower half of the damper is an air seal to retard airflow in the volume between blade necks. Author

N87-22799*# State Univ. of New York, Buffalo.
DEVELOPMENT OF AN INTEGRATED BEM (BOUNDARY ELEMENT MESH) FOR HOT FLUID-STRUCTURE INTERACTION
G. F. Dargush and P. K. Banerjee *In* NASA. Lewis Research Center Structural Integrity and Durability of Reusable Space Propulsion Systems 1987 p 219-222 (For primary document see N87-22766 16-20)
Avail: NTIS HC A10/MF A01 CSCL 21H

A boundary integral representation for a coupled approach to fluid flow and solid deformation problems associated with the design of hot-section components such as those in the Space Shuttle Main Engine is discussed. The formulation is based on the fundamental analytical solution of the Navier-Stokes equation for fluid velocity in an infinite domain. This fundamental solution was obtained by decomposing a Navier-Stokes equation into vorticity and dilation transport equations. A boundary integral involving convolutions in time was then constructed in which the convective terms appear in the volume integral. R.J.F.

N87-22800# Air Force Systems Command, Wright-Patterson AFB, Ohio. Foreign Technology Div.
JOURNAL OF CHINESE SOCIETY OF ASTRONAUTICS (SELECTED ARTICLES)
Xianqi Chang, Weng-An Xu, and Shi-Xue Yang 6 Apr. 1987 87 p Transl. into ENGLISH from Yuhang Xuebao (China), no. 1, Jan. 1987 p 11-23
(AD-A179690; FTD-ID(RS)T-0432-86) Avail: NTIS HC A05/MF A01 CSCL 21H

A numerical solution of the basic equation for one dimensional two-phase nonequilibrium flow in a combustion chamber of solid propellant rocket motors is discussed, the effect of particle size on the flow field in a combustion chamber and pressure-time curves is analyzed, and some useful conclusions are obtained in comparing results of one dimensional two-phase constant lag flow in a combustion chamber. It is useful for predicting pressure-time curves accurately and providing accurate boundary conditions for the calculation of two-phase flow through the nozzle. GRA

N87-22801# Air Force Inst. of Tech., Wright-Patterson AFB, Ohio. School of Engineering.
INVESTIGATION OF ROCKET POWERED, OPEN CYCLE, MAGNETOHYDRODYNAMIC GENERATORS FOR HIGH, PULSED POWER NEEDS IN SPACE M.S. Thesis
John W. Power Nov. 1986 71 p
(AD-A178869; AFIT/GSO/ENP/86D-1) Avail: NTIS HC A04/MF A01 CSCL 10B

This investigation examined the possibility of using a rocket powered magnetohydrodynamic generator for pulse power in space of 300 megawatts (MW). The result is a preliminary design of an MHD generator using an open cycle disk channel and a single superconducting solenoid coil. The disk channel acts as a thrust deflector, and internal vanes counteract induced vorticity. The use of a solid fuel wafer grain design rocket motor is proposed for increased electrical conductivity and pulse operation of the generator. Using conservative parameters, a generator design capable of being carried on one or two space shuttle launches is developed with estimated mass of 24,450kg and estimated power output of 1346MW. The nominal operation time before refurbishment is 115 seconds; the restriction operation time is deterioration of the channel throat. This design exceeds present nuclear and solar cell power systems in power output per unit mass. GRA

N87-22802*# National Aeronautics and Space Administration. Lewis Research Center, Cleveland, Ohio.

IMPACT OF THERMAL ENERGY STORAGE PROPERTIES ON SOLAR DYNAMIC SPACE POWER CONVERSION SYSTEM MASS

Albert J. Juhasz, Carolyn E. Coles-Hamilton, and Dovie E. Lacy 1987 10 p Prepared for presentation at the 22nd Intersociety Energy Conversion Engineering Conference, Philadelphia, Pa., 10-14 Aug. 1987; cosponsored by AIAA, ANS, AMSE, SAE, IEEE, ACS, and AIChE
(NASA-TM-89909; E-3601; NAS 1.15:89909; AIAA-87-9442) Avail: NTIS HC A02/MF A01 CSCL 10C

A 16 parameter solar concentrator/heat receiver mass model is used in conjunction with Stirling and Brayton Power Conversion System (PCS) performance and mass computer codes to determine the effect of thermal energy storage (TES) material property changes on overall PCS mass as a function of steady state electrical power output. Included in the PCS mass model are component masses as a function of thermal power for: concentrator, heat receiver, heat exchangers (source unless integral with heat receiver, heat sink, regenerator), heat engine units with optional parallel redundancy, power conditioning and control (PC and C), PC and C radiator, main radiator, and structure. Critical TES properties are: melting temperature, heat of fusion, density of the liquid phase, and the ratio of solid-to-liquid density. Preliminary results indicate that even though overalll system efficiency increases with TES melting temperature up to 1400 K for concentrator surface accuracies of 1 mrad or better, reductions in the overall system mass beyond that achievable with lithium fluoride (LiF) can be accomplished only if the heat of fusion is at least 800 kJ/kg and the liquid density is comparable to that of LiF (1880 kg/cu m. Author

N87-22803*# Pratt and Whitney Aircraft, West Palm Beach, Fla. Government Products Div.

HIGH HEAT TRANSFER OXIDIZER HEAT EXCHANGER DESIGN AND ANALYSIS Final Report, Jan. 1985 - Oct. 1986

Thomas D. Kmiec, Paul G. Kanic, and Richard J. Peckham May 1987 80 p
(Contract NAS3-24738)
(NASA-CR-179596; NAS 1.26:179596; FR-19289-2) Avail: NTIS HC A05/MF A01 CSCL 21H

The RL10-2B engine, a derivative of the RL10, is capable of multimode thrust operation. This engine operates at two low thrust levels: tank head idle (THI), which is approximately 1 to 2% of full thrust, and pumped idle (PI), which is 10% of full thrust. Operation at THI provides vehicle propellant settling thrust and efficient engine thermal conditioning; PI operation provides vehicle tank pre-pressurization and maneuver thrust for low-g deployment. Stable combustion of the RL10-2B engine during the low thrust operating modes can be accomplished by using a heat exchanger to supply gaseous oxygen to the propellant injector. The oxidizer heat exchanger (OHE) vaporizes the liquid oxygen using hydrogen as the energy source. The design, concept verification testing and analysis for such a heat exchanger is discussed. The design presented uses a high efficiency compact core to vaporize the oxygen, and in the self-contained unit, attenuates any pressure and flow oscillations which result from unstable boiling in the core. This approach is referred to as the high heat transfer design. An alternative approach which prevents unstable boiling of the oxygen by limiting the heat transfer is referred to as the low heat transfer design and is reported in Pratt & Whitney report FR-19135-2. Author

N87-22804*# National Aeronautics and Space Administration. Lewis Research Center, Cleveland, Ohio.

LOW POWER DC ARCJET OPERATION WITH HYDROGEN/NITROGEN/AMMONIA MIXTURES

Terry L. Hardy and Francis M. Curran Jul. 1987 25 p Prepared for presentation at the 23rd Joint Propulsion Conference, San Diego, Calif., 29 Jun. - 2 Jul. 1987; cosponsored by AIAA, SAE, ASME, and ASEE
(NASA-TM-89876; E-3553; NAS 1.15:89876; AIAA-87-1948) Avail: NTIS HC A02/MF A01 CSCL 21C

The effect of gas composition and ambient pressure on arcjet operation was determined. Arcjet operation in different facilities was also compared to determine the validity of tests in small facilities. Volt-ampere characteristics were determined for an arcjet using hydrogen/nitrogen mixtures (simulating both ammonia and hydrazine), hydrogen/nitrogen/ammonia mixtures, and pure ammonia as propellants at various flow rates. The arcjet had a typical performance of 450 sec specific impulse at 1 kW with hydrogen/nitrogen mixures. It was determined that the amount of ammonia present in the gas stream had a significant effect on the arcjet volt-ampere characteristics. Also, hydrogen/nitrogen mixtures simulating ammonia gave arc characteristics approximately the same as those of pure ammonia. Finally, no differences in arc volt-ampere characteristics were seen between low and high ambient pressure operation in the same facility. A 3 to 5 V difference was seen when different facilities were compared, but this difference was probably due to differences in the voltage drops across the current connections, and not due to arcjet operational differences in the two facilities. Author

N87-22805*# National Aeronautics and Space Administration. Lewis Research Center, Cleveland, Ohio.

ELECTROMAGNETIC EMISSION EXPERIENCES USING ELECTRIC PROPULSION SYSTEMS: A SURVEY

James S. Sovey, Lynnette M. Zana, and Steven C. Knowles (Rocket Research Corp., Redmond, Wash.) 1987 37 p Presented at the 23rd Joint Propulsion Conference, San Diego, Calif., 29 Jun. - 2 Jul. 1987; sponsored by AIAA, SAE, ASME and ASEE
(NASA-TM-100120; E-3618; NAS 1.15:100120; AIAA-87-2028) Avail: NTIS HC A03/MF A01 CSCL 21C

As electric propulsion systems become ready to integrate with spacecraft systems, the impact of propulsion system radiated emissions are of significant interest. Radiated emissions from electromagnetic, electrostatic, and electrothermal systems have been characterized and results synopsized from the literature describing 21 space flight programs. Electromagnetic radiated emission results from ground tests and flight experiences are presented with particular attention paid to the performance of spacecraft subsystems and payloads during thruster operations. The impacts to transmission of radio frequency signals through plasma plumes are also reviewed. Author

N87-22806*# National Aeronautics and Space Administration. Lewis Research Center, Cleveland, Ohio.

AN EVALUATION OF METALLIZED PROPELLANTS BASED ON VEHICLE PERFORMANCE

Robert L. Zurawski and James M. Green (Sverdrup Technology, Inc., Cleveland, Ohio.) 1987 27 p Presented at the 23rd Joint Propulsion Conference, San Diego, Calif., 29 Jun. - 2 Jul. 1987; sponsored by AIAA, SAE, ASME and ASEE
(NASA-TM-100104; E-3639; NAS 1.15:100104; AIAA-87-1773) Avail: NTIS HC A03/MF A01 CSCL 21H

An analytical study was conducted to determine the improvements in vehicle performance possible by burning metals with conventional liquid bipropellants. These metallized propellants theoretically offer higher specific impulse, increased propellant density and improved vehicle performance compared with conventional liquid bipropellants. Metals considered were beryllium, lithium, aluminum and iron. Liquid bipropellants were H2/O2, N2H4/N2O4, RP-1/O2 and H2/F2. A mission with a delta V = 4267.2 m/sec (14,000 ft/sec) and vehicle with propellant volume fixed at 56.63 cu m (2000 cu ft) and dry mass fixed at 2761.6 kg (6000 lb) was used, roughly representing the transfer of a chemically propelled upper-stage vehicle from a low-Earth orbit to a geosynchronous orbit. The results of thermochemical calculations and mission analysis calculations for bipropellants metallized with beryllium, lithium, aluminum and iron are presented. Technology issues pertinent to metallized propellants are discussed. Author

N87-22807*# National Aeronautics and Space Administration. Lewis Research Center, Cleveland, Ohio.
LANGMUIR PROBE SURVEYS OF AN ARCJET EXHAUST
Lynnette M. Zana 1987 30 p Presented at the 23rd Joint Propulsion Conference, San Diego, Calif., 29 Jun. - 2 Jul. 1987; sponsored by AIAA, SAE, ASME and ASEE
(NASA-TM-89924; E-3623; NAS 1.15:89924; AIAA-87-1950) Avail: NTIS HC A03/MF A01 CSCL 21C

Electrostatic (Langmuir) probes of both spherical and cylindrical geometry have been used to obtain electron number density and temperature in the exhaust of a laboratory arcjet. The arcjet thruster operated on nitrogen and hydrogen mixtures to simulate fully decomposed hydrazine in a vacuum environment with background pressures less than 0.05 Pa. The exhaust appears to be only slightly ionized (less than 1 percent) with local plasma potentials near facility ground. The current-voltage characteristics of the probes indicate a Maxwellian temperature distribution. Plume data are presented as a function of arcjet operating conditions and also position in the exhaust. Author

23 CHEMISTRY AND MATERIALS (GENERAL)

No abstracts in this category.

24 COMPOSITE MATERIALS

Includes physical, chemical, and mechanical properties of laminates and other composite materials.

For ceramic materials see *27 Nonmetallic Materials*.

N87-22808# National Research Council of Canada, Ottawa (Ontario). Div. of Mechanical Engineering.
ARTIFICIAL COMPOSITES FOR HIGH TEMPERATURE APPLICATIONS: A REVIEW
M. U. Islam, W. Wallace, and A. Y. Kandeil (Qatar Univ., Doha.) Jan. 1987 84 p
(DME-007; NRC-27323) Avail: NTIS HC A05/MF A01

A review is provided of developments in artificial, metal and ceramic matrix composites with potential for high temperature applications such as in the hot sections of gas turbine engines. Emphasis is placed on developments which have occurred since 1975. An attempt is made to assess the current level of activity and to identify outstanding problems and research directions for the future. To provide a basis for these discussions, the status prior to 1975 is also briefly reviewed. Author

N87-22809# Air Force Inst. of Tech., Wright-Patterson AFB, Ohio. School of Engineering.
THERMAL SHOCK RESISTANCE OF MULLITE-BASED SIC-WHISKER COMPOSITES M.S. Thesis
William H. Kelley, II Dec. 1986 114 p
(AD-A179214; AFIT/GAE/AA/86D-6) Avail: NTIS HC A06/MF A01 CSCL 11D

The influence of the addition of silicon carbide (SiC) whiskers and zirconia on the material properties and constants of pure mullite was examined. SiC whisker weight percentages of 0, 10, 20, and 30 were examined, and a zirconia content of 36.1 wt.% was studied. A theoretical approach similar to Hasselman's high-E, low-E theory was used to determine the theoretical values of the material properties which were then compared to experimental results. Using experimental and theoretical values for Young's modulus of elasticity, bend strength, mean coefficient of thermal expansion, thermal diffusivity, and Poisson's ratio, the thermal stress resistance parameters were calculated, and compared to experimental results for critical quench temperatures. Microstructures were characterized by X-ray diffraction (XRD) analysis, chemical analysis, density determinations, light microscopy (LM), and scanning electron microscopy (SEM). The mullite was alumina-rich with particles of silica present. Whisker composites contained 2H, 4H, and 15R polytypes of SiC and impurities from the whisker. GRA

N87-22810# Naval Air Development Center, Warminster, Pa. Aircraft and Crew Systems Technology Directorate.
CHARACTERIZATION OF HYBRIDIZED CONDUCTIVE COMPOSITES Final Report, Feb. 1985 - Feb. 1986
J. J. Reilly, S. J. Thoman, and W. W. Lin 25 Jul. 1986 47 p
(AD-A179689; NADC-86047-60) Avail: NTIS HC A03/MF A01 CSCL 11I

Injection moldable thermoplastics filled with various hybrid conductive reinforcements have been investigated for their physical/mechanical properties. The thermoplastics studied include polyphenylene sulfide (PPS), polyether etherketone (PEEK) and liquid crystal polymers (LCP's). The reinforcements included various combinations and concentrations of graphite (Gr) fibers, stainless steel (SS) fibers, nickel flakes(NiFlk) and nickel plated graphite (NiGr) fibers. Tensile, flexural, and drop weight impact tests were performed. Fracture morphology of tensile specimens was investigated using scanning electron microscopy (SEM). The distribution of fibers and flakes was observed using photomicroscopy. Electromagnetic interference (EMI) shielding effectiveness was determined in the range of 15 MHz to 1 GHz. Water absorption, density and electrical resistivity properties were also determined. Differential scanning calorimetry (DSC) was used to determine thermal properties. Four PPS composites provided at least 80 db of shielding at 80, 100, 150, 200 and 300 MHz respectively. The lowest electrical resisitivity value measured was 0.60 ohm-cm for PPS/30%NiGr/10%SS. Optical microscopy revealed that PEEK Composites with similar loadings to that of PPS composites had lower void contents. Reinforced PEEK performed better mechanically than PPS composites. Composite densities range from 1.98g cc for PPS/30%NiGr/20%NiFlk to 1.47/cm3 for LCP300/30%Gr. GRA

N87-22811*# National Aeronautics and Space Administration. Lewis Research Center, Cleveland, Ohio.
FIBER REINFORCED SUPERALLOYS
Donald W. Petrasek, Robert A. Signorelli, Thomas Caulfield, and John K. Tien (Columbia Univ., New York.) Apr. 1987 62 p
(NASA-TM-89865; E-3533; NAS 1.15:89865) Avail: NTIS HC A04/MF A01 CSCL 11D

Improved performance of heat engines is largely dependent upon maximum cycle temperatures. Tungsten fiber reinforced superalloys (TFRS) are the first of a family of high temperature composites that offer the potential for significantly raising hot component operating temperatures and thus leading to improved heat engine performance. This status review of TFRS research emphasizes the promising property data developed to date, the status of TFRS composite airfoil fabrication technology, and the areas requiring more attention to assure their applicability to hot section components of aircraft gas turbine engines. Author

N87-22812# Oak Ridge National Lab., Tenn.
THERMAL EXPANSION OF EPOXY-FIBERGLASS COMPOSITE SPECIMENS
D. L. McElroy, F. J. Weaver, and C. Bridgman 1986 30 p Presented at the 9th International Thermal Expansion Symposium, Pittsburgh, Pa., 8 Dec. 1986 Prepared in cooperation with Grumman Corp., Bethpage, N.Y.
(Contract DE-AC05-84OR-21400)
(DE87-004273; CONF-861258-1) Avail: NTIS HC A03/MF A01

The thermal expansion behavior of three epoxy-fiberglass composite specimens was measured from 20 to 120°C (70 to 250°F) using a fused quartz push-rod dilatometer. Billets produced by vacuum impregnating layers of two types of fiberglass cloth with an epoxy resin were core-drilled to produce cylindrical specimens. These were used to study expansion perpendicular and parallel to the fiberglass layers. The dilatometer is held at a preselected temperature until steady-state is indicated by stable length and temperature data. Before testing the composite specimens, a reliability check of the dilatometer was performed using a copper secondary standard. This indicated thermal expansion coefficient values within + or -2% of expected values from 20 to 200°C. DOE

N87-22813# Air Force Inst. of Tech., Wright-Patterson AFB, Ohio. School of Engineering.
EFFECTS OF CUTOUT ORIENTATIONS ON NATURAL FREQUENCIES AND MODE SHAPES OF CURVED RECTANGULAR COMPOSITE PANELS M.S. Thesis
Garry J. Cyr Dec. 1986 144 p
(AD-A178638; AFIT/GAE/AA/86D-3) Avail: NTIS HC A07/MF A01 CSCL 11D

STAGSC-1, a finite element code, and holographic interferometry were used to analyze the effects of cutout orientation (O, +45, -45 and 90) on the first five natural frequencies and mode shapes of a curved Gr-Ep panel. The clamped-clamped panels had a quasi-isotropic layup 0, -45, 45, 90s and measured 12 inch high with a 12 inch chord. When the finite element code was compared to the time averaged holograms, the two techniques showed close correlation of both the natural frequencies and mode shapes. It was found that the 0 cutout orientation had a significant effect on the panel stiffness while the other cutout orientations did not adversely affect the stiffness. It was also found that if a large number of elements in the finite element mesh are oriented at an angle other than 0 or 90, then the STAGSC-1 model is artificially stiffened. The phenomenon of mode switching was investigated analytically and determined to be a function of the cutout dimensions. GRA

N87-22814# MSNW, Inc., San Marcos, Calif.
PLASMA JOINING OF METAL MATRIX COMPOSITES Interim Technical Report, Jun. - Jul. 1986
G. H. Reynolds and L. Yang Dec. 1986 13 p
(Contract DAAG29-85-C-0027)
(AD-A178731; ARO-22817.4-MS-S) Avail: NTIS HC A02/MF A01 CSCL 11D

This report describes microstructural and microchemical characterization of low pressure, transferred arc plasma deposits produced on inert substrates using precomposited powder feed (i.e., filler) materials. Also described in the most recent report were the microchemical differences observed between as-produced precomposited powders and those which had been plasma processed and allowed to solidify in free flight. The plasma deposited composite powders described herein impinged on an inert, stainless steel substrate backed by a water-cooled copper chill block to prevent substrate softening and melting. Three types of precomposited powders were used as feed material. These were 1100 aluminum - 30 wt.% silicon carbide powders, aluminum - 5 wt.% Ti - 30 wt.% 30 wt.% silicon carbide powders and aluminum - 3 wt.% Zr - 30 wt.% silicon carbides powders. GRA

N87-22815# Naval Weapons Center, China Lake, Calif.
HYBRID COMPOSITE RESPONSE TO HYDRAULIC RAM Interim Technical Report, Sep. 1985 - Sep. 1986
Todd Anderson, Jamie Childress, and Scott Lang 20 Oct. 1986 52 p Prepared in cooperation with Joint Technical Coordinating Group for Aircraft Survivability, Washington, D.C.
(AD-A178750; JTCG/AS-86-T-001) Avail: NTIS HC A04/MF A01 CSCL 11D

Hydraulic ram is a major damage mechanism in fuel tanks that are impacted by projectiles. Composite materials have proved vulnerable to hydraulic ram in ballistic testing. Hybridizing graphite/epoxy structures with materials such as fiberglass, nylon, or Kevlar shows promise far reducing the vulnerability of composite structures to hydraulic ram. This report presents the results of ballistic testing of small test panels, hybridized with several materials in several different configurations. Many configurations and materials provide significant improvement over baseline graphite panels and are recommended for further testing. GRA

25 INORGANIC AND PHYSICAL CHEMISTRY

Includes chemical analysis, e.g., chromatography; combustion theory; electrochemistry; and photochemistry.

For related information see also *77 Thermodynamics and Statistical Physics.*.

N87-22816# Department of Health, Education, and Welfare, Washington, D.C. Dept. of Health and Human Services.
CROSS-AXIS SYNCHRONOUS FLOW-THROUGH COIL PLANET CENTRIFUGE FREE OF ROTARY SEALS: APPARATUS AND METHOD FOR PERFORMING COUNTERCURRENT CHROMATOGRAPHY Patent Application
Y. Ito, inventor (to HEW) 3 Oct. 1986 26 p
(PB87-126926; PAT-APPL-6-915797) Avail: NTIS HC A03/MF A01 CSCL 07D

A method and apparatus is described for countercurrent chromatography which efficiently mixes solvent phases, avoids the use of rotary seals, and produces a highly asymmetrical force distribution pattern along the X sub b axis and a symmetrical force distribution along the Z sub b axis. GRA

N87-22817*# Southwest Research Inst., San Antonio, Tex.
FAST ION MASS SPECTROMETRY AND CHARGED PARTICLE SPECTROGRAPHY INVESTIGATIONS OF TRANSVERSE ION ACCELERATION AND BEAM-PLASMA INTERACTIONS Final Report
W. C. Gibson, W. M. Tomlinson, and J. A. Marshall Jan. 1987 104 p
(Contract NAS5-27430; SwRI Proj. 15-7435)
(NASA-CR-168348; NAS 1.26:168348) Avail: NTIS HC A06/MF A01 CSCL 07D

Ion acceleration transverse to the magnetic field in the topside ionosphere was investigated. Transverse acceleration is believed to be responsible for the upward-moving conical ion distributions commonly observed along auroral field lines at altitudes from several hundred to several thousand kilometers. Of primary concern in this investigation is the extent of these conic events in space and time. Theoretical predictions indicate very rapid initial heating rates, depending on the ion species. These same theories predict that the events will occur within a narrow vertical region of only a few hundred kilometers. Thus an instrument with very high spatial and temporal resolution was required; further, since different heating rates were predicted for different ions, it was necessary to obtain composition as well as velocity space distributions. The fast ion mass spectrometer (FIMS) was designed to meet these criteria. This instrument and its operation is discussed. E.R.

N87-22818 Paris-Sud Univ., Orsay (France).
INFRARED SPECTROSCOPY USING LASER AND FOURIER TECHNIQUES OF THE UNSTABLE MOLECULES SiH AND NH. DETERMINATION OF THE MOLECULAR CONSTANTS OF THE FUNDAMENTAL ELECTRONIC STATE 3 SIGMA (-) OF NH Ph.D. Thesis [SPECTROSCOPIES INFRAROUGES LASER ET PAR T.F. DES ESPECES INSTABLES SiH ET NH. DETERMINATION DES CONSTANTES MOLECULAIRES DE LETAT ELECTRONIQUE FO NDAMENTAL 3 SIGMA (-) DE NH]
Djamel Boudjaadar 1985 193 p In FRENCH
(ETN-87-99552) Avail: Issuing Activity

An experimental system was assembled to produce and analyze unstable molecules, including a plasma reactor and two spectrometers. The transitions of SiH and NH molecules were observed from 2275 to 3460 mm. The higher levels are in both cases at half the dissociation energy. The modeling and interpretation of the vibration-rotation bands of the NH molecule coincides with the experimental data. A large amount of spectroscopic data is given. ESA

N87-22819# Flow Research, Inc., Kent, Wash. Applied Mechanics Div.
DIRECT NUMERICAL SIMULATIONS OF AN UNPREMIXED TURBULENT JET FLAME Annual Technical Report, 16 Feb. 1986 - 16 Feb. 1987
P. Givi, W.-H. Jou, and R. W. Metcalfe Mar. 1987 21 p
(Contract F49620-85-C-0067)
(AD-A179358; FLOW-TR-401; AFOSR-87-0460TR) Avail: NTIS HC A02/MF A01 CSCL 21B

A hybrid spectral-finite element computer code has been developed for direct numerical simulations of spatially developing three-dimensional turbulent flows under the influence of finite-rate chemical reactions. The spectral element method combines the generality of the finite element methods with the accuracy of the spectral techniques, which permits accurate simulations of flows with realistic boundary conditions. The finite elements are located in the direction of spatial development of the flow, and each element is composed of discrete Chebyshev collocation points. Pseudospectral methods using Fourier transforms have been in the other two directions of the flow. The code has been constructed in a manner that allows the number of data buffering operations to be easily optimized for the memory capabilities of the computer. The algorithm has been tested by comparing the numerical results to some known analytical results. Large-scale simulations are the subject of the present research. GRA

N87-22820# Air Force Inst. of Tech., Wright-Patterson AFB, Ohio. School of Engineering.
FREQUENCY SHIFT MEASUREMENTS OF THE Q(1) AND Q(2) LINES OF H2 USING HIGH RESOLUTION CW COHERENT ANTI-STOKES RAMAN SPECTROSCOPY M.S. Thesis
Mark P. Jelonek 10 Dec. 1986 55 p
(AD-A179390; AFIT/GEP/ENP/86D-5) Avail: NTIS HC A04/MF A01 CSCL 07D

Linear and quadratic frequency shift coefficients were determined for the Q(1) and Q(2) lines of hydrogen using CW Coherent Anti-Stokes Raman Spectroscopy (CARS). The linear coefficients were accurate to three significant digits which is an order of magnitude better than any other published results. The quadratic coefficients were comparable to other reported results because of the range of pressures investigated in this study. Frequency stabilization of the Argon-ion laser allowed accurate measurements of the frequency shifts over a range of 2 to 40 atmospheres. A Fabry-Perot interferometer provides a relative frequency marker and iodine absorption peaks provided an absolute frequency reference. The coefficients determined were compared to those calculated by other researchers using different experimental methods. The high accuracy of the measurements added further credence to the effectiveness of CW CARS as a high resolution spectroscopic tool. GRA

N87-22821# Boeing Aerospace Co., Seattle, Wash.
XAS (X-RAY ABSORPTION SPECTROSCOPY) OF GAS PHASE METAL-CONTAINING CHEMICAL SYSTEMS Technical Report, Sep. 1986 - Aug. 1987
Edward C. Marques, Donald R. Sandstrom, Farrel W. Lytle, and Robert B. Greegor 20 Mar. 1987 9 p
(Contract N00014-85-C-0207)
(AD-A179391; TR-4) Avail: NTIS HC A02/MF A01 CSCL 07D

Our experimental program utilizes x-ray absorption spectroscopy (XAS) to study metal-containing chemical systems, such as metal electrolyte solutions, metal complexes and metal cluster systems. Objectives include the direct experimental measurement of chemical structure in dynamic transient phases and in non-condensed phases. In 1986, emphasis was placed on development of capabilities for detecting metal-containing gas phase XAS. This report describes our progress. GRA

N87-22822# Rockwell International Corp., Canoga Park, Calif. Rocketdyne Div.
BASIC RESEARCH IN ENERGETIC FLUOROCARBONS Final Report, 1 Mar. - 31 Dec. 1986
C. J. Schack and K. O. Christe Feb. 1987 51 p
(Contract F49620-85-C-0037)
(AD-A179676; RI/RD87-139; AFOSR-87-0368TR) Avail: NTIS HC A04/MF A01 CSCL 07C

Reactions of xenon fluoride and trimethyl silyl nitride at low temperatures gave trimethyl silyl fluoride and possibly xenon di nitride as indicated by subsequent decomposition to xenon and nitrogen. These reactions were erratic in either solventless of difluoro dichloro methane solvent systems. Trapping the azide radical from the decomposition with a fluoroolefin was not realized. The interaction of potassium perchlorate and trimethyl silicon chloride gave potassium chloride but the expected Me3SiClO3 was not isolated. It was not possible to duplicate the claimed synthesis of nitryl azide from alkali metal oxides nitrous boron tetra fluoride. An alternate synthesis of nitrous nitride from HN3 and FNO2 in anhydrous HF apparently resulted in an equilibrium involving Nitrile Azide and NO2HF2. Pentafluorosulfuroxide containing fluorocarbons were prepared by the addition of SF5OCl to unsymmetrical fluoroethylenes and also by the addition of SF5OF to CFC1 = CFC1. These new compounds were throughly characterized. Numerous unsuccessful attempts were made to dehalogenate SF5OCFClCF2Cl using zinc and other reducing agents in a variety of solvents and without solvent. Perfluorovinyl cadmium iodide was prepared in DMF solvent and reacted with FNO2. GRA

N87-22823# Sandia National Labs., Albuquerque, N. Mex.
THE AUTOIGNITION OF ISOBUTANE IN A KNOCKING SPARK IGNITION ENGINE
R. M. Green, C. D. Parker, W. J. Pitz, and C. K. Westbrook Nov. 1986 41 p Presented at the Society of Automotive Engineers International Congress and Expo, Detroit, Mich., 23 Feb. 1987 Prepared in cooperation with Jackson State Univ., Miss. and Lawrence Livermore National Lab., Calif.
(Contract W-7405-eng-48)
(DE87-003241; UCRL-95644; CONF-870204-2) Avail: NTIS HC A03/MF A01

The chemical aspects of the autoignition of isobutane are studied experimentally in a spark ignition engine and theoretically using computer simulations with a detailed chemical kinetic mechanism. The results of these studies show that with the relatively knock-resistant fuel, isobutane, there is a significant amount of fuel breakdown in the end gas with a resulting heat release and temperature increase. The ability of the kinetic model to predict this low temperature chemical activity is assessed and the model is modified to more closely simulate the experimental observations. It is clear that a reasonable degree of low-temperature chemical activity precedes the autoignition event. We address the basic question of whether this first stage of combustion accounts for a chemical preconditioning of the end gas which leads to autoignition; or whether it merely provides sufficient heat release in the end gas that the high temperature autoignition is initiated. DOE

N87-22824# Los Alamos National Lab., N. Mex.
ON THE USE OF ADAPTIVE MOVING GRID METHODS IN COMBUSTION PROBLEMS
J. M. Hyman and B. Larrouturou 1986 14 p Presented at the 2nd Workshop on Modelling of Chemical Reaction Systems, Heidelberg, West Germany, 1 Oct. 1986 Prepared in cooperation with Institut National de Recherche en Informatique et en Automatique (INRIA), Valbonne, France
(Contract W-7405-eng-36)
(DE87-003715; LA-UR-86-4043; CONF-8610217-1) Avail: NTIS HC A02/MF A01

The investigators have presented the reasons and advantages of adaptively moving the mesh points for the solution of time-dependent PDEs (partial differential equations) systems developing sharp gradients, and more specifically for combustion problems. Several available adaptive dynamic rezone methods have been briefly reviewed, and the effectiveness of these algorithms for combustion problems has been illustrated by the numerical solution of a simple flame propagation problem. DOE

N87-22825# Argonne National Lab., Ill.
TWO-COLOR, DOPPLER-FREE IONIZATION OF MOLECULAR HYDROGEN FOR ISOTOPIC ANALYSIS
J. P. Hessler and W. L. Glab 1986 7 p Presented at the Resonance Ionization Spectroscopy and its Application, Swansea, England, 7 Sep. 1986
(Contract W-31109-eng-38)
(DE87-004975; CONF-8609132-13) Avail: NTIS HC A02/MF A01

Although resonant ionization techniques have been applied to many atomic systems for ultrasensitive isotopic analysis, very little work has been done on even the simplest molecular system, molecular hydrogen, and its isotopic variants; deuterium hydride, tritium hydride, molecular deuterium, tritium deuteride, and molecular tritium. We present a three-step ionization scheme which will selectively ionize any isotopic variant. The projected isotopic selectivity is sufficient to detect tritium hydride at ambient concentrations without the need of mass analysis. The efficiency of the ionization process is high enough to allow work on small samples. This technique can be applied to many areas of research, e.g., isotopic exchange reactions in the atmosphere and isotopic effects on surfaces. The physical mechanisms which govern the conflicting objectives of both high isotopic selectivity and detection efficiency, discussed below, can be applied to any molecular system. DOE

N87-22826# Oak Ridge National Lab., Tenn.
CHARACTERIZING THE HARDNESS AND MODULUS OF THIN FILMS USING A MECHANICAL PROPERTIES MICROPROBE
W. C. Oliver and C. J. McHargue 1986 7 p Presented at the Materials Research Society Fall Meeting, Boston, Mass., 1 Dec. 1986
(Contract DE-AC05-84OR-21400)
(DE87-006612; CONF-861207-78) Avail: NTIS HC A02/MF A01

A new ultra-low load microindentation system has been acquired in the Metals and Ceramics Division of ORNL. The system's spacial resolution and its data acquisition capabilities allow the determination of several mechanical properties from submicron volumes of materials; hence, the term mechanical properties microprobe (MPM). In this paper we demonstrate the ability of such a system to measure the modulus and hardness of an ion implanted sapphire specimen. The implantation process results in an amorphous surface layer 155 nm thick. The hardness and modulus of the amorphous Al2O3 are 10 and 200 GPa, respectively. This represents a 60% reduction in hardness and a 50% reduction in modulus as compared to the unimplanted material. DOE

N87-22827# Applied Research Corp., Landover, Md.
DECOMPOSITION OF ENERGETIC MATERIALS COMBUSTION OF DECOY MATERIALS Final Report, 14 Feb. 1985 - 30 Sep. 1986
Charles Douglass, Jr. Sep. 1986 8 p
(Contract N00014-85-C-2147)
(AD-A178447; ARC-87-154) Avail: NTIS HC A02/MF A01 CSCL 07C

This report covers an examination of the decomposition of dimethylnitramine using the method of laser powered homogeneous pyrolysis and the spectral and product analysis of the combustion of a series of decoy materials. GRA

N87-22828# Arizona Univ., Tucson. Dept. of Chemistry.
LASER SPECTROSCOPY OF TRANSIENT MOLECULES IMPORTANT IN EXPLOSIONS Final Report, 1 Jan. 1984 - 31 Dec. 1986
Peter F. Bernath 20 Mar. 1987 5 p
(Contract N00014-84-K-0012; RR0-1103)
(AD-A178456; FR-4) Avail: NTIS HC A02/MF A01 CSCL 07B

The high-resolution Fourier transform spectra of the N-H 2 C-H 2 Mg-H 2 Ne-H(+), Cu-H 2, C-P and P-H molecules were observed. The technique of Fourier transform detection of laser-induced fluorescence was applied to free radicals in order to simplify the complex emission spectrum of CCN. A free radical jet source was utilized with a Fourier transform spectrometer to obtain the ultracold emission spectrum of CH N and CD N. A large number of metal-containing free radicals such as calcium nitracarbonate, CaNNN, CaC5H5 and CaOR were discovered by laser-induced fluorescence. GRA

N87-22829# Utah Univ., Salt Lake City. Dept. of Bioengineering.
STOCHASTIC PROCESSES IN CHEMFETs Final Report, 1 Sep. 1983 - 31 Oct. 1986
Jiri Janata and James J. Brophy 16 Jan. 1987 4 p
(Contract N00014-81-K-0664)
(AD-A178841) Avail: NTIS HC A02/MF A01 CSCL 07D

The methodology for evaluation of the electrochemical parameters of both equilibrium and non-equilibrium processes using fluctuation analysis has been fully developed. This paper describing the basic aspects of this technique in a tutorial form has been submitted in hope that the new technique will find broader application within the electrochemical community. As a corrollary to this work we have studied the diffusional impedance of disk and ring microelectrodes and developed theory for the Warburg impedance of these electrodes. Work on chemically modified suspended gate field effects transistor has continued very successfully. We have been able to incorporate nitroarene moieties into polypyrrole and thus create an organic semiconductor with selectivity to arenes. Design of improved top passivation layers for chemical sensors began in January. Deposition and characterization of thin silicon carbide films also began. Fabrication and preliminary testing of the first hole-in-the-rock FETs has been completed. The initial results indicates that this may be a valid technique for study of channel insulators in FET structures. GRA

N87-23398*# Cornell Univ., Ithaca, N.Y. Dept. of Geological Sciences.
MELTING OF TROILITE AT HIGH PRESSURE IN A DIAMOND CELL BY LASER HEATING
William A. Bassett and Maura S. Weathers *In* NASA, Washington Reports of Planetary Geology and Geophysics Program, 1986 May 1987 p 138-140 (For primary document see N87-23341 16-91)
Avail: NTIS HC A24/MF A01 CSCL 07D

N87-23422*# Hawaii Inst. of Geophysics, Honolulu. Planetary Geosciences Div.
SPECTRAL EFFECTS OF DEHYDRATION ON PHYLLOSILICATES
E. A. Bruckenthal and R. B. Singer *In* NASA, Washington Reports of Planetary Geology and Geophysics Program, 1986 May 1987 p 190-192 (For primary document see N87-23341 16-91)
(Grant NsG-7590)
Avail: NTIS HC A24/MF A01 CSCL 07D

N87-23423*# Geological Survey, Denver, Colo.
STUDIES OF THE SCATTERING/ABSORPTION OF MINERALS
Roger N. Clark *In* NASA, Washington Reports of Planetary Geology and Geophysics Program, 1986 May 1987 p 193-195 (For primary document see N87-23341 16-91)
Avail: NTIS HC A24/MF A01 CSCL 07D

N87-23424*# National Aeronautics and Space Administration. Goddard Space Flight Center, Greenbelt, Md.
MID-INFRARED SPECTROSCOPIC INVESTIGATION
Louis Walter, Norma Vergo, and John W. Salisbury (Geological Survey, Denver, Colo.) *In* NASA, Washington Reports of Planetary Geology and Geophysics Program, 1986 May 1987 p 196-198 (For primary document see N87-23341 16-91)
Avail: NTIS HC A24/MF A01 CSCL 07D

N87-23425*# Arizona State Univ., Tempe. Dept. of Geology.
THERMAL-INFRARED SPECTRAL OBSERVATIONS OF GEOLOGIC MATERIALS IN EMISSION
Philip R. Christensen and Sharon J. Luth *In* NASA, Washington Reports of Planetary Geology and Geophysics Program, 1986 May

1987 p 199-201 (For primary document see N87-23341 16-91)
Avail: NTIS HC A24/MF A01 CSCL 07D

N87-23426*# Jet Propulsion Lab., California Inst. of Tech., Pasadena.
BIDIRECTIONAL REFLECTANCE PROPERTIES OF PLANETARY SURFACE MATERIALS
B. Buratti, W. Smythe, R. Nelson, V. Gharakhani, and B. Hapke (Pittsburgh Univ., Pa.) *In* NASA, Washington Reports of Planetary Geology and Geophysics Program, 1986 May 1987 p 202-204 (For primary document see N87-23341 16-91)
(Contract NAS7-918)
Avail: NTIS HC A24/MF A01 CSCL 07D

N87-23427*# Pittsburgh Univ., Pa. Dept. of Geology and Planetary Science.
ATLAS OF REFLECTANCE SPECTRA OF TERRESTRIAL, LUNAR AND METEORITIC POWDERS AND FROSTS FROM 92 TO 1800 (LC2)NM Abstract Only
Jeffrey Wagner, Bruce Hapke, and Eddie Wells *In* NASA, Washington Reports of Planetary Geology and Geophysics Program, 1986 May 1987 p 205 (For primary document see N87-23341 16-91)
Avail: NTIS HC A24/MF A01 CSCL 07D

N87-23428*# Brown Univ., Providence, R. I.
DECONVOLUTION OF SPECTRA FOR INTIMATE MIXTURES
John F. Mustard, Carle M. Pieters, and Stephen F. Pratt *In* NASA, Washington Reports of Planetary Geology and Geophysics Program, 1986 May 1987 p 206-207 (For primary document see N87-23341 16-91)
Avail: NTIS HC A24/MF A01 CSCL 07D

N87-23433*# Pittsburgh Univ., Pa. Dept. of Geology and Planetary Science.
BIDIRECTIONAL REFLECTANCE SPECTROSCOPY Abstract Only
Bruce Hapke *In* NASA, Washington Reports of Planetary Geology and Geophysics Program, 1986 May 1987 p 219 Previously announced in IAA as A87-14645 Submitted for publication (For primary document see N87-23341 16-91)
Avail: NTIS HC A24/MF A01 CSCL 07D

N87-23436*# Cornell Univ., Ithaca, N.Y.
Io: COMPARISON OF PHOTOMETRIC SCANS PRODUCED BY THE MINNAERT AND HAPKE FUNCTIONS
Damon P. Simonelli and Joseph Veverka *In* NASA, Washington Reports of Planetary Geology and Geophysics Program, 1986 May 1987 p 223-225 (For primary document see N87-23341 16-91)
(Grant NsG-7156)
Avail: NTIS HC A24/MF A01 CSCL 07D

N87-23438*# Jet Propulsion Lab., California Inst. of Tech., Pasadena.
SOLID SULFUR IN VACUUM: SUBLIMATION EFFECTS ON SURFACE MICROTEXTURE, COLOR AND SPECTRAL REFLECTANCE, AND APPLICATIONS TO PLANETARY SURFACES
D. B. Nash *In* NASA, Washington Reports of Planetary Geology and Geophysics Program, 1986 May 1987 p 227-228 (For primary document see N87-23341 16-91)
Avail: NTIS HC A24/MF A01 CSCL 07D

26 METALLIC MATERIALS

Includes physical, chemical, and mechanical properties of metals, e.g., corrosion; and metallurgy.

N87-22830# United Kingdom Atomic Energy Authority, Harwell (England). Materials Physics and Metallurgy Div.
HYDROGEN AND TEMPER EMBRITTLEMENT INTERACTIONS IN FATIGUE OF 2 1/4Cr1Mo STEEL
C. A. Hippsley Sep. 1986 45 p
(AERE-R-12322) Avail: NTIS HC A03/MF A01

C. A. Hippsley Sep. 1986 45 p
(AERE-R-12322) Avail: NTIS HC A03/MF A01

The influence of strength, precipitate microstructure, temper embrittlement and environment on fatigue crack growth in 2 1/4 Cr 1Mo steel have been investigated. Particular attention was paid to the interaction between hydrogen embrittlement and temper embrittlement in fatigue. A range of tempered and aged conditions was examined in air, vacuum and gaseous hydrogen environments at growth rates between 10 to the -10 and 10 to the -5 m/cycle. Discussion focuses on effects observed in hydrogen. Author

N87-22831# Admiralty Research Establishment, Portsmouth (England). Dockyard Lab.
CIRCUMFERENTIAL HOT WIRE TIG CLADDING OF CARBON-MANGANESE STEEL WITH INCONEL 625 AND GUN-METAL WITH A TIN BRONZE
K. M. Chipperfield and F. J. Plumb Dec. 1985 18 p
(ARE-TM(UMD)-85574; BR100464; ETN-87-99810) Copyright Avail: NTIS HC A02/MF A01

It is demonstrated that the hot wire TIG process can dramatically increase the deposition rate of weld metal for cladding (and also for thick section joints) of carbon-manganese steel with Inconel 625 to a high quality. The Union Carbide manufactured facility is superior to the lower energy output Mitsubishi clean TIG unit. The major drawback is due to the increase in iron content of clad layer due to the high arc currents employed, but this can be controlled to a level acceptable for marine applications. The lowest iron content level achieved is under conditions comparable to the cold wire spiral TIG conditions determined previously, the latter process being carried out on facilities considerably cheaper than the hot wire TIG facilities. ESA

N87-22832# Materials Quality Assurance Directorate, London (England).
THE EFFECTS OF CANDIDATE CHEMICAL TRAINING AGENTS UPON SERVICE MATERIALS
J. D. Barry, G. R. Clayton, and M. Marshall Jul. 1981 22 p
(MQAD-317; BR79765; ETN-87-99819) Copyright Avail: NTIS HC A02/MF A01

Dowanol DPM and polyethylene glycol (PEG) 300, were evaluated for their effects on service materials. Only PEG 300 can be considered potentially suitable. Limitations on use are recommended. Exposure to PEG 300 of bare steel, magnesium alloy, alkyd paints, transfers, polymethyl methacrylate, and particularly ABS, should be minimized. Decontamination should be performed not more than 6 hr after exposure to PEG 300. ESA

N87-22833# Illinois Univ., Urbana. Dept. of Mechanical and Industrial Engineering.
LASER CLADDING OF Mg AND Nb ALLOYS FOR IMPROVED ENVIRONMENTAL RESISTANCE Annual Report, Jan. 1986 - Jan. 1987
J. Mazumder, J. Singh, and S. Raja Jan. 1987 41 p
(Grant AF-AFOSR-0034-86)
(AD-A179606; AFOSR-87-0441TR) Avail: NTIS HC A03/MF A01 CSCL 11F

The present status of laser cladding of magnesium and niobium has been surveyed. The potential of cladding zirconium onto magnesium and titanium onto niobium for improving environmental resistance have been discussed. In the present project zironium has been cladded onto magnesium by preplaced powder cladding technique. The laser beam encounters the powder first placed on the substrate. A very thin layer on the top of the substrate melts resulting in a cladding of minimum dilution. Corrosion properties of the Zr-clad region was evaluated in a 3.5 percent NaCl solution at room temperature. Substantial improvement in corrosion resistance has been observed. The structural characterization of the clad region was done by optical and electron microscopy. EDAS analysis has been done to identify the phases observed in electron microscopy. GRA

N87-22834# California Univ., Davis. Div. of Materials Science and Engineering.
SUPERPLASTICITY: A FUNDAMENTAL INVESTIGATION ON DEFORMATION MECHANISM AND CAVITATION PHENOMENA Annual Technical Report, 1 Feb. 1986 - 31 Jan. 1987
A. Chokshi, T. Bieler, and A. K. Mukherjee 28 Feb. 1987 38 p
(Grant AF-AFOSR-0091-86)
(AD-A179651; AFOSR-87-0436TR) Avail: NTIS HC A03/MF A01 CSCL 11F

Al-Li alloy and the mechanically alloyed IN91211 were investigated for superplasticity and enhanced plasticity. The optimum test condition for superplastic deformation, the associated grain boundary sliding, and flow localization at non-optimum condition were investigated for Al-Li alloy. The enhanced plasticity at comparatively high strain rates was investigated in IN91211. The mechanical data were analyzed using the concept of threshold stress. The nature and temperature dependence of this threshold stress are being investigated. GRA

N87-22835# Oak Ridge National Lab., Tenn.
CHARACTERIZATION OF RAPIDLY SOLIDIFIED Al-Be-Li AND Al-Be RIBBONS
W. C. Oliver, J. Wadsworth, A. R. Pelton, and T. G. Nieh 1986 7 p Presented at the Materials Research Society Fall Meeting, Boston, Mass., 1 Dec. 1986 Prepared in cooperation with Lockheed Palo Alto Research Labs., Calif., and Notre Dame Univ., Ind.
(Contract DE-AC05-84OR-21400)
(DE87-006613; CONF-861207-80) Avail: NTIS HC A02/MF A01

Rapidly solidified Al-Be and La-Be-Li ribbons have been produced by a melt spinning technique. Differential scanning calorimetry (DSC) measurements were conducted with both binary and ternary ribbons. A direct comparison of DSC results from binary and ternary ribbons indicates that the presence of Be has little or no effect on the precipitation of Li containing phases in the Al matrix (i.e., in this respect the ternary behaves like a pseudo binary Al-Li alloy). Mechanical properties microprobe measurements (MPM) and transmission electron microscopy (TEM) have been carried out on ribbons with a variety of heat treatments. Preliminary results show that the strength of Al-Be-Li ribbons, as a function of aging temperature, exhibits complex behavior. Specifically, the hardness first decreases with increasing annealing temperature up to 185 C, then increases with temperature up to 220 C and then decreases again. The binary alloy is not as hard in the as melt spun condition, but also shows a peak around 220 C. These results are explained in terms of precipitation of Li containing intermetallic compounds and Be from the matrix of the as melt spun alloys. DOE

N87-22836# Massachusetts Inst. of Tech., Cambridge.
MARTENSITIC TRANSFORMATION AS A DEFORMATION PROCESS
G. B. Olson and M. Cohen 1986 23 p Presented at the 115th American Inst. of Mining, Metallurgical and Petroleum Engineers Annual Meeting, New Orleans, La., 2 Mar. 1986
(Contract DE-FG02-84ER-45154)
(DE87-007068; CONF-860340-16) Avail: NTIS HC A02

Constitutive relations for transformation plasticity have been derived from martensitic transformation kinetic theory, predicting flow stress as a function of strain, strain rate, temperature, and stress state. The stress-strain curve can exhibit upward curvature under the combined influence of the softening contribution of the transformation as a deformation mechanism and the hardening contribution of the transformation product. This shape provides a maximum stability of plastic flow and quantitatively accounts for observed enhancement of uniform ductility in TRIP (Transformation-Induced Plasticity) steels. In combination with transformation dilatation effects, the flow stabilizing influence also accounts for a major transformation toughening effect observed when ductile fracture is controlled by plastic shear instability. The principles have now been applied to both homogeneous and dispersed-phase alloy systems. DOE

N87-22837# Sandia National Labs., Albuquerque, N. Mex.
ELECTROCHEMICAL ADJUSTMENT OF THIN FILM Ti-Pd RESISTORS
D. J. Sharp and D. P. Norwood 1987 23 p Presented at the International Conference on Metallurgical Coatings, San Diego, Calif., 23 Mar. 1987
(Contract DE-AC04-76DP-00789)
(DE87-007392; SAND-87-0625C; CONF-870388-3) Avail: NTIS HC A02/MF A01

Thin multilayered films consisting of tantalum nitride (Ta N), titanium, palladium, and gold are used at Sandia to fabricate hybrid microcircuits. From these stock multilayered composites, various circuits can be selectively etched and patterned to provide conductors and two levels of resistor patterns. The tantalum nitride is used to form resistor structures having values ranging from about 20 to 50,000 ohms. In order to provide resistors having values of about 1 to 4 ohms, the palladium, with its underlying titanium and Ta N layers, is used; these were designated as Ti-Pd resistors. Low resistivity tuned strip lines, for example, have this need. We have completed a study of the use of an electrochemical probe which can be used to selectively deposit gold or, alternatively, remove palladium from the surface of the palladium composite film resistors. This permits resistor adjustment to either higher or lower values and does not produce discontinuities which occur with laser trimming. Studies describing accelerated life aging, temperature coefficient of resistance changes, and final adjustment precision are discussed. DOE

N87-22838# Cornell Univ., Ithaca, N.Y.
EXPERIMENTAL AND THEORETICAL STUDIES OF THE STRUCTURE OF GRAIN BOUNDARIES Progress Report
N. W. Ashcroft and S. L. Sass Jan. 1987 17 p
(Contract DE-FG02-85ER-45211)
(DE87-007560; DOE/ER-45211/1) Avail: NTIS HC A02/MF A01

The long range goal of this research project has been to obtain information on the atomic structure of grain boundaries in bcc metals and ceramics, to understand how segregation influences grain boundary structure and causes boundaries to become embrittled in Fe-base alloys, to understand how segregation and ionization state of the solute influences the boundary structure in ceramic materials, and to understand the role of boron and nonstoichiometry in making brittle boundaries in Ni3Al become ductile. A theoretical program was initiated during the period of this grant with the goal of understanding and improving the interatomic potentials that are used to calculate the structure of grain boundaries in metallic systems. DOE

N87-22839# California Univ., Berkeley.
THE ROLE OF PARTICLE SUBSTRUCTURE IN THE SINTERING OF MONOSIZED TITANIA Ph.D. Thesis
L. H. Edelson Dec. 1986 109 p
(Contract DE-AC03-76SF-00098)
(DE87-007600; LBL-22753) Avail: NTIS HC A06

This study examined the sintering behavior of compacts comprised of monodispersed agglomerates and correlates changes in macroscopic dimensions with changes in particle microstructure and chemistry. Monosized titania particles (0.35 microns) prepared by controlled hydrolysis of titanium tetraethoxide in ethanol were found to be porous agglomerates of about 60 A primary particles. The total volume shrinkage during sintering was 84%. Five contributions to the total shrinkage were identified: removal of chemisorbed water about 12% linear shrinkage, from ambient to 250 C, crystallization to anatase about 13% linear shrinkage between 250 and 425 C, intra-agglomerate densification (about 13%, 425 to 600 C), conversion of anatase to rutile (about 5% linear between 600 and 800 C), and intraaglomerate densification (7% linear shrinkage above 800). Thus, about half the compact shrinkage is the result of agglomerate substructure changes. Studies of the agglomerate structural evolution indicate the interagglomerate densification crystallite growth rates, rather than crystallization and the polymorphic transformation, are the secondary factors, after compact packing, that influence microstructure development. This indicates control of intra-agglomerate structure is an important and necessary processing consideration even though particle size and particle packing are tightly controlled. This study indicates that particle substructure can generate unexpected shrinkage and that failure to adequately control intraparticle structure can deleteriously affect the resulting microstructure finished ceramic. DOE

N87-22840# Johns Hopkins Univ., Baltimore, Md. Dept. of Materials Science and Engineering.
INVESTIGATION OF THE ICOSAHEDRAL Z-PHASE IN ALUMINIUM TRANSITION METAL ALLOYS AND RAPIDLY SOLIDIFIED Al-ALLOYS Progress Report
Leo Bendersky, Dan Shechtman, and E. Horowitz Sep. 1986 46 p
(Contract N00014-85-K-0779; DARPA Order 5527)
(AD-A178451) Avail: NTIS HC A03/MF A01 CSCL 11F

The discovery by Shechtman, of five-fold symmetry in rapidly solidified aluminum alloys stimulated world wide interest and activity in the preparation and properties of the materials. Likewise, research on the microstructure of a variety of rapidly solidified aluminum alloys including those containing iron and chromium has been advanced. This report covers the work of two Principal Investigators, Dr. Leo Bendersky and Dr. Dan Shechtman, plus their research collaborators, which has been reported in the scientific literature during the first half of 1986. The five publications reproduced here represent a significant contribution to our understanding of the icosahedral phase and the microstructure of rapidly solidified alloys. GRA

N87-22841# Texas Univ., Austin. Center for Materials Science and Engineering.
MICROSCOPIC STUDY OF THE INFLUENCE OF IMPURITIES ON INTERFACE BONDING Technical Report, 1 Dec. 1983 - 30 Nov. 1986
Harris L. Marcus 30 Jan. 1987 120 p
(Contract N00014-83-K-0143)
(AD-A178510; UTCMSE-87-1) Avail: NTIS HC A06/MF A01 CSCL 11F

In an attempt to evaluate the interface cohesive models of laminate systems, EXAFS was used to probe the interfaces. The advantages of the EXAFS as a probe for these investigations were the use of the beam polarization to probe the directionality of the bonding, the in-situ method of directly probing the nature of the interface, and the ability to localize the impurities at the interface, thus avoiding the masking of the results with background matrix signal. Samples of layered structures of Nickel Titanium-Ni, Cobolt-Ti-Co, Aluminum Gallium-Al, Al-arsenic-Al, and the layered structures with hydrogen added to the interfaces were prepared. Experiments were performed at the Cornell CHESS and the Brookhaven National Laboratory light sources. The ability to get meaningful EXAFS data for multilayered specimens with partial monolayers of impurities was established. The ability of the EXAFS to distinguish between Ti metal, Ti oxide and Ti in TiNi in the interface layers was determined using standards for references. The directional behavior of the bonding within normal to the interface was indicated for the Al-As-Al layered structures. The measurements of hydrogen at the interface were inconclusive. GRA

N87-22842# Stevens Inst. of Tech., Hoboken, N. J.
CORROSION, WEAR AND MECHANICAL PROPERTIES OF PULSE-ELECTRODEPOSITED ALLOYS Final Report, Sep. 1983 - Nov. 1986
Rolf Weil and Wonbeck Kim 1 Mar. 1987 36 p
(Contract DAAG29-83-K-0121)
(AD-A178596; ARO-20642.5-MS) Avail: NTIS HC A03/MF A01 CSCL 11F

Pulse plating to improve the properties of electrodeposits and to develop new materials was investigated. A minitensile device capable of measuring elastic and plastic properties of thin foils over a large range of strain rates was designed and built. A cell for determining hydrogen permeation through electrodeposits was also built. The previously reported reduction of the internal stress in nickel-molybdenum deposits was investigated further as was that in nickel. An observed compressive stress which developed each time that the current was turned on and then changed to tensile was explained in terms of hydrogen expanding the surface layer. Hydrogen was also thought to be responsible for a decreasing stress with increasing pulse frequency when nickel was plated on palladium substrates. The reduction of Mo by hydrogen also during the time the pulsed current was off was the probable cause of a higher alloy content of Ni-Mo deposits and lower stress. The mechanical properties of Ni-Mo deposits were determined. The high ductility exhibited by composites consisting of alternate layers of ordered and disordered beta brass obtained by pulse plating was found to be due to a strain-induced martensitic transformation. GRA

N87-22843# Rockwell International Science Center, Thousand Oaks, Calif.
METALLIDING AS AN ELECTROCHEMICAL PROCESS Final Report, 1 Jun. 1984 - 30 Nov. 1986
M. W. Kendig and D. O. Raleigh Jan. 1987 46 p
(Contract DAAG29-84-C-0006)
(AD-A178744; SC5398.4FR; ARO-21289.3-MS) Avail: NTIS HC A03/MF A01 CSCL 11F

Controlled electrolysis in molten salts can improve the surface properties of metal alloys for wear and corrosion resistance. Surfaces of aluminum 1100 and carbon steel were modified by passage of cathodic current under potentiostatic and galvanostatic control in molten salts variously containing Cerium (3+), Boron tetrafluoride (-), Titanium (3+) ions. Hard, poorly adherent Ceric aluminide and Cerous aluminide layers formed on Al surfaces at potentials which were some 200 to 400 mV positive to the reduction potential of Ce. The deposition occurred by a reductive precipitation mechanism from a KCl/LiCl melt at 560 C containing 1 mole% Ce(3+). Boride and titanide layers were formed on steel in a LiF/KF melt containing the respective ions. A borided layer on steel exhibited a factor of ten improvement in hardness and a titanided layer exhibited a 30% increase in hardness. While the borided steel showed only marginal improvement over the substrate in resistance to corrosion in neutral aerated 0.5M Sodium Chloride, the titanided steel showed a significant improvement in corrosion resistance under these conditions. GRA

N87-22844# Washington Univ., Seattle. Dept. of Aeronautics and Astronautics.
DYNAMIC FRACTURE OF HIGH STRENGTH STEEL Final Report, Jun. 1983 - Nov. 1986
Ian M. Fyfe Jan. 1987 15 p
(Contract DAAG29-83-K-0085)
(AD-A178862; ARO-19785.3-MS) Avail: NTIS HC A02/MF A01 CSCL 11F

Ductile failure under a variety of loading conditions is examined in order to assess the importance of inertia, precompression and mean tensile stress on the failure process. A number of plastic instability concepts are also examined with regard to their ability to provide generality to failure criteria based on void nucleation and growth concepts. It was determined that inertia plays an importance role in localization and can dramatically inhibit the necking process. Precompression appears to be relatively unimportant, unless the material is very highly strain-rate sensitive. It was determined that a viable void volume fraction failure criteria can be established which is applicable over a wide range of impact conditions if the nucleation strains dependence on the mean tensile stress is incorporated in the theory. GRA

N87-22776*# Georgia Inst. of Tech., Atlanta.
DEFORMATION AND FATIGUE BEHAVIOR OF SSME TURBOPUMP BLADE MATERIALS
Walter W. Milligan and Stephen D. Antolovich *In* NASA. Lewis Research Center Structural Integrity and Durability of Reusable Space Propulsion Systems 1987 p 65-81 (For primary document see N87-22766 16-20)
Avail: NTIS HC A10/MF A01 CSCL 11F

N87-22777*# National Aeronautics and Space Administration. Lewis Research Center, Cleveland, Ohio.
FATIGUE DAMAGE INTERACTION BEHAVIOR OF PWA 1480
Michael A. McGaw *In its* Structural Integrity and Durability of Reusable Space Propulsion Systems 1987 p 83-87 (For primary document see N87-22766 16-20)
Avail: NTIS HC A10/MF A01 CSCL 11F

N87-22781*# Rockwell International Corp., Canoga Park, Calif.
MECHANICAL PROPERTIES OF HIGH GRADIENT AND HOT ISOSTATICALLY PRESSED PWA 1480
L. G. Fritzemeier and G. D. Schnittgrund *In* NASA. Lewis Research Center Structural Integrity and Durability of Reusable Space Propulsion Systems 1987 p 107-108 (For primary document see N87-22766 16-20)
Avail: NTIS HC A10/MF A01 CSCL 11F

N87-22782*# Carnegie-Mellon Univ., Pittsburgh, Pa.
EFFECT OF HYDROGEN ON DEFORMATION STRUCTURE AND PROPERTIES OF CMSX-2 NICKEL-BASE SINGLE-CRYSTAL SUPERALLOY
M. Dollar, I. M. Bernstein, S. Walston, F. Prinz, and A. Domnanovich *In* NASA. Lewis Research Center Structural Integrity and Durability of Reusable Space Propulsion Systems 1987 p 109-115 (For primary document see N87-22766 16-20)
Avail: NTIS HC A10/MF A01 CSCL 11F

27 NONMETALLIC MATERIALS

Includes physical, chemical, and mechanical properties of plastics, elastomers, lubricants, polymers, textiles, adhesives, and ceramic materials.
For composite materials see *24 Composite Materials.*

N87-22845* National Aeronautics and Space Administration. Ames Research Center, Moffett Field, Calif.
STRUCTURAL PANELS Patent
John A. Parker, inventor (to NASA), Alvin H. Heimbuch, inventor (to NASA), Ming-Ta S. Hsu, inventor (to NASA), and Timothy S. Chen, inventor (to NASA) (San Jose State Univ., Calif.) 3 Mar. 1987 10 p Filed 22 Apr. 1985 Division of US-Patent-4,526,925, US-Patent-Appl-SN-553339, filed 18 Nov. 1983
(NASA-Case-ARC-11429-2-CU; US-Patent-4,647,615; US-Patent-4,526,925; US-Patent-Appl-SN-725727; US-Patent-Appl-SN-55339; US-Patent-Class-524-548; US-Patent-Class-524-404; US-Patent-Class-525-182; US-Patent-Class-526-262) Avail: US Patent and Trademark Office CSCL 11B

Vinyl pyridines including vinyl stilbazole materials and vinyl styrylpyridine oligomer materials are disclosed. These vinylpyridines form copolymers with bismaleimides which copolymers have good fire retardancy and decreased brittleness. The cure temperatures of the copolymers are substantially below the cure temperatures of the bismaleimides alone. Reinforced composites made from the cured copolymers are disclosed as well.

Official Gazette of the U.S. Patent and Trademark Office

N87-22846# Admiralty Research Establishment, Portland (England).
A SIMPLEX OPTIMISATION TECHNIQUE FOR DEVELOPMENT OF RUBBER FORMULATIONS
R. Lane and B. C. OChiltree Apr. 1986 16 p
(ARE-TM(UMT)-86405; BR100407; ETN-87-99811) Copyright
Avail: NTIS HC A02/MF A01

A Simplex technique for optimization in the presence of error is presented and the use of the technique to develop a rubber formulation for an acoustic application is described. The technique is very useful in the early stages of optimization, permitting a rapid approach to the optimum with minimum experimentation. However, in the later stages, as the optimum is approached, it is doubtful if the Simplex technique offers any advantage over simple extrapolation and one variable optimization. A combination of both techniques seems to be appropriate in most cases with the end of the first, Simplex, phase being reached when oscillation or spiralling of the Simplex plot prevents new combinations from being generated. ESA

N87-22847* National Aeronautics and Space Administration. Langley Research Center, Hampton, Va.
POLYENAMINES FROM AROMATIC DIACETYLENIC DIKETONES AND DIAMINES Patent
Paul M. Hergenrother, inventor (to NASA), Robert G. Bass, inventor (to NASA), Mark S. Sinsky, inventor (to NASA), and John W. Connell, inventor (to NASA) (Virginia Commonwealth Univ., Richmond.) 5 May 1987 7 p Filed 15 May 1985 Supersedes N86-19462 (24 - 10, p 1560)
(NASA-Case-LAR-13444-1-CU; US-Patent-4,663,483; US-Patent-Appl-SN-734366; US-Patent-Class-564-396; US-Patent-Class-564-330; US-Patent-Class-564-430; US-Patent-Class-546-262; US-Patent-Class-546-264; US-Patent-Class-528-229) Avail: US Patent and Trademark Office CSCL 11B

The synthesis and characterization of several polyenamine ketones are discussed wherein conjugated diacetylenic diketones and aromatic diamines are used as a route to the formation of high molecular weight polyenamine ketones which exhibit good mechanical properties and can be cast into creasible films. Typical polymerization conditions involved the reaction of stoichiometric amounts of 1,4- or 1,3-PPPO and a diamine at 60 to 130 C in m-cresol at (w/w) solids content of 8 to 26% for a specified period of time under a nitrogen atmosphere. Novel polyenamine ketones were prepared with inherent viscosities as high as 1.99 dl/g and tough, clear amber films with tensile strengths of 12,400 psi and tensile moduli of 397,000 psi were cast from solutions of the polymers in chloroform. In most cases, the elemental analyses for the polyenamine ketones agree within + or - 0.3% of the theoretical values.

Official Gazette of the U.S. Patent and Trademark Office

N87-22848* National Aeronautics and Space Administration. Langley Research Center, Hampton, Va.
PROCESS FOR CROSSLINKING AND EXTENDING CONJUGATED DIENE-CONTAINING POLYMERS Patent
Vernon L. Bell, inventor (to NASA) and Stephen J. Havens, inventor (to NASA) (Kentron International, Inc., Hampton, Va.) 28 Apr. 1977 8 p Filed 11 May 1986 Supersedes N86-25477 (24 - 16, p 2544)
(NASA-Case-LAR-13452-1; US-Patent-4,661,558; US-Patent-Appl-SN-838655; US-Patent-Class-525-36; US-Patent-Class-528-176; US-Patent-Class-528-184; US-Patent-Class-528-192; US-Patent-Class-528-193) Avail: US Patent and Trademark Office CSCL 11B

A process using a Diels-Alder reaction which increases the molecular weight and/or crosslinks polymers by reacting the polymers with bisunsaturated dienophiles is developed. The polymer comprises at least 75% by weight based on the reaction product, has a molecular weight of at least 5000 and a plurality of conjugated 1,3-diene systems incorporated into the molecular structure. A dienophile reaction with the conjugated 1,3-diene of the polymer is at least 1% by weight based on the reaction product. Examples of the polymer include polyesters, polyamides, polyethers, polysulfones and copolymers. The bisunsaturated dienophiles may include bis-maleimides, bis maleic and bis fumaric esters and amides. This method for expanding the molecular weight chains of the polymers, preferable thermoplastics, is advantageous for processing or fabricating thermoplastics. A low molecular weight thermoplastic is converted to a high molecular weight plastic having improved strength and toughness for use in the completed end use article.

Official Gazette of the U.S. Patent and Trademark Office

N87-22849# Sandia National Labs., Albuquerque, N. Mex.
MOLECULAR REACTIONS AT THE FILM SURFACE IN PLASMA POLYMERIZATION
R. J. Buss 1987 10 p Presented at the 193rd National

Meeting of the American Chemical Society, Denver, Colo., 5 Apr. 1987
(Contract DE-AC04-76DP-00789)
(DE87-002488; SAND-86-2471C; CONF-870410-4) Avail: NTIS HC A02/MF A01

During the plasma polymerization process, the surface of the depositing material is continuously bombarded by a multitude of plasma generated species: ions, photons, radicals and other neutral molecules. In understanding the chemistry of the plasma polymerization process it is desirable to know the way in which these species interact with the film during deposition. Any individual molecule/surface collision may result in growth of the film by an attachment reaction, or in ablation by chemical or physical removal of previously attached atoms. Reported here are results of experiments designed to probe the reaction of molecules undergoing single collisions with the surface of a plasma-polymerized film during the deposition process. The method employed was a molecular beam sampling of all the plasma species and deposition of polymer from the beam onto a substrate. Control of the charged particle fluxes to the surface was used to study the role of ion bombardment. A beam of a probe molecule, incident on the film surface throughout the deposition, was used to investigate the interaction of the probe molecule with the surface. DOE

N87-22850# Sandia National Labs., Albuquerque, N. Mex.
ISOTACTIC POLYSTYRENE PHASE DIAGRAMS AND PHYSICAL GELATION
J. H. Aubert 1987 11 p Presented at the 193rd National Meeting of the American Chemical Society, Denver, Colo., 5 Apr. 1987
(Contract DE-AC04-76DP-00789)
(DE87-002693; SAND-86-2591C; CONF-870410-5) Avail: NTIS HC A02/MF A01

Although the gelation of isotactic polystyrene (iPS) solutions has been studied for a long time, no prior attempt has been made to measure phase diagrams of these solutions. This is surprising because it has been suggested that gelation occurs by liquid-liquid phase separation and knowledge of the phase diagram could support this mechanism. In addition, it has long been known that iPS gels melt at a much higher temperature than where they form. No adequate explanation has been offered for this. We have determined one partial phase diagram for iPS/nitrobenzene(NB) solutions which has allowed us to relate the super-molecular structure of the physical gel to the characteristics of the phase diagram. This is important not only for an adequate explanation of physical gelation but in order to utilize such gels in the manufacture of microporous membranes and foams. DOE

N87-22851# Oak Ridge National Lab., Tenn.
SYNTHESIS OF ALUMINA-ZIRCONIA POWDERS BY SOL-GEL PROCESSING
W. D. Bond and P. F. Becher 1987 18 p Presented at the 3rd International Conference on Ultrastructure Processing of Ceramics, Glasses and Composites, San Diego, Calif., 23 Feb. 1987
(Contract DE-AC05-84OR-21400)
(DE87-005721; CONF-870254-2) Avail: NTIS HC A02/MF A01

The object of this investigation is to determine the feasibility of sol-gel processes for preparing powders of phase-stabilized zirconia. Composites of phase-stabilized zirconia and alumina in which fracture toughening is achieved by the tetragonal to monoclinic transition in ZrO are one of the promising candidate materials for advanced heat engine applications. To achieve superior strength in these composites, structural considerations dictate that the composites be uniform in composition, possess fine-grained microstructures and be highly dense. Sol-gel processes have the potential for the synthesis of powders from which these composites can be fabricated. Yttrium oxide in concentration of 0.5 to 5 mole % (zirconia basis) was used for phase stabilization of zirconia. In the present study particular emphasis was placed on determining the process parameters which control the homogeneity of Y O in the zirconia phase. The stress required to transform tetragonal ZrO during fracture is a function of Y O content. It is well established that gel composition and properties are controlled by the chemistry and processing conditions employed in the individual steps of sol-gel processes. The present study was concerned with the preparation of gel powders of Al O -(ZrO Y O) from precursor aqueous sols containing the codispersed colloidal oxides. DOE

N87-22852# Oak Ridge National Lab., Tenn.
CERAMIC TECHNOLOGY NEWSLETTER NO. 13, OCTOBER - DECEMBER 1986: CERAMIC TECHNOLOGY FOR ADVANCED HEAT ENGINES PROJECT
M. P. Kertesz, ed. and D. A. Douglas, ed. Oct. 1986 4 p
(Contract DE-AC05-84OR-21400)
(DE87-006447; ORNL/M-301) Avail: NTIS HC A02/MF A01

This newsletter describes: the department of ceramic engineering at Illinois University, production of silicon nitride, transformation-toughened ceramics, and various activities in this area. DOE

N87-22853# Oak Ridge National Lab., Tenn.
NEUTRON SCATTERING FROM CHARGED POLYMER LATTICES
J. B. Hayter 1987 10 p Presented at the Materials Research Society Fall Meeting, Boston, Mass., 1 Dec. 1986
(Contract DE-AC05-84OR-21400)
(DE87-006628; CONF-861207-79) Avail: NTIS HC A02/MF A01

Aqueous suspensions of charged polymer latex particles exhibit several forms of ordered structure, the particular form depending on the size, number density and charge of the latex particles, and on the ionic strength of the aqueous medium. At low ionic strength, the inter-particle potential may become sufficiently long-ranged to generate crystalline order, which usually shows bcc symmetry at low density and becomes fcc above about 3% volume fraction of latex in the system. As the ionic strength increases, the crystalline structure melts, and ordered liquid structures develop. This paper reviews some of the recent small-angle neutron scattering experiments on polymer latex suspensions, in the light of new theoretical methods which permit in situ analysis of the particle size and charge. The discussion also encompasses new experimental methods for studying latex structures under dynamic shear conditions. DOE

N87-22854# Colorado Univ., Boulder. Dept. of Chemistry.
HIGH PERFORMANCE POLYMERS: MATRIX RESINS, HIGH STRENGTH POLYQUINOXALINES AND CONDUCTING POLYAROMATICS Final Report, 6 Feb. 1984 - 5 Feb. 1987
J. K. Stille Feb. 1987 16 p
(Contract DAAG29-84-K-0028)
(AD-A178457; ARO-20842.11-CH) Avail: NTIS HC A02/MF A01 CSCL 07C

The synthesis of low molecular weight polyquinolines and polyimides containing biphenylene end-caps, with and without acetylenic units in the main chain, were synthesized and evaluated as matrix resins for fiber reinforced composites. The best composite properties were obtained with an exact equivalent biphenylene groups and acetylenic groups, since these groups generate crosslinks by the formation of phenanthrene units. GRA

N87-22855# McGill Univ., Montreal (Quebec).
PHYSICAL PROPERTIES AND STRUCTURE OF ION-CONTAINING POLYMERS Final Report, 1 Oct. 1983 - 31 Jan. 1987
A. Eisenberg Jan. 1987 39 p
(Contract DAAG29-83-K-0140)
(AD-A178592; ARO-20674.27-CH) Avail: NTIS HC A03/MF A01 CSCL 07C

Research had been concerned with the miscibility enhancement using ion-ion or ion-dipole interactions in simple copolymers as well as the polyurethanes, the synthesis and mechanical property studies of the block copolymers containing short ionic end blocks, structure-property relations covering a wide range of studies ranging from the introduction of hitherto unexplored ion types (such as phenoxy) into polystyrene and preliminary studies of ionic combs and melt rheology investigations of ionomer-diluent systems. GRA

N87-22856# Lockheed Missiles and Space Co., Palo Alto, Calif. Research and Development Div.

LOW-PRESSURE SELF-PROPAGATING HIGH-TEMPERATURE SYNTHESIS Final Report, 1984 - 1986

A. P. Hardt 1 Feb. 1987 31 p
(Contract DAAG29-84-C-0015)
(AD-A178593; LMSC-F145665; ARO-21181.2-MS) Avail: NTIS HC A03/MF A01 CSCL 13H

Self propagating high temperature synthesis (SHS) is discussed. The object was to produce void free refractory bodies by the synthesis of titanium carbide and titanium boride from the elements without applying isostatic pressure. The study was limited to the synthesis of titanium carbide and titanium boride with and without a nickel matrix phase. SHS is now state of the art in the Soviet Union for the production of refractory powders for abrasives and for sintering. The Soviet literature on SHS reports products of higher purity than can be obtained by conventional means. Potential densification is claimed by the addition of an excess of iron. Methods examined include preheating the reaction mixture in an induction furnace, the control of the gas pressure in an autoclave and also the addition of varying amounts of a solvent phase and of excess reactants. The results reported in the Soviet literature cannot be valid; it was found that void free refractory bodies cannot be produced without applying isostatic pressure. The principal value of low pressure SHS is in the synthesis of improved refractory powders. GRA

N87-22857# Air Force Inst. of Tech., Wright-Patterson AFB, Ohio. School of Engineering.

EXAMINATION OF HIGH PERFORMANCE POLYMER FIBERS UNDER COMPRESSIVE DEFORMATION M.S. Thesis

Russell L. Keller Dec. 1986 100 p
(AD-A178640; AFIT/GAE/AA/86D-5) Avail: NTIS HC A05/MF A01 CSCL 11E

High performance polymer fibers are limited in their application due to their relatively low compressive strengths. The Kevlar 49 fiber, for example, has a compressive strength of only twenty percent of its tensile strength. Why does this occur and what mechanism within the fiber is the cause? In order to answer this question, an understanding of the microstructural behavior of the fiber under compression is required. A new technique is developed to study fibers under compression. This is done by embedding a multifilament in an epoxy specimen, having a symmetrically necked cross-section, subjecting it to axial compression, and then examining it using the X-ray diffraction technique. During compression, the deformation of the fibers is a microstructural instability phenomenon known as kink band formation. The X-ray scattering technique is used to determine the molecular structure change in the fibers. A finite element analysis is performed to understand the effect of sample geometry on the axial stress distribution in the fiber. GRA

N87-22858# Cincinnati Univ., Ohio. Dept. of Aerospace Engineering and Engineering Mechanics.

EROSION STUDY OF AM355 AND Al2O3 CERAMICS

W. Tabakoff, A. Hamed, and S. Y. Kang 15 Jan. 1987 94 p
(Contract DAAG29-82-K-0029)
(AD-A178882; Rept-87-58; ARO-18560.30-EG) Avail: NTIS HC A05/MF A01 CSCL 11F

The need for the knowledge and better understanding of material erosion behavior is necessary for the confident use of these materials in future helicopter engines. This investigation presents a detailed study of the erosion behavior of a typical ductile material (steel AM355 alloy) and a nonductile (brittle) material (aluminum oxide). The experimental results show the influence of particle size, particle velocity and temperature on the erosion rate. Electron micrographs of the eroded surfaces under various conditions are presented and compared. Empirical correlations for the erosion results are also presented. GRA

N87-22859# Ultrasystems, Inc., Irvine, Calif. Defense and Space Systems.

PROCESSIBLE BORON NITRIDE PRECERAMIC POLYMERS

K. J. Paciorek, D. H. Harris, W. Krone-Schmidt, and R. H. Kratzer 23 Feb. 1987 19 p
(Contracts N00014-85-C-0659; N00014-82-C-0402)
(AD-A178907; TR-4) Avail: NTIS HC A02/MF A01 CSCL 07C

Synthesis of B-triamino-N-tris(trimethylsily)borazine from the precursor B-trichloro-N-tris(trimethylsilyl)borazine is reported. Thermal condensations of the two borazines are discussed and mechanisms responsible for the results observed are postulated. A structural arrangement for the preceramic polymer obtained from B-triamino-N-tris(trimethylsilyl)-borazine is proposed. Utilization of the above polymer for fiber manufacture, application as fiber coatings and coatings in general are described together with the transformations into boron nitride in ammonia atmosphere. GRA

N87-22860*# National Aeronautics and Space Administration. Lewis Research Center, Cleveland, Ohio.

FRICTION AND WEAR OF SINTERED ALPHA SiC SLIDING AGAINST IN-718 ALLOY AT 25 TO 800 C IN ATMOSPHERIC AIR AT AMBIENT PRESSURE

Daniel L. Deadmore and Harold E. Sliney Jul. 1986 30 p
(NASA-TM-87353; E-3107; NAS 1.15:87353) Avail: NTIS HC A03/MF A01 CSCL 11C

The sliding friction and wear of the SiC-nickel based alloy IN-718 couple under line contact test conditions in atmospheric air at a linear velocity of 0.18 m/sec and a load of 6.8 kg (67N) was investigated at temperatures of 25 to 800 C. It was found that the coefficient of friction was 0.6 up to 350 C then decreased to 0.3 at 500 and 800 C. It is suggested that the sharp decrease in the friction in the range of 350 to 550 C is due to the lubrication value of oxidation products. The wear rate reaches a minimum of 1 x 10 to the -10 to 2 x 10 to the -10 cu cm/cm/kg at 400 to 600 C. Author

N87-22861*# Missouri Univ., Rolla. Dept. of Ceramic Engineering.

CONTAINERLESS PROCESSING OF GLASS FORMING MELTS: D-1, MEA/A-2 EXPERIMENT 81F01 CONDUCTED ON STS-61A FLIGHT, OCTOBER 1985 Final Report

D. E. Day and C. S. Ray 1 Nov. 1986 83 p
(Contract NAS8-34758)
(NASA-CR-179118; NAS 1.26:179118) Avail: NTIS HC A05/MF A01 CSCL 11B

Results of experiment 81F01, which was conducted in the Material Experiment Assembly MEA/A-2 on the D-1 Spacelab Mission (STS-61A), are presented. The general plan of the experiment was to heat, melt, and quench six spherical samples of different glass forming compositions while they were levitated in a single axis acoustic levitator furnace (SAAL). In addition, two non-melting sintered alumina samples were used to check the operational characteristics of the SAAL under reduced gravity conditions. Three of the eight samples were levitated between 1250 and 1500 C before the lack of coolant created an over-temperature condition that caused the SAAL to shut down prematurely. Two of the three samples processed were calcia-gallia-silica and soda-lime-silica glass forming compositions. Evidence of a two to three times increase in the tendency for glass formation was obtained for the calcia-gallia-silica. The final glass appeared reasonably homogeneous even though it was made from hot pressed powders containing deliberate heterogeneities. A photographic record was obtained of the microgravity sample processing sequences. M.G.

28 PROPELLANTS AND FUELS

Includes rocket propellants, igniters, and oxidizers; their storage and handling procedures; and aircraft fuels.

For related information see also *07 Aircraft Propulsion and Power, 20 Spacecraft Propulsion and Power,* and *44 Energy Production and Conversion.*

N87-22862# Systems Research Labs., Inc., Dayton, Ohio.
APPLICATION OF ATOMIC FLUORESCENCE TO MEASUREMENT OF COMBUSTION TEMPERATURE IN SOLID PROPELLANTS Final Report, 1 Aug. 1984 - 31 Jul. 1986
L. P. Goss and A. A. Smith 4 Dec. 1986 66 p
(Contract F49620-83-C-0138)
(AD-A179665; SRL-6809; AFOSR-87-0565TR) Avail: NTIS HC A04/MF A01 CSCL 21I

A method has been developed for nonintrusive collection of surface-temperature data from reactive and nonreactive surfaces. The method relies on the temperature sensitivity of the laser-induced fluorescence of a rare-earth ion which has been seeded into the material under study. The rare-earth ion (dysprosium) doped into a crystal (yttrium-aluminum-garnet) is shown to be an ideal seed, the fluorescence of which is stimulated by the ultra-violet output of a Nd:YAG laser. The fluorescence of the crystal is collected by a linear-array detector, analyzed, and stored for evaluation. Calibration of this method has been made from 300 to 1673 K. Tests have been conducted on reactive and nonreactive surfaces. Additionally, a technique for obtaining temperature depth profiles of reactive materials has been developed, and test results are shown. GRA

N87-22863# Air Force Rocket Propulsion Lab., Edwards AFB, Calif.
AFTERBURNING SUPPRESSION KINETICS Final Report, Mar. 1983 - Feb. 1987
T. S. Singh, D. P. Weaver, and J. D. Eversole Mar. 1987 47 p
(AD-A178967; AFRPL-TR-87-001) Avail: NTIS HC A03/MF A01 CSCL 21B

The inhibition effect of KOH in H2/O2/N2 flames has been studied theoretically. The effect of addition of KOH on laminar burning velocity, peak mole fraction for H and OH, the rate of fuel and oxidizer decay, the rate of production of product species, and the rate of temperature rise has been studied. Computations have been performed for both fuel rich and fuel lean flames. The effect of uncertainties in the data base for rate constants used in the computations has been investigated. Two simplified reaction mechanisms are presented. Comparison of results with experimental data is presented. GRA

N87-22864# Federal Aviation Agency, Atlantic City, N.J. Technical Center.
LABORATORY CHARACTERIZATION TESTS FOR ANTIMISTING FUEL Final Report
Joseph Wilson Mar. 1987 131 p
(DOT/FAA/CT-86/23) Avail: NTIS HC A07/MF A01

Experiments have shown that FM-9 antimisting fuel has the potential for precluding the fine mist and associated fireball generation in aircraft postcrash situations while allowing for the restoration of the filtration and atomizing characteristics required for aircraft operation. Many specialized laboratory characterization tests were developed to evaluate the antimisting properties, the degradability, the composition, and rheological properties of FM-9 antimisting fuel and the physical properties of FM-9 slurry used in the inline blending process for antimisting fuel. All the laboratory characterization tests that were successfully developed and used as a standardized test method are documented. A literature search was done, and a detailed review and analysis of each test method was conducted. This led to the following information: background on the intent and operation of the test method and theory behind the rheological property that the test method is evaluating relative to antimisting fuel; description of the test apparatus along with a general overview of the operational procedure of the test method; equipment specifications for the test apparatus; an accurate and detailed procedure for the test method; and an interpretation of the test results and a discussion of the effectiveness, repeatability, applications, and limitations of the test method. Author

29 MATERIALS PROCESSING

Includes space-based development of products and processes for commercial applications.

For biological materials see *55 Space Biology.*

N87-22865*# Case Western Reserve Univ., Cleveland, Ohio.
THERMOCAPILLARY BUBBLE MIGRATION FOR LARGE MARANGONI NUMBERS Final Report
R. Balasubramaniam May 1987 15 p
(Contract NAG3-567)
(NASA-CR-179628; E-3515; NAS 1.26:179628) Avail: NTIS HC A02/MF A01 CSCL 22A

The thermocapillary motion of spherical bubbles present in an unbounded liquid with a linear temperature distribution, when the Reynolds number and the Marangoni number are large is analyzed. Previous calculations of the terminal velocity performed for this parametric range did not take into complete consideration the thermal boundary layer present near the surface of the bubble. A scaling analysis is presented for this problem. The thermal boundary layer is analyzed by an integral method. The resulting terminal velocity is lower than the one previously calculated, though it is of the same order of magnitude. Author

31 ENGINEERING (GENERAL)

Includes vacuum technology; control engineering; display engineering; cryogenics; and fire prevention.

N87-22866# Atmosphere Furnace Co., Wixom, Pa.
AUSTEMPERED DUCTILE IRON PROCESS DEVELOPMENT Annual Report, Sep. 1985 - Aug. 1986
C. D. Gupta, J. R. Keough, and D. M. Pramstaller Nov. 1986 102 p
(Contract GRI-5085-235-1183)
(PB87-169843; AFC-30001-ANNUAL; GRI-86/0277) Avail: NTIS HC A06/MF A01 CSCL 13H

Pressure from imports and material substitution has severly affected demand for domestic iron industry products. It is estimated that the potential market for Austempered Ductile Iron (ADI) is as large as the market for carburized and/or through hardened forgings. The primary interest in ADI is generated by the economics of process. Improved machinability and reduced processing costs as well as interesting physical properties has created an enormous interest in all metalworking industries towards ADI. The development of gas-fired austempering processes and resoluton of technical and economic uncertainities concerning the process will help improve the outlook for iron founderies. GRA

N87-22867# Texas Univ., Austin. Center for Materials Science and Engineering.
HIGH ENERGY HIGH RATE PULSED POWER PROCESSING OF MATERIALS BY POWDER CONSOLIDATION AND BY RAILGUN DEPOSITION Final Technical Report, 10 Apr. 1985 - 10 Feb. 1987
C. Persad, H. L. Marcus, and W. F. Weldon 31 Mar. 1987 127 p
(Contract N62269-85-C-0222)
(AD-A179289; UT-CMSE-87-02) Avail: NTIS HC A07/MF A01 CSCL 13H

This exploratory research program was initiated to investigate the potential of using pulse power sources for powder consolidation, deposition and other High Energy High Rate Processing. The characteristics of the High Energy High Rate (1MJ/s) powder consolidation using megampere current pulses from a Homopolar Generator, have been defined. Molybdenum Alloy TZM, A Nickel based metallic glass, Copper graphite composites, and P/M Aluminum Alloy X7091 have been investigated. The powder consolidation process produced high densification rates. Density values of 80% to 99% could be obtained with sub second high temperature exposure. Specific energy input and applied pressure were controlling process parameters. Time Temperature Transformation (TTT) concepts underpin a fundamental understanding of pulsed power processing. Deposition experiments were conducted using an exploding foil device (EFD) providing an armature feed to railgun mounted in a vacuum chamber. The material to be deposited - in plasma, gas, liquid or solid state - was accelerated electromagnetically in the railgun and deposited on a substrate. GRA

N87-22868# Rockwell International Corp., Golden, Colo.
CONTROL SYSTEMS DEVELOPMENT, RESEARCH AND DEVELOPMENT Annual Progress Report, Oct. 1983 - Sep. 1984
L. R. Bailey 31 Jul. 1986 27 p
(Contract DE-AC04-76DP-03533)
(DE87-005785; RFP-3814) Avail: NTIS HC A03/MF A01

This report describes design and implementation of several computerized control systems. These implementations include: an ultrasonic weld tester, an automated vacuum oven, a differential pressure gaging system, a die casting control system, a lathe crash prevention and monitoring system, an electric eddy current weld scanner, a bar code scanner, a gage controller, and thermocouple tester. DOE

N87-22869# Rockwell International Corp., Golden, Colo. Space Operations.
HEPA FILTER MONITORING PROGRAM Final Report, September 1985
K. N. Kirchner, C. M. Johnson, W. F. Aiken, J. J. Lucerna, R. L. Barnett, and R. T. Jensen 21 Jul. 1986 22 p
(Contract DE-AC04-76DP-03533)
(RFP-3874) Avail: NTIS HC A02/MF A01

The testing and replacement of HEPA filters, widely used in the nuclear industry to purify process air, are costly and labor-intensive. Current methods of testing filter performance, such as differential pressure measurement and scanning air monitoring, allow determination of overall filter performance but preclude detection of incipient filter failure such as small holes in the filters. Using current technology, a continual in-situ monitoring system was designed which provides three major improvements over current methods of filter testing and replacement. The improvements include: cost savings by reducing the number of intact filters which are currently being replaced unnecessarily; more accurate and quantitative measurement of filter performance; and reduced personnel exposure to a radioactive environment by automatically performing most testing operations. Author

N87-22870*# National Aeronautics and Space Administration. Marshall Space Flight Center, Huntsville, Ala.
MODELING DIGITAL CONTROL SYSTEMS WITH MA-PREFILTERED MEASUREMENTS
Michael E. Polites Jun. 1987 23 p
(NASA-TP-2732; NAS 1.60:2732) Avail: NTIS HC A02/MF A01 CSCL 13H

Three discrete state variable representations are derived for a continuous-time plant driven by a zero-order-hold with a combination of instantaneous measurements and measurements prefiltered by moving-average (MA) digital filters. These representations allow the control system engineer to accurately model plants of this type in a form which permits him to use standard techniques to design digital feedback controllers for them. An example is presented which illustrates how to obtain the coefficient matrices in each representation. Guidelines are presented for choosing the best representation to use for any given point. Author

32 COMMUNICATIONS AND RADAR

Includes radar; land and global communications; communications theory; and optical communications.

For related information see also *04 Aircraft Communications and Navigation* and *17 Space Communications, Spacecraft Communications, Command and Tracking.* For search and rescue see *03 Air Transportation and Safety,* and *16 Space Transportation.*

N87-22871# Stanford Telecommunications, Inc., Reston, Va.
A SYSTEM DESIGN REQUIREMENTS TOOL FOR SATELLITE COMMUNICATIONS THROUGH NUCLEAR-INDUCED SCINTILLATION Final Report, 30 Sep. 1985 - 10 Apr. 1987
Richard S. Orr 10 Apr. 1987 74 p
(Contract F04704-85-C-0147)
(AD-A179272; STI/E-TR-860135; BMO-TR-87-19) Avail: NTIS HC A04/MF A01 CSCL 20N

Nuclear event induced atmospheric scintillation can have an adverse effect on communication systems of all types. Satellite communication systems are particularly susceptible to channel disruption resulting from atmospheric scintillation. This report documents the preliminary results of an effort to develop a tool to assist communication system designers. Various simulation and models attempt to characterize the dynamics of a nuclear perturbed atmosphere. The report focuses on resolving apparent differences of primary interest to the context of Radio Frequency. Phase relationships are addressed relative to a number of commonly used transmission schemes. GRA

N87-22872# Naval Underwater Systems Center, New London, Conn.
ENVELOPE DETECTION OF DISCRETE-TIME BAND-LIMITED SIGNALS USING ANALYTIC SIGNAL REPRESENTATIONS
J. M. Tattersall 6 Feb. 1987 13 p
(AD-A179307; NUSC-TM-861161) Avail: NTIS HC A02/MF A01 CSCL 09D

This memorandum discusses basic concepts relating to analytic signal generation and envelope detection by discrete time methods. The calculation is made of the envelope of a real band pass signal using an analytic signal representation of the signal. Analytic signal representations are common in the development of radar, sonar, and more recently, geophysical signal processing techniques. GRA

N87-22873# Naval Research Lab., Washington, D. C.
WIDEBAND PARALLEL-PLATE WAVEGUIDE, PHASED-ARRAY ANTENNA Final Report
J. B. Rao, S. R. Laxpati, and B. D. Wright 13 Feb. 1987 27 p
(AD-A179402; NRL-9030) Avail: NTIS HC A03/MF A01 CSCL 09E

Presented are the results of experimental studies made on improving bandwidth and scanning range performance of phased array antennas. A parallel plate waveguide element, operating in the S band (2.8 to 4.2 GHz) was used as the radiating element. Such an element permitted the needed less than one-half wavelength interelement spacing for broadband applications and has been found to provide good aperture matching for H plane scanning. The element is fed by a broadband, end on, base fed, coaxial to waveguide transition. H plane waveguide simulators have been used to study aperture match performance and to optimize array parameters to improve bandwidth and scan range. The waveguide simulator results showed that a good aperture match, with voltage standing wave ratio (VSWR) of about 2.1 over a 40% bandwidth and + or - 60 deg scan angle, is achievable for H-plane scanning. Experimentally optimized array parameters are then used to build an 11 x 11 element array. The scanning performance of that array in H and E planes was studied by measuring active element patterns. This does not give precise results, but did show that the aperture match is about equally good, over + or - 60 and 40% bandwidth, for H and E plane scanning. GRA

N87-22874*# National Aeronautics and Space Administration. Lewis Research Center, Cleveland, Ohio.
DETECTION OF REFLECTOR SURFACE ERROR FROM NEAR-FIELD DATA: EFFECT OF EDGE DIFFRACTED FIELD
Alan R. Cherrette, Shong W. Lee (Illinois Univ., Urbana-Champaign.), and Roberto J. Acosta 1987 6 p Presented at the 1987 AP-S International Symposium, Blacksburg, Va., 15-17 Jun. 1987; sponsored by IEEE
(NASA-TM-89920; E-3616; NAS 1.15:89920) Avail: NTIS HC A02/MF A01 CSCL 20N

The surface accuracy of large reflector antennas must be maintained within certain tolerances if high gain/low sidelobe performance is to be achieved. Thus the measurement of the surface profile is an important part of the quality control procedure when constructing antennas of this type. An efficient method for surface profile measurement has been proposed, i.e., the reflector surface is calculated from the measured near-field phase data using the theory of geometric optics. For a surface profile calculation of this kind, it is necessary to know the margin of error built into the method of calculation. This will enable a specification of the tolerance from which the surface profile can be determined. When calculating the surface profile from near-field phase data, there are two main sources of error. The first is the measurement error in near-field phase data. The second arises from the edge diffracted fields that are superimposed on the reflected fields in the measured near-field data. The error in the calculated surface profile produced by the edge diffracted fields is examined. Author

N87-22875# Argonne National Lab., Ill.
THE REGIONAL ELECTROMAGNETICS WORKSHOP IN THE USA
L. R. Turner Nov. 1986 9 p Presented at the International Workshop for Eddy Current Code Comparison, Tokyo, Japan, 20 Dec. 1986
(Contract W-31109-eng-38)
(DE87-004709; CONF-861254-1) Avail: NTIS HC A02/MF A01

At the Second Regional Electromagnetics Workshop, held at Argonne National Laboratory 23 to 24 June 1986, fifteen participants from four countries heard ten presentations on Problems 1, 2, and 6. This note includes information about the workshop and summaries of the results for Problems 1 and 2. DOE

N87-22876# Naval Postgraduate School, Monterey, Calif.
THE EFFECT OF MULTIPATH ON DIGITAL COMMUNICATIONS SYSTEMS: WITH APPLICATION TO SPACE STATION M.S. Thesis
William J. Toti Dec. 1986 98 p
(AD-A178578) Avail: NTIS HC A05/MF A01 CSCL 17B

Analysis of the effect of multipath propagation on digital communications systems was conducted. A brief overview of the root causes of multipath propagation was included in this discussion. Probabilities of error were then derived for a generalized digital communications system experiencing Rician fading due to multipath propagation. Exact results were obtained for equiprobable M-ary Frequency Shift Keyed and M-ary Phase Shift Keyed modulation schemes used to transmit digital data. Furthermore, the probability of error was obtained for a generalized digital communication system experiencing single-bit Intersymbol Interference due to multipath propagation. Finally, the performance of digital communication links for NASA's space station operating in the presence of Intersymbol Interference was evaluated. Results obtained tend to show that severe communication system performance degradation may occur on those links under certain transmitter/receiver and space station geometries. GRA

N87-22877# Air Force Inst. of Tech., Wright-Patterson AFB, Ohio. School of Engineering.
INVESTIGATION OF CONTINUOUSLY VARIABLE SLOPE DELTA (CVSD) MODULATION FOR VOICE COMMUNICATIONS M.S. Thesis
Mark S. Edwards Dec. 1986 175 p
(AD-A178579; AFIT/GE/ENG/86D-52) Avail: NTIS HC A08/MF A01 CSCL 17B

The design of an existing 14 kbps continuously variable slope delta (CVSD) modulation voice communications system is analyzed and documented in an attempt to improve system performance. Design parameters, obtained from the hardware analysis, are used as the input variables to a CVSD computer model which computes output signal-to-noise ratio (SNR). Parameter values are then varied in an attempt to find the setting which produces the best possible SNR for the given data rate. Voice quality is measured using the Diagnostic Rhyme Test for the hardware system operating at various data rates. The results show that data rate and output filter design have the most impact on improving system performance. At the current 14 kbps data, other design parameters have minimal effect on the output SNR. Although noisy, voice quality is acceptable at 14 kbps, but certain consonant sounds, which are distorted by the CVSD processing, could present a problem depending on the system use. Author (GRA)

N87-22878# Air Force Inst. of Tech., Wright-Patterson AFB, Ohio. School of Engineering.
OPTIMIZATION OF THE ANTENNA PATTERN OF A PHASED ARRAY WITH FAILED ELEMENTS M.S. Thesis
Bernard F. Collins, II Dec. 1986 92 p
(AD-A178581; AFIT/GE/ENG/86D-34) Avail: NTIS HC A05/MF A01 CSCL 20N

Using a phased array antenna on a system can add dimensions of flexibility and control. By varying the phase and amplitude of the current exciting each element, the far field antenna pattern can be modified in such a way as to obtain a desired, optimal pattern. The purpose of this thesis is to develop a rapid compensation method for any element failures by varying the currents exciting the remaining elements. Although many methods for optimizing the pattern of a full array are available, this work is unique because it develops methods of finding the optimum pattern of an array which contains failed or missing elements. Optimization methods in the literature which were investigated include thinned array analysis, adaptive array analysis, eigenvalue methods, null displacement techniques, and assorted iterative techniques. Another method discussed in this thesis, the direct technique, originated from the need for a quick optimization method, especially when very large arrays are used. GRA

N87-22879# Ohio State Univ., Columbus. Electroscience Lab.
JOINT SERVICES ELECTRONICS PROGRAM Annual Report, Oct. 1985 - Sep. 1986
Dec. 1986 180 p
(Contract N00014-78-C-0049)
(AD-A178599; ESL-718109-1; AR-9) Avail: NTIS HC A09/MF A01 CSCL 09E

The diffraction studies and the integral equation studies continue to focus on the study of the interaction of electromagnetic energy with penetrable media. GRA

N87-22880# Syracuse Univ., N. Y. Dept. of Electrical and Computer Engineering.
COMPUTER PROGRAM FOR ELECTROMAGNETIC PENETRATION INTO A CONDUCTING CIRCULAR CYLINDER THROUGH A NARROW SLOT, TM CASE Interim Technical Report
Joseph R. Mautz and Roger F. Harrington Feb. 1987 46 p
(Contract DAAG29-84-K-0078)
(AD-A178616; SYRU/DECE/TR-87/1; TR-7; ARO-21378.9-EL) Avail: NTIS HC A03/MF A01 CSCL 20N

A computer program is described and listed which calculates electromagnetic penetration of a TM plane wave into the cylindrical cavity for which rho is less than or = a when the surface (rho = a, phi sub O less than n = phi less than or = 2 pi - rho sub O) is perfectly conducting. Here, rho and phi are cylindrical coordinates. The z directed electric field E sub z in the slot aperture (rho = a, - phi sub less than or = phi less than n = phi sub O) is expressed as a linear combination of 4 even and 4 odd expansion functions. The method of moments is used to obtain the coefficients

of these functions. The elements of the moment matrix are obtained by expressing each expansion function as a Fourier series in phi valid for (0 less than or = phi less than or = 2 pi). Our moment solution remains accurate when the cavity becomes resonant because alternative expansion functions were chosen to prevent the moment matrix from becoming ill-behaved. As the aperture width 2 phi sub O decreases, more and more terms in the Fourier series are needed. Thanks to Debye's asymptotic expansions for Bessel functions, we are able to handle 10,000 terms so as to obtain accurate results for phi sub 0 as small as 1.25 deg.
Author (GRA)

N87-22881# Air Force Inst. of Tech., Wright-Patterson AFB, Ohio. School of Engineering.
SIMULATION MODEL OF A METEOR BURST COMMUNICATION SYSTEM FOR DATA TRANSMISSION PROTOCOL EVALUATION M.S. Thesis
Donald D. Conklin Dec. 1986 233 p
(AD-A178643; AFIT/GE/ENG/86D-29) Avail: NTIS HC A11/MF A01 CSCL 17B

There has been a recent dramatic Air Force interest in meteor burst communications. Due to the ability of a meteor trail to support propagation in the lower VHF band (40 to 100 MHz), it offers the potential for providing relatively survivable communications under disturbed ionospheric conditions. Meteor burst communication system performance and the chances of survivability could be increased if modifications were made in the current data transmission protocol used. A computer simulation model was developed to emulate a high latitude point to point meteor burst communication network. This unique model, written in the Pascal incorporates statistical meteor trial data collected by the High Latitude Meteor Scatter Test Bed, located in Northern Greenland. Measured meteor trail parameters used in the simulation model include average burst durations and interval between bursts for both underdense and oversense type meteor trail occurrences. A description of the developed simulation model is presented, as well as a discussion on how the simulation model was validated and used to test several modifications to the existing data transmission protocol. GRA

N87-22882# Pennsylvania Univ., Philadelphia. Electro-Optics and Microwave-Optics Lab.
STRATEGIES FOR HIGH-RESOLUTION 3-D MILLIMETER WAVE IMAGING Final Report, 15 Aug. 1983 - 31 Oct. 1986
Nabil H. Farhat Feb. 1987 162 p
(Contract DAAG29-83-K-0120)
(AD-A178653; EO/MO-9; ARO-20583.13-EL) Avail: NTIS HC A08/MF A01 CSCL 14E

Two strategies or approaches to millimeter wave (MMW) microwave imaging and recognition are investigated. One approach seeks to produce cost-effective high resolution images of scattering targets and scenes that would resemble as closely as possible their more familiar visual and therefore can be readily recognized and interpreted by a minimally trained observer. In this approach we have extensively studied the principles and methodologies of a 3-D tomographic microwave/MMW diversity imaging where angular, spectral, and polarization degrees of freedom are combined for efficient imaging of remote scattering objects. This work has lead to images with unprecedented quality with near optical resolution employing a unique experimental microwave imaging facility. At such high resolution, image artifact produced by clutter and multiple reflections on the target can be detrimental as these and specially the latter can make the microwave/MMW image depart noticeably in appearance from the visual image in that ghost detail not corresponding to any physical detail on the target can emerge. For this purpose we have conducted a study of the effect of background clutter and multiple reflections on image quality. It was found that microwave/MMW images can be separated from ground or clutter provided that adequate range resolution is available. GRA

N87-22883# Illinois Univ., Urbana. Electromagnetic Communication Lab.
FULL-WAVE ANALYSIS OF ISOLATED AND COUPLED MICROWAVE TRANSMISSION LINES USING THE FINITE ELEMENT METHOD
Zorica Pantic and Raj Mittra Feb. 1987 47 p
(Contract DAAG29-85-K-0183)
(AD-A178805; EMC-87-1; UILU-ENG-87-2542; ARO-22634.5-EL)
Avail: NTIS HC A03/MF A01 CSCL 09A

This paper describes a finite element approach to a hybrid-mode analysis of isolated and coupled microwave transmission lines. Both the first and higher-order ordinary elements, as well as singular and infinite elements, are used to solve for the eigenvalues and eigenvectors of the modes propagating along the line. Once the field distribution in the cross section of the line is known the characteristic impedance of the dominant mode propagating along the line can readily be obtained. A perturbational approach is developed for estimating the losses due to conductor and dielectric dissipation and computing the attenuation constant for each mode. Lines treatable by this method may contain an arbitrary number arbitrarily shaped conductors, including a system of conductors either placed above a single ground plane or between two parallel ground planes, and inhomogeneous dielectric regions that can be approximated locally by a number of homogeneous subregions. The results obtained using the finite element procedure have been compared for various types of microwave transmission lines and have been found to agree well with available data. Author (GRA)

N87-22884# Air Force Inst. of Tech., Wright-Patterson AFB, Ohio. School of Engineering.
ANALYSIS OF LIGHTNING INDUCED MAGNETIC FIELD PENETRATION THROUGH PROTECTIVE METAL SCREENS USING AN EQUIVALENT MAGNETIC DIPOLE MOMENT REPRESENTATION OF AN ARRAY OF ELLIPTIC APERTURES M.S. Thesis
James L. ONeal Dec. 1986 126 p
(AD-A178850; AFIT/GE/ENG/86D-30) Avail: NTIS HC A07/MF A01 CSCL 20N

This investigation analyzed lightning induced magnetic field penetration through protective metal screens using an equivalent magnetic dipole moment representation of an array of elliptic apertures. Two metal screens with differing aperture sizes were modeled. Experiments, using lightning level currents, measured the magnetic field penetration through each screen. A comparison of model versus experimental results was performed. The effect of decreasing mesh sizes on field penetration is also presented. The analysis used linear superposition to sum the contributions from the magnetic dipole moment equivalent of each screen aperture. A computer program was developed to the number of screen model. Results indicate that the model is accurate in predicting the interior magnetic field decay rate with distance from the screen and in accounting for the increased protection provided by decreasing mesh sizes. The only model inaccuracies are the overestimates for interior magnetic field strengths. The overall results indicate that an equivalent magnetic dipole moment representation can be used to model lightning induced magnetic field penetration through protective metal screens. GRA

N87-22885# Air Force Inst. of Tech., Wright-Patterson AFB, Ohio. School of Engineering.
MULTIPLE ANGLE OF INCIDENCE MEASUREMENT TECHNIQUE FOR THE PERMITTIVITY AND PERMEABILITY OF LOSSY MATERIALS AT MILLIMETER WAVELENGTHS M.S. Thesis
John C. Joseph Dec. 1986 104 p
(AD-A178851; AFIT/GE/ENG/86D-58) Avail: NTIS HC A06/MF A01 CSCL 20C

A technique of measuring the permittivity and permeability of lossy, homogeneous, linear, isotropic materials at millimeter wavelengths was developed. The technique was tested by measurement of representative materials at a frequency of 94 GHz. For the type of materials under consideration, the permittivity and permeability are complex and general. Thus there are four unknowns to be determined and a minimum of four measurements are required. The approach taken was to measure the magnitude of the transmission coefficient of a planar material sample in free space at multiple angles of incidence. The system of equations obtained from any four of the angles is solved numerically for the permittivity and permeability of the sample. The equipment consisted primarily of a Gunn phase-locked millimeter-wave oscillator, a pair of conical horn/lens antennae, a sample holder/positioner, and a microwave receiver. Harmonic mixing was employed to convert the test waveform to the operating range of the receiver. GRA

N87-22886# Air Force Inst. of Tech., Wright-Patterson AFB, Ohio. School of Engineering.

FULL POLARIMETRIC NON-SPECULAR SCATTERING OF FLAT PLATE STRUCTURES M.S. Thesis

Jeffrey L. Fath Dec. 1986 109 p
(AD-A178853; AFIT/GE/ENG/86D-26) Avail: NTIS HC A06/MF A01 CSCL 17I

This thesis examined the electromagnetic scattering of a dihedral corner reflector for both monostatic and bistatic source-receiver geometries. The full polarization characteristics of the electromagnetic scattering was maintained while the dihedral corner reflector was modeled on and off the principal (horizontal reference) plane. The dihedral corner reflector was composed of two perfectly conducting 9 inch square flat plates joined along a common edge so that they formed an interior angle of 90 degrees. The frequencies of interest included 2, 3, and 10 GHz. THe theoretical modeling utilized the Uniform Theory of Diffraction and the Method of Moments (MOM). The analysis was performed on a Cray X-MP supercomputer and a VAX 11/785 minicomputer. The results from the models were compared with each other, and with measurements for validation. The measurements were taken on the principal plane for same sense and cross polarization components. The MOM model compared well with measurement for the monostatic and bistatic same sense polarization components. However, differences were noted for the cross polarization component comparison. The MOM model was then extended to off principal plane geometries, which was not measured. A substantial amount of cross polarization scattering was predicted for off principal plane geometries. Author (GRA)

N87-22887# Air Force Inst. of Tech., Wright-Patterson AFB, Ohio. School of Engineering.

CHARACTERIZATION OF THE ERROR PERFORMANCE OF A QPSK (QUADRATURE PHASE SHIFT KEYED) COMMUNICATION SYSTEM IN THE PRESENCE OF LINEAR TRANSMISSION DISTORTION M.S. Thesis

Robert S. Horton Nov. 1986 105 p
(AD-A178855; AFIT/GE/EE/86D-31) Avail: NTIS HC A06/MF A01 CSCL 09D

The purpose of this study was to investigate the effects of linear transmission distortion on a Quadrature Phase Shift Keyed communication system and to calculate the probability of error for a given amount of distortion with different signal-to-noise ratios. The baseband QPSK system was designed to eliminate all intersymbol interference that did not result from distortion or additive white Gaussian noise. The types of transmission distortion investigated were linear amplitude, linear delay, and quadratic delay distortion. Each type of distortion is discussed and modeled. From a range of signal-to-noise ratios, for the given distortion values, a bit error rate is determined. Two types of bit error rates are used. One is the worst case, upper bound, a pessimistic bound that can not be exceeded. The other, is an average probability of error determined by use of center of mass methods. This method provides a bit error rate that may be exceeded but gives an overall first look at the probability of error for that SNR and distortion type and level. The graphs that resulted allow for quick reference of the bit error rate for a range of SNR's at differing values of linear amplitude, linear delay and quadratic delay distortion. GRA

N87-22888# Air Force Inst. of Tech., Wright-Patterson AFB, Ohio. School of Engineering.

DEVELOPMENT OF A MICROCOMPUTER-BASED WORKSTATION FOR ANALYSIS OF DIGITAL SATELLITE LINKS M.S. Thesis

William C. Jackson Dec. 1986 175 p
(AD-A178872; AFIT/GE/ENG/86D-36) Avail: NTIS HC A08/MF A01 CSCL 17B

The product of this thesis is a comprehensive and integrated software package for the analysis of digital satellite links. The system is designed to run on the IBM PC, and should also run on most compatibles. The system performs three basic classes of functions: satellite orbital analysis, antenna gain pattern plotting, and link analysis. The first class includes the computation of such quantities as velocity, orbital period, and coverage area for satellites in circular and elliptical orbits. The second class is concerned with plotting the gain patterns for horns, helixes, parabolic reflectors, and phased arrays of dipoles. The last class represents the major thrust of the system, and entails computing such items as the G/T figure of merit, received useful power, carrier-to-noise ratio, bit error rate, maximum data rate, and power margin. Inherent within this class are mathematical models for computing the attenuation due to rainfall and atmospheric absorption. The link budget itself appears as a color-coded display with two columns: one for the uplink path, and one for the downlink path. The user also has the capability to change certain key inputs, and then have the system automatically recompute the entire link budget with the modified data. Author (GRA)

N87-22889# Ohio State Univ., Columbus. Electroscience Lab.

RADAR TARGET CLASSIFICATION STUDIES Final Report

E. K. Walton, F. D. Garber, D. L. Moffatt, A. J. Kamis, and N. Chamberlain Nov. 1986 184 p
(Contract N00014-85-K-0321)
(AD-A179010; ESL-717220-1) Avail: NTIS HC A09/MF A01 CSCL 17I

Described is the second year of research for the Naval Weapons Center (NWC) in which radar target classification techniques utilizing the resonance region are under investigation. Three specific topics are covered. First, the behavior of the resonance region data base classification algorithms with respect to the polarization state of the radar are studied in detail, including statistical studies of the relative disadvantages of a number of particular polarization states. Also in this part, the polarization of the signal returned from the target is processed by transformation to time domain so that a polarization transient signature is derived. This signature forms the basis of a syntactical target classification concept. Secondly, the complex natural resonance behavior of the signal scattered from the target is studied as a function of polarization. Finally, the features utilized in the classification algorithm are studied to produce an optimization of the feature set from the point of view of the interrogating radar. GRA

N87-22890*# Stanford Univ., Calif. Computer Systems Lab.

CONCURRENT COMMUNICATION AMONG MULTI-TRANSCEIVER STATIONS OVER SHARED MEDIA Ph.D. Thesis

Yitzhak Birk Mar. 1987 218 p Sponsored in part by an IBM Graduate Fellowship
(Grants NAG2-292; NAGw-419)
(NASA-CR-180935; NAS 1.26:180935; CSL-TR-87-321) Avail: NTIS HC A10/MF A01 CSCL 17B

In order to increase a local-area network's throughput beyond a single bus data rate without using dedicated switching nodes, multiple buses and multitransceiver stations are required. The design space of single-hop interconnections is explored among such stations. Interconnections are presented whose throughput can grow quadratically with the number of transmitters and receivers per station. These are referred to as selective broadcast interconnections (SBIs). The performance of various SBIs are studied. A spread-spectrum channel can accommodate several current successful transmission, and a single-transceiver node can thus utilize only a small fraction of the channel capacity. In order to allocate the appropriate fraction of capacity to a busy node, it is proposed to equip it with several transmitters and receivers, thereby turning it into a supernode. Several architectures and operation policies for supernodes are suggested and compared. It is shown that a supernode can significantly outperform a collection of independent conventional nodes with the same total numbers of transmitters and receivers. Packet-radio networks with half-duplex nodes, as well as networks with full-duplex nodes, are considered. B.G.

N87-22610*# Ohio Univ., Athens.
DIGITAL AUTONOMOUS TERMINAL ACCESS COMMUNICATION (DATAC) SYSTEM
Stanley M. Novacki, III *In* NASA. Langley Research Center Joint University Program for Air Transportation Research, 1984 May 1987 p 49-56 (For primary document see N87-22604 16-01)
Avail: NTIS HC A08/MF A01 CSCL 17B

N87-22611*# Ohio Univ., Athens.
FIBER OPTIC DATA TRANSMISSION
Steven T. Shreve *In* NASA. Langley Research Center Joint University Program for Air Transportation Research, 1984 May 1987 p 57-59 (For primary document see N87-22604 16-01)
Avail: NTIS HC A08/MF A01 CSCL 17B

N87-22615*# Ohio Univ., Athens.
GPS ANTENNA DESIGNS
Samuel J. P. Laube *In* NASA. Langley Research Center Joint University Program for Air Transportation Research, 1984 May 1987 p 73-76 (For primary document see N87-22604 16-01)
Avail: NTIS HC A08/MF A01 CSCL 17B

N87-23441*# Hawaii Inst. of Geophysics, Honolulu. Planetary Geosciences Div.
NEW VERY HIGH RESOLUTION RADAR STUDIES OF THE MOON
Peter J. Mouginis-Mark and Bruce Campbell *In* NASA, Washington Reports of Planetary Geology and Geophysics Program, 1986 May 1987 p 237 (For primary document see N87-23341 16-91)
Avail: NTIS HC A24/MF A01 CSCL 17I

N87-23444*# Jet Propulsion Lab., California Inst. of Tech., Pasadena.
GOLDSTONE RADAR OBSERVATIONS OF MARS: THE 1986 OPPOSITION
T. W. Thompson *In* NASA, Washington Reports of Planetary Geology and Geophysics Program, 1986 May 1987 p 243-244 (For primary document see N87-23341 16-91)
Avail: NTIS HC A24/MF A01 CSCL 17I

N87-23445*# Colorado Univ., Boulder. Lab. for Atmospheric and Space Physics.
A DIFFUSE RADAR SCATTERING MODEL FROM MARTIAN SURFACE ROCKS
W. M. Calvin, B. M. Jakosky, and P. R. Christensen (Arizona State Univ., Tempe.) *In* NASA, Washington Reports of Planetary Geology and Geophysics Program, 1986 May 1987 p 245-247 (For primary document see N87-23341 16-91)
Avail: NTIS HC A24/MF A01 CSCL 17I

N87-23446*# Jet Propulsion Lab., California Inst. of Tech., Pasadena.
MARS: SEASONALLY VARIABLE RADAR REFLECTIVITY
L. E. Roth, R. S. Saunders, and T. W. Thompson *In* NASA, Washington Reports of Planetary Geology and Geophysics Program, 1986 May 1987 p 248-250 (For primary document see N87-23341 16-91)
Avail: NTIS HC A24/MF A01 CSCL 17I

N87-23448*# Stanford Univ., Calif. Center for Radar Astronomy.
APPLICATION OF NUMERICAL METHODS TO PLANETARY RADIOWAVE SCATTERING
Richard A. Simpson and G. Leonard Tyler *In* NASA, Washington Reports of Planetary Geology and Geophysics Program, 1986 May 1987 p 253 (For primary document see N87-23341 16-91)
Avail: NTIS HC A24/MF A01 CSCL 20N

33 ELECTRONICS AND ELECTRICAL ENGINEERING

Includes test equipment and maintainability; components, e.g., tunnel diodes and transistors; microminiaturization; and integrated circuitry.

For related information see also *60 Computer Operations and Hardware* and *76 Solid-State Physics.*

N87-22891# Alzeta Corp., Santa Clara, Calif.
CATALYTIC RADIANT TUBE. PHASE 2: PROOF OF CONCEPT Topical Report, Feb. - Aug. 1986
J. Lannutti, R. Schreiber, and R. Tidball Sep. 1986 62 p
(Contract GRI-5086-234-1257)
(PB87-169835; ALZETA-86-722-129; GRI-86/0267) Avail: NTIS HC A04/MF A01 CSCL 09A

The results of Phase 2 research on a radiant tube burner are described. The gas-fired radiant tube concept employs a combustion catalyst, such as platinum, that is coated on the inside surface of a ceramic tube. A preheated, combustible mixture of gas and air passing through the tube burns catalytically on the tube surface. Some of the heat generated conducts through the wall and is transmitted by radiation from the outside surface to the heat sink. When commercialized, the concept could be used in place of the currently popular electric resistance elements. Advantages over existing gas-fired radiant tubes include more uniform tube heating and low NO(sub x) emissions. Phase 2 work was focused on identification of problems associated with these catalysts during prolonged exposure to the surface combustion environment. During the phase, silicon carbide, alumina, and mullite tubes were catalyzed with combinations of platinum and metal oxides and operated in a laboratory combustion test apparatus. The SEM and EDAX post-test analysis indicated that most of the oxides used were severly degraded during their exposure. Performance data indicated a general decrease in combustion efficiency over time. GRA

N87-22892# Department of Energy, Washington, D. C.
LITHIUM DISULFIDE BATTERY Patent Application
T. D. Kaun, inventor (to DOE) (Argonne National Lab., Ill.) 29 May 1986 24 p
(Contract W-31109-eng-38)
(DE87-007183; US-Patent-Appl-SN-868388) Avail: NTIS HC A02/MF A01

Disclosed is a negative electrode-limited secondary electrochemical cell having dense FeS2 positive electrode operating exclusively on the upper plateau, a Li alloy negative electrode and a suitable lithium-containing electrolyte. The electrolyte preferably is 25 mole % LiCl, 38 mole % LiBr and 37 mole % KBr. The cell may be operated isothermally. DOE

N87-22893# Department of Energy, Washington, D. C.
BIPOLAR BATTERY WITH ARRAY OF SEALED CELLS Patent Application
T. D. Kaun and J. A. Smaga, inventors (to DOE) (Argonne National Lab., Ill.) Jul. 1986 20 p
(Contract W-31109-eng-38)
(DE87-007194; US-Patent-Appl-SN-883216) Avail: NTIS HC A02/MF A01

A lithium alloy/metal sulfide battery as a dipolar battery is disclosed with an array of stacked cells with the anode and cathode electrode materials in each cell sealed in a confining structure and separated from one another except across separator material interposed therebetween. The separator material is contained in a module having separate perforated metallic sheets that sandwich opposite sides of the separator material for the cell and an annular insulating spacer that surrounds the separator material beyond the perforations and is also sandwiched between and sealed to the sheets. The peripheral edges of the sheets project outwardly beyond the spacer, traverse the side edges of the adjacent electrode material to form cup-like electrode holders, and are fused to the adjacent current collector or end face members of the array. Electrolyte is infused into the electrolyte cavity through the perforations of one of the metallic sheets with the perforations also functioning to allow ionic conductance across the separator material between the adjacent electrodes. A gas-tight housing provides an enclosure of the array. DOE

N87-22894* National Aeronautics and Space Administration. Pasadena Office, Calif.
METHOD AND APPARATUS FOR MEASURING MINORITY CARRIER LIFETIME IN A DIRECT BAND-GAP SEMICONDUCTOR Patent
Oldwig vonRoos, inventor (to NASA) (Jet Propulsion Lab., California Inst. of Tech., Pasadena.) 28 Apr. 1987 12 p Filed 18 Dec. 1984 Supersedes N85-20251 (23 - 11, p 1628)
(NASA-Case-NPO-16337-1-CU; US-Patent-4,661,770; US-Patent-Appl-SN-683111; US-Patent-Class-324-158-D; US-Patent-Class-324-158-R) Avail: US Patent and Trademark Office CSCL 09A

A direct band-gap semiconductor is exposed to intensity-modulated photon radiation having a characteristic energy at least as great as the energy gap of the semiconductor. This produces a time dependent concentration of excess charge carriers through the material, producing a luminescence signal modulated at the same frequency as the incident radiation but shifted in phase by an amount related to the lifetime of minority carriers. In a preferred embodiment, the phase shift of the luminescence signal is determined by transforming it to a modulated electrical signal and mixing the electrical signal with a reference signal modulated at the same frequency and having a phase which is known relative to the incident radiation. Minority carrier lifetime is calculated by integrating a direct current component of the mixed signal (F sub dc) over a 2 pi range in phase of the reference signal.
Official Gazette of the U.S. Patent and Trademark Office

N87-22895* National Aeronautics and Space Administration. Goddard Space Flight Center, Greenbelt, Md.
PROGRAMMABLE ELECTRONIC SYNTHESIZED CAPACITANCE Patent
Leonard L. Kleinberg, inventor (to NASA) 17 Feb. 1987 7 p Filed 15 Jul. 1985 Supersedes N86-20679 (24 - 11, p 1765)
(NASA-Case-GSC-12961-1; US-Patent-4,644,306; US-Patent-Appl-SN-754707; US-Patent-Class-333-214; US-Patent-Class-307-490; US-Patent-Class-330-107; US-Patent-Class-330-294; US-Patent-Class-331-177-R; US-Patent-Class-333-217) Avail: US Patent and Trademark Office CSCL 09A

A predetermined and variable synthesized capacitance which may be incorporated into the resonant portion of an electronic oscillator for the purpose of tuning the oscillator comprises a programmable operational amplifier circuit. The operational amplifier circuit has its output connected to its inverting input, in a follower configuration, by a network which is low impedance at the operational frequency of the circuit. The output of the operational amplifier is also connected to the noninverting input by a capacitor. The noninverting input appears as a synthesized capacitance which may be varied with a variation in gain-bandwidth product of the operational amplifier circuit. The gain-bandwidth product may, in turn, be varied with a variation in input set current with a digital to analog converter whose output is varied with a command word. The output impedance of the circuit may also be varied by the output set current. This circuit may provide very small ranges in oscillator frequency with relatively large control voltages unaffected by noise.
Official Gazette of the U.S. Patent and Trademark Office

N87-22896# Air Force Systems Command, Wright-Patterson AFB, Ohio. Foreign Technology Div.
KLYSTRON TRANSMITTERS
A. Z. Khaykov 20 Mar. 1987 132 p Transl. into ENGLISH of the mono. "Klystronnyye Peredatchiki" Moscow, USSR, Svyaz, 1967 p 1-63
(AD-A179068; FTD-ID(RS)T-1312-86) Avail: NTIS HC A07/MF A01 CSCL 09E

In contemporary powerful transmitters of decimeter and microwaves multicavity floating klystrons extensively are used. Such klystrons have output power from several watts to tens of kilowatts in the regime of continuous oscillations and to tens of megawatts in pulsed operation. They find basic use as the final stages of transmitters. Large amplification, characteristic to klystrons with four and more cavities (more than 30 dB), leads from previous stages of transmitter work on considerably smaller power level. The construction of these stages is simplified thereby and their energy indices to a small degree affect overall efficiency of transmitter. The qualitative characteristics of the transmitter are also in essence determined by the characteristics of the final stage on the klystron. Therefore, examining the work of klystron transmitters, first of all one should be acquainted with the special features of the multiple cavity klystrons, their parameters and characteristics. In this brochure principles of operation of floating klystrons in final stages of powerful transmitters are stated.
GRA

N87-22897# Massachusetts Inst. of Tech., Cambridge. Microsystems Research Center.
A COHERENT VLSI ENVIRONMENT Semiannual Technical Report, 1 Oct. 1986 - 31 Mar. 1987
Paul Penfield, Jr., William J. Dally, Lance A. Glasser, Thomas F. Knight, Jr., and F. T. Leighton 31 Mar. 1987 84 p
(Contract N00014-80-C-0622; ARPA Order 3872)
(AD-A179303) Avail: NTIS HC A05/MF A01 CSCL 09E

It is important to know how fast a rise time can be achieved, or at what frequencies unwanted oscillations might occur. A set of necessary and sufficient bounds are now possible, in the sense that every point in the s-plane can be easily discovered to be either a frequency at which oscillation cannot occur with any possible combination of components and ideal transformers, or else a point at which a circuit consisting of a few such components and ideal transformers can be made to oscillate. The inclusion of ideal transformers is necessary since otherwise generally only a finite or countable number of natural frequencies can be found. Many new results have been derived for parallel algorithms and complexity, such as a hypercube with a large number of faulty nodes can be used, with high probability, as another perfectly functioning hypercube of half the size, by using reconfiguration algorithms that are simple, fast, and require only local information. The design of a message-driven processor continues. It is now being realized that many different highly parallel architectures require roughly the same sort of processing node, one that can respond quickly (i.e., with low latency) to messages that may require execution of a few (say about ten) instructions. The processor being designed can be considered an experiment in unifying message passing and shared memory architectures. GRA

N87-22898# Air Force Inst. of Tech., Wright-Patterson AFB, Ohio. School of Engineering.
MODELING AND SIMULATION OF THE WFTA (WINOGRAD FOURIER TRANSFORM ALGORITHM) 16 PFA (PRIME FACTOR ALGORITHM) PROCESSOR USING THE VHSIC (VERY HIGH SPEED INTEGRATED CIRCUIT) HARDWARE DESCRIPTION LANGUAGE, VOLUME 1 M.S. Thesis
Charles H. Cooper Dec. 1986 88 p
(AD-A179344; AFIT/GE/ENG/86D-44-Vol-1) Avail: NTIS HC A05/MF A01 CSCL 12A

The VHSIC Hardware Description Language (VHDL) is applied to the problem of modeling and simulating VLSI CMOS components of the WFTA 16 PFA processor. The 16-point PFA processor is one of three PFA processors under design and development for the implementation of the 4080-point PFA pipeline processor by the VLSI design group at the Air Force Institute of Technology. The PFA processor is modeled by applying the hierarchical facilities of the VHDL language to form the top level register component descriptions from combinations of the primary building block hardware element descriptions. Two simple VHDL simulations are performed using the beta test versions of the VHDL simulator and support environment. The simple component simulations are performed on a VHDL Behavioral description of the Parallel-In, Serial-Out register cell and a VHDL structural description of a dynamic MSFF. GRA

N87-22899# Air Force Inst. of Tech., Wright-Patterson AFB, Ohio. School of Engineering.

THE TRANSVERSE DYNAMICS OF SPACE-CHARGE LIMITED DIODES M.S. Thesis

Thomas M. Schaefer Dec. 1986 64 p
(AD-A179389; AFIT/GEP/ENP/86D-10) Avail: NTIS HC A04/MF A01 CSCL 09A

This work critically reviews past analyses of the transverse dynamics in planar space-charge limited diodes. The electrostatic boundary conditions of the diode and their effects on the space-charge are examined. The transverse electric field produced by the space-charge and surface charges are found to be small, in agreement with the assumptions of previous analyses. The diodes used in the Aurora Krypton Flourine excimer laser system provide a baseline for the parameters of this analysis. The relativistic treatment of Belov is extended to predict the transverse constriction of the space-charge trajectories. We derive a simple formula for the amount of constriction by two methods. The relativistic equation agrees with the non-relativistic calculation in the low energy limit. Finally, we derive a formula for the trajectories in the presence of an applied axial magnetic field. GRA

N87-22900# Missouri Univ., Rolla.

RELIABILITY STUDIES OF CERAMIC CAPACITORS Annual Progress Report, 1 Oct. 1984 - 31 Dec. 1986

H. U. Anderson Mar. 1987 156 p
(Contract N00014-82-K-0294)
(AD-A179436) Avail: NTIS HC A08/MF A01 CSCL 09A

This report covers the last year of a contract which studied low voltage degradation, the TSPC/DC spectra of Barium Titanate , and the dielectric and electrical properties of BaTiO3 composites (polymer and air) and the first one and one half years of a project which focussed on: (1) measurements on commercially available relaxor type dielectrics, and (2) organometallic processed relaxor dielectrics synthesis, fabrication and measurement. The measurements to be made are electrical conductivity, dielectric properties, and current-time voltage behavior as a function of chemical composition, temperature, and humidity. GRA

N87-22901# California Univ., Los Angeles. Dept. of Electrical Engineering.

FERROELECTRIC OPTICALLY CONTROLLED MILLIMETER-WAVE DEVICES Final Report, 1 May 1984 - 31 Jul. 1986

H. R. Fetterman 1986 19 p
(Grant AF-AFOSR-0119-84)
(AD-A179524; AFOSR-87-0455TR) Avail: NTIS HC A02/MF A01 CSCL 20F

New materials were tested at cryogenic temperatures for use as modulators, phase shifters and beam steerers of millimeter wave radiation. Cryogenic cooling drastically reduced the absorption and allowed measurement of large electro-optic coefficients at frequencies between 60 and 110 GHz. GRA

N87-22902# Stanford Univ., Calif. Dept. of Materials Science and Engineering.

FUNDAMENTAL STUDIES OF THE MECHANICAL BEHAVIOR OF MICROELECTRONIC THIN FILM MATERIALS Annual Report, 1 Nov. 1985 - 31 Oct. 1986

William D. Nix Mar. 1987 50 p
(Grant AF-AFOSR-0051-86)
(AD-A179699; AFOSR-87-0411TR) Avail: NTIS HC A03/MF A01 CSCL 09E

Research on the mechanical properties of microelectronic thin film materials has been initiated at Stanford University. In this Interim Scientific Report, the progress made during the first year of the program is reviewed, especially in the development of new experimental techniques for measuring mechanical properties. The primary motivation of this work is to understand the mechanical properties of microelectronic thin film materials. Although these materials are not structural materials as such, they are, nevertheless, expected to withstand very high stresses, both during manufacturing and in service. As a consequence, the mechanical properties of materials are almost as important as their electronic properties for successful device applications. Because these materials often exist only as thin films bonded to substrates, it is necessary to study their mechanical properties in that state. Much of this program deals with the development of techniques and methods for studying these properties. Also, these techniques are used to measure various thin film mechanical properties and efforts are being made to understand these in fundamental terms. GRA

N87-22903# Sandia National Labs., Albuquerque, N. Mex.

EXTRINSIC GETTERING FOR VLSI/ULSI PROCESSES

J. W. Medernach and L. L. Witherspoon 1987 2 p Presented at the 171st Electrochemical Society Meeting, Philadelphia, Pa., 10 May 1987 Prepared in cooperation with KMI, Inc., Albuquerque, N. Mex.
(Contract DE-AC04-76DP-00789)
(DE87-002696; SAND-86-1945C; CONF-870513-1) Avail: NTIS HC A02/MF A01

Gettering techniques are employed to reduce metallic impurities that can be accumulated during device processing. The removal of these metallic impurities from active device regions improves device yield, oxide integrity, and other device parameters. Intrinsic (IG) and extrinsic (EG) gettering techniques are reported to be effective, but may not be as effective for small geometry processing because of possible problems regarding reproducibility and uniformity of oxygen precipitation phenomena. The object of this investigation was to develop an EG technique in which a uniform internal defect formation is formed for a n/n+ epitaxial structure. The use of medium and high oxygen content n+ substrates with and without poly/nitride EG layers for a 2.0 micron to 1.0 micron p-well CMOS process is reported. DOE

N87-22904# Argonne National Lab., Ill.

LITHIUM-METAL SULFIDE BATTERY DEVELOPMENT AND SUBMODULE DEMONSTRATION

A. A. Chilenskas, R. L. Biwer, and W. H. DeLuca 1986 9 p Presented at the 8th International Electric Vehicle Symposium, Washington, D.C., 20 Oct. 1986
(Contract W-31109-eng-38)
(DE87-004819; CONF-8610122-9) Avail: NTIS HC A02/MF A01

A program has been initiated by the Electric Power Research Institute to examine the feasibility of using the Li-alloy/FeS battery for electric-vehicle propulsion. In the first phase of the program, a joint effort between Argonne National Laboratory and Gould Research Center resulted in the design, fabrication, and testing of two full-scale 12-V modules and related battery components at Argonne National Battery Test Laboratory. The design of the module and battery components was based upon a van battery design study supported by the US Department of Energy. DOE

N87-22905# Lawrence Livermore National Lab., Calif.

SILICON PULSE SHARPENING DIODES: SWITCHING KILOVOLTS IN 10's OF PICOSECONDS

M. D. Pocha, J. D. Wiedwald, C. G. Dease, and M. M. Contreras Jan. 1987 6 p Presented at the IEEE/OSA Topical Meeting on Picosecond Electronics and Optoelectronics, Lake Tahoe, Nev., 14 Jan. 1987 Prepared in cooperation with New Mexico Univ., Albuquerque
(Contract W-7405-eng-48)
(DE87-005073; UCRL-95276; CONF-870114-3) Avail: NTIS HC A02/MF A01

Numerical analysis was used to determine the physical mechanisms involved in silicon switching diodes. Plots of values for free carrier densities, current density, electric field, etc. were used in visualizing the operation of these devices. It is concluded that the large initial electric field present in the diode is responsible for its behavior. DOE

N87-22906# Oak Ridge National Lab., Tenn.
GAS MIXTURES FOR SPARK GAP CLOSING SWITCHES WITH EMPHASIS ON EFFICIENCY OF OPERATION
L. G. Christophorou, D. L. McCorkle, and S. R. Hunter 1987 9 p Presented at the 5th International Symposium on Gaseous Dielectrics, Knoxville, Tenn., 3 May 1987 Prepared in cooperation with Tennessee Univ., Knoxville.
(Contract DE-AC05-84OR-21400)
(DE87-006624; CONF-870516-2) Avail: NTIS HC A02

The efficient operation of a spark gap closing switch requires a gaseous medium with large breakdown strength, low conduction voltage, and a short formative time lag. Gas properties necessary to achieve these requirements are identified and discussed. Based on available knowledge of such properties, a number of binary (e.g., c-C4F8, or 1-C3F6, or n-C4F10, or C3F8, or C6F6 in Ar or He or H2) and ternary gas mixtures (e.g., c-C4F8, or n-C4F10, or C3F8 in Ar or He + C2H2 or another low ionization onset additive) have been identified which may be suitable for use in spark gap closing switches. DOE

N87-22907# Varian Associates, Palo Alto, Calif.
DESIGN AND OPERATION OF 140 GHz GYROTRON OSCILLATORS FOR POWER LEVELS UP TO 1 MW CW
H. Jory, R. Bier, L. J. Craig, K. Felch, L. Ives, N. Lopez, and S. Spang Dec. 1986 7 p Prepared in cooperation with Lawrence Livermore National Lab., Calif.
(Contract W-7405-eng-48)
(DE87-006683; UCRL-15871) Avail: NTIS HC A02

Varian has designed and tested 140 GHz gyrotron oscillators that have generated output powers of 100 kW CW and 200 kW for 1 ms pulses. Upcoming tubes will be designed to operate at power levels of 200 kW CW and ultimately up to 1 MW CW. The important design considerations which are addressed in the higher power tubes include the design of the electron gun, interaction circuit, and output window. These issues will be discussed and the results of the earlier 140 GHz gyrotron work at Varian will be summarized. DOE

N87-22908# California Univ., Berkeley.
AN INVESTIGATION OF ZINC ELECTRODES RELEVANT TO ZINC-AIR BATTERIES Ph.D. Thesis
H. S. Choi Dec. 1986 83 p
(Contract DE-AC03-76SF-00098)
(DE87-007607; LBL-22705) Avail: NTIS HC A05/MF A01

The particulate electrode (fluidized bed electrode or moving bed electrode) was studied to evaluate its possible application to energy storage. The first part of this study is concerned with the effect of current fluctuation on the morphology of zinc electrodeposited on the rotating disc electrode from alkaline zincate electrolyte. The effect of the fluctuation on the morphology was examined by scanning electron microscopy. The deposits under the condition of fluctuating current density were smoother than those formed under constant current density. The second part is concerned with the electrodeposition of zinc from alkaline electrolyte with the cell employing a fluidized bed electrode which simulates the recharge process of the secondary battery employing a particulate electrode. Except at high current density, energy consumption per unit production was less than 3 to 4 kWh/kg which is the characteristic value of conventional electrowinning from acidic solution. A laboratory cell with a particulate zinc electrode and an air counter electrode was constructed and discharge characteristics were studied to evaluate the cell. Energy efficiencies during discharge at 5 and 2.5 A were about 20 and 30% respectively. DOE

N87-22909# Utah Univ., Salt Lake City. Microwave Device and Physical Electronics Lab.
WAVEGUIDE JUNCTION ANALYSIS INVOLVING ASYMMETRICAL MODES Final Technical Report, Sep. 1982 - Sep. 1985
Cyrus N. Tau Sep. 1986 105 p
(Contract F30602-82-C-0161)
(AD-A178464; UTEC-MD-86-054; RADC-TR-86-129) Avail: NTIS HC A06/MF A01 CSCL 09A

A modal expansion technique is applied to a system of uniform waveguides interconnected by abrupt junctions. Computer codes developed for the asymmetrical modes on-axis transition and all modes off-axis transition have been tested and verified through two separate tests. The three main parts of this work are: (1) The tentative formulation for an abrupt transition from one waveguide to another, where each junction is restricted to having only one input and one output waveguide, while a conducting wall on each side of the junction is accounted for, (2) The development of convergence criteria for the selection of the important modes via symmetry used in each waveguide section, and (3) The numerical implementation of the evaluation of the coupling coefficients for the coupling cases: On-axis asymmetrical modes (circular to circular, circular to coaxial, and coaxial to coaxial waveguide transitions). Off-axis for all modes (circular to circular, circular to coaxial, and coaxial to coaxial waveguide transitions). The implementation of this formulation requires modification of the structure of the matrix equation of the existing code. To expand the capability and the versatility of the code, future work should include the implementation of ridged waveguide, dielectric loaded waveguide, and multiport junctions. Author (GRA)

N87-22910# Electronics Research Lab., Adelaide (Australia).
DESIGN OF GENERALISED CHEBYSHEV SUSPENDED SUBSTRATE STRIPLINE FILTERS
Nick Lioutas Apr. 1986 47 p
(AD-A178505; ERL-0363-TM) Avail: NTIS HC A03/MF A01 CSCL 09A

A method for designing suspended substrate stripline (SSS) lowpass and highpass microwave filters is presented. Such filters can be realized by using a generalized Chebyshev lowpass prototype. An extension of this work is the development of SSS diplexers and multiplexers. The procedure for the design of a SSS contiguous diplexer is given. SSS filters are compact and light-weight. Furthermore, they are not as lossy as microstrip and more conventional stripline microwave filters. GRA

N87-22911# Materials Research Labs., Ascot Vale (Australia).
A FAST, LOW RESISTANCE SWITCH FOR SMALL SLAPPER DETONATORS
D. D Richardson and D. A. Jones Oct. 1986 21 p
(AD-A178562; MRL-R-1030) Avail: NTIS HC A02/MF A01 CSCL 19A

A novel design for a shock compression conduction switch for use with slapper detonators is described. The switch is based on the concept of an explosively driven flyer plate impacting a plastic insulator and producing sufficient pressure within the insulator to produce a conduction transition. An analysis of the functioning of the switch is made using a simple Gurney model for the explosive, and basic shock wave theory to calculate impact pressure and switch closure times. The effect of explosive tamping is considered, and calculations are carried out for two donor explosive thicknesses and a range of flyer plate thicknesses. The new switch has been successfully tested in a series of experimental slapper detonator firings. The results of these tests show trends in overall agreement with those predicted by the calculations. Author (GRA)

N87-22912# Texas Technological Univ., Lubbock. Dept. of Electrical Engineering.
COORDINATED RESEARCH PROGRAM IN PULSED POWER PHYSICS Final Technical Report, 30 Sep. 1985 - 30 Sep. 1986
16 Feb. 1987 191 p
(Contract MIPR/ARO-100-86; Grant AF-AFOSR-0032-84)
(AD-A178625; ARO-21056.34-PH) Avail: NTIS HC A09/MF A01 CSCL 10B

(AD-A178625; ARO-21056.34-PH) Avail: NTIS HC A09/MF A01 CSCL 10B

A report on a coordinated research program in pulsed power physics contains the following: investigation of repetitive e-beam controlled discharges with respect to the influence of different gas properties such as attachment rate coefficient, drift velocity, and Penning ionization - modeling of diffuse discharges, including control mechanisms; investigations of the interaction of discharge and circuit for discharge pulses with short risetimes; investigation of optogalvanic effects with respect to their use as discharge control mechanisms; studies of concepts for optically assisted, externally sustained, diffuse discharge switches; studies of the limitations on high current, high energy switches resulting from electrode erosion; investigation of X-ray ionization of switch gases; investigation of insulator performance when subjected to repetitive surface discharge switching; a new approach to field distortion triggering of spark gaps; design, construction, and testing of two different high voltage line type pulsers; and, an electromagnetic method for injecting a projectile into a mass driver. GRA

N87-22913# Air Force Inst. of Tech., Wright-Patterson AFB, Ohio. School of Engineering.

AN IMPLEMENTATION OF A LANGUAGE ANALYZER FOR THE VERY HIGH SPEED INTEGRATED CIRCUIT HARDWARE DESCRIPTION LANGUAGE M.S. Thesis

Deborah J. Frauenfelder Dec. 1986 172 p
(AD-A178648; AFIT/GCE/MA/86D-1) Avail: NTIS HC A08/MF A01 CSCL 09B

Described is the incremental approach used to develop the first known C-base, UNIX-supported translator/analyzer for the Very High Speed Integrated Circuit (VHSIC) Hardware Description Language (VHDL). This research consisted of defining a VHDL Intermediate Access (VIA) format as a translation target, dividing VHDL into manageable segments, describing VHDL-to-VIA relationships, designing software modules to create those relationships, and evaluating the functional and performance characteristics of the analyzer. The intermediate form, VIA, was based on the Design Data Structure (DDS). Three of the nine VHDL language subsets identified were implemented in the language analyzer. In increments, these subsets were manually translated into specific examples of an enhanced version of DDS represented in a pile file format (VIA). These examples were then used as specifications for designing program modules to automatically translate VHDL code in VIA. After the program modules were written, these same examples were used as formal functional test specifications. GRA

N87-22914# Naval Ocean Systems Center, San Diego, Calif.

OPTICALLY PHASE-LOCKED ELECTRONIC SPECKLE PATTERN INTERFEROMETER (OPL-ESPI) Final Report

Steven E. Moran, Robert L. Law, Peter N. Craig, and Warren M. Goldberg Oct. 1986 35 p
(AD-A178652; NOSC/TR-1119) Avail: NTIS HC A03/MF A01 CSCL 09E

This report describes the design, theory, operation, and characteristics of the OPL-ESPI, which generates real time equal Doppler speckle contours of vibrating objects from unstable sensor platforms with a Doppler resolution of 30 Hz and a maximum tracking range of + or - 5 HMz. The optical phase locked loop compensates for the deleterious effects of ambient background vibration and provides the bases for a new ESPI video signal processing technique, which produces high contrast speckle contours. The OPL-ESPI system has local oscillator phase modulation capability, offering the potential for detection of vibrations with the amplitudes less than lambda/100. GRA

N87-22915# Stevens Inst. of Tech., Hoboken, N. J.

MULTIDIMENSIONAL FILTERING INVESTIGATIONS Final Report, Jan. - Sep. 1986

Sankar Basu Feb. 1987 139 p
(Contract F30602-81-C-0185)
(AD-A178745; RADC-TR-86-231) Avail: NTIS HC A07/MF A01 CSCL 12A

New classes of multivariable polynomials arising in studies of passive multidimensional systems have been identified and their properties have been studied. The problem of structurally passive synthesis of multidimensional digital filters as a cascade interconnection of more elementary building blocks has been addressed via the factorization matrix. The problem of sampling rate alternation of deterministic multidimensional signals is addressed on the basis of frequency domain description of the signal. Experiments with digitized images are also reported to demonstrate the performance of the designed interpolation and decimation schemes. GRA

N87-22916# University of Southern California, Los Angeles. Dept. of Electrical Engineering.

FORMAL MODELS OF HARDWARE AND THEIR APPLICATIONS TO VLSI DESIGN AUTOMATION Final Report, Sep. 1983 - Sep. 1986

Alice C. Parker 24 Dec. 1986 38 p
(Contract DAAG29-83-K-0147)
(AD-A178837; ARO-20637.17-EL) Avail: NTIS HC A03/MF A01 CSCL 09E

This final report describes research in high-level synthesis, and an associated problem, area estimation of integrated circuits. The approach taken is to create formal models of the problem being solved. Four major research results have been produced. First, an accurate technique for estimation of integrated circuit layout area from cell information has been developed. Second, optimal clocking scheme synthesis has been automated. Third, programs to design pipelined and non-pipelined data paths have been developed. Fourth, register allocation of the data paths has also been automated. In addition, a representation for design information which was produced under a previous contract has been used for a number of applications. This research forms part of the ADAM Advanced Design Automation System under construction at the University of Southern California. GRA

N87-22917# EIC, Inc., Norwood, Mass.

DEVELOPMENT OF NICKEL OXIDE/HYDROGEN MULTILAYER BIPOLAR BATTERY FOR PULSED POWER Report, 1 Sep. 1986 - 28 Feb. 1987

24 Mar. 1987 38 p
(Contract N00014-86-C-0803)
(AD-A178844) Avail: NTIS HC A03/MF A01 CSCL 10C

This program is concerned with the development of a nickel oxide/hydrogen battery for pulsed power applications. It is based on thin film nickel oxide cathodes and metal hydride (Lanthanum-Nickel) anodes. Thin film nickel oxides were prepared by reactive RF sputtering, chemical vapor deposition, anodic oxidation of nickel and by cathodic precipitation of nickel hydroxide. Thin LaNi5 films were prepared by RF sputtering from a target of the same composition. Sputtered films showed much more irreversible electrochemical behavior than vapor deposited and anodically formed nickel oxides. Initial nickel oxide pulse currents were several hundred mA/sq. cm. Only a fraction of the electrode capacity was accessible at short times less than 10 msec. The LaNi5 electrodes were electrochemically reversible for the hydrogen storage reaction, and pulse currents of thin film LaNi5H(x) electrodes were of the same magnitude as the non-sputtered NiOx. Rates appear limited by surface reaction kinetics and by bulk diffusion. GRA

N87-22918# Avco-Everett Research Lab., Mass.

MAGNETICALLY INSULATED OPENING SWITCH RESEARCH Final Report, Jun. 1984 - Oct. 1986

M. W. McGeoch and R. Kraft Jan. 1987 52 p
(Contract DAAC29-84-C-0007)
(AD-A178895; ARO-21019.3-PH) Avail: NTIS HC A04/MF A01 CSCL 09A

We examine the feasibility of an opening switch concept based on magnetic insulation in a coaxial thermionic diode. It is found that the impedance ratio between closed and open states of the diode is marginal for efficient energy transfer via this type of switch. The open, or insulated state of the diode is characterized by current leakage across the magnetic field which is associated with the presence of plasma waves. GRA

N87-22919# Air Force Weapons Lab., Kirtland AFB, N. Mex.
TRANSIENT PROTECTION OF ELECTRONIC CIRCUITS Final Report, Jun. 1983 - Jul. 1984
R. B. Standler Feb. 1987 222 p
(AD-A178945; AFWL-TR-85-34) Avail: NTIS HC A10/MF A01 CSCL 09E

Electromagnetic pulses from nuclear weapons, lightning, and electrostatic discharge are three examples of electrical overstress. Such overstress can cause failure, permanent degradation, or temporary malfunction (upset) of electronic devices and systems. This problem and general solutions are briefly reviewed. Nonlinear components and circuits for protection from electrical overstress are discussed in detail, emphasizing spark gaps, metal oxide varistors, and avalanche diodes. However, other components, such as semiconductor diodes, thyristors, resistors, inductors, and optoisolators are also discussed. Applications of these nonlinear components are discussed in the context of signal lines, AC power lines, and DC power supplies. The final chapter discusses specific upset protection circuits. GRA

N87-22920# Massachusetts Inst. of Tech., Cambridge. Microsystems Research Center.
A COHERENT VLSI DESIGN ENVIRONMENT Semiannual Technical Report, 1 Apr. - 30 Sep. 1986
Paul Penfield, Jr., William J. Dally, Lance A. Glasser, Thomas F. Knight, Jr., Charles E. Leiserson, John L. Wyatt, Jr., and Richard E. Zippel 30 Sep. 1986 71 p
(Contract N00014-80-C-0622)
(AD-A179037) Avail: NTIS HC A04/MF A01 CSCL 09E

The CAD frame Schema has been outfitted with a uniform protocol or aggregate data structures, which includes new control structures for examining and searching through the data structures. Circuit simulators installed in Schema can now use their own scratchpad, and call a variety of tools to deal with the pertinent data structures. Waveform bounding results are now beginning to be available for ECL circuits, similar to those reported earlier for MOS interconnect and gates. The principal problem is that a vastly different gate model appears to be necessary for rising and falling transients. So far results within a few percent of SPICE have been obtained for some cases. A new procedure for calculating maximum frequency response of networks made from classes of devices with certain types of small-signal models, connected in arbitrary ways that conserve real and reactive power, has been worked out. This activity required the development of a new procedure to test whether 0 is in the numerical range of a non-Hermitian matrix. GRA

N87-22921*# Stanford Univ., Calif. Computer Systems Lab.
THROUGHPUT ANALYSIS OF THE IEEE 802.4 TOKEN BUS STANDARD UNDER HEAVY LOAD
Joseph Pang and Fouad Tobagi Mar. 1987 45 p
(Grants NAG2-292; NAGw-419)
(NASA-CR-180936; NAS 1.26:180936; CSL-TR-87-331) Avail: NTIS HC A03/MF A01 CSCL 09C

It has become clear in the last few years that there is a trend towards integrated digital services. Parallel to the development of public Integrated Services Digital Network (ISDN) is service integration in the local area (e.g., a campus, a building, an aircraft). The types of services to be integrated depend very much on the specific local environment. However, applications tend to generate data traffic belonging to one of two classes. According to IEEE 802.4 terminology, the first major class of traffic is termed synchronous, such as packetized voice and data generated from other applications with real-time constraints, and the second class is called asynchronous which includes most computer data traffic such as file transfer or facsimile. The IEEE 802.4 token bus protocol which was designed to support both synchronous and asynchronous traffic is examined. The protocol is basically a timer-controlled token bus access scheme. By a suitable choice of the design parameters, it can be shown that access delay is bounded for synchronous traffic. As well, the bandwidth allocated to asynchronous traffic can be controlled. A throughput analysis of the protocol under heavy load with constant channel occupation of synchronous traffic and constant token-passing times is presented. Author

N87-22922# Energy Research Corp., Danbury, Conn.
DEVELOPMENT OF ADVANCED NICKEL-CADMIUM BATTERIES FOR ELECTRIC VEHICLE PROPULSION Annual Report, 1 Apr. 1985 - 31 Mar. 1986
Sep. 1986 83 p
(Contract DE-AC08-84NV-10442)
(DOE/NV/10442-1) Avail: NTIS HC A05/MF A01

Results of a research program to develop an improved, non-sintered, polymer-bonded plate, nickel-cadmium battery are discussed. Major emphases was on cell technology advancement. The effects of adding intercalation compounds to electrolyte and/or active mix were investigated. Experimental cells of 20 Ah size containing various additives were fabricated and tested. Various methods to improve the stability of graphite were evaluated. It was concluded that coating the graphite with spinel oxide is the optimum method to minimize oxidation. R.J.F.

N87-22923*# National Aeronautics and Space Administration. Lewis Research Center, Cleveland, Ohio.
REVISED NASA AXIALLY SYMMETRIC RING MODEL FOR COUPLED-CAVITY TRAVELING-WAVE TUBES
Jeffrey D. Wilson Jan. 1987 17 p
(NASA-TP-2675; E-3220; NAS 1.60:2675) Avail: NTIS HC A02/MF A01 CSCL 09A

A versatile large-signal, two-dimensional computer program is used by NASA to model coupled-cavity travelling-wave tubes (TWTs). In this model, the electron beam is divided into a series of disks, each of which is further divided into axially symmetric rings which can expand and contract. The trajectories of the electron rings and the radiofrequency (RF) fields are determined from the calculated axial and radial space-charge, RF, and magnetic forces as the rings pass through a sequence of cavities. By varying electrical and geometric properties of individual cavities, the model is capable of simulating severs, velocity tapers, and voltage jumps. The calculated electron ring trajectories can be used in designing magnetic focusing and multidepressed collectors. The details of using the program are presented, and results are compared with experimental data. Author

34 FLUID MECHANICS AND HEAT TRANSFER

Includes boundary layers; hydrodynamics; fluidics; mass transfer; and ablation cooling.

For related information see also *02 Aerodynamics* and *77 Thermodynamics and Statistical Physics.*

N87-22924# Messerschmitt-Boelkow-Blohm G.m.b.H., Ottobrunn (West Germany).
THE EFFECT ON THE STRENGTH OF INITIATION ON THE CORNER EFFECT
Manfred Held 1986 9 p Presented at the International Symposium on Intense Dynamic Loading and its Effects, Beijing, China, 3-7 Jun. 1986
(MBB-UA-938/86; ETN-87-99923) Avail: NTIS HC A02/MF A01

It is shown that a minimum radius of curvature for the change in direction of a detonation exists, even in high explosives that detonate well. The obedience of the detonation wave is particularly important in small charges whose size approaches that of the minimum radius of curvature, or when wave shapers are used. The test arrangement for studying these effects is described, and the effects of initiation are summarized. ESA

N87-22925# Air Force Inst. of Tech., Wright-Patterson AFB, Ohio. School of Engineering.
BOUNDARY LAYER DISTURBANCES CAUSED BY PERIODIC HEATING OF A THIN RIBBON M.S. Thesis
Lawrence Kudelka Dec. 1986 73 p
(AD-A179342; AFIT/GAE/AA/86D-7) Avail: NTIS HC A04/MF A01 CSCL 20D

Wind tunnel tests were conducted to generate velocity perturbations in a laminar boundary layer using periodic heating of a flush-mounted ribbon. A thin strip of Nichrome ribbon, flush-mounted on a flat plate, was heated by pulsed voltage of various frequencies with spring tension and used to take up the slack caused by thermal expansion. Vibration of the ribbon was excited by the periodic thermal expansion and contraction due to the pulsed voltage. Sinusiodal velocity fluctuations were detected by a hot wire anemometer when the ribbon was allowed to vibrate during pulsed heating. No effect on the amplitude of the flow disturbances was detected with the spring tension removed and segments of the ribbon firmly fixed to the surface such that no vibration of the ribbon occurred during periodic heating. Pulsed heating of a thin ribbon caused detectable flow disturbances only when the ribbon was allowed to vibrate. The AFIT 9-in wind tunnel had sufficiently low turbulence to detect fluctuations when pulsed voltage was applied to the ribbon. Experiments conducted in AFIT's 14-in wind tunnel were not able to show effects of heating because of the large amount of free stream turbulence. GRA

N87-22926# Army Military Personnel Center, Alexandria, Va.
PREDICTION OF FLUID FLOW IN CURVED PIPE USING THE FINITE ELEMENT METHOD Final Report
Christopher B. Maitin 13 Apr. 1987 87 p
(AD-A179538) Avail: NTIS HC A05/MF A01 CSCL 20D

An analysis of turbulent flow through curved pipes was attempted using the finite element method. A commercial finite element code, FIDAP, which employs the kappa-epsilon model was used. Mesh configurations were developed for three curved pipes with varying bend angles. A pipe with a 180 deg bend was modeled after an experiment to verify the results of the computer code. A 90 deg and 45 deg pipe were modeled at a bend radius of 1 pipe diameter, to simulate standard pipes in ventilation systems. The intent of the study was to examine the flow profiles exiting the bend. The results should give some explanation of the effect of bends on the poor performance of fans placed downstream of bends. The turbulent model failed to converge for a steady-state analysis of the curved pipe flow, so a laminar flow analysis was done. The results show the expected distortion in the velocity profiles exiting from the bends. Also some conclusions were drawn about attaining better convergence with curved pipe flow. GRA

N87-22927# Scientific Research Associates, Inc., Glastonbury, Conn.
FLOW DYNAMICS STIMULATED BY HAIRPIN-LIKE VORTICES IN INITIALLY LAMINAR BOUNDARY LAYERS Annual Report, 1 Feb. 1986 - 31 Jan. 1987
N. S. Liu, S. J. Shamroth, and H. McDonald 28 Feb. 1987 22 p
(Contract F49620-86-C-0028)
(AD-A179578; AFOSR-87-0563TR) Avail: NTIS HC A02/MF A01 CSCL 20D

Time marching spatial simulations of flow events stimulated by hairpin like vortices in the near wall region of initially laminar boundary layers will be carried out. The behavioral flow characteristics and the underlying physical mechanisms will be elucidated by using three distinct but related methods of analysis. During the current reporting period, the development and improvement of the simulation and analysis tools have been completed. Simulations through the direct solution of time dependent, three dimensional, compressible Navier-Stokes equations are being initiated. The successful completion of this effort will provide more insight into the cyclic turbulence production and transport in turbulent boundary layers. A better understanding of wall turbulence may lead to techniques of turbulence management and control which can impact upon a variety of current important technical problem areas. GRA

N87-22928# Pennsylvania State Univ., University Park. Dept. of Mechanical Engineering.
EXPERIMENTAL RESEARCH ON COMPRESSIBLE TURBULENT SHEAR LAYERS, VISCOUS-INVISCID INTERACTIONS, AND FLOW SEPARATION Final Report
Gary S. Settles 9 Apr. 1986 14 p
(Grant AF-AFOSR-0184-84)
(AD-A179579; PSU-ME-86-R-0113; AFOSR-87-0452TR) Avail: NTIS HC A02/MF A01 CSCL 20D

This report describes the DoD-University Research Instrumentation Program Equipment Acquisition for Pennsylvania Univ. The thrust of this effort has been to outfit and upgrade Penn State's Supersonic Wind Tunnel Laboratory with modern instrumentation so that research in support of national defense can be conducted. The subject area of this research is viscous-inviscid interactions in supersonic flight. GRA

N87-22929# Cincinnati Univ., Ohio. Coll. of Engineering.
COMPOSITE VELOCITY PROCEDURES FOR FLOWS WITH PRESSURE INTERACTION Annual Technical Report, 1 Feb. 1985 - 1 Feb. 1986
Stanley G. Rubin and Prem K. Khosla 17 Mar. 1986 44 p
(Contract F49620-85-C-0027)
(AD-A179602; AFOSR-87-0357TR) Avail: NTIS HC A03/MF A01 CSCL 20D

The composite velocity formulation for the Euler and Reduced Navier-Stokes system of equations has been investigated. For transonic steady flow over airfoils a combination of conservative and nonconservative flux directional systems of difference equations have been developed and applied to obtain full potential, Euler and Reduced Navier Stokes solutions. The Enquist Osher procedure for shock capturing has been adapted for these applications to obtain sharp shock waves for both potential and Euler equations. For two dimensional transient flows and for three dimensional global relaxation computations, the coupled strongly implicit matrix inversion algorithm has been reformulated in order to allow for time consistency and space marching efficieny, respectively. GRA

N87-22930# Mississippi State Univ., Mississippi State. Dept. of Mechanical and Nuclear Engineering.
EQUIPMENT FOR TURBULENT HEAT TRANSFER TEST APPARATUS Final Report
Hugh W. Coleman Aug. 1986 9 p
(Grant AF-AFOSR-0075-85)
(AD-A179612; AFOSR-87-0555TR) Avail: NTIS HC A02/MF A01 CSCL 14B

This grant was made for the purpose of acquiring the equipment and constructing a wind tunnel facility called the Turbulent Heat Transfer Test Apparatus (THTTA). The THTTA was designed specifically to provide quality heat transfer and fluid dynamics data for turbulent flow over rough surfaces. GRA

N87-22931# California Univ., Davis. Dept. of Mechanical Engineering.
CONDITIONAL SECOND ORDER CLOSURE FOR TURBULENT SHEAR FLOWS Annual Technical Report, 1 Jul. 1985 - 30 Jun. 1986
Wolfgang Kollmann 27 Jul. 1986 38 p
(Grant AF-AFOSR-0219-84)
(AD-A179661; AFOSR-87-0428TR) Avail: NTIS HC A03/MF A01 CSCL 20D

The properties of scalar variables, permitting distinction between turbulent and nonturbulent zones of shear flows, are investigated. The dynamics of the probability density function (pdf) of such a scalar is considered and a numerical solution technique based on stochastic simulation is developed. The second order closure is extended to axisymmetric shear flows and different closures for the turbulent transport of Reynolds stresses are evaluated. GRA

N87-22932*# National Aeronautics and Space Administration. Ames Research Center, Moffett Field, Calif.
CONSERVATIVE ZONAL SCHEMES FOR PATCHED GRIDS IN 2 AND 3 DIMENSIONS
Kristin A. Hessenius Apr. 1987 97 p
(NASA-TM-88326; A-86317; NAS 1.15:88326) Avail: NTIS HC A05/MF A01 CSCL 20D

The computation of flow over complex geometries, such as realistic aircraft configurations, poses difficult grid generation problems for computational aerodynamicists. The creation of a traditional, single-module grid of acceptable quality about an entire configuration may be impossible even with the most sophisticated of grid generation techniques. A zonal approach, wherein the flow field is partitioned into several regions within which grids are independently generated, is a practical alternative for treating complicated geometries. This technique not only alleviates the problems of discretizing a complex region, but also facilitates a block processing approach to computation thereby circumventing computer memory limitations. The use of such a zonal scheme, however, requires the development of an interfacing procedure that ensures a stable, accurate, and conservative calculation for the transfer of information across the zonal borders. Author

N87-22933# Lawrence Livermore National Lab., Calif.
A GODUNOV METHOD FOR LAGRANGIAN HYDRODYNAMICS IN 1D
W. P. Crowley 15 Jan. 1987 17 p
(Contract W-7405-eng-48)
(DE87-005204; UCID-20966) Avail: NTIS HC A02/MF A01

For transient problems involving strong shocks, the artificial viscosity method has been the standard in numerical hydrodynamics for many years. An alternative approach was suggested by Godunov and it is gaining acceptance. We consider a Godunov method for 1D Lagrangian calculations and show that in the case of a strong shock moving through a nonuniform mesh the Godunov solution is superior to the artificial viscosity solution. For uniform mesh shock problems in spherical geometry the two methods give comparable results. DOE

N87-22934# Stanford Univ., Calif. Dept. of Mechanical Engineering.
HEAT TRANSFER EFFECTS OF LONGITUDINAL VORTICES EMBEDDED IN A TURBULENT BOUNDARY LAYER Final Report
J. K. Eaton 31 Aug. 1986 12 p
(Contract DE-AS03-83ER-13081)
(DE87-006002; DOE/ER-13081/T2) Avail: NTIS HC A02/MF A01

The objective of the present experiment is to study a stronger boundary layer perturbation induced by a vortex pair rather than a single vortex. The data include spatially resolved heat transfer measurements as well as detailed measurements of all six components of the Reynolds stress tensor. The data focus on the variations of the boundary layer structure which are caused by the vortex. This paper presents the heat transfer and skin friction data for several vortex pair cases along with detailed boundary layer velocity profiles for one case. DOE

N87-22935# Massachusetts Inst. of Tech., Cambridge. Dept. of Chemical Engineering.
NUMERICAL CALCULATION OF THE DRAG FORCE INDUCED BY NATURAL CONVECTION OF SPHERES AT LOW GRASHOF NUMBERS
D. Dudek and T. H. Fletcher Feb. 1987 29 p Prepared in cooperation with Sandia National Labs., Livermore, Calif.
(Contract DE-AC04-76DR-00789)
(DE87-006791; SAND-87-8201) Avail: NTIS HC A03/MF A01

When a heated solid sphere is introduced into an ambient fluid, a natural convective flow occurs which results in a drag force on the sphere. This study involves the numerical calculation of both the steady-state and the transient natural convective drag force around spheres at low Grashof numbers. Numerical techniques are taken from Geoola and Cornish. An empirical expression is suggested for the total drag coefficient for Grashof numbers ranging from 4×10^{-4} to 0.5 and Prandtl number = 0.72: log C sub DT = 1.25 + 0.31 log Gr - 0.097(log Gr)^2. The dimensionless time required to reach 90% of the steady-state drag force can be approximated by the second-order polynomial: log t sub 90% = 1.32 - log Gr - 0.11(Gr)^2. DOE

N87-22936# Lawrence Livermore National Lab., Calif.
LAGRANGIAN-LIKE EQUATIONS OF HYDRODYNAMICS WITH MASS DIFFUSION
W. P. Crowley 14 Oct. 1986 8 p
(Contract W-7405-eng-48)
(DE87-007522; UCID-21006) Avail: NTIS HC A02/MF A01

The relation between mean kinetic energy and acceleration is derived by using an Eulerian representation of inviscid hydrodynamics. DOE

N87-22937# Ballistic Research Labs., Aberdeen Proving Ground, Md.
AXISYMMETRIC INVISCID SHOCK TUBE FLOW SIMULATION
Ameer G. Mikhail and Charles J. Nietubicz Dec. 1986 48 p
(AD-A178494; BRL-MR-3559) Avail: NTIS HC A03/MF A01 CSCL 20D

An axisymmetric flow simulation was made for the highly transient flow in a variable cross-section area shock tube at pressure ratio of 16. The shock tube has a varying diameter driver section and a convergent divergent nozzle. A large and sudden area increase exists at the divergent section of the nozzle which leads to the driven section. Euler equations are solved using a time dependent implicit finite difference scheme. A validation computation was made for a constant area tube, at pressure ratio of 6.5 and the result was in good agreement with the corresponding experiment. These results were improved when the tube diaphragm effects were simulated and the divergent nozzle geometry was better modeled. However, four areas of necessary improvement were identified for achieving an accurate simulation: first, the proper modeling of the exact sudden area increase; second, better coordinates near the sudden large area increase; third, inclusion of physical viscosity in the numerical simulation (i.e., use of Navier Stokes solver rather than an Euler's solver); fourth, mininization and examination of the role of the second order implicit numerical dissipation for a time accurate computation. The present procedure can only be used satisfactorily for shock tubes with continuous and mild area changes. Without these improvements, an inviscid, quasi-one-dimensional flow simulation can, and does, yield more accurate results in general. GRA

N87-22938# Air Force Inst. of Tech., Wright-Patterson AFB, Ohio. School of Engineering.
A STUDY OF FLUID-DYNAMIC PRESSURE FIELDS ON COMPRESSOR REED VALVES M.S. Thesis
Clarence J. Coleman, Jr. Dec. 1986 112 p
(AD-A178584; AFIT/GAE/AA/86-02) Avail: NTIS HC A06/MF A01 CSCL 20D

Reed values are spring-metal plates which commonly serve as intake and exhaust valves in refrigeration Compressor units. This thesis reports on an analytic and experimental study of flow through reed-valve-like inlet geometries. In the latter, with reservoir pressures up to 2 1/4 times ambient, the flow passed through a hole in a base plate, stagnated, and turned 90 degrees by a disk centered over the hole, and directed radially outward between the base plate and the disk. Cover-plate-like geometries up to 3 times the diameter of the hole in the base plate, as well as modified base-plate geometries, were investigated. The analytic model used one dimensional (radially symmetric) compressible flow relations to model the inlet geometries in an initial supersonic region which accounted for friction and possible separation. Shock matching techniques were then employed to locate a shock and predict the properties of the flow just behind the shock. Finally, subsonic, isentropic, compressible equations were used to model the flow from the shock to the exit. The analytic modelling was compared with the experimental results and found to satisfactorily explain the qualitative and even quantitative nature of the flows. The results of this study suggest that reed-valve inlet geometries should have relatively thin and high-lipped inlet configurations so as to minimize total pressure loss. Author (GRA)

N87-22939# Stanford Univ., Calif. Dept. of Mechanical Engineering.

DUAL CYLINDRICAL WAVE LASER-DOPPLER METHOD FOR MEASUREMENT OF SKIN FRICTION IN FLUID FLOW

Amir A. Naqwi and William C. Reynolds Jan. 1987 273 p
(Contract DAAG29-83-K-0056)
(AD-A178629; TR-TF-28; ARO-19976.3-EG) Avail: NTIS HC A12/MF A01 CSCL 20D

The objective of the present work is to overcome the inadequacies of conventional skin friction measuring methods in terms of temporal and spatial resolution. An instrument has been developed for measurement of the instantaneous velocity gradient in a boundary layer at a solid surface, from which the instantaneous wall shear stress can be deduced. The principle of the device is akin to that of dual beam Laser Doppler Anemometer. Instead of crossing two laser beams to produce the measuring volume, the present technique uses interference between two closely spaced cylindrical waves emanating from the solid surface. The interference fringes which constitute the measuring volume appear to be radiating from a point on surface. GRA

N87-22940# Air Force Inst. of Tech., Wright-Patterson AFB, Ohio. School of Engineering.

NUMERICAL STUDY OF HIGH SPEED VISCOUS FLOWS M.S. Thesis

Keith B. Jochum Dec. 1986 80 p
(AD-A178639; AFIT/GAE/AA/86D-4) Avail: NTIS HC A05/MF A01 CSCL 20D

Thermal deformations induced by aerodynamic heating on high speed vehicles are an important concern in design. Since aerodynamic heating may have a significant effect on the performance of the vehicle, effective techniques for predicting the heat transfer and flow properties are required. The accuracy of numerical solutions depends on the grid used. Usually accurate prediction requires clustering of grid points near the surface of the body. Using an explicit algorithm to solve such problems results in the stability requirement for very small time steps to satisfy the stability bounds. To remove the time step retriction, fully implicit methods were investigated. Results for high speed flow past a circular wedge using an implicit flux splitting scheme are shown. Viscous blunt body flows are also computed and qualitative comparisons with the existing experimental data are given. In an effort to decrease the computational costs associated with the implicit algorithms for the Navier-Stokes equations, a relaxation algorithm is developed for the Approximate Navier-Stokes equations. Results for Couette flow and supersonic flow over a flat plate are obtained using this relaxation algorithm and compared to analytical and other numerical solutions. GRA

N87-22941# Arnold Engineering Development Center, Arnold Air Force Station, Tenn.

INTERACTION OF A THREE-DIMENSIONAL ROUGHNESS ELEMENT WITH A LAMINAR BOUNDARY LAYER Final Report, 1 Jun. 1982 - 31 Jan. 1987

P. S. Klebanoff, W. G. Cleveland, Jr., and K. D. Tidstron Mar. 1987 120 p Prepared in cooperation with National Bureau of Standards, Gaithersburg, Md.
(AD-A178668; AEDC-TR-87-7) Avail: NTIS HC A06/MF A01 CSCL 20D

An experimental investigation is described that is directed toward extending the technical database and furthering our understanding of boundary layer transition induced by three-dimensional roughness elements. The investigation was carried out in an unsteady wind tunnel, principally with hemispherical roughness elements, in a well characterized zero-pressure gradient laminar boundary layer on a flat plate. Attention was directed toward the following aspects of the behavior of a three dimensional roughness element: (1) the critical Reynolds number of transition and the effect of aspect ratio thereon, (2) eddy generation is steady and unsteady flows, (3) is the fundamental process stability governed, and (4) the evolutionary change in mean velocity and intensity of the velocity fluctuation associated with the transition to fully developed turbulent flow. GRA

N87-22942# Naval Surface Weapons Center, Silver Spring, Md.

NUMERICAL ANALYSIS OF TERMINAL DOUBLE MACH REFLECTION Final Report

Michael J. Lijewski and Harland M. Glaz 26 Aug. 1986 34 p
(AD-A179041; NSWC-TR-86-286) Avail: NTIS HC A03/MF A01 CSCL 20D

Pseudostationary oblique-shock-wave reflections in real and perfect gases were investigated. In particular, we studied the special case of double Mach reflection known as terminal double Mach reflection. Numerical solutions of the inviscid equations are presented and compared with experimental and analytical results. Disparities between our numerical results and those predicted by the two- and three-shock theory are discussed. Author (GRA)

N87-22943*# National Aeronautics and Space Administration. Ames Research Center, Moffett Field, Calif.

COMPUTATIONAL AEROTHERMODYNAMICS

George S. Deiwert and Michael J. Green Apr. 1987 15 p Presented at the American Astronautical Society's 33rd Annual Meeting, Boulder, Colo., 26-29 Oct. 1986
(NASA-TM-89450; A-87181; NAS 1.15:89450) Avail: NTIS HC A02/MF A01 CSCL 20D

Computational aerothermodynamics (CAT) has in the past contributed to the understanding of real-gas flows encountered by hypervelocity reentry vehicles. With advances in computational fluid dynamics, in the modeling of high temperature phenomena, and in computer capability, CAT is an enabling technology for the design of many future space vehicles. An overview of the current capabilities of CAT is provided by describing available methods and their applications. Technical challenges that need to be met are discussed. Author

N87-22944*# Iowa State Univ. of Science and Technology, Ames. Coll. of Engineering.

A THREE-DIMENSIONAL DUAL POTENTIAL PROCEDURE WITH APPLICATIONS TO WIND TUNNEL INLETS AND INTERACTING BOUNDARY LAYERS Final Report

K. V. Rao, R. H. Pletcher, J. L. Steger, and W. R. VanDalsem Jun. 1987 165 p
(NCA2-17)
(NASA-CR-180939; NAS 1.26:180939; HTL-47; CFD-18; ISU-ERI-Ames-87296) Avail: NTIS HC A08/MF A01 CSCL 20D

A dual potential decomposition of the velocity field into a scalar and a vector potential function is extended to three dimensions and used in the finite-difference simulation of steady three-dimensional inviscid rotational flows and viscous flow. The finite-difference procedure was used to simulate the flow through the 80 by 120 ft wind tunnel at NASA Ames Research Center. Rotational flow produced by the stagnation pressure drop across vanes and screens which are located at the entrance of the inlet is modeled using actuator disk theory. Results are presented for two different inlet vane and screen configurations. The numerical predictions are in good agreement with experimental data. The dual potential procedure was also applied to calculate the viscous flow along two and three dimensional troughs. Viscous effects are simulated by injecting vorticity which is computed from a boundary layer algorithm. For attached flow over a three dimensional trough, the present calculations are in good agreement with other numerical predictions. For separated flow, it is shown from a two dimensional analysis that the boundary layer approximation provides an accurate measure of the vorticity in regions close to the wall; whereas further away from the wall, caution has to be exercised in using the boundary-layer equations to supply vorticity to the dual potential formulation. Author

N87-22945# Los Alamos National Lab., N. Mex.
NUMERICAL SIMULATION OF THE DECAY OF SWIRLING FLOW IN A CONSTANT VOLUME ENGINE SIMULATOR
Lawrence D. Cloutman May 1986 22 p
(Contract W-7405-eng-36)
(LA-10728-MS) Avail: NTIS HC A02/MF A01

The KIVA and COYOTE computer programs were used to simulate the decay of turbulent swirling flow in a constant-volume combustion bomb. The results are in satisfactory agreement with the measurement of both swirl velocity and temperature. Predictions of secondary flows and suggestions for future research also are presented. Author

N87-22946# Los Alamos National Lab., N. Mex.
HEAT TRANSFER IN AN ORGANIC HEAT PIPE
F. Haug 1987 18 p
(Contract W-7405-eng-36)
(LA-10781-MS) Avail: NTIS HC A02/MF A01

An experimental study of heat transfer characteristics in a cylindrical gravity assisted heat pipe with an organic working fluid is described. External coolant heat transfer coefficient is given for a temperature range from 25 to 45 C and for radial heat fluxes from around .065 to 1.0 W/sq cm. Observations on the condensate flow were carried out and provisions were made to ensure that no instationary condensate flow occurred which may lead to uncertainties in heat transfer characteristics. Almost complete wetting of the evaporator heat transfer area could be confirmed. Author

N87-22947# Atomic Weapons Research Establishment, Aldermaston (England).
BODY WAVE MAGNITUDES AND LOCATIONS OF FRENCH UNDERGROUND EXPLOSIONS AT THE MURUROA TEST SITE
P. D. Marshall, R. C. Lilwall, and Penelope J. Warburton Nov. 1985 17 p
(BR-97934; AWRE-0-12/85; ISBN-0-85518166-4) Avail: NTIS HC A02/MF A01; HMSO 4 pounds

Since 1975 the French have conducted underground nuclear weapon tests beneath the Mururoa atoll in the Tuamotu Archipelago in the Southern Pacific. A least squares joint estimate of origin time and epicenter together with a least squares joint estimate of magnitude is presented from bulletins of the International Seismological Center. Some seismogram, recorded in Canada, are included to illustrate the nature of the P waves from these presumed explosions. Author

N87-22948*# Massachusetts Inst. of Tech., Cambridge. Dept. of Aeronautics and Astronautics.
A LINEARIZED EULER ANALYSIS OF UNSTEADY FLOWS IN TURBOMACHINERY Final Report
Kenneth C. Hall and Edward F. Crawley Jun. 1987 183 p
(Grant NsG-3079)
(NASA-CR-180987; NAS 1.26:180987) Avail: NTIS HC A09/MF A01 CSCL 20D

A method for calculating unsteady flows in cascades is presented. The model, which is based on the linearized unsteady Euler equations, accounts for blade loading shock motion, wake motion, and blade geometry. The mean flow through the cascade is determined by solving the full nonlinear Euler equations. Assuming the unsteadiness in the flow is small, then the Euler equations are linearized about the mean flow to obtain a set of linear variable coefficient equations which describe the small amplitude, harmonic motion of the flow. These equations are discretized on a computational grid via a finite volume operator and solved directly subject to an appropriate set of linearized boundary conditions. The steady flow, which is calculated prior to the unsteady flow, is found via a Newton iteration procedure. An important feature of the analysis is the use of shock fitting to model steady and unsteady shocks. Use of the Euler equations with the unsteady Rankine-Hugoniot shock jump conditions correctly models the generation of steady and unsteady entropy and vorticity at shocks. In particular, the low frequency shock displacement is correctly predicted. Results of this method are presented for a variety of test cases. Predicted unsteady transonic flows in channels are compared to full nonlinear Euler solutions obtained using time-accurate, time-marching methods. The agreement between the two methods is excellent for small to moderate levels of flow unsteadiness. The method is also used to predict unsteady flows in cascades due to blade motion (flutter problem) and incoming disturbances (gust response problem). M.G.

N87-22949*# National Aeronautics and Space Administration. Lewis Research Center, Cleveland, Ohio.
THERMODYNAMIC ANALYSIS AND SUBSCALE MODELING OF SPACE-BASED ORBIT TRANSFER VEHICLE CRYOGENIC PROPELLANT RESUPPLY
David M. DeFelice and John C. Aydelott Jul. 1987 21 p
Prepared for presentation at the 23rd Joint Propulsion Conference, San Diego, Calif., 29 Jun. - 2 Jul. 1987; cosponsored by AIAA, SAE, ASME, and ASEE
(NASA-TM-89921; E-3617; NAS 1.15:89921; AIAA-87-1764) Avail: NTIS HC A02/MF A01 CSCL 20D

The resupply of the cryogenic propellants is an enabling technology for spacebased orbit transfer vehicles. As part of the NASA Lewis ongoing efforts in microgravity fluid management, thermodynamic analysis and subscale modeling techniques were developed to support an on-orbit test bed for cryogenic fluid management technologies. Analytical results have shown that subscale experimental modeling of liquid resupply can be used to validate analytical models when the appropriate target temperature is selected to relate the model to its prototype system. Further analyses were used to develop a thermodynamic model of the tank chilldown process which is required prior to the no-vent fill operation. These efforts were incorporated into two FORTRAN programs which were used to present preliminary analyticl results. Author

N87-22950* National Aeronautics and Space Administration. Lyndon B. Johnson Space Center, Houston, Tex.
PUMPED TWO-PHASE HEAT TRANSFER LOOP Patent
Fred Edelstein, inventor (to NASA) (Grumman Aerospace Corp., Bethpage, N.Y.) 12 May 1987 7 p Filed 15 Jul. 1985
Supersedes N86-20721 (24 - 11, p 1771
(NASA-Case-MSC-20841-1; US-Patent-4,664,177; US-Patent-Appl-SN-755288; US-Patent-Class-165-1; US-Patent-Class-165-34; US-Patent-Class-165-104.26; US-Patent-Class-165-104.25; US-Patent-Class-165-104.14) Avail: US Patent and Trademark Office CSCL 20D

A pumped loop two-phase heat transfer system, operating at a nearly constant temperature throughout, includes a plurality of independently operating grooved capillary heat exchanger plates supplied with working fluid through independent flow modulation valves connected to a liquid supply line, a vapor line for collecting vapor from the heat exchangers, a condenser between the vapor and the liquid lines, and a fluid circulating pump between the condenser and the heat exchangers.
Official Gazette of the U.S. Patent and Trademark Office

N87-22951*# Stanford Univ., Calif. Dept. of Aeronautics and Astronautics.
A THEORY FOR TURBULENT CURVED WALL JETS
Leonard Roberts Mar. 1986 21 p
(Contracts NCC2-173; NCC2-55)
(NASA-CR-181019; NAS 1.26:181019; JIAA-TR-70) Avail: NTIS HC A02/MF A01 CSCL 20D

A simple theoretical model is proposed to describe the flow of a turbulent wall jet along a curved surface into a quiescent atmosphere. An integral method is used to solve the momentum equation and identifies three contributions to the spreading rate of the wall jet: (1) turbulent diffusion in the wall jet; (2) wall curvature; and (3) rate of change of wall curvature. Closed from approximate solutions are found for the case of a plane wall, a circular cylinder, and a logarithmic spiral surface. Comparison with experimental data for these three cases is made showing good agreement. Author

N87-22767*# National Aeronautics and Space Administration. Lewis Research Center, Cleveland, Ohio.
UNSTEADY STATOR/ROTOR INTERACTION
Philip C. E. Jorgenson and Rodrick V. Chima *In its* Structural Integrity and Durability of Reusable Space Propulsion Systems 1987 p 5-11 (For primary document see N87-22766 16-20)
Avail: NTIS HC A10/MF A01 CSCL 20D

N87-22768*# National Aeronautics and Space Administration. Lewis Research Center, Cleveland, Ohio.
SIMULATION OF MULTISTAGE TURBINE FLOWS
John J. Adamczyk and Richard A. Mulac (Sverdrup Technology, Inc., Middleburg Heights, Ohio.) *In its* Structural Integrity and Durability of Reusable Space Propulsion Systems 1987 p 13-20 (For primary document see N87-22766 16-20)
Avail: NTIS HC A10/MF A01 CSCL 20D

N87-22769*# National Aeronautics and Space Administration. Lewis Research Center, Cleveland, Ohio.
PROGRESS IN THE PREDICTION OF UNSTEADY HEAT TRANSFWE ON TURBINES BLADES
T. Cebeci, R. J. Simoneau, A. Krainer, and M. F. Platzer (Naval Postgraduate School, Monterey, Calif.) *In its* Structural Integrity and Durability of Reusable Space Propulsion Systems 1987 p 21-27 (For primary document see N87-22766 16-20)
Avail: NTIS HC A10/MF A01 CSCL 20D

N87-22770*# Calspan-Buffalo Univ. Research Center, N.Y.
EXPERIMENTAL AND THEORETICAL STUDIES OF TIME-AVERAGED AND TIME RESOLVED ROTOR HEAT TRANSFER
M. G. Dunn, W. J. Rae, and D. L. Rigby *In* NASA. Lewis Research Center Structural Integrity and Durability of Reusable Space Propulsion Systems 1987 p 29-32 (For primary document see N87-22766 16-20)
Avail: NTIS HC A10/MF A01 CSCL 20D

N87-23454*# Washington Univ., Seattle. Dept. of Mathematics.
WIND RIPPLES IN LOW DENSITY ATMOSPHERES
J. S. Miller, J. R. Marshall, and R. Greeley (Arizona State Univ., Tempe.) *In* NASA, Washington Reports of Planetary Geology and Geophysics Program, 1986 May 1987 p 268-270 (For primary document see N87-23341 16-91)
Avail: NTIS HC A24/MF A01 CSCL 20D

N87-23457*# Arizona State Univ., Tempe. Dept. of Geology and Geography.
DEVELOPMENT OF WIND TUNNEL TECHNIQUES FOR THE SOLUTION OF PROBLEMS IN PLANETARY AEOLIAN PROCESSES
Robert Sullivan, Jeffrey Lee, and Ronald Greeley *In* NASA, Washington Reports of Planetary Geology and Geophysics Program, 1986 May 1987 p 276-278 (For primary document see N87-23341 16-91)
Avail: NTIS HC A24/MF A01 CSCL 20D

N87-23459*# Arizona State Univ., Tempe. Dept. of Geography.
REYNOLDS NUMBER EFFECTS ON SURFACE SHEAR STRESS PATTERNS AROUND ISOLATED HEMISPHERES
J. A. Lee and Ronald Greeley *In* NASA, Washington Reports of Planetary Geology and Geophysics Program, 1986 May 1987 p 282-284 (For primary document see N87-23341 16-91)
Avail: NTIS HC A24/MF A01 CSCL 20D

N87-23460*# Arizona State Univ., Tempe. Dept. of Geography.
DETERMINATION OF SURFACE SHEAR STRESS WITH THE NAPHTHALENE SUBLIMATION TECHNIQUE
J. A. Lee and Ronald Greeley *In* NASA, Washington Reports of Planetary Geology and Geophysics Program, 1986 May 1987 p 285-287 (For primary document see N87-23341 16-91)
Avail: NTIS HC A24/MF A01 CSCL 20D

35 INSTRUMENTATION AND PHOTOGRAPHY

Includes remote sensors; measuring instruments and gages; detectors; cameras and photographic supplies; and holography.

For aerial photography see *43 Earth Resources and Remote Sensing*. For related information see also *06 Aircraft Instrumentation*, and *19 Spacecraft Instrumentation*.

N87-22952*# Alabama Univ., Huntsville. Dept. of Chemistry.
COSMIC RAY DETECTORS Final Report
John C. Gregory Feb. 1987 29 p
(Contract NAS8-36191)
(NASA-CR-179086; NAS 1.26:179086) Avail: NTIS HC A03/MF A01 CSCL 14B

Work on the MSFC emulsion laboratory microscopes in which mechanical modifications previously made were verified is reviewed, as is a design study of a large area hybrid electronic/emulsion chamber balloon flight detector system. This design is built upon the experience obtained with the highly successful MSFC/UAH hybrid instrument flown by the JACEE consortium. The design included overall system design and specification, design and fabrication of a prototype large light diffusion for Cerenkov charge detector or scintillator, design of a multiwire proportional counter array and design of the gondola or flight support system. Author

N87-22953* National Aeronautics and Space Administration. Pasadena Office, Calif.
WATER-ABSORBING CAPACITOR SYSTEM FOR MEASURING RELATIVE HUMIDITY Patent
Eric G. Laue, inventor (to NASA) (Jet Propulsion Lab., California Inst. of Tech., Pasadena.) 5 May 1987 6 p Filed 20 Jun. 1985 Supersedes N86-20755 (24 - 11, p 1776)
(NASA-Case-NPO-16544-1-CU; US-Patent-4,662,220; US-Patent-Appl-SN-746809; US-Patent-Class-73-336.5; US-Patent-Class-324-61-R) Avail: US Patent and Trademark Office CSCL 14B

A method and apparatus using a known water-absorbent polymer as a capacitor which is operated at a dc voltage for measuring relative humidity is presented. When formed as a layer between porous electrically-conductive electrodes and operated in an RC oscillator circuit, the oscillator frequency varies inversely with the partial pressure of the moisture to be measured. In a preferred embodiment, the capacitor is formed from Nafion and is operated at a low dc voltage with a resistor as an RC circuit in an RC oscillator. At the low voltage, the leakage current is proper for oscillation over a satisfactory range. The frequency of oscillation varies in an essentially linear fashion with relative humidity which is represented by the moisture being absorbed into the Nafion. The oscillation frequency is detected by a frequency detector.
Official Gazette of the U.S. Patent and Trademark Office

N87-22954# Department of Energy, Morgantown, W. Va.
PROCEEDINGS OF THE INSTRUMENTATION, COMPONENTS, AND MATERIALS CONTRACTORS MEETING
J. M. Hobday, ed. Jan. 1987 295 p Meeting held at Morgantown, W. Va., 16 Sep. 1986
(DE86-006596; DOE/METC-86-6069; CONF-860961) Avail: NTIS HC A13/MF A01

The first combined Instrumentation, Components, and Materials Contractors Meeting was held September 16 to 17, 1986, at the Sheraton Lakeview Conference Center in Morgantown, West Virginia. Work presented at the meeting was sponsored by the US Department of Energy, Office of Fossil Energy, and directed by the Morgantown Energy Technology Center (METC), which served as host. Attendance included representatives from industry, academia, National Laboratories, and other Government agencies and totaled 85 individuals. This and similar meetings focusing on specific topics are organized periodically by METC to provide a forum for exchange of information between DOE contractors and interested parties. The Proceedings have been reproduced from camera-ready manuscripts furnished by the authors. The manuscripts have not been refereed, nor have they been extensively edited. Papers have been entered individually into EDB and ERA. DOE

N87-22955# Lawrence Livermore National Lab., Calif.

MAGNITUDE AND PHASE CALIBRATION OF MICROWAVE SENSORS

R. R. McLeod, H. G. Hudson, and R. J. King Dec. 1986 16 p Presented at the National Radio Science Meeting, Boulder, Colo., 12 Jan. 1986
(Contract W-7405-eng-48)
(DE87-003466; UCRL-95475; CONF-860198-1) Avail: NTIS HC A02/MF A01

Current network analyzer technology allows both magnitude and phase to be accurately recorded in antenna measurements, raising the possibility of fully characterizing microwave sensors. These calibrated sensors can then take data which may be convolved with arbitrary inputs as well as transformed into the time domain. Such measurements require, however, some standard calibration to measure against: a standard phase horn so to speak. This paper first extends the definitions of several commonplace antenna parameters and equations to include phase. Given these necessary tools, a number of methods are used to derive a phase calibration and the results are presented. While every method used yields the proper results, only a few are easily applicable to phase measurements. Using these results, a calibration curve is derived for the Lawrence Livermore National Laboratory EMPEROR monocone. Comparison with low-frequency D probes shows the calibration to be accurate to within 1 dB and 5 degrees. EMPEROR is then found to be a nearly perfect, flat transmitter from 50 Mhz to 18 GHz. This allows it to be used as magnitude and phase calibration range. In concert with an HP 8510 based measurement system, this allows engineers to quickly and accurately measure the complete response of antennas and other EM systems. DOE

N87-22956*# National Aeronautics and Space Administration. Ames Research Center, Moffett Field, Calif.

REAL-TIME LASER HOLOGRAPHIC INTERFEROMETRY FOR AERODYNAMICS

George Lee Jun. 1987 11 p Presented at the SPIE 1987 International Symposium Southeast on Optics, Electro-Optics and Sensors, Orlando, Fla., 17-22 May 1987
(NASA-TM-89462; A-87205; NAS 1.15:89462) Avail: NTIS HC A02/MF A01 CSCL 14E

Recent developments in thermoplastic recording holograms and advancements in automated image digitalization and analysis make real-time laser holographic interferometry feasible for two-dimensional flows such as airfoil flows. Typical airfoil measurements would include airfoil presssure distributions, wake and boundary layer profiles, and flow field density contours. This paper addresses some of the problems and requirements of a real-time laser holographic interferometer. Author

N87-22957# General Electric Co., Schenectady, N.Y. Knolls Atomic Power Lab.

AN IMPROVED SET OF AUGER DATA ANALYSIS PROGRAMS FOR PHYSICAL ELECTRONICS AUGER SPECTROMETER SYSTEMS

R. A. Mulford, F. S. Austin, and R. W. Merchant Mar. 1986 47 p Presented at the Annual Meeting of the Microbeam Analysis Society, Schenectady, N.Y., 11-15 Aug. 1986
(Contract DE-AC-76-SN-00052)
(DOE/TIC-4500; KAPL-4193) Avail: NTIS HC A03/MF A01

A set of utility programs for the display and analysis of Auger spectral data collected with Physical Electronics (PHI) Auger Spectrometers using the embedded computer data acquisition system is described. These programs are designed to replace the routines supplied by the manufacturer and offer the user greater flexibility. All routines will run on standard PHI systems equipped with HP2648 or HP2623 computer terminals. The major feature of these programs is the windowing capability for quantitative analysis of a list of elements. Spectra are collected and saved to disk using the PHI acquisition system in the usual fashion, except that it is not necessary to specify the elements that are present before the analysis is performed. The spectrum can be divided into any convenient arrangement of energy regions. The procedure permits the energy regions for data acquisition to be larger than the element windows to minimize the effect of the end points on the numerical differentiation. It is also easier to analyze closely spaced peaks, such as oxygen and chromium. When the spectra are processed, each region is automatically differentiated and displayed in sequence, with the energy windows for the Auger peaks marked in reverse video. Results are stored on disks, together with the raw peak-to-peak heights and the sensitivity factors used. These disk files can then be read by simple auxiliary programs to average or tabulate results. Author

N87-22958# National Bureau of Standards, Gaithersburg, Md. Office of Physical Measurement Services.

NBS CALIBRATION SERVICES USERS GUIDE, 1986-1988 EDITION

George A. Uriano, ed., Ernest L. Garner, ed., R. Keith Kirby, ed., and William P. Reed, ed. Jul. 1986 205 p
(NBS-SP-250) Avail: NTIS HC A10/MF A01

The National Bureau of Standards (NBS) Calibration Services Users Guide provides detailed descriptions of currently available NBS calibration services, measurement assurance programs, and special test services. The following measurement areas are covered: (1) dimensional, (2) mechanical including flow, acoustic, and ultrasonic, (3) thermodynamic, (4) optical radiation, (5) ionizing radiation, and (6) electromagnetic including dc, ac, RF, and microwave. A separate Fee Schedule is issued every six months which provides current prices for the services offered, updates on points-of-contact, and information on measurement seminars. Author

N87-22959*# National Aeronautics and Space Administration. Lewis Research Center, Cleveland, Ohio.

LASER ANEMOMETRY TECHNIQUES FOR TURBINE APPLICATIONS

Mark P. Wernet and Lawrence G. Oberle Jun. 1987 17 p Presented at the 32nd International Gas Turbine Conference and Exhibition, Anaheim, Calif., 31 May - 4 Jun. 1987; sponsored by ASME
(NASA-TM-88953; E-3369; NAS 1.15:88953) Avail: NTIS HC A02/MF A01 CSCL 14B

Laser anemometry offers a nonintrusive means for obtaining flow field information. Current research at NASA Lewis Research Center is focused on instrumenting a warm turbine facility with a laser anemometer system. In an effort to determine the laser anemometer system best qualified for the warm turbine environment, the performance of a conventional laser fringe anemometer and a two spot time of flight system were compared with a new, modified time of flight system, called a Four Spot laser anemometer. The comparison measurements were made in highly turbulent flows near walls. The Four Spot anemometer uses elliptical spots to increase the flow acceptance angle to be comparable to that of a Laser Fringe Anemometer. Also, the Four Spot uses an optical code that vastly simplifies the pulse detection processor. The results of the comparison measurements will exemplify which laser anemometer system is best suited to the hostile environment typically encountered in warm rotating turbomachinery. Author

N87-22960*# Sverdrup Technology, Inc., Cleveland, Ohio.

OPTICAL STRAIN MEASUREMENT SYSTEM DEVELOPMENT, PHASE 1 Final Report

Christian T. Lant and Walid Qaqish May 1987 39 p
(Contract NAS3-24105)
(NASA-CR-179619; E-3550; NAS 1.26:179619) Avail: NTIS HC A03/MF A01 CSCL 14B

A laser speckle, differential strain measurement system was built and tested for future applications in hostile environments. One dimensional electronic correlation of speckle pattern movement allows a quasi-real time measure of strain. The system was used successfully to measure uniaxial strain reaching into plastic deformation of a test specimen, at temperatures ranging to 450 C. A resolution of 16 microstrain is given by the photodiode array sensor pitch and the specimen to sensor separation. The strain measurement limit of the gauge is determined by air density perturbations causing decorrelation of the reference and shifted speckle patterns, and may be improved by limiting convective flow in the immediate vicinity of the test specimen. Author

N87-22706*# National Aeronautics and Space Administration. Langley Research Center, Hampton, Va.
MICROPROCESSOR CONTROLLED PROOF-MASS ACTUATOR
Garnett C. Horner *In* NASA. Marshall Space Flight Center Structural Dynamics and Control Interaction of Flexible Structures Apr. 1987 p 101-118 (For primary document see N87-22702 16-15)
Avail: NTIS HC A99/MF E03 CSCL 14B

N87-22772*# National Aeronautics and Space Administration. Lewis Research Center, Cleveland, Ohio.
PROGRESS ON THIN-FILM SENSORS FOR SPACE PROPULSION TECHNOLOGY
Walter S. Kim *In its* Structural Integrity and Durability of Reusable Space Propulsion Systems 1987 p 39-42 (For primary document see N87-22766 16-20)
Avail: NTIS HC A10/MF A01 CSCL 14B

N87-22773*# Sverdrup Technology, Inc., Middleburg Heights, Ohio.
PROGRESS IN OPTICAL STRAIN MEASUREMENT SYSTEM DEVELOPMENT
Christian T. Lant and Walid Qaqish *In* NASA. Lewis Research Center Structural Integrity and Durability of Reusable Space Propulsion Systems 1987 p 45-46 (For primary document see N87-22766 16-20)
Avail: NTIS HC A10/MF A01 CSCL 14B

N87-22775*# Case Western Reserve Univ., Cleveland, Ohio.
NUMERICAL STUDY OF THE EFFECTS OF BOUNDARY CONDITIONS ON THE MEASUREMENT AND CALIBRATION OF GARDON TYPE HEAT FLUX SENSORS
M. Krane and A. Dybbs *In* NASA. Lewis Research Center Structural Integrity and Durability of Reusable Space Propulsion Systems 1987 p 51-57 (For primary document see N87-22766 16-20)
Avail: NTIS HC A10/MF A01 CSCL 14B

N87-23556*# Arizona State Univ., Tempe. Dept. of Geology.
THE MARS OBSERVER CAMERA
M. C. Malin, G. E. Danielson, A. P. Ingersoll, H. Masursky, J. Veverka, T. Soulanille, and M. Ravine (Jet Propulsion Lab., California Inst. of Tech., Pasadena.) *In* NASA, Washington Reports of Planetary Geology and Geophysics Program, 1986 May 1987 p 548-550 (For primary document see N87-23341 16-91)
Avail: NTIS HC A24/MF A01 CSCL 14E

36 LASERS AND MASERS

Includes parametric amplifiers.
For related information see also *76 Solid-State Physics.*

N87-22961# Naval Postgraduate School, Monterey, Calif.
CO2 PULSED LASER DAMAGE MECHANISM AND PLASMA EFFECTS (FOCUSED BEAM) M.S. Thesis
Richard L. Weston Dec. 1986 84 p
(AD-A179201) Avail: NTIS HC A05/MF A01 CSCL 20K

An experiment was conducted (at NPS) with AISI SS 304 stainless steel targets in a 0.000001 Torr vacuum using a CO2 TEA high energy, pulsed laser with a beam focused to 1 sq cm. An investigation of the laser damage mechanism was conducted. The power density required for onset of plasma formation and the start of surface damage were determined. Targets were polished to 0.25 micro finish. Target specimens were examined using a scanning electron microscope to determine damage features of micron size dimensions. Experimental results confirmed that the surface damage was confined solely to unipolar arcing and thermal effects resulting from the arcing process. Several targets were cross-sectioned and chemically etched to determine changes in the microstructure of the stainless steel. At high power densities, the surface was heated sufficiently to cause a change in the stainless steel from austenite to austenite and ferrite. The localized change in the microstructure confirmed that the energy deposition from the plasma was confined to the arcing craters. The power density for onset of plasma was confined to the arcing craters. GRA

N87-22962# Science Applications International Corp., McLean, Va.
OPERATION OF THE INDUCED RESONANCE ELECTRON CYCLOTRON MASER AT HIGHER HARMONICS Interim Report
C. M. Tang, S. Riyopoulos, P. Sprangle, and B. Levush 13 Mar. 1987 15 p Prepared in cooperation with University of Maryland, College Park, Md.
(AD-A179428; NRL-MR-5947) Avail: NTIS HC A02/MF A01 CSCL 20E

The induced resonance electron cyclotron (IREC) maser operates at Doppler unshifted frequencies a = gamma-sq Omega sub 0/gamma, where gamma is the relativistic factor and Omega sub 0 is the cyclotron frequency. The frequency can be further increased by operation at higher cyclotron harmonics. A set of fast-time averaged nonlinear equations of motion is derived for the particle motion near an arbitrary harmonic. Start-up currents are computed from the linear efficiency. The nonlinear efficiency is studied numerically for the first few harmonics. Minimization of the detrimental effects due to pitch angle and energy spread are investigated by selecting the optimum angle between the beam and the resonator. GRA

N87-22963# Wisconsin Univ., Madison. Fusion Technology Inst.
RADIATION DAMAGE TO COATINGS FOR SHORT WAVE LENGTH LASER MIRRORS Final Report, 25 Sep. 1985 - 24 Sep. 1986
D. Pertzborn and G. L. Kulcinski Nov. 1986 15 p
(Contract DE-AS08-85NV-10511)
(DE87-001696; DOE/NV-10511/1) Avail: NTIS HC A02/MF A01

Several specimens of highly reflecting (HR) and anti-reflecting (AR) mirrors have been irradiated at the University of Wisconsin from 1985 to 1986. It is shown that at damage levels of 10 to the 11th power rads and higher, visible optical absorption changes take place. By 10 to the 12th power rads (0.05 dpa in the coating and 0.7 dpa in the substrate), the damage is so severe that the mirror is probably unusable. DOE

N87-22964# Los Alamos National Lab., N. Mex.
APPLICATION OF PICOSECOND CO2 LASERS TO PARTICLE ACCELERATORS
I. J. Bigio, N. A. Kurnit, T. Shimada, and R. F. Harrison 1987 5 p Presented at the OSA/IEEE Conference on Lasers and Electro-optics (CLEO '87), Baltimore, Md., 27 Apr. 1987
(Contract W-7405-eng-36)
(DE87-003711; LA-UR-86-3916; CONF-870401-2) Avail: NTIS HC A02/MF A01

Various advanced accelerator concepts invoke lasers for the generation of very-high-gradient accelerating fields. We introduce the subject and review the application of picosecond CO2 lasers to one such scheme: laser-driven open microstructures. DOE

N87-22965# Sandia National Labs., Albuquerque, N. Mex.
PULSED POWER FOR HIGH POWER ELECTRON-BEAM PUMPED LASERS
M. T. Buttram and R. A. Gerber 1987 11 p Presented at the LASE-13: Pulse Power for Lasers Conference, Los Angeles, Calif., 11 Jan. 1987

(Contract DE-AC04-76DP-00789)
(DE87-004523; SAND-86-2926C; CONF-870132-3) Avail: NTIS HC A02/MF A01

A primary consideration for operation of many high power gas lasers is the generation of a high voltage, large area electron beam. Beam parameters are dictated by laser requirements. DOE

N87-22966# Argonne National Lab., Ill.
WHY GAMMA RAYS ARE DIFFERENT: SOME NOTES FOR PEDESTRIANS
H. J. Lipkin 24 Oct. 1986 10 p Presented at the OSA/APS International Laser Science Conference, Seattle, Wash., 20 Oct. 1986
(Contract W-31109-eng-38)
(DE87-004963; ANL-HEP-CP-86-132; CONF-861038-9) Avail: NTIS HC A02/MF A01

This paper is a critical analysis of some of the problems facing gamma ray laser construction. The physics of optical lasers is compared to that of gasers. The manner in which gamma-ray emission is stimulated is very different from light-emission stimulation in optical lasers. It is concluded that the differences in stimulation methods make effective gaser construction very difficult. DOE

N87-22967# Rochester Univ., N. Y. Lab. for Laser Energetics.
TARGET FABRICATION FOR HIGH DENSITY TARGET EXPERIMENTS AT THE UNIVERSITY OF ROCHESTER'S LABORATORY FOR LASER ENERGETICS
H. Kim and J. M. Soures 1986 8 p Presented at the 5th Annual Target Fabrication Specialists Meeting, Las Vegas, Nev., 24 Mar. 1986
(Contract DE-FC08-85DP-40200)
(DE87-005915; DOE/DP-40200/30; CONF-860330-3) Avail: NTIS MF A01

A theoretical and experimental program is in progress at the University of Rochester's Laboratory for Laser Energetics to demonstrate high density compression using the 351-nm, uniform illumination, OMEGA laser facility. The targets that have the best chance of meeting the objectives of this campaign are low-Z polymer shells with liquid or solid DT layers. Fabrication of such targets is described. These activities include polymer shell fabrication, development of a cryogenic fuel facility, a tritium filling facility, development of low-mass target supports, and development of levitated target coating. DOE

N87-22968# Lawrence Livermore National Lab., Calif.
TIME AND SPACE RESOLVED SPECTROSCOPY OF X-RAY LASER EXPERIMENTS FROM 81A TO 220A
N. M. Ceglio and H. Medecki 12 Jan. 1987 12 p Presented at the 30th SPIE Technical Symposium on Optics and Optoelectronic Engineering, San Diego, Calif., 17 Aug. 1986
(Contract W-7405-eng-48)
(DE87-005946; UCRL-95706; CONF-860880-46) Avail: NTIS HC A02/MF A01

Data are presented from three different x-ray laser inversion schemes tested on the Novette laser facility at LLNL: collisional excitation of neon-like selenium (lambda = 206, 209, 220A); resonant photoexcitation of hydrogen-like fluorine (lambda = 81A); and recombination of hydrogen-like magnesium (lambda = 130A). The data illustrate the measurement capabilities of a new, time resolved imaging spectrometer (TGSS-EM), and provide insight to the dynamics and emission characteristics of a new class of laser produced plasmas. DOE

N87-22969# United Technologies Research Center, East Hartford, Conn.
INVESTIGATION OF LASER DIAGNOSTICS OF PACVD PROCESSES FOR DEPOSITING HARD FACE COATINGS Performance Report, 1 Jul. 1986 - 31 Jan. 1987
W. C. Roman Feb. 1987 4 p
(Contract DE-FG02-86ER-13560)
(DE87-006292; DOE/ER-13560/1) Avail: NTIS HC A02/MF A01

(DE87-006292; DOE/ER-13560/1) Avail: NTIS HC A02/MF A01

The objective is to improve the understanding of the mechanisms which govern the nonequilibrium reactive plasma atomistic or molecular deposition of hard face coatings for erosion resistant applications. The goal is to provide a predictive capability that is severely lacking in the present science base of processing for depositing hard face coatings. Advanced laser diagnostics will be used to probe the plasma. DOE

N87-22970# Allied Corp., Morristown, N.J.
NEW LASER MATERIALS Final Report
Oct. 1986 57 p Prepared in cooperation with Lawrence Livermore National Lab., Calif.
(Contract W-7405-eng-48)
(DE87-006723; UCRL-15867-Vol-2) Avail: NTIS HC A04/MF A01

In the Interim Report No. 1, it was reported that the fluorescence lifetime (greater than or equal to 750 microns) in Nd doped Y(PO3)3 was longer by a factor of three as compared to YAG. This means potentially three times as much energy storage and consequently more efficient for flashlamp pumping. It also makes diode pumping easier. In addition, since the Y site is octahedrally coordinated, there is a possibility of energy transfer using Cr as the sensitizing element. It was decided to explore the trivalent cation metaphosphates systematically. The compounds investigated can be represented by the general formula A(PO3)3 where A = Y, Lu, In, Sc, GA and Al. The object is to study the fluorescence characteristics of Nd and Cr as well as the effectiveness of energy transfer from Cr to Nd. In addition, also investigated were other possible laser host crystals, notably CaMgSi2O6 (diopside), LaBO3 and La(BO2)3. Results on these materials will also be discussed. DOE

N87-22971# JAYCOR, Vienna, Va.
THE USE OF THE KARL SUB-SCALE LASER FOR RAMAN BEAM CLEAN-UP EXPERIMENTS Final Report, 13 Aug. 1985 - 1 Dec. 1986
Alan J. Dudas and Harris R. Burris 27 Mar. 1987 95 p
(Contract N00014-85-C-2376)
(AD-A178463; JAYCOR-J206-87-001/6252) Avail: NTIS HC A05/MF A01 CSCL 20E

The two X-ray preionized discharge pumped front end lasers for the Raman Beam Clean-up Experiment (LARBC) have been examined both optically and electrically in an effort to increase the optical and temporal quality of the injection locked beam produced. The KARL subscale has been successfully injection locked by the front end lasers and preliminary studies of the stability of the injection locking begun. An isolator system has been designed and constructed to prevent damage to system optics from energy moving the wrong way in the system. A gas processing system was tested to remove contaminants in the laser gas. Additional units have been purchased for use on all lasers in the system. Diagnostics for the experiment will be coordinated through the WP3202 digitizing system. GRA

N87-22972# New Mexico Univ., Albuquerque. Center for High Technology Materials.
INVESTIGATION OF THE TRANSVERSE-DISCHARGE COPPER-VAPOR LASER Final Report, 1 Feb. 1983 - 31 May 1986
Jin J. Kim 31 May 1986 19 p
(Contract N00014-83-K-0180)
(AD-A178833) Avail: NTIS HC A02/MF A01 CSCL 20E

A transverse-discharge copper-vapor laser has been developed using a fast flat-plate Blumlein pulse forming circuit. A specific laser energy density of 50 micor J/CC has been achieved. This is an order of magnitude higher than that achieved by conventional copper-vapor lasers. The high electric field to number density ratio allows operation with high temperatures of up to 1800 C and high buffer gas pressures above atmospheric pressure. GRA

N87-22973# Naval Ocean Systems Center, San Diego, Calif.
CALIBRATION OF THE HAND-HELD LIDARS USED BY THE NAVAL OCEAN SYSTEMS CENTER Final Report, 17 - 27 Mar. 1986
J. A. Ferguson and M. R. Paulson Aug. 1986 16 p
(AD-A178965; NOSC/TD-996) Avail: NTIS HC A02/MF A01 CSCL 17I

A program of lidar measurements to determine the characteristics of lidar equipment and to make side-by-side comparisons of lidar returns was conducted. The equipment consisted of the mini lidar developed by the Physics and Electronics Laboratory (FEL) of the Netherlands National Defence Organization and the visioceilometer developed by the US Army's Atmospheric Sciences Laboratory. This report presents results of the program, including the energy output of the laser and the output of the signal-processing unit for varying input powers (calibration), as well as the results of comparative atmospheric measurements. GRA

N87-22974# Air Force Inst. of Tech., Wright-Patterson AFB, Ohio. School of Engineering.
A MULTIPLE MODEL ADAPTIVE TRACKING ALGORITHM FOR A HIGH ENERGY LASER WEAPON SYSTEM M.S. Thesis
David M. Tobin Dec. 1986 302 p
(AD-A178978; AFIT/GE/ENG/86D-37) Avail: NTIS HC A14/MF A01 CSCL 17I

This thesis considers replacing a standard correlation tracker with a hybrid Kalman filter/enhanced correlation tracker in a high energy laser weapon system. Dynamic airborne targets are tracked by a Bayesian multiple model adaptive filtering (MMAF) algorithm, which processes the outputs of a matrix-type array of infrared sensing detectors. Emphasis is placed on extending the adaptive potential of the tracking algorithm. This is accomplished by processing measurements from various field of view (FOV) sizes and shapes, and by incorporating direction-dependent target dynamics in some of the elemental Kalman filters within the multiple model structure. A sensor to target range tuning algorithm is derived which can be used for on-line adaptive filter tuning should the tracker be provided range information, (even at low sample rates and/or precision), possibly via laser ranging. Also, the problem of initial target acquisition is explored through an algorithm which acquires the target in the center of the field of view despite initial sensor pointing errors. Two different target dynamics models are considered for the elemental Kalman filters: a linear, Gauss-Markov acceleration model, and a nonlinear, constant turn-rate model. GRA

N87-22975# Los Alamos National Lab., N. Mex.
A HIGH-TEMPERATURE QUADRUPOLE MASS SPECTROMETER FOR STUDYING VAPORIZATION FROM MATERIALS HEATED BY A CO2 LASER
Leif Fredin, George P. Hansen, Madeline P. Sampson, John L. Margrave, Robert G. Behrens, Mary J. Mann, ed., and Debbie Vigil Sep. 1986 20 p Prepared in cooperation with Rice Univ.,Houston, Tex.
(Contract W-7405-eng-36)
(LA-10744) Avail: NTIS HC A02/MF A01

To evaluate the effectiveness of mass spectroscopy techniques in studying vaporization from selected materials, a mass spectrometer was designed that can be used either with a continuous wave or pulsed laser heating system or with a conventional furnace heating system. The experimental apparatus, the components of which are described in detail, consisted of a quadrupole mass spectrometer positioned in a crossed-beam configuration, controlling electronics, a data acquisition system, a vacuum system, a cryogenic collimation system, and a laser heating system. Results of mass spectral scans taken during laser pyrolysis of polymeric materials and laser vaporization of graphite were compatible with data reported in other studies. Results of mass spectral studies of laser induced combustion in the Ti+C system are also presented. Author

37 MECHANICAL ENGINEERING

Includes auxiliary systems (nonpower); machine elements and processes; and mechanical equipment.

N87-22976* National Aeronautics and Space Administration. Langley Research Center, Hampton, Va.
DAZE FASTENERS Patent
L. Robert Jackson, inventor (to NASA), Randall C. Davis, inventor (to NASA), and Allan H. Taylor, inventor (to NASA) 17 Mar. 1987 9 p Filed 5 Feb. 1985 Division of US-Patent-4,572,699, US-Patent-Appl-SN-495380, filed 17 May 1983
(NASA-Case-LAR-13009-2; US-Patent-4,650,385; US-Patent-4,572,699; US-Patent-Appl-SN-698279; US-Patent-Appl-SN-495380; US-Patent-Class-411-166; US-Patent-Class-411-368; US-Patent-Class-411-424; US-Patent-Class-411-427; US-Patent-Class-411-531) Avail: US Patent and Trademark Office CSCL 13E

A daze fastener system for connecting two or more structural elements wherein the structural elements and fastener parts have substantially different coefficient of thermal expansion physical property characteristics is employed in this invention. By providing frusto-conical abutting surfaces between the structural elements and fastener parts any differences in thermal expansion/contraction between the parts is translated to sliding motion and avoids deleterious thermal stresses in the connection. An essential feature for isotropic homogeneous material connections is that at least two sets of mating surfaces are required wherein each set of mating surfaces has line element extensions that pass through a common point.
Official Gazette of the U.S. Patent and Trademark Office

N87-22977* National Aeronautics and Space Administration. Marshall Space Flight Center, Huntsville, Ala.
TUBE COUPLING DEVICE Patent
William N. Myers, inventor (to NASA) and Leopold A. Hein, inventor (to NASA) 7 May 1987 8 p Filed 10 Apr. 1986 Continuation of US-Patent-Appl-SN-692801, filed 18 Jan. 1985, abandoned
(NASA-Case-MFS-25964-2; US-Patent-4,655,482; US-Patent-Appl-SN-853361; US-Patent-Appl-SN-692801; US-Patent-Class-285-81; US-Patent-Class-285-85; US-Patent-Class-285-91; US-Patent-Class-285-305; Avail: US Patent and Trademark Office CSCL 13E

A first annular ring of a tube coupling device has a keyed opening sized to fit around the nut region of a male coupling, and a second annular ring has a keyed opening sized to fit around the nut of a female coupling. Each ring has mating ratchet teeth and these rings are biased together, thereby engaging these teeth and preventing rotation of these rings. This in turn prevents the rotation of the male nut region with respect to the female nut. For tube-to-bulkhead locking, one facet of one ring is notched, and a pin is pressed into an opening in the bulkhead. This pin is sized to fit within one of the notches in the ring, thereby preventing rotation of this ring with respect to the bulkhead.
Official Gazette of the U.S. Patent and Trademark Office

N87-22978*# National Aeronautics and Space Administration. Lewis Research Center, Cleveland, Ohio.
HELICOPTER TRANSMISSION TESTING AT NASA LEWIS RESEARCH CENTER
David G. Lewicki and John J. Coy Jun. 1987 18 p Presented at the Testing of Aerospace Transmissions Conference, Derby, England, 10 Jun. 1987; sponsored by the Institute of Mechanical Engineers
(NASA-TM-89912; E-3603; NAS 1.15:89912; AVSCOM-TR-87-C-10) Avail: NTIS HC A02/MF A01 CSCL 13I

The helicopter has evolved into a highly valuable air mobile vehicle for both military and civilian needs. The helicopter transmission requires advanced studies to develop a technology base for future rotorcraft advances. A joint helicopter transmission research program between the NASA Lewis Research Center and the U.S. Army Aviation Systems Command has existed since 1970. Program goals are to reduce weight and noise and to increase life and reliability. The current experimental activities at Lewis consist of full-scale helicopter transmission testing, a base effort in gearing technology, and a future effort in noise reduction technology. The experimental facilities at Lewis for helicopter transmission testing are described. A description of each of the rigs is presented along with some significant results and near-term plans. Author

N87-22979# Sandia National Labs., Albuquerque, N. Mex.

IN SITU FRICTION, WEAR AND ELECTRICAL CONTACT RESISTANCE OF PRECIOUS METAL ALLOYS

L. E. Pope and D. E. Peebles 1986 33 p Presented at the Annual Meeting of the American Society of Lubrication Engineers, Anaheim, Calif., 11 May 1987
(Contract DE-AC04-76DP-00789)
(DE87-001423; SAND-86-1849C; CONF-870510-1) Avail: NTIS HC A03/MF A01

An in situ friction, wear and electrical contact resistance pin-on-plate system has been assembled and installed in a scanning Auger microprobe. Friction coefficients and electrical contact resistance were measured continuously as wear progressed. The surface composition and the topography of a wear track were measured intermittently without exposure of the surface to contaminating environments or removal of the pin from the wear track. Experiments were completed with known and controlled gaseous contaminants in the ambient. For a palladium based alloy pin (ASTM B540) sliding on a gold based alloy plate (ASTM B541), three stages of wear have been identified. The composition of the prow was essentially that of plate material during the first two stages of wear but was a mixture of pin and plate materials during the third stage of wear. In a helium ambient high electrical contact resistance occurred concomitantly with a transition to the third stage of wear. DOE

N87-22980# Oak Ridge National Lab., Tenn.

A 3-D WORLD MODELING BASED ON COMBINATORIAL GEOMETRY FOR AUTONOMOUS ROBOT NAVIGATION

M. Goldstein, F. G. Pin, G. deSaussure, and C. R. Weisbin 1987 21 p Presented at the IEEE International Conference on Robotics and Automation, Raleigh, N.C., 30 Mar. 1987
(Contract DE-AC05-84OR-21400)
(DE87-002814; CONF-870354-1) Avail: NTIS HC A02/MF A01

In applications of robotics to surveillance and mapping at nuclear facilities, the scene to be described is fundamentally three-dimensional. Usually, only partial information concerning the 3-D environment is known a-priori. Using an autonomous robot, this information may be updated using range data to provide an accurate model of the environment. Range data quantify the distances from the sensor focal plane to the object surface. In other words, the 3-D coordinates of discrete points on the object surface are known. The approach proposed herein for 3-D world modeling is based on the Combinatorial Geometry (CG) Method which is widely used in Monte Carlo particle transport calculations. First, each measured point on the object surface is surrounded by a small solid sphere with a radius determined by the range to that point. Then, the 3-D shapes of the visible surfaces are obtained by taking the (Boolean) union of all the spheres. The result is a concise and unambiguous representation of the object's boundary surfaces. The distances from discrete points on the robot's boundary surface to various objects are calculated effectively using the C.G. type of representation. This feature is particularly useful for navigation purposes. . DOE

N87-22981# Sandia National Labs., Albuquerque, N. Mex.

CORRELATIONS BETWEEN ELECTRICAL CONTACT RESISTANCE AND STAGES OF WEAR IN 700 TORR HELIUM FOR PRECIOUS METAL ELECTRICAL CONTACTS

D. E. Peebles and L. E. Pope 1987 5 p Presented at the 171st Electrochemical Society Meeting, Philadelphia, Pa., 10 May 1987
(Contract DE-AC04-76DP-00789)
(DE87-003499; SAND-86-2797C; CONF-870513-2) Avail: NTIS HC A02/MF A01

In situ pin-on-plate studies of wear between a gold based alloy plate and a palladium based alloy pin in a 700 Torr helium ambient demonstrate that irreversible and erratic increases in contact resistance arise as a result of incorporation of pin material and a corresponding increase in contaminant composition within the wear track. DOE

N87-22982# Sandia National Labs., Albuquerque, N. Mex.

ADVANCED TECHNOLOGY MOBILE ROBOTICS VEHICLE FLEET

D. E. McGovern Mar. 1987 31 p
(Contract DE-AC04-76DP-00789)
(DE87-007526; SAND-87-0033) Avail: NTIS HC A03/MF A01

A fleet of vehicles is being developed and maintained by Sandia National Laboratories (SNL) for studies in remote control and autonomous operation. The vehicles range from modified commercial vehicles to specially constructed mobile platforms and are utilized as testbeds for developing concepts in the areas of remote control (teleoperation) and computer control (autonomy). Actuators control the vehicle speed, brakes, and steering via manual input from a remote driving station or through some level of digital computer control. On-board processing may include simple vehicle control functions or may allow for unmanned, autonomous operation. Communication links are provided for digital communication between control computers, television transmission for vehicle vision, and voice for local control. SNL can develop, test, and evaluate sensors, processing requirements, various methods of actuator implementation, operator controlled feedback requirements, and vehicle operations. A description of the major features and uses for each of the vehicles in the fleet is provided. DOE

N87-22983# SEACO, Inc., Kailua, Hawaii.

TACTILE FEEDBACK FOR TELEOPERATOR SYSTEMS Final Report, Aug. 1985

M. Vercruyssen Nov. 1986 18 p
(Contract N66001-85-D-0023)
(AD-A179054; Rept-85-08-01; NOSC-TD-1018) Avail: NTIS HC A02/MF A01 CSCL 06D

Teleoperators or telerobots are semi-intelligent remote controlled operators that perform a variety of tasks and provide feedback in the form of audio, visual, and tactile information to the human operator with a complete array of displays and controls in a remote locale. These teleoperators exist in a crude form today as industry's robots. If the computer was the single most significant invention of the twentieth century, the area of technology to benefit most from the advent of microcomputer chips is teleoperators. A glimpse further into the future reveals a time when human will be sheltered from adverse environments by telerobots/teleoperators. Teleoperators will be used in environments too hostile or too remote for humans. These include, for dangerous jobs such as cleaning radioactive spills or other toxic wastes. In addition, the quality of life for handicapped people can be improved through research and development of teleoperators in the form of artificial limbs. The purpose of this paper is to introduce the reader to teleoperators, telepresence, developments in the areas of kinesthetic and tactile feedback and the necessity for more research in the area of tactile feedback in teleoperators. GRA

N87-22984# Rockwell International Corp., Golden, Colo. Space Operations.

A NOVEL ROLLABILITY TEST

Ross J. Jackson and Salli L. Prybylowski 25 May 1986 26 p
(Contract DE-AC04-76DP-03533)
(RFP-3901) Avail: NTIS HC A03/MF A01

A novel rollability test was developed and applied to unalloyed uranium metal in the alpha, beta, and gamma states. The test was empirical in origin and development, i.e., based on experiment and observation, not on theory or first principles. The test was based on the experimental observation in coupon rolling of uranium that once a base elasticity is exceeded, the percent gap reduction is always linear with respect to percent thickness reduction at all roll gap settings. This suggested the possibility of measuring a plastic index, P (the slope), and an elastic index, E (the x-intercept), and combining both to obtain a rollability index. The rollability, R, was defined as R = (P/E)0.1. The prescribed test experimentally yields the plastic index, P, and the elastic index, E. The test was validated for 23 sets of process variables and found to easily and quantitatively discriminate small changes in process variables. The source of errors, partitioning of rollability, test logic, and reasons the test works are discussed. Author

N87-22985* National Aeronautics and Space Administration. Lyndon B. Johnson Space Center, Houston, Tex.
APPARATUS AND METHOD OF CAPTURING AN ORBITING SPACECRAFT Patent
William D. Harwell, inventors (to NASA) and Dale A. Gardner, inventors (to NASA) 12 May 1987 13 p Filed 7 Nov. 1985 Supersedes N86-19614 (24 - 10, p 1584)
(NASA-Case-MSC-20979-1; US-Patent-4,664,344; US-Patent-Appl-SN-796053; US-Patent-Class-244/161) Avail: US Patent and Trademark Office CSCL 13I

Apparatus and a method of capturing an orbiting spacecraft by attaching a grapple fixture are discussed. A probe is inserted into an opening, such as a rocket nozzle, in the spacecraft until a stop on the prove mechanism contacts the spacecraft. A lever is actuated releasing a spring loaded rod which moves axially along the probe removing a covering sleeve to expose spring loaded toffle fingers which pivot open engaging the side of the opening. The probe is shortened and tensioned by turning a screw thread, pressing the fingers inside of the opening to compress the spacecraft between the toggle fingers and the stop. A grapple fixture attached to the probe, which is thus secured to the spacecraft, is engaged by appropriate retrieval means such as a remote manipulator arm.
Official Gazette of the U.S. Patent and Trademark Office

38 QUALITY ASSURANCE AND RELIABILITY

Includes product sampling procedures and techniques; and quality control.

N87-22986# United Kingdom Atomic Energy Authority, Harwell (England). Materials Physics and Metallurgy Div.
AUTOMATED NON-DESTRUCTIVE TESTING USING AN INDUSTRIAL ROBOT
B. C. Haywood and J. Gulliver Jul. 1986 14 p
(AERE-R-12308) Avail: NTIS HC A02/MF A01

Described is the use of an industrial robot in the nondestructive testing of workpieces of complex geometry. The requirements and specifications of a system which can be used for this purpose are discussed. Also described is the work performed to realize these requirements. Author

N87-22987# Materials Quality Assurance Directorate, London (England).
EFFECTS OF MACHINE VARIABLES ON THE QUALITY OF INJECTION MOULDINGS. AN INTERLABORATORY TRIAL, 2: HIGH DENSITY POLYETHYLENE
D. G. M. Wright, R. L. Tickner, and R. W. Tobias Mar. 1984 59 p
(MQAD-328; BR99605; PERME-278; ETN-87-99818) Copyright Avail: NTIS HC A04/MF A01

High-density, polyethylene tensile test pieces were produced at three establishments on different injection molding machines using specified conditions and a single injection mold. Large related differences in impact strength and reversion are found between batches of moldings, while no changes in tensile strength and morphology are detected. It is suggested that for crystalline materials, closer control of the cooling cycle may be necessary for the production of moldings with a reproducible standard of quality. ESA

N87-22988# Army Armament Research and Development Command, Dover, N. J. Product Assurance Directorate.
METHODOLOGY FOR VERIFICATION OF ULTRASONIC INSPECTION
Edward J. Mihok Apr. 1987 20 p
(AD-A179694; ARPAD-TR-87001) Avail: NTIS HC A02/MF A01 CSCL 13H

Periodically, manufacturers of large caliber projectiles have lost valuable time due to failure during calibration checkout of ultrasonic inspection systems, after which the bonded production is recalled for reinspection. Ultrasonic inspection provides a means for verification during and/or after inspection of each part. Implementation of such methods yields immediate release of inspected parts for further processing. Ultrasonic inspection systems that are presently operating have limited fail safe functions. The fail safe features in the present systems are related more to mechanical functions and operations than to the most critical part, the ultrasonic flaw detection loop which includes the electronic system and the transducers. The only part of the latter system presently monitored is the pulser/receiver and only as far as its operation is concerned. The effort addressed in this report concerns use of reflectors and electronic monitoring to assure proper system calibration during each inspection cycle. GRA

39 STRUCTURAL MECHANICS

Includes structural element design and weight analysis; fatigue; and thermal stress.

For applications see *05 Aircraft Design, Testing and Performance* and *18 Spacecraft Design, Testing and Performance.*

N87-22989# Giltspur Packaging Ltd., Totton (England). Research and Development Dept. and Testing House.
ACCELERATIONS EXPERIENCED BY PACKAGED MATERIEL DURING FORK LIFT TRUCK HANDLING Final Report
R. J. Pearce Jan. 1985 127 p
(Contract MOD(PE)-A94c/2196)
(RDI-284/45/3; CP/8/34-507; BR98642; ETN-87-99456) Copyright Avail: NTIS HC A07/MF A01

The shock and vibration environment imposed upon material when subjected to handling by a fork lift truck was studied using a representative range of fork lift trucks on a number of different surfaces including stores areas, perimeter roadways, and test tracks. Shock and vibration were recorded with an instrumented package weighing nominally 900 kg. The results are presented graphically as bar charts of acceleration amplitude against occurrence rate, and as a spectra plot of acceleration against frequency for the test track runs. ESA

N87-22990# California Inst. of Tech., Pasadena. Graduate Aeronautical Labs.
MEASUREMENT OF THE J INTEGRAL WITH CAUSTICS: AN EXPERIMENTAL AND NUMERICAL INVESTIGATION
Alan T. Zehnder, Ares J. Rosakis, and R. Narasimhan 1986 34 p
(Contract N00014-85-K-0596; Grant NSF MEA-83-07785)
(AD-A177273; SM-86-8) Avail: NTIS HC A03/MF A01 CSCL 20K

The optical method of caustics as applied to the measurement of the J integral in plastically deforming materials was studied numerically and experimentally. The numerical calculations modeled a cracked body loaded under Mode 1, plane stress, small scale yielding conditions. The results were used to generate simulated optical patterns for caustics obtained from both inside and outside the crack tip plastic zone. These caustics were compared with corresponding caustics observed experimentally. In addition, the region of dominance of the plane stress, HRR field was investigated, and the effect of plasticity on the accuracy of caustics from the elastic region outside the plastic zone was determined. The extent of the region of three dimensionally near the crack tip and its effect on the method of caustics was also investigated. Author (GRA)

N87-22991# United Kingdom Atomic Energy Authority, Harwell (England). Materials Physics and Metallurgy Div.

A STUDY INTO THE GENERATION OF TEMPERATURE GRADIENTS IN MATERIALS FOR DETECTING AND MEASURING THE DEPTH OF SUB-SURFACE CRACKS

J. M. Milne and P. Carter Oct. 1986 31 p
(AERE-R-12382) Avail: NTIS HC A03/MF A01

This paper describes how a thermal imager and heat source can be used to reveal the presence of and measure the depth below the surface of a sub-surface crack in a thin plate 6mm thick, by measuring the temperature drop across its ligament, i.e., the remaining metal between the surface and the crack tip. A finite difference program has been applied to the experimental model and has shown very good agreement. Author

N87-22992# Cambridge Univ. (England). Dept. of Engineering.

RESIDUAL STRESSES IN GIRTH BUTT WELDED PIPES: RESULTS AND IMPLICATIONS

A. Scramangas 1984 102 p
(CUED/D-Struct/TR.109; BR97667; ETN-87-99821) Avail: NTIS HC A06/MF A01

Experimental through-thickness residual stress distributions obtained from three Grade 50D structural steel girth butt welded pipes (9.1, 15.0, and 19.5 mm thickness, 1 m diameter) were compared with predictions of a thermostructural computational model. Good agreement between theory and experiment is achieved. Extrapolations beyond the range of experimental data were compared with published results. All available evidence is gathered, and the underlying trends are identified. Simple empirical formulas for predicting local values of axial residual stress, in particular the axial stress at the critical location of the weld root are presented. It is shown that, where the linear heat input per pass per unit pipe thickness is less than 90 J/sqmm, through-thickness axial stress distributions tend to be complex. Linear interpolation between surface stress values will be in error. It is also shown that, for heat inputs less than 70 J/sqmm, the root axial stress does not exceed half yield tension. ESA

N87-22993# Air Force Inst. of Tech., Wright-Patterson AFB, Ohio. School of Engineering.

TWO-DIMENSIONAL ELASTIC ANALYSIS BY THE BOUNDARY ELEMENT METHOD M.S. Thesis

Foster R. Harris Dec. 1986 148 p
(AD-A179213; AFIT/GA/AA/86D-6) Avail: NTIS HC A07/MF A01 CSCL 20K

This thesis analyzed a crack from a blunt notch and several classic fracture mechanics problems using the Boundary Element Method. Alternative formulations were considered, including direct and indirect methods, special crack tip elements, and higher order formulations. The indirect, or displacement discontinuity method was selected as most appropriate. To fully evaluate the technique before attacking the major problem, a series of classical problems was solved, including a hole in a plate under uniaxial tension, a center crack plate and a crack eminating from a hole. Each problem was analyzed first considering an infinite plate boundary and again considering a finite plate boundary. Agreement with analytic solutions from various sources was excellent. A stress intensity analysis of the crack eminating from a blunt notch was performed and compared to an elastic finite element solution. This complicated problem is not published in the literature, and therefore comparison to finite element solution is indicated. The two solution techniques agreed to within a few percent and confirm that the indirect boundary element technique is applicable to this type of elastic solution. GRA

N87-22994# Texas Univ., Austin. Geotechnical Engineering Center.

INVESTIGATION OF LOW-AMPLITUDE SHEAR WAVE VELOCITY IN ANISOTROPIC MATERIAL Final Technical Report, 1 Feb. 1983 - 15 Jun. 1986

Shannon H. Lee and Kenneth H. Stokoe, II Aug. 1986 262 p
(Grant AF-AFOSR-0062-83)
(AD-A179563; AFOSR-87-0483TR) Avail: NTIS HC A12/MF A01 CSCL 08M

An understanding of the relationship between low-amplitude shear wave velocity and state of stress is necessary for correctly measuring and properly utilizing seismic shear waves in geotechnical engineering. Theoretically, the mean effective stress has been shown to be the stress state controlling shear wave velocity in an isotropic, homogeneous, particulate medium. Mean effective stress has been assumed to be the stress state controlling anisotropic, particulate material even though several researches have shown discrepancies with this assumption. Therefore, a 7-ft cubical sample of dry sand was constructed in a large-scale triaxial device. Instrumentation was embedded in the sample during construction so that shear waves could be excited and monitored within the sand while loaded under true triaxial conditions. Extensive seismic tests were conducted under isotropic, biaxial and triaxial confinements in order to compare measured shear wave velocities with previous research and to investigate the influence of anisotropic stress state on velocity. The behavior of shear waves under isotropic loading agrees with the results of previous investigations and indicates the importance of mean effective stress in estimating shear wave velocity. GRA

N87-22995# Anamet Labs., Inc., San Carlos, Calif.

NUMERICAL METHODS FOR IMPERFECTION SENSITIVITY ANALYSIS OF STIFFENED CYLINDRICAL SHELLS. VOLUME 1: DEVELOPMENT AND APPLICATIONS Interim Report, Jun. 1984 - May 1986

Richard L. Citerley and Narendra S. Khot Sep. 1986 72 p
(Contract F33615-84-C-3216)
(AD-A179686; ANAMET-ASIAC-585.1A-Vol-1; AFWAL-TR-86-3032-Vol-1) Avail: NTIS HC A04/MF A01 CSCL 13M

This report contains documentation for four computer programs used in the imperfection sensitivity analysis of cylindrical shells. The four programs are based upon Donnell's equation for cylindrical shells. The formulation of each program is worked in detail so others may make modification. Input and output instructions, together with the program listings, are provided. This report is in two volumes. Volume 1 discusses the development and applications of the programs, and Volume 2 is the user's manual. GRA

N87-22996*# Pratt and Whitney Aircraft, East Hartford, Conn.

ON 3-D INELASTIC ANALYSIS METHODS FOR HOT SECTION COMPONENTS. VOLUME 1: SPECIAL FINITE ELEMENT MODELS Annual Status Report, 14 Feb. 1985 - 14 Feb. 1986

S. Nakazawa Mar. 1987 102 p
(Contract NAS3-23697)
(NASA-CR-179494; NAS 1.26:179494; PWA-5940-46-Vol-1; ASR-3) Avail: NTIS HC A06/MF A01 CSCL 20K

This Annual Status Report presents the results of work performed during the third year of the 3-D Inelastic Analysis Methods for Hot Section Components program (NASA Contract NAS3-23697). The objective of the program is to produce a series of new computer codes that permit more accurate and efficient three-dimensional analysis of selected hot section components, i.e., combustor liners, turbine blades, and turbine vanes. The computer codes embody a progression of mathematical models and are streamlined to take advantage of geometrical features, loading conditions, and forms of material response that distinguish each group of selected components. This report is presented in two volumes. Volume 1 describes effort performed under Task 4B, Special Finite Element Special Function Models, while Volume 2 concentrates on Task 4C, Advanced Special Functions Models. Author

N87-22997# Edgerton, Germeshausen and Grier, Inc., Idaho Falls, Idaho.

DETERMINATION OF CRACK INITIATION SITES USING A DIGITAL NDE WORKSTATION

B. A. Barna, J. A. Johnson, and R. T. Allemeier Nov. 1986 6 p

Presented at the SEM Fall Meeting, Keystone, Colo., 2 Nov. 1986
(Contract DE-AC07-76ID-01570)
(DE87-001444; EGG-M-32586; CONF-8611110-2) Avail: NTIS HC A02/MF A01

A digital acoustic emission data acquisition and analysis system has been configured to dynamically follow and record the acoustic emissions generated by individual crack initiation sites during fracture. The purpose of this research is to analyze the dynamics of the growing fracture and to discriminate between fracture mechanisms through pattern analysis of the received signals. The work described in this paper is the preliminary experiments using a laser as a simulated AE source for calibration and two experiments in which data were collected from a three-point-bend titanium fracture test. DOE

N87-22998# Lawrence Livermore National Lab., Calif.
DYNA3D: A COMPUTER CODE FOR CRASHWORTHINESS ENGINEERING
J. O. Hallquist and D. J. Benson Sep. 1986 20 p Presented at the 15th International Finite Element Congress, Baden-Baden, West Germany, 17 Nov. 1986
(Contract W-7405-eng-48)
(DE87-003818; UCRL-95152; CONF-8611126-1) Avail: NTIS HC A02/MF A01

A finite element program with crashworthiness applications has been developed at LLNL. DYNA3D, an explicit, fully vectorized, finite deformation structural dynamics program, has four capabilities that are critical for the efficient and realistic modeling crash phenomena: (1) fully optimized nonlinear solid, shell, and beam elements for representing a structure; (2) a broad range of constitutive models for simulating material behavior; (3) sophisticated contact algorithms for impact interactions; (4) a rigid body capability to represent the bodies away from the impact region at a greatly reduced cost without sacrificing accuracy in the momentum calculations. Basic methodologies of the program are briefly presented along with several crashworthiness calculations. Efficiencies of the Hughes-Liu and Belytschko-Tsay shell formulations are considered. DOE

N87-22999# Argonne National Lab., Ill.
EXPERIMENTAL STUDY OF COUPLING BETWEEN EDDY CURREN OF TOKAMAK LIMITERS OF TOKAMAK LIMITERS
L. R. Turner and T. Q. Hua 1986 6 p Presented at the IUTAM Conference: Electromagnetomechanical Interactions in Deformable Solids and Structures, Tokyo, Japan, 12 Oct. 1986
(Contract W-31109-eng-38)
(DE87-004938; CONF-8610240-1) Avail: NTIS HC A02/MF A01

The coupling between eddy current and motion in a cantilevered beam is examined. The beam, which provides a simple model for the limiter blades of a Tokamak fusion reactor, was subjected to simultaneous orthogonal time-varying and constant magnetic fields. The dynamic deformation of the beam includes two different modes: a bending mode and a torsional mode. Interaction of current with each mode and with the combined modes of vibration is described. Experimental verification of the case without torsional motion was performed with the FELIX facility. The peak deflection and stresses are much less than those predicted without consideration given to the coupling. DOE

N87-23000# Aeronautical Research Labs., Melbourne (Australia).
AN EVALUATION OF MICROGRIDDING TECHNIQUES FOR DETERMINING LOCAL PLASTIC STRAIN DISTRIBUTIONS
P. W. Beaver Nov. 1986 33 p
(AD-A178518; ARL/STRUC-TM-454) Avail: NTIS HC A03/MF A01 CSCL 11F

The fatigue and fracture properties of most engineering metals are determined by localized plastic deformation in the vicinity of defects such as cracks and/or geometric discontinuities such as notches. Local stresses in these regions may exceed the yield stress even through the bulk of the material is deforming elastically. A knowledge of the local plastic strain distribution at cracks and notches is fundamental to improve our understanding of the fatigue and fracture properties of laboratory specimens, and to correlate these properties with those of structures and components of the same material. The local plastic strain distributions at crack tips and geometric discontinuities have been examined using a variety of methods which fall into two general categories: (1) direct observations of the displacements associated with the strains, and (2) indirect methods in which measurements are compared with a set of calibrated standards. GRA

N87-23001# Brown Univ., Providence, R. I. Div. of Engineering.
DYNAMIC FRACTURE UNDER PLANE WAVE LOADING Interim Report
G. Ravichandran and R. J. Clifton Dec. 1986 152 p
(Contract DAAG29-85-K-0003)
(AD-A178594; ARO-22306.7-EG) Avail: NTIS HC A08/MF A01 CSCL 20K

A new plate impact experiment is described to study dynamic fracture processes occurring under sub-microsecond loading. The experiment is designed to make the measurements amenable to interpretation within the framework of fracture mechanics. A disc containing a mid-plane, pre-fatigued, edge crack that has been propagated halfway across the diameter is impacted by a thin flyer plate of the same material. A comprehensive pulse propagates through the specimen and reflects from the rear surface as a step, tensile pulse with a duration of 1 microsecond. This plane wave loads the crack and causes initiation and propagation of the crack. The motion of the rear surface is monitored during this event using a laser interferometer system. The location of the crack front is mapped before and after the experiment using a focussed ultrasonic transducer. Experiments have been conducted on a hardened 4340 VAR steel at temperatures ranging from room temperature to - 100 C. Crack advance increases monotonically with increasing impact velocity and with decreasing temperature. A finite difference method is used for numerical simulation of the experiments. GRA

N87-23002# Brown Univ., Providence, R. I. Div. of Engineering.
ANALYTICAL CHARACTERIZATION OF SHEAR LOCALIZATION IN THERMOVISCOPLASTIC MATERIALS
A. Molinari and R. J. Clifton Dec. 1986 48 p
(Contract DAAG29-85-K-0003)
(AD-A178597; ARO-22306.8-EG) Avail: NTIS HC A03/MF A01 CSCL 11F

Critical conditions for shear localization in thermoviscoplastic materials are obtained in closed form for idealized models of simple shearing deformations. The idealizations, which include the neglect of heat conduction, inertia, and elasticity, are viewed as quite acceptable for many applications in which shear bands occur. Explicit results obtained for the idealized, but fully nonlinear problem show the roles of strain rate sensitivity, strain hardening, and initial imperfection on the localization behavior. Numerical solutions for two steels are shown to exhibit the principal features reported for torsional Kolsky bar experiments on these steels. Mathematically exact critical conditions obtained for the fully nonlinear problem are compared with critical conditions obtained by means of linear perturbation analysis gives better agreement with the predictions to the fully nonlinear analysis. GRA

N87-23003# Alabama Univ., Huntsville. Dept. of Mechanical Engineering.
VIBRATION ANALYSIS USING SHADOW SPECKLE METROLOGY AND LINE BROADENING TECHNIQUES
David L. Lehner, T. D. Dudderar, Donald R. Matthys, and John A. Gilbert 1987 9 p
(Contract DAAL03-86-K-0014)
(AD-A178626; ARO-23573.15-EG) Avail: NTIS HC A02/MF A01 CSCL 20K

The application of two different computer based optical methods for locating the positions and amplitudes of nodes and antinodes in vibrating members is described. In a technique called shadow speckle metrology, artificial speckles are projected at an angle onto a vibrating surface using a 35mm projector and a speckled slide. In the second technique called line broadening, a single line is used for projection. The vibrating surface and the projected images are captured either directly using a vidicon camera/digitizer system, or indirectly using an ordinary camera to record a time average photograph which is digitized subsequently. Computer programs compare these images to images recorded prior to excitation in order to determine the mode shape and the amplitude of vibration. GRA

N87-23004# Army Aviation Systems Command, St. Louis, Mo.
ANALYSIS OF STRUCTURES WITH ROTATING, FLEXIBLE SUBSTRUCTURES
A. S. Hopkins and Peter Likins 1987 11 p
(AD-A178903) Avail: NTIS HC A02/MF A01 CSCL 20K

A new methodology has been developed for the dynamic analysis of flexible structures, parts of which may be experiencing discrete motion relative to other parts. It can represent the continuum deformations typically treated using finite element methods. In addition, it can also represent the discrete motion at joints traditionally available with multibody methods. After decomposing the structure into substructures and associating a frame of reference with each substructure, the equations of motion for each substructure can be written explicitly including contributions due to the frame of reference generalized coordinates. By expanding the set of constraints to include those that eliminate the redundancy introduced by the frame generalized coordinates, the equations of motion become amenable to solution. The first digital computer program using this methodology is the General Rotorcraft Aeromechanical Stability Program (GRASP). GRASP is limited to applications involving steady state rotation, but extension to arbitrary motions (including spin up) can be accomplished by the selective retention of nonlinear terms in this formulation. GRA

N87-23005# Dayton Univ., Ohio. Research Inst.
BODNER-PARTOM VISCOPLASTIC MODEL IN STEALTH FINITE DIFFERENCE CODE Interim Report, Apr. 1985 - Apr. 1986
A. M. Rajendran and D. J. Grove Jan. 1987 55 p
(Contract F33615-84-C-5045)
(AD-A178994; UDR-TR-86-22; AFWAL-TR-86-4098) Avail: NTIS HC A04/MF A01 CSCL 20K

Most of the state of the art finite difference codes are still incapable of describing strain rate and loading history dependent plastic flow behaviors in metals. The main objective of our work was to develop a computational algorithm for describing viscoplastic constitutive model in a finite difference code. A subincremental time stepping, iterative numerical scheme was used to describe Bodner Partom viscoplastic model in the STEALTH finite difference code. Several special purpose subroutines were developed and incorporated into the code. The new routines were validated by comparing the solutions obtained for several model problems with the already available solutions of those problems. This report also describes in detail the input preparations for the Bodner Partom model and the flowcharts associated with the numerical algorithms. GRA

N87-23006# Pennsylvania State Univ., State College. Applied Research Lab.
NON-LINEAR FINITE ELEMENT ANALYSIS PROGRAM
Shirish N. Kher 10 Dec. 1986 148 p
(Contract N00024-85-C-6041)
(AD-A179038; ARL/PSU-TM-86-215) Avail: NTIS HC A07/MF A01 CSCL 12A

The Non-Linear Finite Element Analysis Program NOFEAP is designed for applications which require frequency modifications. The program, developed for VAX 11/730 running under VMS Version 4.3 operating system, is modular in structure. The problem solution module is designed around a macro programming language concept in which the solution algorithm is written by the user. There are sufficient macro commands in the program for many applications in structural mechanics. The element library of NOFEAP contains elements to model linear and non-linear problems for axisymmetric bodies and bodies in plane strain or plane stress. Nonlinear elements are available for elastic-plastic and/or geometrically non-linear analysis. Surface nonlinearities are modeled by using a contact problem formulation provided in the problem for two-dimensional bodies. This manual contains NOFEAP user manuals for mesh generation, macro commands' definition and the element library description. GRA

N87-23007# Virginia Univ., Charlottesville. Dept. of Mechanical and Aerospace Engineering.
AUTOMATED TRANSIENT ANALYSIS OF STRUCTURAL MEMBERS Final Report, 1 Sep. 1982 - 31 Aug. 1983
Walter D. Pilkey 4 Mar. 1987 16 p
(Contract N00014-75-C-0374)
(AD-A179042; UVA/525303/MAE86/101) Avail: NTIS HC A02/MF A01 CSCL 13M

The trend in structural analysis in the past two decades has been the development of the finite element methodology. The state-of-the-art of the finite element method is such that most linear structural problems can be solved, provided time and cost are not of concern. For many engineering problems of interest to the Navy, a finite element model may not be as appropriate as a structural member model. The latter may be adequate and, indeed, even more accurate. Hence, there is a pressing need for efficient, accurate structural member solutions. The goal of this project has been to develop structural member dynamic response technology so that it is as reliable as static response methodology, even for complex geometric, material, and loading situations. The technology being developed is computational. Reanalysis formulations, which were developed primarily for discrete systems, are extended to structural members. Studies of design sensitivity, synthesis for prescribed dynamic characteristics, and optimizations under dynamic constraints were performed. GRA

N87-23008*# National Aeronautics and Space Administration, Washington, D.C.
INFLUENCE OF SUPPORTING CONDITIONS ON STRESS INTENSITY FACTORS FOR SINGLE-EDGE-CRACKED SPECIMENS UNDER BENDING
Hiromobu Nisitani and Kazuya Mori Jun. 1987 14 p Transl. into ENGLISH from Kyushu Univ. Technology Reports (Japan), v. 58, Oct. 1985 p 751-755 Original language document was announced in IAA as A86-31212 Transl. by Scitran, Inc., Santa Barbara, Calif.
(Contract NASw-4004)
(NASA-TT-20016; NAS 1.77:20016; ISSN-0023-2718) Avail: NTIS HC A02/MF A01 CSCL 20K

The stress intensity factors for single-edge-cracked (SEC) specimens under three- or four-point bending are analyzed by the body force doublet method, and the influence of supporting conditions on K1 is considered. The difference between the values of K1 under pure bending and three-point bending is discussed, based on the difference between the stress distributions of the specimens without cracks under these two loading conditions. The approximate expression for Ki of SEC specimens under three-point bending is also given. Author

N87-23009*# National Aeronautics and Space Administration. Ames Research Center, Moffett Field, Calif.
PREDICTION OF SERVICE LIFE OF AIRCRAFT STRUCTURAL COMPONENTS USING THE HALF-CYCLE METHOD
William L. Ko May 1987 27 p
(NASA-TM-86812; H-1352; NAS 1.15:86812) Avail: NTIS HC A03/MF A01 CSCL 20K

The service life of aircraft structural components undergoing random stress cycling was analyzed by the application of fracture mechanics. The initial crack sizes at the critical stress points for the fatigue-crack growth analysis were established through proof load tests. The fatigue-crack growth rates for random stress cycles were calculated using the half-cycle method. A new equation was developed for calculating the number of remaining flights for the structural components. The number of remaining flights predicted by the new equation is much lower than that predicted by the conventional equation. Author

N87-23010*# National Aeronautics and Space Administration. Lewis Research Center, Cleveland, Ohio.

FINITE ELEMENT IMPLEMENTATION OF ROBINSON'S UNIFIED VISCOPLASTIC MODEL AND ITS APPLICATION TO SOME UNIAXIAL AND MULTIAXIAL PROBLEMS

V. K. Arya and A. Kaufman Jun. 1987 20 p
(NASA-TM-89891; E-3583; NAS 1.15:89891) Avail: NTIS HC A02/MF A01 CSCL 20K

A description of the finite element implementation of Robinson's unified viscoplastic model into the General Purpose Finite Element Program (MARC) is presented. To demonstrate its application, the implementation is applied to some uniaxial and multiaxial problems. A comparison of the results for the multiaxial problem of a thick internally pressurized cylinder, obtained using the finite element implementation and an analytical solution, is also presented. The excellent agreement obtained confirms the correct finite element implementation of Robinson's model. Author

N87-23011# Aeronautical Research Labs., Melbourne (Australia).

ON THE APPLICATION OF THE STRAIN ENERGY DENSITY THEORY IN PREDICTING CRACK INITIATION AND ANGLE OF GROWTH

A. K. Wong Sep. 1986 22 p
(AR-004-493; ARL-STRUC-R-421) Copyright Avail: NTIS HC A02/MF A01

Until recently, the one-parameter singular expression for stresses near a crack-tip was widely thought to be sufficiently accurate over a reasonable region for any geometry and loading conditions. This view is fast changing due to the growing evidence that the inclusion of higher order terms can significantly affect the solution, particularly under certain biaxial loading conditions. In this context, the strain energy density criterion for fracture, and the consequences of the assumption of a I/r energy singularity in the formulation on its application were examined. It is found that this assumption imposes a rather severe restriction on the region for which the criterion is applicable, and that its application on an arbitrarily selected small distance from the crack-tip (a proceduce which was adopted by many experimentalists and finite element analysis), can lead to erroneous results. Author

N87-22707*# Tennessee Univ. Space Inst., Tullahoma.

A GENERAL METHOD FOR DYNAMIC ANALYSIS OF STRUCTURES OVERVIEW

Remi C. Engels *In* NASA. Marshall Space Flight Center Structural Dynamics and Control Interaction of Flexible Structures Apr. 1987 p 119-132 (For primary document see N87-22702 16-15) (Contract F29601-85-K-0054)
Avail: NTIS HC A99/MF E03 CSCL 20K

N87-22712*# Jet Propulsion Lab., California Inst. of Tech., Pasadena.

VERIFICATION OF LARGE BEAM-TYPE SPACE STRUCTURES

Choon-Foo Shih, Jay C. Chen, and John A. Garba *In* NASA. Marshall Space Flight Center Structural Dynamics and Control Interaction of Flexible Structures Apr. 1987 p 247-254 (For primary document see N87-22702 16-15)
Avail: NTIS HC A99/MF E03 CSCL 20K

N87-22713*# Jet Propulsion Lab., California Inst. of Tech., Pasadena.

VERIFICATION OF FLEXIBLE STRUCTURES BY GROUND TEST

Ben K. Wada and C. P. Kuo *In* NASA. Marshall Space Flight Center Structural Dynamics and Control Interaction of Flexible Structures Apr. 1987 p 255-274 (For primary document see N87-22702 16-15)
Avail: NTIS HC A99/MF E03 CSCL 20K

N87-22720*# National Aeronautics and Space Administration. Langley Research Center, Hampton, Va.

AN OVERVIEW OF CONTROLS RESEARCH ON THE NASA LANGLEY RESEARCH CENTER GRID

Raymond C. Montgomery *In* NASA. Marshall Space Flight Center Structural Dynamics and Control Interaction of Flexible Structures Apr. 1987 p 435-456 (For primary document see N87-22702 16-15)
Avail: NTIS HC A99/MF E03 CSCL 20K

N87-22724*# Boeing Aerospace Co., Seattle, Wash.

DYNAMICS OF TRUSSES HAVING NONLINEAR JOINTS

J. M. Chapman, F. H. Shaw, and W. C. Russell *In* NASA. Marshall Space Flight Center Structural Dynamics and Control Interaction of Flexible Structures Apr. 1987 p 539-566 (For primary document see N87-22702 16-15)
Avail: NTIS HC A99/MF E03 CSCL 20K

N87-22725*# Boeing Aerospace Co., Seattle, Wash.

EQUIVALENT BEAM MODELING USING NUMERICAL REDUCTION TECHNIQUES

J. M. Chapman and F. H. Shaw *In* NASA. Marshall Space Flight Center Structural Dynamics and Control Interaction of Flexible Structures Apr. 1987 p 567-594 (For primary document see N87-22702 16-15)
Avail: NTIS HC A99/MF E03 CSCL 20K

N87-22726*# National Aeronautics and Space Administration. Marshall Space Flight Center, Huntsville, Ala.

DYNAMIC CHARACTERISTICS OF A VIBRATING BEAM WITH PERIODIC VARIATION IN BENDING STIFFNESS

John S. Townsend *In its* Structural Dynamics and Control Interaction of Flexible Structures Apr. 1987 p 595-624 (For primary document see N87-22702 16-15)
Avail: NTIS HC A99/MF E03 CSCL 20K

N87-22727*# Jet Propulsion Lab., California Inst. of Tech., Pasadena.

STRUCTURAL DYNAMICS SYSTEM MODEL REDUCTION

J. C. Chen, T. L. Rose, and B. K. Wada *In* NASA. Marshall Space Flight Center Structural Dynamics and Control Interaction of Flexible Structures Apr. 1987 p 625-668 (For primary document see N87-22702 16-15)
Avail: NTIS HC A99/MF E03 CSCL 20K

N87-22728*# National Aeronautics and Space Administration. Marshall Space Flight Center, Huntsville, Ala.

WORKSHOP ON STRUCTURAL DYNAMICS AND CONTROL INTERACTION OF FLEXIBLE STRUCTURES

L. P. Davis, J. F. Wilson (Sperry Corp., Phoenix, Ariz.), and R. E. Jewell *In its* Structural Dynamics and Control Interaction of Flexible Structures Apr. 1987 p 669-690 Reprinted from Vibration Damping Workshop, 6 Mar. 1986 (For primary document see N87-22702 16-15)
Avail: NTIS HC A99/MF E03 CSCL 20K

N87-22730*# California Inst. of Tech., Pasadena.

VIBRATION SUPPRESSION BY STIFFNESS CONTROL

James Fanson, Thomas Caughey, and Jay Chen *In* NASA. Marshall Space Flight Center Structural Dynamics and Control Interaction of Flexible Structures Apr. 1987 p 693-758 (For primary document see N87-22729 16-15)
Avail: NTIS HC A99/MF E03 CSCL 20K

N87-22735*# National Aeronautics and Space Administration. Marshall Space Flight Center, Huntsville, Ala.

A TREETOPS SIMULATION OF THE HUBBLE SPACE TELESCOPE-HIGH GAIN ANTENNA INTERACTION

John P. Sharkey *In its* Structural Dynamics and Control Interaction of Flexible Structures Apr. 1987 p 881-902 (For primary document see N87-22729 16-15)
Avail: NTIS HC A99/MF E03 CSCL 20K

N87-22742*# Lockheed Missiles and Space Co., Sunnyvale, Calif. Space Systems Div.

VIBRATION ISOLATION FOR LINE OF SIGHT PERFORMANCE IMPROVEMENT

J. J. Rodden, H. J. Dougherty, and W. B. Haile *In* NASA.

Marshall Space Flight Center Structural Dynamics and Control Interaction of Flexible Structures Apr. 1987 p 1071-1078 (For primary document see N87-22729 16-15)
Avail: NTIS HC A99/MF E03 CSCL 20K

N87-22743*# Auburn Univ., Ala. Dept. of Aerospace Engineering.
A NEW APPROACH FOR VIBRATION CONTROL IN LARGE SPACE STRUCTURES
K. Kumar and J. E. Cochran, Jr. *In* NASA. Marshall Space Flight Center Structural Dynamics and Control Interaction of Flexible Structures Apr. 1987 p 1079-1094 (For primary document see N87-22729 16-15)
Avail: NTIS HC A99/MF E03 CSCL 20K

N87-22746*# DYNACS Engineering Co., Inc., Clearwater, Fla.
NOTES ON IMPLEMENTATION OF COULOMB FRICTION IN COUPLED DYNAMICAL SIMULATIONS
R. J. VanderVoort and R. P. Singh *In* NASA. Marshall Space Flight Center Structural Dynamics and Control Interaction of Flexible Structures Apr. 1987 p 1197-1213 (For primary document see N87-22729 16-15)
Avail: NTIS HC A99/MF E03 CSCL 20K

N87-22747*# Jet Propulsion Lab., California Inst. of Tech., Pasadena.
ON THE CONTROL OF STRUCTURES BY APPLIED THERMAL GRADIENTS
Don Edberg and Jay-C. Chen *In* NASA. Marshall Space Flight Center Structural Dynamics and Control Interaction of Flexible Structures Apr. 1987 p 1214-1250 (For primary document see N87-22729 16-15)
Avail: NTIS HC A99/MF E03 CSCL 20K

N87-22748*# National Aeronautics and Space Administration. Marshall Space Flight Center, Huntsville, Ala.
FINITE ELEMENT MODELS OF WIRE ROPE FOR VIBRATION ANALYSIS
J. E. Cochran, Jr., N. G. Fitz-Coy, and M. A. Cutchins *In* NASA. Marshall Space Flight Center Structural Dynamics and Control Interaction of Flexible Structures Apr. 1987 p 1251-1270 (For primary document see N87-22729 16-15)
Avail: NTIS HC A99/MF E03 CSCL 20K

N87-22749*# Boeing Aerospace Co., Seattle, Wash.
EXPERIMENTAL CHARACTERIZATION OF DEPLOYABLE TRUSSES AND JOINTS
R. Ikegami, S. M. Church, D. A. Keinholz, and B. L. Fowler (CSA Engineering, Inc., Palo Alto, Calif.) *In* NASA. Marshall Space Flight Center Structural Dynamics and Control Interaction of Flexible Structures Apr. 1987 p 1271-1288 (For primary document see N87-22729 16-15)
Avail: NTIS HC A99/MF E03 CSCL 20K

N87-22771*# Argonne National Lab., Ill.
ANALYTICAL AND EXPERIMENTAL STUDIES OF FLOW-INDUCED VIBRATION OF SSME COMPONENTS
S. S. Chen, J. A. Jendrzejczyk, and M. W. Wambsganss *In* NASA. Lewis Research Center Structural Integrity and Durability of Reusable Space Propulsion Systems 1987 p 33-36 Sponsored in part by DOE (For primary document see N87-22766 16-20)
Avail: NTIS HC A10/MF A01 CSCL 20K

N87-22778*# Case Western Reserve Univ., Cleveland, Ohio.
A NEW FORMULATION OF MEAN STRESS EFFECTS IN FATIGUE
S. S. Manson and K. R. Heidmann (Steelcase Corp., Grand Rapids, Mich.) *In* NASA. Lewis Research Center Structural Integrity and Durability of Reusable Space Propulsion Systems 1987 p 89-93 (For primary document see N87-22766 16-20)
Avail: NTIS HC A10/MF A01 CSCL 20K

N87-22779*# National Aeronautics and Space Administration. Lewis Research Center, Cleveland, Ohio.
NONLINEAR HEAT TRANSFER AND STRUCTURAL ANALYSES OF SSME TURBINE BLADES
A. Abdul-Aziz (Sverdrup Technology, Inc., Middleburg Heights, Ohio.) and A. Kaufman *In its* Structural Integrity and Durability of Reusable Space Propulsion Systems 1987 p 95-104 (For primary document see N87-22766 16-20)
Avail: NTIS HC A10/MF A01 CSCL 20K

N87-22780*# General Electric Co., Cincinnati, Ohio.
STRUCTURAL ANALYSIS DEMONSTRATION OF CONSTITUTIVE AND LIFE MODELS
G. Bechtel, T. S. Cook, M. T. Tipton, and R. L. McKnight *In* NASA. Lewis Research Center Structural Integrity and Durability of Reusable Space Propulsion Systems 1987 p 105-106 (For primary document see N87-22766 16-20)
Avail: NTIS HC A10/MF A01 CSCL 20K

N87-22785*# MARC Analysis Research Corp., Palo Alto, Calif.
THE NESSUS FINITE ELEMENT CODE
J. B. Dias, J. C. Nagiegaal, and S. Nakazawa *In* NASA. Lewis Research Center Structural Integrity and Durability of Reusable Space Propulsion Systems 1987 p 127-131 (For primary document see N87-22766 16-20)
(Contract NAS3-24389)
Avail: NTIS HC A10/MF A01 CSCL 20K

N87-22786*# Rockwell International Corp., Canoga Park, Calif. Rocketdyne Div.
PROBABILISTIC STRUCTURAL ANALYSIS VERIFICATION STUDIES
K. R. Rajagopal *In* NASA. Lewis Research Center Structural Integrity and Durability of Reusable Space Propulsion Systems 1987 p 133-137 (For primary document see N87-22766 16-20)
Avail: NTIS HC A10/MF A01 CSCL 20K

N87-22787*# Southwest Research Inst., San Antonio, Tex.
NESSUS/EXPERT AND NESSUS/FPI IN THE PROBABILISTIC STRUCTURAL ANALYSIS METHODS (PSAM) PROGRAM
O. H. Burnside *In* NASA. Lewis Research Center Structural Integrity and Durability of Reusable Space Propulsion Systems 1987 p 139-143 (For primary document see N87-22766 16-20)
Avail: NTIS HC A10/MF A01 CSCL 20K

N87-22789*# Georgia Inst. of Tech., Atlanta.
STOCHASTIC AND HYBRID-STRESS PLATE/SHELL FINITE ELEMENTS FOR HOT-SECTION COMPONENTS
S. N. Atluri *In* NASA. Lewis Research Center Structural Integrity and Durability of Reusable Space Propulsion Systems 1987 p 151-152 (For primary document see N87-22766 16-20)
Avail: NTIS HC A10/MF A01 CSCL 20K

N87-22790*# Northwestern Univ., Evanston, Ill.
PROBABILISTIC FINITE ELEMENTS
Ted Belytschko and Kam Liu Wing *In* NASA. Lewis Research Center Structural Integrity and Durability of Reusable Space Propulsion Systems 1987 p 153-159 (For primary document see N87-22766 16-20)
(Grant NAG3-535)
Avail: NTIS HC A10/MF A01 CSCL 20K

N87-22796*# Georgia Inst. of Tech., Atlanta.
NONISOTHERMAL ELASTO-VISCO-PLASTIC RESPONSE OF SHELL-TYPE STRUCTURES
G. J. Simitses, R. L. Carlson, and R. Riff *In* NASA. Lewis Research Center Structural Integrity and Durability of Reusable Space Propulsion Systems 1987 p 207-214 (For primary document see N87-22766 16-20)
(Grant NAG3-534)
Avail: NTIS HC A10/MF A01 CSCL 20K

N87-22797*# Sverdrup Technology, Inc., Middleburg Heights, Ohio.
DYNAMIC CHARACTERISTICS OF SINGLE CRYSTAL SSME BLADES
L. A. Moss and T. E. Smith *In* NASA. Lewis Research Center Structural Integrity and Durability of Reusable Space Propulsion Systems 1987 p 211-214 (For primary document see N87-22766 16-20)
Avail: NTIS HC A10/MF A01 CSCL 20K

42 GEOSCIENCES (GENERAL)

No abstracts in this category.

43 EARTH RESOURCES AND REMOTE SENSING

Includes remote sensing of earth resources by aircraft and spacecraft; photogrammetry; and aerial photography.

For instrumentation see *35 Instrumentation and Photography.*

N87-23012# Air Force Geophysics Lab., Hanscom AFB, Mass.
ATMOSPHERIC REMOTE SENSING IN ARCTIC REGIONS
Gerald W. Felde, James T. Bunting, and Kenneth R. Hardy 1986 10 p Reprinted from the Department of Defense Symposium and Workshop on Arctic and Arctic-Related Environmental Sciences, 1986 p 1-8
(AD-A179550; AFGL-TR-87-0128) Avail: NTIS HC A02/MF A01 CSCL 08L

The particular features which must be considered when sensing arctic regions from space platforms include a generally dry atmosphere, thin and low water content clouds which often cover large areas, a highly reflective snow or ice background in the visible spectrum, and weak thermal contrast between snow and cloud in the thermal infrared spectrum. In recent years, more attention has been given to the problem of identifying clouds in arctic regions. An investigation of operational cloud analysis programs for arctic regions has been initiated; results from this study have shown that clouds are often specified in regions which turn out to be generally cloud-free and vice versa. Some possible reasons for this error will be presented. Results of discriminating clouds from a snow background using multi spectral visible and near Infrared sensors will also be given. A new Special Sensor Microwave/Imager (SSM/I) operating at four frequencies from 19 to 85 GHz is designed to provide estimates of several surface and atmospheric characteristics. Several parameters which will be estimated from SSM/I data are of particular interest to arctic regions. These include snow parameters, sea ice attributes, cloud amount over snow, cloud liquid water content, soil moisture, and land surface temperature. GRA

N87-23013* National Aeronautics and Space Administration, Washington, D.C.
EARTH RESOURCES: A CONTINUING BIBLIOGRAPHY WITH INDEXES (ISSUE 53)
May 1987 165 p
(NASA-SP-7041(53); NAS 1.21:7041(53)) Avail: NTIS HC A08 CSCL 05B

This bibliography lists 604 reports, articles, and other documents introduced into the NASA scientific and technical information system between January 1 and March 31, 1987. Emphasis is placed on the use of remote sensing and geophysical instrumentation in spacecraft and aircraft to survey and inventory natural resources and urban areas. Subject matter is grouped according to agriculture and forestry, environmental changes and cultural resources, geodesy and cartography, geology and mineral resources, hydrology and water management, data processing and distribution systems, instrumentation and sensors, and economic analysis. Author

N87-23014# Army Cold Regions Research and Engineering Lab., Hanover, N. H.
AN EVALUATION OF THE POLAR ICE PREDICTION SYSTEM Final Report
W. B. Tucker, III and W. D. Hibler, III Feb. 1987 98 p
(AD-A178522) Avail: NTIS HC A05/MF A01 CSCL 08L

The Polar Ice Prediction System (PIP) is a numerical ice forecasting system that has been implemented at the U.S. Navy Fleet Numerical Oceanographic Center (FNOC). The PIPS model is run as a 24-hr timestep out to 144 hours (6 days) on a 47 x 25 grid at a resolution of 127 Km. This grid covers the entire Arctic basin as well as the Greenland and Norwegian Seas. Graphic forecast products are transmitted via the Naval Environmental Display Systems to the Naval Polar Oceanographic Center (NPOC) for guidance in preparation of weekly ice forecasts. Primary products are ice drift, thickness, concentration and divergence. A two-phased evaluation of PIPS was conducted. The first extended from 15 Nov 1985 until 15 March 1986 while the second phase ran from 15 June until 15 Oct 1986. As well as covering periods of ice growth and decay, the model was initialized differently for the two phases. During Phase I, the model self-generated its initial concentration field from analysis atmospheric forcing fields. For Phase II, the digitized ice analysis prepared by NPOC was used to update the model each week. GRA

N87-23015# Louisiana State Univ., Baton Rouge. Remote Sensing and Image Processing Lab.
THE INTEGRATION OF SPECTRAL AND SPATIAL ANALYSIS FOR LAND USE CLASSIFICATION Final Report, 27 Sep. 1982 - 30 Sep. 1986
Charles A. Harlow Dec. 1986 24 p
(Contract DAAG29-82-K-0189)
(AD-A178703; ARO-19327.9-GS) Avail: NTIS HC A02/MF A01 CSCL 17H

This report describes the research conducted through September 1986 on the investigation of vision systems for aerial scenes. The projects reported on include: (1) Defining Measures Related to Perceptual Properties, (2) Texture Operators and their Application to Vision Systems, (3) Structure of Vision Systems for Aerial Scenes, and (4) General Purpose Spatial Operators. GRA

N87-23016# Naval Postgraduate School, Monterey, Calif.
LASER REFLECTANCE AS A FUNCTION OF ROUGH WATER GLITTER PROFILE M.S. Thesis
Carlton M. Bourne Mar. 1987 67 p
(AD-A178774) Avail: NTIS HC A04/MF A01 CSCL 17H

A new remote sensing technique was developed for predicting the expected mean laser radar return from a rough water surface. This technique involved measuring the standard deviations of the upwind and crosswind profiles of the elliptical glitter patterns occurring for illumination of the water surface with a point source near the laser radar system. A pencil beam laser radar from a companion project simultaneously measured the reflected signals from the water surface. The glitter pattern images were recorded with a video camera and recorder. The images for each run were later digitized along their major and minor elliptic axes and averaged over 256 images to produce smooth intensity curvers from which the standard deviations were measured. The radar return fluctuated over a large range because of the rapid variation of individual water surface facets, and so was recorded and time averaged for the same interval as the video images. Data sufficient for empirical preduction of expected mean laser return signal were obtained. This is necessary to permit evaluation of the performance of a given laser radar design. The data obtained approximated the predictions of a new model proposed in this work. GRA

N87-23017# SRI International Corp., Menlo Park, Calif.
COMPUTER VISION RESEARCH AND ITS APPLICATIONS TO AUTOMATED CARTOGRAPHY Final Report, 11 Jun. 1984 - 31 May 1986
Martin A. Fischler Mar. 1987 19 p
(Contract MDA903-83-C-0027; ARPA Order 5355)
(AD-A178815) Avail: NTIS HC A02/MF A01 CSCL 17H

The SRI Image Understanding program is a broad effort spanning the entire range of machine vision research. Three major concerns are: (1) to develop a computational description of the physics and mathematics of the vision process; (2) to develop a knowledge-based framework for interpreting sensed (imaged) data; and (3) to develop a machine-based environment for effective experimentation, demonstration, and evaluation of our theoretical results, as well as providing a vehicle for technology transfer. This final report summarizes progress in these and related areas. Author (GRA)

N87-23018*# National Aeronautics and Space Administration. Goddard Space Flight Center, Greenbelt, Md.
QUICK-LOOK GUIDE TO THE CRUSTAL DYNAMICS PROJECT'S DATA INFORMATION SYSTEM
Carey E. Noll, Jeanne M. Behnke, and Henry G. Linder Jun. 1987 82 p
(NASA-TM-87818; NAS 1.15:87818) Avail: NTIS HC A05/MF A01 CSCL 08G

Described are the contents of the Crustal Dynamics Project Data Information System (DIS) and instructions on the use of this facility. The main purpose of the DIS is to store all geodetic data products acquired by the Project in a central data bank and to maintain information about the archive of all Project-related data. Access and use of the DIS menu-driven system is described as well as procedures for contacting DIS staff and submitting data requests. Author

N87-23440*# Geological Survey, Flagstaff, Ariz.
A COMPILATION SYSTEM FOR VENUS RADAR MISSION (MAGELLAN)
Sherman S. C. Wu, Francis J. Schafer, and Annie-Elpis Howington *In* NASA, Washington Reports of Planetary Geology and Geophysics Program, 1986 May 1987 p 233-236 (For primary document see N87-23341 16-91)
Avail: NTIS HC A24/MF A01 CSCL 08B

N87-23442*# Jet Propulsion Lab., California Inst. of Tech., Pasadena.
HIGH RESOLUTION RADAR MAP OF THE MOON
T. W. Thompson *In* NASA, Washington Reports of Planetary Geology and Geophysics Program, 1986 May 1987 p 238-239 (For primary document see N87-23341 16-91)
Avail: NTIS HC A24/MF A01 CSCL 08B

N87-23443*# Geological Survey, Menlo Park, Calif.
LANDFORM IDENTIFICATION: LUNAR RADAR IMAGES
Henry J. Moore and T. W. Thompson (Jet Propulsion Lab., California Inst. of Tech., Pasadena.) *In* NASA, Washington Reports of Planetary Geology and Geophysics Program, 1986 May 1987 p 240-242 (For primary document see N87-23341 16-91)
Avail: NTIS HC A24/MF A01 CSCL 08B

N87-23461*# University of Southern Illinois, Carbondale. Dept. of Geology.
GROUNDWATER SAPPING CHANNELS: SUMMARY OF EFFECTS OF EXPERIMENTS WITH VARIED STRATIGRAPHY
R. Craig Kochel and David W. Simmons *In* NASA, Washington Reports of Planetary Geology and Geophysics Program, 1986 May 1987 p 291-293 (For primary document see N87-23341 16-91)
Avail: NTIS HC A24/MF A01 CSCL 08H

N87-23464*# Oregon State Univ., Corvallis. College of Oceanography.
THE APPLICATION OF FLOW COMPETENCE EVALUATIONS TO THE ASSESSMENT OF FLOOD-FLOW VELOCITIES AND STRESSES
Paul D. Komar *In* NASA, Washington Reports of Planetary Geology and Geophysics Program, 1986 May 1987 p 300-302 (For primary document see N87-23341 16-91)
Avail: NTIS HC A24/MF A01 CSCL 08H

N87-23540*# Lawrence Livermore National Lab., Calif.
CREEP OF ICE: FURTHER STUDIES
H. C. Heard, W. B. Durham, and S. H. Kirby (Geological Survey, Menlo Park, Calif.) *In* NASA, Washington Reports of Planetary Geology and Geophysics Program, 1986 May 1987 p 511-513 (For primary document see N87-23341 16-91)
Avail: NTIS HC A24/MF A01 CSCL 08L

N87-23558*# Geological Survey, Flagstaff, Ariz.
ENHANCED LANDSAT IMAGES OF ANTARCTICA AND PLANETARY EXPLORATION
B. K. Lucchitta, J. A. Bowell, K. Edwards, E. M. Eliason, and H. M. Ferguson *In* NASA, Washington Reports of Planetary Geology and Geophysics Program, 1986 May 1987 p 554 Submitted for publication (For primary document see N87-23341 16-91)
Avail: NTIS HC A24/MF A01 CSCL 08B

44 ENERGY PRODUCTION AND CONVERSION

Includes specific energy conversion systems, e.g., fuel cells; global sources of energy; geophysical conversion; and windpower.

For related information see also *07 Aircraft Propulsion and Power, 20 Spacecraft Propulsion and Power,* and *28 Propellants and Fuels.*

N87-23019# Ceramatec, Inc., Salt Lake City, Utah.
THERMOELECTRIC CONVERSION WITH ION CONDUCTORS Quarterly Technical Progress Report, 1 Nov. 1986 - 15 Jan. 1987
15 Jan. 1987 12 p
(Contract N00014-86-C-0827)
(AD-A179353; QTPR-2) Avail: NTIS HC A02/MF A01 CSCL 07D

This report highlights progress accomplished during the second quarter: Electrolyte conductivity versus composition studies are continuing on both zirconia and bismuth oxide compounds. Electrode studies were initiated to find an efficient electrode to operate at high temperatures (i.e., 1000 C) for the high temperature side of the heat engine. A Bi-element thermoelectric cell was constructed and tested to identify the critical design considerations for efficient energy conversion. GRA

N87-23020*# National Aeronautics and Space Administration. Lewis Research Center, Cleveland, Ohio.
HIGH TEMPERATURE SOLID OXIDE REGENERATIVE FUEL CELL FOR SOLAR PHOTOVOLTAIC ENERGY STORAGE
David J. Bents 1987 19 p Prepared for presentation at the 22nd Intersociety Energy Conversion Engineering Conference, Philadelphia, Pa., 10-14 Aug. 1987; sponsored in part by AIAA, ANS, ASME, SAE, IEEE, ACS, and AIChE
(NASA-TM-89872; E-3549; NAS 1.15:89872; AIAA-87-9203) Avail: NTIS HC A02/MF A01 CSCL 10C

A hydrogen-oxygen regenerative fuel cell (RFC) energy storage system based on high temperature solid oxide fuel cell (SOFC) technology is described. The reactants are stored as gases in lightweight insulated pressure vessels. The product water is stored as a liquid in saturated equilibrium with the fuel gas. The system functions as a secondary battery and is applicable to darkside energy storage for solar photovoltaics. Author

N87-23021# Midwest Research Inst., Golden, Colo.
A COMPARISON OF PREDICTED WIND TURBINE BLADE LOADS TO TEST MEASUREMENTS
A. D. Wright and R. W. Thresher Jan. 1987 10 p Presented at the ASME/JSME/ISES Solar Energy Conference, Honolulu,

Hawaii, 22 Mar. 1987
(Contract DE-AC02-83CH-10093)
(DE87-001130; SERI/TP-217-3070; CONF-870307-9) Avail: NTIS HC A02

The accurate prediction of wind turbine blade loads and response is important in predicting the fatigue life of wind machines. At the SERI Wind Energy Research Center, a rotor code called FLAP (Force and Loads Analysis Program) is currently being validated by comparing predicted results to machine measurements. The FLAP code has been modified to allow the teetering degrees of freedom. This paper describes these modifications and comparisons of predicted blade bending moments to test measurements. Wind tunnel data for a 1/20th scale model will be used to compare FLAP predictions for the cyclic flap-bending moments at the 33% spanwise station for three different wind speeds. The comparisons will be made for both rigid and teetering hubs. Currently, the FLAP code accounts for deterministic excitations such as wind shear, tower shadow, gravity, and prescribed yawing motions. Conclusions will be made regarding the code's accuracy in predicting the cyclic bending moments. DOE

N87-23022# Sandia National Labs., Albuquerque, N. Mex.
STRUCTURAL DESIGN AND FABRICATION OF THE SANDIA 34-METER VERTICAL AXIS WIND TURBINE
T. D. Ashwill 1987 7 p Presented at the ASME/JSME/ISES Solar Energy Conference, Honolulu, Hawaii, 22 Mar. 1987
(Contract DE-AC04-76DP-00789)
(DE87-003503; SAND-86-1322C; CONF-870307-7) Avail: NTIS MF A01

The Wind Energy Research Division of Sandia National Laboratories has been funded by the Wind/Ocean Technology Division of the Department of Energy (DOE) to design and build a 34-meter diameter Vertical Axis Wind Turbine (VAWT). The turbine design incorporates the results of recent VAWT research in aerodynamics and structural dynamics. Initial system concept studies identified several blade options that met the required power rating of 500 kW. The final blade and rotor configurations were chosen based on finite element calculations that determined the turbine modes of response, their frequency of vibration, and stress levels. Parked survival turbine components were designed to withstand the loading of a 150 mph (67.0 m/s) wind coupled with maximum cable tensions. Specific areas of design discussed include the rotor, cables, bearings, brakes, and foundations. DOE

N87-23023# Sandia National Labs., Albuquerque, N. Mex.
THE STATUS OF THE VERTICAL AXIS WIND TURBINE RESEARCH TEST BED
H. M. Dodd, Jr. 1987 15 p Presented at the Energy Technology Conference, Albuquerque, N. Mex., 15 Apr. 1987
(Contract DE-AC04-76DP-00789)
(DE87-005524; SAND-87-0214C; CONF-870477-1) Avail: NTIS HC A02

The Sandia National Laboratories has designed, procured, and is presently erecting in Bushland, Texas, a Vertical Axis Wind Turbine (VAWT) research Test Bed in order to develop and demonstrate the improved technologies necessary for the next generation of commercial VAWTs. Of particular interest are the significant improvements predicted by analytical models in the areas of aerodynamic performance, structural dynamics, fatigue life and control strategies. The Test Bed is specifically designed to be a modular research tool rather than a commercial prototype unit; however, the research seeks to directly impact the cost of energy through increased energy capture, more efficient structures (i.e., lower initial cost), increased component lifetimes and improved operating procedures. As is befitting research hardware, the Test Bed is heavily instrumented in order to precisely define its performance and to accurately record the impact of various hardware and operational changes. DOE

N87-23024# New Mexico Solar Energy Inst., Las Cruces.
RELIABILITY OF INTERMEDIATE SIZED PHOTOVOLTAIC SYSTEMS
Jan. 1987 63 p Prepared in cooperation with Sandia National Labs., Albuquerque, N. Mex.
(Contract DE-AC04-76DP-00789)
(DE87-006328; SAND-86-7039) Avail: NTIS HC A04/MF A01

An investigation of the reliability of installed intermediate sized photovoltaic systems identifies interconnection and corrosion losses as the most significant problems. This was determined by performing ten systematic field evaluations on eight different systems using consistent test techniques and recording methods. Simple computer programs were also developed to (1) normalize I-V field data, (2) determine array ratings, (3) predict failure rates and effects, (4) demonstrate the impact of maintenance, and (5) store the data base for future comparison studies. This investigation provides credible field test data on PV components reliability and failure rates. DOE

N87-23025# ENTECH Corp., Dallas-Fort Worth Airport, Tex.
EVALUATION OF A HELIOSTAT TRACKER FOR LINEAR FRESNEL LENS PHOTOVOLTAIC CONCENTRATORS
Dec. 1986 30 p Prepared in cooperation with Sandia National Labs., Albuquerque, N. Mex.
(Contract DE-AC04-76DP-00789)
(DE87-006331; SAND-86-7038) Avail: NTIS HC A03/MF A01

This report presents the results of an evaluation of a heliostat tracking structure used as a two-axis tracking platform for ENTECH's linear focus Fresnel lens photovoltaic collectors. The study included the installation and operation of a heliostat tracker populated with 30 modules (1 operational and 29 non-operational) on a 32-ft x 32-ft platform. Details of the array installation, collector mounting, and array tracking accuracy are provided. Test results demonstrate that the heliostat tracker meets the performance requirements imposed by the collector. The evaluation includes a comparison of the heliostat tracker approach with the current tracker approach (a roll/tilt array). Results of the comparison do not identify a clearly superior option. DOE

N87-23026# Sandia National Labs., Albuquerque, N. Mex.
EVALUATION OF SPHERICAL CERAMIC PARTICLES FOR SOLAR THERMAL TRANSFER MEDIA
J. R. Hellmann, M. O. Eatough, P. F. Hlava, and A. R. Mahoney Jan. 1987 61 p
(Contract DE-AC04-76DP-00789)
(DE87-007432; SAND-86-0981) Avail: NTIS HC A04/MF A01

Two ceramic materials, spheroidized sintered bauxite and fused zircon, were evaluated for potential use as thermal transfer media in an advanced high temperature solid particle solar receiver. Both materials were sufficiently resistant to aggregation via sintering to permit repeated cycling of the particle charge to temperatures approaching 1400°C provided no pressure was applied to the particle bed. Application of pressure dramatically enhanced sintering above 1100°C and yielded non-flowable sintered particle masses. This indicates that moving particle bed storage configurations must be employed for temperatures in excess of 1100°C. The sintered bauxite material exhibited a higher solar absorptance (0.94) than the fused zircon (0.74) for all conditions investigated. Extended thermal treatments in air markedly degraded the solar absorptance of both materials. Degradation was attributed to modifications in crystalline phase assemblages and distribution of multi-valent iron and titanium cations. High solar absorptances could be restored by reheating the oxidized specimens in mildly reducing atmospheres. Potential improvements in the solar absorptance of the fused zircon material may be possible through doping the material with higher concentrations of transition metal and rare Earth cations. DOE

N87-23027*# National Aeronautics and Space Administration. Lewis Research Center, Cleveland, Ohio.
SP-100 ADVANCED TECHNOLOGY PROGRAM
Ronald J. Sovie 1987 12 p Proposed for presentation at the 22nd Intersociety Energy Conversion Engineering Conference,

Philadelphia, Pa., 10-14 Aug. 1987; sponsored by AIAA, ANS, ASME, SAE, IEEE, ACS and AIChE
(NASA-TM-89888; E-3576; NAS 1.15:89888; AIAA-87-9232) Avail: NTIS HC A02/MF A01 CSCL 10B

The goal of the triagency SP-100 Program is to develop long-lived, compact, lightweight, survivable nuclear reactor space power systems for application to the power range 50 kWe to 1 MWe. The successful development of these systems should enable or significantly enhance many of the future NASA civil and commercial missions. The NASA SP-100 Advanced Technology Program strongly augments the parallel SP-100 Ground Engineering System Development program and enhances the chances for success of the overall SP-100 program. The purpose of this paper is to discuss the key technical elements of the Advanced Technology Program and the progress made in the initial year and a half of the project. Author

N87-23028*# National Aeronautics and Space Administration. Lewis Research Center, Cleveland, Ohio.
PERFORMANCE CHARACTERISTICS OF A COMBINATION SOLAR PHOTOVOLTAIC HEAT ENGINE ENERGY CONVERTER
Donald L. Chubb 1987 14 p Prepared for presentation at the 22nd Intersociety Energy Conversion Engineering Conference, Philadelphia, Pa. 10-14 Aug. 1987; cosponsored by AIAA, ANS, ASME, SAE, IEEE, ACS, AIChE
(NASA-TM-89908; E-3591; NAS 1.15:89908; AIAA-87-9035) Avail: NTIS HC A02/MF A01 CSCL 10A

A combination solar photovoltaic heat engine converter is proposed. Such a system is suitable for either terrestrial or space power applications. The combination system has a higher efficiency than either the photovoltaic array or the heat engine alone can attain. Advantages in concentrator and radiator area and receiver mass of the photovoltaic heat engine system over a heat-engine-only system are estimated. A mass and area comparison between the proposed space station organic Rankine power system and a combination PV-heat engine system is made. The critical problem for the proposed converter is the necessity for high temperature photovoltaic array operation. Estimates of the required photovoltaic temperature are presented. Author

N87-23029*# National Aeronautics and Space Administration. Lewis Research Center, Cleveland, Ohio.
COMPONENT VARIATIONS AND THEIR EFFECTS ON BIPOLAR NICKEL-HYDROGEN CELL PERFORMANCE
Michelle A. Manzo, Randall F. Gahn, Olga D. Gonzalez-Sanabria, Robert L. Cataldo, and Russel P. Gemeiner 1987 6 p Prepared for presentation at the 22nd Intersociety Energy Conversion Engineering Conference, Philadelphia, Pa., 10-14 Aug. 1987; cosponsored by AIAA, ANS, ASME, SAE, IEEE, ACS, and AIChE
(NASA-TM-89907; E-3600; NAS 1.15:89907; AIAA-87-9260) Avail: NTIS HC A02/MF A01 CSCL 10C

A 50 cell bipolar nickel-hydrogen battery was assembled to demonstrate the feasibility of constructing a high voltage stack of cells. Various component combinations were tested in this battery. The battery had approximately 1 ampere-hour of capacity and was constructed from components with an active area of 2' X 2'. The components were parametrically varied to give a comparison of nickel electrodes, hydrogen electrodes, separators, fill procedures and electrolyte reservoir plate thicknesses. Groups of five cells were constructed using the same components; ten combinations were tested in all. The battery was thoroughly characterized at various change and discharge rates as well as with various pulse patterns and rates. Over a period of 1400 40% DOD LEO cycles some of the groups began to exhibit performance differences. In general, only separator variations had a significant effect on cell performance. It also appears that shunt currents may have been operating within the stack, resulting in electrolyte transfer from one cell to another, thus contributing to cell performance variations. Author

N87-23030*# Solavolt International, Phoenix, Ariz.
DESIGN, DEVELOPMENT AND DEPLOYMENT OF PUBLIC SERVICE PHOTOVOLTAIC POWER/LOAD SYSTEMS FOR THE GABONESE REPUBLIC Final Report
William J. Kaszeta Apr. 1987 235 p
(Contract DEN3-347)
(NASA-CR-179603; NAS 1.26:179603) Avail: NTIS HC A11/MF A01 CSCL 10B

Five different types of public service photovoltaic power/load systems installed in the Gabonese Republic are discussed. The village settings, the systems, performance results and some problems encountered are described. Most of the systems performed well, but some of the systems had problems due to failure of components or installation errors. The project was reasonably successful in collecting and reporting data for system performance evaluation that will be useful for guiding officials and system designers involved in village power applications in developing countries. R.J.F.

N87-22722*# National Aeronautics and Space Administration. Marshall Space Flight Center, Huntsville, Ala.
SOLAR ARRAY FLIGHT DYNAMIC EXPERIMENT
Richard W. Schock *In its* Structural Dynamics and Control Interaction of Flexible Structures Apr. 1987 p 487-504 (For primary document see N87-22702 16-15)
Avail: NTIS HC A99/MF E03 CSCL 10A

45 ENVIRONMENT POLLUTION

Includes atmospheric, noise, thermal, and water pollution.

N87-23031# Edgerton, Germeshausen and Grier, Inc., Idaho Falls, Idaho.
AN ASSESSMENT OF NITROGEN OXIDE FORMATION IN PREHEATED HIGH-TEMPERATURE COMBUSTION AIR IN INDUSTRIAL PROCESSES
Stephen J. Priebe, Scott L. Richlen, Paul D. Ritter, and Dan F. Suciu Sep. 1986 56 p
(Contract DE-AC07-76ID-01570)
(EGG-2439) Avail: NTIS HC A04/MF A01

To assess the impact of high temperature burner duct recuperator (HTBDR) technology on air quality, researchers at the Idaho National Engineering Laboratory reviewed information on nitrogen oxide (NOx) formation in burners using high temperature combustion air. Increasing combustion air temperature increases burner efficiency, but also generally increases NOx formation. Information was gathered on regulations and standards for NOx emission, industrial burner technology, NOx formation as a function of burner design and combustion air temperature, and the role of computer modeling in low-NOx burner design. Previous work is summarized on laminar and turbulent diffusion flames, staged combustion, kinetics and mechanism of NOx formation, the addition of steam to combustion air, and methods for postcombustion control of NOx formation. Recommendations are made to conduct additional research and development needed to allow the installation of new, and retrofit of, advanced energy-conserving, low-NOx burners. Author

N87-23032# Missouri Univ., Columbia. Dept. of Atmospheric Sciences.
THE IMPACT OF CLIMATE CHANGE FROM INCREASED ATMOSPHERIC CARBON DIOXIDE ON AMERICAN AGRICULTURE
Wayne L. Decker, Vernon K. Jones, and Rao Achutuni May 1986 108 p
(Contract W-7405-eng-48)
(DOE/NBB-0077) Avail: NTIS HC A06/MF A01

The impact of climate change on crop production and animal production are discussed. Genetic selection, cropping patterns, farm management techniques, pest management, forage production and water availability are among the topics considered. R.J.F.

46 GEOPHYSICS

Includes aeronomy; upper and lower atmosphere studies; inospheric and magnetospheric physics; and geomagnetism.

For space radiation see *93 Space Radiation.*

N87-23033*# Texas Univ., Austin. Center for Space Research.
ALTIMETER MEASUREMENTS FOR THE DETERMINATION OF THE EARTH'S GRAVITY FIELD Annual Research Technical Report, 18 Mar. 1986 - 14 Mar. 1987
B. D. Tapley, B. E. Schutz, and C. K. Shum 29 Apr. 1987 15 p
(Grant NAG5-746)
(NASA-CR-180520; NAS 1.26:180520) Avail: NTIS HC A02/MF A01 CSCL 08G

The ability of satellite-borne radar altimeter data to measure the global ocean surface with high precision and dense spatial coverage provides a unique tool for the mapping of the Earth's gravity field and its geoid. The altimeter crossover measurements, created by differencing direct altimeter measurements at the subsatellite points where the orbit ground tracks intersect, have the distinct advantage of eliminating geoid error and other nontemporal or long period oceanographic features. In the 1990's, the joint U.S./French TOPEX/POSEIDON mission and the European Space Agency's ERS-1 mission will carry radar altimeter instruments capable of global ocean mapping with high precision. This investigation aims at the development and application of dynamically consistent direct altimeter and altimeter crossover measurement models to the simultaneous mapping of the Earth's gravity field and its geoid, the ocean tides and the quasi-stationary component of the dynamic sea surface topography. Altimeter data collected by SEASAT, GEOS-3, and GEOSAT are used for the investigation. Author

N87-23034# World Climate Programme, Geneva (Switzerland).
WORKSHOP ON COMPARISON OF SIMULATIONS BY NUMERICAL MODELS OF THE SENSITIVITY OF THE ATMOSPHERIC CIRCULATION TO SEA SURFACE TEMPERATURE ANOMALIES
Jul. 1986 204 p Workshop presented in Boulder, Colo., 9-12 Dec. 1985 Prepared in cooperation with ICSU, Rome, Italy
(WCP-121; WMO-TD-138; ETN-87-99182) Avail: NTIS MF A01; print copy available from WMO, Geneva, Switzerland

Experiments are reported which were carried out with atmospheric general circulation models on the effects of sea surface temperature anomalies on the atmospheric circulation and, in particular, the simulated rainfalls and models derived estimates of surface heat fluxes and surface wind stress. Experiments are also reported with ocean general circulation models on the effects of wind stress and heat flux anomalies on predicted sea surface temperature and ocean circulation. Maps of a variety of parameters such as global precipitation, stream function and velocity potential, zonal mean cross sections of wind components, temperature and specific humidity, mean surface pressure, geopotential heights at a number of standard pressure levels and ocean-atmosphere fluxes of sensible and latent heat and momentum are presented. For individual titles, see N87-23035 through N87-23055.

N87-23035# Canadian Climate Centre, Downsview (Ontario).
SIMULATED AND OBSERVED BUDGETS AND BALANCES DURING THE 82/83 ENSO EVENT
G. J. Boer *In* World Climate Program Workshop on Comparison of Simulations by Numerical Models of the Sensitivity of the Atmospheric Circulation to Sea Surface Temperature Anomalies Jul. 1986 p 12-18 (For primary document see N87-23034 16-46)
Avail: NTIS MF A01; print copy available from WMO, Geneva, Switzerland

The behavior of the atmosphere during an El Nino event was analyzed in terms of global vertically integrated budgets of mass, moisture, and energy. Comparison of the results of a simulation of the 1982 to 1983 event with data from the NMC objective analysis system shows that the major features of this phenomena in the tropical region are captured in the simulation and the observations. The anomalous divergent mass, moisture, and energy fluxes and their associated source/sink distribution make a consistent picture which bears out the phenomenological description of the phenomena given by Bjerknes (1969). ESA

N87-23036# California Univ., Los Angeles. Dept of Atmospheric Sciences.
NUMERICAL EXPERIMENTS ON THE ATMOSPHERIC RESPONSE TO A SEA SURFACE TEMPERATURE ANOMALY OVER THE EQUATORIAL EASTERN PACIFIC OCEAN
Carlos R. Mechoso, Akio Kitoh, Shrinivas Moorthi, and Akio Arakawa *In* World Climate Program Workshop on Comparison of Simulations by Numerical Models of the Sensitivity of the Atmospheric Circulation to Sea Surface Temperature Anomalies Jul. 1986 p 19-28 (For primary document see N87-23034 16-46)
(Grant NSF ATM-82-18215)
Avail: NTIS MF A01; print copy available from WMO, Geneva, Switzerland

Differences between selected fields obtained in simulations performed with several versions of the UCLA General Circulation Model (GCM) for normal and anomalous sea surface temperature (SSTA) are presented. The SSTA pattern resembles that observed during the mature phase of El Nino, and is kept constant in time. Simulations used the 9-layer with low and high horizontal resolutions, and the 15-layer with low horizontal resolution versions of the UCLA GCM. The SSTA results in anomalous precipitation in the tropics which is mostly balanced by anomalous moisture flux convergence. The anomalous moisture fluxes in the planetary boundary layer (PBL) and the free atmosphere have comparable magnitude with different geographical distributions. Consistently, the pattern for the moisture flux convergence in the entire atmospheric column, which is very similar to that to anomalous precipitation, is not similar to any of these two components. Findings suggest that a correct simulation of the moisture flux both in the PBL and the free atmosphere may be crucial in determining the distribution of anomalous precipitation. ESA

N87-23037# Oregon State Univ., Corvallis. Climatic Research Inst.
ENSO EXPERIMENTS WITH A TWO-LEVEL AGCM
Steven K. Esbensen *In* World Climate Program Workshop on Comparison of Simulations by Numerical Models of the Sensitivity of the Atmospheric Circulation to Sea Surface Temperature Anomalies Jul. 1986 p 29-34 (For primary document see N87-23034 16-46)
Avail: NTIS MF A01; print copy available from WMO, Geneva, Switzerland

It is shown that the Oregon State University general circulation model can qualitatively represent many of the observed features of El Nino Southern Oscillation (ENSO) events. Maxima in the anomalies of cloudiness and precipitation occur in regions of maxima of the SST anomaly field with the largest response occurring in regions of warmest sea surface temperatures. The upper-level circulation in the vicinity of the simulated equatorial heating anomaly is qualitatively realistic and the remote response appears to be consistent with observations over the northeast Pacific and North America. There are, however, serious discrepancies that must be corrected before a realistic representation of ENSO events can be obtained, especially the lack of response of the lower tropospheric circulation in the equatorial region, and the unrealistic remote response over the Northwestern Pacific during the simulated 1982 to 1983 ENSO event. ESA

N87-23038# Miami Univ., Fla. Rosenstiel School of Marine and Atmospheric Science.
ATMOSPHERIC SIMULATIONS OF THE 1982-83 ENSO EPISODE
Eric J. Pitcher and Maurice L. Blackmon (National Center for Atmospheric Research, Boulder, Colo.) *In* World Climate Program Workshop on Comparison of Simulations by Numerical Models of the Sensitivity of the Atmospheric Circulation to Sea Surface

Temperature Anomalies Jul. 1986 p 35-39 Sponsored by NSF (For primary document see N87-23034 16-46)
Avail: NTIS MF A01; print copy available from WMO, Geneva, Switzerland

Atmospheric simulations with the NCAR Community Climate Model of the 1982 to 1983 El Nino/Southern Oscillation (ENSO) episode are summarized. Five simulations of the response to the tropical sea surface temperature anomaly pattern evolving through the 20-month period beginning in September, 1981 were completed. Each simulation began from a different year in a 5 yr control run. Ensemble-averaged fields were formed by taking at each grid point the average of the variable over all five realizations. For selected fields, maps of the difference between the ensemble averages for the experiment and the control were generated. Evolution of the seasonal (3 month) average of the precipitation anomaly, vector wind anomaly, and 200 mb height anomaly for winter is shown. ESA

N87-23039# National Center for Atmospheric Research, Boulder, Colo.

SENSITIVITY OF TROPICAL AND MID-LATITUDE TIME-AVERAGED ATMOSPHERIC STATES TO INTERANNUALLY VARYING GLOBAL OCEAN SURFACE TEMPERATURE DISTRIBUTION

Robert M. Chervin *In* World Climate Program Workshop on Comparison of Simulations by Numerical Models of the Sensitivity of the Atmospheric Circulation to Sea Surface Temperature Anomalies Jul. 1986 p 40-47 Sponsored by NSF (For primary document see N87-23034 16-46)
Avail: NTIS MF A01; print copy available from WMO, Geneva, Switzerland

A parallel pair of 15-yr integrations was performed with an annual cycle version of the original NCAR Community Climate Model with lower boundary forcing prescribed by the May 1958 to April 1973 monthly mean global ocean surface temperature analyses from Oort (1983), to study the effect of anomalous forcing from ocean surface temperatures on time averaged atmospheric states. The first experiment features the exact month-by-month evolution of analyzed temperatures while the second was forced by the 15-yr monthly means of the analyses during each model year. Thus, the mean forcing is identical in each experiment but one allows interannual variability in forcing with concomitant evolving global distributions of anomalous ocean surface temperatures. The extent to which such anomalous boundary forcing could produce anomalous time-averaged atmospheric states more extreme than those attainable from unforced internal dynamics acting alone is shown. ESA

N87-23040# Hamburg Univ. (West Germany). Inst. fuer Meteorologie.

PRELIMINARY RESULTS FROM A TROPICAL OCEAN GLOBAL ATMOSPHERE (TOGA) RELATED EXPERIMENT PERFORMED AT HAMBURG (WEST GERMANY) WITH THE ECWME GENERAL CIRCULATION MODEL (GCM) WITH T21 RESOLUTION

Hans vonStorch, Ulrich Schlese, and Edilbert Kirk *In* World Climate Program Workshop on Comparison of Simulations by Numerical Models of the Sensitivity of the Atmospheric Circulation to Sea Surface Temperature Anomalies Jul. 1986 p 48-55 (For primary document see N87-23034 16-46)
Avail: NTIS MF A01; print copy available from WMO, Geneva, Switzerland

An atmospheric circulation model was used to study to what extent fluctuations of the tropical Pacific sea surface temperature (SST) induce low frequency variability in midlatitudes; whether normal El Nino events as the 1972 to 1973 or 1976 to 1977 events excite a significant and stable extratropical flow anomaly; if it is possible to identify in spring and summer a relevant response to strong El Nino events; and to what extent inadequate tropical Pacific SST destroys midlatitude potential predictability. The experiment comprises a control experiment covering a total range of up to 20 annual cycles; a continuous 15 yr simulation forced in an equatorial Pacific strip by actually observed (1970 to 1984) SST instead of climatologically fixed SST; a series of 5-month runs, forced with winter 1972 to 1973 and 1976 to 1977 SST (for both El Ninos) 5 integrations are done, initialized with November 1st conditions as simulated in the years 2, 4, 6, 8, and 10 of the control run; and a series of five November to August integrations with 1982 to 1983 equatorial Pacific SST. ESA

N87-23041# Princeton Univ., N. J. Geophysical Fluid Dynamics Lab.

PRINCIPAL CIRCULATION ANOMALIES IN MODEL ATMOSPHERES WITH AND WITHOUT INTERANNUAL VARIATIONS OF TROPICAL PACIFIC SST

In-Sik Kang and Ngar-Cheung Lau *In* World Climate Program Workshop on Comparison of Simulations by Numerical Models of the Sensitivity of the Atmospheric Circulation to Sea Surface Temperature Anomalies Jul. 1986 p 56-62 (For primary document see N87-23034 16-46)
Avail: NTIS MF A01; print copy available from WMO, Geneva, Switzerland

The issue of external forcing versus internal atmospheric processes in causing circulation changes in the winter Northern Hemisphere was studied in extended general circulation model (GCM) experiments. In a 15-yr experiment (control run), no interannual variability in the external forcing was introduced. Another experiment was performed with the SST conditions in the tropical Pacific being prescribed to follow the actual month-to-month changes observed during a 15-year period. Results imply that internal atmospheric processes and external forcing can impart a considerable level of variability to the atmospheric circulation. Outside of the tropics, the amplitudes of the patterns associated with SST changes and with zonal/eddy interaction are quite comparable. Variability in the tropics is seen to be strongly influenced by the presence of tropical Pacific SST anomalies, the effect being manifest in the fluctuation amplitude and in the character of the spatial pattern. ESA

N87-23042# Princeton Univ., N. J. Geophysical Fluid Dynamics Lab.

DIAGNOSIS OF INTRASEASONAL OSCILLATIONS APPEARING IN GCM EXPERIMENTS CONDUCTED AT GFDL

Ngar-Cheung Lau *In* World Climate Program Workshop on Comparison of Simulations by Numerical Models of the Sensitivity of the Atmospheric Circulation to Sea Surface Temperature Anomalies Jul. 1986 p 63-68 (For primary document see N87-23034 16-46)
Avail: NTIS MF A01; print copy available from WMO, Geneva, Switzerland

The 40 to 50 day oscillation in the tropical atmosphere is discussed. The many similarities that exist between the structure of the intraseasonal oscillations and that of the circulation anomalies associated with El Nino-Southern Oscillations (ENSO) also suggest that the two phenomena might be linked to each other. For a better understanding of the interaction between perturbations with such disparate time scales, monitoring of ENSO events in the real atmosphere should therefore also encompass monitoring of the intraseasonal oscillations. However, the presence of the intraseasonal oscillations in a GCM integration with no SST anomalies imposed infers that the preferred time scale of such oscillations is determined internally within the model atmosphere itself. The presence of a strong intraseasonal signal in the model integration indicates that the essential dynamical and physical processes associated with these oscillations are adequately incorporated in the GCM. ESA

N87-23043# Utah Univ., Salt Lake City. Dept. of Meteorology.

THE 30-60 DAY OSCILLATION IN A PERPETUAL JANUARY SIMULATION WITH THE NCAR GENERAL CIRCULATION MODEL

J. E. Geisler and E. J. Pitcher (Miami Univ., Fla.) *In* World Climate Program Workshop on Comparison of Simulations by Numerical Models of the Sensitivity of the Atmospheric Circulation to Sea Surface Temperature Anomalies Jul. 1986 p 69-71 (For primary document see N87-23034 16-46)

Avail: NTIS MF A01; print copy available from WMO, Geneva, Switzerland

A 1200-day, perpetual January simulation with the NCAR Community Climate Model was analyzed for the presence of an oscillation in the tropics having a period in the 30 to 60 day range. This general circulation model is a q level, sigma coordinate, spectral model with R15 truncation. Convective precipitation and heating is parameterized by a moist convective adjustment process. The model generates its own clouds. The 200 mb velocity potential, 200 mb zonal wind, 500 mb convective heating, outgoing longwave radiation (ORL), and precipitation were examined. The model 30 to 60 day oscillation does not stand out well from spatially incoherent noise in the 200 mb zonal wind field and does not stand out at all in the fields associated with convective activity. The reason for these differences between simulated and observed behavior of the oscillation may be lack of coupling in the model between the large-scale moisture convergence field of the oscillation and the field of convective heating. The model parameterizes tropical convection as moist convective adjustment, a process whose connection to large scale moisture convergence is a statistical one with very low spatial coherence. ESA

N87-23044*# National Aeronautics and Space Administration. Goddard Space Flight Center, Greenbelt, Md.

A PRELIMINARY THEORY OF THE ORIGIN OF THE 40-50 DAY OSCILLATION

K. M. Lau and L. Peng *In* World Climate Program Workshop on Comparison of Simulations by Numerical Models of the Sensitivity of the Atmospheric Circulation to Sea Surface Temperature Anomalies Jul. 1986 p 72-76 Presented at Workshop on Model Intercomparison, Boulder, Colorado, Dec. 1985 (For primary document see N87-23034 16-46)

Avail: NTIS MF A01; print copy available from WMO, Geneva, Switzerland

A theory of the 40 to 50 day oscillation in the tropical atmosphere which encompasses predominantly eastward propagation along the equator, spatial scales of wavenumber 1 and 2, slow time scales (20 to 70 days), and strong amplitude modulation in associated large-scale convective activity as a function of geographical location, i.e., pronounced convection is confined to the Indian Ocean and western Pacific, is presented. An initial disturbance generated near the equator disperses away from the source region, eastward by Kelvin waves and westward by Rossby waves. When the eastward disturbance passes over warm water it is expected to amplify by CISK due to enhanced supply of moisture from the ocean surface. Over cold water, its amplitude is expected to reduce due to decreased moisture supply. The climatological sea surface temperature contrast between the Indian Ocean/western Pacific and the eastern Pacific sets the spatial scale of the wave and its modulation to low wavenumbers and confines pronounced convection to the warm sector. If the eastward propagating wave can maintain itself over dissipation one circuit around the globe, it has a good chance to continue the process indefinitely, provided it is rejuvenated over the warm water with enough energy to go around for the next cycle. ESA

N87-23045# Meteorological Office, Bracknell (England).

FORECAST AND SENSITIVITY EXPERIMENTS ON THE UK METEOROLOGICAL OFFICE GCM WITH EL NINO SST ANOMALIES

T. N. Palmer and J. A. Owen *In* World Climate Program Workshop on Comparison of Simulations by Numerical Models of the Sensitivity of the Atmospheric Circulation to Sea Surface Temperature Anomalies Jul. 1986 p 81-93 (For primary document see N87-23034 16-46)

Avail: NTIS MF A01; print copy available from WMO, Geneva, Switzerland

Model experiments were run to determine equilibrium and transient response to El Nino SST anomalies. In the first set of experiments, 540 day perpetual January integrations with a 2x composite El Nino anomaly and the observed December to February 1982 to 1983 El Nino anomaly were compared with a 540 day mean control integration. To study the transient response, 2 ensembles of 90 day forecast experiments were run from 12z ECMWF analyses for the 15th, 16th and 17th December 1982. One ensemble had seasonally varying climatological SSTs the other had observed SST anomalies added to these climatological values. In both ensembles SSTs were updated every 5 days. One of the major systematic errors in the 11-layer model is excessive wintertime Northern Hemisphere westerlies. These errors can be substantially alleviated by parametrizing the effects of subgridscale topography, through envelope orography or orographic gravity wave drag. The effect on including envelope orography on the zonal wind cross-section from 540 day perpetual January runs (with climatological SST) is shown. Gravity wave drag has a similar effect (although there are important differences). ESA

N87-23046# European Centre for Medium-Range Weather Forecasts, Reading (England).

THE IMPACT OF INITIAL CONDITIONS AND SST ANOMALIES ON EXTENDED RANGE PREDICTIONS FOR THE EL NINO PERIOD c48

Ulrich Cubasch *In* World Climate Program Workshop on Comparison of Simulations by Numerical Models of the Sensitivity of the Atmospheric Circulation to Sea Surface Temperature Anomalies Jul. 1986 p 110-116 (For primary document see N87-23034 16-46)

Avail: NTIS MF A01; print copy available from WMO, Geneva, Switzerland

The El Nino sea surface temperature (SST) anomaly observed during 1982 to 1983 was used to investigate the impact of anomalous forcing at the lower boundary on the predictability of the atmosphere. In order to test the impact of the SST as a function of the initial conditions, forecasts using the observed or climatological SST adjusted every 5th day, were run starting on December 15, 16, and 17 1982. All experiments were run up to 90 days with the ECMWF spectral model and a resolution of T42L16 (i.e., with a Gaussian grid of 2.8125 deg) from the ECMWF operational 12z analysis. Results show that precipitation can be used as a diagnostic tool for the effect of El Nino on the tropical atmosphere. The difference between the experiments with the observed moving and climatological SST indicates the impact of the El Nino SST anomaly on the atmosphere. ESA

N87-23047# European Centre for Medium-Range Weather Forecasts, Reading (England).

A LAGGED-AVERAGE 60-DAY FORECAST EXPERIMENT DURING THE 1982-83 EL NINO PERIOD

F. Molteni and S. Tibaldi *In* World Climate Program Workshop on Comparison of Simulations by Numerical Models of the Sensitivity of the Atmospheric Circulation to Sea Surface Temperature Anomalies Jul. 1986 p 117-123 (For primary document see N87-23034 16-46)

Avail: NTIS MF A01; print copy available from WMO, Geneva, Switzerland

The role of surface thermal forcing in increasing the predictability of low-frequency large-scale atmospheric anomalies was assessed using model runs of winter 1982 to 1983, with the strong El-Nino event. The experiment is composed of two lagged-average forecasting sets of integrations, each consisting of 9 forecasts initiated from adjacent analysis separated by 6-hr intervals. It is concluded that it is plausible that, during the central part of the integration period, the Northern Hemisphere extratropical atmosphere switched from a regime dominated by internal dynamics variability to a regime driven mainly by anomalous boundary forcing. The model integrations seem to be unable to reproduce the former while they show considerable skill in representing the latter. ESA

N87-23048# National Meteorological Center, Washington, D.C.

SENSITIVITY OF THE NMC SPECTRAL MODE TO THE JANUARY 1983 EL NINO SST c48

Robert E. Kistler and J. Shukla (Maryland Univ., College Park.) *In* World Climate Program Workshop on Comparison of Simulations by Numerical Models of the Sensitivity of the Atmospheric Circulation to Sea Surface Temperature Anomalies Jul. 1986

p 124-130 (For primary document see N87-23034 16-46)
Avail: NTIS MF A01; print copy available from WMO, Geneva, Switzerland

The National Meteorological Center (NMC) spectral model was twice integrated to 30 days from the NMC analysis of 00Z, Dec 1982. In one prediction climatological sea surface temperatures (SST) for January were used; in the second the blended SST analysis for January 1983 was used. In both runs, the SST was held fixed throughout the prediction. The impact of the implied SST anomaly on the 30 day mean precipitation was examined. The difference field indicates that the rainfall maxima over the maritime continent and the Andes are insensitive to the SST anomaly. The rainfall differences in the mid-Pacific correspond well with the SST anomalies. The northern branch of the ITCZ is shifted southward in the western Pacific, while in the mid-Pacific it is intensified in place. In the eastern half of the Pacific, the ITCZ remains split with the northern branch producing more rainfall in place, and the southern branch expanding eastward and increasing in intensity in concert with the expanded warmer SST. ESA

N87-23049# Maryland Univ., College Park. Dept. of Meteorology.
TROPICAL PACIFIC SST EXPERIMENTS WITH THE GLAS CLIMATE MODEL **c47**
M. Fennessy *In* World Climate Program Workshop on Comparison of Simulations by Numerical Models of the Sensitivity of the Atmospheric Circulation to Sea Surface Temperature Anomalies Jul. 1986 p 131-136 (For primary document see N87-23034 16-46)
Avail: NTIS MF A01; print copy available from WMO, Geneva, Switzerland

The observed 1982 to 1983 mature phase Pacific SST anomalies were used for control simulations started from observed initial conditions of 15, 16, 17 Dec. 1982. Model control simulation of precipitation is reasonable. For the tropical diabatic heating field, the 3 case average 11 to 60 day model difference field shows a large positive anomaly in the central Pacific of up to 3 deg/day with a negative region of -2 deg/day over Indonesia. The increase in skill in the tropics and extratropics obtained by using observed initial conditions with observed boundary conditions of SST is encouraging. ESA

N87-23050# Canadian Climate Centre, Downsview (Ontario).
AN EXTENDED FORECAST EXPERIMENT WITH THE CCC GCM
G. J. Boer *In* World Climate Program Workshop on Comparison of Simulations by Numerical Models of the Sensitivity of the Atmospheric Circulation to Sea Surface Temperature Anomalies Jul. 1986 p 137-143 (For primary document see N87-23034 16-46)
Avail: NTIS MF A01; print copy available from WMO, Geneva, Switzerland

Enhanced predictability under the strong boundary forcing during El Nino was assessed. A forecast experiment for January 1983 indicates that the divergent flow anomaly is a response to the anomalous boundary forcing and not to the initial conditions. The rotational component of the flow in the tropics is also sensitive to the sea surface temperature anomaly. In the extratropics strong anomalies are present in both hemispheres with and without anomalous boundary conditions. These may represent the consequences of the initial conditions at these latitudes or could be an accidental correspondence between model drift and the observed anomaly for this month. It appears that tropical atmospheric features can be reasonably well predicted as a consequence of the El Nino sea surface boundary forcing while in the extratropics the situation is less clear. Extended predictability may at least partially reside in the initial condition information at these latitudes. ESA

N87-23051# Meteorological Research Inst., Tsukuba (Japan).
THE IMPACT OF SST ANOMALIES AND INITIAL CONDITIONS ON EXTENDED RANGE PREDICTIONS WITH AN ATMOSPHERIC GENERAL CIRCULATION MODEL: A CASE STUDY IN EARLY SUMMER OF 1983
T. Tokioka *In* World Climate Program Workshop on Comparison of Simulations by Numerical Models of the Sensitivity of the Atmospheric Circulation to Sea Surface Temperature Anomalies Jul. 1986 p 144-153 (For primary document see N87-23034 16-46)
Avail: NTIS MF A01; print copy available from WMO, Geneva, Switzerland

Numerical experiments were performed to study the impact of SST anomalies and initial conditions on predictions up to 2 months with an atmospheric general circulation model for a period in the early summer of 1983, when the 1982 to 1983 El Nino was still active and strong impacts of SST anomalies are expected. Results for low latitudes, and extratropical latitudes of the Northern Hemisphere are summarized. ESA

N87-23052# Laboratoire de Meteorologie Dynamique, Paris (France).
SENSITIVITY OF JANUARY 1983 SEA SURFACE TEMPERATURE (SST)-EXPERIMENTS TO THE FORMULATION OF LATERAL DIFFUSION
R. Michaud and R. Sadourny *In* World Climate Program Workshop on Comparison of Simulations by Numerical Models of the Sensitivity of the Atmospheric Circulation to Sea Surface Temperature Anomalies Jul. 1986 p 154-164 (For primary document see N87-23034 16-46)
Avail: NTIS MF A01; print copy available from WMO, Geneva, Switzerland

In order to study medium resolution general circulation model sensitivity to orography, lateral diffusion of temperature and velocity were formulated in such a way that the quantities damped are isobaric gradients. The capacity of the formulation to improve the representation of quasi-stationary planetary waves is evaluated. Monthly mean forecasts of January 1983 were performed using the model with improved lateral diffusion. The sensitivity of such forecasts to the use of observed instead of climatic average temperatures is described. Using lateral diffusion, many large-scale structures are better simulated, in midlatitudes and tropics; variability is also improved, as shown by the displacement towards Central Pacific of the upper level Indonesian monsoon diffluence, in prediction experiments involving the observed field of sea surface temperatures. ESA

N87-23053# Lamont-Doherty Geological Observatory, Palisades, N.Y.
MODELLING AND FORECASTING EL NINO **c48**
S. E. Zebiak and M. A. Cane *In* World Climate Program Workshop on Comparison of Simulations by Numerical Models of the Sensitivity of the Atmospheric Circulation to Sea Surface Temperature Anomalies Jul. 1986 p 167-176 (For primary document see N87-23034 16-46)
Avail: NTIS MF A01; print copy available from WMO, Geneva, Switzerland

In order to reproduce the salient features of the El Nino Southern Oscillation cycle with as simple a model as the essential physics allow, a nonlinear model for the perturbations about a basic state derived from monthly mean climatologies of SST, surface winds, and thermocline depths was formulated. Although the physics of this simple one-mode linear response model can be justified only with great difficulty, it gives surprisingly good results for the low level tropical winds, especially when the heating is known. The heating in the model depends not only on mean and perturbation SST, but also on the mean and perturbation convergence. The most important effect of the convergence feedback is to make the response sensitive to the pattern of divergence and convergence in the mean wind field. The seasonal migration of the Intertropical Convergence Zone becomes especially important. ESA

N87-23054# Max-Planck-Inst. fuer Meteorologie, Hamburg (West Germany).
SENSITIVITY OF AN OCEAN GENERAL CIRCULATION MODEL (OCGM) TO WIND FORCING
M. Latif *In* World Climate Program Workshop on Comparison of Simulations by Numerical Models of the Sensitivity of the Atmospheric Circulation to Sea Surface Temperature Anomalies Jul. 1986 p 179-184 (For primary document see N87-23034 16-46)
Avail: NTIS MF A01; print copy available from WMO, Geneva, Switzerland

A primitive equation model of the tropical Pacific Ocean was forced by realistic wind stress fields over decades. Experiments were performed by using two differently analyzed wind fields. There are 18 common years of integration, which can be compared directly. The results indicate a strong sensitivity of the model to the choice of the wind field. Sea surface temperature anomalies in the eastern Pacific show strong differences between the two model runs. ESA

N87-23055# Oxford Univ. (England). Clarendon Lab.
THE DEVELOPMENT OF A COUPLED GCM SUITABLE FOR MODELLING STUDIES IN TOGA c48
C. Gordon *In* World Climate Program Workshop on Comparison of Simulations by Numerical Models of the Sensitivity of the Atmospheric Circulation to Sea Surface Temperature Anomalies Jul. 1986 p 184-188 (For primary document see N87-23034 16-46)
Avail: NTIS MF A01; print copy available from WMO, Geneva, Switzerland

A coupled model in which the tropical Pacific Ocean is represented by a high resolution version of Cox's (1984) ocean general circulation model (GCM) and the global atmosphere by the UK Meteorological Office 11-layer atmospheric GCM is outlined. The ocean model and experiments using it are described. The quality of the interface fluxes of heat and momentum simulated by the atmospheric model are discussed. ESA

N87-23056# Lowell Univ., Mass. Center for Atmospheric Research.
PRELIMINARY INVESTIGATION OF IONOSPHERIC MODIFICATION USING OBLIQUE INCIDENCE HIGH POWER HF RADIO WAVES
Gary S. Sales, Bodo W. Reinisch, and Claude G. Dozois Sep. 1986 44 p
(Contract F19628-83-C-0092)
(AD-A179174; ULRF-435/CAR; AFGL-TR-86-0203; SR-6) Avail: NTIS HC A03/MF A01 CSCL 04A

A special experiment was carried out using a high powered transmitter and a high gain rhombic antenna to heat the ionosphere at a distance of 1300 km from the transmitter. A Digisonde ionospheric sounder was located at the midpoint to sense any changes that might occur in the ionosphere at the heating cycle period of ten minutes. The measured phase data was processed using spectrum analysis in an attempt to detect this ten minute period. The results are not conclusive but there is some indication that the heating period was detected only during the nighttime in agreement with the theoretical. GRA

N87-23057# Bedford Research Associates, Mass.
INVESTIGATE AND VERIFY THE VALIDITY OF MATHEMATICAL FORMULAS AND PROCEDURES IN RELATION TO DATA OBTAINED FROM THEORETICAL INVESTIGATIONS AND EXPERIMENTAL OBSERVATIONS Final Report, Sep. 1983 - Sep. 1986
F. Battles, P. Burkhardt, H. McAvoy, M. Moses, and K. Chatterjee 30 Sep. 1986 73 p
(Contract F19628-83-C-0090)
(AD-A179564; AFGL-TR-86-0213) Avail: NTIS HC A04/MF A01 CSCL 04A

A report on the use of mathematical formulation to forecast weather trends contains the following: Calculation and Plotting of Cloud Cover Statistics; Computation of Energies Associated with Meteorological circulation; The Contributions of Atmospheric Density on the Drop Off Rate of (C sub n)squared; The Identification of Factors Influencing Turbopause Height; and Themis User Guide for the Purchase Request System. GRA

N87-23058# Washington Univ., Seattle. Dept. of Geophysics.
TWO AND THREE-DIMENSIONAL INVERSION OF MAGNETOTELLURIC DATA Annual Performance Report
J. R. Booker 15 Jan. 1987 50 p
(Contract DE-FG06-86ER-13472)
(DE87-005553; DOE/ER-13472/1) Avail: NTIS HC A03/MF A01

Structure in terms of norms of the derivative of the conductivity (sigma) or logsigma with respect to a function of depth are measured. Models that minimize these norms for chosen levels of chi-squared misfit are found, using an iterative linearized algorithm. In most cases, the models found are very likely the global minima of these norms, as they do not depend on the starting model. It is demonstrated that overfitting data requires extraneous structure. Some choices of the depth function result in systematic overfitting of high frequencies, a blue fit, and extraneous shallow structure. Others result in systematic overfitting of low frequencies, a red fit, and extraneous deep structure. A robust statistic is used to test for whiteness, and show how to make the fit acceptably white by varying the depth function that defines the norm. Using artificial data, it is shown that the optimum norm produces an inversion which does not introduce false structure and which approaches the true structure in a reasonable way as data errors decrease. For models of sigma (but not logsigma) linearization errors are often so small that models may be reasonably interpreted as the true conductivity averaged through known resolution functions. DOE

N87-23059# International Centre for Theoretical Physics, Trieste (Italy).
PERTURBATIVE AND GLOBAL ANOMALIES IN SUPERGRAVITY THEORIES
E. Sezgin Sep. 1986 17 p
(DE87-701562; IC-86/329) Avail: NTIS (US Sales Only) HC A02/MF A01

Perturbative and global anomalies in supergravity theories are reviewed. The existence of a matter and gauge coupled supergravity theory in six dimensions with E/sub 6/xE/sub 7/xU(1) symmetry and highly nontrivial anomaly cancellations is emphasised. The possible string origin of this theory is posed as an open problem, study of which may lead to discovery of new ways to construct/compactify heterotic superstrings. DOE

N87-23060# Rome Air Development Center, Griffiss AFB, N.Y.
MEASUREMENT OF THE ATMOSPHERIC PHASE COHERENCE LENGTH, rSUBo In-House Report, Jan. 1983 - May 1984
Gary D. Wilkins Dec. 1986 33 p
(AD-A178468; RADC-TR-86-192) Avail: NTIS HC A03/MF A01 CSCL 04A

This report provides a method of measuring the atmospheric phase coherence length, r sub o, (also referred to as the diffraction limited aperture of the atmosphere), directly by using a telescope, a few optical instruments, a photomultiplier tube, a spinning reticle wheel, an A to D converter and a computer. Chapter 1 explains the meaning of r sub o and how it limits the performance of optical equipment viewing objects through the atmosphere. The second chapter is an explanation of the modulation transfer function of the atmosphere, and how it can be obtained using a telescope, collimators and a spinning reticle wheel. Chapter 3 describes how analog signal which is produced by the photomultiplier is digitized into an 8 bit digital signal by a device known as a datagrabber, and then fed into the computer. Chapter 4 describes how the data is used to calculate r sub o. The final chapter explains the problems encountered and suggestions to improve the experiment. GRA

N87-23061# Aerospace Corp., El Segundo, Calif. Space Sciences Lab.

ON THE THINNING OF THE PLASMA SHEET DURING SUBSTORMS

E. W. Hones, Jr., S. J. Bame, J. F. Fennell, and D. R. Croley, Jr. 17 Mar. 1987 75 p
(Contract F04701-85-C-0086)
(AD-A178484; TR-0086(6940-05)-17; SD-TR-87-13) Avail: NTIS HC A04/MF A01 CSCL 04A

Concurrent measurements of plasma by the SCATHA satellite in near synchronous orbit and by ISEE 2 in the near magnetotail are used to examine the phenomenon of plasma sheet thinning associated with substorms. Results show that thinning occurs in two stages, thought to be attributable to two different processes. For 30-60 minutes before expansive phase offset, gradual thinning occurred over the region from geosynchronous orbit out to 20 RE in the tail. This was attributable to the tail like configuration thought to lead to neutral line formation and the beginning of magnetic reconnection within the plasma sheet. At expansive phase onset, extreme thinning was seen and is thought to occur as a portion of the plasma sheet (a plasmoid), severed by magnetic connection at a near Earth neutral line, quickly departs tailward. Earthward of the neutral line, the plasma sheet expanded. Results generally support the neutral line model of substorms. GRA

N87-23062# Viz Ability, Corvallis, Oreg.

NEW METHODS FOR OBTAINING SCATTERING AND ABSORPTION FROM TROPOSPHERIC VISIBLE SPECTRUM DATA Final Report, 1 Jul. 1984 - 31 Dec. 1986

Jacqueline I. Gordon 28 Feb. 1987 155 p
(Contract DAAG29-84-C-0014)
(AD-A178590; VA187-1; ARO-21655.8-GS-S) Avail: NTIS HC A08/MF A01 CSCL 20F

During the contract period, new methods for obtaining absorption, aerosol and total scattering optical thickness, and single scattering albedo from tropospheric visible spectrum data were published and then used on two extant sets of tropospheric optical data in the visible spectrum. One ground based set of measurements predated heavy atmospheric pollution. The other set of airborne measurements was from a metropolitan area containing pollution sources. Application of the methods to these data sets further developed the methods, provided substantial examples of their use, served to update the data, and provided a means to access all the atmospheric optical data measured prior to 1976. A significant finding was that the aerosol scattering optical thickness of the total atmosphere or of separate haze layers can be described by a modified Angstrom equation in which the constant is a function of the power of the wavelength. GRA

N87-23063*# Iowa Univ., Iowa City. Dept. of Physics and Astronomy.

LATITUDINAL MOTIONS OF THE AURORA DURING SUBSTORMS

J. D. Craven and L. A. Frank Jan. 1986 37 p
(Contracts N00014-85-K-0404; NAG5-483; Grant NGL-16-001-002)
(NASA-CR-180930; NAS 1.26:180930; AD-A178651; U-of-IOWA-86-04) Avail: NTIS HC A03/MF A01 CSCL 04A

Sequences of auroral images obtained with Dynamics Explorer 1 are used to investigate latitudinal motions of the aurora in substorms. Average speeds of poleward motion are about 230 m/s near local midnight for two isolated, small substorms and about 1000 m/s during an intensification within a previously active auroral oval. The speed of poleward expansion measured at about 6 minute temporal resolution can differ greatly from the average speed due to the episodic development of substorms. This poleward motion may be influenced by the sign of the z component of the interplanetary magnetic field. Recovery of the high latitude boundary of the aurora to presubstorm latitudes is first observed in the post midnight sector. In the premidnight sector the discrete aurora can become stationary for a period of time or even continue further poleward before a retreat to lower latitudes begins. For these substorms the expansion and recovery phases are not separated by about 5 deg poleward leap of the aurora. During the recovery period, a prominent decrease in luminosities is first observed at intermediate latitudes within the auroral distribution. Given that magnetic field lines threading these auroral distributions map to the plasma sheet boundary layer and to the central plasma sheet, respectively, magnetic field lines at the intermediate auroral latitudes then map to the plasma sheet at distances somewhat greater than 22 R sub E. GRA

N87-23064# Rome Air Development Center, Griffiss AFB, N.Y.

CALCULATION OF RAY PATHS IN THE IONOSPHERE USING AN ANALYTIC RAYTRACING TECHNIQUE Technical Report, Feb. 1985 - Feb. 1986

Stanford P. Yukon Jul. 1986 21 p
(AD-A178888; RADC-TR-86-125) Avail: NTIS HC A02/MF A01 CSCL 20N

A method for tracing rays in the ionosphere using analytic solutions to approximate path varying ionospheric potentials is outlined in this report. Using the ionospheric parameters generated by IONCAP and approximating the E-F2 and ground-E layer potential wells by a scaled Morse potential and a linear potential respectively, known solutions to these potentials are promoted to final ray paths by using methods developed for solving the time dependent Schroedinger equation. The computer code necessary to fit the potentials, connect the solutions at the E layer peak, and trace arbitrarily launched rays is described. GRA

N87-23065*# Johns Hopkins Univ., Baltimore, Md. Dept. of Earth and Planetary Sciences.

THE DELINEATION AND INTERPRETATION OF THE EARTH'S GRAVITY FIELD Annual Report, 1 Jun. 1986 - 31 May 1987

Bruce D. Marsh 25 Jun. 1987 17 p
(Grant NAG5-32)
(NASA-CR-181015; NAS 1.26:181015) Avail: NTIS HC A02/MF A01 CSCL 08G

The geoid and topographic fields of the central Pacific were delineated and shown to correlate closely at intermediate wavelengths (500 to 2500 km). The associated admittance shows that anomalies having wavelengths less than about 1000 km are probably supported by the elastic strength of the lithosphere. Larger wavelength anomalies are due to dynamic effects in the sublithosphere. Direct modeling of small scale convection in the asthenosphere shows that the amplitudes of observed geoid and topographic anomalies can be independently matched, but that the observed admittance cannot. Only by imposing an initial regional variation in the thermal regime is it possible to match the admittance. It is proposed that this variation may be due to differences in the onset time of convection beneath the lithosphere of different ages. That is, convection beneath thickening lithosphere is strongly dependent on the rate of thickening (V) relative to the rise time for convection. The critical Rayleigh number contains the length scale K/V, where K is thermal diffusivity. Young, fast growing lithosphere stabilizes the underlying asthenosphere unless it has an unusually low viscosity. Lithosphere of different age, separated by fracture zones, will go unstable at different times, producing regional horizontal temperature gradient that may strongly influence convection. Laboratory and numerical experiments are proposed to study this form of convection and its influence on the geoid. Author

N87-23066*# Massachusetts Inst. of Tech., Cambridge. Plasma Fusion Center.

A PRELIMINARY STUDY OF EXTENDED MAGNETIC FIELD STRUCTURES IN THE IONOSPHERE Status Report

James D. Sullivan, Barton G. Lane, and Richard S. Post 18 Jun. 1987 21 p
(Grant NAG5-874)
(NASA-CR-181004; NAS 1.26:181004) Avail: NTIS HC A02/MF A01 CSCL 04A

Several plasma phenomena which are to be expected around a magnet in LEO were identified and analyzed qualitatively. The ASTROMAG cusp magnet will create an extended field whose strength drops to the ambient level over a scale length of approx.

15 m; the combined field has a complex topology with ring nulls and open and closed field lines. The entire configuration is moving through the partially ionized F-layer of the ionosphere at a speed slow compared to the local Alfven speed but fast compared to the ion sound speed. The ambient plasma crosses the extended field structure in a time short compared to the ion Larmor period yet long relative to the electron Larmor period. Thus, electrons behave as a magnetized fluid while ions move ballistically until reflected from higher fields near the cusp. Since the Debye length is short compared to the field scale length, an electrostatic shock-like structure forms to equilibrate the flows and achieve quasi-neutrality. The ambient plasma will be excluded from a cavity near the magnet. The size and nature of the strong interaction region in which the magnet significantly perturbs the ambient flow were determined by studying ion orbits numerically. Lecture viewgraphs summarizing these results are presented. M.G.

N87-23321*# Minnesota Univ., Minneapolis. School of Physics and Astronomy.
EFFECT OF DOUBLE LAYERS ON MAGNETOSPHERE-IONOSPHERE COUPLING
Robert L. Lysak and Mary K. Hudson (Dartmouth Coll., Hanover, N.H.) *In* NASA. Marshall Space Flight Center Double Layers in Astrophysics May 1987 p 147-166 (For primary document see N87-23313 16-88)
Avail: NTIS HC A14/MF A01 CSCL 04A

N87-23325*# Science Applications International Corp., McLean, Va. Plasma Physics Div.
ANOMALOUS TRANSPORT IN DISCRETE ARCS AND SIMULATION OF DOUBLE LAYERS IN A MODEL AURORAL CIRCUIT
Robert A. Smith *In* NASA. Marshall Space Flight Center Double Layers in Astrophysics May 1987 p 211-223 (For primary document see N87-23313 16-88)
(Contract NASw-3947)
Avail: NTIS HC A14/MF A01 CSCL 04A

N87-23326*# Dartmouth Coll., Hanover, N.H. Dept. of Physics and Astronomy.
WEAK DOUBLE LAYERS IN THE AURORAL IONOSPHERE
M. K. Hudson, T. L. Crystal, W. Lotko, and C. Barnes (Los Alamos National Lab., N. Mex.) *In* NASA. Marshall Space Flight Center Double Layers in Astrophysics May 1987 p 225-245 (For primary document see N87-23313 16-88)
(Grant NSF ATM-84-45010)
Avail: NTIS HC A14/MF A01 CSCL 04A

N87-23327*# Princeton Univ., N. J. Physics Lab.
PARTICLE SIMULATION OF AURORAL DOUBLE LAYERS
Bruce L. Smith and Hideo Okuda *In* NASA. Marshall Space Flight Center Double Layers in Astrophysics May 1987 p 247-263 Sponsored in part by the Aerospace Sponsored Research Program (For primary document see N87-23313 16-88)
Avail: NTIS HC A14/MF A01 CSCL 04A

N87-23328*# Aerospace Corp., Los Angeles, Calif. Space Sciences Lab.
CONDITIONS FOR DOUBLE LAYERS IN THE EARTH'S MAGNETOSPHERE AND PERHAPS IN OTHER ASTROPHYSICAL OBJECTS
L. R. Lyons *In* NASA. Marshall Space Flight Center Double Layers in Astrophysics May 1987 p 265-273 Sponsored in part by the Aerospace Sponsored Research Program (For primary document see N87-23313 16-88)
(Contract NASw-861; Grant NAGw-853)
Avail: NTIS HC A14/MF A01 CSCL 04A

N87-23329*# Lockheed Missiles and Space Co., Palo Alto, Calif. Research Lab.
SOME ASPECTS OF DOUBLE LAYER FORMATION IN A PLASMA CONSTRAINED BY A MAGNETIC MIRROR
W. Lennartsson *In* NASA. Marshall Space Flight Center Double Layers in Astrophysics May 1987 p 275-285 Sponsored in part by the Lockheed Independent Research Program (For primary document see N87-23313 16-88)
(Grant NSF ATM-83-17710)
Avail: NTIS HC A14/MF A01 CSCL 04A

N87-23330*# National Oceanic and Atmospheric Administration, Boulder, Colo.
ELECTRIC POTENTIAL DISTRIBUTIONS AT THE INTERFACE BETWEEN PLASMASHEET CLOUDS
D. S. Evans, M. Roth, and J. Lemaire (Institut d'Aeronomie Spatiale de Belgique, Brussels.) *In* NASA. Marshall Space Flight Center Double Layers in Astrophysics May 1987 p 287-294 (For primary document see N87-23313 16-88)
Avail: NTIS HC A14/MF A01 CSCL 04A

N87-23331*# California Univ., Berkeley. Space Sciences Lab.
DOUBLE LAYERS ABOVE THE AURORA
M. Temerin and F. S. Mozer *In* NASA. Marshall Space Flight Center Double Layers in Astrophysics May 1987 p 295-303 (For primary document see N87-23313 16-88)
(Contract N00014-81-C-0006)
Avail: NTIS HC A14/MF A01 CSCL 04A

N87-23401*# Arizona Univ., Tucson. Lunar and Planetary Lab.
THE ORIGIN OF POLARITY ASYMMETRIES IN THE HISTORY OF THE GEOMAGNETIC FIELD Abstract Only
E. H. Levy *In* NASA, Washington Reports of Planetary Geology and Geophysics Program, 1986 May 1987 p 147 (For primary document see N87-23341 16-91)
Avail: NTIS HC A24/MF A01 CSCL 08G

N87-23404*# Arizona Univ., Tucson. Lunar and Planetary Lab.
THE STEADY STATE TOROIDAL MAGNETIC FIELD AT THE CORE-MANTLE BOUNDARY Abstract Only
S. J. Pearce and E. H. Levy *In* NASA, Washington Reports of Planetary Geology and Geophysics Program, 1986 May 1987 p 148 (For primary document see N87-23341 16-91)
Avail: NTIS HC A24/MF A01 CSCL 08G

N87-23463*# Arizona Univ., Tucson. Dept. of Geosciences.
VALLEY DEVELOPMENT ON HAWAIIAN VOLCANOES
Victor R. Baker and Virginia C. Gulick *In* NASA, Washington Reports of Planetary Geology and Geophysics Program, 1986 May 1987 p 297-299 (For primary document see N87-23341 16-91)
Avail: NTIS HC A24/MF A01 CSCL 08G

N87-23479*# Arizona State Univ., Tempe. Dept. of Geology.
STUDIES OF FLUID INSTABILITIES IN FLOWS OF LAVA AND DEBRIS
Jonathan H. Fink *In* NASA, Washington Reports of Planetary Geology and Geophysics Program, 1986 May 1987 p 345-347 (For primary document see N87-23341 16-91)
Avail: NTIS HC A24/MF A01 CSCL 08K

N87-23480*# Hawaii Inst. of Geophysics, Honolulu.
LONG, PAIRED A'A/PAHOEHOE FLOWS OF MAUNA LOA: VOLCANOLOGICAL SIGNIFICANCE AND INSIGHTS THEY PROVIDE INTO VOLCANO PLUMBING SYSTEMS
Scott K. Rowland and George P. L. Walker *In* NASA, Washington Reports of Planetary Geology and Geophysics Program, 1986 May 1987 p 348-350 (For primary document see N87-23341 16-91)
Avail: NTIS HC A24/MF A01 CSCL 08K

N87-23481*# Geological Survey, Menlo Park, Calif.
THE 1984 MAUNA LOA ERUPTION AND PLANETARY GEOLGOY
Henry J. Moore *In* NASA, Washington Reports of Planetary Geology and Geophysics Program, 1986 May 1987 p 351-353 (For primary document see N87-23341 16-91)
Avail: NTIS HC A24/MF A01 CSCL 08K

N87-23482*# Jet Propulsion Lab., California Inst. of Tech., Pasadena.
CALCULATED VISCOSITY-DISTANCE DEPENDENCE FOR SOME ACTIVELY FLOWING LAVAS
David Pieri *In* NASA, Washington Reports of Planetary Geology and Geophysics Program, 1986 May 1987 p 354-356 (For primary document see N87-23341 16-91)
Avail: NTIS HC A24/MF A01 CSCL 08K

N87-23483*# Jet Propulsion Lab., California Inst. of Tech., Pasadena.
TOWARD A MODEL FOR LEVEED LAVA FLOWS
Stephen Baloga *In* NASA, Washington Reports of Planetary Geology and Geophysics Program, 1986 May 1987 p 357-359 (For primary document see N87-23341 16-91)
Avail: NTIS HC A24/MF A01 CSCL 08K

N87-23484*# Hawaii Inst. of Geophysics, Honolulu.
STUDIES OF VESICLE DISTRIBUTION PATTERNS IN HAWAIIAN LAVAS
George P. L. Walker *In* NASA, Washington Reports of Planetary Geology and Geophysics Program, 1986 May 1987 p 360-361 (For primary document see N87-23341 16-91)
Avail: NTIS HC A24/MF A01 CSCL 08K

N87-23485*# Sul Ross State Univ., Alpine, Tex. Dept. of Geology.
CRUSTAL AND SUBCRUSTAL NODULES IN EJECTA FROM KILBOURNE HOLE MAAR, NEW MEXICO
J. L. Whitford-Stark *In* NASA, Washington Reports of Planetary Geology and Geophysics Program, 1986 May 1987 p 362-364 (For primary document see N87-23341 16-91)
Avail: NTIS HC A24/MF A01 CSCL 08G

N87-23486*# State Univ. of New York, Buffalo. Dept. of Geological Sciences.
GEOLOGY OF THE MOHON MOUNTAIN VOLCANIC FIELD, YAVAPAI AND MOHAVE COUNTIES, ARIZONA: A PRELIMINARY REPORT
Ardyth M. Simmons and John S. King *In* NASA, Washington Reports of Planetary Geology and Geophysics Program, 1986 May 1987 p 365-367 (For primary document see N87-23341 16-91)
Avail: NTIS HC A24/MF A01 CSCL 08G

N87-23487*# State Univ. of New York, Buffalo. Dept. of Geological Sciences.
THE GEOLOGY OF PINE AND CRATER BUTTES: TWO BASALTIC CONSTRUCTS ON THE FAR EASTERN SNAKE RIVER PLAIN
Paul F. Mazierski and John S. King *In* NASA, Washington Reports of Planetary Geology and Geophysics Program, 1986 May 1987 p 368-370 (For primary document see N87-23341 16-91)
Avail: NTIS HC A24/MF A01 CSCL 08G

N87-23488*# State Univ. of New York, Buffalo. Dept. of Geological Sciences.
THE GEOLOGY OF PICACHO BUTTE, A SILICIC VOLCANIC DOME IN NORTHWEST ARIZONA
Andrew P. Kisiel and John S. King *In* NASA, Washington Reports of Planetary Geology and Geophysics Program, 1986 May 1987 p 371-373 (For primary document see N87-23341 16-91)
Avail: NTIS HC A24/MF A01 CSCL 08G

N87-23489*# Geological Survey, Flagstaff, Ariz.
COMPUTER SIMULATIONS OF 10-km-DIAMETER ASTEROID IMPACTS INTO OCEANIC AND CONTINENTAL SITES: PRELIMINARY RESULTS ON ATMOSPHERIC PASSAGE, CRATERING AND EJECTA DYNAMICS
D. J. Roddy, S. H. Schuster, Martin Rosenblatt, L. B. Grant, P. J. Hassig, and K. N. Kreyenhagen (California Research and Technology, Inc., Chatsworth.) *In* NASA, Washington Reports of Planetary Geology and Geophysics Program, 1986 May 1987 p 377-379 (For primary document see N87-23341 16-91)
Avail: NTIS HC A24/MF A01 CSCL 08G

N87-23490*# Brown Univ., Providence, R. I. Dept. of Geological Sciences.
IMPACTS OF HEMISPHERICAL GRANULAR TARGETS: IMPLICATIONS FOR GLOBAL IMPACTS
P. H. Schultz, D. E. Gault (Murphys Center of Planetology, Calif.), and D. Crawford *In* NASA, Washington Reports of Planetary Geology and Geophysics Program, 1986 May 1987 p 380-381 (For primary document see N87-23341 16-91)
Avail: NTIS HC A24/MF A01 CSCL 08G

N87-23491*# Brown Univ., Providence, R. I. Dept. of Geological Sciences.
IMPACT VAPORIZATION: LATE TIME PHENOMENA FROM EXPERIMENTS
P. H. Schultz and D. E. Gault (Murphys Center of Planetology, Calif.) *In* NASA, Washington Reports of Planetary Geology and Geophysics Program, 1986 May 1987 p 382-383 (For primary document see N87-23341 16-91)
Avail: NTIS HC A24/MF A01 CSCL 08G

N87-23492*# Murphys Center of Planetology, Calif.
OBLIQUE IMPACT: PROJECTILE RICHOCHET, CONCOMITANT EJECTA AND MOMENTUM TRANSFER
Donald E. Gault and Peter H. Schultz (Brown Univ., Providence, R. I.) *In* NASA, Washington Reports of Planetary Geology and Geophysics Program, 1986 May 1987 p 384-385 (For primary document see N87-23341 16-91)
Avail: NTIS HC A24/MF A01 CSCL 08G

N87-23493*# Brown Univ., Providence, R. I. Dept. of Geological Sciences.
MOMENTUM TRANSFER FROM OBLIQUE IMPACTS
Peter H. Schultz and Donald E. Gault (Murphys Center of Planetology, Calif.) *In* NASA, Washington Reports of Planetary Geology and Geophysics Program, 1986 May 1987 p 386-387 (For primary document see N87-23341 16-91)
Avail: NTIS HC A24/MF A01 CSCL 08G

N87-23494*# Planetary Science Inst., Tucson, Ariz.
EXPERIMENTAL STUDIES OF COLLISION AND FRAGMENTATION PHENOMENA
William K. Hartmann, D. R. Davis, and S. J. Weidenschilling *In* NASA, Washington Reports of Planetary Geology and Geophysics Program, 1986 May 1987 p 388-390 (For primary document see N87-23341 16-91)
Avail: NTIS HC A24/MF A01 CSCL 08G

N87-23495*# Boeing Aerospace Co., Seattle, Wash.
CENTRIFUGE IMPACT CRATERING EXPERIMENTS: SCALING LAWS FOR NON-POROUS TARGETS Abstract Only
Robert M. Schmidt *In* NASA, Washington Reports of Planetary Geology and Geophysics Program, 1986 May 1987 p 391 (For primary document see N87-23341 16-91)
Avail: NTIS HC A24/MF A01 CSCL 08G

N87-23496*# Washington Univ., Seattle.
IMPACT CRATER SCALING LAWS
K. A. Holsapple *In* NASA, Washington Reports of Planetary Geology and Geophysics Program, 1986 May 1987 p 392-393 (For primary document see N87-23341 16-91)
Avail: NTIS HC A24/MF A01 CSCL 08G

N87-23497*# Brown Univ., Providence, R. I. Dept. of Geological Sciences.
EXPERIMENTAL EVIDENCE FOR NON-PROPORTIONAL GROWTH OF LARGE CRATERS
Peter H. Schultz and Donald E. Gault (Murphys Center of Planetology, Calif.) *In* NASA, Washington Reports of Planetary Geology and Geophysics Program, 1986 May 1987 p 394-395 (For primary document see N87-23341 16-91)
Avail: NTIS HC A24/MF A01 CSCL 08G

N87-23498*# Boeing Aerospace Co., Seattle, Wash.
CENTRIFUGE IMPACT CRATERING EXPERIMENTS: SCALING LAWS FOR NON-POROUS TARGETS
Robert M. Schmidt *In* NASA, Washington Reports of Planetary Geology and Geophysics Program, 1986 May 1987 p 396-398 (For primary document see N87-23341 16-91)
Avail: NTIS HC A24/MF A01 CSCL 08G

N87-23513*# Arizona State Univ., Tempe. Dept. of Geology.
SHATTER CONES IN ILLINOIS: EVIDENCE FOR METOERITIC IMPACTS AT GLASFORD AND DES PLAINES
John F. McHone, Michael L. Sargent, and W. John Nelson (Illinois State Geological Survey, Champaign.) *In* NASA, Washington Reports of Planetary Geology and Geophysics Program, 1986 May 1987 p 438 (For primary document see N87-23341 16-91)
Avail: NTIS HC A24/MF A01 CSCL 08G

N87-23514*# Lawrence Univ., Appleton, Wis.
SEARCH FOR, AND STUDY OF, PALEOZOIC IMPACT EJECTA: PROGRESS MADE DURING THE PAST YEAR
William F. Read *In* NASA, Washington Reports of Planetary Geology and Geophysics Program, 1986 May 1987 p 439-440 (For primary document see N87-23341 16-91)
(Grant NAGw-658)
Avail: NTIS HC A24/MF A01 CSCL 08G

N87-23519*# Massachusetts Inst. of Tech., Cambridge. Dept. of Earth, Atmospheric and Planetary Sciences.
SECULAR COOLING OF EARTH AS A SOURCE OF INTRAPLATE STRESS
Sean C. Solomon *In* NASA, Washington Reports of Planetary Geology and Geophysics Program, 1986 May 1987 p 455-457 (For primary document see N87-23341 16-91)
Avail: NTIS HC A24/MF A01 CSCL 08G

N87-23520*# Massachusetts Inst. of Tech., Cambridge. Dept. of Earth, Atmospheric and Planetary Sciences.
A TEST OF THE HYPOTHESIS THAT IMPACT-INDUCED FRACTURES ARE PREFERRED SITES FOR LATER TECTONIC ACTIVITY
Sean C. Solomon and Elizabeth D. Duxbury *In* NASA, Washington Reports of Planetary Geology and Geophysics Program, 1986 May 1987 p 458-460 (For primary document see N87-23341 16-91)
Avail: NTIS HC A24/MF A01 CSCL 08G

N87-23535*# Colorado State Univ., Fort Collins. Dept. of Earth Resources.
THE EFFECT OF OVERBURDEN THICKNESS ON TENSION FRACTURE PATTERNS ABOVE AN UPLIFTING DOME
H. Pranger, II *In* NASA, Washington Reports of Planetary Geology and Geophysics Program, 1986 May 1987 p 497-498 (For primary document see N87-23341 16-91)
Avail: NTIS HC A24/MF A01 CSCL 08G

N87-23536*# California State Polytechnic Univ., Pomona. Dept. of Geological Sciences.
NATURAL FRACTURE SYSTEMS ON PLANETARY SURFACES: GENETIC CLASSIFICATION AND PATTERN RANDOMNESS
Lisa A. Rossbacher *In* NASA, Washington Reports of Planetary Geology and Geophysics Program, 1986 May 1987 p 499-501 (For primary document see N87-23341 16-91)
Avail: NTIS HC A24/MF A01 CSCL 08G

47 METEOROLOGY AND CLIMATOLOGY

Includes weather forecasting and modification.

N87-23067# Federal Aviation Administration, Washington, D.C.
INTEGRATED FAA WIND SHEAR PROGRAM PLAN
Apr. 1987 95 p
(DOT/FAA/DL-87/1; DOT/FAA/VS-87/1; DOT/FAA/AT-87/1)
Avail: NTIS HC A05/MF A01

Wind shear can have serious and sometimes disastrous effects on the flight path of an aircraft, especially when encountered below 1,000 feet above the ground. In the last 10 years, wind shear was found to be a contributing factor in 14 major aircraft accidents, 4 of which resulted in a total of 401 casualties. Following these accidents, the National transportation Safety Board (NTSB) issued a number of recommendations urging the Federal Aviation Administration (FAA) to address the wind shear problem. Recommendations pertaining to wind shear were also issued by the National Research Council (NRC) in an in-depth study on wind shear published in 1983. The NTSB and NRC recommendations serve as a backdrop to the development of the Integrated FAA Wind Shear Program Plan. Program elements include education and training, ground sensors, airborne sensors and flight guidance systems, terminal information systems, and low-level meteorological hazard characterization. The plan emphasizes how each program element operationally relates to the others and incrementally adds to the overall National Airspace System safety. Author

N87-23068# World Meteorological Organization, Geneva (Switzerland).
PROCEEDINGS OF THE CONFERENCE ON THE SCIENTIFIC RESULTS OF THE ALPINE EXPERIMENT (ALPEX), VOLUME 2
Global Atmospheric Research Program
Jul. 1986 376 p Proceedings held in Venice, Italy, 26 Oct.-1 Nov. and 4-6 Nov. 1985 Sponsored by ICSU, Rome, Italy
(WMO-TD-108-Vol-2; GARP-Publ-Ser-27-Vol-2; ETN-87-99180)
Copyright Avail: NTIS MF A01; print copy available from WMO, Geneva, Switzerland

Frontal modification of Alpine meteorology; air-sea interaction; mesoscale mountain circulation; and local orographic phenomena were among the areas of concern which were discussed in this volume of the conference. For individual titles, see N87-23069 through N87-23094.

N87-23069# Yale Univ., New Haven, Conn. Dept. of Geology and Geophysics.
MESOSCALE MOUNTAIN METEOROLOGY
Ronald B. Smith *In* WMO Proceedings of the Conference on the Scientific Results of the Alpine Experiment (ALPEX), Volume 2 Jul. 1986 p 407-423 (For primary document see N87-23068 16-47)
Copyright Avail: NTIS MF A01; print copy available from WMO, Geneva, Switzerland

Research on mesoscale wind systems in the Alpine region is reviewed. Phenomena such as frontal passage, shallow foehn, mistral, lee waves, and bora are described, and the state of knowledge is discussed. For each of these, dynamical analogies in other mountainous regions are identified. ESA

N87-23070# Eidgenoessische Technische Hochschule, Zurich (Switzerland). Dept. of Atmospheric Physics.
DIAGNOSTIC STUDIES OF MESO-ALPHA SCALE FLOW ON THE ALPINE NORTHSIDE
H. C. Davies *In* WMO Proceedings of the Conference on the Scientific Results of the Alpine Experiment (ALPEX), Volume 2 Jul. 1986 p 425-436 (For primary document see N87-23068 16-47)
Copyright Avail: NTIS MF A01; print copy available from WMO, Geneva, Switzerland

Diagnostic studies undertaken to examine meso-alpha scale atmospheric flow processes over the central Alpine region are summarized. Results from studies designed to examine: the flow features during incidents of quasi-steady northerly flow, the progression of cold fronts on the northern foreland, the pressure drag across the Gotthard, and the kinematic properties of the free atmosphere are presented. The examples illustrate modes of influence of the Alps upon the dynamical climatology of the region. ESA

N87-23071# Colorado Univ., Boulder.
FRONTAL INTERACTION WITH OROGRAPHY

William Blumen, Craig Hartsough, and Brian Gross *In* WMO Proceedings of the Conference on the Scientific Results of the Alpine Experiment (ALPEX), Volume 2 Jul. 1986 p 437-444 (For primary document see N87-23068 16-47)
(Grant NSF ATM-84-18625)
Copyright Avail: NTIS MF A01; print copy available from WMO, Geneva, Switzerland

Two-dimensional (vertical-horizontal) cross-section analyses through an Alpine cold front are presented. They show the frontal movement from relatively level terrain onto the northern slope of the Alps. The depictions are constructed by the Sharpiro and Hastings (1973) isentropic analysis scheme, modified to include orography. Surface and radiosonde data are used. Since pressure is analyzed on isentropic surfaces, the vertical velocity, defined as omega = dp/dt, may be computed on isentropic surfaces as a by-product of the analysis. The distribution of omega, above a saturated surface-based layer, appears to be consistent with the low-level frontal movement. ESA

N87-23072# Deutsche Forschungs- und Versuchsanstalt fuer Luft- und Raumfahrt, Oberpfaffenhofen (West Germany). Inst. of Atmospheric Physics.
ON THE DIAGNOSIS OF A COLD FRONT OBSERVED DURING ALPINE EXPERIMENT (ALPEX)
K. P. Hoinka *In* WMO Proceedings of the Conference on the Scientific Results of the Alpine Experiment (ALPEX), Volume 2 Jul. 1986 p 445-453 (For primary document see N87-23068 16-47)
Copyright Avail: NTIS MF A01; print copy available from WMO, Geneva, Switzerland

A cold front which passed through the dense network of the Alpine Experiment was investigated. This cold front was connected with the generation of an intense lee cyclone. Rawinsonde data, collected above central Europe, are analyzed objectively. The analysis is focused on frontogenetical effects disturbed by the orography, to extract from the data effects of the Alps on this front. The data analysis shows the retardation of the cold air by the Alps. The vertical component of the vorticity connected with the cold front decreases in magnitude as soon as the front approaches the Alps. The frontogenesis due to the deformation and the convergence of the flow field weakens with decreasing distance from the Alps. ESA

N87-23073# State Committee on Hydrometeorology and Control of the Natural Environment, Moscow (USSR).
AIR-SEA INTERACTION OVER THE MEDITERRANEAN SEA DURING THE ALPINE EXPERIMENT (ALPEX) SPECIAL OBSERVING PERIOD
Yu. Vakalyuk, P. Gudz, and Yu. Popov *In* WMO Proceedings of the Conference on the Scientific Results of the Alpine Experiment (ALPEX), Volume 2 Jul. 1986 p 457-466 (For primary document see N87-23068 16-47)
Copyright Avail: NTIS MF A01; print copy available from WMO, Geneva, Switzerland

The response of the Mediterranean Sea to major atmospheric disturbances was studied. Major atmospheric disturbances affecting the Mediterranean Sea surface in winter-spring period are intimately connected with position and intensity of the northwesterly jet stream in the upper troposphere. The western part of the Mediterranean Sea is the region of baroclinic instability with active development of cyclogenesis and associated outbreaks of cold polar air from northwest. Statistical studies show that 70% to 75% of all cyclones are generated in this region. The significant temperature difference between air and water and strong wind cause considerable heat flux and evaporation into the atmosphere. A large dynamic stress under such conditions can lead to amplifying waves and turbulent mixing in the upper layer, masking convective processes. During the Special Observing Period total duration of storm conditions exceeded 100 hr. The sea was subjected to considerable cooling through evaporation and heat flux, and intensive convective mixing down to the bottom of the Ligurian sea took place. ESA

N87-23074# Technische Univ., Munich (West Germany). Inst. of Meteorology.
WINDS IN THE INN VALLEY (AUSTRIA)
Josef Egger *In* WMO Proceedings of the Conference on the Scientific Results of the Alpine Experiment (ALPEX), Volume 2 Jul. 1986 p 469-477 (For primary document see N87-23068 16-47)
Copyright Avail: NTIS MF A01; print copy available from WMO, Geneva, Switzerland

The wind regime in the Inn valley, characterized by a pronounced diurnal cycle with mountain winds down the valley at night and up-valley wind during the day (if the flow situation at larger scales has little impact on the flow in the valley) was studied in the Alpine Experiment. Heat transfer to the main valley by slope winds and side valley circulations, which is linked to the size and shape of the mountains, is studied using a hierarchy of flow models. Very simple models help in understanding the basic mechanism of valley winds. In these models the effect of side valley circulations is parameterized by a K-ansatz. An explicit calculation of both slope and valley winds is attempted using a high-resolution mesoscale flow model. ESA

N87-23075# Innsbruck Univ. (Austria). Dept. of Meteorology.
AN ELEMENTARY VALLEY WIND MODEL
I. Vergeiner *In* WMO Proceedings of the Conference on the Scientific Results of the Alpine Experiment (ALPEX), Volume 2 Jul. 1986 p 479-488 (For primary document see N87-23068 16-47)
Copyright Avail: NTIS MF A01; print copy available from WMO, Geneva, Switzerland

An Alpine valley was modeled as a three-box model which consists of the foreland, one basin, and one valley tube connecting the basin to the foreland. Horizontal variations in each of the boxes, and internal circulations are neglected. The model is used to study quasi-periodic valley winds. ESA

N87-23076# Technische Univ., Munich (West Germany). Inst. of Meteorology.
ENERGY BUDGET OF AN ALPINE VALLEY
Barbara Hennemuth *In* WMO Proceedings of the Conference on the Scientific Results of the Alpine Experiment (ALPEX), Volume 2 Jul. 1986 p 491-500 (For primary document see N87-23068 16-47)
Copyright Avail: NTIS MF A01; print copy available from WMO, Geneva, Switzerland

Measurements in a small Alpine end valley were used to compute the energy budget of the valley and to examine the heat exchange between the different valleys. The measured data are processed to two-dimensional fields of the surface energy balance terms and to three-dimensional fields of temperature and wind. A general energy budget estimation indicates that up to midday the sensible heat flux heats the valley atmosphere, whereas in the afternoon heat is exported out of the small valley. The heat transport is accomplished by a valley wind circulation system with ascending motion in the small valley and subsidence in the next larger valley. ESA

N87-23077# Eidgenoessische Technische Hochschule, Zurich (Switzerland).
VALLEY CIRCULATIONS AS MEASURED IN THE HIMALAYA BY INSTRUMENTED MOTOR GLIDER
B. Neininger, M. Reinhardt, and J. Kuettner (National Center for Atmospheric Research, Boulder, Colo.) *In* WMO Proceedings of the Conference on the Scientific Results of the Alpine Experiment (ALPEX), Volume 2 Jul. 1986 p 501-508 (For primary document see N87-23068 16-47)
Copyright Avail: NTIS MF A01; print copy available from WMO, Geneva, Switzerland

The three dimensional wind, temperature, and humidity field in the Kali-Gandaki Valley (the deepest valley in the world) was measured by an instrumented motorglider along four daily multilevel traverses. In premonsoon time, the intense up-valley winds reach 40 to 60 knots near the ground and were already strong during the tropical spring time of the expedition. A three layered wind system which exchanges air of very different characteristics between Nepal and China is found. ESA

N87-23078# Consiglio Nazionale delle Ricerche, Bologna (Italy). Ist. FISBAT.

ANALYSIS OF STABLY STRATIFIED ATMOSPHERIC FLOW OVER THE DINARIC ALPS DURING THE ALPINE EXPERIMENT (ALPEX)

F. Trombetti and F. Tampieri *In* WMO Proceedings of the Conference on the Scientific Results of the Alpine Experiment (ALPEX), Volume 2 Jul. 1986 p 509-518 (For primary document see N87-23068 16-47)

Copyright Avail: NTIS MF A01; print copy available from WMO, Geneva, Switzerland

Cases of blocking upstream of the Dinaric Alps were analyzed to estimate the dividing streamline height. These critical heights, plotted as a function of the average upwind Froude number, show a slower decrease than that observed for three-dimensional obstacles, and in most cases are greater than those predicted by the inviscid theory, due to friction and wind shear effects (often present) in dipping the streamlines. The upstream influence is detectable at Froude numbers as high as 2, in agreement with results for smaller obstacles. Therefore, the dividing streamline concept may be applied also to mesoscale mountains, giving a good estimate of the height of the layer in which separate circulation or blocking is present. ESA

N87-23079# Colorado Univ., Boulder.

DYNAMICS AND EVOLUTION OF THE PYRENEES LEE WAVE EVENT DURING 21-23 MARCH 1982

K. W. Cox and W. Blumen *In* WMO Proceedings of the Conference on the Scientific Results of the Alpine Experiment (ALPEX), Volume 2 Jul. 1986 p 519-530 (For primary document see N87-23068 16-47)

(Grant NSF ATM-86-17797)

Copyright Avail: NTIS MF A01; print copy available from WMO, Geneva, Switzerland

Scorer's (1949) model of two-dimensional, inviscid, steady-state flow over a mountain ridge is utilized to examine the wave structure at selected times during a sustained northerly flow over the Pyrenees that initiated and maintained lee-wave activity over Spain during 21 to 23 March 1982. Satellite observations of cloud patterns on 21 March reveal a train of waves extending 350 km downstream of the Pyrenees. On 23 March, however, instrumented aircraft observations reveal the continued existence of wave activity in the troposphere and lower stratosphere. Upstream radiosonde reports are used to represent the continuous vertical profiles of the static stability and northerly wind at 12 hr intervals over the 72 hr period. ESA

N87-23080# Centre National de Recherches Meteorologiques, Toulouse (France).

A CONTRIBUTION TO BORA STUDIES USING ALPINE EXPERIMENT (ALPEX) AIRCRAFT DATA

Paul Pettre *In* WMO Proceedings of the Conference on the Scientific Results of the Alpine Experiment (ALPEX), Volume 2 Jul. 1986 p 531-540 (For primary document see N87-23068 16-47)

Copyright Avail: NTIS MF A01; print copy available from WMO, Geneva, Switzerland

A fine scale analysis of the effect of the Bora wind on its environment is presented. A Zagreb-Senj vertical cross-section of the flow is drawn, showing the horizontal and vertical wind field, and the potential temperature field, for two cases. By carefully positioning of flight legs, and assuming that the flow is quasi-stationary, the vertical propagation of the perturbation is derived. The mean values of the components of the velocity and potential temperature are computed on leg sections of 10 km to establish the characteristics of the mean flow. The vertical momentum fluxes are computed along the legs with 1 sec resolution data. ESA

N87-23081# Colorado Univ., Boulder.

AN ANALYSIS OF DOWNSLOPE WINDS IN THE LEE OF THE PYRENEES ON 23 MARCH 1982

William Blumen and Craig S. Hartsough *In* WMO Proceedings of the Conference on the Scientific Results of the Alpine Experiment (ALPEX), Volume 2 Jul. 1986 p 541-548 (For primary document see N87-23068 16-47)

(Grants NSF ATM-84-18625; NSF ATM-82-17797)

Copyright Avail: NTIS MF A01; print copy available from WMO, Geneva, Switzerland

The Klemp and Lilly (1975) model of downslope windstorms was modified to explain the onset and maintenance of the northerly flow at Jaca in the Pyrenees. All variables are continuous functions of height above the surface, but in other respects the models are the same. The present model employs the Bordeaux upstream radiosonde soundings to construct the basic state wind and static stability distributions, and a 2 km high bell-shaped mountain is used to represent a two-dimensional cross-section of the Pyrenees. The model predicts higher winds than those observed. When upstream blocking of the flow, below the ridge, is taken into account the wind predictions are more in line with the reported value. This circumstance arises from a reduction in the effective amplitude of the ridge and an alteration of the reflection coefficient. ESA

N87-23082# Centre National de Recherches Meteorologiques, Toulouse (France).

NUMERICAL STUDY OF THE MISTRAL WITH A MESOSCALE MODEL

Christian Blondin and Bernard Bret *In* WMO Proceedings of the Conference on the Scientific Results of the Alpine Experiment (ALPEX), Volume 2 Jul. 1986 p 549-563 (For primary document see N87-23068 16-47)

(Contract INAG-APT-RA-82.4622)

Copyright Avail: NTIS MF A01; print copy available from WMO, Geneva, Switzerland

For two typical Mistral situations, the experimental results are compared with numerical predictions using a 3-D mesoscale model. Numerical simulations show that the structure of the flow in the southern part of the Rhone Valley (France) results from the katabatic gravity component and from a large scale wave induced by the airflow over the mountains. ESA

N87-23083# National Meteorological Inst., Madrid (Spain).

CIERZO: NORTHWESTERLY WIND ALONG THE EBRO VALLEY (SPAIN) AS A MESOSCALE EFFECT INDUCED ON THE LEE OF THE PYRENEES MOUNTAIN RANGE; A CASE STUDY DURING THE ALPINE EXPERIMENT (ALPEX) SPECIAL OBSERVING PERIOD

R. Riosalido, L. Vazquez, A. Gordo, and A. Jansa *In* WMO Proceedings of the Conference on the Scientific Results of the Alpine Experiment (ALPEX), Volume 2 Jul. 1986 p 565-575 (For primary document see N87-23068 16-47)

Copyright Avail: NTIS MF A01; print copy available from WMO, Geneva, Switzerland

The geographical, climatological, and synoptical patterns of Cierzo are described as a mesoscale phenomenon induced by orographical effect on the lee of the Pyrenees mountain range. The evolution of the vertical profiles of wind and temperature in Zaragoza is shown, emphasizing the maximum winds at low levels, which structure recalls the low level jet. The change of the surface pressure in the Ebro valley, on the lee of the Pyrenees, is analyzed and a relationship between the surface pressure anomaly across the mountain range and the evolution of the wind field is established. An objective analysis of the surface wind which takes into account the mesoscale pressure anomaly on both sides of the Pyrenees, induced by orographical effect of the mountainous barrier, is made. ESA

N87-23084# National Meteorological Inst., Madrid (Spain). Centro Meteorologico Zonal de Palma de Mallorca.

THE MISTRAL-TRAMUNTANA SHEAR LINE. A SATELLITE OBSERVATION

Agustin Jansa *In* WMO Proceedings of the Conference on the

Scientific Results of the Alpine Experiment (ALPEX), Volume 2 Jul. 1986 p 577-590 (For primary document see N87-23068 16-47)
Copyright Avail: NTIS MF A01; print copy available from WMO, Geneva, Switzerland

A satellite picture in a visible channel, showing many significant mesoscale details in the spatial distribution of the Mistral-Tramuntana wind system is presented. A shear line shows clearly as the western limit of the wind. Mistral distribution based on conventional surface data is discussed. Information relating to Balearic Islands Tramuntana distribution is given. Brightness of the sea as viewed from the satellite, according to astronomical and astronautical conditions and assuming the state of the sea (or wave profile) is known, is discussed. Rough waves darken the sea in bright areas (where the angular difference between satellite line of vision and reflected Sun ray is small), but rough seas illuminate dark zones where satellite line of vision is 10 deg below reflected Sun beam. These criteria allow rough sea and/or strong wind zones to be determined. ESA

N87-23085# Institute of Meteorology and Water Management, Zakopane (Poland).

THE INFLUENCE OF OROGRAPHY ON THE TEMPERATURE AND WIND REGIME IN THE MOUNTAINS

Maria Klapowa *In* WMO Proceedings of the Conference on the Scientific Results of the Alpine Experiment (ALPEX), Volume 2 Jul. 1986 p 591-600 (For primary document see N87-23068 16-47)
Copyright Avail: NTIS MF A01; print copy available from WMO, Geneva, Switzerland

Characteristics of air temperature and wind during the Alpine Experiment experiment for days with northern and southern air flow along the selected sections that crosses the Tatra Mountains (Poland) are analyzed. A relationship between temperature and wind near the surface and topography and large-scale air flow was established. During Special Observing Period typical cases of the orographic phenomena were defined and described. ESA

N87-23086# Bern Univ. (Switzerland). Inst. of Geography.

MESOSCALE ANALYSES OF TEMPERATURE, PRESSURE AND WIND FIELDS OVER SWITZERLAND: A CASE STUDY OF A FOEHN

M. Furger, H. Wanner, and J. Engel *In* WMO Proceedings of the Conference on the Scientific Results of the Alpine Experiment (ALPEX), Volume 2 Jul. 1986 p 603-613 Sponsored by the Swiss National Science Foundation (For primary document see N87-23068 16-47)
Copyright Avail: NTIS MF A01; print copy available from WMO, Geneva, Switzerland

Streamline analysis was proposed for the study of air mass exchange between the Swiss Plateau and the Alpine valleys. In view of the complexity of the terrain, with numerous effects on the airflow, the density of existing observing stations is not sufficient. To fill the gaps in the network, a wind observation campaign was organized. Together with pressure and temperature analysis, the resulting data allow a decoupling of the different flow regimes in certain cases. As an example, a Foehn is discussed. ESA

N87-23087# Deutsche Forschungs- und Versuchsanstalt fuer Luft- und Raumfahrt, Wesseling (West Germany). Inst. of Atmospheric Physics.

FINE STRUCTURE OF THE ATMOSPHERIC BOUNDARY LAYER ACROSS THE ALPS DURING A HIGH PRESSURE PERIOD IN THE ALPINE EXPERIMENT (ALPEX). A CASE STUDY ON APRIL 22, 1982

T. A. Hafner, M. E. Reinhardt, E. L. Weisel, and H. P. Fimpel *In* WMO Proceedings of the Conference on the Scientific Results of the Alpine Experiment (ALPEX), Volume 2 Jul. 1986 p 615-626 (For primary document see N87-23068 16-47)
Copyright Avail: NTIS MF A01; print copy available from WMO, Geneva, Switzerland

High pressure influence in the whole inner-ALPEX area gave an opportunity to study the effects of differential radiative heating introduced by the Alpine mountain range due to elevation, topographic features, and albedo. The fine structure and diurnal evolution of the boundary layer are documented by cross-sectional analysis of the potential temperature, mixing ratio, and the 3 wind components from 1 Hz aircraft data along the traverses. In addition, 15 aircraft soundings were selected to evaluate the vertical distribution of the turbulent variances and fluxes on both sides of the Alps. The differences of the structure and temporal evolution of the Alpine boundary layer on the north and south side of the Alps, as well as the differences between the Alpine boundary layer and the boundary layer over homogenous terrain are significant. ESA

N87-23088# Utah Univ., Salt Lake City. Dept. of Meteorology.

ON THE PREDICABILITY OF LOW-LEVEL FLOW DURING ALPEX

Jan Paegle and Tomislava Vukicevic *In* WMO Proceedings of the Conference on the Scientific Results of the Alpine Experiment (ALPEX), Volume 2 Jul. 1986 p 627-637 (For primary document see N87-23068 16-47)
Copyright Avail: NTIS MF A01; print copy available from WMO, Geneva, Switzerland

It is shown that the local air flow bound by topography and dissipated by friction is highly predictable with respect to initial data uncertainties. The predictions involve a rather complicated evolution toward diurnally fluctuating flows and not merely steady balance of forcing, dissipation and boundary conditions. The uncertainties associated with initial data damp rapidly with time in these prognoses. The influence of boundary conditions grows with time. The sensitivity to parameterized forcings, dissipation, and conductive capacitance also grows with time. However, the physically evolving signal through 36 hr in the interior of the 19 x 19 grid point region of the local domain in all the integrations is larger by at least a factor of 2 than is the influence of the uncertainty of any of these parameterizations within the tested range. ESA

N87-23089# Karlsruhe Univ. (West Germany). Inst. fuer Meteorologie und Klimaforschung.

SYNOPTIC-SCALE INFLUENCE ON THE VARIABILITY OF THE ALPINE EXPERIMENT (ALPEX) LOW-LEVEL JET

E. L. Weisel *In* WMO Proceedings of the Conference on the Scientific Results of the Alpine Experiment (ALPEX), Volume 2 Jul. 1986 p 639-653 (For primary document see N87-23068 16-47)
(Grant DFG-Fi-165/21-3)
Copyright Avail: NTIS MF A01; print copy available from WMO, Geneva, Switzerland

The near synoptic-scale factors contributing to jet-formation during the Alpine Experiment (ALPEX) were assessed via analysis of geopotential, wind, and temperature at 700 and 850 hPa surfaces, and calculation of terms of the horizontal momentum budgets. The low level jet observed during ALPEX is a nonstationary and horizontal inhomogeneous phenomenon. Analysis of wind and temperature fields on pressure surfaces shows common synoptic scale features. Calculation of terms of the horizontal momentum budget quantify the contribution by temporal variations, advective accelerations, and baroclinity to the jet. ESA

N87-23090# Eidgenoessische Technische Hochschule, Zurich (Switzerland). Lab. for Atmospheric Physics.

LAGRANGIAN TURBULENCE MEASUREMENTS WITH CONSTANT DENSITY BALLOONS

Bruno Neininger and Hans Richner *In* WMO Proceedings of the Conference on the Scientific Results of the Alpine Experiment (ALPEX), Volume 2 Jul. 1986 p 655-664 Sponsored by the Swiss National Science Foundation (For primary document see N87-23068 16-47)
Copyright Avail: NTIS MF A01; print copy available from WMO, Geneva, Switzerland

During the Alpine Experiment (ALPEX) Special Observing Period, and during post-ALPEX Foehn events, 79 constant level balloons (CLBs) were flown and radar tracked a few hundred meters above the hills of North Central Switzerland under different meteorological conditions: 44 of the flights meet the quality needs for spectral analysis within the frame of interest. The buoyancy corrected data represents the three dimensional flow in a Lagrangian system. Additional data was collected using radiosondes and powered gliders; its represents the wind and temperature-fields in the region of the CLB-trajectories. Topographical data on a 250 m grid are included in the analyses. For turbulent stress measurements, mixing length (time) theory was applied in concurrence to the direct measurement of the u'w'-term of the Navier-Stokes-equation. During crosswind situations, momentum fluxes of several Pascals are found. The average value is on the order of 0.2 Pascal (strongly depending on which cases are included). ESA

N87-23091# National Aeronautics and Space Administration, Washington, D.C.

FIELD STUDY OF THE EFFECT OF OROGRAPHIC FEATURES ON PLANETARY BOUNDARY LAYER MODELS

Walter Frost, John S. Theon, Kao-Huah Huang, and Robert E. Turner (FWG Associates, Inc., Tullahoma, Tenn.) *In* WMO Proceedings of the Conference on the Scientific Results of the Alpine Experiment (ALPEX), Volume 2 Jul. 1986 p 665-685 (For primary document see N87-23068 16-47)
(Contract NAS5-28558)
Copyright Avail: NTIS MF A01; print copy available from WMO, Geneva, Switzerland

A flight program to measure the influence of orographic features on turbulent momentum, heat, and moisture fluxes was carried out. Characteristic wake flow patterns were observed in laboratory studies. While the upper level winds (above 10,000 ft msl) blow from west to east (perpendicular to the mountain range), flow patterns similar to flow from a backward-facing step are observed. When the upper level winds blow at 301 and 312 deg from true north (slightly oblique to the mountain range), experimental evidence suggests flow patterns typical of a vortex shed from the mountain range similar to a leading edge vortex from a delta wing aircraft. The observed flow patterns are analyzed. It is concluded that wake flow very similar to those observed in laboratory facilities can occur due to winds over mountain ranges. Results of studies in the laboratory may shed considerable insight to atmospheric boundary layer winds obstructed by orographic features. ESA

N87-23092# Air Force Geophysics Lab., Hanscom AFB, Mass.

CHARACTERISTICS OF OROGRAPHICALLY INITIATED CONVECTION

Crystal Barker Schaaf and Robert M. Banta *In* WMO Proceedings of the Conference on the Scientific Results of the Alpine Experiment (ALPEX), Volume 2 Jul. 1986 p 687-696 (For primary document see N87-23068 16-47)
Copyright Avail: NTIS MF A01; print copy available from WMO, Geneva, Switzerland

Satellite imagery was used to investigate the initiation of mountain thunderstorms and identify the topographies that encourage these initiations. The initiation sites are often clustered together in identifiable genesis regions. The genesis zones can be caused by lifting and channeling, by the effects of isolated peaks, or by leeside convergence zones that form in leeward valleys and basins. Three major ridgetop flow regimes are recognized (northwest, southwest, and flow that switches from southeast in the southern Rockies to southwest in the northern Rockies). Westerly flows (north and south) produce convergence and thunderstorm genesis along the Sangre de Cristo Mountains. Numerical model runs stress the importance of ridgetop wind speeds on the leeside convergence mechanism. Weaker winds aloft produce stronger longer-lived convergence zones than strong ridgetop winds. ESA

N87-23093# Technische Univ., Vienna (Austria). Inst. of Meteorology.

FRACTAL ANALYSIS OF RADAR PRECIPITATION DATA OVER HILLY TERRAIN

Georg Skoda *In* WMO Proceedings of the Conference on the Scientific Results of the Alpine Experiment (ALPEX), Volume 2 Jul. 1986 p 697-703 (For primary document see N87-23068 16-47)
Copyright Avail: NTIS MF A01; print copy available from WMO, Geneva, Switzerland

The favorable geographical position of the Vienna Airport weather radar, with plain regions in the eastern parts of its panorama range and mountainous areas in the west and in the southwest, was exploited for comparisons of the precipitation structure in these different orographic regions. Radar echoes within a range of 150 km confirm the general thesis of fractal structure with dimension $D = 4/3$, but deviations in space and in time from the expected fractal dimension exist. As D should be determined by the physical processes (including interaction with orography) which shape clouds, the data set was split up according to orographic region (e.g., upstream side, ridge, lee-side) and weather process type (e.g., prefrontal, frontal, postfrontal; type of organization of precipitation). A moderate reduction in fractal dimension on the upwind side, and a substantial growth of D on the lee-side, especially in situations with strong vertical shear of flow velocities follows. ESA

N87-23094# Institute of Meteorology and Water Management, Krakow (Poland).

THE EFFECT OF THE TATRA MOUNTAINS (POLAND) ON THE ATMOSPHERIC PRECIPITATION AND AIR HUMIDITY DURING THE NORTHERN AND SOUTHERN AIR FLOW

D. Limanowka *In* WMO Proceedings of the Conference on the Scientific Results of the Alpine Experiment (ALPEX), Volume 2 Jul. 1986 p 705-710 (For primary document see N87-23068 16-47)
Copyright Avail: NTIS MF A01; print copy available from WMO, Geneva, Switzerland

Precipitation and humidity on both slopes of the Tatra mountains when the airflow was oriented towards the mountain range were determined during the Alpine Experiment; the north wind occurred on 79 days and the southern wind 51 days. Results show that the largest amount and time variation of precipitation are observed on the northern slopes of the Tatra mountains during the north winds. The amount and variation of precipitation are not so large during the southern winds and, in particular, its significant decrease is observed in Podhale Basin due to Foehn effects. The change of humidity is well manifested during the occurrence of Foehn. In one case of southern wind, the relative humidity was observed as low as 6%. The mean value of relative humidity is 15% to 20% less during the southern wind than during the north wind. ESA

N87-23095# National Severe Storms Lab., Norman, Okla.

OKLAHOMA DOWNBURSTS AND THEIR ASYMMETRY Final Report

Michael D. Eilts and Richard J. Doviak Nov. 1986 50 p
(Contract DTFA01-80-Y-10524)
(DOT/FAA/PM-87/7) Avail: NTIS HC A03/MF A01

Data collected each spring in 1979 to 1984 by the two Doppler radars operated by the National Severe Storms Laboratory (NSSL) are used to investigate the asymmetry of low-altitude divergent outflows of convective storm downbursts in central Oklahoma. These outflows can be highly asymmetric with horizontal shear along the axis of maximum divergence as much as 5.5 times the shear along the axis of minimum divergence. The downbursts observed in central Oklahoma, all large-scale (4 to 10 km) events, were superposed with the maximum reflectivity core of the storms. However, scanning strategies may have precluded detection of smaller scale (less than 4 km) microbursts. Typical downbursts observed during the Joint Airport Weather Studies (JAWS) Project were of smaller scale (less than 4 km) and were often associated with little or no rain on the surface. The mechanisms for the initiation of the majority of the JAWS microbursts was most likely evaporative cooling, which occurred when precipitation fell into a dry, deep and nearly adiabatic boundary layer; it appears that, because of a lower cloud base and a moister and slightly more stable boundary layer, the mechanisms for the initiation of the observed Oklahoma downbursts include low-level melting, as well as evaporation of precipitation, low-level precipitation loading, and evaporational cooling at middle levels due to entrainment of dry air. Author

N87-23096# Argonne National Lab., Ill.

MEASUREMENT OF HIGH RESOLUTION WIND PROFILES WITH A MINISODAR

R. L. Coulter and T. J. Martin 1987 15 p Presented at the 6th Symposium on Meteorological Observations and Instrumentation, New Orleans, La., 12 Jan. 1987
(Contract W-31109-eng-38)
(DE87-007001; CONF-870128-2) Avail: NTIS HC A02/MF A01

The minisodar has proven to be a valuable tool in surface and boundary layer investigations, particularly in complex terrain, nocturnal boundary layer, and precipitation conditions. Data from low heights and fine resolution have proven to be accurate and dependable. An increased sampling rate of about a factor of ten over conventional sodars has been realized. It should be noted, however, that due to its limited maximum range, operation with other remote sensors is often desirable. For example, with the computational power available presently, a combination of mini- and conventional sodars could be operated simultaneously with the same operating system with relative ease. DOE

N87-23097# Air Force Geophysics Lab., Hanscom AFB, Mass.

VALIDATION OF A SURFACE-LAYER WINDFLOW MODEL USING CLIMATOLOGY AND METEOROLOGICAL TOWER DATA FROM VANDENBERG AFB, CALIFORNIA

John M. Lanicci and Harald Weber 30 Sep. 1986 96 p
(AD-A178480; AFGL-TR-86-0210; AFGL-ERP-963) Avail: NTIS HC A05/MF A01 CSCL 04B

The 2nd phase of a study involving a surface-layer windflow model is described. The model produces a two-dimensional (x-y plane) variational analysis of windflow by employing Gauss' principle of least constraints to adjust an initial windfield to effects of topography, stability, momentum advection, and mass conservation. It used detailed terrain data (100 to 200 m horizontal resolution) to compensate for sparse meteorological data available over the small areas for which the model is run (25 to 250 sq km). The first phase involved testing of the model to effects of stability and vegetation using terrain, vegetation, and climate for Ft. Polk, La. The 2nd phase involves further model development, including changes in meteorological data input as well as changes in wind and stability initializations. Model experiments using artificially-produced terrain were conducted to test these changes. A two-part model validation was then performed using climate data and archived meteorological tower data from Vandenberg AFB, California. The area of interest is 11 x 12 km, and covers the South Vandenberg Launch Complex. GRA

N87-23098# Miami Univ., Fla. Div. of Physical Oceanography.

MILLIMETER WAVE DOPPLER RADAR OBSERVATION OF CLOUD AND BOUNDARY LAYER STRUCTURE Final Report, 1 Aug. 1984 - 1 Oct. 1986

Roger M. Lhermitte 28 Jan. 1987 11 p
(Contract DAAG29-85-K-0145)
(AD-A178679; ARO-21830.9-GS) Avail: NTIS HC A02/MF A01 CSCL 17I

The project was concerned initially with the development of a Doppler radar operating a 94 GHz (3 mm wavelength) primarily for the study of dynamical processes in clouds in the early stages of their development. The observation of other weak targets such as particulates suspended in the Earth's atmosphere was also included in the research as well as the study of snow cover done in cooperation with the University of Massachusetts. The radar was tested and extensively used for the observation of cloud and precipitation, including observation of: cirrus density and motion, melting layer in a stratified cloud, particle vertical velocity in storms, and small cumulus kinematics and development. GRA

N87-23099# Air Force Inst. of Tech., Wright-Patterson AFB, Ohio. School of Engineering.

INVESTIGATIONS OF THE POLAR RAIN: POLAR CAP ELECTRON PRECIPITATION M.S. Thesis

Kevin B. Riehl Dec. 1986 94 p
(AD-A178876; AFIT/GEP/ENP/86D-8) Avail: NTIS HC A05/MF A01 CSCL 04A

A study of the characteristics of the polar rain using data from the SSJ/4 sensor on the Defense Meteorological Satellite Program F6 satellite Dawn/Dusk flux gradients are verified as being controlled by the interplanetary magnetic field (IMF) Y component at least 84% of the time. The IMF Z component is shown to play a role in generating flux gradients. The polar rain is best characterized by a double Maxwellian distribution with typical temperatures of 80 to 90 eV for the low energy component and 3.6 to 4.8 KeV for the high energy component. The characteristics of the low energy component of the polar rain strongly match those of the solar wind strahl component, suggesting the polar rain is of strahl origin. But correlations with IMF sector structure and solar wind parameters do not show the relationships proposed since the unpreferred cap generally has the same polar rain characteristics as the preferred cap. GRA

N87-23100*# National Aeronautics and Space Administration. Ames Research Center, Moffett Field, Calif.

HIGH ALTITUDE TURBULENCE FOR SUPERSONIC CRUISE VEHICLES

L. J. Ehernberger May 1987 18 p Presented at the 33rd Annual Meeting of the American Astronautical Society, Boulder, Colo., 26-29 Oct. 1986
(NASA-TM-88285; H-1399; AAS-86-418; NAS 1.15:88285) Avail: NTIS HC A02/MF A01 CSCL 04B

The characterisitics of high altitude turbulence and its associated meteorological features are reviewed. Findings based on data from NASA flight research programs with prototype military aircraft, the XB-70 and YF-12A, are emphasized. An example of detailed numerical atmospheric simulations, which amy provide greatly increased understanding of these earlier turbulence observations, is presented. Comparisons between observation and numerical simulation should help to delineate the limitations of analysis techniques and improve our understanding of atmospheric processes in the stratosphere. Author

N87-23101*# National Aeronautics and Space Administration. Langley Research Center, Hampton, Va.

STANDARD-RESOLUTION TOVS OBSERVATIONS FOR THE FIRE/SRB WISCONSIN EXPERIMENT REGION FROM OCTOBER 9 THROUGH NOVEMBER 2, 1986

Charles H. Whitlock, Stuart R. LeCroy (PRC Kentron, Inc., Hampton, Va.), and Wayne L. Darnell May 1987 134 p
(NASA-TM-89151; NAS 1.15:89151) Avail: NTIS HC A07/MF A01 CSCL 04B

Maps and concise tables are presented which show TIROS Operational Vertical Sounder (TOVS) box centroid locations, box size, and vertical sounding products from the NOAA-6 and -9 satellites for the FIRE/SRB (First ISCCP Regional Experiment/Surface Radiation Budget) Wisconsin experiment region during October 9 through November 2, 1986. In addition to the operational standard products, relative reflectance is calculated and presented based on values from HIRS/2 Band 20 measurements. Author

N87-23049# Maryland Univ., College Park. Dept. of Meteorology.

TROPICAL PACIFIC SST EXPERIMENTS WITH THE GLAS CLIMATE MODEL

M. Fennessy *In* World Climate Program Workshop on Comparison of Simulations by Numerical Models of the Sensitivity of the Atmospheric Circulation to Sea Surface Temperature Anomalies Jul. 1986 p 131-136 (For primary document see N87-23034 16-46)
Avail: NTIS MF A01; print copy available from WMO, Geneva, Switzerland

48 OCEANOGRAPHY

Includes biological, dynamic, and physical oceanography; and marine resources.

For related information see also *43 Earth Resources and Remote Sensing.*

N87-23102# Admiralty Research Establishment, Portland (England).
THE SIR-B MISSION: TOWARDS AN UNDERSTANDING OF INTERNAL WAVES IN THE OCEAN
M. T. Bagg, A. C. Edwards, J. R. Perry, J. C. Scott, J. A. Stacey, and J. O. Thomas Dec. 1986 51 p
(Contract MOD(PE)-NUW-72A/1287)
(ARE-TR-86122; ACCN-74513; BR101469; ETN-87-99809) Copyright Avail: NTIS HC A04/MF A01

An internal wave sea truch experiment was conducted in conjunction with SIR-B overflights. Using knowledge obtained from sea truth and radar imagery of internal waves computational and theoretical procedures to model observed surface signatures are presented. The procedures are intended to predict the changing wave action spectral density of the ocean surface short wavelength surface gravity waves as they propagate across the straining region induced at the surface by the underlying internal wave. Variants of the Phillips (1984) formulation of the wave action source and sink terms are used to account for the effects of the wind and wave breaking on the development of the wave action spectral density. Considerable success is achieved in understanding how various signatures arise. ESA

N87-23103# Royal Australian Navy Research Lab., Edgecliff.
STUDIES OF THE EAST AUSTRALIAN CURRENT OFF NORTHERN NEW SOUTH WALES
P. J. Mulheran Aug. 1986 73 p
(AD-A178461; RANRL-TN-6/86) Avail: NTIS HC A04/MF A01 CSCL 08C

Cruises in November 1982 and May 1983 were conducted to investigate the structure of the front on the near-shore edge of the East Australian Current off northern New South Wales. Concurrent satellite data were also obtained. From this work it was found that the front could move in the east-west direction at speeds of order 10 to 20 km/day, that the surface mixed layer became very shallow near the surface front, and that the front's structure was at times affected by fresh water outflow from the Clarence River. It was also found that LANDSAT Imagery could be useful in frontal investigations and that it is feasible to obtain depth - averaged currents with a geomagnetic electro-kinetograph (GEK). Author (GRA)

N87-23104# Oregon State Univ., Corvallis. Coll. of Oceanography.
OPTICAL DYNAMICS EXPERIMENT (ODEX) DATA REPORT R/V ACANIA EXPEDITION 10 OCTOBER-17 NOVEMBER 1982. VOLUME 2: PARTICLE SIZE DISTRIBUTIONS. VOLUME 6: SCALAR SPECTRAL-RADIOMETER DATA
Hasong Pak, David W. Menzies, and James C. Kitchen Sep. 1986 408 p
(Contract N00014-84-C-0218)
(AD-A178535; DATA-124-Vol-2/6; REF-86-10-Vol-2/6) Avail: NTIS HC A18/MF A01 CSCL 08J

The Optical Dynamics Experiment (ODEX) was an interdisciplinary experiment to study the relation of physical forcing, biological processes, and the structure of optical parameters in the open ocean. This data report presents the data collected with the spectral radiometer package, and the particle size analysis of discrete water samples taken from CTD casts by the Oregon State Univ. Optical Oceanography Group. The ODEX cruise of Oct. and Nov. 1982 occupied 1984 stations along a transect from the California coast at 35 deg N to a study area covering the subtropical front near 32 deg N, 142 deg W. Plots are presented of hydrographic parameters, beam attenuation, percentage of surface irradiance at 9 wave-lengths, and diffuse attenuation at 5 wavelengths. Lists of the same parameters as well as discrete and total visible irradiance are presented. GRA

N87-23105# Coastal Engineering Research Center, Vicksburg, Miss.
A WIND- AND WAVE-DRIVEN NEARSHORE CURRENT MODEL, THE ONE-DIMENSIONAL MODEL Final Report
Jon M. Hubertz Feb. 1987 29 p
(AD-A178751; CERC-87-4) Avail: NTIS HC A03/MF A01 CSCL 08C

A model to calculate the longshore component of currents resulting from winds and waves is described. The model is one-dimensional in the sense that it calculates variables at a number of grid points along a line normal to shore. The user of the model must supply the depth at each grid point along the line; a wave height, period, and mean direction at the seaward end of the line; and the wind speed and direction. The model then calculates the steady-state free surface elevation, longshore and cross-shore current, and wave height and direction at each grid point. Input parameters are described, and a sample application is provided. The model is intended for use where a quick but accurate estimate of the longshore current at an unobstructed, relatively straight shoreline is needed. For more complicated coastal configurations, a two-dimensional model is recommended. Author (GRA)

N87-23046# European Centre for Medium-Range Weather Forecasts, Reading (England).
THE IMPACT OF INITIAL CONDITIONS AND SST ANOMALIES ON EXTENDED RANGE PREDICTIONS FOR THE EL NINO PERIOD
Ulrich Cubasch *In* World Climate Program Workshop on Comparison of Simulations by Numerical Models of the Sensitivity of the Atmospheric Circulation to Sea Surface Temperature Anomalies Jul. 1986 p 110-116 (For primary document see N87-23034 16-46)
Avail: NTIS MF A01; print copy available from WMO, Geneva, Switzerland

N87-23048# National Meteorological Center, Washington, D.C.
SENSITIVITY OF THE NMC SPECTRAL MODE TO THE JANUARY 1983 EL NINO SST
Robert E. Kistler and J. Shukla (Maryland Univ., College Park.) *In* World Climate Program Workshop on Comparison of Simulations by Numerical Models of the Sensitivity of the Atmospheric Circulation to Sea Surface Temperature Anomalies Jul. 1986 p 124-130 (For primary document see N87-23034 16-46)
Avail: NTIS MF A01; print copy available from WMO, Geneva, Switzerland

N87-23053# Lamont-Doherty Geological Observatory, Palisades, N.Y.
MODELLING AND FORECASTING EL NINO
S. E. Zebiak and M. A. Cane *In* World Climate Program Workshop on Comparison of Simulations by Numerical Models of the Sensitivity of the Atmospheric Circulation to Sea Surface Temperature Anomalies Jul. 1986 p 167-176 (For primary document see N87-23034 16-46)
Avail: NTIS MF A01; print copy available from WMO, Geneva, Switzerland

N87-23055# Oxford Univ. (England). Clarendon Lab.
THE DEVELOPMENT OF A COUPLED GCM SUITABLE FOR MODELLING STUDIES IN TOGA
C. Gordon *In* World Climate Program Workshop on Comparison of Simulations by Numerical Models of the Sensitivity of the Atmospheric Circulation to Sea Surface Temperature Anomalies Jul. 1986 p 184-188 (For primary document see N87-23034 16-46)
Avail: NTIS MF A01; print copy available from WMO, Geneva, Switzerland

51 LIFE SCIENCES (GENERAL)

N87-23128# Joint Publications Research Service, Arlington, Va.
SPLIT CIRCADIAN RHYTHM OF SIMIAN BODY TEMPERATURE DURING ANTIORTHOSTATIC HYPOKINESIA
A. M. Alpatov and V. Ya. Klimovitskiy *In its* USSR Report: Space Biology and Aerospace Medicine, Volume 20, No. 5, September - October 1986 16 Dec. 1986 p 50-55 Transl. into ENGLISH from Kosmicheskaya Biologiya i Aviakosmicheskaya Meditsina (Moscow, USSR), v. 20, no. 5, Sep. - Oct. 1986 p 37-41 (For primary document see N87-23120 16-52)
Copyright Avail: NTIS HC A07/MF A01

N87-23129# Joint Publications Research Service, Arlington, Va.
EFFECT OF HYPOKINESIA ON INTENSITY OF GLUCONEOGENESIS IN CORTICAL LAYER OF RAT KIDNEY
S. M. Yershikov *In its* USSR Report: Space Biology and Aerospace Medicine, Volume 20, No. 5, September - October 1986 16 Dec. 1986 p 56-61 Transl. into ENGLISH from Kosmicheskaya Biologiya i Aviakosmicheskaya Meditsina (Moscow, USSR), v. 20, no. 5, Sep. - Oct. 1986 p 41-44 (For primary document see N87-23120 16-52)
Copyright Avail: NTIS HC A07/MF A01

N87-23130# Joint Publications Research Service, Arlington, Va.
CORTICAL ULTRASTRUCTURE OF RAT CEREBELLAR NODULUS FOLLOWING FLIGHT ABOARD COSMOS-1514 BIOSATELLITE
I. B. Krasnov and L. N. Dyachkova *In its* USSR Report: Space Biology and Aerospace Medicine, Volume 20, No. 5, September - October 1986 16 Dec. 1986 p 62-66 Transl. into ENGLISH from Kosmicheskaya Biologiya i Aviakosmicheskaya Meditsina (Moscow, USSR), v. 20, no. 5, Sep. - Oct. 1986 p 45-48 (For primary document see N87-23120 16-52)
Copyright Avail: NTIS HC A07/MF A01

N87-23133# Joint Publications Research Service, Arlington, Va.
REACTION TO VIBRATION OF RAT KINESTHETIC ANALYZER NEUROCYTES
V. V. Antipov, V. I. Drobyshev, I. B. Ushakov, and T. P. Stepanova *In its* USSR Report: Space Biology and Aerospace Medicine, Volume 20, No. 5, September - October 1986 16 Dec. 1986 p 86-92 Transl. into ENGLISH from Kosmicheskaya Biologiya i Aviakosmicheskaya Meditsina (Moscow, USSR), v. 20, no. 5, Sep. - Oct. 1986 p 60-64 (For primary document see N87-23120 16-52)
Copyright Avail: NTIS HC A07/MF A01

N87-23138# Joint Publications Research Service, Arlington, Va.
DISTINCTIONS IN FORMATION OF MICROBIAL COMPLEX IN NUTRIENT SOLUTIONS OF HIGHER PLANTS AFTER USE OF STRAW MINERALIZATION PRODUCTS
N. A. Drugova, L. S. Yunusova, and Yu. I. Shaydorov *In its* USSR Report: Space Biology and Aerospace Medicine, Volume 20, No. 5, September - October 1986 16 Dec. 1986 p 117-122 Transl. into ENGLISH from Kosmicheskaya Biologiya i Aviakosmicheskaya Meditsina (Moscow, USSR), v. 20, no. 5, Sep. - Oct. 1986 p 81-84 (For primary document see N87-23120 16-52)
Copyright Avail: NTIS HC A07/MF A01

N87-23141# Joint Publications Research Service, Arlington, Va.
SOME BIOCHEMICAL AND MORPHOLOGICAL CHANGES IN RAT BLOOD WITH EXPOSURE TO VARIABLE MAGNETIC FIELD AT INFRALOW FREQUENCY
V. G. Sidyakin, N. A. Temuryants, and Ye. V. Yevstafyeva *In its* USSR Report: Space Biology and Aerospace Medicine, Volume 20, No. 5, September - October 1986 16 Dec. 1986 p 132-133 Transl. into ENGLISH from Kosmicheskaya Biologiya i Aviakosmicheskaya Meditsina (Moscow, USSR), v. 20, no. 5, Sep. - Oct. 1986 p 90-91 (For primary document see N87-23120 16-52)
Copyright Avail: NTIS HC A07/MF A01

52 AEROSPACE MEDICINE

Includes physiological factors; biological effects of radiation; and effects of weightlessness on man and animals.

N87-23106# Air Force Systems Command, Wright-Patterson AFB, Ohio. Foreign Technology Div.
SPECIAL FEATURES IN REGULATING RESPIRATION UNDER NORMAL CONDITIONS AND CONDITIONS OF ALTERED GAS MEDIUM
M. V. Sergiyevskiy 25 Mar. 1987 24 p Transl. into ENGLISH from Fiziologicheskiy Zhurnal SSSR (USSR), v. 57, no. 12, Dec. 1971 p 1780-1787
(AD-A179216; FTD-ID(RS)T-0189-87) Avail: NTIS HC A02/MF A01 CSCL 06P

Arguments are presented for these conclusions: Under physiological conditions an automatic and adaptable control of the respiratory functional system is provided by an elaborate complex of reflex reactions at different levels. When the gaseous medium is changed against the background of developing hypoxia the products of partial oxidation have a significant effect on the cerebral cortex of brain, and then on the medulla oblongata. Under the conditions of hypoxia the receptor zones in the tissues of the brain, including in the venous sinuses and bulbus venae jungularis acquire special importance. They are the first receptors to receive the effect of the products of partial oxidation, which are generated in the cortex, and because of them the preferential oxygen supply to the cells of the cortex occurs. With changed gaseous medium first of all the activity of the cortex is disturbed, which ensures formation of functionally mobile constellations of nerve centers, which integrate the adaptation of the functional systems to varied conditions of vital activity. GRA

N87-23107# Oxford Univ. (England). Dept. of Physiology.
THE PERCEPTION OF BRIGHTNESS AND COLOUR: NEUROPHYSIOLOGY, PSYCHOPHYSICS AND COMPUTATION Final Scientific Report, 1 Sep. 1985 - 31 Aug. 1986
A. J. Parker, M. J. Hawken, and C. B. Blakemore 27 Feb. 1987 69 p
(Contract F12878-85-C-00014; Grant AF-AFOSR-0296-85)
(AD-A179217; KK-8F-161; EOARD-85-0056) Avail: NTIS HC A04/MF A01 CSCL 06P

Progress in research in 3 areas of computational visual neuroscience is summarized. The first project has assessed the receptive field organization of neurons in the primate striate cortex. A new model is proposed for cortical receptive fields based on linear combinations of difference of Gaussian functions. The second project is directed towards measuring the chromatic properties of cortical cell receptive fields. The third project is assessing current computational models of the perception of three dimensional surfaces using psychophysical techniques with human observers. GRA

N87-23108# Dayton Univ., Ohio. Research Inst.
ASYMMETRIES IN THE CONTROL OF SACCADIC EYE MOVEMENTS TO BIFURCATING TARGETS Final Report, Mar. 1983 - Mar. 1984
Yehoshua Y. Zeevi, Paul A. Wetzel, and George A. Geri Apr. 1987 21 p
(Contract F33615-84-C-0066)
(AD-A179270; AFHRL-TR-86-54) Avail: NTIS HC A02/MF A01 CSCL 05I

The task of responding to one of two simultaneously presented targets often reveals unexpected yet profound preferences in the direction of saccadic eye movements. A simple experimental paradigm is used in which a single point of light bifurcates symmetrically to the left and right of the fixation point. Under these conditions, most subjects show an eye movement response preference to either the left or right. Data show that this preference can be eliminated by delaying the onset of the target, presented in the preferred direction, by about 40 milliseconds. This indicates that in the sequence of events occurring prior to the execution of a saccade, a window of time of this duration is allocated for decisions concerning direction, of response even when targets are presented to both visual hemifields. It was also found that the bifurcating targets interact to significantly increase response latencies in both the preferred and nonpreferred directions. Further, the interaction is asymmetrical, in that a target presented in the preferred direction has a greater effect than a target in the nonpreferred direction on responses in the counter direction. Results suggest an asymmetry in hemispheric interaction. GRA

N87-23109# Army Research Inst. of Environmental Medicine, Natick, Mass.

RELATIONSHIP BETWEEN A TWO MILE RUN AND MAXIMAL OXYGEN UPTAKE

Robert P. Mello, Michelle M. Murphy, and James A. Vogel Feb. 1987 25 p
(AD-A179343) Avail: NTIS HC A02/MF A01 CSCL 06P

The relationship between a maximal effort two-mile run for time and maximal oxygen uptake (VO2 max) as measured by treadmill running is examined. Subjects were 44 males (aged 20-51) and 17 females (aged 20-37) of various fitness and activity levels. All subjects performed a timed two mile run and a treadmill running test for maximal oxygen uptake. The coefficient of correlation between the treadmill maximal test and the two mile run test for all subjects was -0.91. Separate regression analyses for male and female data also displayed significant correlations (r sub m -0.91, r sub f -0.89). The addition of such variables as age, height, weight, and % body fat did not improve the predictability of the equations. However, inclusion of body weight in the male equation did increase its predictive accuracy (SEE = 3.31 to 2.69). The high degree of correlation between VO2 max and two mile run time thus permits the estimation of either component with significant accuracy from the direct measurement of the other. This study confirms the usefulness and validity of a timed 2 mile run test to indicate the level of aerobic fitness capacity when the test is properly supervised and the subjects are well motivated. GRA

N87-23110# Anthropology Research Project, Yellow Springs, Ohio.

SELECTION OF DIMENSIONS FOR AN ANTHROPOMETRIC DATA BASE. VOLUME 2: DIMENSION EVALUATION SHEETS Final Report, Sep. 1984 - Oct. 1985

Charles E. Clauser, John T. McConville, Claire C. Gordon, and Ilse O. Tebbetts 30 May 1986 420 p
(Contract DAAK60-84-C-0086)
(AD-A179472; NATICK-TR-86/054) Avail: NTIS HC A18/MF A01 CSCL 06N

Anthropometric dimensions measured in 14 major foreign and domestic military and civilian surveys were reviewed in detail for possible inclusion in an anthropometric survey of U.S. Army men and women. Detailed review of each dimension included the following information: a description of the dimension, subject position, and landmarks required; type of instrument used; significant technique differences among different surveys; alternative dimensions that could serve the same function in a data base; summary statistics from surveys that included the dimensions; notation of significant gender or racial differences for the dimension; ease of reproducibility, and factors contributing to reproducibility problems (if any); and a rating (with rationale) of the dimension's relative utility for a U.S. Army data base. Review sheets summarizing this information comprise Volume 2 of this report. GRA

N87-23111# Boston Univ., Mass. Center for Adaptive Systems.

WORKSHOP SYMPOSIUM ON NEURAL MODELS OF SENSORY-MOTOR CONTROL Final Report, 1 Jul. 1986 - 30 Jun. 1987

Daniel Bullock and Stephen Grossberg 6 Mar. 1987 222 p
Workshop held in Cambridge, Mass., 19-20 Aug. 1986
(Grant AF-AFOSR-0228-86)
(AD-A179501; AFOSR-87-0457TR) Avail: NTIS HC A10/MF A01 CSCL 05J

The Symposium on Neural Models of Sensory-Motor Control was held on August 19 and 20, 1986, at Harvard University as part of the annual meeting of the Society for Mathematical Psychology. The Symposium was divided into two sessions, each with four 50-minute presentations. The first session focused on neural models of the human oculo-motor system. The second session began with two papers on arm movement planning. GRA

N87-23112# Anthropology Research Project, Yellow Springs, Ohio.

SELECTION OF DIMENSIONS FOR AN ANTHROPOMETRIC DATA BASE. VOLUME 1: RATIONALE, SUMMARY, AND CONCLUSIONS Final Report, Sep. 1984 - Oct. 1985

Charles E. Clauser, John T. McConville, Claire C. Gordon, and Ilse O. Tebbetts May 1986 65 p
(Contract DAAK60-84-C-0086)
(AD-A179566; NATICK-TR-86/053-Vol-1) Avail: NTIS HC A04/MF A01 CSCL 06N

A large number of body size variables were examined and rated for their usefulness in an anthropometric data base designed to serve present and future needs of the U.S. Army. These dimensions are assembled in groups representing various uses to which the Army might put these data, ranging from the design of clothing, personal protective equipment, and workspaces, to the development of link systems and human analogs. A total of 362 dimensions analyzed in this study were rated as marginal, useful or essential to one or more of these applications. Some 194 dimensions are suggested as candidates for measurement in a proposed new large-scale multipurpose survey of Army personnel. Sources for the study included 34 anthropometric surveys of U.S. and foreign military and civilian subjects, as well as questionnaire surveys and interviews with clothiers, modelers, design engineers, physical anthropologists, and others experienced in the application of anthropometric data to military design problems. Dimension lists from fourteen large-scale surveys were selected for detailed review. Descriptions and analyses of all the dimensions measured in these surveys appear in Volume 2 of this report. GRA

N87-23113# Washington Univ., Seattle. Dept. of Psychology.

IMAGE SIZE AND RESOLUTION IN FACE RECOGNITION

Amy Jo Bilson 1987 128 p
Avail: NTIS HC A07/MF A01

The effect of image size on the resolution threshold for face recognition is investigated using a large and relatively heterogeneous set of faces. Three experiments were run: a two alternative forced choice (2AFC) study, yes/no (Y/N) study, and a sixteen alternative forced choice (16AFC) study. The results of these three studies indicated that, for images subtending 1 to 4 deg, the resolution threshold for face recognition is approximately 4 cycles per face width (c/fw), and that this value is independent of image size. Images subtending 0.5 deg were not reliably recognized at any resolution. This lower bound on scale invariant image recognition, 0.5 deg, can be at least partially explained in terms of the Contrast Sensitivity Function (CSF) for human foveal vision. Author

N87-23114* National Aeronautics and Space Administration, Washington, D.C.

AEROSPACE MEDICINE AND BIOLOGY: A CONTINUING BIBLIOGRAPHY WITH INDEXES (SUPPLEMENT 298)

Jun. 1987 64 p
(NASA-SP-7011(298); NAS 1.21:7011(298)) Avail: NTIS HC A04 CSCL 06E

This bibliography lists 173 reports, articles, and other documents introduced into the NASA scientific and technical information system in May, 1987. Author

N87-23115# Cornell Univ., New York, N.Y. Dept. of Applied Physics.

FUNDAMENTAL STUDIES IN THE MOLECULAR BASIS OF LASER INDUCED RETINAL DAMAGE Annual Report, 1 May 1985 - 30 Apr. 1986

Aaron Lewis 31 Dec. 1986 35 p
(Contract DAMD17-85-C-5136; DA Proj. 3E1-62772-A-878)
(AD-A178453) Avail: NTIS HC A03/MF A01 CSCL 06R

Progress on the fundamental effects of femtosecond laser pulses with retinal pigments, new insights into the detailed interactions of light with photoreceptor cells, and tremendous advances in new forms of super-resolution microscopy are discussed. The common Nd:YAG laser pumping a dye laser is used. GRA

N87-23116# School of Aerospace Medicine, Brooks AFB, Tex.

F-16 CONTROL STICK RESPONSE DURING +G SUB z-INDUCED LOSS OF CONSCIOUSNESS Interim Report, Dec. 1985 - Apr. 1986

James E. Whinnery Nov. 1986 19 p
(AD-A178474; USAFSAM-TR-86-26) Avail: NTIS HC A02/MF A01 CSCL 06B

The stick input has been analyzed during deliberate self-induced +Gz loss of consciousness (G-LOC) on the USAF School of Aerospace Medicine human centrifuge. An F-16A stick was utilized with output of + or - pitch, + or - roll, an on-off binary sensory being obtained in 1/8-second intervals during G-LOC and recovery. The results are applicable to emerging aircraft autorecovery technology. The currently known physiologic aspects of G-LOC and their time relationships are viewed in relation to the potential use of stick force as a rather simplistic G-LOC physiologic monitoring technique. GRA

N87-23117# Naval Aerospace Medical Research Lab., Pensacola, Fla.

VISUAL ACUITY AND REACTION TIME IN NAVY FIGHTER PILOTS

A. Morris and P. V. Hamilton Dec. 1986 32 p
(AD-A178485; NAMRL-1324) Avail: NTIS HC A03/MF A01 CSCL 06P

This report summarizes data on selected visual measures for Navy fighter pilots. The vision of 163 pilots was measured using an Automated Vision Test Battery housed in a Mobile Field Laboratory. All pilots were involved in training at the Tactical Air Combat Training System (TACTS) range, NAS Oceana, Va. Data on simple visual reaction time, spot detection ability, static visual acuity under several conditions are reported, and the influences of age and spectacles on vision are examined. The average high contrast acuity score was 0.40 minutes of visual angle, or 20/8 Snellen; no pilot had worse than 20/15 acuity. These findings, together with other data, suggest that Navy fighter pilots have better vision than non-aviators of the same age, and possibly better vision than Student Naval Aviators. Correlational analyses suggest that acuity threshold, simple visual reaction time, and threshold stressed reaction time, are independent measures of visual functioning. Spectacled pilots had poorer vision than non-spectacled pilots, and older pilots tended to have poorer vision than younger pilots. GRA

N87-23118# Wright State Univ., Dayton, Ohio. Div. of Human Biology.

IDENTIFICATION AND VALIDATION OF NEW ANTHROPOMETRIC TECHNIQUES FOR QUANTIFYING BODY COMPOSITION Final Report, Aug. 1984 - Jul. 1985

Alexander F. Roche, William C. Chumlea, and Shumei Guo 16 Oct. 1986 231 p
(Contract DAAK60-84-C-0054)
(AD-A178753) Avail: NTIS HC A11/MF A01 CSCL 06N

This study validates estimates of body composition from bioelectrical impedance (RJL Model BIA-101) against corresponding estimates of body composition from densitometry in a sample of 177 young men and women, of whom 14% were black. Also, comparisons are made between measures of subcutaneous adipose tissue thickness using a portable ultrasound machine (EchoScan 1502) and Lange skinfold calipers in the same sample. In separate samples, measures of machine reliability were conducted between pairs of impedance machines and between pairs of ultrasound machines. In addition, tests were made of the possible effects of physiological noise factors on measures of impedance. Bioelectric impedance is highly reliable as are measures of subcutaneous adipose tissue with Lange skinfold calipers. Ultrasonic measures of subcutaneous adipose tissue are not reliable and do not improve predictions of body composition over that of corresponding skinfold measurements. Bioelectric impedance is not affected by physiological factors such as diet, time of day, exercise of the menstrual cycle. However, in those women who do not participate in some form of regular exercise, predictions of body composition from Stature/Resistance plus anthropometry do differ significantly from those of women who do exercise regularly. The addition of bioelectric impedance does improve the predictions of body composition from anthropometry alone compared to corresponding estimates from densitometry. GRA

N87-23119# Air Force Inst. of Tech., Wright-Patterson AFB, Ohio. School of Engineering.

A COLLECTION AND STATISTICAL ANALYSIS OF BIOPHYSICAL DATA TO PREDICT MOTION SICKNESS INCIDENCE M.S. Thesis

Michael R. McPherson Dec. 1986 187 p
(AD-A178874; AFIT/GCS/ENG/86D-21) Avail: NTIS HC A09/MF A01 CSCL 06S

Biophysical data were collected on humam volunteers to study the effects of the motion sickness syndrome. Physiological parameters were analyzed by descriptive statistical methods and by means of a spectrum analyzer. Descriptive statistical analysis showed at least five separate physiological parameters were linearly correlated to a motion sickness symptom index. Spectral analysis showed definite frequency and amplitude shifts during the onset of motion sickness for various parameters. Low frequency brain wave activity on the order of 0.1 Hz was discovered as the subject approached nausea. A multiple linear regression model was constructed from the correlated data obtained by descriptive statistics. Six separate physiological parameters were useful in describing a predictive motion sickness model that can be used as a major construct in developing a complete biofeedback system for countering effects of motion sickness. GRA

N87-23120# Joint Publications Research Service, Arlington, Va.

USSR REPORT: SPACE BIOLOGY AND AEROSPACE MEDICINE, VOLUME 20, NO. 5, SEPTEMBER - OCTOBER 1986

16 Dec. 1986 147 p Transl. into ENGLISH of Kosmicheskaya Biologiya i Aviakosmicheskaya Meditsina (Moscow, USSR), v. 20, no. 5, Sep. - Oct. 1986 96 p
(JPRS-USB-86-007) Copyright Avail: NTIS HC A07/MF A01

The translation of a Russian journal is presented. The articles mainly concern themselves with the biological effects of space flight on humans. Methods of testing for these effects are also given. Extensive coverage of experimental and general theoretical research is presented. For individual titles, see N87-23121 through N87-23142.

N87-23121# Joint Publications Research Service, Arlington, Va.

PROBLEMS AND FEASIBILITY OF DRUG CORRECTION OF ORTHOSTATIC TOLERANCE IN SPACE MEDICINE

V. S. Shashkov and A. Yu. Modin *In its* USSR Report: Space Biology and Aerospace Medicine, Volume 20, No. 5, September - October 1986 16 Dec. 1986 p 1-11 Transl. into ENGLISH from Kosmicheskaya Biologiya i Aviakosmicheskaya Meditsina (Moscow, USSR), v. 20, no. 5, Sep.-Oct. 1986 p 4-11 (For primary document see N87-23120 16-52)
Copyright Avail: NTIS HC A07/MF A01

Published data concerning physiological mechanisms of man's orthostatic tolerance and its decline under the influence of space flight factors are reviewed. The principles, goals and potentialities of drug correction of orthostatic intolerance are presented. The applicability of selected drugs used separately or in combination with traditional countermeasures is discussed. Author

N87-23122# Joint Publications Research Service, Arlington, Va.
STRUCTURE AND FUNCTION OF OTOLITHS
A. A. Shipov and A. V. Kondrachuk *In its* USSR Report: Space Biology and Aerospace Medicine, Volume 20, No. 5, September - October 1986 16 Dec. 1986 p 12-22 Transl. into ENGLISH from Kosmicheskaya Biologiya i Aviakosmicheskaya Meditsina (Moscow, USSR), v. 20, no. 5, Sep. - Oct. 1986 p 11-19 (For primary document see N87-23120 16-52)
Copyright Avail: NTIS HC A07/MF A01

Current data on the structure and function of the otoliths are reviewed. The function of the otolith organ in microgravity is discussed. Biophysical approaches to its study are presented. Theoretical and practical theories, which may be important, because they may help clarify certain aspects of space motion sickness are presented. Author

N87-23123# Joint Publications Research Service, Arlington, Va.
INVESTIGATION OF HEMOSTASIS SYSTEM IN AIR TRAFFIC CONTROLLERS AS RELATED TO DIFFERENT AIR TRAFFIC CONDITIONS
I. V. Kuznetsova *In its* USSR Report: Space Biology and Aerospace Medicine, Volume 20, No. 5, September - October 1986 16 Dec. 1986 p 23-28 Transl. into ENGLISH from Kosmicheskaya Biologiya i Aviakosmicheskaya Meditsina (Moscow, USSR), v. 20, no. 5, Sep. - Oct. 1986 p 19-23 (For primary document see N87-23120 16-52)
Copyright Avail: NTIS HC A07/MF A01

The system of hemostasis of air traffic controllers responsible for the control of air traffic of varying intensity was investigated. The response of the system depended on its initial state: a higher workload led to hypercoagulation and a lower workload, to hypocoagulation. Author

N87-23124# Joint Publications Research Service, Arlington, Va.
TOLERANCE TO FRUSTRATION AS A FACTOR IN OPERATOR PERFORMANCE **c54**
O. F. Makarevich *In its* USSR Report: Space Biology and Aerospace Medicine, Volume 20, No. 5, September - October 1986 16 Dec. 1986 p 29-32 Transl. into ENGLISH from Kosmicheskaya Biologiya i Aviakosmicheskaya Meditsina (Moscow, USSR), v. 20, no. 5, Sep. - Oct 1986 p 24-26 (For primary document see N87-23120 16-52)
Copyright Avail: NTIS HC A07/MF A01

Frustration tolerance is a personality trait that contributes to the reliable performance of an air traffic controller. The results of a psychological examination of air traffic controllers using the Rosenzweig frustration test are presented and a correlation between the predominant behavior type in frustrating circumstances and professional success is emphasized. Examples of realistic observations over air traffic controllers are given which confirm experimental data. Author

N87-23125# Joint Publications Research Service, Arlington, Va.
EFFECT OF SHORT-TERM SPACEFLIGHTS ON ACTIVITY OF RENIN-ANGIOTENSION-ALDOSTERONE SYSTEM, CONCENTRATION OF CYCLIC NUCLEOTIDES AND PROSTAGLANDINS IN BLOOD
B. V. Afonin, A. I. Grigoryev, and E. A. Pavlova *In its* USSR Report: Space Biology and Aerospace Medicine, Volume 20, No. 5, September - October 1986 16 Dec. 1986 p 33-38 Transl. into ENGLISH from Kosmicheskaya Biologiya i Aviakosmicheskaya Meditsina (Moscow, USSR), v 20, no. 5, Sep. - Oct. 1986 p 27-30 (For primary document see N87-23120 16-52)
Copyright Avail: NTIS HC A07/MF A01

After short term flights renal excretion of aldosterone increased, thus suggesting its enhanced production and metabolism. An adequate increase of aldosterone synthesis was accompanied by an increase of its concentration in blood. An inadequate activation of mineralocorticoids manifested as a lower concentration of blood aldosterone and greater excretion of aldosterone in the urine. These differences in the mineralocorticoid activity were determined by the renin-angiotensin system whose activity was associated not only with fluid-electrolyte metabolism but also with changes in the concentration of cyclic nucleotides and prostaglandins that reflect the vascular tone and sympatho-adrenal activity. An increase activity of the renin-angiotensin system seen in most cosmonauts at an acute stage of readaptation was correlated with a higher concentration of cAMP and a lower concentration of depressor prostaglindins. The acitivity of the renin-angiotensin system declined in parallel with the decrease of the blood content of cAMP. Author

N87-23126# Joint Publications Research Service, Arlington, Va.
NUTRITIONAL CORRECTION OF HISTAMINE AND SEROTONIN LEVELS AS RELATED TO EXPOSURE TO HYPOKINESIA AND NEURO-EMOTIONAL STRESS
S. Kalandarov, V. P. Bychkov, and I. D. Frenkel *In its* USSR Report: Space Biology and Aerospace Medicine, Volume 20, No. 5, September - October 1986 16 Dec. 1986 p 39-44 Transl. into ENGLISH from Kosmicheskaya Biologiya i Aviakosmicheskaya Meditsina (Moscow, USSR), v. 20, no. 5, Sep. - Oct. 1986 p 31-34 (For primary document see N87-23120 16-52)
Copyright Avail: NTIS HC A07/MF A01

The content of histamine and serotonin was measured in test of subject exposed to: (1) bed rest at an angle of +6, -2, or -6 deg; (2) neuro-emotional stress; (3) an increased concentration of ammonium in the enclosure. The exposure to the factors that simulated space flight stress (i.e., orthostatic hypokinesia at -6 deg and neuro-emotional stress and anticipation of rotation in the centrifuge) led to an increase of histamine and serotonin and a decrease of histaminepectic activity. Consumption of selected nutritional agents a day before and on the day of exposure to the neuro-emotional stress improved the content of histamine and serotonin as well as histaminepectic activity. Author

N87-23127# Joint Publications Research Service, Arlington, Va.
SOME PARAMETERS OF HUMAN LIPID METABOLISM DURING ANTIORTHOSTATIC HYPOKINESIA AND THEIR CORRECTION
K. V. Smirnov, I. L. Medkova, O. V. Zhiznevskaya, V. P. Bychkov, L. I. Mosyakina, and O. S. Khokhlova *In its* USSR Report: Space Biology and Aerospace Medicine, Volume 20, No. 5, September - October 1986 16 Dec. 1986 p 45-49 Transl. into ENGLISH from Kosmicheskaya Biologiya i Aviakosmicheskaya Meditsina (Moscow, USSR), v. 20, no. 5, Sep. - Oct. 1986 p 34-37 (For primary document see N87-23120 16-52)
Copyright Avail: NTIS HC A07/MF A01

Twenty-one test subjects exposed to head down tilt for 120 days were subdivided to four groups: (1) nine subjects used as controls; (2) three bed rested subjects who performed regular exercises; (3) four bed rested subjects who were given selected drugs, including Vitamin F-99 that influenced lipid metabolism; (4) four bed rested subjects who performed regular exercised and received Vitamin F-99. At different stages of bed rest and recovery the content of lipoprotein fractions and lipids of different classes in serum was measured by thin layer chromatography. The concentration of cholesterol in biliary lipids was determined. In group 1 and 2 subjects bed rest led to a drastic and significant increase of cholesterol esters in blood, a decrease of phospholipids, variations of triglycerides and nonesterified fatty acids, and a lower percentage content of alpha-lipoproteins. The use of Vitamin F-99 produced positive changes in the above parameters of lipid metabolism. In group 4 subjects the effect of exercises combined with drugs was most distinct. Author

N87-23128# Joint Publications Research Service, Arlington, Va.
SPLIT CIRCADIAN RHYTHM OF SIMIAN BODY TEMPERATURE DURING ANTIORTHOSTATIC HYPOKINESIA **c51**
A. M. Alpatov and V. Ya. Klimovitskiy *In its* USSR Report: Space Biology and Aerospace Medicine, Volume 20, No. 5, September - October 1986 16 Dec. 1986 p 50-55 Transl. into ENGLISH from Kosmicheskaya Biologiya i Aviakosmicheskaya Meditsina (Moscow, USSR), v. 20, no. 5, Sep. - Oct. 1986 p 37-41 (For primary document see N87-23120 16-52)
Copyright Avail: NTIS HC A07/MF A01

37-41 (For primary document see N87-23120 16-52)
Copyright Avail: NTIS HC A07/MF A01

A rhesus monkey was restrained in the prone position with the head kept at -6 deg. The day:night cycle was 16:8 and an ambient temperature 20 to 22 C. Skin temperature (ST) in the ankle area and body temperatue (BT) in the armpit were measured by thermistors every 16 min during 14 days. Mean daily values of both temperatures decreased continuously beginning with day 5 and reached a minimum on day 11. Between days 5 and 11 the BT rhythm was split into two components, i.e., morning and evening (with the 12 hour periodicity being predominant in the spectrum). The amplitude of the ST rhythm declined and reached a minimum on day 4. On that day the rhythm phase was sharply shifted and thereafter the amplitude and phase of the ST rhythm gradually restored. The above effects can be explained by a transient attenuation of the relationship of circadian oscillators due to a greater load of the mechanisms of adaptation to simulated microgravity. Author

N87-23129# Joint Publications Research Service, Arlington, Va.
EFFECT OF HYPOKINESIA ON INTENSITY OF GLUCONEOGENESIS IN CORTICAL LAYER OF RAT KIDNEY
c51
S. M. Yershikov *In its* USSR Report: Space Biology and Aerospace Medicine, Volume 20, No. 5, September - October 1986 16 Dec. 1986 p 56-61 Transl. into ENGLISH from Kosmicheskaya Biologiya i Aviakosmicheskaya Meditsina (Moscow, USSR), v. 20, no. 5, Sep. - Oct. 1986 p 41-44 (For primary document see N87-23120 16-52)
Copyright Avail: NTIS HC A07/MF A01

The rate of gluconeogenesis was measured in the cortical layer of kidneys of 95 white rats on hypokinesia days 1, 3, 7, 15, 30, and 60. At early stages of hypokinesia the rate of glucose formation from aspartic, glutamic, pyruvic, alpha-ketoglutaric acids and glycerol increased, specifically on hypokinesia day 3. The rate of glucose formation from the amino acids on hypokinesia day 30 was identical to that in the controls. The rate of glucose formation frcm alpha-ketoglutaric and succinic acids increased and that from pyruvic acid significantly decreased. On hypokinesia day 30 the rate of glucose formation from every substrate used, except for pyruvic acid, increased. The glucose concentration in serum was higher on hypokinesia days 1 to 7 and lower on hypokinesia days 15 to 60. The changes in the rate of glucose formation in the kidneys make inexplicable stable hypoglycemia seen at later stages of hypokinesia. Author

N87-23130# Joint Publications Research Service, Arlington, Va.
CORTICAL ULTRASTRUCTURE OF RAT CEREBELLAR NODULUS FOLLOWING FLIGHT ABOARD COSMOS-1514 BIOSATELLITE c51
I. B. Krasnov and L. N. Dyachkova *In its* USSR Report: Space Biology and Aerospace Medicine, Volume 20, No. 5, September - October 1986 16 Dec. 1986 p 62-66 Transl. into ENGLISH from Kosmicheskaya Biologiya i Aviakosmicheskaya Meditsina (Moscow, USSR), v. 20, no. 5, Sep. - Oct. 1986 p 45-48 (For primary document see N87-23120 16-52)
Copyright Avail: NTIS HC A07/MF A01

The ultrastructure of moss fibers and granule cells of the cortex of the cerebellum nodulus of rats flown for 5 day onboard the biosatellite Cosmos-1514 and exposed to 1 g for 6 to 8 hours upon return to Earth is indicative of an excess excitation of terminals of moss fibers and excitation of granule cells. The excitation of moss fiber terminals reflects the excitatory state of hair cells of the otolith apparatus and neurons of the vestibular ganglion produced by the effect of 1 g after exposure to microgravity. This state can be viewed as evidence of a greater sensitivity of the hair cell of the otolith organ - neuron of the vestibular ganglion system during exposure to microgravity. It is hypothesized that the sensitivity of this system of other mammals may also increase in microgravity. Author

N87-23131# Joint Publications Research Service, Arlington, Va.
CHEMICAL SENSITIVITY OF MEDIAL VESTIBULAR NUCLEAR NEURONS TO ENKEPHALINS, ACETYLCHOLINE, GABA AND L-GLUTAMATE
V. V. Yasnetsov and V. A. Pravdivtsev *In its* USSR Report: Space Biology and Aerospace Medicine, Volume 20, No. 5, September - October 1986 16 Dec. 1986 p 75-81 Transl. into ENGLISH from Kosmicheskaya Biologiya i Aviakosmicheskaya Meditsina (Moscow, USSR), v. 20, no. 5, Sep. - Oct. 1986 p 53-57 (For primary document see N87-23120 16-52)
Copyright Avail: NTIS HC A07/MF A01

The effect of enkephalins, morphine and some neurotransmitters on spontaneous and evoked activity of neurons of the medial ventricular nucleus was investigated. The evoked activity was produced by an adequate stimulation of the vestibular apparatus. It was shown that neurons of this nucleus were highly sensitive to enkephalins, morphine, acetylcholine, GABA, and L-glutamate. It was found that activation and depression effects of opioid peptides and morphine occurred due to the stimulation of mu- and delta-opiate receptors. It can be concluded that enkephalins modulate cholinergic and glutamatergic synaptic transfer in the medial vestibular nucleus. Together with opiate receptors, they participate in the perception and processing of vestibular information at the level of neurons of this nucleus. Author

N87-23132# Joint Publications Research Service, Arlington, Va.
PHARMACOLOGICAL CORRECTION OF CENTRAL NERVOUS SYSTEM FUNCTIO DURING EXPOSURE TO CORIOLIS ACCELERATIONS
N. N. Karkishchenko, N. A. Dimitriadi, and V. V. Molchanovskiy *In its* USSR Report: Space Biology and Aerospace Medicine, Volume 20, No. 5, September - October 1986 16 Dec. 1986 p 82-85 Transl. into ENGLISH from Kosmicheskaya Biologiya i Aviakosmicheskaya Meditsina (Moscow, USSR), v. 20, no. 5, Sep. - Oct. 1986 p 57-59 (For primary document see N87-23120 16-52)
Copyright Avail: NTIS HC A07/MF A01

Healthy volunteers with a low vestibular tolerance were exposed to Coriolis acceleration. Potassium orotate, pyracetame and riboxine were used as prophylactic measures against disorders in the function of the vestibular apparatus and higher compartments of the higher nervous system. The central nervous system function was assessed with respect to the spectral powder of electroencephalograms, short term memory and mental performance. Potassium orotate given at a dose of 40 mg/kg body weight/day during 12 to 14 days as well as pyracetame given at a dose of 30 mg/kg body weight/day during 3 or 7 days increased significantly statokinetic tolerance and produced a protective effect on the central nervous function against Coriolis acceleration. Author

N87-23133# Joint Publications Research Service, Arlington, Va.
REACTION TO VIBRATION OF RAT KINESTHETIC ANALYZER NEUROCYTES c51
V. V. Antipov, V. I. Drobyshev, I. B. Ushakov, and T. P. Stepanova *In its* USSR Report: Space Biology and Aerospace Medicine, Volume 20, No. 5, September - October 1986 16 Dec. 1986 p 86-92 Transl. into ENGLISH from Kosmicheskaya Biologiya i Aviakosmicheskaya Meditsina (Moscow, USSR), v. 20, no. 5, Sep. - Oct. 1986 p 60-64 (For primary document see N87-23120 16-52)
Copyright Avail: NTIS HC A07/MF A01

By neurohistological, morphometric and electron microscopic methods the effect of vibration of 80 Hz applied at an acceleration of 8 m/sq sec on the nerve cell and conduction components of the kinesthetic analyzer was investigated. After a single exposure to vibration nerve cells of the sensorimotor cortex showed some changes. Exposure to vibration for as long as a week caused reactive changes in every structure of the kinesthetic analyzer investigated. After 1 month exposure the changes were more disseminated and became destructive, after 2 month exposure the process developed at a slower rate, and after 3 month exposure it remained at the same level. However, after 3 month exposure the morphological equivalent of compensatory adaptive reactions was seen. Author

N87-23134# Joint Publications Research Service, Arlington, Va.
EVALUATION OF EFFECT OF POSITIVE INTRAPULMONARY PRESSURE ON RESPIRATORY FUNCTION OF MAN
I. S. Breslav, G. G. Isayev, A. V. Kochubeyev, and Ye. A. Sokol *In its* USSR Report: Space Biology and Aerospace Medicine, Volume 20, No. 5, September - October 1986 16 Dec. 1986 p 93-99 Transl. into ENGLISH from Kosmicheskaya Biologiya i Aviakosmicheskaya Meditsina (Moscow, USSR), v. 20, no. 5, Sep. - Oct. 1986 p 64-69 (For primary document see N87-23120 16-52)
Copyright Avail: NTIS HC A07/MF A01

The parameters characterizing lung ventilation and electrical activity of expiratory muscles were investigated in six healthy young men exposed to the positive intrapulmonary pressure 20, 30 or 40 mm Hg. Gas mixtures with a varying oxygen content were used. The effect of two compensatory devices that applied different counterpressures to the body surface was evaluated. It was found that the parameter that can best characterize the respiratory function in the case of a positive intrapulmonary pressure is electrical activity of expiratory muscles. The hypoxic effect makes no important contribution to the change of respiratory pressure 20, 30 or 40 mm Hg. The different methods of applying compensation do not influence changes in the above respiratory parameters. Author

N87-23135# Joint Publications Research Service, Arlington, Va.
EVALUATION OF SKELETOMUSCULAR SYSTEM FUNCTION IN SELF-CONTAINED LIFE-SUPPORT SYSTEM ON THE BASIS OF BLOOD BIOCHEMISTRY
V. V. Makarovskiy, A. F. Khalangot, Yu. A. Shafranskiy, and G. F. Kryzhanovskaya *In its* USSR Report: Space Biology and Aerospace Medicine, Volume 20, No. 5, September - October 1986 16 Dec. 1986 p 100-107 Transl. into ENGLISH from Kosmicheskaya Biologiya i Aviakosmicheskaya Meditsina (Moscow, USSR), v. 20, no. 5, Sep. - Oct. 1986 p. 69-75 (For primary document see N87-23120 16-52)
Copyright Avail: NTIS HC A07/MF A01

The functional state of the musculoskeletal system of healthy male volunteers of three ages group was evaluated. The subjects were kept in an enclosure for 30 days. Creatine phosphokinase (CPK), lactate dehydrogenase (LDH), alkaline phosphatase, aspartate aminotransferase (AAT), calcium, P sub 1 were measured in blood. The test subjects of the three groups showed a decrease of CPK, LDH, AAT and creatinine. The correlation coefficient between the enzymes varied from 0.64 to 1.00. By the end of the study alkaline phosphatase increased in the group 1 and 2 subjects and decreased in the group 3 subjects. Calcium variations were less distinct. The P sub 1 content declined significantly in the group 3 subjects. Some of the group 3 subjects who performed regular exercises during the study exhibited smaller decreases of CPK, LDH, AAT and greater stability of calcium and phosphorus. Author

N87-23136# Joint Publications Research Service, Arlington, Va.
INVESTIGATION OF CAUSES OF HYDROGEN SULFIDE FORMATION IN RECLAIMED WATER c54
I. G. Popov, V. V. Vlodavets, S. V. Chizhov, Yu. Ye. Sinyak, M. I. Shikina, L. A. Vinogradova, and N. B. Kolesina *In its* USSR Report: Space Biology and Aerospace Medicine, Volume 20, No. 5, September - October 1986 16 Dec. 1986 p 108-111 Transl. into ENGLISH from Kosmicheskaya Biologiya i Aviakosmicheskaya Meditsina (Moscow, USSR), v. 20, no. 5, Sep. - Oct. 1986 p 75-78 (For primary document see N87-23120 16-52)
Copyright Avail: NTIS HC A07/MF A01

The factors responsible for the formation of hydrogen sulphide in the water reclaimed from the atmospheric condensate were investigated. It was found that hydrogen sulphide developed in reclaimed water due to microorganisms which in the presence of inorganic sulphur acquired the capacity to produce hydrogen sulphide, although normally they are not sulphur reducing. Among the microorganisms studied, E. coli showed the highest capacity (100%) and Streptococcus faecalis and Citrobacter freundii showed the lowest capacity (10 to 20%) to produce hydrogen sulphide. Author

N87-23137# Joint Publications Research Service, Arlington, Va.
EXPERIMENTAL INVESTIGATION OF THE PROCESS OF CO2-CO-H2O-H2-N2 GAS MIXTURE BREAKDOWN IN ELECTROLYSIS CELL WITH SOLID ELECTROLYTE c54
B. G. Grishayenkov and N. G. Zorina *In its* USSR Report: Space Biology and Aerospace Medicine, Volume 20, No. 5, september - October 1986 16 Dec. 1986 p 112-116 Transl. into ENGLISH from Kosmicheskaya Biologiya i Aviakosmicheskaya Meditsina (Moscow, USSR), v. 20, no. 5, Sep. - Oct. 1986 p 78-81 (For primary document see N87-23120 16-52)
Copyright Avail: NTIS HC A07/MF A01

The experimental investigation was carried out in an electrolytic cell having the form of a short tube and containing a solid electrolyte of the following composition: 0.9 ZrO2-0.1Y2O3. The concentration of the gaseous mixtures investigated varied in range 0.22 to 18.0. The cathode polarization of the cell with platinum electrodes was measured as a function of the composition of the gaseous mixture and oxygen content at the temperatures 800, 900 and 1000 C. The measurements demonstrated that the cell cathode polarization decreased as the water concentration in the starting mixture decreased. The dependence of the cell cathode polarization on the oxygen content had minima in a specific range of the values. Simultaneously, the cell cathode polarization decreased as the water content in the starting gaseous mixture increased. Author

N87-23138# Joint Publications Research Service, Arlington, Va.
DISTINCTIONS IN FORMATION OF MICROBIAL COMPLEX IN NUTRIENT SOLUTIONS OF HIGHER PLANTS AFTER USE OF STRAW MINERALIZATION PRODUCTS c51
N. A. Drugova, L. S. Yunusova, and Yu. I. Shaydorov *In its* USSR Report: Space Biology and Aerospace Medicine, Volume 20, No. 5, September - October 1986 16 Dec. 1986 p 117-122 Transl. into ENGLISH from Kosmicheskaya Biologiya i Aviakosmicheskaya Meditsina (Moscow, USSR), v. 20, no. 5, Sep. - Oct. 1986 p 81-84 (For primary document see N87-23120 16-52)
Copyright Avail: NTIS HC A07/MF A01

The effect of a product of wheat straw mineralization, e.g., ecothole, on the formation of a microbial complex that is concomitant with lettuce plants during 7 vegetations (i.e., 189 days) was investigated. The plants were grown by the subirrigation-aeroponic method on nutrient solutions that were not replaced throughout the study. It was found that in the course of lettuce ontogenesis the count of microorganisms, fungi and actinomycetes varied in the range of 100,000 to 1,000,000, 100 to 10,000 and 100 to 100,000 cells per ml solution, respectively. During all lettuce vegetations 19 bacterial species were isolated. During the first vegetation a stable microbial complex with predominant gram-negative bacteria developed. However, addition of ecothole caused an increase in the count of spore forming bacteria, whereas in the control the count of nitrogen fixing bacteria grew. Author

N87-23139# Joint Publications Research Service, Arlington, Va.
HORMONAL AND METABOLIC STATUS OF MAN IN THE EXTREME NORTH
Yu. F. Krylov and R. A. Tigranyan *In its* USSR Report: Space Biology and Aerospace Medicine, Volume 20, No. 5, September - October 1986 16 Dec. 1986 p 123-127 Transl. into ENGLISH from Kosmicheskaya Biolgoiya i Aviakosmicheskaya Meditsina (Moscow, USSR), v. 20, no. 5, Sep. - Oct. 1986 p 85-88 (For primary document see N87-23120 16-52)
Copyright Avail: NTIS HC A07/MF A01

The concentrations of hormones (ACTH, cortisol, aldosterone, thyrotrophin, thyroxine, triiodothyronine, growth hormone, insulin, prolactine and testosterone), electrolytes (Na and K) as well glucose and triglycerides were measured in 10 athletes who made a 380 km ski expedition in the Far North at ambient temperatures of -32 to -34 C. Human adaptation to the geographic and climatic conditions of high latitudes was accompanied by noticeable changes in the incretory function of the adenopituitary, thyroid gland, adrenals and gonads. The data obtained indicate that a ski trip in the Far North produces a distinct stress with physical and cold components being predominant. Author

N87-23140# Joint Publications Research Service, Arlington, Va.
HUMAN BLOOD SERUM PROTEOLYTIC ENZYME ACTIVITY AFTER STAY IN HYPOXIC ENVIRONMENT
V. D. Vlasov, I. G. Dlusskaya, V. V. Krashutskiy, and A. A. Domnikova *In its* USSR Report: Space Biology and Aerospace Medicine, Volume 20, No. 5, September - October 1986 16 Dec. 1986 p 128-131 Transl. into ENGLISH from Kosmicheskaya Biologiya i Aviakosmicheskaya Meditsina (Moscow, USSR), v. 20, no. 5, Sep. - Oct. 1986 p 88-90 (For primary document see N87-23120 16-52)
Copyright Avail: NTIS HC A07/MF A01

Diminished appetite, various dyspeptic manifestations and temporary weight loss in man and animals submitted to chronic and intermittent hypoxic hypoxia at low barometric pressure are indicative of disturbances in processes of digestion, assimilation and resynthesis of proteins in the body. This is confirmed by development of a negative nitrogen balance in man and animals under hypoxic conditions. Changes in activity of proteolytic and certain other enzymes in blood serum of healthy males 19 to 21 years of age after exposure to hypoxic environment at low barometric pressure was investigated. Brief details concerning methods, results and conclusions are given. Author

N87-23141# Joint Publications Research Service, Arlington, Va.
SOME BIOCHEMICAL AND MORPHOLOGICAL CHANGES IN RAT BLOOD WITH EXPOSURE TO VARIABLE MAGNETIC FIELD AT INFRALOW FREQUENCY c51
V. G. Sidyakin, N. A. Temuryants, and Ye. V. Yevstafyeva *In its* USSR Report: Space Biology and Aerospace Medicine, Volume 20, No. 5, September - October 1986 16 Dec. 1986 p 132-133 Transl. into ENGLISH from Kosmicheskaya Biologiya i Aviakosmicheskaya Meditsina (Moscow, USSR), v. 20, no. 5, Sep. - Oct. 1986 p 90-91 (For primary document see N87-23120 16-52)
Copyright Avail: NTIS HC A07/MF A01

In recent years it was found that a variable magnetic field (VMF) at a frequency of 8 Hz at a voltage 10 to 100 times greater than that of the geomagnetic field causes some biological functional changes varying in complexity. Experiments were conducted on white rats to investigate these findings. Author

N87-23142# Joint Publications Research Service, Arlington, Va.
BIOCHEMICAL ASPECTS OF SOME NEUROHUMORAL SYSTEM FUNCTIONS DURING LONG-TERM ANTIORTHOSTATIC HYPOKINESIA
N. A. Davydova, S. K. Shishkina, N. V. Korneyeva, Ye. V. Suprunova, and A. S. Ushakov *In its* USSR Report: Space Biology and Aerospace Medicine, Volume 20, No. 5, September - October 1986 16 Dec. 1986 p 134-140 Transl. into ENGLISH from Koshmicheskaya Biologiya i Aviakosmicheskaya Meditsina (Moscow, USSR), v. 20, no. 5, Sep. - Oct. 1986 p 91-95 (For primary document see N87-23120 16-52)
Copyright Avail: NTIS HC A07/MF A01

The sympathoadrenal (SAS) and cholinergic (CS) systems play an important part in processes of neurohumoral regulation of changes that occur during long term restriction of motor activity. Investigation of these system using modern methods and criteria for evaluating their functional activity makes it possible to find approaches to the solution of some problems of prevention and correction of metabolic changes. The objective was to investigate human SAS and CS activity during long term antiorthostatic hypokinesia. A brief account of the methods used are given along with results and discussion of those results. Author

53 BEHAVIORAL SCIENCES

Includes psychological factors; individual and group behavior; crew training and evaluation; and psychiatric research.

No abstracts in this category.

54 MAN/SYSTEM TECHNOLOGY AND LIFE SUPPORT

Includes human engineering; biotechnology; and space suits and protective clothing.

For related information see also *16 Space Transportation.*

N87-23143# Illinois Univ., Champaign. Cognitive Psychophysiology Lab.
THE EVENT RELATED BRAIN POTENTIAL AS AN INDEX OF INFORMATION PROCESSING AND COGNITIVE ACTIVITY: A PROGRAM OF BASIC RESEARCH Annual Progress Report, 1 Jan. - 31 Dec. 1986
Emanuel Donchin, Michael Coles, and Arthur Kramer 23 Feb. 1987 334 p
(Contract F49620-85-C-0041)
(AD-A179310; CPL-87-1; AFOSR-87-0322TR) Avail: NTIS HC A15/MF A01 CSCL 05J

Research designed to understand the event related potential (ERP) can be used as a tool in the study of human information processing and in the assessment of man machine systems. The present contract year has focussed on (1) the use of measures of the P300 and motor potentials in the chronometric analysis of human information processing, (2) the use of P300 in the study of memory, (3) the use of various ERP components in the study of the structure of human cognitive resources as a function of task difficulty, priority, and automaticity, and (4) the use of ERP components in lie detection and mental prosthesis. GRA

N87-23144# Human Engineering Labs., Aberdeen Proving Ground, Md.
HUMAN FACTORS ENGINEERING DATA MANAGEMENT HANDBOOK Final Report
R. B. McCommons Mar. 1987 75 p
(AD-A179691; HEL-TM-6-87) Avail: NTIS HC A04/MF A01 CSCL 05B

For some time, serious concerns have existed regarding how the Government acquires data. The questions most frequently asked include, how much data should we buy, when should we ask for it, how should we use it, and how do we acquire it so it is both timely and useful? This document was written with the above concerns and questions in mind. It is intended for use by HEL and other personnel who are engaged in HFE program management activities in support of materiel acqusitions. The document is presented as guidance for determining data requirements and specifying and scheduling their timely delivery. Accordingly, the objectives are to provide a basic understanding of data acquisition as part of the materiel development process. It should be considered a living document and, after evaluation and/or implementation by users, one which will be updated or modified, as required, to reflect field experience and changes in relevant policy. Last, while written from an HFE perspective, the author recognizes that HFE is most properly considered not as a discipline in and unto itself, but as a predominant element of the much larger initiative called MANPRINT (Manpower and Personnel Integration). GRA

N87-23145# Oak Ridge National Lab., Tenn.
ALTERNATIVE KNOWLEDGE ACQUISITION: DEVELOPING A PULSE CODED NEURAL NETWORK
W. B. Dress Jan. 1987 12 p Presented at the Long Island

University Computer Technology Symposium, Brookville, N.Y., 23 Jan. 1987
(Contract DE-AC05-84OR-21400)
(DE87-005192; CONF-870150-1) Avail: NTIS HC A02/MF A01

After a Rip-van-Winkle nap of more than 20 years, the ideas of biologically motivated computing are re-emerging. Instrumental to this awakening have been the highly publicized contributions of John Hopfield and major advances in the neurosciences. In 1982, Hopfield showed how a system of maximally coupled neutron-like elements described by a Hamiltonian formalism (a linear, conservative system) could behave in a manner startlingly suggestive of the way humans might go about solving problems and retrieving memories. Continuing advances in the neurosciences are providing a coherent basis in suggesting how nature's neurons might function. A particular model is described for an artificial neural system designed to interact with (learn from and manipulate) a simulated (or real) environment. The model is based on early work by Iben Browning. The Browning model, designed to investigate computer-based intelligence, contains a particular simplification based on observations of frequency coding of information in the brain and information flow from receptors to the brain and back to effectors. The ability to act on and react to the environment was seen as an important principle, leading to self-organization of the system. DOE

N87-23146# Air Force Human Resources Lab., Brooks AFB, Tex.
AIRCREW TASK SURVEYS: SELECTION CRITERIA FOR LOW-COST TRAINING TECHNOLOGY APPLICATIONS Interim Technical Paper, Mar. 1983 - Feb. 1986
Bernell J. Edwards Mar. 1987 39 p
(AD-A178473; AFHRL-TR-86-52) Avail: NTIS HC A03/MF A01 CSCL 05I

This paper documents the first phase of a research and development effort to obtain opinion data from Air Force operational aircrews to support the selection of training tasks as candidates for the development of several high technology, low cost, part task trainer demonstrations. The overall goal of the effort is to develop and combine scientifically derived, advanced part task training methods with state-of-the-art training technology. Several surveys of aircrews who fly tanker, transport, or bomber type aircraft were conducted to elicit their opinions regarding training issues which bear on the matching of task characteristics with low cost training technology. Survey results provide a general guide to the selection of appropriate tasks for further analysis. GRA

N87-23147# Naval Aerospace Medical Research Lab., Pensacola, Fla.
EFFECT OF THE NEUTRAL DENSITY HELMET VISOR ON THE VISUAL ACUITY OF NAVY FIGHTER PILOTS
P. V. Hamilton and A. Morris Dec. 1986 27 p
(AD-A178486; NAMRL-1325) Avail: NTIS HC A03/MF A01 CSCL 06P

The visual acuity of 63 Navy fighter pilots was measured under four viewing conditions in an Automated Vision Test Battery housed in a Mobile Field Laboratory operated by the Naval Aerospace Medical Research Laboratory (NAMRL). These and other pilots were also interviewed concerning their visor usage habits. Use of the 12% neutral density visor resulted in an average acuity loss of about 0.51 minutes of visual angle (mva) for low contrast targets under high-luminance laboratory conditions. The visor may cause an operationally significant reduction in visual acuity in the presence of luminance levels encountered at typical flight altitudes. Pilots range widely in their sensitivities to reduced contrast and glare, so a single optical density visor would not be optimal for many pilots. Pilot attempts to identify individually-optimal strategies for using visors and sunglasses often have no objective or systematic basis. Recommendations are presented for improving the vision of aviators wearing visors. GRA

N87-23148# Air Force Wright Aeronautical Labs., Wright-Patterson AFB, Ohio.
PROCEEDINGS OF THE 22ND ANNUAL CONFERENCE ON MANUAL CONTROL Annual Report, 15 - 16 Jul. 1986
Frank L. George Dec. 1986 374 p Conference held in Dayton, Ohio, 15-16 Jul. 1986
(AD-A178627; AFWAL-TR-86-3093) Avail: NTIS HC A16/MF A01 CSCL 05H

The Twenty-Second Annual Conference on Manual Controls emphasized human-machine system design methodology and the impact of automation on the human-machine interface. GRA

N87-22636*# Harvard Univ., Cambridge, Mass.
GROUP-LEVEL ISSUES IN THE DESIGN AND TRAINING OF COCKPIT CREWS
J. Richard Hackman *In* NASA. Ames Research Center Cockpit Resource Management Training May 1987 p 23-39 (For primary document see N87-22634 16-03)
(Contract NCC2-324)
Avail: NTIS HC A14/MF A01 CSCL 05H

N87-23124# Joint Publications Research Service, Arlington, Va.
TOLERANCE TO FRUSTRATION AS A FACTOR IN OPERATOR PERFORMANCE
O. F. Makarevich *In its* USSR Report: Space Biology and Aerospace Medicine, Volume 20, No. 5, September - October 1986 16 Dec. 1986 p 29-32 Transl. into ENGLISH from Kosmicheskaya Biologiya i Aviakosmicheskaya Meditsina (Moscow, USSR), v. 20, no. 5, Sep. - Oct 1986 p 24-26 (For primary document see N87-23120 16-52)
Copyright Avail: NTIS HC A07/MF A01

N87-23136# Joint Publications Research Service, Arlington, Va.
INVESTIGATION OF CAUSES OF HYDROGEN SULFIDE FORMATION IN RECLAIMED WATER
I. G. Popov, V. V. Vlodavets, S. V. Chizhov, Yu. Ye. Sinyak, M. I. Shikina, L. A. Vinogradova, and N. B. Kolesina *In its* USSR Report: Space Biology and Aerospace Medicine, Volume 20, No. 5, September - October 1986 16 Dec. 1986 p 108-111 Transl. into ENGLISH from Kosmicheskaya Biologiya i Aviakosmicheskaya Meditsina (Moscow, USSR), v. 20, no. 5, Sep. - Oct. 1986 p 75-78 (For primary document see N87-23120 16-52)
Copyright Avail: NTIS HC A07/MF A01

N87-23137# Joint Publications Research Service, Arlington, Va.
EXPERIMENTAL INVESTIGATION OF THE PROCESS OF CO2-CO-H2O-H2-N2 GAS MIXTURE BREAKDOWN IN ELECTROLYSIS CELL WITH SOLID ELECTROLYTE
B. G. Grishayenkov and N. G. Zorina *In its* USSR Report: Space Biology and Aerospace Medicine, Volume 20, No. 5, september - October 1986 16 Dec. 1986 p 112-116 Transl. into ENGLISH from Kosmicheskaya Biologiya i Aviakosmicheskaya Meditsina (Moscow, USSR), v. 20, no. 5, Sep. - Oct. 1986 p 78-81 (For primary document see N87-23120 16-52)
Copyright Avail: NTIS HC A07/MF A01

55 SPACE BIOLOGY

Includes exobiology; planetary biology; and extraterrestrial life.

No abstracts in this category.

59 MATHEMATICAL AND COMPUTER SCIENCES (GENERAL)

No abstracts in this category.

60 COMPUTER OPERATIONS AND HARDWARE

Includes hardware for computer graphics, firmware, and data processing.

For components see *33 Electronics and Electrical Engineering.*

N87-23149# Air Force Inst. of Tech., Wright-Patterson AFB, Ohio. School of Engineering.
PERFORMANCE COMPARISON OF FOUR STATE-OF-THE-ART COMPUTER ARCHITECTURES M.S. Thesis
Ronald W. Lee Dec. 1986 220 p
(AD-A179071; AFIT/GCS/ENG/86D-17) Avail: NTIS HC A10/MF A01 CSCL 09B

This study determined the relative performance trends of sequential, vector, and multiprocessor architectures solving computationally intense problems. The problem time complexity of sequential matrix multiplication and inversion algorithms on a Cyber 845, a Vax-11/785, and a Cray X-MP/12 were compared with parallelizations of the algorithms on an Intel Personal Supercomputer (iPSC). In addition, sequential and parallel sort algorithms were run on the Vax and iPSC, respectively. The implementations were run with a range of data sizes. The relative time complexities were determined by computing the factor of execution time increase in relation to the factor of data size increase. By analyzing the problem time complexity, the machine-specific influences on execution speed were partially accounted for, thus enabling generalizations to the corresponding architectural classes to be drawn. It was shown that the multiprocessor was the only architecture to allow a reduction in the problem time complexity, and speedups from vector operations were constant. GRA

N87-23150# Massachusetts Inst. of Tech., Cambridge.
IMAGE PROCESSING FOR VISION: AN EQUIPMENT REQUESTS TO DOD Final Report, 15 Jun. 1983 - 17 Jan. 1985
Whitman Richards 19 Feb. 1987 8 p
(Grant AF-AFOSR-0266-83)
(AD-A179261; AFOSR-87-0463TR) Avail: NTIS HC A02/MF A01 CSCL 14E

The report lists items of scientific instrumentation acquired under the DOD University Research Instrumentation Program. These items, used for basic research on human vision, include an image processor and associated color display monitors, a computer disk drive, a computer magnetic tape storage, and a color video camera. GRA

N87-23151# Sandia National Labs., Albuquerque, N. Mex.
CONSIDERATIONS IN DEVELOPING A COMPREHENSIVE COMPUTER SECURITY SUPPORT DATABASE SYSTEM
J. J. Clever 1987 18 p Presented at the Department of Energy Computer Security Group Conference, Albuquerque, N. Mex., 5 May 1987
(Contract DE-AC04-76DP-00789)
(DE87-005527; SAND-86-2543C; CONF-870565-1) Avail: NTIS HC A02/MF A01

In the past several years, computer technology has mushroomed on all fronts. This has resulted in the computer security professional encountering the problem of an ever increasingly complex demand for control, audit, and countermeasure efforts, with concomitantly greater demands on scarce personal time. This paper examines the background of the problem in the practical context of an existing larger organization. It then looks at some of the managerial, technical and economic considerations involved in achieving a higher level of individual productivity at minimal personnel costs. In this instance, the methodology reviewed considerations for developing support from an automated database. Finally, it provides an overview of the database schema, a summary of the initial applications design, and a review of some concerns encountered at implementation of the concept. DOE

N87-23152# Sandia National Labs., Albuquerque, N. Mex.
ELEMENTS OF A PROPOSED SECURITY METHODOLOGY FOR NETWORKS OF COMPUTERS
L. G. Pierson and E. L. Witzke Oct. 1986 13 p
(Contract DE-AC04-76DP-00789)
(DE87-006769; SAND-86-2453) Avail: NTIS HC A02/MF A01

Described are the components or elements of a proposed security methodology for networks of computers. This general security methodology separates the security life of a computer network into two phases; the design, review, and accreditation phase, and the operational phase. The first phase deals with system security planning, implementation, certification, and accreditation for operation. The second phase deals with the processing of unusual events which may be of security interest during the operation of a computer network. The unusual events are processed through a series of filters to determine if the event is associated with a loss or unauthorized activity. Detection and processing of certain kinds of unusual events may cause the update and review of the elements in the first phase (design, review, and accreditation). DOE

N87-23153# Sandia National Labs., Albuquerque, N. Mex.
THE USE OF REAL-TIME OPTICAL PROCESSORS IN EMBEDDED COMPUTING
K. T. Stalker, P. A. Molley, J. H. Stichman, and S. L. Humphreys 1987 10 p Presented at the Computing Conference, Anaheim, Calif., 1 May 1987
(Contract DE-AC04-76DP-00789)
(DE87-006895; SAND-87-0587C; CONF-870574-2) Avail: NTIS HC A02/MF A01

Optical processing technology can be applied to embedded computer systems to perform specialized tasks and general computation. An overview of several processing architectures will be presented. In particular, a class of architectures which uses one-dimensional acousto-optic devices (AOD) to achieve two-dimensional processing has been studied. These architectures are applicable to radar image formation and 2-D correlation coprocessors for real-time embedded computers. Real-time radar image formation by such a system has been achieved in the laboratory with components that can be applied in an embedded computer environment. Data on the performance of this coprocessor will be presented, along with a discussion of the potential extensions of this technology to other embedded computer problems. DOE

N87-23154# City Coll. of the City Univ. of New York. Dept. of Electrical Engineering.
OPTICAL ACQUISITION, IMAGE AND DATA COMPRESSION Progress Report, Jun. 1985 - May 1986
George Eichmann Jun. 1986 75 p
(Grant AF-AFOSR-0212-85)
(AD-A178508; CCEE-447222-1; AFOSR-86-1041TR) Avail: NTIS HC A04/MF A01 CSCL 09B

In this report a new shape classification scheme is proposed which uses the image processing formalism of associative memory mapping. This scalar transform technique is applied to two-dimensional (2D) images. The shape description is the centrodial profile which is the radius as a function of arc length parametrization of the boundary. Other one-dimensional (ID) representations are also discussed. The scheme is applicable to both full-and partial-view recognition problems. The restoration of degraded images, either due to occulsion or other forms of information loss, is optimal in the least squares sense. Two different approaches to decision aids are explored. In one, forced binary decisions are made. In the other, a set of a posteriori probabilities is calculated. In both cases fast inferences can be calculated by optical matrix operations. There are many cases, both in signal and in image processing applications, where the eigenvalues and vectors of particular matrix operators are required. Furthermore, in many situations, on a particular matrix operator, there is a priori information available. GRA

N87-23155# Naval Postgraduate School, Monterey, Calif.
THE DESIGN OF A REAL TIME OPERATING SYSTEM FOR A FAULT TOLERANT MICROCOMPUTER M.S. Thesis
Robert J. Voigt Dec. 1986 103 p
(AD-A178577) Avail: NTIS HC A06/MF A01 CSCL 09B

The design and implementation of a real time operating system kernel for a fault tolerant microcomputer is presented. The operating system is designed for a real time imbedded system. The particular design is for a Motorola MC68000 microprocessor; however, the majority of the operating system is implemented using the C programming language for portability to other microprocessors. The C source for the kernel is presented. The source code is modular so that it may be used in part or as a whole operating system kernel. A heap implementation of a priority ready queue is used for task management. Performance measurements are included for parts of the ready queue. Author (GRA)

N87-22617*# Ohio Univ., Athens. Dept. of Electrical and Computer Engineering.
A MICRO-COMPUTER-BASED SYSTEM TO COMPUTE MAGNETIC VARIATION
Rajan Kaul *In* NASA. Langley Research Center Joint University Program for Air Transportation Research, 1984 May 1987 p 87-112 Previously anounced as N84-20506 (For primary document see N87-22604 16-01)
(OU-TM-91) Avail: NTIS HC A08/MF A01 CSCL 09B

61 COMPUTER PROGRAMMING AND SOFTWARE

Includes computer programs, routines, alogorithms, and specific applications, e.g., CAD/CAM.

N87-23156*# National Aeronautics and Space Administration. Goddard Space Flight Center, Greenbelt, Md.
SIXTH ANNUAL USERS' CONFERENCE
Martha Szczur, ed. and Elfrieda Harris, ed. (Science Applications Research, Lanham, Md.) Oct. 1986 228 p Conference held in Pasadena, Calif., 8-10 Oct. 1986; sponsored by JPL and NASA. Goddard Space Flight Center
(NASA-CP-2463; Rept-87B0176; NAS 1.55:2463) Avail: NTIS HC A11/MF A01 CSCL 09B

Conference papers and presentation outlines which address the use of the Transportable Applications Executive (TAE) and its various applications programs are compiled. Emphasis is given to the design of the user interface and image processing workstation in general. Alternate ports of TAE and TAE subsystems are also covered. For individual titles, see N87-23157 through N87-23169.

N87-23157*# National Aeronautics and Space Administration. Goddard Space Flight Center, Greenbelt, Md.
TAE PLUS: A CONCEPTUAL VIEW OF TAE IN THE SPACE STATION ERA
Martha Szczur *In its* Sixth Annual Users' Conference Oct. 1986 p 19-30 (For primary document see N87-23156 16-61)
Avail: NTIS HC A11/MF A01 CSCL 09B

The use of the Transportable Applications Executive (TAE) for prototyping user interfaces has been the prime force behind the new TAE research and development work. The Data Systems Technology Division at GSFC is developing prototypes of user interfaces for different functions involved in the operation, analysis and data communication of space station payloads. TAE is a valuable prototyping tool because it enables a developer to build an entire application user interface model and run it without writing a single line of application code. One force driving new development is the need to update TAE's user interface to support the latest interactive graphic device technology. The current TAE, TAE Classic, uses interface techniques designed for an 80x24 character monochrome alphanumeric terminal, but does not effectively utilize features such as windowing, graphics, color, and selection devices available on newer workstations. To meet our needs, development of a TAE Plus began in FY-86 and involves augmenting TAE with three different sets of tools: a user interface toolkit; an application toolkit; and run-time service subroutines. A phased approach is being used to develop TAE Plus. In the first phase, we have met the needs of the user community and provided some support for rapid prototyping by developing a TAE Facelift, which adds an enhanced TAE interface (with windowing, mouse interaction, pull-down menus, etc.) to a select set of graphic workstations. The TAE Facelift allows many new concepts to be tested quickly for feedback and performance. In the second phase, a fully-integrated user interface management system, TAE Plus, will be built that supports the separation of interface from application, with the concomitant ability to prototype and rapidly change interfaces. This robust functionality will support, in an integrated manner, an application's development cycle from the prototype step through to the fully operational system. M.G.

N87-23158*# Jet Propulsion Lab., California Inst. of Tech., Pasadena.
THE EVALUATION AND EXTENSION OF TAE IN THE DEVELOPMENT OF A USER INTERFACE MANAGEMENT SYSTEM
Brenda Burkhart and Ross Sugar (Century Computing, Inc., Laurel, Md.) *In* NASA. Goddard Space Flight Center Sixth Annual Users' Conference Oct. 1986 p 31-37 (For primary document see N87-23156 16-61)
Avail: NTIS HC A11/MF A01 CSCL 09B

The development of a user interface management system (UIMS) for an information gathering and display system is discussed. The system interface requirements are outlined along with the UIMS functional characteristics. Those systems requirements which are supported by the current Transportable Applications Executive (TAE) are listed and necessary modifications to the TAE are described. M.G.

N87-23159*# EROS Data Center, Sioux Falls, S. Dak.
A DESIGN FOR A NEW CATALOG MANAGER AND ASSOCIATED FILE MANAGEMENT FOR THE LAND ANALYSIS SYSTEM (LAS)
Cheryl Greenhagen *In* NASA. Goddard Space Flight Center Sixth Annual Users' Conference Oct. 1986 p 53-60 (For primary document see N87-23156 16-61)
Avail: NTIS HC A11/MF A01 CSCL 09B

Due to the larger number of different types of files used in an image processing system, a mechanism for file management beyond the bounds of typical operating systems is necessary. The Transportable Applications Executive (TAE) Catalog Manager was written to meet this need. Land Analysis System (LAS) users at the EROS Data Center (EDC) encountered some problems in using the TAE catalog manager, including catalog corruption, networking difficulties, and lack of a reliable tape storage and retrieval capability. These problems, coupled with the complexity of the TAE catalog manager, led to the decision to design a new file management system for LAS, tailored to the needs of the EDC user community. This design effort, which addressed catalog management, label services, associated data management, and enhancements to LAS applications, is described. The new file management design will provide many benefits including improved system integration, increased flexibility, enhanced reliability, enhanced portability, improved performance, and improved maintainability. M.G.

N87-23160*# Washington Univ., St. Louis, Mo.
NASA REGIONAL PLANETARY IMAGE FACILITY IMAGE RETRIEVAL AND PROCESSING SYSTEM
Susan Slavney *In* NASA. Goddard Space Flight Center Sixth Annual Users' Conference Oct. 1986 p 61-66 (For primary document see N87-23156 16-61)
Avail: NTIS HC A11/MF A01 CSCL 09B

The general design and analysis functions of the NASA Regional Planetary Image Facility (RPIF) image workstation prototype are described. The main functions of the MicroVAX II based workstation will be database searching, digital image retrieval, and image processing and display. The uses of the Transportable Applications Executive (TAE) in the system are described. File access and image processing programs use TAE tutor screens to receive parameters from the user and TAE subroutines are used to pass parameters to applications programs. Interface menus are also provided by TAE. M.G.

N87-23161*# National Aeronautics and Space Administration. Goddard Space Flight Center, Greenbelt, Md.
SOT: A RAPID PROTOTYPE USING TAE WINDOWS
Mark Stephens, David Eike, Elfrieda Harris (Science Applications Research, Lanham, Md.), and Dana Miller *In its* Sixth Annual Users' Conference Oct. 1986 p 97-110 (For primary document see N87-23156 16-61)
Avail: NTIS HC A11/MF A01 CSCL 09B

The development of the window interface extension feature of the Transportable Applications Executive (TAE) is discussed. This feature is being used to prototype a space station payload interface in order to demonstrate and assess the benefits of using windows on a bit mapped display and also to convey the concept of telescience, the control and operation of space station payloads from remote sites. The prototype version of the TAE with windows operates on a DEC VAXstation 100. This workstation has a high resolution 19 inch bit mapped display, a keyboard and a three-button mouse. The VAXstation 100 is not a stand-alone workstation, but is controlled by software executing on a VAX/8600. A short scenario was developed utilizing the Solar Optical Telescope (SOT) as an example payload. In the scenario the end-user station includes the VAXstation 100 plus an image analysis terminal used to display the CCD images. The layout and use of the prototype elements, i.e., the root menu, payload status window, and target acquisition menu is described. M.G.

N87-23162*# Computer Sciences Corp., Mountain View, Calif. Systems Sciences Div.
THE 2GCHAS: A HIGH PRODUCTIVITY SOFTWARE DEVELOPMENT ENVIRONMENT
Larry Babb *In* NASA. Goddard Space Flight Center Sixth Annual Users' Conference Oct. 1986 p 111-123 (For primary document see N87-23156 16-61)
Avail: NTIS HC A11/MF A01 CSCL 09B

To the user, the most visible feature of the Transportable Applications Executive (TAE) is its very powerful user interface. To the programmer, TAE's user interface, proc concept, standardized interface definitions, and hierarchy search provide a set of tools for rapidly prototyping or developing production software. The 2GCHAS (Second Generation Comprehensive Helicopter Analysis System) project has extended and enhanced these mechanisms, creating a powerful and high productivity programming environment where the 2GCHAS development environment is 2GCHAS itself and where a sustained rate for certified, documented, and tested software above 30 delivered source instructions per programmer day has been achieved. The 2GCHAS environment is not limited to helicopter analysis, but is applicable to other disciplines where software development is important. Author

N87-23163*# Science Applications Research, Lanham, Md.
AN OVERVIEW OF THE CATALOG MANAGER
Frederick M. Irani *In* NASA. Goddard Space Flight Center Sixth Annual Users' Conference Oct. 1986 p 127-152 (For primary document see N87-23156 16-61)
Avail: NTIS HC A11/MF A01 CSCL 09B

The Catalog Manager (CM) is being used at the Goddard Space Flight Center in conjunction with the Land Analysis System (LAS) running under the Transportable Applications Executive (TAE). CM maintains a catalog of file names for all users of the LAS system. The catalog provides a cross-reference between TAE user file names and fully qualified host-file names. It also maintains information about the content and status of each file. A brief history of CM development is given and a description of naming conventions, catalog structure and file attributes, and archive/retrieve capabilities is presented. General user operation and the LAS user scenario are also discussed. M.G.

N87-23164*# National Aeronautics and Space Administration. Goddard Space Flight Center, Greenbelt, Md.
DISPLAY MANAGEMENT SUBSYSTEM, VERSION 1: A USER'S EYE VIEW
Dolores Parker *In its* Sixth Annual Users' Conference Oct. 1986 p 153-166 (For primary document see N87-23156 16-61)
Avail: NTIS HC A11/MF A01 CSCL 09B

The structure and application functions of the Display Management Subsystem (DMS) are described. The DMS, a subsystem of the Transportable Applications Executive (TAE), was designed to provide a device-independent interface for an image processing and display environment. The system is callable by C and FORTRAN applications, portable to accommodate different image analysis terminals, and easily expandable to meet local needs. Generic applications are also available for performing many image processing tasks. M.G.

N87-23165*# Imperial Coll. of Science and Technology, London (England). Atmospheric Physics Group.
RATIONALIZING VICAR WITHIN A TAE FRAMEWORK: SOME PROBLEMS AND SOME SOLUTIONS
Colin P. Harris *In* NASA. Goddard Space Flight Center Sixth Annual Users' Conference Oct. 1986 p 169-178 (For primary document see N87-23156 16-61)
Avail: NTIS HC A11/MF A01 CSCL 09B

Transportable Applications Executive (TAE) implementation may impose a strain on centers with modest resources. This may be eased in a number of ways. The balance of a small number of expert users and a large number of computing novices at the Interactive Planetary Image-Processing System (IPIPS) imposes special constraints. Some solutions to these and other particular problems are described. Author

N87-23166*# Washington Univ., Seattle. Dept. of Electrical Engineering.
POTENTIAL MEDICAL APPLICATIONS OF TAE
J. Ben Fahy, Robert Kaucic, and Yongmin Kim *In* NASA. Goddard Space Flight Center Sixth Annual Users' Conference Oct. 1986 p 179-192 (For primary document see N87-23156 16-61)
Avail: NTIS HC A11/MF A01 CSCL 09B

In cooperation with scientists in the University of Washington Medical School, a microcomputer-based image processing system for quantitative microscopy, called DMD1 (Digital Microdensitometer 1) was constructed. In order to make DMD1 transportable to different hosts and image processors, we have been investigating the possibility of rewriting the lower level portions of DMD1 software using Transportable Applications Executive (TAE) libraries and subsystems. If successful, we hope to produce a newer version of DMD1, called DMD2, running on an IBM PC/AT under the SCO XENIX System 5 operating system, using any of seven target image processors available in our laboratory. Following this implementation, copies of the system will be transferred to other laboratories with biomedical imaging applications. By integrating those applications into DMD2, we hope to eventually expand our system into a low-cost general purpose biomedical imaging workstation. This workstation will be useful not only as a self-contained instrument for clinical or research applications, but also as part of a large scale Digital Imaging Network and Picture Archiving and Communication System, (DIN/PACS). Widespread application of these TAE-based image processing and analysis systems should facilitate software exchange and scientific cooperation not only within the medical community, but between the medical and remote sensing communities as well. Author

N87-23167*# Global Imaging, Inc., Solana Beach, Calif.
NAVAL APPLICATIONS OF A TAE-DERIVED EXECUTIVE
Michael Guberek, Stephen Borders, and Serge Masse *In* NASA. Goddard Space Flight Center Sixth Annual Users' Conference Oct. 1986 p 193-196 (For primary document see N87-23156 16-61)
Avail: NTIS HC A11/MF A01 CSCL 09B

Global Imaging introduced an interactive image processing system in 1985, featuring the Global Applications Executive (GAE) which is a modified Transportable Applications Executive (TAE) environment. The executive plus a large variety of image processing functions, known commercially as the System 9000, are designed to operate on the Hewlett-Packard as its standard desktop computer (NSDTC), the System 9000 has found easy acceptance for Naval image processing applications. The Department of Oceanography at the Naval Academy, Annapolis, Maryland, has installed an NSDTC with an image processing upgrade. This interactive digital image processing workstation is used by the midshipmen and staff for training and research in remote sensing oceanography. The turn-key system provides the capability to process imagery from commonly used Earth observation spacecraft, in conjunction with in situ data sets. The Acoustic Group at the Naval Research Laboratory, Washington, D.C. has acquired its first System 9000 to interactively process ocean acoustic data gathered by shipboard sensors. Finally, the Naval Oceanographic Facility in Bay St. Louis, Mississippi has acquired a System 9000 to provide a second generation Tactical Environmental Support System (TESS 2) prototype with image processing capabilities. This will permit merging of conventional data with polar orbiting spacecraft imagery. A brief description of these applications and the TAE-derived system is presented. M.G.

N87-23168*# National Aeronautics and Space Administration. Goddard Space Flight Center, Greenbelt, Md.
AN OVERVIEW OF THE LAND ANALYSIS SYSTEM (LAS)
Yun-Chi Lu *In its* Sixth Annual Users' Conference Oct. 1986 p 197-210 (For primary document see N87-23156 16-61)
Avail: NTIS HC A11/MF A01 CSCL 09B

An outline covering the history, development methodology, and major hardware/software components of the Land Analysis System (LAS) is presented. System support services including the Transportable Applications Executive (TAE), Catalog Manager, history files, and applications services are briefly described along with the general functional capabilities of the 224 available applications programs. Example interface menus are given and desired enhancements to the LAS system are listed. M.G.

N87-23169*# EROS Data Center, Sioux Falls, S. Dak.
DEVELOPMENT OF LAND ANALYSIS SYSTEM DISPLAY MODULES
Douglas Gordon, Douglas Hollaren, and Laurie Huewe *In* NASA. Goddard Space Flight Center Sixth Annual Users' Conference Oct. 1986 p 211-225 (For primary document see N87-23156 16-61)
Avail: NTIS HC A11/MF A01 CSCL 09B

The Land Analysis System (LAS) display modules were developed to allow a user to interactively display, manipulate, and store image and image related data. To help accomplish this task, these modules utilize the Transportable Applications Executive and the Display Management System software to interact with the user and the display device. The basic characteristics of a display are outlined and some of the major modifications and additions made to the display management software are discussed. Finally, all available LAS display modules are listed along with a short description of each. M.G.

N87-23170# National Bureau of Standards, Gaithersburg, Md. Center for Programming Science and Technology.
PROGRAMMING LANGUAGES FOR KNOWLEDGE-BASED SYSTEMS
J. V. Cugini Feb. 1987 82 p
(PB87-157228; NBS/SP-500/145; LC-86-600602) Avail: HC A05/MF A01; also available SOD HC $4.00 as 003-003-02783-9 CSCL 09B

Knowledge-Based Systems (KBS) represent a new software methodology which can broaden the scope of computer applications. When developing such software at the programming level, symbolic languages offer features to the programmer not provided by traditional procedural languages. The three most widespread symbolic languages are LISP, PROLOG, and OPS5. An abstract model for a basic KBS and associated terminology is described. This provides a framework for evaluation of the languages. There are several critieria by which one may assess the relative merits of these languages for a given knowledge-based application. Some are related to the language's expressiveness for typical KBS techniques, others to the user's requirements. An extensive set of these criteria is discussed, and the languages are evaluated in light of them. GRA

N87-23171# National Bureau of Standards, Gaithersburg, Md. Statistical Engineering Div.
OMNITAB 80: AN INTERPRETIVE SYSTEM FOR STATISTICAL AND NUMERICAL DATA ANLYSIS Final Report
S. T. Peavy, S. G. Bremer, R. N. Varner, and D. Hogben Nov. 1986 357 p
(PB87-172235; NBS/SP-701; LC-86-600589) Avail: HC A16/MF A01: also available SOD HC $17.00 as 003-003-02775-8 CSCL 09B

OMNITAB 80 is a highly integrated, general purpose programming language and statistical software computing system. The system permits the use of a digital computer to perform statistical and numerical data analysis without having any prior knowledge of computers or programming languages. The system responds to simple instructions to obtain accurate results since reliable, varied and sophisticated algorithms for data analysis and manipulation are referenced. It may be used either interactively or in batch mode. OMNITAB 80 has been installed nationally and internationally. It has been written to make it as machine independent as possible. This document describes Version 6.0. Details are presented so that the user can easily find the specific information needed in any instance. Part A is a simple compact introduction to OMNITAB. Part B describes the general and special features of the OMNITAB system. Part C gives explanations, with short examples, for the use of specifc instructions. Part D is a complete alphabetical list of the instructions in the system. GRA

N87-23172# Honeywell, Inc., Bloomington, Minn. Physical Sciences Center.
OPTICAL SYMBOLIC PROCESSOR FOR EXPERT SYSTEM EXECUTION Quarterly Status Report, 1 Dec. 1986 - 28 Feb. 1987
Matthew Derstine 13 Mar. 1987 5 p
(Contract F49620-86-C-0082; ARPA Order 5794; DA Proj. 230-5)
(AD-A179375; AFOSR-87-0461TR; QSR-3) Avail: NTIS HC A02/MF A01 CSCL 09B

The goal of this program is to develop a concept for an optical computer architecture for symbolic computing by defining a computation model of a high level computer language, examining the possible devices for the ultimate construction of a processor, and by defining required optical operations. The major accomplishments (in chronological order) of this quarter include: Definition of Five level hierarchy; Linear Array representation of processor; Node/Network partitioning; Primitive definitions for distributed execution; and Recursion. GRA

N87-23173# Department of Defense, Fort Meade, Md.
PARALLEL GRAPH REDUCTION ON A SUPERCOMPUTER Status Report
R. Michelsen, L. Smith, E. Williams, and B. Yantis 1986 6 p

Presented at the Santa Fe Graph Reduction Workshop, Santa Fe, N. Mex., 1 Oct. 1986 Prepared in cooperation with Los Alamos National Lab., N. Mex.
(Contract W-7405-eng-36)
(DE87-006066; LA-UR-87-673; CONF-8610257-1) Avail: NTIS HC A02/MF A01

An ongoing effort to develop a parallel graph reduction run-time system hosted on a multiprocessor supercomputer is described. This run-time system is presently augmented by the functional language compiler of the ALFALFA system. Admittedly, parallel graph reduction is hardly a novel idea. The interesting notion is the provision of a parallel execution environment sufficiently powerful to support development of large prototypical scientific and symbolic codes in a functional language. This will allow the investigation of the functional programming paradigm within these application domains in an empirical fashion. In this paper, we discuss the motivation for the effort, describe the basic elements of the implementation, and provide some preliminary insight distilled from our experience with an initial version of the run-time system. DOE

N87-23174# Lawrence Livermore National Lab., Calif.
READING PATTERNS IN ONLINE DOCUMENTATION: HOW TRANSCRIPT ANALYSIS REFLECTS TEXT DESIGN, SOFTWARE CONSTRAINTS, AND USER PREFERENCES
T. R. Girill, C. H. Luk, and S. Norton Feb. 1987 6 p Presented at the 34th International Technical Communication Conference, Denver, Colo., 10 May 1987
(Contract W-7405-eng-48)
(DE87-006466; UCRL-96188; CONF-870538-4) Avail: NTIS HC A02

Text design and text-delivery software together influence the effectiveness of online computer documentation. To explore this relationship, we analyzed transcripts for a typical month of sessions in which users of a supercomputer network consulted online documentation by means of very flexible software. We found that most readers displayed relatively small passages from single documents, often checking a subject index to select those passages. This strong reference-reading pattern confirms and clarifies results from other, more limited studies of online text use. The reference pattern appears even stronger when users accessed task-oriented documents that included many examples. DOE

N87-23175# Lawrence Livermore National Lab., Calif.
PATTERNS FROM MODELS OF DISSIPATIVE SYSTEMS
P. Keller and M. Duong-van Feb. 1987 4 p Presented at the International Conference on Physics of Chaos and Systems Far From Equilibrium, Monterey, Calif., 11 Jan. 1987
(Contract W-7405-eng-48)
(DE87-006823; UCRL-96070; CONF-870159-1) Avail: NTIS HC A02/MF A01

We use various computer graphics techniques to study complex systems. Computer graphics help us to decide what and how to measure. We use a recursion relationship as a way of generating instabilities and turbulence on a two-dimensional lattice. We have been successful in recovering many patterns observed in recent experiments, and mathematical analyses of some experiments also corroborate the mathematical analyses of some of our pictures. DOE

N87-23176# Argonne National Lab., Ill.
FORMAL MODELING AND ANALYSIS OF FAULT-TOLERANCE PROPERTIES FOR SOFTWARE
G. H. Chisholm, J. Kljaich, B. T. Smith, and A. S. Wojcik 1987 16 p Presented at the 9th International Conference on Software Engineering, Boulder, Colo., 30 Mar. 1987 Prepared in cooperation with Michigan State Univ., East Lansing.
(Contract W-31-109-eng-38)
(DE87-007006; CONF-870399-1) Avail: NTIS HC A02/MF A01

This paper describes the application of modeling and analysis techniques to software that is designed to execute on the Charles Stark Draper Laboratory (CSDL) Fault-Tolerant Processor (FTP). The software performs sensor validation of four independent measures (signals) from the Experimental Breeder Reactor-II operated by Argonne National Laboratory. From the validated signals, a flow trip signal is formulated for the reactor safety system. We demonstrate that previously developed modeling and analysis techniques apply to proving the fault-tolerance of the software in the hardware, provided the validation algorithms DOE

N87-23177# University of Southern California, Redondo Beach. Behavioral Technology Labs.
RESEARCH ON COMPUTER AIDED DESIGN FOR MAINTAINABILITY Technical Report, Jun. 1980 - Oct. 1986
Douglas M. Towne and Mark C. Johnson 28 Feb. 1987 69 p
(Contract N00014-80-C-0493; RF5-7525)
(AD-A178460; TR-109-ONR) Avail: NTIS HC A04/MF A01 CSCL 09B

The objective of this research was to investigate methods for measuring and predicting equipment maintainability as a consequence of internal structure and the design of the man-machine interface. A computer-based technique has been developed for projecting maintenance workload which is sensitive to design characteristics such as selection for test points and from panel indicators, modularization, internal system architecture and circuitry, and physical packaging of the hardware. The report summarizes the operation of the performance model which generates projected diagnostic sequences for sample failures; it presents a complete example of a maintainability analysis of a system; and it discusses the current application of the technique within an intelligent tutoring system. GRA

N87-23178# Rensselaer Polytechnic Inst., Troy, N.Y. School of Management.
ROBUST DATA ANALYSIS BASED ON CHARACTERISTIC FUNCTIONS
A. S. Paulson 1986 28 p
(Contract DAAG29-81-K-0110)
(AD-A178544; WP-37-86-P22; ARO-18072.18-MA) Avail: NTIS HC A03/MF A01 CSCL 12A

Simultaneous estimators of location and scale parameters of a Gaussian population are obtained from an analog to weighted least squares by placing the sample characteristic function and the population characteristic function in the role of observed and expected quantities. The advantage to such a scheme is that the error and structural model play a direct role in the analysis. The analog to the usual sum of squares, the sum of moduli squared, then depends on a nonstochastic nuisance variable u. Removal of the nuisance variable is effected by integration over u. A simulation study provides some small sample properties of the location and scale estimators. An example showing the potential for complementing response surface methodology is provided. GRA

N87-23179# Rensselaer Polytechnic Inst., Troy, N.Y. School of Management.
AN ALGORITHM FOR THE COMPUTATION OF GENERALIZED LIKELIHOOD OR SELF-CRITICAL ESTIMATORS FOR BINARY DATA
T. A. Delahanty and A. S. Paulson 1986 41 p
(Contract DAAG29-81-K-0110)
(AD-A178545; WP-37-86-P26; ARO-18072.20-MA) Avail: NTIS HC A03/MF A01 CSCL 09B

This paper describes the computational algorithms for computing generalized likelihood estimators for parametric proportional hazards models. Subroutine BINARY is an implementation of the self-critical estimation procedure of Paulson, Pressor and Lawrence (1983). The logistic, Gaussian or Type 1 extreme value distribution may be selected as tolerance distribution. Estimates are expressed in location-scale form on entry and exit, but results may be printed out in regression form, location-scale form, or in both forms. It is possible to hold location parameters constant during the estimation procedure. Estimation is accomplished by a Newton-Raphson method. GRA

N87-23180# Air Force Inst. of Tech., Wright-Patterson AFB, Ohio. School of Engineering.

THE GRAPHICAL KERNEL SYSTEM: A STANDARDS IMPLEMENTATION M.S. Thesis

Michael W. Denny Dec. 1986 134 p

(AD-A178583; AFIT/GCS/ENG/86D-19) Avail: NTIS HC A07/MF A01 CSCL 09B

A subset of the Graphical Kernel System (GKS) is implemented to provide a device independent graphics application development environment. The host development system consists of an Intel 310 microcomputer operating under XENIX with C as the development language. The major input and output functions of a level Oa GKS implementation are supported. The requirement for device independence, portability, and system extensibility were met through the development of a well structured, modular system. A centralized device control structure was established allowing quick and simple upgrades. A graphical modelling environment providing hierarchically-structured, object-oriented operations and metafile archiving capability was postulated. This modelling environment was developed as a specific application for this GKS implementation; however, it could be modified to work with any system supporting interactive graphics. This GKS implementation and proposed modelling environment serves as an effective base for development of future implementations. More advanced graphics systems in concert with the evolution of graphical standards can be developed and integrated by using some of these implementation techniques. GRA

N87-23181# Air Force Inst. of Tech., Wright-Patterson AFB, Ohio. School of Engineering.

AUTOMATIC SCENE ANALYSIS USING HIERARCHICAL SPATIAL FREQUENCY DOMAIN CORRELATION WITH ENERGY NORMALIZATION AND HEURISTIC NOISE REDUCTION M.S. Thesis

Eugene F. Kelly Oct. 1986 133 p

(AD-A178589; AFIT/GCS/ENG/86D-8) Avail: NTIS HC A07/MF A01 CSCL 05H

Described is the development of software to perform automatic scene analysis using a correlation process. The scene analysis software is designed to locate a given target within a scene image. The operation of the scene analysis software proceeds in a hierarchical manner. The original scene undergoes analysis and sub-sections of the original scene are further evaluated as appropriate. To improve the accuracy of the correlation software, two preprocessing techniques were programmed and tested. The first technique is one used in earlier research efforts. This technique, edging, proved successful in improving the performance of the correlation software. The second noise-reduction technique, a heuristic technique called the Queen Victoria Method (QVM), was also programmed and tested. The result of tests, although nonconclusive, indicates that the QVM does not improve the results of the correlation process. GRA

N87-23182# Air Force Inst. of Tech., Wright-Patterson AFB, Ohio. School of Engineering.

A GRAPHICS ENVIRONMENT SUPPORTING THE RAPID PROTOTYPING OF PICTORIAL COCKPIT DISPLAYS M.S. Thesis

Alan J. Braaten Dec. 1986 168 p

(AD-A178636; AFIT/GCS/MA/86D-1) Avail: NTIS HC A08/MF A01 CSCL 09B

Attention was focused on the interactive construction of pictorial type cockpit displays from libraries of cockpit displays and symbology. Implementation was based on an object-oriented programming paradigm. This approach provided a natural and consistent means of mapping abstract design specifications into functional software. Implementation was supported by an object-oriented extension to the C programming language. Although this investigation addressed a specific application, the resulting graphic environment is applicable to other areas requiring the rapid prototyping of pictorial displays. Author (GRA)

N87-23183# Air Force Inst. of Tech., Wright-Patterson AFB, Ohio. School of Engineering.

DEVELOPMENT OF AN IMAGE ANALYSIS PROGRAM FOR THE IBM PC/XT/AT M.S. Thesis

Richard W. Kroll Dec. 1986 191 p

(AD-A178644; AFIT/GE/ENG/86D-25) Avail: NTIS HC A09/MF A01 CSCL 09B

Development of an image analysis environment for an IBM PC suitable for experimentation and prototyping in areas of pattern recognition and human visual system understanding was explored. Requirements for the spatial Fourier transform and its inverse, correlation, histogram, and spatial and frequency filtering, with a variety of graphic displays are established. An image analysis environment is formed by using the analysis functions and operations as primitive functions of a higher level language. Turbo Pascal was used as the development language because of its user friendly environment and fast compiler. Program size restrictions were eliminated by use of virtual arrays provided in the Turbo Extender package from TurboPower Software. Additional graphics capabilities were obtained with MetaWINDOR from MetaGraphics Software Corp. Only the frequency analysis, display picture, and print picture sections were completed. The completed portion of the program makes extensive use of graphics to create pop-up menus and windows that combine picture displays and graphs for maximum flexibility. As an operational system Turbo Pascal is not suitable. Virtual arrays which eliminate the 64KB memory restriction have very slow access. Completion of this program in another dialect of Pascal without the size restriction should result in a usable environment. GRA

N87-23184# Carnegie-Mellon Univ., Pittsburgh, Pa. Software Engineering Inst.

SUMMARY OF THE SEI (SOFTWARE ENGINEERING INSTITUTE) WORKSHOP ON SOFTWEAR CONFIGURATION MANAGEMENT

Katherine E. Harvey Dec. 1986 14 p Workshop held in Pittsburgh, Pa., 16 Jul. 1986

(AD-A178770; CMU/SEI-86-TR-5; ESD-TR-86-209) Avail: NTIS HC A02/MF A01 CSCL 09B

It is apparent to me that Software Configuration Management (SCM) courses are essential to progress within Software Engineering today. SCM is tied to every stage of software product development. A good configuration management team could make the difference between products coming in on time and within cost, and those coming in late, full of bugs, and with greater costs. Education seems to be the place to start, but there seems to be much more involved than classroom development alone. What the group tried to do was begin a program that would teach software engineers that they need to learn the concepts of Software Configuration Management wherever that education may be available (whether learning in the classroom or gaining experience in the field). It is concluded that what seems to be wrong in Software Configuration Management today is that too many software engineers don't seem to think they are missing much without a solid knowledge of SCM. If they can be shown the importance of SCM, then perhaps they will be more eager to learn its concepts and to use it more often and more effectively. GRA

N87-23185# Carnegie-Mellon Univ., Pittsburgh, Pa. Software Engineering Inst.

THE HETEROGENEOUS MACHINE SIMULATOR Final Report

Robert G. Stockton Dec. 1986 23 p

(Contracts F33615-84-K-1520; ARPA Order 4976)

(AD-A178771; CMU/SEI-86-TR-6; ESD-TR-86-212) Avail: NTIS HC A02/MF A01 CSCL 09B

The heterogeneous machine simulator is a program which attempts to simulate the proposed hardware for the heterogeneous machine at a high level, along with the low level programming abstractions which have been proposed. This will, hopefully, provide: (1) a reasonable basis for programmers to evaluate application designs in the absence of the actual machine; and (2) a testbed for designers to experiment with various reconfigurations which might be difficult to perform on the machine itself. This document presents a basic description of the system and an example of how a simulation may be run. GRA

N87-23186# New York Univ., New York. Inst. of Mathematical Sciences.

CUSTOM-MADE PYRAMIDS

Shmuel Peleg, Orna Federbusch, and Robert A. Hummel Nov. 1986 22 p Sponsored in part by the Israel Academy of Sciences
(Contract N00014-85-K-0077)
(AD-A178955; TR-255; ROBOTICS-85) Avail: NTIS HC A02/MF A01 CSCL 09B

Pyramids are data structures used to store and process images at multiple levels of resolution. The bottom level of a pyramid is used to represent data at a fine level of resolution, while higher levels of the pyramid are used for data stored at coarser levels of resolution. For example, in the Gaussian pyramid data structure, each successive level is obtained by local averaging and subsampling of the immediately lower level in the pyramid. In nearly all pyramid implementations to date, the size reduction in each dimension between levels of the pyramid is a constant factor of two. This paper describes a scheme that permits construction of pyramids with arbitrary size reductions between levels. The reduction factors can be different in each dimension, and differ between levels, to adapt to a given application. The user can thus specify a sequence of decreasing rectangular image sizes, and construct pyramids conforming to those sizes. Further, the reduction factors can be made adaptive to region properties, enabling smooth regions to be reduced more than busy regions. GRA

N87-23187# Air Force Inst. of Tech., Wright-Patterson AFB, Ohio. School of Engineering.

DESIGN OF FAULT TOLERANT PRIME FACTOR ALGORITHM ARRAY ELEMENTS M.S. Thesis

Gary D. Hedrick Dec. 1986 83 p
(AD-A178977; AFIT/GE/ENG/86D-45) Avail: NTIS HC A05/MF A01 CSCL 09B

The calculation of the discrete Fourier transform (DFT) has long been a significant bottleneck in many Digital Signal Processing applications. This thesis contributes to the goal of implementing a very large-scale integrated (VLSI) circuit which uses the Winograd and Good-Thomas algorithms for computing DFTs with composite blocklengths. Winograd processors use both the small and large Winograd algorithms to compute DFTs with blocklengths of 15, 16, and 17. Longer blocklength DFTs (240, 255, 272, and 4080 are computed using a pipeline of Winograd processors, dual-port memories, and a controller. The pipeline used the Good-Thomas Prime Factor Algorithm. Fault tolerance was enhanced by the use of watchdog processors to provide concurrent fault detection and error control coding to provide fault masking. A pipeline controller was designed as a Reduced Instruction Set Computer to control the pipeline and regulate the flow of data. Also, a dual ported, double buffered random access memory was designed to provide intra-pipeline data storage. GRA

N87-23188# Michigan Univ., Ann Arbor. Technical Communication Program.

A DEVELOPMENT SYSTEM FOR AUGMENTED TRANSITION NETWORK GRAMMARS AND A LARGE GRAMMAR FOR TECHNICAL PROSE

John Mayer and David E. Kieras 15 Mar. 1987 48 p
(Contract N00014-85-K-0385; RR0-4206)
(AD-A179009; TR-87/ONR-25) Avail: NTIS HC A03/MF A01 CSCL 05G

This report is in two major sections. The first presents a High-Level Grammer Specification Language (HGSL) which greatly simplifies the development of a complex augmented transition network grammar (ATN). A compiler converts HGSL expressions into a transition network which a simple interpreter uses for parsing. The algorithms used by the compiler and interpreter are presented. The second section presents the HGSL for a large grammar for technical prose. The grammar was developed to allow parsing of technical training materials in the draft stage of writing, as part of a computer-based comprehensible writing aid. Some results on the coverage of the grammar are presented to show that the grammer is close to being practically useful. GRA

N87-23189*# National Aeronautics and Space Administration. Goddard Space Flight Center, Greenbelt, Md.

MEASURING SOFTWARE DESIGN

Nov. 1986 77 p
(NASA-TM-89372; SEL-86-005; NAS 1.15:89372) Avail: NTIS HC A05/MF A01; single copies available from NASA/GSFC, Code 552, Greenbelt, Md. 20771 CSCL 09B

An extensive series of studies of software design measures conducted by the Software Engineering Laboratory is described. Included are the objectives and results of the studies, the method used to perform the studies, and the problems encountered. The document should be useful to researchers planning similar studies as well as to managers and designers concerned with applying quantitative design measures. Author

N87-23190*# National Aeronautics and Space Administration. Goddard Space Flight Center, Greenbelt, Md.

GENERAL OBJECT-ORIENTED SOFTWARE DEVELOPMENT

Edwin V. Seidewitz and Mike Stark Aug. 1986 97 p
(NASA-TM-89375; SEL-86-002; NAS 1.15:89375) Avail: NTIS HC A05/MF A01; single copies available from NASA/GSFC, Code 552, Greenbelt, Md. 20771 CSCL 09B

Object-oriented design techniques are gaining increasing popularity for use with the Ada programming language. A general approach to object-oriented design which synthesizes the principles of previous object-oriented methods into the overall software life-cycle, providing transitions from specification to design and from design to code. It therefore provides the basis for a general object-oriented development methodology. Author

N87-23191*# National Aeronautics and Space Administration. Goddard Space Flight Center, Greenbelt, Md.

Ada STYLE GUIDE (VERSION 1.1)

Edwin V. Seidewitz, William Agresti, Daniel Ferry, David LaVallee, Paul Maresca, Robert Nelson, Kelvin Quimby, Jacob Rosenberg, Daniel Roy, Allyn Shell (Computer Sciences Corp., Greenbelt, Md.) et al. May 1987 106 p
(NASA-TM-89376; SEL-87-002; NAS 1.15:89376) Avail: NTIS HC A06/MF A01; single copies available from NASA/GSFC, Code 552, Greenbelt, Md. 20771 CSCL 09B

Ada is a programming language of considerable expressive power. The Ada Language Reference Manual provides a thorough definition of the language. However, it does not offer sufficient guidance on the appropriate use of Ada's powerful features. For this reason, the Goddard Space Flight Center Ada User's Group has produced this style guide which addresses such program style issues. The guide covers three areas of Ada program style: the structural decomposition of a program; the coding and the use of specific Ada features; and the textural formatting of a program. Author

N87-23192*# National Aeronautics and Space Administration. Goddard Space Flight Center, Greenbelt, Md.

PRODUCT ASSURANCE POLICIES AND PROCEDURES FOR FLIGHT DYNAMICS SOFTWARE DEVELOPMENT

Sandra Perry, Leon Jordan, William Decker, Gerald Page (Computer Sciences Corp., Greenbelt, Md.), Frank E. McGarry, and Jon Valett Mar. 1987 107 p
(NASA-TM-89377; SEL-87-001; NAS 1.15:89377) Avail: NTIS HC A06/MF A01; single copies available from NASA/GSFC, Code 552, Greenbelt, Md. 20771 CSCL 09B

The product assurance policies and procedures necessary to support flight dynamics software development projects for Goddard Space Flight Center are presented. The quality assurance and configuration management methods and tools for each phase of the software development life cycles are described, from requirements analysis through acceptance testing; maintenance and operation are not addressed. Author

N87-23193*# National Aeronautics and Space Administration. Goddard Space Flight Center, Greenbelt, Md.
GUIDELINES FOR APPLYING THE COMPOSITE SPECIFICATION MODEL (CSM)
William Agresti (Computer Sciences Corp., Greenbelt, Md.) Jun. 1987 59 p
(NASA-TM-89374; SEL-87-003; NAS 1.15:89374) Avail: NTIS HC A04/MF A01; single copies available from NASA/GSFC, Code 552, Greenbelt, Md. 20771 CSCL 09B

The Composite Specification Model (CSM) is an approach to representing software requirements. Guidelines are provided for applying CSM and developing each of the three descriptive views of the software: the contextual view, using entities and relationships; the dynamic view, using states and transitions; and the function view, using data flows and processes. Using CSM results in a software specification document, which is outlined. Author

N87-23194*# Computer Sciences Corp., Hampton, Va.
DESCRIPTION OF AN AERONAUTICAL GEOMETRY CONVERSION PACKAGE: WAVE-DRAG TO LANGLEY WIREFRAME GEOMETRY STANDARD (LAWGS) TO SUPERSONIC IMPLICIT MARCHING POTENTIAL (SIMP)
Michael R. Wiese Mar. 1987 42 p
(Contract NAS1-17999)
(NASA-CR-178299; NAS 1.26:178299; TAO-50015) Avail: NTIS HC A03/MF A01 CSCL 09B

Documented is an aeronautical geometry conversion package which translates wave-drag geometry into the Langley Wireframe Geometry Standard (LaWGS) format and then into a format which is used by the Supersonic Implicit Marching Potential (SIMP) program. The programs described were developed by Computer Sciences Corporation for the Advanced Vehicles Division/Advanced Concepts Branch at NASA Langley Research Center. Included also are the input and output from a benchmark test case. Author

N87-22618*# Ohio Univ., Athens. Dept. of Electrical and Computer Engineering.
A PROGRAM DOWNLOADER AND OTHER UTILITY SOFTWARE FOR THE DATAC BUS MONITOR UNIT
Stanley M. Novacki, III *In* NASA. Langley Research Center Joint University Program for Air Transportation Research, 1984 May 1987 p 113-129 (For primary document see N87-22604 16-01)
(OU-TM-92) Avail: NTIS HC A08/MF A01 CSCL 09B

N87-22710*# Engineering Mechanics Association, Inc., Torrance, Calif.
A COMPUTER PROGRAM FOR MODEL VERIFICATION OF DYNAMIC SYSTEMS
J. D. Chrostowski and T. K. Hasselman *In* NASA. Marshall Space Flight Center Structural Dynamics and Control Interaction of Flexible Structures Apr. 1987 p 199-214 (For primary document see N87-22702 16-15)
Avail: NTIS HC A99/MF E03 CSCL 09B

N87-22738*# Boeing Aerospace Co., Seattle, Wash.
HIGH SPEED SIMULATION OF FLEXIBLE MULTIBODY DYNAMICS
A. D. Jacot, R. E. Jones, and C. D. Juengst *In* NASA. Marshall Space Flight Center Structural Dynamics and Control Interaction of Flexible Structures Apr. 1987 p 979-998 (For primary document see N87-22729 16-15)
Avail: NTIS HC A99/MF E03 CSCL 09B

62 COMPUTER SYSTEMS

Includes computer networks and special application computer systems.

N87-23195# California Univ., Berkeley. Dept. of Computer Sciences.
AN EXPERIMENTAL STUDY OF LOAD BALANCING PERFORMANCE Technical Report, 7 Aug. 1984 - 6 Aug. 1987
Songnian Zhou and Domenico Ferrari Jan. 1987 28 p
(Contract N00039-84-C-0089; ARPA Order 4871)
(AD-A179322) Avail: NTIS HC A03/MF A01 CSCL 09B

The design and implementation of a prototype load balancer on a loosely-coupled distributed system are discussed, and the results of a large number of measurement experiments performed on the system under artificial workloads we constructed using frequently executed system commands are presented. The impacts on the system's performance of the load balancing algorithms, as well as of the values of their adjustable parameters, and of the various types of workloads, are evaluated. The effects of load balancing on the performances of individual hosts and on each type of job are also quantitatively investigated using measurements. The results of our study show that automatic load balancing at the job level can have very beneficial effects on the mean and standard deviation of job response times while causing little overhead and requiring no modification to the system kernel or to applications programs. This is the case even when only a relatively small fraction of the jobs can be executed remotely, and the reduction in response time is uniform across all job types, including those that are not moved for execution to another machine. GRA

N87-23196# Air Force Inst. of Tech., Wright-Patterson AFB, Ohio. School of Engineering.
PERFORMANCE EVALUATION OF PARALLEL BRANCH AND BOUND SEARCH WITH THE INTEL IPSC (INTEL PERSONAL SUPERCOMPUTER) HYPERCUBE COMPUTER M.S. Thesis
Richard T. Mraz Dec. 1986 202 p
(AD-A179384; AFIT/GCE/ENG/86D-2) Avail: NTIS HC A10/MF A01 CSCL 09B

With the recent availability of commercial parallel computers, researchers are examining new classes of problems for benefits from parallel processing. This report presents results of an investigation of the set of problems classified as search intensive. The specific problems discussed in this report are the backtracking search method of the N-queens problem and the Least-Cost Branch and Bound search of deadline job scheduling. The object-oriented design methodology was used to map the problem into a parallel solution. While the initial design was good for a prototype, the best performance resulted from fine tuning the algorithms for a specific computer. The experiments of the N-queens and deadline job scheduling included an analysis of the computation time to first solution, the computation time to all solutions, the speed up over a VAX 11/785, and the load balance of the problem when using an Intel Personal SuperComputer(iPSC). The iPSC is a loosely couple multiprocessor system based on a hypercube architecture. Results are presented which compare the performance of the iPSC and VAX 11/785 for these classes of problems. GRA

N87-23197# Stanford Univ., Calif. Dept. of Computer Science.
AN EXPERIMENT IN KNOWLEDGE-BASED SIGNAL UNDERSTANDING USING PARALLEL ARCHITECTURES
Harold D. Brown, Eric Schoen, and Bruce A. Delagi Oct. 1986 42 p
(Contract F30602-85-C-0012)
(AD-A179407; STAN-CS-86-1136) Avail: NTIS HC A03/MF A01 CSCL 17I

Documented is an investigation of the potential of a parallel computing architecture to enhance the performance of a knowledge-based signal understanding system. The experiment consisted of implementing and evaluating an application encoded in a parallel programming extension of LISP and executed on a simulated multiprocessor system. The chosen application for the experiment was a knowledge-based system for interpreting pre-processed, passively acquired radar emissions from aircraft. The application was implemented in an experimental concurrent, asynchronous object-oriented framework. This framework, in turn, relied on the services provided by the underlying hardware system. The hardware system for the experiment was a simulation of various sized grids of processors with inter-processor communication via message-passing. The experiment investigated the effects of various high-level control strategies on the quality of the problem solution, the speedup of the overall system performance as a function of the number of processors in the grid, and some of the issues in implementing and debugging a knowledge-based system on a message-passing multiprocessor system. Author (GRA)

N87-23198# Argonne National Lab., Ill. Mathematics and Computer Science Div.
EXPERIMENTS WITH OR-PARALLEL LOGIC PROGRAMS
T. Disz, E. Lusk, and R. Overbeek Feb. 1987 31 p
(Contract W-31109-eng-38)
(DE87-006882; ANL/MCS-TM-87) Avail: NTIS HC A03/MF A01

We present here the results of several experiments involving OR-parallelism, based on the implementation of a parallel Warren Abstract Machine at Argonne National Laboratory. The experiments illustrate a variety of effects resulting from various types of programs, and raise issues that must be dealt with in any parallel implementation. We also demonstrate a tool for obtaining a visual representation of the parallelism. DOE

N87-23199# Naval Postgraduate School, Monterey, Calif.
JANUS/Ada SOFTWARE IMPLEMENTATION OF A STAR CLUSTER LOCAL AREA NETWORK OF PERSONAL COMPUTERS M.S. Thesis
Thomas V. Works Dec. 1986 158 p
(AD-A178681) Avail: NTIS HC A08/MF A01 CSCL 09B

This thesis describes the detailed design and implementation of a star cluster local area network among multiple Zenith Z-100 microcomputers. The Z-100s are linked together by the Concentrator, a server system consisting of a power supply, an iSBC 86/12A single board computer, and three BLC 8538 eight channel I/O expansion boards, through RS232c USART ports. The local area network software consists of a server program resident in the Concentrator which provides the communication links between the Z-100s and the utility programs resident in each microcomputer. These utilities include file and message transfer (both point to point and broadcast), directory listing transfer, and online user identification. The program and utilities are written in JANUS/Ada, with assembly language sub-routines for machine specific functions, and are designed to run with the CP/M-86 operating system. Author (GRA)

N87-23200# Colorado Univ., Boulder. Dept. of Computer Science.
PARALLEL BRANCH AND BOUND ON AN MIMD (MULTIPLE INSTRUCTION STREAM, MULTIPLE DATA STREAM) SYSTEM
Harry W. Trienekens 16 Feb. 1987 29 p
(Contract DAAG29-84-K-0140)
(AD-A178816; CU-CS-360-87; ARO-21453.8-MA) Avail: NTIS HC A03/MF A01 CSCL 09B

This paper gives a classification of parallel branch and bound algorithms and develops a class of asynchronous branch and bound algorithms for execution on an MIMD system. We develop sufficient conditions to prevent the anomalies that can occur due to the parallelism, the asynchronicity or the nondeterminism, from degrading the performance of the algorithm. Such conditions were known already for the synchronous case. It turns out that these conditions are sufficient for asynchronous alogrithms as well. We also investigate the consequences of nonhomogeneous processing elements in a parallel computer system. We introduce the notions of perfect parallel time and achieved efficiency to empirically measure the effects of parallelism, because the traditional notions of speedup and efficiency are not capable of fully characterizing the actual execution of an asynchronous parallel algorithm. Finally we present some computational results obtained for the symmetric traveling salesman problem. Author (GRA)

N87-23201*# National Aeronautics and Space Administration. Ames Research Center, Moffett Field, Calif.
A STATIC DATA FLOW SIMULATION STUDY AT AMES RESEARCH CENTER
Eric Barszcz and Lauri S. Howard Jun. 1987 23 p Prepared for presentation at the International Conference on Parallel Processing, St. Charles, Ill., 17-21 Aug. 1987
(NASA-TM-89434; A-87129; NAS 1.15:89434) Avail: NTIS HC A02/MF A01 CSCL 09B

Demands in computational power, particularly in the area of computational fluid dynamics (CFD), led NASA Ames Research Center to study advanced computer architectures. One architecture being studied is the static data flow architecture based on research done by Jack B. Dennis at MIT. To improve understanding of this architecture, a static data flow simulator, written in Pascal, has been implemented for use on a Cray X-MP/48. A matrix multiply and a two-dimensional fast Fourier transform (FFT), two algorithms used in CFD work at Ames, have been run on the simulator. Execution times can vary by a factor of more than 2 depending on the partitioning method used to assign instructions to processing elements. Service time for matching tokens has proved to be a major bottleneck. Loop control and array address calculation overhead can double the execution time. The best sustained MFLOPS rates were less than 50% of the maximum capability of the machine. Author

N87-23202*# National Aeronautics and Space Administration. Lewis Research Center, Cleveland, Ohio.
APPLICATIONS AND REQUIREMENTS FOR REAL-TIME SIMULATORS IN GROUND-TEST FACILITIES
Dale J. Arpasi and Richard A. Blech Dec. 1986 26 p
(NASA-TP-2672; E-3189; NAS 1.60:2672) Avail: NTIS HC A03/MF A01 CSCL 09B

This report relates simulator functions and capabilities to the operation of ground test facilities, in general. The potential benefits of having a simulator are described to aid in the selection of desired applications for a specific facility. Configuration options for integrating a simulator into the facility control system are discussed, and a logical approach to configuration selection based on desired applications is presented. The functional and data path requirements to support selected applications and configurations are defined. Finally, practical considerations for implementation (i.e., available hardware and costs) are discussed. Author

63 CYBERNETICS

Includes feedback and control threory, artificial intelligence, robotics and expert systems.

For related information see also *54 Man/System Technology and Life Support.*

N87-23203# Air Force Inst. of Tech., Wright-Patterson AFB, Ohio. School of Engineering.
A PROTOTYPE KNOWLEDGE-BASED SYSTEM TO AID SPACE SYSTEM RESTORATION MANAGEMENT M.S. Thesis
Barbara A. Phillips Dec. 1986 348 p
(AD-A179336; AFIT/GOR/OS/86-12) Avail: NTIS HC A15/MF A01 CSCL 22B

This research effort investigates the application of Artificial Intelligence knowledge-based techniques to the problem of space system restoration management. A prototype decision aid was developed to demonstrate the feasibility of a knowledge-based decision aid capable of assisting the Commander of the US Space Command in maximizing the use of remaining space resources following wartime losses and degradation of space systems. Programmed with the Automated Reasoning Tool (ART), the prototype decision aid generates alternative restoration plans based on the mission priorities specified by the user. To rank the alternative plans by their effectiveness, the prototype uses an objective function which encompasses the multiple objectives of restoring communications, navigation and weather mission capabilities. The prototype decision aid also contains provisions to handle uncertain data and uses a branch and bound pruning algorithm to eliminate inferior partial plans and thereby hasten the solution process. GRA

N87-23204# Air Force Inst. of Tech., Wright-Patterson AFB, Ohio. School of Engineering.
MULTI/INPUT-OUTPUT DESIGNATED EIGENSTRUCTURE (MODES): A COMPUTER-AIDED CONTROL SYSTEM DESIGN PROGRAM M.S. Thesis
Michael E. Hopper Mar. 1987 211 p
(AD-A179341; AFIT/GAE/AA/87M-2) Avail: NTIS HC A10/MF A01 CSCL 12B

The design engineer can specify the closed-loop response of a system, including both the modes and mode shapes, with the eigenstructure assignment approach to system synthesis. This effort was to create an interactive computer-aided control system design program to enable the designer to use the modern control approach to design a control system with specified response characteristics, or to come as close to the ideal as possible. With the program MODES, the design engineer can easily calculate the feedback gains needed to give the controlled system the optimum response characteristics by specifying the desired eigenvalues and eigenvectors. The singular value decomposition is used to accomplish this. GRA

N87-23205# Florida Univ., Gainesville. Dept. of Electrical Engineering.
CONTROL OF LINEAR SYSTEMS OVER COMMUTATIVE NORMED ALGEBRAS WITH APPLICATIONS Final Report, 1 Jul. 1984 - 30 Jun. 1986
Edward W. Kamen Feb. 1987 8 p
(Contract DAAG29-84-K-0081)
(AD-A178765; ARO-20803.7-MA) Avail: NTIS HC A02/MF A01 CSCL 09C

The development of a control theory for various classes of complex linear systems, including systems with time delays, systems with unknown parameters and time-varying systems is discussed. In the case of time delays, we have been able to prove that systems with one or more noncommensurate time delays can always be stabilized using a lumped (finite-dimensional) compensator. In many cases, such as delays in control or delays in measurements, we have developed explicit constructive procedures for designing lumped compensators. In systems with unknown parameters, we have developed an indirect adaptive control scheme that does not require a persistent excitation to achieve global stability. The scheme is based on a new parameter estimation algorithm forcing the estimates of the unknown system parameters to converge to pre-specified intervals. In linear time-varying systems, we have developed a new approach to control based on a type of system augmentation. Via this approach, we have derived a number of results on the existence of canonical forms such as the control canonical form. We have also developed a pole-placement algorthim for time-varying systems. Author (GRA)

N87-23206# Carnegie-Mellon Univ., Pittsburgh, Pa. Software Engineering Inst.
SPECIFYING FUNCTIONAL AND TIMING BEHAVIOR FOR REAL-TIME APPLICATIONS Final Report
Mario R. Barbacci and Jeannette M. Wing Dec. 1986 21 p
(Contracts F33615-84K-1520; ARPA Order 4976)
(AD-A178769; CMU/SEI-86-TR-4; ESD-TR-86-208) Avail: NTIS HC A02/MF A01 CSCL 09B

We present a notation and a methodology for specifying the functional and timing behavior of real-time applications for a heterogeneous machine. In our methodology we build upon well-defined, though isolated, pieces of previous work: Larch and Real Time Logic. In our notation, we strive to keep separate the functional specification from the timing specification so that a task's functionality can be understood independent of its timing behavior. We show that while there is a clean separation of concerns between these two specifications, the semantics of both pieces as well as their combination are simple. GRA

N87-23207# New York Univ., New York. Inst. of Mathematical Sciences.
A STATISTICAL VIEWPOINT ON THE THEORY OF EVIDENCE, REVISION
Robert A. Hummel and Michael S. Landy May 1986 25 p
(Contract N00014-85-K-0077; Grant NSF DCR-84-03300)
(AD-A178958; TR-194-Rev; ROBOTICS-57-Rev) Avail: NTIS HC A02/MF A01 CSCL 09D

This document describes a viewpoint on the Dempster/Shafer Theory of Evidence, and provides an interpretation which regards the combination formulas as statics of the opinions of experts. This is done by introducing spaces with binary operations that are simpler to interpret or simpler to implement than the standard combination formula, and showing that these spaces can be mapped homomorphically onto the Dempster/Shafer theory of evidence space. The experts in the space of opinions of experts combine information in a Bayesian fashion. Presented are alternative spaces for the combination of evidence suggested by this viewpoint. GRA

N87-23208*# National Aeronautics and Space Administration. Langley Research Center, Hampton, Va.
CHANDRASEKHAR EQUATIONS FOR INFINITE DIMENSIONAL SYSTEMS. PART 2: UNBOUNDED INPUT AND OUTPUT CASE Final Report
Kazufumi Ito and Robert K. Powers (Arkansas Univ., Fayetteville.) May 1987 56 p Submitted for publication
(Contracts NAS1-17070; NAS1-18107; Grants NAG1-517; AF-AFOSR-0039-84; AF-AFOSR-0303-85)
(NASA-CR-178303; ICASE-87-32; NAS 1.26:178303) Avail: NTIS HC A04/MF A01 CSCL 09B

A set of equations known as Chandrasekhar equations arising in the linear quadratic optimal control problem is considered. In this paper, we consider the linear time-invariant system defined in Hilbert spaces involving unbounded input and output operators. For a general class of such systems, the Chandrasekhar equations are derived and the existence, uniqueness, and regularity of the results of their solutions established. Author

N87-22621*# Princeton Univ., N. J.
INTELLIGENT FAULT-TOLERANT CONTROLLERS
Chien Y. Huang *In* NASA. Langley Research Center Joint University Program for Air Transportation Research, 1984 May 1987 p 149-160 (For primary document see N87-22604 16-01)
Avail: NTIS HC A08/MF A01 CSCL 09B

64 NUMERICAL ANALYSIS

Includes iteration, difference equations, and numerical approximation.

N87-23209# Illinois Univ., Urbana. Dept. of Computer Science.
DIFFERENTIAL-ALGEBRAIC EQUATION INDEX TRANSFORMATIONS
C. W. Gear Dec. 1986 19 p Presented at the 1st International Conference on Industrial and Applied Mathematics, Paris, France, 1 Jul. 1987
(Contract DE-FG02-87ER-25026)
(DE87-005543; DOE/ER-25026/1; UIUCDCS-R-86-1314; UILU-ENG-86-1780; CONF-870726-1) Avail: NTIS HC A02/MF A01

Techniques are discussed for the reduction of higher index problems of general differential-algebraic equations (DAEs) by differentiation to lower index ones that can be solved numerically while not introducing any constants of integration. Furthermore, we will give transformations between general DAEs and ones in semi-explicit form, and, by these techniques, show how a problem can be reduced to an index 1 semi-explicit form that can be reduced to an implicit differential equation from whose solution the solution to the original problem can be retrieved by at most a differentiation and a linear transformation. DOE

N87-23210# Illinois Univ., Urbana. Dept. of Computer Science.
A METHOD FOR THE SPATIAL DISCRETIZATION OF PARABOLIC EQUATIONS IN ONE SPACE VARIABLE
R. D. Skeel and M. Berzins Feb. 1987 57 p
(Contracts DE-FG02-87ER25026; DE-AC02-76ER-02383)
(DE87-005991; DOE/ER-25026/2; UIUCDCS-R-87-1319; UILU-ENG-87-1705) Avail: NTIS MF A01

The aim of this paper is to describe and analyze a new spatial discretization method for parabolic equations in one space variable. Ordinary and parabolic partial differential equations in one space variable x often have a singularity due to the use of polar cylindrical or spherical coordinates. The method we propose is a simple piecewise nonlinear Galerkin/Petrov-Galerkin method which is second order accurate in space. (It supersedes the method proposed by Skeel). The case $m = 1$ involves the use of the logarithm function, which is probably the only accurate way to model the logarithmic singularity present in the solution. A code based on a variant of the proposed method has already been included as part of the SPRINT package of Berzins, Dew, and Furzeland. The method that we propose here will be distributed in the next release of the D03P (parabolic equations) section of the NAG Library. DOE

N87-23211# Atlanta Univ., Ga. Dept. of Physics.
INVESTIGATION OF PERTURBATION TECHNIQUES FOR NONLINEAR DIFFERENCE EQUATIONS AND OTHER RELATED TOPICS Final Technical Report
R. E. Mickens 29 Oct. 1986 7 p
(Contract DE-AS05-83ER-13123)
(DE87-006663; DOE/ER-13123/3) Avail: NTIS HC A02/MF A01

Investigations in mathematical physics are summarized for projects concerning a nonlinear wave equation; a second-order nonlinear difference equation; singular, nonlinear oscillators; and numerical instabilities. All of the results obtained through these research efforts have been presented in seminars and professional meetings and conferences. Further, all of these results have been published in the scientific literature. A list of references is given in the appendices. DOE

N87-23212# International Centre for Theoretical Physics, Trieste (Italy).
OSCILLATORY BEHAVIOUR OF SOLUTIONS OF FIRST-ORDER ORDINARY AND DELAY DIFFERENTIAL EQUATIONS
N. Parhi Aug. 1986 13 p
(DE87-701552; IC-86/238) Avail: NTIS (US Sales Only) HC A02/MF A01

In this work, sufficient conditions have been obtained for oscillation-non-oscillation of solutions of non-linear non-homogeneous first-order ordinary and delay differential equations. DOE

N87-23213# Catholic Univ. of America, Washington, D.C.
ON NON-PARAMETRIC DISCRIMINATION USING SERIES EXPANSIONS AND PROJECTION PURSUIT Final Report
Lee K. Jones 26 Feb. 1987 24 p
(Contract N00014-84-C-2245)
(AD-A178455) Avail: NTIS HC A02/MF A01 CSCL 17H

This article develops a rigorous non parametric theory of optimal binary discrimination using series expansions. A relationship is presented between minimum scatter and limiting nearest neighbor error rate and its pertinence of optimal discrimination. A general consistency result for series expansions is then given. This motivates a data driven consistent projection pursuit algorithm for constructing an orthonormal basis for discriminant expansions. It is seen for projection pursuit discrimination that limiting nearest neighbor error rate plays an important role as mean squared residual error and relative entropy do in projection pursuit regression and density estimation, respectively. Finally an application to motion detection of optical point sources is given and a numerical experiment is carried out. GRA

N87-23214# Rensselaer Polytechnic Inst., Troy, N.Y. School of Management.
A FAMILY OF ALGORITHMS FOR THE ESTIMATION OF THE PARAMETERS OF THE STABLE LAWS AND THE PARAMETERS OF ATTRACTING STABLE LAWS
T. A. Delehanty and A. S. Paulson 1986 52 p
(Contract DAAG29-81-K-0110)
(AD-A178542; WP-37-86-P34; ARO-18072.25-MA) Avail: NTIS HC A04/MF A01 CSCL 12A

This document presents an iteractive and adaptive algorithm for joint estimation of stable law parameters, using the empirical characteristic function. The algorithm is flexible in that either of two procedures may be selected, and subsets of the parameters may be allowed to vary freely, with others constrained or held constant. The algorithm may also be used to provide informal estimates of the parameters of the law to which a sample distribution is attracted. GRA

N87-23215# Air Force Inst. of Tech., Wright-Patterson AFB, Ohio. School of Engineering.
A PARTIAL DIFFERENTIAL EQUATION MODEL DESCRIBING THE THREAT TO AN AIRCRAFT IN A ONE-ON-MANY SCENARIO M.S. Thesis
Henry G. Birkdale Dec. 1986 100 p
(AD-A178641; AFIT/GOR/MA/86D-2) Avail: NTIS HC A05/MF A01 CSCL 15G

This research investigates the feasibility of describing the threat potential at a point in a specified air defense zone as a function of position and time while stipulating that the function is a solution to a partial differential equation. The mission, the aircraft, and the hostility of the air defense zone are incorporated into the forcing function, as well as the initial and boundary conditions which are needed to solve the partial differential equation. A constant speed and altitude of the aircraft is assumed. In order to validate the partial differential equation used to generate the threat data a scheme for determining the path of least threat through the threat data is proposed. The calculus of variations, a branch of mathematics concerned with the optimization of an integral, is used to find the curve x(t) and y(t) which minimizes the total threat of the flight path. Preliminary results indicate that it does appear feasible to describe the threat as above but further validation is required. GRA

N87-23216# Air Force Inst. of Tech., Wright-Patterson AFB, Ohio. School of Engineering.
LINEAR TIME INVARIANT SYSTEM IDENTIFICATION USING A RESULT OF THE BUSSGANG THEOREM M.S. Thesis
Timothy H. Lewis Dec. 1986 66 p
(AD-A178642; AFIT/GE/ENG/86D-49) Avail: NTIS HC A04/MF A01 CSCL 12A

This investigation applied the Bussgang theorem to the cross correlation method of linear, time invariant (LTI) system identification. In this procedure a Gaussian signal is passed through an LTI system and the output is cross correlated with a nonlinearly distorted version of the original Gaussian signal. If the Gaussian noise were white the correlation would be equal to the impulse response of the LTI system within a constant of proportionality. With the use of bandlimited Gaussian noise this relationship is only approximately satisfied. The analysis compared the performance of the cross-correlation method with the nonlinearity to that of the cross-correlation method without the non linearity. The experimental results indicate that the introduction of the nonlinearity degrades the performance of the method, but this can be improved by correcting for the effects of several quantities associated with the time varying statistics of the Gaussian noise. GRA

N87-23217# Naval Postgraduate School, Monterey, Calif.
A SEPARABLE PIECEWISE LINEAR UPPER BOUND FOR STOCHASTIC LINEAR PROGRAMS

John R. Birge and Stein W. Wallace Feb. 1987 28 p
(AD-A178694; NPS55-67-001) Avail: NTIS HC A03/MF A01
CSCL 12A

Stochastic linear programs require the evaluation of an integral in which the integrand is itself the value of a linear program. This integration is often approximated by discrete distributions that bound the integral from above or below. A difficulty with previous upper bounds is that they generally require a number of function evaluations that grows exponentially in the number of variables. We give a new upper bound that requires operations that only grow polynomially in the number of random variables. We show that this bound is sharp if the function is linear and give computational results to illustrate its performance. GRA

N87-23218# Rensselaer Polytechnic Inst., Troy, N.Y. School of Management.

GOODNESS-OF-FIT BASED ON INTEGRATED SQUARED DISCREPANCIES BETWEEN SAMPLE AND POPULATION CHARACTERISTIC FUNCTIONS

J. L. Bryant and A. S. Paulson 1986 39 p
(Contract DAAG29-81-K-0110)
(AD-A178763; ARO-18072.19-MA) Avail: NTIS HC A03/MF A01 CSCL 12A

This document assesses the feasibility of a goodness-of-fit test based on an integral of the weighted squared modulus of the discrepancy between the sample and population characteristic functions. The resulting statistic is therefore analogous to the Cramer-von Mises statistic and is shown to reduce to it as a special case. A number of properties of the test have been derived, including the asymptotic null distribution of its statistic. It is shown that under mild regularity conditions the test is consistent. A number of approximations to the null distribution of the test statistic are considered, and are found to be successful in simplifying its application without due loss of accuracy. Author (GRA)

N87-23219# Johns Hopkins Univ., Baltimore, Md. Dept. of Electrical Engineering and Computer Science.

CONVERGENCE OF RELAXATION ALGORITHMS BY AVERAGING Interim Report, 1 Jan. - 16 Mar. 1987

Gerard G. Meyer 16 Mar. 1987 13 p
(Grant AF-AFOSR-0097-85)
(AD-A178784; JHU/ECE-87/04) Avail: NTIS HC A02/MF A01
CSCL 12A

Adaptive relaxation algorithms use anti-jamming schemes that require either a large amount of computation or a large amount of memory. This paper presents a non-adaptive approach that possesses substantial computational and memory advantages over the adaptive schemes. The approach uses averaging and may be applied whenever the relaxation algorithm's point-to-set maps satisfy appropriate assumptions. GRA

N87-23220# Rensselaer Polytechnic Inst., Troy, N.Y. School of Management.

SOME ROBUST ESTIMATES OF COVARIANCE STRUCTURE BASED ON PARAMETRIC DENSITY ESTIMATION

A. S. Paulson, T. A. Delehanty, and N. J. Delaney 1987 30 p
(Contract DAAG29-81-K-0110)
(AD-A178806; WP-37-86-P27; ARO-18072.21-MA) Avail: NTIS HC A03/MF A01 CSCL 12A

A new family of Fourier-based estimators of the parameters of the multivariate Gaussian distribution is presented. The estimators are equivalent to parametric density estimators. Three distinct estimators arise, each of which is robust and reduces to the maximum likelihood estimator as a special case. By varying the window width of a parametric density estimator, a set of diagnostics which are useful in problems of outlier detection and clustering are obtained. An example, using a trivariate data set, is given. GRA

N87-23221# Rensselaer Polytechnic Inst., Troy, N.Y. School of Management.

SELF-CRITICAL AND ROBUST PROCEDURES FOR THE ANALYSIS OF BINARY DATA

A. S. Paulson, M. A. Presser, and C. E. Lawrence 1987 74 p
(Contract DAAG29-81-K-0110)
(AD-A178935; WP-37-86-P23; ARO-18072.26-MA) Avail: NTIS HC A04/MF A01 CSCL 12A

A new and general method for the critical analysis of binary data is given. Since the method invokes a memory of the distributions and structural model assumed in the processing of the data it is termed self-critical. A single parameter c generates a family of critical estimator - and tests of hypotheses, if warranted. When $c=0$, the procedure reduces to that of maximum likelihood. The method is derived from primitive considerations exactly parallel to those which result in critical methods for complete data. Both symmetric and asymmetric quantal distributions are considered for regression-type models. A critical procedure for the proportional hazards model, an alternative to the logistic regression model, is introduced and successfully applied. Asymptotic results are given. Experience with live data is reported in the examples. GRA

N87-23222# New York Univ., New York. Inst. of Mathematical Sciences.

THE SCALE-SPACE FORMULATION OF PYRAMID DATA STRUCTURES

Robert A. Hummel Aug. 1986 17 p
(Contract N00014-85-K-0077; Grant NSF DCR-84-03300)
(AD-A178960; TR-239; ROBOTICS-77) Avail: NTIS HC A02/MF A01 CSCL 09D

Pyramid data structures for image processing are usually defined using discrete grids and discrete levels. It has proven useful to formulate pyramids in terms of continuous variables. When the level of the pyramid is changed to be a continuous variable, we talk of the resulting domain as scale-space. When both the image domain and level are treated as continuous, the resulting pyramid structures are most naturally viewed in terms of partial differential equations governing their formation. This viewpoint allows one to generalize new kinds of pyramid data structures, analyze their information content, and develop rational methods for treating borders and other problems in the discrete construction of pyramids. Author (GRA)

N87-23223# Naval Postgraduate School, Monterey, Calif.

THE POTENTIAL GRADIENT OF A PLANE SOURCE Final Report, Aug. 1985 - Dec. 1986

A. V. Hershey Dec. 1986 23 p
(AD-A178976; NPS012-86-011) Avail: NTIS HC A02/MF A01
CSCL 20D

Direct integration leads to the potential gradient of a rectangular plate. Lines with equal spacing form a grid for integration over the infinite plane. A source distribution is approximated by pattern functions which are centered over each grid point. The pattern functions are based upon the sine quotient function. Fourier analysis replaces integration in physical space with integration in wave number space. The range of integration is limited to lines of finite length in wave number space. The computation of potential gradient is provided by subroutines. GRA

N87-23224# Rensselaer Polytechnic Inst., Troy, N.Y. School of Management.

SOME INTEGRATED SQUARED ERROR PROCEDURES FOR MULTIVARIATE NORMAL DATA

A. S. Paulson, N. J. Delaney, H. L. Hwang, and C. E. Lawrence 1986 45 p
(Contract DAAG29-81-K-0110)
(AD-A178985; ARO-18072.23-MA) Avail: NTIS HC A03/MF A01 CSCL 12A

Two methods of estimation for the parameters of the multivariate normal distribution based on the sample characteristic function are given. These methods are shown to have an equivalent basis in terms of Parzen kernel-like density estimation. The estimators for the mean vector and covariance matrix are dependent on a user-specified parameter. Variation of the user-specified parameter produces a response surface in the parameter estimates and therefore allows for an informal sensitivity analysis of the data with respect to a tentative working model.

The informal sensitivity analysis is intricately related to formal tests of fit of the model. The estimators of mean vector and covariance matrix have desirable robustness properties, are easy to compute and use, are relatively efficient at the multivariate normal, and are useful in identifying potential outliers and inconsistencies in some statistical assumptions. These methods are directly applicable to structured data such as multivariate experimental designs. Several illustrations are provided. GRA

N87-23225# Rensselaer Polytechnic Inst., Troy, N.Y. School of Management.

GOODNESS OF FIT BASED ON INTEGRATED SQUARED ERRORS IN CHARACTERISTIC FUNCTIONS OR DENSITIES

A. S. Paulson, Ho-Ling Hwang, and J. L. Bryant 1986 22 p
(Contract DAAG29-81-K-0110)
(AD-A179027; WP-37-86-P32; ARO-18072.24-MA) Avail: NTIS HC A02/MF A01 CSCL 12A

This paper is concerned mainly with tests of goodness of fit that a random sample x sub 1, x sub 2,..., x sub n is from a completely specified distribution function. The test is based on the integral of the weighted squared modulus of the difference between sample and population characteristic functions. This integral expression is equivalent to the integral of the squared difference between a density and its Parzen kernel estimate. The asymptotic null distribution of the statistic is that of an infinite weighted sum of mutually independent chi squared variates. An approximation to the asymptotic null distribution is given and applied to give the percentage points of a test of fit of p-variate normality. The test of fit is consistent under mild regularity conditions. GRA

N87-23226# Air Force Inst. of Tech., Wright-Patterson AFB, Ohio. School of Engineering.

A MODIFIED GOODNESS-OF-FIT TEST FOR THE LOGNORMAL DISTRIBUTION WITH UNKNOWN SCALE AND LOCATION PARAMETERS M.S. Thesis

Lynnette T. Whitsel Dec. 1986 105 p
(AD-A179049; AFIT/GOR/MA/86D-6) Avail: NTIS HC A06/MF A01 CSCL 12A

This thesis developed modified goodness-of-fit tests for the three parameter lognormal distribution when the location and scale parameters must be estimated from the sample. The critical values were generated for the Kolmogorov-Smirnov, Anderson-Darling, and Cramer-von Mises goodness-of-fit tests, using the Monte Carlo methods of 5000 repetitions to simulate samples of size 5,10,...,30. The second part of the research also involved a Monte Carlo simulation of 5000 repetitions for sample sizes of 5, 15, and 25. From these observations, the power of the test was determined by counting the number of times the modified goodness-of-fit tests incorrectly accepted null hypothesis that the distribution was lognormally distributed. The data used in this power comparison came from the lognormal distribution (shape = 1.0 and 3.0), Weibull, gamma, beta, exponential, and normal distributions. The third and final phase of research was to determine the functional relationship, in any, between the known shape parameter and the new modified critical values. Author (GRA)

N87-23227# General Electric Co., Schenectady, N.Y. Knolls Atomic Power Lab.

WIELANDT ITERATION AS APPLIED TO THE NODAL EXPANSION METHOD

T. M. Sutton Jun. 1986 13 p Presented at the American Nuclear Society Topical Meeting, Saratoga Springs, N.Y., 17-19 Sep. 1986
(Contract DE-AC-76-SN-00052)
(KAPL-4194) Avail: NTIS HC A02/MF A01

An implementation of Wielandt's method of eigenvalue shifting to accelerate the convergence of Nodal Expansion Method (NEM) reactor calculations is presented. This particular formulation of the method greatly decreases the number of source iterations required for a particular degree of convergence while retaining most of the efficiency of a group-wise solution procedure for the inner iterations. The nature of the NEM equations causes Wielandt's method to behave somewhat differently than when it is applied to the finite difference equations, and this is discussed. Results are presented for well known two and three dimensional benchmark problems. Author

N87-23228# Royal Inst. of Tech., Stockholm (Sweden). Dept. of Numerical Analysis and Computing Science.

THE EXPONENTIAL METHOD

Gustaf Soederlind 1987 14 p
(TRITA-NA-8517) Avail: NTIS HC A02/MF A01

A continuous analog of the power method is presented. The exponential method is a dynamic system with the properties that the solution converges to a unit eigenvector of the matrix corresponding to the eigenvalue with maximum real part. The rate of convergence is determined by the gap between the largest and next largest real parts of the spectrum. Author

N87-23229*# National Aeronautics and Space Administration. Langley Research Center, Hampton, Va.

A SURVEY OF MIXED FINITE ELEMENT METHODS Final Report

F. Brezzi (Consiglio Nazionale delle Ricerche, Pavia, Italy) Mar. 1987 33 p Submitted for publication
(Contract NAS1-18107)
(NASA-CR-178267; ICASE-87-15; NAS 1.26:178267) Avail: NTIS HC A03/MF A01 CSCL 12A

This paper is an introduction to and an overview of mixed finite element methods. It discusses the mixed formulation of certain basic problems in elasticity and hydrodynamics. It also discusses special techniques for solving the discrete problem. Author

N87-23230*# National Aeronautics and Space Administration. Langley Research Center, Hampton, Va.

EFFICIENT IMPLEMENTATION OF ESSENTIALLY NON-OSCILLATORY SHOCK CAPTURING SCHEMES Final Report

Chi-Wang Shu and Stanley Osher (California Univ., Los Angeles.) May 1987 74 p Submitted for publication
(Contract NAS1-18107; Grants NAG1-270; NSF DMS-85-03294; DAAG29-85-K-0190; N00014-86-K-0691)
(NASA-CR-178304; ICASE-87-33; NAS 1.26:178304) Avail: NTIS HC A04/MF A01 CSCL 12A

In the computation of discontinuous solutions of hyperbolic conservation laws, TVD (total-variation-diminishing), TVB (total-variation-bounded) and the recently developed ENO (essentially non-oscillatory) schemes have proven to be very useful. In this paper two improvements are discussed: a simple TVD Runge-Kutta type time discretization, and an ENO construction procedure based on fluxes rather than on cell averages. These improvements simplify the schemes considerably -- especially for multi-dimensional problems or problems with forcing terms. Preliminary numerical results are also given. Author

N87-22719*# Auburn Univ., Ala. Dept. of Electrical Engineering.

IMPROVING STABILITY MARGINS IN DISCRETE-TIME LOG CONTROLLERS

B. Tarik Oranc and Charles L. Phillips *In* NASA. Marshall Space Flight Center Structural Dynamics and Control Interaction of Flexible Structures Apr. 1987 p 417-434 (For primary document see N87-22702 16-15)
Avail: NTIS HC A99/MF E03 CSCL 12A

65 STATISTICS AND PROBABILITY

Includes data sampling and smoothing; Monte Carlo method; and stochastic processes.

N87-23231# Essex Corp., Orlando, Fla.

INVESTIGATION INTO THE USE OF NORMAL AND HALF-NORMAL PLOTS FOR INTERPRETING RESULTS FROM SCREENING EXPERIMENTS Final Report, 25 Apr. 1986 - 25 Apr. 1987

Charles W. Simon 25 Mar. 1987 155 p
(Contract N61339-85-D-0026)
(AD-A179082; EOTR-87-2) Avail: NTIS HC A08/MF A01 CSCL 12A

Daniel, in 1959, proposed the use of half-normal probability plots as a means of interpreting the results from unreplicated factorial experiments. Zahn, in 1975, suggested modifications to Daniel's approach and investigated some operating characteristics of the plots, along with techniques for estimating population sigma from the slope of the standardized contrasts plotted on half-normal probability paper. That work is reviewed here. This project examines some properties and the usefulness of both normal and half-normal probability plots when applied to the interpretation of experiment is to select from a very large number of potentially critical factors and the ones that do have an important effect on the performance of a particular task, so that these may be investigated in depth. GRA

N87-23232# Pennsylvania State Univ., University Park. Dept. of Statistics.
ESTIMATING THE STANDARD ERROR OF ROBUST REGRESSION ESTIMATES
Simon J. Sheather and Thomas P. Hettmansperger Mar. 1987 17 p Prepared in cooperation with Melbourne Univ., Parkville, Australia
(Contract N00014-80-C-0741)
(AD-A179099; TR-70) Avail: NTIS HC A02/MF A01 CSCL 12A

Over the last two decades there has been much interest in the statistical literature in alternative methods to least squares for fitting equations to data. During this time a large number of estimates of regression coefficients have been proposed that are not unduly affected by a small percentage of the data (so-called robust estimates). Although the robustness properties of these estimates have been studied in great detail, little attention has been paid to the problem of estimating the asymptotic covariance matrices of these estimates. Such estimates are necessary if inferences are to be made about the unknown regression parameters. This paper provides a brief description of two popular robust regression estimates, namely-M- and l sub 1 -estimates. It reviews the available methods for estimating the asymptotic covariance matrices of each of these estimates. In the case of M-estimates, it is shown how to use MINITAB to compute the robust estimates along with an estimated of their asymptotic covariance matrix. Finally, the different robust estimates and their estimated covariance matrices are compared via an example. GRA

N87-23233# North Carolina Univ., Chapel Hill. Center for Stochastic Processes.
EXTREME VALUE THEORY FOR SUPREMA OF RANDOM VARIABLES WITH REGULARLY VARYING TAIL PROBABILITIES Technical Report, Sep. 1984 - Aug. 1985
Tailen Hsing Jul. 1986 13 p
(Contract F49620-82-C-0009)
(AD-A179126; TR-140; AFOSR-87-0319TR) Avail: NTIS HC A02/MF A01 CSCL 12A

Extreme value theory concerns the joint tail behavior and related problems of random variables (r.v.'s). Recent emphasis has been the extension of the classical theory, which considers independent and identically distributed (i.i.d.) r.v.'s to the more general setting of stationarity. Progress has been made on topics such as notions of asymptotic independence, general extremal type theorems, studies of related point processes, etc. The author is interested in the extremal properties of stationary sequences whose members are certain functions of identically distributed random variables. In this direction, previous documents investigated moving average sequences under various assumptions. Through the particular structure of the sequences, these studies provided invaluable insights into the theory in general. This paper considers a stationary sequence (X sub j) consisting of the weighted suprema -- instead of sums as in the case of moving average -- of certain i.i.d. r.v.'s whose tail probabilities are regularly varying. A sequence with this structure may be used to model random exchanges and is a useful tool in studying multivariate extreme value theory. GRA

N87-23234# Purdue Univ., West Lafayette, Ind. Dept. of Statistics.
ON THE LEAST FAVORABLE CONFIGURATION OF A SELECTION PROCEDURE BASED ON RANKS
Shanti S. Gupta and Takashi Matsui Jan. 1987 21 p Prepared in cooperation with Dokkyo Univ., Saitama, Japan
(Contract N00014-84-C-0167)
(AD-A178454; TR-87-2) Avail: NTIS HC A02/MF A01 CSCL 12A

The problem of selection of the population with the largest parameter is considered using the subset selection as well as the indifference zone approach for distributions that belong to a location or a scale parameter family. The procedures are based on the sums of combined (Wilcoxon type) ranks and vector (Friedman type) ranks. The least favorable configurations are obtained in an asymptotic framework under certain order relations between the gaps of parameters. The asymptotic theory is based on exact moments of the rank sum statistics. GRA

N87-23235# Purdue Univ., West Lafayette, Ind. Dept. of Statistics.
ON BAYES SELECTION RULES FOR THE BEST EXPONENTIAL POPULATION WITH TYPE-I CENSORED DATA
Shanti S. Gupta and TaChen Liang Feb. 1987 17 p
(Contract N00014-84-C-0167; Grant NSF DMS-86-06964)
(AD-A178472; TR-87-4) Avail: NTIS HC A02/MF A01 CSCL 12A

The problem of selecting the exponential population having the largest mean life among several exponential populations is investigated. A Bayes rule based on type I censored data is derived. A monotone property of the Bayes selection rule is discussed. An early selection rule is also proposed. Finally, an example is presented to illustrate the implementation of these two selection rules. GRA

N87-23236# Rensselaer Polytechnic Inst., Troy, N.Y. School of Management.
ESTIMATION OF THE PARAMETERS OF A MODIFIED COMPOUND POISSON DISTRIBUTION
J. L. Bryant and A. S. Paulson 1986 37 p
(Contract DAAG29-81-K-0110)
(AD-A178540; WP-37-86-P21; ARO-18072.17-MA) Avail: NTIS HC A03/MF A01 CSCL 12A

This paper addresses the problem of estimation of the parameters of the Poisson sum of Gaussian random variables imbedded in a background of Gaussian noise when only realizations of the sum are observable. Cumulant matching, maximum likelihood, and an empirically orthogonalized characteristic function procedures are considered. The characteristic function and the maximum likelihood procedures produce similar results in a simulation study. However, the characteristic function procedure is computationally superior. Conditions under which all procedures are incapable of parameter estimation are discussed. GRA

N87-23237# Rensselaer Polytechnic Inst., Troy, N.Y. School of Management.
A TEST OF GOODNESS OF FIT FOR MULTIVARIATE NORMALITY
A. S. Paulson, P. J. Roohan, H. L. Hwang, and M. Fuller 1986 41 p
(Contract DAAG29-81-K-0110)
(AD-A178543; WP-37-85-P31; ARO-18072.14-MA) Avail: NTIS HC A03/MF A01 CSCL 12A

This paper presents a procedure for testing the composite hypothesis of p-variate normality, 1 less than or = P less than or = 10, when the parameters are estimated from the data. The test is based on the weighted and integrated modulus squared of discrepancies between sample and population characteristic functions. This measure is shown to be equivalent to the integral of the squared difference between a population density and an empirical estimate. Tables of percentage points are provided. The performances of our density-based or characteristic function-based test statistic, the multivariate skewness, the multivariate kurtosis, a multivariate Shapiro-Wilk, a multivariate Cramer-von Mises, and the multivariate-Anderson-Darling test statistic are compared under several alternatives. The density-based omnibus test is shown to be generally better that the competitors examined.

Author (GRA)

N87-23238# Rensselaer Polytechnic Inst., Troy, N.Y. School of Management.

THE APPLICABILITY OF THE STABLE LAWS IN COLLECTIVE RISK THEORY AND PRACTICE

A. S. Paulson, R. V. Deekshit, R. A. Derrig, and G. W. Ulseth 1986 47 p

(Contract DAAG29-81-K-0110)

(AD-A178546; WP-37-86-P28; ARO-18072.22-MA) Avail: NTIS HC A03/MF A01 CSCL 12A

This paper examines the potential applicability of the stable laws to collective risk theory and practice. The applicability is indirect: it centers on the use of a generalized central limit theorem. If partial sums of losses behave in essentially the same way as complete sums of losses, then stable laws will be useful in the collective risk setting; if partial sums of losses do not behave in essentially the same way as complete sums then the stable laws will not only be useful in a a collective risk setting, but may also be misleading. The overall conclusion is that the stable laws generally can be useful in collective risk settings but that they cannot be used universally and non-discriminantly. GRA

N87-23239# Naval Postgraduate School, Monterey, Calif.

PROBLEMS OF IDENTIFICATION

Donald P. Gaver, Patricia A. Jacobs, I. OMuircheartaigh, and A. Meldrum Nov. 1986 45 p

(AD-A178555; NPS55-86-021) Avail: NTIS HC A03/MF A01 CSCL 12A

Several (I in number) observers cooperate to identify the member of a population of items (J in number) transmitting. The observers' measurements of basic item-identifying (known) parameters are error-prone; errors are frequently non-Gaussian (gross-error-prone). Various methods are introduced and studied for combining the observers; observations so as to achieve as high a probability of correct identification as possible. Linear combinations of observations are shown to be less than satisfactory in the environment described. Continuation and generalization of the work is in progress. GRA

N87-23240# Stanford Univ., Calif. Dept. of Operations Research.

SENSITIVITY ANALYSIS FOR STATIONARY PROBABILITIES OF A MARKOV CHAIN

Peter W. Glynn Aug. 1986 19 p

(Contract DAAG29-84-K-0030; Grants NSF ECS-84-04809; NSF DCK-85-09668)

(AD-A178556; TR-14; ARO-20927.17-MA) Avail: NTIS HC A02/MF A01 CSCL 12A

This paper considers the problem of evaluating the sensitivity of a steady state cost alpha (Theta) to underlying uncertainty in a parameter vector 0 governing the probabilistic dynamics of the system under consideration. We show that the gradient grad alpha (Theta) plays a fundamental role in the parametric statistical theory for Markov processes. We then survey numerical methods available for evaluating grad alpha (Theta) and introduce a new Monte Carlo estimator for grad alpha (Theta), which is applicable to Markov processes of substantial generality. GRA

N87-23241# Rensselaer Polytechnic Inst., Troy, N.Y. School of Management.

ESTIMATION OF THE PARAMETERS OF MIXTURES VIA DISTANCE BETWEEN DENSITIES OR CHARACTERISTIC FUNCTIONS

J. L. Bryant and A. S. Paulson 1986 98 p

(Contract DAAG29-81-K-0110)

(AD-A178623; WP-37-86-P19; ARO-18072.15-MA) Avail: NTIS HC A05/MF A01 CSCL 12A

The integrated weighted distance between the sample characteristic function and the assumed characteristic function, or equivalently, the integrated distance between the smoothed assumed density and its kernel-estimate, is shown to be an effective procedure for estimation of mixing proportions and for estimating all parameters of a modified compound Poisson distribution. These procedures are compared against their competitors in terms of efficiency, mean square error, and computational time. The characteristic function-based procedures are generally superior in terms of computation time for each of two types of procedures. The procedure introduced for the modified compound distribution is widely applicable since it is basically nonlinear modified x squared minimum. The role of the sampling interval in estimating the parameters of the modified compound distribution is discussed and recommendations are made. Information matrices associated with this distribution are given for a spectrum of parameter values. GRA

N87-23242# Ohio State Univ., Columbus.

A BAYESIAN STATISTICS YEAR AT THE OHIO STATE UNIVERSITY Final Report, 24 Feb. - 23 Aug. 1986

Prem K. Goel and Mark Berliner Feb. 1987 16 p Presented at Columbus, Ohio, 18-19 May 1986

(Grant DAAL03-86-G-0074)

(AD-A178762; ARO-23568.1-MA-CF) Avail: NTIS HC A02/MF A01 CSCL 12A

The workshop featured eleven talks concerning various issues and applications of computational Bayesian analysis. All presentations were followed by informal, often lively, discussions. In the spirit of a workshop atmosphere, a two hour working lunch was devoted to an open forum on Bayesian computing. The issues raised focused on which computing environments are desirable for Bayesian statistical analyses, and what are the potentials for a Bayesian software package. In the beginning, there was division of opinions about suitable environment for interactive Bayesian analyses and the question of how to start the process. However, an overwhelming majority of participants agreed with the idea that is too early to push for a new statistical package. Instead we should all push for new software to be compatible with a package like S (an AT&T trademark) so that one could use its data handling and graphics capabilities. Furthermore, we should start a Bayesian Bulletin Board which will give news about Bayesian programs as they are developed and a Bayesian Software Data Base which could be accessed via networks popular among academia. This would be done either at Carnegie-Mellon University's Statistics VAX or at The Ohio State University's Math-Stat PYRAMID.

GRA

N87-23243# Rensselaer Polytechnic Inst., Troy, N.Y. School of Management.

THE PERCENTILES OF THE STABLE LAWS

A. S. Paulson, T. A. Delehanty, and K. M. Brothers 1986 111 p

(Contract DAAG29-81-K-0110)

(AD-A179025; ARO-18072.27-MA) Avail: NTIS HC A06/MF A01 CSCL 12A

This document provides tables to five significant figures of the percentiles x sub p, o less than or = p less than or = 1 of the stable distributions for characteristic exponent alpha = .1(.1)1.9, skewness beta = -1(.1)om and p = .0001(.0001).001 (.001).01(.01).99(.001).999(.0001).9999. The percentiles are accurate to all places given. Examples of the use of the table are given. GRA

N87-23244*# National Aeronautics and Space Administration. Langley Research Center, Hampton, Va.

DEVELOPMENT OF CONFIDENCE LIMITS BY PIVOTAL FUNCTIONS FOR ESTIMATING SOFTWARE RELIABILITY

Kelly J. Dotson Jun. 1987 12 p

(NASA-TP-2709; L-16264; NAS 1.60:2709) Avail: NTIS HC A02/MF A01 CSCL 12A

(NASA-TP-2709; L-16264; NAS 1.60:2709) Avail: NTIS HC A02/MF A01 CSCL 12A

The utility of pivotal functions is established for assessing software reliability. Based on the Moranda geometric de-eutrophication model of reliability growth, confidence limits for attained reliability and prediction limits for the time to the next failure are derived using a pivotal function approach. Asymptotic approximations to the confidence and prediction limits are considered and are shown to be inadequate in cases where only a few bugs are found in the software. Departures from the assumed exponentially distributed interfailure times in the model are also investigated. The effect of these departures is discussed relative to restricting the use of the Moranda model. Author

66 SYSTEMS ANALYSIS

Includes mathematical modeling; network analysis; and operations research.

N87-23245# Sandia National Labs., Albuquerque, N. Mex.
A NEW LIHE (LIGHT INITIATED HIGH EXPLOSIVE) TEST CAPABILITY FOR SPHERICAL TARGETS
R. A. Benham 1987 2 p Presented at the Annual SDI Technical Achievements Symposium, Washington, D.C., 1 Mar. 1987
(Contract DE-AC04-76DP-00789)
(DE87-003035; SAND-86-2366C; CONF-870398-1-Summ) Avail: NTIS HC A02/MF A01

A goal of the Defense Nuclear Agency Lethality and Target Hardening (LTH-3) Program is to assess the lethality of the x-ray laser against the SDI threat entourage of boosters, post-boost vehicles (PBVs), reentry vehicles, and defense suppression weapons (DSWs). A principal characteristic of the effects of the x-ray laser on such threats is the delivery of a cosine distributed impulsive load to exposed curved surfaces of the targets. The LTH-3 program is using test and analysis techniques to investigate the structural response of models of typical targets and target components subjected to impulsive flood loads. A new capability for testing spherical targets using Light Initiated High Explosive (LIHE) is the subject of this paper. DOE

N87-23246# Air Force Inst. of Tech., Wright-Patterson AFB, Ohio. School of Engineering.
MANAGING UNCERTAINTY IN EXPERT SYSTEMS: A PROBABILISTIC APPROACH M.S. Thesis
David C. Knue Dec. 1986 120 p
(AD-A178582; AFIT/GOR/MA/86D-5) Avail: NTIS HC A06/MF A01 CSCL 12B

A study of the use of probability to manage uncertainty in expert systems is presented. The study begins with a comprehensive summary of the literature on applying numeric techniques to manage uncertainty in expert systems. In addition to probability, fuzzy sets, certainty factors, and belief functions are addressed. Basic principles and rules of information combination for each technique are discussed. The Lindley scoring rule argument for why probability is mathematically and realistically more sound for managing uncertainty than the nonprobabilistic techniques is reviewed. The issues why using probability is considered to be a hindrance to managing uncertainty in expert systems are also reviewed. A simple expert system is developed using a state of the art expert system building tool called ALTERID. ALTERID is unique in that it unifies logical and probabilistic inference. This simple expert system is used to explore how probability theory can be used to manage the uncertainty in expert systems. The simple ALTERID based expert system is also used to evaluate the aforementioned issues for using probability to manage uncertainty in expert systems. GRA

67 THEORETICAL MATHEMATICS

Includes topology and number theory.

No abstracts in this category.

70 PHYSICS (GENERAL)

For precision time and time interval (PTTI) see *35 Instrumentation and Photography;* for geophysics, astrophysics or solar physics see *46 Geophysics, 90 Astrophysics,* or *92 Solar Physics.*

N87-23247# Wisconsin Univ., Madison.
PROGRAM AND ABSTRACTS OF THE 39TH ANNUAL GASEOUS ELECTRONICS CONFERENCE Final Report
D. W. Heddle, C. C. Lin, L. W. Anderson, Francis A. Sharpton, and M. B. Schulman 1986 194 p Conference held in Madison, Wisc., 7-10 Oct. 1986
(Contract N00014-86-G-0083)
(AD-A178598) Avail: NTIS HC A09/MF A01 CSCL 09C

The Thirty-ninth Gaseous Electronics Conference was held October 7-10, 1986 at the Wisconsin Center on the campus of the University of Wisconsin, Madison. At the conference papers were presented on fundamental processes such as electron collisions, recombination, and attachment, metastable and excited-state energy transfer, photon interactions, ion and neutral collision, distribution functions, transport properties of ions and electrons, and fundamental processes in gas discharge lasers. Papers were also presented on the properties of discharges including papers on corona, glow discharges, arcs, plasma boundary interactions, plasma chemistry, plasma etching, and atmospheric chemistry. This conference provided a strong interaction between researchers in fundamental processes and applied research on gas discharge physics. Two hundred ten reports were presented. GRA

71 ACOUSTICS

Includes sound generation, transmission and attenuation. For noise pollution see *45 Environmental Pollution.*

N87-23248# Westland Helicopters Ltd., Yeovil (England).
ACOUSTIC TESTING OF SIMPLIFIED CABIN BOX, PHASE 1 Final Report
A. W. Rossall Feb. 1986 58 p
(Contract MOD-K/A12/1668)
(RP-698; BR100264; ETN-87-99820) Copyright Avail: NTIS HC A04/MF A01

Acoustic transmission loss and radiation efficiency properties of three different types of skin panels fitted to a simple box shaped framework (plain aluminum, aluminum with stringers, fibrelam) were measured. The plain aluminum skin is superior to the aluminum skin with stringers, which is superior to fibrelam (although doubts are expressed as to the validity and appropriateness of radiation efficiency measurements on a structure such as the box). Data was provided for correlation with SEA predictions, and the box is found to respond in a linear fashion to various levels of input force. ESA

N87-23249# Catholic Univ. of America, Washington, D.C. Dept. of Civil Engineering.
PHASE SPACE METHODS AND PATH INTEGRATION: A MICROSCOPIC APPROACH TO DIRECT AND INVERSE WAVE PROPAGATION Final Report, Nov. 1984 - Nov. 1986
Louis Fishman 5 Feb. 1987 22 p
(Contract DAAG29-85-K-0002)
(AD-A178557; ARO-20910.6-MA) Avail: NTIS HC A02/MF A01 CSCL 20A

This project focuses on the development of new, multidimensional algorithms for direct acoustic propagation and generalized acoustic tomography at the level of the scalar Helmholtz equation. The general aim is the continued detailed development of the ideas originally outlined. Phase space, or microscopic methods, and path (functional) integral representations provide the appropriate framework to extend homogeneous Fourier methods to inhomogeneous environments. The path integrals furnish the principal representation of the Helmholtz propagator and, subsequently, through direct computation, the basis for the direct numerical algorithms. There are two complementary approaches to the analysis and computation of the n-dimensional Helmholtz propagator. GRA

N87-23250# Army Aviation Research and Development Command, Moffett Field, Calif. Aeroflightdynamics Directorate.
PREDICTION OF HIGH-SPEED ROTOR NOISE WITH A KIRCHHOFF FORMULA
Timothy W. Purcell, Roger C. Strawn, and Yung H. Yu 1987 10 p
(AD-A178982) Avail: NTIS HC A02/MF A01 CSCL 20A

A new method has been developed to predict the impulsive noise generated by a transonic rotor blade. The formulation uses a full-potential finite-difference method to obtain the pressure field close to the blade. A Kirchhoff integral formulation is then used to extend these finite difference results into the far field. This Kirchhoff formula, written in a blade-fixed coordinate system, requires initial data across a plane at the sonic radius. This data is provided by the finite-difference solution. Acoustic pressure predictions show excellent agreement with hover experimental data for two hover cases of 0.88 and 0.90 tip Mach number, the latter of which has delocalized transonic flow. These results represent the first successful prediction technique for peak pressure amplitudes using a computational code. GRA

72 ATOMIC AND MOLECULAR PHYSICS

Includes atomic structure, electron properties, and molecular spectra.

N87-23251# Oregon Univ., Eugene. Dept. of Physics.
RELATIVISTIC CALCULATIONS AND MEASUREMENTS OF ENERGIES, AUGER RATES, AND LIFETIMES Final Technical Report, 15 Dec. 1982 - 14 Jan. 1987
B. Crasemann 15 Jan. 1987 12 p
(Contract F49620-85-C-0040)
(AD-A179137; AFOSR-87-0329TR) Avail: NTIS HC A02/MF A01 CSCL 20J

Experimental and theoretical research on atomic inner-shell physics has been performed. Relativistic calculations of energy levels and transition rates have been performed, including configuration interaction and quantum electrodynamic effects. Cross sections for inner-shell ionization by slow protons have been computed relativistically. The dynamics of inner-shell processes has been studied through experiments with synchrotron radiation. Based on resonant scattering theory, a unified theory has been developed that describes resonant Raman processes at threshold, post-collision interaction above threshold, and the traditional two-step excitation-deexcitation model in the high-energy limit. A study of multiphoton multiionization in strong laser fields has been initiated. GRA

73 NUCLEAR AND HIGH-ENERGY PHYSICS

Includes elementary and nuclear particles; and reactor theory.

For space radiation see *93 Space Radiation.*

N87-23252# Argonne National Lab., Ill.
CONSIDERATIONS PERTINENT TO THE DOPPLER EFFECT FOR SPACE REACTORS
R. N. Hwang 1987 7 p Presented at the 4th Symposium on Space Nuclear Power Systems, Albuquerque, N. Mex., 12 Jan. 1987
(Contract W-31109-eng-38)
(DE87-007032; CONF-870102-13) Avail: NTIS HC A02/MF A01

Because of the potential importance of the Doppler effect to the safety considerations of compact fast spectrum reactors for space applications, extensive investigations have been carried out. The purpose of this paper is two-fold. First, the magnitude of the Doppler reactivity of such reactors will be estimated. Secondly, some relevant questions concerning the fundamental nature of the problems will be addressed. In the present study, a generic space reactor design having features of current designs is examined. In R-Z geometry, the reactor consists of 3 core regions which are made of UN with various enrichments mixed in with a W/Re matrix and coolant channels filled with ALi and surrounded by Mo-vessel and beryllium oxide reflector along with external control drums made of BC in the radial direction and accompanied by axial regions. The axial region above the core contains BeO with W/Re structure. The enrichment increases as a function of radius to provide an approximately constant power distribution in the core regions. Hence, the temperature distribution is also expected to be approximately constant in various core regions. The Doppler reactivities will be given for various radial and axial regions. DOE

N87-23253# Aerospace Corp., El Segundo, Calif. Electronics Research Lab.
DOSE ENHANCEMENT EFFECTS IN THE AEROSPACE CORPORATION Co-60 IRRADIATOR
Thomas C. Zietlow 17 Mar. 1987 26 p
(Contract F04701-85-C-0086)
(AD-A178481; TR-0086(6925-07)-6; SD-TR-87-11) Avail: NTIS HC A03/MF A01 CSCL 18F

The magnitude of the low energy component of the radiation energy spectrum inside The Aerospace Corporation Co-60 irradiator has been determined. Thermoluminescent detectors and a specialized ionization gauge were used to verify the usefulness of a lead (0.06) and aluminum (0.03) sample shielding box to harden the Co-60 photon energy spectrum. The area of uniform dose as a function of distance from the Co-60 source inside the irradiator has also been determined. The results suggest two recommendations for use of the irradiator: The Pb/Al box should be used for all irradiated samples where low energy radiation can be a factor, and samples should be placed as close to the source as possible, within the constraints of a homologous radiation field. GRA

N87-23254# Naval Postgraduate School, Monterey, Calif.
FREQUENCY SPECTRUM OF SOFT X-RAY EMISSION FROM TRANSITION RADIATION M.S. Thesis
Seog K. Yoon Dec. 1986 61 p
(AD-A178858) Avail: NTIS HC A04/MF A01 CSCL 07D

The absolute differential production efficiencies from foil stack materials for an electron beam energy of 65 MeV were measured. The spectra shapes and the absolute differential production efficiencies for each of the four foil stacks are well matched by the calculated values. The transition radiation cone was measured using a motor driven detector. The measured apex angle is in agreement with the optimum radiation cone angle. Aluminum bandwidth narrowing associated with K edge absorption was observed. The production intensity was compared with the theoretical prediction and interpreted in terms of absorption and coherence. GRA

N87-23255# Naval Postgraduate School, Monterey, Calif.
ANGULAR DISTRIBUTION OF TRANSITION RADIATION IN THE SOFT X-RAY SPECTRUM M.S. Thesis
Chang H. Yim 18 Dec. 1986 61 p
(AD-A178859) Avail: NTIS HC A04/MF A01 CSCL 07D

The angular distribution of transition radiation has been investigated theoretically and experimentally. The theoretical prediction and the computer graphic analysis are presented in families of plots which illustrate the dependence of the intensity on the emission angle. Although the experimental method used had limited resolution, the optimum cone angles of the X-ray radiation were in agreement with the theoretical values. Problems encountered during the experiment are discussed for continuing work. This work may have several important applications in electron beam diagnostics. These include monitoring of the beam emittance and energy. GRA

74 OPTICS

Includes light phenomena; and optical devices.
For lasers see *36 Lasers and Masers.*

N87-23256# Messerschmitt-Boelkow-Blohm G.m.b.H., Ottobrunn (West Germany). Dynamics Div.
DETERMINING THE KINEMATIC PARAMETERS OF A MOVING IMAGING SENSOR BY PROCESSING SPATIAL AND TEMPORAL INTENSITY CHANGES
Helmut Zinner 1986 32 p Repr. from the Journal of the Optical Society of America, vol. 3, no. 9, 1986 Sponsored by the German Ministry of Defence
(MBB-UA-914/85; ETN-87-99924) Avail: NTIS HC A03/MF A01

A method for extracting information from optical flow is proposed. The approach derives algorithms analytically from the way in which events in the environment affect the image. The method determines the kinematic quantities of a moving observer without computing the optical flow directly. It combines spatial and temporal derivatives of intensity in the projection plane of an imaging sensor connected to the observer. It applies to systems with six degrees of freedom, such as aircraft. Systems with simpler dynamics are treated as a special case. ESA

N87-23257*# Stanford Univ., Calif. Center for Materials Research.
INFRARED FIBER OPTIC MATERIALS Final Technical Report, 1 Jan. 1983 - 31 Dec. 1985
Robert S. Feigelson 21 May 1987 47 p
(Contract NCC-2-22)
(NASA-CR-180604; NAS 1.26:180604; SU-CMR-87-3) Avail: NTIS HC A03/MF A01 CSCL 20F

The development of IR fiber optics for use in astronomical and other space applications is summarized. Candidate materials were sought for use in the 1 to 200 micron and the 200 to 1000 micron wavelength range. Synthesis and optical characterization were carried out on several of these materials in bulk form. And the fabrication of a few materials in single crystal fiber optic form were studied. E.R.

N87-23258# Los Alamos National Lab., N. Mex.
OPTICO-MECHANICAL SCANNING RADIOMETER
I. K. Kupriianov, E. A. Lustberg, N. S. Lapushkin, A. V. Koroleva, and A. D. Galpern 1987 6 p Transl. into ENGLISH from Russian Patent No. 236807 (2 Oct. 1969)
(Contract W-7405-eng-36)
(DE87-007075; LA-tr-87-9) Avail: NTIS HC A02/MF A01

An opto-mechanical scanning radiometer is described. The optical systems (lenses and mirrors) are installed on a rotating drum so that the focal planes of all elements are coincident with the axis of rotation. The sensitive surface of the photodetector is located on the axis of rotation and is coupled to a drive system which displaces it along the axis synchronously with the drum's rotation. The optical systems turn about the axis of rotation in a plane at an angle equal to one-half the field of view of each objective for the purpose of simplification of the scanning mechanism and increasing coordinate reading accuracy. DOE

N87-23259*# National Aeronautics and Space Administration. Pasadena Office, Calif.
CLOSED LOOP FIBER OPTIC ROTATION SENSOR Patent
Willis C. Goss, inventor (to NASA), Bruce R. Youmans, inventor (to NASA), Noble M. Nerheim, inventor (to NASA), and Randall K. Bartman, inventor (to NASA) (Jet Propulsion Lab., California Inst. of Tech., Pasadena) 5 May 1987 12 p Filed 24 Sep. 1985 Supersedes N86-20129 (24 - 10, p 1670)
(NASA-Case-NPO-16558-1-CU; US-Patent-4,662,751; US-Patent-Appl-SN-779744; US-Patent-Class-356-350; US-Patent-Class-250-231-GY) Avail: US Patent and Trademark Office CSCL 20F

An improved optical gyroscope is provided, of the type that passes two light components in opposite directions through an optic fiber coil, and which adds a small variable frequency to one of the light components to cancel the phase shift due to rotation of the coil. The amount of coil rotation from an initial orientation, is accurately determined by combining the two light components, one of which has a slightly increased frequency, to develop beats that each represent a predetermined angle of rotation. The direction of rotation is obtained by combining the two light components on a photodetector, intermittently phase shifting a single light component by 90 deg and comparing the direction of change of photodetector output (+ or -) caused by the 90 deg shift, with the slope (+ or -) of the photodetector output at about the same time, when there is a 90 deg shift.
Official Gazette of the U.S. Patent and Trademark Office

N87-23260# Pennsylvania State Univ., University Park. Dept. of Electrical Engineering.
WHITE-LIGHT OPTICAL INFORMATION PROCESSING AND HOLOGRAPHY Final Report, 15 Feb. 1981 - 14 May 1986
Francis T. Yu 23 Jan. 1987 312 p
(Grants AF-AFOSR-0140-83; AF-AFOSR-0148-81)
(AD-A179489; AFOSR-87-0456TR) Avail: NTIS HC A14/MF A01 CSCL 20F

A report on white-light optical information processing and holography contains the following: Smeared Image Deblurring; Image Subtraction; Visualization of Phase Object; Coherence Requirement; Apparent Transfer Function; Source Encoding and Signal Sampling; Broadband Image Deblurring; Color Image Subtraction; Rainbow Holographic Aberration; Pseudocolor Encoding with Three Primary Colors; Partial Coherent Measurement; Restoration of Out of Focused Color Image; Solar Light Optical Signal Processing; White light Processing with Magnetooptic Device; Measurement of Noise Performance; White Light Fourier Holography; Optical Generation of Speech Spectrogram with White-Light Source; Progress on Archival Color Film Storage; Generating False Color Composites for LANDSAT data; Developed a Low Cost White-Light Processor; White Light Talbot Interferometer; Analysis of Cross Spectral Density Function for White Light Processing; Computer Generated Filters in White Light Processor; Holographic Tomography for 3 D Object Field; Medical Imaging with White Light; Dual Aperture Sampling with Partially Coherent Light; Application of LCTV; and Computer Generated Tricolor Sampling and Application. GRA

N87-23261# Rochester Univ., N. Y. Dept. of Physics and Astronomy.
COLLECTIVE EFFECTS IN INTENSE-FIELD ELECTRODYNAMICS 1981-1986 Final Report, 15 Jun. 1981 - 14 Jun. 1986 14 Jun. 1986
J. H. Eberly 10 Dec. 1986 16 p
(Grant AF-AFOSR-0204-81)
(AD-A179490; AFOSR-87-0494TR) Avail: NTIS HC A02/MF A01 CSCL 07D

Research Objectives were to accumulate evidence for collective and coherent effects in the interaction of optical and near-optical radiation with matter, and to develop a theoretical understanding of these effects that is adequate for predictive modeling. The focus of this effort was on continuum transitions such as atomic ionization, molecular dissociation and broadband transitions in solids, where coherence phenomena are not commonly found. GRA

N87-23262# Stanford Univ., Calif.

WORKSHOP REPORT ON NEW DIRECTIONS IN X-RAY SCATTERING

George Brown, Nancy Kerr DelGrande, ed., Paul Fuoss, John H. Mallett, Richard Pratt, ed., and David Templeton 1 Feb. 1987 47 p Workshop held at Pacific Grove, Calif., 2-5 Apr. 1987 Prepared in cooperation with Lawrence Livermore National Lab., Calif., Bell Labs., Holmdel, N.J., Pittsburgh Univ., Pa. and Lawrence Berkeley Lab., Calif.
(Contract W-7405-eng-48)
(DE87-006305; CONF-870459) Avail: NTIS HC A03/MF A01

Presented is a summary of the Workshop on New Directions in X-Ray Scattering held at the Asilomar Conference Center, Pacific Grove, California, April 2-5, 1985. The report primarily consists of the edited transcript of the final review session of the workshop. It is clear that we are close to achieving an accurate theory of scattering in independent particle approximation, but for edge regions, there is need to go beyond this approach. Much of what is experimentally interesting in scattering is occurring between the photoabsorption edge and the photoelectric threshold. Applications in condensed matter and biological and chemical material studies are expanding, exploiting higher intensity sources and faster time resolution as in magnetic scattering and surface studies. Storage rings are now conventional sources, and new high-intensity beam lines are under development; the free electron laser is one of the more speculative sources. Recent work in x-ray scattering has led to advances in x-ray optics, and conversely, advances in x-ray optics have benefited our understanding of x-ray scattering. DOE

N87-23263# Hughes Aircraft Co., El Segundo, Calif. Display Systems Lab.

DEVELOPMENT OF A HOLOGRAPHIC BEAMSPLITTER FOR USE WITH A CONVENTIONAL FRESNEL LENS

Feb. 1987 48 p Prepared in cooperation with Sandia National Labs., Albuquerque, N. Mex.
(Contract DE-AC04-76DP-00789)
(DE87-006770; SAND-86-7049) Avail: NTIS HC A03/MF A01

A holographic beamsplitter module is designed to be used with Si/1.72 eV AlGaAs cell pairs to achieve enhanced solar efficiencies. The hologram plate, when laminated to a Fresnel lens, was intended to focus less than 1.72 eV radiation onto the Si cell and greater than 1.72 eV radiation onto the AlGaAs cell. The baseline concept for the holographic beamsplitter consisted of two singly exposed volume phase holograms laminated together. Analysis revealed that an ideal beamsplitter would yield 21.1% solar efficiency for series-connected cells. However, it was discovered that the optimum holographic beamsplitter theoretically yielded only 15.6% efficiency for series-connected cells, compared to 16.6% efficiency for a single Si cell. The limited performance was primarily due to the unavoidable rolloff of hologram response with wavelength inherent in singly exposed holograms. Independently connecting the cells and optimizing the AlGaAs band gap were not expected to yield significant improvement in solar efficiency. These results were corroborated by a 1985 West German study, which suggested that flattening the hologram response spectrum by double exposure might yield substantial improvements in solar efficiency. In conclusion, the current holographic technology is not capable of providing a beamsplitter that will significantly improve the solar collection efficiency in Si/AlGaAs systems. DOE

N87-23264# Chicago Univ., Ill.

FUNDAMENTALS AND TECHNIQUES OF NONIMAGING OPTICS RESEARCH AT THE UNIVERSITY OF CHICAGO Technical Progress Report

R. Winston and J. OGallagher Nov. 1986 21 p
(Contract DE-FG02-84ER-13178)
(DE87-006917; DOE/ER-13178/3) Avail: NTIS HC A02/MF A01

Nonimaging Optics differs from conventional approaches in its relaxation of unnecessary constraints on energy transport imposed by the traditional methods for optimizing image formation and its use of more broadly based analytical techniques such as phase space representations of energy flow, radiative transfer analysis, thermodynamic arguments, etc. Based on these means, techniques for designing optical elements which approach and in some cases attain the maximum concentration permitted by the Second Law of Thermodynamics were developed. The most widely known of these devices are the family of Compound Parabolic Concentrators (CPC's) and their variants and the so called Flow-Line concentrator derived from the geometric vector flux formalism developed under this program. Applications of these and other such ideal or near-ideal devices permits increases of typically a factor of four (though in some cases as much as an order of magnitude) in the concentration above that possible with conventional means. In the most recent phase, our efforts can be classed into two main areas; (a) "classical" geometrical nonimaging optics; and (b) logical extensions of nonimaging concepts to the physical optics domain. DOE

N87-23265# EOTec Corp., West Haven, Conn.

DEVELOPMENT OF RADIATION HARD GRADED INDEX OPTICAL FIBERS Final Technical Report, Sep. 1985 - Mar. 1986

Mokhtar S. Maklad Nov. 1986 41 p
(Contract F19628-85-C-0143)
(AD-A178465; RADC-TR-86-182) Avail: NTIS HC A03/MF A01 CSCL 20F

The objective of this investigation is to reduce the optical fiber radiation sensitivity by doping with multivalent elements. Optical fibers, doped with arsenic under different redox conditions were prepared. Arsenic additions under slightly reducing conditions lowered the fiber radiation sensitivity, without influencing the intrinsic optical loss. This observation proved that arsenic can be used to improve optical fiber radiation hardening if optimized processing conditions are used. Further, development effort is needed to determine the effect of different parameters on radiation response. The parameters include, dopants and dopant levels, redox and fiber drawing conditions. GRA

N87-23266# GTE Labs., Inc., Waltham, Mass.

RADIATION HARDENED SILICA-BASED OPTICAL FIBERS Interim Report, Mar. 1985 - Mar. 1986

W. J. Miniscalco, T. Wei, and P. I. Onorato Oct. 1986 51 p
(Contract F19628-85-C-0050)
(AD-A178466; RADC-TR-86-181) Avail: NTIS HC A04/MF A01 CSCL 20F

For the defect passivation approach, we have completed the evaluation of the effects of hydrogen treatment. Considerable reduction in radiation-induced absorption at long wavelengths (lamba greater than 1 micron) has been observed for hydrogen-treated fibers. Posttreatment of irradiated fibers by hydrogen also increases the hardness of the fibers under subsequent irradiation. In addition, we found photoluminescence to be an effective characterization tool which provides additional evidence for the passivating effect of hydrogen treatment. GRA

N87-23267# Rochester Univ., N. Y. Inst. of Optics.

AUTOMATIC PATTERN RECOGNITION AND RELATED TOPICS Final Report, 19 Sep. 1983 - 18 Sep. 1986

Nicholas George Jan. 1987 41 p
(Contract DAAG29-83-K-0166)
(AD-A178595; ARO-21051.13-PH) Avail: NTIS HC A03/MF A01 CSCL 20F

Research in the field of opto-electronic systems research is summarized for the contract period September 1983 to September 1986. The goal has been to contribute solutions to problems of basic research importance which also have an underlying significance in systems for automatic pattern recognition, electronic imaging, and remote sensing. In theoretical and experimental research, excellent progress is reported in five major topic areas. Abstracts of publications and brief overview remarks are included on each of the following subjects: Image Retrieval, Holographic Optical Elements, Transforms in Incoherent Illumination, Diffraction Theory, and Speckle. GRA

N87-23268# Alabama Univ., Huntsville. Dept. of Mechanical Engineering.

APPLICATIONS OF FIBER OPTICS IN EXPERIMENTAL MECHANICS

J. A. Gilbert and T. D. Dudderar 1987 10 p
(Contracts DAAL03-86-K-0014; DAAG29-84-K-0183; Grant DAAG29-84-K-0045)
(AD-A178683; ARO-21671.6-EG; ARO-22148.3-EG; ARO-23573.13-EG) Avail: NTIS HC A02/MF A01 CSCL 20F

Fiber optics provide a powerful new tool for use in experimental mechanics. Applications range from excitation to illumination to detection to information transmission. Interesting examples include applications in holo-interferometry, laser speckle photography, laser Doppler velocimetry, photoelastic spectral analysis and numerous other experimental techniques in which fiber optics may be used to manipulate light. In addition, fiber optics are finding uses in a wide variety of strain, pressure, crack, temperature, displacement and motion sensing transducers. This presentation will review the special characteristics of various types of optical fibers that fit them to these non-communications related roles. A few applications will be described in detail and many others mentioned briefly in order to illustrate the numerous advantages to be realized from the use of fiber optics in experimental mechanics. GRA

N87-23269# Georgia Inst. of Tech., Atlanta. School of Geophysical Sciences.

SIGNATURES FROM IN-SITU LIGHT SCATTERING OF NON-HOMOGENEOUS NON-SPHERICAL PARTICLES Final Technical Report, 1 Jul. 1984 - 31 Jan. 1987

Alessandro Coletti 6 Feb. 1987 70 p
(Contract DAAG29-84-K-0115)
(AD-A178761; ARO-21016.1-GS) Avail: NTIS HC A04/MF A01 CSCL 20F

The research preformed under this program has focused on studying the angular light scattering of monodisperse quasi spherical non homogeneous particles. For that purpose specific laboratory techniques are developed suitable for the generation of these particles and for properly collecting the data. For comparing the measurements with the light scattering theories for spheres and spheroids we have formulated a new kind of algorithm that is innovative in many aspects and has useful application. The method might be advantageous for inversions of physical parameters from experimental data, and for estimating their statistical significance. GRA

N87-23270# Rochester Univ., N. Y. Inst. of Optics.

STATIONARY PHASE APPROXIMATIONS IN FRESNEL-ZONE MAGNITUDE-ONLY RECONSTRUCTIONS

Robert Rolleston and Nicholas George Jan. 1987 8 p
(Contract DAAG29-83-K-0166)
(AD-A178812; ARO-21051.10-PH) Avail: NTIS HC A02/MF A01 CSCL 05H

An analytic approximation of an iterative method of image reconstruction from Fresnel zone magnitude data is discussed. The method of stationary phase is used to estimate both the Fresnel zone transform and the inverse Fresnel zone transform. With this theory we can explain why fewer iterations are needed for good images to be obtained at locations in the Fresnel zone region of an optical processor that are farther from the Fourier transform. GRA

N87-23271# Air Force Inst. of Tech., Wright-Patterson AFB, Ohio. School of Engineering.

TWO-POINT RESOLUTION CRITERION FOR MULTI-APERTURE OPTICAL SYSTEMS M.S. Thesis

Steven M. Watson Mar. 1987 92 p
(AD-A178980; AFIT/GEP/ENP/87M-1) Avail: NTIS HC A05/MF A01 CSCL 20F

Two point resolution criteria is the classic way of comparing telescopes. However, the standard two point resolution criterion is not appropriate for multi-aperture systems. This paper proposes a new two point resolution criterion based on the idea of thresholding the irradiances of the resulting far field diffraction patterns of multi-aperture optical systems. The threshold was defined as a fraction of the central lobe irradiance. The thresholds varied from 0.1 to 0.9 of the central lobe irradiance of the far field diffraction patterns. Theoretical data of normalized irradiance versus point separation for various multi-aperture optical systems were presented. The two point resolution for these configurations was analyzed. The two point resolution criterion using thresholds was demonstrated. The threshold criterion provided the information necessary to compare the two point resolution performance of a particular multi-aperture optical system illuminated coherently and incoherently. Also, this criterion allowed the comparison of the two point resolution performance of systems composed of three, four, and six subapertures illuminated incoherently. GRA

N87-23272# TRW, Inc., Redondo Beach, Calif. Electro Optics Research Center.

ANALOG FIBER OPTIC RECIRCULATING DELAY LINE Final Report, Sep. 1983 - Mar. 1987

Thomas R. Joseph and Alan Jackson 31 Mar. 1987 37 p
(Contract N00014-83-C-2322)
(AD-A179050) Avail: NTIS HC A03/MF A01 CSCL 09A

The goal of this effort was to develop and demonstrate a fiber optic analog recirculating delay line. The wavelength was 1.3 micrometers, and the bandwidth was 1GHz. Transmitters, receivers and the interface amplifiers for two recirculating delay lines were fabricated and tested. Open loop data showed amplitude ripple of less than + or - 15dB. Problems with the diode lasers precluded fully meeting all of the performance goals for the hardware. GRA

N87-23273*# Stanford Univ., Calif. Computer Systems Lab.

CHANNEL ACCESS SCHEMES AND FIBER OPTIC CONFIGURATIONS FOR INTEGRATED-SERVICES LOCAL AREA NETWORKS Ph.D. Thesis

M. Mehdi Nassehi Mar. 1987 162 p Sponsored in part by an IBM Graduate Fellowship
(Grants NAG2-292; NAGw-419)
(NASA-CR-180934; NAS 1.26:180934; CSL-TR-87-322) Avail: NTIS HC A08/MF A01 CSCL 20F

Local Area Networks are in common use for data communications and have enjoyed great success. Recently, there is a growing interest in using a single network to support many applications in addition to traditional data traffic. These additional applications introduce new requirements in terms of volume of traffic and real-time delivery of data which are not met by existing networks. To satisfy these requirements, a high-bandwidth tranmission medium, such as fiber optics, and a distributed channel access scheme for the efficient sharing of the bandwidth among the various applications are needed. As far as the throughput-delay requirements of the various application are concerned, a network structure along with a distributed channel access are proposed which incorporate appropriate scheduling policies for the transmission of outstanding messages on the network. A dynamic scheduling policy was devised which outperforms all existing policies in terms of minimizing the expected cost per message. A broadcast mechanism was devised for the efficient dissemination of all relevant information. Fiber optic technology is considered for the high-bandwidth transmisison medium. B.G.

N87-23377*# Jet Propulsion Lab., California Inst. of Tech., Pasadena.
ASTEROID LIGHTCURVE INVERSION
Steven J. Ostro and Robert Connelly (Cornell Univ., Ithaca, N.Y.) *In* NASA, Washington Reports of Planetary Geology and Geophysics Program, 1986 May 1987 p 90-91 (For primary document see N87-23341 16-91)
Avail: NTIS HC A24/MF A01 CSCL 20F

75 PLASMA PHYSICS

Includes magnetohydrodynamics and plasma fusion.
For ionospheric plasmas see *46 Geophysics*. For space plasmas see *90 Astrophysics*.

N87-23274# Nagoya Univ. (Japan). Inst. of Plasma Physics.
A SYSTEM FOR LONG PULSE REB GENERATION
Tetsuya Tsuzuki, Mitsuru Hasegawa, Kazumichi Narihara, Yukihiro Tomita, Shin Kubo, Tadasuke Kobata (Tokyo Univ., Japan), and Akihiro Mohri Feb. 1987 29 p
(IPPJ-812; ISSN-0469-4732) Avail: NTIS HC A03/MF A01

A high voltage pulse generator system producing intense relativistic electron beams (REB) (1 microsecond pulse width, 30 kA peak current, 1 MeV energy) was developed to the use of REB ring formation. The system consists of a Marx generator, a transmission line with plastics-water hybrid insulators, and a magnetically insulated transmission line connected with a cathode. The system was well operated more than twenty thousand shots without trouble. Author

N87-23275# Massachusetts Inst. of Tech., Cambridge.
NUMERICAL STUDY OF HYBRID PLUME Annual Progress Report, 1 Sep. 1985 - 30 Aug. 1986
F. R. Chang and T. F. Yang 1 Aug. 1986 29 p
(Grant AF-AFOSR-0190-84)
(AD-A179561; AFOSR-87-0524TR) Avail: NTIS HC A03/MF A01 CSCL 21C

The fluid modeling of plasma-gas kinetics including momentum transfer and charge exchange reaction, the study of parametric dependence of ion cyclotron range of frequency heating efficiency, and conceptual design of the tandem mirror plasma source has been accomplished. A preliminary study was carried out by using a much simpler fluid model to investigate the feasibility of the hybrid plume concept. It was demonstrated that the exhaust duct can be protected by a supersonic gas jet from the hot plasma core. The code was expanded to include momentum transfer and recombination reaction. It was found that the ions are cooled down further at the end of the exhaust duct with the inclusion of additional physics properties. Thrust contour can now be calculated. Presently, the steady state fluid model and uniform magnetic field are assumed. A slab model for ion cyclotron range of frequency heating has also been developed. The parametric dependence of the loading resistance of the plasma on the antenna was analyzed. The conceptual design of the plasma rocket was obtained. GRA

N87-23276# Illinois Univ., Urbana. Nuclear Engineering Lab.
OPENING SWITCH RESEARCH ON A DENSE PLASMA FOCUS Final Report, 30 Sep. 1984 - 29 Sep. 1986
G. Gerdin 23 Feb. 1987 72 p
(Grant AF-AFOSR-0391-84)
(AD-A179693; AFOSR-87-0414TR) Avail: NTIS HC A04/MF A01 CSCL 20I

Experiments were performed to enhance power coupling to the load by placing the load electrode opposite the muzzle end of the Dense Plasma Focus plasma gun. The impaler concept, whereby the current sheath is run into a knife edge insulator, was tested in two configurations. However, the power coupled to the load was always less than one tenth that of the experiments where the load was coupled to the breach of the gun. Other load coupling schemes where the load electrode was brought near the outside of the central electrode prevented pinches (voltage surges) when placed too close and the power coupled to the load was reduced when the load electrodes were moved away. The results were not as good as those of the impaler concept. Measurements of the dynamics of the current sheath in various stages were performed and compared with theory. Generally the velocity of the current sheath falls below theoretical expectations suggesting the presence of electrode drag, a phenomenon not present in the model. During the radial collapse phase the model and the experimental estimates of dL/dt are in substantiaL agreement before pinch time but disagree afterward due to two dimensional effects not present in the theory. GRA

N87-23277# Pennsylvania State Univ., University Park.
ANALYSIS OF THE EFFECTS OF IMPURITY BUILDUP ON THE PERFORMANCE OF A REVERSED FIELD PINCH Final Report
E. H. Klevans 30 Oct. 1986 42 p
(Contract DE-FG02-86ER-53219)
(DE87-005438; DOE/ER-53219/1) Avail: NTIS HC A03/MF A01

A Zero-Dimensional code has been developed and used for parametric studies of ZT-40M behavior and the projected behavior of CPRF(ZT-H). The code includes equations for energy balance for electrons and ions. Particle density and current are specified quantities. Impurities are treated using a coronal equilibrium model. The energy confinement times for electrons and ions are permitted through the use of multiplicative coefficients. Ohmic heating includes an anomaly factor, and an experimentally observed ion heating is modeled by use of a multiplicative factor times Ohmic heating. The data from ZT-40M is used to obtain a reasonable set of coefficients, and the effect on T(sub e) and T(sub i) of varying these coefficients is examined. Various levels and kinds of impurities are introduced and their effects are examined. Both flat top and ramp current waveforms are studied. The results are then applied to study a ramp startup of CPRF for a current level of 1 MA. DOE

N87-23278# Washington Univ., Seattle. Dept. of Nuclear Engineering.
CONFINEMENT AND HEATING OF HIGH BETA PLASMAS WITH EMPHASIS ON COMPACT TOROIDS. TASK 2: STELLARATOR AND HELIAC RESEARCH Annual Report, 1 Oct. 1985 - 30 Sep. 1986
F. L. Ribe 31 Dec. 1986 63 p
(Contract DE-AT06-72ET-53047)
(DE87-005554; DOE/ET-53047/25) Avail: NTIS HC A04/MF A01

Progress over the past year has enabled us to complete the comprehensive experimental investigation of the equilibrium and stability of the linear heliac and the linear $l = 1$ stellarator configuration. In the case of the heliac work, we discoverd axisymmetric hot plasma near the axial conductor (hardcore) in amounts which are comparable to the helically symmetric hot plasma centered on the magnetic axis. From this result came the motivation for an extended investigation which concentrates on the details of high-beta heliac formation. Important first results of the formation study have been obtained. In the case of the stellarator work, we have observed the flute-like $m = 1$ instability for a specific set of experimental parameters and, for a different set, we have observed the mode stabilized by the combined effects of a finite ion Larmor radius and a nearby conducting wall. The single-discharge CV ion-temperature diagnostic system has been debugged and has yielded a heliac temperature measurement of (90 + or - 10)eV. The plasma density diagnostic system based on cross-tube interferometry has been modified from its previous design for use with the somewhat wrinkly helical discharge tube. DOE

N87-23279# Rochester Univ., N. Y. Lab. for Laser Energetics.
DIRECT-DRIVE LASER-FUSION IN THE US
R. L. McCrory, J. M. Soures, P. Audebert, O. Barnouin, R. S. Craxton, J. Delettrez, R. Epstein, L. Forsley, R. J. Hutchison, and S. Jacobs 1986 9 p Presented at the IAEA International Conference on Plasma Physics and Controlled Nuclear Fusion Research, Kyoto, Japan, 12 Nov. 1986 Prepared in cooperation

with NRL, Washington, D.C. and IAEA, Vienna, Austria
(Contract DE-FC08-85DP-40200)
(DE87-005916; DOE/DP-40200/31; IAEA-CN-47/B-I-5; CONF-861106-21) Avail: NTIS HC A02/MF A01

Direct-drive experiments at the University of Rochester's Laboratory for Laser Energetics (LLE) and the Naval Research Laboratory (NRL) are presently addressing issues in pellet compression and heating: efficiency of coupling of laser energy to the target and the coupling of absorbed energy to the fuel, drive uniformity, hydrodynamic stability, preheat arising from laser plasma instabilities and X-rays, and target diagnostics. The 24-beam, 2500-Joule, 351 nm OMEGA laser system at LLE has been used in an experimental effort to achieve high compressed DT fuel densities. Detailed hydrodynamic computer simulations at NRL predict that the growth rate of the ablative Rayleigh-Taylor instability is less than the classical values. Recent Rayleigh-Taylor experiments at NRL are testing these predictions. DOE

N87-23280# State Univ. of New York, Buffalo.
PLASMA DIAGNOSIS BY DYE LASER INTRACAVITY ABSORPTION Final Report, 1 Jan. 1982 - 31 May 1986
G. O. Brink May 1986 28 p
(Contract DE-AC02-81ER-53122)
(DE87-006407; DOE/ER-53122/3) Avail: NTIS HC A03/MF A01

Dye laser intracavity absorption (ICA) has been studied as a potential diagnostic for plasma or neutral beam systems. For magnetic field measurements it is necessary to make Zeeman effect measurements on the resonance transition of atomic lithium on a millisecond time scale, or to make motional Stark Effect measurements on an injected fast atomic beam of hydrogen. To do this it may be necessary to sweep the dye laser in wavelength at a rapid rate so that the absorber can be sampled many times during the measurement. We have examined both of these possibilities during this contract. A rather detailed absorption spectrum of molecular hydrogen and deuterium arising in the 2c ^{3}Piu and other electronic states has been obtained and analyzed. This has provided new information on the types of molecular species that may be detected in a plasma by ICA, and may provide a basis for the application of ICA for the diagnosis of the edge plasma in a Tokamak or in the end regions of a mirror machine. DOE

N87-23281# Air Force Inst. of Tech., Wright-Patterson AFB, Ohio. School of Engineering.
DEVELOPMENT OF A GENERALIZED MODEL FOR A THREE COMPONENT PLASMA M.S. Thesis
John C. Lucas Jan. 1987 88 p
(AD-A178979; AFIT/GNE/EN/87M-4) Avail: NTIS HC A05/MF A01 CSCL 20I

This theses develops a generalized model of a three component plasma which predicts the density profiles of the charged particles. The plasma was modeled using a finite difference solution to the charged particle continuity and momentum equations. The plasma sheath boundary is treated by applying the Bohm criterion. The code developed was successful in modeling one component diffusion. However attempts to apply the model to two component plasmas resulted in numerical instabilities and therefore prevented application of the model to a three component plasma. GRA

N87-23282# Colorado Univ., Boulder. Dept. of Astrophysical, Planetary and Atmospheric Sciences.
THE GENERATION OF ELECTROSTATIC NOISE IN THE PLASMA SHEET BOUNDARY LAYER
P. B. Dusenberry and L. R. Lyons 1 Sep. 1986 38 p Prepared in cooperation with Aerospace Corp., El Segundo, Calif.
(ATR-86(8433)-4) Avail: NTIS HC A03/MF A01

The one and two ion beam instability is considered as a possible explanation for the observations of broad band electrostatic noise in the plasma sheet region of the geomagnetic tail. When only hot streaming plasma sheet boundary layer ions are present, no broad band waves are excited. Cold, streaming ionospheric ions can generate electrostatic broad band waves propagating in the slow beam acoustic mode, but the growth rates of the waves are significantly enhanced when hot boundary layer ions are present. (Both the slow and fast beam acoustic modes can be excited, depending on the relative ion drift.) This model predicts that the wave intensity of the broad band noise should peak in the plasma sheet boundary layer. Observations of less intense electrostatic waves in the lobes and plasma sheet are likely a result of the absence of hot ion beams or large ion temperatures, respectively, which result in smaller growth rates. The ion beam instability may play an important role in the formation of the central plasma sheet. Author

N87-23314*# Northeastern Univ., Boston, Mass. Center for Electromagnetics Research.
FORMATION MECHANISMS OF LABORATORY DOUBLE LAYERS
Chung Chan *In* NASA. Marshall Space Flight Center Double Layers in Astrophysics May 1987 p 35-53 Sponsored in part by NSF (For primary document see N87-23313 16-88)
Avail: NTIS HC A14/MF A01 CSCL 20I

N87-23315*# Iowa Univ., Iowa City. Dept. of Physics.
SOME DYNAMICAL PROPERTIES OF VERY STRONG DOUBLE LAYERS IN A TRIPLE PLASMA DEVICE
T. Carpenter and S. Torven (Royal Inst. of Tech., Stockholm, Sweden) *In* NASA. Marshall Space Flight Center Double Layers in Astrophysics May 1987 p 55-72 (For primary document see N87-23313 16-88)
Avail: NTIS HC A14/MF A01 CSCL 20I

N87-23316*# Wisconsin Univ., Madison. Dept. of Nuclear Engineering.
PUMPING POTENTIAL WELLS
N. Hershkowitz, C. Forest, E. Y. Wang, and T. Intrator *In* NASA. Marshall Space Flight Center Double Layers in Astrophysics May 1987 p 73-88 (For primary document see N87-23313 16-88) (Grant NAGw-275)
Avail: NTIS HC A14/MF A01 CSCL 20I

N87-23317*# Jet Propulsion Lab., California Inst. of Tech., Pasadena.
A LABORATORY INVESTIGATION OF POTENTIAL DOUBLE LAYERS
Philip Leung *In* NASA. Marshall Space Flight Center Double Layers in Astrophysics May 1987 p 89-103 (For primary document see N87-23313 16-88)
Avail: NTIS HC A14/MF A01 CSCL 20I

N87-23318*# Physical Research Lab., Ahmedabad (India). Plasma Physics Programme.
EXPERIMENTAL OBSERVATION OF ION-ACOUSTIC DOUBLE LAYERS IN LABORATORY PLASMA Abstract Only
Y. C. Saxena *In* NASA. Marshall Space Flight Center Double Layers in Astrophysics May 1987 p 105 (For primary document see N87-23313 16-88)
Avail: NTIS HC A14/MF A01 CSCL 20I

N87-23319*# Iowa Univ., Iowa City. Dept. of Physics and Astronomy.
A NEW HYDRODYNAMIC ANALYSIS OF DOUBLE LAYERS
Heinrich Hora *In* NASA. Marshall Space Flight Center Double Layers in Astrophysics May 1987 p 109-137 (For primary document see N87-23313 16-88)
Avail: NTIS HC A14/MF A01 CSCL 20I

N87-23320*# Riso National Lab., Roskilde (Denmark). Physics Dept.
ION PHASE-SPACE VORTICES AND THEIR RELATION TO SMALL AMPLITUDE DOUBLE LAYERS
Hans L. Pecseli *In* NASA. Marshall Space Flight Center Double Layers in Astrophysics May 1987 p 139-145 (For primary document see N87-23313 16-88)
Avail: NTIS HC A14/MF A01 CSCL 20I

N87-23322*# Centre National d'Etudes des Telecommunications, Issy-les-Moulineaux (France).
CURRENT DRIVEN WEAK DOUBLE LAYERS
Gerard Chanteur *In* NASA. Marshall Space Flight Center Double Layers in Astrophysics May 1987 p 167-181 (For primary document see N87-23313 16-88)
Avail: NTIS HC A14/MF A01 CSCL 20I

N87-23323*# Utah State Univ., Logan. Center for Atmospheric and Space Sciences.
ELECTRIC FIELDS AND DOUBLE LAYERS IN PLASMAS
Nagendra Singh, H. Thiemann, and R. W. Schunk *In* NASA. Marshall Space Flight Center Double Layers in Astrophysics May 1987 p 183-208 (For primary document see N87-23313 16-88)
(Grants NAGw-77; NSF ATM-84-17880)
Avail: NTIS HC A14/MF A01 CSCL 20I

N87-23324*# Dartmouth Coll., Hanover, N.H.
ELECTRON ACCELERATION IN STOCHASTIC DOUBLE LAYERS Abstract Only
William Lotko *In* NASA. Marshall Space Flight Center Double Layers in Astrophysics May 1987 p 209 (For primary document see N87-23313 16-88)
Avail: NTIS HC A14/MF A01 CSCL 20I

N87-23334*# National Aeronautics and Space Administration. Marshall Space Flight Center, Huntsville, Ala.
ACCRETION ONTO NEUTRON STARS WITH THE PRESENCE OF A DOUBLE LAYER Abstract Only
A. C. Williams, M. C. Weisskopf, R. F. Elsner, W. Darbro, and P. G. Sutherland (McMaster Univ., Hamilton, Ontario) *In its* Double Layers in Astrophysics May 1987 p 317 Previously announced in IAA as A86-43296 (For primary document see N87-23313 16-88)
Avail: NTIS HC A14/MF A01 CSCL 20I

N87-23335*# National Aeronautics and Space Administration. Marshall Space Flight Center, Huntsville, Ala.
THE FORMATION OF A DOUBLE LAYER LEADING TO THE CRITICAL VELOCITY PHENOMENON
A. C. Williams *In its* Double Layers in Astrophysics May 1987 p 319-328 (For primary document see N87-23313 16-88)
Avail: NTIS HC A14/MF A01 CSCL 20I

76 SOLID-STATE PHYSICS

Includes superconductivity.
For related information, see also *33 Electronics and Electrical Engineering* and *36 Lasers and Masers.*

N87-23283# Tsentralnyj Nauchno-Issledovatelskij Inst. Informatsii i Tekhniko-Ehkonomicheskikh Issledovanij po Atomnoj Nauke i Tekhnike, Moscow (USSR).
POWDER. COMPLEX OF PROGRAMS FOR STRUCTURAL ANALYSIS OF POLYCRYSTALS
V. P. Serykh 1985 29 p In RUSSIAN; In RUSSIAN
(DE87-701211; KFTI-85-5) Avail: NTIS (US Sales Only) HC A03/MF A01

Possibilities of a powder method, as applied to the first step of structural investigations, are studied. Ratios, used as a reliability criterion, are obtained. Algorithms for full-profile difractogram processing, identification, Bravais parallelepiped redetermination, regeneration of the ordered spectrum of possible reflections, induction are described. Program operation is illustrated by examples. Instructions for a user are given. Programs are realized on the FORTRAN-4 language fitting the HBESM-6 computer. DOE

N87-23284# Argonne National Lab., Ill.
MOLECULAR-DYNAMICS SIMULATION OF THIN-FILM GROWTH
M. Schneider, I. K. Schuller, and A. Rahman (Minnesota Univ., Minneapolis.) Jan. 1987 8 p Presented at the Materials Research Society Fall Meeting, Boston, Mass., 1 Dec. 1986
(Contract W-31109-eng-38)
(DE87-006973; CONF-861207-88) Avail: NTIS HC A02/MF A01

The epitaxial growth of thin films has been studied by molecular-dynamics computer simulation. In these simulations atoms are projected towards a temperature-controlled substrate, and the equations of motion of all atoms are solved for a given interaction potential. The calculations give insight into the microscopic structure of thin films, the dynamics of the adsorption process, and they help answer the way in which substrate temperature, form of the substrate, flux of impinging atoms, and form of the interaction potential, affect epitaxial growth. Simulations were performed for monatomic and binary systems with spherically symmetric atomic interactions, and for systems in which the atoms are interacting via a three-body potential to simulate the epitaxial growth of silicon. DOE

N87-23285# Sandia National Labs., Albuquerque, N. Mex.
A STATISTICAL STUDY OF THE COMBINED EFFECTS OF SUBSTRATE TEMPERATURE, BIAS, ANNEALING, AND A Cr3Si2 UNDERCOATING ON THE TRIBOLOGICAL PROPERTIES OF RF-SPUTTERED MoS2 COATINGS
J. K. G. Panitz, L. E. Pope, C. R. Hills, J. E. Lyons, and D. J. Staley 1987 16 p Presented at the International Conference on Metallurgical Coatings, San Diego, Calif., 23 Mar. 1987
(Contract DE-AC04-76DP-00789)
(DE87-007086; SAND-86-2555C; CONF-870388-2) Avail: NTIS HC A02/MF A01

A study is completed of the effects of (1) substrate temperature, (2) substrate bias, (3) post-deposition annealing, and (4) the presence of a Cr3Si2 undercoating on the tribological properties of 300 to 500 nm thick MoS2 coatings which were rf-sputter deposited on annealed 304 stainless steel substrates. It was determined that a Cr3Si2 undercoating and substrate bias are the most important individual factors in order to obtain MoS2 coatings with low coefficients of friction, 0.07. The highest coefficients of friction, 0.12, occurred for coatings which were not heated during deposition nor annealed afterwards and which were deposited onto substrates that were not biased during deposition or precoated with Cr3Si2. Coatings which were deposited onto substrates that were precoated with Cr3Si2, subjected to deposition temperatures of 300 C, biased during deposition and annealed afterwards were able to withstand the most wear. The best MoS2 coatings with regards to both coefficient of friction and wear occur over a broad range of substrate biases from -50 to -100 V. Transmission electron microscopy indicates that there are significant differences in the deposition morphology of the MoS2 coatings. DOE

N87-23286* National Aeronautics and Space Administration. Pasadena Office, Calif.
TOTAL IMMERSION CRYSTAL GROWTH Patent
Andrew D. Morrison, inventor (to NASA) (Jet Propulsion Lab., California Inst. of Tech., Pasadena.) 31 Mar. 1987 9 p Filed 21 Nov. 1984 Supersedes N85-22178 (23 - 12, p 1939) Continuation-in-part of US-Patent-Appl-SN-442815, dated 18 Nov. 1982, abandoned
(NASA-Case-NPO-15800-2; US-Patent-4,654,110; US-Patent-Appl-SN-674395; US-Patent-Appl-SN-442815; US-Patent-Class-156-607; US-Patent-Class-156-617-H; US-Patent-Class-156-617-SP) Avail: US Patent and Trademark Office CSCL 20L

Crystals of wide band gap materials are produced by positioning a holder receiving a seed crystal at the interface between a body of molten wide band gap material and an overlying layer of temperature-controlled, encapsulating liquid. The temperature of the layer decreases from the crystallization temperature of the crystal at the interface with the melt to a substantially lower temperature at which formation of crystal defects does not occur, suitably a temperature of 200 to 600 C. After initiation of crystal growth, the leading edge of the crystal is pulled through the layer until the leading edge of the crystal enters the ambient gas headspace which may also be temperature controlled. The length

of the column of liquid encapsulant may exceed the length of the crystal such that the leading edge and trailing edge of the crystal are both simultaneously with the column of the crystal. The crystal can be pulled vertically by means of a pulling-rotation assembly or horizontally by means of a low-angle withdrawal mechanism.
Official Gazette of the U.S. Patent and Trademark Office

N87-23287# Hughes Research Labs., Malibu, Calif.
NONLINEAR OPTICAL PROPERTIES AND SUBPICOSECOND DYNAMICS OF EXCITONS AND ELECTRON-HOLE PLASMAS IN MULTIPLE QUANTUM WELL STRUCTURES Bimonthy Progress Report, Jan. - Feb. 1987
A. L. Smirl, R. A. McFarlane, and J. F. Lam 16 Mar. 1987 11 p
(Contract F49620-84-C-0083)
(AD-A179124; HAC-REF-F4767; AFOSR-87-0332TR) Avail: NTIS HC A02/MF A01 CSCL 07D

Time resolved photoluminescence measurements are reported for MBE-grown Aluminum, Gallium, Arsenide samples having alloy compositions which result in both direct gap and indirect gap materials. Quantitative results have been obtained for bandgap renormalization induced at high carrier densities and the results compared with a theoretical model. Detailed studies are reported of a marginally indirect sample displaying stimulated emission from both direct and indirect bandgaps. GRA

N87-23288# Stanford Univ., Calif. Dept. of Applied Physics.
SUPERCONDUCTING THIN FILMS, COMPOSITES AND JUNCTIONS Annual Report, 1 Oct. 1985 - 30 Sep. 1986
T. H. Geballe Dec. 1986 9 p
(Contract F49620-82-C-0014)
(AD-A179346; GL-4157; AFOSR-87-0341TR) Avail: NTIS HC A02/MF A01 CSCL 20C

Low energy ion beam cleaning of the substrates prior to deposition has been found to enhance the quality of ultrathin (less than 100A) refractory superconducting Niobium, Vanadium films. Nb film as thin as 7A has been grown from which it has been possible to fabricate good superconducting tunnel junctions. Both the native films and the tunnel junctions can be thermally recycled without any degradation. In-situ surface studies along with transmission electron microscopy (EM) suggest the removal of the carbon atoms from the surface of the substrate and possibly that increased chemical reactivity of the substrate atoms are the causes of the improvement. Electron microscopy (EM) results indicate that the Nb films grow perfectly lattice matched to the sapphire substrate when the substrate is ion-beam cleaned. This strained-layer epitaxy is observed up to 40A, the maximum thickness investigated through EM. Good-quality tunnel junctions have been fabricated on ultrathin films of Nb. Absolute specific-heat measurements have been made through the metal-insulator transition in thin film Molybdenum (X) Germanium (1-X) determining the thermodynamic electronic density of states. Nb/Tantalum multilayered films prepared by magnetron sputtering have been studied by critical field measurements. The effects of substrate orientation and deposition temperature on the properties of the films has been determined. Considerable progress has been made in the design and construction of the new advance electron beam deposition facility. GRA

N87-23289# Harry Diamond Labs., Adelphi, Md.
ANGULAR MOMENTUM THEORY APPLIED TO INTERACTIONS IN SOLIDS Summary Progress Report
Clyde A. Morrison Feb. 1987 164 p
(DA Proj. 1L1-61102-AH-44)
(AD-A179366; HDL-SR-87-1) Avail: NTIS HC A08/MF A01 CSCL 20L

Concepts of group theory applied to the spectra of impurity ions in crystals are discussed. Beginning with the simple hydrogen atom, spectroscopic notation and angular momentum operators are discussed. This is followed by a general discussion of angular momentum theory including Clebsch Gordon coefficients, the Wigner Eckart theorem, unit spherical tensors, and Racah coefficients. The extension of these techniques to the electronic configuration, (nl to the Nth power), for N equivalent electrons is discussed. The theory of point groups as applied to ions in solids is introduced, along with the use of the International Tables of Crystallography and character tables. The phenomenological theory of crystal fields is discussed in some detail along with the so-called free ion parameters characterizing the Coulomb interaction, the spin-orbit interaction, and the interconfiguration interaction. The use of tables of 3-j and 6-j symbols in the calculation of the matrix elements of the various interactions is presented, along with other tables and aids in the computation of the energy levels. The point ion model of crystal-field interaction is discussed with particular emphasis on the work done at the Harry Diamond Laboratories (HDL) on its development. The earlier work at HDL was applied to triply ionized rare earth ions (l to the Nth power electronic configuration), and the preliminary extensions presently being undertaken at HDL are applied to the transit. GRA

N87-23290# Air Force Inst. of Tech., Wright-Patterson AFB, Ohio. School of Engineering.
THE CHARACTERIZATION OF WHISKERS PRODUCED BY ELECTROMIGRATION ON SUSPENDED ALUMINUM LINESTRIPES M.S. Thesis
Scott L. Linder 8 Dec. 1986 118 p
(AD-A179383; AFIT/GE/ENG/86D-35) Avail: NTIS HC A06/MF A01 CSCL 11F

Studies have shown that aluminum whiskers resulting from electromigration are as threatening to device reliability as void formation. Comparatively little research has been conducted to study their morphology or formation. This study generates whiskers on suspended aluminum tests stripes. The aluminum is evaporated onto 9 mil thick silicon wafers with a 5000 A layer of thermally grown silicon dioxide. Normal photolithography techniques are used to produce serpentine test patterns. The silicon substrate is chemically etched to produce aluminum stripes suspended on a thin layer of silicon dioxide. A current density of approximately 450,000 A/sq. cm is applied to induce electromigration. The whiskers are examined with a Cambridge MK II Scanning Electron Microscope and analyzed with a JEOL 2000FX Scanning Transmission Electron Microscope. The results of the analysis show that aluminum whiskers grow in a less than 110 greater than direction along the crystal axis. Additional morphological observations reveal internal dislocations and mass accumulation beneath the stripe surface at the whisker's nucleation site. GRA

N87-23291# Utah Univ., Salt Lake City.
STRUCTURE AND PROPERTIES OF NOVEL COMPOUNDS OF SILICON GERMANIUM AND TIN Final Technical Report, 1 Jun. 1985 - 1 Aug. 1986
Josef Michl 31 Jan. 1987 6 p
(Grant AF-AFOSR-0065-84)
(AD-A179433; AFOSR-87-0521TR) Avail: NTIS HC A02/MF A01 CSCL 07C

Work on silanimines has been continued in collaboration with Professor R. West (Madison, Wisconsin). A highly sterically hindered derivative has been found to be stable in solutions at low temperature. The controversy concerning the assignment of the structure of dimethylsilylene by Drahnak, West, and Michl has now been settled. The pyrolysis of phenyltriaxidosilane yields phenysilaisonitrile and this has been confirmed by chemical trapping as well as UV and IR matrix-isolation spectroscopy. We have discovered that the photolysis of PhSi(N3)3 in matrix isolation produces not only PhNSi, but also the isomer, benxosilanitrile. This is the first representative of a triply bonded compound to tetravelant silicon. GRA

N87-23292# State Univ. of New York, Buffalo. Dept. of Chemistry.
NON-MARKOVIAN LINE SHAPES OF PHYSISORBED ATOMS ON A CRYSTAL
Henk F. Arnoldus and Thomas F. George Apr. 1987 38 p
(Contract N00014-86-K-0043)
(AD-A179525; UBUFFALO/DC/87/TR-35) Avail: NTIS HC A03/MF A01 CSCL 07D

An atom adsorbed on the surface of a harmonic crystal is considered. The binding potential well supports many vibrational bound-harmonic and the coupling of the motion of the atom with the substrate gives rise to phonon-exchange reactions, which subsequently amount to atomic transitions between the bound states. This process of thermal relaxation of the adatom density operator is commonly described with reservoir theory, in which the crystal is regarded as a thermal bath with an extremely short correlation time. The latter property then justifies the neglect of any memory in the interaction, which is usually referred to as the Markov approximation. It is shown, however, that the reservoir correlation time is not necessarily small in comparison with the inverse (relaxation) frequencies of the system, which implies a breakdown of this approach. The equation of motion for the adatom density-operator is then solved without line profile for absorption of infrared radiation. Essentially different results are obtained than with the approximate theory, but it turns out that the solutions can be expressed in terms of the same parameters. GRA

N87-23293# Virginia Univ., Charlottesville. Dept. of Electrical Engineering.

SIS (SUPERCONDUCTOR-INSULATOR-SUPERCONDUCTOR) MIXER RESEARCH Final Report, 15 Nov. 1985 - 14 Nov. 1986

M. J. Feldman 17 Mar. 1987 12 p

(Grant AF-AFOSR-0056-86)

(AD-A179604; UVA/525657/EE87/101; AFOSR-87-0447TR) Avail: NTIS HC A02/MF A01 CSCL 09A

Theoretical and experimental research has been conducted to elucidate the basic physics behind the properties of superconductor-insulator- superconductor (SIS) tunnel junction receiving devices. The quantum theory of mixing was employed to calculate the saturation behavior of the SIS mixer and the SIS direct detector. The direct detector was found to saturate at far higher powers than previously believed, permitting practical application of this device. Experiments verified the saturation theory. The mixer saturation expression led to the formulation of frequency scaling regions. The origin of quantum noise sources is completely minimized. The mixer quantum noise limit was shown to be reached in only two special cases. Computer calculations determined that the behavior of SIS receivers divides into two regimes, low and high frequencies, the cross-over frequency depending upon junction quality. The properties of these two regimes were delineated. All previous SIS receivers have operated in the low frequency regime. Plasma-etched niobium nitride edge junctions have been fabricated using a novel barrier formation process. These junctions have excellent current-voltage characteristics. Author (GRA)

N87-23294# Oak Ridge National Lab., Tenn.

A MICROCRYSTALLINE GROWTH STUDY OF SOLVENT EFFECTS IN ALKOXIDES BY DYNAMIC LASER LIGHT SCATTERING

C. H. Byers and M. T. Harris Feb. 1987 16 p Presented at the 3rd International Conference on Ultrastructure Processing of Ceramics, Glasses and Composites, San Diego, Calif., 23 Feb. 1987

(Contract DE-AC05-84OR-21400)

(DE87-005710; CONF-870254-1) Avail: NTIS HC A02

The hydrolysis and condensation reactions which result in homogeneous precipitation of alkoxides, such as silicon ethoxide, are studied in a laser light scattering facility in which a thermally-controlled quartz cell is used as a crystallization vessel. Rapid, nonintrusive monitoring of the growth of the particles in 0.005-to-1 micron range is achieved. A study of particle growth and powder characteristics of the titania and silica indicates that a major contributing factor to the ultimate particle size and morphology is the nature of alcohol solvent medium for the reaction. Results for ethanol propanols and three butanols indicate that particle characteristics are improved by choosing the proper solvent. DOE

N87-23295# Mount Holyoke Coll., South Hadley, Mass.

THE STUDY OF PHOTOCHEMISTRY AT SEMICONDUCTOR SURFACES USING TOTAL INTERNAL REFLECTION TECHNIQUES Final Report, 1 Jun. 1984 - 31 May 1986

M. T. Spitler Jan. 1987 10 p

(Contract DE-FG02-84ER-13209)

(DE87-006259; DOE/ER-13209/1) Avail: NTIS HC A02/MF A01

The photochemistry and photoelectrochemistry of organic dyes has been studied using internal reflection spectroscopy and standard photoelectrochemical techniques. The causes of the low efficiency for dye sensitized photocurrent at semiconductors have been established and systems found where sensitization is highly efficient. Internal reflection flash photolysis techniques have been perfected and demonstrated through the study of the photochemistry of the dye eosin adsorbed at semiconductor surfaces. The photochemical attachment of dyes to the electrode surface has also been demonstrated. DOE

N87-23296# Purdue Univ., West Lafayette, Ind. Dept. of Chemistry.

NOVEL POLYMERIC LIT AND DIVALENT CATION FAST ION CONDUCTING MATERIALS Annual Technical Report

C. A. Angell 1986 16 p

(Contract DE-FG02-84ER-45102)

(DE87-006294; DOE/ER-45102/T1) Avail: NTIS HC A02/MF A01

Solid state energy devices require a component which conducts electricity by ionic migration. The conductivity of this element of the system must be very high. Four types of materials show the promise to provide the necessary conductivity characteristics, while offering other desirable features such as the ability to distort in shape under mechanical stresses: (1) crystalline; (2) plastic crystal; (3) inorganic glassy; and (4) polymer salt solutions. This document reports on the following materials: lead halide-containing fast ion conducting glasses (LiF-PbF2-Al(PO3)3), mixed ionic electronic conduction (Na2O-V2O5-TeO2), alpha relaxation in ionic glasses, glass transition in P2O2, and conductivity transition between all-halide and all-oxide glasses. DOE

N87-23297# Sandia National Labs., Albuquerque, N. Mex.

ATOMISTIC SIMULATION OF STABILITY PROPERTIES AND GROWTH OF STRAINED LAYER STRUCTURES

P. A. Taylor and B. W. Dodson 1987 21 p Presented at the SPIE Conference on Growth of Compound Semiconductors, Bay Point, Fla., 22 Mar. 1987

(Contract DE-AC04-76DP-00789)

(DE87-006712; SAND-86-2213C; CONF-870385-1) Avail: NTIS HC A02/MF A01

Monte Carlo based microscopic techniques were used to study the stability and metastability of thin coherently strained layers of mismatched silicon-like semiconductor material grown on the (111) silicon surface. The structural energy was calculated using three-body empirical potentials. For layers greater than roughly 20 A in thickness, the critical layer thickness associated with thermodynamic stability agrees quantitatively with continuum theory. For thinner layers, however, considerable variations from the continuum theory are found. For a strained layer six monolayers thick, the test system is found to be metastable against the nucleation of misfit dislocations to a lattice mismatch of approximately 11%, compared to the 4% equilibrium stability limit. Additionally, simulation of strained layer growth of two-dimensional Lennard-Jones crystal lattices has been performed using molecular dynamics. In particular, we have studied the influences of lattice mismatch and substrate temperature on the growth, from the vapor phase, of overlayer material possessing a different bulk lattice constant than that of the substrate material. Simulation results predict that at substrate temperatures less than 50% of melting, epitaxial growth occurs for mismatch values less than 4% whereas above this value, defective growth is observed. At temperatures above 50% of the melt temperature, mass transport occurs across the layer interface and rapid diffusion is observed in the top-most atomic layers, resulting in liquid-like behavior in a thin layer over ordered strained layer crystal. DOE

N87-23298# Lawrence Livermore National Lab., Calif.
SEMICONDUCTOR RESEARCH CAPABILITIES AT THE LAWRENCE BERKELEY LABORATORY
Feb. 1987 12 p
(Contract DE-AC03-76SF-00098)
(DE87-006931; LBL-PUB-606) Avail: NTIS HC A02/MF A01

This document discusses semiconductor research capabilities (advanced materials, processing, packaging) and national user facilities (electron microscopy, heavy-ion accelerators, advanced light source). DOE

N87-23299# Sandia National Labs., Albuquerque, N. Mex.
TEMPERATURE DEPENDENCE OF IMPLANTATION DAMAGE IN STRAINED-LAYER SUPERLATTICES
D. R. Myers, G. W. Arnold, L. R. Dawson, R. M. Biefeld, C. R. Hills, and B. L. Doyle 1987 8 p Presented at the Spring Meeting of the Materials Research Society, Anaheim, Calif., 21 Apr. 1987
(Contract DE-AC04-76DP-00789)
(DE87-007678; SAND-86-2581C; CONF-870438-1) Avail: NTIS HC A02/MF A01

We have characterized damage production in both (InGa)As/GaAs and Ga(AsP)/GaP strained-layer superlattices for silicon implants at 80 K, 300 K or 673 K at fluences sufficient to induce compositional disordering of the superlattice layers. Implants at low temperatures (80 K for the (InGa)As/GaAs system, 300 K and below in the Ga(AsP)/GaP system) are characterized by well-drained amorphous layers at depths consistent with the predictions of ion range codes. Implants at higher temperatures are characterized by greatly reduced damage levels with substantial densities of extended defects located near the mean ion range. Point defect clusters are preferentially located in the ternary layers in the (InGa)As/GaAs SLS at the deepest part of the implanted zone. Despite the absence of amorphous layer formation, precipitous stress relief still occurs for the Si-implanted (InGa)As/GaAs SLS. DOE

N87-23300# International Centre for Theoretical Physics, Trieste (Italy).
ORBITAL REMOVAL METHOD FOR THE NEUTRAL VACANCY IN SEMICONDUCTORS
V. K. Bashenov, D. L. Kardashev, and D. I. Marvakov Jul. 1986 8 p
(DE87-701537; IC-86/197) Avail: NTIS (US Sales Only) HC A02/MF A01

A study of the orbital removal method for vacancy states in semiconductors is presented. It is shown that the bound and resonance states are zeroes of the local perfect-crystal Green function. We suggest that the generalized localized orbitals generate a vacancy potential, when the atom has been removed from the lattice site, which leads to the appearance of a bound state. This is demonstrated for diamond. DOE

N87-23301# Arizona State Univ., Tempe. Dept. of Physics.
SUBMICRON CHARACTERIZATION OF THE ATOMIC AND ELECTRONIC STRUCTURE OF DEFECTS IN SEMICONDUCTORS Final Report, 1 Jun. 1983 - 30 Sep. 1986
J. C. Spence 3 Feb. 1987 6 p
(Contract DAAG29-83-K-0087)
(AD-A178458; ARO-20088.14-MS) Avail: NTIS HC A02/MF A01 CSCL 20L

New submicron defect characterization techniques have been developed, including energy loss spectroscopy and cathodoluminesence in TEM. This has allowed the first observations of infra-red emission from groups of well characterized dislocations in silicon, and the spatial mapping of luminescence in GaAs. The basic theory and corresponding experiments have been developed for coherent bremsstrahlung and electron energy loss spectroscopy (ELS) (in Be2C in particular). ELS allows chemical and structural information to be obtained from subnanometer regions of material. GRA

N87-23302# Aerospace Corp., El Segundo, Calif. Chemistry and Physics Lab.
UNPINNING OF THE FERMI LEVEL ON GaAs BY FLOWING WATER
Neil A. Ives, Gary W. Stupian, and Martin S. Leung 1 Mar. 1987 14 p
(Contract F04701-85-C-0086)
(AD-A178489; TR-0086(6945-09)-3; SD-TR-87-08) Avail: NTIS HC A02/MF A01 CSCL 20L

Unpinning of the Fermi level on Gallium Arsenide (100) surfaces by photochemical reactions resulting from simultaneous exposure of specimens to flowing water and light was recently reported. A series of experiments is carried out to provide further information on the changes in surface electronic structure responsible for unpinning of the Fermi level under these conditions. The present work supports the conclusion that the surface states which pin the Fermi level are associated with elemental arsenic and arsenic sesquioxide (As2O3). Effects of each of these two species on pinning are distinguished experimentally. In addition to photochemical reactions, exposure to flowing water alone can result in Fermi level unpinning under certain conditions. The oxygen content of the wash water and the specimen preparation are shown to be important variables. GRA

N87-23303# Stanford Univ., Calif. Electronics Lab.
MODELING OF SUBSTRATE AND IMPLANTATION EFFECTS ON THE THRESHOLD VOLTAGE OF MESFET STRUCTURES FABRICATED IN SEMI-INSULATING GaAs Final Report, Sep. 1984 - May 1986
Thomas W. Sigmon Dec. 1986 67 p
(Contract F33615-84-C-5072)
(AD-A178550; AFWAL-TR-86-4103) Avail: NTIS HC A04/MF A01 CSCL 20L

The primary objective of this process modeling program was to identify Semi-Insulating Gallium Arsenide (SI-GaAs) substrate and implantation parameters that affect device behavior. Three major areas were investigated: (1) Predicting the two-dimensional distribution of the EL2 anti-site defect; (2) Modeling changes in the two-dimensional 2/EL2 distribution resulting from the annealing of Si-GaAs; and (3) Determining the electrical characteristics of SI-GaAs substrate and the thermal stability of these characteristics. A two-dimensional computer model was developed to predict the thermally induced stress in a growing Czochralski GaAs boule from fundamental growth parameters. A stress-conversion coefficient was obtained from experimental data and was applied to the stress results to predict two-dimensional EL2 profiles. These predicted profiles were compared with experimental results. GRA

N87-23304*# National Aeronautics and Space Administration. Lewis Research Center, Cleveland, Ohio.
AlGaAs GROWTH BY OMCVD USING AN EXCIMER LASER
Joseph D. Warner, David M. Wilt, John J. Pouch, and Paul R. Aron Dec. 1986 11 p Presented at the Fall Meeting of the Materials Research Society, Boston, Mass., 1-5 Dec. 1986
(NASA-TM-88937; E-3379; NAS 1.15:88937) Avail: NTIS HC A02/MF A01 CSCL 20B

AlGaAs has been grown on GaAs by laser assisted OMCVD using an excimer laser, wavelength 193 nm, and a Cambridge OMCVD reactor. Films were grown at temperatures of 450 and 500 C with the laser beam parallel to the surface and impinging onto the surface at 15 deg from parallel. The samples were heated by RF coils while the laser beam was perpendicular to the gas flow. Typical gas flow parameters are 12 slm of H2, 15 sccm of Ga(CH3)3, 13 sccm of Al(CH3)3, and a pressure of 250 mbar. The initial energy density of the beam at the surface was 40 mJ/sq cm, the pulse rate was 20 pps, and the growth time was 7 min. The films were analyzed by Auger electron spectroscopy for the aluminum concentration and by TEM for the surface morphology. Author

77 THERMODYNAMICS AND STATISTICAL PHYSICS

Includes quantum mechanics; theoretical physics; and Bose and Fermi statistics.

For related information see also *25 Inorganic and Physical Chemistry* and *34 Fluid Mechanics and Heat Transfer.*

N87-23305 Paris-Sud Univ., Orsay (France).
THE CHIRAL SYMMETRY ASPECTS OF SUPERSYMMETRIC CONFINING GAUGE THEORIES Ph.D. Thesis [ASPECTS DE LA SYMMETRIE CHIRALE DANS LES THEORIES DE JAUGE CONFINANTES SUPERSYMMETRIQUES]
Marc Knecht 1985 99 p In FRENCH; ENGLISH summary
(ETN-87-99553) Avail: Issuing Activity

The interplay between chiral symmetry and supersymmetry was analyzed. In the frame of quantic chromodynamics a general method leading to exact results on quark mass dependences of physical qualities such as bounded state masses is described. The commutation relations satisfied by the supersymmetric and chiral charges in presence of the soft breaking due to quark masses is established. It is shown that if the chiral limit is unique, the global symmetry is not spontaneously broken. ESA

N87-23306# Argonne National Lab., Ill.
THERMODYNAMIC PROPERTIES OF MOLTEN SALT SOLUTIONS
M. Blander 15 Aug. 1986 39 p Presented at the Advanced Study Institute on Molten Salt Chemistry, Camerino, Italy, 3 Aug. 1986
(Contract W-31109-eng-38)
(DE87-004948; CONF-8608157-2) Avail: NTIS HC A03/MF A01

Why is it important to understand the thermodynamic properties of molten salt solutions, and what aspect of these properties is most important? In technologies and sciences where molten salts, slags or magmas are used or studied, one often must calculate the extent of a chemical reaction or of phase equilibria. In order to do this we need to know an equilibrium constant which can be generally written as $G^\circ = RT1nK$. The equilibrium constant K is a function of compositions and activity coefficients, the two quantities necessary to define chemical potentials, $K = K(X,A)$. Thus, in order to calculate the concentrations of the final equilibrium product, X, one needs a knowledge of G° and of the activity coefficients A. The calculation of G°, the standard free energy change for reactants and products in their standard states (generally the pure salts) is obtained from calorimetric data or other types of equilibrium data on pure compounds. This paper investigates a way to calculate activity coefficients using chemical potentials. Mathematical models are presented for binary and ternary mixtures. DOE

N87-23307# International Centre for Theoretical Physics, Trieste (Italy).
GENERALIZED QUANTAL EQUATION OF MOTION
M. W. Morsy and M. Embaby Jul. 1986 11 p
(DE87-701531; IC-86/182) Avail: NTIS (US Sales Only) HC A02/MF A01

In the present paper, an attempt is made for establishing a generalized equation of motion for quantal objects, in which intrinsic self adjointness is naturally built in, independently of any prescribed representation. This is accomplished by adopting Hamilton's principle of least action, after incorporating, properly, the quantal features and employing the generalized calculus of variations, without being restricted to fixed end points representation. It turns out that our proposed equation of motion is an intrinsically self-adjoint Euler-Lagrange's differential equation that ensures extremization of the quantal action as required by Hamilton's principle. Time dependence is introduced and the corresponding equation of motion is derived, in which intrinsic self adjointness is also achieved. Reducibility of the proposed equation of motion to the conventional Schroedinger equation is examined. The corresponding continuity equation is established, and both of the probability density and the probability current density are identified. DOE

80 SOCIAL SCIENCES (GENERAL)

Includes educational matters.

No abstracts in this category.

81 ADMINISTRATION AND MANAGEMENT

Includes management planning and research.

N87-23308# British Aerospace Public Ltd. Co., Kingston-upon-Thames (England).
BRITISH AEROSPACE: A KINGSTON PERSPECTIVE
Bernard Harbor Aug. 1986 82 p
(ETN-87-99823) Avail: NTIS HC A05/MF A01

The commercial and industrial environment of British Aerospace is reviewed, and the possibilities of converting its Kingston (UK) plant to non defense related production if government arms spending is cut are assessed. ESA

N87-23309# National Bureau of Standards, Gaithersburg, Md.
COOPERATIVE RESEARCH OPPORTUNITIES AT NBS (NATIONAL BUREAU OF STANDARDS)
Dec. 1986 57 p
(PB87-157236; NBS/SP-723; LC-86-600570) Avail: HC A04/MF A01; also available SOD HC $2.75 as 003-003-02788-0 CSCL 05A

A report on Cooperative Research Opportunities at the National Bureau of Standards (NBS) has the following contents: Cooperative Research At NBS; Research opportunities; Analytical chemistry; Applied mathematics; Basic standards; Building technology; Ceramics; Chemical engineering; Chemical physics; Computer sciences and technology; Electronics and electrical engineering; Fire research; Fracture and deformation; Manufacturing engineering; Matallurgy; Neutron scattering and refraction; Nondestructive evaluation; Polymers; Product standards; Radiation research; Standards reference data. GRA

N87-23310# Air Force Inst. of Tech., Wright-Patterson AFB, Ohio. School of Engineering.
LRS: A KNOWLEDGE BASED APPROACH TO LAUNCH RESOURCE SCHEDULING M.S. Thesis
Fred H. Koch Dec. 1986 214 p
(AD-A179426; AFIT/GSO/ENS/86D-4) Avail: NTIS HC A10/MF A01 CSCL 22D

This work describes a knowledge based prototype launch resource scheduling tool called Launch Resources Scheduling (LRS). The tool was requested by US Space Command for use by planners to evaluate future space launch resource requirements. A knowledge based approach to the launch resource scheduling problem is used due to its knowledge intensive nature. The LRS prototype is implemented using a knowledge system tool called Insight 2+ on an IBM PC compatible microcomputer. LRS uses menus and explanation screens to make it simple to operate. LRS matches launch resources to launch requirements. A launch schedule is produced which shows how the resources meet the launch requirements. At completion of the matching process, LRS provides a list of unsatisfied requirements and available resources. This list may be used by the planner to determine how well the planned launch resources meet the estimated launch requirements. GRA

N87-22641*# Pan American World Airways, Inc., San Francisco, Calif.
PAN AMERICAN WORLD AIRWAYS FLIGHT TRAINING: A NEW DIRECTION. FLIGHT OPERATIONS RESOURCE MANAGEMENT
Roy Butler *In* NASA. Ames Research Center Cockpit Resource Management Training May 1987 p 61-67 (For primary document see N87-22634 16-03)
Avail: NTIS HC A14/MF A01 CSCL 05A

N87-22645*# Trans-Australia Airlines, Melbourne. Flight Standards Div.
AIRCREW TEAM MANAGEMENT PROGRAM
Charles Margerison, Dick McCann, and Rod Davies (Queensland Univ., Brisbane, Australia) *In* NASA. Ames Research Center Cockpit Resource Management Training May 1987 p 90-107 (For primary document see N87-22634 16-03)
Avail: NTIS HC A14/MF A01 CSCL 05A

82 DOCUMENTATION AND INFORMATION SCIENCE

Includes information management; information storage and retrieval technology; technical writing; graphic arts; and micrography.

For computer documentation see *61 Computer Programming and Software.*

N87-23311# Air Force Inst. of Tech., Wright-Patterson AFB, Ohio. School of Engineering.
A DECISION SUPPORT SYSTEM FOR DATABASE MANAGEMENT SYSTEM SELECTION M.S. Thesis
Dennis R. Davidson Dec. 1986 76 p
(AD-A179339; AFIT/CS/ENG/86D-12) Avail: NTIS HC A05/MF A01 CSCL 05B

An interactive micro-computer based decision support system was designed and developed to aid in the evaluation of Database Management Systems (DBMS). DBMS attributes were researched in order to develop a hierarchy of attributes that reflect the important factors that must be considered when implementing a DBMS. After the hierarchy was established, different DBMS were evaluated relative to the attributes, and a base knowledge was established. The Decision Support System for DBMS Selection used the Analytical Hierarchy Process to allow the user to create a scenario that represents his requirements, and then evaluated this scenario against the base of knowledge. Several problems including an incomplete hierarchy and excessive input requirements were identified and solutions were implemented in the system. A preliminary evaluation indicates that users with database experience find the system responsive and usable, while those without database experience were easily confused. Several suggestions for further research are proposed. Author (GRA)

N87-23312# Sci-Tech Knowledge Systems, Scotia, N.Y.
MATERIALS INFORMATION FOR SCIENCE AND TECHNOLOGY (MIST). PROJECT OVERVIEW: PHASE 1 AND 2 AND GENERAL CONSIDERATIONS
W. Grattidge, J. Westbrook, J. McCarthy, C. Northrup, Jr., and J. Rumble, Jr. Nov. 1986 128 p Prepared in cooperation with Lawrence Berkeley Lab., Calif., Sandia National Labs., Albuquerque, N. Mex., and the National Bureau of Standards, Washington, D.C.
(DE87-006799; NBS-SP-726) Avail: NTIS HC A07/MF A01

The National Bureau of Standards and the Department of Energy have embarked on a program to build a demonstration computerized materials data system called Materials Information for Science and Technology (MIST). This report documents the first two phases of the project. The emphasis of the first phase was on determining what information was needed and how it could impact user productivity. The second phase data from the Aerospace Metal Handbook on a set of alloys was digitized and incorporated into the system. DOE

83 ECONOMICS AND COST ANALYSIS

Includes cost effectiveness studies.

No abstracts in this category.

84 LAW, POLITICAL SCIENCE AND SPACE POLICY

Includes NASA appropriation hearings; aviation law; space law and policy; international law; international cooperation; and patent policy.

No abstracts in this category.

85 URBAN TECHNOLOGY AND TRANSPORTATION

Includes applications of space technology to urban problems; technology transfer; technology assessment; and surface and mass transportation.

For related information see also *03 Air Transportation and Safety, 16 Space Transportation,* and *44 Energy Production and Conversion.*

No abstracts in this category.

88 SPACE SCIENCES (GENERAL)

N87-23313*# National Aeronautics and Space Administration. Marshall Space Flight Center, Huntsville, Ala.
DOUBLE LAYERS IN ASTROPHYSICS
Alton C. Williams, ed. and Tauna W. Moorehead, ed. May 1987 321 p Workshop held in Huntsville, Ala., 17-19 Mar. 1986; sponsored by NASA, Washington and USRA
(NASA-CP-2469; M-560; NAS 1.55:2469) Avail: NTIS HC A14/MF A01 CSCL 03B

Topics addressed include: laboratory double layers; ion-acoustic double layers; pumping potential wells; ion phase-space vortices; weak double layers; electric fields and double layers in plasmas; auroral double layers; double layer formation in a plasma; beamed emission from gamma-ray burst source; double layers and extragalactic jets; and electric potential between plasma sheet clouds. For individual titles, see N87-23314 through N87-23335.

N87-23314*# Northeastern Univ., Boston, Mass. Center for Electromagnetics Research.
FORMATION MECHANISMS OF LABORATORY DOUBLE LAYERS c75
Chung Chan *In* NASA. Marshall Space Flight Center Double Layers in Astrophysics May 1987 p 35-53 Sponsored in part by NSF (For primary document see N87-23313 16-88)
Avail: NTIS HC A14/MF A01 CSCL 20I

The evolution processes of double layers were studied in a series of laboratory experiments. It was found that the existence of virtual cathode-type potential wells at the electron injection boundary was the dominant triggering mechanism. The rapid growth of the potential wells led to collisionless ion trapping and the establishment of the necessary trapped ion population. For double layers with small potential drops, collisionless ion trapping actually induced ion-ion streaming instabilities and the formation of ion phase-space vortices. In this regime, the system often exhibited relaxation-type oscillations which correspond to the disruption and the recovery of the double layers. Author

N87-23315*# Iowa Univ., Iowa City. Dept. of Physics.

SOME DYNAMICAL PROPERTIES OF VERY STRONG DOUBLE LAYERS IN A TRIPLE PLASMA DEVICE **c75**

T. Carpenter and S. Torven (Royal Inst. of Tech., Stockholm, Sweden) *In* NASA. Marshall Space Flight Center Double Layers in Astrophysics May 1987 p 55-72 (For primary document see N87-23313 16-88)

Avail: NTIS HC A14/MF A01 CSCL 20I

Dynamical properties of very strong double layers seen in a differentially pumped triple plasma device are reported. These double layers are V-shaped. The following findings are discussed: (1) Disruptions in the double layer potential and in the plasma current occur when an inductance is placed in series with the bias supply between the sources in the external circuit. These disruptions, which can be highly periodic, are the result of a negative resistance region. (2) When reactances in the circuit are minimized, the double layer exhibits a jitter motion in position approximately equal to the double layer thickness. (3) When the bias between the sources is rapidly turned on, the initial phase in the double layer formation is the occurrence of a constant electric field for the first few microseconds. First the apparatus used in all of the work is discussed and then each of the three phenomena are considered. B.G.

N87-23316*# Wisconsin Univ., Madison. Dept. of Nuclear Engineering.

PUMPING POTENTIAL WELLS **c75**

N. Hershkowitz, C. Forest, E. Y. Wang, and T. Intrator *In* NASA. Marshall Space Flight Center Double Layers in Astrophysics May 1987 p 73-88 (For primary document see N87-23313 16-88) (Grant NAGw-275)

Avail: NTIS HC A14/MF A01 CSCL 20I

Nonmonotonic plasma potential structures are a common feature of many double layers and sheaths. Steady state plasma potential wells separating regions having different plasma potentials are often found in laboratory experiments. In order to exist, all such structures must find a solution to a common problem. Ions created by charge exchange or ionization in the region of the potential well are electrostatically confined and tend to accumulate and fill up the potential well. The increase in positive charge should eliminate the well. Nevertheless, steady state structures are found in which the wells do not fill up. This means that it is important to take into account processes which pump ions from the well. As examples of ion pumping of plasma wells, potential dips in front of a positively biased electron collecting anode in a relatively cold, low density, multidipole plasma are considered. Pumping is provided by ion leaks from the edges of the potential dip or by oscillating the applied potential. In the former case the two-dimensional character of the problem is shown to be important. Author

N87-23317*# Jet Propulsion Lab., California Inst. of Tech., Pasadena.

A LABORATORY INVESTIGATION OF POTENTIAL DOUBLE LAYERS **c75**

Philip Leung *In* NASA. Marshall Space Flight Center Double Layers in Astrophysics May 1987 p 89-103 (For primary document see N87-23313 16-88)

Avail: NTIS HC A14/MF A01 CSCL 20I

In a triple plasma device, the injection of electron current from the source chamber to the target chamber causes the formation of a potential double layer. At a low current density, the space charge of the injected current produces a virtual cathode-type potential double layer. This double layer is stable, and various wave instabilities are observed to associate with this double layer. As the current density is increased, the double layer becomes unstable, and a moving double layer results. As the current density is increased further, the enhanced ionization causes the neutralization of the space charge of the electron beam, and the beam plasma discharge is ignited. Author

N87-23318*# Physical Research Lab., Ahmedabad (India). Plasma Physics Programme.

EXPERIMENTAL OBSERVATION OF ION-ACOUSTIC DOUBLE LAYERS IN LABORATORY PLASMA Abstract Only **c75**

Y. C. Saxena *In* NASA. Marshall Space Flight Center Double Layers in Astrophysics May 1987 p 105 (For primary document see N87-23313 16-88)

Avail: NTIS HC A14/MF A01 CSCL 20I

Experimental results on the observation of ion-acoustic double layers in laboratory plasma are presented. In a double-plasma device, modified suitably to inject an electron beam into the target plasma, modulation of the beam through a step potential leads to excitation of ion-acoustic fluctuations. The fluctuations, growing away from the separating grids, develop into weak asymmetric ion-acoustic double layers. The observations are compared with the scenario emerging out of the computer simulations and analytical results on ion-acoustic double layers. Author

N87-23319*# Iowa Univ., Iowa City. Dept. of Physics and Astronomy.

A NEW HYDRODYNAMIC ANALYSIS OF DOUBLE LAYERS **c75**

Heinrich Hora *In* NASA. Marshall Space Flight Center Double Layers in Astrophysics May 1987 p 109-137 (For primary document see N87-23313 16-88)

Avail: NTIS HC A14/MF A01 CSCL 20I

A genuine two-fluid model of plasmas with collisions permits the calculation of dynamic (not necessarily static) electric fields and double layers inside of plasmas including oscillations and damping. For the first time a macroscopic model for coupling of electromagnetic and Langmuir waves was achieved with realistic damping. Starting points were laser-produced plasmas showing very high dynamic electric fields in nonlinear force-produced cavitous and inverted double layers in agreement with experiments. Applications for any inhomogeneous plasma as in laboratory or in astrophysical plasmas can then be followed up by a transparent hydrodynamic description. Results are the rotation of plasmas in magnetic fields and a new second harmonic resonance, explanation of the measured inverted double layers, explanation of the observed density-independent, second harmonics emission from laser-produced plasmas, and a laser acceleration scheme by the very high fields of the double layers. Author

N87-23320*# Riso National Lab., Roskilde (Denmark). Physics Dept.

ION PHASE-SPACE VORTICES AND THEIR RELATION TO SMALL AMPLITUDE DOUBLE LAYERS **c75**

Hans L. Pecseli *In* NASA. Marshall Space Flight Center Double Layers in Astrophysics May 1987 p 139-145 (For primary document see N87-23313 16-88)

Avail: NTIS HC A14/MF A01 CSCL 20I

The properties of ion phase-space vortices are reviewed with particular attention to their role in the formation of small amplitude double layers in current-carrying plasmas. In a one-dimensional analysis, many such double layers simply add up to produce a large voltage drop. A laboratory experiment is carried out in order to investigate the properties of ion phase-space vortices in three dimensions. Their lifetime is significantly reduced as compared with similar results from one-dimensional numerical simulations of the problem. Author

N87-23321*# Minnesota Univ., Minneapolis. School of Physics and Astronomy.

EFFECT OF DOUBLE LAYERS ON MAGNETOSPHERE-IONOSPHERE COUPLING **c46**

Robert L. Lysak and Mary K. Hudson (Dartmouth Coll., Hanover, N.H.) *In* NASA. Marshall Space Flight Center Double Layers in Astrophysics May 1987 p 147-166 (For primary document see N87-23313 16-88)

Avail: NTIS HC A14/MF A01 CSCL 04A

The Earth's auroral zone contains dynamic processes occurring on scales from the length of an auroral zone field line which characterizes Alfven wave propagation to the scale of microscopic processes which occur over a few Debye lengths. These processes interact in a time-dependent fashion since the current carried by the Alfven waves can excite microscopic turbulence which can in turn provide dissipation of the Alfven wave energy. This review will first describe the dynamic aspects of auroral current structures with emphasis on consequences for models of microscopic turbulence. A number of models of microscopic turbulence will be introduced into a large-scale model of Alfven wave propagation to determine the effect of various models on the overall structure of auroral currents. In particular, the effects of a double layer electric field which scales with the plasma temperature and Debye length is compared with the effect of anomalous resistivity due to electrostatic ion cyclotron turbulence in which the electric field scales with the magnetic field strength. It is found that the double layer model is less diffusive than in the resistive model leading to the possibility of narrow, intense current structures. Author

N87-23322*# Centre National d'Etudes des Telecommunications, Issy-les-Moulineaux (France).

CURRENT DRIVEN WEAK DOUBLE LAYERS **c75**

Gerard Chanteur *In* NASA. Marshall Space Flight Center Double Layers in Astrophysics May 1987 p 167-181 (For primary document see N87-23313 16-88)

Avail: NTIS HC A14/MF A01 CSCL 20I

Double layers in plasmas can be created by different means. For example, a potential difference forms between two plasmas with different temperatures, in a plasma jet flowing along a converging magnetic field, in a quiescent plasma submitted to an external difference of potential, or in a turbulent plasma carrying an electric charge. The first three cases can be current-free, but not necessarily, although the numerical simulations were made under such conditions for the first two points. Apart from the third case, which is mainly of interest for laboratory experiments, these double layers are good candidates for accelerating the auroral electrons to the few kiloelectron volts observed. Author

N87-23323*# Utah State Univ., Logan. Center for Atmospheric and Space Sciences.

ELECTRIC FIELDS AND DOUBLE LAYERS IN PLASMAS **c75**

Nagendra Singh, H. Thiemann, and R. W. Schunk *In* NASA. Marshall Space Flight Center Double Layers in Astrophysics May 1987 p 183-208 (For primary document see N87-23313 16-88)

(Grants NAGw-77; NSF ATM-84-17880)

Avail: NTIS HC A14/MF A01 CSCL 20I

Various mechanisms for driving double layers in plasmas are briefly described, including applied potential drops, currents, contact potentials, and plasma expansions. Some dynamical features of the double layers are discussed. These features, as seen in simulations, laboratory experiments, and theory, indicate that double layers and the currents through them undergo slow oscillations which are determined by the ion transit time across an effective length of the system in which double layers form. It is shown that a localized potential dip forms at the low potential end of a double layer, which interrupts the electron current through it according to the Langmuir criterion, whenever the ion flux into the double is disrupted. The generation of electric fields perpendicular to the ambient magnetic field by contact potentials is also discussed. Two different situations were considered; in one, a low-density hot plasma is sandwiched between high-density cold plasmas, while in the other a high-density current sheet permeates a low-density background plasma. Perpendicular electric fields develop near the contact surfaces. In the case of the current sheet, the creation of parallel electric fields and the formation of double layers are also discussed when the current sheet thickness is varied. Finally, the generation of electric fields and double layers in an expanding plasma is discussed. Author

N87-23324*# Dartmouth Coll., Hanover, N.H.

ELECTRON ACCELERATION IN STOCHASTIC DOUBLE LAYERS Abstract Only **c75**

William Lotko *In* NASA. Marshall Space Flight Center Double Layers in Astrophysics May 1987 p 209 (For primary document see N87-23313 16-88)

Avail: NTIS HC A14/MF A01 CSCL 20I

Transversely localized double layers evolve randomly in turbulent regions of strongly magnetized plasma carrying current along the magnetic field. Results from numerical simulations and spacecraft observations in the auroral plasma indicate that the parallel electric field in such regions is microscopically intermittent or stochastic. The implications of stochastic double layer fields on electron acceleration will be discussed in terms of a statistical process involving ensemble averages over test particle motion. A Fokker-Planck equation can be derived for the electron phase space density, which depends on the mean and rms amplitudes of the double layers, the mean double layer density, and the initial electron velocity distribution. It is shown that the resulting electron acceleration is very sensitive to the ratio of the initial electron energy to the rms double layer amplitude. When this ratio is large, the acceleration process differs little from that expected in a dc electric field. When it is small, stochastic heating competes with directed acceleration. Evidence for both cases can be found in the auroral ionosphere in association with so-called inverted-V precipitation and collimated edge precipitation. Author

N87-23325*# Science Applications International Corp., McLean, Va. Plasma Physics Div.

ANOMALOUS TRANSPORT IN DISCRETE ARCS AND SIMULATION OF DOUBLE LAYERS IN A MODEL AURORAL CIRCUIT **c46**

Robert A. Smith *In* NASA. Marshall Space Flight Center Double Layers in Astrophysics May 1987 p 211-223 (For primary document see N87-23313 16-88)

(Contract NASw-3947)

Avail: NTIS HC A14/MF A01 CSCL 04A

The evolution and long-time stability of a double layer (DL) in a discrete auroral arc requires that the parallel current in the arc, which may be considered uniform at the source, be diverted within the arc to charge the flanks of the U-shaped double layer potential structure. A simple model is presented in which this current redistribution is effected by anomalous transport based on electrostatic lower hybrid waves driven by the flank structure itself. This process provides the limiting constraint on the double layer potential. The flank charging may be represented as that of a nonlinear transmission line. A simplified model circuit, in which the transmission line is represented by a nonlinear impedance in parallel with a variable resistor, is incorporated in a one-dimensional simulation model to give the current density at the DL boundaries. Results are presented for the scaling of the DL potential as a function of the width of the arc and the saturation efficiency of the lower hybrid instability mechanism. Author

N87-23326*# Dartmouth Coll., Hanover, N.H. Dept. of Physics and Astronomy.

WEAK DOUBLE LAYERS IN THE AURORAL IONOSPHERE **c46**

M. K. Hudson, T. L. Crystal, W. Lotko, and C. Barnes (Los Alamos National Lab., N. Mex.) *In* NASA. Marshall Space Flight Center Double Layers in Astrophysics May 1987 p 225-245 (For primary document see N87-23313 16-88)

(Grant NSF ATM-84-45010)

Avail: NTIS HC A14/MF A01 CSCL 04A

Previous work on the evolution of weak double layers in a hydrogen plasma was extended to include H(+) and O(+) with relative drift. The relative drift between hydrogen and oxygen ions due to a quasi-static parallel electric field gives rise to a strong linear fluid instability which dominates the ion-acoustic mode at the bottom of the auroral acceleration region. This ion-ion instability can modify ion distributions at lower altitudes and the subsequent nonlinear evolution of weak double layers at higher altitudes in the ion-acoustic regime. Ion hole formation can occur for smaller relative electron-ion drifts than seen in previous simulations, due to the hydrogen-oxygen two-stream instability. This results in local modification of the ion distributions in phase space, and a partial filling of the valley between the hydrogen and oxygen peaks, which would be expected at higher altitudes on auroral field lines. The observed velocity diffusion does not necessarily preclude ion hole and double layer formation in hydrogen in the ion-acoustic regime. These simulation results are consistent with the experimentally measured persistence of separate hydrogen and oxygen peaks, and the observation of weak double layers above an altitude of 3000 km on auroral field lines. Author

N87-23327*# Princeton Univ., N. J. Physics Lab.
PARTICLE SIMULATION OF AURORAL DOUBLE LAYERS **c46**
Bruce L. Smith and Hideo Okuda *In* NASA. Marshall Space Flight Center Double Layers in Astrophysics May 1987 p 247-263 Sponsored in part by the Aerospace Sponsored Research Program (For primary document see N87-23313 16-88)
Avail: NTIS HC A14/MF A01 CSCL 04A

Work on the simulation of auroral double layers (DLs) with realistic particle-in-cell models is presented. An early model simulated weak DLs formed in a self-consistent circuit but under conditions subject to the ion-acoustic instability. Recent work has focused on strong DLs formed when currentless jets are injected into a dipole magnetic field. Author

N87-23328*# Aerospace Corp., Los Angeles, Calif. Space Sciences Lab.
CONDITIONS FOR DOUBLE LAYERS IN THE EARTH'S MAGNETOSPHERE AND PERHAPS IN OTHER ASTROPHYSICAL OBJECTS **c46**
L. R. Lyons *In* NASA. Marshall Space Flight Center Double Layers in Astrophysics May 1987 p 265-273 Sponsored in part by the Aerospace Sponsored Research Program (For primary document see N87-23313 16-88)
(Contract NASw-861; Grant NAGw-853)
Avail: NTIS HC A14/MF A01 CSCL 04A

Double layers form along auroral field lines in the Earth's magnetosphere. They form in order to maintain current continuity in the ionosphere in the presence of a magnetospheric electric field E with nabla x E is not equal to 0. Features which govern the formation of the double layers are: (1) the divergence of E, (2) the conductivity of the ionosphere, and (3) the current-voltage characteristics of auroral magnetic field lines. Astrophysical situations where nabla x E is not equal to 0 is applied to a conducting plasma similar to the Earth's ionosphere are potential candidates for the formation of double layers. The region with nabla x E is not equal to 0 can be generated within, or along field lines connected to, the conducting plasma. In addition to nabla x E, shear neutral flow in the conducting plasma can also form double layers. Author

N87-23329*# Lockheed Missiles and Space Co., Palo Alto, Calif. Research Lab.
SOME ASPECTS OF DOUBLE LAYER FORMATION IN A PLASMA CONSTRAINED BY A MAGNETIC MIRROR **c46**
W. Lennartsson *In* NASA. Marshall Space Flight Center Double Layers in Astrophysics May 1987 p 275-285 Sponsored in part by the Lockheed Independent Research Program (For primary document see N87-23313 16-88)
(Grant NSF ATM-83-17710)
Avail: NTIS HC A14/MF A01 CSCL 04A

The shift from wave-generated anomalous resistivity toward the more large-scale effects of magnetic confinement of current carrying plasmas was inspired by the more extensive data on auroral particle distribution functions that were made available, data that may often seem consistent with a dissipation-free acceleration of auroral electrons over an extended altitude range. Efforts to interpret these data have brought new vigor to the concept that a smooth and static electric field can be self-consistently generated by suitable pitch angle anisotropies among the high altitude particle populations, different for electrons and ions, and that such an electric field is both necessary and sufficient to maintain the plasma in a quasi-neutral steady state. Certain aspects of this concept are reviewed and criticized, both from a general theoretical standpoint and from the standpoint of what is known about the magnetospheric environment. It is argued that this concept has flaws and that the actual physical problem is considerably more complicated, requiring a more complex electric field, possibly including double layer structures. Author

N87-23330*# National Oceanic and Atmospheric Administration, Boulder, Colo.
ELECTRIC POTENTIAL DISTRIBUTIONS AT THE INTERFACE BETWEEN PLASMASHEET CLOUDS **c46**
D. S. Evans, M. Roth, and J. Lemaire (Institut d'Aeronomie Spatiale de Belgique, Brussels.) *In* NASA. Marshall Space Flight Center Double Layers in Astrophysics May 1987 p 287-294 (For primary document see N87-23313 16-88)
Avail: NTIS HC A14/MF A01 CSCL 04A

At the interface between two plasma clouds with different densities, temperatures, and/or bulk velocities, there are large charge separation electric fields which can be modeled in the framework of a collisionless theory for tangential discontinuities. Two different classes of layers were identified: the first one corresponds to (stable) ion layers which are thicker than one ion Lamor radius; the second one corresponds to (unstable) electron layers which are only a few electron Larmor radii thick. It is suggested that these thin electron layers with large electric potential gradients (up to 400 mV/m) are the regions where large-amplitude electrostatic waves are spontaneously generated. These waves scatter the pitch angles of the ambient plasmasheet electron into the atmospheric loss cone. The unstable electron layers can therefore be considered as the seat of strong pitch angle scattering for the primary auroral electrons. Author

N87-23331*# California Univ., Berkeley. Space Sciences Lab.
DOUBLE LAYERS ABOVE THE AURORA **c46**
M. Temerin and F. S. Mozer *In* NASA. Marshall Space Flight Center Double Layers in Astrophysics May 1987 p 295-303 (For primary document see N87-23313 16-88)
(Contract N00014-81-C-0006)
Avail: NTIS HC A14/MF A01 CSCL 04A

Two different kinds of double layers were found in association with auroral precipitation. One of these is the so-called electrostatic shock, which is oriented at an oblique angle to the magnetic field in such a way that the perpendicular electric field is much larger than the parallel electric field. This type of double layer is often found at the edges of regions of upflowing ion beams and the direction of the electric fields in the shock points toward the ion beam. The potential drop through the shock can be several kV and is comparable to the total potential needed to produce auroral acceleration. Instabilities associated with the shock may generate obliquely propagating Alfven waves, which may accelerate electrons to produce flickering auroras. The flickering aurora provides evidence that the electrostatic shock may have large temporal fluctuations. The other kind of double layer is the small-amplitude double layer found in regions of upward flowing in beams, often in association with electrostatic ion cyclotron waves. The parallel and perpendicular electric fields in these structures are comparable in magnitude. The associated potentials are a few eV. Since many such double layers are found in regions of upward flowing ion beams, the combined potential drop through a set of these double layers can be substantial. Author

N87-23332*# Los Alamos National Lab., N. Mex.
BEAMED EMISSION FROM GAMMA-RAY BURST SOURCES Abstract Only **c93**
R. Epstein *In* NASA. Marshall Space Flight Center Double Layers in Astrophysics May 1987 p 305 (For primary document see N87-23313 16-88)
Avail: NTIS HC A14/MF A01 CSCL 03B

Gamma-ray bursts are intense fluxes of radiation in the 100 keV to several MeV energy range which typically persist for between a fraction of a second to several seconds. The observed spectral shape of these bursts suggest that the radiation is emitted as highly collimated beams emanating from neutron stars. This inference is based on the lack of significant gamma-gamma absorption (which are produced when gamma rays interact with stellar surfaces). The gamma-ray beams may be a consequence of a particle acceleration in double layers in neutron star magnetospheres. Author

N87-23333*# Los Alamos National Lab., N. Mex. Space Plasma Physics Group.
DOUBLE LAYERS AND PLASMA-WAVE RESISTIVITY IN EXTRAGALACTIC JETS: CAVITY FORMATION AND RADIO-WAVE EMISSION **c93**
Joseph E. Borovsky *In* NASA. Marshall Space Flight Center Double Layers in Astrophysics May 1987 p 307-315 Sponsored in part by DOE (For primary document see N87-23313 16-88)
Avail: NTIS HC A14/MF A01 CSCL 03B

For estimated values of the currents carried by extragalactic jets, current-driven electrostatic-wave- and electromagnetic-wave-produced resistivities do not occur. Strong plasma double layers, however, may exist within self-maintained density cavities, the relativistic double-layer-emitted electron, and ion beams driving plasma-wave resistivities in the low- and high-potential plasma adjacent to the double layers. The double-layer-emitted electron beams may also emit polarized radio waves via a collective bremsstrahlung process mediated by electrostatic two-stream instabilities. Author

N87-23334*# National Aeronautics and Space Administration. Marshall Space Flight Center, Huntsville, Ala.
ACCRETION ONTO NEUTRON STARS WITH THE PRESENCE OF A DOUBLE LAYER Abstract Only **c75**
A. C. Williams, M. C. Weisskopf, R. F. Elsner, W. Darbro, and P. G. Sutherland (McMaster Univ., Hamilton, Ontario) *In its* Double Layers in Astrophysics May 1987 p 317 Previously announced in IAA as A86-43296 (For primary document see N87-23313 16-88)
Avail: NTIS HC A14/MF A01 CSCL 20I

It is known, from laboratory experiments, that double layers will form in plasmas, usually in the presence of an electric current. It is argued that a double layer may be present in the accretion column of a neutron star in a binary system. It is suggested that the double layer may be the predominant deceleration mechanism for the accreting ions, especially for sources with X-ray luminosities of less than about 10 to the 37th erg/s. Previous models have involved either a collisionless shock or an assumed gradual deceleration of the accreting ions to thermalize the energy of the infalling matter. Author

N87-23335*# National Aeronautics and Space Administration. Marshall Space Flight Center, Huntsville, Ala.
THE FORMATION OF A DOUBLE LAYER LEADING TO THE CRITICAL VELOCITY PHENOMENON **c75**
A. C. Williams *In its* Double Layers in Astrophysics May 1987 p 319-328 (For primary document see N87-23313 16-88)
Avail: NTIS HC A14/MF A01 CSCL 20I

The formation of a double layer is proposed as the mechanism which produces the critical velocity phenomenon. This hypothesis was examined qualitatively and it was found that the double layer can be a very efficient mechanism for transferring the kinetic energy of the neutral gas into the kinetic energy of electrons which, in turn, will ionize the neutral gas if the critical velocity was reached or exceeded. Author

89 ASTRONOMY

Includes radio, gamma-ray, and infrared astronomy, and astrometry.

N87-23336*# Wisconsin Univ., Madison.
A STUDY OF THE FUNDAMENTAL CHARACTERISTICS OF 2175A EXTINCTION Semiannual Progress Report
Jason A. Cardelli and Blair D. Savage 11 Jun. 1987 45 p
(Grant NAG5-832)
(NASA-CR-180926; NAS 1.26:180926) Avail: NTIS HC A03/MF A01 CSCL 03A

(NASA-CR-180926; NAS 1.26:180926) Avail: NTIS HC A03/MF A01 CSCL 03A

The characteristics of interstellar extinction were studied in the region of the 2175 A feature for lines of sight which appear to exhibit unusually weak ultraviolet extinction. The analysis was based upon a parameterization of the observed extinction via fitting specific mathematical functions in order to determine the position and width of the 2175 A feature. The data are currently being analyzed. B.G.

N87-23421*# Hawaii Inst. of Geophysics, Honolulu. Planetary Geosciences Div.
REFLECTANCE SPECTRA OF MAFIC SILICATES AND PHYLLOSILICATES FROM .6 TO 4.6 MICRONS
Ted L. Roush, Robert B. Singer, and Thomas B. McCord *In* NASA, Washington Reports of Planetary Geology and Geophysics Program, 1986 May 1987 p 187-189 (For primary document see N87-23341 16-91)
(Grants NsG-7590; NsG-7312)
Avail: NTIS HC A24/MF A01 CSCL 03A

90 ASTROPHYSICS

Includes cosmology; celestial mechanics; space plasmas; and interstellar and interplanetary gases and dust.
For related information see also *75 Plasma Physics.*

N87-23337# Royal Inst. of Tech., Stockholm (Sweden). Dept. of Plasma Physics.
THE EARTH'S MAGNETOSPHERE AS A SAMPLE OF THE PLASMA UNIVERSE
Carl-Gunne Faelthammar Sep. 1986 24 p Presented at the NASA-OAST Workshop on Space Technology Plasma Issues in 2001, Pasadena, Calif., 24-26 Sep. 1986
(TRITA-EPP-86-12; ISSN-0348-7539; ETN-87-99786) Avail: NTIS HC A02/MF A01

Observations and experiments in the near-Earth plasma are discussed. They can clarify the dynamics of the sapce environment and widen our understanding of matter. They can form a basis interpretating remote observations of astrophysical objects, thereby helping to reconstruct events that led to the evolution of our solar system. They can provide know-how required for adapting space-based technology to the plasma environment. ESA

N87-23338# Air Force Inst. of Tech., Wright-Patterson AFB, Ohio. School of Engineering.
PERIODIC ORBITS ABOUT ROTATING ASTEROIDS IN FREE SPACE M.S. Thesis
Kerry D. Hicks Dec. 1986 75 p
(AD-A179387; AFIT/GA/AA/86D-7) Avail: NTIS HC A04/MF A01 CSCL 03C

In this investigation of periodic orbits about asteroids rotating in free space, oscillatory orbits about equilibrium points as well as those orbits encircling the body were found. While a method was derived for finding orbits of all inclinations, only equatorial orbits are presented. The major emphasis is on stable, periodic orbits, but certain unstable orbits are presented where appropriate. The analysis assumed that asteroids could be represented by triaxial ellipsoidal bodies rotating about their major axis of inertia. Hamilton's canonical equations were derived to describe the dynamics. An algorithm was then developed and used to solve the equations of motion in such a way as to find closed, periodic orbits. GRA

N87-23339# International Centre for Theoretical Physics, Trieste (Italy).
POSSIBLE INFLATIONARY SOLUTION TO THE SHORT DISTANCE GRAVITY MODEL
K. G. Akdeniz, A. Hacinliyan, and J. Kalayci Sep. 1986 8 p
(DE87-701559; IC-86/291) Avail: NTIS (US Sales Only) HC A02/MF A01

We find a solution involving a time dependent cosmological constant to the short distance gravity model which may be interpreted as inflationary. DOE

N87-23340*# California Univ., Santa Cruz.
NUMERICAL STUDIES OF COLLAPSING INTERSTELLAR CLOUDS Final Technical Report
Peter Bodenheimer, Karen R. Villere (California Univ., Santa Cruz.), and David C. Black 1 May 1987 25 p
(Grant NAG2-368)
(NASA-CR-180933; NAS 1.26:180933) Avail: NTIS HC A02/MF A01 CSCL 03B

Numerical simulation of the structure and evolution of interstellar clouds was conducted. Steps were taken toward an integrated treatment of the dynamical, thermal, and chemical processes entering model calculations, and a detailed study was made of radiative transfer in molecular lines to allow model predictions to be tested against empirical data. It is shown that the shapes of molecular lines are sensitive to details of the cloud structure and evolutionary state and are thus useful in inferring the cloud density, temperature, chemical composition, age, and initial conditions. The calculations have successfully reproduced and explained several observed cloud properties, including abundances of complex molecular species and the apparent depletion of CO in dense cores. Author

N87-23366*# Jet Propulsion Lab., California Inst. of Tech., Pasadena.
COMET THERMAL MODELING
Paul R. Weissman and Hugh H. Kieffer (Geological Survey, Flagstaff, Ariz.) *In* NASA, Washington Reports of Planetary Geology and Geophysics Program, 1986 May 1987 p 66-68 (For primary document see N87-23341 16-91)
Avail: NTIS HC A24/MF A01 CSCL 03B

N87-23367*# Hawaii Inst. of Geophysics, Honolulu. Planetary Geosciences Div.
THE LOSS AND DEPTH OF CO2 ICE IN COMET NUCLEI
F. P. Fanale and J. R. Salvail *In* NASA, Washington Reports of Planetary Geology and Geophysics Program, 1986 May 1987 p 69 (For primary document see N87-23341 16-91)
Avail: NTIS HC A24/MF A01 CSCL 03B

N87-23368*# Jet Propulsion Lab., California Inst. of Tech., Pasadena. Earth and Space Sciences Div.
DYNAMICS OF LONG PERIOD COMETS
Paul R. Weissman *In* NASA, Washington Reports of Planetary Geology and Geophysics Program, 1986 May 1987 p 70-71 (For primary document see N87-23341 16-91)
Avail: NTIS HC A24/MF A01 CSCL 03B

N87-23369*# Geological Survey, Flagstaff, Ariz.
OBSERVATIONS ON THE MAGNITUDE-FREQUENCY DISTRIBUTION OF EARTH-CROSSING ASTEROIDS
Eugene M. Shoemaker and Carolyn S. Shoemaker (Arizona Research and Technology, Flagstaff.) *In* NASA, Washington Reports of Planetary Geology and Geophysics Program, 1986 May 1987 p 72-74 (For primary document see N87-23341 16-91)
Avail: NTIS HC A24/MF A01 CSCL 03B

N87-23370*# Jet Propulsion Lab., California Inst. of Tech., Pasadena.
ASTEROID FAMILIES, DYNAMICS AND ASTROMETRY
J. G. Williams and J. Gibson *In* NASA, Washington Reports of Planetary Geology and Geophysics Program, 1986 May 1987 p 75-76 (For primary document see N87-23341 16-91)
Avail: NTIS HC A24/MF A01 CSCL 03B

N87-23371*# Hawaii Inst. of Geophysics, Honolulu. Planetary Geosciences Div.
THE 1986 DA AND 1986 EB: M-CLASS ASTEROIDS IN NEAR-EARTH ORBITS
Jonathan Gradie and Edward Tedesco (Jet Propulsion Lab., California Inst. of Tech., Pasadena.) *In* NASA, Washington Reports of Planetary Geology and Geophysics Program, 1986 May 1987 p 77-79 (For primary document see N87-23341 16-91)
Avail: NTIS HC A24/MF A01 CSCL 03B

N87-23373*# Rensselaer Polytechnic Inst., Troy, N.Y. Dept. of Geology.
METEORITE SPECTROSCOPY AND CHARACTERIZATION OF ASTEROID SURFACE MATERIALS
Michael J. Gaffey *In* NASA, Washington Reports of Planetary Geology and Geophysics Program, 1986 May 1987 p 81-83 (For primary document see N87-23341 16-91)
Avail: NTIS HC A24/MF A01 CSCL 03B

N87-23374*# Brown Univ., Providence, R. I. Dept. of Geological Sciences.
SOURCE OF THE OPTICAL RED-SLOPE IN IRON-RICH METEORITES
Daniel T. Britt, Carle M. Pieters, and Peter H. Schultz *In* NASA, Washington Reports of Planetary Geology and Geophysics Program, 1986 May 1987 p 84 (For primary document see N87-23341 16-91)
Avail: NTIS HC A24/MF A01 CSCL 03B

N87-23376*# National Aeronautics and Space Administration. Lyndon B. Johnson Space Center, Houston, Tex.
ANALYTICAL ELECTRON MICROSCOPY OF FINE-GRAINED PHASES IN PRIMITIVE INTERPLANETARY DUST PARTICLES AND CARBONACEOUS CHONDRITES
Ian D. R. Mackinnon, Frans J. M. Rietmeijer (New Mexico Univ., Albuquerque.), and David S. McKay *In* NASA, Washington Reports of Planetary Geology and Geophysics Program, 1986 May 1987 p 87-89 (For primary document see N87-23341 16-91)
Avail: NTIS HC A24/MF A01 CSCL 03B

N87-23381*# Virginia Univ., Charlottesville.
FORMATION OF GIANT MOLECULAR CLOUDS IN GLOBAL SPIRAL STRUCTURES: THE ROLE OF ORBITAL DYNAMICS AND CLOUD-CLOUD COLLISIONS
W. W. Roberts, Jr. and G. R. Stewart *In* NASA, Washington Reports of Planetary Geology and Geophysics Program, 1986 May 1987 p 101 (For primary document see N87-23341 16-91)
(Grants NAGw-929; NSF AST-82-04256)
Avail: NTIS HC A24/MF A01 CSCL 03B

N87-23385*# National Aeronautics and Space Administration, Washington, D.C.
A SCALING LAW FOR ACCRETION ZONE SIZES Abstract Only
Yuval Greenzweig and Jack J. Lissauer *In* NASA, Washington Reports of Planetary Geology and Geophysics Program, 1986 May 1987 p 108 (For primary document see N87-23341 16-91)
Avail: NTIS HC A24/MF A01 CSCL 03B

N87-23387*# Planetary Science Inst., Tucson, Ariz.
COLLISIONAL AND DYNAMICAL PROCESSES IN MOON AND PLANET FORMATION
C. R. Chapman, D. R. Davis, S. J. Weidenschilling, W. K. Hartmann, and D. Spaute *In* NASA, Washington Reports of Planetary Geology and Geophysics Program, 1986 May 1987 p 112-114 (For primary document see N87-23341 16-91)
Avail: NTIS HC A24/MF A01 CSCL 03B

N87-23388*# National Aeronautics and Space Administration, Washington, D.C.
DYNAMICAL CONSTRAINTS ON THE ORIGIN OF THE MOON Abstract Only
A. P. Boss and S. J. Peale (California Univ., Santa Barbara.) *In* NASA, Washington Reports of Planetary Geology and Geophysics Program, 1986 May 1987 p 115 Previously announced in IAA as A87-20628 (For primary document see N87-23341 16-91)
Avail: NTIS HC A24/MF A01 CSCL 03B

N87-23390*# Massachusetts Inst. of Tech., Cambridge. Dept. of Earth, Atmospheric and Planetary Sciences.
SOLAR SYSTEM DYNAMICS
Jack Wisdom *In* NASA, Washington Reports of Planetary Geology and Geophysics Program, 1986 May 1987 p 117-119 (For primary document see N87-23341 16-91)
Avail: NTIS HC A24/MF A01 CSCL 03B

N87-23392*# Cornell Univ., Ithaca, N.Y.
DYNAMICS OF SATELLITES, ASTEROIDS, AND RINGS
Stanley F. Dermott *In* NASA, Washington Reports of Planetary Geology and Geophysics Program, 1986 May 1987 p 121-123 (For primary document see N87-23341 16-91)
Avail: NTIS HC A24/MF A01 CSCL 03B

N87-23393*# Virginia Univ., Charlottesville.
HAMILTONIAN THEORY OF NONLINEAR WAVES IN PLANETARY RINGS Abstract Only
G. R. Stewart *In* NASA, Washington Reports of Planetary Geology and Geophysics Program, 1986 May 1987 p 124 (For primary document see N87-23341 16-91)
(Grants NAGw-929; NSF AST-82-004256)
Avail: NTIS HC A24/MF A01 CSCL 03B

N87-23394*# National Aeronautics and Space Administration. Ames Research Center, Moffett Field, Calif.
PLANETARY RING DYNAMICS AND MORPHOLOGY
Jeffrey N. Cuzzi, Richard H. Durisen, and Frank H. Shu (California Univ., Berkeley.) *In* NASA, Washington Reports of Planetary Geology and Geophysics Program, 1986 May 1987 p 125-127 (For primary document see N87-23341 16-91)
Avail: NTIS HC A24/MF A01 CSCL 03B

N87-23402*# Arizona Univ., Tucson. Lunar and Planetary Lab.
MAGNETIC FLARES IN THE PROTOPLANETARY NEBULA AND THE ORIGIN OF METEORITE CHONDRULES Abstract Only
E. H. Levy and S. Araki *In* NASA, Washington Reports of Planetary Geology and Geophysics Program, 1986 May 1987 p 147 (For primary document see N87-23341 16-91)
Avail: NTIS HC A24/MF A01 CSCL 03B

N87-23403*# Arizona Univ., Tucson. Lunary and Planetary Lab.
GENERATION OF A DYNAMO MAGNETIC FIELD IN A PROTOPLANETARY ACCRETION DISK Abstract Only
T. Stepinski and E. H. Levy *In* NASA, Washington Reports of Planetary Geology and Geophysics Program, 1986 May 1987 p 148 (For primary document see N87-23341 16-91)
Avail: NTIS HC A24/MF A01 CSCL 03B

N87-23434*# Pittsburgh Univ., Pa.
ON THE SPUTTER ALTERATION OF REGOLITHS OF OUTER SOLAR SYSTEM BODIES Abstract Only
Bruce Hapke *In* NASA, Washington Reports of Planetary Geology and Geophysics Program, 1986 May 1987 p 220 Submitted for publication (For primary document see N87-23341 16-91)
Avail: NTIS HC A24/MF A01 CSCL 03B

N87-23435*# Virginia Univ., Charlottesville.
CHARGED PARTICLE MODIFICATION OF SURFACES IN THE OUTER SOLAR SYSTEM
R. E. Johnson *In* NASA, Washington Reports of Planetary Geology and Geophysics Program, 1986 May 1987 p 221-222 (For primary document see N87-23341 16-91)
(Grant NAGw-186)
Avail: NTIS HC A24/MF A01 CSCL 03B

N87-23499*# Planetary Science Inst., Tucson, Ariz.
IMPACT AND CRATERING PROCESSES ON ASTEROIDS, SATELLITES, AND PLANETS
Clark R. Chapman, Donald R. Davis, and Stuart J. Weidenschilling *In* NASA, Washington Reports of Planetary Geology and Geophysics Program, 1986 May 1987 p 399-401 (For primary document see N87-23341 16-91)
Avail: NTIS HC A24/MF A01 CSCL 03B

N87-23500*# Geological Survey, Flagstaff, Ariz.
CRATER PRODUCTION ON VENUS AND EARTH BY ASTEROID AND COMET IMPACT
Eugene M. Shoemaker and Ruth F. Wolfe *In* NASA, Washington Reports of Planetary Geology and Geophysics Program, 1986 May 1987 p 402-404 (For primary document see N87-23341 16-91)
Avail: NTIS HC A24/MF A01 CSCL 03B

91 LUNAR AND PLANETARY EXPLORATION

Includes planetology; and manned and unmanned flights. For spacecraft design or space stations see *18 Spacecraft Design, Testing and Performance.*

N87-23341*# National Aeronautics and Space Administration, Washington, D.C.
REPORTS OF PLANETARY GEOLOGY AND GEOPHYSICS PROGRAM, 1986
May 1987 558 p
(NASA-TM-89810; NAS 1.15:89810) Avail: NTIS HC A24/MF A01 CSCL 03B

Abstracts compiled from reports from Principal Investigators of the NASA Planetary Geology and Geophysics Program, Office of Space Science and Applications are presented. The purpose is to document in summary form work conducted in this program during 1986. Each report reflects significant accomplishments within the area of the author's funded grant or contract. For individual titles, see N87-23342 through N87-23559.

N87-23342*# Arizona Univ., Tucson. Dept. of Planetary Sciences.
THE CRATERING RECORD AT URANUS: IMPLICATIONS FOR SATELLITE EVOLUTION AND THE ORIGIN OF IMPACTING OBJECTS
Robert G. Strom *In* NASA, Washington Reports of Planetary Geology and Geophysics Program, 1986 May 1987 p 3-5 (For primary document see N87-23341 16-91)
Avail: NTIS HC A24/MF A01 CSCL 03B

The crater size/frequency distributions on the major Uranian satellites show two distinctly different crater populations of different ages. Any hypothesis on the origin of the objects responsible for the period of heavy bombardment must account for the occurrence of different crater populations (size/frequency distributions) in different parts of the solar system. A computerized simulation using short-period comet impact velocities and a modified Holsapple-Schmidt crater scaling law was used to recover the size distribution of cometary nuclei from the observed cratering record. The most likely explanation for the cratering record is that the period of heavy bombardment was caused by different families of accretional remnants indigenous to the system in which the different crater populations occurred. B.G.

N87-23343*# Arizona Univ., Tucson. Lunar and Planetary Lab.
CRATER MORPHOLOGY AND MORPHOMETRY ON THE URANIAN SATELLITES
Steven K. Croft *In* NASA, Washington Reports of Planetary Geology and Geophysics Program, 1986 May 1987 p 6-8 (For primary document see N87-23341 16-91)
Avail: NTIS HC A24/MF A01 CSCL 03B

Fresh craters on the icy Uranian satellites exhibit a range of morphologies similar to craters on the icy satellites of Jupiter and Saturn. The general structural features found in the craters are described. Estimates of transition diameters from simple to complex crater morphologies are given for the five large Uranian satellites and 1985U1, and plotted with transition diameters on other bodies against surface gravity. Possible large-scale impacts are discussed. B.G.

N87-23344*# National Aeronautics and Space Administration, Washington, D.C.
CRATERING HISTORY OF MIRANDA
J. B. Plescia (Geological Survey, Flagstaff, Ariz.) and J. M. Boyce *In its* Reports of Planetary Geology and Geophysics Program, 1986 May 1987 p 9-11 (For primary document see N87-23341 16-91)
Avail: NTIS HC A24/MF A01 CSCL 03B

The surface of the southern hemisphere of Miranda imaged by Voyager 2 is divisible into two general types of terrain: cratered terrain, characterized by numerous craters and undulating intercrater plains; and basins, circular to rectangular areas of complex morphology having large-scale albedo markings. To determine the relative ages of the terrains and the length of geological activity, crater-frequency data were compiled for various parts of the cratered terrain and basins. Crater-frequency data indicate that the cratered terrain is the oldest terrain on Miranda and that it was locally resurfaced. B.G.

N87-23345*# National Aeronautics and Space Administration. Ames Research Center, Moffett Field, Calif.
THE VISCOSITY OF MIRANDA
P. J. Thomas, R. T. Reynolds, S. W. Squyres, and P. M. Cassen *In* NASA, Washington Reports of Planetary Geology and Geophysics Program, 1986 May 1987 p 12-14 (For primary document see N87-23341 16-91)
Avail: NTIS HC A24/MF A01 CSCL 03B

Voyager 2 images of Miranda revealed a significant history of geological activity. Overlying an apparently ancient cratered terrain are assemblages of concentric ridges, scarps, and dark banded material. The problems that evolutionary thermal and structural modes of Miranda must face, to provide a convincing explanation for such topographic complexity, are examined. B.G.

N87-23346*# Arizona Univ., Tucson. Lunar and Planetary Lab.
MECHANICAL AND THERMAL PROPERTIES OF PLANETOLOGICALLY IMPORTANT ICES
Steven K. Croft *In* NASA, Washington Reports of Planetary Geology and Geophyiscs Program, 1986 May 1987 p 15-17 (For primary document see N87-23341 16-91)
Avail: NTIS HC A24/MF A01 CSCL 03B

Two squences of ice composition were proposed for the icy satellites: a dense nebula model and a solar nebula model. Careful modeling of the structure, composition, and thermal history of satellites composed of these various ices requires quantitative information on the density, compressibility, thermal expansion, heat capacity, and thermal conductivity. Equations of state were fitted to the density data of the molecular ices. The unusual thermal and mechanical properties of the molecular and binary ices suggest a larger range of phenomena than previously anticipated, sufficiently complex perhaps to account for many of the unusual geologic phenomena found on the icy satellites. B.G.

N87-23347*# California Univ., Santa Barbara.
COULD ARIEL HAVE BEEN HEATED BY TIDAL FRICTION?
S. J. Peale *In* NASA, Washington Reports of Planetary Geology and Geophysics Program, 1986 May 1987 p 18 (For primary document see N87-23341 16-91)
Avail: NTIS HC A24/MF A01 CSCL 03B

For significant dissipation in Ariel, the past existence of an orbital resonance to force and maintain a substantial eccentricity in the orbit is hypothesized. The absolute maximum dissipation rate would be reduced both by the time necessary to establish the resonance in the first place and by a consequently larger minimum Q. The actual heating rate was much less than this maximum so even the existence of a 2/1 resonance may not be sufficient to account for Ariel's smooth sufrace. B.G.

N87-23348*# National Aeronautics and Space Administration, Washington, D.C.
GEOLOGY AND CRATERING HISTORY OF ARIEL
J. B. Plescia (Geological Survey, Flagstaff, Ariz.) and J. M. Boyce *In its* Reports of Planetary Geology and Geophysics Program, 1986 May 1987 p 19-21 (For primary document see N87-23341 16-91)
Avail: NTIS HC A24/MF A01 CSCL 03B

The surface of Ariel imaged by Voyager 2 can be divided into several types of terrain on the basis of morphology: cratered terrain, subdued terrain, ridged terrain, and plains. Crater statistics were compiled for each of the terrain types. Despite differing morphology, the various terrains on Ariel do not exhibit large variations in crater frequency. None of the observed surfaces on Ariel record the period of accretion. It seems that conditions appropriate for resurfacing could have occurred during the early history of Ariel. B.G.

N87-23349*# California Univ., Santa Barbara.
ON THE LACK OF COMMENSURABILITIES IN THE MEAN MOTIONS OF THE SATELLITES OF URANUS AND THE RESURFACING OF ARIEL
S. J. Peale *In* NASA, Washington Reports of Planetary Geology and Geophysics Program, 1986 May 1987 p 22 (For primary document see N87-23341 16-91)
Avail: NTIS HC A24/MF A01 CSCL 03B

The lack of commensurabilites among the mean motion of the satellites of Uranus is investigated by determining the probabilities of capture into those orbital resonances which might be encountered as the satellite orbits expand differentially from tidal torques. An alternate to this is investigated to evaluate the conditions necessary to allow sufficient tidal heating of Ariel for the observed resurfacing. B.G.

N87-23350*# Geological Survey, Flagstaff, Ariz.
ORBITAL DYNAMICS OF THE URANIAN SATELLITES BASED ON VOYAGER DATA
J. B. Plescia *In* NASA, Washington Reports of Planetary Geology and Geophysics Program, 1986 May 1987 p 23-25 (For primary document see N87-23341 16-91)
Avail: NTIS HC A24/MF A01 CSCL 03B

The satellites of Uranus all have significant non-zero eccentricities and in the case of Miranda a significant inclination as well. The Voyager 2 encounter with Uranus in January 1986, provided more accurate estimates of the masses and sizes of the satellites. Orbital history and possible tidal heating were reexamined by using the Voyager data. The relevant orbital dynamics equations are described. B.G.

N87-23351*# California Univ., Santa Barbara.
WHY NO ORBITAL RESONANCES AMONG THE SATELLITES OF URANUS?
S. J. Peale *In* NASA, Washington Reports of Planetary Geology and Geophysics Program, 1986 May 1987 p 26 (For primary document see N87-23341 16-91)
Avail: NTIS HC A24/MF A01 CSCL 03B

Most of the orbital resonances among the satellites of the major planets are thought to be assembled by differential tidal expansion of their orbits. Why this has not occurred for the Uranus system can be investigated by determining the resonances which would be encountered for various values of Uranus' tidal effective Q. The comparison and the possible escape of Ariel-Umbriel from the 5:3 resonance mean that it is not unreasonable that no orbital resonances are found among these satellites. B.G.

N87-23352*# Cornell Univ., Ithaca, N.Y.
VOYAGER OBSERVATIONS OF 1985U1
P. Thomas and J. Veverka *In* NASA, Washington Reports of Planetary Geology and Geophysics Program, 1986 May 1987 p 27-29 (For primary document see N87-23341 16-91)
(Grants NsG-7156; NAGw-111)
Avail: NTIS HC A24/MF A01 CSCL 03B

Of the 10 small Uranian satellites, 1985U1 is the largest and the only one for which a resolved image was obtained by Voyager 2. In terms of albedo, the other nine satellites seem to be similar. Thus the single image of 1985U1 is important in suggesting what these other objects may be like. Size, shape, surface features, and photometry are examined. B.G.

N87-23353*# Massachusetts Inst. of Tech., Cambridge. Dept. of Earth, Atmospheric and Planetary Sciences.

KINEMATICS AND DYNAMICS OF THE URANIAN RINGS

Richard G. French *In* NASA, Washington Reports of Planetary Geology and Geophysics Program, 1986 May 1987 p 30-32 (For primary document see N87-23341 16-91)
Avail: NTIS HC A24/MF A01 CSCL 03B

The self-gravity model of apse alignment was tested by comparing its predictions about structure within the epsilon ring with an extensive set of observed occultation profiles covering a wide range of ring longitudes. The self-gravity model as presently constructed is inconsistent with the observations. The Lindblad resonance survey and Shepherd satellite ring perturbation are discussed. The kinematic model of the Uranian ring orbit was enhanced to accommodate Voyager observations as well as ground-based occultation observations. B.G.

N87-23354*# Cornell Univ., Ithaca, N.Y.

SHAPES OF SMALL SATELLITES

P. Thomas *In* NASA, Washington Reports of Planetary Geology and Geophysics Program, 1986 May 1987 p 35-36 (For primary document see N87-23341 16-91)
(Grant NAGw-111)
Avail: NTIS HC A24/MF A01 CSCL 03B

The accurate measurement of limb coordinates on small satellite is the major technique for evaluating their sizes and shapes in the absence of good stereoscopic image coverage. The shapes of satellites may be clues to their internal structure if they are relaxed into ellipsoids. The distinction between irregular and ellipsoidal satellites can now be made quantitatively with the availability of many accurate limb profiles of satellites. The residuals from these fit ellipses provide a convenient and quantitative measure of the topography on the satellites. Departures from gravitational (and tidal) equipotentials would be greater, but on the average this is a good measure of the relaxed or nonrelaxed nature of the shape of the objects. The limb topography is also related to specific forms on the objects, and a systematic survey of these forms on small and larger objects is underway. Author

N87-23355*# National Aeronautics and Space Administration. Ames Research Center, Moffett Field, Calif.

ACCRETIONAL HEATING OF THE SATELLITES OF SATURN AND URANUS

Steven W. Squyres, Ray T. Reynolds, Audrey L. Summers, and Felix Shung (Sterling Software, Palo Alto, Calif.) *In* NASA, Washington Reports of Planetary Geology and Geophysics Program, 1986 May 1987 p 37-39 (For primary document see N87-23341 16-91)
Avail: NTIS HC A24/MF A01 CSCL 03B

Voyager images of the satellites of Saturn and Uranus have shown that these bodies are characterized by remarkable diversity and surprisingly complex geologic histories. Despite their small sizes, a number of the satellites show unambiguous evidence for resurfacing. The goal was to develop a detailed model for heating of these small satellites, and then to explore the consequences of variations in the free parameters in the model. Specifically an attempt was made to determine for what range of conditions melting will occur in these satellites. Along with varying a number of model parameters, the important effects of inclusion of small amounts of ammonia and methane in the system were considered. B.G.

N87-23356*# California Univ., Los Angeles. Dept. of Earth and Space Sciences.

INVESTIGATIONS OF THE SURFACES AND INTERIORS OF OUTER PLANET SATELLITES

Gerald Schubert *In* NASA, Washington Reports of Planetary Geology and Geophysics Program, 1986 May 1987 p 40-42 (For primary document see N87-23341 16-91)
Avail: NTIS HC A24/MF A01 CSCL 03B

Studies during 1985/86 include tidal heating and the structure and evolution of Io and Europa, crater relaxation on icy satellites using realistic non-Newtonian ice rheology, and convection through phase transition in the interiors of icy satellites. The abstracts of published papers on these subjects are reproduced. Author

N87-23357*# Jet Propulsion Lab., California Inst. of Tech., Pasadena.

FAILURE STRENGTH OF ICY LITHOSPHERES

M. P. Golombek and W. B. Banerdt *In* NASA, Washington Reports of Planetary Geology and Geophysics Program, 1986 May 1987 p 43-45 (For primary document see N87-23341 16-91)
Avail: NTIS HC A24/MF A01 CSCL 03B

Lithospheric strengths derived from friction on pre-existing fractures and ductile flow laws show that the tensile strength of intact ice under applicable conditions is actually an order of magnitude stronger than widely assumed. It is demonstrated that this strength is everywhere greater than that required to initiate frictional sliding on pre-existing fractures and faults. Because the tensile strength of intact ice increases markedly with confining pressure, it actually exceeds the frictional strength at all depths. Thus, icy lithospheres will fail by frictional slip along pre-existing fractures at yeild stresses greater than previously assumed rather than opening tensile cracks in intact ice. B.G.

N87-23358*# Washington Univ., St. Louis, Mo. Dept. of Earth and Planetary Sciences.

STUDIES OF OUTER PLANET SATELLITES, MERCURY AND URANUS

William B. McKinnon and Paul M. Schenk *In* NASA, Washington Reports of Planetary Geology and Geophysics Program, 1986 May 1987 p 46-48 (For primary document see N87-23341 16-91)
(Grant NAGw-432)
Avail: NTIS HC A24/MF A01 CSCL 03B

Arguments were made, based on geometry, for both an impact and an internal origin for the ancient, partially preserved furrow system of Ganymede. It was concluded that furrows were not concentric, but could be impact related if multiringed structures on icy satellites are initially noncircular. The geometry of the Valhalla ring structure on Callisto was examined in order to assess the circularity of an unmodified ring system. The Ganymede furrow system was remapped to make use of improvements in coordinate control. The least-squares center of curvature for all furrows in the Marius and Galileao Regio is -20.7, and 179.2 degrees. Furrows in Marius and Galileo Regio are reasonably concentric, and are much more circular than previously estimated. The perceived present nonalignment of the assumed originally concentric furrows were used to argue for large-scale lateral motion of dark terrain blocks in Ganymede's crust, presumably in association with bright terrain formation., The overall alignment of furrows as well as the inherent scatter in centers of curvature from subregions of Galileo and Marius do not support this hypothesis. B.G.

N87-23359*# Hawaii Inst. of Geophysics, Honolulu. Planetary Geosciences Div.

SO2 ON IO: A THERMODYNAMIC PERSPECTIVE

Aaron P. Zent and Fraser P. Fanale *In* NASA, Washington Reports of Planetary Geology and Geophysics Program, 1986 May 1987 p 49-51 (For primary document see N87-23341 16-91)
Avail: NTIS HC A24/MF A01 CSCL 03B

The presence of condensed SO2 on Io mandates a finite abundance of SO2 vapor which must be present, regardless of plume activity. The absorption of SO2 was measured on particulate sulfur and the equilibrium between absorbed SO2, SO2 vapor, and SO2 ice examined, based upon measurements and simple thermodynamic considerations. B.G.

N87-23360*# Cornell Univ., Ithaca, N.Y.

INVESTIGATIONS OF PLANETARY RING PHENOMENA

Joseph A. Burns *In* NASA, Washington Reports of Planetary Geology and Geophysics Program, 1986 May 1987 p 52-54 (For primary document see N87-23341 16-91)
Avail: NTIS HC A24/MF A01 CSCL 03B

Faint planetary rings, their dynamical behavior and physical properties, were the main focus of the research efforts. The motion of weakly-charged dust through the gravitational and magnetic fields of Jupiter were examined. Several topics concerning features of Saturn's rings were addressed. The origin and fate of the Uranian ring dust is presently being studied. B.G.

N87-23361*# National Aeronautics and Space Administration, Washington, D.C.
SUBCENTIMETER-SIZE PARTICLE DISTRIBUTION FUNCTIONS IN PLANETARY RINGS FROM VOYAGER RADIO AND PHOTOPOLARIMETER OCCULTATION DATA
Howard A. Zebker, Leonard G. Tyler, and Essam A. Marouf *In* NASA, Washington Reports of Planetary Geology and Geophysics Program, 1986 May 1987 p 55-56 (For primary document see N87-23341 16-91)
Avail: NTIS HC A24/MF A01 CSCL 03B

Analysis of measurements of the scattered and direct components of Voyager 1 radio occultation signals at 3.5 and 13 cm wavelengths yield estimates of the distribution functions of supracentimeter-size particles and thickness of relatively broad regions in Saturn's rings. If mearurements of signal amplitude at a shorter wavelength are combined with the previously analyzed data, the shape of the distribution functions characterizing the smaller particles can be constrained. If size distributions of arbitrary form were considered, many solutions are found that are consistent with the three available observations of signal amplitude. The best-fit power law was calculated to the three observations at three wavelengths for several of the embedded Saturn ringlets. Mie scattering theory predicts that the measured phase of the radio occultation signal is highly sensitive to particles ranging from 0.1 to 1.0 wavelengths in size, thus additional constraints on the subcentimeter-size distribution functions for both the Saturn and Uranus rings can in principle be derived from radio phase measurements. B.G.

N87-23362*# Arizona Univ., Tucson. Lunar and Planetary Lab.
OBSERVATIONAL STUDIES OF SATURN'S RINGS
Carolyn C. Porco *In* NASA, Washington Reports of Planetary Geology and Geophysics Program, 1986 May 1987 p 57-58 (For primary document see N87-23341 16-91)
Avail: NTIS HC A24/MF A01 CSCL 03B

Several noteworthy phenomena in Saturn's rings were investigated which have until now received an inadequate amount of attention. Among these are the periodic variation of the spokes in the B ring and eccentric features throughout the rings. One of the major discoveries by Voyager was the existence of eccentric features within the predominantly circular rings of Saturn. Several of these nonaxisymmetric features are narrow elliptical rings which share many characteristics with the rings of Uranus. In recent work, two narrow ringlets were added to the list of eccentric features in the rings of Saturn. Voyager imaging and occultation data are now in hand, as well as image-processing software which allows accurate absolute positional measurements to be made in Voyager imaging data. Work is in progress to re-examine this region of Saturn's rings and to study the possibility of a dynamical interaction between the outer B ring edge, the Huygens ringlet and the nearby Mimas 2:1 resonance. An understanding of the kinematics and dynamics of this region promises to yield important clues to a matter of great interest in both theoretical and observation ring studies. B.G.

N87-23363*# California Univ., Santa Barbara.
THE PRODUCTION OF BRAIDS IN SATURN'S F RING
Jack J. Lissauer and Stanton J. Peale *In* NASA, Washington Reports of Planetary Geology and Geophysics Program, 1986 May 1987 p 59 Previously announced in IAA as A87-19040 (For primary document see N87-23341 16-91)
Avail: NTIS HC A24/MF A01 CSCL 03B

The braided structure noted in Voyager images of the Saturn F ring is presently addressed by two models. In the first, the pattern is generated by a narrow and initially uniform ring's passing of a nearby satellite, followed by an embedded moonlet gravitational acceleration-induced doubling back so that trajectories of the ring particles traverse one end of the classic horseshoe orbit. In the second model, the F ring is composed of two separated strands before the Moon's passage, so that a long braided pattern can be generated by the subsequent drift in relative phase; the embedded moonlet is thereby obviated. IAA

N87-23364*# California Univ., Santa Cruz. Dept. of Physics.
EXPERIMENTAL STUDIES ON THE IMPACT PROPERTIES OF WATER ICE
F. G. Bridges, D. N. C. Lin, and A. P. Hatzes *In* NASA, Washington Reports of Planetary Geology and Geophysics Program, 1986 May 1987 p 60-61 (For primary document see N87-23341 16-91)
Avail: NTIS HC A24/MF A01 CSCL 03B

Experimental studies on the impact of ice particles at very low velocity were continued. These measurements have applications in the dynamics of Saturn's rings. Initially data were obtained on the coefficient of restitution for ice spheres of one radius of curvature. The type of measurements were expanded to include restitution data for balls with a variety of surfaces as well as sticking forces between ice particles. Significant improvements were made to this experiment, the most important being the construction of a new apparatus. The new apparatus consists of a smaller version of the disk pendulum and a stainless steel, double-walled cryostat. The apparatus has proved to be a significant improvement over the old one. Measurements can now be made at temperatures near 90 K, comparable to the temperature of the environment of Saturn's rings, and with much greater temperature stability. It was found that a roughened contact surface or the presence of frost can cause a much larger change in the restitution measure than the geometrical effect of the radius of curvature. B.G.

N87-23365*# Hawaii Inst. of Geophysics, Honolulu.
TEMPERATURES AND MINIMUM THICKNESS OF THE INACTIVE SURFACE LAYER OF COMET HALLEY
F. P. Fanale and J. R. Salvail *In* NASA, Washington Reports of Planetary Geology and Geophysics Program, 1986 May 1987 p 65 (For primary document see N87-23341 16-91)
Avail: NTIS HC A24/MF A01 CSCL 03B

The effects of a nonvolatile mantle on the thermal state of a comet nucleus are investigated. The original computer model was modified so that temperatures can be computed through a thin dust mantle to the center of a 5 km spherical nucleus in the orbit of P/Halley. No attempt is made to simulate the formation of the mantle. Results are obtained for various specified values of initial mantle thickness and thermal conductivity to determine their effects on temperature profiles through the mantle. The minimum thickness of mantle that can withstand ejection by sublimating gasses is also calculated as a function of mantle thermal conductivity. Calculations were performed for ten or more orbits until temperatures in the mantle reached a near steady state. Results indicate that mantles as thin as 4 cm and 14 cm, for thermal conductivities of 600 and 6000 ergs/cm/s K, respectively, will remain intact. Surface temperatures as high as 511 K at perihelion and 400 K at the position of spacecraft encounter were computed at 0 degree latitude for an upright, rotating nucleus. Ice interface temperatures were raised by different amounts during each orbit, depending on mantle thickness and thermal conductivity, until steady state was reached. These results imply that relatively small nonvolatile masses emplaced randomly in comet nuclei could produce an irregular, permanently mantled surface and could also account for the apparently random location of active areas. Author

N87-23366*# Jet Propulsion Lab., California Inst. of Tech., Pasadena.
COMET THERMAL MODELING c90
Paul R. Weissman and Hugh H. Kieffer (Geological Survey, Flagstaff, Ariz.) *In* NASA, Washington Reports of Planetary Geology and Geophysics Program, 1986 May 1987 p 66-68 (For primary document see N87-23341 16-91)
Avail: NTIS HC A24/MF A01 CSCL 03B

The past year was one of tremendous activity because of the appearance of Halley's Comet. Observations of the comet were collected from a number of sources and compared with the detailed predictions of the comet thermal modeling program. Spacecraft observations of key physical parameters for cometary nucleus were incorporated into the thermal model and new cases run. These results have led to a much better understanding of physical processes on the nucleus and have pointed the way for further improvements to the modeling program. A model for the large-scale structure of cometary nuclei was proposed in which comets were envisioned as loosely bound agglomerations of smaller icy planetesimals, essentially a rubble pile of primordial dirty snowballs. In addition, a study of the physical history of comets was begun, concentrating on processes during formation and in the Oort cloud which would alter the volatile and nonvolatile materials in cometary nuclei from their pristine state before formation. B.G.

N87-23367*# Hawaii Inst. of Geophysics, Honolulu. Planetary Geosciences Div.

THE LOSS AND DEPTH OF CO2 ICE IN COMET NUCLEI c90

F. P. Fanale and J. R. Salvail *In* NASA, Washington Reports of Planetary Geology and Geophysics Program, 1986 May 1987 p 69 (For primary document see N87-23341 16-91)
Avail: NTIS HC A24/MF A01 CSCL 03B

An analytical model was developed to simulate the material differentiation of a cometary nucleus composed of water ice, putative unclathrated CO2 ice and silicate dust in specified proportions. Selective sublimation of any free CO2 ice present in a comet would produce a surface layer of water ice and dust overlying the original CO2 rich material. This surface layer reduces the temperature of buried CO2 ice and restricts the outflow of gaseous CO2. On each orbit, water sublimation at smaller heliocentric distances temporarily reduces the thickness of the water ice and dust layer and liberates dust. The model includes the effects of nucleus rotation, arbitrary orientation of the rotation axis, latitude, heat conduction into the deep interior of the nucleus and restriction of CO2 gas outflow by the water ice and dust layer. The effects of the permeability of the surface water ice layer, the nucleus rotation rate, and the latitude were investigated. Comparison of these and similar results with observations could yield information regarding the permeability and chemical composition of cometary material and suggest sampling strategies to minimize fractionation effects. Author

N87-23368*# Jet Propulsion Lab., California Inst. of Tech., Pasadena. Earth and Space Sciences Div.

DYNAMICS OF LONG PERIOD COMETS c90

Paul R. Weissman *In* NASA, Washington Reports of Planetary Geology and Geophysics Program, 1986 May 1987 p 70-71 (For primary document see N87-23341 16-91)
Avail: NTIS HC A24/MF A01 CSCL 03B

The appearance of Halley's Comet in 1985 to 1986 and the related emphasis on research on physical models of cometary nuclei, led to a more moderate pace for the dynamical studies of the Oort cloud and the motion of long-period comets this year. Specific areas studied included the dynamical evolution of cometary showers as a result of stars passages through the inner Oort cloud and the possible relationship to observed stepwise mass extinctions at geological boundaries, revised estimates for the total mass of comets in the Oort cloud as a result of lessons learned from the spacecraft encounters with Halley's Comet, and study of the possible dynamical sources for the short-period comets in the solar system as part of a wider study of physical processing of cometary nuclei prior to their becoming visible comets. The work on cometary showers used a Monte Carlo simulation of the evolution of cometary orbits under a combination of planetary, nongravitational, and stellar perturbations, and with physical removal by disruption, sublimation of all volatiles, and collision. B.G.

N87-23369*# Geological Survey, Flagstaff, Ariz.

OBSERVATIONS ON THE MAGNITUDE-FREQUENCY DISTRIBUTION OF EARTH-CROSSING ASTEROIDS c90

Eugene M. Shoemaker and Carolyn S. Shoemaker (Arizona Research and Technology, Flagstaff.) *In* NASA, Washington Reports of Planetary Geology and Geophysics Program, 1986 May 1987 p 72-74 (For primary document see N87-23341 16-91)
Avail: NTIS HC A24/MF A01 CSCL 03B

1987 p 72-74 (For primary document see N87-23341 16-91)
Avail: NTIS HC A24/MF A01 CSCL 03B

During the past decade, discovery of Earth-crossing asteroids has continued at the pace of several per year; the total number of known Earth crossers reached 70 as of September, 1986. The sample of discovered Earth crossers has become large enough to provide a fairly strong statistical basis for calculations of mean probabilities of asteroid collision with the Earth, the Moon, and Venus. It is also now large enough to begin to address the more difficult question of the magnitude-frequency distribution and size distribution of the Earth-crossing asteroids. Absolute V magnitude, H, was derived from reported magnitudes for each Earth crosser on the basis of a standard algorithm that utilizes a physically realistic phase function. The derived values of H range from 12.88 for (1627) Ivar to 21.6 for the Palomar-Leiden object 6344, which is the faintest and smallest asteroid discovered. B.G.

N87-23370*# Jet Propulsion Lab., California Inst. of Tech., Pasadena.

ASTEROID FAMILIES, DYNAMICS AND ASTROMETRY c90

J. G. Williams and J. Gibson *In* NASA, Washington Reports of Planetary Geology and Geophysics Program, 1986 May 1987 p 75-76 (For primary document see N87-23341 16-91)
Avail: NTIS HC A24/MF A01 CSCL 03B

The proper elements and family assignments for the 1227 Palomar-Leiden Survey asteroids of high quality were tabulated. In addition to the large table, there are also auxiliary tables of Mars crossers and commensurate objects, histograms of the proper element distributions, and a discussion. Probably the most important part of the discussion describes the Mars crossing boundary, how the closest distances of approach to Mars and Jupiter are calculated, and why the observed population of Mars crossers should bombard that planet episodically rather than uniformly. Analytical work was done to derive velocity distributions of family forming events from proper element distributions subject to assumptions which may be appropriate for cratering events. Software was developed for a microcomputer to permit plotting of the proper elements. Three orthogonal views are generated and stereo pairs can be printed when desired. This program was created for the study of asteroid families. The astrometry task is directed toward measuring and reducing positions on faint comets and the minor planets with less common orbits. The observational material is CCD frames taken with the Palomar 1.5 m telescope. Positions of 10 comets and 16 different asteroids were published on the Minor Planet Circulars. B.G.

N87-23371*# Hawaii Inst. of Geophysics, Honolulu. Planetary Geosciences Div.

THE 1986 DA AND 1986 EB: M-CLASS ASTEROIDS IN NEAR-EARTH ORBITS c90

Jonathan Gradie and Edward Tedesco (Jet Propulsion Lab., California Inst. of Tech., Pasadena.) *In* NASA, Washington Reports of Planetary Geology and Geophysics Program, 1986 May 1987 p 77-79 (For primary document see N87-23341 16-91)
Avail: NTIS HC A24/MF A01 CSCL 03B

The Earth-approaching asteroid population is composed of asteroids in orbits with short lifetimes compared with the age of the solar system. These objects which are comprised of Aten, Apollo, and Amor asteroids must be replenished from either cometary or mainbelt asteroid sources since lifetimes against collision with or ejection by a planet are on the order of 10 to 100 million years. The physical study of Earth-approaching asteroids is constrained by the generally long period between favorable apparitions and poorly known orbits. Broadband spectrophotometry on the Johnson UBVR system and the Eight-Color Asteroid Survey system were obtained at Kitt Peak National Observatory and on the Johnson JHK system and at 10 and 20 microns at the NASA Infrared Telescope Facility at Mauna Kea Observatory. These observations were used to determine the absolute visual magnitudes and to derive the visual geometric albedos and diameters on the IRAS system. The spectral reflectance properties and geometric albedos of the M-class asteroids are consistent compositions analogous to the iron nickel meteorites or the enstatite-metal assemblages of the enstatite chondrites. The issue of the source(s) of the near-Earth asteroids population was examined by comparing the classifications on the scheme employed by Gradie and Tedesco of 38 such asteroids. Most of the near-Earth objects is indeed the asteroid belt as the observations suggest, then a method for removing extinct nuclei of short period comets must be found since the rate of production of short period comets from the long period comets is relatively large. B.G.

N87-23372*# Rensselaer Polytechnic Inst., Troy, N.Y. Dept. of Geology.

EVOLUTION OF THE INNER ASTEROID BELT: PARADIGMS AND PARADOXES FROM SPECTRAL STUDIES

Michael J. Gaffey *In* NASA, Washington Reports of Planetary Geology and Geophysics Program, 1986 May 1987 p 80 (For primary document see N87-23341 16-91)
Avail: NTIS HC A24/MF A01 CSCL 03B

Recent years have witnessed a significant increase in the sophistication of asteroidal surface material characterizations derived from spectral data. An extensive data base of moderate to high spectral resolution, visible and near-infrared asteroid spectra is now available. Interpretive methodologies and calibrations were developed to determine phase abundance and composition in olivine-pyroxene assemblages and to estimate NiFe metal abundance from such spectra. A modified version of the asteroid classifications system more closely parallels the mineralogic variations of the major inner belt asteroid types. These improvements permit several general conclusions to be drawn concerning the nature of inner belt objects; their history, and that of the inner solar system; and the relationship between the asteroids and meteorites. Essentially all large belt asteroids have or are fragments of parent bodies which have undergone strong post-accretionary heating, varying degrees of melting and magmatic differentiation, and subsequent collisional disruption. These asteroids show a systematic, but not yet well characterized, mineralogic variation with semi-major axis. This suggests that the S-type asteroid families represent relatively recent collisions onto the cores of previously disrupted parent bodies. Author

N87-23373*# Rensselaer Polytechnic Inst., Troy, N.Y. Dept. of Geology.

METEORITE SPECTROSCOPY AND CHARACTERIZATION OF ASTEROID SURFACE MATERIALS c90

Michael J. Gaffey *In* NASA, Washington Reports of Planetary Geology and Geophysics Program, 1986 May 1987 p 81-83 (For primary document see N87-23341 16-91)
Avail: NTIS HC A24/MF A01 CSCL 03B

The purpose of this research effort is to improve the understanding of the origin, evolution, and interrelationships of the asteroids; of their relationships to the meteorites; and of the conditions and processes in the early inner solar system. The surface mineral assemblage and the surface heterogeneity of selected minor planets is determined from analysis of telescopic spectra to provide the data base to accomplish these goals. The analysis of asteroidal visible and near-infrared (VNIR) reflectance spectra compliments meteorite studies as a means of probing the late nebular through the early post-accretionary period of solar system history. To date, essentially all available spectral evidence has strongly indicated that the large S-type asteroids are predominantly thermally evolved, magmatically differentiated bodies. B.G.

N87-23374*# Brown Univ., Providence, R. I. Dept. of Geological Sciences.

SOURCE OF THE OPTICAL RED-SLOPE IN IRON-RICH METEORITES c90

Daniel T. Britt, Carle M. Pieters, and Peter H. Schultz *In* NASA, Washington Reports of Planetary Geology and Geophysics Program, 1986 May 1987 p 84 (For primary document see N87-23341 16-91)
Avail: NTIS HC A24/MF A01 CSCL 03B

The relationship between ordinary chondrites and S-type asteroids is an unresolved issue in meteorite science. S-type asteroids exhibit a positively red-sloped spectrum that is interpreted to indicate the presence of elemental iron on the surfaces. The characteristic red-sloped spectrum of iron-rich meteorites is produced by only the specular component of the reflectance. Complex metallic surfaces can be modeled as linear mixtures of specular and nonspecular components. It is the geometry of the metal on a surface and its interaction with surrounding material, rather than the absolute amount of metal, that determine the redness of resulting spectra. In order to distinguish between ordinary chondrite and differentiated parent bodies it is important to understand how regolith processes affect the nature and form of metal on asteroid surfaces. B.G.

N87-23375*# National Aeronautics and Space Administration, Washington, D.C.

A SEARCH FOR SPECTRAL ALTERATION EFFECTS IN CHONDRITIC GAS-RICH BRECCIAS

J. F. Bell and Klaus Keil (New Mexico Univ., Albuquerque.) *In* NASA, Washington Reports of Planetary and Geology and Geophysics Program, 1986 May 1987 p 85-86 (For primary document see N87-23341 16-91)
Avail: NTIS HC A24/MF A01 CSCL 03B

Several samples of gas-rich breccias were selected, including slabs of the Kapoeta howardite, the ordinary chondrites Dubrovnik, Cangas de Onis, and Dimmit. Numerous 0.8 to 2.5 micron reflection spectra of selected areas on sawed or broken surfaces were measured with the Planetary Geosciences Division spectrogoniometer. While these spectra are not directly comparable to those of powered samples, comparisons within the data set should reveal any spectral differences due to weathering. These results indicate that unknown regolith processes do not confer the ordinary-chondrite parent bodies with an altered layer exhibiting S-class spectral properties. This is consistent with recent interpretations of the new Q-class of asteroids as the ordinary-chondrite parent bodies. However, significant spectral effects do occur in asteroid regoliths: darkening and suppression of absorption bands in highly shocked material, as seen previously in the so-called black chondrites; and segregation of metal in large impact melt pools on chondritic asteroids, which may have achondritic spectra. Neither of these effects is likely to be significant in interpreting current integral-disk spectra, but should be searched for in spectral maps returned by future spacecraft. B.G.

N87-23376*# National Aeronautics and Space Administration. Lyndon B. Johnson Space Center, Houston, Tex.

ANALYTICAL ELECTRON MICROSCOPY OF FINE-GRAINED PHASES IN PRIMITIVE INTERPLANETARY DUST PARTICLES AND CARBONACEOUS CHONDRITES c90

Ian D. R. Mackinnon, Frans J. M. Rietmeijer (New Mexico Univ., Albuquerque.), and David S. McKay *In* NASA, Washington Reports of Planetary Geology and Geophysics Program, 1986 May 1987 p 87-89 (For primary document see N87-23341 16-91)
Avail: NTIS HC A24/MF A01 CSCL 03B

In order to describe the total mineralogical diversity within primitive extraterrestrial materials, individual interplanetary dust particles (IDPs) collected from the stratosphere as part of the JSC Cosmic Dust Curatorial Program were analyzed using a variety of AEM techniques. Identification of over 250 individual grains within one chondritic porous (CP) IDP shows that most phases could be formed by low temperature processes and that heating of the IDP during atmospheric entry is minimal and less than 600 C. In a review of the mineralogy of IDPs, it was suggested that the occurrence of other silicates such as enstatite whiskers is consistent with the formation in an early turbulent period of the solar nebula. Experimental confirmation of fundamental chemical and physical processes in a stellar environment, such as vapor phase condensation, nucleation, and growth by annealing, is an important aspect of astrophysical models for the evolution of the Solar System. A detailed comparison of chondritic IDP and carbonaceous chondrite mineralogies shows significant differences between the types of silicate minerals as well as the predominant oxides. B.G.

N87-23377*# Jet Propulsion Lab., California Inst. of Tech., Pasadena.

ASTEROID LIGHTCURVE INVERSION c74

Steven J. Ostro and Robert Connelly (Cornell Univ., Ithaca, N.Y.) *In* NASA, Washington Reports of Planetary Geology and Geophysics Program, 1986 May 1987 p 90-91 (For primary document see N87-23341 16-91)

Avail: NTIS HC A24/MF A01 CSCL 20F

One of the most fundamental physical properties of any asteroid is its shape. Lightcurves provide the only source of shape information for most asteroids. Unfortunately, the functional form of a lightcurve is determined by the viewing/illumination geometry and the asteroid's light scattering characteristics as well as its shape, and in general it is impossible to determine an asteroid's shape from lightcurves. A technique called convex-profile inversion (CPI) that obtains a convex profile, P, from any lightcurve is introduced. If certain ideal conditions are satisfied, then P is an estimator for the asteroid's mean cross section, C, a convex set defined as the average of all cross sections C(z) cut by planes a distance z above the asteroids's equatorial plane. C is therefore a 2-D average of the asteroid's 3-D shape. B.G.

N87-23378*# Carnegie Institution of Washington, D. C.

ACCUMULATION OF THE PLANETS

G. W. Wetherill *In* NASA, Washington Reports of Planetary Geology and Geophysics Program, 1986 May 1987 p 92-94 (For primary document see N87-23341 16-91)

Avail: NTIS HC A24/MF A01 CSCL 03B

In modeling the accumulation of planetesimals into planets, it is appropriate to distinguish between two stages: an early stage, during which approximately 10 km diameter planetesimals accumulate locally to form bodies approximate 10 to the 25th g in mass; and a later stage in which the approximately 10 to the 25th g planetesimals accumulate into the final planets. In the terrestrial planet region, an initial planetesimal swarm corresponding to the critical mass of dust layer gravitational instabilities is considered. In order to better understand the accumulation history of Mercury-sized bodies, 19 Monte-Carlo simulations of terrestrial planet growth were calculated. A Monte Carlo technique was used to investigate the orbital evolution of asteroidal collision debris produced interior to 2.6 AU. It was found that there are two regions primarily responsible for production of Earth-crossing meteoritic material and Apollo objects. The same techniques were extended to include the origin of Earth-approaching asteroidal bodies. It is found that these same two resonant mechanisms predict a steady-state number of Apollo-Amor about 1/2 that estimated based on astronomical observations. B.G.

N87-23379*# National Aeronautics and Space Administration. Ames Research Center, Moffett Field, Calif.

PROTOSTELLAR DISKS AND THE PRIMITIVE SOLAR NEBULA c92

P. M. Cassen, J. B. Pollack, T. Bunch, O. Hubickyj, P. Moins, and C. Yuan (City Coll. of the City Univ. of New York.) *In* NASA, Washington Reports of Planetary Geology and Geophysics Program, 1986 May 1987 p 97-99 (For primary document see N87-23341 16-91)

Avail: NTIS HC A24/MF A01 CSCL 03B

The objective is to obtain quantitative information on the turbulent transport of mass, angular momentum, and energy under the conditions that characterize the solar nebula, by direct numerical calculations. These calculations were made possible by research conducted on supercomputers (Cray XMP and Cray 2) by the Ames Computational Fluid Dynamics Branch. Techniques were developed that permitted the accurate representation of turbulent flows over the full range of important eddy sizes. So far, these techniques were applied (and verified) primarily in mundane laboratory situations, but they have a strong potential for astrophysical applications. A sequence of numerical experiments were conducted to evaluate the Reynold's stress tensor, turbulent heat transfer rate, turbulent dissipation rate, and turbulent kinetic energy spectrum, as functions of position, for conditions relevant to the solar nebula. Emphasis is placed on the variation of these properties with appropriate nondimensional quantities, so that relations can be derived that will be useful for disk modeling under a variety of hypotheses and initial conditions. B.G.

N87-23380*# California Univ., Santa Barbara.

TIMESCALES FOR PLANETARY ACCRETION AND THE STRUCTURE OF THE PROTOPLANETARY DISK

Jack J. Lissauer *In* NASA, Washington Reports of Planetary Geology and Geophysics Program, 1986 May 1987 p 100 (For primary document see N87-23341 16-91)

Avail: NTIS HC A24/MF A01 CSCL 03B

Models of planetary accretion which assume the mass of condensable matter in the protoplanetary disk was equal to that present in the planets today predict accretion timescales for the outer planets approximately or less than 10 to the 8th years. Such timescales are inconsistent with observations of star forming regions, which suggest that most of the gas in disks around one solar mass is removed in a few x 10 to the 6th years. A unified scenario was outlined for solar system formation consistent with astrophysical constraints. Jupiter's core could have grown by runaway accretion of planetesimals to a mass sufficient to initiate rapid accretion of gas in times of order of 500,000 to 5,000,000 years, provided the surface density of solids in its accretion zone was at least 5 to 10 times greater than that required by minimum mass models of the protoplanetary disk. The inner planets and the asteroids can be accounted for in this picture if the surface density of the solar nebula was relatively uniform out to Jupiter's orbit. The formation of such a protoplanetary disk requires significant transport of mass and angular momentum, and is consistent with viscous accretion disk models of the solar nebula. Author

N87-23381*# Virginia Univ., Charlottesville.

FORMATION OF GIANT MOLECULAR CLOUDS IN GLOBAL SPIRAL STRUCTURES: THE ROLE OF ORBITAL DYNAMICS AND CLOUD-CLOUD COLLISIONS c90

W. W. Roberts, Jr. and G. R. Stewart *In* NASA, Washington Reports of Planetary Geology and Geophysics Program, 1986 May 1987 p 101 (For primary document see N87-23341 16-91) (Grants NAGw-929; NSF AST-82-04256)

Avail: NTIS HC A24/MF A01 CSCL 03B

The different roles played by orbital dynamics and dissipative cloud-cloud collisions in the formation of giant molecular clouds (GMCs) in a global spiral structure are investigated. The interstellar medium (ISM) is simulated by a system of particles, representing clouds, which orbit in a spiral-perturbed, galactic gravitational field. The overall magnitude and width of the global cloud density distribution in spiral arms is very similar in the collisional and collisionless simulations. The results suggest that the assumed number density and size distribution of clouds and the details of individual cloud-cloud collisions have relatively little effect on these features. Dissipative cloud-cloud collisions play an important steadying role for the cloud system's global spiral structure. Dissipative cloud-cloud collisions also damp the relative velocity dispersion of clouds in massive associations and thereby aid in the effective assembling of GMC-like complexes. B.G.

N87-23382*# California Univ., Los Angeles.

ANALYSIS OF PLANETARY EVOLUTION WITH EMPHASIS ON DIFFERENTIATION AND DYNAMICS

William M. Kaula and William I. Newman *In* NASA, Washington Reports of Planetary Geology and Geophysics Program, 1986 May 1987 p 102-104 (For primary document see N87-23341 16-91)

Avail: NTIS HC A24/MF A01 CSCL 03B

In order to address the early stages of nebula evolution, a three-dimensional collapse code which includes not only hydrodynamics and radiative transfer, but also the effects of ionization and, possibly, magnetic fields is being addressed. As part of the examination of solar system evolution, an N-body code was developed which describes the latter stages of planet formation from the accretion of planetesimals. To test the code for accuracy and run-time efficiency, and to develop a stronger theoretical foundation, problems were studied in orbital dynamics. A regional analysis of the correlation in the gravity and topography fields of Venus was performed in order to determine the small and intermediate scale subsurface structure. B.G.

N87-23383*# Virginia Univ., Charlottesville.
EVOLUTION OF PLANETESIMAL VELOCITIES Abstract Only
Glen R. Stewart and George W. Wetherill (Carnegie Institution of Washington, D. C.) *In* NASA, Washington Reports of Planetary Geology and Geophysics Program, 1986 May 1987 p 105 (For primary document see N87-23341 16-91)
(Grants NsG-7437; NAGw-398; NAGw-929; NSF AST-82-04256; NSF MCS-83-04459)
Avail: NTIS HC A24/MF A01 CSCL 03B

A self-consistent set of equations for the velocity evolution of a general planetesimal population is presented. The equations are given in a form convenient for calculations of the early stages of planetary accumulation when it is necessary to model the planetesimal swarm by methods of gas dynamics, rather than follow the orbital evolution of individual bodies. Steady state velocities of a simple planetesimal population consisting of two different sizes of bodies are calculated. Dynamical friction is found to be an important mechanism for transferring kinetic energy from the larger planetesimals to the smaller ones. When the small planetesimals are relatively abundant, gas drag and inelastic collisions among the smaller bodies are of comparable importance for dissipating energy from the population. Author

N87-23384*# Planetary Science Inst., Tucson, Ariz.
ACCUMULATION OF SOLID BODIES IN THE SOLAR NEBULA c92
S. J. Weidenschilling and D. R. Davis *In* NASA, Washington Reports of Planetary Geology and Geophysics Program, 1986 May 1987 p 106-107 (For primary document see N87-23341 16-91)
(Contract NASw-3214)
Avail: NTIS HC A24/MF A01 CSCL 03B

Research on the accumulation of solid bodies in the solar nebula is discussed. Studies of the earliest stage of accumulation of solid bodies in the solar system, which occured in the presence of the gaseous component of the solar nebula, are discussed. The combined effects of gas drag and gravitational perturbations of a planetary embryo on the orbital evolution of planetesimals, the effects of resonant trapping on planetesimals, and planetary mass accretion are discussed. R.J.F.

N87-23385*# National Aeronautics and Space Administration, Washington, D.C.
A SCALING LAW FOR ACCRETION ZONE SIZES Abstract Only c90
Yuval Greenzweig and Jack J. Lissauer *In* NASA, Washington Reports of Planetary Geology and Geophysics Program, 1986 May 1987 p 108 (For primary document see N87-23341 16-91)
Avail: NTIS HC A24/MF A01 CSCL 03B

Current theories of runaway planetary accretion require small random velocities of the accreted particles. Two body gravitational accretion cross sections which ignore tidal perturbations of the Sun are not valid for the slow encounters which occur at low relative velocities. Wetherill and Cox have studied accretion cross sections for rocky protoplanets orbiting at 1 AU. Using analytic methods based on Hill's lunar theory, one can scale these results for protoplanets that occupy the same fraction of their Hill sphere as does a rocky body at 1 AU. Generalization to bodies of different sizes is achieved here by numerical integrations of the three-body problem. Starting at initial positions far from the accreting body, test particles are allowed to encounter the body once, and the cross section is computed. A power law is found relating the cross section to the radius of the accreting body (of fixed mass). R.J.F.

N87-23386*# National Aeronautics and Space Administration. Ames Research Center, Moffett Field, Calif.
URANUS AND NEPTUNE: QUESTIONS AND POSSIBLE ANSWERS
R. T. Reynolds and M. Podolak *In* NASA, Washington Reports of Planetary Geology and Geophysics Program, 1986 May 1987 p 109-111 Previously announced as N85-23495 (For primary document see N87-23341 16-91)
Avail: NTIS HC A24/MF A01 CSCL 03B

Uranus and Neptune form a special class of planetary objects; intermediate in mass and composition between the giant hydrogen-rich planets of Jupiter and Saturn, and the small, rocky terrestrial planets, their structure and composition are not only of intrinsic importance, but also should provide information regarding the nature of the protoplanetary nebula and the processes of planetary formation. A detailed set of theoretical models of these planets within the framework of two and three shell models was costructed. The ratio of ice to rock was varied. The three shell model fits the data on the two planets best. R.J.F.

N87-23387*# Planetary Science Inst., Tucson, Ariz.
COLLISIONAL AND DYNAMICAL PROCESSES IN MOON AND PLANET FORMATION c90
C. R. Chapman, D. R. Davis, S. J. Weidenschilling, W. K. Hartmann, and D. Spaute *In* NASA, Washington Reports of Planetary Geology and Geophysics Program, 1986 May 1987 p 112-114 (For primary document see N87-23341 16-91)
Avail: NTIS HC A24/MF A01 CSCL 03B

Research on a variety of dynamical processes relevant to the formation of planets, satellites and ring systems is discussed. The main focus is on studies of accretionary formation of early protoplanets using a numerical model, structures and evolution of ring systems and individual bodies within planetary rings, and theories of lunar origin. R.J.F.

N87-23388*# National Aeronautics and Space Administration, Washington, D.C.
DYNAMICAL CONSTRAINTS ON THE ORIGIN OF THE MOON Abstract Only c90
A. P. Boss and S. J. Peale (California Univ., Santa Barbara.) *In* NASA, Washington Reports of Planetary Geology and Geophysics Program, 1986 May 1987 p 115 Previously announced in IAA as A87-20628 (For primary document see N87-23341 16-91)
Avail: NTIS HC A24/MF A01 CSCL 03B

Six different categories of models for the formation of the moon within the context of the general theory of terrestial planet formation by the accumulation of protoplanets are discussed. These catagories are: (1) rotational fission; (2) precipitation fission; (3) intact capture; (4) disintegrative capture; (5) binary accretion; and (6) giant impact accretion. It appears that the only plausable mechanism proposed thus far involves the formation of the Moon following a giant impact that ejects portions of the differentiated Earth's mantle and parts of the impacting body into circumterrestrial orbit. R.J.F.

N87-23389*# Jet Propulsion Lab., California Inst. of Tech., Pasadena.
LUNAR SCIENCE FROM LUNAR LASER RANGING Abstract Only
J. G. Williams, X. X. Newhall, and J. O. Dickey *In* NASA, Washington Reports of Planetary Geology and Geophysics Program, 1986 May 1987 p 116 (For primary document see N87-23341 16-91)
Avail: NTIS HC A24/MF A01 CSCL 03B

Seventeen years of lunar ranging data have been analyzed to determine lunar second-degree moment differences, third-degree gravitational harmonics, Love number, rotational dissipation and retroreflector coordinates. R.J.F.

N87-23390*# Massachusetts Inst. of Tech., Cambridge. Dept. of Earth, Atmospheric and Planetary Sciences.
SOLAR SYSTEM DYNAMICS c90
Jack Wisdom *In* NASA, Washington Reports of Planetary Geology and Geophysics Program, 1986 May 1987 p 117-119 (For primary document see N87-23341 16-91)
Avail: NTIS HC A24/MF A01 CSCL 03B

The rotational dynamics of irregularly shaped satellites and the origin of Kirkwood Gaps are discussed. The chaotic tumbling of Hyperion and the anomalously low eccentricity of Deimos are examined. The Digital Orrery is used to explore the phase space of the ellipic restricted three body problem near the principal commensurabilities (2/1, 5/2, 3/1, and 3/2). The results for the 3/1 commensurability are in close agreement with those found earlier with the algebraic mapping method. Large chaotic zones are associated with the 3/1, 2/1 and 5/2 resonances, where there are gaps in the distribution of asteroids. The region near the 3/2 resonance, where the Hilda group of asteroids is located, is largely devoid of chaotic behavior. Thus, there is a qualitative agreement between the character of the motion and the distribution of asteroids. R.J.F.

N87-23391*# California Univ., Santa Barbara.
ORBITAL RESONANCES, UNUSUAL CONFIGURATIONS AND EXOTIC ROTATION STATES AMONG PLANETARY SATELLITES Abstract Only
S. J. Peale *In* NASA, Washington Reports of Planetary Geology and Geophysics Program, 1986 May 1987 p 120 (For primary document see N87-23341 16-91)
Avail: NTIS HC A24/MF A01 CSCL 03B

Several examples of satellite dynamics are presented where significant progress has been made in understanding a complex problem, where a long-standing problem has finally been solved, where newly discovered configurations have motivated novel descriptions or where an entirely new phenomenon has been revealed. The origin of orbital resonances in satellites and the solution of the problem of the origin and evolution of the three body Laplace resonance among the Galilean satellites are among the topics discussed. R.J.F.

N87-23392*# Cornell Univ., Ithaca, N.Y.
DYNAMICS OF SATELLITES, ASTEROIDS, AND RINGS c90
Stanley F. Dermott *In* NASA, Washington Reports of Planetary Geology and Geophysics Program, 1986 May 1987 p 121-123 (For primary document see N87-23341 16-91)
Avail: NTIS HC A24/MF A01 CSCL 03B

Work is reported on: (1) the shapes and the internal structures of satellites; (2) the tidal heating of Miranda; (3) the dynamics of arc-like rings; and (4) the structure of the zodiacal cloud that was revealed by the Infrared Astronomy Satellite. Significant progress was made in determining the shape and internal structure of Mimas and in understanding the dynamical evolution of Miranda's orbit. R.J.F.

N87-23393*# Virginia Univ., Charlottesville.
HAMILTONIAN THEORY OF NONLINEAR WAVES IN PLANETARY RINGS Abstract Only c90
G. R. Stewart *In* NASA, Washington Reports of Planetary Geology and Geophysics Program, 1986 May 1987 p 124 (For primary document see N87-23341 16-91)
(Grants NAGw-929; NSF AST-82-004256)
Avail: NTIS HC A24/MF A01 CSCL 03B

The derivation of a Hamiltonian field theory for nonlinear density waves in Saturn's rings is discussed. Starting with a Hamiltonian for a discrete system of gravitating streamlines, an averaged Hamiltonian is obtained by successive applications of Lie transforms. The transformation may be carried out to any desired order in q, where q is the nonlinearity parameter defined in the work of Shu, et al (1985) and Borderies et al (1985). Subsequent application of the Wentzel-Kramer-Brillouin Method approximation yields an asymptotic field Hamiltonian. Both the nonlinear dispersion relation and the wave action transport equation are easily derived from the corresponding Lagrangian by the standard variational principle. R.J.F.

N87-23394*# National Aeronautics and Space Administration. Ames Research Center, Moffett Field, Calif.
PLANETARY RING DYNAMICS AND MORPHOLOGY c90
Jeffrey N. Cuzzi, Richard H. Durisen, and Frank H. Shu (California Univ., Berkeley.) *In* NASA, Washington Reports of Planetary Geology and Geophysics Program, 1986 May 1987 p 125-127 (For primary document see N87-23341 16-91)
Avail: NTIS HC A24/MF A01 CSCL 03B

Evidence for a moonlet belt in the region between Saturn's close-in moonrings Pandora and Prometheus is discussed. It is argued that little-known observations of magnetospheric electron density by Pioneer 11 imply substantial, ongoing injections of mass into the 2000 km region which surrounds the F ring. A hypothesis is presented that these events result naturally from interparticle collisions between the smaller members of an optically thin belt of moonlets. Also discussed is work on Uranus ring structure and photometry, image processing and analysis of the Jonian ring strucure, photometric and structural studies of the A ring of Saturn, and improvements to an image processing system for ring studies. R.J.F.

N87-23395*# Cornell Univ., Ithaca, N.Y. Dept. of Astronomy.
DYNAMICAL STUDIES OF SATURN'S RINGS
Philip D. Nicholson and Carolyn C. Porco (Arizona Univ., Tucson.) *In* NASA, Washington Reports of Planetary Geology and Geophysics Program, 1986 May 1987 p 128-129 (For primary document see N87-23341 16-91)
Avail: NTIS HC A24/MF A01 CSCL 03B

Several investigations of Saturn's rings employing data from three Voyager experiments are discussed. These investigations concentrated on the regularily organized C ring. A search for eccentric or inclined features, a photometric study of regions of different optical depth, an analysis of wavelike structures at three locations, and a study of the size distribution of meter-sized particles are dicussed. R.J.F.

N87-23396*# California Univ., Los Angeles. Dept. of Chemistry and Biochemistry.
HIGH PRESSURE COSMOCHEMISTRY OF MAJOR PLANETARY INTERIORS: LABORATORY STUDIES OF THE WATER-RICH REGION OF THE SYSTEM AMMONIA-WATER
Malcolm Nicol, Mary Johnson, Steven Boone, and Hyunchee Cynn *In* NASA, Washington Reports of Planetary Geology and Geophysics Program, 1986 May 1987 p 133-135 (For primary document see N87-23341 16-91)
Avail: NTIS HC A24/MF A01 CSCL 03B

Several studies relative to high pressure cosmochemistry of major planetary interiors are summarized. The behavior of gas-ice mixtures at very high pressures, studies of the phase diagram of (NH3) sub x (H2O) sub 1-x at pressures to 5GPa and temperatures from 240 to 370 K, single crystal growth of ammonia dihydrate at room temperature in order to determine their structures by x-ray diffraction, spectroscopy of chemical reactions during shock compression in order to evaluate how the reactions affect the interpretation of equation of state data obtained by shock methods, and temperature and x-ray diffraction measurements made on resistively heated wire in diamond anvil cells in order to obtain phase and structural data relevant to the interiors of terrestrial planets are among the studies discussed. R.J.F.

N87-23397*# California Univ., Berkeley. Dept. of Geology and Geophysics.
EXPERIMENTS PERTAINING TO THE FORMATION AND EQUILIBRATION OF PLANETARY CORES
Raymond Jeanloz, Elise Knittle, and Quentin Williams *In* NASA, Washington Reports of Planetary Geology and Geophysics Program, 1986 May 1987 p 136-137 (For primary document see N87-23341 16-91)
Avail: NTIS HC A24/MF A01 CSCL 03B

The phase diagram of FeO was experimentally determined to pressures of 155 GPa and temperatures of 4000 K using shock wave and diamond-cell techniques. Researchers discovered a metallic phase of FeO at pressures greater than 70 GPa and temperatures exceeding 1000 K. The metallization of FeO at high pressures implies that oxygen can be present as the light alloying element of the Earth's outer core, in accord with the geochemical predictions of Ringwood. The high pressures necessry for this metallization suggest that the core has acquired its composition well after the initial stages of the Earth's accretion. The core forming alloy can react chemically with oxides such as those forming the mantle. The core and mantle may never have reached complete chemical equilibrium, however. If this is the case, the core-mantle boundary is likely to be a zone of active chemical reactions. R.J.F.

N87-23398*# Cornell Univ., Ithaca, N.Y. Dept. of Geological Sciences.

MELTING OF TROILITE AT HIGH PRESSURE IN A DIAMOND CELL BY LASER HEATING **c25**

William A. Bassett and Maura S. Weathers *In* NASA, Washington Reports of Planetary Geology and Geophysics Program, 1986 May 1987 p 138-140 (For primary document see N87-23341 16-91)
Avail: NTIS HC A24/MF A01 CSCL 07D

A system for measuring melting temperatures at high pressures is described. The sample is heated with radiation from a YAG laser. The beam is reflected downward through a microscope objective, through the upper diamond anvil, and focused onto the sample. Hense, intense heating is produced only at the sample and not within the diamond anvils. A vidicon system is used to observe the sample during heating. Incandescent light from the heated sample passes back through the objective lens into a grating spectrometer. The spectrum of the incandescent light is received by the photodiode array and stored in the multichannel analyzer. These data can then be transferred to floppy disk for analysis. A curve fitting program is used to compare the spectra with standard blackbody curves and to determine the temperature. Pressure is measured by the ruby fluorescence method. The system was used to study the melting behavior of natural troilite (FeS). R.J.F.

N87-23399*# Lawrence Livermore National Lab., Calif.

PROPERTIES OF PLANETARY FLUIDS AT HIGH PRESSURE AND TEMPERATURE

W. J. Nellis, D. C. Hamilton, N. C. Holmes, H. B. Radousky, F. H. Ree, M. Ross, D. A. Young, and M. Nicol (California Univ., Los Angeles.) *In* NASA, Washington Reports of Planetary Geology and Geophysics Program, 1986 May 1987 p 141-143 (For primary document see N87-23341 16-91)
(Contract W-7405-eng-48)
Avail: NTIS HC A24/MF A01 CSCL 03B

In order to derive models of the interiors of Uranus, Neptune, Jupiter and Saturn, researchers studied equations of state and electrical conductivities of molecules at high dynamic pressures and temperatures. Results are given for shock temperature measurements of N2 and CH4. Temperature data allowed demonstration of shock induced cooling in the the transition region and the existence of crossing isotherms in P-V space. R.J.F.

N87-23400*# Jet Propulsion Lab., California Inst. of Tech., Pasadena.

GRAVITY DATA ANALYSIS

William L. Sjogren *In* NASA, Washington Reports of Planetary Geology and Geophysics Program, 1986 May 1987 p 144-146 (For primary document see N87-23341 16-91)
Avail: NTIS HC A24/MF A01 CSCL 03B

Work on three different efforts related to gravity data analysis is discussed. The reduction of raw Doppler data from the Apollo 15 subsatellite to produce acceleration profiles as a function of latitude, longitude and altitude; an investigation related to fitting long arcs of Pioneer Venus Orbiter tracking data; and a study of gravity/topography ratios which were found to have a linear trend with longitude are discussed. R.J.F.

N87-23401*# Arizona Univ., Tucson. Lunar and Planetary Lab.

THE ORIGIN OF POLARITY ASYMMETRIES IN THE HISTORY OF THE GEOMAGNETIC FIELD Abstract Only **c46**

E. H. Levy *In* NASA, Washington Reports of Planetary Geology and Geophysics Program, 1986 May 1987 p 147 (For primary document see N87-23341 16-91)
Avail: NTIS HC A24/MF A01 CSCL 08G

The behavior of magnetohydrodynamic stationary modes in the presence of an imposed weak magnetic field originating separately from the dynamo is studied. A rare class of stationary states is found that exhibit high sensitivity to the presence of weak imposed fields. The amplitude of the difference between the total fields of opposite polarity is much larger than the amplitude of the imposed nondynamo fields. It is proposed that Earth's magnetic field operates in such a mode, highly sensitive to the presence of an ambient field. An argument is given to explain why the terrestrial dynamo should choose to operate in one of these rare states. Implications are discussed for the general mechanism of dynamo magnetic field equilibrium in planets. Author

N87-23402*# Arizona Univ., Tucson. Lunar and Planetary Lab.

MAGNETIC FLARES IN THE PROTOPLANETARY NEBULA AND THE ORIGIN OF METEORITE CHONDRULES Abstract Only **c90**

E. H. Levy and S. Araki *In* NASA, Washington Reports of Planetary Geology and Geophysics Program, 1986 May 1987 p 147 (For primary document see N87-23341 16-91)
Avail: NTIS HC A24/MF A01 CSCL 03B

This study proposes and analyzes a model for the chondrule forming heating events based on magnetohydrodynamic flares in the corona of the protoplanetary nebula which precipitate energy in the form of energetic plasma along magnetic field lines down toward the face of the nebula. It is found that flare energy release rates sufficient to melt the prechondrular matter, leading to the formation of the chondrules, can occur in the tenuous corona of a protostellar disk. Energy release rates sufficient to achieve melting require that the ambient magnetic field strength be in the range that has been inferred separately from independent meteorite remanent magnetization studies. Author

N87-23403*# Arizona Univ., Tucson. Lunary and Planetary Lab.

GENERATION OF A DYNAMO MAGNETIC FIELD IN A PROTOPLANETARY ACCRETION DISK Abstract Only **c90**

T. Stepinski and E. H. Levy *In* NASA, Washington Reports of Planetary Geology and Geophysics Program, 1986 May 1987 p 148 (For primary document see N87-23341 16-91)
Avail: NTIS HC A24/MF A01 CSCL 03B

A new computational technique is developed that allows realistic calculations of dynamo magnetic field generation in disk geometries corresponding to protoplanetary and protostellar accretion disks. The approach is of sufficient generality to allow, in the future, a wide class of accretion disk problems to be solved. Here, basic modes of a disk dynamo are calculated. Spatially localized oscillatory states are found to occur in Keplerain disks. A physical interpretation is given that argues that spatially localized fields of the type found in these calculations constitute the basic modes of a Keplerian disk dynamo. Author

N87-23404*# Arizona Univ., Tucson. Lunar and Planetary Lab.

THE STEADY STATE TOROIDAL MAGNETIC FIELD AT THE CORE-MANTLE BOUNDARY Abstract Only **c46**

S. J. Pearce and E. H. Levy *In* NASA, Washington Reports of Planetary Geology and Geophysics Program, 1986 May 1987 p 148 (For primary document see N87-23341 16-91)
Avail: NTIS HC A24/MF A01 CSCL 08G

Recent measurements indicate that the strength of the toroidal magnetic field at Earth's core-mantle boundary is comparable in strength to the poloidal field - 5 to 10 gauss. Calculations are given to show that this is an inevitable result of the external boundary condition on the core, in which the mantle electrical conductivity is several orders of magnitude lower than that of the core. The measurements are shown to imply that the internal core magnetic field is in the range of several hundred gauss. Thus the measurements imply that the Earth's core contains a strong toroidal magnetic field. They also support the idea that Earth's dynamo, and by implication, other planetary magnetic fields, involves efficient toroidal magnetic field generation through strong differential rotation. Author

N87-23405*# California Univ., Berkeley. Space Sciences Lab.

LUNAR MAGNETIZATION CONCENTRATIONS (MAGCONS) ANTIPODAL TO YOUNG LARGE IMPACT BASINS

R. P. Lin, K. A. Anderson, and L. L. Hood (Arizona Univ., Tucson.) *In* NASA, Washington Reports of Planetary Geology and Geophysics Program, 1986 May 1987 p 149-150 (For primary document see N87-23341 16-91)

Avail: NTIS HC A24/MF A01 CSCL 03B

Electron reflection measurements from Apollo 15 and 16 subsatellites show that patches of strong surface magnetic fields ranging in size from less than about 7 km to greater than 500 km are distributed over the surface of the Moon. With the exception of a few regions, no obvious association to surface geology has been found. Researchers examined the antipodes of 23 winged impact basins for which electron reflection measurements are available. It was concluded that the apparent temporal variations for the basin antipodes may reflect real variations in the lunar magnetic field. R.J.F.

N87-23406*# Cornell Univ., Ithaca, N.Y. Dept. of Geological Sciences.

IMPLICATIONS OF CONVECTION IN THE MOON AND THE TERRESTRIAL PLANETS

Donald L. Turcotte *In* NASA, Washington Reports of Planetary Geology and Geophysics Program, 1986 May 1987 p 151 (For primary document see N87-23341 16-91)

Avail: NTIS HC A24/MF A01 CSCL 03B

The early thermal and chemical evolution of the Moon is discussed. The rubidium-strontium, neodymium-samarium, and uranium-thorium-lead systems were studied. The relation of source region heterogeneity to the mixing associated with mantle convection is considered. Work on the application of fractal concepts to planetary geology and geophysics is also discussed. The fractal concept was applied to fragmentation, including the frequency-size distribution of meteorites, asteroids and particulate matter produced by impacts. R.J.F.

N87-23407*# Geological Survey, Flagstaff, Ariz. Branch of Astrogeology.

GLOBAL PETROLOGIC VARIATIONS OF THE MOON: A TERNARY-DIAGRAM APPROACH

Philip A. Davis and Paul D. Spudis *In* NASA, Washington Reports of Planetary Geology and Geophysics Program, 1986 May 1987 p 152-154 (For primary document see N87-23341 16-91)

Avail: NTIS HC A24/MF A01 CSCL 03B

A ternary-diagram approach is used to show on a single map as much detailed geochemical information concerning petrologic variations within the lunar crust as is possible. The classification map shows the global spatial distributions of end-member compositions, the transitional spatial relations between end-member compositions, and quantitative estimates of relative proportions of each end member at each pixel location within the orbital groundtracks. The use of elemental ratios in this analysis, instead of the commonly used elemental bivariate diagrams, shows geologic information that is otherwise hidden in individual elemental databases. R.J.F.

N87-23408*# National Aeronautics and Space Administration, Washington, D.C.

A CHEMICAL AND PETROLOGICAL MODEL OF THE LUNAR CRUST

Paul D. Spudis and Philip A. Davis *In* NASA, Washington Reports of Planetary Geology and Geophysics Program, 1986 May 1987 p 155-157 (For primary document see N87-23341 16-91)

Avail: NTIS HC A24/MF A01 CSCL 03B

Information is given on the composition and structure of the lunar crust. A lunar model is illustrated, indicating that it has essentially two layers, anorthositic mixed rocks overlaying a generally noritic crystalline basement. Implications relative to lunar evolution are discussed. R.J.F.

N87-23409*# National Aeronautics and Space Administration. Lyndon B. Johnson Space Center, Houston, Tex.

CALCIUM CARBONATE AND CALCIUM SULFATE IN MARTIAN METEORITE EETA79001

J. L. Gooding and S. J. Wentworth (Lockheed Engineering and Management Services Co., Inc., Houston, Tex.) *In* NASA, Washington Reports of Planetary Geology and Geophysics Program, 1986 May 1987 p 158-159 (For primary document see N87-23341 16-91)

Avail: NTIS HC A24/MF A01 CSCL 03B

Chips of glassy Lithology C of EETA79001 were studied by scanning electron microscopy and energy dispersive X-ray spectroscopy to determine the mineralogy and petrogenesis of the glass that was shown by others to contain trapped Mars-like gases. Calcium carbonite was identified as massive to acicular crystals for which Ca, C, and O were the major elements. Calcium sulfate was identified as prismatic-acicular crystals with Ca and S as the major elements. R.J.F.

N87-23410*# National Aeronautics and Space Administration. Ames Research Center, Moffett Field, Calif.

THE CASE FOR A WET, WARM CLIMATE ON EARLY MARS Abstract Only

J. B. Pollack, J. F. Kasting, S. M. Richardson, and K. Poliakoff (IMI, Inc., San Jose, Calif.) *In* NASA, Washington Reports of Planetary Geology and Geophysics Program, 1986 May 1987 p 160 (For primary document see N87-23341 16-91)

Avail: NTIS HC A24/MF A01 CSCL 03B

Arguments are presented in support of the idea that Mars possessed a dense CO2 atmosphere and a wet, warm climate early in its history. The plausibility of a CO2 greenhouse is tested by formulating a simple model of the CO2 geochemical cycle on early Mars. By scaling the rate of silicate weathering on Earth, researchers estimated a weathering time constant of the order of several times 10 to the 7th power years for early Mars. Thus, a dense atmosphere could have existed for a geologically significant time period (approx. 10 to the 9th power years) only if atmospheric CO2 was being continuously resupplied. The most likely mechanism by which this could have been accomplished is the thermal decomposition of carbonate rocks induced directly or indirectly by intense, global scale volcanism. R.J.F.

N87-23411*# Hawaii Inst. of Geophysics, Honolulu. Planetary Geosciences Div.

THE ROLE OF REGOLITH ADSORPTION IN THE TRANSITION FROM EARLY TO LATE MARS CLIMATE

F. P. Fanale, S. E. Postawko, A. P. Zent, and J. R. Salvail *In* NASA, Washington Reports of Planetary Geology and Geophysics Program, 1986 May 1987 p 161-162 (For primary document see N87-23341 16-91)

Avail: NTIS HC A24/MF A01 CSCL 03B

Researchers reexamined radiative transfer models of early Mars that were advanced to show the existance of a greenhouse effect. These models were reexamined with regard to the effect that regolith adsorption may have had. It is argued that while the precipitation of carbonates has probably been an important process during Mars history, the rates at which this process could have taken place under early Mars conditions would have dropped sharply once liquid water was fairly scarce. Furthermore, conditions under which liquid water was available may have involved efficient recycling of carbonate so that steady state conditions rather than irreversible CO2 removal prevailed. In contrast, the growth of regolith surface area demands corresponding and predictable CO2 removal from the atmosphere-cap system and is fully capable of terminating any enhanced temperature regime on early Mars in the absence of any other effects. R.J.F.

N87-23412*# National Aeronautics and Space Administration. Goddard Space Flight Center, Greenbelt, Md.

OXIDIZED BASALTS ON THE SURFACE OF VENUS: COMPOSITIONAL IMPLICATIONS OF MEASURED SPECTRAL PROPERTIES

C. M. Pieters, W. Patterson, S. Pratt, J. W. Head (Brown Univ.,

Providence, R. I.), and J. Garvin *In* NASA, Washington Reports of Planetary Geology and Geophysics Program, 1986 May 1987 p 165-166 (For primary document see N87-23341 16-91)
Avail: NTIS HC A24/MF A01 CSCL 03B

Venera Lander reflectance data are compared with high temperature spectra of the same basaltic materials. The dark, flat unoxidized basalts are still inconsistent with the Venera data in the near-infrared. Basaltic material with a ferric component, however, would satisfy both the increase in reflectance beyond 0.7 microns as well as the dark, relatively colorless character in the visible. Therefore, it is concluded that besaltic surfaces of Venus represented by these measurements either contain minerals with uncommon characteristics, or, more likely, are relatively oxidized. R.J.F.

N87-23413*# Arizona State Univ., Tempe. Dept. of Geology.

VARIATIONS OF MARTIAN SURFACE ALBEDO: EVIDENCE FOR YEARLY DUST DEPOSITION AND REMOVAL

Philip R. Christensen *In* NASA, Washington Reports of Planetary Geology and Geophysics Program, 1986 May 1987 p 167-169 (For primary document see N87-23341 16-91)
Avail: NTIS HC A24/MF A01 CSCL 03B

The purpose is to determine the degree, spatial distribution and timing of the deposition and removal of dust storm fallout, and to relate the current patterns of dust deposition and removal to the long-term evolution of the Martian surface. Southern Hemisphere dark areas are found to quickly return to close to their pre-storm albedos, suggesting rapid removal of any dust that was deposited. Northern Hemisphere dark regions are brighter post-storm, but gradually darken to pre-storm levels over the Mars year. In doing so they act as local sources of dust during otherwise clear periods. Dust does not appear to be removed from bright regions, resulting in the 1 to 2 m thick deposits observed today. R.J.F.

N87-23414*# Washington Univ., St. Louis, Mo. Center for the Space Sciences.

ON THE SPECTRAL REFLECTANCE PROPERTIES OF MATERIALS EXPOSED AT THE VIKING LANDING SITES

E. Guinness, R. Arvidson, M. Dale-Bannister, R. Singer, and E. Bruckenthal (Hawaii Inst. of Geophysics, Honolulu.) *In* NASA, Washington Reports of Planetary Geology and Geophysics Program, 1986 May 1987 p 170-172 (For primary document see N87-23341 16-91)
Avail: NTIS HC A24/MF A01 CSCL 03B

Reflectance data derived from Viking Lander multispectral data were used to characterize the types of soils and blocks exposed at the landing sites and to search for evidence of relatively unaltered igneous rocks. A comprehensive effort was mounted to examine multispectral data that combines testing of camera radiometric calibrations, explicitly removing the effects of atmospheric attenuation and skylight, and quantitatively comparing the corrected data to reflectance data from laboratory materials. Bi-directional reflectances for blue, green and red channels were determined for 31 block and soil exposures at Viking landing sites. R.J.F.

N87-23415*# Washington Univ., Seattle. Dept. of Geological Sciences.

SPECTRAL MIXTURE MODELING: FURTHER ANALYSIS OF ROCK AND SOIL TYPES AT THE VIKING LANDER SITES

John B. Adams and Milton O. Smith *In* NASA, Washington Reports of Planetary Geology and Geophysics Program, 1986 May 1987 p 173-174 (For primary document see N87-23341 16-91)
Avail: NTIS HC A24/MF A01 CSCL 03B

A new image processing technique was applied to Viking Lander multispectral images. Spectral endmembers were defined that included soil, rock and shade. Mixtures of these endmembers were found to account for nearly all the spectral variance in a Viking Lander image. R.J.F.

N87-23416*# Massachusetts Inst. of Tech., Cambridge. Dept. of Earth, Atmospheric and Planetary Sciences.

HISINGERITE AND IDDINGSITE ON MARS: DEGRADATION OF IRON-RICH BASALTS

Roger G. Burns *In* NASA, Washington Reports of Planetary Geology and Geophysics Program, 1986 May 1987 p 175 (For primary document see N87-23341 16-91)
Avail: NTIS HC A24/MF A01 CSCL 03B

Paragenetic evidence that indicates that hisingerite may have formed during the evolution of Martian regolith is summarized. Hisingerite was once regarded as poorly crystalline iron-rich smectite or nontronite. However, recent electron microscopy and X-ray studies have revealed hisingerite to have an amorphous or gel structure containing a disordered array of (FeO6) octahedra and (SiO4) tetrahedra. It is just this coordination environment and degree of crystallinity that matches materials simulating the spectral properties of the bright regions of Mars. Therefore, hisingerite and basic ferric sulfate minerals appear to be major contributers to remote sensed reflectance spectral profiles of Mars. R.J.F.

N87-23417*# Massachusetts Inst. of Tech., Cambridge. Dept. of Earth, Atmospheric and Planetary Sciences.

GOSSANS ON MARS: SPECTRAL FEATURES ATTRIBUTED TO JAROSITE

Roger G. Burns *In* NASA, Washington Reports of Planetary Geology and Geophysics Program, 1986 May 1987 p 176-177 (For primary document see N87-23341 16-91)
Avail: NTIS HC A24/MF A01 CSCL 03B

Jarosites, which are present in terrestrial gossans capping oxidized sulfides associated with mafic igneous rocks, may also be present in Martian regolith. Spectral characteristics of jarosites are displayed in remote sensed reflectance spectra of bright regions of Mars surface. The occurrence of jarosite in the regolith would imply that acidic permafrost and sulfide ores exist beneath the surface of Mars. R.J.F.

N87-23418*# Washington Univ., Seattle. Center for the Space Sciences.

CHARACTERIZATION OF SURFICIAL UNITS ON MARS USING VIKING ORBITER MULTISPECTRAL IMAGE AND THERMAL DATA

M. A. Presley, R. E. Arvidson, and P. R. Christensen (Arizona State Univ., Tempe.) *In* NASA, Washington Reports of Planetary Geology and Geophysics Program, 1986 May 1987 p 178-180 (For primary document see N87-23341 16-91)
Avail: NTIS HC A24/MF A01 CSCL 03B

Albedo and thermal property correlations of the topography of Mars were conducted with emphases upon the types and origins of materials exposed in the central equatorial region. This area displays a wide variation in color, albedo and thermal properties, and is relatively free of dust and haze. The physical, mineralogical and elemental characteristics of this area are discussed. R.J.F.

N87-23419*# Hawaii Inst. of Geophysics, Honolulu. Planetary Geosciences Div.

CO2: ADSORPTION ON PALAGONITE AND THE MARTIAN REGOLITH

Aaron P. Zent, Fraser P. Fanale, and Susan E. Postawko *In* NASA, Washington Reports of Planetary Geology and Geophysics Program, 1986 May 1987 p 181-183 (For primary document see N87-23341 16-91)
Avail: NTIS HC A24/MF A01 CSCL 03B

Possible scenarios for the evolution of the Martian climate are discussed. In the interest of determining an upper limit on the absorptive capacity of the Martian regolith, researchers examined the results of Fanale and Cannon (1971, 1974) for CO2 adsorption on nontronite and basalt. There appeared to be a strong proportionality between the capacity of the absorbent and its specific surface area. A model of the Martian climate is given that allows the researchers to make some estimates of exchangeable CO2 abundances. R.J.F.

N87-23420*# Cornell Univ., Ithaca, N.Y.
INVESTIGATION OF MARTIAN H2O AND CO2 VIA GAMMA-RAY SPECTROSCOPY
Steven W. Squyres and Larry G. Evans (Computer Sciences Corp., Beltsville, Md.) *In* NASA, Washington Reports of Planetary Geology and Geophysics Program, 1986 May 1987 p 184-186 (For primary document see N87-23341 16-91)
Avail: NTIS HC A24/MF A01 CSCL 03B

The evolution and present state of water and carbon dioxide on Mars are discussed. Researchers wished to determine how effectively questions regarding the distribution of water and carbon dioxide on Mars may be addressed with orbital gamma ray spectrometer data. Several simple, multi-layer models of the Martian surface were formulated to address problems such as the ice/dust ratio of layered deposits; the distribution, depth and concentration of ground ice; the thickness of north polar perennial ice; the thickness of the carbon dioxide layer over the south polar cap; the thickness of the seasonal carbon dioxide frost cap; and the water content of the seasonal frost cap. The results indicate that the Mars Observer gamma ray spectrometer will be a powerful tool for investigating the distribution and stratigraphy of volatiles on Mars. R.J.F.

N87-23421*# Hawaii Inst. of Geophysics, Honolulu. Planetary Geosciences Div.
REFLECTANCE SPECTRA OF MAFIC SILICATES AND PHYLLOSILICATES FROM .6 TO 4.6 MICRONS c89
Ted L. Roush, Robert B. Singer, and Thomas B. McCord *In* NASA, Washington Reports of Planetary Geology and Geophysics Program, 1986 May 1987 p 187-189 (For primary document see N87-23341 16-91)
(Grants NsG-7590; NsG-7312)
Avail: NTIS HC A24/MF A01 CSCL 03A

The results of spectral measurements for mafic silicates are given. The study provided valuable spectral reflectance information about mafic silicates and phyllosilicates in the 2.5 to 4.6 micron wavelength region. It was shown that the reflectance of these materials is strongly affected by the presence of H2O and OH. Therefore, the identification of these absorbing species is greatly enhanced. R.J.F.

N87-23422*# Hawaii Inst. of Geophysics, Honolulu. Planetary Geosciences Div.
SPECTRAL EFFECTS OF DEHYDRATION ON PHYLLOSILICATES c25
E. A. Bruckenthal and R. B. Singer *In* NASA, Washington Reports of Planetary Geology and Geophysics Program, 1986 May 1987 p 190-192 (For primary document see N87-23341 16-91)
(Grant NsG-7590)
Avail: NTIS HC A24/MF A01 CSCL 07D

Six phyllosilicates were progressively dehydrated under controlled conditions in an effort to study the spectral effects of their dehydration. The spectra obtained at each level of hydration provide information that may be used in future spectroscopic observations of the planets, as well as a data set which compliments the existing body of terrestrial soil knowledge. R.J.F.

N87-23423*# Geological Survey, Denver, Colo.
STUDIES OF THE SCATTERING/ABSORPTION OF MINERALS c25
Roger N. Clark *In* NASA, Washington Reports of Planetary Geology and Geophysics Program, 1986 May 1987 p 193-195 (For primary document see N87-23341 16-91)
Avail: NTIS HC A24/MF A01 CSCL 07D

Reflectance spectra were computed for water ice and ammonia ice mixtures as functions of weight fraction, grain size, and viewing geometry to simulate possible outer solar system satellite surfaces. Reflectance spectra of planetary surfaces are most affected by the weight fraction and grain sizes of the minerals in the surface. The reflectance can range from 1.0 to about 0.01 by changing the grain size or weight fraction, a factor of 100. Viewing geometry changes the reflectance by about 25 percent or less. R.J.F.

N87-23424*# National Aeronautics and Space Administration. Goddard Space Flight Center, Greenbelt, Md.
MID-INFRARED SPECTROSCOPIC INVESTIGATION c25
Louis Walter, Norma Vergo, and John W. Salisbury (Geological Survey, Denver, Colo.) *In* NASA, Washington Reports of Planetary Geology and Geophysics Program, 1986 May 1987 p 196-198 (For primary document see N87-23341 16-91)
Avail: NTIS HC A24/MF A01 CSCL 07D

Mid-infrared spectroscopic research efforts are discussed. The development of a new instrumentation to permit advanced measurements in the mid-infrared region of the spectrum, the development of a special library of well-characterized mineral and rock specimens for interpretation of remote sensing data, and cooperative measurements of the spectral signatures of analogues of materials that may be present on the surfaces of asteroids, planets or their Moons are discussed. R.J.F.

N87-23425*# Arizona State Univ., Tempe. Dept. of Geology.
THERMAL-INFRARED SPECTRAL OBSERVATIONS OF GEOLOGIC MATERIALS IN EMISSION c25
Philip R. Christensen and Sharon J. Luth *In* NASA, Washington Reports of Planetary Geology and Geophysics Program, 1986 May 1987 p 199-201 (For primary document see N87-23341 16-91)
Avail: NTIS HC A24/MF A01 CSCL 07D

The thermal-infrared spectra of geologic materials in emission were studied using the prototype Thermal Emission Spectrometer (TES). A variety of of processes and surface modifications that may influence or alter the spectra of primary rock materials were studied. It was confirmed that thermal emission spectra contain the same absorption features as those observed in transmission and reflection spectra. It was confirmed that the TES instrument can be used to obtain relevant spectra for analysis of rock and mineral composition. R.J.F.

N87-23426*# Jet Propulsion Lab., California Inst. of Tech., Pasadena.
BIDIRECTIONAL REFLECTANCE PROPERTIES OF PLANETARY SURFACE MATERIALS c25
B. Buratti, W. Smythe, R. Nelson, V. Gharakhani, and B. Hapke (Pittsburgh Univ., Pa.) *In* NASA, Washington Reports of Planetary Geology and Geophysics Program, 1986 May 1987 p 202-204 (For primary document see N87-23341 16-91)
(Contract NAS7-918)
Avail: NTIS HC A24/MF A01 CSCL 07D

Laboratory measurements using a spectrogoniometer to separate the effects of surficial texture and albedo in the characterization of planetary surface materials are discussed. An investigation of the surface of Io is discussed. A number of technical improvements to the goniometer are summarized. R.J.F.

N87-23427*# Pittsburgh Univ., Pa. Dept. of Geology and Planetary Science.
ATLAS OF REFLECTANCE SPECTRA OF TERRESTRIAL, LUNAR AND METEORITIC POWDERS AND FROSTS FROM 92 TO 1800 (LC2)NM Abstract Only c25
Jeffrey Wagner, Bruce Hapke, and Eddie Wells *In* NASA, Washington Reports of Planetary Geology and Geophysics Program, 1986 May 1987 p 205 (For primary document see N87-23341 16-91)
Avail: NTIS HC A24/MF A01 CSCL 07D

The reflectance spectra of powdered samples of selected minerals, meteorites, lunar materials and frosts are presented as an aid in the interpretation of present and future remote sensing data of solar system objects. Spectra obtained in separate wavelength regions have been combined and normalized, yielding coverage from 92 to 1800 nm. Spectral features include reflectance maxima in the far UV region produced by valence-conduction interband transitions, and reflectance minima in the near UV, visible and near IR regions, produced by charge transfer and crystal field transitions. Specific maxima and minima are diagnostic of mineral type and composition; additionally, the minerals present in mixtures such as meteorites and lunar samples can be determined. Author

N87-23428*# Brown Univ., Providence, R. I.
DECONVOLUTION OF SPECTRA FOR INTIMATE MIXTURES
c25
John F. Mustard, Carle M. Pieters, and Stephen F. Pratt *In* NASA, Washington Reports of Planetary Geology and Geophysics Program, 1986 May 1987 p 206-207 (For primary document see N87-23341 16-91)
Avail: NTIS HC A24/MF A01 CSCL 07D

Visible to near infrared reflectance spectra of macroscopic mixtures have been shown to be linear combinations of the reflections of the pure mineral components in the mixture. However, for microscopic mixtures the mixing systematics are in general nonlinear. The systematics may be linearized by conversion of reflectance to single scattering albedo (w), where the equations which relate reflectance to w depend on the method of data collection. Several proposed mixing models may be used to estimate mineral abundances from the reflectance spectra of intimate mixtures. These models are summarized and a revised model is presented. A noniterative (linear) least squares approach was used for curve fitting and the data, measured as bi-directional reflectance with incidence and emergence angles of 30 and 0 deg were converted to w by a simplified version of Hapke's equation for bi-directional reflectance. This model was tested with two mixture series composed of 45 to 75 micron particles: an anorthite-enstatite series and an olivine-magnetite series. The data indicate that the simplified Hapke's equation may be used to convolve reflectance spectra into mineral abundances if appropriate endmembers are known or derived from other techniques. For surfaces that contain a significant component of very low albedo material, a somewhat modified version of this technique will need to be developed. Since the abundances are calculated using a noniterative approach, the application of this method is especially efficient for large spectral data sets, such as those produced by mapping spectrometers. M.G.

N87-23429*# National Aeronautics and Space Administration, Washington, D.C. Dept. of Geological Sciences.
COMPOSITIONAL INFORMATION FOR THE MOON: SOME CHARACTERISTICS OF CURRENT NEAR-IR SPECTRA (TELESCOPIC AND LABORATORY)
Carle M. Pieters *In* NASA, Washington Reports of Planetary Geology and Geophysics Program, 1986 May 1987 p 208-209 (For primary document see N87-23341 16-91)
Avail: NTIS HC A24/MF A01 CSCL 03B

For the last decade telescopic near infrared spectra have been obtained for small lunar areas. Such spectra, with the ground truth foundation from lunar samples, have been used extensively to address a multitude of problems in lunar science. Much of the near infrared spectral reflectance data from both laboratory and telescopic measurements have recently been compiled in comparable formats and an initial comparative assessment of the available data using selected spectral parameters has been made. The objective is to develop a framework for the systematics of lunar near-IR spectra in order to better interpret spectra of unknown materials in terms of useful compositional information. Each spectrum was first classified according to its general character then a variety of parameters sensitive to mineralogy and alteration products were measured for each spectrum: band width, band strength, absorption band center near 1 micron, band symmetry, continuum slope, etc. The telescopic and laboratory data sets are briefly described. The comparative analysis shows that a few well known lunar spectral properties are evident in both sets, such as the systematic variation in pyroxene composition between the highlands and the mare. However, an additional gabbroic component can be detected in many highland craters. M.G.

N87-23430*# Hawaii Inst. of Geophysics, Honolulu. Planetary Geosciences Div.
PRELIMINARY RESULTS OF SPECTRAL REFLECTANCE STUDIES OF TYCHO CRATER
B. R. Hawke, C. R. Coombs, P. G. Lucey, J. F. Bell, R. Jaumann, G. Neukum, and Carle M. Pieters (Brown Univ., Providence, R. I.) *In* NASA, Washington Reports of Planetary Geology and Geophysics Program, 1986 May 1987 p 211-213 (For primary document see N87-23341 16-91)
Avail: NTIS HC A24/MF A01 CSCL 03B

The preliminary analysis and interpretation of near infrared spectra obtained for both the interior and exterior deposits associated with the Tycho crater is presented. Specific objectives were: (1) to determine the composition and stratigraphy of the highland crust in the Tycho target site; (2) to determine the likely composition of the primary ejecta which may be present in ray deposits; (3) to investigate the nature of spectral units defined in previous studies; (4) to further investigate the nature and origin of both the bright and dark haloes around the rim crest; and (5) to compare the compositions determined for the Tycho units with those of the Aristarchus crater as well as typical highland deposits. The spectra obtained for the interior areas exhibit similar spectral features. These include relatively strong 1 micron absorption bands whose minima are centered between 0.97 and 0.99 microns and shallow to intermediate continuum slopes. The spectra generally exhibit indications of a 1.3 micron feature consistent with the presence of Fe(2+) bearing plagioclase feldspar. The strong 1 micron absorption features indicate a dominant high Ca clinopyroxene component. Results obtained from the ejecta deposits show that the spectrum of the inner, bright halo is almost identical with those obtained for interior units. The spectrum of the dark halo exhibits a wide, relatively shallow absorption feature centered at 1.01 microns, a 1.3 micron absorption, and a steep continuum slope. This spectrum is interpreted as indicating the presence of pyroxene, Fe-bearing feldspar, and a significant component of Fe-bearing impact melt glass. Finally, the spectra of spots inside Tycho show similarity with certain spectra for Aristarchus. However, the suite of spectra obtained for Tycho exhibits a different trend in terms of band center versus width. M.G.

N87-23431*# Hawaii Inst. of Geophysics, Honolulu. Planetary Geosciences Div.
PRELIMINARY RESULTS OF GEOLOGIC AND REMOTE SENSING STUDIES OF RIMA MOZART
C. R. Coombs and B. R. Hawke *In* NASA, Washington Reports of Planetary Geology and Geophysics Program, 1986 May 1987 p 214-216 (For primary document see N87-23341 16-91)
Avail: NTIS HC A24/MF A01 CSCL 03B

In order to better understand the processes responsible for the formation of lunar sinuous rilles, a study of Rima Mozart was conducted using a variety of geologic, photographic, and remote sensing data. The apparent source of this rille is located in a highlands unit of known composition and it is hypothesized that thermal and mechanical erosion played an important role in the formation of Rima Mozart. Excellent photographic, topographic, multispectral, and radar data exist for this rille. The preliminary results of an analysis of this data are presented. Photographic data indicates the presence of two volcanic source vents for Rima Mozart: Kathleen and Ann. It is suggested that Rima Mozart, like many other lunar sinuous rilles, was most likely formed by a combination of events. Rima Mozart does follow a pre-existing, dominant NW/SE structural trend suggesting the influence of structural features on the rille, however, the tectonic influence is not the sole source for the formation of the rille, as suggested by the presence of the two source vents and the spatter around Ann. It is suggested that the rille formation began with an explosive eruption at Kathleen which later calmed down to a pulsating, high volume, low-viscosity lava flow. The rapid effusion rate of the magma as well as its high temperature and turbid nature helped carve the sinuous rille into the fractured and structurally weak Apennine Bench Formation underneath. Similar eruptions and subsequent flows were also created at Ann and joined to the main channel by a NE-trending secondary rille. M.G.

N87-23432*# Cornell Univ., Ithaca, N.Y. Center for Radiophysics and Space Research.
PHOTOMETRIC PROPERTIES OF LUNAR TERRAINS DERIVED FROM HAPKE'S EQUATION
Paul Helfenstein and Joseph Veverka *In* NASA, Washington

Reports of Planetary Geology and Geophysics Program, 1986 May 1987 p 217-218 (For primary document see N87-23341 16-91) (Grant NsG-7606)
Avail: NTIS HC A24/MF A01 CSCL 03B

Hapke's bidirectional reflectance equations provide the most rigorous available description of photometric behavior in terms of physically meaningful parameters. The primary objective of this study was to derive Hapke parameters for the lunar surface from both disk-integrated and disk-resolved photometric data. Hapke's equation was fit to the disk-integrated phase curves and disk-resolved data for dark, average, and bright terrain classes using an iterative, nonlinear least squares algorithm described by Helfenstein. Parameters were initially determined from the disk-integrated data, and the result was applied as a first guess to the iterative solution of parameters for individual terrain classes. Plots are presented of the disk-resolved data normalized to corresponding brightnesses predicted from the disk-integrated solution under the same illumination and viewing geometries. Systematic trends in disk-resolved parameters can be identified. Values for single scattering albedo (w) of the dominantly anorthositic average and bright terrains are significantly larger than the value for the basaltic dark terrains (mare). Values for surge brightness parameters, particle phase function, and average topographic slope angle are also discussed. M.G.

N87-23433*# Pittsburgh Univ., Pa. Dept. of Geology and Planetary Science.
BIDIRECTIONAL REFLECTANCE SPECTROSCOPY Abstract Only **c25**
Bruce Hapke *In* NASA, Washington Reports of Planetary Geology and Geophysics Program, 1986 May 1987 p 219 Previously announced in IAA as A87-14645 Submitted for publication (For primary document see N87-23341 16-91)
Avail: NTIS HC A24/MF A01 CSCL 07D

An analytical model is developed for the opposition effects (heiligenshein) in the case of light scattering from a semi-infinite, particulate medium with particles that are large relative to the wavelength. The effect is common for natural materials, and comprises a bright surge in light diffusively reflected from a surface at near zero phase. A generalized expression is devised for the extinction coefficient of a particulate medium. Models are developed for step function and hyperbolic tangent distributions of light scattered from a stratified medium and exhibiting the opposition effect. A maximum brightness amplitude increase of 0.753 is projected for the effect. Greater values must have other causes. To illustrate the theory it is fitted to observations of the Moon, an asteroid, and a satellite of Uranus; Europa is also discussed. ESA

N87-23434*# Pittsburgh Univ., Pa.
ON THE SPUTTER ALTERATION OF REGOLITHS OF OUTER SOLAR SYSTEM BODIES Abstract Only **c90**
Bruce Hapke *In* NASA, Washington Reports of Planetary Geology and Geophysics Program, 1986 May 1987 p 220 Submitted for publication (For primary document see N87-23341 16-91)
Avail: NTIS HC A24/MF A01 CSCL 03B

Several processes that are expected to occur when the porous regoliths of outer solar system bodies (without atmospheres) are subjected to energetic ion bombardment are discussed. The conclusions reached in much of the literature addressing sputtering are quantitatively or qualitatively incorrect because effects of soil porosity have been neglected. It is shown theoretically and experimentally that porosity reduces the effective sputtering yield of a soil by more than an order of magnitude. Between 90 and 97% of the sputtered atoms are trapped within the regolith, where they are factionated by differential desorption. Experiments indicate that more volatile species have higher desorption probabilities. This process is the most important way in which alteration of chemical and optical properties occurs when a regolith is sputtered. When a basic silicate soil is irradiated these effects lead to sputter-deposited films enriched in metallic iron, while O, Na and K are preferentially lost. The Na and K are present in the atmosphere above the sputtered silicate in quantities much greater than their abundances in the regolith. Icy regoliths of SO2 should be enriched in elemental S and/or S2O. This prediction is supported by the probable identification of S2O and polysulfur oxide bands in the IR spectra of H-sputtered SO2 reported by Moore. When porous mixtures of water, ammonia and methane frosts are sputtered, the loss of H and surface reactions of C, N and O in the deposits should produce complex hydrocarbons and carbohydrates, some of which may be quite dark. Such reactions may have played a role in the formation of the matrix material of carbonaceous chondrites prior to agglomeration. M.G.

N87-23435*# Virginia Univ., Charlottesville.
CHARGED PARTICLE MODIFICATION OF SURFACES IN THE OUTER SOLAR SYSTEM **c90**
R. E. Johnson *In* NASA, Washington Reports of Planetary Geology and Geophysics Program, 1986 May 1987 p 221-222 (For primary document see N87-23341 16-91)
(Grant NAGw-186)
Avail: NTIS HC A24/MF A01 CSCL 03B

Voyager reflectance spectra data have indicated clear leading/trailing differences in the albedo of the icy Galilean and Saturnian satellites. For the Galilean satellites, these have been analyzed by Nelson, et al. and, more recently, by McEwen. They have described the longitudinal dependence of this data and attempted to interpret this in terms of plasma and meteorite modification of the surface. Primary attention has been paid to Europa at which the leading/trailing differences are the largest. This data was reanalyzed extracting the single grain albedo (w) and constructing the Espat-function, W = (1-w)/w from this. Because w is near unity, W is approximately 2(alpha)D where alpha is the absorption coefficient and D is the grain size. In doing so, a direct comparison to the longitudinal plasma bombardment flux was found for the first time. This occurs primarily in the UV and is probably due to an absorption associated with implanted S, as the UV band of Voyager overlaps the IUE data of Lane et al. The relative importance of grain size effects and implant impurity effects can now be studied. Author

N87-23436*# Cornell Univ., Ithaca, N.Y.
Io: COMPARISON OF PHOTOMETRIC SCANS PRODUCED BY THE MINNAERT AND HAPKE FUNCTIONS **c25**
Damon P. Simonelli and Joseph Veverka *In* NASA, Washington Reports of Planetary Geology and Geophysics Program, 1986 May 1987 p 223-225 (For primary document see N87-23341 16-91) (Grant NsG-7156)
Avail: NTIS HC A24/MF A01 CSCL 07D

Experience has shown that the empirical Minnaert function is a very useful approximation to real photometric behavior near opposition (phase angle = 0), but that in general it cannot accurately model photometric scans across the face of even a homogeneous planet at higher phase angles. Given recent work on fitting the rigorous Hapke function to Voyager data for Io, we can test to what degree the Minnaert function breaks down in the case of Ionian materials by comparing photometric scans produced by the two approaches. At phase angles 2, 20, 30, 60, and 90 deg, we have computed scans of the reflectance along the photometric equator and mirror meridian that would be expected for a homogeneous planet whose surface obeys Hapke's law. The values used for the Hapke parameters omega(0), h, g, and bar-theta were derived for Io by Simonelli and Veverka in both the Voyager narrow angle camera violet filter and orange filter. Each calculated Hapke scan is compared with the corresponding scan predicted by Minnaert's law for various values of the Minnaert limb-darkening parameter k. For a Minnaert scan at a particular k, the value of the reflectance parameter B(0) is arbitrarily chosen so that the Minnaert and Hapke scans coincide at the so-called specular point (the point where the photometric equator and mirror meridian intersect). The violet filter photometric scans that result from this process are shown. Results indicate that the empirical Minnaert function, while not a perfect model of real photometric behavior, does provide a very useful parameterization of limb darkening at phase angles out to 90 deg, and is especially useful near opposition. Author

N87-23437*# Jet Propulsion Lab., California Inst. of Tech., Pasadena.

SULFUR-OXYGEN PROCESSES ON Io

Robert M. Nelson and William D. Smythe *In* NASA, Washington Reports of Planetary Geology and Geophysics Program, 1986 May 1987 p 226 (For primary document see N87-23341 16-91)
Avail: NTIS HC A24/MF A01 CSCL 03B

Laboratory studies of irradiated sulfur dioxide frost have found that sulfur trioxide should be formed as a consequence of the irradiation process. The spectral reflectance of solid sulfur trioxide was measured in the laboratory and it was found that the compound has strong absorption features at 3.37 and 3.70 microns. These features are not present in the spectral geometric albedo of Io. This is interpreted as an indication that sulfur trioxide may exist in such limited abundance that it is undetectable in disk averaged spectrophotometry. It is suggested that the Near-Infrared Mapping Spectrometer on the Galileo spacecraft should be able to identify condensed sulfur trioxide on Io particularly in regions bordering the sulfur dioxide deposits. The presence of elemental sulfur on Io's surface has been questioned on several grounds, most notably the suggested production process (quenched molten sulfur extrusions) and the effect of radiation (particularly X-rays) on some of the allotropes. Mixtures of sulfur allotropes were produced in the laboratory by quenching molten sulfur and it was found that the spectra indicate the presence of certain red-colored allotropes which are preserved upon quenching. The color of the sulfur glass produced is redder when the temperature of the original melt is higher. This is consistent with the suggestion that Io's spectral geometric albedo can be partly explained by the presence of quenched sulfur glasses. M.G.

N87-23438*# Jet Propulsion Lab., California Inst. of Tech., Pasadena.

SOLID SULFUR IN VACUUM: SUBLIMATION EFFECTS ON SURFACE MICROTEXTURE, COLOR AND SPECTRAL REFLECTANCE, AND APPLICATIONS TO PLANETARY SURFACES c25

D. B. Nash *In* NASA, Washington Reports of Planetary Geology and Geophysics Program, 1986 May 1987 p 227-228 (For primary document see N87-23341 16-91)
Avail: NTIS HC A24/MF A01 CSCL 07D

A form of sulfur that is white at room temperature and very fluffy in texture has been found in laboratory experiments on the effects of vacuum sublimation (evaporation) on solid sulfur. This work is an outgrowth of proton sputtering experiments on sulfur directed toward understanding Jovian magnetospheric effects on the surface of Io. Fluffy white sulfur is formed on the surface of solid yellow, tan, or brown sulfur melt freezes in vacuum by differential (fractional) evaporation of two or more sulfur molecular species present in the original sulfur; S(8) ring sulfur is thought to be the dominant sublimination phase lost to the vacuum sink, and polymeric chain sulfur S(u) the dominant residual phase that remains in place, forming the residual fluffy surface layer. The reflectance spectrum of the original sulfur surface is greaty modified by formation of the fluffy layer: the blue absorption band-edge and shoulder move 0.05 to 0.06 microns toward shorter wavelengths resulting in a permanent increase in reflectivity near 0.42 to 0.46 microns; the UV reflectivity below 0.40 microns is reduced. This form of sulfur should exist in large quantity on the surface of Io, especially in hotspot regions if there is solid free sulfur there that has solidified from a melt. Its color and spectra will indicate relative crystallization age on a scale of days to months and/or surface temperature distribution history. M.G.

N87-23439*# Pittsburgh Univ., Pa. Dept. of Geology and Planetary Science.

A PRELIMINARY ANALYSIS OF THE MARINER 10 COLOR RATIO MAP OF MERCURY Abstract Only

Barry Rava and Bruce Hapke *In* NASA, Washington Reports of Planetary Geology and Geophysics Program, 1986 May 1987 p 229 (For primary document see N87-23341 16-91)
Avail: NTIS HC A24/MF A01 CSCL 03B

A preliminary geological analysis of the Mariner 10 orange/UV color ratio map of Mercury is given, assuming a basaltic crust. Certain errors in the map are pointed out. The relationship between color and terrain are distinctly non-lunar. Rays and ejecta are bluer than average on Mercury, whereas they are redder on the Moon. This fact, along with the lack of the ferrous band in Mercury's spectral reflectance and smaller albedo contrasts, implies that the crust is low in Fe and Ti. There is no correlation between color boundaries and the smooth plains on Mercury, in contrast with the strong correlation between color and maria-highlands contacts on the Moon. The smooth plains are not Mercurian analogs of lunar maria, and a lunar-type of second wave melting did not occur. Ambiguous correlations between color and topography indicate that older, redder materials underlie younger, bluer rocks in many places on the planet, implying that the last stages of volcanism involved low-Fe lavas covering higher-Fe rocks. There is some evidence of late Fe-rich pyroclastic activity. Author

N87-23440*# Geological Survey, Flagstaff, Ariz.

A COMPILATION SYSTEM FOR VENUS RADAR MISSION (MAGELLAN) c43

Sherman S. C. Wu, Francis J. Schafer, and Annie-Elpis Howington *In* NASA, Washington Reports of Planetary Geology and Geophysics Program, 1986 May 1987 p 233-236 (For primary document see N87-23341 16-91)
Avail: NTIS HC A24/MF A01 CSCL 08B

A synthetic aperture radar (SAR) compilation system was developed for extraction of topographic information of Venus from stereoradar imagery to be obtained from the Magellan mission. The system was developed for an AS-11AM analytical stereoplotter. Extensive tests were made on this compilation software by using stereo images from various radar systems, both spaceborne and airborne. Maps were compiled and the precision of planimetry and contour measurement was evaluated. Digital data of some models were also collected for processing orthophoto or perspective views by using the original radar images. M.G.

N87-23441*# Hawaii Inst. of Geophysics, Honolulu. Planetary Geosciences Div.

NEW VERY HIGH RESOLUTION RADAR STUDIES OF THE MOON c32

Peter J. Mouginis-Mark and Bruce Campbell *In* NASA, Washington Reports of Planetary Geology and Geophysics Program, 1986 May 1987 p 237 (For primary document see N87-23341 16-91)
Avail: NTIS HC A24/MF A01 CSCL 17I

As part of an effort to further understand the geologic utility of radar studies of the terrestrial planets, investigators at the Hawaii Institute of Geophysics are collaborating with NEROC Haystack Observatory, MIT and the Jet Propulsion Laboratory in the analysis of existing 3.8 and 70 cm radar images of the Moon, and in the acquisition of new data for selected lunar targets. The intent is to obtain multi-polarization radar images at resolutions approaching 75 meters (3.8 cm wavelength) and 400 meters (70 cm wavelength) for the Apollo landing sites (thereby exploiting available ground truth) or regions covered by the metric camera and geochemical experiments onboard the command modules of Apollos 15, 16 and 17. These data were collected in both like- and cross-polarizations, and, in the case of the 70 cm data, permit the phase records to be used to assess the scattering properties of the surface. The distribution of surface units on the Moon that show a mismatch between the surface implied by like- and cross-polarized scattering data is being analyzed, based on the scattering models of Evans and Hagfors. M.G.

N87-23442*# Jet Propulsion Lab., California Inst. of Tech., Pasadena.

HIGH RESOLUTION RADAR MAP OF THE MOON c43

T. W. Thompson *In* NASA, Washington Reports of Planetary Geology and Geophysics Program, 1986 May 1987 p 238-239 (For primary document see N87-23341 16-91)
Avail: NTIS HC A24/MF A01 CSCL 08B

Previous radar mappings of the Moon at 70 cm wavelength in the late 1960's by Thompson have been replaced with a new set of observations using the 430 MHz radar at the Arecibo Observatory, Puerto Rico. Radar resolution was reduced to 2 to 5 km radar cell size and a beam-sweep, limb-to-limb calibration was conducted. Advances in computer technology provided the principle means of improving lunar radar mapping at this wavelength. Observation techniques and data processing are described and scattering differences found in the orthographic projection of the radar data are discussed. M.G.

N87-23443*# Geological Survey, Menlo Park, Calif.
LANDFORM IDENTIFICATION: LUNAR RADAR IMAGES **c43**
Henry J. Moore and T. W. Thompson (Jet Propulsion Lab., California Inst. of Tech., Pasadena.) *In* NASA, Washington Reports of Planetary Geology and Geophysics Program, 1986 May 1987 p 240-242 (For primary document see N87-23341 16-91)
Avail: NTIS HC A24/MF A01 CSCL 08B

Three sets of polarized radar-echo images of the Moon were examined to establish the relation between radar resolution and landform-identification resolution. After comparison with lunar maps and photographs, real and apparent landforms on the radar images were grouped into one of seven classes. Results show strong relations between radar resolution and diameter or relief of landforms that are clearly identified and those that would probably be correctly identified (class 1 and class 2). Landforms are not detected (class 5) at all diameters and reliefs, but the percentage of undetected landforms decreases with increasing mean diameter and mean relief. Landforms are simply detected (class 4) at most mean diameters and reliefs. Ambiguous arrays (class 6) portrayed by the radar constitute up to about 16, 22, and 15% of the landforms at various diameters and relief values for the 3.8 cm, 70 cm high resolution, and 70 cm low resolution images, respectively. Only a few percent of the landforms portrayed by the radar images at various diameters and relief values are fictitious (class 7). Author

N87-23444*# Jet Propulsion Lab., California Inst. of Tech., Pasadena.
GOLDSTONE RADAR OBSERVATIONS OF MARS: THE 1986 OPPOSITION **c32**
T. W. Thompson *In* NASA, Washington Reports of Planetary Geology and Geophysics Program, 1986 May 1987 p 243-244 (For primary document see N87-23341 16-91)
Avail: NTIS HC A24/MF A01 CSCL 17I

Radar echoes from the planet Mars were obtained on 27 S-band (wavelength = 12.5 cm) and 2 X-band (wavelength = 3.5 cm) tracks using the Goldstone Solar System Radar. These observations took advantage of the favorable 1986 opposition since the Earth-Mars distance was 0.40 AU at opposition and radar echo strength is proportional to inverse-fourth-power of the distance to the target. The coverages of the Goldstone observations are summarized. The observations were conducted via the CW-spectra techniques described by Harmon et al. A continuous tone was transmitted at Mars and the radar echo was sampled to obtain a Doppler spread spectrum. Each received event was separated into polarized (opposite sense circular) and depolarized (same sense circular) periods. There was one successful ranging run which had a resolution of 2 microseconds. This should yield surface heights accurate to 300 meters. M.G.

N87-23445*# Colorado Univ., Boulder. Lab. for Atmospheric and Space Physics.
A DIFFUSE RADAR SCATTERING MODEL FROM MARTIAN SURFACE ROCKS **c32**
W. M. Calvin, B. M. Jakosky, and P. R. Christensen (Arizona State Univ., Tempe.) *In* NASA, Washington Reports of Planetary Geology and Geophysics Program, 1986 May 1987 p 245-247 (For primary document see N87-23341 16-91)
Avail: NTIS HC A24/MF A01 CSCL 17I

Remote sensing of Mars has been done with a variety of instrumentation at various wavelengths. Many of these data sets can be reconciled with a surface model of bonded fines (or duricrust) which varies widely across the surface and a surface rock distribution which varies less so. A surface rock distribution map from -60 to +60 deg latitude has been generated by Christensen. Our objective is to model the diffuse component of radar reflection based on this surface distribution of rocks. The diffuse, rather than specular, scattering is modeled because the diffuse component arises due to scattering from rocks with sizes on the order of the wavelength of the radar beam. Scattering for radio waves of 12.5 cm is then indicative of the meter scale and smaller structure of the surface. The specular term is indicative of large scale surface undulations and should not be causally related to other surface physical properties. A simplified model of diffuse scattering is described along with two rock distribution models. The results of applying the models to a planet of uniform fractional rock coverage with values ranging from 5 to 20% are discussed. M.G.

N87-23446*# Jet Propulsion Lab., California Inst. of Tech., Pasadena.
MARS: SEASONALLY VARIABLE RADAR REFLECTIVITY **c32**
L. E. Roth, R. S. Saunders, and T. W. Thompson *In* NASA, Washington Reports of Planetary Geology and Geophysics Program, 1986 May 1987 p 248-250 (For primary document see N87-23341 16-91)
Avail: NTIS HC A24/MF A01 CSCL 17I

Since reflectivity is a quantity characteristic of a given target at a particular geometry, the same (temporally unchanging) target examined by radar on different occasions should have the same reflectivity. Zisk and Mouginis-Mark noted that the average reflectivities in the Goldstone Mars data increased as the planet's S hemisphere passed from the late spring into early summer. The same data set was re-examined and the presence of the phenomenon of the apparent seasonal variability of radar reflectivity was confirmed. Two objections to these findings are addressed: (1) reflectivity variations may be present in the Goldstone Mars data as a result of an instrument/calibration error; and (2) the variations were introduced into the analysis through comparing reflectivities from two incompatible subsets of the data. M.G.

N87-23447*# Jet Propulsion Lab., California Inst. of Tech., Pasadena.
MEASUREMENTS OF THE DIELECTRIC CONSTANTS FOR PLANETARY VOLATILES
Vincent G. Anicich and Wesley T. Huntress, Jr. *In* NASA, Washington Reports of Planetary Geology and Geophysics Program, 1986 May 1987 p 251-252 (For primary document see N87-23341 16-91)
Avail: NTIS HC A24/MF A01 CSCL 03B

The model of Titan at present has the surface temperature, pressure, and composition such that there is a possibility of a binary ethane-methane ocean. Proposed experiments for future Titan flybys include microwave mappers. Very little has been measured of the dielectric properties of the small hydrocarbons at these radar frequencies. An experiment was conducted utilizing a slotted line to measure the dielectric properties of the hydrocarbons, methane to heptane, from room temperature to -180 C. Measurements of the real part of the dielectric constants are accurate to + or - 0.006 and the imaginary part (the loss tangent) of the liquids studied is less than or equal to 0.001. In order to verify this low loss tangent, the real part of the dielectric constant of hexane at 25 C was studied as a function of the frequency range of the slotted line system used. The dielectric constant of hexane at room temperature, between 500 MHz and 3 MHz, is constant within experimental error. M.G.

N87-23448*# Stanford Univ., Calif. Center for Radar Astronomy.
APPLICATION OF NUMERICAL METHODS TO PLANETARY RADIOWAVE SCATTERING **c32**
Richard A. Simpson and G. Leonard Tyler *In* NASA, Washington Reports of Planetary Geology and Geophysics Program, 1986 May 1987 p 253 (For primary document see N87-23341 16-91)
Avail: NTIS HC A24/MF A01 CSCL 20N

Existing numerical techniques for the solution of scattering problems were investigated to determine those which might be applicable to planetary surface studies, with the goal of improving the interpretation of radar data from Venus, Mars, the Moon, and icy satellites. The general characteristics of the models are described along with computational concerns. In particular, the Numerical Electrogmatics Code (NEC) developed at the Lawrence Livermore Laboratory is discussed. Though not developed for random rough surfaces, the NEC contains elements which may be generalized and which could be valuable in the study of scattering by planetary surfaces. M.G.

N87-23449*# Arizona State Univ., Tempe. Dept. of Geology.
BRIGHT SAND/DARK DUST: THE IDENTIFICATION OF ACTIVE SAND SURFACES ON THE EARTH AND MARS
H. G. Blount, II, R. Greeley, P. R. Christensen, and R. Arvidson (Washington Univ., St. Louis, Mo.) *In* NASA, Washington Reports of Planetary Geology and Geophysics Program, 1986 May 1987 p 257-258 (For primary document see N87-23341 16-91)
Avail: NTIS HC A24/MF A01 CSCL 03B

Field studies and analysis of LANDSAT Thematic Mapper data in the Gran Desierto, Mexico may shed light on a technique to distinguish active from inactive (relict) sand surfaces. Active sand bodies in the study area are consistently brighter (by an average of 20%) at visual and near infrared wavelengths and darker at thermal infrared wavelengths than compositionally similar inactive sands. The reasons for the albedo difference between active and inactive sands are reviewed and the mixing model of Johnson et al. is examined for tracing the provenance of sands based on albedo and spectral variations. Portions of the wavelengths covered by the Mars Orbiter correspond to the Thematic Mapper data. The identification of active sands on Earth, with a priori knowledge of bulk composition and grain size distribution, may allow the remote mapping of active sand surfaces on Mars. In conjuction with thermal infrared remote sensing for composition, it may also provide a method for the remote determination of grain size distributions within sand/silt mixtures. M.G.

N87-23450*# Arizona State Univ., Tempe. Dept. of Geology.
REGIONAL SOURCES AND SINKS OF DUST ON MARS: VIKING OBSERVATIONS OF CERBERUS, SOLIS PLANUM AND SYRTIS MAJOR
Steven W. Lee *In* NASA, Washington Reports of Planetary Geology and Geophysics Program, 1986 May 1987 p 259-260 (For primary document see N87-23341 16-91)
Avail: NTIS HC A24/MF A01 CSCL 03B

A study of seasonal variations of albedo features in the Cerberus, Solis Planum, and Syrtis Major regions was based on Viking Orbiter data obtained over more than one complete Martian year. Contour maps of Lambert albedo and single-point thermal inertia were constructed from the Infrared Thermal Mapper (IRTM) experiment data, and Orbiter images were used to determine the pattern and variability of regional winds (inferred from wind streak orientations). Coupled with ground-based radar data, these data allow the regional sediment transport direction, surface properties (texture, morphology, and roughness), and the implications of the observed seasonal and longer term dust redistribution to be investigated. Results are outlined. M.G.

N87-23451*# Arizona State Univ., Tempe. Dept. of Geology.
HIGH RESOLUTION THERMAL INFRARED MAPPING OF MARTIAN CHANNELS
R. A. Craddock, R. Greeley, and P. R. Christensen *In* NASA, Washington Reports of Planetary Geology and Geophysics Program, 1986 May 1987 p 261-263 (For primary document see N87-23341 16-91)
Avail: NTIS HC A24/MF A01 CSCL 03B

Viking Infrared Thermal Mapper (IRTM) high resolution (2 to 5 km) data were compiled and compared to Viking Visual Imaging Subsystem (VIS) data and available 1:5M geologic maps for several Martian channels including Dao, Harmakhis, Mangala, Shalbatana, and Simud Valles in an effort to determine the surface characteristics and the processes active during and after the formation of these channels. Results show a dominance of aeolian processes active in and around the channels. These processes have left materials thick enough to mask any genuine channel deposits. Results also indicate that very comparable Martian channels and their surrounding terrain are blanketed by deposits which are homogeneous in their thermal inertia values. However, optimum IRTM data does not cover the entire Martian surface and because local deposits of high thermal inertia material may not be large enough in areal extent or may be in an unfavorable location on the planet, a high resolution data track may not always occur over these deposits. Therefore, aeolian processes may be even more active than the IRTM data tracts can always show.
M.G.

N87-23452*# Arizona State Univ., Tempe. Dept. of Geology.
MARS: MORPHOLOGY OF SOUTHERN HEMISPHERE INTRACRATER DUNEFIELDS
N. Lancaster and R. Greeley *In* NASA, Washington Reports of Planetary Geology and Geophysics Program, 1986 May 1987 p 264-265 (For primary document see N87-23341 16-91)
Avail: NTIS HC A24/MF A01 CSCL 03B

Viking Orbiter images of intracrater dunefields in the Noachis Terra region were examined in order to study the morphology of these landforms and to assess their relationship to local geological settings. The sizes of the dunefields range from 40 to 3600 sq km and vary directly with crater size. Preliminary studies reveal dunefields of two varieties. The most common type is composed of massed straight to slightly wavy crescentic dunes similar to those described by Breed. Dunefields of this type occupy more than 20% of the area of the crater floor, with the dunefield margins often marked by a large dune wall or rampart. Dune spacing ranges between 0.7 and 1.2 km. The second type of dune accumulation consists of clusters of large, widely spaced straight or curved ridges, which often intersect to create rectilinear patterns. Dunes are typically spaced 1.6 to 4 km apart. Earth terrestrial analogs for these dunes are discussed. M.G.

N87-23453*# Cornell Univ., Ithaca, N.Y.
TIMING OF FROST DEPOSITION ON MARTIAN DUNES: A CLUE TO PROPERTIES OF DUNE PARTICLES?
P. Thomas *In* NASA, Washington Reports of Planetary Geology and Geophysics Program, 1986 May 1987 p 266-267 (For primary document see N87-23341 16-91)
(Grant NAGw-111)
Avail: NTIS HC A24/MF A01 CSCL 03B

Scans were made across the Martian dunes found in images taken at several different times to determine the time history of the dune albedo. Atmospheric contributions were estimated using optical depth data and the brightness of shadows in some images. The data show that the dunes brighten very substantially between L(s) = 10 and 40 deg, depending on the latitude. Bright coverings on dunes form outliers 1 to 5 deg north of the cap edge. Formation of the general cap then sometimes reverses the contrast of the dune field with the surrounding area. Causes for the early deposition of frost on dunes relative to surroundings are discussed. M.G.

N87-23454*# Washington Univ., Seattle. Dept. of Mathematics.
WIND RIPPLES IN LOW DENSITY ATMOSPHERES c34
J. S. Miller, J. R. Marshall, and R. Greeley (Arizona State Univ., Tempe.) *In* NASA, Washington Reports of Planetary Geology and Geophysics Program, 1986 May 1987 p 268-270 (For primary document see N87-23341 16-91)
Avail: NTIS HC A24/MF A01 CSCL 20D

The effect of varying fluid density (rho) on particle transport was examined by conducting tests at atmospheric pressures between 1 and 0.004 bar in the Martian Surface Wind Tunnel (MARSWIT). This study specifically concerns the effect of varying rho on the character of wind ripples, and elicits information concerning generalized ripple models as well as specific geological circumstances for ripple formation such as those prevailing on Mars. Tests were conducted primarily with 95 micron quartz sand, and for each atmospheric pressure chosen, tests were conducted at two freestream wind speeds: 1.1 U*(t) and 1.5 U*(t), where U*(t) is saltation threshold. Preliminary analysis of the data suggests: (1) ballistic ripple wavelength is not at variance with model predictions; (2) an atmospheric pressure of approximately 0.2 bar could represent a discontinuity in ripple behavior; and (4) ripple formation on Mars may not be readily predicted by extrapolation of terrestrial observations. M.G.

N87-23455*# Geological Survey, Flagstaff, Ariz.
EOLIAN SALTATION ON MARS
D. J. MacKinnon *In* NASA, Washington Reports of Planetary Geology and Geophysics Program, 1986 May 1987 p 271-273 (For primary document see N87-23341 16-91)
Avail: NTIS HC A24/MF A01 CSCL 03B

A computer model was developed in order to examine the effects of the wind field and surface collisions on the Martian saltation cloud. The distribution of incidence speeds and angles assumed by one grain in this model characterizes reasonably well the quantitative physical processes in the saltation cloud. Saltating grains that transfer small fractions of their horizontal momentum to the surface attain higher speeds, rise higher above the surface, and achieve longer trajectories than do saltating grains that transfer larger amounts of momentum; relatively small differences in the coefficients of restitution yield significant differences in the saltation cloud. It is also shown that grains can both assume long trajectories and transfer large amounts of momentum to the surface for the rapid development of the saltation cloud. M.G.

N87-23456*# Arizona State Univ., Tempe. Dept. of Geology.
MASS TRANSPORT BY AEOLIAN SALTATION ON EARTH, MARS AND VENUS: THE EFFECTS OF FULL SALTATION CLOUD DEVELOPMENT AND CHOKING
S. H. Williams and R. Greeley *In* NASA, Washington Reports of Planetary Geology and Geophysics Program, 1986 May 1987 p 274-275 (For primary document see N87-23341 16-91)
Avail: NTIS HC A24/MF A01 CSCL 03B

Wind tunnel tests were conducted to study the characteristics of particle motion and the quantity transported by wind under a variety of planetary environmental conditions. Analysis of the results indicates that, on Earth, saltation fully develops at near-threshold wind speeds and rarely chokes (retarding of saltation due to high particle concentration and subsequent increase of mid-air collisions). On Mars, saltation becomes fully developed only at favorable locations and at wind speeds well above threshold. The Martian saltation cloud has an insufficient particle concentration to cause choking, particularly over a partially rocky surface. On Venus, full saltation occurs at wind speeds very near threshold, but saltation flux increases less rapidly than expected at relatively modest wind speeds due to choking. M.G.

N87-23457*# Arizona State Univ., Tempe. Dept. of Geology and Geography.
DEVELOPMENT OF WIND TUNNEL TECHNIQUES FOR THE SOLUTION OF PROBLEMS IN PLANETARY AEOLIAN PROCESSES **c34**
Robert Sullivan, Jeffrey Lee, and Ronald Greeley *In* NASA, Washington Reports of Planetary Geology and Geophysics Program, 1986 May 1987 p 276-278 (For primary document see N87-23341 16-91)
Avail: NTIS HC A24/MF A01 CSCL 20D

Kutzbach reports wind profiles over a series of roughness elements on a frozen lake and how the wind profile changed as the surface roughness was varied. The approach of the current study was to duplicate Kutzbach's roughness arrays in the wind tunnel at 1/20 and 1/40 scales, and to compare the wind profiles over these scale models to those derived by Kutzbach at full scale in the field. The effects of scale differences and data reduction techniques are discussed. Although the study suggests that wind tunnel scale models can predict parameters measured in the field, the development of more definitive guidelines requires a field experiment designed specifically for comparison with wind tunnel results. M.G.

N87-23458*# Arizona State Univ., Tempe. Dept. of Geology.
AEOLIAN ABRASION ON VENUS: PRELIMINARY RESULTS FROM THE VENUS SIMULATOR
J. R. Marshall, Ronald Greeley, D. W. Tucker, and J. B. Pollack *In* NASA, Washington Reports of Planetary Geology and Geophysics Program, 1986 May 1987 p 279-281 (For primary document see N87-23341 16-91)
Avail: NTIS HC A24/MF A01 CSCL 03B

The role of atmospheric pressure on aeolian abrasion was examined in the Venus Simulator with a constant temperature of 737 K. Both the rock target and the impactor were fine-grained basalt. The impactor was a 3 mm diameter angular particle chosen to represent a size of material that is entrainable by the dense Venusian atmosphere and potentially abrasive by virtue of its mass. It was projected at the target 10 to the 5 power times at a velocity of 0.7 m/s. The impactor showed a weight loss of approximately 1.2 x 10 to the -9 power gm per impact with the attrition occurring only at the edges. Results from scanning electron microscope analysis, profilometry, and weight measurement are summarized. It is concluded that particles can incur abrasion at Venusian temperatures even with low impact velocities expected for Venus. M.G.

N87-23459*# Arizona State Univ., Tempe. Dept. of Geography.
REYNOLDS NUMBER EFFECTS ON SURFACE SHEAR STRESS PATTERNS AROUND ISOLATED HEMISPHERES **c34**
J. A. Lee and Ronald Greeley *In* NASA, Washington Reports of Planetary Geology and Geophysics Program, 1986 May 1987 p 282-284 (For primary document see N87-23341 16-91)
Avail: NTIS HC A24/MF A01 CSCL 20D

Obstacles projecting into the wind stream alter the shear stress on the surface around them, thus altering the erosion, transportation, and deposition of aeolian sediment. The effect of Reynolds number on the pattern of shear stress on the surface around an isolated hemisphere was investigated. An understanding of Reynolds number effects is necessary if wind tunnel results are to be scaled up to natural situations for meaningful applications. The experiment shows that the surface shear stress pattern is strongly affected by Reynolds number, at least within the range of Re used (1360 to 2977). This is presumably due to a decrease in flow around the sides of the hemisphere and an increase in flow over the object as the Reynolds number increases. M.G.

N87-23460*# Arizona State Univ., Tempe. Dept. of Geography.
DETERMINATION OF SURFACE SHEAR STRESS WITH THE NAPHTHALENE SUBLIMATION TECHNIQUE **c34**
J. A. Lee and Ronald Greeley *In* NASA, Washington Reports of Planetary Geology and Geophysics Program, 1986 May 1987 p 285-287 (For primary document see N87-23341 16-91)
Avail: NTIS HC A24/MF A01 CSCL 20D

Aeolian entrainment and transport are functions of surface shear stress and particle characteristics. Measuring surface shear stress is difficult, however, where logarithmic wind profiles are not found, such as regions around large roughness elements. An outline of a method whereby shear stress can be mapped on the surface around an object is presented. The technique involves the sublimation of naphthalene (C10H8) which is a function of surface shear stress and surface temperature. This technique is based on the assumption that the transfer of momentum, heat and mass are analogous (Reynolds analogy). If the Reynolds analogy can be shown to be correct for a given situation, then knowledge of the diffusion of one property allows the determination of the others. The analytical framework and data acquisition for the method are described. The technique was tested in the Planetary Geology Wind Tunnel. Results show that the naphthalene sublimation technique is a reasonably accurate method for determining shear stress, particularly around objects where numerous point values are needed. M.G.

N87-23461*# University of Southern Illinois, Carbondale. Dept. of Geology.
GROUNDWATER SAPPING CHANNELS: SUMMARY OF EFFECTS OF EXPERIMENTS WITH VARIED STRATIGRAPHY **c43**
R. Craig Kochel and David W. Simmons *In* NASA, Washington Reports of Planetary Geology and Geophysics Program, 1986 May

1987 p 291-293 (For primary document see N87-23341 16-91)
Avail: NTIS HC A24/MF A01 CSCL 08H

Experiments in the recirculating flume sapping box have modeled valley formation by groundwater sapping processes in a number of settings. The effects of the following parameters on sapping channel morphology were examined: surface slope; stratigraphic variations in permeability cohesion and dip; and structure of joints and dikes. These kinds of modeling experiments are particularly good for: testing concepts; developing a suite of distinctive morphologies and morphometries indicative of sapping; helping to relate process to morphology; and providing data necessary to assess the relative importance of runoff, sapping, and mass wasting processes on channel development. The observations from the flume systems can be used to help interpret features observed in terrestrial and Martian settings where sapping processes are thought to have played an important role in the development of valley networks. B.G.

N87-23462*# Arizona Univ., Tucson. Dept. of Geosciences.
FLUVIAL VALLEYS ON MARTIAN VOLCANOES
Victor R. Baker and Virginia C. Gulick *In* NASA, Washington Reports of Planetary Geology and Geophysics Program, 1986 May 1987 p 294-296 (For primary document see N87-23341 16-91)
Avail: NTIS HC A24/MF A01 CSCL 03B

Channels and valleys were known on the Martian volcanoes since their discovery by the Mariner 9 mission. Their analysis has generally centered on interpretation of possible origins by fluvial, lava, or viscous flows. The possible fluvial dissection of Martian volcanoes has received scant attention in comparison to that afforded outflow, runoff, and fretted channels. Photointerpretative, mapping, and morphometric studies of three Martian volcanoes were initiated: Ceraunius Tholus, Hecate Tholus, and Alba Patera. Preliminary morphometric results indicate that, for these three volcanoes, valley junction angles increase with decreasing slope. Drainage densities are quite variable, apparently reflecting complex interactions in the landscape-forming factors described. Ages of the Martian volcanoes were recently reinterpreted. This refined dating provides a time sequence in which to evaluate the degradational forms. An anomaly has appeared from the initial study: fluvial valleys seem to be present on some Martian volcanoes, but not on others of the same age. Volcanic surfaces characterized only by high permeability lava flows may have persisted without fluvial dissection. B.G.

N87-23463*# Arizona Univ., Tucson. Dept. of Geosciences.
VALLEY DEVELOPMENT ON HAWAIIAN VOLCANOES c46
Victor R. Baker and Virginia C. Gulick *In* NASA, Washington Reports of Planetary Geology and Geophysics Program, 1986 May 1987 p 297-299 (For primary document see N87-23341 16-91)
Avail: NTIS HC A24/MF A01 CSCL 08G

Work in progress on Hawaiian drainage evolution indicates an important potential for understanding drainage development on Mars. Similar to Mars, the Hawaiian valleys were initiated by surface runoff, subsequently enlarged by groundwater sapping, and eventually stabilized as aquifers were depleted. Quantitative geomorphic measurements were used to evaluate the following factors in Hawaiian drainage evolution: climate, stream processes, and time. In comparing regions of similar climate, drainage density shows a general increase with the age of the volcani island. With age and climate held constant, sapping dominated valleys, in contrast to runoff-dominated valleys, display the following: lower drainage densities, higher ratios of valley floor width to valley height, and more positive profile concavities. Studies of stream junction angles indicate increasing junction angles with time on the drier leeward sides of the major islands. The quantitative geomorphic studies and earlier field work yielded important insights for Martian geomorphology. The importance of ash mantling in controlling infiltration on Hawaii also seems to apply to Mars. The Hawaiian valley also have implications for the valley networks of Martian heavily cratered terrains. B.G.

N87-23464*# Oregon State Univ., Corvallis. College of Oceanography.
THE APPLICATION OF FLOW COMPETENCE EVALUATIONS TO THE ASSESSMENT OF FLOOD-FLOW VELOCITIES AND STRESSES c43
Paul D. Komar *In* NASA, Washington Reports of Planetary Geology and Geophysics Program, 1986 May 1987 p 300-302 (For primary document see N87-23341 16-91)
Avail: NTIS HC A24/MF A01 CSCL 08H

The concept of flow competence is generally employed to evaluate the velocities, discharges, and bottom stresses of river floods inferred from the size of the largest sediment particles transported. Flow competence has become an important tool for evaluating the hydraulics of exceptional floods on Earth, including those which eroded the Channeled Scabland of eastern Washington, and has potential for similar evaluations of the floods which carved the outflow channels on Mars. For the most part, flow-competence evaluations were empirical, based on data compiled from a variety of sources including major terrestrial floods caused by natural processes or dam failures. Such flow-competence relationships would appear to provide a straight-forward assessment of flood-flow stresses and velocities based on the maximum size of gravel and boulders transported. However, a re-examination of the data base and comparisons with measurements of selective entrainment and transport of gravel in rivers open to question such evaluations. Analyses of the forces acting on the grain during entrainment by pivoting, rolling, or sliding, an approach which focuses more on the physical processes than the purely empirical relationships can be demonstrated. These derived equations require further testing by flume and field measurements before being applied to flow-competence evaluations. Such tests are now underway. B.G.

N87-23465*# Hawaii Inst. of Geophysics, Honolulu. Planetary Geosciences Div.
POSSIBLE ORIGIN OF SOME CHANNELS ON ALBA PATERA, MARS
S. E. Postawko and P. Mouginis-Mark *In* NASA, Washington Reports of Planetary Geology and Geophysics Program, 1986 May 1987 p 303-304 (For primary document see N87-23341 16-91)
Avail: NTIS HC A24/MF A01 CSCL 03B

Several alternative models were proposed for the origin and mode of formation of channels and valley networks on Martian volcanoes, notably Hecates Tholus, Ceraunius Tholus, and Alba Patera. Early interpretations of Mariner 9 and Viking images suggested that these features on Alba were lava channels, while those on Ceraunius Tholus were interpreted as fluvial or volcanic debris channels. Subsequent mapping of Tyrrehna Patera and Hecate Tholus has suggested that pyroclastic activity may have characterized eruptions on these volcanoes, and that at least for Hecates the channels were probably formed by fluvial erosion of unconsolidated ash deposits on the flanks of the volcano. As part of a continuing program to better understand the eruptive history of the young volcanic centers on Mars, numerous channels were identified on the flanks of Alba Patera that resemble the channels on Hecates. As a result, the possibility is being explored that some of the small channels on the flanks of Alba Patera may be fluvial in origin and potentail water sources and modes of formation are being explored. B.G.

N87-23466*# National Aeronautics and Space Administration. Lyndon B. Johnson Space Center, Houston, Tex.
NON-EQUILIBRIUM FREEZING OF WATER-ICE IN SANDY BASALTIC REGOLITHS AND IMPLICATIONS FOR FLUIDIZED DEBRIS FLOWS ON MARS
J. L. Gooding *In* NASA, Washington Reports of Planetary Geology and Geophysics Program, 1986 May 1987 p 305-306 (For primary document see N87-23341 16-91)
Avail: NTIS HC A24/MF A01 CSCL 03B

Many geomorphic features on Mars were attributed to Earth-analogous, cold-climate processes involving movement of water or ice lubricated debris. Clearly, knowledge of the behavior of water in regolith materials under Martian conditions is essential to understanding the postulated geomorphic processes. Experiments were performed with sand-sized samples of natural basaltic regoliths in order to further elucidate how water/regolith interactions depend upon grain size and mineralogy. The data reveal important contrasts with data for clay-mineral substrates and suggest that the microphysics of water/mineral interactions might affect Martian geomorphic processes in ways that are not fully appreciated. Sand and silt sized fractions of two soils from the summit of Mauna Kea were used as Mars-analogous regolith materials. Temperatures were measured for water/ice phase transitions as wet slurries of individual soil fractions which were cooled or heated at controlled rates under a carbon dioxide atmosphere. Freezing and melting of ice was studied as a function of water/soil mass ratio, soil particle size, and thermal-cycle rate. Comparison tests were done under the same conditions with U.S. Geological Survey standard rock powders. B.G.

N87-23467*# Brigham Young Univ., Provo, Utah.

VOLATILE RESERVOIRS BELOW THE SURFACE OF THE ELYSIUM REGION OF MARS: GEOMORPHIC EVIDENCE

Eric H. Christiansen and Jennifer A. Hopler (Iowa Univ., Iowa City.) *In* NASA, Washington Reports of Planetary Geology and Geophysics Program, 1986 May 1987 p 307-309 (For primary document see N87-23341 16-91)

Avail: NTIS HC A24/MF A01 CSCL 03B

The Elysium volcanic province contains a variety of geomorphic evidence for the existence of large volatile reservoirs of subsurface volatiles. Study of these landforms yields insight into the distribution and size of these reservoirs and how they interact with the surface environment and will ultimately place constraints on the geometry, constitution, origin, time of formation, and temporal evolution of these important components of the Martian crust. Three principal types of landforms appear to be related to subsurface volatile reservoirs in the Elysium region of Mars: small outflow channels; large lahars; and vast expanses of knobby terranes around the margins of the Elysium dome. The evidence provided by these landforms is internally consistent with the presence of a large relatively shallow volatile reservoir in the Elysium region. If the geologic features described are reliable indicators of subsurface volatiles, they imply that: volatile reservoirs lie relatively close to the surface and underlie millions of sq km in this region; there is no apparent latitudinal variation in the depth or thickness of the volatile reservoirs; the precursors of the knobby terranes are or were important volatile reservoirs; volatiles may be lost in a variety of ways from these reservoirs; and volatiles were incorporated in an easily eroded surficial deposit in the middle history of Mars. The ultimate origin of water in this reservoir is uncertain. A model to explain the preferential entrapment of volatiles into the region's surface materials may be required. B.G.

N87-23468*# Texas A&M Univ., College Station.

EVIDENCE FOR GLACIATION IN ELYSIUM

Duwayne M. Anderson *In* NASA, Washington Reports of Planetary Geology and Geophysics Program, 1986 May 1987 p 310-312 (For primary document see N87-23341 16-91)

Avail: NTIS HC A24/MF A01 CSCL 03B

Evidence for the existence of permafrost and the surface modification due to frost effects and the presence of ice on Mars dates from early observations. Later analysis of the Viking Orbiter imagery produced evidence suggesting the former presence of ice sheets that could have played a part in shaping the surface of Mars. Similarities were pointed out between a number of streamlined Martian channel features and similar streamlined landforms created by Antarctic ice sheet movement. A study of Viking Orbiter imagery of Granicus Valles and the surrounding terrain in Elysium has produced further evidence of glaciation on Mars. Volcanism has played an important role in developing the landscapes of the Elysium region. A possible explanation is that subsidence occurred during formation of the Martian moberg ridges due to the melting of ground ice near the eruption area while at a distance most of the ground ice in the permafrost is still present and the original elevation was preserved. Meltwater during and following eruptions might be suddenly released during subglacial volcanism into Granicus Valles in one case and into Hrad Valles in the other. Fluvial erosion thus could have played a role in shaping both. B.G.

N87-23469*# Geological Survey, Flagstaff, Ariz.

WATER AND ICE ON MARS: EVIDENCE FROM VALLES MARINERIS

B. K. Lucchitta *In* NASA, Washington Reports of Planetary Geology and Geophysics Program, 1986 May 1987 p 313-315 (For primary document see N87-23341 16-91)

Avail: NTIS HC A24/MF A01 CSCL 03B

An important contribution to the volatile history of Mars comes from a detailed study of Valles Marineris, where excellent stereoimages and a three-dimensional view of the upper Martian crust permit unusual insights. The evidence that ground water and ice existed until relatively recently or still exist in the equatorial area comes from observations of landslides, wall rock, and dark volcanic vents. Valles Marineris landslides are different in efficiency from large catastrophic landslides on Earth. One explanation for the difference might be that the Martian slides are lubricated by water. A comparison of landslide speeds also suggests that the Martian slides contain water. That Valles Marineris wall rock contained water or ice is further suggested by its difference from the interior layered deposits. Faults and fault zones in Valles Marineris also shed light on the problem of water content in the walls. Because the main evidence for water and ice in the wall rock comes from landslides, their time of emplacement is important. The landslides in Valles Marineris date from the time of late eruptions of the Tharsis volcanoes and thus were emplaced after the major activity of Martian outflow channels. None of the observations conclusively demonstrate that water or ice existed in the wall rock of Valles Marineris, but altogether the evidence is highly suggestive. B.G.

N87-23470*# National Aeronautics and Space Administration. Ames Research Center, Moffett Field, Calif.

FORMATION OF THE LAYERED DEPOSITS IN THE VALLES MARINERIS, MARS

Susan S. Nedell and Steven W. Squyres (Cornell Univ., Ithaca, N.Y.) *In* NASA, Washington Reports of Planetary Geology and Geophysics Program, 1986 May 1987 p 316-318 (For primary document see N87-23341 16-91)

Avail: NTIS HC A24/MF A01 CSCL 03B

Thick sequences of layered deposits are found in the Valles Marineris, which exhibit fine, nearly horizontal layering, and are present as isolated plateaus of what were once more extensive deposits. It was argued that the morphology of the deposits is most consistent with origin in standing bodies of water. The conditions necessary for the existence of ice-covered Martian paleolakes are examined in detail and mechanisms for sediment deposition in them are considered. It was concluded that there are several geologically feasible mechanisms that could have led to the formation of thick deposits in ice-covered paleolakes in the Valles Marineris. Present data are insufficient to choose conclusively among the various possibilities. Several types of data from the Mars Observer mission will be useful in further characterizing the deposits and clarifying the process of their origin. The deposits should be considered important targets for a future Mars sample return mission. B.G.

N87-23471*# Jet Propulsion Lab., California Inst. of Tech., Pasadena.

GEOMORPHIC EVIDENCE FOR ANCIENT SEAS IN WEST DEUTERONILUS MENSAE, MARS-1: REGIONAL GEOMORPHOLOGY

Timothy J. Parker, Dale M. Schneeberger, David C. Pieri, and R. Stephen Saunders *In* NASA, Washington Reports of Planetary Geology and Geophysics Program, 1986 May 1987 p 319-321 (For primary document see N87-23341 16-91)

Avail: NTIS HC A24/MF A01 CSCL 03B

The fretted terrain in west Deuteronilus Mensae consists of extensive cratered upland penninsulas or isolated plateaus cut by long, finger-like canyons typically 10 to 20 km wide and upwards of 300 km long. The longest of these canyons trend roughly north-south to north-northeast, which may reflect some local structural and/or topographic control. At least three geomorphic zones roughly parallel to the lowland/upland boundary, suggestive of increasing modification northward, can be recognized on the fretted region of the region. The southern-most zone (zone A) consists of sharply defined fretted terrain. The middle zone (zone B) consists of well defined fretted terrain in which the plateau surfaces appear smoother, with a somewhat darker and much less varied albedo surface than those of zone A. The northern-most zone (zone C) consists of rounded or softened fretted terrain. The zones were interpreted as surface exposures of successively lower stratigraphic units. B.G.

N87-23472*# Jet Propulsion Lab., California Inst. of Tech., Pasadena.

GEOMORPHIC EVIDENCE FOR ANCIENT SEAS IN WEST DEUTERONILUS MENSAE, MARS-2: FROM VERY HIGH RESOLUTION VIKING ORBITER IMAGES

Timothy J. Parker, Dale M. Schneeberger, David C. Pieri, and R. Stephen Saunders *In* NASA, Washington Reports of Planetary Geology and Geophysics Program, 1986 May 1987 p 322-324 (For primary document see N87-23341 16-91)
Avail: NTIS HC A24/MF A01 CSCL 03B

Very high resolution Viking Orbiter images of the Martian surface, though rare, make it possible to examine specific areas at image scales approaching those of high altitude terrestrial aerial photographs. Twenty three clear images lie within west Deuteronilus Mensae. The northernmost images which constitute an almost unbroken mosaic of the west wall of a long fingerlike canyon are examined. Morphological details on the plateau surface within zone B, not detectable at low resolution, make it possible to divide the zone into two distinct subzones separated by an east-west escarpment. The morphology of the canyon floor is described in detail. B.G.

N87-23473*# Arizona State Univ., Tempe. Dept. of Geology.

EXPLOSIVE VOLCANIC DEPOSITS ON MARS: PRELIMINARY INVESTIGATIONS

D. A. Crown, L. A. Leshin, and Ronald Greeley *In* NASA, Washington Reports of Planetary Geology and Geophysics Program, 1986 May 1987 p 327-329 (For primary document see N87-23341 16-91)
Avail: NTIS HC A24/MF A01 CSCL 03B

Two investigations were undertaken to examine possible large scale explosive volcanic deposits on Mars. The first includes an analysis of Viking Infrared Thermal Mapper (IRTM) data covering the vast deposits in the Amazonis, Memnonia, and Aeolis regions. These postulated ignimbrites have been previously mapped, and at least five high resolution nighttime IRTM data tracks cross the deposits. Preliminary analysis of the data covering Amazonis Planitia show that local features have anomalous thermal inertias but the ignimbrites as a whole do not consistently have significantly different thermal inertias from their surroundings. Preliminary photogeologic and IRTM studies of the large and small highland paterae have also begun. The purpose of IRTM studies of postulated Martian explosive volcanic deposits is to determine the physical properties of the proposed ignimbrites. If volcanic deposits are exposed at the surface, high thermal inertias, as are observed for Apollinaris Patera, should be present. E.R.

N87-23474*# National Aeronautics and Space Administration. Goddard Space Flight Center, Greenbelt, Md.

PSEUDOCRATERS AS INDICATORS OF GROUND ICE ON MARS

Herbert Frey *In* NASA, Washington Reports of Planetary Geology and Geophysics Program, 1986 May 1987 p 330-332 (For primary document see N87-23341 16-91)
Avail: NTIS HC A24/MF A01 CSCL 03B

Positive identification of Martian pseudocraters would be a strong indication of past occurrence of ice at or near the surface of Mars. The basis for suggesting that small cones on Mars are pseudocraters includes: (1) small size, (2) abundant but patchy distribution on what appear to be volcanic plains, (3) presence of other features suggestive of surface or subsurface ice, (4) morphological similarities to Icelandic pseudocraters, and (5) the similarity in distribution of crater/cone diameter ratios to Icelandic pseudocraters. This last morphometric parameter may be the most important, since other possible small terrestrial volcanic analogs have very different crater/cone diameter ratio distributions. In a survey of the available high resolution Viking Orbiter imagery, abundant fields of possible pseudocraters were found. However, only a small fraction of the plains forming units imaged at high resolution were found to contain the small cones. This low discovery rate, combined with the limited high resolution imagery, restrict Martian pseudocraters as global indicators of surface or subsurface ice. The meanings of this terrain analysis are discussed. E.R.

N87-23475*# Geological Survey, Flagstaff, Ariz.

ERUPTIVE HISTORY OF THE ELYSIUM VOLCANIC PROVINCE OF MARS

Kenneth L. Tanaka and David H. Scott *In* NASA, Washington Reports of Planetary Geology and Geophysics Program, 1986 May 1987 p 333-335 (For primary document see N87-23341 16-91)
Avail: NTIS HC A24/MF A01 CSCL 03B

New geologic mapping of the Elysium volcanic province at 1:2,000,000 scale and crater counts provide a basis for describing its overall eruptive history. Four stages are listed and described in order of their relative age. They are also distinguished by eruption style and location. Stage 1: Central volcanism at Hecates and Albor Tholi. Stage 2: Shield and complex volcanism at Elysium Mons and Elysium Fossae. Stage 3: Rille volcanism at Elysium Fossae and Utopia Planitia. Stage 4: Flood lava and pyroclastic eruptions at Hecates Tholus and Elysium Mons. Tectonic and channeling activity in the Elysium region is intimately associated with volcanism. Recent work indicates that isostatic uplift of Tharsis, loading by Elysium Mons, and flexural uplift of the Elysium rise produced the stresses responsible for the fracturing and wrinkle-ridge formation in the region. Coeval faulting and channel formation almost certainly occurred in the pertinent areas in Stages 2 to 4. Older faults east of the lava flows and channels on Hecates Tholus may be coeval with Stage 1. E.R.

N87-23476*# Geological Survey, Flagstaff, Ariz.

LATE-STAGE FLOOD LAVAS IN THE ELYSIUM REGION, MARS

J. B. Plescia *In* NASA, Washington Reports of Planetary Geology and Geophysics Program, 1986 May 1987 p 336-338 (For primary document see N87-23341 16-91)
Avail: NTIS HC A24/MF A01 CSCL 03B

In the southeastern part of the Elysium region is a unit that exhibits little texture and a generally low albedo and that has a very low crater frequency. This unit has been mapped as smooth plains material and previously interpreted as an eolian deposit on the basis of Mariner 9 images. More recently, the unit was mapped as material deposited during a channeling episode. The author interprets the smooth plains unit as being a volcanic deposit composed of low viscosity lava flows: both flood lavas and individual flows. The reasons for these conclusions are given and briefly discussed. E.R.

N87-23477*# Jet Propulsion Lab., California Inst. of Tech., Pasadena.

RELATIVE AGES OF LAVA FLOWS AT ALBA PATERA, MARS

Dale M. Schneeberger and David C. Pieri *In* NASA, Washington Reports of Planetary Geology and Geophysics Program, 1986 May 1987 p 339-341 (For primary document see N87-23341 16-91)
Avail: NTIS HC A24/MF A01 CSCL 03B

Many large lava flows on the flanks of Alba Patera are astonishing in their volume and length. As a suite, these flows suggest tremendously voluminous and sustained eruptions, and provide dimensional boundary conditions typically a factor of 100 larger than terrestrial flows. One of the most striking features associated with Alba Patera is the large, radially oriented lava flows that exhibit a variety of flow morphologies. These include sheet flows, tube fed and tube channel flows, and undifferentiated flows. Three groups of flows were studied; flows on the northwest flank, southeast flank, and the intracaldera region. The lava flows discussed probably were erupted as a group during the same major volcanic episode as suggested by the data presented. Absolute ages are poorly constrained for both the individual flows and shield, due in part to disagreement as to which absolute age curve is representative for Mars. A relative age sequence is implied but lacks precision due to the closeness of the size frequency curves. E.R.

N87-23478*# Arizona State Univ., Tempe. Dept. of Geology.
MARTIAN VOLCANISM: FESTOON-LIKE RIDGES ON TERRESTRIAL BASALT FLOWS AND IMPLICATIONS FOR MARS
E. Theilig and Ronald Greeley *In* NASA, Washington Reports of Planetary Geology and Geophysics Program, 1986 May 1987 p 342-344 (For primary document see N87-23341 16-91)
Avail: NTIS HC A24/MF A01 CSCL 03B

The Fink and Fletcher, and Fink model was used to assess and compare flow rheology for two terrestrial basalt flows and one Martian flow with previous studies. Based on the morphologic similarities between the Martian flows and the Icelandic flows and knowledge of the emplacement of the terrestrial flows, the flows west of Arsia Mons are considered to have been emplaced as large sheet flows from basaltic flood style eruptions. Festoon ridges represent folding of the surface crust in the last stages of emplacement when viscosities would be high due to cooling. Alternatively, the lava may have had a high crystallinity or was erupted at low temperatures. In addition, increased compressive stress behind halted flow fronts or in ponded areas may have contributed to ridge formation. E.R.

N87-23479*# Arizona State Univ., Tempe. Dept. of Geology.
STUDIES OF FLUID INSTABILITIES IN FLOWS OF LAVA AND DEBRIS **c46**
Jonathan H. Fink *In* NASA, Washington Reports of Planetary Geology and Geophysics Program, 1986 May 1987 p 345-347 (For primary document see N87-23341 16-91)
Avail: NTIS HC A24/MF A01 CSCL 08K

At least two instabilities have been identified and utilized in lava flow studies: surface folding and gravity instability. Both lead to the development of regularly spaced structures on the surfaces of lava flows. The geometry of surface folds have been used to estimate the rheology of lava flows on other planets. One investigation's analysis assumed that lava flows have a temperature-dependent Newtonian rheology, and that the lava's viscosity decreased exponentially inward from the upper surface. The author reviews studies by other investigators on the analysis of surface folding, the analysis of Taylor instability in lava flows, and the effect of surface folding on debris flows. E.R.

N87-23480*# Hawaii Inst. of Geophysics, Honolulu.
LONG, PAIRED A'A/PAHOEHOE FLOWS OF MAUNA LOA: VOLCANOLOGICAL SIGNIFICANCE AND INSIGHTS THEY PROVIDE INTO VOLCANO PLUMBING SYSTEMS **c46**
Scott K. Rowland and George P. L. Walker *In* NASA, Washington Reports of Planetary Geology and Geophysics Program, 1986 May 1987 p 348-350 (For primary document see N87-23341 16-91)
Avail: NTIS HC A24/MF A01 CSCL 08K

The long lava flows of Mauna Loa, Hawaii have been cited as Earth's closed analogs to the large Martian flows. It is therefore important to understand the flow mechanics and characteristics of the Mauna Loa flows and to make use of these in an attempt to gain insights into Martian eruptive processes. Two fundamentally different kinds of long lava flows can be distinguished on Hawaiian volcanoes as in Martian flows. The two kinds may have identical initial viscosities, chemical compositions, flow lengths, and flow volumes, but their flow mechanisms and thermal energy budgets are radically different. One travels a distance set by the discharge rate as envisaged by Walker and Wadge, and the other travels a distance set mainly by the eruption duration and ground slope. In the Mauna Loa lavas, yield strength becomes an important flow morphology control only in the distal part of a'a lavas. The occurrence of paired flows on Mauna Loa yields insights into the internal plumbing systems of the volcano, and it is significant that all of the volume of the a'a flow must be stored in a magma chamber before eruption, while none of the volume of the pahoehoe needs to be so stored. Differentiation between the two kinds of flows on images of Martian volcanoes is possible and hence an improved understanding of these huge structures is acquired. E.R.

N87-23481*# Geological Survey, Menlo Park, Calif.
THE 1984 MAUNA LOA ERUPTION AND PLANETARY GEOLGOY **c46**
Henry J. Moore *In* NASA, Washington Reports of Planetary Geology and Geophysics Program, 1986 May 1987 p 351-353 (For primary document see N87-23341 16-91)
Avail: NTIS HC A24/MF A01 CSCL 08K

In planetary geology, lava flows on the Moon and Mars are commonly treated as relatively simple systems. Some of the complexities of actual lava flows are illustrated using the main flow system of the 1984 Mauna Loa eruption. The outline, brief narrative, and results given are based on a number of sources. The implications of the results to planetary geology are clear. Volume flow rates during an eruption depend, in part, on the volatile content of the lava. These differ from the volume flow rates calculated from post eruption flow dimensions and the duration of the eruption and from those using models that assume a constant density. Mass flow rates might be more appropriate because the masses of volatiles in lavas are usually small, but variable and sometimes unknown densities impose severe restrictions on mass estimates. E.R.

N87-23482*# Jet Propulsion Lab., California Inst. of Tech., Pasadena.
CALCULATED VISCOSITY-DISTANCE DEPENDENCE FOR SOME ACTIVELY FLOWING LAVAS **c46**
David Pieri *In* NASA, Washington Reports of Planetary Geology and Geophysics Program, 1986 May 1987 p 354-356 (For primary document see N87-23341 16-91)
Avail: NTIS HC A24/MF A01 CSCL 08K

The importance of viscosity as a gauge of the various energy and momentum dissipation regimes of lava flows has been realized for a long time. Nevertheless, despite its central role in lava dynamics and kinematics, it remains among the most difficult of flow physical properties to measure in situ during an eruption. Attempts at reconstructing the actual emplacement viscosities of lava flows from their solidified topographic form are difficult. Where data are available on the position of an advancing flow front as a function of time, it is possible to calculate the effective viscosity of the front as a function of distance from the vent, under the assumptions of a steady state regime. As an application and test of an equation given, relevant parameters from five recent flows on Mauna Loa and Kilauea were utilized to infer the dynamic structure of their aggregate flow front viscosity as they advanced, up to cessation. The observed form of the viscosity-distance relation for the five active Hawaiian flows examined appears to be exponential, with a rapid increase just before the flows stopped as one would expect. E.R.

N87-23483*# Jet Propulsion Lab., California Inst. of Tech., Pasadena.
TOWARD A MODEL FOR LEVEED LAVA FLOWS **c46**
Stephen Baloga *In* NASA, Washington Reports of Planetary Geology and Geophysics Program, 1986 May 1987 p 357-359 (For primary document see N87-23341 16-91)
Avail: NTIS HC A24/MF A01 CSCL 08K

Many lava flows have two distinct volumetric components during emplacement. First, there is a component actively flowing in accordance with Newtonian or other constitutive relations. Second, there may be an inactive, stationary component that is no longer participating in the forward movement of the flow. Such passive components may take the form of flow-confining levees, solidified lateral margins, overspilling, plating, small ponds and sidestreams, or a lava tube. To describe the conservation of flow volume for the active component, governing equations are given and discussed. E.R.

N87-23484*# Hawaii Inst. of Geophysics, Honolulu.

STUDIES OF VESICLE DISTRIBUTION PATTERNS IN HAWAIIAN LAVAS c46

George P. L. Walker *In* NASA, Washington Reports of Planetary Geology and Geophysics Program, 1986 May 1987 p 360-361 (For primary document see N87-23341 16-91)
Avail: NTIS HC A24/MF A01 CSCL 08K

Basaltic lava flows are generally vesicular, and the broader facts relating to vesicle distribution have long been established; few studies have yet been made with a view to determining how and when vesicles form in the cooling history of the lava, explaining vesicle shape and size distribution, and gaining enough understanding to employ vesicles as a geological tool. Various avenues of approach exist by which one may seek to gain a better understanding of these ubiquitous structures and make a start towards developing a general theory, and three such avenues have recently been explored. One avenue involves the study of pipe vesicles; these are a well known feature of lava flows and are narrow pipes which occur near the base of many pahoehoe flow units. Another avenue of approach is that presented by the distinctive spongy pahoehoe facies of lava that is common in distal locations on Hawaiian volcanoes. A third avenue of approach is that of the study of gas blisters in lava. Gas blisters are voids, which can be as much as tens of meters wide, where the lava split along a vesicle-rich layer and the roof up-arched by gas pressure. These three avenues are briefly discussed. E.R.

N87-23485*# Sul Ross State Univ., Alpine, Tex. Dept. of Geology.

CRUSTAL AND SUBCRUSTAL NODULES IN EJECTA FROM KILBOURNE HOLE MAAR, NEW MEXICO c46

J. L. Whitford-Stark *In* NASA, Washington Reports of Planetary Geology and Geophysics Program, 1986 May 1987 p 362-364 (For primary document see N87-23341 16-91)
Avail: NTIS HC A24/MF A01 CSCL 08G

Nodules retrieved from the ejecta of volcanic craters serve as the source of two major items of information. The first is in providing details of the geochemistry and mineralogy of the Earth's interior by supplying samples of materials that cannot be obtained by existing drilling techniques. The other is in providing information regarding the process which led to their transport from the Earth's interior to the surface. The primary purpose of the present study was to examine the morphology of the nodules in an attempt to place some constraints on the process that brought them to the surface. This attempt is briefly discussed. E.R.

N87-23486*# State Univ. of New York, Buffalo. Dept. of Geological Sciences.

GEOLOGY OF THE MOHON MOUNTAIN VOLCANIC FIELD, YAVAPAI AND MOHAVE COUNTIES, ARIZONA: A PRELIMINARY REPORT c46

Ardyth M. Simmons and John S. King *In* NASA, Washington Reports of Planetary Geology and Geophysics Program, 1986 May 1987 p 365-367 (For primary document see N87-23341 16-91)
Avail: NTIS HC A24/MF A01 CSCL 08G

Field mapping has produced a preliminary picture of Mohon Mountain as a composite volcano, in which pyroclastic ash and larger tephra erupted alternately with flows of rhyodacite and dacite. An analog study which uses imagery of lunar and Martian features will compare the overall shape of the vent complex, including its breached southern flank and satellite vents, to similar landforms found on Mars and the Moon which are believed to have formed similar processes. Ash flow sheets were hypothesized to comprise the outer slopes of Olympus Mons suggesting that explosive eruptions which are more volatile-rich than those which produce basalt flows are not confined to terrestrial settings but may also be found on bodies such as Mars, which have a thicker crust and deeper magma source in the mantle. The analog study will explore further evidence for explosive eruptions on Mars and the Moon. Author

N87-23487*# State Univ. of New York, Buffalo. Dept. of Geological Sciences.

THE GEOLOGY OF PINE AND CRATER BUTTES: TWO BASALTIC CONSTRUCTS ON THE FAR EASTERN SNAKE RIVER PLAIN c46

Paul F. Mazierski and John S. King *In* NASA, Washington Reports of Planetary Geology and Geophysics Program, 1986 May 1987 p 368-370 (For primary document see N87-23341 16-91)
Avail: NTIS HC A24/MF A01 CSCL 08G

The emplacement history and petrochemical evolution of the volcanics associated with Pine Butte, Crater Butte, and other nearby vents are developed and described. Four major vents were identified in the study area and their associated eruptive products were mapped. All of the vents show a marked physical elongation or linear orientation coincident with the observed rift set. Planetary exploration has revealed the importance of volcanic processes in the genesis and modification of extraterrestrial surfaces. Interpretation of surface features has identified plains-type basaltic volcanism in various mare regions of the Moon and the volcanic provinces of Mars. Identification of these areas with features that appear analogous to those observed in the Pine Butte area suggests similar styles of eruption and mode of emplacement. Such terrestrial analogies serve as a method to interpret the evolution of volcanic planetary surfaces on the inner planets. E.R.

N87-23488*# State Univ. of New York, Buffalo. Dept. of Geological Sciences.

THE GEOLOGY OF PICACHO BUTTE, A SILICIC VOLCANIC DOME IN NORTHWEST ARIZONA c46

Andrew P. Kisiel and John S. King *In* NASA, Washington Reports of Planetary Geology and Geophysics Program, 1986 May 1987 p 371-373 (For primary document see N87-23341 16-91)
Avail: NTIS HC A24/MF A01 CSCL 08G

The purpose of this investigation was to determine the geologic history of Picacho Butte and vicinity through careful mapping of a 38 square kilometer area surrounding the peak. A detailed analysis of the geochemistry and petrology will aid in the development of a petrogenetic model for the area. The relationship of Picacho Butte to regional volcanism in Arizona, and more specifically to nearby volcanic centers can thus be established. Furthermore, in conjunction with this study a search will be made for possible planetary analogs exhibiting photogeologic characteristics similar to those in northern Arizona. Author

N87-23489*# Geological Survey, Flagstaff, Ariz.

COMPUTER SIMULATIONS OF 10-km-DIAMETER ASTEROID IMPACTS INTO OCEANIC AND CONTINENTAL SITES: PRELIMINARY RESULTS ON ATMOSPHERIC PASSAGE, CRATERING AND EJECTA DYNAMICS c46

D. J. Roddy, S. H. Schuster, Martin Rosenblatt, L. B. Grant, P. J. Hassig, and K. N. Kreyenhagen (California Research and Technology, Inc., Chatsworth.) *In* NASA, Washington Reports of Planetary Geology and Geophysics Program, 1986 May 1987 p 377-379 (For primary document see N87-23341 16-91)
Avail: NTIS HC A24/MF A01 CSCL 08G

A series of analytical calculations of large scale cratering events for both oceanic and continental sites were made in order to examine their effects on the target media and atmosphere. The first analytical studies that were completed consists of computer simulations of the dynamics of: (1) the passage of a 10 km diameter asteroid moving at 20 km/sec through the Earth's atmosphere, and (2) the impact cratering events in both oceanic and continental environments. Calculation of the dynamics associated with the passage of the asteroid through the atmosphere showed strong effects on the surrounding air mass. The calculations of the impact cratering events showed equally dramatic effects on the oceanic and continental environments. These effects are briefly discussed. E.R.

N87-23490*# Brown Univ., Providence, R. I. Dept. of Geological Sciences.

IMPACTS OF HEMISPHERICAL GRANULAR TARGETS: IMPLICATIONS FOR GLOBAL IMPACTS c46

P. H. Schultz, D. E. Gault (Murphys Center of Planetology, Calif.), and D. Crawford *In* NASA, Washington Reports of Planetary Geology and Geophysics Program, 1986 May 1987 p 380-381 (For primary document see N87-23341 16-91)

Avail: NTIS HC A24/MF A01 CSCL 08G

As impact excavation diameters subtend a nontrivial fraction of a planetary body, both the excavation process and ejecta emplacement may depart form the classical description of impacts into a planar surface. Hemispherical particulate targets were impacted at the NASA-Ames Vertical Gun Range in order to trace the evolution of the ejecta curtain and to document the effects of slope and surface curvature on crater shape and cratering efficiency. The experiments suggest that basin size impacts or large craters on small bodies may be shallower than their counterparts on a planar surface but may have displaced a larger relative mass. Moreover, the increased ejecta curtain angle with distance may result in a change in ejecta emplacement style with distance. Although the ejecta curtain is vertical, ejecta within the curtain impact the surface at 45 deg and the time between first and last arrival within the curtain increases. This increased interaction time as the ejecta curtain density decreases should result in a more chaotic style of implacement. E.R.

N87-23491*# Brown Univ., Providence, R. I. Dept. of Geological Sciences.

IMPACT VAPORIZATION: LATE TIME PHENOMENA FROM EXPERIMENTS c46

P. H. Schultz and D. E. Gault (Murphys Center of Planetology, Calif.) *In* NASA, Washington Reports of Planetary Geology and Geophysics Program, 1986 May 1987 p 382-383 (For primary document see N87-23341 16-91)

Avail: NTIS HC A24/MF A01 CSCL 08G

While simple airflow produced by the outward movement of the ejecta curtain can be scaled to large dimensions, the interaction between an impact-vaporized component and the ejecta curtain is more complicated. The goal of these experiments was to examine such interaction in a real system involving crater growth, ejection of material, two phased mixtures of gas and dust, and strong pressure gradients. The results will be complemented by theoretical studies at laboratory scales in order to separate the various parameters for planetary scale processes. These experiments prompt, however, the following conclusions that may have relevance at broader scales. First, under near vacuum or low atmospheric pressures, an expanding vapor cloud scours the surrounding surface in advance of arriving ejecta. Second, the effect of early-time vaporization is relatively unimportant at late-times. Third, the overpressure created within the crater cavity by significant vaporization results in increased cratering efficiency and larger aspect ratios. Author

N87-23492*# Murphys Center of Planetology, Calif.

OBLIQUE IMPACT: PROJECTILE RICHOCHET, CONCOMITANT EJECTA AND MOMENTUM TRANSFER c46

Donald E. Gault and Peter H. Schultz (Brown Univ., Providence, R. I.) *In* NASA, Washington Reports of Planetary Geology and Geophysics Program, 1986 May 1987 p 384-385 (For primary document see N87-23341 16-91)

Avail: NTIS HC A24/MF A01 CSCL 08G

Experimental studies of oblique impact indicate that projectile richochet occurs for trajectory angles less than 30 deg and that the richocheted projectile, accompanied by some target material, are ejected at velocities that are a large fraction of the impact velocity. Because the probability of occurrence of oblique impact less than 30 deg on a planetary body is about one out of every four impact events, oblique impacts would seem to be a potential mechanism to provide a source of meteorites from even the largest atmosphere-free planetary bodies. Because the amount of richocheted target material cannot be determined from previous results, additional experiments in the Ames Vertical Gun laboratory were undertaken toward that purpose using pendulums; one to measure momentum of the richocheted projectile and concomitant target ejecta, and a second to measure the momentum transferred from projectile to target. These experiments are briefly discussed. Author

N87-23493*# Brown Univ., Providence, R. I. Dept. of Geological Sciences.

MOMENTUM TRANSFER FROM OBLIQUE IMPACTS c46

Peter H. Schultz and Donald E. Gault (Murphys Center of Planetology, Calif.) *In* NASA, Washington Reports of Planetary Geology and Geophysics Program, 1986 May 1987 p 386-387 (For primary document see N87-23341 16-91)

Avail: NTIS HC A24/MF A01 CSCL 08G

A completely satisfactory experiment would be in a low gravity environment where the effect of momentum imparted by ejecta impacting the surface can be removed or controlled from momentum transfer during impact. Preliminary estimates can be made using a ballistic pendulum. Such experiments were initiated at the NASA-Ames Vertical Gun Range in order to examine momentum transfer due to impact vaporization for oblique impacts. The preliminary results indicate that momentum from oblique impacts is very inefficient: decreasing with increasing impact velocity and perhaps size; increasing with decreasing density; and increasing with increasing impact angle. At face value, such results minimize the effect of momentum transfer by grazing impact; the more probable impact angles of 30 deg would have a greater effect, contrary to the commonly held impression. E.R.

N87-23494*# Planetary Science Inst., Tucson, Ariz.

EXPERIMENTAL STUDIES OF COLLISION AND FRAGMENTATION PHENOMENA c46

William K. Hartmann, D. R. Davis, and S. J. Weidenschilling *In* NASA, Washington Reports of Planetary Geology and Geophysics Program, 1986 May 1987 p 388-390 (For primary document see N87-23341 16-91)

Avail: NTIS HC A24/MF A01 CSCL 08G

The reduction and publication of an extensive data set collected in experiments over several years at Ames and PSI is briefly examined. Hartmann has been assembling data sets from his experiments on catastrophic fragmentation of various materials, including basalt, other igneous rock, ice, and weak dirt clods. Weidenschilling and Davis have continued to gather and reduce data on oblique impacts. The data indicate a power law distribution of ejecta mass vs. velocity, with a slope that is independent of azimuth, and does not vary with impact angle from normal impacts to at least 75 deg from vertical. In order to improve models of coagulation of dust aggregates in the solar nebula, SJW developed an apparatus for drop tests of fragile projectiles. Davis and Weidenschilling continued to collect and analyze experimental data on collisional catastrophic disruption at the Ames Vertical Gun Range. E.R.

N87-23495*# Boeing Aerospace Co., Seattle, Wash.

CENTRIFUGE IMPACT CRATERING EXPERIMENTS: SCALING LAWS FOR NON-POROUS TARGETS Abstract Only c46

Robert M. Schmidt *In* NASA, Washington Reports of Planetary Geology and Geophysics Program, 1986 May 1987 p 391 (For primary document see N87-23341 16-91)

Avail: NTIS HC A24/MF A01 CSCL 08G

A geotechnical centrifuge was used to investigate large body impacts onto planetary surfaces. At elevated gravity, it is possible to match various dimensionless similarity parameters which were shown to govern large scale impacts. Observations of crater growth and target flow fields have provided detailed and critical tests of a complete and unified scaling theory for impact cratering. Scaling estimates were determined for nonporous targets. Scaling estimates for large scale cratering in rock proposed previously by others have assumed that the crater radius is proportional to powers of the impactor energy and gravity, with no additional dependence on impact velocity. The size scaling laws determined from ongoing centrifuge experiments differ from earlier ones in three respects. First, a distinct dependence of impact velocity is recognized, even for constant impactor energy. Second, the present energy exponent for low porosity targets, like competent rock, is lower than earlier estimates. Third, the gravity exponent is recognized here as being related to both the energy and the velocity exponents. Author

N87-23496*# Washington Univ., Seattle.
IMPACT CRATER SCALING LAWS c46
K. A. Holsapple *In* NASA, Washington Reports of Planetary Geology and Geophysics Program, 1986 May 1987 p 392-393 (For primary document see N87-23341 16-91)
Avail: NTIS HC A24/MF A01 CSCL 08G

Impact craters are numerous on planetary bodies and furnish important information about the composition and past histories of those bodies. The interpretation of that information requires knowledge about the fundamental aspects of impact cratering mechanics. Since the typical conditions of impacts are at a size scale and velocity far in excess of experimental capabilities, direct simulations are precluded. Therefore, one must rely on extrapolation from experiments of relatively slow impacts of very small bodies, using physically based scaling laws, or must study the actual cases of interest using numerical code solutions of the fundamental physical laws that govern these processes. A progress report is presented on research on impact cratering scaling laws, on numerical studies that were designed to investigate those laws, and on various applications of the scaling laws developed by the author and his colleagues. These applications are briefly reviewed. Author

N87-23497*# Brown Univ., Providence, R. I. Dept. of Geological Sciences.
EXPERIMENTAL EVIDENCE FOR NON-PROPORTIONAL GROWTH OF LARGE CRATERS c46
Peter H. Schultz and Donald E. Gault (Murphys Center of Planetology, Calif.) *In* NASA, Washington Reports of Planetary Geology and Geophysics Program, 1986 May 1987 p 394-395 (For primary document see N87-23341 16-91)
Avail: NTIS HC A24/MF A01 CSCL 08G

Evidence from laboratory impact experiments is indicating that increasing crater aspect ratios (diameter:depth) can result from increasing both velocity and projectile size without invoking unusual impactor conditions. An extensive data base of experimental impact cratering was analyzed for a variety of impactors and impact velocities for low strength targets. These data indicate a change in cratering efficiency that appears to be related to the onset of projectile deformation or rupture. When all projectile types and sizes are considered, one finds two contrasting relationships between crater aspect ratio and impactor parameter. These relationships are briefly considered. E.R.

N87-23498*# Boeing Aerospace Co., Seattle, Wash.
CENTRIFUGE IMPACT CRATERING EXPERIMENTS: SCALING LAWS FOR NON-POROUS TARGETS c46
Robert M. Schmidt *In* NASA, Washington Reports of Planetary Geology and Geophysics Program, 1986 May 1987 p 396-398 (For primary document see N87-23341 16-91)
Avail: NTIS HC A24/MF A01 CSCL 08G

This research is a continuation of an ongoing program whose objective is to perform experiments and to develop scaling relationships for large body impacts onto planetary surfaces. The development of the centrifuge technique has been pioneered by the present investigator and is used to provide experimental data for actual target materials of interest. With both powder and gas guns mounted on a rotor arm, it is possible to match various dimensionless similarity parameters, which have been shown to govern the behavior of large scale impacts. Current work is directed toward the determination of scaling estimates for nonporous targets. The results are presented in summary form. Author

N87-23499*# Planetary Science Inst., Tucson, Ariz.
IMPACT AND CRATERING PROCESSES ON ASTEROIDS, SATELLITES, AND PLANETS c90
Clark R. Chapman, Donald R. Davis, and Stuart J. Weidenschilling *In* NASA, Washington Reports of Planetary Geology and Geophysics Program, 1986 May 1987 p 399-401 (For primary document see N87-23341 16-91)
Avail: NTIS HC A24/MF A01 CSCL 03B

A new model for scaling the outcome of catastrophic collisions from laboratory scale experiments was developed and applied to large bodies where gravitational binding is dominant. This algorithm includes a pressure dependent impact strength which predicts that large asteroids behave as intrinsically strong objects due to compressive loading of overburden throughout their interiors. For small bodies, where the gravitational loading is negligible, this model assumes that the impact strength is independent of size. There was considerable discussion of scaling laws for disruption when these results were presented to one authors colleagues. The pressure strengthening impact strength model was viewed as physically quite plausible; however, it was argued that the impact strength should decrease with increasing size in the size range where gravitational compression is negligible. Author

N87-23500*# Geological Survey, Flagstaff, Ariz.
CRATER PRODUCTION ON VENUS AND EARTH BY ASTEROID AND COMET IMPACT c90
Eugene M. Shoemaker and Ruth F. Wolfe *In* NASA, Washington Reports of Planetary Geology and Geophysics Program, 1986 May 1987 p 402-404 (For primary document see N87-23341 16-91)
Avail: NTIS HC A24/MF A01 CSCL 03B

New calculations of the collision probabilities of asteroids and comets with Venus were carried out based on the orbits of the known Venus-crossing asteroids and comets. For comparison, asteroid and comet collision probabilities and cratering rates on the Earth and Moon were recalculated and the estimated cratering rates on Venus were normalized to those of the Earth. Author

N87-23501*# Geological Survey, Flagstaff, Ariz.
THE SURFACE AGE OF VENUS: APPLYING THE TERRESTRIAL CRATERING RATE
Gerald G. Schaber, Eugene M. Shoemaker, and Richard C. Kozak *In* NASA, Washington Reports of Planetary Geology and Geophysics Program, 1986 May 1987 p 405-407 (For primary document see N87-23341 16-91)
Avail: NTIS HC A24/MF A01 CSCL 03B

The population of Venusian craters having suspected impact crater morphology has been reported from 115 x 10 to the 6th power sq km of the northern hemisphere of the planet with the estimated average age of the surface to be approx. 1 b.y. (+ or - 0.5 b.y.) on the basis of lunar crater production curves corrected for Venus. Such an old average age is somewhat difficult to reconcile with the similarity in size and mass of Venus and Earth and with Earth's high heat flow and crustal resurfacing rate. Given the present uncertainties in the role of both active and inactive comet nuclei in the cratering history of Earth, it is concluded that the average age of the observed surface in the northern hemisphere of Venus could be as great as the 450 m.y. mean age of the Earth's crust. The surface of Venus might be even older, but no evidence from the crater observations support an age as great as 1 b.y. Author

N87-23502*# Houston Univ., Tex.
A STATISTICAL STUDY OF MERCURIAN CRATER CLASSES APPLIED TO THE EMPLACEMENT OF THE INTERCRATER PLAINS
Alex Woronow and Karen Love *In* NASA, Washington Reports of Planetary Geology and Geophysics Program, 1986 May 1987 p 408-410 (For primary document see N87-23341 16-91)
Avail: NTIS HC A24/MF A01 CSCL 03B

Two principal processes have been invoked for emplacement of the intercrater plains: (1) basin ejecta and autochthonous surface materials reworked by that ejecta or (2) volcanic flows. A new approach was taken: the multivariate statistical analysis of crater class. The results of the analysis constrain the formative process of the intercrater plains units to have affected craters on both terrains in a similar manner. Any emplacement process brief in temporal extent (compared to the period of late heavy bombardment), such as emplacement of ejecta from a single event or a brief period of extensive volcanism, violates this constraint. This analysis is briefly discussed. Author

N87-23503*# Planetary Science Inst., Tucson, Ariz.
STUDIES OF EARLY INTENSE CRATERING AND POSSIBLE SATURATION EFFECTS
William K. Hartmann *In* NASA, Washington Reports of Planetary Geology and Geophysics Program, 1986 May 1987 p 411-412 (For primary document see N87-23341 16-91)
Avail: NTIS HC A24/MF A01 CSCL 03B

Crater counts on Rhea were completed, to be compared and combined with independent counts by Steve Squyres; the material is now being integrated into a study of cratering on Rhea and other Saturn satellites by Squyres, Lissauer, and Hartmann. Special attention is being paid to lighting and other effects on the apparent changes in crater density from one region to another. An earlier proposal by the author on crater density was further tested. Brief preliminary results are given. Author

N87-23504*# Arizona Univ., Tucson. Lunar and Planetary Lab.
REVISION OF THE MARTIAN RELATIVE AGE CHRONOLOGY
Nadine G. Barlow *In* NASA, Washington Reports of Planetary Geology and Geophysics Program, 1986 May 1987 p 413-415 (For primary document see N87-23341 16-91)
Avail: NTIS HC A24/MF A01 CSCL 03B

This study has provided a more detailed chronology than currently exists in the literature and has created some changes to the currently accepted geological evolutionary sequence of Mars. The period of heavy bombardment, although dominated by impact processes, experienced many forms of volcanic activity and at least one episode of intense fracturing. Most small volcanic constructs and the ridged plains regions are found to date from this early period, contrary to common belief. The fracturing and dissection of the highlands helps to provide further constraints on the timing of events such as the formation of the hemispheric dichotomy and the formation of the Tharsis Bulge. The northern plains are found to consist of a number of differently aged regions. The difference in age between the chaotic terrain and the outflow channels together with differences in the distribution curves among craters of various erosional states found on the channels support the theory of episodic periods of flooding. Author

N87-23505*# Brown Univ., Providence, R. I. Dept. of Geological Sciences.
EARLY CHANGES IN GRADATION STYLES AND RATES ON MARS
Peter H. Schultz and D. Britt *In* NASA, Washington Reports of Planetary Geology and Geophysics Program, 1986 May 1987 p 416-417 (For primary document see N87-23341 16-91)
Avail: NTIS HC A24/MF A01 CSCL 03B

The wide annulus of massifs and knobs of Isidis and Argyre provided sufficiently large areas for meaningful crater statistics of large craters. Counts were made over adjacent and nested areas in order to test consistency and to derive relative age of each basin. Within the Isidis annulus, charateristic terrains provided counting areas for dating contrasting surface process: channeled hummocky terrain, etched terrains, and intermassif channeled plains. The channeled hummocky terrain contains a high channel density of narrow valley networks cutting both primary Isidis features and old craters. The etched terrains represent a broad region outside the inner high relief massifs of southwestern Isidis where numerous irregular plateaus, mesas, and relict craters indicate a different style of erosion. The intermassif channeled plains occur along the inner mountainous ring. Shallow meandering channels form a large integrated drainage system that is linked to numerous smaller intermountainous basins. These ponds and interconnected tributaries extend beyond the primary inner massif ring through broad canyons. Author

N87-23506*# Washington Univ., St. Louis, Mo. Center for the Space Sciences.
CRATERING AND OBLITERATION HISTORY OF THE SOUTH POLAR REGION OF MARS
J. J. Plaut, R. E. Arvidson, E. A. Guinness, and R. Kahn *In* NASA, Washington Reports of Planetary Geology and Geophysics Program, 1986 May 1987 p 418-419 (For primary document see N87-23341 16-91)
Avail: NTIS HC A24/MF A01 CSCL 03B

Results are presented from a comprehensive analysis of crater size frequency distributions compiled from Viking Orbiter images of Martian south polar terrains. Depositional histories for the various terrain units are modelled based on deviations of cumulative crater size frequency plots from an assumed production function. Stratigraphic and morphologic data obtained from visual examination of Viking images are also used, primarily to corroborate inferences concerning ages and obliteration histories derived from the crater data. Author

N87-23507*# Hawaii Inst. of Geophysics, Honolulu. Planetary Geosciences Div.
MARTIAN RAMPART CRATERS: MORPHOLOGIC CLUES FOR THE PHYSICAL STATE OF THE TARGET AT TIME OF IMPACT
Peter J. Mouginis-Mark *In* NASA, Washington Reports of Planetary Geology and Geophysics Program, 1986 May 1987 p 420-422 (For primary document see N87-23341 16-91)
Avail: NTIS HC A24/MF A01 CSCL 03B

Current research attempts to describe morphologic features seen in very high resolution Viking Orbiter images of crater ejecta blankets and interiors, in order to constrain the most likely target properties at the time of crater formation. The Viking Orbiter image data set contains approximately 400 frames at a spatial resolution of better than 10 meters per pixel, and 2,200 frames at a resolution of better than 20 meters per pixel, for which the atmosphere was either clear or only slightly obscured. A search is being conducted of all these images and so far has revealed several examples of both interior and exterior features of impact craters that bear on the nature of the ejecta fluidizing medium. Preliminary observations and speculations on the physical state of the Martian regolith at the time of crater formation are given and briefly discussed. E.R.

N87-23508*# Brown Univ., Providence, R. I. Dept. of Geological Sciences.
CRATER EJECTA MORPHOLOGY AND THE PRESENCE OF WATER ON MARS
Peter H. Schultz *In* NASA, Washington Reports of Planetary Geology and Geophysics Program, 1986 May 1987 p 423-425 (For primary document see N87-23341 16-91)
Avail: NTIS HC A24/MF A01 CSCL 03B

The purpose of this contribution is to review the possible effects of projectile, target, and environment on the cratering process. The discussion presented suggests that contradictions in interpreting Martian crater ejecta morphologies reflect oversimplifying the process as a singular consequence of buried water. It seem entirely possible that most ejecta facies could be produced without the presence of liquid water. However, the combination of extraordinary ejecta fluidity, absence of secondaries, and high ejection angles all would point to the combined effects of atmosphere and fluid rich substrates. Moreover, recent experiments revealing the broad scour zone associated with rapid vapor expansion may account for numerous craters in the circum-polar regions with subtle radial grooving extending 10 crater radii away with faint distal ramparts. Thus certain crater ejecta morphologies may yet provide fundamental clues for the presence of unbound water. Author

N87-23509*# Arizona State Univ., Tempe. Dept. of Geology.
THERMAL INERTIA CHARACTERISTICS OF THE MARTIAN CRATER CURIE
V. M. Horner and J. R. Zimbelman (Lunar and Planetary Inst., Houston, Tex.) *In* NASA, Washington Reports of Planetary Geology and Geophysics Program, 1986 May 1987 p 426-428 (For primary document see N87-23341 16-91)
Avail: NTIS HC A24/MF A01 CSCL 03B

Thermal inertia characteristics have been determined for the martian crater Curie from high resolution groundtracks of Viking

Thermal Infrared Mapper (IRTM) data. Flow features near the southeastern edge of the ejecta indicate that at least part of the Curie ejecta was emplaced in a manner similar to the ejecta of rampart craters. Within the study region there appears to be a general southeastern trend towards lower thermal inertia values. This trend may be related to the proximity of the Arabia region, which is mainly to the south and east of Curie. Curie is in a region where the overall thermal inertias change over relatively short distances radial to Arabia. Therefore, the observed general decrease in thermal inertia may represent increasing regional dust accumulation in the direction of Arabia. E.R.

N87-23510*# Arizona State Univ., Tempe. Dept. of Geology.
DOME CRATERS ON GANYMEDE
J. M. Moore and M. C. Malin *In* NASA, Washington Reports of Planetary Geology and Geophysics Program, 1986 May 1987 p 429-431 (For primary document see N87-23341 16-91)
Avail: NTIS HC A24/MF A01 CSCL 03B

Voyager observations reveal impact craters on Ganymede that are characterized by the presence of broad, high albedo, topographic domes situated within a central pit. Fifty-seven craters with central domes were identified in images covering approx. 50% of the surface. Owing to limitations in resolution, and viewing and illumination angles, the features identified are most likely a subset of dome craters. The sample appears to be sufficiently large to infer statistically meaningful trends. Dome craters appear to fall into two distinct populations on plots of the ratio of dome diameter to crater rim diameter, large-dome craters and small-dome craters. The two classes are morphologically distinct from one another. In general, large dome craters show little relief and their constituent landforms appear subdued with respect to fresh craters. The physical attributes of small-dome craters are more sharply defined, a characteristic they share with young impact craters of comparable size observed elsewhere in the solar system. Both types of dome craters exhibit central pits in which the dome is located. As it is difficult to produce domes by impact and/or erosional processes, an endogenic origin for the domes is reasonably inferred. Several hypotheses for their origin are proposed. These hypotheses are briefly reviewed. E.R.

N87-23511*# National Aeronautics and Space Administration. Ames Research Center, Moffett Field, Calif.
NON-NEWTONIAN ICE RHEOLOGY AND THE RETENTION OF CRATERS ON GANYMEDE
Paul J. Thomas and Gerald Schubert (California Univ., Los Angeles.) *In* NASA, Washington Reports of Planetary Geology and Geophysics Program, 1986 May 1987 p 432-434 (For primary document see N87-23341 16-91)
Avail: NTIS HC A24/MF A01 CSCL 03B

Calculations carried out for craters of varying sizes in a medium with constant temperature T = 173 K yield values for the crater relaxation time t sub e (defined as the time required for the crater depth to become 1/e of its original value) that appear to be too small to account for the observed retention of craters on Ganymede and the other icy satellites. Such a calculation is seriously in conflict with the observed crater population of the surfaces of the icy satellites. In an attempt to reconcile this conflict, possible explanations for the much slower relaxation rate of craters on the icy satellites are considered. It is possible that an admixture of silicates in the surface ice regions of the icy satellites may raise the viscosity to some extent. This possible explanation and others are briefly discussed. E.R.

N87-23512*# Arizona State Univ., Tempe. Dept. of Geology.
EJECTA TYPES ON GANYMEDE AND CALLISTO
V. M. Horner and Ronald Greeley *In* NASA, Washington Reports of Planetary Geology and Geophysics Program, 1986 May 1987 p 435-437 (For primary document see N87-23341 16-91)
Avail: NTIS HC A24/MF A01 CSCL 03B

Ejecta types on Ganymede and Callisto have been identified from Voyager 1 and 2 images. Image resolution used range from approx. 0.6 to approx. 4 km/pxl, which allowed the surveying of almost all of the mappable surface of the two satellites. Seven ejecta classes were identified on Voyager images of Ganymede on the basis of albedo pattern and type of terminus. The ejecta of different terrains on ejecta characteristics were investigated for the most populated ejecta types. Two major ejecta types were identified on Callisto; both have counterparts on Ganymede. Type C1 has a uniformly high albedo and a sharp terminus. Type C2 has a gradational terminus and a moderate albedo. The similarity in ejecta types on Ganymede and Callisto may indicate similarities in the near surface environment of the two satellites, with different ejecta types representing several possible conditions for the impact environment. E.R.

N87-23513*# Arizona State Univ., Tempe. Dept. of Geology.
SHATTER CONES IN ILLINOIS: EVIDENCE FOR METOERITIC IMPACTS AT GLASFORD AND DES PLAINES c46
John F. McHone, Michael L. Sargent, and W. John Nelson (Illinois State Geological Survey, Champaign.) *In* NASA, Washington Reports of Planetary Geology and Geophysics Program, 1986 May 1987 p 438 (For primary document see N87-23341 16-91)
Avail: NTIS HC A24/MF A01 CSCL 08G

Shatter cone fragments were recovered from rock cores at two previously suspected, but heretofore unverified, impact structures in Illinois. Both sites are buried features known from geophysical surveys and drill holes. Shatter cones are accepted widely as field criteria of meteoritic impact. Detection of these shock indicators in both the Glasford Structure and the Des Plains Disturbance upgrades these sites in Earth's inventory of known and suspected impact structures from possible impact sites with compatible structure and morphology to probable impact structures which possess also evidence of shock metamorphism. E.R.

N87-23514*# Lawrence Univ., Appleton, Wis.
SEARCH FOR, AND STUDY OF, PALEOZOIC IMPACT EJECTA: PROGRESS MADE DURING THE PAST YEAR c46
William F. Read *In* NASA, Washington Reports of Planetary Geology and Geophysics Program, 1986 May 1987 p 439-440 (For primary document see N87-23341 16-91)
(Grant NAGw-658)
Avail: NTIS HC A24/MF A01 CSCL 08G

Nodule-like objects which the author believes to be impact bombs had been found in Middle Ordovician rocks of southeastern Wisconsin and northern Illinois. In northern Illinois, rock fragments containing oolith-like spherules, which the author believes to be solidified impact droplets, and numerous large bubble-holes, had been found at the same stratigraphic level. The discovery of bomb-like nodules in Lower Ordovician rocks of southeastern Wisconsin was reported. Bomb-type nodules associated with droplet-type spherules have been found in Lower Ordovician rocks of central Pennsylvania. These discoveries, in the authors opinion, suffice to show that impact ejecta are widespread in marine sediments of Ordovician age and are likely to be widespread also in marine sediments of other ages. Unfortunately, according to the author, there is little indication so far that this evidence has been accepted as valid by the concerned scientific community. E.R.

N87-23515*# Geological Survey, Flagstaff, Ariz.
COMMENTS ON THE TECTONISM OF VENUS
R. C. Kozak and G. G. Schaber *In* NASA, Washington Reports of Planetary Geology and Geophysics Program, 1986 May 1987 p 443-445 (For primary document see N87-23341 16-91)
Avail: NTIS HC A24/MF A01 CSCL 03B

Preliminary tectonic mapping of Venus from Venera 15/16 images shows unquestionable evidence of at least limited horizontal tectonism. The majority of tectonic features on Venus have no relation to topography. In fact, many axes of disruption interconnect, and cross sharp topographic boundaries at large angles, thereby discounting gravity as the driving force. Compressional zones (CZ's), unlike Extensional zones (EZ's), tend to be discontinuous, and, whereas EZ's cross tectonic and topographic boundaries at various angles, many CZ's on Venus are subparallel to these boundaries. Strike-like faulting is curiously lacking from the mapping, possible due to the steep incidence angle of the radar, which is far from optimal for detecting faults of small throw. A chronology of horizontal crustal movements, and hence the analysis of Venus' thermal development, is large dependent on understanding the crater form features. Regardless of their uncertain origin, the craters still could hold the answer to whether, and to what extent, crustal shuffling is occurring on Venus. E.R.

N87-23516*# Jet Propulsion Lab., California Inst. of Tech., Pasadena.

LITHOSPHERIC STRUCTURE ON VENUS FROM TECTONIC MODELLING OF COMPRESSIONAL FEATURES

W. B. Banerdt and M. P. Golombek *In* NASA, Washington Reports of Planetary Geology and Geophysics Program, 1986 May 1987 p 446-448 (For primary document see N87-23341 16-91)
Avail: NTIS HC A24/MF A01 CSCL 03B

In previous studies, extensional models were used that incorporated realistic rheologies in order to constrain lithospheric structure. Lithospheric modelling is considered herein from the standpoint of compressional deformation. Features of presumed compressional tectonic origin are reviewed and a model for compressional folding based on lithospheric strength envelopes are presented that include the effects of both brittle and ductile yielding as well as finite elastic strength. Model predictions are then compared with the widths and spacings of observed tectonic features and it is concluded that the results are consistent with a thin crust overlying a relatively stronger mantle, with thermal gradients probably in the range of 10 to 15 deg/km. Author

N87-23517*# Southern Methodist Univ., Dallas, Tex. Dept. of Geological Sciences.

VENUSIAN TECTONICS: CONVECTIVE COUPLING TO THE LITHOSPHERE?

R. J. Phillips *In* NASA, Washington Reports of Planetary Geology and Geophysics Program, 1986 May 1987 p 449-451 (For primary document see N87-23341 16-91)
Avail: NTIS HC A24/MF A01 CSCL 03B

The relationship between the dominant global heat loss mechanism and planetary size has motivated the search for tectonic style on Venus. Prior to the American and Soviet mapping missions of the past eight years, it was thought that terrestrial style plate tectonics was operative on Venus because this planet is approximately the size of the Earth and is conjectured to have about the same heat source content per unit mass. However, surface topography mapped by the altimeter of the Pioneer Venus spacecraft did not show any physiographic expression of terrestrial style spreading ridges, trenches, volcanic arcs or transform faults, although the horizontal resolution was questionable for detection of at least some of these features. The Venera 15 and 16 radar missions mapped the northern latitudes of Venus at 1 to 2 km resolution and showed that there are significant geographic areas of deformation seemingly created by large horizontal stresses. These same high resolution images show no evidence for plate tectonic features. Thus a fundamental problem for venusian tectonics is the origin of large horizontal stresses near the surface in the apparent absence of plate tectonics. Author

N87-23518*# Brown Univ., Providence, R. I. Dept. of Geological Sciences.

BILATERAL SYMMETRY ACROSS APHRODITE TERRA

L. S. Crumpler, J. W. Head, and D. B. Campbell (Arecibo Ionospheric Observatory, Puerto Rico.) *In* NASA, WAshington Reports of Planetary Geology and Geophysics Program, 1986 May 1987 p 452-454 (For primary document see N87-23341 16-91)
Avail: NTIS HC A24/MF A01 CSCL 03B

There are three main highland areas on Venus: Beta Regio, Ishtar Terra and Aphrodite Terra. The latter is least known and the least mapped, yet existing analyses of Aphrodite Terra based on available Pioneer-Venus orbiter data suggest that it may be the site of extensive rifting. Some of the highest resolution (30 km) PV data (SAR) included most of the western half of Aphrodite Terra. Recent analysis of the SAR data together with Arecibo range-doppler topographic profiling (10 X 100 km horizontal and 10 m vertical resolution) across parts of Aphrodite, further characterized the nature of possible tectonic processes in the equatorial highlands. The existence of distinct topographic and radar morphologic linear discontinuities across the nearly east-west strike of Aphrodite Terra is indicated. Another prominent set of linear features is distinctly parallel to and orthogonal to the ground tracks of the PV spacecraft and are not included because of the possibility that they are artifacts. Study of the northwest trending cross-strike discontinuities (CSD's) and the nature of topographic and morphologic features along their strike suggest the presence of bilateral topographic and morphologic symmetry about the long axis of Aphrodite Terra. Author

N87-23519*# Massachusetts Inst. of Tech., Cambridge. Dept. of Earth, Atmospheric and Planetary Sciences.

SECULAR COOLING OF EARTH AS A SOURCE OF INTRAPLATE STRESS c46

Sean C. Solomon *In* NASA, Washington Reports of Planetary Geology and Geophysics Program, 1986 May 1987 p 455-457 (For primary document see N87-23341 16-91)
Avail: NTIS HC A24/MF A01 CSCL 08G

The once popular idea that changes in planetary volume play an important role in terrestrial orogeny and tectonics was generally discarded with the acceptance of plate tectonics. It is nonetheless likely that the Earth has been steadily cooling over the past 3-4 billion years, and the global contraction that accompanied such cooling would have led to a secular decrease in the radius of curvature of the plates. The implications of this global cooling and contraction are explored here for the intraplate stress field and the evolution of continental plates. Author

N87-23520*# Massachusetts Inst. of Tech., Cambridge. Dept. of Earth, Atmospheric and Planetary Sciences.

A TEST OF THE HYPOTHESIS THAT IMPACT-INDUCED FRACTURES ARE PREFERRED SITES FOR LATER TECTONIC ACTIVITY c46

Sean C. Solomon and Elizabeth D. Duxbury *In* NASA, Washington Reports of Planetary Geology and Geophysics Program, 1986 May 1987 p 458-460 (For primary document see N87-23341 16-91)
Avail: NTIS HC A24/MF A01 CSCL 08G

Impact cratering has been an important process in the solar system. The cratering event is generally accompanied by faulting in adjacent terrain. Impact-induced faults are nearly ubiquitous over large areas on the terrestrial planets. The suggestion is made that these fault systems, particularly those associated with the largest impact features are preferred sites for later deformation in response to lithospheric stresses generated by other processes. The evidence is a perceived clustering of orientations of tectonic features either radial or concentric to the crater or basin in question. An opportunity exists to test this suggestion more directly on Earth. The terrestrial continents contain more than 100 known or probable impact craters, with associated geological structures mapped to varying levels of detail. Prime facie evidence for reactivation of crater-induced faults would be the occurrence of earthquakes on these faults in response to the intraplate stress field. Either an alignment of epicenters with mapped fault traces or fault plane solutions indicating slip on a plane approximately coincident with that inferred for a crater-induced fault would be sufficient to demonstrate such an association. Author

N87-23521*# Jet Propulsion Lab., California Inst. of Tech., Pasadena.

PHYSIOGRAPHIC CONSTRAINTS ON THE ORIGIN OF LUNAR WRINKLE RIDGES

M. P. Golombek and B. J. Franklin *In* NASA, Washington Reports of Planetary Geology and Geophysics Program, 1986 May 1987 p 461-463 (For primary document see N87-23341 16-91)
Avail: NTIS HC A24/MF A01 CSCL 03B

Wrinkle ridges are linear asymmetric topographic highs with considerable morphologic complexity that are commonly found on the lunar maria and the smooth plains of Mars and Mercury. The origin of planetary wrinkle ridges has been a much argued and debated topic. Early ideas suggested that wrinkle ridges resulted from volcanic intrusion and extrusion of high viscosity lavas; these early ideas were countered with suggestions that wrinkle ridges formed from tectonic processes involving folding and faulting. Combined volcanic and tectonic mechanisms have also been suggested. The identification and analysis of a number of morphologically similar structures on the earth has helped in the recent interpretation of wrinkle ridges as thrust faults that deform surface rocks. Nevertheless, there remains the uncertainty of the dominant role of thrusting versus folding in the formation of planetary wrinkle ridges. Presented is a detailed physiographic analysis of lunar wrinkle ridges in an effort to help distinguish the dominant deformation mechanism. Results agree with the findings of the earth analog study and support the hypothesis that wrinkle ridges form from thrust faults that deform surface rocks. Author

N87-23522*# Massachusetts Inst. of Tech., Cambridge. Dept. of Earth, Atmospheric and Planetary Sciences.

LITHOSPHERIC LOADING AND TECTONICS OF THE LUNAR IRREGULAR MARIA

J. Lynn Hall and Sean C. Solomon *In* NASA, Washington Reports of Planetary Geology and Geophysics Program, 1986 May 1987 p 464-466 (For primary document see N87-23341 16-91)
Avail: NTIS HC A24/MF A01 CSCL 03B

Many of the tectonic features associated with the circular maria are the result of stresses generated by loading of the lunar lithosphere by mare basalt units. The hypothesis is tested that the irregular lunar maria share with the circular maria the processes leading to the formation of associated graben and mare ridge systems. A formulation of the lithospheric flexure problem that accounts for the variable distribution of basalt loads for the irregular maria is applied. On the basis of the tectonic structures and geologic history of each of the major irregular maria, as well as models for the distribution of mare basalt for each region, the predicted stress fields are compared with the distribution of tectonic features for a range of assumed values of the thickness of the elastic lithosphere. The best fitting values for lithospheric thickness beneath the regular maria are then compared with those previously inferred for the circular maria. Author

N87-23523*# National Aeronautics and Space Administration. Goddard Space Flight Center, Greenbelt, Md.

CHARACTERISTIC STRUCTURES OF THE HIGHLAND BOUNDARY ON MARS: EVIDENCE AGAINST A SINGLE MEGA-IMPACT EVENT?

Ann Marie Semeniuk (Maryland Univ., College Park.) and Herbert Frey *In* NASA, Washington Reports of Planetary Geology and Geophysics Program, 1986 May 1987 p 467-468 (For primary document see N87-23341 16-91)
Avail: NTIS HC A24/MF A01 CSCL 03B

It has been suggested that an early mega-impact event might explain the fumdamental crustal dichotomy on Mars. Detailed morphological mapping of the structures which characterize the boundary between the cratered highlands and northern plains does not support this idea: the distribution of these features along and especially away from the boundary is more consistent with a larger number of smaller but overlapping impacts. A data base was assembled for the study of the highland boundary through quantitative mapping (including crater counts) based on the 1:2 M controlled photomosaics. Whole and partial craters larger than 10 km in diameter, knobby terrain, detached plateaus and intervening plains-forming units have been identified wherever they occur on Mars between +65 and -45 deg latitude. There is evidence for occurrences of possible old cratered terrain (or its remanents) at high latitudes well north of the current or likely former location of the proposed Borealis Basin rim which are difficult to reconcile with an impact structure of the proposed size and location. Author

N87-23524*# National Aeronautics and Space Administration. Goddard Space Flight Center, Greenbelt, Md.

THE MARTIAN CRUSTAL DICHOTOMY: PRODUCT OF ACCRETION AND NOT A SPECIFIC EVENT?

Herbert Frey, R. A. Schultz, and T. A. Maxwell (National Air and Space Museum, Washington, D.C.) *In* NASA, Washington Reports of Planetary Geology and Geophysics Program, 1986 May 1987 p 469-471 (For primary document see N87-23341 16-91)
Avail: NTIS HC A24/MF A01 CSCL 03B

Attempts to explain the fundamental crustal dichotomy on Mars range from purely endogenic to extreme exogenic processes, but to date no satisfactory theory has evolved. What is accepted is: (1) the dichotomy is an ancient feature of the Martian crust, and (2) the boundary between the cratered highlands and northern plains which marks the dichotomy in parts of Mars has undergone significant and variable modification during the observable parts of Martian history. Some ascribe it to a single mega-impact event, essentially an instantaneous rearrangement of the crustal structures (topography and lithospheric thickness). Others prefer an internal mechanism: a period of vigorous convection subcrustally erodes the northern one third of Mars, causing foundering and isostatic lowering of that part of Mars. The evidence for each theory is reviewed, with the conclusion that there is little to recommend either. An alternative is suggested: the formation of the crustal dichotomy on Mars was not a specific tectonic event but a byproduct of the accretionary process and therefore a primordial characteristic of the Martian crust, predating the oldest recognizable landforms. Author

N87-23525*# National Air and Space Museum, Washington, D.C.

IMPLICATIONS OF VIKING COLOR DATA FOR EVOLUTION OF THE AMENTHES REGION, MARS

Ted A. Maxwell *In* NASA, Washington Reports of Planetary Geology and Geophysics Program, 1986 May 1987 p 472-473 (For primary document see N87-23341 16-91)
Avail: NTIS HC A24/MF A01 CSCL 03B

In the Eastern Hemisphere of Mars, where the hemispheric dichotomy is not overlain by relatively recent flows from the Tharsis volcanoes, the Mars cratered terrain boundary (CTB) now exists as highly fractured terrain juxtaposed with the smooth plains of the Northern Hemisphere. Based on Mariner 9 photography, the southern cratered terrain in the Amenthes region (0 to 30 deg N, 225 to 270 deg W) is approximately 3 to 4 km above the northern plains, and the transition zone is marked by both broad plateaus and knobby terrain. In the Amenthes Southest quadrangle, in particular, the continuum between large detached plateaus, smaller smooth topped plateaus and knobby hills can be seen. To define the previous position and evolution of the boundary, the distribution of cratered terrain, characteristic landforms (knobby terrain and detached plateaus) have been mapped, as well as structural features across the boundary. Structural mapping indicates that geological formations parallel the boundary in the Eastern Hemisphere with the conclusion that CTB evolution involved normal faulting through extension perpendicular to the boundary. Author

N87-23526*# National Aeronautics and Space Administration, Washington, D.C. Dept. of Geological Sciences.

TIMING OF ANCIENT EXTENSIONAL TECTONIC FEATURES ON MARS

R. Wichman and Peter H. Schultz *In* NASA, Washington Reports of Planetary Geology and Geophysics Program, 1986 May 1987 p 474-475 (For primary document see N87-23341 16-91)
Avail: NTIS HC A24/MF A01 CSCL 03B

Although numerous studies have delineated the Tharsis and post-Tharsis volcanic/tectonic history on Mars, only a few attempts have examined the earlier epochs. This is not an easy task since unambiguous crater ages for pre-Tharsis and early Tharsis units are difficult to determine owing to a variety of active surface processes. Ancient tectonic features, however, have a sufficiently large superposed crater population that should permit relative dating. A technique for crater counting along linear features analagous to areal crater density is proposed. A modification of this approach has been tested and applied to a variety of ancient tectonic features. Author

N87-23527*# Massachusetts Univ., Amherst. Dept. of Geology and Geography.

STRESS HISTORY OF THE THARSIS REGION, MARS

Robert A. Francis *In* NASA, Washington Reports of Planetary Geology and Geophysics Program, 1986 May 1987 p 476-477 (For primary document see N87-23341 16-91)
Avail: NTIS HC A24/MF A01 CSCL 03B

The Tharsis topographic rise of Mars is roughly 5000 km wide and 10 km high and is believed to have originated more than 3.5 BY ago. Within its boundaries lie the four largest volcanoes on the planet. It is also the locus of a series of fracture traces which extend over approximately a hemisphere. The events leading to the formation of the Tharsis region continue to generate debate. Three geophysical models of the formation of Tharsis are now in general contention and each of these models has been used to predict a characteristic stress-field. These models are: the volcanic construct model, the isostatic compensation model, and the lithospheric uplift model. Each has been used by its proponents to predict some of the features observed in the Tharsis region but none accurately accounts for all of the fracture features observed. This is due, in part, to the use of fractures too young to be directly related to the origin of Tharsis. To constrain the origin of Tharsis, as opposed to its later history, one should look for the oldest fractures related to Tharsis and compare these to the predictions made by the models. Mapping of old terrains in and around the Tharsis rise has revealed 175 hitherto unknown old fracture features. Author

N87-23528*# Geological Survey, Flagstaff, Ariz.
HISTORY AND MORPHOLOGY OF FAULTING IN THE NOCTIS LABYRINTHUS-CLARITAS FOSSAE REGION OF MARS
Kenneth L. Tanaka and Philip A. Davis *In* NASA, Washington Reports of Planetary Geology and Geophysics Program, 1986 May 1987 p 478-480 (For primary document see N87-23341 16-91)
Avail: NTIS HC A24/MF A01 CSCL 03B

The topographically high areas cut by Noctis Labyrinthus, Noctis Fossae, and Claritas Fossae were subjected to only minor resurfacing during and following local tectonic activity. Principal resurfacing materials consist of lava flows from Syria Planum and Tharsis Montes. Thus, these areas preserve much of the fault record produced by tectonism in this region. Although recent geologic maps of the area have been produced from Viking images, the only detailed fault histories available until now were described from Mariner 9 images. Much of the faulting in the Tharsis tectonic province was centered in Syria Planum; therefore, understanding the fault history in this region is critical to understanding the stress history and tectonism of Tharsis as a whole. Author

N87-23529*# National Air and Space Museum, Washington, D.C.
THIN AND THICK-SKINNED DEFORMATION IN THE THARSIS REGION OF MARS
Thomas R. Watters *In* NASA, Washington Reports of Planetary Geology and Geophysics Program, 1986 May 1987 p 481-483 (For primary document see N87-23341 16-91)
Avail: NTIS HC A24/MF A01 CSCL 03B

The ridge system of the Tharsis Plateau is a dominant structural form equaled only by the radial fracture system. The structural interpretation of the ridges are: (1) folds formed by regional or local compressional stress; (2) the surface manifestation of reverse or thrust faults; or (3) folds with thrust faulting developing as a result of fold geometry. It has been suggested that the compressional events that generated the ridges occurred after the emplacement of the ridged plains volcanic units, but before the episode of faulting that generated the majority of the observed ridge-fault crosscutting relationships on the ridged plains and that it did not continue beyond the emplacement of the Syria Planum Formation or the basal units of the Tharsis Montes Formation. Models for the origin of the regional stresses involving a combination of isostatic uplift and flexural loading were proposed. Author

N87-23530*# Southern Methodist Univ., Dallas, Tex. Dept. of Geological Sciences.
FLEXURALLY-RESISTED UPLIFT OF THE THARSIS PROVINCE, MARS
R. J. Phillips and N. H. Sleep (Stanford Univ., Calif.) *In* NASA, Washington Reports of Planetary Geology and Geophysics Program, 1986 May 1987 p 484-486 (For primary document see N87-23341 16-91)
Avail: NTIS HC A24/MF A01 CSCL 03B

The tectonic style of Mars is dominated by vertical motion, perhaps more than any of the terrestrial planets. The imprint of this tectonic activity has left a surface widely faulted even though younger volcanism has masked the expression of tectonism in many places. Geological activity associated with the Tharsis and, to a lesser extent, Elysium provinces is responsible for a significant portion of this faulting, while the origins of the remaining features are enigmatic in many cases. The origin and evolution of the Tharsis and Elysium provinces, in terms of their great elevation, volcanic activity, and tectonic style, has sparked intense debate over the last fifteen years. Central to these discussions are the relative roles of structural uplift and volcanic construction in the creation of immense topographic relief. For example, it is argued that the presence of very old and cratered terrain high on the Tharsis rise, in the vicinity of Claritas Fossae, points to structural uplift of an ancient crust. Others have pointed out, however, that there is no reason that this terrain could not be of volcanic origin and thus part of the constructional mechanism. Author

N87-23531*# National Air and Space Museum, Washington, D.C. Center for Earth and Planetary Studies.
TECTONIC DOMAINS IN THE EASTERN HEMISPHERE OF MARS
Ted A. Maxwell and C. E. Leff *In* NASA, Washington Reports of Planetary Geology and Geophysics Program, 1986 May 1987 p 487-488 (For primary document see N87-23341 16-91)
Avail: NTIS HC A24/MF A01 CSCL 03B

The definition of boundaries of discrete structural provinces on the surface of Mars has previously been made by the assumptions of circular or radial symmetry (in the case of the Tharsis olateau), by artificial quadrangle boundaries for regional studies, or simply by regional geographical features. Much of the planetary structural mapping has been presented in a line or spot format in existing consortium data. Methods are being generated to convert the detailed maps of tectonic features to a format that can be used with standard image processing techniques. In this manner such data can be more readily compared to age and other attributes deduced from geological mapping, gravity results, and topography. The 24 photomosaics covering the Eastern Hemisphere of Mars have already been examined for four types of structural features: erosional remnants, ridges, graben, and scarps. When digitized, each feature was flagged according to feature type, azimuth and length. These values were stored as text files on a quad-by-quad basis for each quad studied. Author

N87-23532*# National Air and Space Museum, Washington, D.C. Center for Earth and Planetary Studies.
AGE OF FRACTURING AND MESA DEVELOPMENT IN THE ELYSIUM AREA, NORTHERN MARTIAN PLAINS
George E. McGill *In* NASA, Washington Reports of Planetary Geology and Geophysics Program, 1986 May 1987 p 489-491 (For primary document see N87-23341 16-91)
Avail: NTIS HC A24/MF A01 CSCL 03B

One of the fundamental questions of Martian crustal history is the origin of the crustal dichotomy between northern plains and southern highlands. Hypotheses for the origin of the dichotomy may be constrained by global scale, geophysical considerations, or by detailed geological studies of the genesis and relative ages of materials and landforms in the northern plains of Mars and along the boundary between the plains and the highlands. This abstract summarizes progress on one aspect of a long-range geological study intended to constrain hypotheses for the dichotomy by tracing the history of the northern plains from the most recent events backward -- essentially the same approach used to understand old events in Earth history. Both the giant impact and the mantle convection models for the crustal dichotomy imply a major coeval fracturing event. As has been known for some time, the present dichotomy boundary lies well south of its original position, at least in some places. Nevertheless, there is severe fracturing of this present dichotomy boundary in many places. The specific objectives of this study are to determine the ages of fracturing along the present dichotomy boundary. Author

N87-23533*# Massachusetts Univ., Amherst. Dept. of Geology and Geography.

GEOMETRY AND RELATIVE AGE OF LARGE PATTERNED FRACTURES IN SOUTHERN ACIDALIA PLANITIA, MARS

Murray C. Borrello *In* NASA, Washington Reports of Planetary Geology and Geophysics Program, 1986 May 1987 p 492-494 (For primary document see N87-23341 16-91)
Avail: NTIS HC A24/MF A01 CSCL 03B

Extraordinary patterned fractures occur in Elysium, Utopia, and Acidalia Planitiae of Mars. Theories as to their origin range from permafrost patterning to tectonic fracturing. Recent studies indicate the patterned fractures may be a surface reflection of rough, buried terrane in which fracturing occurs as a result of differential compaction. The patterned terrane in the southern portion of the Acidalia region (MC4-SE, MC4-SC) is being studied to determine its age relative to other terranes and events, and to constrain models for the origin of the fractures. Fracturing in this area occurs between 5 and 25 degrees west longitude and 37 and 50 degrees north latitude. Many fracture patterns are roughly polygonal, with polygons ranging in size from approximately 11 to 32 km in diameter. Fracture traces range from the limit of resolution (10's of meters) to 35 km in length. Author

N87-23534*# Massachusetts Univ., Amherst. Dept. of Geology and Geography.

ORIGIN OF FRACTURES, MARTIAN POLYGONAL TERRAIN

L. Scott Hills *In* NASA, Washington Reports of Planetary Geology and Geophysics Program, 1986 May 1987 p 495-496 (For primary document see N87-23341 16-91)
Avail: NTIS HC A24/MF A01 CSCL 03B

It has been proposed that the origin of the polygonally fractured terrain on Mars is due to stress caused by differential settling of material deposited over an irregular base topography. The eventual goal of this study is to evaluate this proposal by construction of mathematical models for this process. These models will attempt to determine what combinations of base topography, covering material composition, and depositional rate would cause the fractures observed. Because fracture formation would largely be a function of generated stress, the first step in modeling is calculation of stresses created during settlement. Author

N87-23535*# Colorado State Univ., Fort Collins. Dept. of Earth Resources.

THE EFFECT OF OVERBURDEN THICKNESS ON TENSION FRACTURE PATTERNS ABOVE AN UPLIFTING DOME c46

H. Pranger, II *In* NASA, Washington Reports of Planetary Geology and Geophysics Program, 1986 May 1987 p 497-498 (For primary document see N87-23341 16-91)
Avail: NTIS HC A24/MF A01 CSCL 08G

Four experiments demonstrate that tension-fracture patterns above an uplifting dome depend on the thickness of the overburden layer being deformed. Four layers of increasing thicknesses (4.92 cm, 6.92 cm, 9.05 cm, and 11.12 cm) of a very fine sand (85%) and silt-clay (15%) mixture were updomed by slowly inflating a 1.22 m-diameter circular rubber pillow. The upper 2 cm of each layer was wetted and air dried to make it brittle and susceptible to fracture. The fractures that formed during these experiments exhibited a continuum of patterns from dominantly arcuate to dominantly radial as the overburden thickness increased. However, fracture density remained constant in each case for a given amount of surface deformation. Author

N87-23536*# California State Polytechnic Univ., Pomona. Dept. of Geological Sciences.

NATURAL FRACTURE SYSTEMS ON PLANETARY SURFACES: GENETIC CLASSIFICATION AND PATTERN RANDOMNESS c46

Lisa A. Rossbacher *In* NASA, Washington Reports of Planetary Geology and Geophysics Program, 1986 May 1987 p 499-501 (For primary document see N87-23341 16-91)
Avail: NTIS HC A24/MF A01 CSCL 08G

One method for classifying natural fracture systems is by fracture genesis. This approach involves the physics of the formation process, and it has been used most frequently in attempts to predict subsurface fractures and petroleum reservoir productivity. This classification system can also be applied to larger fracture systems on any planetary surface. One problem in applying this classification system to planetary surfaces is that it was developed for ralatively small-scale fractures that would influence porosity, particularly as observed in a core sample. Planetary studies also require consideration of large-scale fractures. Nevertheless, this system offers some valuable perspectives on fracture systems of any size. Author

N87-23537*# Jet Propulsion Lab., California Inst. of Tech., Pasadena.

CURVILINEAR RIDGES AND RELATED FEATURES IN SOUTHWEST CYDONIA MENSAE, MARS

Timothy J. Parker, Dale M. Schneeberger, David C. Pieri, and R. Stephen Saunders *In* NASA, Washington Reports of Planetary Geology and Geophysics Program, 1986 May 1987 p 502-504 (For primary document see N87-23341 16-91)
Avail: NTIS HC A24/MF A01 CSCL 03B

Examined is a region on Mars in southwest Cydonia Mensae (32 deg lat., 17 deg long.) just northwest of the lowland/upland boundary escarpment. The dominant morphological features in this region are the clusters of large massifs and plateau outliers (Pl), knobby material (K), and smooth lowland plains (Ps). Surrounding the clusters and linking many isolated knobs is a system of curvilinear ridges and arcuate terrain boundaries which tend to separate the massifs and knobs from the smooth plains. Curvilinear ridges are arcuate to nearly linear and smoother in plan than wrinkle ridges and show no apparent correlation with regional structural grain. They are typically 5 to 10 km long but can range from as little as 2 or 3 km to greater than 50 km long. The widths vary from about 100 m to as much as 2 km. Curvilinear ridges are most numerous within 100 km of the lowland/upland boundary escarpment and are associated with massifs and knobby terrain. Arcuate terrain boundaries appear between units of different apparent albedo or arcuate breaks in slope. Author

N87-23538*# Brown Univ., Providence, R. I. Dept. of Geological Sciences.

LOCAL-SCALE STRATIGRAPHY OF GROOVED TERRAIN ON GANYMEDE

Scott L. Murchie, James W. Head, Paul Helfenstein, and Jeffrey B. Plescia (Geological Survey, Flagstaff, Ariz.) *In* NASA, Washington Reports of Planetary Geology and Geophysics Program, 1986 May 1987 p 505-507 (For primary document see N87-23341 16-91)
Avail: NTIS HC A24/MF A01 CSCL 03B

The surface of the Jovian satellite, Ganymede, is divided into two main units, dark terrain cut by arcuate and subradial furrows, and light terrain consisting largely of areas with pervasive U-shaped grooves. The grooved terrain may be subdivided on the basis of pervasive morphology of groove domains into four terrain types: (1) elongate bands of parallel grooves (groove lanes); (2) polygonal domains of parallel grooves (grooved polygons); (3) polygonal domains of two orthogonal groove sets (reticulate terrain); and (4) polygons having two to several complexly cross-cutting groove sets (complex grooved terrain). Reticulate terrain is frequently dark and not extensively resurfaced, and grades to a more hummocky terrain type. The other three grooved terrain types have almost universally been resurfaced by light material during their emplacement. The sequence of events during grooved terrain emplacement has been investigated. An attempt is made to integrate observed geologic and tectonic patterns to better constrain the relative ages and styles of emplacement of grooved terrain types. A revised model of grooved terrain emplacement is proposed and is tested using detailed geologic mapping and measurement of crater density. Author

N87-23539*# Northeast Louisiana State Coll., Monroe. Dept. of Geosciences.

STRATIGRAPHY OF THE SOUTH POLAR REGION OF GANYMEDE

R. A. DeHon *In* NASA, Washington Reports of Planetary Geology and Geophysics Program, 1986 May 1987 p 508-510 (For primary document see N87-23341 16-91)

Avail: NTIS HC A24/MF A01 CSCL 03B

A preliminary assessment is made of the stratigraphy and geology in the south polar region of the Jovian satellite, Ganymede. Geologic mapping is based on inspection of Voyager images and compilation on an airbrush base map at a scale of 1:5M. Illumination and resolution vary greatly in the region. Approximately half of the quadripole is beyond the terminator. Low angle illumination over a large part of the area precludes distinction of some units by albedo characteristics. Several types of grooved terrain and groove related terrain occur in the southern polar region. Grooves typically occur in straight to curvilinear sets or lanes. Bright lanes and grooved lanes intersect at high angles outlining polygons of dark cratered terrain. Groove sets exhibit a range of ages as shown by superposition or truncation and by crater superposition ages. Author

N87-23540*# Lawrence Livermore National Lab., Calif.

CREEP OF ICE: FURTHER STUDIES c43

H. C. Heard, W. B. Durham, and S. H. Kirby (Geological Survey, Menlo Park, Calif.) *In* NASA, Washington Reports of Planetary Geology and Geophysics Program, 1986 May 1987 p 511-513 (For primary document see N87-23341 16-91)

Avail: NTIS HC A24/MF A01 CSCL 08L

Detailed studies have been done of ice creep as related to the icy satellites, Ganymede and Callisto. Included were: (1) the flow of high-pressure water ices II, III, and V, and (2) frictional sliding of ice I sub h. Work was also begun on the study of the effects of impurities on the flow of ice. Test results are summarized. Author

N87-23541*# Arizona State Univ., Tempe. Dept. of Geology.

OBSERVATIONS OF INDUSTRIAL SULFUR FLOWS AND IMPLICATIONS FOR Io

S. W. Lee, D. A. Crown, N. Lancaster, and R. Greeley *In* NASA, Washington Reports of Planetary Geology and Geophysics Program, 1986 May 1987 p 514-516 (For primary document see N87-23341 16-91)

(Grant NAGw-132)

Avail: NTIS HC A24/MF A01 CSCL 03B

The possibility of sulfur flows on the Jovian satellite Io is discussed. Although the primary problem is lack of sufficient information to resolve the issue, interpretations of existing data are hampered by poor knowledge of the thermal properties and rheologic behavior of sulfur flows, especially under conditions present on Io. Relatively few natural sulfur flows occur on Earth and only one has been seen in active flow. However, recent observations of industrial sulfur flows, which are much larger than those produced experimentally, may provide important information concerning natural sulfur flows on both Earth and Io. Author

N87-23542*# Arizona State Univ., Tempe. Dept. of Geology.

GEOLOGY OF Io

R. Greeley, R. A. Craddock, D. A. Crown, L. A. Leshin, and G. G. Schaber (Geological Survey, Flagstaff, Ariz.) *In* NASA, Washington Reports of Planetary Geology and Geophysics Program, 1986 May 1987 p 519-521 (For primary document see N87-23341 16-91)

Avail: NTIS HC A24/MF A01 CSCL 03B

Geologic mapping of the Jovian satellite Io has been completed at 1:15,000,000 scale for an area lying between +40 and -90 deg latitude and 230 and 45 deg longitude, which includes portions of the Ruwa Patera quadrangle (Ji2) and the Lerna Region (Ji4) and the westernmost section of the Colchis Region (Ji3). Image resolution in the mapped area is commonly 0.5 to 2 km/pxl. High resolution areas (less than .5 km/pxl) are located near the south pole (Lerna Region) and in eastern Ruwa Patera quadrangle. Geologic maps for the Ruwa Patera quadrangle (Ji2) and the Lerna Region (Ji4) have been produced at 1:5,000,000 scale. The present effort reexamines the previously mapped areas and synthesizes the geology of Io on a global scale. Author

N87-23543*# Jet Propulsion Lab., California Inst. of Tech., Pasadena.

LARGE SCALE TOPOGRAPHY OF Io

R. W. Gaskell and S. P. Synnott *In* NASA, Washington Reports of Planetary Geology and Geophysics Program, 1986 May 1987 p 522-523 (For primary document see N87-23341 16-91)

Avail: NTIS HC A24/MF A01 CSCL 03B

To investigate the large scale topography of the Jovian satellite Io, both limb observations and stereographic techniques applied to landmarks are used. The raw data for this study consists of Voyager 1 images of Io, 800x800 arrays of picture elements each of which can take on 256 possible brightness values. In analyzing this data it was necessary to identify and locate landmarks and limb points on the raw images, remove the image distortions caused by the camera electronics and translate the corrected locations into positions relative to a reference geoid. Minimizing the uncertainty in the corrected locations is crucial to the success of this project. In the highest resolution frames, an error of a tenth of a pixel in image space location can lead to a 300 m error in true location. In the lowest resolution frames, the same error can lead to an uncertainty of several km. Author

N87-23544*# Geological Survey, Flagstaff, Ariz.

THE GALILEAN SATELLITE GEOLOGICAL MAPPING PROGRAM, 1986 Abstract Only

B. K. Lucchitta *In* NASA, Washington Reports of Planetary Geology and Geophysics Program, 1986 May 1987 p 524 (For primary document see N87-23341 16-91)

Avail: NTIS HC A24/MF A01 CSCL 03B

The Galilean Satellite Geological Mapping Program was established to illuminate detailed geologic relations on the four large satellites of Jupiter. The program involves some 40 investigators from various universities, research institutes, and government offices in the United States, U.K., West Germany, and Italy. A total of 24 researchers was assigned to map 15 quadrangles on Ganymede, 15 to map 6 quadrangles on Io, and 3 to map 2 quadrangles on Europa. Maps of these three bodies are at a scale of 1:5 M except for three on Io that cover selected areas where high-resolution pictures permit compilation at 1:2 and 1:1 M scales. A 1:15,000,000 scale map of Callisto has been assigned; from it, quadrangles containing useful geologic information will be extracted later for mapping at a scale of 1:5,000,000. Author

N87-23545*# Geological Survey, Flagstaff, Ariz.

CARTOGRAPHY OF IRREGULARLY SHAPED SATELLITES

R. M. Batson and Kathleen Edwards *In* NASA, Washington Reports of Planetary Geology and Geophysics Program, 1986 May 1987 p 525-526 (For primary document see N87-23341 16-91)

Avail: NTIS HC A24/MF A01 CSCL 03B

Irregularly shaped satellites, such as Phobos and Amalthea, do not lend themselves to mapping by conventional methods because mathematical projections of their surfaces fail to convey an accurate visual impression of the landforms, and because large and irregular scale changes make their features difficult to measure on maps. A digital mapping technique has therefore been developed by which maps are compiled from digital topographic and spacecraft image files. The digital file is geometrically transformed as desired for human viewing, either on video screens or on hard copy. Digital files of this kind consist of digital images superimposed on another digital file representing the three-dimensional form of a body. Author

N87-23546*# Geological Survey, Flagstaff, Ariz.

VOYAGER CARTOGRAPHY

R. M. Batson, E. M. Lee, and K. F. Mullins *In* NASA, Washington Reports of Planetary Geology and Geophysics Program, 1986 May 1987 p 527 (For primary document see N87-23341 16-91)

Avail: NTIS HC A24/MF A01 CSCL 03B

1987 p 527 (For primary document see N87-23341 16-91)
Avail: NTIS HC A24/MF A01 CSCL 03B

The Jovian and Saturnian satellites are being mapped at several scales from Voyager 1 and 2 data. The maps are especially formatted color mosaics, controlled photomosaics, and airbrush maps. At 1:5,000,000 scale, mapping of Io, Europa, and Ganymede is complete. At 1:15,000,000 scale, mapping of Io and Europa is complete, and mapping of Ganymede is approximately complete. A controlled mosaic of Rhea has been compiled as a Digital Image Model (DIM) in the same format as is being used for Mars. The mosaic is being formatted for publication as a two-sheet set (Lambert Azimuthal Equal Area, Mercator, and Polar Stereographic projections). Magnetic tape copies of the DIM have been distributed to regional Planetary Image Facilities and other interested users. The DIM has a scale of 1/16 degree/pixel, corresponding to approximately 833 m/pixel on Rhea. Details of the status of the various map series are reported quarterly to Planetary Geology Principal Investigators. Author

N87-23547*# Geological Survey, Flagstaff, Ariz.
ASPECTS OF VOYAGER PHOTOGRAMMETRY
Sherman S. C. Wu, Francis J. Schafer, Raymond Jordan, and Annie-Elpis Howington *In* NASA, Washington Reports of Planetary Geology and Geophysics Program, 1986 May 1987 p 528-529 (For primary document see N87-23341 16-91)
Avail: NTIS HC A24/MF A01 CSCL 03B

In January 1986, Voyager 2 took a series of pictures of Uranus and its satellites with the Imaging Science System (ISS) on board the spacecraft. Based on six stereo images from the ISS narrow-angle camera, a topographic map was compiled of the Southern Hemisphere of Miranda, one of Uranus' moons. Assuming a spherical figure, a 20-km surface relief is shown on the map. With three additional images from the ISS wide-angle camera, a control network of Miranda's Southern Hemisphere was established by analytical photogrammetry, producing 88 ground points for the control of multiple-model compilation on the AS-11AM analytical stereoplotter. Digital terrain data from the topographic map of Miranda have also been produced. By combining these data and the image data from the Voyager 2 mission, perspective views or even a movie of the mapped area can be made. The application of these newly developed techniques to Voyager 1 imagery, which includes a few overlapping pictures of Io and Ganymede, permits the compilation of contour maps or topographic profiles of these bodies on the analytical stereoplotters. Author

N87-23548*# Geological Survey, Flagstaff, Ariz.
PROGRESS IN COMPILATION OF THE 1:2,000,000-SCALE TOPOGRAPHIC MAP Abstract Only
Sherman S. C. Wu, Raymond Jordan, and Francis J. Schafer *In* NASA, Washington Reports of Planetary Geology and Geophysics Program, 1986 May 1987 p 530 (For primary document see N87-23341 16-91)
Avail: NTIS HC A24/MF A01 CSCL 03B

The application of special photogrammetric techniques has enabled the systematic mapping of Mars' topography at a scale of 1:2,000,000, using high-altitude Viking Orbiter pictures. In fiscal 86, compilation was completed of the 24 subquadrangles that make up the quadrangles MC-12, MC-13, MC-14, MC-15, MC-20, and MC-21. This work completes compilation of the 60 topographic maps covering the equatorial belt (lat. + or - 30 deg). The remaining 80 subquadrangles of Mars are planned to be completed within 3 years (27, 27 and 26 subquadrangles, in fiscal 87, 88, and 89, respectively). Elevations on all topographic maps are relative to the Mars topographic datum. The maps have a contour interval of 1 km and a precision of + or - 1 km. The equatorial-belt maps are Mercator projections having true scale at lat. + or - 27.476 deg. These maps provide more precise information than do those previously available and they will help in understanding the geologic processes that have shaped the Martian surface. Author

N87-23549*# Geological Survey, Flagstaff, Ariz.
MARS DIGITAL TERRAIN MODEL
Sherman S. C. Wu and Annie-Elpis Howington *In* NASA, Washington Reports of Planetary Geology and Geophysics Program, 1986 May 1987 p 531-533 (For primary document see N87-23341 16-91)
Avail: NTIS HC A24/MF A01 CSCL 03B

The Mars Digital Terrain Model (DTM) is the result of a new project to: (1) digitize the series of 1:2,000,000-scale topographic maps of Mars, which are being derived photogrammetically under a separate project, and (2) reformat the digital contour information into rasters of elevation that can be readily registered with the Digital Image Model (DIM) of Mars. Derivation of DTM's involves interpolation of elevation values into 1/64-degree resolution and transformation of them to a sinusoidal equal-area projection. Digital data are produced in blocks corresponding with the coordinates of the original 1:2,000,000-scale maps, i.e., the dimensions of each block in the equatorial belt are 22.5 deg of longitude and 15 deg of latitude. This DTM is not only compatible with the DIM, but it can also be registered with other data such as geologic units or gravity. It will be the most comprehensive record of topographic information yet compiled for the Martian surface. Once the DTM's are established, any enhancement of Mars topographic information made with updated data, such as data from the planned Mars Observer Mission, will be by mathematical transformation of the DTM's, eliminating the need for recompilation. Author

N87-23550*# Geological Survey, Flagstaff, Ariz.
DIGITAL CARTOGRAPHY OF MARS
R. M. Batson *In* NASA, Washington Reports of Planetary Geology and Geophysics Program, 1986 May 1987 p 534-535 (For primary document see N87-23341 16-91)
Avail: NTIS HC A24/MF A01 CSCL 03B

A medium-resolution Digital Image Model (DIM) of Mars is being compiled. A DIM is a mosaic of radiometrically corrected, photometrically modelled spacecraft images displaying accurate reflectance properties at uniform resolution, and geometrically tied to the best available control. The Mars medium-resolution DIM contains approximately 4700 Viking Orbiter image frames that were used to compile the recently completed 1:2,000,000-scale controlled photomosaic series of Mars. This DIM provides a planimetric control base to which all other Mars maps will be registered. A similar control base of topographic elevations (Digital Terrain Model, or DTM) is also being compiled. These products are scheduled for completion in 1989. Author

N87-23551*# RAND Corp., Santa Monica, Calif.
THE CONTROL NETWORK OF MARS: OCTOBER 1986
Merton E. Davies *In* NASA, Washington Reports of Planetary Geology and Geophysics Program, 1986 May 1987 p 536 (For primary document see N87-23341 16-91)
Avail: NTIS HC A24/MF A01 CSCL 03B

The control network of Mars is composed of Mariner 9 frames which essentially give full coverage of the planet at low resolution. Superimposed on and tied to this network are strips of Viking mapping frames (resolution 100 to 250 m per pixel) which encircle the equator and 60 deg north latitude and multiple longitude ties between these latitude strips. There are multiple ties between these strips and the Viking 1 lander site. In the future another strip will be established at 60 deg south latitude. Because the Viking 1 lander site has been accurately located, the coordinates of points in its vicinity can be determined with an error of less than 100 m relative to an inertial coordinate system. Author

N87-23552*# RAND Corp., Santa Monica, Calif.
A UNIFIED LUNAR CONTROL NETWORK
Merton E. Davies, Tim R. Colvin, and Donald L. Meyer (Defense Mapping Agency Aerospace Center, St. Louis, Mo.) *In* NASA, Washington Reports of Planetary Geology and Geophysics Program, 1986 May 1987 p 537-538 (For primary document see N87-23341 16-91)
Avail: NTIS HC A24/MF A01 CSCL 03B

Mapping network control on the Moon is composed of a number of independent regional networks. These networks frequently have different origins but never have common ties, even in overlapping areas. The objective of the unified network program is to tie the regional networks into a single consistent planetwide control network. The plan is to start with the best defined regions, create common ties with neighboring data sets, and then expand into poorly defined regions. The most accurately defined points on the Moon are locations of the laser ranging retroreflectors and the VLBI measurements of the locations of the Apollo 15, 16, 17 ALSEP stations. Recent values for the coordinates of the retroreflectors have been received. The accuracy of these locations is about 30 m and their locations are used to define the center-of-mass and, hence, the origin of the unified lunar coordinate system. The coordinates of the retroreflectors are given in both principal axis and mean Earth/Polar axis systems. Mean Earth/Polar axis coordinates have been recommended by the IAU for the Moon. The difference in the coordinates is important, more than 600 m in latitude and longitude. Author

N87-23553*# RAND Corp., Santa Monica, Calif.

THE CONTROL NETWORKS OF THE SATELLITES OF JUPITER Abstract Only

Merton E. Davies *In* NASA, Washington Reports of Planetary Geology and Geophysics Program, 1986 May 1987 p 539 (For primary document see N87-23341 16-91)
Avail: NTIS HC A24/MF A01 CSCL 03B

Geodetic control networks are being computed photogrammetrically for the large satellites of Jupiter, using pictures from the Voyager 1 and 2 encounters. Control points have been identified on the satellites and their coordinates computed by single-block analytical triangulation. The data sets have been converted from the B1950 to the J2000 inertial coordinate system to be compatible with future flight missions. Author

N87-23554*# Washington Univ., St. Louis, Mo. Center for the Space Sciences.

MICROVAX-BASED DATA MANAGEMENT AND REDUCTION SYSTEM FOR THE REGIONAL PLANETARY IMAGE FACILITIES

R. Arvidson, E. Guinness, S. Slavney, and B. Weiss *In* NASA, Washington Reports of Planetary Geology and Geophysics Program, 1986 May 1987 p 543-544 (For primary document see N87-23341 16-91)
Avail: NTIS HC A24/MF A01 CSCL 03B

Presented is a progress report for the Regional Planetary Image Facilities (RPIF) prototype image data management and reduction system being jointly implemented by Washington University and the USGS, Flagstaff. The system will consist of a MicroVAX with a high capacity (approx 300 megabyte) disk drive, a compact disk player, an image display buffer, a videodisk player, USGS image processing software, and SYSTEM 1032 - a commercial relational database management package. The USGS, Flagstaff, will transfer their image processing software including radiometric and geometric calibration routines, to the MicroVAX environment. Washington University will have primary responsibility for developing the database management aspects of the system and for integrating the various aspects into a working system. Author

N87-23555*# Geological Survey, Flagstaff, Ariz.

MARTIAN TERRAINS

Harold Masursky, M. G. Chapman, P. A. Davis, A. L. Dial, Jr., and M. E. Strobell *In* NASA, Washington Reports of Planetary Geology and Geophysics Program, 1986 May 1987 p 545-547 (For primary document see N87-23341 16-91)
Avail: NTIS HC A24/MF A01 CSCL 03B

Terrain studies of candidate landing sites for a future rover/sample-return mission to Mars are being conducted to evaluate the geologic and trafficability aspects of each site. An optimum site should have geologic units of widely diverse ages and chemical compositions occurring in close enough proximity and in smooth enough terrain so that a roving vehicle of limited traverse ability (+ or - 100 km) could collect representative samples. In FY 1986, geologic maps were compiled at 1:500,000 and 1:2 million scales of the Mangala Valles, Kasei Valles, Chasma Boreale (north polar), and Planum Australe (south polar) areas, and a study was begun of the topography and surface roughness characteristics of the Mangala Valles site. Geologic mapping has been greatly facilitated by specially enhanced, high-resolution Viking photographs, which clarify stratigraphic relations of units unrecognized earlier. Photoclinometric profiles of topographic features provide width and depth measurements of four classes of channels, the thickness of some volcanic units, and the throw on some faults. Estimates of the surface roughness of units are calculated using a newly developed USGS computer program and using measurements derived from Earth-based radar. Author

N87-23556*# Arizona State Univ., Tempe. Dept. of Geology.

THE MARS OBSERVER CAMERA c35

M. C. Malin, G. E. Danielson, A. P. Ingersoll, H. Masursky, J. Veverka, T. Soulanille, and M. Ravine (Jet Propulsion Lab., California Inst. of Tech., Pasadena.) *In* NASA, Washington Reports of Planetary Geology and Geophysics Program, 1986 May 1987 p 548-550 (For primary document see N87-23341 16-91)
Avail: NTIS HC A24/MF A01 CSCL 14E

A camera designed to operate under the extreme constraints of the Mars Observer Mission was selected by NASA in April, 1986. Contingent upon final confirmation in mid-November, the Mars Observer Camera (MOC) will begin acquiring images of the surface and atmosphere of Mars in September-October 1991. The MOC incorporates both a wide angle system for low resolution global monitoring and intermediate resolution regional targeting, and a narrow angle system for high resolution selective surveys. Camera electronics provide control of image clocking and on-board, internal editing and buffering to match whatever spacecraft data system capabilities are allocated to the experiment. The objectives of the MOC experiment follow. Author

N87-23557*# Geological Survey, Flagstaff, Ariz.

PLANETARY NOMENCLATURE

M. E. Strobell and Harold Masursky *In* NASA, Washington Reports of Planetary Geology and Geophysics Program, 1986 May 1987 p 551-553 (For primary document see N87-23341 16-91)
Avail: NTIS HC A24/MF A01 CSCL 03B

In fiscal 1986, names were chosen for prominent features on the five previously known Uranian satellites and for features on the largest of the 10 satellites discovered by Voyager 2. The names of the five large satellites are taken mostly from Shakespeare, and most are spirits; therefore, Shakespearean and spirit themes were used to choose names for topographic features on the satellites. Crater names and most other feature names on Miranda, Oberon, and Titania are from Shakespeare; features on Ariel are named for bright spirits and those on Umbriel for dark, all taken from universal mythology. Preliminary coordinates for these features are derived from shaded relief maps of the satellites to be published in 1987. Orbital elements have been established for the 10 new satellites, and a paper describing this work is in progress; satellite positions are under review by Commission 16 of the IAU. The moon 1985 U1 is informally designated Puck. The nine small satellites discovered in 1986 are to be named for Shakespearean heroines; these names are to be listed in the 1987 edition of the Annual Gazetteer of Planetary Nomenclature. Author

N87-23558*# Geological Survey, Flagstaff, Ariz.

ENHANCED LANDSAT IMAGES OF ANTARCTICA AND PLANETARY EXPLORATION c43

B. K. Lucchitta, J. A. Bowell, K. Edwards, E. M. Eliason, and H. M. Ferguson *In* NASA, Washington Reports of Planetary Geology and Geophysics Program, 1986 May 1987 p 554 Submitted for publication (For primary document see N87-23341 16-91)
Avail: NTIS HC A24/MF A01 CSCL 08B

Since early in the LANDSAT program, black-and-white paper prints of band 7 (near infrared) of the LANDSAT multispectral scanner have been used extensively to prepare semicontrolled maps of Antarctica. Image-processing techniques are now employed to enhance fine detail and to make controlled image-mosaic maps in color. LANDSAT multispectral images of Antarctica help to expand our knowledge of extraterrestrial bodies by showing bare-ice areas as bright blue patches; on such patches

meteorites tend to be concentrated and are collected. Many subtle flow features in Antarctic ice streams resemble features at the mouths of Martian outflow channels, which suggests that the channels also contained ice. Furthermore, flow lines in Antarctic ice sheets that merge with ice shelves resemble Martian flow features associated with dissected terrain along the Martian northern highland margin, and support the concept that ice was involved in the transport of material from the southern highlands to the northern lowland plains. In Antarctica, as on Mars, the virtual absence of fluvial activity over millions of years has permitted the growth of glacial and eolian features to unusually large sizes.
Author

N87-23559*# National Aeronautics and Space Administration, Washington, D.C. Dept. of Geological Sciences.
COMPOSITIONAL STRATIGRAPHY OF CRUSTAL MATERIAL FROM NEAR-INFRARED SPECTRA
Carle M. Pieters *In* NASA, Washington Reports of Planetary Geology and Geophysics Program, 1986 May 1987 p 210
(For primary document see N87-23341 16-91)
Avail: NTIS HC A24/MF A01 CSCL 03B

An Earth-based telescopic program to acquire near-infrared spectra of freshly exposed lunar material now contains data for 17 large impact craters with central peaks. Noritic, gabbroic, anorthositic and troctolitic rock types can be distinguished for areas within these large craters from characteristic absorptions in individual spectra of their walls and central peaks. Norites dominate the upper lunar crust while the deeper crustal zones also contain significant amounts of gabbros and anorthosites. Data for material associated with large craters indicate that not only is the lunar crust highly heterogeneous across the nearside, but that the compositional stratigraphy of the lunar crust is nonuniform. Crustal complexity should be expected for other planetary bodies, which should be studied using high spatial and spectral resolution data in and around large impact craters. J.P.B.

92 SOLAR PHYSICS

Includes solar activity, solar flares, solar radiation and sunspots.
For related information see *93 Space Radiation.*

N87-23560# Tufts Univ., Medford, Mass. Dept. of Physics and Astronomy.
SOLAR ACTIVE REGION PHYSICAL PARAMETERS INFERRED FROM A THERMAL CYCLOTRON LINE AND SOFT X-RAY SPECTRAL LINES
Kenneth R. Lang, Robert F. Willson, Kermit L. Smith, and Keith T. Strong 1986 22 p Prepared in cooperation with Lockheed Missile and Space Co., Palo Alto, Calif.
(Contract N00014-86-K-0068; Grant AF-AFOSR-0019-83)
(AD-A179650) Avail: NTIS HC A02/MF A01 CSCL 03B

Simultaneous high resolution observations of coronal loops are presented at 20 cm wavelength with the Very Large Array and at soft X ray wavelengths. The images at 20 cm and soft X-ray wavelengths have nearly identical sizes and ellipsoidal shapes, with a linear extent of about 5 cm. This emission stretches between and across regions of opposite magnetic polarity in the underlying photosphere. Complete X ray coronal loops can therefore be imaged at 20 cm, and the VLA maps describe the radio wavelength counterpart of X ray coronal loops. X ray spectral lines were used to obtain values of electron temperature and electron density averaged over the emitting area. The absence of detectable circular polarization is consistent with an optically thick plasma. The observed brightness temperature was roughly equal to the electron temperature of the coronal plasma. The VLA maps at 10 closely spaced frequencies between 1440 and 1720 MHz describe the same coronal loops or arcades of loops. A plot of the maximum brightness temperature of these loops as a function of observing frequency exhibits a line like feature with a central frequency of 1650 MHz and a half width of 80 MHz. This spectral feature is attributed to a thermal cyclotron line. GRA

N87-23561*# Tufts Univ., Medford, Mass. Dept. of Physics.
J. VLA (VERY LARGE ARRAY) OF A SOLAR NOISE STORM
Kenneth R. Lang and Robert F. Willson 1986 20 p
(Grant NAG5-501)
(NASA-CR-180219; NAS 1.26:180219; AD-A179664) Avail: NTIS HC A02/MF A01 CSCL 03B

The first Very Large Array (VLA) observations of the Sun at 92 cm wavelength (328 MHz) are presented. A 3-hr solar noise storm was detected; it consisted of burst-like spikes superimposed on a slowly varying background, and both storm components were 95 + or - 5% right-hand circularly polarized. A long duration soft X ray event preceded the radio radiation by 30 m, suggesting a disturbance moving outwards at a velocity of v = 78 km/s. The 92 cm noise storm was resolved with an angular resolution of 9 sec for time intervals as short as 13 s. During the onset and early phases, the storm consisted of four compact sources, each with an angular diameter of 40 sec, oriented within an elongated source with angular dimensions of 40 sec by 200 sec. During the subsequent hour the most intense emission was located in two 40 sec sources separated by 100 sec. Snapshot maps revealed a persistent elongated source at successive peaks, with a scatter in the source position. A systematic position shift of Deta Theta sub I greater than or = 15 sec can be produced by the Earth's ionosphere, but these effects can be removed by frequent observations of a nearby calibrator source. The observations confirm previously reported trends for a decrease in source size at higher frequencies, but they suggest a hitherto unresolved complexity in source structure. GRA

N87-23562# Tufts Univ., Medford, Mass. Dept. of Physics and Astronomy.
SIMULTANEOUS SMM FLAT CRYSTAL SPECTROMETER AND VERY LARGE ARRAY OBSERVATIONS OF SOLAR ACTIVE REGIONS
Kenneth R. Lang, Robert F. Willson, Kermit L. Smith, and Keith T. Strong 1986 27 p Prepared in cooperation with Lockheed Missile and Space Co., Palo Alto, Calif.
(Contract N00014-86-K-0068; Grant AF-AFOSR-0019-83)
(AD-A179698) Avail: NTIS HC A03/MF A01 CSCL 03B

High-resolution images of the quiescent emission from two solar active regions at 20 cm (VLA) and soft X-ray (SMM-FCS) wavelengths are compared. There are regions where the X-ray coronal loops have been completely imaged at 20 cm wavelength. In other regions, the X-ray radiation was detected without detectable 20 cm radiation, and vice versa. The X-ray data were used to infer average electron temperatures Te of about 3,000,000 K and average electron densities of about 2.5 x ten to the ninth power cu cm for the X-ray emitting plasma in the two active regions. The thermal bremsstrahlung of the X-ray emitting plasma is probably optically thin at 20 cm wavelength. Although the 20-cm brightness temperatures TB were always less than Te, suggesting optically thin layers, the thermal gyroresonance radiation from the X-ray emitting plasma ought to be optically thick at 20 cm wavelength. The low TB can be explained if a higher, cooler plasma covers the hotter X-ray emitting plasma. Thermal gyroresonance radiation must account for the intense 20-cm radiation near and above sunspots where no X-ray radiation is detected. The potential of 20 cm (VLA) and soft X-ray (SMM-FCS) comparisons is discussed. GRA

N87-23563*# California Univ., Berkeley. Space Sciences Lab.
A PRELIMINARY SUMMARY OF THE OBSERVATIONS OF THE 16 FEBRUARY 1984 SOLAR FLARE (STIP INTERVAL XV, 12-21 FEBRUARY 1984)
S. R. Kane and H. W. Urbarz (Tuebingen Univ., West Germany) [1987] 10 p Sponsored in part by AFGL
(Grants NAG5-376; NGL-05-003-017; NAG2-393)
(NASA-CR-180929; NAS 1.26:180929) Avail: NTIS HC A02/MF A01 CSCL 03B

The solar flare on 16 Feb. 1984 (0900 UT) and the associated photon and particle emissions were perhaps the most interesting solar and interplanetary phenomena during STIP Interval XV, 12 to 21 Feb. 1984. The X-ray and microwave radio emissions, as observed from the Earth, were relatively weak and no optical flare was reported. However, the hard X-ray and low energy gamma-ray observations made with the Pioneer Venus Orbiter spacecraft behind the west limb of the Sun indicate that the flare was, in reality, very intense. There is evidence that the flare was located approx 40 deg behind the west limb of the Sun and hence, for instruments located near the Earth, the most intense parts of the X-ray and microwave radio sources were occulted by the photosphere. However, the effect of occultation on the metric type II, type III, and type IV and decimetric (type DCIM) radio sources appeared to be relatively small. Following the flare, a large increase in the counting rates was recorded by several ground level neutron monitors and energetic particle detectors located in interplanetary space. A preliminary analysis of the 16 Feb. 1984 flare observations follows. Author

N87-23564*# California Univ., Berkeley. Space Sciences Lab.
X-RAY AND LOW ENERGY GAMMA-RAY OBSERVATIONS OF THE 16 FEBRUARY 1984 SOLAR FLARE
S. R. Kane, R. W. Klebesadel, E. E. Fenimore, and J. G. Laros (Los Alamos National Lab., N. Mex.) 1987 4 p Sponsored in part by DOE
(Grants NAG5-376; NAG2-393)
(NASA-CR-180928; NAS 1.26:180928) Avail: NTIS HC A02/MF A01 CSCL 03B

The February 16, 1984 (0900 UT) solar flare was very energetic and produced a variety of emissions. The X-ray and gamma ray continuum measurement, made aboard the International Cometary Explorer (ICE) and the Pioneer Venus Orbiter (PVO), are briefly described. B.G.

N87-23565# Naval Research Lab., Washington, D. C.
NONLINEAR ASPECTS OF PLANAR CONDENSATIONAL INSTABILITY
R. B. Dahlburg, C. R. DeVore, J. M. Picone, J. T. Mariska, and J. T. Karpen 27 Feb. 1987 62 p
(AD-A178998; NRL-MR-5922) Avail: NTIS HC A04/MF A01 CSCL 03B

The numerical simulation of the nonlinear evolution of a radiation driven thermally unstable planar fluid, using a semi-implicit finite difference algorithm is discussed. When the equilibrium state of the fluid is perturbed by random initial excitation of the velocity field, dense, cool, two dimensional structures are observed forming in a rarer, warmer, surrounding medium. The nonlinear phase of evolution is characterized by the turbulent contraction of the condensed region, accompanied by a significant increase in the amount of energy radiated. If the random velocity perturbation has a sufficiently large amplitude, the fluid will not form condensed structures. Finally, the relationship of these results to observations of the solar chromosphere, transition region and corona is discussed. GRA

N87-23566# Herzberg Inst. of Astrophysics, Ottawa (Ontario).
OBSERVATIONS OF SOLAR FLUX AT THE ALGONQUIN RADIO OBSERVATORY ON 2800 MHz AND THE DOMINION RADIO ASTROPHYSICAL OBSERVATORY ON 2700 MHz Monthly Reports, Jan. - Dec. 1985
M. B. Bell, H. P. Gagnon, and J. D. Moore Feb. 1986 67 p
(ARO-15; NRCC-25417) Avail: NTIS HC A04/MF A01

Daily tabulations of the radio flux at 2800 MHz from the Algonquin Radio Observatory (ARO) and at 2700 MHz from the Dominion Radio Astrophysical Observatory (DRAO) are presented for the year 1985. This period marks the tenth year into sunspot cycle 21. Author

N87-23567# Herzberg Inst. of Astrophysics, Ottawa (Ontario).
EAST-WEST SOLAR SCANS AT 10-CM WAVELENGTH TAKEN AT THE ALGONQUIN RADIO OBSERVATORY, JAN. 1980 TO DECEMBER 1985
M. B. Bell, H. P. Gagnon, and J. D. Moore Mar. 1986 82 p
(ARO-16; NRCC-25466) Avail: NTIS HC A05/MF A01

Solar scans at 10-cm wavelength and 1.5 minutes of arc east-west resolution, taken at the Algonquin Radio Observatory between January 1980 and December 1985 are presented. Also given is a list to date of all publications pertaining to the ARO solar multielement interferometer. Author

N87-23379*# National Aeronautics and Space Administration. Ames Research Center, Moffett Field, Calif.
PROTOSTELLAR DISKS AND THE PRIMITIVE SOLAR NEBULA
P. M. Cassen, J. B. Pollack, T. Bunch, O. Hubickyj, P. Moins, and C. Yuan (City Coll. of the City Univ. of New York.) *In* NASA, Washington Reports of Planetary Geology and Geophysics Program, 1986 May 1987 p 97-99 (For primary document see N87-23341 16-91)
Avail: NTIS HC A24/MF A01 CSCL 03B

N87-23384*# Planetary Science Inst., Tucson, Ariz.
ACCUMULATION OF SOLID BODIES IN THE SOLAR NEBULA
S. J. Weidenschilling and D. R. Davis *In* NASA, Washington Reports of Planetary Geology and Geophysics Program, 1986 May 1987 p 106-107 (For primary document see N87-23341 16-91)
(Contract NASw-3214)
Avail: NTIS HC A24/MF A01 CSCL 03B

93 SPACE RADIATION

Includes cosmic radiation; and inner and outer earth's radiation belts.

For biological effects of radiation see *52 Aerospace Medicine.* For theory see *73 Nuclear and High-Energy Physics.*

N87-23568# Los Alamos National Lab., N. Mex.
DETECTION OF 10-eV GAMMA RAYS FROM CYGNUS X-3 DURING 1986
D. E. Nagle, R. D. Bolton, R. L. Burman, K. B. Butterfield, R. Cady, R. D. Carlini, V. D. Sandberg, R. A. Williams, C. Wilkinson, C. Y. Chang et al. Jan. 1987 6 p Presented at the Relativistic Astrophysics Conference, Pasadena, Ca., 4 Jan. 1987 Prepared in cooperation with Maryland Univ., College Park. Tata Inst. of Fundamental Research, Bombay, India, George Mason Univ., Fairfax, Va., New Mexico Univ., Albuquerque and California Univ., Irvine
(Contract W-7405-eng-36)
(DE87-006054; LA-UR-87-409; CONF-870157-1) Avail: NTIS HC A02/MF A01

Cosmic ray muons associated with extensive air showers were detected by a scintillator array. Data were collected within a 30 degree cone centered about the zenith. About 20,000 showers per day were recorded. DOE

N87-23332*# Los Alamos National Lab., N. Mex.
BEAMED EMISSION FROM GAMMA-RAY BURST SOURCES Abstract Only
R. Epstein *In* NASA. Marshall Space Flight Center Double Layers in Astrophysics May 1987 p 305 (For primary document see N87-23313 16-88)
Avail: NTIS HC A14/MF A01 CSCL 03B

N87-23333*# Los Alamos National Lab., N. Mex. Space Plasma Physics Group.
DOUBLE LAYERS AND PLASMA-WAVE RESISTIVITY IN EXTRAGALACTIC JETS: CAVITY FORMATION AND RADIO-WAVE EMISSION
Joseph E. Borovsky *In* NASA. Marshall Space Flight Center Double Layers in Astrophysics May 1987 p 307-315 Sponsored in part by DOE (For primary document see N87-23313 16-88)
Avail: NTIS HC A14/MF A01 CSCL 03B

99 GENERAL

N87-23569# Air Force Systems Command, Brooks AFB, Tex. Human Systems Div.

AIR FORCE TECHNICAL OBJECTIVES DOCUMENT, FISCAL YEAR 1988 Annual Report, Jan. 1986 - Jan. 1987

Jan. 1987 27 p
(AD-A179163; HSD-TR-87-005) Avail: NTIS HC A03/MF A01
CSCL 15B

This Technical Objective Document (TOD) describes the planning methodology used within two of Human Systems Division (HSD) laboratories to achieve technical goals. Specifically, efforts are directed in the biotechnology program to man's adaptability, survivability, and performance capabilities within his operational environment. This research and development of HSD's functions is accomplished as interdisciplinary work by teams of biomedical scientists, engineers, and physical scientists within the Air Force laboratories and the industrial and academic communities.

GRA

☆ U.S. GOVERNMENT PRINTING OFFICE: 1987—181-546/60014

FEDERAL REGIONAL DEPOSITORY LIBRARIES

ALABAMA

AUBURN UNIV. AT MONTGOMERY LIBRARY
Documents Department
Montgomery, AL 36193
(205) 271-9650

UNIV. OF ALABAMA LIBRARY
Documents Dept.-Box S
University, AL 35486
(205) 348-6046

ARIZONA

DEPT. OF LIBRARY, ARCHIVES AND PUBLIC RECORDS
Third Floor—State Cap.
1700 West Washington
Phoenix, AZ 85007
(602) 255-4121

UNIVERSITY OF ARIZONA LIB.
Government Documents Dept.
Tucson, AZ 85721
(602) 621-6433

ARKANSAS

ARKANSAS STATE LIBRARY
One Capitol Mall
Little Rock, AR 72201
(501) 371-2326

CALIFORNIA

CALIFORNIA STATE LIBRARY
Govt. Publications Section
P.O. Box 2037
Sacramento, CA 95809
(916) 324-4863

COLORADO

UNIV OF COLORADO LIB.
Government Pub. Division
Campus Box 184
Boulder, CO 80309
(303) 492-8834

DENVER PUBLIC LIBRARY
Govt. Pub. Department
1357 Broadway
Denver, CO 80203
(303) 571-2131

CONNECTICUT

CONNECTICUT STATE LIBRARY
Government Documents Unit
231 Capitol Avenue
Hartford, CT 06106
(203) 566-7029

FLORIDA

UNIV. OF FLORIDA LIBRARIES
Library West
Documents Department
Gainesville, FL 32611
(904) 392-0367

GEORGIA

UNIV. OF GEORGIA LIBRARIES
Government Reference Dept.
Athens, GA 30602
(404) 542-8949

HAWAII

UNIV. OF HAWAII LIBRARY
Govt. Documents Collection
2550 The Mall
Honolulu, HI 96822
(808) 948-8230

IDAHO

UNIV. OF IDAHO LIBRARY
Documents Section
Moscow, ID 83843
(208) 885-6344

ILLINOIS

ILLINOIS STATE LIBRARY
Information Services Branch
Centennial Building
Springfield, IL 62756
(217) 782-5185

INDIANA

INDIANA STATE LIBRARY
Serials Documents Section
140 North Senate Avenue
Indianapolis, IN 46204
(317) 232-3686

IOWA

UNIV. OF IOWA LIBRARIES
Govt. Documents Department
Iowa City, IA 52242
(319) 353-3318

KANSAS

UNIVERSITY OF KANSAS
Doc. Collect—Spencer Lib.
Lawrence, KS 66045-2800
(913) 864-4662

KENTUCKY

UNIV. OF KENTUCKY LIBRARIES
Govt. Pub. Department
Lexington, KY 40506-0039
(606) 257-3139

LOUISIANA

LOUISIANA STATE UNIVERSITY
Middleton Library
Govt. Docs. Dept.
Baton Rouge, LA 70803
(504) 388-2570

LOUISIANA TECHNICAL UNIV. LIBRARY
Documents Department
Ruston, LA 71272-0046
(318) 257-4962

MAINE

UNIVERSITY OF MAINE
Raymond H. Fogler Library
Tri-State Regional Documents Depository
Orono, ME 04469
(207) 581-1680

MARYLAND

UNIVERSITY OF MARYLAND
McKeldin Lib.—Doc. Div.
College Park, MD 20742
(301) 454-3034

MASSACHUSETTS

BOSTON PUBLIC LIBRARY
Government Docs. Dept.
Boston, MA 02117
(617) 536-5400 ext.226

MICHIGAN

DETROIT PUBLIC LIBRARY
Sociology Department
5201 Woodward Avenue
Detroit, MI 48202-4093
(313) 833-1409

MICHIGAN STATE LIBRARY
P.O. Box 30007
Lansing, MI 48909
(517) 373-1593

MINNESOTA

UNIVERSITY OF MINNESOTA
Government Pubs. Division
409 Wilson Library
309 19th Avenue South
Minneapolis, MN 55455
(612) 373-7870

MISSISSIPPI

UNIV. OF MISSISSIPPI LIB.
Documents Department
University, MS 38677
(601) 232-5857

MONTANA

UNIV. OF MONTANA
Mansfield Library
Documents Division
Missoula, MT 59812
(406) 243-6700

NEBRASKA

UNIVERSITY OF NEBRASKA - LINCOLN
Love Library
Documents Department
Lincoln, NE 68588-0410
(402) 472-2562

NEVADA

UNIVERSITY OF NEVADA LIB.
Govt. Pub. Department
Reno, NV 89557-0044
(702) 784-6579

NEW JERSEY

NEWARK PUBLIC LIBRARY
5 Washington Street
Newark, NJ 07101-0630
(201) 733-7812

NEW MEXICO

UNIVERSITY OF NEW MEXICO
Zimmerman Library
Government Pub. Dept.
Albuquerque, NM 87131
(505) 277-5441

NEW MEXICO STATE LIBRARY
Reference Department
325 Don Gaspar Avenue
Santa Fe, NM 87503
(505) 827-3826

NEW YORK

NEW YORK STATE LIBRARY
Empire State Plaza
Albany, NY 12230
(518) 474-5563

NORTH CAROLINA

UNIVERSITY OF NORTH CAROLINA AT CHAPEL HILL
Davis Library
BA/SS Documents Division
Chapel Hill, NC 27515
(919) 962-1151

NORTH DAKOTA

UNIVERSITY OF NORTH DAKOTA
Chester Fritz Library
Documents Department
Grand Forks, ND 58202
(701) 777-4629
In cooperation with North Dakota State Univ. Library

OHIO

STATE LIBRARY OF OHIO
Documents Department
65 South Front Street
Columbus, OH 43266-0334
(614) 462-7051

OKLAHOMA

OKLAHOMA DEPT. OF LIB.
Government Documents
200 NE 18th Street
Oklahoma City, OK 73105
(405) 521-2502, ext. 252

OKLAHOMA STATE UNIV. LIB.
Documents Department
Stillwater, OK 74078
(405) 624-6546

OREGON

PORTLAND STATE UNIV. LIB.
Documents Department
P.O. Box 1151
Portland, OR 97207
(503) 229-3673

PENNSYLVANIA

STATE LIBRARY OF PENN.
Government Pub. Section
P.O. Box 1601
Harrisburg, PA 17105
(717) 787-3752

TEXAS

TEXAS STATE LIBRARY
Public Services Department
P.O. Box 12927—Cap. Sta.
Austin, TX 78711
(512) 475-2996

TEXAS TECH. UNIV. LIBRARY
Govt. Documents Department
Lubbock, TX 79409
(806) 742-2268

UTAH

UTAH STATE UNIVERSITY
Merrill Library, U.M.C. 30
Logan, UT 84322
(801) 750-2682

VIRGINIA

UNIVERSITY OF VIRGINIA
Alderman Lib.—Public Doc.
Charlottesville, VA 22903-2498
(804) 924-3133

WASHINGTON

WASHINGTON STATE LIBRARY
Documents Section
Olympia, WA 98504
(206) 753-4027

WEST VIRGINIA

WEST VIRGINIA UNIV. LIB.
Documents Department
Morgantown, WV 26506-6069
(304) 293-3640

WISCONSIN

MILWAUKEE PUBLIC LIBRARY
814 West Wisconsin Avenue
Milwaukee, WI 53233
(414) 278-3065

ST. HIST LIB. OF WISCONSIN
Government Pub. Section
816 State Street
Madison, WI 53706
(608) 262-4347

WYOMING

WYOMING STATE LIBRARY
Supreme Ct. & Library Bld.
Cheyenne, WY 82002
(307) 777-5919

National Aeronautics and
Space Administration
Code NTT-4
Washington, D.C.
20546

Official Business
Penalty for Private Use, $300

SPECIAL FOURTH-CLASS RATE
POSTAGE & FEES PAID
NASA
PERMIT No. G 27

NASA

POSTMASTER: If Undeliverable (Section 158
Postal Manual) Do Not Return